N76-33525

CONIT

A Service of:

National Aeronautics and Space Administration

Scientific and Technical Information Office

NASA CR-134991

(NASA-CR-134991) ASSESSMENT OF NDE RELIABILITY DATA Final Report, Jul. 1974 - Sep. 1975 (General Dynamics/Fort Worth) HC $11.75 CSCL 14D

N76-33525

Unclas

G3/38 05376

ASSESSMENT OF NDE RELIABILITY DATA

B. G. W. Yee, F. H. Chang,
J. C. Couchman and G. H. Lemon

General Dynamics
Fort Worth Division
Fort Worth, Texas

and

P. F. Packman

Vanderbilt University
Nashville, Tennessee

Prepared for

NATIONAL AERONAUTICS AND SPACE ADMINISTRATION

NASA Lewis Research Center
Contract NAS 3-18907

N O T I C E

1. Report No.
NASA CR-134991

2. Government Accession No.

3. Recipient's Catalog No.

4. Title and Subtitle

ASSESSMENT OF NDE RELIABILITY DATA

5. Report Date
October 1976

6. Performing Organization Code

7. Author(s) B. G. W. Yee, F. H. Chang, J. C. Couchman and G. H. Lemon of General Dynamics and P. F. Packman, Vanderbilt University

8. Performing Organization Report No.

10. Work Unit No.
YHG 6780

9. Performing Organization Name and Address
General Dynamics/Fort Worth Division
Fort Worth, Texas and
Vanderbilt University, Nashville, Tennessee

11. Contract or Grant No.
NAS3-18907

12. Sponsoring Agency Name and Address
National Aeronautics and Space Administration
Washington, D. C. 20546

13. Type of Report and Period Covered
Contractor Report
July 1974 - Sept 1975

14. Sponsoring Agency Code

15. Supplementary Notes
Project Manager, S. J. Klima, Materials & Structures Division
NASA Lewis Research Center, Cleveland, Ohio

16. Abstract

Twenty sets of relevant NDE reliability data have been identified, collected, compiled, and categorized. Three relevant on-going programs are being monitored for future usage. A criterion for the selection of data for statistical analysis considerations has been formulated. A model to grade the quality and validity of the data sets has been developed. Data input formats, which record the pertinent parameters of the defect/specimen and inspection procedures, have been formulated for each NDE method. A comprehensive computer program has been written to calculate the probability of flaw detection at several confidence levels by the binomial distribution. This program also selects the desired data sets for pooling and tests the statistical pooling criteria before calculating the composite detection reliability. Probability of detection curves at 95 and 50 percent confidence levels have been plotted for individual sets of relevant data as well as for several sets of merged data with common sets of NDE parameters.

17. Key Words (Suggested by Author(s))
NDE
Reliability
Probability of Detection
Confidence Level
Fatigue Cracks

18. Distribution Statement
Unclassified

19. Security Classif. (of this report)
Unclassified

20. Security Classif. (of this page)
Unclassified

ASSESSMENT OF NDE RELIABILITY DATA

B. G. W. Yee, F. H. Chang,
J. C. Couchman and G. H. Lemon

General Dynamics
Fort Worth Division
Fort Worth, Texas

and

P. F. Packman

Vanderbilt University
Nashville, Tennessee

Final Report

Prepared for

NATIONAL AERONAUTICS & SPACE ADMINISTRATION
Lewis Research Center
Cleveland, Ohio

Contract NAS 3-18907

Foreword

This final report covers the work performed under Contract NAS-3-18907 from July 1974 to September 1975. The study was accomplished by General Dynamics Corporation, Fort Worth Division, Fort Worth, Texas and Vanderbilt University, Nashville, Tennessee. The program was managed by Dr. B. G. W. Yee of General Dynamics, with Dr. J. C. Couchman and Dr. F. H. Chang serving as principal investigators. Valuable contributions were made to the development of the statistical analysis by Dr. G. H. Lemon and computer programming by J. S. Kunselman and T. Walker. Dr. P. F. Packman of Vanderbilt University served as associate program manager. The program was under the technical direction of Mr. S. J. Klima, NASA Lewis Research Center, Cleveland, Ohio.

Participants in this program are indebted to many people in the NDE community for furnishing data to this program and for providing consultation.

Thank you!

TABLE OF CONTENTS

TABLE OF CONTENTS
(CONTINUED)

LIST OF FIGURES

LIST OF TABLES

SUMMARY

The overall objective of this program is to assess available nondestructive testing data for the determination of the sensitivity and reliability of state-of-the-art production NDE methods for flaw detection on metallic materials. This program was separated into four different tasks. They were:

Task I	Acquisition of Information
Task II	Screening and Separation of Data by NDE Method and Material
Task III	Statistical Determination of NDE Reliability
Task IV	Reporting

Twenty sets of relevant NDE reliability data have been identified, collected, compiled, and categorized. Three relevant on-going programs have also been identified. A criterion for the selection of data for statistical analysis considerations has been formulated. A model to grade the quality and validity of the data sets has been developed. Data input formats, which record the pertinent parameters of the defect/specimen and inspection procedures, have been formulated for each NDE method. A comprehensive computer program has been written to calculate the probability of flaw detection at several confidence levels by the binomial distribution. This program also selects the desired data sets for pooling, and tests the statistical pooling criteria before calculating the composite detection reliability. Probability of detection curves at 95 and 50 percent confidence levels have been plotted by NDE technique and material type for individual sets of data as well as for merged data.

I. INTRODUCTION

In order to apply linear-elastic fracture mechanics to structural design, NDE has to show at a high level of confidence that no flaw larger than a specific size exists in the structure. To establish the minimum detectable flaw size, many companies and organizations have conducted NDE demonstration programs. Most of these demonstration programs have been conducted in the production and field-service environment, but some have been conducted in the laboratory environment.

The results obtained from demonstration programs are lacking in universal agreement. This lack of agreement is not surprising because each company or organization may use a different NDE procedure, different personnel, different procedures and parameters to generate the test flaws, different flaws and material types, and even different statistical analysis procedures. There appears to be a need to (1) collect much of the available NDE reliability data, (2) closely examine all the parameters that could affect the detection reliability, (3) compare the parameters used by each organization to obtain the data, and (4) attempt to identify the parameters that most likely cause observable differences in detection reliability. It appears worthwhile to obtain a composite detection reliability for each NDE method, material type, and flaw type by pooling data obtained from several sources. At the same time, the merits and shortcomings of several statistical analysis procedures should be carefully examined and the procedure most suitable for the analysis of NDE reliability data should be selected. Any needs for improved methods should be identified.

The program reported on in this document was intended to collect all available NDE data, screen and separate the data by NDE method and material, perform statistical analyses, and evaluate the state-of-the-art in NDE reliability.

II. ACQUISITION OF INFORMATION

The acquisition of NDE reliability related data, identification of on-going programs, and preparation of a bibliography of the acquired data is discussed in this section.

2.1 Acquisition of NDE Reliability Related Data

Twenty-three sets of potentially useful data have been identified during this program and twenty sets were acquired. Three sets of data involve on-going programs and the data were not made available for inclusion in this study. Of the twenty sets of data received, only seven sets were statistically analyzed. The thirteen sets of data that were not statistically analyzed were rejected because they did not satisfy the selection criterion discussed in Section III of this report or the owner refused to permit the data to be used.

2.2 Bibliography

The twenty sets of NDE reliability related data that have been acquired are listed below. Some of the references are private data in which case only company or committee report numbers are available. Several references to government funded programs, which have not been published can only be identified by sponsoring agencies and the name of an individual at the company where the work was conducted. Copies of these data can be obtained by either contacting an individual within the sponsoring agency or an individual associated with the company.

References

1. Pettit, D. E. and Hoeppner, D. W., "Fatigue Flaw Growth and NDI Evaluation for Preventing Through Cracks in Spacecraft Tankage Structures," NASA CR-128600 (NAS-9-11722), September 25, 1972, Lockheed, CA.

2. Rummel, W. D.,Todd, P. H. Jr., Frecska, S. A. and Rathke, R. A., "The Detection of Fatigue Cracks by Nondestructive Test Methods," NASA CR-2369 (NAS-9-12276), February 1974, Martin Marietta.

3. Packman, P. F., et al, "The Applicability of Fracture Mechanics Nondestructive Testing Design Criterion," AFML-TR68-32, May 1968.

4. Anderson, R. T., Delacy, T. J., and Stewart, R. C., "Detection of Fatigue Cracks by Nondestructive Testing Methods," NASA CR-128946 (NAS-9-12326), March 1973.

5. Buchanan, R. A., "Analysis of Test Data on PVRC specification No. 3, Ultrasonic Examination of Forgings, Revisions I and II, January 14, 1974 (PVRC Committee on ND Examination of Mat. for Pressure Components, PVRC Welding Research Council).

6. Buchanan, R. A., and Talbot, T. F., "Analysis of ND Examination of PVRC Plate-Weld Specimen 251J," May 21, 1973. (PVRC Committee on ND Examination of Mat. for Pressure Components, PVRC WRC).

7. Yee, B. G. W., et al, "Evaluation and Optimization of the Advanced Signal Counting Technique on Weldments," General Dynamics/FWD, FZM-5917, January 31, 1972.

8. Bishop, C. R., "Nondestructive Evaluation of Fatigue Cracks," Rockwell International-Space Division SD73-SH-0219 (NAS-9-14000), September 1973.

9. Sattler, F. J., "Nondestructive Flaw Definition Techniques for Critical Defect Determination," NASA-CR-72602 (NAS-3-11221), January 1970.

10. Southworth, H. L., Steele, N. W., Torelli, P. P., et al, "Practical Sensitivity Limits of Production Nondestructive Testing Methods in Aluminum and Steel," AFML-TR-74-241, November 1974.

11. Moyzis, J. W., Jr., "Reliability of Airframe Inspections at the Depot Maintenance Level," Boeing, Wichita, Kansas. (Eddy current inspection of bolt holes in KC-135A wings). Boeing No. 1554, (No date).

12. Hannah, K. J., Cross, B. T., and Tooley, W. M., "Development of the Ultrasonic Delta Technique for Aluminum Welds and Materials," NASA CR-61952 (NAS 8-18009), May 15, 1968.

13. Sproat, W. H., "Reliability Analysis of C-5A Pylon Inspection," Lockheed-Georgia Internal Document No. LG-72-ER0107, (No date).

14. Sproat, W. H., "Reliability Evaluation of Nondestructive Inspection Methods Using C-130 Wing Boxes," Lockheed-Georgia Internal Document No. LG-72-ER0107, (No date).

15. Lord, R. J., "Evaluation of the Reliability and Sensitivity of NDT Methods for Titanium Alloys," AFML-TR-73-107, June 1974.

16. B-1 USAF/Rockwell International NDI Demonstration Program, E. L. Caustin, Director of Quality & Reliability Assurance, Los Angeles Division, (Set of Reports) 1972-1973.

17. A10 USAF/Fairchild Hiller NDI Demonstration Program, Ted Renshaw of Fairchild Hiller, (Set of Reports), Sept. 1973.

18. F-111 USAF/General Dynamics NDI Human Factors Study Program. Bill Kloster of General Dynamics, Fort Worth Division, (Set of Reports) 1971.

19. AFML Round Robin Results on (1) Delta Scan and (2) Magnetic Particle, Lee Gulley, AFML, WPAFB, Dayton, Ohio, March 1971.

20. Raatz, C. F., Senske, R. A. Woodmansee, W. E., et al. "Detection of Cracks Under Installed Fasteners," AFML-TR-74-80, April 1974.

2.3 On-Going Programs

There are several on-going programs that are currently known. Of these, only three are government funded and their results will be available to the public for analysis. The data from the privately funded programs may never be made available for public analysis.

The three government funded on-going programs are:

1. Crack detection reliability on welded plates and structures, Martin Marietta, Ward Rummel, sponsored by NASA/Johnson Space Center, NAS 9-13578.

2. Crack detection reliability on actual aircraft structures at the depot level, Lockheed, GA., W. Lewis, sponsored by Kelly Air Force Base.

3. Crack detection reliability on bolt holes on F-111 fatigue tested structures, General Dynamics, Fort Worth Division, B. G. W. Yee, Sponsored by SMALC.

III. SCREENING AND SEPARATION OF DATA BY NDE METHOD AND MATERIAL

This section describes the development of data selection criteria, separation and categorization of data, development of a model to grade quality of the data, and the development of a data input format for each NDE method.

3.1 Criteria for Selection of Data for Statistical Analysis

All of the reliability related NDE data are not necessarily suitable for statistical analysis. Some are lacking in the documentation of certain key pertinent parameters, such as the defect dimension, defect type, NDE method, etc. Statistical analysis of data when the key pertinent parameters are not documented would be marginal in value. A data selection criteria is needed to screen the data and prejudge the suitability of the data for statistical analysis. Such a criteria is necessarily subjective because it involves human judgment of data value or usefulness. It is felt that such a subjective criteria will still be useful to screen out data having marginal statistical value and to eliminate lost time in processing the data.

To be eligible for statistical analysis, a set of data must satisfy the following conditions:

a) An NDE procedure or specification must accompany the data which clearly describes the equipment and the parameters used so that the data may be reproduced in other facilities (assuming the same equipment or its equivalent is used).

b) The defect dimensions and specimen geometry must be well documented so that data may be statistically analyzed and compared to defect detection in the proper defect size range. When artificial methods of defect fabrication are used, at least ten percent (10%) of all defects in a given set must be destructively tested to obtain the defect dimensions. For methods that are used to produce multiple defects in a specimen or methods that are questionable for producing controllable defect dimensions, at least fifty percent (50%) of all defects in a given set must be destructively tested to verify the defect dimensions.

The model that was developed to grade the quality of the data was very subjective. It consisted of assigning weighting factors and summing up the weighting factors to obtain an overall factor that is an index of data quality. The model is included in Appendix A.

Data pooling tests that were coded in the NASA data processing code (reproduced in Appendix B) provided a means for isolating input errors and identifying any data set that may be suspect. The tests are derived from binomial statistics equations which are developed in the next section.

The computer code developed for processing the NDE reliability data is described in Appendix C. Included is a complete description of data input formats and parameter keys.

3.2 Separation and Categorization of Data Sets

The twenty sets of data listed in the Bibliography in Subsection 2.2 can be separated into three categories. Table 3-1 describes the data separated into the three categories and the status of these data sets. The first category is the data that appear to satisfy the criteria discussed in Subsection 3.1, and they will be considered for statistical analysis. There are seven (7) sets of data in this category. The second category is data that probably could be used if permission to use the data is granted by the rightful owner of the data. There are two sets of data in this category. The third category is the data that are either lacking in the inspection procedure documentation or defect dimension documentation. There are eleven sets of data in this category. The data sets in each of the three categories are presented in Table 3-1.

A large majority of the data were obtained on thin flat plates which contain fatigue cracks or weld defects. There are few sets of data that were obtained with relatively complex shaped specimens such as a T, I, or H shape. In order to gain a better understanding of the availability of data on material type, defect type, and specimen complexity, a table (Table 3-2) is constructed to categorize the data sets according to test specimen complexity. Within each data set, a brief description of the material type, NDE methods, and defect type is presented.

The materials and shapes for which valid data were obtained and statistical analysis results are computed are tabulated later in Section V (RESULTS).

Table 3-1 STATUS AND CATEGORY OF DATA CONSIDERED FOR NDE RELIABILITY ASSESSMENT

Data that satisfy the criteria discussed in Subsection 3.1 and were statistically analyzed	Data that lack owner permission use	Data that were not statistically analyzed due to the lack of sufficient inspection procedure or defect dimension documentation or both
References:	References:	References:
2 3 4 8 10 11 16	5 Pressure Vessel Research Committee approval needed before data can be used 6 Same as 5 above	1 7 9 12 13 14 15 17 18 19 20

Table 3-2 Data Grouping According to Specimen Thickness and Complexity

Flat Plates and Simple Shape	Cylindrical, I, H, T and other Moderately Complex Shapes	Actual Aircraft Structures
References:	References:	References:
1 2219-T87 Al up to 1 cm thick o Cracks in plates and welded plates o Ultrasonics, penetrant, eddy current, and X-ray o Laboratory environment	3 7075-T6511 Al o Fatigue cracks in cylindrical tubes o Ultrasonic, penetrant, and X-ray 4300 V Steel o Fatigue cracks in cylindrical tubes o Ultrasonics, penetrant, X-ray, and magnetic particle o Laboratory environment	11 7178-T651 Al o Naturally occurring fatigue cracks in bolt holes o Eddy current o Laboratory and depot level
2 2219-T87 Al up to 1 cm thick o Fatigue cracks in flat plates o Ultrasonic, penetrant, eddy current, and X-ray o Laboratory environment (mostly)	10 2024 Al o Forged defects o Ultrasonic, penetrant, eddy current, X-ray o Production environment 4340 M Steel o Forged defects o Ultrasonics, penetrant eddy current, X-ray, and magnetic particles o Production environment Some grinding cracks and hydrogen embrittlement cracks	13 6Al-4V-Ti and 7075-T6Al o Fatigue cracks off C-5A Pylon (actual and simulated) o Ultrasonics and X-ray
4 2219-T87 Al up to 1 cm thick o Fatigue cracks in flat plates o Ultrasonic, penetrant, eddy current, and X-ray o Laboratory environment (mostly)		14 7075-T6 Al o Fatigue cracks off C-130 wing boxes (actual and simulated) o Ultrasonics and eddy current 20 KC-135 lower wing skin panel and laboratory specimens with fatigue cracks under installed fastener o Ultrasonic o Laboratory and field environment

Table 3-2 (Continued)

Flat Plates and Simple Shape	Cylindrical, I, H, T and other Moderately Complex Shapes	Actual Aircraft Structure
5 Steel forging up to 25 cm thick o Induced and naturally occurring defects o Ultrasonics o Laboratory environment	15 6A1-4V-Ti o Induced forging defects o Ultrasonics, penetrant X-ray o Most production environment	
6 Steel welded-plates up to 28 cm thick o Induced weld defects o Ultrasonics and X-ray o Laboratory environment	18 D6ac Steel o Induced forging defects o Ultrasonics, magnetic particle and rubber o Production environment	
7 2219-T87 welded plates of 0.62 and 1.25 cm thick o All types of weld defects o Ultrasonic and X-ray		
8 2219-T87 Al up to 1 cm thick o Fatigue cracks in flat plates o Ultrasonic, penetrant, eddy current, and X-ray o Production environment (mostly)		
9 2219-T87 and 2014-T6A1 up to 2.5 cm thick 6A1-4V-Ti and 5A1-2.5 Sn Ti up to 1½ cm thick o Fatigue cracks in flat plates weld defects in plates		

Table 3-2 (Continued

Flat Plates and Simple Shape	Cylindrical, I, H, T and other Moderately Complex Shapes	Actual Aircraft Structure
o Ultrasonic, penetrant, X-ray, and eddy current o Laboratory environment 12 2219-T87 Welded plates of 1.25 and 2.5 cm thick o All types of weld defects o Ultrasonic and X-ray 16 6Al-4V-Ti up to 13 cm thick o Ultrasonic o Flat bottom holes and induced defects 6Al-4V-Ti Diffusion Bonded thin plates o Induced defects o Penetrant Al Samples o Fatigue cracks in flat plates o Penetrant 6Al-4V-Ti o Fatigue cracks in flat plates o Penetrant Steel o Induced weld defects o Ultrasonics		

Table 3-2 (Continued)

Flat Plates and Simple Shape	Cylindrical, I, H, T and other Moderately Complex Shapes	Actual Aircraft Structure
Al, Ti, and Steel Plates (multiple) o Cracks in fastener holes o Eddy current All in production environment		
17 Similar to those described in Reference 16		
19 o D6ac Steel Plate Delta Scan Ultrasonics		19 o D6ac, 4340, and other Steel Alloys Actual Aircraft Structure Magnetic Particle

IV STATISTICAL DETERMINATION OF NDE RELIABILITY

This section describes the binomial statistical method, cumulative schemes, statistical pooling procedure, and digital computer code for computing NDE reliability.

4.1 Introduction

There are four possible outcomes from any nondestructive inspection of an item: (1) detection of a defect that is present, (2) non-detection of a defect that is present, (3) detection of a defect that is not present (false indication), and (4) non-detection of a defect that is not present. Because of these four possible outcomes, any single inspection may be called a quadrinomial event. Although it is recognized that false indications of defects and true indications of non-defective items (cases 3 and 4) are of practical significance to both the manufacturer and the customer, it is beyond the scope of this investigation to develop a straightforward statistical method for handling the quadrinomial event.

Preliminary indications show that most NDE reliability investigations have neglected to report information concerning either false indications of defects, or true indications that specimens contained no intentionally induced flaws. However, the data input format discussed in the previous section provides for storage of information concerning false indications for future use when more of these data become available.

Cases (1) and (2) involve either a detection or non-detection of a defect that is known to exist. This event can best be described statistically by applying the binomial distribution. The Normal, Chi-square, and Poisson distributions are sometimes used as approximations to the binomial. Their applicability to the problem of NDE reliability is to be considered in the later sections of this report.

4.2 Application of Binomial Distribution

An event that has only two possible outcomes is referred to as a binomial event. Suppose, for example, an experiment in NDE is performed where N specimens, all containing identical

flaws, are routed through an ultrasonic inspection system. Suppose further, that the system capability does not change throughout the entire inspection process, i.e., each specimen is evaluated independently of the others. Let p equal the true,(but as yet unknown) probability of detecting each flaw and q=1-p be the probability of missing each flaw. Assuming p remains the same for all specimens, the random variable X can be defined as being the number of flaws that are detected in any given experiment. X, then, is referred to as a binomial random variable with parameters N and p. Its possible values are 0, 1, 2, ..., N. Equivalently, it can be said that X has a binomial distribution. The probability of obtaining any one of the N+1 possible values of X from such an experiment is described by the following equation:

$$P(X=n) = \binom{N}{n} p^n \quad q^{N-n}, \qquad n=0,1,\ldots,N \tag{1}$$

where $\binom{N}{n} = \frac{N!}{n!(N-n)!}$.

The sum of all the possible values for equation (1) is equal to unity and can be written as follows:

$$(p+q)^N = \sum_{n=o}^{N} \binom{N}{n} \; p^n \; q^{N-n} = 1 \tag{2}$$

The probability of detecting n or more flaws can be found by summing equation (1) over all the values of X for which $X \geq n$. Thus,

$$P(X \geq n) = \sum_{i=n}^{N} \binom{N}{i} p^i \; q^{N-i}. \tag{3}$$

4.2.1 Confidence Interval Estimates of the True Probability of Detection

The objective is to estimate the true proportion of defects of a particular type and size that can be detected by a given NDE method. The best single estimate, $\bar{p}$, of the true

detectable proportion is the number of flaws detected divided by the total number of flaws present:

$$\bar{p} = \frac{n}{N} \tag{4}$$

If the binomial experiment (N, n_k^*, p) is repeated an infinite number of times and if P_k is computed each time, then the average of all the p_ks will be equal to p. So $\bar{p}$ is an unbiased estimator of the true probability of crack detection.

Since the probability is small that $\bar{p}$ will exactly equal p on any specific replication of the experiment, an interval estimator that will contain p most of the time is considered useful. A lower one-sided confidence interval can be used to estimate a lower bound on the true probability of crack detection. The lower bound, p_1, for n detections of N cracks is computed as follows:

$$\text{Solve} \quad \alpha = \sum_{i=n}^{N} \binom{N}{i} p_1^{\,i} (1-p_1)^{N-i} \tag{5}$$

for p_1, where

$$\alpha = 1 - G \tag{6}$$

The following interpretation can be given for a 100G percent lower binomial confidence interval. If the binomial experiment (N, n_k, p) is repeated many times (theoretically infinite), and if p_{1_k} is computed each time, then 100G percent of these lower confidence intervals will be equal to or lower than p. Thus, there is 100G percent "confidence" that the lower bound, p_1, computed for any specific binomial experiment will be less than or equal to the true probability of crack detection. The choice of G is arbitrary and depends on how sure one needs to be that the true probability of detection is in the interval from p_1 to 1, (the larger the value of G, the smaller the calculated lower bound p_1 will be).

---

* n_k is the number of successes in the K^{th} replication of a binomial experiment consisting of N measurements.

4.2.2 Sample Size Determination

The objective is to determine the sample size required to estimate the lower confidence limit and confidence level. This can be accomplished by utilizing equation (6). By specifying the confidence level, G, and the lower confidence limit p_1, a set of values (which must be integers) can be computed for N and n. Each combination of N and n in this set indicates the number of inspections and the number of detections required to achieve the specified probability of detection (POD) at the stated confidence level. For example, if G and p_1 are chosen to be 0.95 and 0.9 respectively, equation (5) becomes

$$0.95 = 1 - \sum_{i=n}^{N} \binom{N}{i} (0.9)^{i}(0.1)^{N-i}. \tag{7}$$

One of the combinations of N and n is 29 and 29 respectively. This represents the smallest sample size that can be utilized to meet the minimum specified values for G and p_1. The next smallest sample size is N=46. In this case n must equal at least 45 to achieve 90% probability of detection at 95% confidence level. The higher the reliability requirements, of course, the larger the sample size required.

Equation (5) can also be used to calculate the number of added NDE tests required to upgrade an existing batch of data in the hope of achieving higher reliability estimates. Equation (5) takes on the form

$$1-G = \sum_{i=n+\delta-\epsilon}^{N+\delta} \binom{N+\delta}{i} p_1^i \quad (1-p_1)^{N+\delta-i} \tag{8}$$

where δ is the required number of additional tests and ϵ is the maximum number of additional misses (nondetections). For example, if an experiment consisting of 29 inspections and 28 detections was performed, the reliability (equation 5) is 90% probability of detection at 80% confidence level. If a 95% confidence level is desired, the additional data requirements are indicated by equation (8). Thus, δ = 17 with ϵ = 0 represents the minimum added sample required to upgrade the existing data.

4.3 Comparison of Alternative Statistical Procedures

Table 4-1 lists the probability of detection at the 95% confidence level for four commonly used probability analysis methods, (Binomial, Normal, Poisson, and Chi-Square). The comparison is on the basis of 30 trials with 10, 15, 20, 25, 29 and 30 detections. The Binomial gives the exact results. The Normal approximation gives confidence values greater than the Binomial for large successes (30/30), and very nearly equal to the Binomial for intermediate successes (15 or 20/30). The Poisson approximation gives values less than the Binomial method. It is a good approximation only for cases with large number of trials with small number of successes. For 30 trials, the Chi-Square method gives values less than the Binomial for 10 to 30 successes. Like the Poisson, the Chi-Square values approach those of the Binomial for less than 10 successes in 30 trials.

However, a closer approximation to the Binomial for both the Poisson and Chi-Square can be achieved by using a conditional approach. By first calculating the upper one-sided confidence limit for the probability of missing a flaw (q_μ), the lower one-sided confidence limit for $P_1 = 1 - q_\mu$ can then be approximated when $1 - n < n$. By using this conditional approach, a new set of values is calculated and included in Table 4-1 under the conditional approach column. These new values give a much better approximation to the Binomial when the number of successes is high.

Since the Poisson and Chi-Square approximations yield almost the same values, only one set of values was calculated under the new conditional approach.

For larger or smaller number of trials, the above comparisons is not necessarily true but the comparison generally shows the importance of analyzing binomial measurements with binomial statistics.

Table 4-1 Comparison of Probability of Detection Values Obtained by Approximation to the Binomial Distribution

NUMBER OF SUCCESSFUL DETECTIONS IN 30 TRIALS	POINT ESTIMATE OF PROBABILITY OF DETECTION ($\bar{p}$)	LOWER ONE SIDED CONFIDENCE LIMITS AT 95% CL				CONDITIONAL APPROACH
		BINOMIAL (Exact)	NORMAL	POISSON*	CHI-SQUARE*	POISSON AND CHI-SQUARE
10	0.333	0.193	0.192	0.181	0.181	0.181
15	0.500	0.339	0.350	0.308	0.308	0.308
20	0.667	0.501	0.525	0.441	0.442	0.435
25	0.833	0.681	0.721	0.578	0.579	0.650
29	0.967	0.851	0.913	0.691	0.691	0.842
30	1.000	0.905	1.000	0.715	0.720	0.900

*No conditional information was used in obtaining these numbers, see "Reliability Management Methods and Mathematics," Lloyd and Litow, Prentice Hall, 1962, pp. 218-219

4.4 Data Cumulation Methods

The calculated value for the lower confidence limit (probability of detection, p_1, at some selected confidence level, CL) is influenced by the total number of measurements (sample size). In order achieve a high POD at a high CL, such as 90% at 95% confidence level, a minimum of 29 measurements have to be made without a miss for a given flaw size. Because of the high costs involved, it is generally not economical to make 29 or more measurements for each flaw size for the entire range of flaw sizes of interest. At the same time, in the inspection of actual structural components, it is unlikely to have 29 or more measurements at any specific flaw size. As a result, size interval grouping has been used in order to obtain a sufficient number of measurements to compute a high p_1 at a high CL and to smooth over the flaw sizes that have no measurements. A cumulation plan permits the accumulation of data over a range of flaw sizes for computing a p_1 which is representative of that range.

Several cumulation procedures were considered. These procedures include (1) the range interval "RI", (2) the overlapping 60 points "OSP" and (3) the procedure developed under this contract which will be called the optimized probability method "OPM." Other procedures evaluated are reported in Reference 1. For the same set of data, the computed p_1 can be considerably different depending on which of these cumulative procedures is used. Generally, NDE reliability is demonstrated by inspecting specimens containing flaws distributed uniformly over a wide flaw size range. The smallest flaws should be virtually nondetectable and the largest flaws should be 100% detectable. First, the raw data set is arranged in order of increasing flaw size with the appropriate outcome indicated for each measurement. The various cumulative procedures are applied as follows:

(a) Range interval method. The data are separated into groups of equal flaw size increments. The probability of detection at the one sided lower confidence limit is computed for each group separately and plotted as a histogram bar. A conservative p_1 curve can be obtained by connecting the upper right hand corner of the bars. This procedure is most appropriate for computing probabilities of detection and confidence limits when large numbers of data are available so that all histogram bars represent large data samples. It is important to note that sample size (N) may vary widely between intervals.

(b) Overlapping sixty point method (N = 60). One begins by combining detection results for the largest sixty crack sizes. The POD is calculated for this interval and plotted at the largest flaw size within the size range spanned. The next data increment is obtained by starting at the median flaw size of the first interval and combining the data for the next smaller 60 cracks. The POD of the second set is plotted at its largest flaw size and the process is repeated until all data have been combined. Each interval overlaps its adjacent interval by 30 data points. Note that the sample size is the same for each interval, but the breadth of the interval can vary widely.

(c) Optimized Probability Method. The ordered NDE data are grouped into J (a computer input number) intervals of successively increasing size range. The POD of the largest size range is computed at some desired confidence level. The next smaller size range data are combined with the first and the POD of the second grouping is computed. This process is continued until J probabilities of detection are computed, and the largest value of POD obtained is plotted at the largest flaw size contained in the corresponding composite grouping. The largest flaw size interval is removed from consideration and this procedure is repeated starting from the next to largest flaw size grouping. The pattern is repeated until J probability of detections can be plotted. Note that if J is sufficiently large, the POD curve produced by this method will be the upper envelope of either the RI or the OSP method. The advantage to this method is that the sample size (N) is maximized, and results in the maximum possible value of p_1 for the available data. A basic assumption is that the larger the flaw, the more detectable it is.

V. RESULTS

Of the twenty sets of data collected, only seven sets were statistically analyzed. These seven sets appeared to meet the criteria stated in Section III of this report. Each of these seven sets, in turn, was subdivided into subsets and analyzed according to the NDE method and material types. Appendix D contains a computer listing of NDE data and detection reliability results that were analyzed during this program. Table 5-1 summarizes the results of the statistical analysis. There is a total of one hundred and twelve subsets and the subset number is given in the first column of Table 5-1. The second column gives data source. The third and fourth columns identify the material and defect type respectively. The fifth and sixth columns identify the specimen geometry and NDE method respectively. The seventh column lists some of the pertinent parameters, and the eighth column gives the crack length at which 90% probability of detection at 95% confidence level POD90(CL95) was first achieved. The shortest crack length that reached POD90(CL95) by either the OPM or OSP scheme was used and is herein referred to as the threshold level. In many instances, the POD(CL95) became smaller than 90% at crack lengths above the threshold level. This is particularly true for the OSP scheme (see Appendix D). For more details on the NDE parameters and inspection procedures that were used to acquire each set or subset of data, one has to refer to the original data reference.

The first set of data analyzed is from Martin Marietta (Contract NAS 9 12276). Four subsets, one by ultrasonic surface wave, one by penetrant, one by eddy current, and one by the X-ray method, were available before the specimens were chemically etched and another four subsets were available after chemically etching the test specimens.

The second and third sets of data analyzed are from Rockwell International-Space Division (Contract NAS 9-14000) and General Dynamics, Convair Aerospace Division (Contract NAS 9-12326). This set of data includes data from Contract NAS 9-12276 with the specimens in the "after-etched" condition.

TABLE 5-1 SUMMARY OF NDE DATA STATISTICALLY ANALYZED

CAUTION: The crack lengths in the POD90(CL95) column are not intended to be used for design purposes unless the user demonstrates a similar capability

DATA* SUB-SET	DATA SOURCE	MATERIAL TYPE	DEFECT TYPE	SPECIMEN GEOMETRY	NDE METHOD	PERTINENT PARAMETERS	CRACK LENGTH POD90(CL95) cm
1	Martin Marietta NAS 9 12276	2219-T87 Al	Fatigue Cracks	Flat Plates	Ultrasonic-Surface Wave	Before Etch, and with 3 Ops; 10 MHz	.345
2					Liquid Penetrant	Same as above, Uresco P151,K410,D499C	.665
3					Eddy Current	Same as above;NDT-3; 100KHz	.274
4					X-ray	Same as above	-
5					Ultrasonic-Surface Wave	After Etch, and with 3 Ops.	.211
6					Liquid Penetrant	Same as above	.274
7					Eddy Current	Same as above	-
8					X-ray	Same as above	.665
9	Rockwell Inter. Space Div. (NAS9-14000); Martin Marietta, and GD Convair	2219-T87	Fatigue Cracks	Flat Plates	Ultrasonic-Shear Wave (Surface Wave)	After Etch, and by Operator O	.737
10					f = 2.25 MHz	Operator P	.221
11					for RI-SD	Operator Q	.699
12					f = 10 MHz	Operator R	.699
13					for GD Convair	Operator S	.358
14					Liquid Penetrant P-133,D495A for RI - SD	After Etch, and by Operator H	.282
15						Operator I	.737
16						Operator J	.737
17						Operator K	.333
18						Operator L	.737
19						Operator M	.340
20						Operator N	1.36
21					Eddy Current Defectometer Model 2.154	After Etch, and by Operator T	.665
22					f = 2 MHz	Operator U	.201
23					for RI - SD	Operator V	-
24						Operator W	.333
25						Operator X	.320

*Data Set Numbers are Included on the Corresponding Computer Output in Appendix D.

TABLE 5-1 SUMMARY OF NDE DATA STATISTICALLY ANALYZED (Continued)

DATA SUB-SET	DATA SOURCE	MATERIAL TYPE	DEFECT TYPE	SPECIMEN GEOMETRY	NDE METHOD	PERTINENT PARAMETERS	CRACK LENGTH POD90 (CL95) cm
26					X-ray	After Etch and by Operator A	-
27						Operator B	-
28						Operator C	-
29						Operator D	-
30						Operator E	.737
31						Operator F	-
32						Operator G	-
33	RI-SD, Martin Marietta, &GDC	2219-T87 A1	Fatigue Cracks	Flat Plate	Ultrasonics	After Etch and Merged Results of 5 Operators	.201
34					Liquid Penetrant	After Etch and Merged Results of 7 Operators	.237
35					Eddy Current	After Etch and Merged Results of 5 Operators	.282
36	RI-B-1 Division (TFD-72-925)	Ti-6A1-4V	Fatigue Cracks	Flat Plate	Liquid Pene.	Used P5F-1 Penetrant	.183
37	(TFD-72-1005)					Used P5F-2	.170
38	(TFD-72-1515)					Used P5F-2 and D100 Developer	.178
39	(TFD-72-793)					Used P5F-2.5	.127
40	(TFD-72-767)	7075-T6511 A1	Fatigue Cracks	Flat Plates		Used P5F-2.5	.173
41	(TFD-73-532)					Used P5F-2.5, NQ-1	.203
42	(TFD-73-532)					Used P5F-2.5, D100	
43	(TFD-73-496)	PH13-8 Mo. St.	Fatigue Cracks	Flat Plates		Used P5F-2 and NQ-1 Developer	
44	(TFD-73-371)	Ti-6A1-4V	Fatigue/ Cracks Corroded	Welded Flat Plates	Ultrasonic, Shear Wave		.173
45	(TFD-73-372)	4330V St.				Simulate Welded Flaws	.211
46	(TFD-73-140)	PH17-4 St.				Simulate Flaws in Wrought St.	.218
47	(TFD-72-768)	PH17-4 St.	Fagigue Cracks	Flat Plates			-
48	RI-SD, MM, GDC, and RI-B1	2219-T87 and 7075-T6511 A1	Fatigue Cracks	Flat Plates	Liquid Penetrant	Merged Results from the Four Data Source on A1	.241

TABLE 5-1 SUMMARY OF NDE DATA STATISTICALLY ANALYZED (Continued)

DATA SUB-SET	DATA SOURCE	MATERIAL TYPE	DEFECT TYPE	SPECIMEN GEOMETRY	NDE METHOD	PERTINENT PARAMETERS	CRACK LENGTH POD90(CL95) cm
49	Lockheed GA	4330V St.	Fatigue Cracks	Cylindrical	Liquid Penetrant	Laboratory Condition	-
50	(TR-68-32)			Shell	Magniflux ZL-2, ZE-3, and ZP-4	Production Condition	-
51		7075-T6511 Al		7.62 cm in dia.		Laboratory Condition	-
52		4330V St.		0.64 cm thick	Mag. Particle	" "	-
53		4330V St.			Ultrasonic Shear Wave 5 MHz	" "	-
54		7075-T6511 Al			Ultrasonic Shear Wave	" "	-
55		7075-T6511 Al			X-ray	" "	-
56		4330V St.			X-ray	" "	-
57	Boeing, W.Kan.	7178-T651 Al	Fatigue Cracks	KC-135 Wings	Eddy Current	Hand Held E.C. Probe at Tear Down Insp. at Depot Level	
						Results of Team 2 (Atypical of 3 more teams)	-
58						Results of Team 4 (A-typical)	-
59						Merged results of 5 teams	-
60	Boeing Comm.	2024-T6 Al	Forge Closed	Tandem T	Liquid Penetrant	Production Insp.	-
61	Airplane Co.	4340 M St	"	Solid Cyl., Threaded	ZL-2A and 30A;	" "	-
62	(TR-74-241)	"	"	Hollow Cyl., Filleted	ZE-4B;	" "	-
63		"	"	Hollow Cyl.,	ZP-9B	" "	-
64		"	"	Solid Cyl.	Plus Others	" "	-
65		2074-T6 Al	"	Tandem T	Liquid Penetrant	Laboratory Insp.	.178

TABLE 5-1 SUMMARY OF NDE DATA STATISTICALLY ANALYZED (Continued)

DATA SUB-SET	DATA SOURCE	MATERIAL TYPE	DEFECT TYPE	SPECIMEN GEOMETRY	NDE METHOD	PERTINENT PARAMETERS	CRACK LENGTH POD90(CL95) cm
66		4340 M St	Forged Closed EDM" Slots	Solid Cyl., Threaded	ZL-2A and 30A;	Laboratory Insp.	.584
67		"		Hollow Cyl., Filleted	ZE-4B;	" "	.787
68		"	"	Hollow Cyl.,	ZP-9B;		-
69		"	"	Solid Cyl.,Fil.	Plus Others		.229
70		"	"	" "			.406
71		2024-T6 Al	"	Tandem T	Ultrasonics	Production Insp.	.533
72		4340 M St.	"	Solid Cyl.Threaded	5 and 10 MHz		-
73		"	"	Hollow Cyl. Filleted	Shear and Surface		.330
74		"	"	Hollow Cyl.	Wave		-
75		"	"	Solid Cyl., Filleted			.178
76		"	"	" "			.356
77		"	"	Solid Cyl.	Ultrasonics	Laboratory Insp.	.356
78		"	"	" " Filleted	5 and 10 MHz		.229
79		"	"	Hollow Cyl.	Shear and Surface		.254
80		"	"	" " Filleted	Wave		.330
81		2024-T6 Al	"	Tandem T			.432
82		4340 M St.	"	Solid Cyl.	X-ray	Production Insp.	-
83			"	" ", Filleted			-
84			"	Hollow "			-
85			"	" " "			-
86			"	Solid ", Threaded			-
87		2024-T6 Al	"	Tandem T			-
88		4340 M St	"	Solid Cyl.	X-ray	Laboratory Insp.	-
89		4340 M St		Hollow ", Filleted			-
90		"		Solid ", Filleted			-
91		"		Hollow ",			-

TABLE 5-1 SUMMARY OF NDE DATA STATISTICALLY ANALYZED (Continued)

DATA SUB-SET	DATA SOURCE	MATERIAL TYPE	DEFECT TYPE	SPECIMEN GEOMETRY	NDE METHOD	PERTINENT PARAMETERS	CRACK LENGTH POD90 (CL95) cm
92		2024-T6 Al		Tandem T			.279
93		4340 M St.	Forge	Solid Cyl.	Mag. Particle	Production Insp.	.305
94		"	Closed	" " , Filleted			.330
95		"	EDM Slots	Hollow "			-
96		"	"	" " , Filleted			-
97		"	"	Solid " , Threaded			-
98		"	"	Solid Cyl.	Mag. Particle	Laboratory Insp.	.305
99		"	"	Hollow " , Filleted			.329
100		"	"	Solid ", Threaded			-
101		"	"	" ", Filleted			.178
102		"	"	Hollow "			.254
103		"	"	Solid Cyl.	Eddy Current	Production Insp.	.400
104		"	"	" " , Filleted	ED400 and 520 at f=100 KHz		.762
105		"	"	Hollow Cyl.			-
106		"	"	" " , Filleted			-
107		2024-T6 Al	"	Tandem T			.330
108		"	"	Tandem T	Eddy Current	Laboratory Insp.	.457
109		4340 M St.	"	Solid Cyl.	ED400 and 520		.508
110		"	"	Hollow Cyl.,Fil.	at f=100 KHz		.356
111		"	"	Solid ", Filleted			.584
112		"	"	Hollow Cyl.			-

There are five subsets of data obtained with the ultrasonic method, each subset for a different inspector, three inspectors for Contract NAS 9-12276, one for NAS 9-14000, and one for NAS 9-12326. There are seven subsets of data obtained with the liquid penetrant method, each subset by a different inspector, three inspectors for NAS 9-12276, three for NAS 9-14000, and one for NAS 9-12326. There are five subsets of data obtained with the eddy current method, each subset by a different inspector, three inspectors for NAS 9-12276, one for NAS 9-14000, and one for NAS 9-12326. There are seven subsets of data obtained with the X-ray method, each subset by a different inspector: three inspectors for NAS 9-12276, three for NAS 9-14000, and one for NAS 9-12326. Subsets 33, 34 and 35 were obtained by merging the data of five ultrasonic inspectors, seven penetrant inspectors, and five eddy current inspectors. The X-ray data were not merged because the results are not worthy of further consideration.

The fourth set of data analyzed is from Rockwell International B-1 Division, B-1 NDI Demonstration Program. There were twelve subsets of data in this set. The fifth set of data analyzed is from Lockheed, Georgia, AFML Report No. TR-68-32. There are eight subsets in this data set. The sixth set of data analyzed is from Boeing Company of Wichita, Kansas. This set of data was obtained from eddy current inspection of bolt holes, after pulling off the bolts, from actual aircraft parts.

The seventh set of data analyzed is from the Boeing Commercial Airplane Company, AFML Report No. TR-74-241. There are fifty-three subsets in this set of data.

Data subset number 48 was obtained by merging the data from Martin Marietta (NAS 9-12276), Rockwell Int.-Space Division (NAS 9-14000), General Dynamics' Convair Division (NAS 9 12326), and Rockwell Int.-B-1 Division for aluminum for the liquid penetrant method.

All the data described in this report were taken from a total of nine alloys of aluminum, titanium, and steel. These alloys are described in Table 5-2. The predominant amount of data were taken with the four aluminum alloys.

Table 5-2 Alloys with Valid Data

Aluminum	Steel	Titanium
2219-T87	PH13-8MO	6A1-4V
7075-T6511	4330V	
2024-T6	PH17-4	
7178-T651	4340M	

VI. DISCUSSION OF RESULTS

The tabulated and graphical computer output format (Appendix D), is convenient for assessing the state-of-the-art in NDE reliability. It contains:

(1) the binomial experiment results (N,n) in each of 32 crack size intervals (tabulated in units of Mils and plotted in both Mils and cm.);

(2) the 50 percent lower confidence limit for each interval POD(CL50

(3) the 95 percent lower confidence limit POD(CL95); and

(4) the number of new measurements required in each interval to demonstrate a 90 percent probability of detection at a 95 percent confidence level "POD90(CL95)".

These data are useful for comparing the effects of material, inspector, and inspection parameters on NDE reliability and seeing where data deficiencies lie.

As can be seen in Figure D-1a the POD fluctuates widely throughout 32 ranges for this set of data because of the variation in the number of measurements, N, reported in each range. Twenty of the ranges contain less than 29 measurements while six ranges contained no measurements at all. The number of measurements per range can be increased by broadening the flaw size interval per range, but there is still no assurance that all of the broader ranges will contain measurements. Fluctuation in the probability of detection due to the variation in the number of measurements in a range is a shortcoming of the range interval method.

Figure D-1b shows the tabulated and graphic results obtained by using the optimized probability method (OPM) for the set of data in Figure D-1a. As can be seen, the number of measurements available for each interval is much larger than for the range scheme. The thirty-first interval lists 183 detections out of 183 measurements resulting in a POD of 98% plotted at 1.18 cm. The POD computed with the OPM increases monotonically with increasing crack length and does not fluctuate as in the range scheme. The POD at 95% CL reaches 89% for the first time at .32 cm for the OPM versus .358 cm for the range scheme.

Figure D-1c shows graphic and tabulated results using the overlapping 60 points scheme. In this scheme, the number of measurements for each POD calculation is constant (60). Fluctuation in the POD can be attributed primarily to human operator and inspection process variations. The POD at 95% CL reaches 89% for the first time at .328 cm, which is intermediate between the OPM and the RI results.

6.1 Effects of Material, Source, and Inspection Parameters

It is apparent from data subsets 1 through 8 in Table 5-1 that the sensitivity is increased for ultrasonic, liquid penetrant, and X-ray techniques after the test specimens were chemically etched. This increase is reasonable since the crack openings are enlarged. The sensitivity is decreased, however, for eddy current method after chemically etching the specimens. This effect is difficult to explain.

Data subsets 9 through 32 show that the difference in the POD90(CL95) obtained by different inspection operators within a company vary as much as those obtained by companies which use different inspection parameters and procedures. Several observations can be made with subsets 9 - 14: (1) Operators P and S in subsets 10 and 13 can be considered to be model operators. Not only did they achieve a smaller POD90(CL95) <u>threshold level</u> than other operators, they were able to maintain the POD(CL95) at a relatively constant (and high) level for crack lengths above the threshold level (Figures D-10 and D-13). (2) Subsets 10 and 13 show that the sensitivity of the ultrasonic method increases or remains constant for increasing crack length, particularly for crack lengths above the threshold level. (3) Fluctuations in the POD(CL95) for crack lengths above the threshold level are primarily caused by fluctuations in operator efficiency and less likely by the sensitivity of the NDE method.

Subsets 14-20 (Figures D-14 to D-20) show more fluctuation in the POD(CL95) due to variation in operator efficiency than to types of penetrant or procedures used by the three different companies that made the measurements. There is a large variation in the threshold level of the seven operators. Three operators demonstrated threshold levels around .33 cm, another three demonstrated the level at .737 cm, and the seventh one demonstrated it at 1.35 cm. One should keep in mind that most of these POD (CL95) curves are relatively flat and the POD(CL95) is greater than 80% from .254 cm on to the longer crack length.

Like the ultrasonic and penetrant results, the eddy current results showed considerable differences in the threshold level for the five different operators. In fact Operator V did not demonstrate POD90(CL95). However, he did demonstrate POD88(CL95) at a crack length of .737 cm. Operator T demonstrated POD90(CL95) at a crack length of .665 cm. However, he reached POD88(CL95) at a crack length of .399 cm.

X-ray is not a good inspection technique for reliably detecting fatigue cracks. Data sets, 26 to 32 show that only one operator can achieve POD90(CL95). This forecasts that X-ray techniques will not be viable procedures for detecting fatigue cracks. However, this does not necessarily mean that the technique should not be used to detect other defects such as porosity.

Merging data provides a means for observing overall detection reliability trends. When the data for five ultrasonic operators were merged (subset No. 33) and calculated with the OSP scheme the POD(CL95) reached 95% at a crack length of 0.66 cm (see Figure D-33c). However, it fell below 95% at higher crack length, and it reached a minimum of 79% at a crack length of 0.810 cm. When the results of seven penetrant operators were merged (subset No. 34) and calculated with the OSP scheme, the POD(CL95) reached 92% at a crack length of 0.26 cm (see Figure D-34c), but it fell below 90% between 0.26 cm and 0.63 cm. It peaked to 95% at 0.65 cm, then fell below 90% and reached a minimum of 81% at a crack length of 1.12 cm. When the results of five eddy current operators were merged (subset No. 35) and calculated with the OSP scheme, the POD(CL95) reached 92% at a crack length of 0.32 cm (see Figure D-35c). But like the ultrasonic and penetrant results, the POD(CL95) for the eddy current fell below 90% at higher crack length and it reached a minimum of 81% at 0.88 cm.

Data subsets 36 through 47 (Figures D-36 to D- 47) are from the B-1 NDI demonstration program. These data show that the POD(CL95) either increases monotonically or remains constant with increasing crack length once the threshold level is reached. In several data sets no further measurements were made once the desired threshold level was demonstrated. It is interesting that the threshold level as well as a large portion of the POD(CL95) curve does not differ greatly for several types

of penetrant applied to materials such as Ti-6Al-4V, 7075-T6511 Al, PH 13-8 Mo steel, 4330V steel, and PH 17-4 steel.

Data subset 48 represents the merged results of four data sources (RI-Space Division, Martin Marietta, General Dynamics Convair, and RI-B-1) on 2219-T87 Al by the liquid penetrant method on flat plates.

Data subsets 49 through 56 were obtained with fatigue cracks in 4330V steel and 7075-T6511 Al having a cylindrical shape (7.62 cm in diameter and .62 cm thick). Data were taken in both the laboratory and production environments. None of the curves for these 8 sets of data attained POD90(CL95), however, the penetrant results for 7075-T6511 Al did demonstrate POD87(CL95) at a crack length of 1.0 cm, POD87(CL95) at a crack length of 1.17 cm, and POD89(CL95) at 1.47 cm. The POD for ultrasonic shear wave reached a value of POD86(CL95) at a crack length of .80 cm and POD87(CL95) at a 1.27 cm.

Data subsets 57, 58, and 59 were obtained with eddy current inspection of bolt holes during tear-down inspection of KC-135 wings at the depot level. The same holes were inspected by five separate inspection teams. The inspection results from four of the five teams were about the same. Figure D-57 shows the results of team number two which is representative of the four teams. Figure D-58 shows that the detection reliability of team number four is considerably different than the other four teams. Figure D-59 shows the merged results of the five teams. None of the five teams achieved POD90(CL95).

Data subsets 60 through 112 (Figures D-60 to D-112) were obtained from the Practical Sensitivity Limits program which was conducted by Boeing Commercial Airplane Company and supported by the NDE Branch of Air Force Materials Laboratory. The inspection results were obtained in both the laboratory and production lines of several Boeing Divisions. Divisions used different NDI procedure or specification, as well as different NDI techniques. For example, ultrasonic shear and surface waves of 5 and 10 MHz were used, different liquid penetrant systems in either the Group V or VI category were used, etc. Because the results were obtained under different NDE procedures, it is difficult to make comparison between results from different data sources. Furthermore, the majority of the defects used in this program were forging cracks instead of fatigue cracks, nevertheless the length of the crack at POD90(CL95) found by each of the NDI techniques is comparable, in most cases, to those found at other companies using fatigue cracks.

6.2 Statistical Analysis Procedures

All NDE measurements are considered to be binomial and describable by binomial distribution functions and binomial statistics. Because of this consideration, lower one sided confidence limits and data deficiencies can be rigorously computed.

The only factor which reduces mathematical rigor is the crack length parameter. It is necessary to group NDE data into a size interval that will contain a population of 29 successes without a miss in order to show 95 percent confidence that the probability of detection exceeds 90 percent. If a miss is encountered, it is necessary to have a higher population (see Table 6-1) in order to demonstrate POD90(CL95).

Table 6-1

Interval Sample Size and
Successes Required to Achieve POD90(CL95)

No. of Misses	Interval Population Required, N	No. of Successes, n
0	29	29
1	46	45
2	61	59
3	76	73
4	89	85
5	103	98
6	116	110
7	129	122
8	142	134
9	154	145
10	167	157

Once an acceptable size interval has been chosen that will produce a reasonable population, there remains a problem of selecting the crack length within the range at which to plot the computed POD(CL95). For conservatism, the POD curves in this report are plotted through the maximum crack length in the interval. The crack interval is also indicated by a horizontal line connecting maximum and minimum crack sizes.

Three procedures for determining the probability of detection for the lower one-sided confidence level are compared in this report. Described earlier in Section 4.3, they were the range interval (RI) method, the optimized probability method (OPM) and the overlapping sixty point method (OSP). The optimized probability method is preferred over the RI or OSP but requires more computational time. The main claim to success for the OSP method is that it forces groupings to be large enough to provide the capability for achieving POD95 (CL95). The OPM should provide the upper envelope to both the RI and the OSP methods.

6.3 Data Deficiencies

The data described in this report represents more than 30,000 measurements, yet there are many gaps in the probability of detection for different defect types, material types, and specimen geometry by the five NDE methods (ultrasonics, liquid penetrant, eddy current, X-ray, and magnetic particle). The most data are available for fatigue cracks in flat plates of 2219-T87 aluminum which reasonably characterize the reliability of all five NDE methods. There are also several sets of data for fatigue cracks in aluminum cylinders, forging cracks in extruded aluminum (tandem T configuration), and fatigue cracks in bolt holes of actual aluminum aircraft parts. There is a notable data deficiency for steel. Most of the steel data are for fatigue and forged cracks in cylinders. There are, however, four sets of data for fatigue cracks in flat plates of steel. Only five sets of data are available for titanium and all of them were taken on flat plates.

With the exception of the B-1 NDE demonstration data most of the data exhibit a gap over some range of the crack lengths. A perfect example of this is the data from Martin Marietta, Rockwell International-Space Division, and General Dynamics-Convair Division. All these three companies made measurements using the same set of specimens which contains two gaps. As can be seen from the crack size distribution curve in Figure 6-1, there are no cracks with length between 0.47 to 0.59 cm and between 1.03 to 1.17 cm. Thus, no cracks can be detected in these two gaps and the probability of detection, regardless of which cumulative scheme is being used, is affected. A set of specimens without gaps in the crack size distribution curve is needed to study the actual probability of detection in future programs.

6.4 Application to Fracture Mechanics

The threshold crack length (the shortest crack length that reached to POD90(CL95)) that was detected by the different NDE techniques is given in Table 5-1. However, as can be seen from the curves in Appendix D, the POD (CL95) in many instances falls below 90% for some crack length longer than the threshold level. Thus the potential user is cautioned against using these threshold crack lengths in the design process. In the first place, the POD can vary from company to company even when the same inspection procedures were used because of training procedures and using different inspectors. In the second place, some of these POD curves do not have a zero or positive slope for crack length above the threshold level. The decrease in the POD above the threshold level could be a real phenomenon and might not necessarily be attributed to human factors. There are scatter reports, in the case of liquid penetrant, that indicate penetrant washes out of wide cracks before the developer is applied.

In the fracture mechanics design process, one must be assured with some probability at some confidence level that no cracks larger than the assumed size can be present in the structure. Thus, for fracture mechanics to be a viable design process, the probability of detection as a function of crack length must be monotonically increasing or at least levels off above some selected threshold crack length.

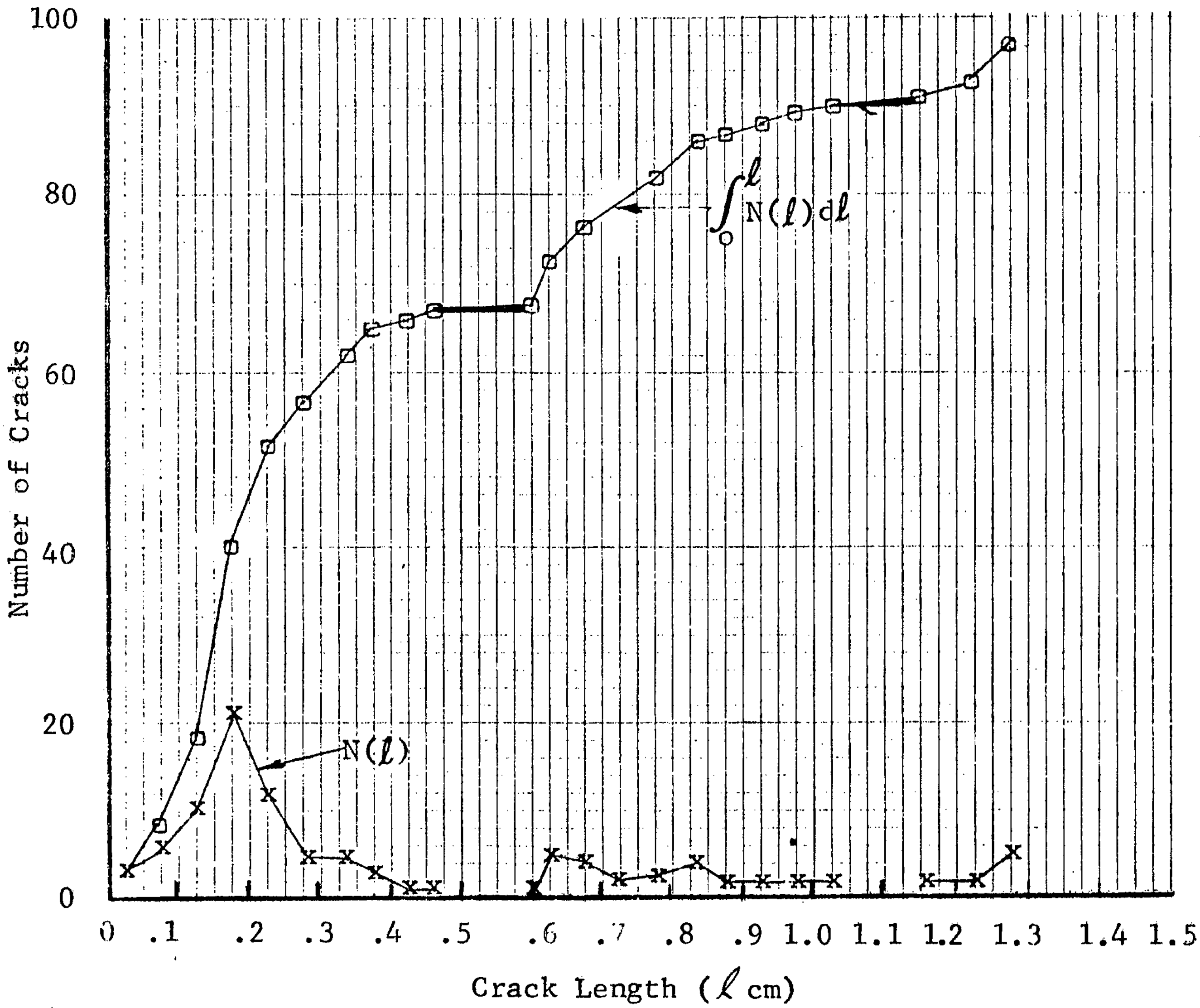

Figure 6-1 Differential and Integral Crack Distribution Function for the Martin Marietta Demonstration Program. 2219-T87.

6.5 Optimum Demonstration Program

In order to determine the reliability of an NDE technique without operator influence, the optimum demonstration program will have to employ computer automation in scanning specimens and interpreting NDE signals. It should incorporate ultrasonic, eddy current and penetrant inspection into each demonstration program.

The data in this report can be used to estimate the sample size required for the optimum demonstration program. For example, if one can afford to test 100 specimens and requires a 50-50 chance of success in demonstrating POD90/CL95 then one would have to select a data set representative of this expected capability and select a crack length for his demonstration program for which the probability of detection is at least 95%. If he can afford only 45 specimens then he must choose a crack length for which the probability of detection is at least 98%. This can be seen in Figure 6-5 where number of misses corresponding to POD90(CL95) is plotted against the number of specimens tested. The shaded region is the region of success for which POD 90(CL95) has been met or exceeded. The broken lines show the number of failures expected for various values of POD (98, 95, 94, 93, 92, and 90%).

Assume that data set # 1 (Figure D-1) is for a geometry and NDE method that is most representative of those required in a demonstration program. These data demonstrate a POD(CL95) at .345 cm. Figure D-1a would lead one to believe that POD 90(CL95) might be demonstrated at about .27 cm for which 38 out of 39 cracks were detected. Figure D-1a shows that one can be 50 percent confident that the probability of detection exceeds 95% for this case if his NDE techniques are as good as those used to produce data set # 1. Figure 6-2 shows that if 110 test cracks were fabricated and tested and that less than 5 cracks were missed, then the demonstration program would be successful.

The previous example is indicative of the usefulness of these data as a means for minimizing the number of specimens required for achieving a successful demonstration program. The common practice of manufacturing a large number of crack specimens for which there is little chance to achieve POD 90(CL95) will be eliminated by this approach to designing an optimum demonstration program.

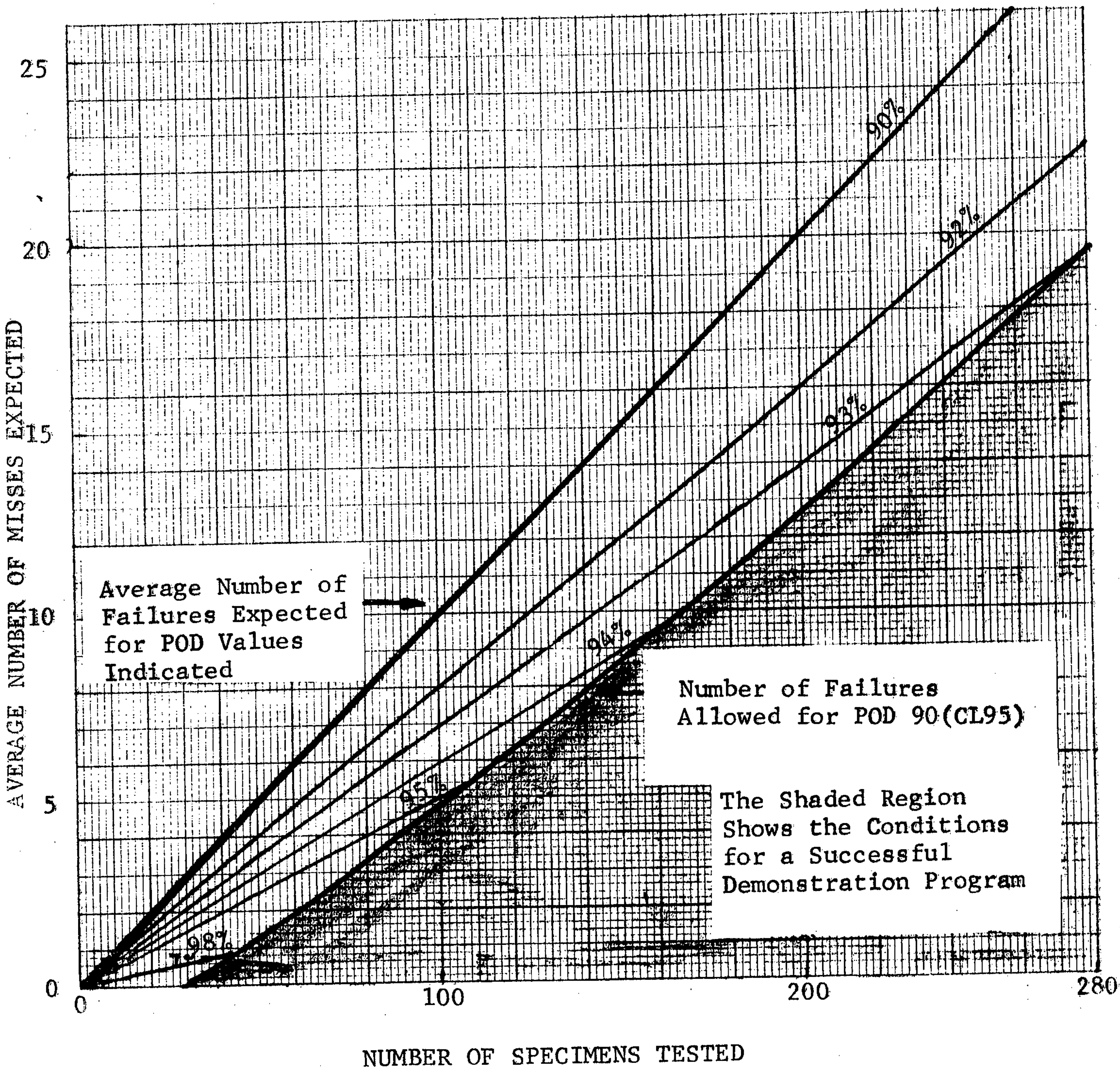

Figure 6-2 Conditions for Success in Selecting a Sample Size that will Potentially Demonstrate POD90(CL95)

VII. CONCLUSIONS

This program was sponsored by NASA as a service to the new fracture mechanics approach to structural design whereby system reliability may be related to the expectation that flaws larger than a specific size may exist in the structure. The program objectives were to (1) collect all available NDE reliability data, (2) examine the validity of the data, (3) select and computerize a statistical procedure for analyzing the data, and (4) generally assess the current state-of-the-art in NDE. We feel that the surface has been broken by this program but vigorous follow-on work would be very valuable to the field of structural design.

Some of the specific conclusions that can be drawn from the contents of this report and the experience gained in performing this study are:

(1) The human factors influence stands out as dominating in influencing NDE reliability. Although a company can demonstrate a 90 percent probability of detecting a crack at a lower one sided confidence limit at the 95 percent confidence level, there is no guarantee that this is indicative of a continuing capability unless some form of automation has replaced human judgment. This then indicates a need for some type of periodic audit of capability.

(2) Although more than 30,000 measurements have been filed in a computer library and analyzed to determine the NDE reliability of X-ray, ultrasonics, eddy current, and penetrants, there are still many gaps in the data: There are no eddy current data in the data bank for titanium nor are there much data for crack lengths near .5 or near 1.2 cm. These data deficiencies cause large uncertainties in the POD plots for these crack lengths.

(3) Binomial statistics are recommended for analyzing NDE reliability data. This report contains a comprehensive discussion of the preferred analysis model.

(4) The optimized probability method (OPM) of data cumulation is preferred over the range interval or the overlapping sixty point scheme for computing probability of detection. The optimum probability model which was developed during this program is discussed in this report.

(5) Data show that the X-ray technique is not viable for detecting tight fatigue cracks.

(6) In order to obtain optimum results from an NDE demonstration program, special care must be taken in the design of flaw size distribution. The cumulative distribution must always maintain a positive slope or there will be gaps without data which can have deleterious effects on the POD curves as a function of flaw sizes.

(7) The data presented in this report are offered as a guide for manufacturers who intend to perform an NDE reliability demonstration program and can identify data sets that represent their expected NDE capabilities. However, due to the human factor influence on POD, the data cannot be used as design information. Each company must develop reliability numbers for their own use.

(8) A continuing program to maintain an NDE reliability data file and to optimize the data processing procedures formulated during this program would be useful to the field of fracture mechanics. As the data base becomes larger it will begin to support parametric studies of the influence of NDE variables.

APPENDIX A

A MODEL TO GRADE THE QUALITY OF THE DATA SETS

The thoroughness of the characterization of the defect-specimen and the documentation of the inspection procedures affects the quality and the usefulness of the data sets. A designer will not have confidence in using the data unless the inspection procedures and defect dimensions are sufficiently documented so that it can be reproduced in future inspections.

The model described in this section will only relate to the quality of each set of data. It will not address the question of applicability. That is, a set of data obtained on flat plates will not be graded on the basis of its applicability to the design of complex structures.

The model is empirical and the weighting factors assigned to the various known pertinent parameters are rather arbitrary. However, it does represent a first attempt to quantitatively evaluate the quality of a data set. Each of the pertinent parameters in this model is listed in the Input Data Format which will be discussed in the next subsection. The grade for a given set of data can be tallied in the computer by checking the entries to the columns containing these pertinent parameters. A score of one hundred (100) corresponds to a perfect set of data. A perfect set of data is one where all the pertinent parameters are documented.

The preliminary model to grade the data quality for the ultrasonic, eddy current, liquid penetrant, magnetic particle, and X-ray methods is given in Table A-1. The model is divided into two major groups. Group A is the characterization of specimens and defects and it is common to all techniques. Group B is the documentation of the inspection and is different for different NDE techniques. The first eight parameters in this last group are common to all techniques. Each technique has about eleven parameters that are considered pertinent to adequately document the inspection. Parameter A1 is the description of the specimen geometry and defect location. This is considered a key parameter and a value of 7 points is arbitrarily assigned to it. If no description about the specimen geometry and defect location is given, that data point or set of data will receive no points. Those parameters that are marked by an asterisk are considered key parameters. If any of them is not recorded, the data point or set will be considered for possible exclusion from statistical analysis.

Table A-1

THE GRADING FACTORS USED TO GRADE NDE DATA QUALITY

A.	Specimen - Defect Characterization Information		35
	1. Specimen geometry complexity and defect location	*	7
	2. Crack dimension verification	*	10
	3. Defect type	*	3
	4. Specimen surface condition	*	3
	5. Material characterization (thermo-mechanical history)		3
	6. Material inside defect	*	3
B.	Inspection Documentation		65
	1. False indication recording		4
	2. Inspector qualification level		3
	3. Knowledge of defect orientation, location, and presence by inspector	*	9
	4. Use of proof load	*	3
	5. Use of control specimens without crack		3
	6. Method of data recording		3
	7. Method of scanning specimens		3
	8. Insp. environment	*	3
	9. Number of insp. prior to this insp.		3
	10. Parameters recorded by nondestructive testing standards		
	a. Radiography		38
	1) Radiographic source	*	3
	2) Ref. standard		3

10. (Continued)

3)	Detector type	*	4
4)	Voltage	*	4
5)	Current	*	4
6)	Exposure time	*	4
7)	Source/film distance	*	4
8)	Angle of entry	*	3
9)	Film development parameters		3
10)	Radiograph density	*	3
11)	Radiographic equipment type		3
b.	Ultrasonics		38
1)	Ultrasonic method	*	4
2)	Frequency	*	4
3)	Transducer type and size	*	4
4)	Reference standard type and size	*	4
5)	Angle of incidence (inside the material)	*	3
6)	Equipment type		3
7)	Gate alarm level (% of ref. signal)	*	4
8)	Gain setting (% of screen saturation)	*	4
9)	Type of coupling		3
10)	Index interval	*	3
11)	Contact or Immersion		3

10. (Continued)

c.	Eddy Current			38
	1)	Method of Scan	*	3
	2)	Coil size	*	4
	3)	Coil arrangement and shape	*	3
	4)	Frequency	*	4
	5)	Reference type and size	*	4
	6)	Equipment type		3
	7)	Index interval	*	3
	8)	% of meter response (Real Part)	*	4
	9)	% of meter response (Imaginary Part)	*	4
	10)	Lift-off compensation		3
	11)	Signal processing		3
d.	Penetrant			38
	1)	Penetrant type	*	4
	2)	Developer type	*	4
	3)	Classification of penetrant (group no.)		2
	4)	Emulsifier type	*	4
	5)	Pre-insp. surface cleaning and penetrant removal	*	3
	6)	Method of penetrant application		3
	7)	Dwell time	*	4
	8)	Development time	*	4

10. (Continued)

9)	Wash time		4
10)	Light type and intensity at specimen surface		3
11)	Reference standard type		3
e.	Magnetic Particle		38
1)	Type of current used	*	4
2)	Current level (Amperes)	*	4
3)	Method of magnetization		4
4)	Direction of magnetization	*	4
5)	Magnetic flux density	*	4
6)	Magnetic particle type and size	*	3
7)	Magnetic particle density		3
8)	Type of liquid vehicle		3
9)	Method of particle application		3
10)	Equipment type		3
11)	Dwell time (seconds)	*	4

APPENDIX B

DATA POOLING

B.1 Data Pooling by NDE Method and Parameters

Data that meet the preliminary criterion as described in Subsection 3.1 are input to the computer for statistical analysis. Then data from several sets are pooled and analyzed if they have a common set of parameters. Data from different NDE methods are not to be pooled. For a given NDE method such as ultrasonic shear wave at 5 MHz, reliability curves will be plotted for a material type, a defect type, an environment, a specimen geometry and defect location, and either before or after some enhancement such as a proof test. Composite reliability curves can be plotted by pooling data with different parameters, such as pooling 5 and 10 MHz shear wave data, laboratory and production data, flat plate and cylindrical shell data, etc.

B.2 Statistical Pooling Criteria

The NDE data that is compiled for this contract was collected from different sources using different calibration factors, different equipment, different personnel, different environments, etc. Each set of data therefore contains unique source characteristics that preclude indiscriminate pooling for reliability calculations.

A statistical pooling criteria has been developed to safeguard against mistakes or inconsistencies in the data which would produce abnormal statistical results. The data pooling technique is based solely on the binomial distribution and is described below as a procedure which can be implemented on a computer. The procedure consists of the following four steps.

(1) The best single estimate, $\bar{p}_c$, for probability of detection

$$\bar{p}_c = \frac{\sum_{k=1}^{M} n_k}{\sum_{k=1}^{M} N_k} \quad , \qquad (9)$$

where M is the number of data sets to be pooled.

(2) The best single estimate of the true probability

$$\bar{p}_k = \frac{n_k}{N_k} \quad , \tag{10}$$

of each of the data subsets is computed.

(3) Consider the binomial distribution function for each data set (N_k, n_k) having a true probability of detection given by $\bar{p}_c$. The two-sided probability, α_2, that (N_k, n_k) and all less likely outcomes are possible is computed from

$$\alpha_2 = 2 \sum_{i=0}^{n_k} \binom{N_k}{i} \bar{p}_c^{\,i} \; (1-\bar{p}_c)^{N_k - i} \tag{11}$$

$$\text{if} \quad \frac{n_k}{N_k} < \bar{p}_c$$

or by

$$\alpha_2 = \sum_{i = n_k}^{N_k} \binom{N_k}{i} \bar{p}_c^{\,i} \; (1-\bar{p}_c)^{N_k - i} \tag{12}$$

$$\text{if} \quad \frac{n_k}{N_k} > \bar{p}_c \quad .$$

(4) All data sets having a value of α_2 less than a reference value α' (computer input value) are removed as candidates for pooling.

The choice of α' is somewhat arbitrary and depends upon the acceptable risk. The data sets that will be rejected from pooling for a given α' value will be reviewed. If no abnormalties are found within each set of data (i.e., no mistakes in data recording, or other possible means of causing the probability of detection to be normally high or low),

a new value of α' will be tried and one that will permit the data sets to be pooled with the data base will be selected. Thus, the value for α' may be governed by operator judgment of the validity of the data.

Table B-1 is an example which contains six hypothetical binomial experiments (assuming all sets have the same measurement parameters). (For this example α' was chosen to be .05). The α_2 values for sets C, E, and F are very low. The α_2 values for sets C and E were calculated using Equation (11) and for set F was calculated using Equation (12). For set C one is only 2.22% confident that one out of eight measurements is successful. For set E one is only 0.86% confident that one out of ten measurements is successful. For set F one is only 0.11% confident that seven out of seven measurements are successful. The confidence is too low for measurements to be pooled with those of sets A, B, and D.

Upon rejecting sets C, E, and F, new α_2 values are calculated for sets A, B, and D using the $\bar{p}_c$ (16/40). These three sets have comparable confidence limits and they will be pooled.

Table B-1

SIX SETS OF DATA FROM DIFFERENT SOURCES (A-F) TESTED FOR POOLING

Source	N Number of Measurements	n Number of Successes	α_2 (Alpha)
A	24	9	.4085 (accepted)
B	8	3	.3612 (accepted)
C	8	1	.0222 (rejected)
D	8	4	.3572 (accepted)
E	10	1	.0086 (rejected)
F	7	7	.0011 (rejected)
TOTAL	65	25	
A	24	9	.3641 (accepted)
B	8	3	.3361 (accepted)
D	8	4	.3834 (accepted)
TOTAL	40	16	

APPENDIX C

NASA. FTN COMPUTER CODE

NASA. FTN is written in Fortran and organized with a main routine performing all executive functions. Main does no data manipulation, it simply calls other routines which manipulate the data.

The flow diagram Figure C-1 illustrates the run sequence of the program. Two inputs required for the program are the Master Data File and a Problem Input Deck. At the end of a production run, the program lists the computational results.

C-1 Master Data File

The master data file consists of a sequence of 'data sets'. Each data set grouping has a common combination of conditions under which a series of specimens were inspected. These conditions are described in two 256 word records (header records). The results of the inspection are called data points and are stored after the two header records. Each data point is 8 words long and contains: crack ID, detect code, crack length, crack depth, measured crack length, measured crack depth, surface finish and thickness. The 'data records' consists of 256 words which contain 32 data points in each. Each data set is labeled by a number which is unique to the data set. The data set number and the number of data records per data set are stored in the header records of each data set. The master data file is stored on magnetic tape in binary format, 256 words per record.

C-2 Program Flow (Ref. to Table C-1)

The first step in running the program is to read all the program options. The subroutine then reads the master data file to extract, data points for analysis. These data are stored on a local disk file for up to 10,000 data points. Each data point on this data file is described by four words, crack size, detect/no detect, crack ID, and data set number. The input options have already (either implicitly or explicitly) described a set of common conditions. Subroutine Order then rewrites the local data file in increasing crack size.

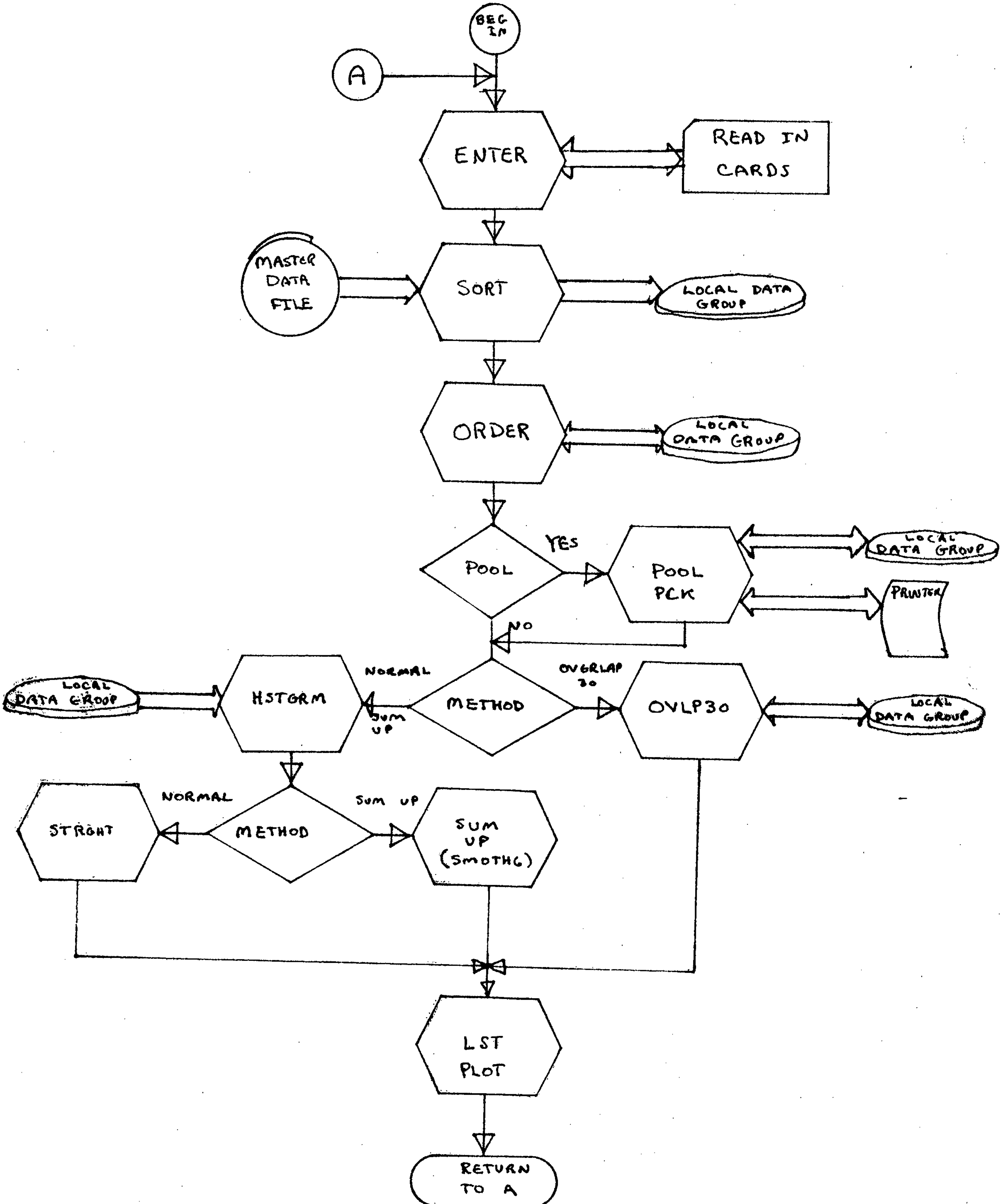

C-2

Figure C-1 Structure of Main Routine in NASA. FTN Code

Table C-1

Glossary of Programs and Subroutines
Used in NASA. FTN

NASA	-	Main program to control the program steps flow in Figure
ENTER	-	Routine to read in cards which contain the program options. The options are stored in commons for use by other routines.
SORT	-	Routine that reads the master data file, sorts out data for analysis, then writes this data on local disk file.
ORDER	-	Routine to sort the data on the local data file so that the order of the data will be by increasing crack size.
POOL	-	Routing to determine whether a particular data set belongs to the rest of the sets being considered.
POOLR	-	Routine to calculate probability of data sample belonging to a group having a known probability of detection.
RJCT	-	Routine to zero out data points of a data set that has been rejected on statistical grounds.
PCK	-	Routine to remove 'holes' in the local data file that are created by RJCT and to form a packed data file.
HSTGRM	-	Routine to sort data into 32 size interval groups.
OVLP30	-	Routine to perform an analysis of the data by using the procedure known as the "OSP" scheme.
SMOTHG	-	Routine to perform an analysis of the data by using the procedure known as the OPM.

Table C-1 (Continued)

STRGHT	-	Routine to perform analysis of the data by using the procedure known as the "RI" scheme.
BIN	-	Routine to calculate POD at a specific confidence limit for a binomial experiment consisting of N measurements and n successes.
DEFJC	-	Routine to calculate the number of successful experiments which must be performed in order to know the lower limit probability of detection within a given confidence limit.
LST	-	Routine to list the results of the analysis.
CKNRT	-	Routine which performs paging of the local data file.

If pooling is desired, routine POOL can be used to calculate the probability that each data set statistically belongs to the rest of the data sets that are collected together. Any data set that gets rejected is removed from the local data file by zeroing the data points. Routine PCK takes the local data file and re-packs it so that there are no zeroed points. All data sets removed are listed on the printer. The method of analysis determines the route the program takes next. If 'overlapping 60' is chosen routing OVLP30 "OSP" takes the local data file and processes the data directly. Routing HSTGRM is used to divide the data points into 32 groups which have equal crack size intervals ranging between a minimum and maximum input crack size. All crack sizes falling below the minimum are included in the first interval and all data falling above the maximum are included in the thirty second interval. Either the routine STRGHT "RI" or the SMOTHG "OPM" analysis procedure can be selected to analyze the data. The results are then listed. The program then returns to the beginning to read more cards. If there are no more problems to be solved, the program terminates.

C-3 Sorting Option

The program has two sort options. The first option uses the data set number directly. (See Figure 4-2). The user specifies the number of data sets to be considered, then specifies the data set numbers. The second option (Figure 4-3), makes use of the header card information which includes 26 words or numerical codes for the alphanumeric data that is contained in the header records. By supplying values for these words, each header record can be compared to this 'master' input. No zero values are compared. Each time a match is made, that data set is stored on the local data file. A maximum of 5 master header records can be combined per run.

C-4 Program Limitations

The maximum crack size that can be stored and analyzed is 2.54 cm. The maximum number of data points that can be combined into a set is 1000. The maximum number of measurements that can be analyzed by the subroutine "DEFIC" which computes data deficiencies is 120.

IDSN = NUMBER OF DATA SETS TO BE SELECTED

JDSN = ARRAY CONTAINING THE DATA SET NUMBERS

DSN = DATA SET NUMBER (READ FROM MASTER DATA FILE)

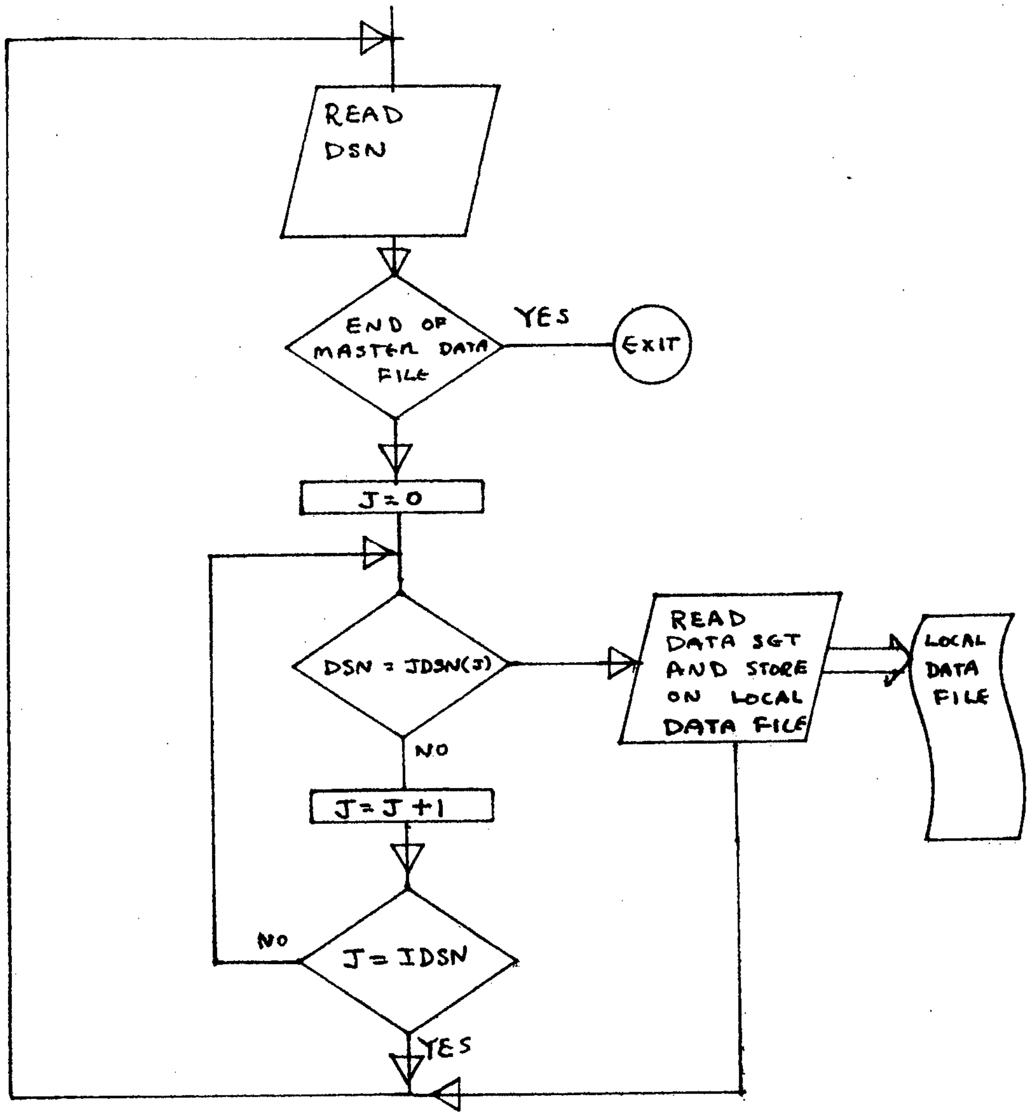

Figure C-2 Sort Subroutine Flow When Using Data Set Number Only for Sorting

C-5 Local Data File

The local data file is a direct access file which occupies a continuous block or disk space. A paging method has been incorporated to avoid executive disk I/O. The subroutine CKNXT is used for paging. At any given time, 1024 data points may be held in the core, therefore a disk access does not have to be made each time a new data point is addressed. The local data file has ten pages available for program use.

C-6 Ordering Method

A subroutine names "ORDER" reorders the local data file entries in increasing crack length then rewrites the ordered data file in place of the original unordered local data file. This ordered data is then used as input for data pooling and statistical analysis.

C-7 Lower One-Sided Confidence Limits Calculations

The binomial Equation (5) is solved by setting G equal to the confidence level desired and determining the value of p_1 which satisfies the equation. A Fortran IV program which has been made operable in a PDO 11/45 computer to perform this function is given in Figure 4-5. p_1 is the probability of detection at the lower confidence limit.

The procedure used to determine how many more measurements are required in each interval for the 95% confidence curve to reach the 90% probability of detection level is to solve Equation 8 for and . Figure 4-6 gives the listing of a Fortran IV program to perform this calculation.

ICCN = NUMBER OF CONTROL CARDS (MAXIMUM OF 5)

JCCN(26, ICCN) = ARRAY OF CONTROL CARD INFORMATION THAT IS INPUT

KCC(26) = ARRAY OF CONTROL CARD INFORMATION FOR EACH DATA SET

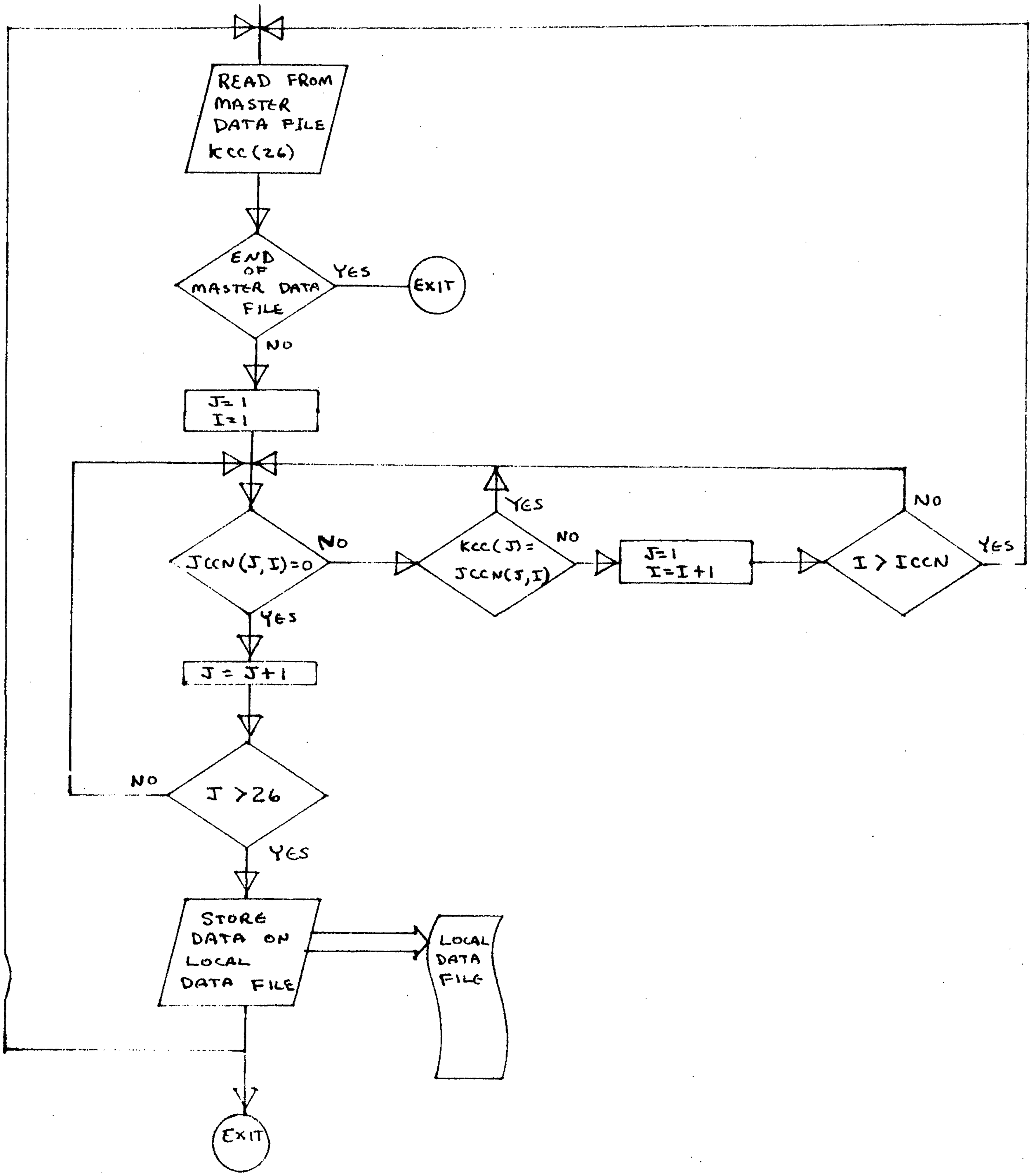

Figure C-3 Sort Subroutine Flow When Using Master Control Records to Sort on Master Data File

```
   SUBROUTINE BIN(AR1,AR2,AR3,AR10)
 1 IF(AR2)2,2,4
 2 AR10=0.0
 3 RETURN
 4 IF(AR2-AR1)7,5,5
 5 AR10=(1.0-AR3)**(1.0/AR1)
 6 RETURN
 7 ATT=2.0*AR2
 8 IF(ATT-AR1)9,9,12
 9 AR4=AR2-1.0
10 AR5=-1.0
11 GO TO 15
12 AR4=AR1-AR2
13 AR3=1.0-AR3
14 AR5=-1.0
15 AR10=0.5
16 AR6=1.0
17 AR8=0.0
18 AR9=1.0
19 AR11=AR1
20 AR7=(AR10**AR8)*((1.0-AR10)**(AR1-AR8))
21 IF(AR8-AR4)22,27,22
22 AR8=AR8+1.0
23 AR9=AR9*AR11/AR8
24 AR11=AR11-1.0
25 AR7=AR7+AR9*(AR10**AR8)*((1.0-AR10)**(AR1-AR8))
26 GO TO 21
27 IF(AR3-AR7)28,28,30
28 AR20=AR10-AR5/(2.0**(AR6+1.0))
29 GO TO 31
30 AR20=AR10+AR5/(2.0**(AR6+1.0))
31 CCC=ABS(AR7-AR3)
32 IF(CCC-0.0001)36,36,33
33 AR6=AR6+1.0
34 AR10=AR20
35 GO TO 17
36 IF(ATT-AR1)6,6,37
37 AR10=1.0-AR10
38 RETURN
39 END
```

Figure C-4 Computer Code Used to Calculate Lower One-Sided Confidence Limit

```
   SUBROUTINE DEFIC(AR1,AR2,FFF,AR4)
 1 A=AR1-AR2+FFF
 2 AR4=0.0
 3 IF(A)4,4,9
 4 AR4=29.0-AR1
 5 IF(AR4)6,6,7
 6 AR4=0.0
 7 RETURN
 9 X=1.0
10 AR5=0.0
11 C=1.0
12 CCC=AR1+AR4
13 AR5=0.9**CCC
14 C=(C/X)*(AR1+AR4+1.0-X)
15 DDD=AR1+AR4-X
16 AR5=AR5+(0.1**X)*C*(0.9**DDD)
17 IF(A-X)18,18,21
18 IF(0.05-AR5)19,19,7
19 AR4=AR4+1.0
   IF ( AR4 .EQ. 100. ) RETURN
20 GO TO 9
21 X=X+1.0
22 GO TO 14
23 END
```

Figure C-5 Computer Code Used to Calculate Additional Measurements Required to Achieve 90% Probability of Detection at 95% Confidence Limit

C-8 DATA INPUT FORMAT

The data are filed in mass memory by using a 'data set' concept. All the common control parameters for a group of data points are loaded together. There are 26 such control parameters. The first 14 are the same for all NDE methods, the next 12 are different for each of the five NDE methods. The results of the inspection follow the control parameters. Eight numbers are used to describe each point. (Crack ID, detect code, crack length, crack depth, measured crack length, measured crack depth, surface finish, thickness).

A typical control parameter listing is shown in Table C-1. Nine hundred eighty four flaw measurements have these parameters in common. The data in Table C-1 can be compacted for computer storage into the format shown in Table C-2. A special data set listing like that shown in Table C-1 can be prepared from the line of integers shown in Table C-2 by using the parameter key included at the end of this appendix. Four of the 984 data points for data set # 1 were entered onto each of 246 lines in the format depicted in Table C-3. Each complete data set is terminated by a 0000 entry in Columns 1 through 4 of the digital computer data sheet.

Table C-1 Data Set Parameters
for Data Set Number 1

DATA SET NUMBER : 1

1)	5	NDE METHOD	: ULTRASONIC
2)	4	COMPANY NAME	: MARTIN MARIETTA
3)	2	PROGRAM ID	: DETECTION OF FATIGUE CRACKS
4)	1	MATERIAL	: ALUMINUM 2219-T87
5)	1	DEFECT TYPE	: FATIGUE CRK./NO CYCLE/REMOVE EDM
6)	0	OPERATOR ID	: NA
7)	7	QUALIFICATION	: QUALIFIED ACCORDING TO MIL-STD-453
8)	1	INSP. ENVIRONMENT	: PRODUCTION
9)	2	INSP. PROCEDURE	: STD. INSP. / MULTIPLE FLAW SPEC.
10)	4	DATA RECORD TYPE	: RECORD OF METER OR SCOPE DISPLAY
11)	3	MODE OF SCAN	: MECHANICAL SCAN AND INDEX
12)	3	REFERENCE STANDARD	: FLAT BOTTOM HOLE
13)	1	DEFECT MATERIAL	: AIR
14)	1	PART GEOMETRY	: FLAT PLATE
15)	1	ULTRASONIC METHOD	: SHEAR : PULSE ECHO
16)	4	FREQUENCY	: 10 MEG HZ.
17)	1	XMITTER TYPE/SIZE	: FLAT FACE , .95 CM
18)	1	RECEIVER TYPE/SIZE	: FLAT FACE , .95 CM
19)	1	EQUIPMENT TYPE	: UM 715 , 10N PULSER/RECIEVER
20)	0	GAIN SET % OF SS	: NA
21)	0	ALARM SET % OF SS	: NA
22)	1	TYPE OF COUPLING	: WATER IMERSION
23)	1	ANGLE OF INCIDENCE	: 27.25 DEG.
24)	1	INDEX INTERVAL	: .318 CM (.125 IN)

Table C-2 Data Set Entry for Compact Storage of Data Set Parameters

Computer Input:

DIGITAL COMPUTER DATA SHEET

1	2	3	4	5	6	7	8	9	10	11	12	13	14	15	16	17	18	19	20	21	22	23	24	25	26	27	28	29	30	31	32	33	34	35	36	37	38	39	40	41	42	43	44	45	46	47	48	49	50	51	52
	5		4		2		1		1		0		7		1		2		4		3		3		1		1		1		4		1		1		1		0		0		1		1		1				

Computer Output:

5 4 2 1 1 Ø 7 1 2 4 3 3 1 1 1 4 1 1 1 Ø Ø 1 1 1

Table C-3 Flaw Size Data Entry Format
Showing Last Four Entries with End of
File Designated by "0000"

Computer Input:

1	2	3	4	5	6	7	8	9	10	11	12	13	14	15	16	17	18	19	20
			2	1		5	0		0		1	0		0	1	1	0	0	
0	0	0	0																

21	22	23	24	25	26	27	28	29	30	31	32	33	34	35	36	37	38	39	40
		5	0	6		9	0	1	0		2	0		5	2		5	0	

41	42	43	44	45	46	47	48	49	50	51	52	53	54	55	56	57	58	59	60
1	0	0	0	6	1	0	0	2	0		1	0		2	2	2	0	0	

61	62	63	64	65	66	67	68	69	70	71	72	73	74	75	76	77	78	79	80
		9	0	6	9	5	0	9	0		2	0		5	4		5	0	

Crack I.D.
Detect Code
Crack Length
Measured Crack Length
Crack Depth
Measured Crack Depth
Surface Finish
Thickness
Blank

Computer Listing

```
    21  50  Ø  Ø  1Ø  Ø11ØØ    5Ø6 9Ø1Ø 2Ø 52 5Ø 1ØØØ61ØØ2Ø 1Ø 222ØØ    9Ø695Ø9Ø 2Ø 54 5Ø
ØØØØ
```

Table C-4 Data Key

NDI METHOD

NDE	METHOD
1	EDDY CURRENT
2	PENETRANT
3	MAGNETIC PARTICLE
4	RADIOGRAPHY
5	ULTRASONIC
6	
7	
8	
9	
10	
11	
12	
13	
14	
15	
16	
17	
18	
19	
20	
21	
22	
23	
24	

DATA SOURCE

COMPANY	NAME
1	GENERAL DYNAMICS FW
2	CONVAIR/SAN DIEGO
3	BOEING COMMERCIAL
4	MARTIN MARIETTA
5	ROCKWELL INTER. B-1
6	LOCKHEED GA.
7	MCDONNELL DOUGLAS
8	AFML
9	TRW
10	GE , EVENDALE OHIO
11	FAIRCHILD HILLER
12	LOCKHEED CALIF.
13	ROCKWELL INTER. SPACE CENTER
14	BOEING WICHITA
15	
16	
17	
18	
19	
20	
21	
22	
23	
24	

PROGRAM ID

```
PROGRAM ID
 1  SENSI. LIMITS OF PROD. NDE METHODS
 2  DETECTION OF FATIGUE CRACKS
 3  EVAL OF RELI. & SENSI OF NDE METHODS
 4  USAF A10 SPO DEMO PROGRAM
 5  USAF B-1 SPO DEMO PROGRAM
 6  DETECTION OF TIGHTLY CLOSED FLAWS
 7
 8
 9
10
11
12
13
14
15
16
17
18
19
20
21
22
23
24
```

MATERIAL

```
MATERIAL
 1  ALUMINUM 2219-T87
 2  ALUMINUM 2024
 3  4340M STEEL 270-300 KSI
 4  TI-6AL-4V
 5
 6
 7
 8
 9
10
11
12
13
14
15
16
17
18
19
20
21
22
23
24
```

DEFECT TYPE

DEFECT TYPE	
1	FATIGUE CRK./NO CYCLE/REMOVE EDM
2	ELOX SLOT
3	SAW CUR
4	WELD DEFECT (LACK OF FUSION)
5	WELD DEFECT (LACK OF PENETRATION)
6	WELD DEFECT (POROSITY)
7	FORGING FLAWS WITH OXIDE IN FLAW
8	HYDROGEN EMBRITTLEMENT
9	HYDROGEN INDUCTED GRINDING CRACK
10	FATIGUE CRACK / ADD. CYCLES / REMOVE EDM
11	
12	
13	COMPRESSED NOTCH FLAW
14	FATIGUE CRACKED WELDS
15	
16	
17	
18	
19	
20	
21	
22	
23	
24	

OPERATOR ID

OPERATOR ID	
1	A
2	B
3	C
4	D
5	E
6	F
7	G
8	H
9	I
10	J
11	K
12	L
13	M
14	N
15	O
16	P
17	Q
18	R
19	S
20	T
21	U
22	V
23	W
24	X

QUALIFICATION

QUALIFICATION	
1	LEVEL 1
2	LEVEL 2
3	LEVEL 3
4	FIELD SERVICE TECHNICIAN
5	LABORATORY TECHNICIAN
6	LABORATORY ENGINEER
7	QUALIFIED ACCORDING TO MIL-STD-453
8	TECHNICALLY QUALIFIED
9	
10	CERTIFIED UNDER BOIENG A.C. 5953
11	
12	
13	
14	
15	
16	
17	
18	
19	
20	
21	
22	
23	
24	

INSP. ENVIRONMENT

INSP. ENVIRONMENT	
1	PRODUCTION
2	LABORATORY
3	FIELD SERVICE
4	
5	
6	
7	
8	
9	
10	
11	
12	
13	
14	
15	
16	
17	
18	
19	
20	
21	
22	
23	
24	

INSP. PROCEDURE

INSP.	PROCEDURE
1	STD. INSP. / SINGLE FLAW SPEC.
2	STD. INSP. / MULTIPLE FLAW SPEC.
3	NON STD. INSP. , SINGLE FLAW SPEC.
4	NON STD. INSP. , MULTIPLE FLAW SPEC.
5	
6	
7	
8	
9	
10	MIL-STD-453 / MULTIPLE FLAW
11	
12	
13	
14	
15	
16	
17	
18	
19	
20	
21	
22	
23	
24	

DATA RECORD TYPE

DATA	RECORD TYPE
1	MANUAL RECORD OF VISUAL DISPLAY
2	MANUAL RECORD OF METER OR SCOPE DISPLAY
3	MECHANICAL RECORD OF VISUAL DISPLAY
4	RECORD OF METER OR SCOPE DISPLAY
5	COMPUTER RECORD OF METER OR SCOPE DISPLA
6	
7	
8	
9	
10	
11	
12	
13	
14	
15	
16	
17	
18	
19	
20	
21	
22	
23	
24	

MODE OF SCAN

MODE OF SCAN	
1	MANUAL HAND SCAN
2	MECHANICAL SCAN , HAND INDEX
3	MECHANICAL SCAN AND INDEX
4	COMPUTER CONTROLLED SCAN
5	
6	
7	
8	
9	
10	
11	
12	
13	
14	
15	
16	
17	
18	
19	
20	
21	
22	
23	
24	

REFERENCE STANDARD

REFERENCE STANDARD	
1	ELOX SLOT
2	FATIGUE CRACK
3	FLAT BOTTOM HOLE
4	FORGING FLAW
5	SAW CUT
6	SIDE DRILLED HOLE
7	VERTICAL DRILLED HOLE
8	0.039687 (1/64) FBH
9	0.079375 (2/64) FBH
10	0.119063 (3/64) FBH
11	0.15875 (4/64) FBH
12	0.198437 (5/64) FBH
13	REF. PANEL USED / DESCRIP. NOT KNOWN
14	
15	
16	
17	
18	
19	
20	
21	
22	
23	
24	

DEFECT MATERIAL

DEFECT MATERIAL	
1	AIR
2	WATER
3	
4	
5	
6	
7	
8	
9	
10	
11	
12	
13	
14	
15	
16	
17	
18	
19	
20	
21	
22	
23	
24	

PART GEO.

PART GEOMETRY	
1	FLAT PLATE
2	
3	
4	
5	
6	WELDED BUTT JOINT WITHOUT CROWNS
7	INTEGERALLY STIFFENED PANEL (ISP)
8	WELDED BUTT JOINT WITH CROWNS
9	I.S.P. RIVETED TO FLAT PLATE
10	SOLID CYLINDER
11	FILLETED SOLID CYLINDER
12	TANDEM 'T'
13	HOLLOW CYLINDER
14	HOLLOW FILLETED CYLINDER
15	FLAT BAR
16	
17	
18	
19	
20	
21	
22	
23	
24	

SPECIAL
KEY FOR EDDY CURRENT
DATA

1 NDE METHOD
2 COMPANY NAME
3 PROGRAM ID
4 MATERIAL
5 DEFECT TYPE
6 OPERATOR ID
7 QUALIFICATION
8 INSP. ENVIRONMENT
9 INSP. PROCEDURE
10 DATA RECORD TYPE
11 MODE OF SCAN
12 REFERENCE STANDARD
13 DEFECT MATERIAL
14 PART GEOMETRY

15 EQUIPMENT TYPE
16 DIAMETER OF COIL
17 CONF./SHAPE OF COIL
18 FREQUENCY
19 TYPE OF EC RESPONSE
20 LIFT-OFF COMP.
21 SIGNAL PROCESSING
22 INDEX INTERVAL

15 EQUIPMENT TYPE

16 DIAMETER OF COIL

EQUIPMENT TYPE
1 NORTER NDT-3
2
3
4
5 MAGNATEST ED-400 & ED-520
6 VECTOR 3 SR 150 BUDD , ULTA BRIDGE
7
8
9
10
11
12
13
14
15
16
17
18
19
20
21
22
23
24

17 CONF./SHAPE OF COIL

CONF./SHAPE OF COIL	
1	DUAL COIL , AIR CORE
2	SINGLE COIL HELICALLY WOUND
3	
4	
5	BOLT HOLE & SURFACE PROBE
6	
7	
8	
9	
10	
11	
12	
13	
14	
15	
16	
17	
18	
19	
20	
21	
22	
23	
24	

18 FREQUENCY

FREQUENCY	
1	100 KHZ
2	20 KHZ
3	
4	
5	
6	
7	
8	
9	
10	
11	
12	
13	
14	
15	
16	
17	
18	
19	
20	
21	
22	
23	
24	

19 TYPE OF EC RESPONSE

TYPE OF EC RESPONSE
1 AMPLITUDE
2 PHASE
3
4
5
6
7
8
9
10
11
12
13
14
15
16
17
18
19
20
21
22
23
24

20 LIFT-OFF COMP.

LIFT-OFF COMP.
1 NO LIFT-OFF COMPENSATION
2 LIFT-OFF COMPENSATED FOR (3MIL SHIM)
3
4
5
6
7
8
9
10
11
12
13
14
15
16
17
18
19
20
21
22
23
24

21 SIGNAL PROCESSING

SIGNAL PROCESSING
1 STRAIGHT AMPLIFICATION
2
3
4
5
6
7
8
9
10
11
12
13
14
15
16
17
18
19
20
21
22
23
24

22 INDEX INTERVAL

INDEX INTERVAL
1 3048 CM (.125 IN)
2 .0508 CM (.020 IN)
3
4
5
6
7
8
9
10
11
12
13
14
15
16
17
18
19
20
21
22
23
24

SPECIAL
KEY FOR LIQUID PENETRANT
DATA

1 NDE METHOD
2 COMPANY NAME
3 PROGRAM ID
4 MATERIAL
5 DEFECT TYPE
6 OPERATOR ID
7 QUALIFICATION
8 INSP. ENVIRONMENT
9 INSP. PROCEDURE
10 DATA RECORD TYPE
11 MODE OF SCAN
12 REFERENCE STANDARD
13 DEFECT MATERIAL
14 PART GEOMETRY

15 PENETRANT TYPE
16 DEVELOPER TYPE
17 CLASS OF PENETRANT
18 REMOVER/EMULSIFER
19 APPLICATION METHOD
20 DWELL TIME
21 DEVELOPING TIME
22 WASH TIME
23 LIGHT INTENSITY
24 REMOVAL/PRE-CLEANING

15 PENETRANT TYPE

PENETRANT TYPE	
1	URESCO P-151
2	
3	
4	ZL-2A , URESCO P-133 & P-134
5	URESCO P-149
6	
7	
8	
9	
10	
11	
12	
13	
14	
15	
16	
17	
18	
19	
20	
21	
22	
23	
24	

16 DEVELOPER TYPE

DEVELOPER TYPE	
1	URESCO D499C
2	
3	
4	MAGNAFLUX ZP-4A ,-5,&-13, & URESCO 499B
5	URESCO D499C
6	
7	
8	
9	
10	
11	
12	
13	
14	
15	
16	
17	
18	
19	
20	
21	
22	
23	
24	

17 CLASS OF PENETRANT

CLASS OF PENETRANT	
1	GROUP 1
2	GROUP 2
3	GROUP 3
4	GROUP 4
5	GROUP 5
6	GROUP 6
7	GROUP 7
8	
9	
10	
11	
12	
13	
14	
15	
16	
17	
18	
19	
20	
21	
22	
23	
24	

18 REMOVER/EMULSIFER

REMOVER/EMULSIFER	
1	URESCO K410
2	
3	
4	ZE-4A AND ZE-4B
5	
6	
7	
8	
9	
10	
11	
12	
13	
14	
15	
16	
17	
18	
19	
20	
21	
22	
23	
24	

19 APPLICATION METHOD

APPLICATION METHOD	
1	HAND BRUSH
2	
3	
4	
5	
6	
7	
8	
9	
10	
11	
12	
13	
14	
15	
16	
17	
18	
19	
20	
21	
22	
23	
24	

20 DWELL TIME

DWELL TIME	
1	30. MINUTES
2	
3	
4	
5	
6	
7	
8	
9	
10	
11	
12	
13	
14	
15	
16	
17	
18	
19	
20	
21	
22	
23	
24	

21 DEVELOPING TIME

DEVELOPING TIME
1 30 MINUTES
2
3
4
5
6
7
8
9
10
11
12
13
14
15
16
17
18
19
20
21
22
23
24

22 WASH TIME

WASH TIME
1 60 MINUTES
2
3
4
5
6
7
8
9
10
11
12
13
14
15
16
17
18
19
20
21
22
23
24

23 LIGHT INTENSITY

LIGHT INTENSITY
1350 LUMENS/SQ METER
125 FT-CANDLES , 15 IN FROM FILTER

24 REMOVAL/PRE-CLEANING

REMOVAL/PRE-CLEANING
MARTIN MARIETTA (PER. NASA CR-2369)
CLEANED BY ALCOHOL IN ULTRASONIC CLEANE

SPECIAL
KEY FOR MAGNETIC PARTICLE
DATA

1 NDE METHOD
2 COMPANY NAME
3 PROGRAM ID
4 MATERIAL
5 DEFECT TYPE
6 OPERATOR ID
7 QUALIFICATION
8 INSP. ENVIRONMENT
9 INSP. PROCEDURE
10 DATA RECORD TYPE
11 MODE OF SCAN
12 REFERENCE STANDARD
13 DEFECT MATERIAL
14 PART GEOMETRY

15 EQUIPMENT
16 PROCEDURE
17 MAG. PARTICAL TYPE
18 SUSPENSION TYPE

15 EQUIPMENT

EQUIPMENT
1 TYPICAL AERO-SPACE EQUIP.
2 PARKER RESEARCH CO. (MOD DA-200)
3
4
5
6
7
8
9
10
11
12
13
14
15
16
17
18
19
20
21
22
23
24

16 PROCEDURE

PROCEDURE
1 WET CONTINUOUS FLUORESCENT PRCE.
2
3
4
5
6
7
8
9
10
11
12
13
14
15
16
17
18
19
20
21
22
23
24

17 MAG. PARTICAL TYPE

MAG.	PARTICAL TYPE
1	MAGNAFLUX 14A
2	MAGNAFLUX 14A & 14AM
3	
4	
5	
6	
7	
8	
9	
10	
11	
12	
13	
14	
15	
16	
17	
18	
19	
20	
21	
22	
23	
24	

18 SUSPENSION TYPE

SUSPENSION	TYPE
1	OIL & WATER BASE
2	14A IN OIL / 14AM IN AEROSOL CANS
3	
4	
5	
6	
7	
8	
9	
10	
11	
12	
13	
14	
15	
16	
17	
18	
19	
20	
21	
22	
23	
24	

SPECIAL
KEY FOR RADIOGRAPHY
DATA

1 NDE METHOD
2 COMPANY NAME
3 PROGRAM ID
4 MATERIAL
5 DEFECT TYPE
6 OPERATOR ID
7 QUALIFICATION
8 INSP. ENVIRONMENT
9 INSP. PROCEDURE
10 DATA RECORD TYPE
11 MODE OF SCAN
12 REFERENCE STANDARD
13 DEFECT MATERIAL
14 PART GEOMETRY

15 RADIOGRAPHY
16 EQUIIPMENT TYPE
17 SOURCE ENERGY
18 SOUPCE STRENGTH
19 WINDOW MATERIAL
20 TYPE OF FILM
21 EXPOSURE TIME
22 SOURCE TO FILM DISTA
23 ANGLE OF INCIDENCE
24 DENSITOMETER READING

15 RADIOGRAPHY

RADIOGRAPHY	
1	X-RAY
2	NEUTRON
3	
4	
5	
6	
7	
8	
9	
10	
11	
12	
13	
14	
15	
16	
17	
18	
19	
20	
21	
22	
23	
24	

16 EQUIIPMENT TYPE

EQUIIPMENT TYPE	
1	
2	
3	
4	BALTOSPOT X-RAY
5	NORELCO X-RAY 150 KV 24MA
6	
7	
8	
9	
10	
11	
12	
13	
14	
15	
16	
17	
18	
19	
20	
21	
22	
23	
24	

17 SOURCE ENERGY

```
SOURCE ENERGY
 1  30 KV FOR .1524 CM AL PANEL
 2  40 KV FOR .5207 CM AL PANEL
 3  45 KV FOR .3300 CM  , 70 KV FOR  1.27 CM
 4
 5
 6
 7
 8
 9
10
11
12
13
14
15
16
17
18
19
20
21
22
23
24
```

18 SOUPCE STRENGTH

```
SOUPCE STRENGTH
 1  20 MILLI-AMPS
 2  3 MILLI-AMPS
 3
 4
 5
 6
 7
 8
 9
10
11
12
13
14
15
16
17
18
19
20
21
22
23
24
```

19 WINDOW MATERIAL

WINDOW MATERIAL	
1	BERYLLIUM
2	
3	
4	
5	
6	
7	
8	
9	
10	
11	
12	
13	
14	
15	
16	
17	
18	
19	
20	
21	
22	
23	
24	

20 TYPE OF FILM

TYPE OF FILM	
1	KODAK , TYPE M
2	
3	
4	
5	
6	
7	
8	
9	
10	
11	
12	
13	
14	
15	
16	
17	
18	
19	
20	
21	
22	
23	
24	

21 EXPOSURE TIME

```
EXPOSURE TIME
 1  7 MIN. FOR .1524 CM AL
 2  15 MIN. FOR .5207 CM AL
 3  1.5-3.0 MIN. (THICK-ENERGY DEPEND.)
 4  1.5-2.25 MIN. (THICK-ENERGY DEPEND.)
 5
 6
 7
 8
 9
10
11
12
13
14
15
16
17
18
19
20
21
22
23
24
```

22 SOURCE TO FILM DISTA

```
SOURCE TO FILM DISTA
 1  117 CM.
 2  122 CM.
 3
 4
 5
 6
 7
 8
 9
10
11
12
13
14
15
16
17
18
19
20
21
22
23
24
```

23 ANGLE OF INCIDENCE

ANGLE OF INCIDENCE	
1	0.0 DEG (NORMAL)
2	
3	
4	
5	
6	
7	
8	
9	
10	
11	
12	
13	
14	
15	
16	
17	
18	
19	
20	
21	
22	
23	
24	

24 DENSITOMETER READING

DENSITOMETER READING	
1	2.5-3.5
2	
3	
4	
5	
6	
7	
8	
9	
10	
11	
12	
13	
14	
15	
16	
17	
18	
19	
20	
21	
22	
23	
24	

SPECIAL
KEY FOR ULTRASONICS
DATA

1 NDE METHOD
2 COMPANY NAME
3 PROGRAM ID
4 MATERIAL
5 DEFECT TYPE
6 OPERATOR ID
7 QUALIFICATION
8 INSP. ENVIRONMENT
9 INSP. PROCEDURE
10 DATA RECORD TYPE
11 MODE OF SCAN
12 REFERENCE STANDARD
13 DEFECT MATERIAL
14 PART GEOMETRY

15 ULTRASONIC METHOD
16 FREQUENCY
17 XMITTER TYPE/SIZE
18 RECEIVER TYPE/SIZE
19 EQUIPMENT TYPE
20 GAIN SET % OF SS
21 ALARM SET % OF SS
22 TYPE OF COUPLING
23 ANGLE OF INCIDENCE
24 INDEX INTERVAL

15 ULTRASONIC METHOD

ULTRASONIC METHOD

1 SHEAR : PULSE ECHO
2 SHEAR : PITCH CATCH
3 DELTA SCAN
4 COMPRESSIONAL WAVE : PULSE ECHO
5 COMPRESSIONAL WAVE : THROUGH TRANS.
6 SURFACE WAVE
7 SHEAR + SURFACE : PULSE ECHO
8 SHEAR + SURFACE + LONG. : PULSE ECHO
9
10
11
12
13
14
15
16
17
18
19
20
21
22
23
24

16 FREQUENCY

FREQUENCY

1 1 MEG. HERTZ
2 2.25 MEG HZ.
3 5 MEG HZ.
4 10 MEG HZ.
5 15 MEG HZ.
6
7
8
9
10
11
12
13
14
15
16
17
18
19
20
21
22
23
24

17 XMITTER TYPE/SIZE

XMITTER TYPE/SIZE

1	FLAT FACE , .95 CM
2	FLAT FACE , .635 CM
3	FLAT FACE , 1.27 CM
4	
5	
6	
7	
8	
9	
10	
11	
12	
13	
14	
15	
16	
17	
18	
19	
20	
21	
22	
23	
24	

18 RECEIVER TYPE/SIZE

RECEIVER TYPE/SIZE

1	FLAT FACE , .95 CM
2	FLAT FACE , .635 CM
3	FLAT FACE , 1.27 CM
4	
5	
6	
7	
8	
9	
10	
11	
12	
13	
14	
15	
16	
17	
18	
19	
20	
21	
22	
23	
24	

19 EQUIPMENT TYPE

	EQUIPMENT TYPE
1	UM 715 , 10N PULSER/RECIEVER
2	
3	
4	
5	
6	
7	
8	
9	
10	UM 715 , USIP 11 , 424D
11	
12	
13	
14	
15	
16	
17	
18	
19	
20	
21	
22	
23	
24	

20 GAIN SET % OF SS

	GAIN SET % OF SS
1	80 % SCREEN SATURATION
2	
3	
4	
5	
6	
7	
8	
9	
10	
11	
12	
13	
14	
15	
16	
17	
18	
19	
20	
21	
22	
23	
24	

21 ALARM SET % OF SS

ALARM SET % OF SS
1 33 % SCREEN SATURATION
2 50 % SCREEN STAURATION
3
4
5
6
7
8
9
10
11
12
13
14
15
16
17
18
19
20
21
22
23
24

22 TYPE OF COUPLING

TYPE OF COUPLING
1 WATER IMERSION
2 OIL IMERSION
3 WATER CONTACT
4 OIL CONTACT
5
6
7
8
9
10
11
12
13
14
15
16
17
18
19
20
21
22
23
24

23 ANGLE OF INCIDENCE

```
ANGLE OF INCIDENCE
 1  27.25 DEG.
 2  18.00 DEG
 3  27.00-27.75 DEG.
 4  32.00 DEG.
 5  90.0 DEG. (NORMAL)
 6
 7
 8
 9
10
11
12
13
14
15
16
17
18
19
20
21
22
23
24
```

24 INDEX INTERVAL

```
INDEX INTERVAL
 1  .318 CM (.125 IN.)
 2  .081 CM  (.032 IN)
 3  .051 CM. (.020 IN)
 4  .076 CM. (.030 IN)
 5
 6
 7
 8
 9
10
11
12
13
14
15
16
17
18
19
20
21
22
23
24
```

APPENDIX D

COMPUTER OUTPUT - NDE RELIABILITY DATA

The data for Figures D-1a, D-1b, and D-1c were obtained with an ultrasonic surface wave technique and at a frequency of 10 MHz. The abscissa is the surface length of a fatigue crack. The NDE technique (ultrasonics) is given on the upper left hand corner of the figures immediately after the date when the curves were plotted. Test 1, Test 2, or Test 3 is written on the same top line of the page. Test 1 refers to the range scheme where the lower one-sided confidence limit, p_1, was calculated for equal flaw size intervals. In Figure D-1a the flaw size interval is 0.038 cm. Test 2 (Figure D-1b) refers to the use of the optimized probability method to calculate the p_1. Test 3 (Figure D-1c) refers to the use of the overlapping sixty point scheme to calculate the p_1. The top line of the computer output also contains the name of the company or the agency that published the report from which the data were taken. In Figure D-1 the company is Martin Marietta of Denver, Colorado. The test specimen martial type is identified in the figure caption on the bottom of the page or in Table 5-1 of Section V where the data set number can be matched with the number in parenthesis in the upper right hand side of each figure.

The first column of the tabulated results in these figures lists the range numbers. The second column gives the minimum crack length of each range and the third column gives the maximum crack length of each range.* The fourth column gives the total number of measurements or observations (N) for each size range and the fifth column gives the number of detections (n) for each size range. The probability of detection at 50% and 95% confidence level** is given in the sixth and seventh columns respectively. The last two columns list the number of new measurements that must be made with no misses and with one miss, respectively, to achieve 90% probability of detection at a 95% confidence level. The zeroes in these last two columns indicate that either no measurements need to be made or the number is too large for practical consideration.

---

* Tabulated data give crack lengths in mils while the graphs give both mils and cm scales. This dual labeling is offered as a convenience for the design engineer.

** Hereafter POD90(CL95) will be used to refer to a 95 percent confidence that the true probability of detection equals or exceeds 90 percent.

All the reliability curves discussed in this appendix are presented in the above format. Additional information such as flaw, type, material alloy type, contract or report identification number, and other pertinent parameters associated with the data used to generate these reliability curves and tables are included wherever possible.

(a) Range Interval Method of Data Cumulation

02-JUL-75 ULTRASONIC BY LENGTH TEST 1 , MARTIN (1)

RANGE	MIN LN *	MAX LN *	N	DET	50%	95%	0 MISS	RANGE 1 MISS
1	7	21	39	4	9	3	0	0
2	25	36	48	15	30	20	0	[illegible]
3	38	52	72	40	54	45	0	[illegible]
4	54	67	120	98	81	74	0	0
5	68	82	132	117	88	83	0	[illegible]
6	83	97	87	72	82	74	0	0
7	98	108	39	38	95	88	7	22
8	115	126	33	31	91	82	28	43
9	129	141	42	41	96	89	4	19
10	146	153	18	17	90	76	28	43
11	158	171	9	8	82	57	0	0
12	182	184	9	8	82	57	0	0
13	0	0	0	0	0	0	0	0
14	0	0	0	0	0	0	0	0
15	0	0	0	0	0	0	0	0
16	241	247	12	11	86	66	0	0
17	248	262	51	51	98	94	0	0
18	268	275	9	9	92	71	0	0
19	279	290	15	15	95	81	14	31
20	295	306	15	15	95	81	14	31
21	310	322	27	27	97	89	2	19
22	323	336	30	30	97	90	0	16
23	338	347	18	18	96	84	11	[illegible]
24	362	362	3	3	79	36	0	[illegible]
25	381	381	3	3	79	36	0	[illegible]
26	393	393	3	3	79	36	0	[illegible]
27	408	408	3	3	79	36	0	[illegible]
28	0	0	0	0	0	0	0	[illegible]
29	0	0	0	0	0	0	[illegible]	[illegible]
30	0	0	0	0	0	0	[illegible]	[illegible]
31	459	466	6	6	89	60	[illegible]	[illegible]
32	475	979	90	89	99	94	[illegible]	[illegible]

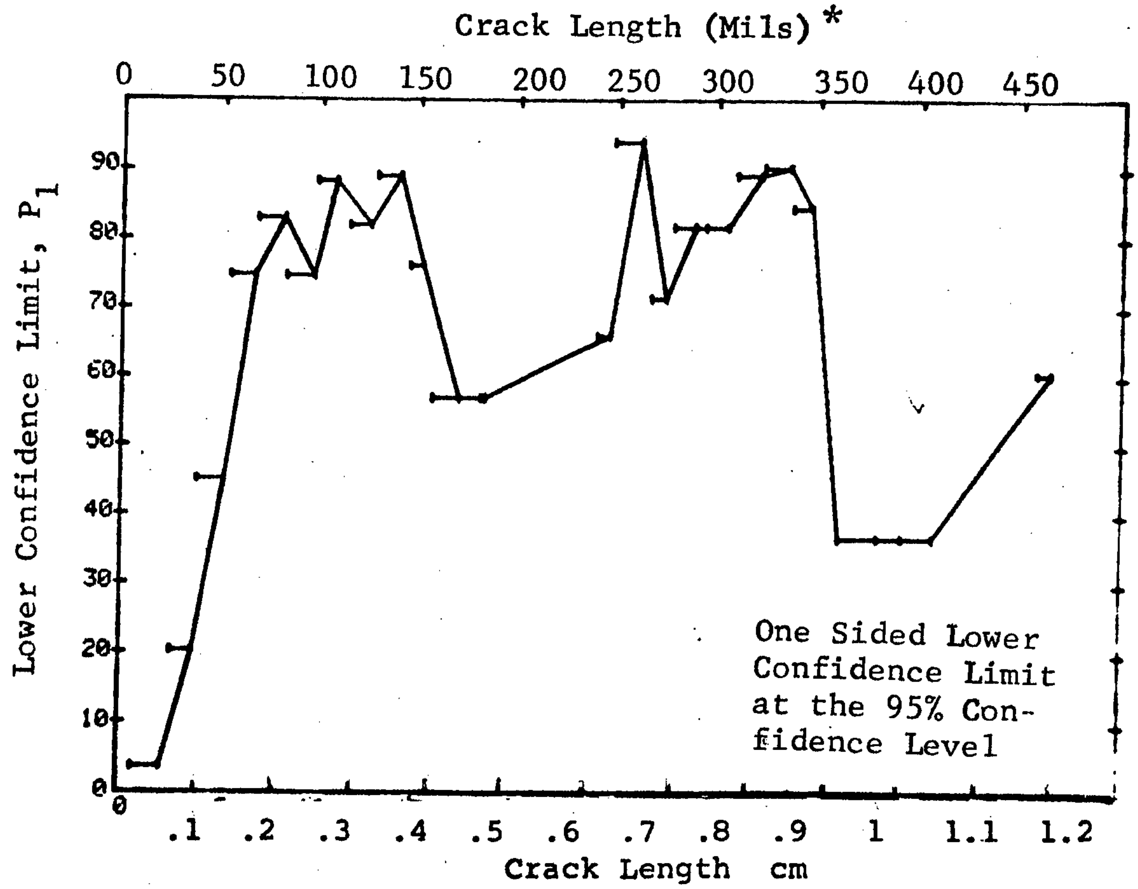

Figure D-1 Probability of Detection for 2219-T87 Al Using Ultrasonic Surface Waves. Fatigue Cracks in Flat Plates. Lab. Env.

(b) Optimum Probability Method of Data Cumulation

02-JUL-75 ULTRASONIC BY LENGTH TEST 2 , MARTIN (i') . MCD

RANGE	MIN LN	MAX LN	N	DET	50%	95%	0 MISS	1 MISS
1	7*	21 *	39	4	0	3	0	0
2	25	36	48	15	0	20	0	0
3	38	52	72	40	0	45	0	0
4	54	67	120	98	0	74	0	0
5	68	82	132	117	0	83	0	0
6	68	97	219	189	0	81	0	0
7	98	108	39	38	0	88	7	22
8	98	126	72	69	0	99	4	17
9	98	141	114	110	0	92	0	0
10	98	153	132	127	0	92	0	0
11	98	171	141	135	0	91	0	0
12	98	184	150	143	0	91	0	0
13	0	0	0	0	0	0	0	0
14	0	0	0	0	0	0	0	0
15	0	0	0	0	0	0	0	0
16	98	247	162	154	0	91	0	0
17	248	262	51	51	0	94	0	0
18	248	275	60	60	0	95	0	0
19	248	290	75	75	0	96	0	0
20	248	306	90	90	0	96	0	0
21	248	322	117	117	0	97	0	0
22	248	336	147	147	0	97	0	0
23	248	347	165	165	0	98	0	0
24	248	362	168	168	0	98	0	0
25	248	381	171	171	0	98	0	0
26	248	393	174	174	0	98	0	0
27	248	408	177	177	0	98	0	0
28	0	0	0	0	0	0	0	0
29	0	0	0	0	0	0	0	
30	0	0	0	0	0	0	0	[illegible]
31	248	466	183	183	0	98	0	[illegible]
32	248	979	273	272	0	98	0	[illegible]

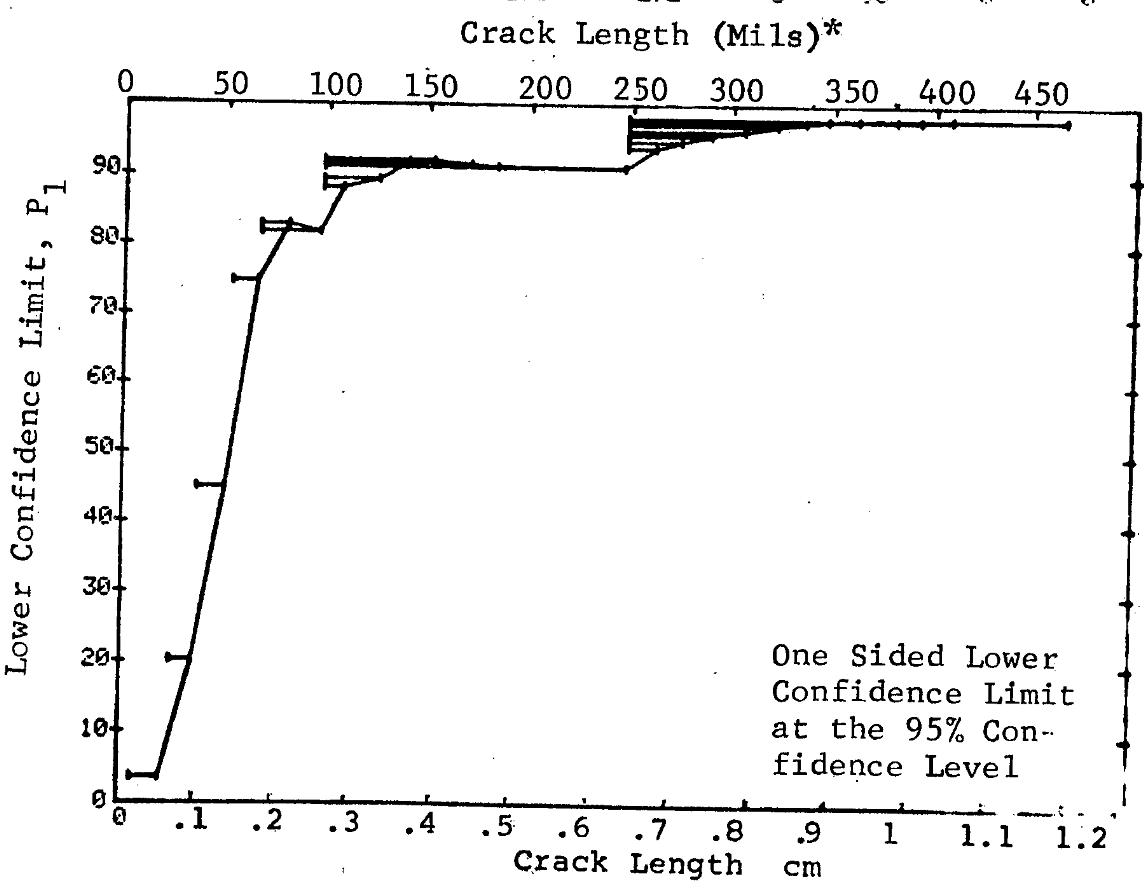

Figure D-1 (Continued)

(c) Overlapping Sixty Point Method of Data Cumulation

02-JUL-75 ULTRASONIC BY LENGTH TEST 3 MARTIN (1)

RANGE	MIN LN	MAX LN	N	DET	50%	95%	0 MISS	1 MISS
1	0 *	0 *	0	0	0	0	0	0
2	0	0	0	0	0	0	0	0
3	0	0	0	0	0	0	0	0
4	7	20	33	4	11	4	0	0
5	8	30	60	10	16	9	0	0
6	21	40	60	16	25	17	0	0
7	31	45	60	20	32	23	0	0
8	40	51	60	33	54	43	0	0
9	45	58	60	42	69	58	0	0
10	52	61	60	43	70	60	0	0
11	58	64	60	53	87	79	69	82
12	62	67	60	56	92	85	29	43
13	64	70	60	53	87	79	69	82
14	67	73	60	52	85	77	82	94
15	70	77	60	50	82	73	0	0
16	74	80	60	52	85	77	82	94
17	77	83	60	56	92	85	29	43
18	80	87	60	53	87	79	69	82
19	84	95	60	52	85	77	82	94
20	90	102	60	51	83	75	94	100
21	96	115	60	52	85	77	82	94
22	103	129	60	58	95	89	1	16
23	117	136	60	60	98	95	0	0
24	129	158	60	58	95	89	1	[illegible]
25	138	248	60	55	90	83	43	56
26	162	258	60	57	93	87	16	[illegible]
27	249	279	60	60	98	95	0	0
28	258	310	60	60	98	95	0	0
29	279	326	60	60	98	95	0	
30	310	340	60	60	98	95	0	[illegible]
31	326	466	60	60	98	95	0	[illegible]
32	342	500	60	60	98	95	[illegible]	[illegible]

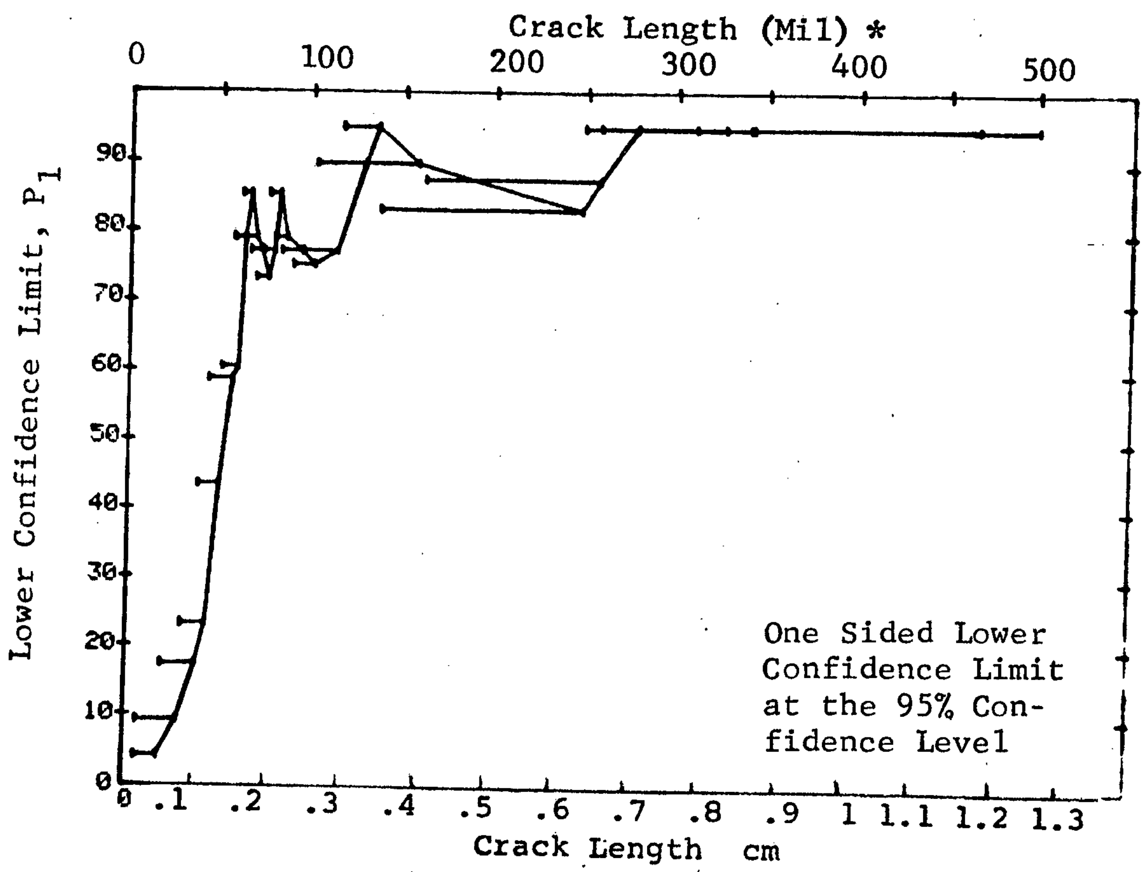

Figure D-1 (Concluded)

(a) Range Interval Method of Data Cumulation

02-JUL-75 TEST 1 , PENET , [illegible] (2)

RANGE	MIN LN	MAX LN	N	DET	50%	95%	[illegible]	RANGE
1	7*	21 *	39	4	9	3	0	[illegible]
2	25	36	48	13	26	15	0	[illegible]
3	38	52	72	23	31	22	0	[illegible]
4	54	67	120	63	52	44	0	[illegible]
5	68	82	132	91	68	61	0	[illegible]
6	83	97	87	60	68	59	0	0
7	98	108	39	23	57	44	0	0
8	115	126	33	15	43	30	0	0
9	129	141	42	26	60	48	0	0
10	146	153	18	11	58	39	0	0
11	158	171	9	3	28	9	0	0
12	182	185	9	5	50	25	0	0
13	0	0	0	0	0	0	0	0
14	0	0	0	0	0	0	0	0
15	0	0	0	0	0	0	0	0
16	241	247	12	12	94	77	17	34
17	248	262	51	50	96	91	0	10
18	268	275	9	7	71	45	0	0
19	279	290	15	13	82	63	0	0
20	295	306	15	14	89	72	0	0
21	310	322	27	19	68	52	0	0
22	323	336	30	27	87	76	46	59
23	338	347	18	15	79	62	0	0
24	362	362	3	3	79	36	0	0
25	381	381	3	3	79	36	0	0
26	393	393	3	3	79	36	0	0
27	408	408	3	3	79	36	0	0
28	0	0	0	0	0	0	0	0
29	0	0	0	0	0	0	0	0
30	0	0	0	0	0	0	0	0
31	459	466	6	4	57	27	0	0
32	474	979	90	83	91	85	[illegible]	[illegible]

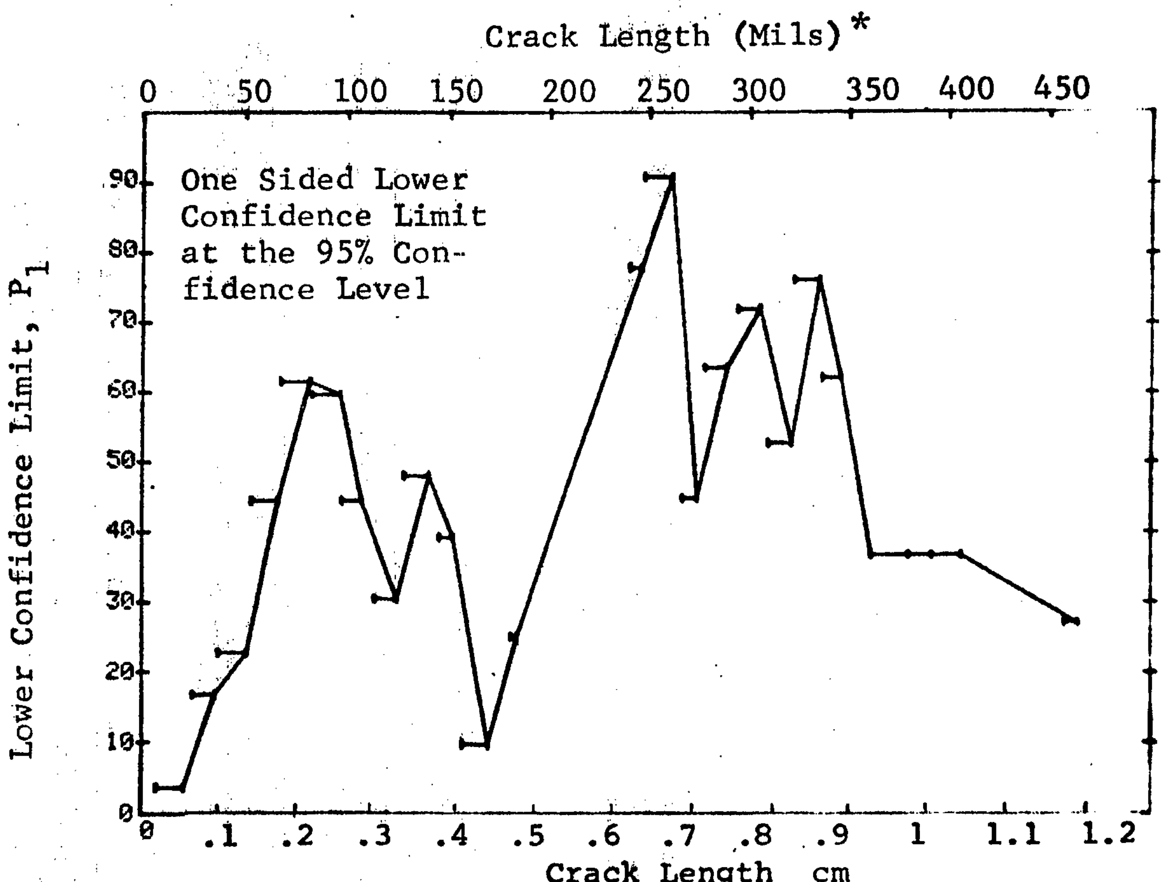

Figure D-2 Probability of Detection for 2219-T87 Al Using Liquid Penetrant. Fatigue Cracks in Flat Plates. Lab. Env.

(b) Optimum Probability Method of Data Cumulation

02-JUL-75 PENETRANT TEST 2 , PENET , MARTIN (2) MCD

RANGE	MIN LN	MAX LN	N	DET	50%	95%	0 MISS	MCD
1	7 *	21 *	39	4	0	3	0	[illegible]
2	25	36	48	13	0	16	0	[illegible]
3	25	52	120	36	0	23	0	[illegible]
4	54	67	120	63	0	44	0	[illegible]
5	68	82	132	91	0	61	0	[illegible]
6	68	97	219	151	0	63	0	0
7	68	108	258	174	0	62	0	0
8	54	126	411	252	0	57	0	0
9	68	141	333	215	0	60	0	0
10	68	153	351	226	0	59	0	0
11	68	171	360	229	0	59	0	0
12	68	185	369	234	0	59	0	0
13	0	0	0	0	0	0	0	0
14	0	0	0	0	0	0	0	0
15	0	0	0	0	0	0	0	0
16	241	247	12	12	0	77	0	0
17	241	262	63	62	0	92	0	0
18	241	275	72	69	0	89	4	17
19	241	290	87	82	0	88	16	[illegible]
20	241	306	102	96	0	88	0	0
21	241	322	129	115	0	83	0	0
22	241	336	159	142	0	84	0	0
23	241	347	177	157	0	84	0	0
24	241	362	180	160	0	84	0	[illegible]
25	241	381	183	163	0	84	0	0
26	241	393	186	166	0	84	0	0
27	241	408	189	169	0	84	0	0
28	0	0	0	0	0	0	0	0
29	0	0	0	0	0	0	[illegible]	[illegible]
30	0	0	0	0	0	0	0	[illegible]
31	241	466	195	173	0	84	0	0
32	241	979	285	256	0	[illegible]	0	0

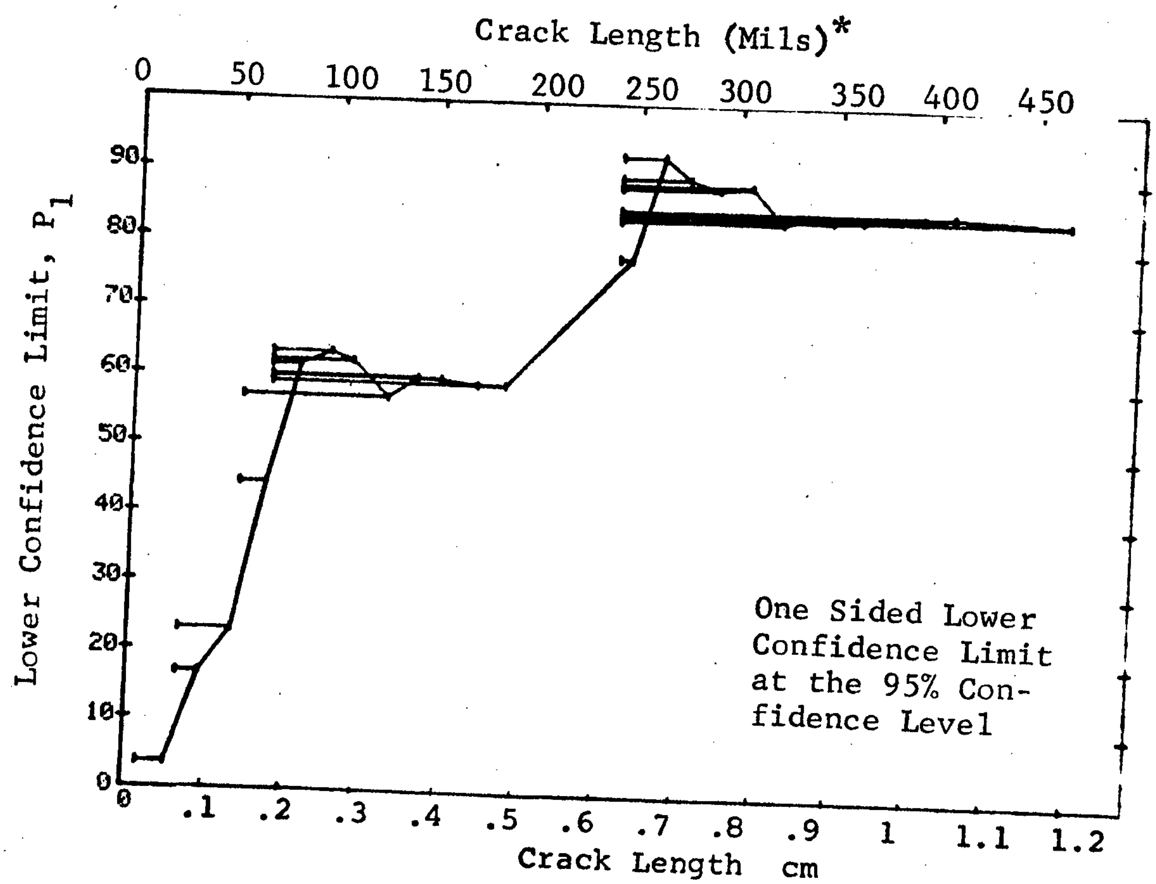

Figure D-2 (Continued)

(c) Overlapping Sixty Point Method of Data Cumulation

02-JUL-75 PENETRANT TEST 3 , MARTIN (2)

RANGE	MIN LN	MAX LN	N	DET	50%	95%	0 MI[illegible]	[illegible]
1	0	0	0	0	0	0	0	[illegible]
2	0	0	0	0	0	0	0	[illegible]
3	0	0	0	0	0	0	0	[illegible]
4	7	20	33	2	5	1	0	[illegible]
5	8	30	60	11	17	10	0	[illegible]
6	21	40	60	15	24	16	0	0
7	31	45	60	15	24	16	0	0
8	40	51	60	21	34	24	0	0
9	45	58	60	24	39	29	0	0
10	52	61	60	28	45	35	0	0
11	56	64	60	34	55	45	0	0
12	62	67	60	32	52	41	0	0
13	64	70	60	35	57	46	0	0
14	67	73	60	38	62	51	0	0
15	70	77	60	31	50	40	0	0
16	74	80	60	40	65	55	0	0
17	77	83	60	56	92	85	29	43
18	80	87	60	55	90	83	43	56
19	84	95	60	41	67	57	0	0
20	90	102	60	29	47	37	0	0
21	96	115	60	31	50	40	0	0
22	103	129	60	34	55	45	0	0
23	117	136	60	34	55	45	0	0
24	129	158	60	37	60	50	0	[illegible]
25	138	248	60	40	65	55	0	0
26	162	258	60	51	83	75	94	100
27	249	279	60	57	93	87	16	29
28	258	310	60	52	85	77	82	94
29	279	326	60	49	80	71	0	[illegible]
30	310	340	60	49	80	71	0	0
31	326	466	60	52	85	77	82	94
32	342	500	60	53	87	79	[illegible]	[illegible]

*

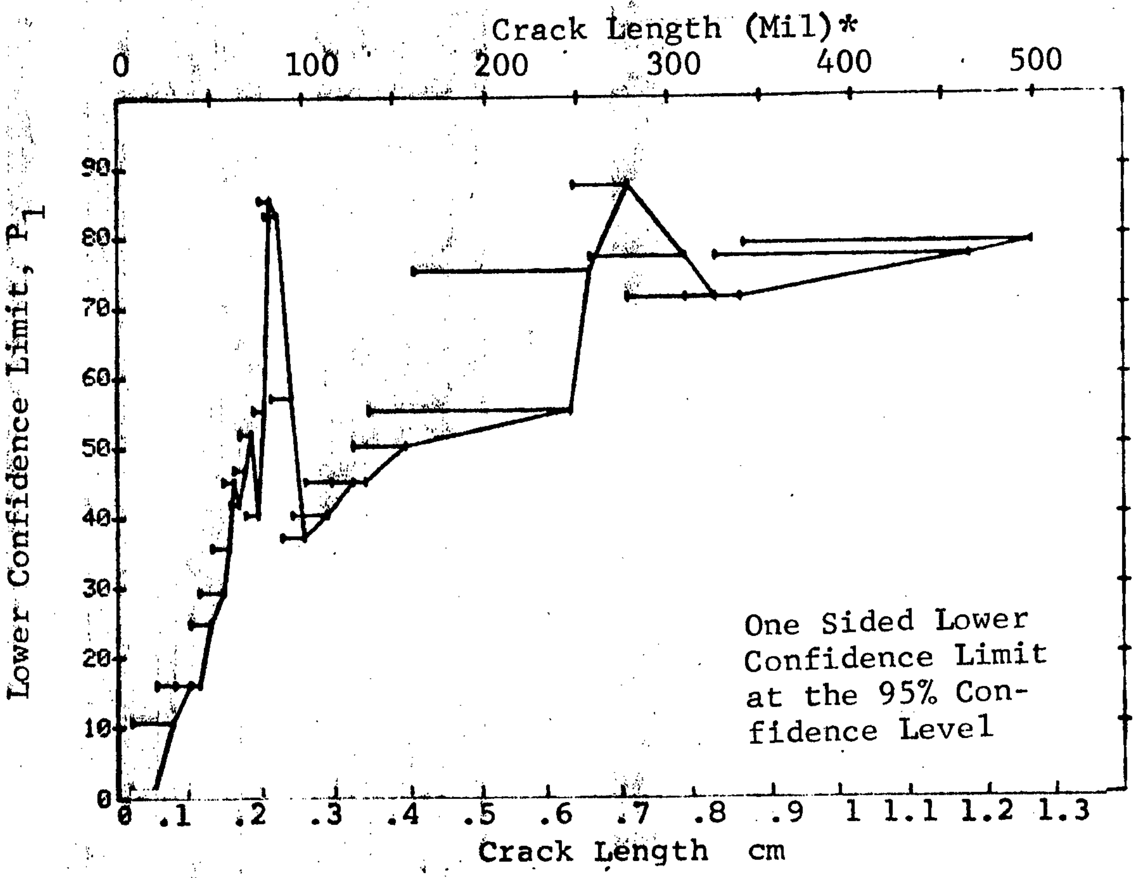

Figure D-2 (Concluded)

(a) Range Interval Method of Data Cumulation

02-JUL-75 EDDY CURRENT TEST 1 , EDDY CURRENT [illegible] (3)RANGE

RANGE	MIN LN *	MAX LN **	N	DET	50%	95%	0 MI[illegible]	
1	7	21	39	5	11	5	0	
2	25	36	48	10	20	11	0	
3	38	52	72	40	54	45	0	[illegible]
4	54	67	120	85	70	63	0	[illegible]
5	68	82	133	109	81	75	0	[illegible]
6	83	97	87	78	88	82	67	[illegible]
7	98	108	39	39	98	92	0	[illegible]
8	115	126	33	30	88	78	43	[illegible]
9	129	141	42	39	91	82	34	[illegible]
10	146	153	18	18	96	84	11	[illegible]
11	158	171	9	9	92	71	0	0
12	182	185	9	7	71	45	0	0
13	0	0	0	0	0	0	0	0
14	0	0	0	0	0	0	0	0
15	0	0	0	0	0	0	0	0
16	241	247	12	11	86	66	0	0
17	248	262	51	51	98	94	0	0
18	268	275	9	9	92	71	0	0
19	279	290	14	13	88	70	0	0
20	295	306	15	14	89	72	0	0
21	310	322	27	26	93	83	19	34
22	323	336	30	30	97	90	0	16
23	338	347	18	16	85	68	0	[illegible]
24	362	362	3	3	79	36	0	[illegible]
25	381	381	3	3	79	36	0	0
26	393	393	3	3	79	36	0	[illegible]
27	408	408	3	3	79	36	0	0
28	0	0	0	0	0	0	0	0
29	0	0	0	0	0	0	[illegible]	
30	0	0	0	0	0	0	0	[illegible]
31	459	466	6	6	89	60	0	[illegible]
32	475	979	90	85	93	88	13	[illegible]

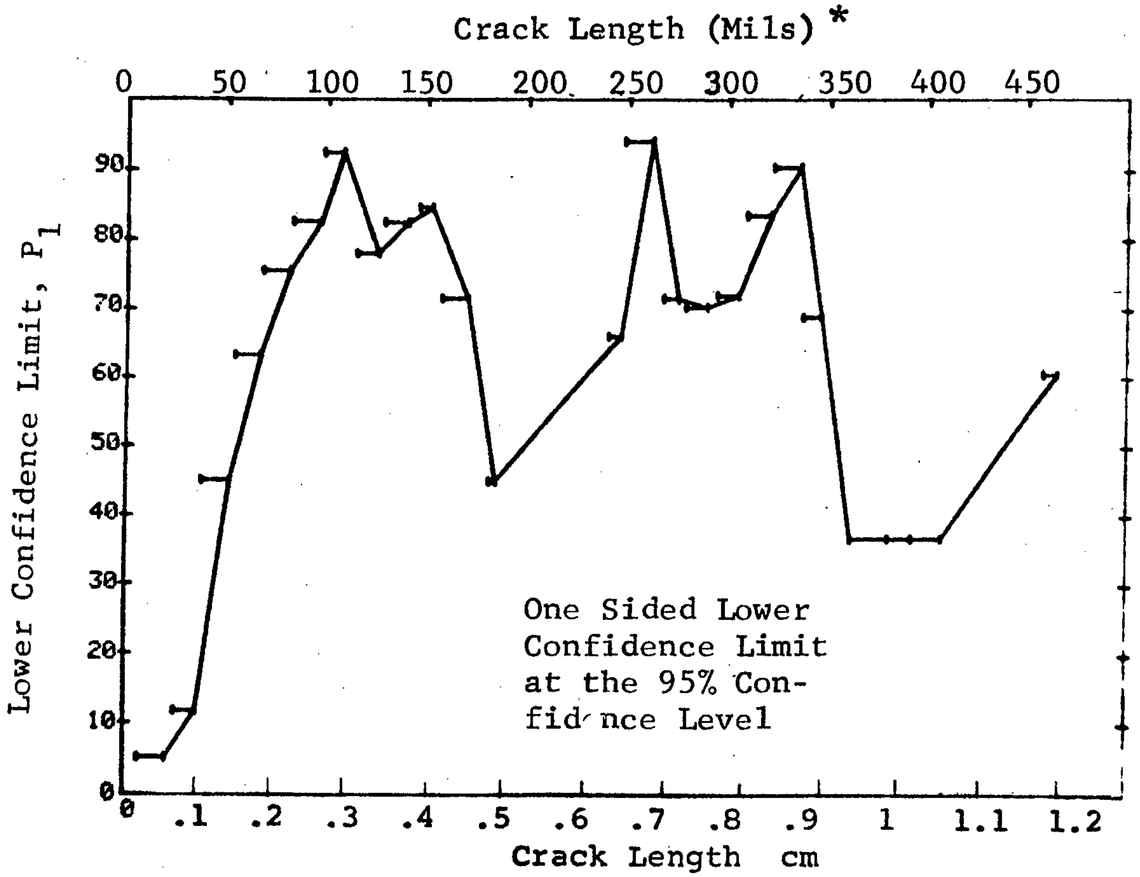

Figure D-3 Probability of Detection for 2219-T87 Al Using Eddy Current. Fatigue Cracks in Flat Plates. Lab. Env.

(b) Optimum Probability Method of Data Cumulation

07-JUL-75 EDDY CURRENT TEST 2, MARTIN , (3)

RANGE	MIN LN	MAX LN	N	DET	50%	95%	0 MISS	MCD 1 MISS
1	7*	21*	39	5	0	5	0	0
2	25	36	48	10	0	11	0	0
3	38	52	72	40	0	45	0	0
4	54	67	120	84	0	62	0	0
5	68	82	133	109	0	75	0	0
6	83	97	87	78	0	82	67	80
7	98	108	39	39	0	92	0	7
8	98	126	72	69	0	89	4	17
9	98	141	113	107	0	89	0	0
10	98	153	131	125	0	91	0	0
11	98	171	140	134	0	91	0	0
12	98	185	149	141	0	90	0	0
13	0	0	0	0	0	0	0	0
14	0	0	0	0	0	0	0	0
15	0	0	0	0	0	0	0	0
16	98	247	161	152	0	90	0	0
17	248	262	51	51	0	94	0	0
18	248	275	60	60	0	95	0	0
19	248	290	74	73	0	93	0	0
20	248	306	89	87	0	93	0	0
21	248	322	116	113	0	93	0	0
22	248	336	146	143	0	94	0	0
23	248	347	164	159	0	93	0	0
24	248	362	167	162	0	93	0	0
25	248	381	170	165	0	93	0	0
26	248	393	173	168	0	94	0	0
27	248	408	176	171	0	94	0	0
28	0	0	0	0	0	0	0	0
29	0	0	0	0	0	0	0	0
30	0	0	0	0	0	0	0	0
31	248	466	182	177	0	94	0	0
32	248	979	272	261	0	93	0	0

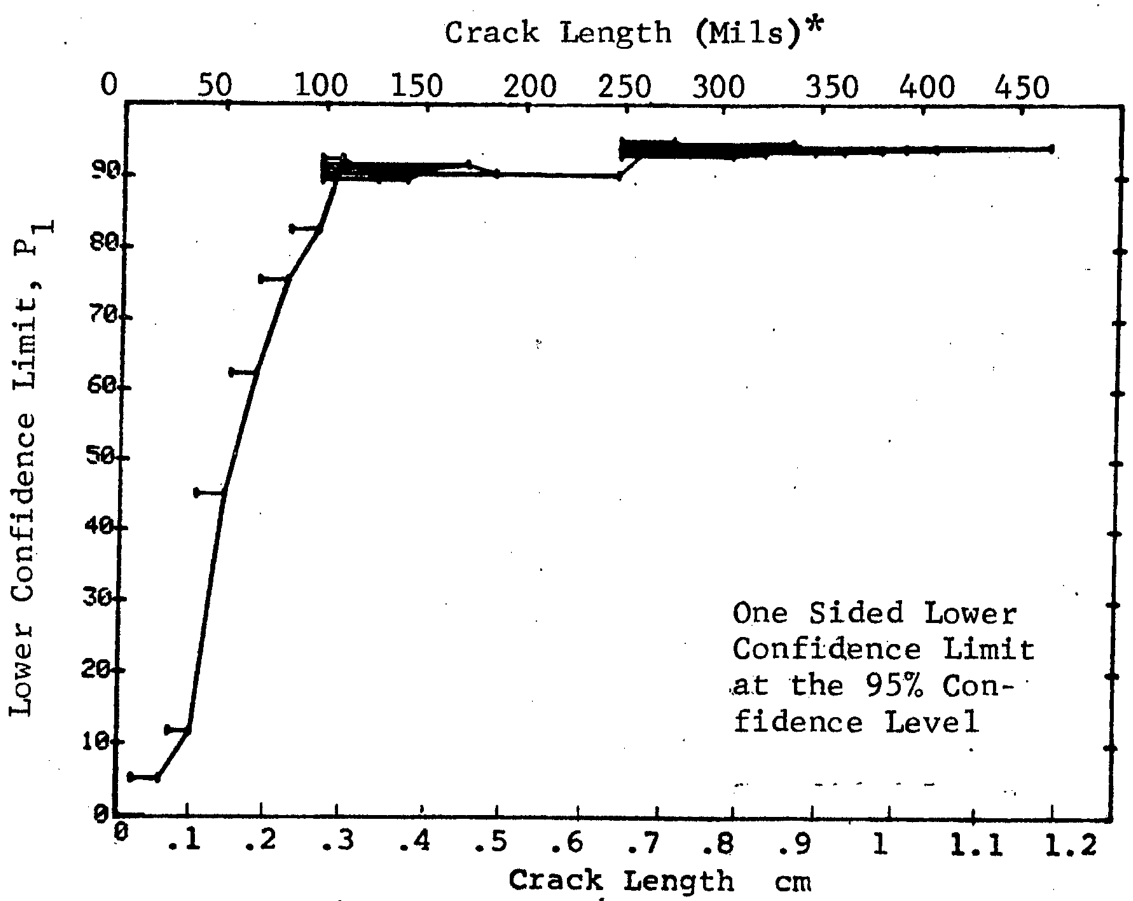

Figure D-3 (Continued)

(c) Overlapping Sixty Point Method of Data Cumulation

02-JUL-75 TEST 3 EDDY CURRENT [illegible] (3)

RANGE	MIN LN	MAX LN	N	DET	50%	95%	0 MISS	[illegible]
1	0 *	0 *	0	0	0	0	0	[illegible]
2	0	0	0	0	0	0	0	
3	0	0	0	0	0	0	0	[illegible]
4	7	20	33	4	11	4	0	[illegible]
5	8	30	60	11	17	10	0	[illegible]
6	21	40	60	14	22	14	0	0
7	31	45	60	22	35	26	0	0
8	40	51	60	33	54	43	0	0
9	45	58	60	36	59	48	0	0
10	52	61	60	38	62	51	0	0
11	58	64	60	44	72	62	0	0
12	62	67	60	47	77	67	0	0
13	64	70	60	46	75	65	0	0
14	67	73	60	43	70	60	0	0
15	70	77	60	43	70	60	0	0
16	74	80	60	52	85	77	82	94
17	77	83	60	57	93	87	16	[illegible]
18	80	87	60	54	88	81	56	[illegible]
19	83	95	60	55	90	83	43	56
20	87	102	60	56	92	85	29	47
21	95	115	60	54	88	81	56	[illegible]
22	102	129	60	56	92	85	29	43
23	115	136	60	58	95	89	1	[illegible]
24	129	158	60	58	95	89	1	[illegible]
25	136	248	60	56	92	85	29	47
26	158	258	60	57	93	87	16	[illegible]
27	248	279	60	60	98	95	0	0
28	258	310	60	58	95	89	1	16
29	279	326	60	57	93	87	[illegible]	[illegible]
30	310	340	60	57	93	87	[illegible]	[illegible]
31	326	466	60	58	95	89	1	[illegible]
32	342	500	60	58	95	89	1	[illegible]

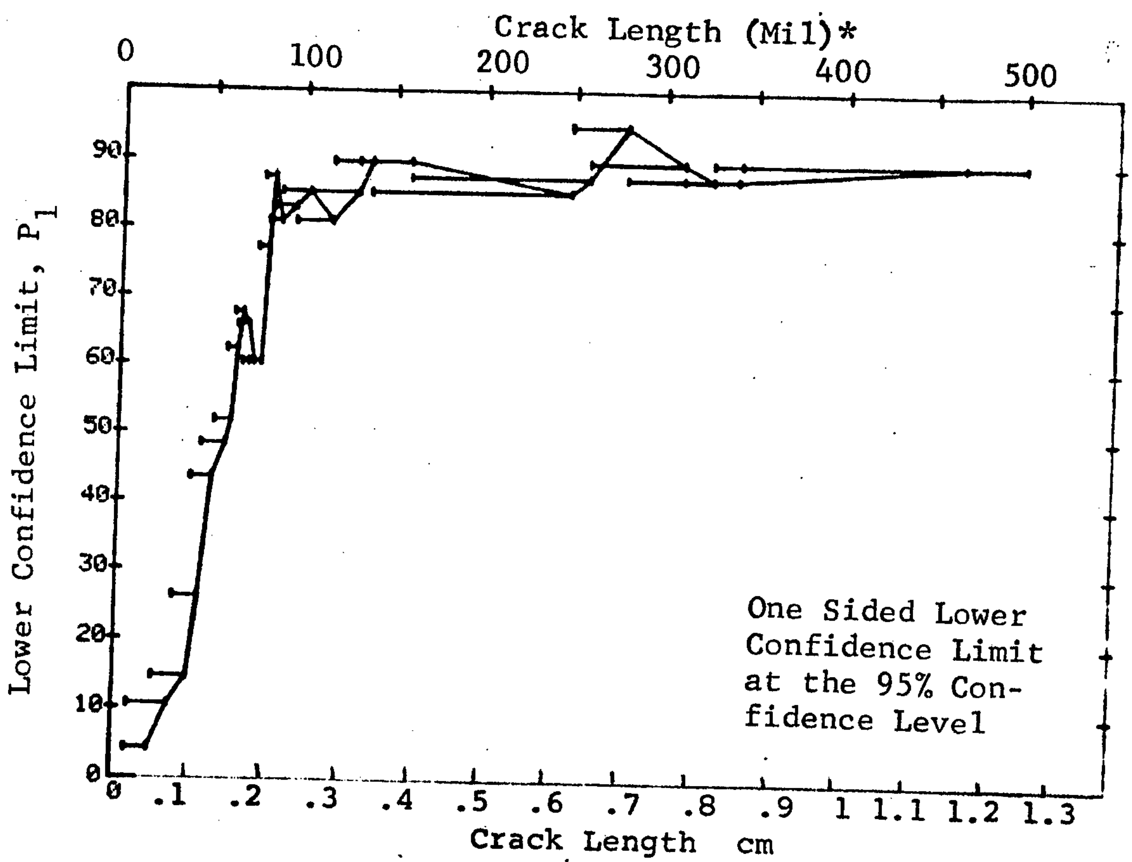

Figure D-3 (Concluded)

(a) Range Interval Method of Data Cumulation

02-JUL-75 RADIOGRAPHY TEST 1 , X-RAY , MARTIN 4

RANGE	MIN LN	MAX LN	N	DET	50%	95%	0 MISS	[illegible]
1	7 *	21 *	39	1	1	0	0	[illegible]
2	25	36	48	0	0	0	0	[illegible]
3	38	52	71	2	2	0	0	[illegible]
4	54	67	116	2	1	0	0	[illegible]
5	68	82	134	2	1	0	0	[illegible]
6	83	97	86	1	0	0	0	0
7	98	108	39	1	1	0	0	0
8	115	126	33	0	0	0	0	0
9	129	141	42	1	1	0	0	0
10	146	153	18	1	3	0	0	0
11	158	171	9	0	0	0	0	0
12	182	185	9	1	7	0	0	0
13	0	0	0	0	0	0	0	0
14	0	0	0	0	0	0	0	0
15	0	0	0	0	0	0	0	0
16	241	247	12	0	0	0	0	0
17	248	262	51	4	7	2	0	0
18	268	275	9	0	0	0	0	0
19	279	290	16	0	0	0	0	0
20	295	306	14	1	4	0	0	0
21	310	322	27	2	6	1	0	0
22	323	336	30	1	2	0	0	0
23	338	347	18	0	0	0	0	0
24	362	362	3	0	0	0	0	[illegible]
25	381	381	3	0	0	0	0	0
26	393	393	3	0	0	0	0	[illegible]
27	408	408	3	0	0	0	0	0
28	0	0	0	0	0	0	0	0
29	0	0	0	0	0	0	[illegible]	[illegible]
30	0	0	0	0	0	0	0	[illegible]
31	459	466	6	1	10	0	0	[illegible]
32	475	979	94	71	74	67	[illegible]	[illegible]

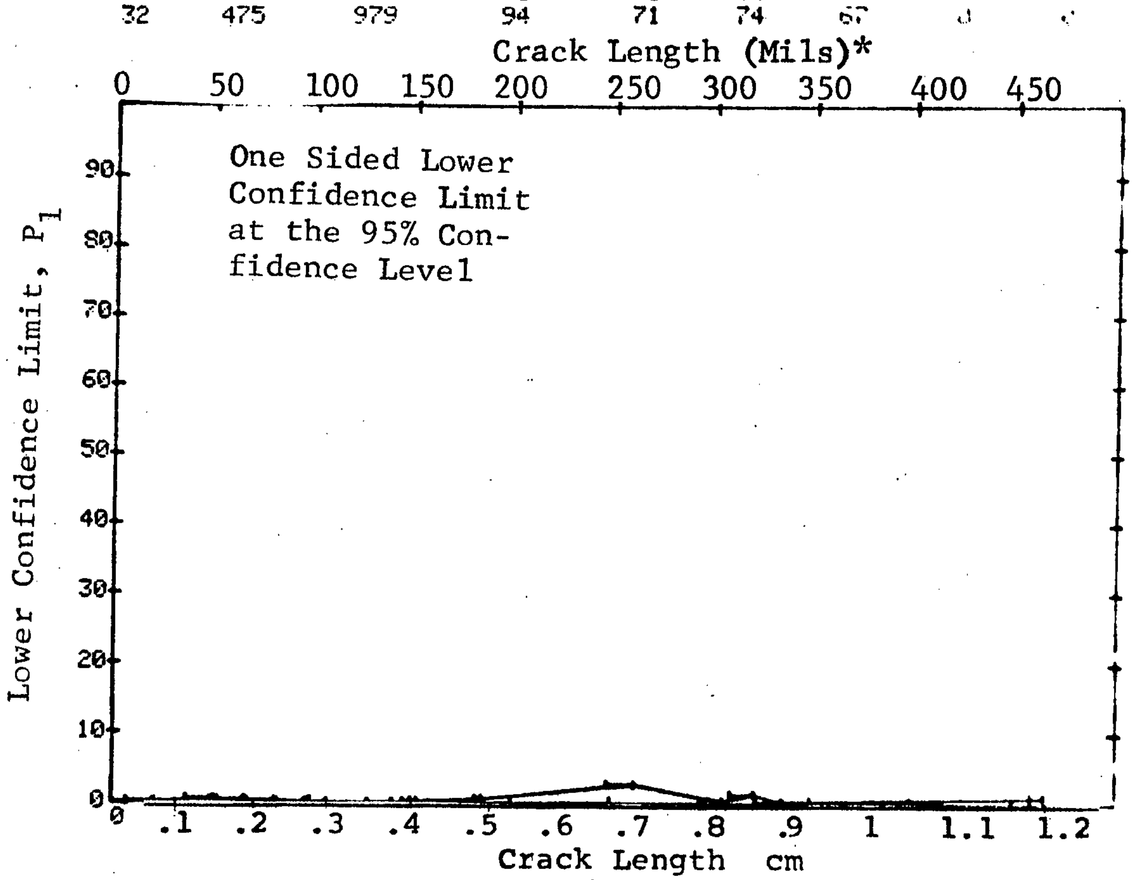

Figure D-4 Probability of Detection for 2219-T87 Al Using X-ray. Fatigue Cracks in Flat Plates. Lab. Env.

(b) Optimum Probability Method of Data Cumulation

02-JUL-75 TEST 2 , X-RAY , MARTIN (4)

RANGE	MIN LN *	MAX LN *	N	DET	50%	95%	0 MISS	1 MISS
1	7	21	39	1	0	0	0	[illegible]
2	7	36	87	1	0	0	0	[illegible]
3	7	52	158	3	0	0	0	[illegible]
4	38	67	187	4	0	0	0	[illegible]
5	38	82	321	6	0	0	0	[illegible]
6	38	97	407	7	0	0	0	0
7	38	108	446	8	0	0	0	0
8	38	126	479	8	0	0	0	0
9	38	141	521	9	0	0	0	0
10	38	153	539	10	0	0	0	0
11	38	171	548	10	0	1	0	0
12	38	185	557	11	0	0	0	0
13	0	0	0	0	0	1	0	0
14	0	0	0	0	0	0	0	0
15	0	0	0	0	0	0	0	0
16	38	247	569	11	0	0	0	0
17	182	262	72	5	0	1	0	0
18	182	275	81	5	0	2	0	0
19	146	290	124	6	0	2	0	0
20	146	306	138	7	0	2	0	0
21	182	322	138	8	0	2	0	0
22	182	336	168	9	0	2	0	0
23	146	347	213	10	0	2	0	0
24	146	362	216	10	0	2	0	0
25	146	381	219	10	0	2	0	0
26	146	393	222	10	0	2	0	0
27	146	408	225	10	0	2	0	0
28	0	0	0	0	0	2	0	0
29	0	0	0	0	0	0	0	0
30	0	0	0	0	0	0	[illegible]	[illegible]
31	146	466	231	11	0	0	[illegible]	[illegible]
32	475	979	94	71	0	[illegible]	[illegible]	[illegible]

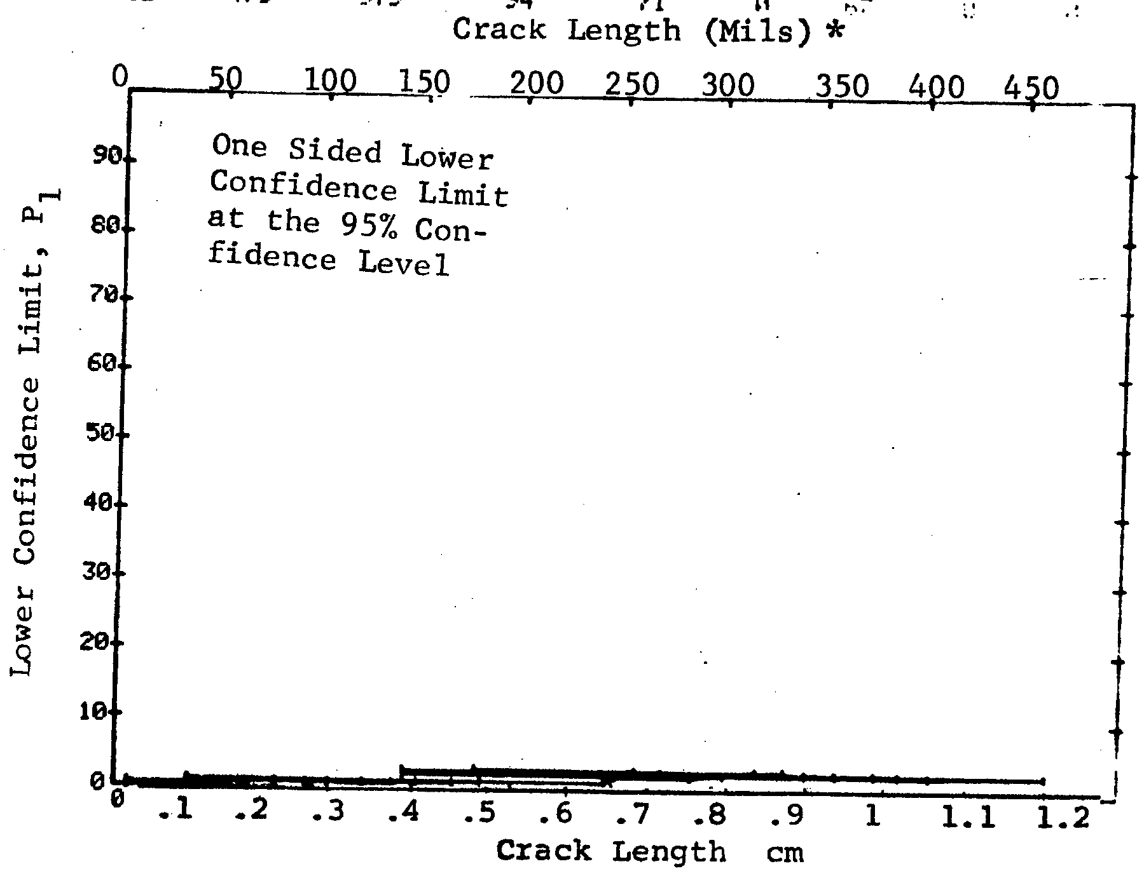

Figure D-4 (Continued)

(c) Overlapping Sixty Point Method of Data Cumulation

02-JUL-75 TEST 3 , X-RAY , MARTIN

RANGE	MIN LN*	MAX LN*	N	DET	50%	95%	0 MISS	[illegible]
1	0	0	0	0	0	0	0	[illegible]
2	0	0	0	0	0	0	0	[illegible]
3	0	0	0	0	0	0	0	[illegible]
4	0	0	0	0	0	0	0	[illegible]
5	7	30	59	1	1	0	0	[illegible]
6	20	38	60	0	0	0	0	0
7	30	45	60	1	1	0	0	0
8	38	50	60	2	2	0	0	0
9	45	58	60	1	1	0	0	0
10	51	61	60	1	1	0	0	0
11	58	64	60	1	1	0	0	0
12	61	67	60	1	1	0	0	0
13	64	70	60	1	1	0	0	0
14	67	74	60	1	1	0	0	0
15	70	77	60	1	1	0	0	0
16	74	80	60	1	1	0	0	0
17	77	83	60	1	1	0	0	0
18	80	87	60	1	1	0	0	0
19	83	95	60	1	1	0	0	0
20	87	102	60	1	1	0	0	0
21	95	115	60	1	1	0	0	0
22	103	129	60	1	1	0	0	0
23	117	136	60	1	1	0	0	0
24	129	158	60	1	1	0	0	0
25	138	248	60	1	1	0	0	[illegible]
26	162	258	60	2	2	0	0	0
27	249	279	60	5	7	3	0	0
28	258	310	60	4	6	2	0	0
29	279	326	60	1	1	0	0	0
30	310	340	60	3	4	1	[illegible]	[illegible]
31	326	466	60	3	4	1	[illegible]	[illegible]
32	342	500	60	2	2	0	0	[illegible]
				26	42	[illegible]	[illegible]	[illegible]

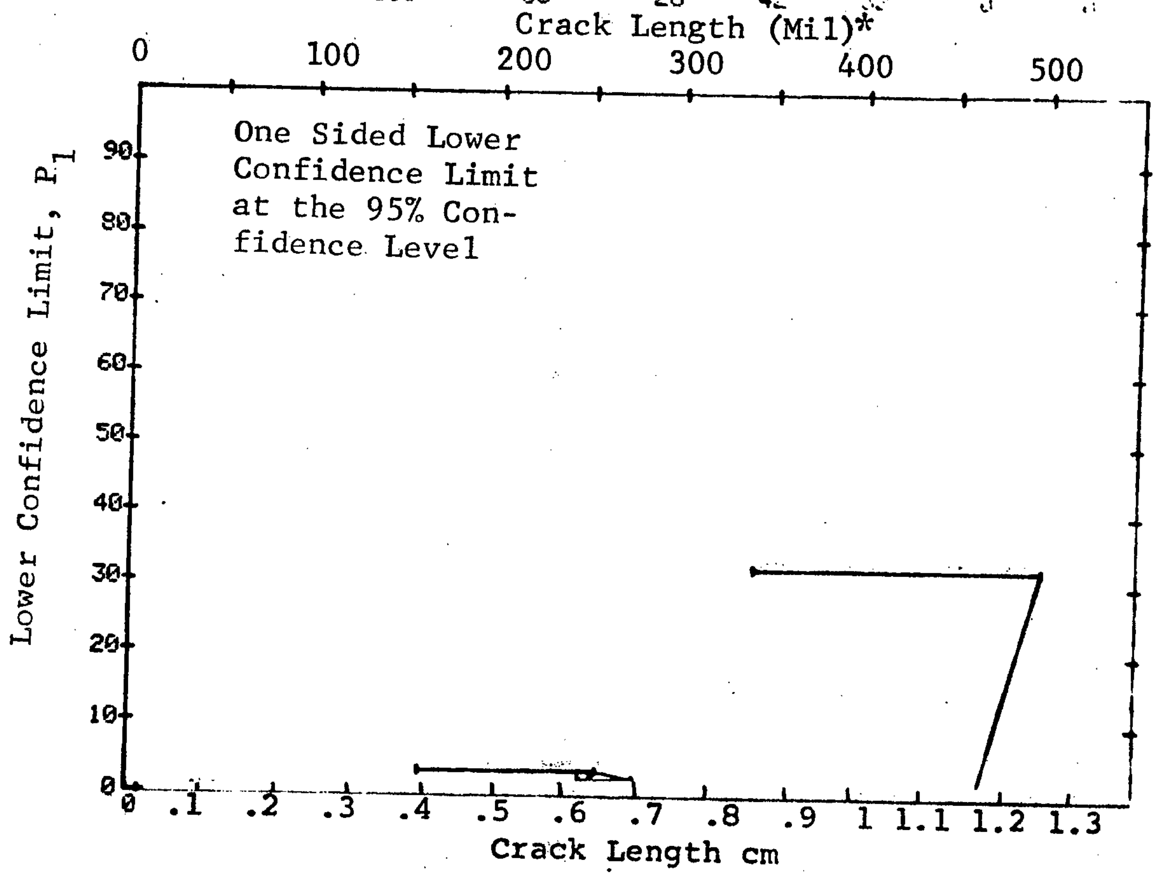

Figure D-4 (Concluded)

(a) Range Interval Method of Data Cumulation

03-JUL-75 ULTRASONIC BY LENGTH TEST 1, MARTIN 5

RANGE	MIN LN *	MAX LN *	N	DET	50%	95%	0 MISS	RANGE 1 MISS
1	7	21	39	12	29	18	0	0
2	25	36	48	35	71	60	0	[illegible]
3	38	52	72	58	79	71	0	0
4	54	67	120	101	83	77	0	0
5	68	82	132	119	89	84	0	0
6	83	97	87	76	86	79	92	100
7	98	108	39	33	83	71	0	0
8	115	126	33	27	79	67	0	0
9	129	141	42	37	86	76	61	74
10	146	153	18	16	85	68	0	0
11	158	171	9	7	71	45	0	0
12	182	185	9	9	92	71	0	0
13	0	0	0	0	0	0	0	0
14	0	0	0	0	0	0	0	0
15	0	0	0	0	0	0	0	0
16	241	247	12	11	86	66	0	0
17	248	262	51	51	98	94	0	0
18	268	275	9	9	92	71	0	0
19	279	290	15	14	89	72	0	0
20	295	306	15	15	95	81	14	31
21	310	322	27	25	90	78	34	[illegible]
22	323	336	29	28	94	84	17	[illegible]
23	338	347	18	16	85	68	0	[illegible]
24	362	362	3	3	79	36	0	[illegible]
25	381	381	3	3	79	36	0	0
26	393	393	3	3	79	36	0	[illegible]
27	408	408	3	3	79	36	0	0
28	0	0	0	0	0	0	0	0
29	0	0	0	0	0	0	[illegible]	[illegible]
30	0	0	0	0	0	0	0	[illegible]
31	459	466	6	6	89	60	[illegible]	[illegible]
32	475	979	90	83	91	85	[illegible]	[illegible]

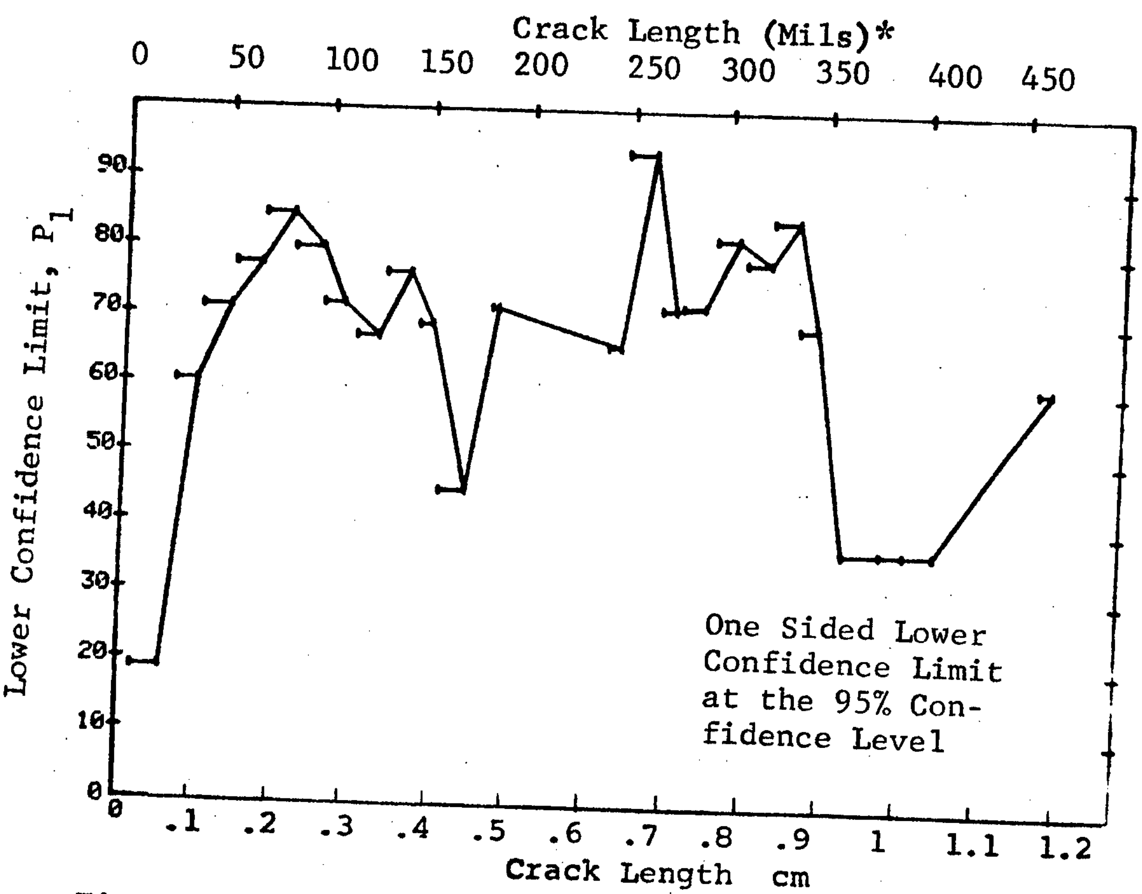

Figure D-5 Probability of Detection for 2219-T87 Al Using Ultrasonic Surface Waves. Etched Fatigue Cracks in Flat Plates. Lab. Env.

(b) Optimum Probability Method of Data Cumulation

03-JUL-75 ULTRASONIC BY LENGTH TEST 2, MARTIN (5).

RANGE	MIN LN *	MAX LN *	N	DET	50%	95%	MCD 0 MISS	MCD 1 MISS
1	7	21	39	12	0	18	0	0
2	25	36	48	35	0	60	0	[illegible]
3	38	52	72	58	0	71	0	0
4	38	67	192	159	0	77	0	0
5	68	82	132	119	0	84	0	0
6	68	97	219	195	0	84	0	0
7	68	108	258	228	0	84	0	0
8	68	126	291	255	0	83	0	0
9	68	141	333	292	0	84	0	0
10	68	153	351	308	0	84	0	0
11	68	171	360	315	0	84	0	0
12	68	185	369	324	0	84	0	0
13	0	0	0	0	0	0	0	0
14	0	0	0	0	0	0	0	0
15	0	0	0	0	0	0	0	0
16	68	247	381	335	0	84	0	0
17	248	262	51	51	0	94	0	0
18	248	275	60	60	0	95	0	0
19	248	290	75	74	0	93	0	0
20	248	306	90	89	0	94	0	0
21	248	322	117	114	0	93	0	0
22	248	336	146	142	0	93	0	0
23	182	347	185	178	0	93	0	0
24	182	362	188	181	0	93	0	0
25	182	381	191	184	0	93	0	[illegible]
26	182	393	194	187	0	93	0	0
27	182	408	197	190	0	93	0	[illegible]
28	0	0	0	0	0	0	0	0
29	0	0	0	0	0	0	[illegible]	[illegible]
30	0	0	0	0	0	0	0	[illegible]
31	182	466	203	196	0	93	0	[illegible]
32	182	979	293	279	0	[illegible]	[illegible]	[illegible]

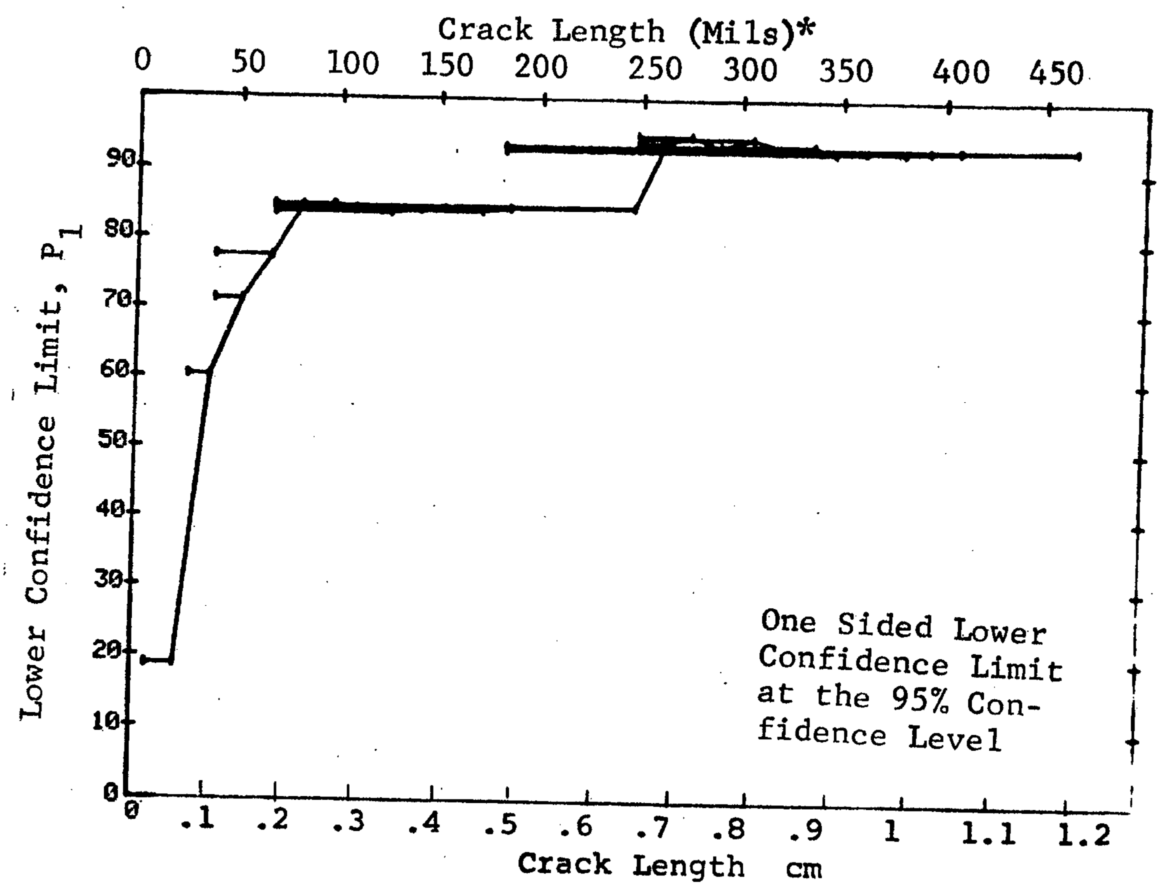

Figure D-5 (Continued)

(c) Overlapping Sixty Point Method of Data Cumulation

03-JUL-75 ULTRASONIC BY LENGTH TEST 3, MARTIN 5

RANGE	MIN LN	MAX LN	N	DET	50%	95%	0 MISS	1 MISS
1	0 *	0 *	0	0	0	0	0	0
2	0	0	0	0	0	0	0	[illegible]
3	0	0	0	0	0	0	0	0
4	7	20	32	8	23	13	0	[illegible]
5	7	30	60	29	47	37	0	[illegible]
6	20	40	60	42	69	58	0	0
7	30	45	60	43	70	60	0	0
8	40	51	60	48	79	69	0	0
9	45	58	60	47	77	67	0	0
10	51	61	60	49	80	71	0	0
11	58	64	60	57	93	87	16	29
12	61	67	60	53	87	79	69	82
13	64	70	60	51	83	75	94	100
14	67	73	60	53	87	79	69	82
15	70	77	60	50	82	73	0	0
16	73	80	60	53	87	79	69	82
17	77	83	60	59	97	92	0	1
18	80	87	60	55	90	83	43	56
19	83	95	60	53	87	79	69	82
20	87	102	60	51	83	75	94	100
21	95	115	60	47	77	67	0	0
22	102	129	60	51	83	75	94	100
23	115	136	60	53	87	79	69	[illegible]
24	129	158	60	53	87	79	[illegible]	[illegible]
25	136	248	60	54	88	81	56	[illegible]
26	158	258	60	57	93	87	16	[illegible]
27	248	279	60	60	98	95	0	0
28	258	310	60	59	97	92	0	[illegible]
29	279	326	60	57	93	[illegible]	[illegible]	[illegible]
30	310	340	60	56	92	85	[illegible]	[illegible]
31	326	466	60	57	93	87	[illegible]	[illegible]
32	342	500	60	56	92	85	[illegible]	[illegible]

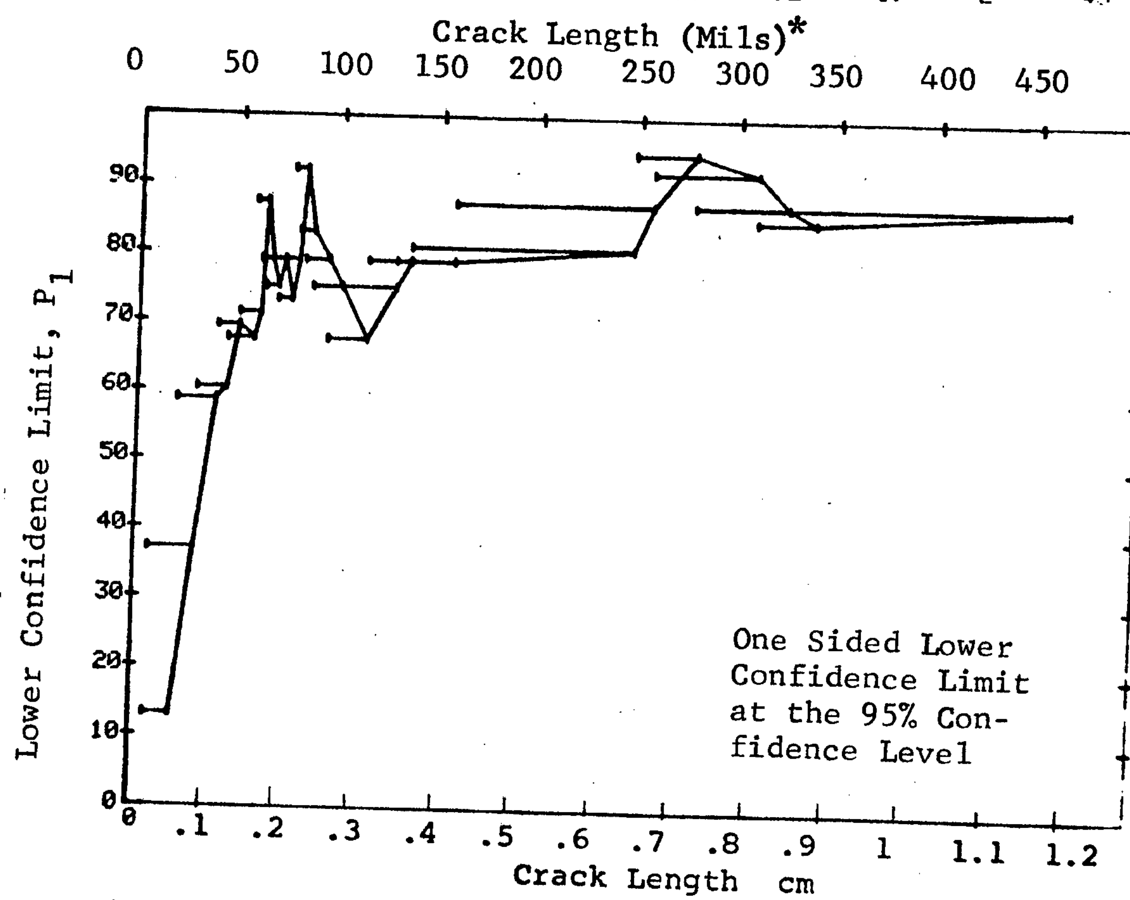

Figure D-5 (Concluded)

(a) Range Interval Method of Data Cumulation

02-JUL-75	PENETRANT			TEST 1 . PENET .			MARTIN 6	RANGE
RANGE	MIN LN	MAX LN	N	DET	50%	95%	0 MIS	[illegible]
1	7 *	21 *	39	10	24	14	0	[illegible]
2	25	36	48	31	63	51	0	[illegible]
3	38	52	72	57	78	69	0	[illegible]
4	54	67	119	98	81	75	0	[illegible]
5	68	82	132	113	85	79	0	[illegible]
6	83	97	87	79	90	84	55	67
7	98	108	39	39	98	92	0	[illegible]
8	115	126	33	27	79	67	0	[illegible]
9	129	141	42	41	96	89	4	19
10	146	153	18	16	85	68	0	0
11	158	171	9	9	92	71	0	0
12	182	185	9	9	92	71	0	0
13	0	0	0	0	0	0	0	0
14	0	0	0	0	0	0	0	0
15	0	0	0	0	0	0	0	0
16	241	247	12	11	86	66	0	0
17	248	262	51	51	98	94	0	0
18	268	275	9	9	92	71	0	0
19	279	290	15	15	95	81	14	31
20	295	306	15	15	95	81	14	31
21	310	322	27	25	90	78	34	49
22	323	336	30	30	97	90	0	16
23	338	347	18	16	85	68	0	[illegible]
24	362	362	3	3	79	36	0	[illegible]
25	381	381	3	3	79	36	0	[illegible]
26	393	393	3	2	50	13	0	[illegible]
27	408	408	3	3	79	36	0	0
28	0	0	0	0	0	0	0	0
29	0	0	0	0	0	0	[illegible]	[illegible]
30	0	0	0	0	0	0	0	[illegible]
31	459	466	6	6	89	60	0	[illegible]
32	475	979	91	91	99	96	[illegible]	0

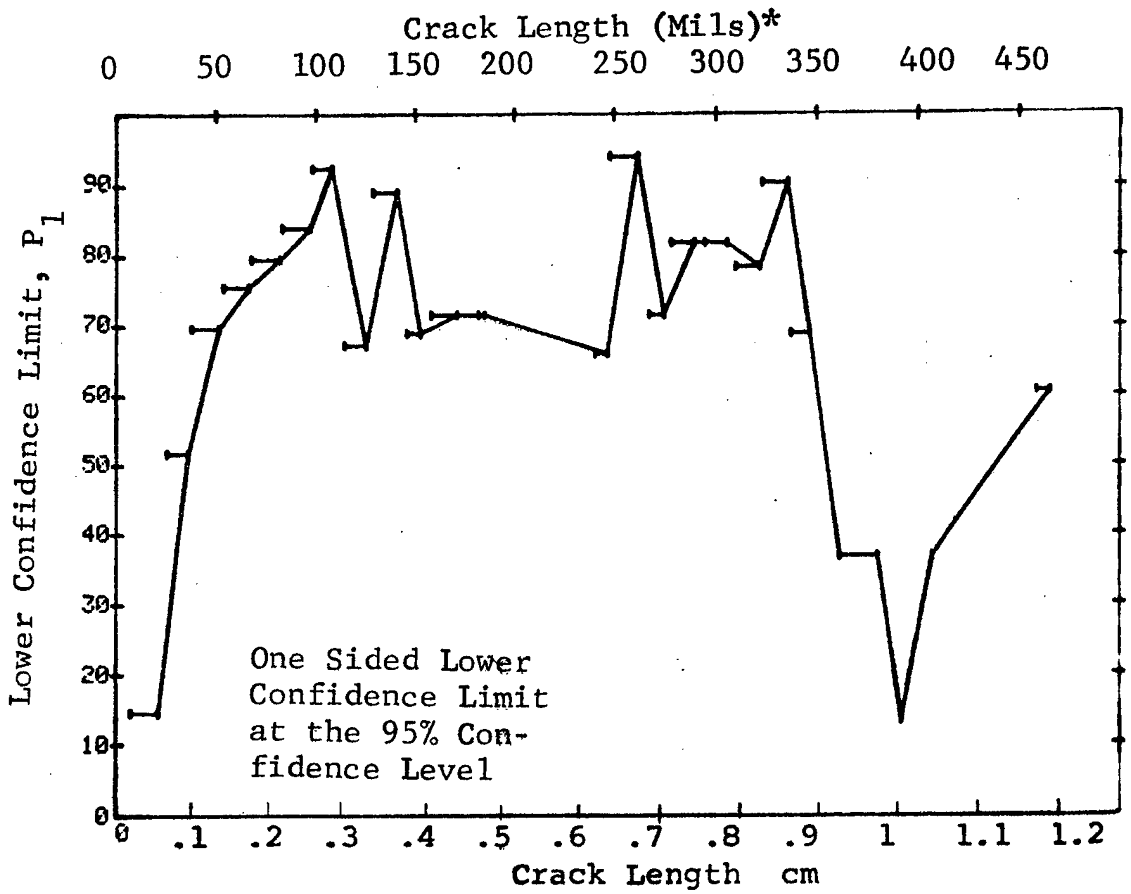

Figure D-6 Probability of Detection for 2219-T87 Al Using Liquid Penetrant. Etched Fatigue Cracks in Flat Plates. Lab. Env.

(b) Optimum Probability Method of Date Cumulation

02-JUL-75 PENETRANT TEST 2 , PENET , MAR[illegible] 6 MCD

RANGE	MIN LN	MAX LN	N	DET	50%	95%	0 MISS	1 MISS
1	7	21	39	10	0	14	0	0
2	25	36	48	31	0	51	0	[illegible]
3	38	52	72	57	0	69	0	[illegible]
4	38	67	191	155	0	75	0	[illegible]
5	54	82	251	211	0	79	0	[illegible]
6	83	97	87	79	0	84	55	67
7	98	109	39	39	0	92	0	[illegible]
8	83	126	159	145	0	86	0	0
9	129	141	42	41	0	89	4	19
10	83	153	219	202	0	88	0	0
11	129	171	69	66	0	89	7	20
12	129	185	78	75	0	90	0	11
13	0	0	0	0	0	0	0	0
14	0	0	0	0	0	0	0	0
15	0	0	0	0	0	0	0	0
16	129	247	90	86	0	90	0	13
17	248	262	51	51	0	94	0	0
18	248	275	60	60	0	95	0	0
19	248	290	75	75	0	96	0	0
20	248	306	90	90	0	96	0	0
21	158	322	147	144	0	94	0	0
22	248	336	147	145	0	95	0	0
23	158	347	195	190	0	94	0	[illegible]
24	158	362	198	193	0	94	0	[illegible]
25	158	381	201	196	0	94	0	0
26	158	393	204	198	0	94	0	[illegible]
27	158	408	207	201	0	94	0	0
28	0	0	0	0	0	0	0	0
29	0	0	0	0	0	0	[illegible]	[illegible]
30	0	0	0	0	0	0	[illegible]	[illegible]
31	158	466	213	207	0	94	0	0
32	403	979	199	199	0	97	[illegible]	[illegible]

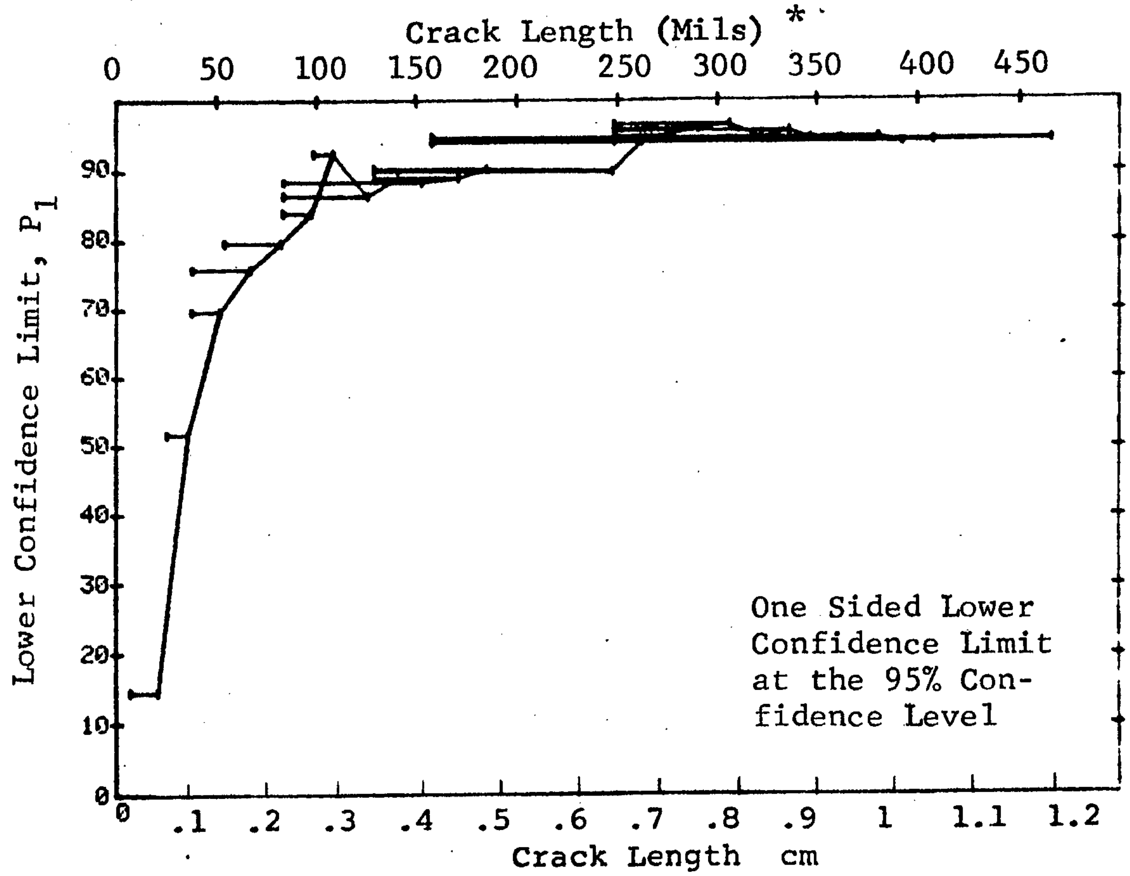

Figure D-6 (Continued)

(c) Overlapping Sixty Point Method of Data Cumulation

02-JUL-75 TEST 3 , PENET . MNFTIH(6)

RANGE	MIN LN *	MAX LN *	N	DET	50%	95%	0 MI[illegible]	1 [illegible]
1	0	0	0	0	0	0	0	[illegible]
2	0	0	0	0	0	0	0	[illegible]
3	0	0	0	0	0	0	0	[illegible]
4	7	20	32	7	20	10	0	[illegible]
5	7	30	60	24	39	29	0	[illegible]
6	20	40	60	38	62	51	0	[illegible]
7	30	45	60	42	69	58	0	[illegible]
8	40	51	60	47	77	67	0	[illegible]
9	45	58	60	48	79	69	0	[illegible]
10	51	61	60	48	79	69	0	[illegible]
11	58	64	60	53	87	79	69	[illegible]
12	62	67	60	50	82	73	0	0
13	64	70	60	48	79	69	0	0
14	67	73	60	48	79	69	0	0
15	70	77	60	48	79	69	0	0
16	74	80	60	53	87	79	69	82
17	77	83	60	58	95	89	1	16
18	80	87	60	57	93	87	16	[illegible]
19	84	95	60	56	92	85	29	47
20	90	102	60	55	90	83	43	56
21	96	115	60	53	87	79	69	82
22	103	129	60	54	88	81	56	69
23	117	136	60	56	92	85	29	43
24	129	158	60	57	93	87	16	[illegible]
25	138	248	60	57	93	87	16	29
26	162	258	60	59	97	92	0	1
27	249	279	60	60	98	95	0	0
28	258	310	60	60	98	95	0	0
29	279	326	60	58	95	[illegible]	[illegible]	[illegible]
30	310	340	60	56	92	85	29	43
31	326	466	60	57	93	87	16	[illegible]
32	342	500	60	59	97	92	0	1

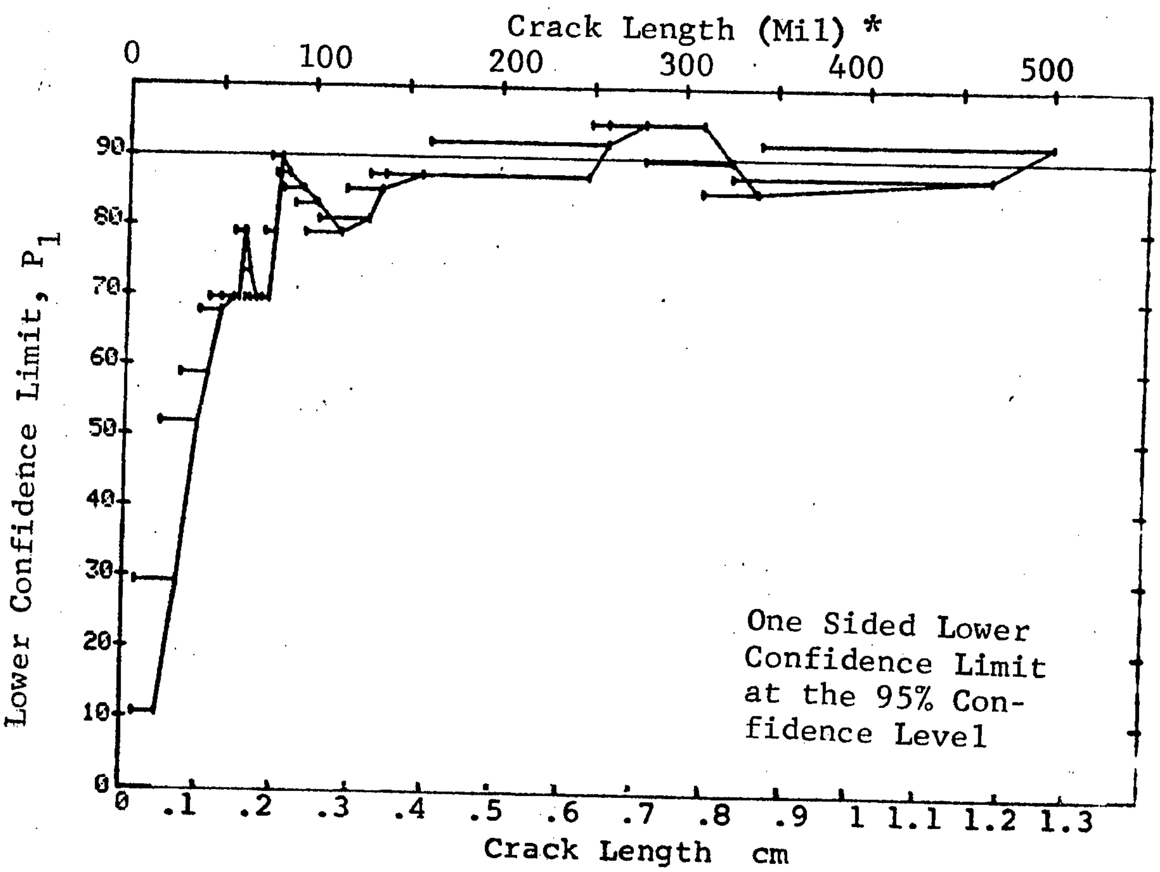

Figure D-6 (Concluded)

(a) Range Interval Method of Data Cumulation

22-JUL-75		EDDY CURRENT SEQ II		TEST 1		MARTIN (7)		
RANGE	MIN LN	MAX LN	N	DET	50%	95%	0 MISS	1 MISS
1	7 *	21*	39	6	14	6	0	0
2	25	36	48	6	11	5	0	0
3	38	52	72	17	23	15	0	0
4	54	67	121	62	50	43	0	0
5	68	82	131	80	60	53	0	0
6	83	97	87	69	78	70	0	0
7	98	108	39	31	77	66	0	0
8	115	126	34	30	86	75	55	69
9	129	141	42	38	88	79	47	61
10	146	153	18	16	85	68	0	0
11	158	171	9	9	92	71	0	0
12	182	185	9	7	71	45	0	0
13	0	0	0	0	0	0	0	0
14	0	0	0	0	0	0	0	0
15	0	0	0	0	0	0	0	0
16	241	247	12	11	86	66	0	0
17	248	262	51	47	90	82	38	52
18	268	275	9	9	92	71	0	0
19	279	290	15	14	89	72	0	0
20	295	306	15	13	82	63	0	0
21	310	322	27	26	93	83	13	34
22	323	336	30	29	94	85	15	71
23	339	347	18	15	79	62	0	0
24	362	362	3	3	79	36	0	0
25	381	381	3	3	79	36	0	0
26	393	393	3	3	79	36	0	0
27	408	408	3	2	50	13	0	0
28	0	0	0	0	0	0	0	0
29	0	0	0	0	0	0	0	0
30	0	0	0	0	0	0	0	0
31	459	466	6	6	89	60	0	0
32	475	979	90	86	94	90	0	13

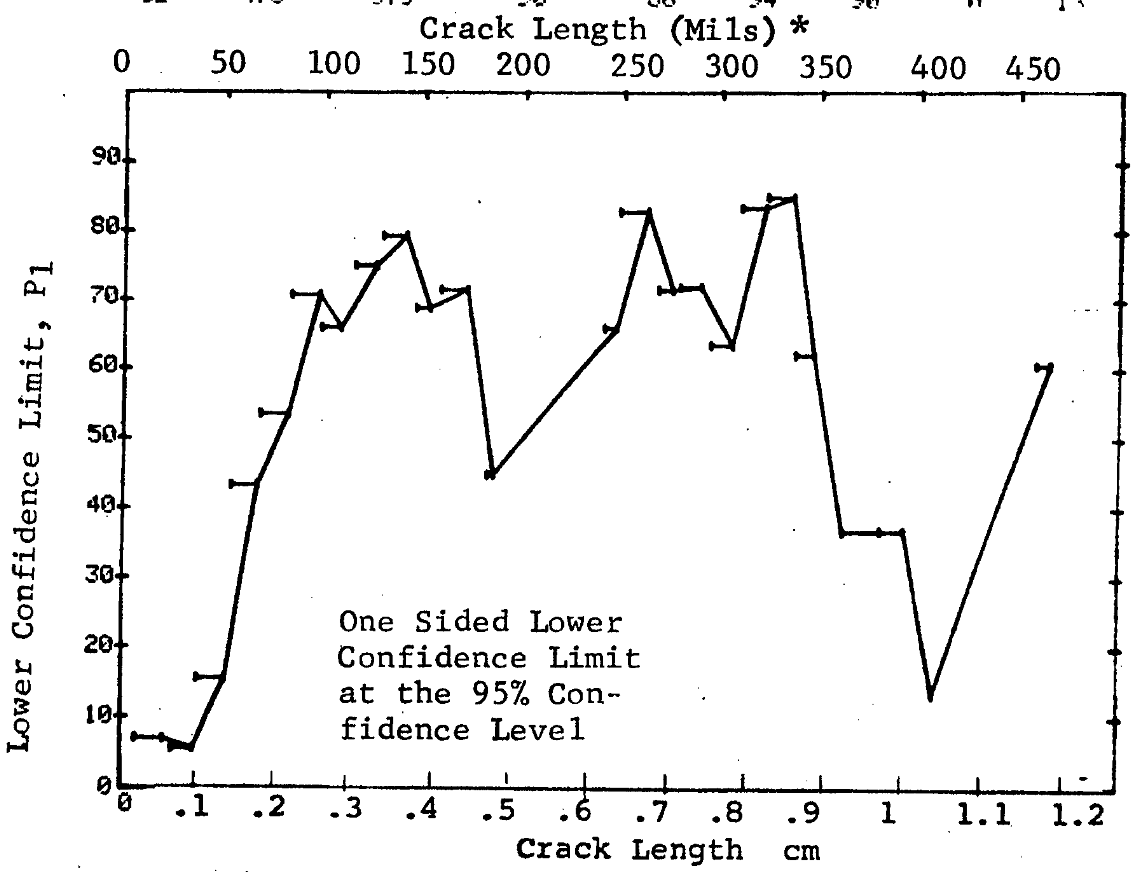

Figure D-7 Probability of Detection for 2219-T87 Al Using Eddy Current. Etched Fatigue Cracks in Flat Plates. Lab. Env.

(b) Optimum Probability Method of Data Cumulation

22-JUL-75 EDDY CURRENT SEQ II TEST 2 MARTIN (7)

RANGE	MIN LN *	MAX LN *	N	DET	50%	95%	0 MISS	1 MISS
1	7	21	39	6	0	6	0	[illegible]
2	[illegible]	36	57	12	0	8	0	[illegible]
3	38	52	72	17	0	15	0	[illegible]
4	54	67	121	52	0	43	0	[illegible]
5	68	82	131	80	0	53	0	[illegible]
6	83	97	87	69	0	70	0	[illegible]
7	83	108	126	100	0	72	0	[illegible]
8	83	126	160	130	0	75	0	[illegible]
9	115	141	76	68	0	81	0	[illegible]
10	115	153	94	84	0	82	65	[illegible]
11	115	171	103	93	0	84	73	[illegible]
12	115	185	112	100	0	83	0	[illegible]
13	0	0	0	0	0	0	0	[illegible]
14	0	0	0	0	0	0	0	[illegible]
15	0	0	0	0	0	0	0	[illegible]
16	115	247	124	111	0	83	0	[illegible]
17	115	262	175	158	0	85	0	[illegible]
18	129	275	150	137	0	86	0	[illegible]
19	129	290	165	151	0	87	0	[illegible]
20	129	306	180	164	0	86	0	[illegible]
21	241	322	129	120	0	88	0	[illegible]
22	241	336	159	149	0	89	0	[illegible]
23	241	347	177	164	0	88	0	[illegible]
24	241	362	180	167	0	88	0	[illegible]
25	241	381	183	170	0	88	0	[illegible]
26	241	393	186	173	0	89	0	[illegible]
27	241	408	189	175	0	88	0	[illegible]
28	0	0	0	0	0	0	0	[illegible]
29	0	0	0	0	0	0	0	[illegible]
30	0	0	0	0	0	0	0	[illegible]
31	241	466	195	181	0	89	0	[illegible]
32	310	979	183	173	0	90	0	[illegible]

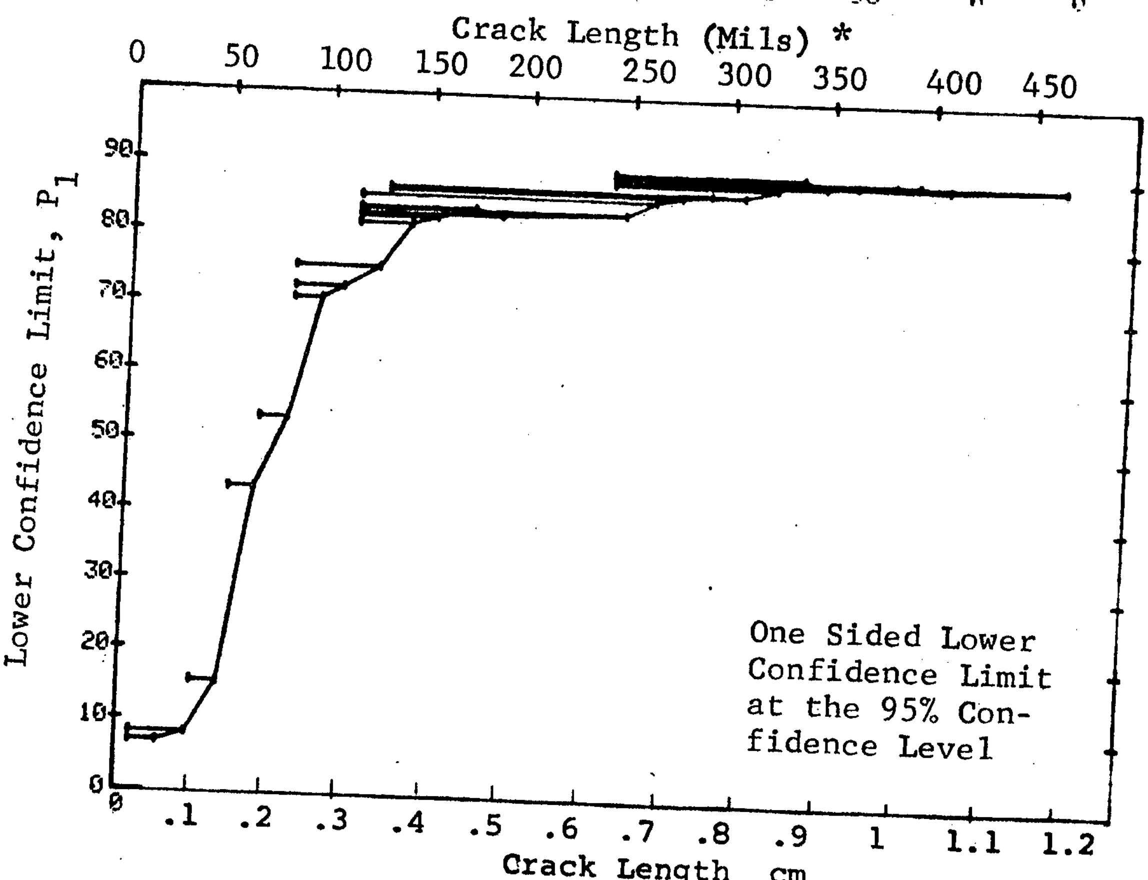

Figure D-7 (Continued)

(c) Overlapping Sixty Point Method of Data Cumulation

22-JUL-75 EDDY CURRENT SEQ II TEST 3 MARTIN (7)

RANGE	MIN LN *	MAX LN *	N	DET	50%	95%	0 MISS	1 MISS
1	0	0	0	0	0	0	0	0
2	0	0	0	0	0	0	0	0
3	0	0	0	0	0	0	0	0
4	7	21	34	5	13	5	0	0
5	8	31	60	9	14	8	0	0
6	21	40	60	9	14	8	0	0
7	31	45	60	8	12	6	0	0
8	40	52	60	14	22	14	0	0
9	45	58	60	19	30	21	0	0
10	52	61	60	26	42	32	0	0
11	58	64	60	38	62	51	0	0
12	62	67	60	35	57	46	0	0
13	64	70	60	27	44	33	0	0
14	67	74	60	30	49	38	0	0
15	70	77	60	32	52	41	0	0
16	74	80	60	37	60	50	0	0
17	77	84	60	49	80	71	0	0
18	80	90	60	50	82	73	0	0
19	84	96	60	46	75	65	0	0
20	90	103	60	45	74	64	0	0
21	96	115	60	46	75	65	0	0
22	103	129	60	52	85	77	83	[illegible]
23	117	136	60	55	90	83	43	[illegible]
24	129	158	60	55	90	83	43	[illegible]
25	138	248	60	54	88	81	56	[illegible]
26	162	258	60	54	88	81	56	[illegible]
27	249	279	60	57	93	87	16	29
28	258	310	60	56	92	85	29	43
29	279	326	60	56	92	85	[illegible]	43
30	310	340	60	56	92	85	29	43
31	326	466	60	55	90	83	43	56
32	342	500	60	57	93	87	16	29

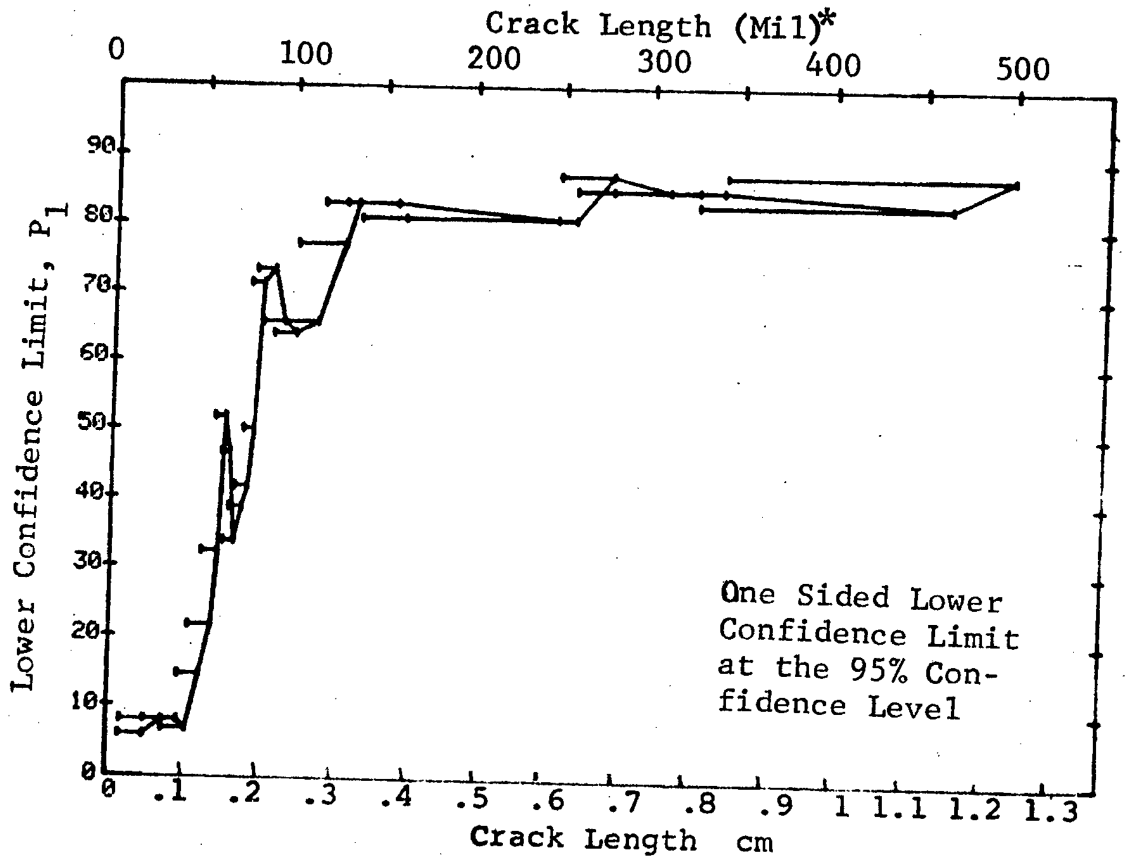

Figure D-7 (Concluded)

(a) Range Interval Method of Data Cumulation

02-JUL-75 RANGE	RADIOGRAPHY MIN LN*	MAX LN*	N	TEST 1 DET	X-RAY 50%	95%	MARTIN 8 0 MISS	1 MISS
1	7	21	39	1	1	0	0	[illegible]
2	23	36	49	8	15	8	0	[illegible]
3	38	52	72	18	24	16	0	[illegible]
4	54	67	120	41	33	27	0	[illegible]
5	68	82	131	60	45	39	0	[illegible]
6	83	97	87	54	61	52	0	[illegible]
7	98	108	39	15	37	25	0	0
8	115	126	33	7	20	10	0	[illegible]
9	129	141	42	11	25	15	0	0
10	146	153	18	11	58	39	0	0
11	158	171	9	6	60	34	0	0
12	182	185	9	3	28	9	0	0
13	0	0	0	0	0	0	0	0
14	0	0	0	0	0	0	0	0
15	0	0	0	0	0	0	0	0
16	241	247	12	12	94	77	0	0
17	248	262	51	50	96	91	17	34
18	268	275	9	9	92	71	0	10
19	279	290	15	13	82	63	0	0
20	295	306	15	12	76	56	0	0
21	310	322	27	13	46	31	0	0
22	323	336	30	23	74	60	0	0
23	338	347	18	15	79	62	0	0
24	362	362	3	1	20	1	0	[illegible]
25	381	381	3	2	50	13	0	[illegible]
26	393	393	3	3	79	36	0	0
27	408	408	3	3	79	36	0	[illegible]
28	0	0	0	0	0	0	0	0
29	0	0	0	0	0	0	0	0
30	0	0	0	0	0	0	[illegible]	[illegible]
31	459	466	6	6	89	60	0	[illegible]
32	475	979	90	88	97	93	[illegible]	[illegible]

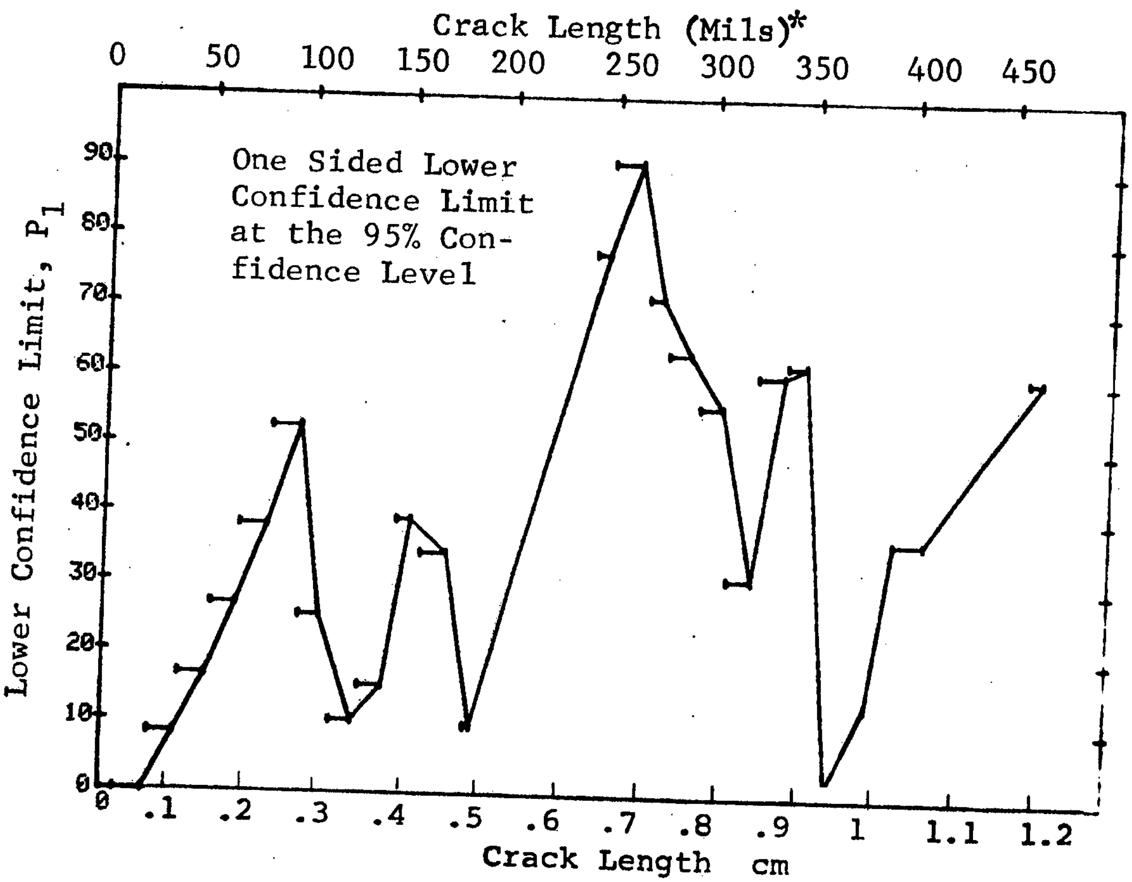

Figure D-8 Probability of Detection for 2219-T87 Al Using X-ray. Etched Fatigue Cracks in Flat Plates. Lab. Env.

(b) Optimum Probability Method of Data Cumulation

02-JUL-75 TEST 2 , X-RAY , MARTIN (8)

RANGE	MIN LN	MAX LN	N	DET	50%	95%	0 MISS	1 MISS
1	7 *	21*	39	1	0	0	0	[illegible]
2	23	36	49	8	0	8	0	[illegible]
3	38	52	72	18	0	16	0	[illegible]
4	54	67	120	41	0	27	0	[illegible]
5	68	82	131	60	0	38	0	[illegible]
6	83	97	87	54	0	52	0	0
7	83	108	126	69	0	47	0	0
8	68	126	290	136	0	41	0	0
9	68	141	332	147	0	39	0	0
10	68	153	350	158	0	40	0	0
11	146	171	27	17	0	45	0	0
12	68	185	368	167	0	41	0	0
13	0	0	0	0	0	0	0	0
14	0	0	0	0	0	0	0	0
15	0	0	0	0	0	0	0	0
16	241	247	12	12	0	77	0	0
17	241	262	63	62	0	92	0	0
18	241	275	72	71	0	93	0	0
19	241	290	87	84	0	91	0	0
20	241	306	102	96	0	88	0	0
21	241	322	129	109	0	78	0	0
22	241	336	159	132	0	77	0	0
23	241	347	177	147	0	77	0	0
24	241	362	180	148	0	76	0	[illegible]
25	241	381	183	150	0	76	0	[illegible]
26	241	393	186	153	0	77	0	[illegible]
27	241	408	189	156	0	77	0	0
28	0	0	0	0	0	0	0	0
29	0	0	0	0	0	0	[illegible]	[illegible]
30	0	0	0	0	0	0	0	[illegible]
31	241	466	195	162	0	78	0	[illegible]
32	393	979	102	100	0	[illegible]	[illegible]	[illegible]

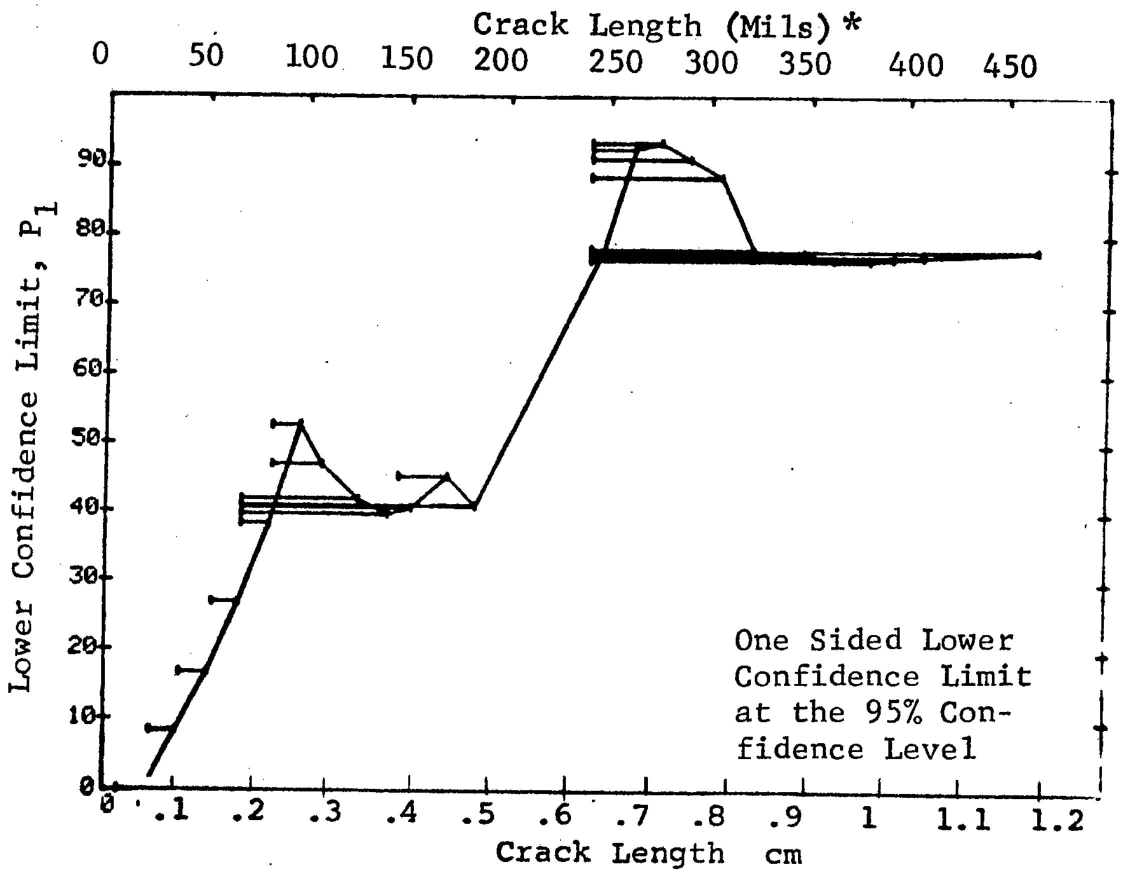

Figure D-8 (Continued)

(c) Overlapping Sixty Point Method of Data Cumulation

02-JUL-75

TEST 3 , X-RAY , MARTIN (8)

RANGE	MIN LN	MAX LN	N	DET	50%	95%	0 MISS	1 MISS
1	0*	0*	0	0	0	0	0	[illegible]
2	0	0	0	0	0	0	0	[illegible]
3	0	0	0	0	0	0	0	0
4	7	20	32	0	0	0	0	0
5	7	30	60	7	11	5	0	0
6	20	40	60	10	16	9	0	0
7	30	45	60	8	12	6	0	0
8	40	50	60	13	20	13	0	0
9	45	58	60	16	25	17	0	0
10	51	61	60	21	34	24	0	0
11	58	64	60	26	42	32	0	0
12	61	67	60	19	30	21	0	0
13	64	70	60	23	37	27	0	0
14	67	73	60	28	45	35	0	0
15	70	77	60	18	29	20	0	0
16	73	80	60	25	40	30	0	0
17	77	83	60	41	67	57	0	0
18	80	87	60	45	74	64	0	0
19	83	95	60	37	60	50	0	0
20	87	102	60	27	44	33	0	0
21	95	115	60	21	34	24	0	0
22	102	129	60	18	29	20	0	0
23	115	136	60	16	25	17	0	0
24	129	158	60	21	34	24	0	[illegible]
25	136	248	60	36	59	48	0	[illegible]
26	158	258	60	51	83	75	0	0
27	248	279	60	59	97	92	94	100
28	258	310	60	55	90	83	0	1
29	279	326	60	40	65	55	43	56
30	310	340	60	36	59	48	[illegible]	[illegible]
31	326	466	60	48	79	69	0	[illegible]
32	340	500	60	55	90	83	43	56

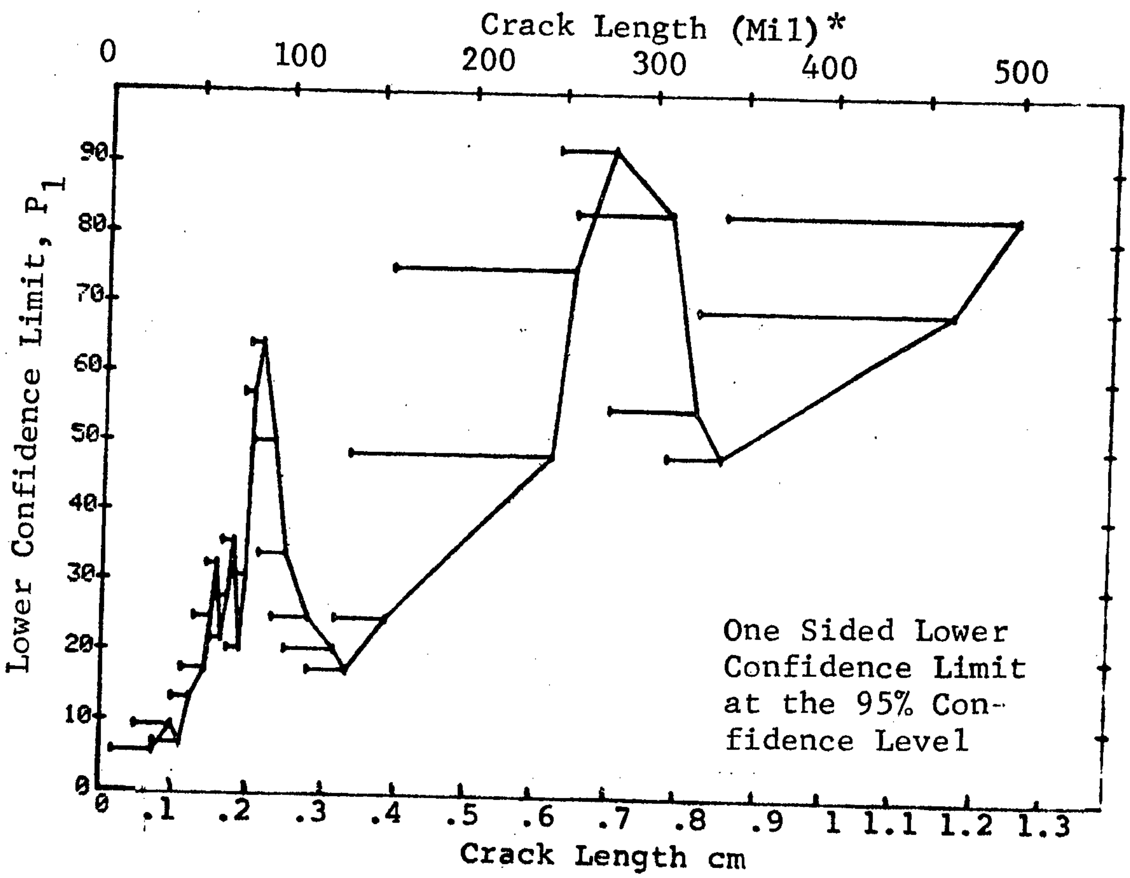

Figure D-8 (Concluded)

(a) Range Interval Method of Data Cumulation

03-JUL-75 ULTRASONIC TEST 1 , ROCKWELL SC, "O" (9)

RANGE	MIN LN	MAX LN	N	DET	50%	95%	0 MISS	1 MISS
1	7*	22*	13	4	27	11	0	0
2	25	36	49	11	58	39	0	0
3	38	52	23	19	79	64	0	0
4	54	67	46	32	68	56	0	0
5	68	82	53	38	70	59	0	0
6	83	97	39	27	67	54	0	0
7	98	111	17	13	73	53	0	0
8	115	126	17	13	73	53	0	0
9	129	141	19	16	81	64	0	0
10	143	157	15	13	82	63	0	0
11	158	171	3	3	79	36	0	0
12	182	185	3	2	50	13	0	0
13	190	197	2	1	29	2	0	0
14	0	0	0	0	0	0	0	0
15	0	0	0	0	0	0	0	0
16	241	247	4	4	84	47	0	0
17	248	262	17	17	96	83	12	29
18	268	275	3	3	79	36	0	0
19	279	290	7	7	90	65	0	0
20	295	306	6	5	73	41	0	0
21	310	322	10	10	93	74	0	0
22	323	336	12	12	94	77	17	34
23	338	352	11	10	85	63	0	0
24	356	362	4	4	84	47	0	0
25	370	381	5	5	87	54	0	0
26	384	393	2	2	70	22	0	0
27	408	408	1	0	0	0	0	0
28	426	426	1	1	50	5	0	0
29	442	442	1	1	50	5	0	0
30	444	444	1	1	50	5	0	0
31	458	472	8	8	91	68	0	0
32	474	979	59	57	95	89	2	17

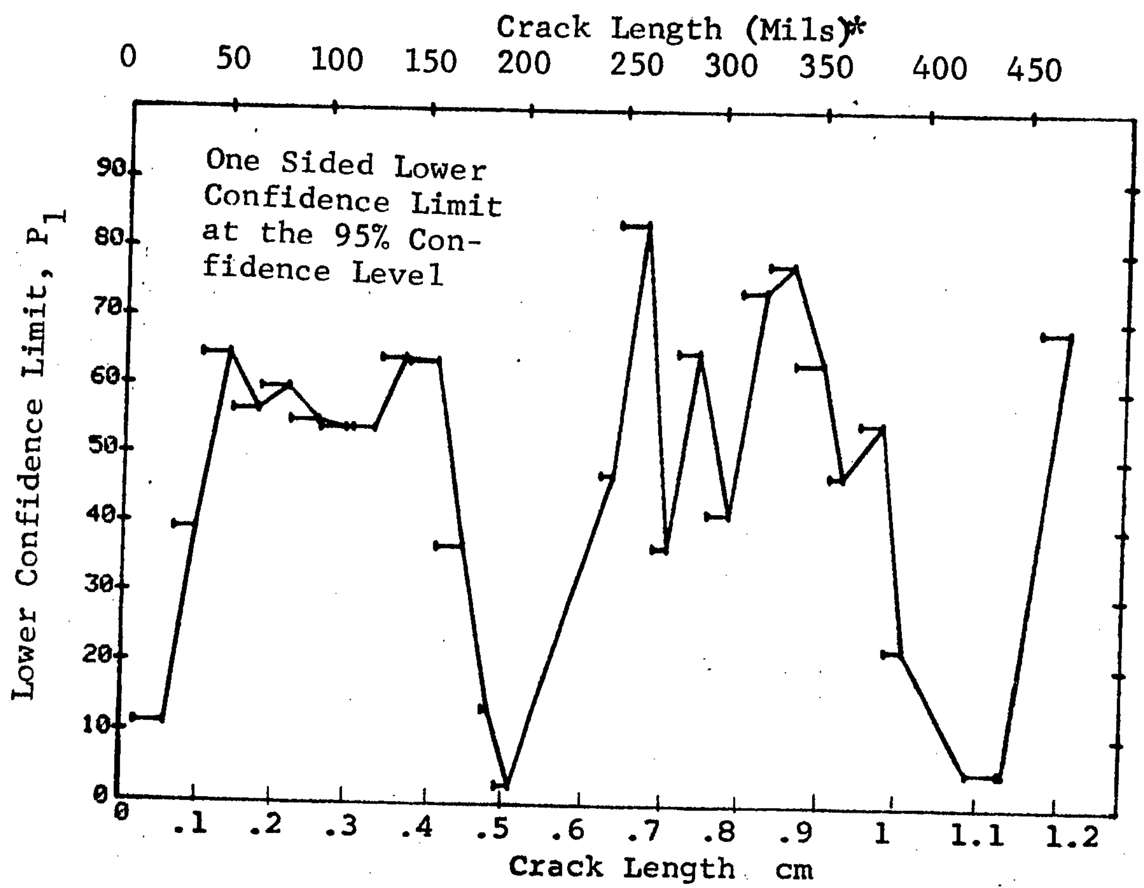

Figure D-9 Probability of Detection for 2219-T87 Al Using Ultrasonic Shear Wave. Etched-Fatigue Cracks in Flat Plates Measured by Operator O. Lab. Env.

(b) Optimum Probability Method of Data Cumulation

03-JUL-75 ULTRASONIC TEST 2 ROCKWELL SC, 'U' (9)

RANGE	MIN LN	MAX LN	N	DET	50%	95%	0 MISS	1 MISS
1	7*	22 *	13	4	0	11	0	0
2	25	36	18	11	0	39	0	0
3	38	52	23	19	0	64	0	0
4	38	67	69	51	0	63	0	0
5	38	82	122	89	0	65	0	0
6	38	97	161	116	0	65	0	0
7	38	111	178	129	0	66	0	0
8	38	126	195	142	0	67	0	0
9	38	141	214	158	0	68	0	0
10	129	157	34	29	0	71	0	0
11	129	171	37	32	0	73	0	0
12	129	185	40	34	0	72	0	0
13	98	197	76	61	0	71	0	0
14	0	0	0	0	0	0	0	0
15	0	0	0	0	0	0	0	0
16	129	247	46	39	0	73	0	0
17	241	262	21	21	0	86	8	25
18	241	275	24	24	0	88	5	22
19	241	290	31	31	0	90	0	15
20	241	306	37	36	0	87	9	24
21	241	322	47	46	0	90	0	14
22	241	336	59	58	0	92	0	2
23	241	352	70	68	0	91	0	6
24	241	362	74	72	0	91	0	2
25	241	381	79	77	0	92	0	0
26	241	393	81	79	0	92	0	0
27	241	408	82	79	0	90	0	7
28	241	426	83	80	0	90	0	6
29	241	442	84	81	0	91	0	5
30	241	444	85	82	0	91	0	4
31	241	472	93	90	0	91	0	0
32	241	979	152	147	0	93 *	0	0

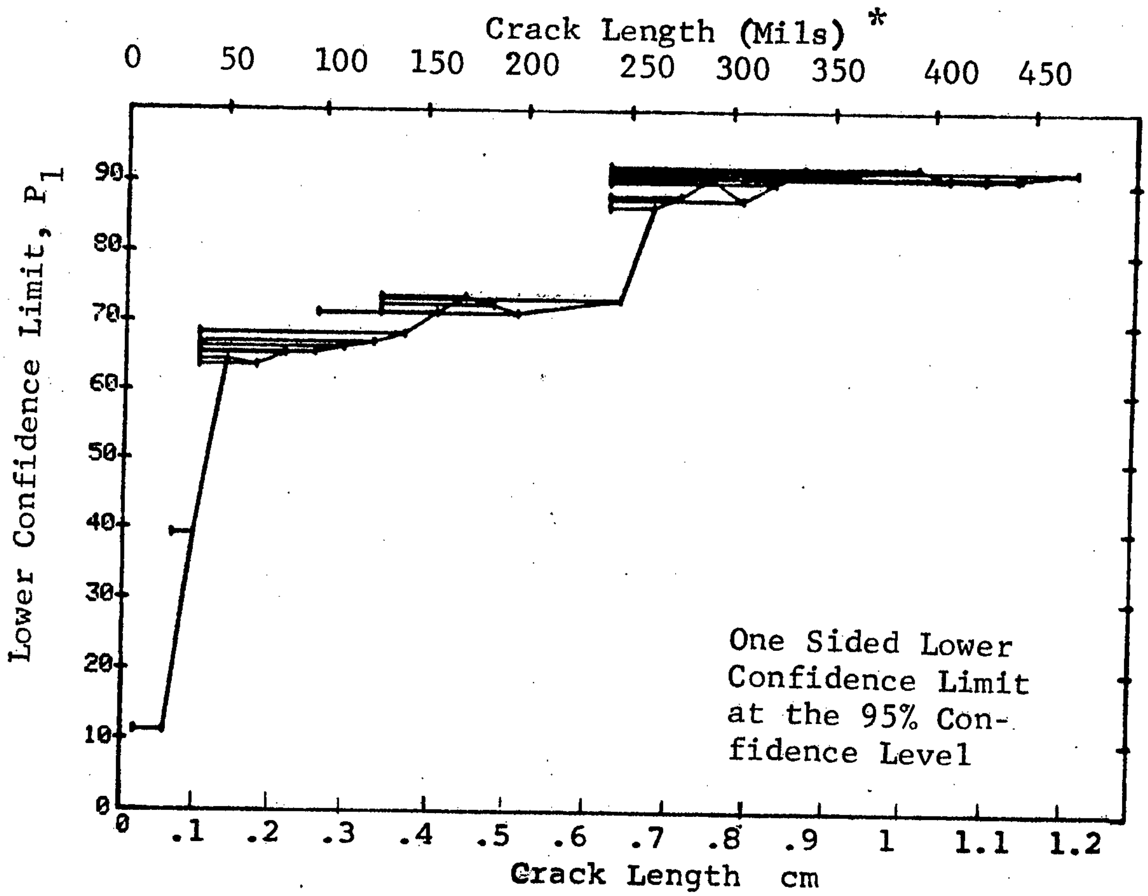

Figure D-9 (Continued)

(c) Overlapping Sixty Point Method of Data Cumulation

03-JUL-75 ULTRASONIC TEST 3 , ROCKWELL SG. 'O' (9)

RANGE	MIN LN *	MAX LN *	N	OPT	50%	95%	0 MISS	1 MISS
1	0	0	0	0	0	0	0	0
2	0	0	0	0	0	0	0	0
3	0	0	0	0	0	0	0	0
4	0	0	0	0	0	0	0	0
5	0	0	0	0	0	0	0	0
6	0	0	0	0	0	0	0	0
7	0	0	0	0	0	0	0	0
8	0	0	0	0	0	0	0	0
9	0	0	0	0	0	0	0	0
10	0	0	0	0	0	0	0	0
11	0	0	0	0	0	0	0	0
12	0	0	0	0	0	0	0	0
13	0	0	0	0	0	0	0	0
14	0	0	0	0	0	0	0	0
15	0	0	0	0	0	0	0	0
16	0	0	0	0	0	0	0	0
17	0	0	0	0	0	0	0	0
18	0	0	0	0	0	0	0	0
19	0	0	0	0	0	0	0	0
20	0	0	0	0	0	0	0	0
21	7	49	52	33	62	51	0	0
22	31	63	60	44	72	62	0	0
23	51	70	60	40	65	55	0	0
24	64	79	60	44	72	62	0	0
25	70	87	60	44	72	62	0	0
26	79	105	60	40	65	55	0	0
27	88	131	60	45	74	64	0	0
28	105	162	60	50	82	73	0	0
29	132	275	60	54	88	81	56	69
30	171	330	60	57	93	87	16	29
31	279	442	60	57	93	87	16	29
32	331	500	60	56	92	85	29	43

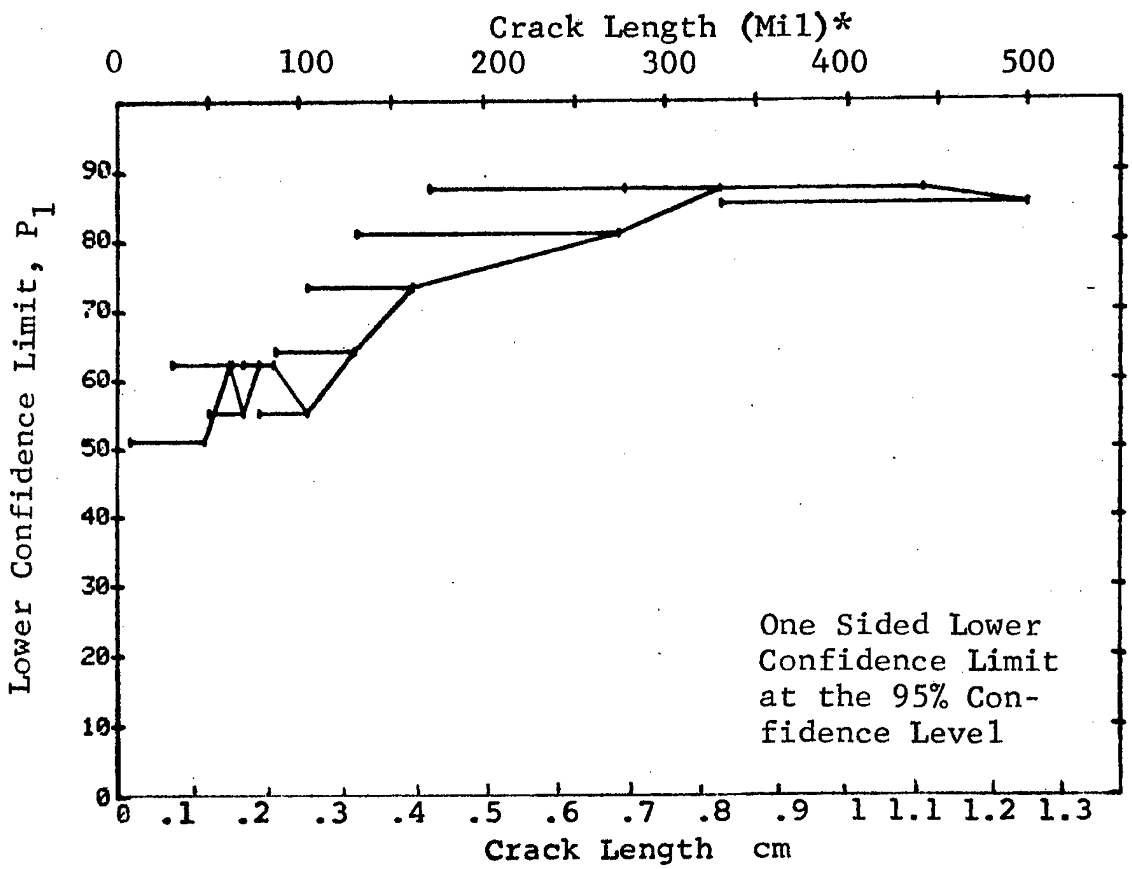

Figure D-9 (Concluded)

(a) Range Interval Method of Data Cumulation

03-JUL-75 ULTRASONIC TEST 1 , ROCKWELL [illegible] , "P" (10)

RANGE	MIN LN *	MAX LN *	N	DET	50%	95%	0 MISS	1 MISS
1	7	22	13	4	27	11	0	0
2	25	36	18	15	79	62	0	0
3	38	52	23	19	79	64	0	0
4	54	67	46	39	83	73	0	0
5	68	82	53	51	94	88	8	23
6	83	97	39	39	98	92	0	7
7	98	111	17	16	90	75	29	44
8	115	126	17	17	96	83	12	29
9	129	141	19	19	96	85	10	27
10	143	157	15	15	95	81	14	31
11	158	171	3	3	79	36	0	0
12	182	185	3	3	79	36	0	0
13	190	197	2	2	70	22	0	0
14	207	207	1	1	50	5	0	0
15	0	0	0	0	0	0	0	0
16	241	247	4	4	84	47	0	0
17	248	262	17	17	96	83	12	29
18	268	275	3	3	79	36	0	0
19	279	290	6	6	89	60	0	0
20	295	306	6	6	89	60	0	0
21	310	322	10	10	93	74	0	0
22	323	336	12	12	94	77	17	34
23	338	352	11	11	93	76	18	35
24	356	362	4	4	84	47	0	0
25	370	381	5	5	87	54	0	0
26	384	393	2	2	70	22	0	0
27	408	408	1	1	50	5	0	0
28	426	426	1	1	50	5	0	0
29	442	442	1	1	50	5	0	0
30	444	450	2	2	70	22	0	0
31	458	472	7	7	90	65	0	0
32	474	979	59	59	98	95	0	0

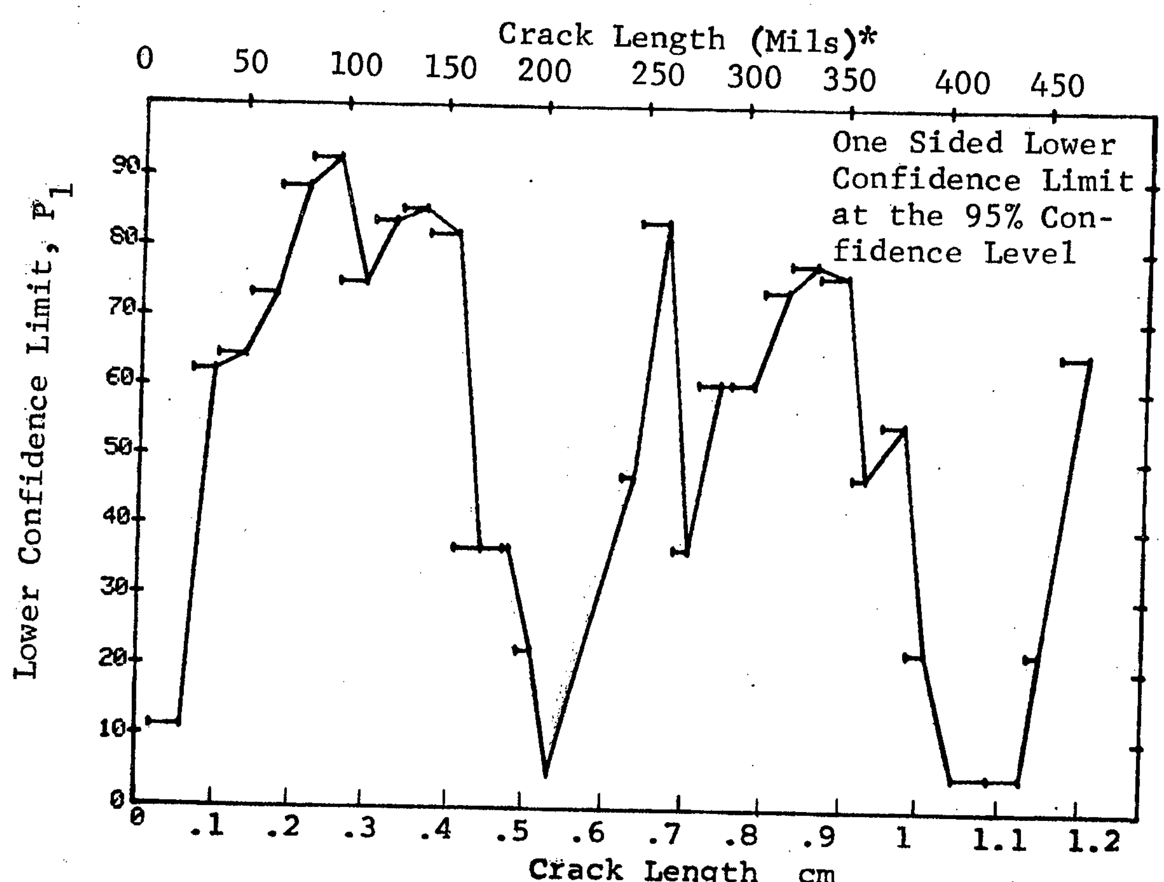

Figure D-10 Probability of Detection for 2219-T87 Al Using Ultrasonic Shear Wave. Etched-Fatigue Cracks in Flat Plates Measured by Operator P. Lab. Env.

(b) Optimum Probability Method of Data Cumulation

03-JUL-75 ULTRASONIC TEST 2 , ROCKWELL ≈C , R (10)

RANGE	MIN LN	MAX LN	N	DET	50%	95%	0 MISS	1 MISS
1	7 *	22 *	13	4	0	11	0	0
2	25	38	18	15	0	62	0	0
3	25	52	41	34	0	70	0	0
4	25	67	87	73	0	75	0	0
5	68	82	53	51	0	88	8	23
6	68	97	92	90	0	93	0	0
7	68	111	109	106	0	93	0	0
8	68	126	126	123	0	93	0	0
9	83	141	92	91	0	94	0	0
10	83	157	107	106	0	95	0	0
11	83	171	110	109	0	95	0	0
12	83	185	113	112	0	95	0	0
13	83	197	115	114	0	95	0	0
14	83	207	116	115	0	95	0	0
15	0	0	0	0	0	0	0	0
16	83	247	120	119	0	96	0	0
17	83	262	137	136	0	96	0	0
18	83	275	140	139	0	96	0	0
19	83	290	146	145	0	96	0	0
20	115	306	96	96	0	96	0	0
21	115	322	106	106	0	97	0	0
22	115	336	118	118	0	97	0	0
23	115	352	129	129	0	97	0	0
24	115	362	133	133	0	97	0	0
25	115	381	138	138	0	97	0	0
26	115	393	140	140	0	97	0	0
27	115	408	141	141	0	97	0	0
28	115	426	142	142	0	97	0	0
29	115	442	143	143	0	97	0	0
30	115	450	145	145	0	97	0	0
31	115	472	152	152	0	98	0	0
32	115	979	211	211	0	98	0	0

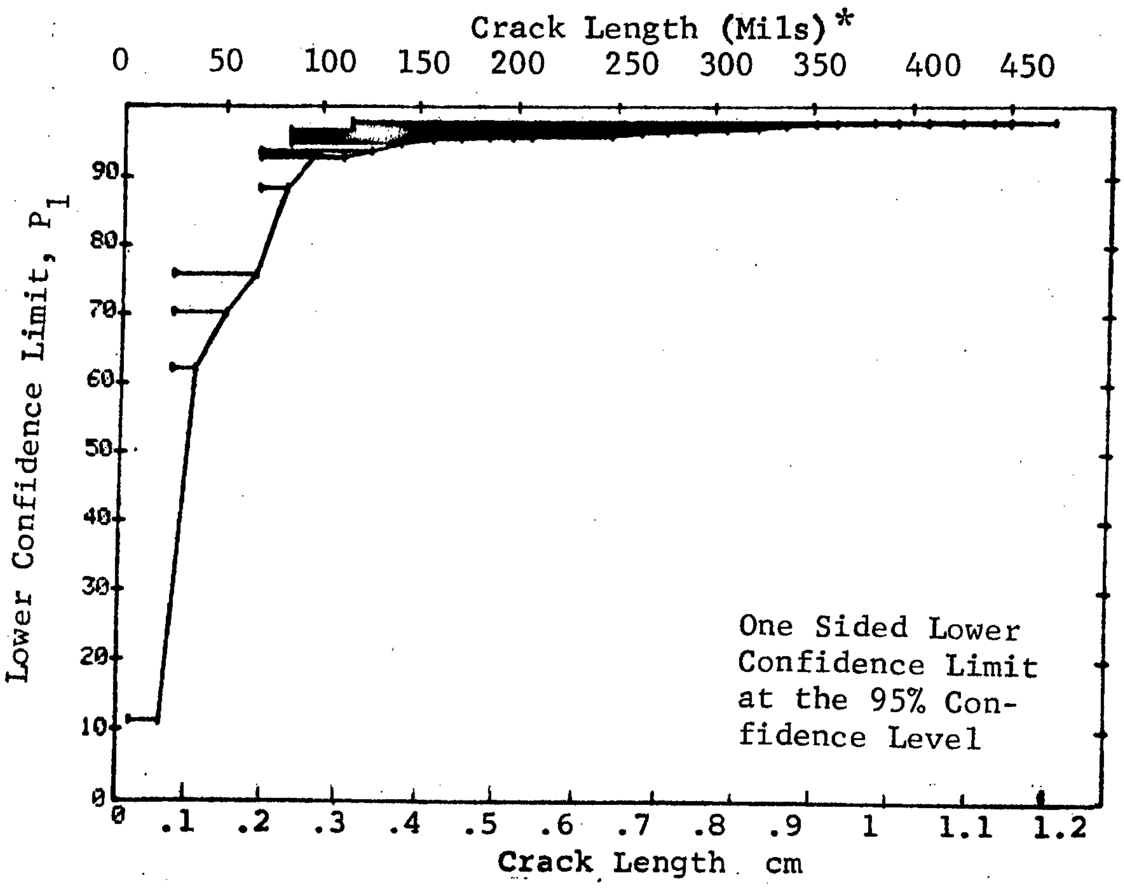

Figure D-10 (Continued)

(c) Overlapping Sixty Point Method of Data Cumulation

03-JUL-75 ULTRASONIC TEST 3 , ROCKWELL 5C , F (10)

RANGE	MIN LN*	MAX LN*	N	DET	50%	95%	0 MISS	1 MISS
1	0	0	0	0	0	0	0	0
2	0	0	0	0	0	0	0	0
3	0	0	0	0	0	0	0	0
4	0	0	0	0	0	0	0	0
5	0	0	0	0	0	0	0	0
6	0	0	0	0	0	0	0	0
7	0	0	0	0	0	0	0	0
8	0	0	0	0	0	0	0	0
9	0	0	0	0	0	0	0	0
10	0	0	0	0	0	0	0	0
11	0	0	0	0	0	0	0	0
12	0	0	0	0	0	0	0	0
13	0	0	0	0	0	0	0	0
14	0	0	0	0	0	0	0	0
15	0	0	0	0	0	0	0	0
16	0	0	0	0	0	0	0	0
17	0	0	0	0	0	0	0	0
18	0	0	0	0	0	0	0	0
19	0	0	0	0	0	0	0	0
20	0	0	0	0	0	0	0	0
21	7	49	52	36	68	57	0	0
22	31	63	60	51	83	75	94	100
23	51	70	60	52	85	77	82	94
24	64	79	60	55	90	83	43	56
25	70	87	60	59	97	92	0	1
26	79	105	60	60	98	95	0	0
27	88	131	60	59	97	92	0	1
28	105	162	60	59	97	92	0	1
29	132	269	60	60	98	95	0	0
30	171	330	60	60	98	95	0	0
31	275	442	60	60	98	95	0	0
32	331	500	60	60	98	95	0	0

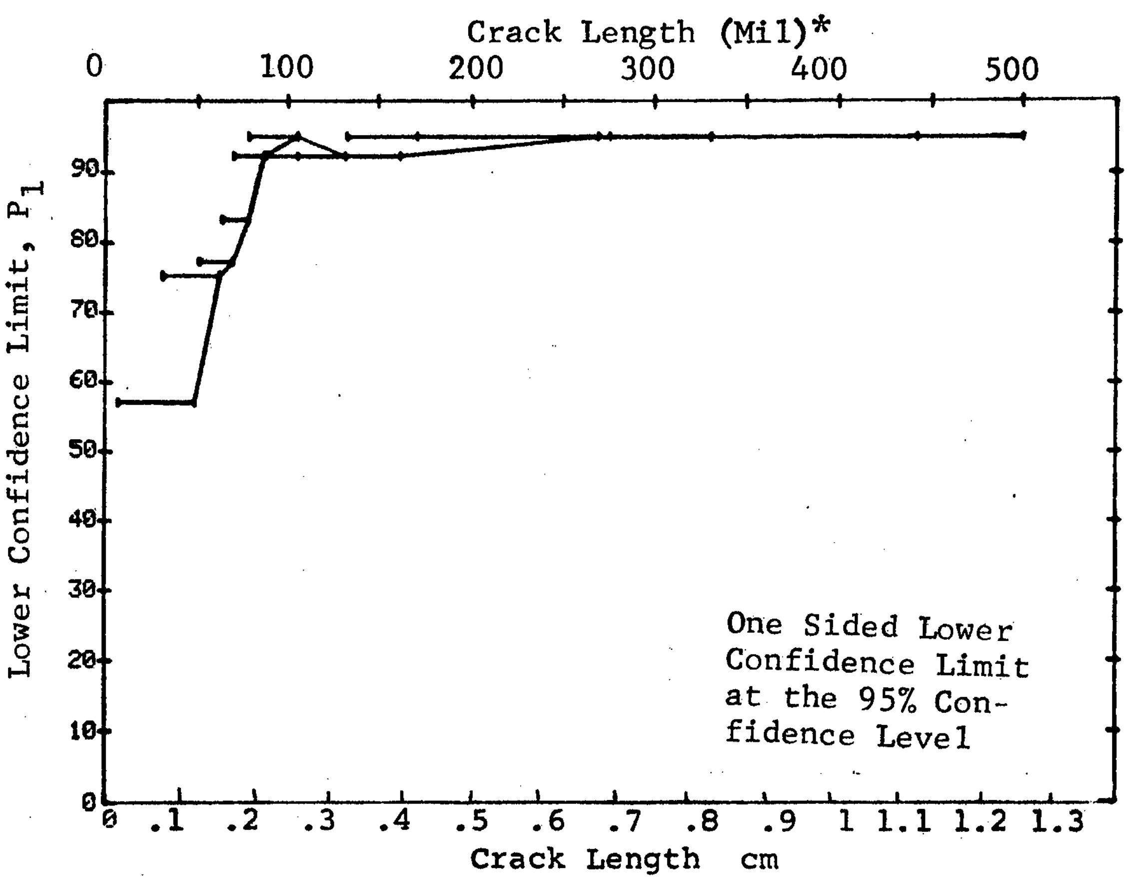

Figure D-10 (Concluded)

(b) Optimum Probability Method of Data Cumulation

03-JUL-75 ULTRASONIC TEST 1 . ROCKWELL SC , 'Q' (11)

RANGE	MIN LN	MAX LN	N	DET	50%	95%	0 MISS	1 MISS
1	7 *	22 *	13	7	20	6	0	0
2	25	36	18	9	47	29	0	0
3	38	52	24	18	72	56	0	0
4	54	67	46	37	79	68	0	0
5	68	82	53	46	85	76	76	89
6	83	97	39	31	77	66	0	0
7	98	111	17	13	73	53	0	0
8	115	126	17	16	90	75	29	44
9	129	141	19	14	70	52	0	0
10	143	157	15	10	63	42	0	0
11	158	171	3	2	50	13	0	0
12	182	185	3	3	79	36	0	0
13	190	197	2	2	70	22	0	0
14	0	0	0	0	0	0	0	0
15	0	0	0	0	0	0	0	0
16	241	247	4	4	84	47	0	0
17	248	262	17	17	96	83	12	29
18	268	275	3	3	79	36	0	0
19	279	290	7	7	90	65	0	0
20	295	306	6	6	89	60	0	0
21	310	322	10	10	93	74	0	0
22	323	336	12	12	94	77	17	34
23	338	352	11	10	85	63	0	0
24	356	362	4	4	84	47	0	0
25	370	381	5	4	68	34	0	0
26	384	393	2	2	70	22	0	0
27	408	408	1	1	50	5	0	0
29	426	426	1	1	50	5	0	0
29	442	442	1	1	50	5	0	0
30	444	444	1	1	50	5	0	0
31	458	472	7	7	90	65	0	0
32	474	979	59	55	92	85	30	44

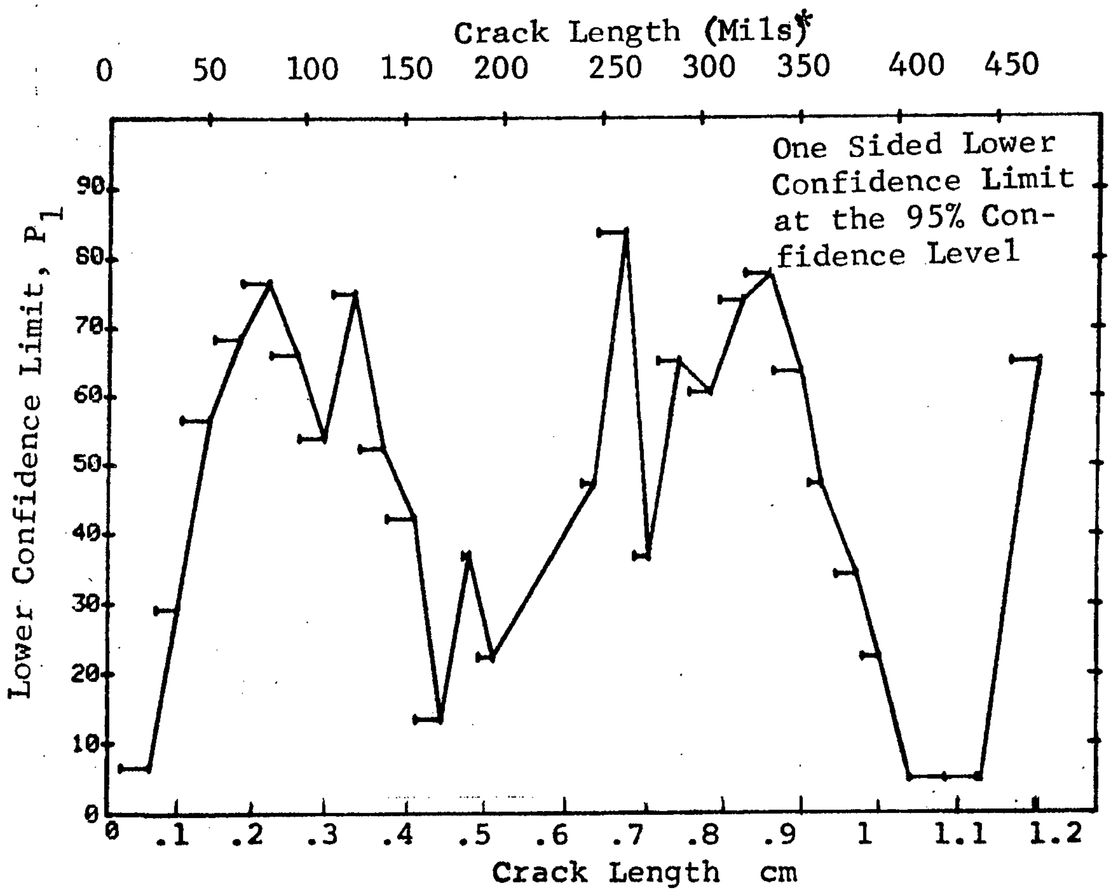

Figure D-11 Probability of Detection for 2219-T87 Al Using Ultrasonic Shear Waves. Etched Fatigue Cracks in Flat Plates Measured by Operator Q. Lab. Env.

(b) Optimum Probability Method of Data Cumulation

03-JUL-75 ULTRASONIC TEST 2 , ROCKWELL SC , '0' (11)

RANGE	MIN LN	MAX LN	N	DET	50%	95%	0 MISS	1 MISS
1	7*	22*	13	3	0	6	0	0
2	25	36	18	9	0	29	0	0
3	38	52	24	18	0	56	0	0
4	38	67	70	55	0	68	0	0
5	68	82	53	46	0	76	0	0
6	54	97	139	114	0	76	0	0
7	54	111	155	127	0	76	0	0
8	68	126	126	106	0	77	0	0
9	54	141	191	157	0	77	0	0
10	54	157	206	167	0	76	0	0
11	54	171	209	169	0	75	0	0
12	54	185	212	172	0	76	0	0
13	54	197	214	174	0	76	0	0
14	0	0	0	0	0	0	0	0
15	0	0	0	0	0	0	0	0
16	54	247	218	178	0	76	0	0
17	182	262	26	26	0	89	3	20
18	182	275	29	29	0	90	0	17
19	182	290	36	36	0	92	0	10
20	182	306	42	42	0	93	0	4
21	182	322	52	52	0	94	0	0
22	182	336	64	64	0	95	0	0
23	182	352	75	74	0	93	0	0
24	182	362	79	78	0	94	0	0
25	182	381	84	82	0	92	0	0
26	182	393	86	84	0	92	0	0
27	182	408	87	85	0	92	0	0
28	182	426	88	86	0	93	0	0
29	182	442	89	87	0	93	0	0
30	182	444	90	88	0	93	0	0
31	182	472	97	95	0	93	0	0
32	182	979	156	150	0	92	0	0

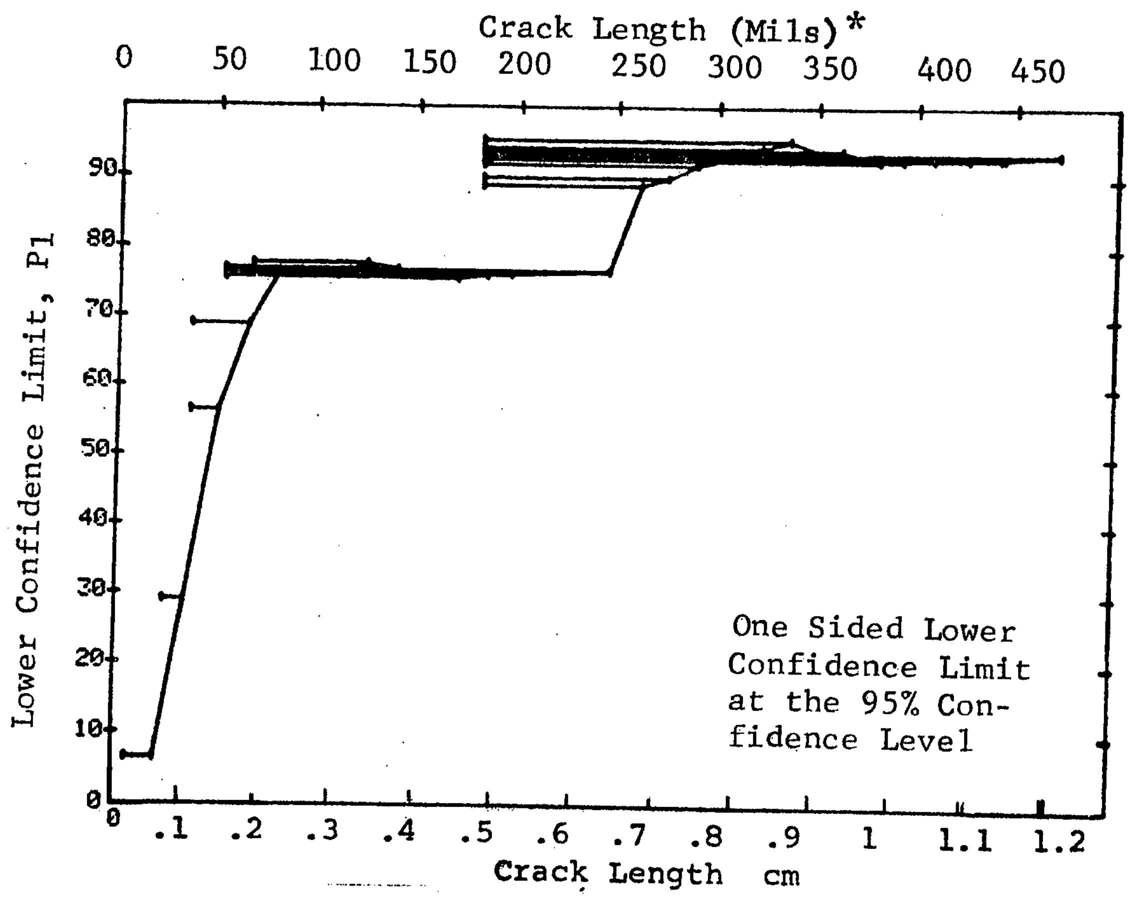

Figure D-11 (Continued)

(c) Overlapping Sixty Point Method of Data Cumulation

03-JUL-75 ULTRASONIC TEST 3 , ROCKWELL SC , 'O' (11)

RANGE	MIN LN	MAX LN	N	DET	50%	95%	0 MISS	1 MISS
1	0	0	0	0	0	0	0	0
2	0	0	0	0	0	0	0	0
3	0	0	0	0	0	0	0	0
4	0	0	0	0	0	0	0	0
5	0	0	0	0	0	0	0	0
6	0	0	0	0	0	0	0	0
7	0	0	0	0	0	0	0	0
8	0	0	0	0	0	0	0	0
9	0	0	0	0	0	0	0	0
10	0	0	0	0	0	0	0	0
11	0	0	0	0	0	0	0	0
12	0	0	0	0	0	0	0	0
13	0	0	0	0	0	0	0	0
14	0	0	0	0	0	0	0	0
15	0	0	0	0	0	0	0	0
16	0	0	0	0	0	0	0	0
17	0	0	0	0	0	0	0	0
18	0	0	0	0	0	0	0	0
19	0	0	0	0	0	0	0	0
20	0	0	0	0	0	0	0	0
21	7	49	52	27	50	39	0	0
22	31	63	60	46	75	65	0	0
23	49	69	60	50	82	73	0	0
24	63	79	60	50	82	73	0	0
25	70	87	60	51	83	75	94	100
26	79	104	60	49	80	71	0	0
27	87	131	60	49	80	71	0	0
28	105	158	60	47	77	67	0	0
29	131	269	60	50	82	73	0	0
30	162	329	60	59	97	92	0	1
31	275	426	60	58	95	89	1	16
32	330	500	60	57	93	87	16	29

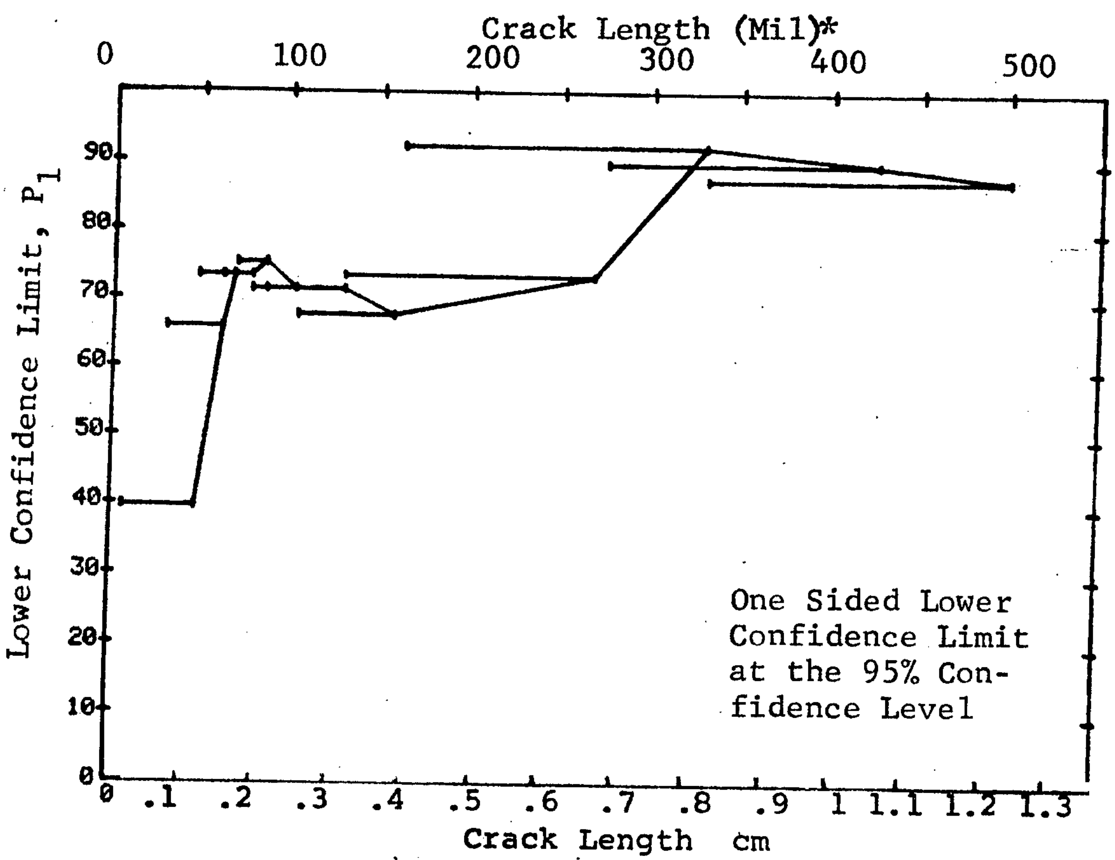

Figure D-11 (Concluded)

(a) Range Interval Method of Data Cumulation

24-JUL-75 ULTRASONIC TEST 1, (12) , ROCKWELL SC R

RANGE	MIN LN	MAX LN	N	DET	50%	95%	0 MISS	1 MISS
1	7 *	22 *	13	6	42	22	0	0
2	25	36	18	13	69	50	0	0
3	38	52	22	18	79	63	0	0
4	54	67	47	42	88	78	56	[illegible]
5	68	82	53	47	87	78	63	75
6	83	97	39	37	93	84	22	37
7	98	111	17	15	84	67	0	0
8	115	126	17	16	90	75	29	44
9	129	141	19	18	91	77	27	42
10	143	157	15	12	76	56	0	0
11	158	171	3	2	50	13	0	0
12	182	185	3	3	79	36	0	0
13	190	197	2	2	70	22	0	0
14	0	0	0	0	0	0	0	0
15	0	0	0	0	0	0	0	0
16	241	247	4	4	84	47	0	0
17	248	262	17	17	96	83	12	29
18	268	275	3	3	79	36	0	0
19	279	290	7	7	90	65	0	0
20	295	306	6	6	89	60	0	0
21	310	322	10	8	74	49	0	0
22	323	336	12	12	94	77	17	34
23	338	352	11	8	67	43	0	0
24	356	362	4	4	84	47	0	0
25	370	381	5	4	68	34	0	0
26	384	393	2	2	70	22	0	0
27	408	408	1	1	50	5	0	0
28	426	426	1	1	50	5	0	0
29	442	442	1	1	50	5	0	0
30	444	444	1	1	50	5	0	0
31	458	472	8	8	91	68	0	0
32	474	979	59	55	92	85	30	44

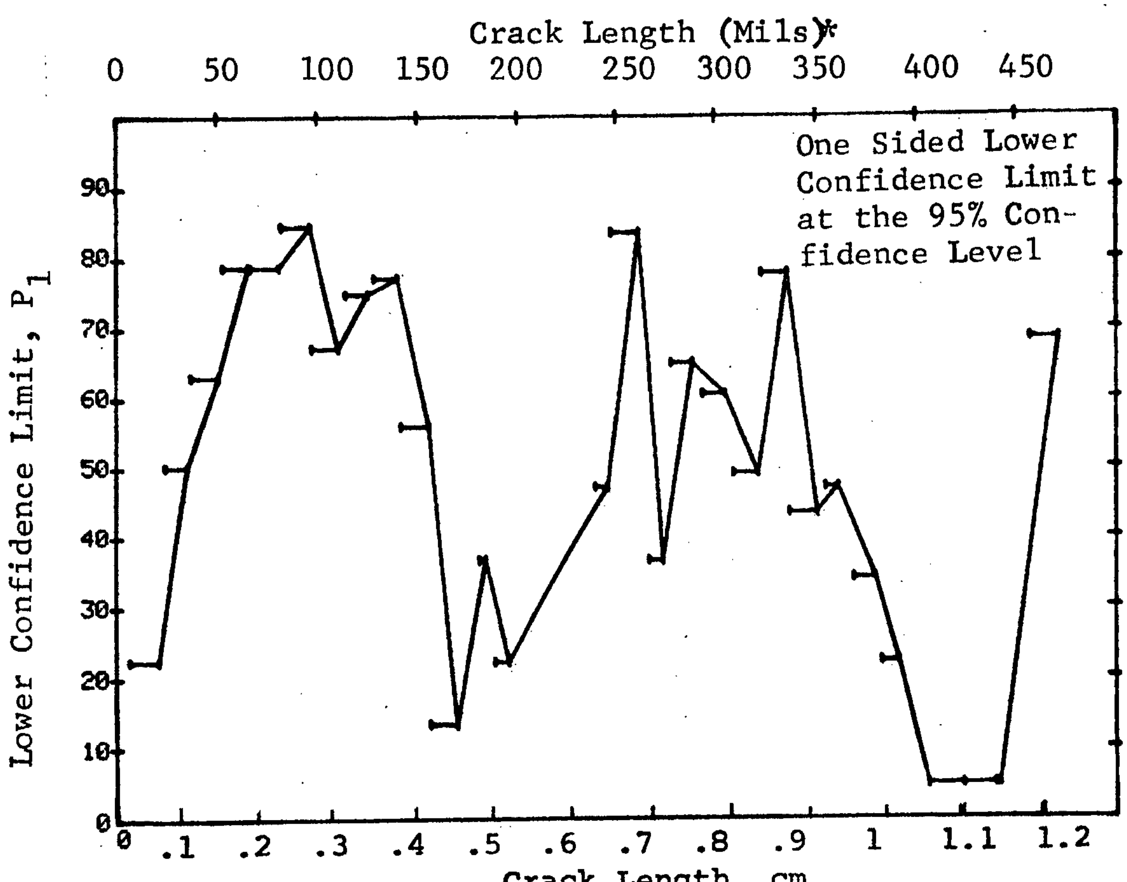

Figure D-12 Probability of Detection for 2219-T87 Al Using Ultrasonic Shear Waves. Etched Fatigue Cracks in Flat Plates Measured by Operator R. Lab. Env.

(b) Optimum Probability Method of Data Cumulation

24-JUL-75 ULTRASONIC TEST 2, (12) , ROCKWELL 5C R

RANGE	MIN LN	MAX LN	N	DET	50%	95%	0 MISS	1 MISS
1	7*	22*	13	6	0	22	0	0
2	25	36	18	13	0	50	0	0
3	25	52	40	31	0	64	0	0
4	54	67	47	42	0	78	0	0
5	54	82	100	89	0	82	79	91
6	54	97	139	126	0	85	0	0
7	54	111	156	141	0	85	0	0
8	83	126	73	68	0	86	30	43
9	83	141	92	86	0	87	24	37
10	68	157	160	145	0	85	0	0
11	54	171	210	189	0	85	0	0
12	54	185	213	192	0	86	0	0
13	68	197	168	152	0	85	0	0
14	0	0	0	0	0	0	0	0
15	0	0	0	0	0	0	0	0
16	54	247	219	198	0	86	0	0
17	182	262	26	26	0	89	3	20
18	182	275	29	29	0	90	0	17
19	182	290	36	36	0	92	0	10
20	182	306	42	42	0	93	0	4
21	182	322	52	50	0	88	9	24
22	182	336	64	62	0	90	0	12
23	83	352	185	170	0	87	0	0
24	83	362	189	174	0	88	0	0
25	83	381	194	178	0	87	0	0
26	83	393	196	180	0	87	0	0
27	83	408	197	181	0	87	0	0
28	83	426	198	182	0	87	0	0
29	68	442	252	230	0	87	0	0
30	83	444	200	184	0	88	0	0
31	83	472	208	192	0	88	0	0
32	182	979	157	147	0	89	0	0

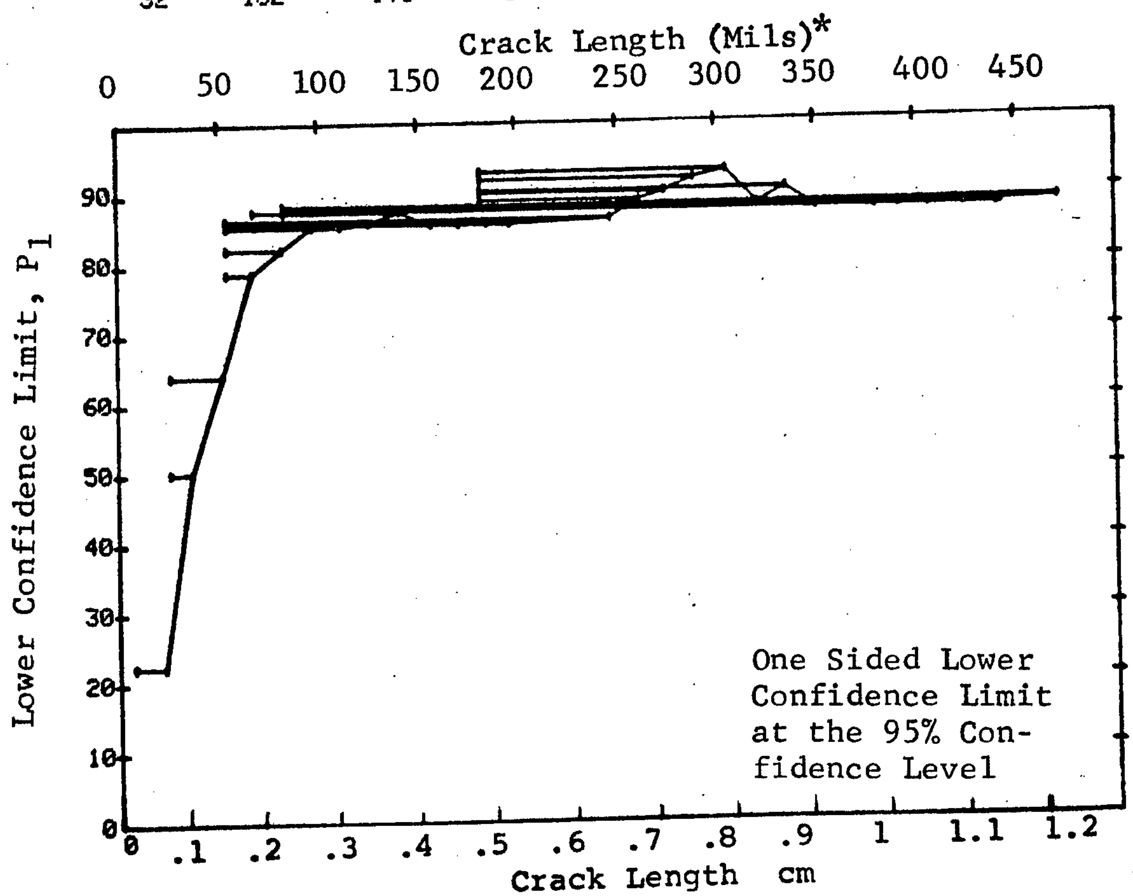

Figure D-12 (Continued)

(c) Overlapping Sixty Point Method of Data Cumulation

24-JUL-75 ULTRASONIC TEST 3, (12) , ROCKWELL SC R

RANGE	MIN LN *	MAX LN *	N	DET	50%	95%	0 MISS	1 MISS
1	0	0	0	0	0	0	0	0
2	0	0	0	0	0	0	0	0
3	0	0	0	0	0	0	0	0
4	0	0	0	0	0	0	0	0
5	0	0	0	0	0	0	0	0
6	0	0	0	0	0	0	0	0
7	0	0	0	0	0	0	0	0
8	0	0	0	0	0	0	0	0
9	0	0	0	0	0	0	0	0
10	0	0	0	0	0	0	0	0
11	0	0	0	0	0	0	0	0
12	0	0	0	0	0	0	0	0
13	0	0	0	0	0	0	0	0
14	0	0	0	0	0	0	0	0
15	0	0	0	0	0	0	0	0
16	0	0	0	0	0	0	0	0
17	0	0	0	0	0	0	0	0
18	0	0	0	0	0	0	0	0
19	0	0	0	0	0	0	0	0
20	0	0	0	0	0	0	0	0
21	7	51	52	36	68	57	0	0
22	31	63	60	49	80	71	0	0
23	52	70	60	51	83	75	94	100
24	64	79	60	53	87	79	69	82
25	70	87	60	57	93	87	16	29
26	79	105	60	56	92	85	29	43
27	88	131	60	56	92	85	29	43
28	105	162	60	54	88	81	56	69
29	132	275	60	55	90	83	43	56
30	171	330	60	58	95	89	1	16
31	279	442	60	54	88	81	56	69
32	331	500	60	54	88	81	56	69

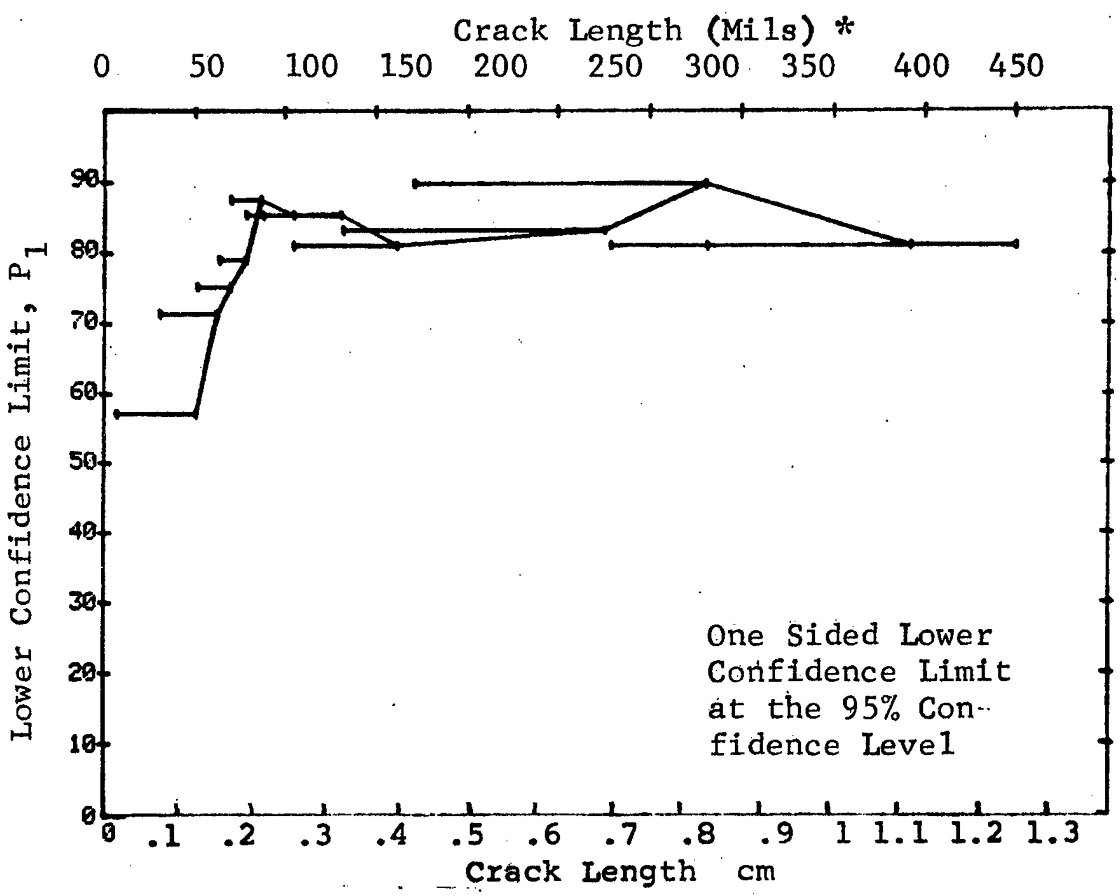

Figure D-12 (Concluded)

(a) Range Interval Method of Data Cumulation

24-JUL-75 ULTRASONIC TEST 1, (13) ROCKWELL SC S

RANGE	MIN LN *	MAX LN *	N	DET	50%	95%	0 MISS	1 MISS
1	7	22	13	4	27	11	0	0
2	25	36	18	13	69	50	0	0
3	38	52	23	17	71	54	0	0
4	54	67	46	38	81	70	0	0
5	68	82	53	50	93	86	23	36
6	83	97	39	36	90	81	37	50
7	98	111	17	17	96	83	12	29
8	115	126	17	16	90	75	29	44
9	129	141	19	18	91	77	27	42
10	143	157	15	14	89	72	0	0
11	158	171	3	3	79	36	0	0
12	182	185	3	3	79	36	0	0
13	190	197	2	2	70	22	0	0
14	0	0	0	0	0	0	0	0
15	0	0	0	0	0	0	0	0
16	241	247	4	3	61	24	0	0
17	248	262	17	17	96	83	12	29
18	268	275	3	3	79	36	0	0
19	279	290	7	6	77	47	0	0
20	295	306	6	6	89	60	0	0
21	310	322	10	10	93	74	0	0
22	323	336	12	10	78	56	0	0
23	338	352	11	10	85	63	0	0
24	356	362	4	4	84	47	0	0
25	370	381	5	4	68	34	0	0
26	384	393	2	2	70	22	0	0
27	408	408	1	1	50	5	0	0
28	426	426	1	1	50	5	0	0
29	442	442	1	1	50	5	0	0
30	444	444	1	1	50	5	0	0
31	458	472	8	8	91	68	0	0
32	474	979	59	59	98	95	0	0

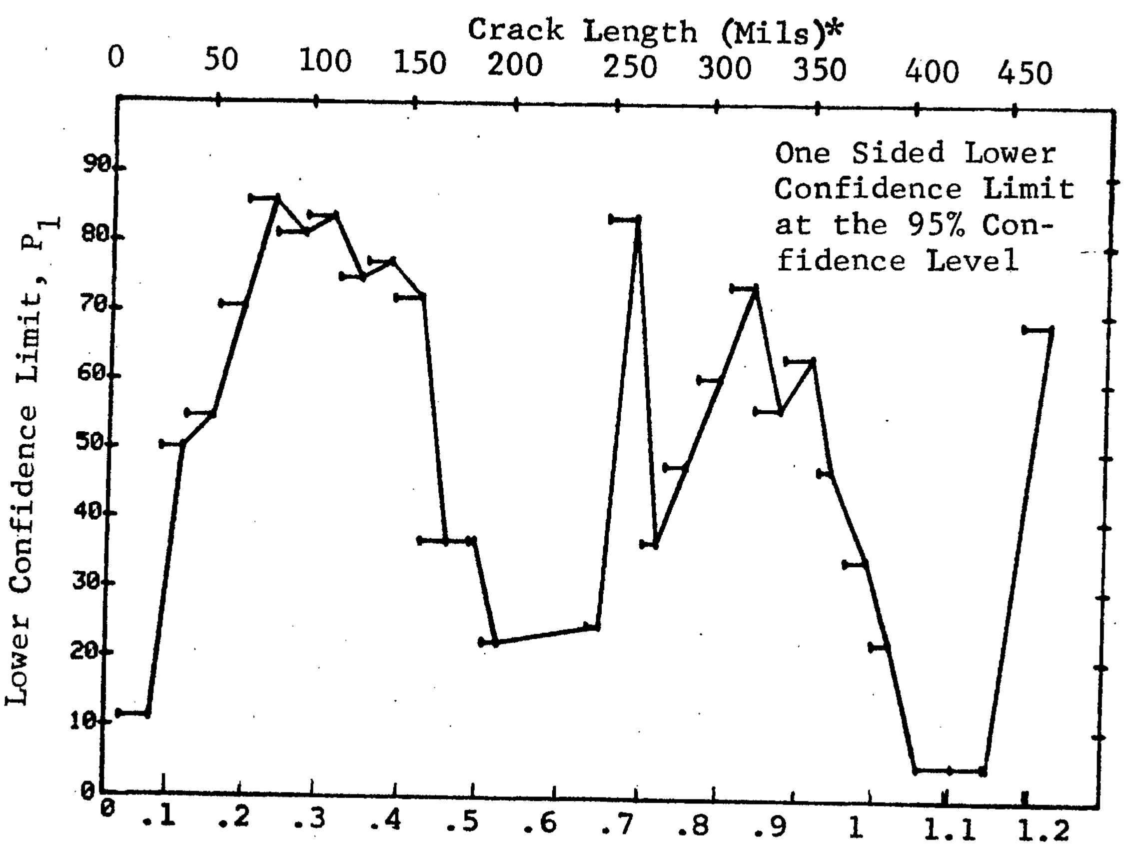

Figure D-13 Probability of Detection for 2219-T87 Al Using Ultrasonic Shear Waves. Etched Fatigue Cracks in Flat Plates Measured by Operator S. Lab. Env.

(b) Optimum Probability Method of Data Cumulation

24-JUL-75 ULTRASONIC TEST 2, (13) ROCKWELL 5C

RANGE	MIN LN	MAX LN	N	DET	50%	95%	0 MISS	1 MISS
1	7 *	22 *	13	4	0	11	0	0
2	25	36	18	13	0	50	0	0
3	25	52	41	30	0	59	0	0
4	54	67	46	38	0	70	0	0
5	68	82	53	50	0	86	23	35
6	68	97	92	86	0	87	24	37
7	68	111	109	103	0	89	0	0
8	68	126	126	119	0	89	0	0
9	68	141	145	137	0	90	0	0
10	68	157	160	151	0	90	0	0
11	68	171	163	154	0	90	0	0
12	68	185	166	157	0	90	0	0
13	68	197	168	159	0	90	0	0
14	0	0	0	0	0	0	0	0
15	0	0	0	0	0	0	0	0
16	68	247	172	162	0	90	0	0
17	68	262	189	179	0	91	0	0
18	68	275	192	182	0	91	0	0
19	68	290	199	188	0	91	0	0
20	68	306	205	194	0	91	0	0
21	68	322	215	204	0	91	0	0
22	68	336	227	214	0	91	0	0
23	68	352	238	224	0	90	0	0
24	68	362	242	228	0	91	0	0
25	68	381	247	232	0	90	0	0
26	68	393	249	234	0	90	0	0
27	68	408	250	235	0	90	0	0
28	68	426	251	236	0	90	0	0
29	68	442	252	237	0	90	0	0
30	68	444	253	238	0	91	0	0
31	68	472	261	246	0	91	0	0
32	384	979	73	73	0	95	0	0

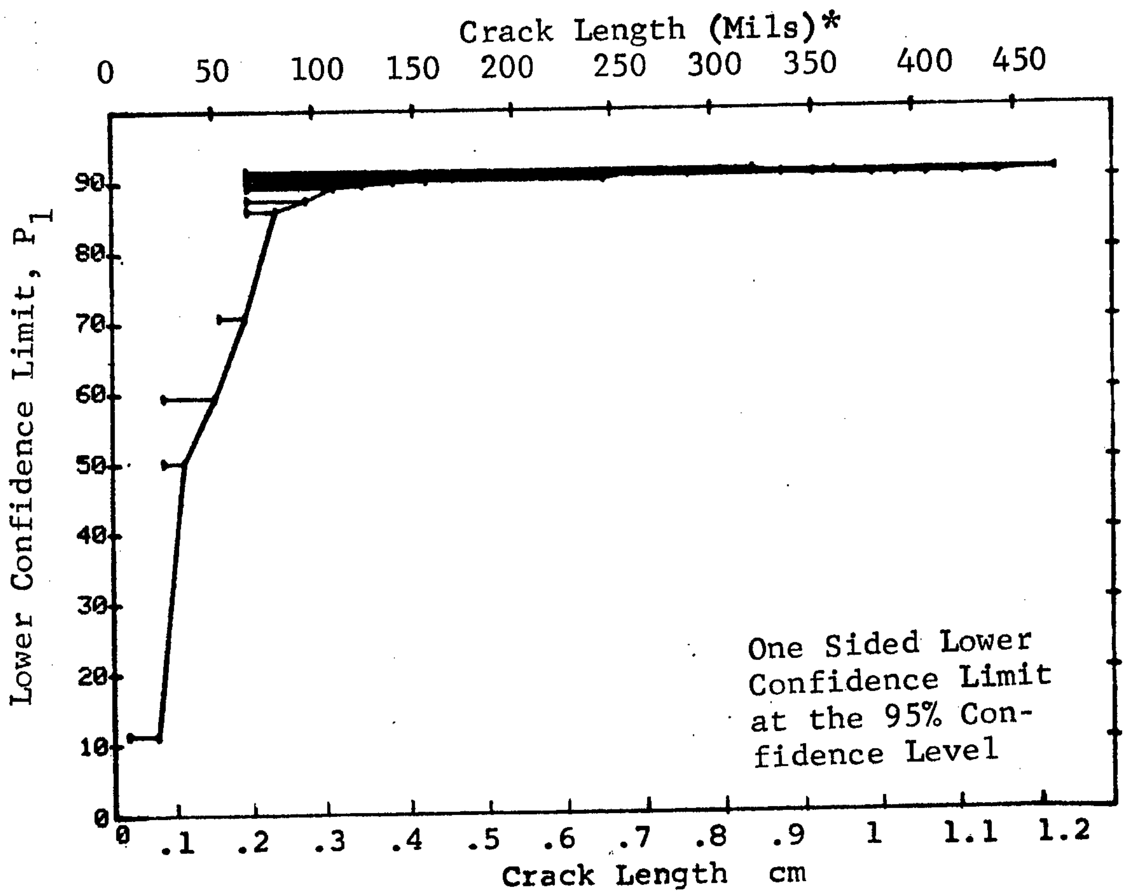

Figure D-13 (Continued)

(c) Overlapping Sixty Point Method of Data Cumulation

24-JUL-75 ULTRASONIC TEST 3, (13) . ROCKWELL SC s

RANGE	MIN LN *	MAX LN *	N	DET	50%	95%	0 MISS	1 MISS
1	0	0	0	0	0	0	0	0
2	0	0	0	0	0	0	0	0
3	0	0	0	0	0	0	0	0
4	0	0	0	0	0	0	0	0
5	0	0	0	0	0	0	0	0
6	0	0	0	0	0	0	0	0
7	0	0	0	0	0	0	0	0
8	0	0	0	0	0	0	0	0
9	0	0	0	0	0	0	0	0
10	0	0	0	0	0	0	0	0
11	0	0	0	0	0	0	0	0
12	0	0	0	0	0	0	0	0
13	0	0	0	0	0	0	0	0
14	0	0	0	0	0	0	0	0
15	0	0	0	0	0	0	0	0
16	0	0	0	0	0	0	0	0
17	0	0	0	0	0	0	0	0
18	0	0	0	0	0	0	0	0
19	0	0	0	0	0	0	0	0
20	0	0	0	0	0	0	0	0
21	7	49	52	32	60	49	0	0
22	31	63	60	46	75	65	0	0
23	51	70	60	51	83	75	94	100
24	64	79	60	54	88	81	56	69
25	70	87	60	57	93	87	16	29
26	79	105	60	57	93	87	16	29
27	88	131	60	56	92	85	29	43
28	105	162	60	57	93	87	16	29
29	132	275	60	58	95	89	1	16
30	171	330	60	58	95	89	1	16
31	279	442	60	55	90	83	43	56
32	331	500	60	56	92	85	29	43

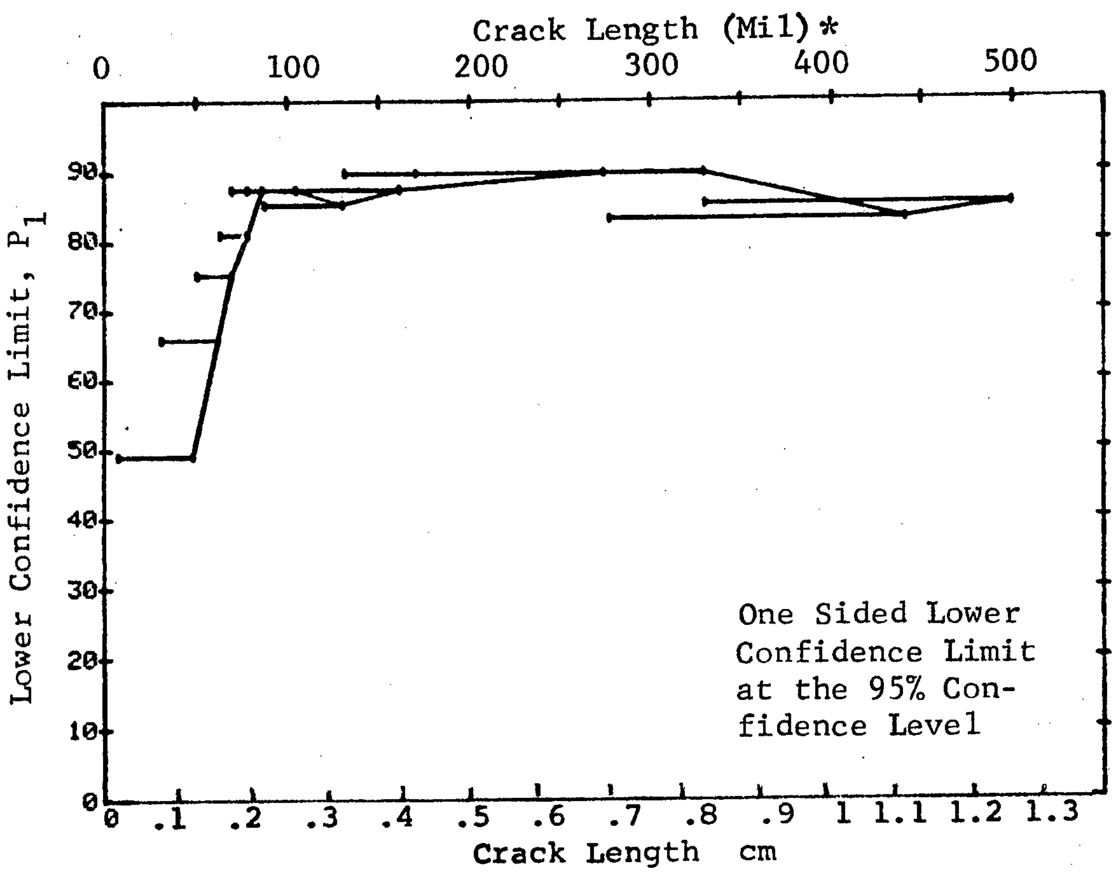

Figure D-13 (Concluded)

(a) Range Interval Method of Data Cumulation

24-JUL-75 PENETRANT TEST 1, (14), ROCKWELL SC H

RANGE	MIN LN	MAX LN	N	DET	50%	95%	0 MISS	1 MISS
1	7 *	22 *	13	4	27	11	0	0
2	25	36	18	9	47	29	0	0
3	38	52	23	21	88	75	38	53
4	54	67	46	39	83	73	0	0
5	68	82	53	47	87	78	63	75
6	83	97	38	37	95	88	8	23
7	98	111	17	17	96	83	12	29
8	115	126	17	15	84	67	0	0
9	129	141	19	18	91	77	27	42
10	143	157	15	14	89	72	0	0
11	158	171	3	3	79	36	0	0
12	182	185	3	3	79	36	0	0
13	190	197	2	2	70	22	0	0
14	0	0	0	0	0	0	0	0
15	0	0	0	0	0	0	0	0
16	241	247	4	4	84	47	0	0
17	248	262	17	17	96	83	12	29
18	268	275	3	3	79	36	0	0
19	279	290	7	7	90	65	0	0
20	295	306	6	6	89	60	0	0
21	310	322	10	10	93	74	0	0
22	323	336	12	11	86	66	0	0
23	338	352	11	11	93	76	18	35
24	356	362	4	4	84	47	0	0
25	370	381	5	4	68	34	0	0
26	384	393	2	2	70	22	0	0
27	408	408	1	1	50	5	0	0
28	426	426	1	1	50	5	0	0
29	442	442	1	1	50	5	0	0
30	444	444	1	1	50	5	0	0
31	458	472	8	8	91	68	0	0
32	474	979	59	59	98	95	0	0

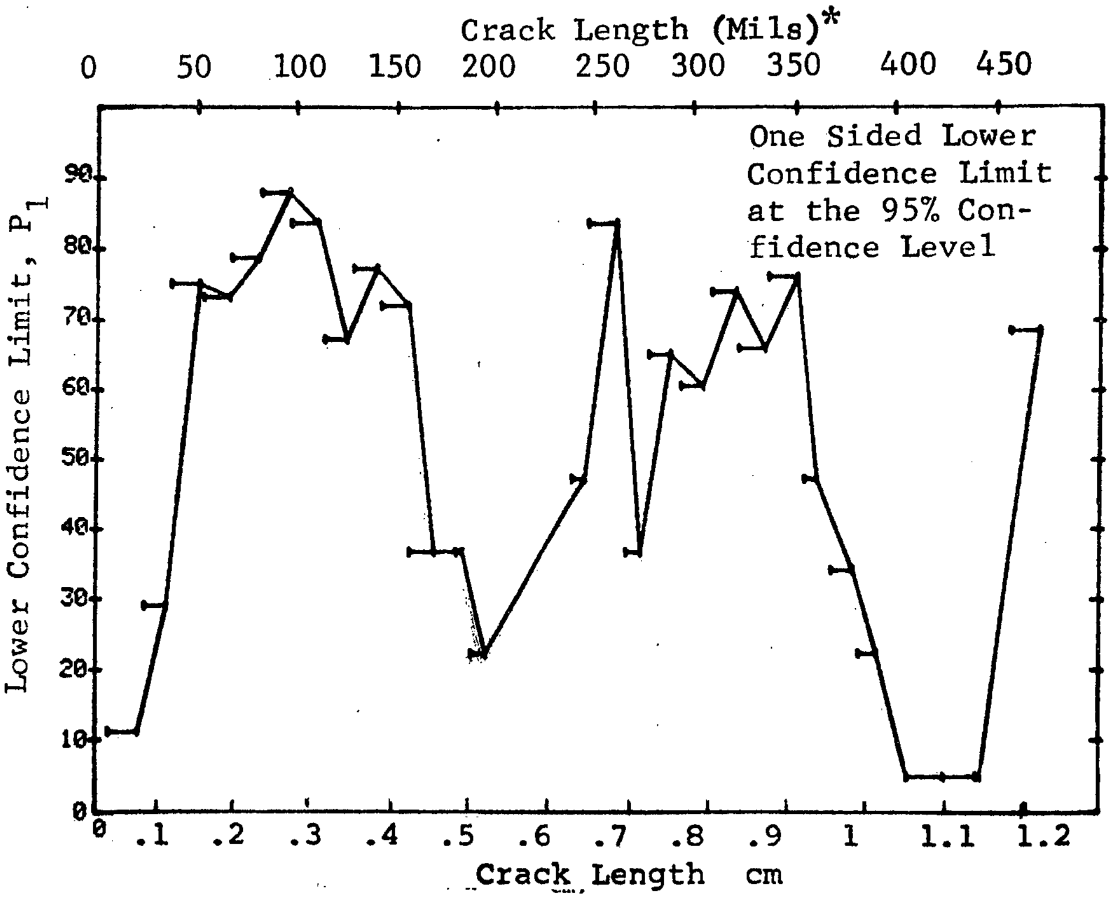

Figure D-14 Probability of Detection for 2219-T87 Al Using Liquid Penetrant. Etched Fatigue Cracks in Flat Plates Measured by Operator H. Lab. Env.

(b) Optimum Probability Method of Data Cumulation

24-JUL-75 PENETRANT TEST 2, (14) ROCKWELL 9 H

RANGE	MIN LN	MAX LN	N	DET	50%	95%	0 MISS	1 MISS
1	7 *	22 *	13	4	0	11	0	0
2	25	36	18	9	0	29	0	0
3	38	52	23	21	0	75	0	0
4	38	67	69	60	0	78	0	0
5	38	82	122	107	0	81	0	0
6	83	97	38	37	0	88	8	23
7	83	111	55	54	0	91	0	6
8	83	126	72	69	0	89	4	17
9	83	141	91	87	0	90	0	12
10	83	157	106	101	0	90	0	0
11	83	171	109	104	0	90	0	0
12	83	185	112	107	0	90	0	0
13	83	197	114	109	0	90	0	0
14	0	0	0	0	0	0	0	0
15	0	0	0	0	0	0	0	0
16	83	247	118	113	0	91	0	0
17	83	262	135	130	0	92	0	0
18	83	275	138	133	0	92	0	0
19	83	290	145	140	0	92	0	0
20	158	306	45	45	0	93	0	1
21	158	322	55	55	0	94	0	0
22	83	336	173	167	0	93	0	0
23	158	352	78	77	0	94	0	0
24	158	362	82	81	0	94	0	0
25	83	381	193	186	0	93	0	0
26	83	393	195	188	0	93	0	0
27	83	408	196	189	0	93	0	0
28	83	426	197	190	0	93	0	0
29	83	442	198	191	0	93	0	0
30	83	444	199	192	0	93	0	0
31	158	472	101	99	0	93	0	0
32	158	979	160	158	0	96	0	0

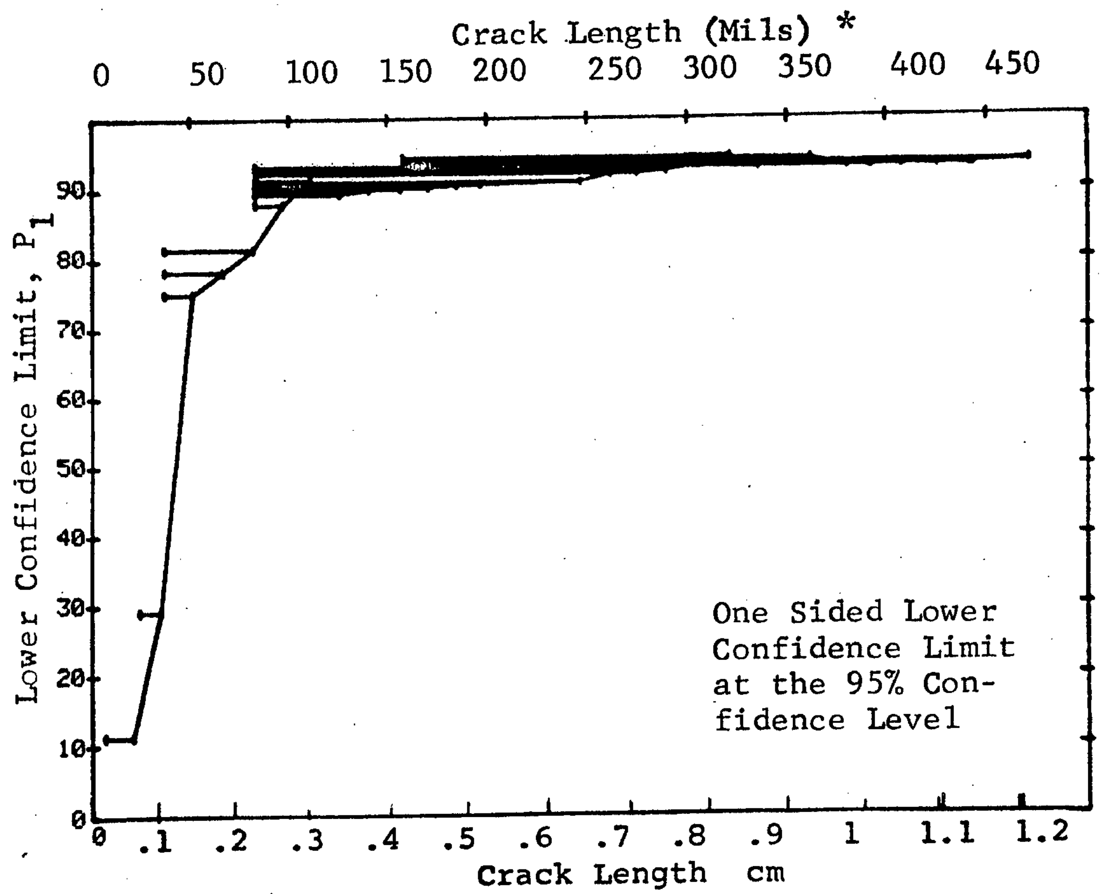

Figure D-14 (Continued)

(c) Overlapping Sixty Point Method of Data Cumulation

24-JUL-75 PENETRANT TEST 3, (14) ROCKWELL H

RANGE	MIN LN	MAX LN	N	DET	50%	95%	0 MISS	1 MISS
1	0 *	0 *	0	0	0	0	0	0
2	0	0	0	0	0	0	0	0
3	0	0	0	0	0	0	0	0
4	0	0	0	0	0	0	0	0
5	0	0	0	0	0	0	0	0
6	0	0	0	0	0	0	0	0
7	0	0	0	0	0	0	0	0
8	0	0	0	0	0	0	0	0
9	0	0	0	0	0	0	0	0
10	0	0	0	0	0	0	0	0
11	0	0	0	0	0	0	0	0
12	0	0	0	0	0	0	0	0
13	0	0	0	0	0	0	0	0
14	0	0	0	0	0	0	0	0
15	0	0	0	0	0	0	0	0
16	0	0	0	0	0	0	0	0
17	0	0	0	0	0	0	0	0
18	0	0	0	0	0	0	0	0
19	0	0	0	0	0	0	0	0
20	0	0	0	0	0	0	0	0
21	7	49	51	31	59	48	0	0
22	30	63	60	50	82	73	0	0
23	49	69	60	50	82	73	0	0
24	63	79	60	54	88	81	56	69
25	70	87	60	56	92	85	29	43
26	79	105	60	56	92	85	29	43
27	87	131	60	58	95	89	1	16
28	105	162	60	56	92	85	29	43
29	132	275	60	58	95	89	1	16
30	171	330	60	59	97	92	0	1
31	279	442	60	58	95	89	1	16
32	331	500	60	59	97	92	0	1

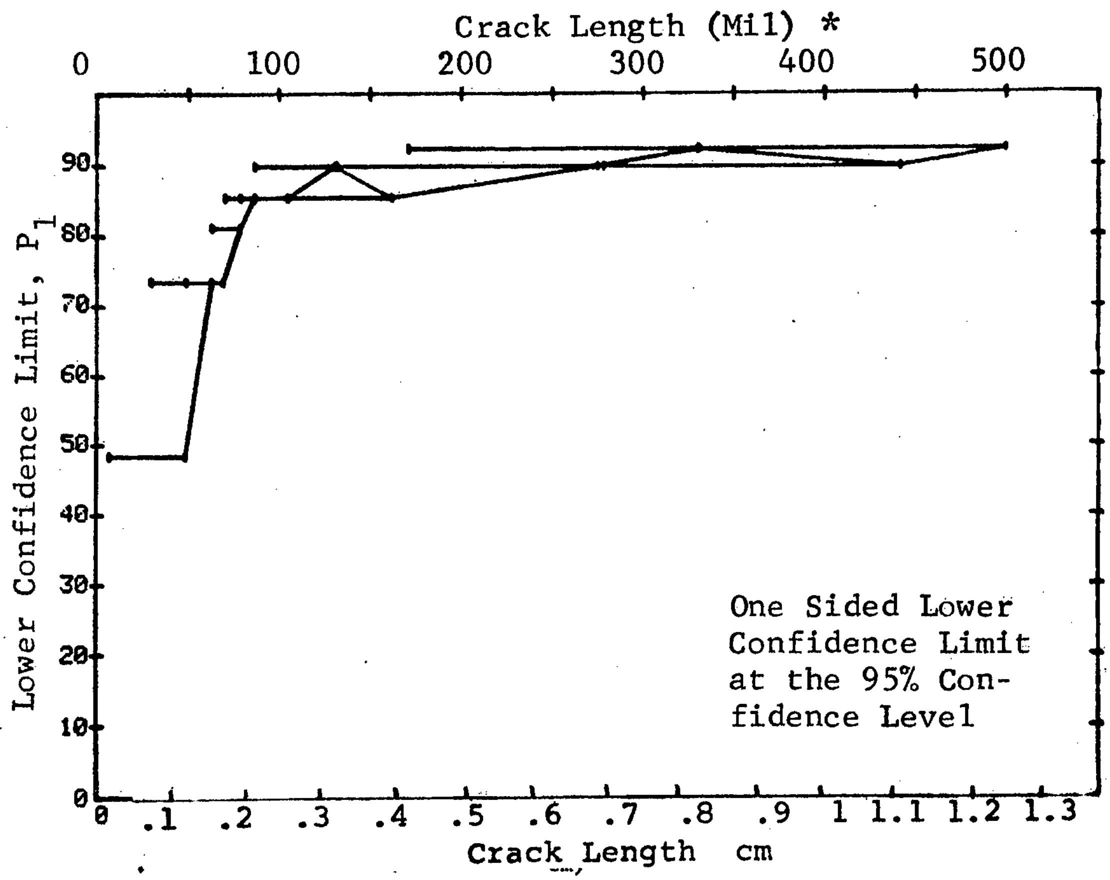

Figure D-14 (Concluded)

(a) Range Interval Method of Data Cumulation

24-JUL-75 PENETRANT TEST 1, (15) , ROCKWELL SG I

RANGE	MIN LN	MAX LN	N	DET	50%	95%	0 MISS	1 MISS
1	7 *	22 *	13	0	0	0	0	0
2	25	36	18	9	47	29	0	0
3	38	52	23	17	71	54	0	0
4	54	67	46	32	68	56	0	0
5	68	82	53	44	81	72	0	0
6	83	97	39	35	88	78	50	64
7	98	111	17	15	84	67	0	0
8	115	126	17	14	78	60	0	0
9	129	141	19	18	91	77	27	42
10	143	157	15	13	82	63	0	0
11	158	171	3	3	79	36	0	0
12	182	185	3	3	79	36	0	0
13	190	197	2	1	29	2	0	0
14	0	0	0	0	0	0	0	0
15	0	0	0	0	0	0	0	0
16	241	247	4	4	84	47	0	0
17	248	262	17	17	96	83	12	29
18	268	275	3	3	79	36	0	0
19	279	290	7	7	90	65	0	0
20	295	306	6	6	89	60	0	0
21	310	322	10	10	93	74	0	0
22	323	336	12	12	94	77	17	34
23	338	352	11	11	93	76	18	35
24	356	362	4	4	84	47	0	0
25	370	381	5	5	87	54	0	0
26	384	393	2	2	70	22	0	0
27	408	408	1	1	50	5	0	0
28	426	426	1	1	50	5	0	0
29	442	442	1	1	50	5	0	0
30	444	444	1	1	50	5	0	0
31	458	472	8	8	91	68	0	0
32	474	979	59	58	97	92	0	2

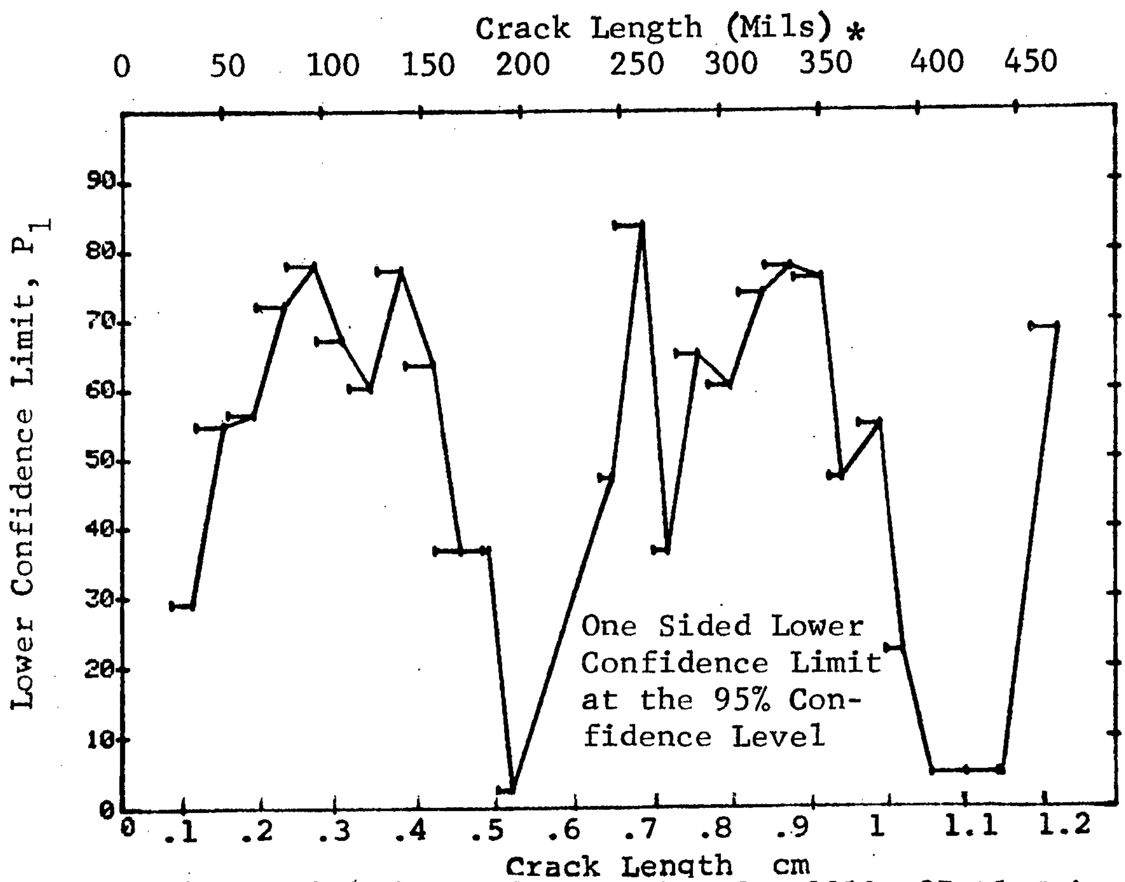

Figure D-15 Probability of Detection for 2219-T87 Al Using Liquid Penetrant. Etched Fatigue Cracks in Flat Plates Measured by Operator I. Lab. Env.

(b) Optimum Probability Method of Data Cumulation

24-JUL-75 PENETRANT TEST 2. .(15) ROCKWELL SC I

RANGE	MIN LN	MAX LN	N	DET	50%	95%	0 MI	MISS
1	7 *	22 *	13	0	0	0	0	0
2	25	36	18	9	0	29	0	0
3	38	52	23	17	0	54	0	0
4	38	67	69	49	0	60	0	0
5	68	82	53	44	0	72	0	0
6	68	97	92	79	0	78	0	0
7	83	111	56	50	0	79	0	0
8	68	126	126	103	0	79	0	0
9	83	141	92	82	0	82	75	87
10	83	157	107	95	0	82	0	0
11	83	171	110	98	0	82	0	0
12	83	185	113	101	0	83	0	0
13	83	197	115	102	0	82	0	0
14	0	0	0	0	0	0	0	0
15	0	0	0	0	0	0	0	0
16	83	247	119	106	0	83	0	0
17	241	262	21	21	0	86	8	25
18	241	275	24	24	0	88	5	22
19	241	290	31	31	0	90	0	15
20	241	306	37	37	0	92	0	9
21	241	322	47	47	0	93	0	0
22	241	336	59	59	0	95	0	0
23	241	352	70	70	0	95	0	0
24	241	362	74	74	0	96	0	0
25	241	381	79	79	0	96	0	0
26	241	393	81	81	0	96	0	0
27	241	408	82	82	0	96	0	0
28	241	426	83	83	0	96	0	0
29	241	442	84	84	0	96	0	0
30	241	444	85	85	0	96	0	0
31	241	472	93	93	0	96	0	0
32	241	979	152	151	0	96	0	0

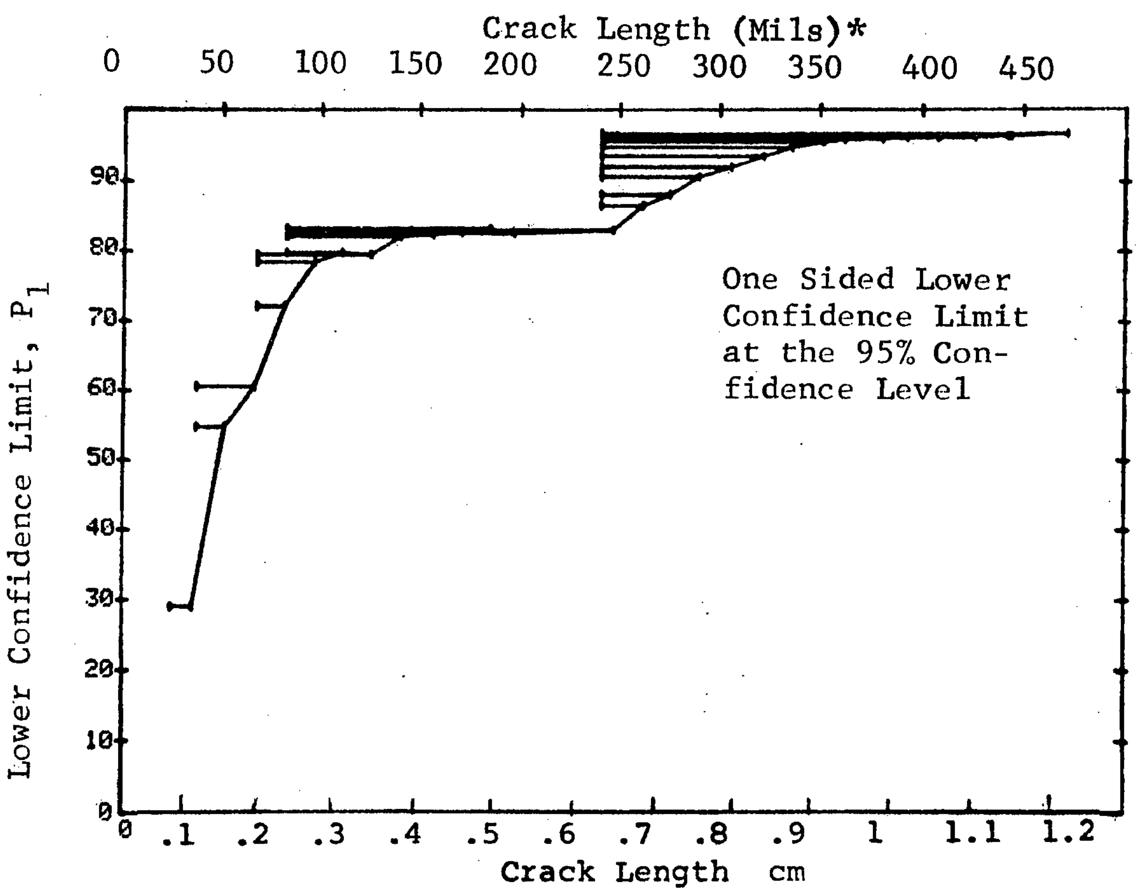

Figure D-15 (Continued)

(c) Overlapping Sixty Point Method of Data Cumulation

24-JUL-75 PENETRANT TEST 3, (15) , ROCKWELL SLI

RANGE	MIN LN	MAX LN	N	DET	50%	95%	0 MISS	1 MISS
1	0 *	0 *	0	0	0	0	0	0
2	0	0	0	0	0	0	0	[illegible]
3	0	0	0	0	0	0	0	0
4	0	0	0	0	0	0	0	0
5	0	0	0	0	0	0	0	0
6	0	0	0	0	0	0	0	0
7	0	0	0	0	0	0	0	0
8	0	0	0	0	0	0	0	0
9	0	0	0	0	0	0	0	0
10	0	0	0	0	0	0	0	0
11	0	0	0	0	0	0	0	0
12	0	0	0	0	0	0	0	0
13	0	0	0	0	0	0	0	0
14	0	0	0	0	0	0	0	0
15	0	0	0	0	0	0	0	0
16	0	0	0	0	0	0	0	0
17	0	0	0	0	0	0	0	0
18	0	0	0	0	0	0	0	0
19	0	0	0	0	0	0	0	0
20	0	0	0	0	0	0	0	0
21	7	49	52	25	47	36	0	0
22	31	63	60	42	69	58	0	0
23	51	70	60	43	70	60	0	0
24	64	79	60	46	75	65	0	0
25	70	87	60	50	82	73	0	0
26	79	105	60	53	87	79	69	82
27	88	131	60	54	88	81	56	69
28	105	162	60	53	87	79	69	82
29	132	275	60	56	92	85	29	43
30	171	330	60	59	97	92	0	1
31	279	442	60	60	98	93	0	0
32	331	500	60	59	97	92	0	1

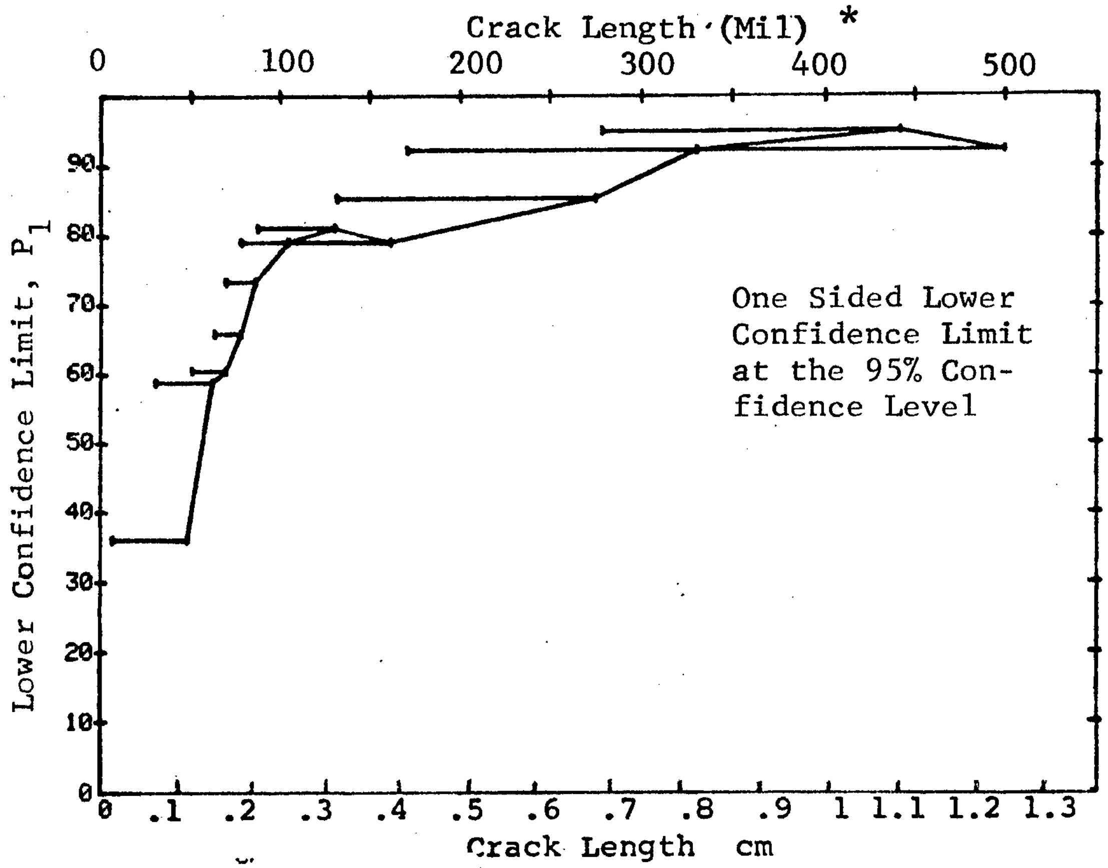

Figure D-15 (Concluded)

(a) Range Interval Method of Data Cumulation

24-JUL-75 PENETRANT TEST 1. . (16) ROCKWELL [illegible] J

RANGE	MIN LN	*MAX LN *	N	DET	50%	95%	0 MI[illegible]	[illegible] MISS
1	7	22	13	3	20	6	0	0
2	25	36	18	6	30	15	0	[illegible]
3	38	52	23	9	37	22	0	0
4	54	67	46	29	61	49	0	0
5	68	82	53	36	66	55	0	0
6	83	97	39	30	75	63	0	0
7	98	111	17	16	90	75	29	44
8	115	126	17	15	84	67	0	0
9	129	141	19	17	86	70	0	0
10	143	157	15	13	82	63	0	0
11	158	171	3	3	79	36	0	0
12	182	185	3	3	79	36	0	0
13	190	197	2	1	29	2	0	0
14	0	0	0	0	0	0	0	0
15	0	0	0	0	0	0	0	0
16	241	247	4	4	84	47	0	0
17	248	262	17	17	96	83	12	29
18	268	275	3	3	79	36	0	0
19	279	290	7	7	90	65	0	0
20	295	306	6	6	89	60	0	0
21	310	322	10	9	83	60	0	0
22	323	336	12	12	94	77	17	34
23	338	352	11	10	65	63	0	0
24	356	362	4	4	84	47	0	0
25	370	381	5	5	87	54	0	0
26	384	393	2	2	70	22	0	0
27	408	408	1	1	50	5	0	0
28	426	426	1	1	50	5	0	0
29	442	442	1	1	50	5	0	0
30	444	444	1	1	50	5	0	0
31	458	472	9	9	91	68	0	0
32	474	979	60	59	97	92	0	1

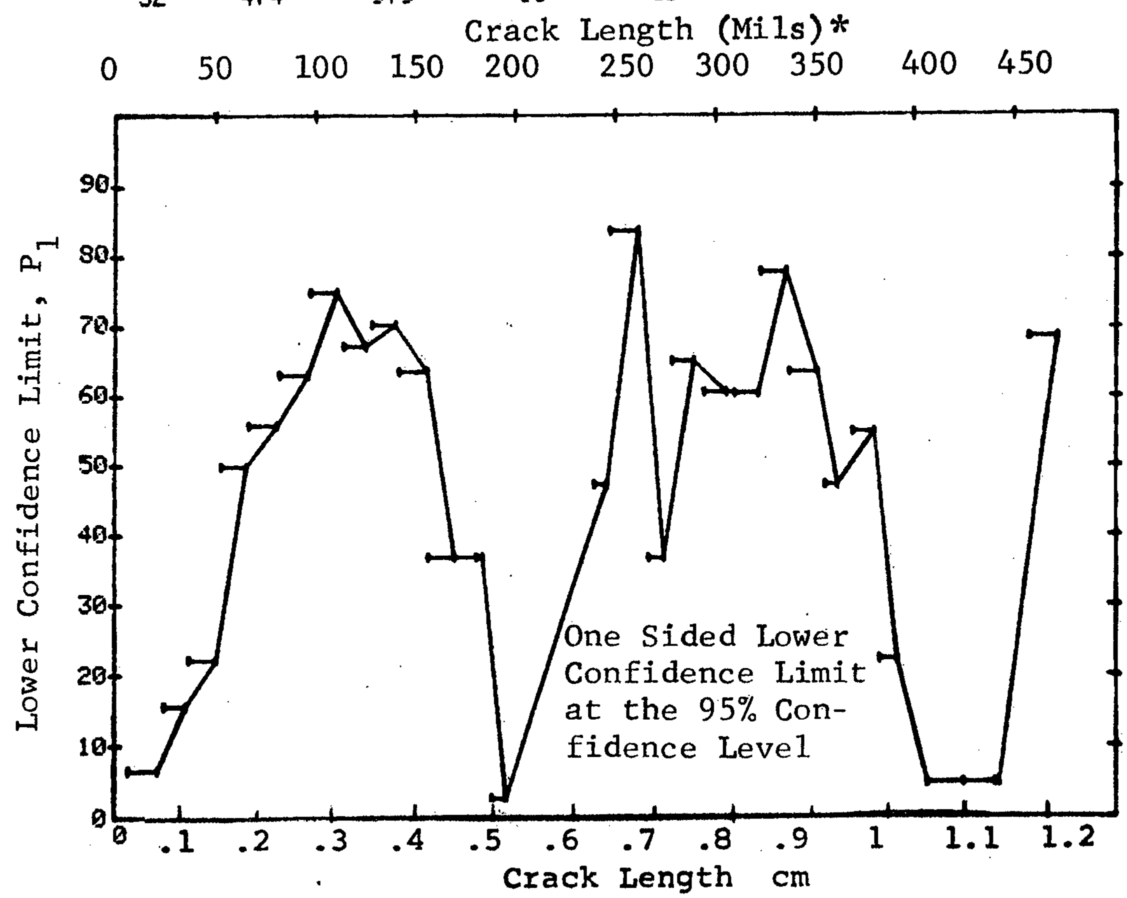

Figure D-16 Probability of Detection for 2219-T87 Al Using Liquid Penetrant. Etched Fatigue Cracks in Flat Plates Measured by Operator J D-48 Lab. Env.

(b) Optimum Probability Method of Data Cumulation

24-JUL-75 PENETRANT TEST 2, (16) ROCKWELL

RANGE	MIN LN	MAX LN	N	DET	50%	95%	0 MIL	
1	7	* 22*	13	3	0	6	0	0
2	7	36	31	9	0	16	0	0
3	25	52	41	15	0	24	0	0
4	54	67	46	29	0	49	0	0
5	54	82	99	65	0	57	0	0
6	83	97	39	30	0	63	0	0
7	98	111	17	16	0	75	0	0
8	98	126	34	31	0	78	0	0
9	98	141	53	48	0	81	50	63
10	98	157	68	61	0	81	61	[illegible]
11	98	171	71	64	0	82	58	71
12	98	185	74	67	0	82	55	66
13	98	197	76	68	0	81	66	[illegible]
14	0	0	0	0	0	0	0	0
15	0	0	0	0	0	0	0	0
16	98	247	80	72	0	83	62	74
17	241	262	21	21	0	86	8	25
18	241	275	24	24	0	88	5	22
19	241	290	31	31	0	90	0	15
20	241	306	37	37	0	92	0	9
21	241	322	47	46	0	90	0	14
22	241	336	59	58	0	92	0	2
23	241	352	70	68	0	91	0	6
24	241	362	74	72	0	91	0	2
25	241	381	79	77	0	92	0	0
26	241	393	81	79	0	92	0	0
27	241	408	82	80	0	92	0	0
28	241	426	83	81	0	92	0	0
29	241	442	84	82	0	92	0	0
30	241	444	85	83	0	92	0	0
31	241	472	93	91	0	93	0	0
32	241	979	153	150	0	95	0	0

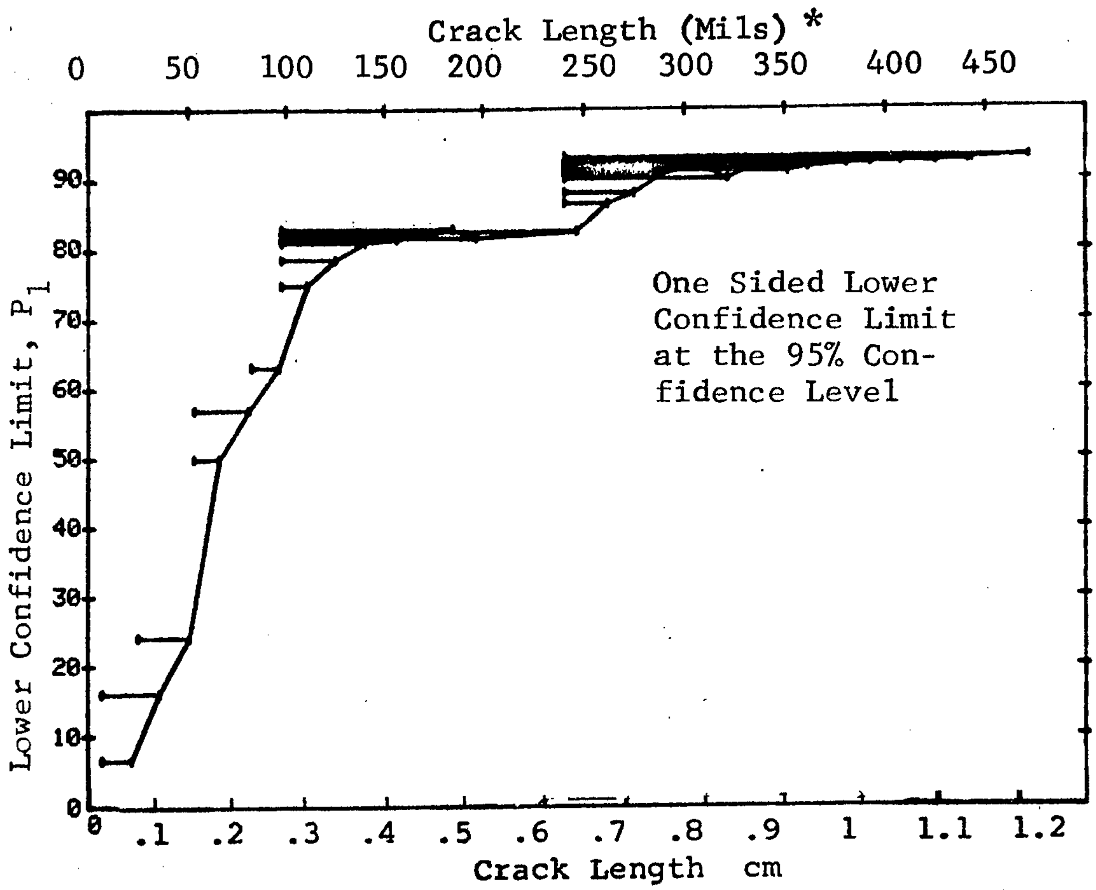

Figure D-16 (Continued)

(c) Overlapping Sixty Point Method of Data Cumulation

24-JUL-75 PENETRANT TEST 3, (16) ROCKWELL 50 J

RANGE	MIN LN *	MAX LN *	N	DET	50%	95%	0 MISS	1 MISS
1	0	0	0	0	0	0	0	0
2	0	0	0	0	0	0	0	0
3	0	0	0	0	0	0	0	0
4	0	0	0	0	0	0	0	0
5	0	0	0	0	0	0	0	0
6	0	0	0	0	0	0	0	0
7	0	0	0	0	0	0	0	0
8	0	0	0	0	0	0	0	0
9	0	0	0	0	0	0	0	0
10	0	0	0	0	0	0	0	0
11	0	0	0	0	0	0	0	0
12	0	0	0	0	0	0	0	0
13	0	0	0	0	0	0	0	0
14	0	0	0	0	0	0	0	0
15	0	0	0	0	0	0	0	0
16	0	0	0	0	0	0	0	0
17	0	0	0	0	0	0	0	0
18	0	0	0	0	0	0	0	0
19	0	0	0	0	0	0	0	0
20	0	0	0	0	0	0	0	0
21	7	49	52	16	29	20	0	0
22	31	63	60	29	47	37	0	0
23	51	70	60	37	60	50	0	0
24	64	79	60	42	69	58	0	0
25	70	87	60	40	65	55	0	0
26	79	105	60	45	74	64	0	0
27	88	131	60	57	93	87	16	29
28	105	162	60	54	88	81	56	69
29	132	275	60	55	90	83	43	56
30	171	330	60	58	95	89	1	16
31	279	442	60	58	95	89	1	16
32	331	500	60	58	95	89	1	16

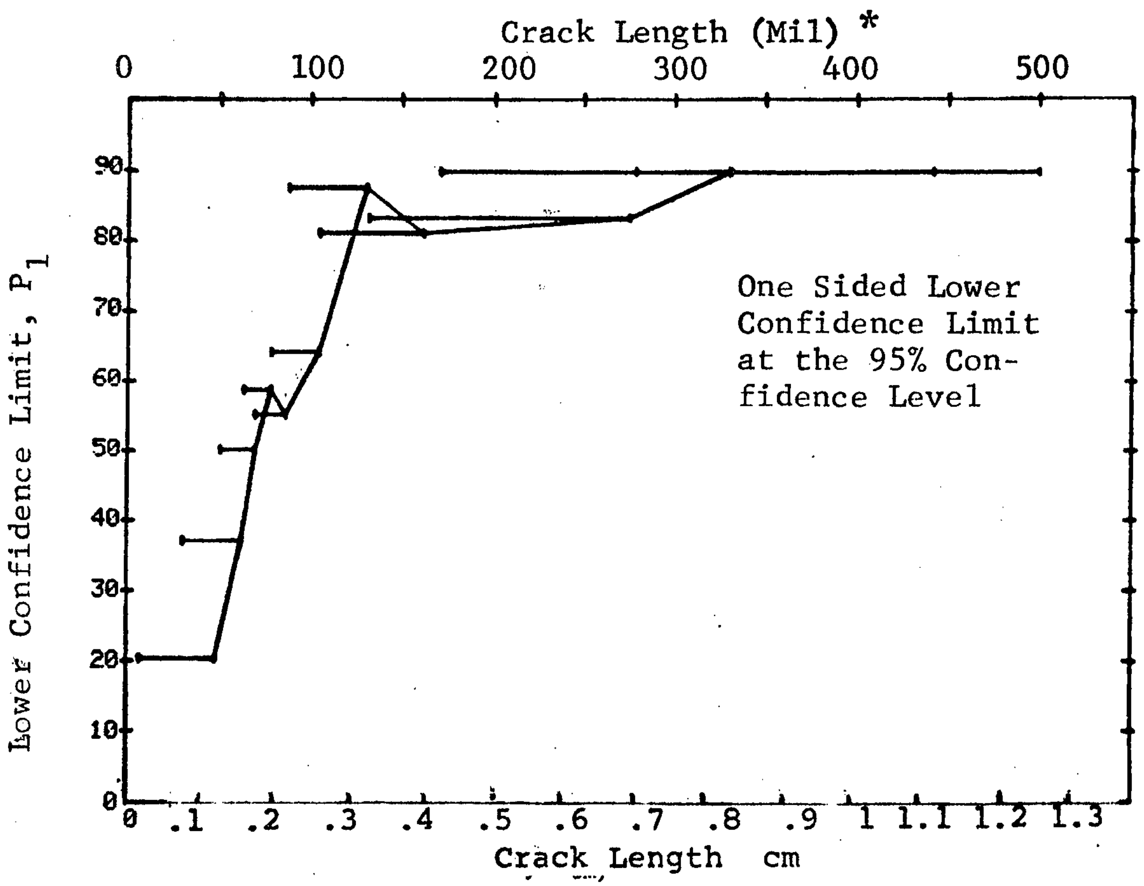

Figure D-16 (Concluded)

(a) Range Interval Method of Data Cumulation

24-JUL-75 PENETRANT TEST 1, · (17) ROCKWELL

RANGE	MIN LN	MAX LN	N	DET	50%	95%	0 MISS	1 MISS
1	7 *	22 *	13	3	20	6	0	0
2	25	36	18	9	47	29	0	0
3	38	52	23	16	67	50	0	0
4	54	67	46	37	79	68	0	0
5	68	82	54	46	84	74	0	0
6	83	97	39	37	93	84	22	37
7	98	111	17	17	96	83	12	29
8	115	126	17	16	90	75	29	44
9	129	141	19	19	96	85	10	27
10	143	157	15	15	95	81	14	31
11	158	171	3	3	79	36	0	0
12	182	185	3	3	79	36	0	0
13	190	197	2	2	70	22	0	0
14	0	0	0	0	0	0	0	0
15	0	0	0	0	0	0	0	0
16	241	247	4	4	84	47	0	0
17	248	262	17	17	96	83	12	29
18	268	275	3	3	79	36	0	0
19	279	290	7	7	90	65	0	0
20	295	306	6	6	89	60	0	0
21	310	322	10	10	93	74	0	0
22	323	336	12	12	94	77	17	34
23	338	352	11	11	93	76	18	35
24	356	362	4	4	84	47	0	0
25	370	381	5	5	87	54	0	0
26	384	393	2	2	70	22	0	0
27	408	408	1	1	50	5	0	0
28	426	426	1	1	50	5	0	0
29	442	442	1	1	50	5	0	0
30	444	444	1	1	50	5	0	0
31	458	472	8	8	91	68	0	0
32	474	979	59	59	98	95	0	0

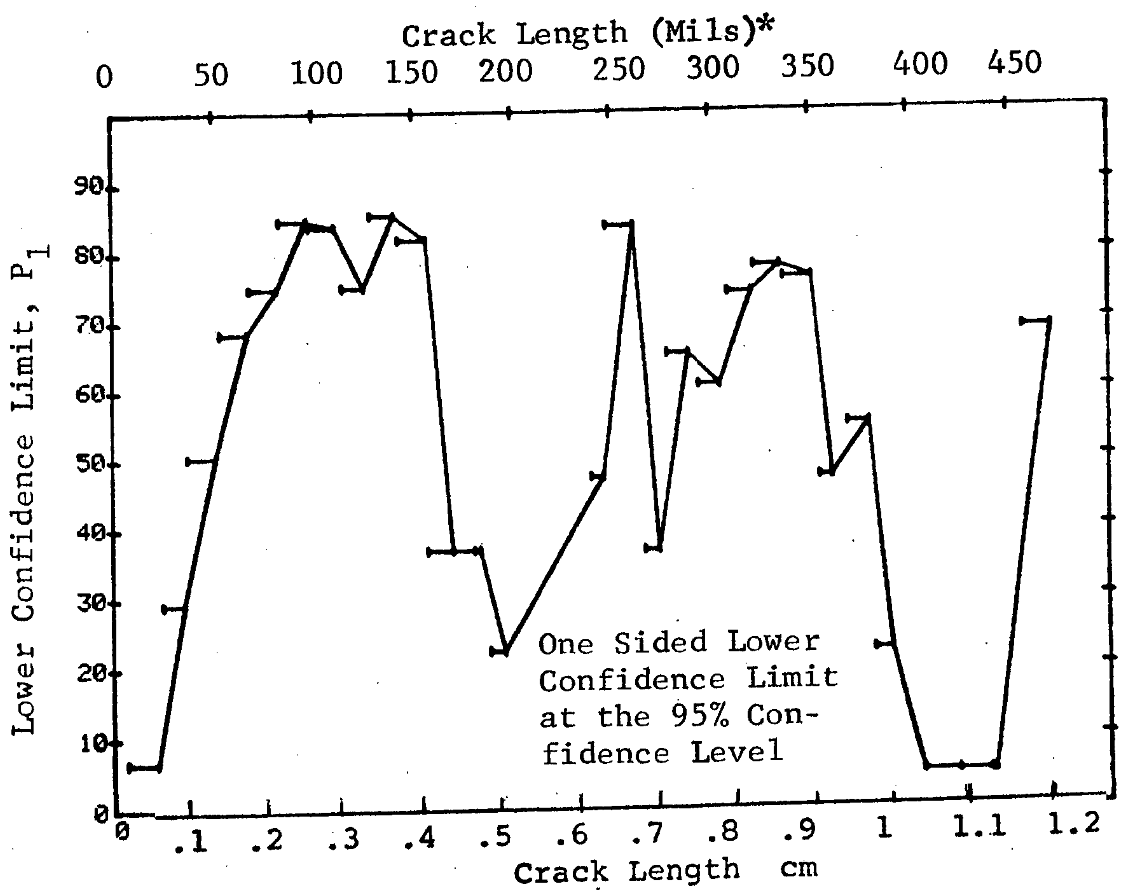

Figure D-17 Probability of Detection for 2219-T87 Al Using Liquid Penetrant. Etched Fatigue Cracks in Flat Plates Measured by Operator K Lab. Env.

(b) Optimum Probability Method of Data Cumulation

24-JUL-75 PENETRANT TEST 2, (17) ROCKWELL 3C K

RANGE	MIN LN	MAX LN	N	DET	50%	95%	0 MISS	1 MISS
1	7 *	22 *	13	3	0	6	0	0
2	25	36	18	9	0	29	0	0
3	38	52	23	16	0	50	0	0
4	54	67	46	37	0	68	0	0
5	54	82	100	83	0	75	0	0
6	83	97	39	37	0	84	22	37
7	83	111	56	54	0	89	5	30
8	83	126	73	70	0	89	3	16
9	83	141	92	89	0	91	0	0
10	98	157	68	67	0	93	0	0
11	98	171	71	70	0	93	0	0
12	98	185	74	73	0	93	0	0
13	98	197	76	75	0	93	0	0
14	0	0	0	0	0	0	0	0
15	0	0	0	0	0	0	0	0
16	98	247	80	79	0	94	0	0
17	129	262	63	63	0	95	0	0
18	129	275	66	66	0	95	0	0
19	129	290	73	73	0	95	0	0
20	129	306	79	79	0	96	0	0
21	129	322	89	89	0	96	0	0
22	129	336	101	101	0	97	0	0
23	129	352	112	112	0	97	0	0
24	129	362	116	116	0	97	0	0
25	129	381	121	121	0	97	0	0
26	129	393	123	123	0	97	0	0
27	129	408	124	124	0	97	0	0
28	129	426	125	125	0	97	0	0
29	129	442	126	126	0	97	0	0
30	129	444	127	127	0	97	0	0
31	129	472	135	135	0	97	0	0
32	129	979	194	194	0	98	0	0

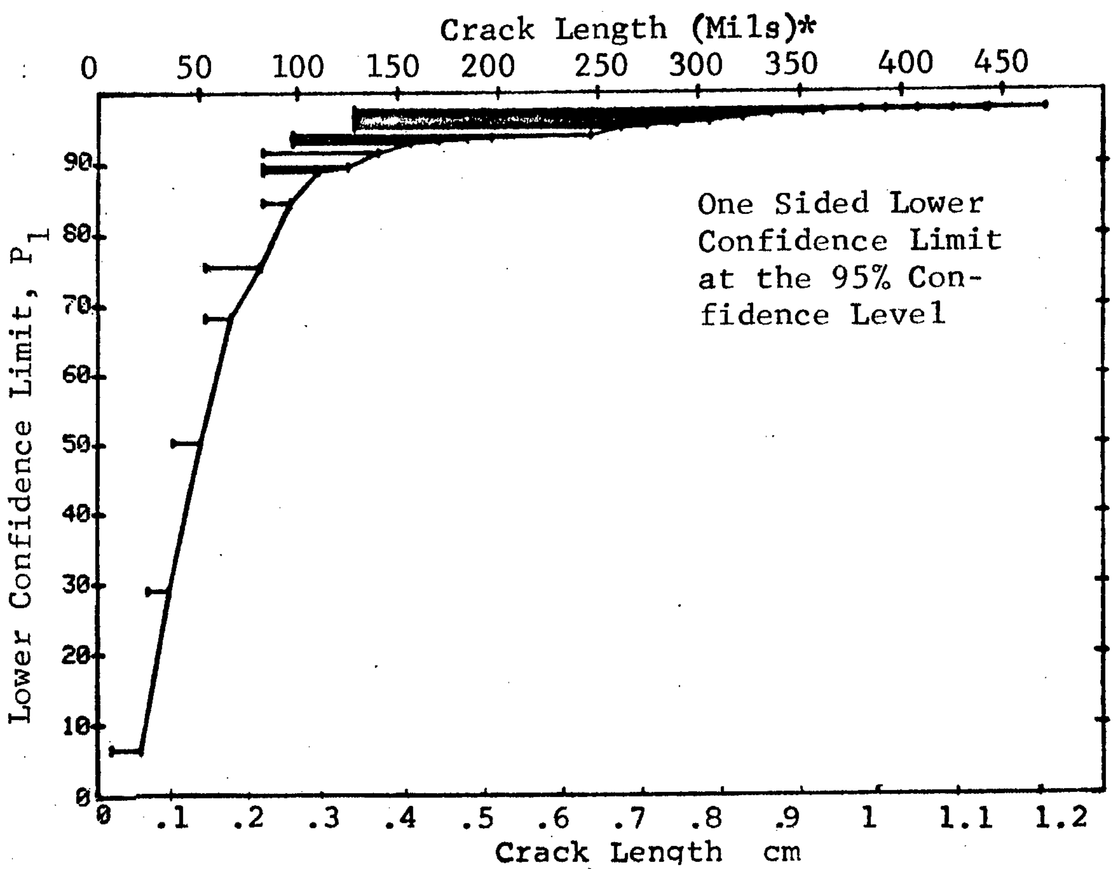

Figure D-17 (Continued)

(c) Overlapping Sixty Point Method of Data Cumulation

24-JUL-75 PENETRANT TEST 3, (17) ROCKWELL 56 K

RANGE	MIN LN	MAX LN	N	DET	50%	95%	0 MISS	1 MISS
1	0 *	0 *	0	0	0	0	0	0
2	0	0	0	0	0	0	0	0
3	0	0	0	0	0	0	0	0
4	0	0	0	0	0	0	0	0
5	0	0	0	0	0	0	0	0
6	0	0	0	0	0	0	0	0
7	0	0	0	0	0	0	0	0
8	0	0	0	0	0	0	0	0
9	0	0	0	0	0	0	0	0
10	0	0	0	0	0	0	0	0
11	0	0	0	0	0	0	0	0
12	0	0	0	0	0	0	0	0
13	0	0	0	0	0	0	0	0
14	0	0	0	0	0	0	0	0
15	0	0	0	0	0	0	0	0
16	0	0	0	0	0	0	0	0
17	0	0	0	0	0	0	0	0
18	0	0	0	0	0	0	0	0
19	0	0	0	0	0	0	0	0
20	0	0	0	0	0	0	0	0
21	7	51	53	27	50	38	0	0
22	32	64	60	45	74	64	0	0
23	52	70	60	47	77	67	0	0
24	64	79	60	51	83	75	94	100
25	70	87	60	54	88	81	56	69
26	79	105	60	56	92	85	29	43
27	88	131	60	59	97	92	0	1
28	105	162	60	59	97	92	0	1
29	132	275	60	60	98	95	0	0
30	171	330	60	60	98	95	0	0
31	279	442	60	60	98	95	0	0
32	331	500	60	60	98	95	0	0

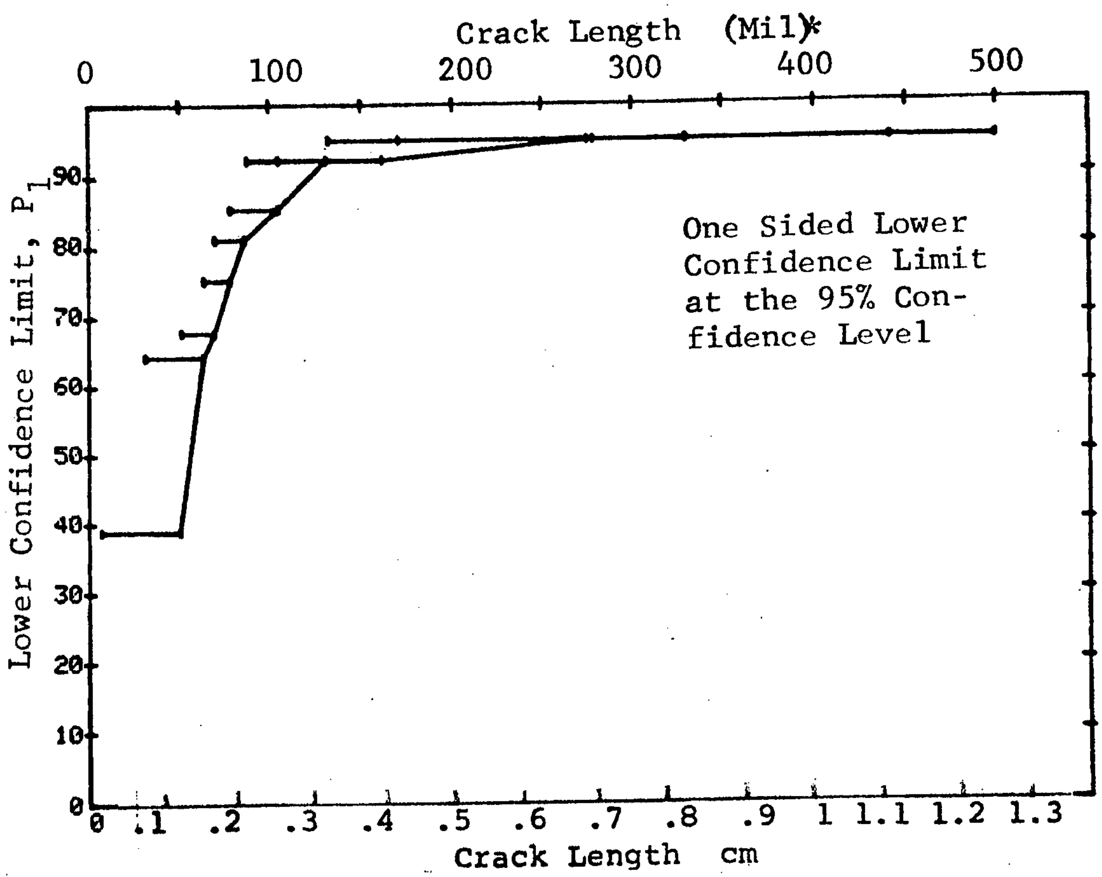

Figure D-17 (Concluded)

(a) Range Interval Method of Data Cumulation

24-JUL-75 PENETRANT TEST 1, (18) ROCKWELL SC L

RANGE	MIN LN *	MAX LN *	N	DET	50%	95%	0 MISS	1 MISS
1	7	22	13	3	20	6	0	0
2	25	36	18	13	69	50	0	0
3	38	52	23	15	62	45	0	0
4	54	67	46	34	72	61	0	0
5	68	82	53	46	85	76	76	89
6	83	97	39	34	85	74	0	0
7	98	111	17	15	84	67	0	0
8	115	126	17	15	84	67	0	0
9	129	141	19	15	75	58	0	0
10	143	157	15	11	69	48	0	0
11	158	171	3	3	79	36	0	0
12	182	185	3	3	79	36	0	0
13	190	197	2	1	29	2	0	0
14	0	0	0	0	0	0	0	0
15	0	0	0	0	0	0	0	0
16	241	247	4	4	84	47	0	0
17	248	262	17	17	96	83	12	29
18	268	275	3	3	79	36	0	0
19	279	290	7	7	90	65	0	0
20	295	306	6	5	73	41	0	0
21	310	322	10	10	93	74	0	0
22	323	336	12	11	86	66	0	0
23	338	352	11	7	58	34	0	0
24	356	362	4	4	84	47	0	0
25	370	381	5	2	31	7	0	0
26	384	393	2	1	29	2	0	0
27	408	408	1	1	50	5	0	0
28	426	426	1	1	50	5	0	0
29	442	442	1	0	0	0	0	0
30	444	444	1	1	50	5	0	0
31	458	472	8	6	67	40	0	0
32	474	979	59	54	90	83	44	57

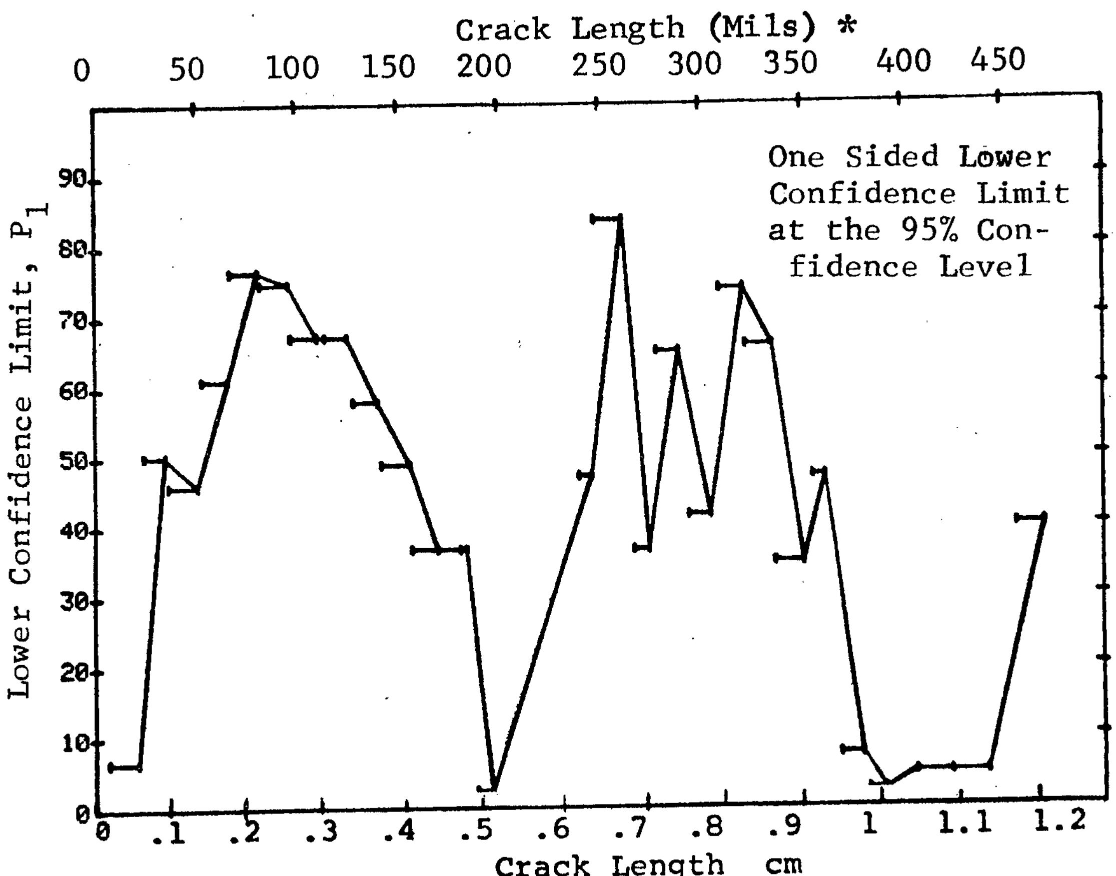

Figure D-18 Probability of Detection for 2219-T87 Al Using Liquid Penetrant. Etched Fatigue Cracks in Flat Plates Measured by Operator L. Lab. Env.

(b) Optimum Probability Method of Data Cumulation

24-JUL-75 PENETRANT TEST 2. (18)" ROCKWELL

RANGE	MIN LN	MAX LN	N	DET	50%	95%	0 MISS	1 MISS
1	7	* 22 *	13	3	0	6	0	0
2	25	36	18	13	0	50	0	0
3	25	52	41	28	0	54	0	0
4	25	67	87	62	0	62	0	0
5	68	82	53	46	0	76	0	0
6	68	97	92	80	0	79	0	0
7	68	111	109	95	0	80	0	0
8	68	126	126	110	0	81	0	0
9	68	141	145	125	0	80	0	0
10	68	157	160	136	0	79	0	0
11	68	171	163	139	0	79	0	0
12	68	185	166	142	0	80	0	0
13	68	197	168	143	0	79	0	0
14	0	0	0	0	0	0	0	0
15	0	0	0	0	0	0	0	0
16	68	247	172	147	0	80	0	0
17	241	262	21	21	0	86	8	25
18	241	275	24	24	0	88	5	22
19	241	290	31	31	0	90	0	15
20	241	306	37	36	0	87	9	24
21	241	322	47	46	0	90	0	14
22	241	336	59	57	0	89	2	17
23	241	352	70	64	0	83	46	59
24	241	362	74	68	0	84	42	55
25	68	381	247	213	0	82	0	0
26	68	393	249	214	0	81	0	0
27	68	408	250	215	0	81	0	0
28	68	426	251	216	0	81	0	0
29	68	442	252	216	0	81	0	0
30	68	444	253	217	0	81	0	0
31	68	472	261	223	0	81	0	0
32	159	979	160	141	0	83	0	0

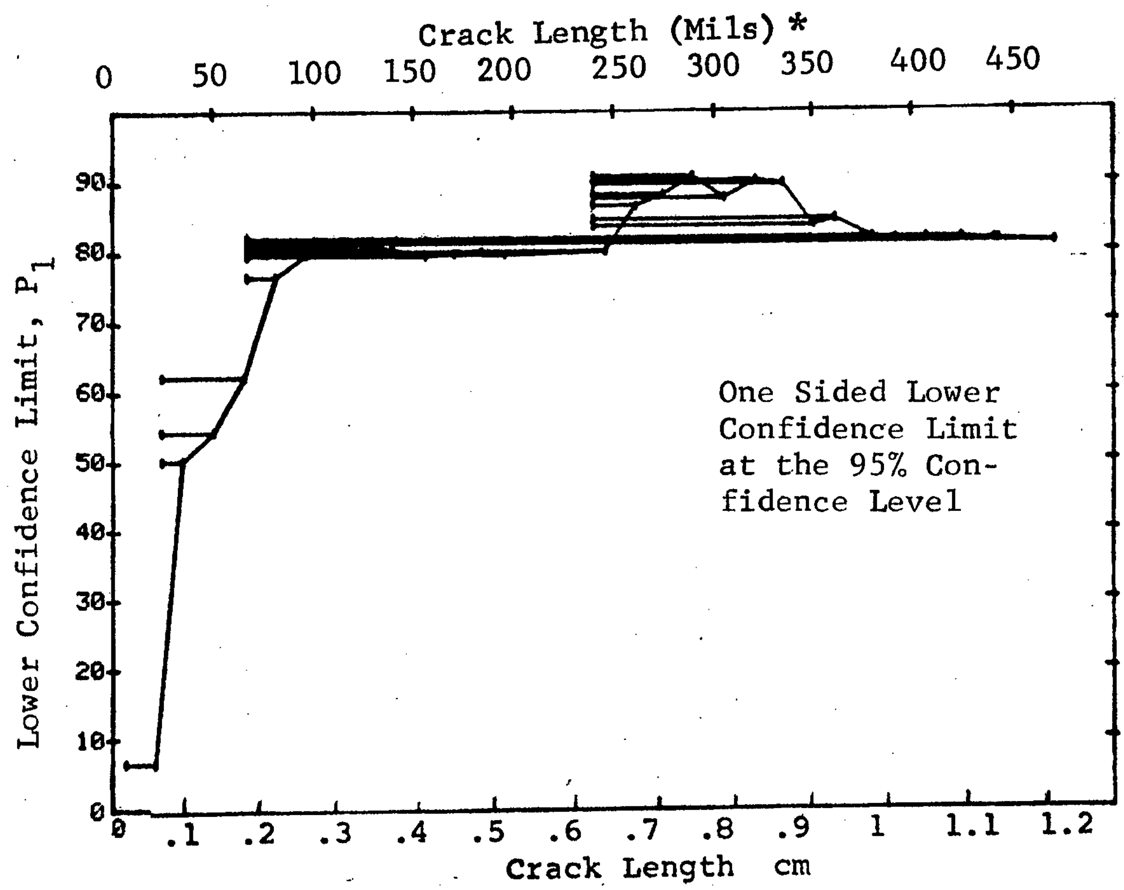

Figure D-18 (Continued)

(c) Overlapping Sixty Point Method of Data Cumulation

24-JUL-75	PENETRANT			TEST 3, (18)		ROCKWELL SL L		
RANGE	MIN LN	MAX LN	N	DET	50%	95%	0 MISS	1 MISS
1	0*	0 *	0	0	0	0	0	0
2	0*	0	0	0	0	0	0	0
3	0	0	0	0	0	0	0	0
4	0	0	0	0	0	0	0	0
5	0	0	0	0	0	0	0	0
6	0	0	0	0	0	0	0	0
7	0	0	0	0	0	0	0	0
8	0	0	0	0	0	0	0	0
9	0	0	0	0	0	0	0	0
10	0	0	0	0	0	0	0	0
11	0	0	0	0	0	0	0	0
12	0	0	0	0	0	0	0	0
13	0	0	0	0	0	0	0	0
14	0	0	0	0	0	0	0	0
15	0	0	0	0	0	0	0	0
16	0	0	0	0	0	0	0	0
17	0	0	0	0	0	0	0	0
18	0	0	0	0	0	0	0	0
19	0	0	0	0	0	0	0	0
20	0	0	0	0	0	0	0	0
21	7	49	52	30	56	45	0	0
22	31	63	60	44	72	62	0	0
23	51	70	60	43	70	60	0	0
24	64	79	60	47	77	67	0	0
25	70	87	60	55	90	83	43	56
26	79	105	60	53	87	79	69	82
27	88	131	60	52	85	77	82	94
28	105	162	60	49	80	71	0	0
29	132	275	60	52	85	77	82	94
30	171	330	60	58	95	89	1	16
31	279	442	60	49	80	71	0	0
32	331	500	60	46	75	65	0	0

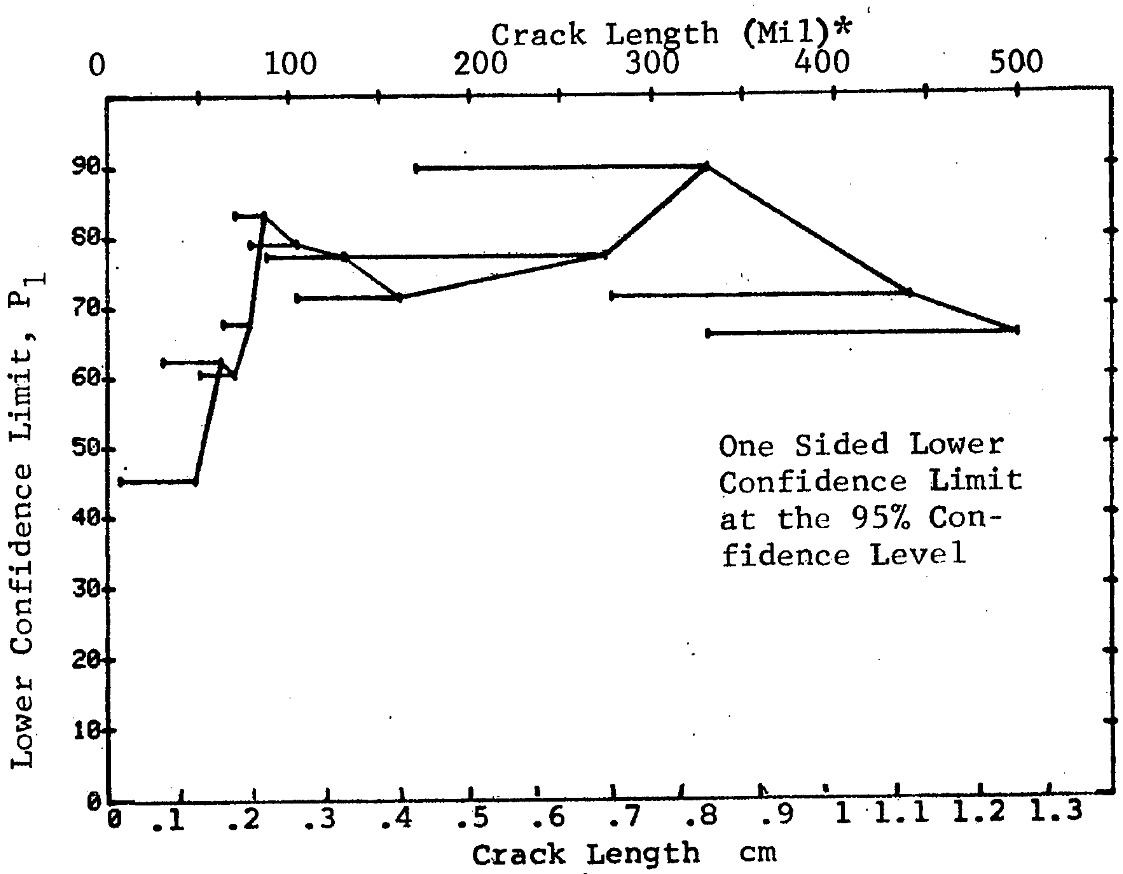

Figure D-18 (Concluded)

(a) Range Interval Method of Data Cumulation

18-SEP-75 PENETRANT P-1 (19) M

RANGE	MIN LN *	MAX LN *	N	DET	50%	95%	0 MISS	1 MISS
1	10	41	36	17	45	32	0	[illegible]
2	42	72	80	65	80	72	[illegible]	[illegible]
3	73	103	82	78	94	89	7	21
4	104	134	36	34	92	83	25	4
5	135	162	26	21	78	63	0	[illegible]
6	171	190	4	4	84	47	0	0
7	197	197	1	1	50	5	0	0
8	241	258	16	16	95	82	13	30
9	259	288	13	13	94	79	15	77
10	290	318	16	16	95	82	17	[illegible]
11	321	347	23	22	92	80	23	78
12	352	381	11	10	85	63	0	[illegible]
13	384	408	3	3	79	36	0	[illegible]
14	426	444	3	3	79	36	0	0
15	458	475	11	11	93	76	18	35
16	478	506	22	22	96	87	7	24
17	508	535	25	25	97	88	4	21
18	538	568	6	6	89	60	0	[illegible]
19	0	0	0	0	0	0	0	0
20	610	610	1	1	50	5	0	0
21	0	0	0	0	0	0	0	0
22	0	0	0	0	0	0	0	0
23	710	710	1	1	50	5	0	0
24	0	0	0	0	0	0	0	0
25	0	0	0	0	0	0	0	0
26	0	0	0	0	0	0	0	[illegible]
27	0	0	0	0	0	0	0	0
28	0	0	0	0	0	0	0	0
29	0	0	0	0	0	0	[illegible]	0
30	0	0	0	0	0	0	[illegible]	0
31	0	0	0	0	0	0	[illegible]	0
32	979	979	1	1	50	5	[illegible]	0

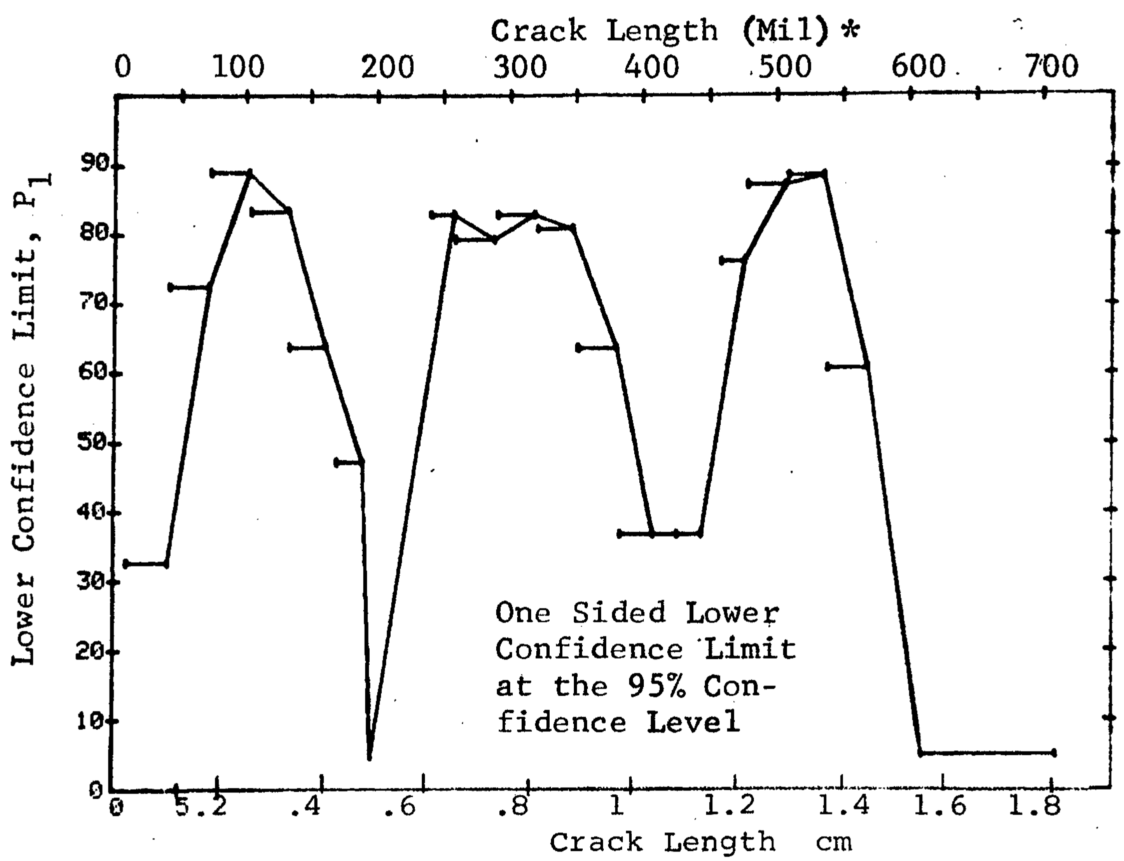

Figure D-19 Probability of Detection for 2219-T87 Al Using Liquid Penetrant. Etched Fatigue Cracks in Flat Plates Measured by Operator M. Lab. Env.

(b) Optimum Probability Method of Data Cumulation

18-SEP-75 RANGE	MIN LN	PENETRANT MAX LN	N	P-2. (19) DET	50%	M 95%	0 MI[illegible]	1 M[illegible]
1	10 *	41 *	36	17	0	32	0	[illegible]
2	42	72	80	65	0	72	0	[illegible]
3	73	103	82	78	0	89	[illegible]	[illegible]
4	73	134	118	112	0	90	0	0
5	73	162	144	133	0	87	0	[illegible]
6	73	190	148	137	0	87	0	0
7	73	197	149	138	0	88	0	0
8	73	258	165	154	0	89	0	0
9	171	288	34	34	0	91	0	[illegible]
10	171	318	50	50	0	94	0	0
11	171	347	73	72	0	93	0	0
12	171	381	84	82	0	92	0	0
13	171	408	87	85	0	92	0	0
14	171	444	90	88	0	93	0	0
15	171	475	101	99	0	93	0	0
16	171	506	123	121	0	94	0	0
17	171	535	148	146	0	95	0	0
18	171	568	154	152	0	95	0	0
19	0	0	0	0	0	0	0	0
20	171	610	155	153	0	95	0	0
21	0	0	0	0	0	0	0	0
22	0	0	0	0	0	0	0	0
23	171	710	156	154	0	96	0	0
24	0	0	0	0	0	0	0	0
25	0	0	0	0	0	0	0	0
26	0	0	0	0	0	0	0	0
27	0	0	0	0	0	0	0	0
28	0	0	0	0	0	0	0	0
29	0	0	0	0	0	0	[illegible]	0
30	0	0	0	0	0	0	0	0
31	0	0	0	0	0	0	0	0
32	171	979	157	155	0	96	0	0

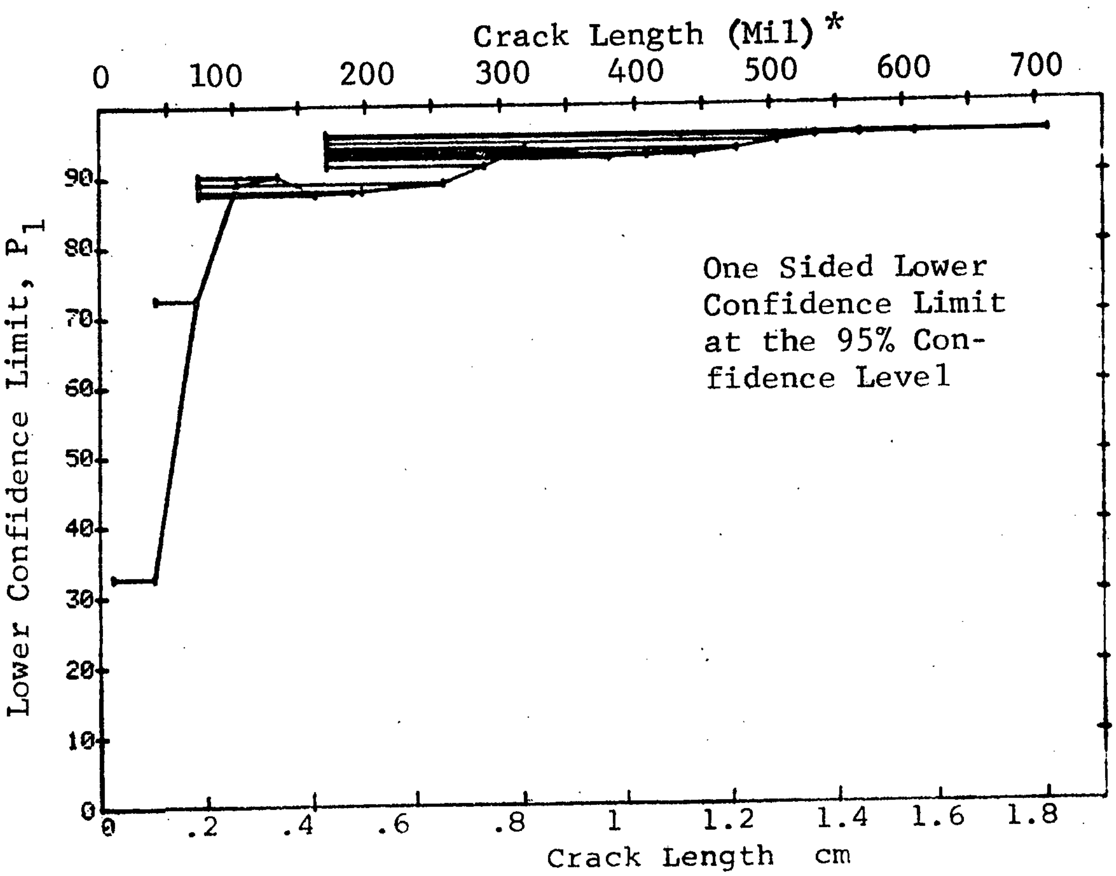

Figure D-19 (Continued) for A[illegible]

(c) Overlapping Sixty Point Method of Data Cumulation

18-SEP-75 PENETRANT P-[illegible] (19) M

RANGE	MIN LN	MAX LN	N	DET	50%	95%	0 MI[illegible]	[illegible]
1	0*	0*	0	0	0	0	0	
2	0	0	0	0	0	0	[illegible]	
3	0	0	0	0	0	0	0	
4	0	0	0	0	0	0	0	[illegible]
5	0	0	0	0	0	0	[illegible]	
6	0	0	0	0	0	0	0	0
7	0	0	0	0	0	0	0	0
8	0	0	0	0	0	0	0	0
9	0	0	0	0	0	0	0	[illegible]
10	0	0	0	0	0	0	0	0
11	0	0	0	0	0	0	0	0
12	0	0	0	0	0	0	0	0
13	0	0	0	0	0	0	0	0
14	0	0	0	0	0	0	0	0
15	0	0	0	0	0	0	0	0
16	0	0	0	0	0	0	0	0
17	0	0	0	0	0	0	0	0
18	0	0	0	0	0	0	0	[illegible]
19	0	0	0	0	0	0	0	[illegible]
20	10	52	52	30	56	45	0	[illegible]
21	32	64	60	46	75	65	0	[illegible]
22	54	70	60	49	80	71	0	[illegible]
23	64	80	60	52	85	77	82	[illegible]
24	71	89	60	55	90	83	43	[illegible]
25	80	106	60	58	95	89	1	[illegible]
26	89	134	60	58	95	89	1	[illegible]
27	106	182	60	53	87	79	69	82
28	134	283	60	55	90	83	43	56
29	183	333	60	60	98	[illegible]	[illegible]	
30	287	458	60	58	95	89	1	[illegible]
31	334	506	60	58	95	89	1	[illegible]
32	459	550	60	60	98	95	0	[illegible]

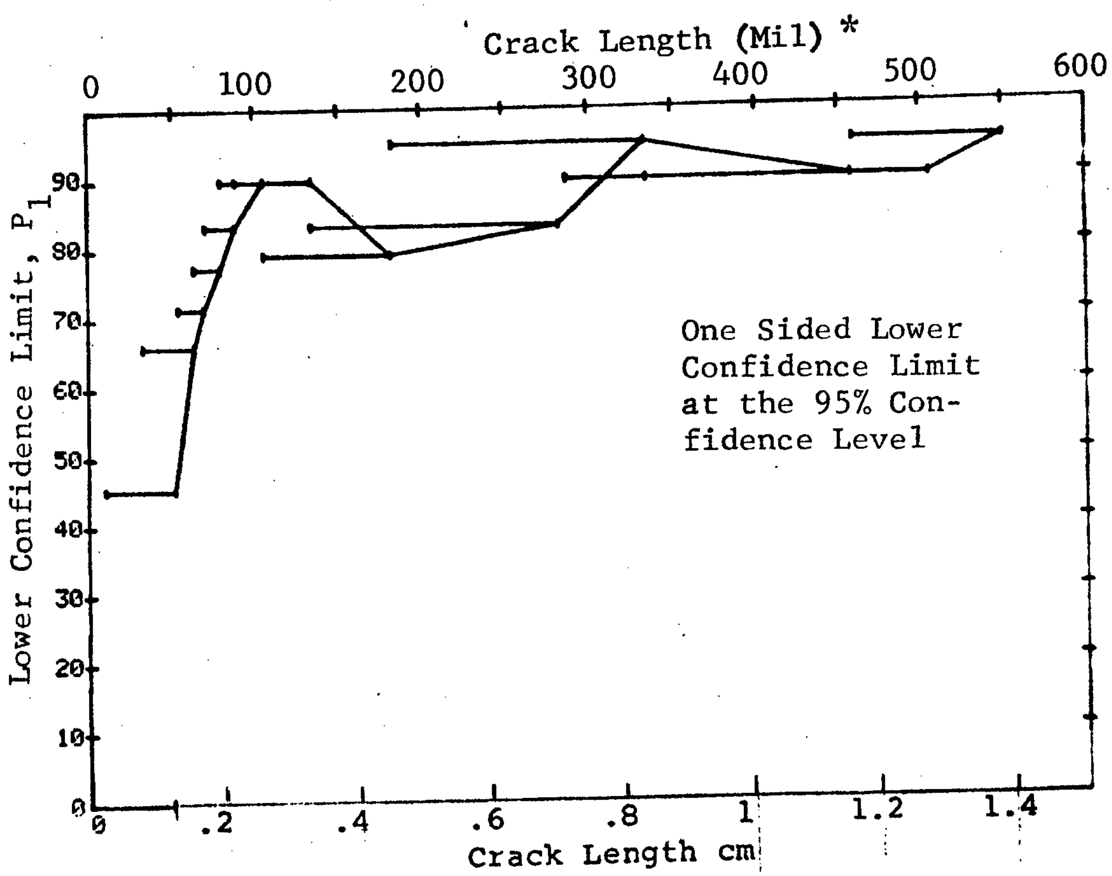

Figure D-19 (Concluded)

(a) Range Interval Method of Data Cumulation

18-SEP-75 PENETRANT F-1, (20) N

RANGE	MIN LN *	MAX LN *	N	DET	50%	95%	0 MI[illegible]	1 [illegible]
1	10	41	37	12	31	19	0	[illegible]
2	42	2	[illegible]80	60	74	65	0	
3	73	103	82	72	87	80	85	[illegible]
4	104	134	36	32	87	76	53	[illegible]
5	135	162	26	20	74	59	0	
6	171	190	5	5	87	54	0	0
7	197	197	1	1	50	5	0	0
8	241	258	16	15	89	73	0	0
9	259	288	13	13	94	79	16	37
10	290	318	16	15	89	73	0	0
11	321	347	23	20	84	69	0	0
12	352	381	11	10	85	63	0	0
13	384	408	3	3	79	36	0	0
14	426	444	3	3	79	36	0	0
15	458	475	11	11	93	76	18	35
16	478	506	22	21	92	80	24	[illegible]
17	508	535	25	25	97	88	4	21
18	538	568	6	6	89	60	0	0
19	0	0	0	0	0	0	0	0
20	610	610	1	1	50	5	0	0
21	0	0	0	0	0	0	0	0
22	0	0	0	0	0	0	0	0
23	710	710	1	1	50	5	0	0
24	0	0	0	0	0	0	0	0
25	0	0	0	0	0	0	0	0
26	0	0	0	0	0	0	0	0
27	0	0	0	0	0	0	0	0
28	0	0	0	0	0	0	0	0
29	0	0	0	0	0	0	0	0
30	0	0	0	0	0	0	0	0
31	0	0	0	0	0	0	0	0
32	979	979	1	1	50	5	0	0

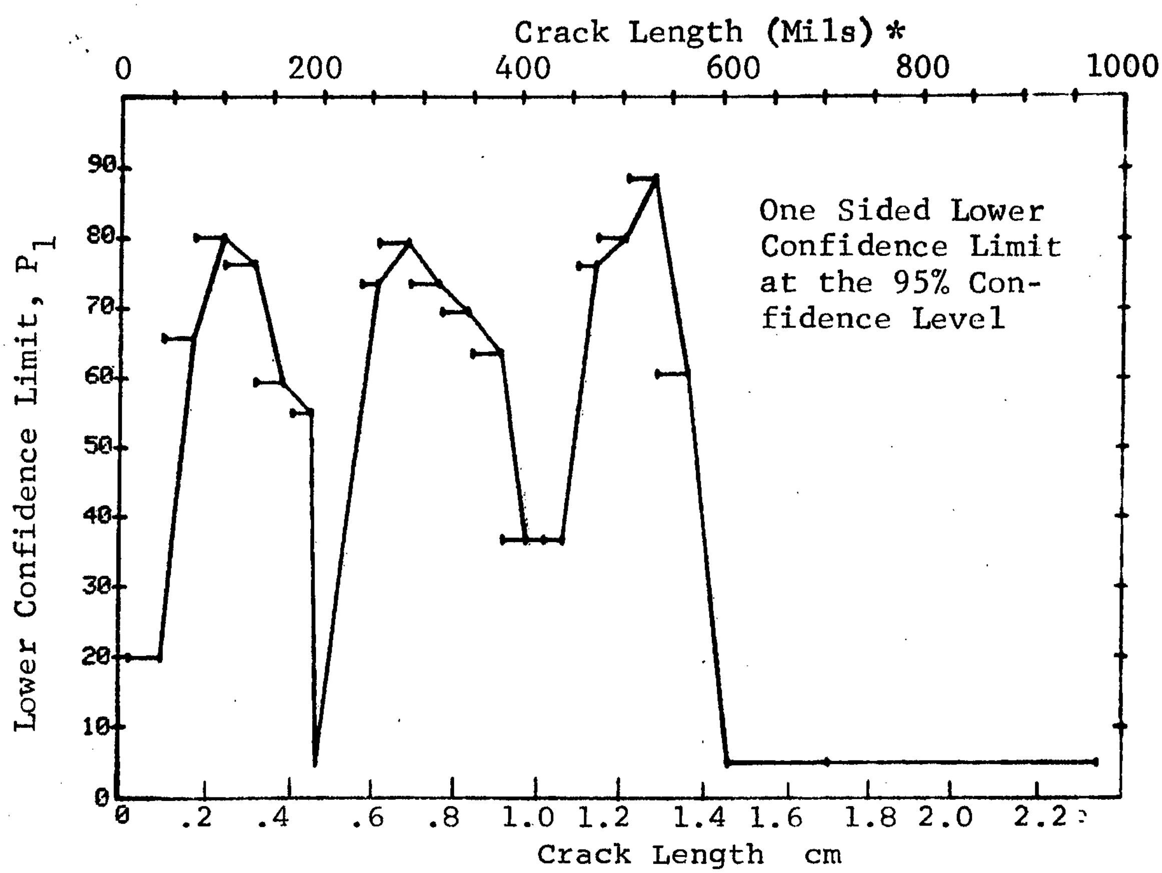

Figure D-20 Probability of Detection for 2219-T87 Al Using Liquid Penetrant. Etched Fatigue Cracks in Flat Plates Measured by Operator N. Lab. Env.

(b) Optimum Probability Method of Data Cumulation

18-SEP-75 PENETRANT P-2, (20) N

RANGE	MIN LN	MAX LN	N	DET	50%	95%	0 MISS	[illegible]
1	10 *	41 *	37	12	0	19	0	[illegible]
2	42	72	80	60	0	65	0	[illegible]
3	73	103	82	72	0	80	85	[illegible]
4	73	134	118	104	0	82	0	[illegible]
5	73	162	144	124	0	80	0	
6	73	190	149	129	0	81	0	0
7	73	197	150	130	0	81	0	[illegible]
8	73	258	166	145	0	82	0	0
9	171	288	35	34	0	87	11	[illegible]
10	171	318	51	49	0	88	10	[illegible]
11	171	347	74	69	0	86	29	[illegible]
12	171	381	85	79	0	86	31	44
13	171	408	88	82	0	86	28	[illegible]
14	171	444	91	85	0	87	25	[illegible]
15	171	475	102	96	0	88	0	[illegible]
16	171	506	124	117	0	89	0	[illegible]
17	384	535	64	63	0	92	0	[illegible]
18	384	568	70	69	0	93	0	[illegible]
19	0	0	0	0	0	0	0	[illegible]
20	384	610	71	70	0	93	0	[illegible]
21	0	0	0	0	0	0	0	[illegible]
22	0	0	0	0	0	0	0	[illegible]
23	384	710	72	71	0	93	0	[illegible]
24	0	0	0	0	0	0	0	[illegible]
25	0	0	0	0	0	0	0	[illegible]
26	0	0	0	0	0	0	0	[illegible]
27	0	0	0	0	0	0	0	0
28	0	0	0	0	0	0	0	0
29	0	0	0	0	0	0	[illegible]	[illegible]
30	0	0	0	0	0	0	[illegible]	[illegible]
31	0	0	0	0	0	0	[illegible]	[illegible]
32	384	979	73	72	0	93	[illegible]	[illegible]

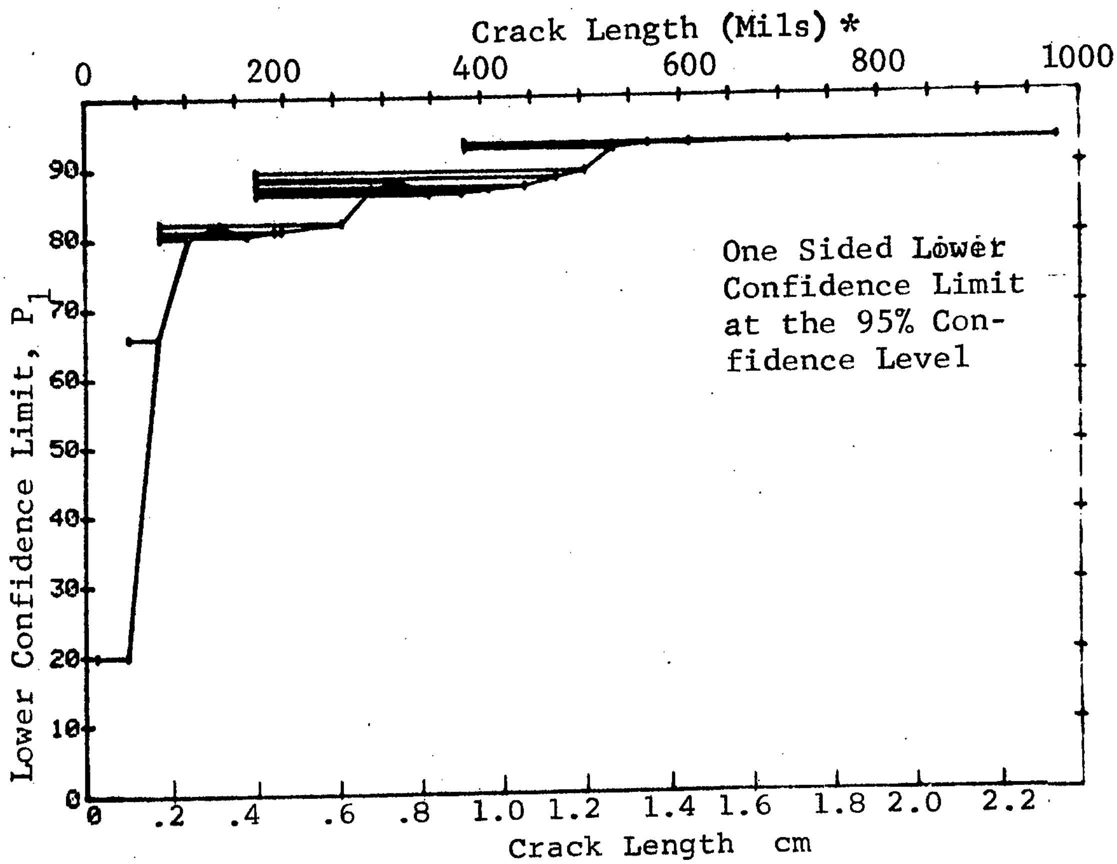

Figure D-20 (Continued)

(c) Overlapping Sixty Point Method of Data Cumulation

18-SEP-75 RANGE	MIN LN	PENETRANT * MAX LN *	N	P-3, DET	(20) 50%	N 95%	0 MI[illegible]	[illegible]
1	0	0	0	0	0	0	0	0
2	0	0	0	0	0	0	[illegible]	[illegible]
3	0	0	0	0	0	0	0	[illegible]
4	0	0	0	0	0	0	0	[illegible]
5	0	0	0	0	0	0	0	[illegible]
6	0	0	0	0	0	0	0	0
7	0	0	0	0	0	0	0	0
8	0	0	0	0	0	0	0	0
9	0	0	0	0	0	0	0	0
10	0	0	0	0	0	0	0	0
11	0	0	0	0	0	0	0	0
12	0	0	0	0	0	0	0	0
13	0	0	0	0	0	0	0	[illegible]
14	0	0	0	0	0	0	0	0
15	0	0	0	0	0	0	0	0
16	0	0	0	0	0	0	0	0
17	0	0	0	0	0	0	0	0
18	0	0	0	0	0	0	0	0
19	0	0	0	0	0	0	0	0
20	10	54	54	26	47	36	0	0
21	33	64	60	44	72	62	0	0
22	55	71	60	45	74	64	0	0
23	64	80	60	45	74	64	0	0
24	71	89	60	50	82	73	0	0
25	80	106	60	55	90	83	43	56
26	90	134	60	54	88	81	56	[illegible]
27	108	183	60	50	82	73	0	0
28	134	283	60	53	87	79	69	82
29	185	333	60	57	93	87	[illegible]	[illegible]
30	287	459	60	55	90	83	43	[illegible]
31	334	506	60	56	92	85	29	43
32	459	550	60	59	97	92	0	1

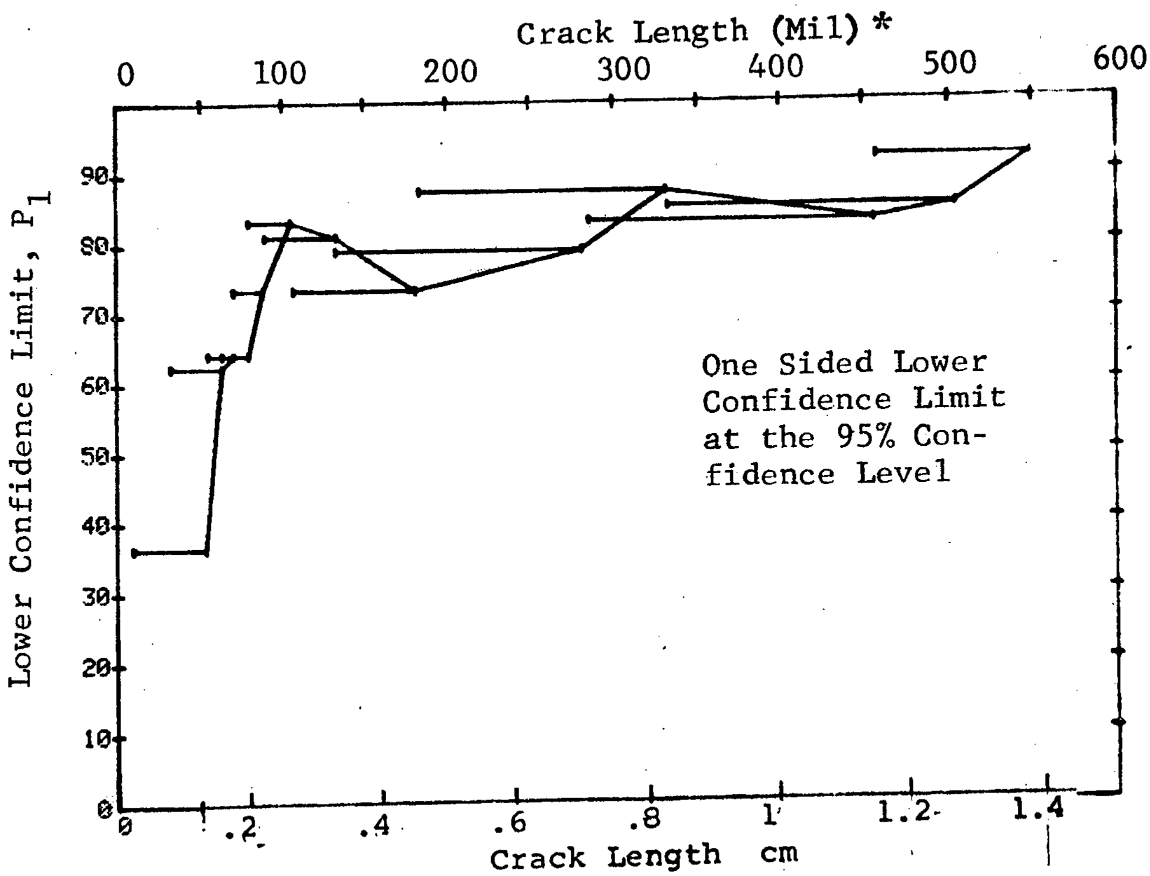

Figure D-20 (Concluded)

(a) Range Interval Method of Data Cumulation

24-JUL-75 EDDY CURRENT TEST 1, (21) T

RANGE	MIN LN	* MAX LN *	N	DET	50%	95%	0 MISS	1 MISS
1	7	22	13	1	5	0	0	0
2	25	36	18	2	9	2	0	0
3	38	51	23	3	11	3	0	0
4	54	67	46	30	64	52	0	0
5	68	82	53	36	66	55	0	0
6	83	97	38	36	93	84	23	38
7	98	111	18	16	85	68	0	0
8	115	126	17	16	90	75	29	44
9	129	141	19	17	86	70	0	0
10	143	157	15	15	95	81	14	31
11	158	171	3	3	79	36	0	0
12	182	185	3	3	79	36	0	0
13	190	197	2	2	70	22	0	0
14	0	0	0	0	0	0	0	0
15	232	232	1	1	50	5	0	0
16	241	247	3	3	79	36	0	0
17	248	262	17	17	96	83	12	29
18	268	275	3	3	79	36	0	0
19	279	290	7	7	90	65	0	0
20	295	304	6	6	89	60	0	0
21	310	322	10	10	93	74	0	0
22	323	336	12	12	94	77	17	34
23	338	352	11	11	93	76	18	35
24	356	362	4	4	84	47	0	0
25	370	381	5	5	87	54	0	0
26	384	393	2	2	70	22	0	0
27	408	408	1	1	50	5	0	0
28	426	426	1	1	50	5	0	0
29	442	442	1	1	50	5	0	0
30	444	444	1	1	50	5	0	0
31	458	472	8	8	91	68	0	0
32	474	979	59	59	98	95	0	0

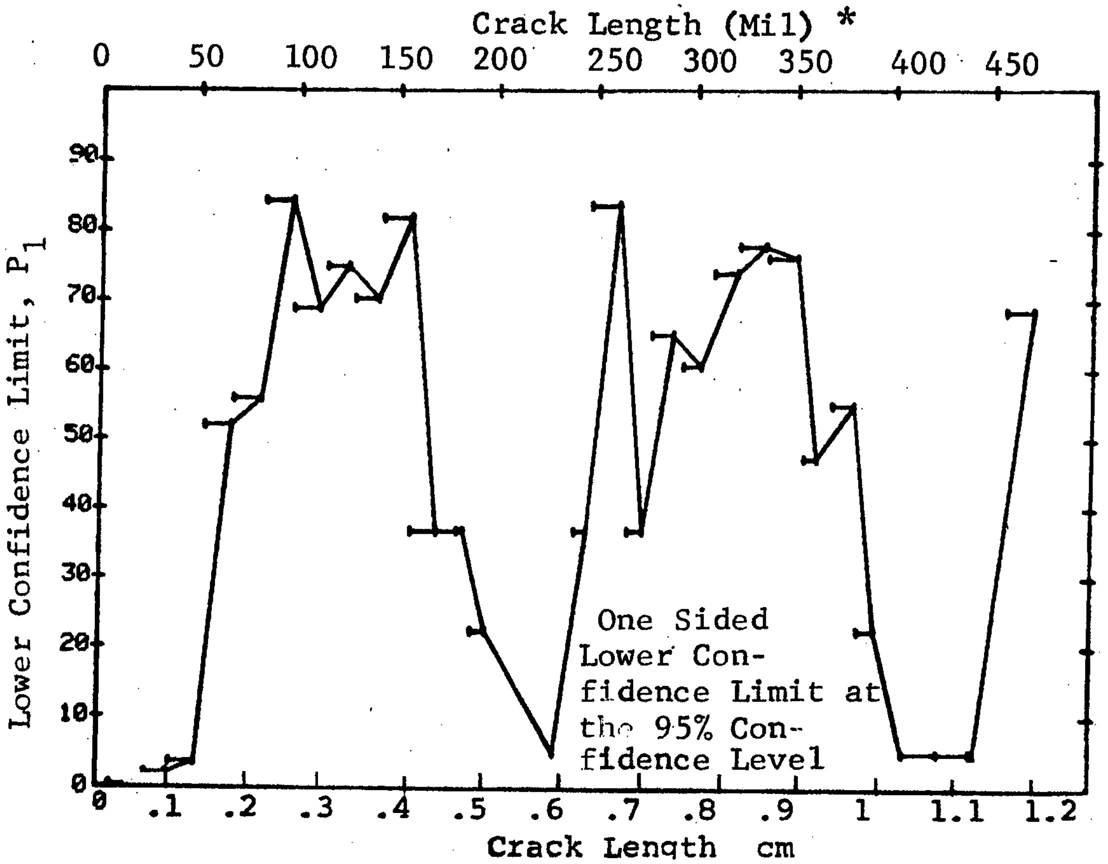

Figure D-21 Probability of Detection for 2219-T87 Al Using Eddy Current. Etched Fatigue Cracks in Flat Plates Measured by Operator T. Lab. Env.

(b) Optimum Probability Method of Data Cumulation

24-JUL-75 EDDY CURRENT TEST 2, (21) ROCKWELL SC T

RANGE	MIN LN	* MAX LN *	N	DET	50%	95%	0 MISS	1 MISS
1	7	22	13	1	0	0	0	0
2	7	36	31	3	0	2	0	0
3	7	51	54	6	0	4	0	0
4	54	67	46	30	0	52	0	0
5	54	82	99	66	0	58	0	0
6	83	97	38	36	0	84	23	38
7	83	111	56	52	0	84	33	47
8	83	126	73	68	0	86	30	43
9	83	141	92	85	0	86	37	50
10	83	157	107	100	0	88	0	0
11	83	171	110	103	0	88	0	0
12	83	185	113	106	0	88	0	0
13	83	197	115	108	0	88	0	0
14	0	0	0	0	0	0	0	0
15	83	232	116	109	0	88	0	0
16	143	247	27	27	0	89	2	19
17	143	262	44	44	0	93	0	2
18	143	275	47	47	0	93	0	0
19	143	290	54	54	0	94	0	0
20	143	304	60	60	0	95	0	0
21	143	322	70	70	0	95	0	0
22	143	336	82	82	0	96	0	0
23	143	352	93	93	0	96	0	0
24	143	362	97	97	0	96	0	0
25	143	381	102	102	0	97	0	0
26	143	393	104	104	0	97	0	0
27	143	408	105	105	0	97	0	0
28	143	426	106	106	0	97	0	0
29	143	442	107	107	0	97	0	0
30	143	444	108	108	0	97	0	0
31	143	472	116	116	0	97	0	0
32	143	979	175	175	0	98	0	0

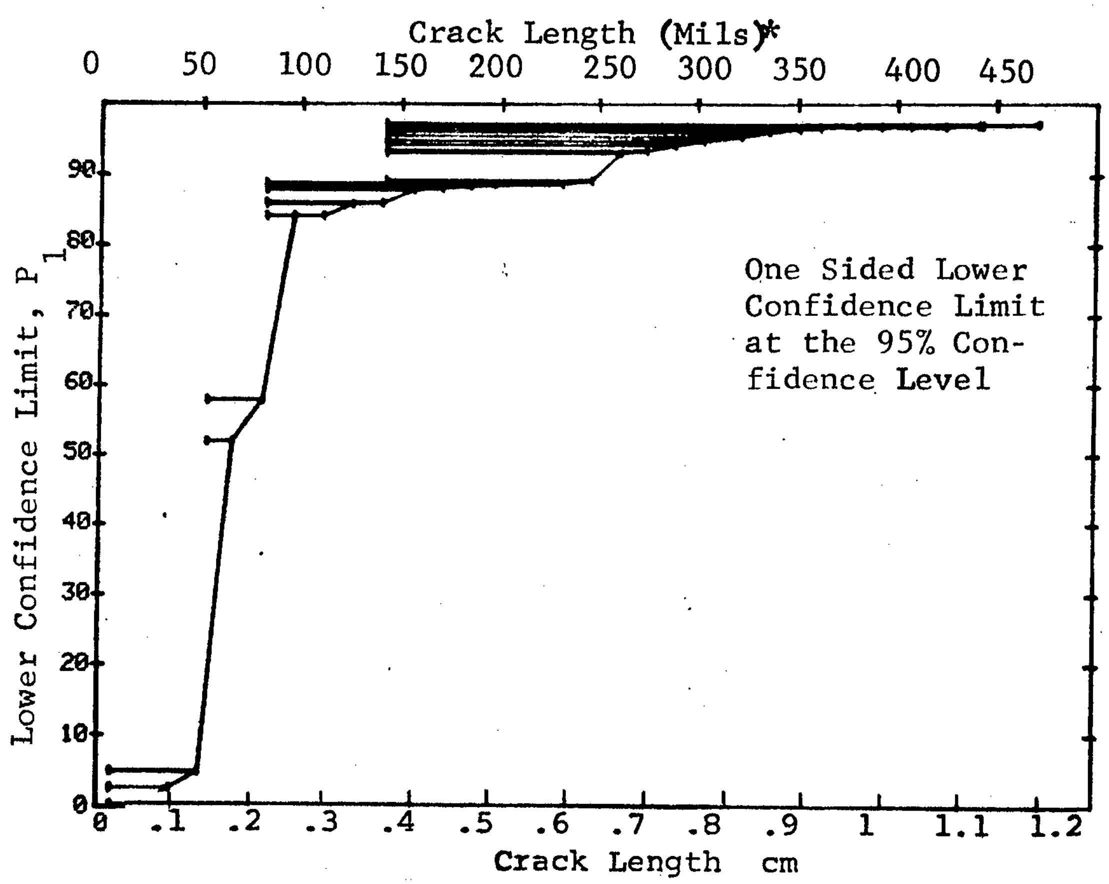

Figure D-21 (Continued) for

(c) Overlapping Sixty Point Method of Data Cumulation

24-JUL-75 EDDY CURRENT TEST 3 (21) ROCKWELL SC T

RANGE	MIN LN *	MAX LN *	N	DET	50%	95%	0 MISS	1 MISS
1	0	0	0	0	0	0	0	0
2	0	0	0	0	0	0	0	0
3	0	0	0	0	0	0	0	0
4	0	0	0	0	0	0	0	0
5	0	0	0	0	0	0	0	0
6	0	0	0	0	0	0	0	0
7	0	0	0	0	0	0	0	0
8	0	0	0	0	0	0	0	0
9	0	0	0	0	0	0	0	0
10	0	0	0	0	0	0	0	0
11	0	0	0	0	0	0	0	0
12	0	0	0	0	0	0	0	0
13	0	0	0	0	0	0	0	0
14	0	0	0	0	0	0	0	0
15	0	0	0	0	0	0	0	0
16	0	0	0	0	0	0	0	0
17	0	0	0	0	0	0	0	0
18	0	0	0	0	0	0	0	0
19	0	0	0	0	0	0	0	0
20	0	0	0	0	0	0	0	0
21	7	49	52	5	8	3	0	0
22	31	63	60	23	37	27	0	0
23	49	70	60	36	59	48	0	0
24	64	79	60	37	60	50	0	0
25	70	87	60	50	82	73	0	0
26	79	105	60	55	90	83	43	56
27	88	131	60	53	87	79	69	82
28	105	162	60	57	93	87	16	29
29	132	275	60	60	98	95	0	0
30	171	330	60	60	98	95	0	0
31	279	442	60	60	98	95	0	0
32	331	500	60	60	98	95	0	0

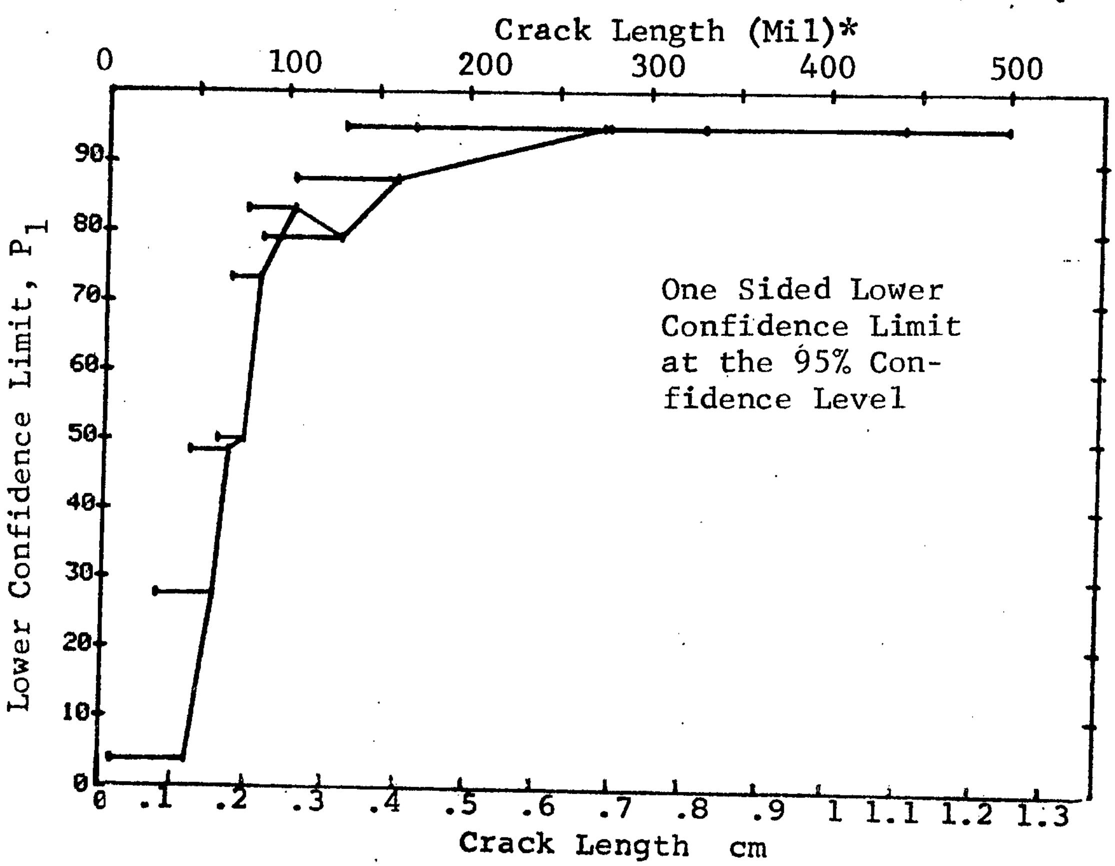

Figure D-21 (Concluded)

(a) Range Interval Method of Data Cumulation

03-JUL-75 EDDY CURRENT TEST 1 . POCKWELL 5C , 'U' (22)

RANGE	MIN LN	*MAX LN*	N	DET	50%	95%	0 MISS	1 MISS
1	7	22	13	3	20	6	0	0
2	25	26	18	6	30	15	0	0
3	38	52	25	13	50	34	0	0
4	54	67	48	42	86	76	0	0
5	68	82	50	50	98	94	68	81
6	83	97	39	35	88	78	0	0
7	98	111	17	16	90	75	50	64
8	115	126	18	18	96	84	29	44
9	129	141	18	18	96	84	11	28
10	143	157	15	15	95	81	11	28
11	158	171	3	3	79	36	14	31
12	182	185	3	3	79	36	0	0
13	190	197	2	2	70	35	0	0
14	0	0	0	0	0	22	0	0
15	0	0	0	0	0	0	0	0
16	241	247	4	4	84	0	0	0
17	248	262	16	16	95	47	0	0
18	268	275	3	3	79	82	13	30
19	279	290	7	7	90	36	0	0
20	295	306	6	6	89	65	0	0
21	310	322	10	10	93	60	0	0
22	323	336	12	12	94	74	0	0
23	338	352	11	11	93	77	17	34
24	356	362	4	4	84	76	18	35
25	370	381	5	5	87	47	0	0
26	384	393	2	2	70	54	0	0
27	408	408	1	1	50	22	0	0
28	426	426	1	1	50	5	0	0
29	442	442	1	1	50	5	0	0
30	444	444	1	1	50	5	0	0
31	458	472	8	8	91	5	0	0
32	474	979	59	59	98	68	0	0
						95		

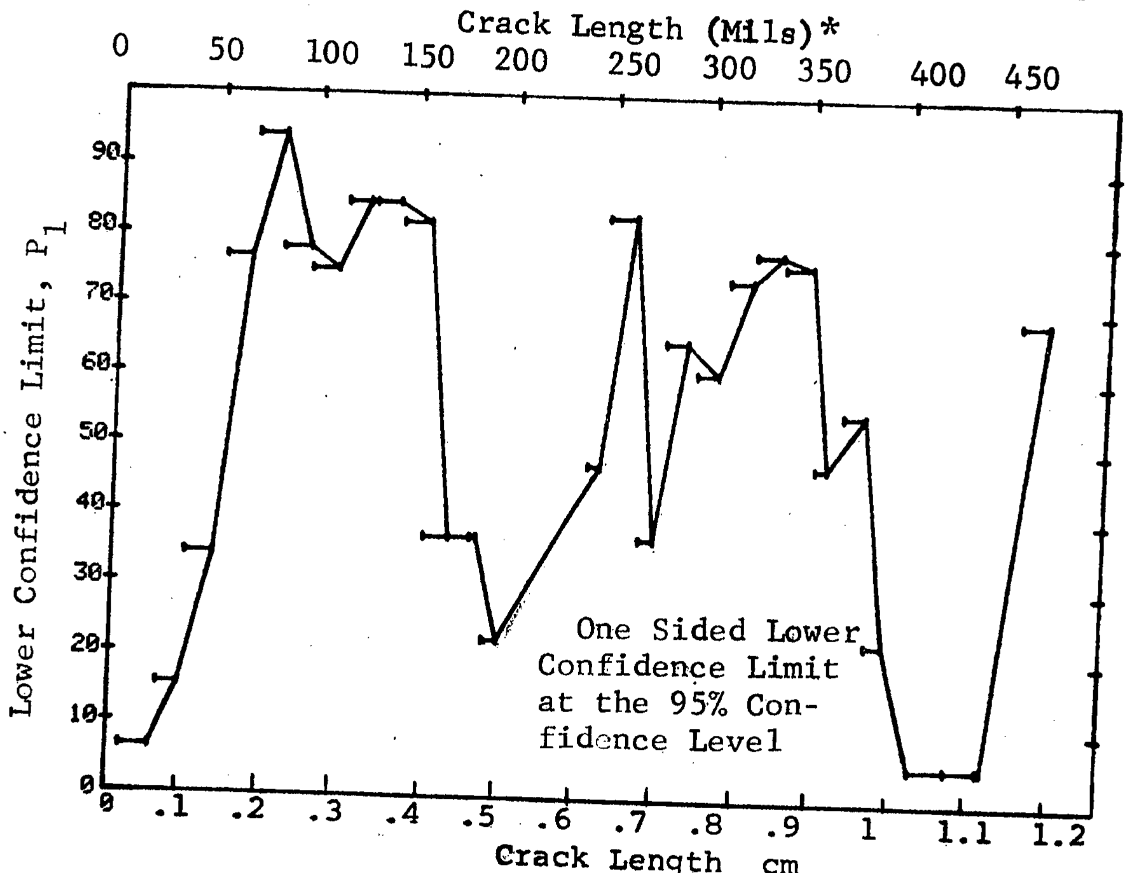

Figure D-22 Probability of Detection for 2219-T87 Al Using Eddy Current. Etched Fatigue Cracks in Flat Plates Measured by Operator U. Lab. Env.

(b) Optimum Probability Method of Data Cumulation

03-JUL-75 EDDY CURRENT TEST 2, ROCKWELL SC, 'U'

RANGE	MIN LN	MAX LN *	N	DET	50%	95%	0 MISS	(22) 1 MISS
1	7	22	13	3	0	6	0	0
2	7	36	31	9	0	16	0	0
3	38	52	25	13	0	34	0	0
4	54	67	48	42	0	76	0	0
5	68	82	50	50	0	94	0	0
6	68	97	89	85	0	90	0	0
7	68	111	106	101	0	90	0	14
8	68	126	124	119	0	91	0	0
9	68	141	142	137	0	92	0	0
10	115	157	51	51	0	94	0	0
11	115	171	54	54	0	94	0	0
12	115	185	57	57	0	94	0	0
13	115	197	59	59	0	95	0	0
14	0	0	0	0	0	0	0	0
15	0	0	0	0	0	0	0	0
16	115	247	63	63	0	95	0	0
17	115	262	79	79	0	96	0	0
18	115	275	82	82	0	96	0	0
19	115	290	89	89	0	96	0	0
20	115	306	95	95	0	96	0	0
21	115	322	105	105	0	97	0	0
22	115	336	117	117	0	97	0	0
23	115	352	128	128	0	97	0	0
24	115	362	132	132	0	97	0	0
25	115	381	137	137	0	97	0	0
26	115	393	139	139	0	97	0	0
27	115	408	140	140	0	97	0	0
28	115	426	141	141	0	97	0	0
29	115	442	142	142	0	97	0	0
30	115	444	143	143	0	97	0	0
31	115	472	151	151	0	97	0	0
32	115	979	210	210	0	98	0	0

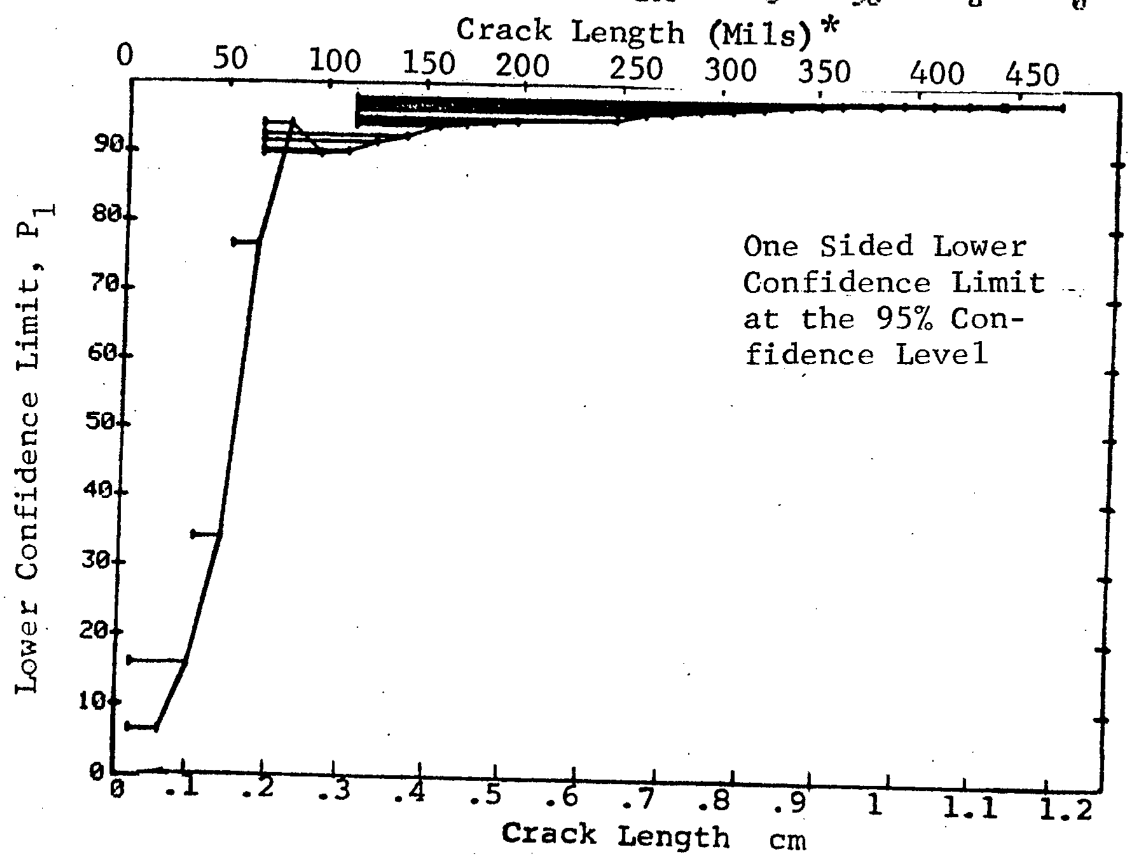

Figure D-22 (Continued)

(c) Overlapping Sixty Point Method of Data Cumulation

03-JUL-75 EDDY CURRENT TEST 3 ROCKWELL SC, 'U' (22)

RANGE	MIN LN	MAX LN	N	DET	50%	95%	0 MISS	1 MISS
1	0*	0*	0	0	0	0	0	0
2	0	0	0	0	0	0	0	0
3	0	0	0	0	0	0	0	0
4	0	0	0	0	0	0	0	0
5	0	0	0	0	0	0	0	0
6	0	0	0	0	0	0	0	0
7	0	0	0	0	0	0	0	0
8	0	0	0	0	0	0	0	0
9	0	0	0	0	0	0	0	0
10	0	0	0	0	0	0	0	0
11	0	0	0	0	0	0	0	0
12	0	0	0	0	0	0	0	0
13	0	0	0	0	0	0	0	0
14	0	0	0	0	0	0	0	0
15	0	0	0	0	0	0	0	0
16	0	0	0	0	0	0	0	0
17	0	0	0	0	0	0	0	0
18	0	0	0	0	0	0	0	0
19	0	0	0	0	0	0	0	0
20	0	0	0	0	0	0	0	0
21	7	49	52	20	37	27	0	0
22	31	63	60	38	62	51	0	0
23	49	69	60	52	85	77	82	94
24	63	79	60	59	97	92	0	1
25	69	87	60	59	97	92	0	1
26	79	104	60	55	90	83	43	56
27	87	131	60	56	92	85	29	43
28	105	158	60	60	98	95	0	0
29	132	275	60	60	98	95	0	0
30	162	330	60	60	98	95	0	0
31	279	442	60	60	98	95	0	0
32	331	500	60	60	98	95	0	0

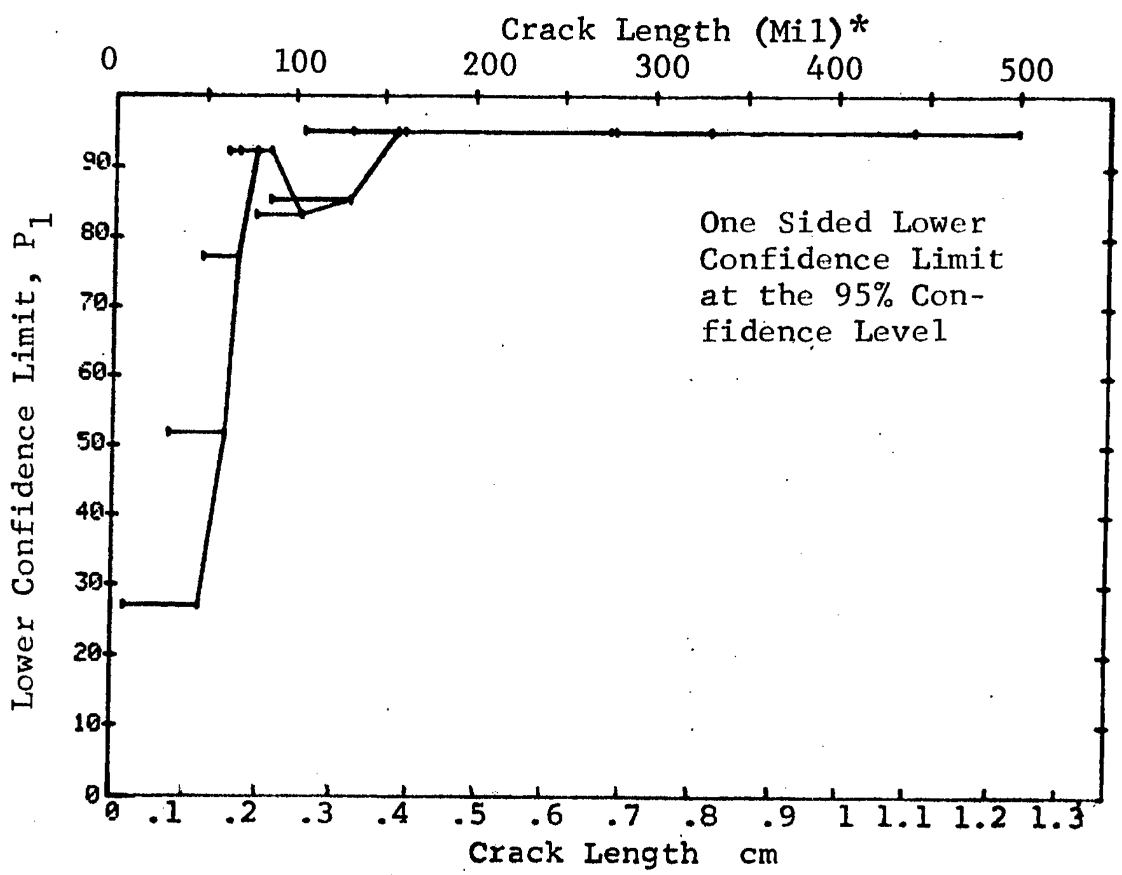

Figure D-22 (Continued)

(a) Range Interval Method of Data Cumulation

03-JUL-75 EDDY CURRENT TEST 1, ROCKWELL SC. 'U' (23)

RANGE	MIN LN	* MAX LN *	N	DET	50%	95%.	0 MISS	1 MISS
1	7	22	13	1	5	0	0	0
2	25	36	18	2	3	2	0	0
3	38	52	23	10	41	25	0	0
4	54	67	47	26	54	42	0	0
5	68	82	53	44	81	72	0	0
6	83	97	38	34	87	77	51	65
7	98	111	17	16	90	75	29	44
8	115	126	17	16	90	75	29	44
9	129	141	19	16	81	64	0	0
10	143	157	15	12	76	56	0	0
11	158	171	3	3	79	36	0	0
12	182	185	3	1	20	1	0	0
13	190	197	2	2	70	22	0	0
14	0	0	0	0	0	0	0	0
15	0	0	0	0	0	0	0	0
16	241	247	4	3	61	24	0	0
17	248	262	16	16	95	82	13	30
18	268	275	3	3	79	36	0	0
19	279	290	6	6	89	60	0	0
20	295	306	7	5	63	34	0	0
21	310	322	10	9	83	60	0	0
22	323	336	12	12	94	77	17	34
23	338	352	11	9	76	52	0	0
24	356	362	4	4	84	47	0	0
25	370	381	5	4	68	34	0	0
26	384	393	2	2	70	22	0	0
27	408	408	1	1	50	5	0	0
28	426	426	1	1	50	5	0	0
29	435	442	3	2	50	13	0	0
30	444	444	1	1	50	5	0	0
31	458	472	8	8	91	68	0	0
32	474	979	57	52	90	92	40	53

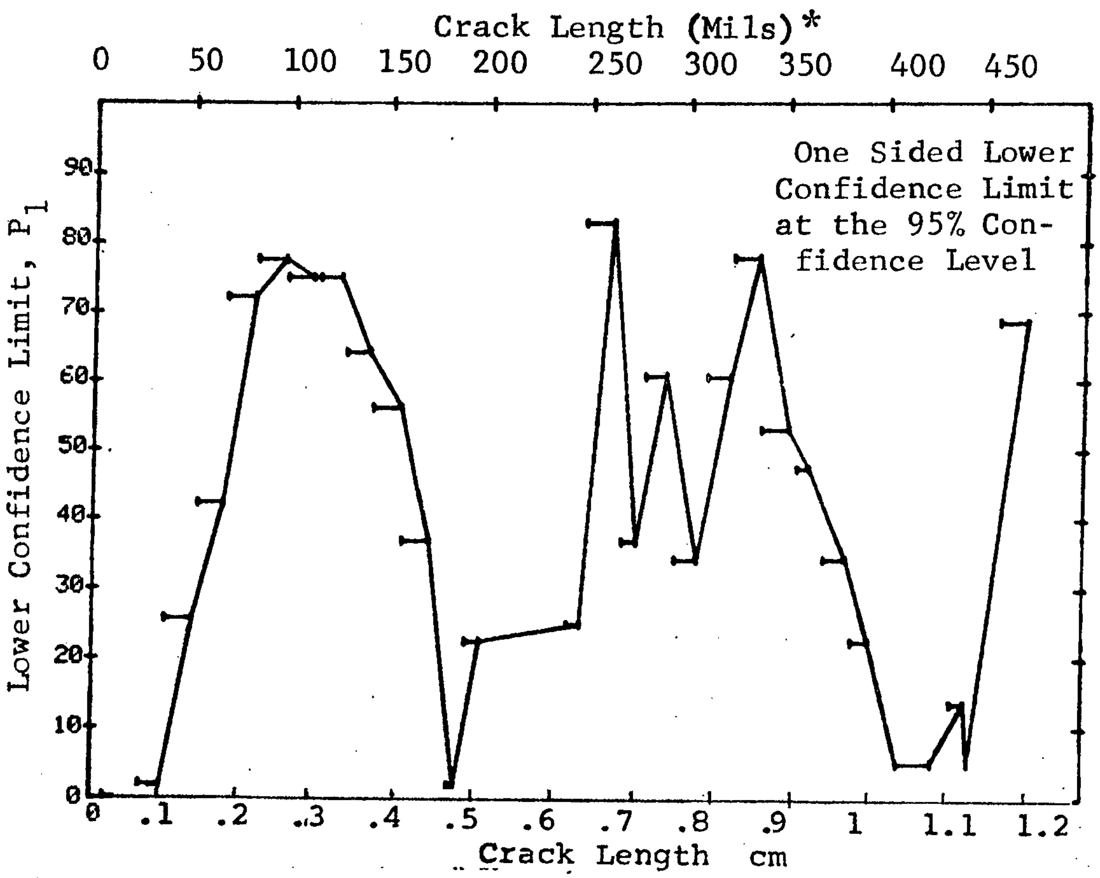

Figure D-23 Probability of Detection for 2219-T87 Al Using Eddy Current. Etched Fatigue Cracks in Flat Plates Measured by Operator V. Lab. Env.

(b) Optimum Probability Method of Data Cumulation

03-JUL-75 EDDY CURRENT TEST 2, ROCKWELL SC, 'U' (23)

RANGE	MIN LN	MAX LN	N	DET	50%	95%	0 MISS	1 MISS
1	7*	22*	13	1	0	0	0	0
2	7	36	31	3	0	2	0	0
3	38	52	23	10	0	25	0	0
4	54	67	47	26	0	42	0	0
5	68	82	53	44	0	72	0	0
6	68	97	91	78	0	78	0	0
7	83	111	55	50	0	81	48	61
8	83	126	72	66	0	84	44	57
9	83	141	91	82	0	83	63	76
10	83	157	106	94	0	82	0	0
11	83	171	109	97	0	82	0	0
12	83	185	112	98	0	81	0	0
13	83	197	114	100	0	81	0	0
14	0	0	0	0	0	0	0	0
15	0	0	0	0	0	0	0	0
16	83	247	118	103	0	81	0	0
17	83	262	134	119	0	83	0	0
18	248	275	19	19	0	85	10	27
19	248	290	25	25	0	88	4	21
20	83	306	150	133	0	83	0	0
21	83	322	160	142	0	83	0	0
22	248	336	54	51	0	86	22	35
23	248	352	65	60	0	84	38	51
24	248	362	69	64	0	85	34	47
25	83	381	192	171	0	84	0	0
26	248	393	76	70	0	85	40	53
27	248	408	77	71	0	85	39	52
28	248	426	78	72	0	85	38	51
29	248	442	81	74	0	84	43	61
30	83	444	200	178	0	84	0	0
31	248	472	90	83	0	85	39	52
32	248	979	147	135	0	87	0	0

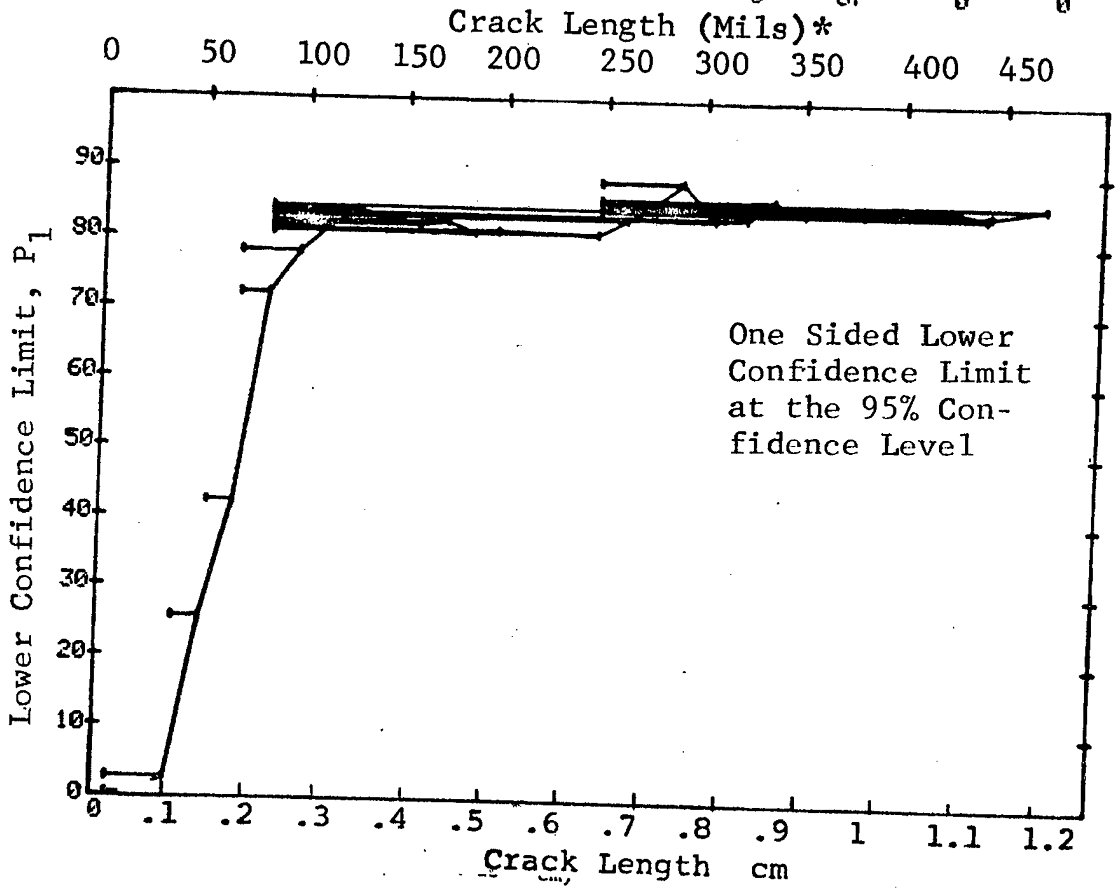

Figure D-23 (Continued)

(c) Overlapping Sixty Point Method of Data Cumulation

03-JUL-75 EDDY CURRENT TEST 3, ROCKWELL SC. 'U' (23)

RANGE	MIN LN	MAX LN	N	DET	50%	95%	0 MISS	1 MISS
1	0 *	0*	0	0	0	0	0	0
2	0	0	0	0	0	0	0	0
3	0	0	0	0	0	0	0	0
4	0	0	0	0	0	0	0	0
5	0	0	0	0	0	0	0	0
6	0	0	0	0	0	0	0	0
7	0	0	0	0	0	0	0	0
8	0	0	0	0	0	0	0	0
9	0	0	0	0	0	0	0	0
10	0	0	0	0	0	0	0	0
11	0	0	0	0	0	0	0	0
12	0	0	0	0	0	0	0	0
13	0	0	0	0	0	0	0	0
14	0	0	0	0	0	0	0	0
15	0	0	0	0	0	0	0	0
16	0	0	0	0	0	0	0	0
17	0	0	0	0	0	0	0	0
18	0	0	0	0	0	0	0	0
19	0	0	0	0	0	0	0	0
20	0	0	0	0	0	0	0	0
21	7	51	53	12	21	13	0	0
22	32	63	60	26	42	32	0	0
23	52	70	60	36	59	48	0	0
24	64	79	60	43	70	60	0	0
25	70	87	60	52	85	77	82	94
26	79	105	60	56	92	85	29	43
27	88	132	60	54	88	81	56	69
28	106	171	60	52	85	77	82	94
29	134	279	60	53	87	79	69	82
30	182	331	60	54	88	81	56	69
31	283	442	60	53	87	79	69	82
32	333	500	60	54	88	81	56	69

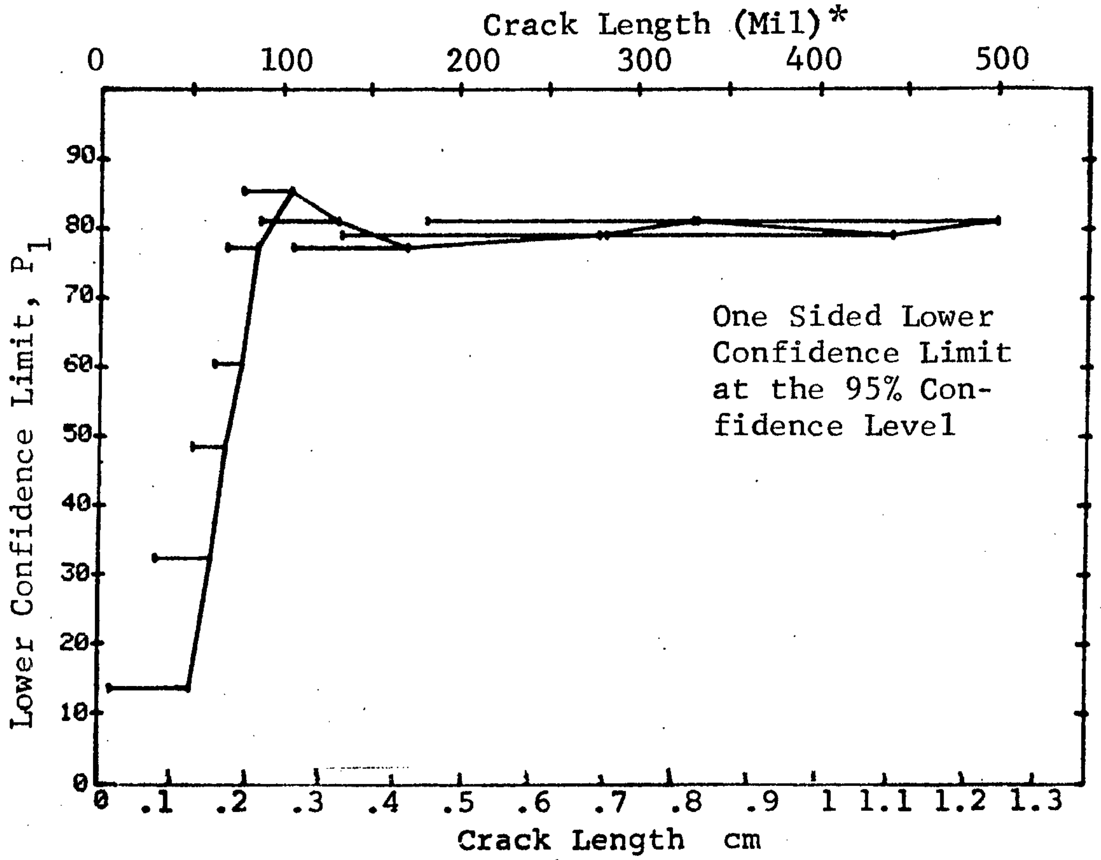

[1]Figure D-23 (Concluded)

(a) Range Interval Method of Data Cumulation

03-JUL-75 EDDY CURRENT TEST 1, ROCKWELL SC, 'W' (24)

RANGE	MIN LN		MAX LN		N	DET	50%	95%	0 MISS	1 MISS
1	7	*	22	*	13	2	12	2	0	0
2	25		36		18	6	30	15	0	0
3	38		52		22	8	34	19	0	0
4	54		67		46	10	20	12	0	0
5	68		82		53	47	87	78	63	76
6	83		97		39	37	93	84	22	37
7	98		111		17	17	96	83	12	29
8	115		126		17	16	90	75	29	44
9	129		141		19	17	36	70	0	0
10	143		157		15	12	76	56	0	0
11	158		171		3	3	79	36	0	0
12	182		185		3	3	79	36	0	0
13	190		197		2	2	70	22	0	0
14	0		0		0	0	0	0	0	0
15	0		0		0	0	0	0	0	0
16	241		247		4	4	84	47	0	0
17	248		262		17	17	96	83	12	29
18	268		275		3	3	79	36	0	0
19	279		290		7	6	77	47	0	0
20	295		306		6	6	89	60	0	0
21	310		322		10	10	93	74	0	0
22	323		336		12	11	86	66	0	0
23	338		352		11	9	76	52	0	0
24	356		362		4	4	84	47	0	0
25	370		381		5	4	68	34	0	0
26	384		393		2	2	70	22	0	0
27	408		408		1	1	50	5	0	0
28	426		426		1	1	50	5	0	0
29	442		442		1	0	0	0	0	0
30	444		444		1	1	50	5	0	0
31	458		472		8	7	79	52	0	0
32	474		979		58	53	90	82	45	58

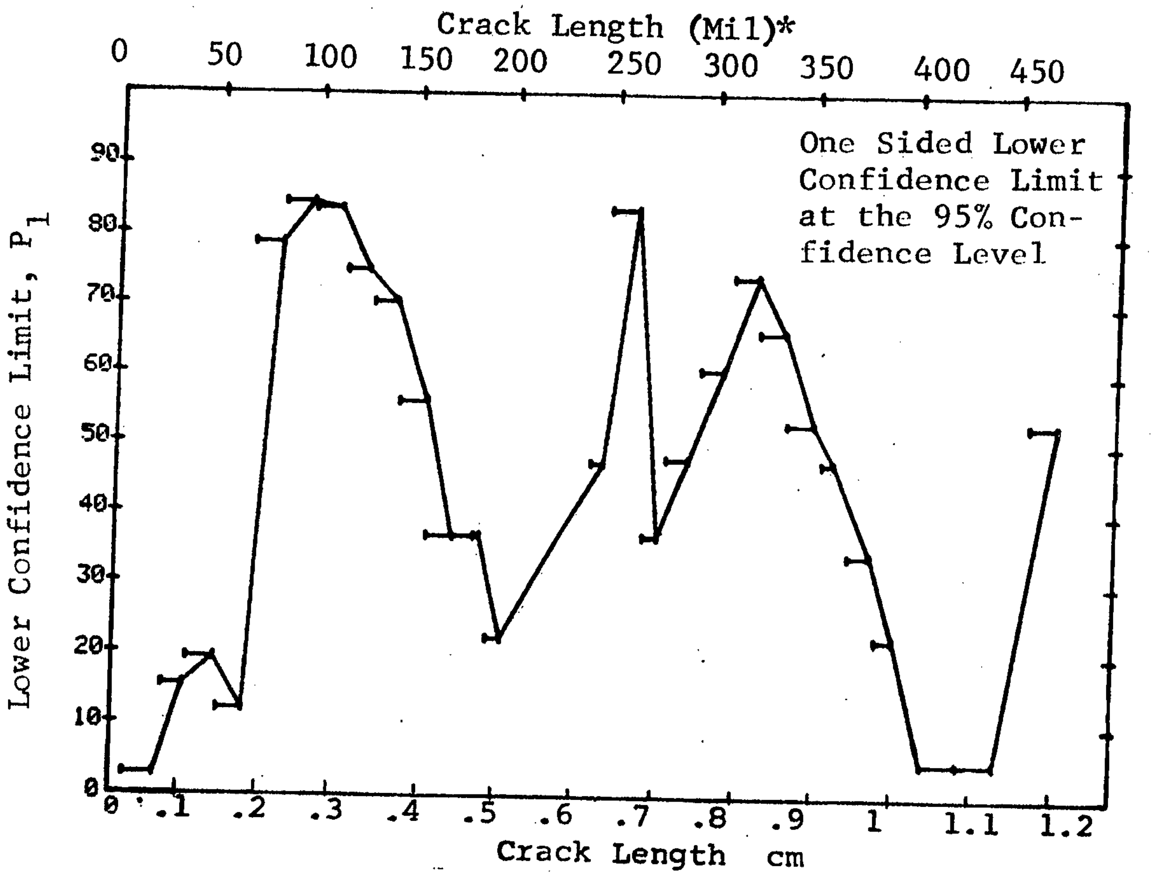

Figure D-24 Probability of Detection for 2219-T87 Al Using Eddy Current. Etched Fatigue Cracks in Flat Plates Measured by Operator W. Lab. Env.

(b) Optimum Probability Method of Data Cumulation

03-JUL-75 EDDY CURRENT TEST 2, ROCKWELL SC. 'W' (24)

RANGE	MIN LN	MAX LN	N	DET	50%	95%	0 MISS	1 MISS
1	7*	23 *	13	2	0	2	0	0
2	25	36	18	6	0	15	0	0
3	25	52	40	14	0	22	0	0
4	25	67	86	24	0	20	0	0
5	68	82	53	47	0	78	0	0
6	68	97	92	84	0	84	50	62
7	83	111	56	54	0	89	5	20
8	83	126	73	70	0	89	3	16
9	83	141	92	87	0	88	11	24
10	83	157	107	99	0	86	0	0
11	83	171	110	102	0	87	0	0
12	83	185	113	105	0	87	0	0
13	83	197	115	107	0	87	0	0
14	0	0	0	0	0	0	0	0
15	0	0	0	0	0	0	0	0
16	83	247	119	111	0	88	0	0
17	158	262	29	29	0	90	0	17
18	158	275	32	32	0	91	0	14
19	83	290	146	137	0	89	0	0
20	158	306	45	44	0	89	1	16
21	158	322	55	54	0	91	0	6
22	158	336	67	65	0	90	0	9
23	83	352	185	173	0	89	0	0
24	83	362	189	177	0	89	0	0
25	83	381	194	181	0	89	0	0
26	83	393	196	183	0	89	0	0
27	83	408	197	184	0	89	0	0
28	83	426	198	185	0	89	0	0
29	68	442	252	232	0	89	0	0
30	83	444	200	186	0	[illegible]	0	0
31	83	472	208	193	0	89	0	0
32	83	979	266	246	0	89	0	0

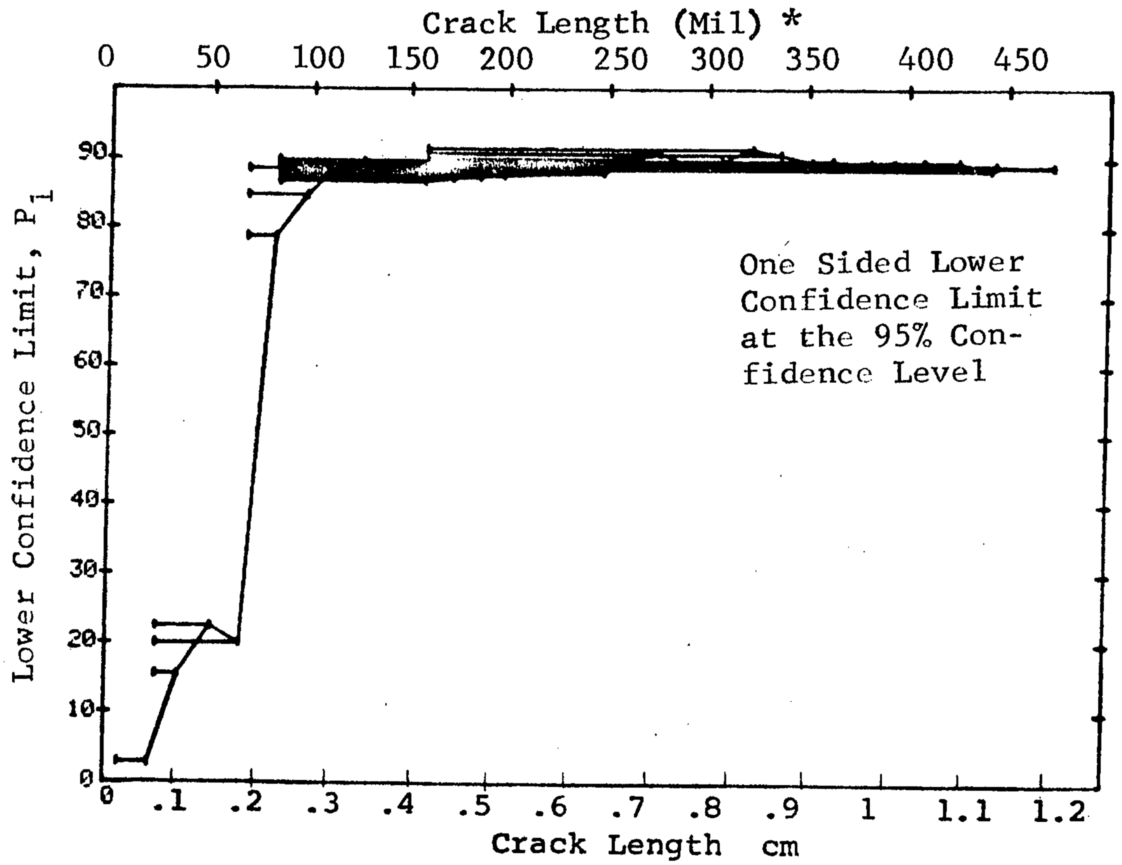

Figure D-24 (Continued)

(c) Overlapping Sixty Point Method of Data Cumulation

03-JUL-75 EDDY CURRENT TEST 3, ROCKWELL SC, 'W' (24)

RANGE	MIN LN	MAX LN *	N	DET	50%	95%	0 MISS	1 MISS
1	0	0	0	0	0	0	0	0
2	0	0	0	0	0	0	0	0
3	0	0	0	0	0	0	0	0
4	0	0	0	0	0	0	0	0
5	0	0	0	0	0	0	0	0
6	0	0	0	0	0	0	0	0
7	0	0	0	0	0	0	0	0
8	0	0	0	0	0	0	0	0
9	0	0	0	0	0	0	0	0
10	0	0	0	0	0	0	0	0
11	0	0	0	0	0	0	0	0
12	0	0	0	0	0	0	0	0
13	0	0	0	0	0	0	0	0
14	0	0	0	0	0	0	0	0
15	0	0	0	0	0	0	0	0
16	0	0	0	0	0	0	0	0
17	0	0	0	0	0	0	0	0
18	0	0	0	0	0	0	0	0
19	0	0	0	0	0	0	0	0
20	0	0	0	0	0	0	0	0
21	7	49	51	16	30	20	0	0
22	30	63	60	16	25	17	0	0
23	51	70	60	19	30	21	0	0
24	64	79	60	43	70	60	0	0
25	70	87	60	55	90	83	43	56
26	79	105	60	57	93	87	16	29
27	87	131	60	59	97	92	0	1
28	106	162	60	54	88	81	56	69
29	132	275	60	55	90	83	43	56
30	171	330	60	59	97	92	0	1
31	279	442	60	54	88	81	56	69
32	331	500	60	52	85	77	82	94

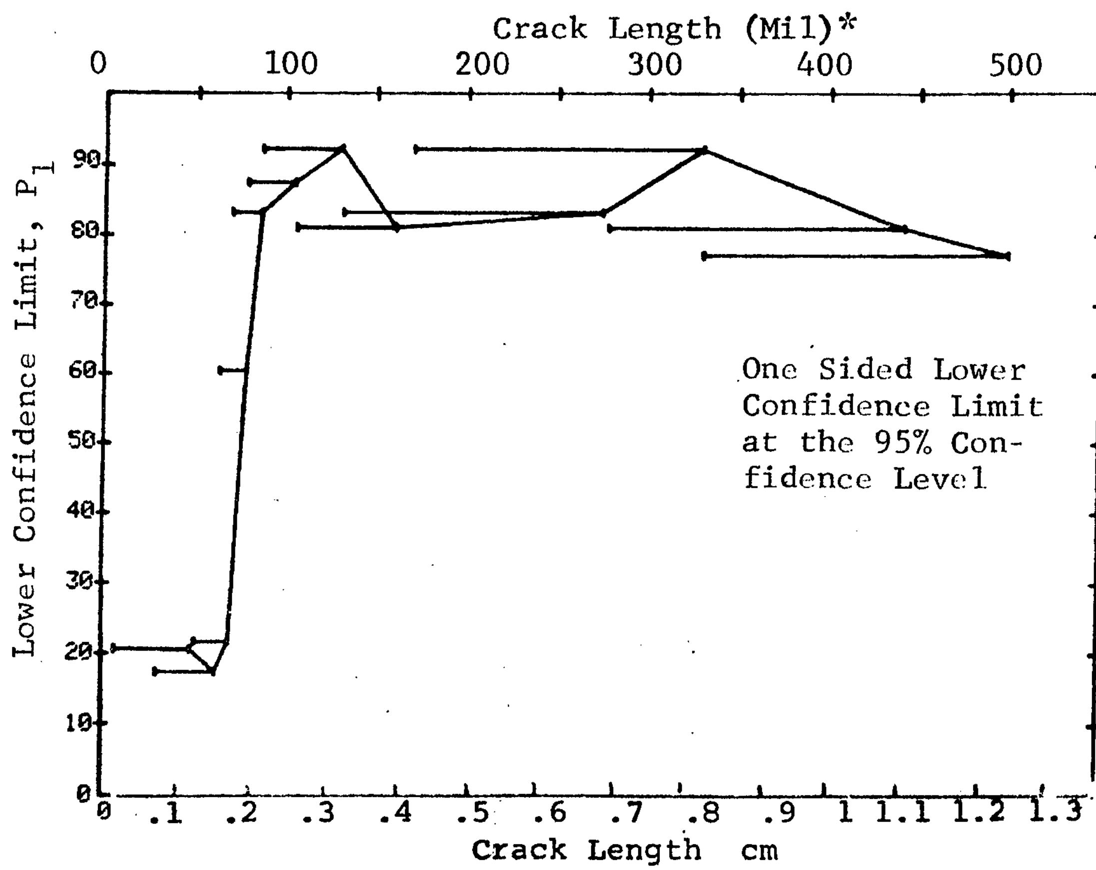

Figure D-24 (Concluded)

(a) Range Interval Method of Data Cumulation

03-JUL-75 EDDY CURRENT TEST 1, ROCKWELL SC, 'X' (25)

RANGE	MIN LN	MAX LN	N	DET	50%	95%	0 MISS	1 MISS
1	7 *	22 *	13	1	5	0	0	0
2	25	36	18	3	14	4	0	0
3	38	52	23	8	32	18	0	0
4	54	67	47	31	64	52	0	0
5	68	82	53	21	38	28	0	0
6	83	97	39	36	90	81	37	50
7	98	111	17	17	96	83	12	29
8	115	126	17	17	96	83	12	29
9	129	141	19	19	96	85	10	27
10	143	157	14	13	88	70	0	0
11	158	171	3	3	79	36	0	0
12	182	185	3	3	79	36	0	0
13	190	197	2	2	70	22	0	0
14	0	0	0	0	0	0	0	0
15	0	0	0	0	0	0	0	0
16	241	247	4	4	84	47	0	0
17	248	261	16	16	95	82	13	30
18	268	275	3	3	79	36	0	0
19	279	290	7	7	90	65	0	0
20	295	306	6	6	89	60	0	0
21	310	322	10	10	93	74	0	0
22	323	336	12	12	94	77	17	34
23	338	352	11	10	85	63	0	0
24	356	362	5	4	68	34	0	0
25	370	381	4	4	84	47	0	0
26	384	393	2	2	70	22	0	0
27	408	408	1	1	50	5	0	0
28	426	426	1	1	50	5	0	0
29	442	442	1	1	50	5	0	0
30	444	444	1	1	50	5	0	0
31	458	472	8	8	91	68	0	0
32	474	979	59	58	97	92	0	2

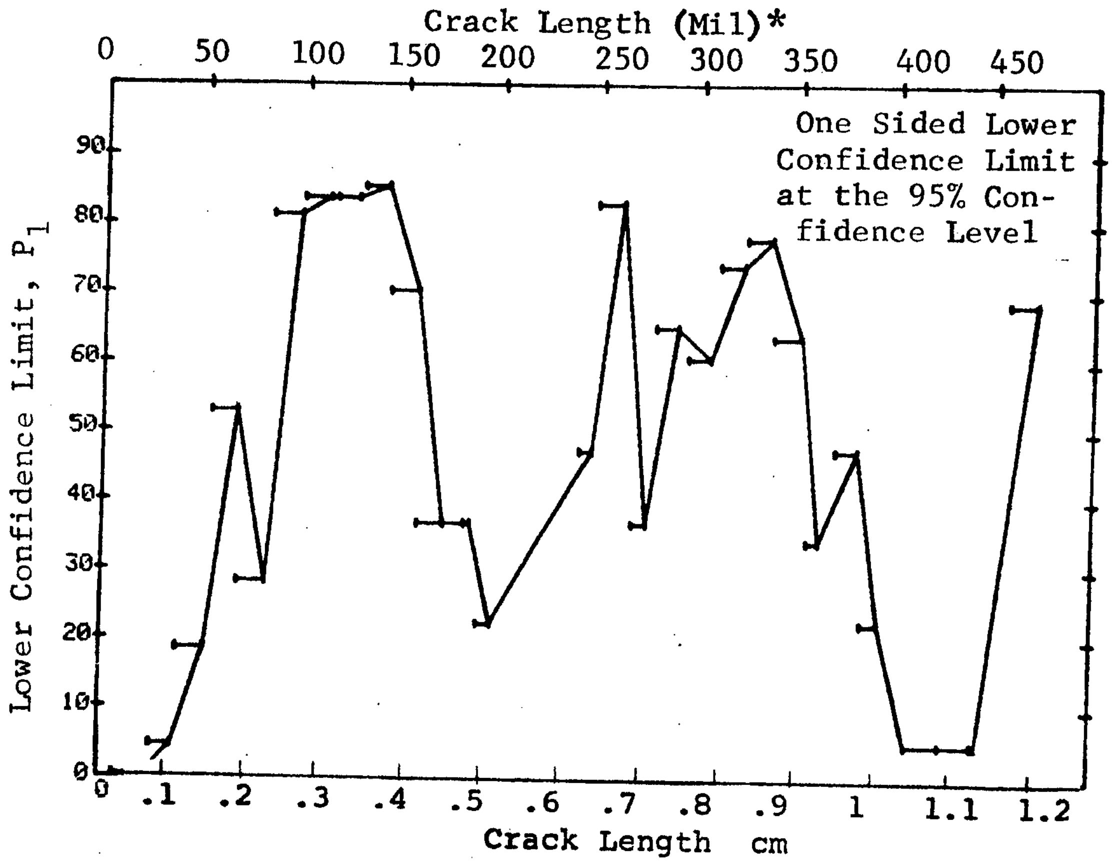

Figure D-25 Probability of Detection for 2219-T87 Al Using Eddy Current. Etched Fatigue Cracks in Flat Plates Measured by Operator X. Lab. Env.

(b) Optimum Probability Method of Data Cumulation

03-JUL-75 EDDY CURRENT TEST 2, ROCKWELL SC, 'X' (25)

RANGE	MIN LN	MAX LN	N	DET	50%	95%	0 MISS	1 MISS
1	7 *	22 *	13	1	0	0	0	0
2	25	36	18	3	0	4	0	0
3	38	52	23	8	0	18	0	0
4	54	67	47	31	0	52	0	0
5	54	82	100	52	0	43	0	0
6	83	97	39	36	0	81	37	50
7	83	111	56	53	0	86	20	33
8	98	126	34	34	0	91	0	12
9	98	141	53	53	0	94	0	0
10	98	157	67	66	0	93	0	0
11	98	171	70	69	0	93	0	0
12	98	185	73	72	0	93	0	0
13	98	197	75	74	0	93	0	0
14	0	0	0	0	0	0	0	0
15	0	0	0	0	0	0	0	0
16	98	247	79	78	0	94	0	0
17	98	261	95	94	0	95	0	0
18	98	275	98	97	0	95	0	0
19	98	290	105	104	0	95	0	0
20	98	306	111	110	0	95	0	0
21	98	322	121	120	0	96	0	0
22	98	336	133	132	0	96	0	0
23	98	352	144	142	0	95	0	0
24	98	362	149	146	0	94	0	0
25	98	381	153	150	0	95	0	0
26	98	393	155	152	0	95	0	0
27	98	408	156	153	0	95	0	0
28	98	426	157	154	0	95	0	0
29	98	442	158	155	0	95	0	0
30	98	444	159	156	0	95	0	0
31	98	472	167	164	0	95	0	0
32	98	979	226	222	0	95	0	0

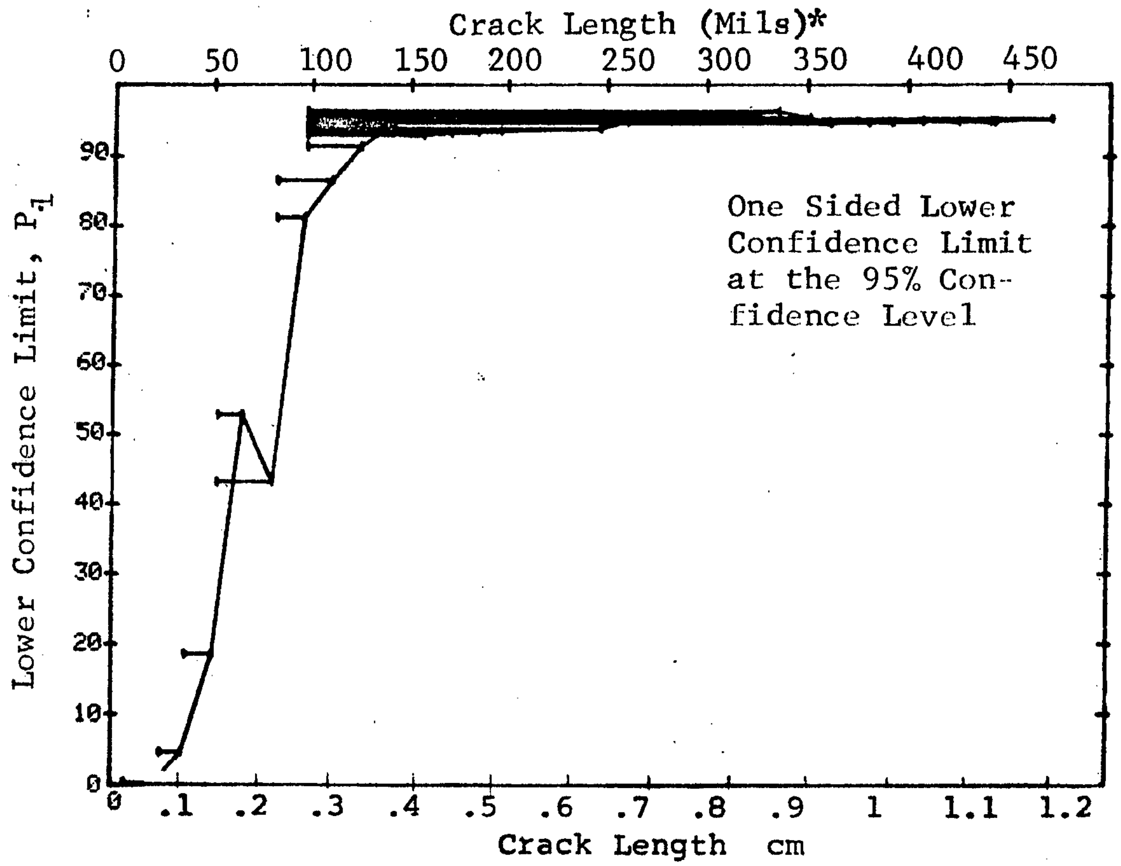

Figure D-25 (Continued)

(c) Overlapping Sixty Point Method of Data Cumulation

03-JUL-75 EDDY CURRENT TEST 3. ROCKWELL SC. 'X' (25)

RANGE	MIN LN	MAX LN	N	DET	50%	95%	0 MISS	1 MISS
1	0 *	0*	0	0	0	0	0	0
2	0	0	0	0	0	0	0	0
3	0	0	0	0	0	0	0	0
4	0	0	0	0	0	0	0	0
5	0	0	0	0	0	0	0	0
6	0	0	0	0	0	0	0	0
7	0	0	0	0	0	0	0	0
8	0	0	0	0	0	0	0	0
9	0	0	0	0	0	0	0	0
10	0	0	0	0	0	0	0	0
11	0	0	0	0	0	0	0	0
12	0	0	0	0	0	0	0	0
13	0	0	0	0	0	0	0	0
14	0	0	0	0	0	0	0	0
15	0	0	0	0	0	0	0	0
16	0	0	0	0	0	0	0	0
17	0	0	0	0	0	0	0	0
18	0	0	0	0	0	0	0	0
19	0	0	0	0	0	0	0	0
20	0	0	0	0	0	0	0	0
21	7	49	51	10	18	11	0	0
22	30	63	60	25	40	30	0	0
23	49	69	60	35	57	46	0	0
24	63	79	60	29	47	37	0	0
25	69	86	60	33	54	43	0	0
26	79	103	60	51	83	75	94	100
27	87	129	60	60	98	95	0	0
28	104	158	60	59	97	92	0	1
29	131	275	60	59	97	92	0	1
30	162	330	60	60	98	95	0	0
31	279	442	60	58	95	89	1	16
32	331	500	60	57	93	87	16	29

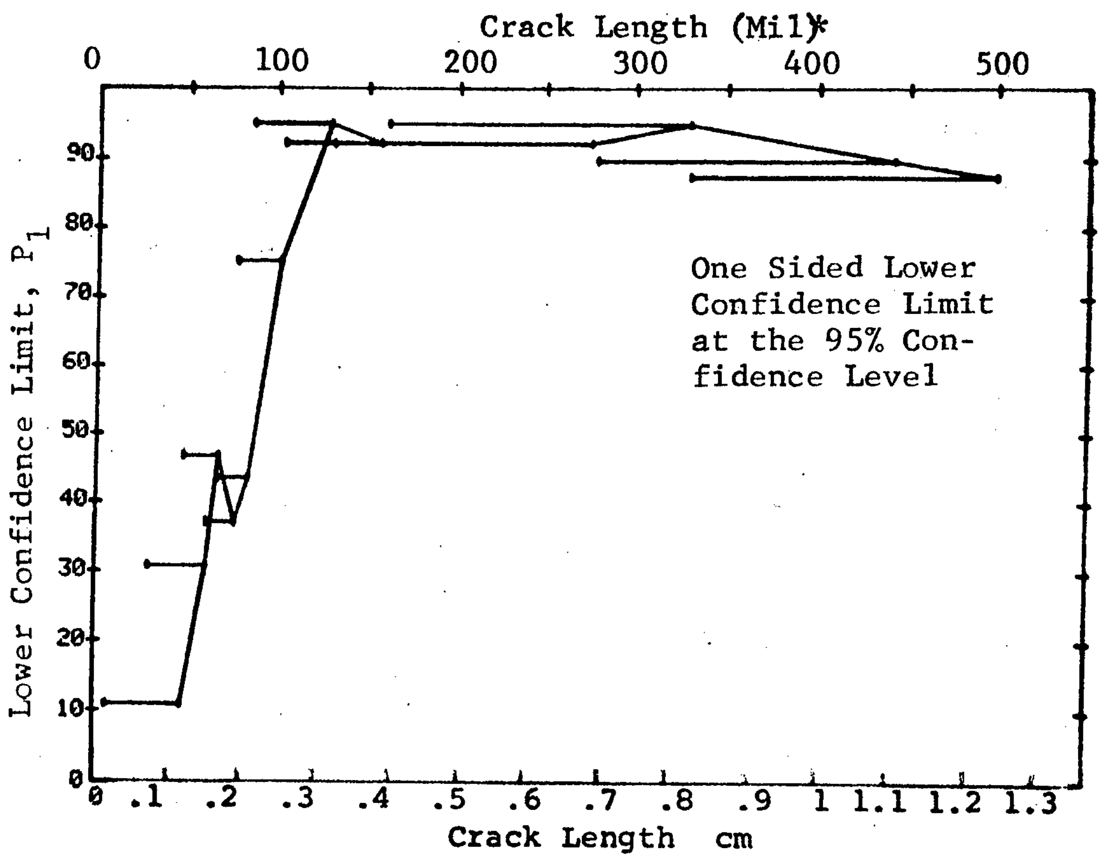

Figure D-25 (Concluded)

(a) Range Interval Method of Data Cumulation

03-JUL-75 RADIOGRAPHY TEST 1, ROCKWELL SC [illegible] (26)

RANGE	MIN LN	MAX LN	N	DET	50%	95%	0 MISS	1 MISS
1	7 *	22 *	13	0	0	0	0	[illegible]
2	25	36	18	2	9	2	0	[illegible]
3	38	52	23	3	11	3	0	[illegible]
4	54	67	46	7	14	3	0	[illegible]
5	68	82	53	12	21	7	0	[illegible]
6	83	97	39	12	29	13	0	0
7	98	111	17	6	32	18	0	0
8	115	126	17	1	3	16	0	0
9	129	141	19	1	3	0	0	0
10	143	157	15	1	4	0	0	0
11	158	171	3	0	0	0	0	0
12	182	185	3	1	20	0	0	0
13	190	197	2	1	29	1	0	0
14	0	0	0	0	0	2	0	0
15	0	0	0	0	0	0	0	0
16	241	247	4	4	84	0	0	0
17	248	262	17	16	90	47	0	0
18	268	275	3	3	79	75	29	44
19	279	290	7	5	63	36	0	0
20	295	306	6	2	26	34	0	0
21	310	322	10	5	45	6	0	0
22	323	336	12	4	29	22	0	0
23	338	352	11	11	93	12	0	0
24	356	362	4	3	61	76	18	[illegible]
25	370	381	5	5	87	24	0	[illegible]
26	384	393	2	2	70	54	0	0
27	408	408	1	0	0	22	0	[illegible]
28	426	426	1	0	0	0	0	0
29	442	442	1	1	50	0	0	[illegible]
30	444	444	1	1	50	[illegible]	[illegible]	[illegible]
31	458	472	8	8	91	5	0	[illegible]
32	474	979	59	54	90	68	0	[illegible]
						83	44	[illegible]

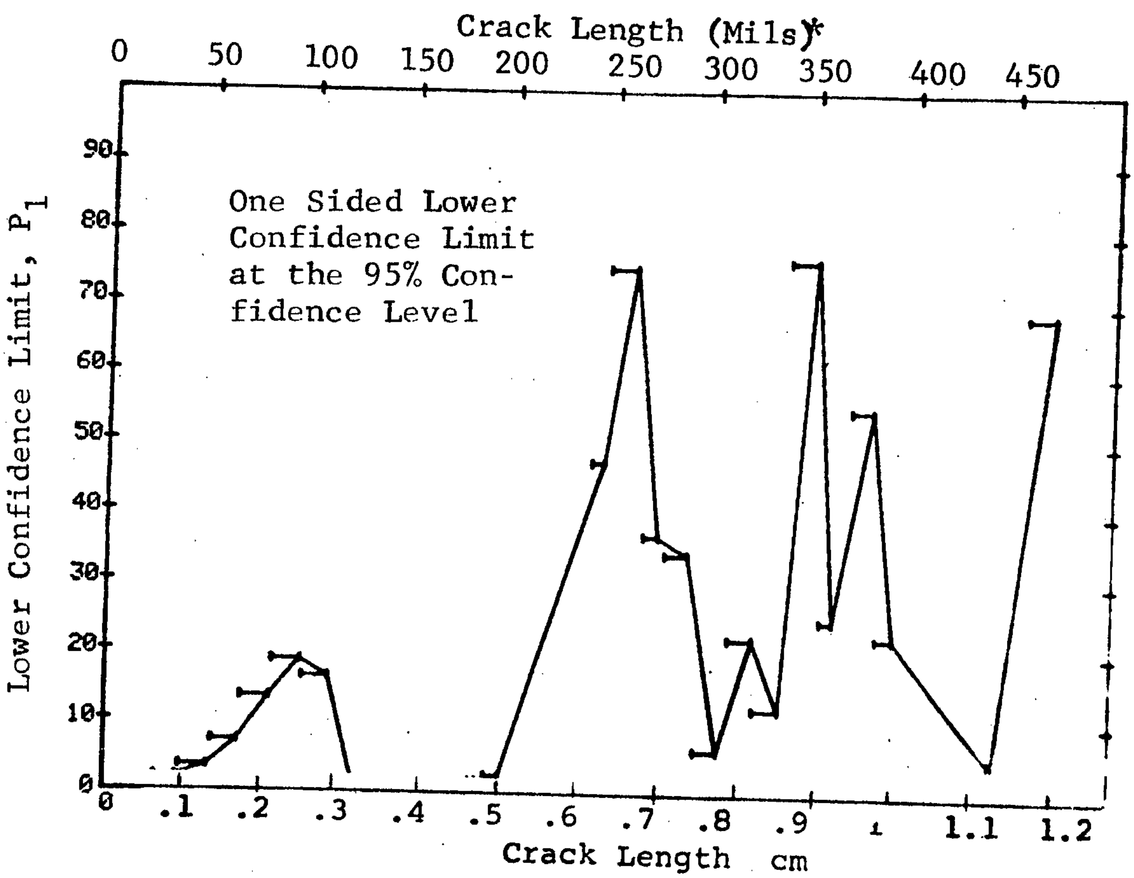

Figure D-26 Probability of Detection for 2219-T87 Al Using X-ray. Etched Fatigue Cracks in Flat Plates Measured by Operator A. Lab. Env.

(b) Optimum Probability Method of Data Cumulation

03-JUL-75 RADIOGRAPHY TEST 2, ROCKWELL 3C, (26)

RANGE	MIN LN	*MAX LN*	N	DET	50%	95%	0 MISS	1 MISS
1	7	22	13	0	0	0	0	[illegible]
2	25	36	18	2	0	2	0	[illegible]
3	25	52	41	5	0	4	0	0
4	25	67	87	12	0	8	0	0
5	68	82	53	12	0	13	0	0
6	83	97	39	12	0	18	0	0
7	83	111	56	18	0	21	0	0
8	68	126	126	31	0	18	0	0
9	68	141	145	32	0	16	0	0
10	68	157	160	33	0	15	0	0
11	68	171	163	33	0	15	0	0
12	68	185	166	34	0	15	0	0
13	68	197	168	35	0	15	0	0
14	0	0	0	0	0	0	0	0
15	0	0	0	0	0	0	0	0
16	241	247	4	4	0	47	0	0
17	241	262	21	20	0	79	0	0
18	241	275	24	23	0	81	0	0
19	241	290	31	28	0	76	22	37
20	241	306	37	30	0	67	0	0
21	241	322	47	35	0	61	0	0
22	241	336	59	39	0	54	0	0
23	338	352	11	11	0	76	0	0
24	338	362	15	14	0	72	0	0
25	338	381	20	19	0	78	0	[illegible]
26	338	393	22	21	0	80	0	0
27	338	408	23	21	0	75	24	[illegible]
28	338	426	24	21	0	70	0	0
29	338	442	25	22	0	71	[illegible]	0
30	338	444	26	23	0	72	0	[illegible]
31	338	472	34	31	0	78	0	[illegible]
32	442	979	69	64	0	85	34	[illegible]

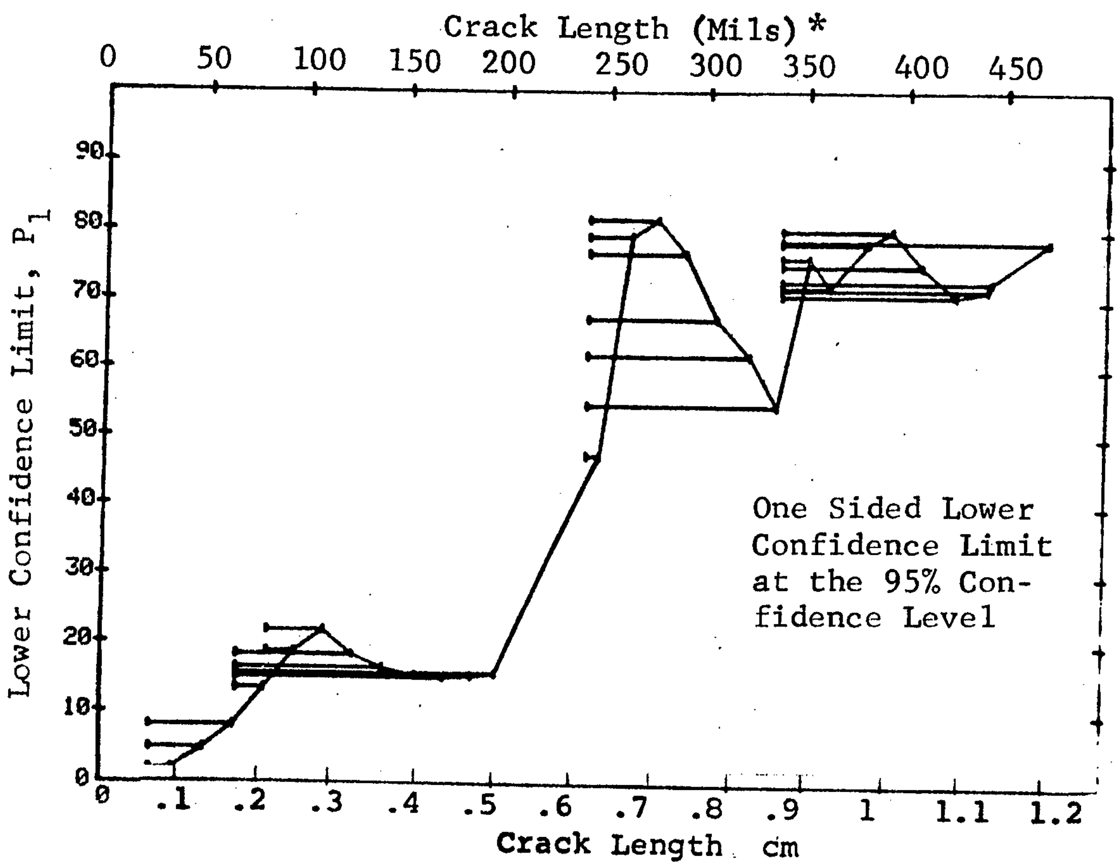

Figure D-26 (Continued)

(c) Overlapping Sixty Point Method of Data Cumulation

03-JUL-75 RADIOGRAPHY TEST 3, ROCKWELL SC, 'H (26)

RANGE	MIN LN*	MAX LN*	N	DET	50%	95%	0 MISS	1 MISS
1	0	0	0	0	0	0	0	0
2	0	0	0	0	0	0	0	0
3	0	0	0	0	0	0	0	0
4	0	0	0	0	0	0	0	0
5	0	0	0	0	0	0	0	0
6	0	0	0	0	0	0	0	0
7	0	0	0	0	0	0	0	0
8	0	0	0	0	0	0	0	0
9	0	0	0	0	0	0	0	0
10	0	0	0	0	0	0	0	0
11	0	0	0	0	0	0	0	0
12	0	0	0	0	0	0	0	0
13	0	0	0	0	0	0	0	0
14	0	0	0	0	0	0	0	0
15	0	0	0	0	0	0	0	0
16	0	0	0	0	0	0	0	0
17	0	0	0	0	0	0	0	0
18	0	0	0	0	0	0	0	0
19	0	0	0	0	0	0	0	0
20	0	0	0	0	0	0	0	0
21	7	49	52	4	7	2	0	0
22	31	63	60	8	12	6	0	0
23	51	70	60	10	16	9	0	0
24	64	79	60	12	19	11	0	[illegible]
25	70	87	60	17	27	18	0	0
26	79	105	60	18	29	20	0	0
27	88	131	60	13	20	13	0	0
28	105	162	60	5	7	3	0	0
29	132	275	60	26	42	[illegible]	[illegible]	
30	171	330	60	40	65	55	0	[illegible]
31	279	442	60	38	62	51	0	[illegible]
32	331	500	60	50	82	73	[illegible]	[illegible]

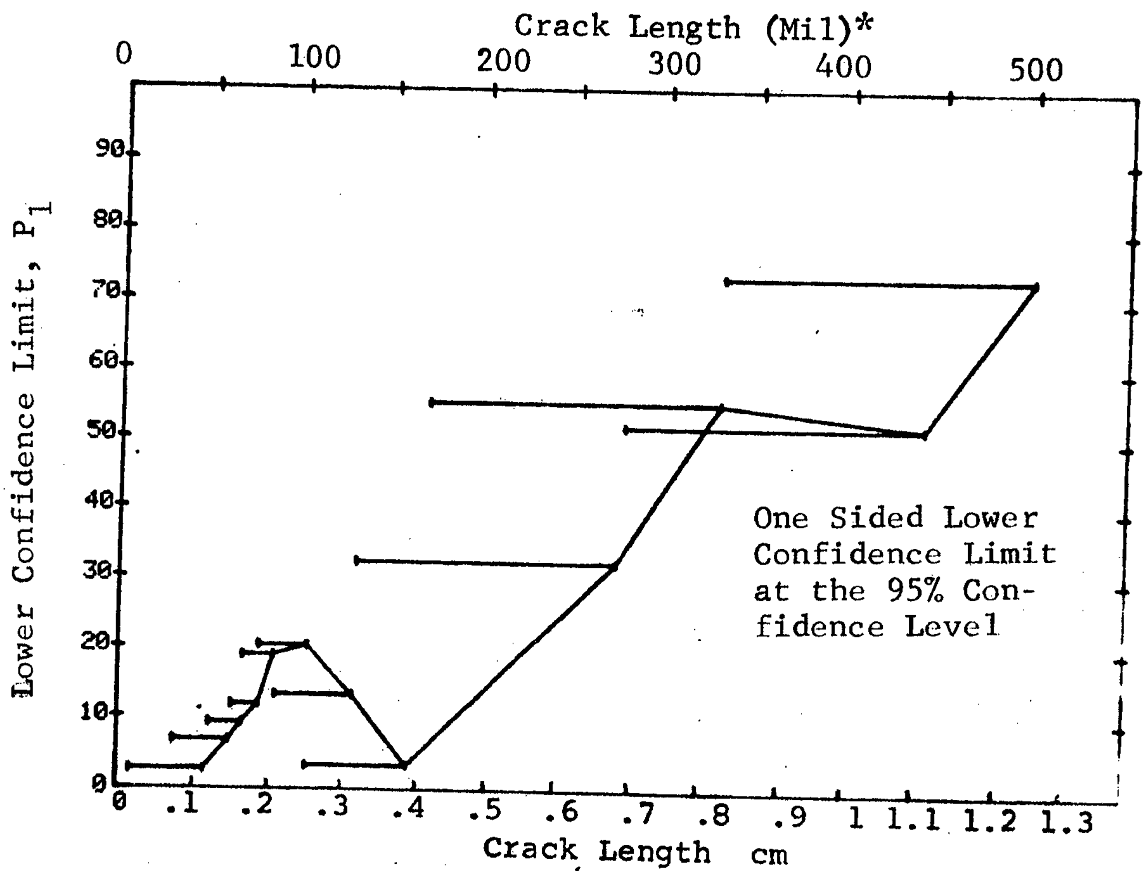

Figure D-26 (Concluded)

(a) Range Interval Method of Data Cumulation

03-JUL-75 RADIOGRAPHY TEST 1, ROCKWELL SC[illegible]E (27)

RANGE	MIN LN	MAX LN	N	DET	50%	95%	0 MISS	1 MISS
1	7 *	22 *	13	1	5	0	0	0
2	25	36	18	1	3	0	0	0
3	38	52	23	1	2	0	0	0
4	54	67	46	5	10	4	0	0
5	68	82	53	9	16	9	0	0
6	33	97	37	8	20	11	0	0
7	98	111	17	2	9	2	0	0
8	115	126	17	0	0	0	0	0
9	129	141	19	0	0	0	0	0
10	143	157	15	1	4	0	0	0
11	158	171	3	0	0	0	0	0
12	182	185	3	0	0	0	0	0
13	190	197	2	0	0	0	0	0
14	0	0	0	0	0	0	0	0
15	0	0	0	0	0	0	0	0
16	241	247	4	4	84	47	0	0
17	248	262	17	16	90	75	29	44
18	268	275	3	3	79	36	0	0
19	279	290	7	6	77	47	0	0
20	295	306	6	2	26	6	0	0
21	310	322	10	4	35	15	0	0
22	323	336	12	3	21	7	0	0
23	338	352	11	10	85	63	0	[illegible]
24	356	362	4	3	61	24	0	[illegible]
25	370	381	5	5	87	54	0	0
26	384	393	2	1	29	2	0	[illegible]
27	408	408	1	1	50	5	0	0
28	426	426	1	0	0	0	0	0
29	442	442	1	1	50	5	[illegible]	[illegible]
30	444	444	1	1	50	5	0	[illegible]
31	458	472	8	8	91	68	[illegible]	[illegible]
32	474	979	59	54	90	83	44	[illegible]

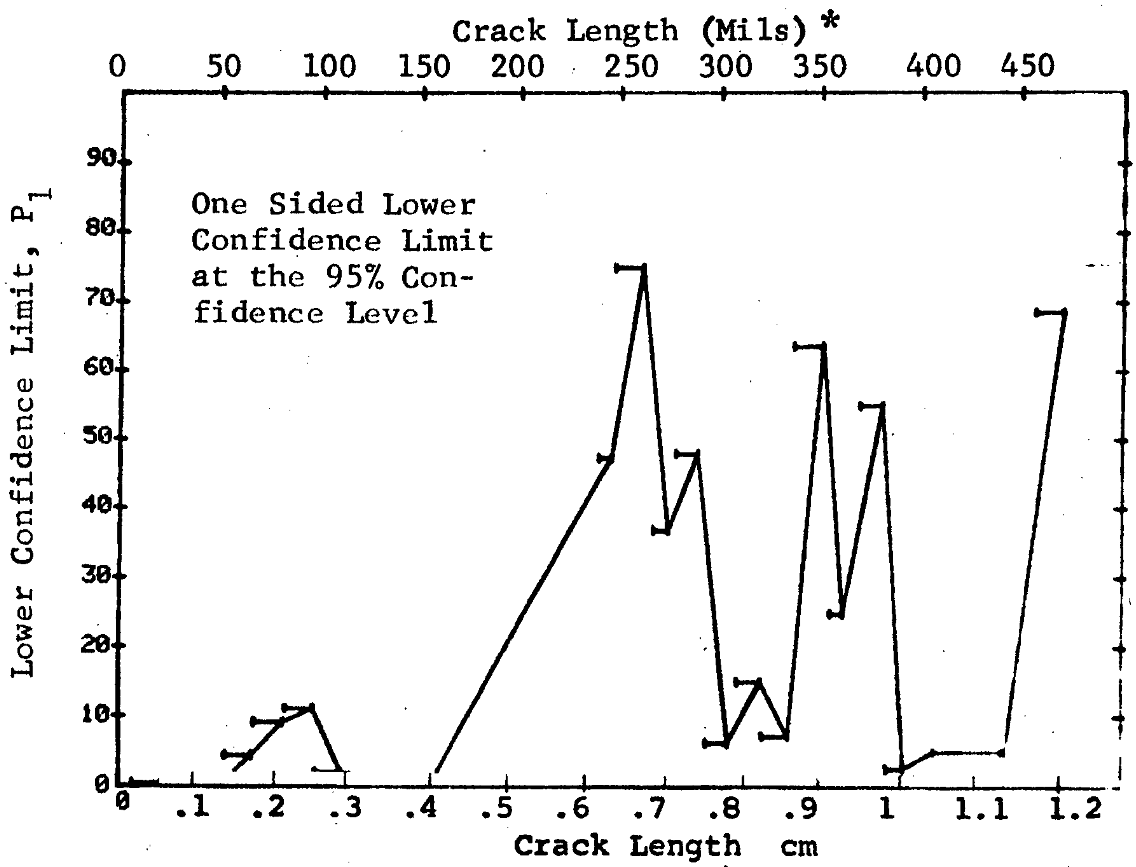

Figure D-27. Probability of Detection for 2219-T87 Al Using X-ray. Etched Fatigue Cracks in Flat Plates Measured by Operator B. Lab. Env.

(b) Optimum Probability Method of Data Cumulation

03-JUL-75 RADIOGRAPHY TEST 2 , ROCKWELL SC. 'C' (27)

RANGE	MIN LN	MAX LN	N	DET	50%	95%	0 MISS	1 MISS
1	7	* 22 *,	13	1	0	0	0	0
2	7	36	31	2	0	1	0	0
3	7	52	54	3	0	1	0	0
4	54	67	46	5	0	4	0	0
5	68	82	53	9	0	9	0	0
6	68	97	90	17	0	12	0	0
7	68	111	107	19	0	11	0	0
8	68	126	124	19	0	10	0	0
9	54	141	189	24	0	8	0	0
10	54	157	204	25	0	8	0	0
11	68	171	161	20	0	8	0	0
12	54	185	210	25	0	8	0	0
13	54	197	212	25	0	8	0	0
14	0	0	0	0	0	0	0	0
15	0	0	0	0	0	0	0	0
16	241	247	4	4	0	47	0	0
17	241	262	21	20	0	79	0	0
18	241	275	24	23	0	81	0	0
19	241	290	31	29	0	81	22	37
20	241	306	37	31	0	70	30	45
21	241	322	47	35	0	61	0	0
22	241	336	59	38	0	52	0	0
23	338	352	11	10	0	63	0	0
24	338	362	15	13	0	63	0	0
25	338	381	20	18	0	71	0	0
26	338	393	22	19	0	68	0	0
27	338	408	23	20	0	69	0	0
28	338	426	24	20	0	65	0	0
29	338	442	25	21	0	66	0	0
30	338	444	26	22	0	68	0	0
31	338	472	34	38	0	75	0	0
32	442	979	69	64	0	85	34	47

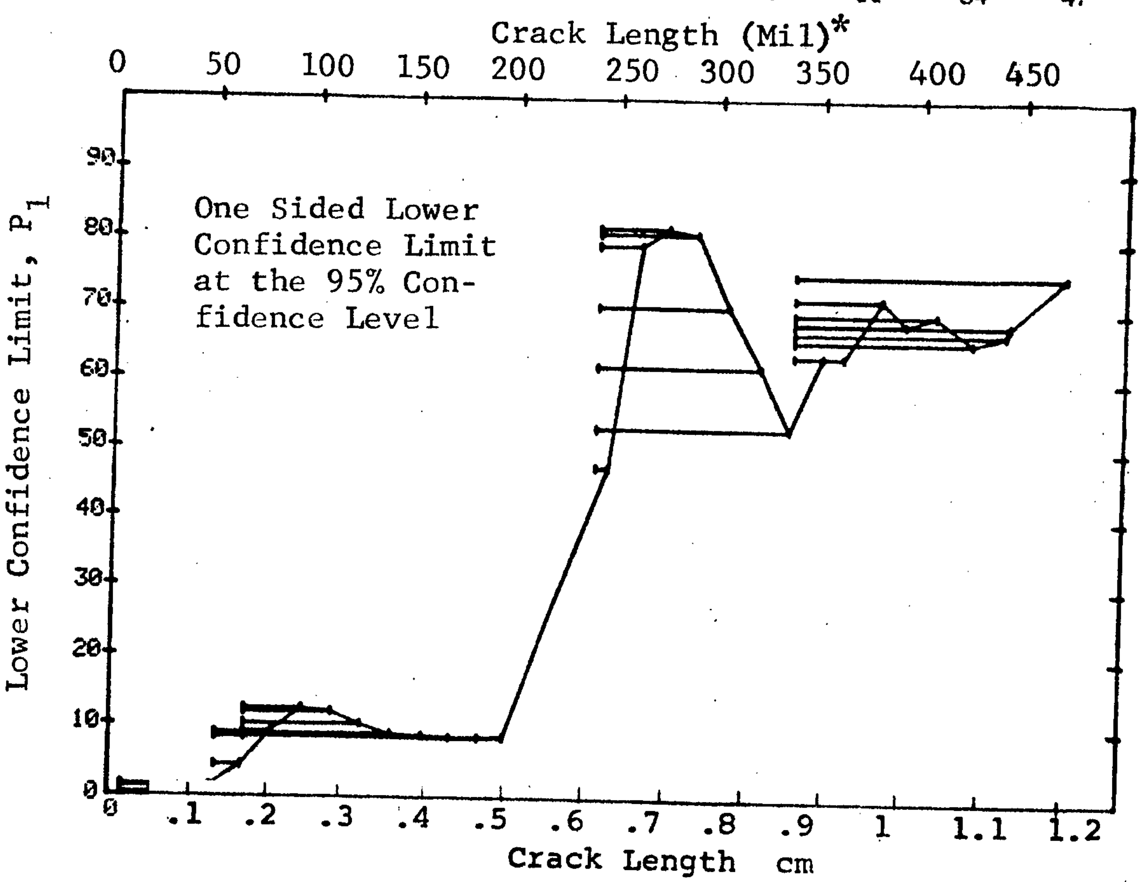

Figure D-27 (Continued)

(c) Overlapping Sixty Point Method of Data Cumulation

03-JUL-75 RADIOGRAPHY TEST 3, ROCKWELL SC (27)

RANGE	MIN LN	* MAX LN *	N	DET	50%	95%	0 MISS	1 MISS
1	0	0	0	0	0	0	0	0
2	0	0	0	0	0	0	0	0
3	0	0	0	0	0	0	0	0
4	0	0	0	0	0	0	0	0
5	0	0	0	0	0	0	0	0
6	0	0	0	0	0	0	0	0
7	0	0	0	0	0	0	0	0
8	0	0	0	0	0	0	0	0
9	0	0	0	0	0	0	0	0
10	0	0	0	0	0	0	0	0
11	0	0	0	0	0	0	0	0
12	0	0	0	0	0	0	0	0
13	0	0	0	0	0	0	0	0
14	0	0	0	0	0	0	0	0
15	0	0	0	0	0	0	0	0
16	0	0	0	0	0	0	0	0
17	0	0	0	0	0	0	0	0
18	0	0	0	0	0	0	0	0
19	0	0	0	0	0	0	0	0
20	0	0	0	0	0	0	0	0
21	7	49	50	3	5	1	0	0
22	30	63	60	5	7	3	0	0
23	49	69	60	5	7	3	0	0
24	63	79	60	7	11	5	0	0
25	69	87	60	13	20	13	0	0
26	79	105	60	14	22	14	0	0
27	88	131	60	6	9	4	0	0
28	105	162	60	1	1	0	0	0
29	132	275	60	24	39	[illegible]	[illegible]	[illegible]
30	171	330	60	36	59	48	[illegible]	[illegible]
31	279	442	60	36	59	48	0	[illegible]
32	331	500	60	50	82	73	[illegible]	[illegible]

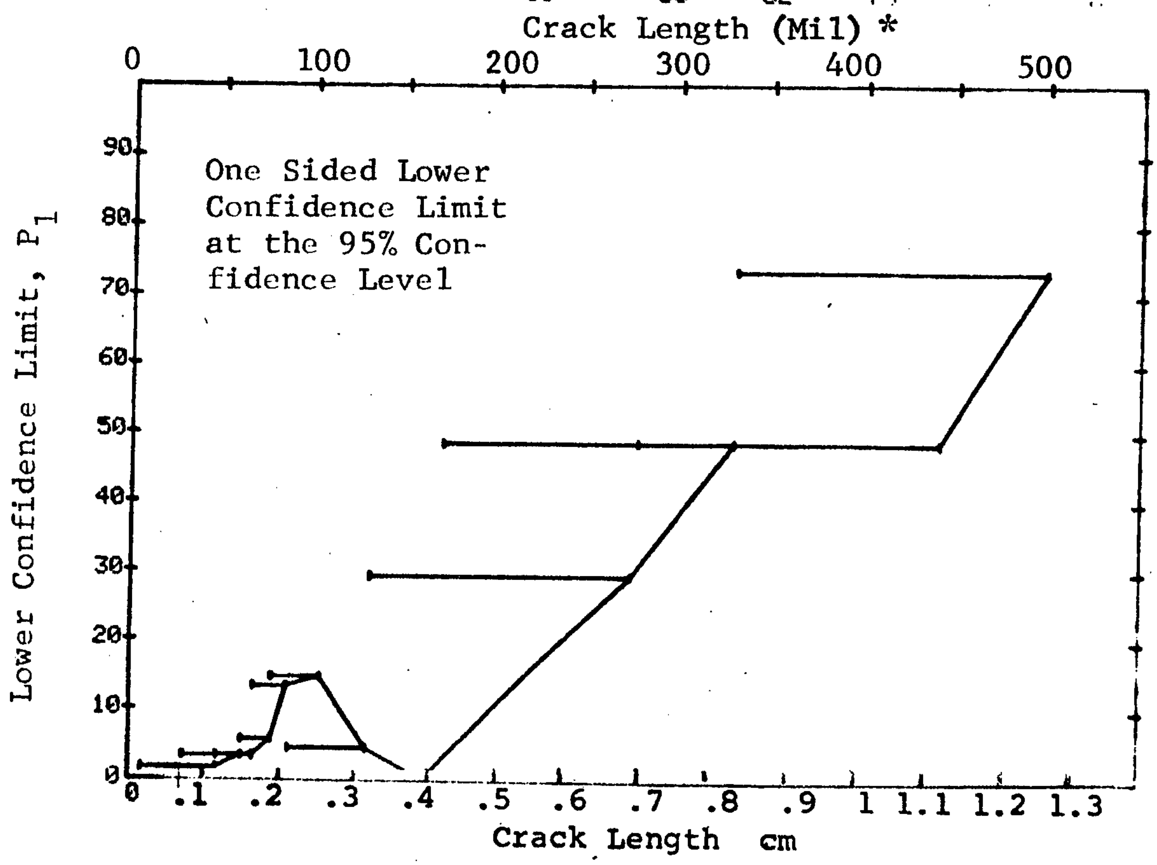

Figure D-27 (Concluded)

(a) Range Interval Method of Data Cumulation

23-JUL-75 RADIOGRAPHY TEST 1. DEN=20. ROCKWELL SC. C (28)

RANGE	MIN LN	MAX LN	N	DET	50%	95%	0 MISS	1 MISS
1	7 *	22 *	13	0	0	0	0	0
2	25	36	18	0	0	0	0	0
3	38	52	23	1	2	0	0	0
4	54	67	46	1	1	0	0	0
5	68	82	53	3	5	1	0	0
6	83	97	39	6	14	6	0	0
7	98	111	17	3	15	4	0	0
8	115	126	17	0	0	0	0	0
9	129	141	19	1	3	0	0	0
10	143	157	15	1	4	0	0	0
11	158	171	3	0	0	0	0	0
12	182	185	3	0	0	0	0	0
13	190	197	2	0	0	0	0	0
14	0	0	0	0	0	0	0	0
15	0	0	0	0	0	0	0	0
16	241	247	4	3	61	24	0	0
17	248	262	17	15	84	67	0	0
18	268	275	3	2	50	13	0	0
19	279	290	7	4	50	22	0	[illegible]
20	295	306	6	1	10	0	0	[illegible]
21	310	322	10	1	6	0	0	[illegible]
22	323	336	12	2	13	3	0	[illegible]
23	338	352	11	9	76	52	0	[illegible]
24	356	362	4	3	61	24	0	[illegible]
25	370	381	5	4	68	34	0	[illegible]
26	384	393	2	2	70	22	0	[illegible]
27	408	408	1	0	0	0	0	[illegible]
28	426	426	1	0	0	0	0	0
29	442	442	1	1	50	5	0	0
30	444	444	1	1	50	5	[illegible]	[illegible]
31	458	472	8	7	79	52	0	[illegible]
32	474	979	59	48	80	71	0	0

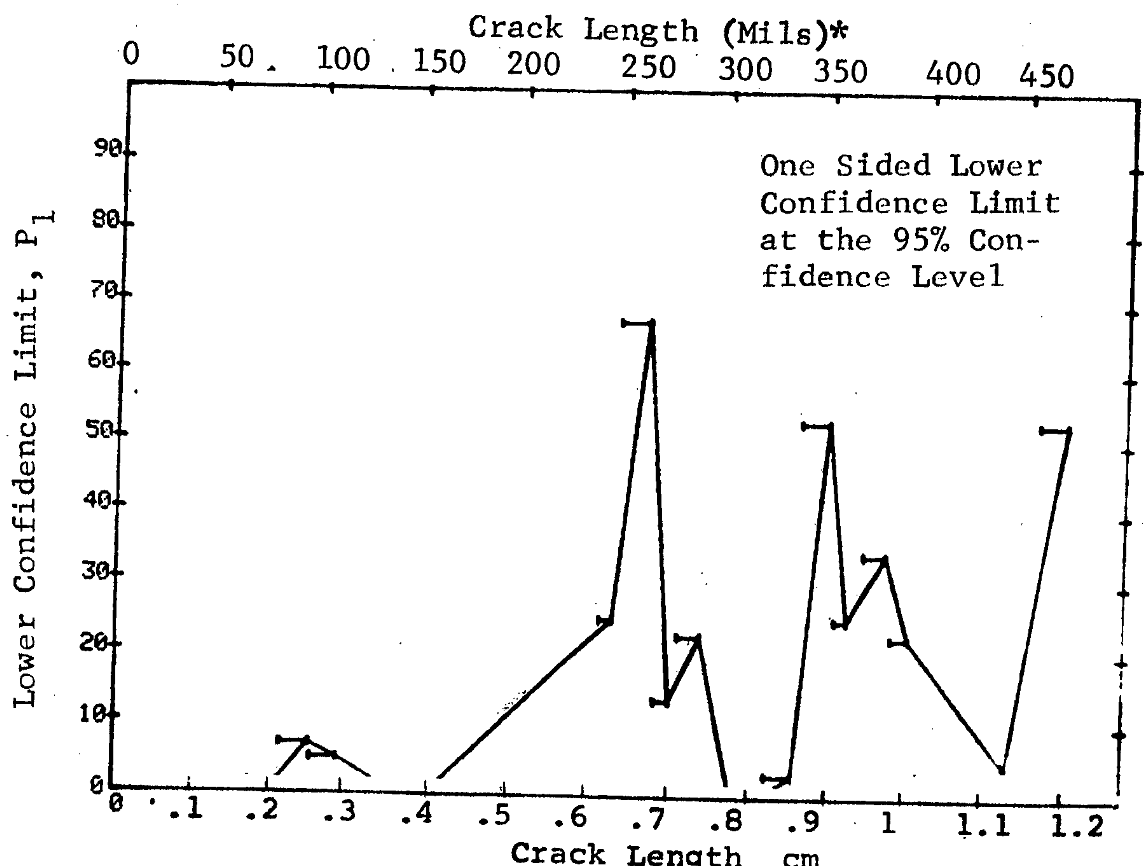

Figure D-28 Probability of Detection for 2219-T87 Al Using X-ray. Etched Fatigue Cracks in Flat Plates Measured by Operator C. Lab. Env.

(b) Optimum Probability Method of Data Cumulation

23-JUL-75 RADIOGRAPHY TEST 2, DSN=20, ROCKWELL SC. C (28)

RANGE	MIN LN	MAX LN	N	DET	50%	95%	0 MISS	1 MISS
1	7 *	22 *	13	0	0	0	0	0
2	25	36	18	0	0	0	0	0
3	38	52	23	1	0	0	0	0
4	38	67	69	2	0	0	0	0
5	38	82	122	5	0	1	0	0
6	83	97	39	6	0	6	0	0
7	83	111	56	9	0	8	0	0
8	83	126	73	9	0	6	0	0
9	83	141	92	10	0	6	0	0
10	83	157	107	11	0	5	0	0
11	83	171	110	11	0	5	0	0
12	83	185	113	11	0	5	0	0
13	83	197	115	11	0	5	0	0
14	0	0	0	0	0	0	0	0
15	0	0	0	0	0	0	0	0
16	241	247	4	3	0	24	0	0
17	248	262	17	15	0	67	0	0
18	241	275	24	20	0	65	0	0
19	241	290	31	24	0	61	0	0
20	241	306	37	25	0	52	0	0
21	241	322	47	26	0	42	0	0
22	241	336	59	28	0	36	0	0
23	338	352	11	9	0	52	0	0
24	338	362	15	12	0	56	0	0
25	338	381	20	16	0	59	0	0
26	338	393	22	18	0	63	0	0
27	338	408	23	18	0	59	0	0
28	338	426	24	18	0	56	0	0
29	338	442	25	19	0	[illegible]	[illegible]	[illegible]
30	338	444	26	20	0	59	[illegible]	[illegible]
31	338	472	34	27	0	64	0	0
32	442	979	69	57	0	73	0	0

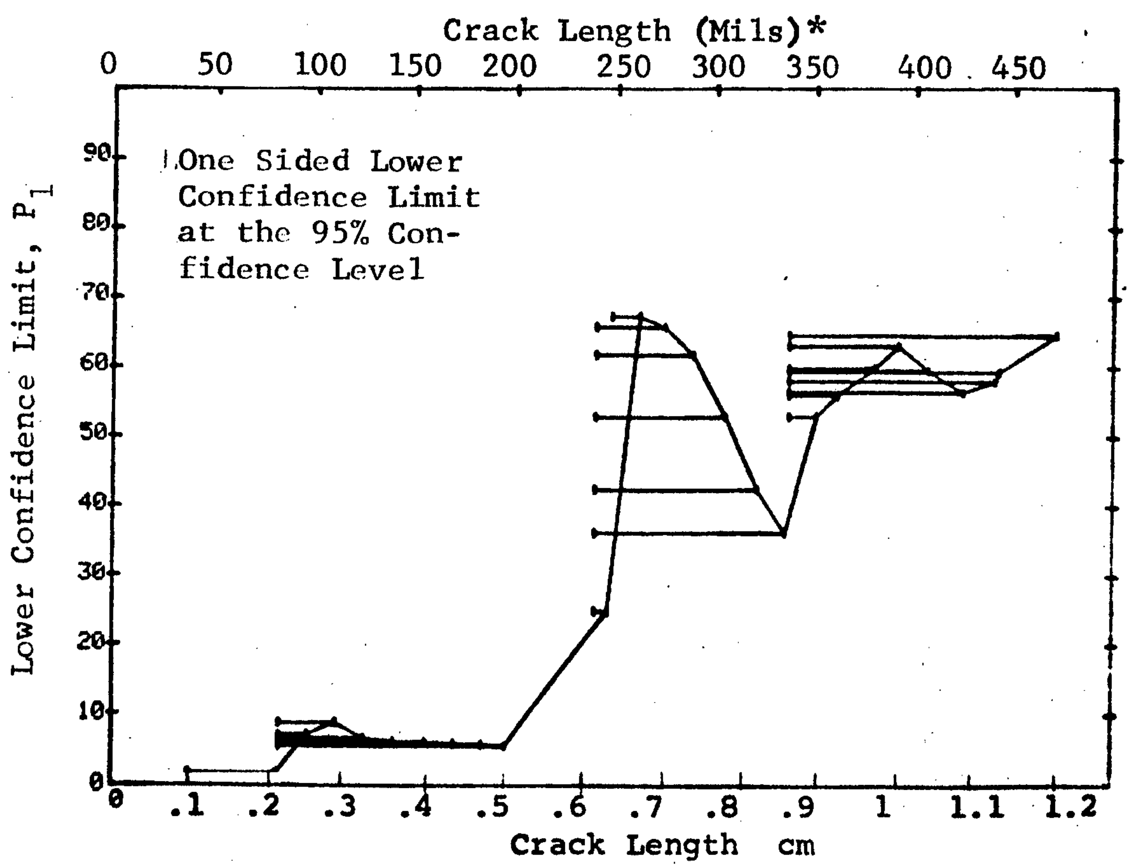

Figure D-28 (Continued)

(c) Overlapping Sixty Point Method of Data Cumulation

23-JUL-75 RADIOGRAPHY TEST 3, DSN=20, ROCKWELL SC. (28) C

RANGE	MIN LN	MAX LN	N	DET	50%	95%	0 MISS	1 MISS
1	0 *	0 *	0	0	0	0	0	0
2	0	0	0	0	0	0	0	0
3	0	0	0	0	0	0	0	0
4	0	0	0	0	0	0	0	0
5	0	0	0	0	0	0	0	0
6	0	0	0	0	0	0	0	0
7	0	0	0	0	0	0	0	0
8	0	0	0	0	0	0	0	0
9	0	0	0	0	0	0	0	0
10	0	0	0	0	0	0	0	0
11	0	0	0	0	0	0	0	0
12	0	0	0	0	0	0	0	0
13	0	0	0	0	0	0	0	0
14	0	0	0	0	0	0	0	0
15	0	0	0	0	0	0	0	0
16	0	0	0	0	0	0	0	0
17	0	0	0	0	0	0	0	0
18	0	0	0	0	0	0	0	0
19	0	0	0	0	0	0	0	0
20	0	0	0	0	0	0	0	0
21	7	49	52	1	1	0	0	0
22	31	63	60	2	2	0	0	0
23	51	70	60	1	1	0	0	0
24	64	79	60	1	1	0	0	0
25	70	87	60	9	14	8	0	0
26	79	105	60	10	16	9	0	0
27	88	131	60	4	6	2	0	0
28	105	162	60	3	4	1	0	0
29	132	275	60	21	34	24	0	0
30	171	330	60	27	44	33	0	0
31	279	442	60	27	44	33	0	0
32	331	500	60	43	70	60	0	0

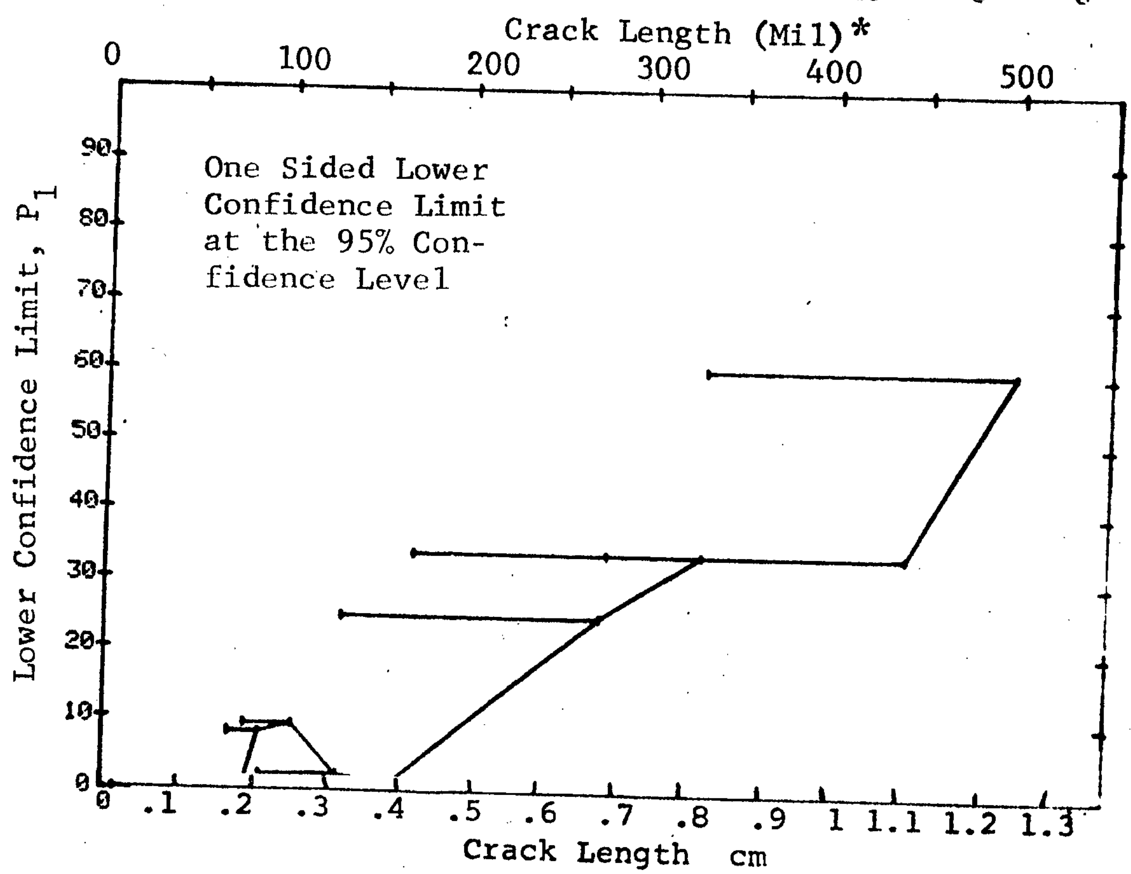

Figure D-28 (Concluded)

(a) Range Interval Method of Data Cumulation

23-JUL-75 RADIOGRAPHY TEST 1, DSN=21, ROCKWELL SC. D (29)

RANGE	MIN LN *	MAX LN *	N	DET	50%	95%	0 MISS	1 MISS
1	7	22	13	1	5	0	0	0
2	25	36	18	2	9	2	0	0
3	38	52	23	2	7	1	0	0
4	54	67	46	7	14	7	0	0
5	68	82	53	9	16	9	0	0
6	83	97	39	16	39	27	0	0
7	98	111	17	6	32	16	0	0
8	115	126	17	1	3	0	0	0
9	129	141	19	3	13	4	0	0
10	143	157	15	2	10	2	0	0
11	158	171	3	0	0	0	0	0
12	182	185	3	0	0	0	0	0
13	190	197	2	1	29	2	0	0
14	0	0	0	0	0	0	0	0
15	0	0	0	0	0	0	0	0
16	241	247	4	3	61	24	0	0
17	248	262	17	16	90	75	29	44
18	268	275	3	3	79	36	0	0
19	279	290	7	3	36	12	0	0
20	295	306	6	1	10	0	0	0
21	310	322	10	3	25	8	0	0
22	323	336	12	4	29	12	0	0
23	338	352	11	8	67	43	0	0
24	356	362	4	3	61	24	0	0
25	370	381	5	5	87	54	0	0
26	384	393	2	2	70	22	0	0
27	408	408	1	0	0	0	0	0
28	426	426	1	0	0	0	0	0
29	442	442	1	1	50	5	0	0
30	444	444	1	1	50	5	0	0
31	458	472	8	8	91	68	0	0
32	474	979	59	58	97	92	0	0

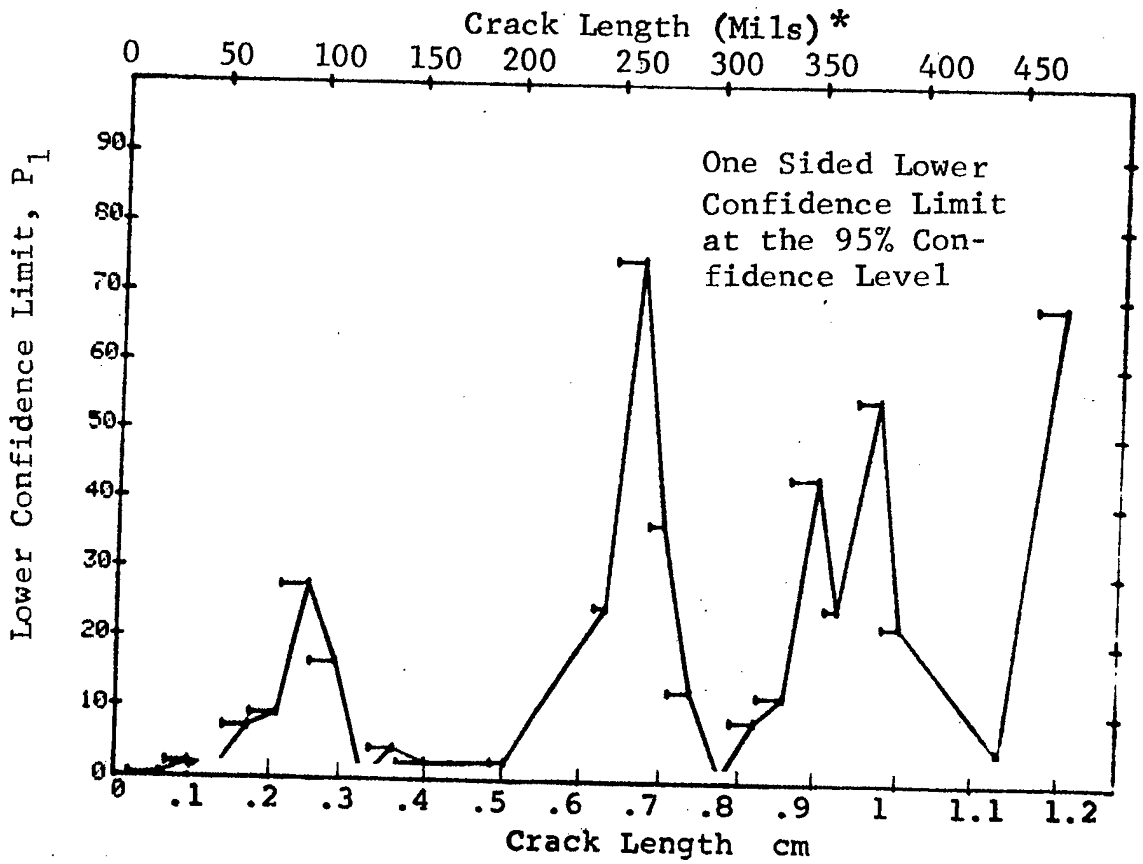

Figure D-29 Probability of Detection for 2219-T87 Al Using X-ray. Etched Fatigue Cracks in Flat Plates Measured by Operator D. Lab. Env.

(b) Optimum Probability Method of Data Cumulation

23-JUL-75 RADIOGRAPHY TEST 2, DSN=21, ROCKWELL [illegible] D' (29)

RANGE	MIN LN		MAX LN		N	DFT	50%	95%	0 MISS	1 MISS
1	7	*	22	*	13	1	0	0	0	0
2	7		36		21	3	0	2	0	0
3	7		52		54	5	0	3	0	0
4	54		67		46	7	0	7	0	0
5	54		82		99	16	0	10	0	0
6	83		97		39	16	0	27	0	0
7	83		111		56	22	0	28	0	0
8	83		126		73	23	0	22	0	0
9	83		141		92	26	0	20	0	0
10	83		157		107	28	0	19	0	0
11	83		171		110	28	0	18	0	0
12	83		185		113	28	0	18	0	0
13	83		197		115	29	0	18	0	0
14	0		0		0	0	0	0	0	0
15	0		0		0	0	0	0	0	0
16	190		247		6	4	0	27	0	0
17	248		262		17	16	0	75	0	0
18	248		275		20	19	0	78	0	[illegible]
19	241		290		31	25	0	65	0	[illegible]
20	241		306		37	26	0	55	0	[illegible]
21	241		322		47	29	0	48	0	
22	241		336		59	33	0	44	0	[illegible]
23	241		352		70	41	0	48	0	[illegible]
24	241		362		74	44	0	49	0	[illegible]
25	338		381		20	16	0	59	0	[illegible]
26	370		393		7	7	0	65	0	[illegible]
27	338		408		23	18	0	59	0	0
28	338		426		24	18	0	56	0	[illegible]
29	338		442		25	19	0	56	[illegible]	[illegible]
30	338		444		26	20	0	59	0	[illegible]
31	442		472		10	10	0	74	0	[illegible]
32	442		979		69	68	0	93	0	0

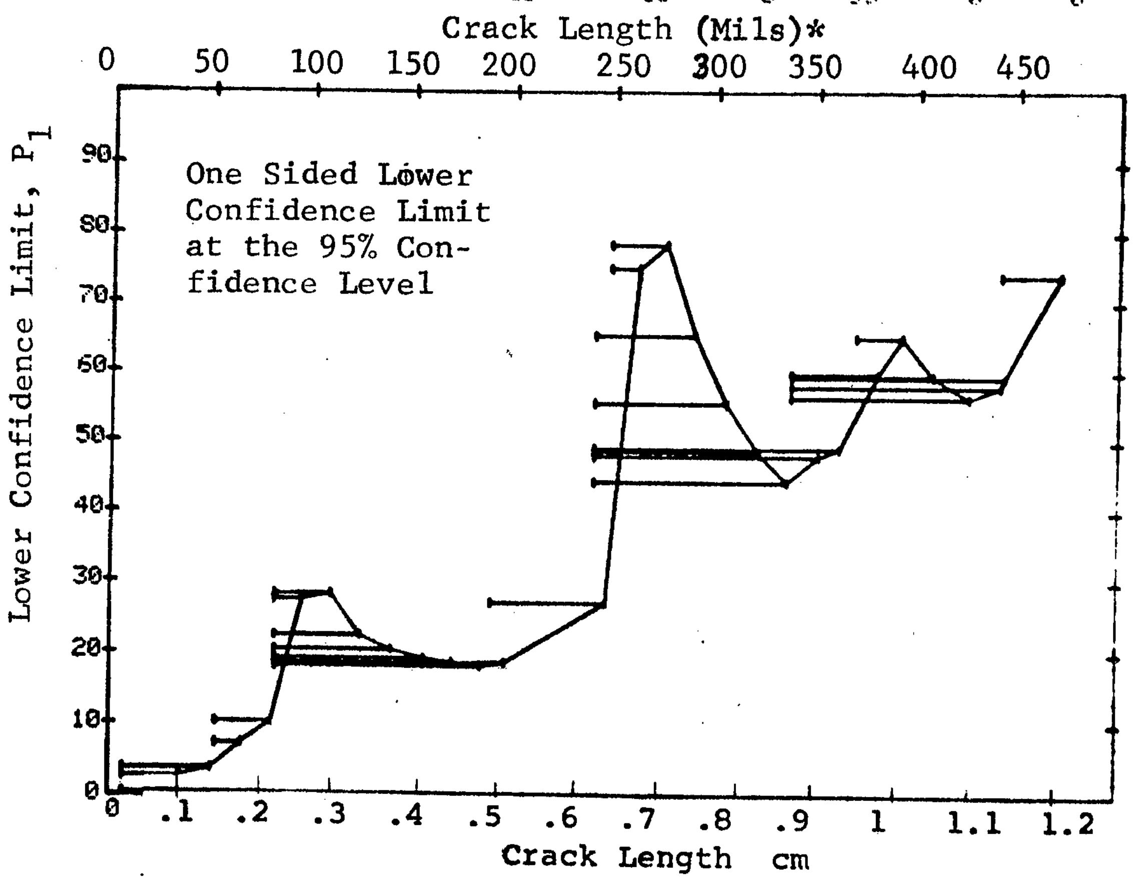

Figure D-29 (Continued)

(c) Overlapping Sixty Point Method of Data Cumulation

23-JUL-75 RADIOGRAPHY TEST 3, DSN=21, ROCKWELL SC D (29)

RANGE	MIN LN	MAX LN	N	DET	50%	95%	0 MISS	1 MISS
1	0 *	0 *	0	0	0	0	0	0
2	0	0	0	0	0	0	0	0
3	0	0	0	0	0	0	0	0
4	0	0	0	0	0	0	0	0
5	0	0	0	0	0	0	0	0
6	0	0	0	0	0	0	0	0
7	0	0	0	0	0	0	0	0
8	0	0	0	0	0	0	0	0
9	0	0	0	0	0	0	0	0
10	0	0	0	0	0	0	0	0
11	0	0	0	0	0	0	0	0
12	0	0	0	0	0	0	0	0
13	0	0	0	0	0	0	0	0
14	0	0	0	0	0	0	0	0
15	0	0	0	0	0	0	0	0
16	0	0	0	0	0	0	0	0
17	0	0	0	0	0	0	0	0
18	0	0	0	0	0	0	0	0
19	0	0	0	0	0	0	0	0
20	0	0	0	0	0	0	0	0
21	7	49	52	4	7	2	0	0
22	31	63	60	10	16	9	0	0
23	51	70	60	9	14	8	0	0
24	64	79	60	7	11	5	0	0
25	70	87	60	16	25	17	0	0
26	79	105	60	24	39	29	0	0
27	88	131	60	15	24	16	0	0
28	105	162	60	7	11	5	0	0
29	132	275	60	28	45	35	0	0
30	171	330	60	32	52	41	0	0
31	279	442	60	30	49	36	0	0
32	331	500	60	51	83	75	94	100

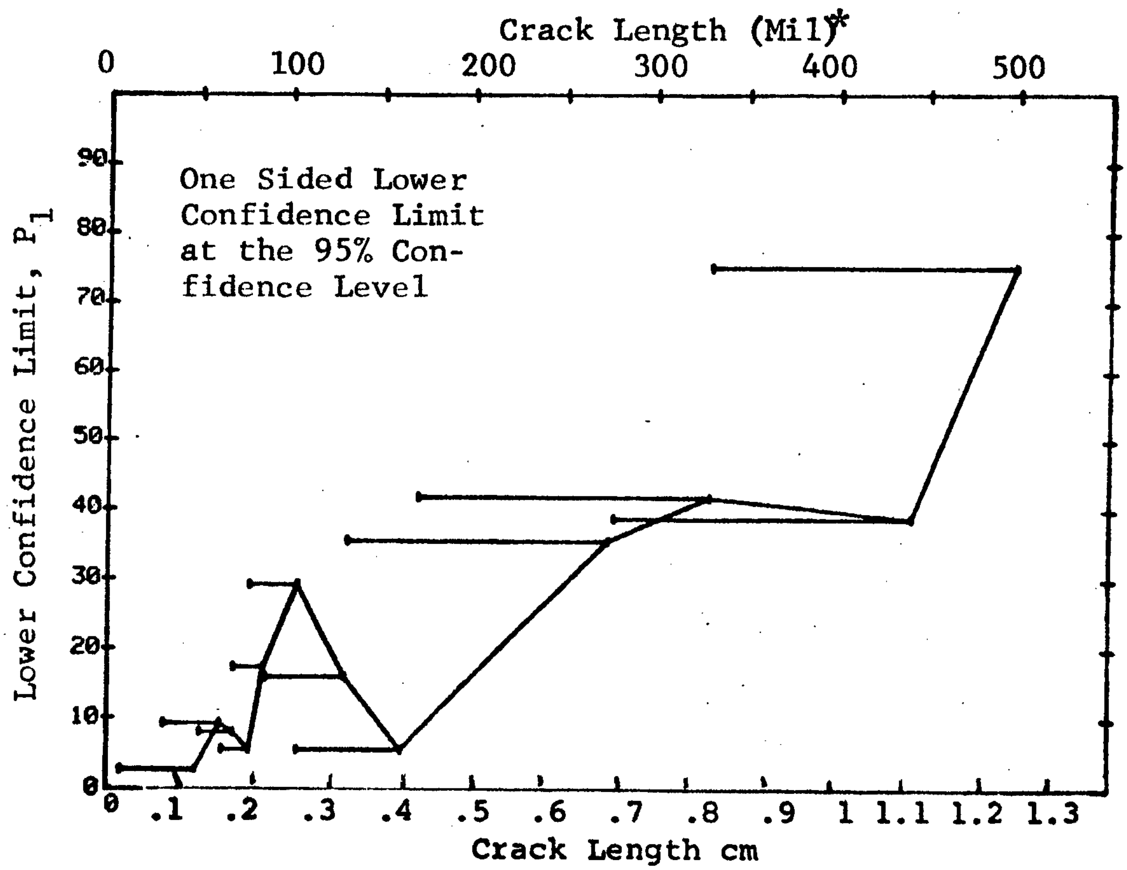

Figure D-29 (Concluded)

(a) Range Interval Method of Data Cumulation

23-JUL-75 RADIOGRAPHY TEST 1, (30) E

RANGE	MIN LN	MAX LN	N	DET	50%	95%	0 MISS	1 MISS
1	7*	18*	8	0	0	0	0	0
2	20	28	11	3	23	7	0	0
3	30	40	15	1	4	0	0	0
4	41	51	19	4	18	7	0	0
5	52	62	26	8	29	16	0	0
6	63	73	43	13	29	18	0	0
7	74	84	38	15	38	26	0	0
8	85	95	26	12	44	29	0	0
9	96	106	19	6	29	14	0	0
10	108	117	8	1	8	0	0	0
11	118	126	13	2	12	2	0	0
12	129	138	16	2	10	2	0	0
13	140	150	13	2	12	2	0	0
14	151	158	6	1	10	0	0	0
15	162	171	2	1	29	2	0	0
16	182	183	2	1	29	2	0	0
17	185	190	2	1	29	2	0	0
18	197	197	1	1	50	5	0	0
19	0	0	0	0	0	0	0	0
20	0	0	0	0	0	0	0	0
21	0	0	0	0	0	0	0	0
22	241	249	7	7	90	65	0	0
23	250	260	11	11	93	76	18	35
24	261	269	5	5	87	54	0	0
25	275	279	3	3	79	36	0	0
26	283	290	5	5	87	54	0	0
27	295	304	5	4	68	34	0	0
28	306	313	7	5	63	34	0	0
29	317	326	8	3	32	11	0	0
30	328	336	8	4	44	19	0	0
31	338	347	9	6	60	34	0	0
32	352	362	4	3	61	24	0	0

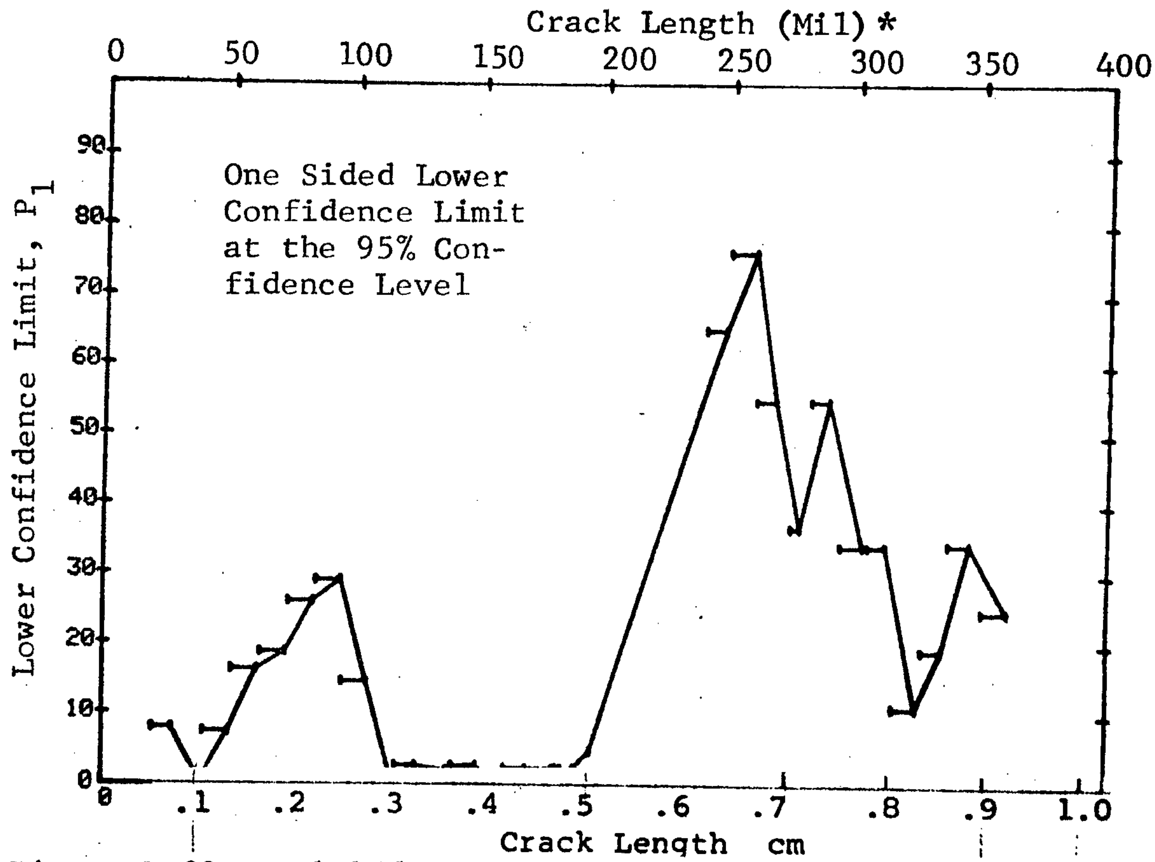

Figure D-30 Probability of Detection for 2219-T87 Al Using X-ray. Etched Fatigue Cracks in Flat Plates Measured by Operator E. Lab. Env.

C3

(b) Overlapping Sixty Point Method of Data Cumulation

23-JUL-75 RADIOGRAPHY TEST 2, ∟ (30). ROCKWELL SC E

RANGE	MIN LN	*MAX LN*	N	DET	50%	95%	0 MISS	1 MISS
1	7	18	8	0	0	0	0	0
2	20	28	11	3	0	7	0	0
3	20	40	26	4	0	5	0	0
4	20	51	45	8	0	9	0	0
5	52	62	26	8	0	16	0	0
6	52	73	69	21	0	21	0	0
7	74	84	38	15	0	26	0	0
8	74	95	64	27	0	31	0	0
9	74	106	83	33	0	30	0	0
10	74	117	91	34	0	28	0	0
11	63	126	147	49	0	26	0	0
12	52	138	189	59	0	25	0	0
13	52	150	202	61	0	24	0	0
14	52	158	208	62	0	24	0	0
15	52	171	210	63	0	24	0	0
16	52	183	212	64	0	25	0	0
17	52	190	214	65	0	25	0	0
18	63	197	189	58	0	25	0	0
19	0	0	0	0	0	0	0	0
20	0	0	0	0	0	0	0	0
21	0	0	0	0	0	0	0	0
22	197	249	8	8	0	68	0	0
23	197	260	19	19	0	85	10	27
24	197	269	24	24	0	88	5	22
25	197	279	27	27	0	89	2	19
26	197	290	32	32	0	91	0	14
27	197	304	37	36	0	87	9	24
28	197	313	44	41	0	83	32	45
29	197	326	52	44	0	73	0	0
30	197	336	60	48	0	69	0	0
31	197	347	69	54	0	68	0	0
32	197	362	73	57	0	68	0	0

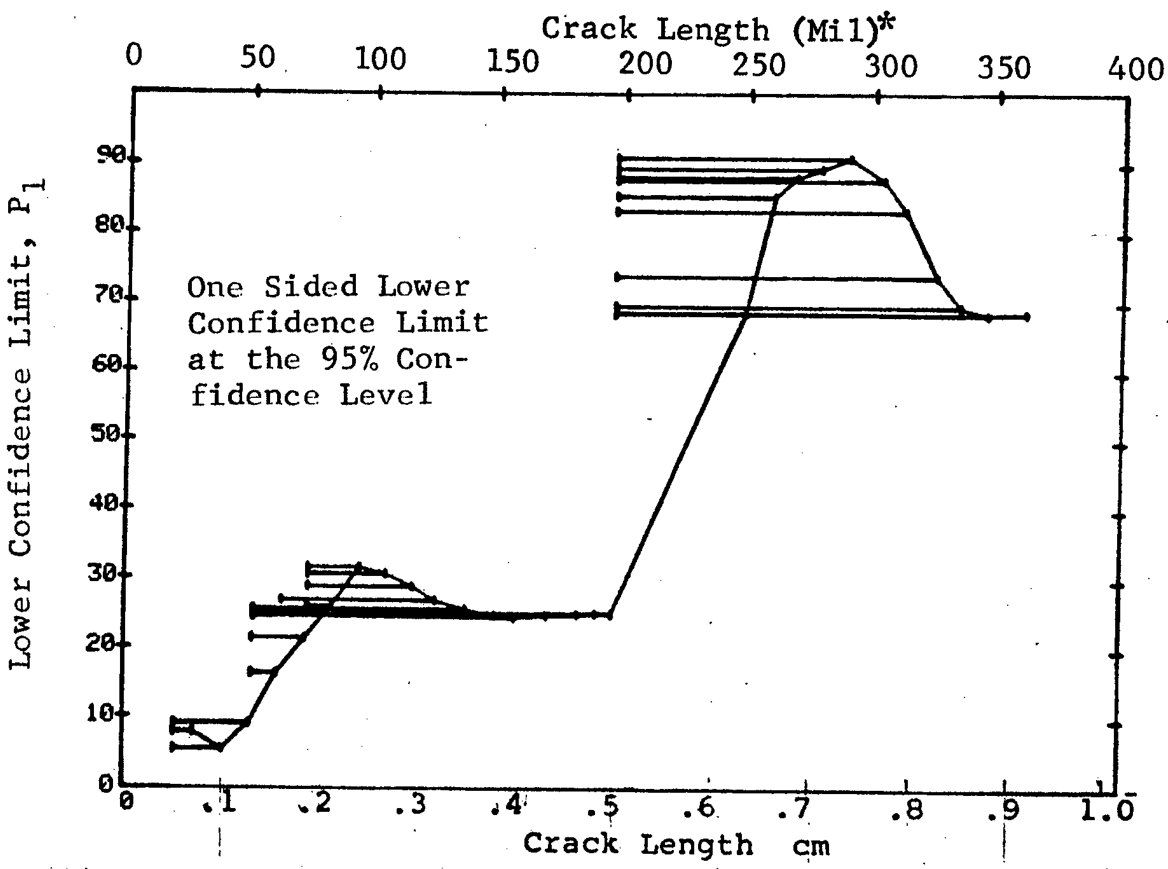

Figure D-30 (Continued)

(c) Overlapping Sixty Point Method of Data Cumulation

23-JUL-75 RADIOGRAPHY TEST 3. (30) ROCKWELL SC E

RANGE	MIN LN	MAX LN	N	DET	50%	95%	0 MISS	1 MISS
1	0	0	0	0	0	0	0	0
2	0	0	0	0	0	0	0	0
3	0	0	0	0	0	0	0	0
4	0	0	0	0	0	0	0	0
5	0	0	0	0	0	0	0	0
6	0	0	0	0	0	0	0	0
7	0	0	0	0	0	0	0	0
8	0	0	0	0	0	0	0	0
9	0	0	0	0	0	0	0	0
10	0	0	0	0	0	0	0	0
11	0	0	0	0	0	0	0	0
12	0	0	0	0	0	0	0	0
13	0	0	0	0	0	0	0	0
14	0	0	0	0	0	0	0	0
15	0	0	0	0	0	0	0	0
16	0	0	0	0	0	0	0	0
17	0	0	0	0	0	0	0	0
18	0	0	0	0	0	0	0	0
19	0	0	0	0	0	0	0	0
20	0	0	0	0	0	0	0	0
21	0	0	0	0	0	0	0	0
22	7	44	40	5	11	5	0	0
23	21	60	60	12	19	11	0	0
24	45	67	60	17	27	18	0	0
25	61	76	60	19	30	21	0	0
26	68	84	60	22	35	26	0	0
27	76	97	60	25	40	30	0	0
28	85	123	60	20	32	23	0	0
29	97	144	60	12	19	11	0	0
30	124	257	60	22	35	26	0	0
31	145	313	60	45	74	64	0	0
32	257	362	60	44	72	62	0	0

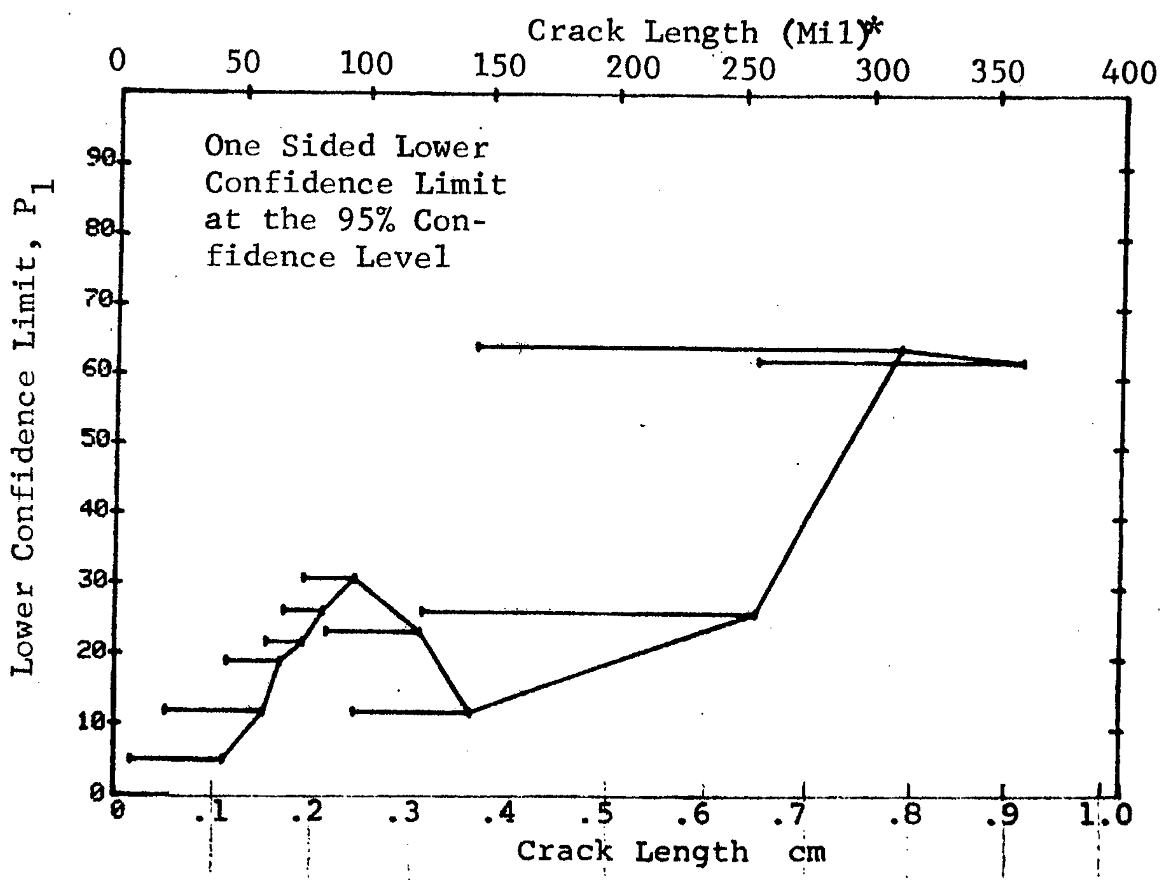

Figure D-30 (Concluded)

(a) Range Interval Method of Data Cumulation

23-JUL-75 RADIOGRAPHY TEST 1, . (31) F

RANGE	MIN LN *	MAX LN *	N	DET	50%	95%	0 MISS	1 MISS
1	7	22	13	2	12	2	0	0
2	25	36	18	3	14	4	0	0
3	38	52	23	7	28	15	0	0
4	54	67	46	13	27	17	0	0
5	68	82	53	23	42	31	0	0
6	83	97	39	18	44	32	0	0
7	98	111	17	5	26	12	0	0
8	115	126	16	4	22	9	0	0
9	129	141	20	5	22	10	0	0
10	143	157	15	8	50	29	0	0
11	158	171	3	2	50	13	0	0
12	182	185	3	2	50	13	0	0
13	190	197	2	1	29	2	0	0
14	0	0	0	0	0	0	0	0
15	0	0	0	0	0	0	0	0
16	241	247	4	4	84	47	0	0
17	248	262	17	16	90	75	29	44
18	268	275	3	3	79	36	0	0
19	279	290	7	6	77	47	0	0
20	295	306	6	5	73	41	0	0
21	310	322	10	4	35	15	0	0
22	323	336	12	9	70	47	0	0
23	338	352	11	9	76	52	0	0
24	356	362	4	2	38	9	0	0
25	370	381	5	4	68	34	0	0
26	384	393	2	2	70	22	0	0
27	408	408	1	1	50	5	0	0
28	426	426	1	0	0	0	0	0
29	442	442	1	1	50	5	0	0
30	444	444	1	0	0	0	0	0
31	458	472	8	6	67	40	0	0
32	474	979	59	51	85	76	83	95

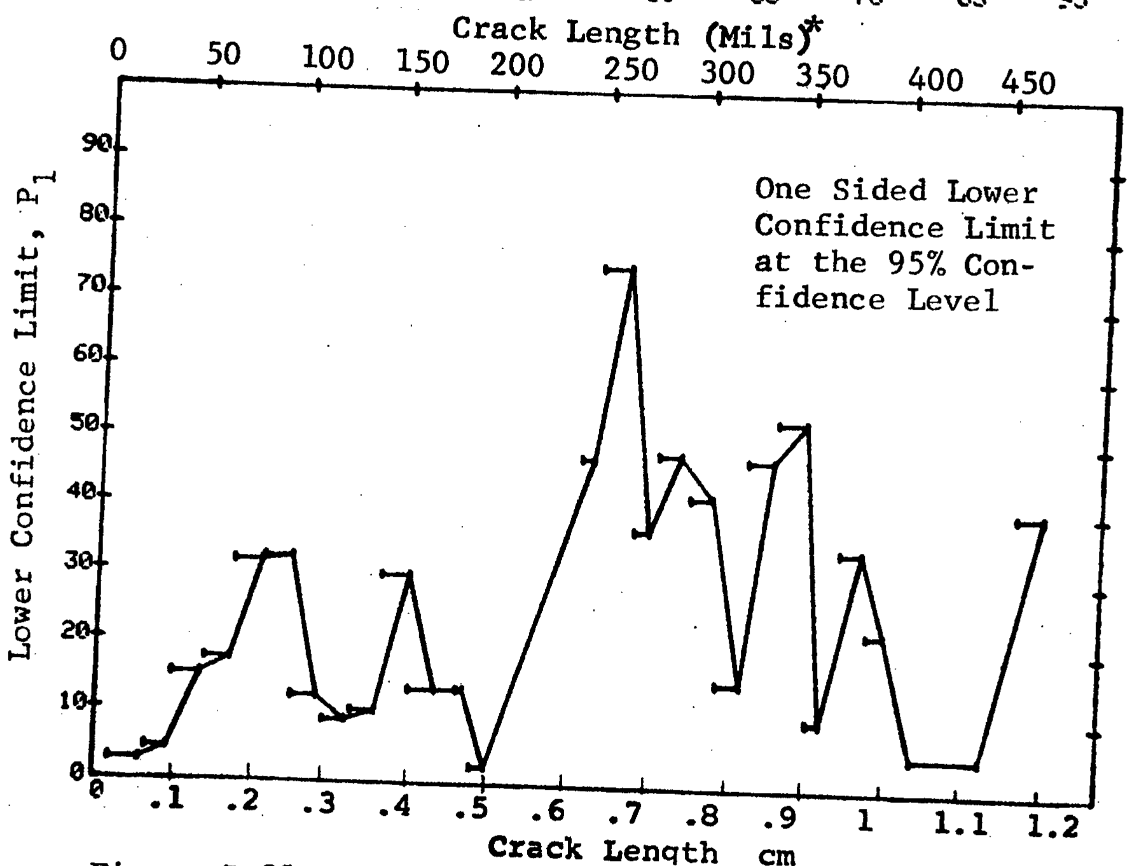

Figure D-31 Probability of Detection for 2219-T87 Al Using X-ray. Etched Fatigue Cracks in Flat Plates Measured by Operator F. Lab. Env.

(b) Optimum Probability Method of Data Cumulation

23-JUL-75 RADIOGRAPHY TEST 2. (31) ROCKWELL SC F

RANGE	MIN LN	MAX LN	N	DET	50%	95%	0 MISS	1 MISS
1	7 *	22 *	13	2	0	2	0	0
2	7	36	31	5	0	6	0	0
3	38	52	23	7	0	15	0	0
4	38	67	69	20	0	20	0	0
5	68	82	53	23	0	31	0	0
6	68	97	92	41	0	35	0	0
7	68	111	109	46	0	34	0	0
8	68	126	125	50	0	32	0	0
9	68	141	145	55	0	31	0	0
10	68	157	160	63	0	32	0	0
11	143	171	18	10	0	34	0	0
12	143	185	21	12	0	37	0	0
13	143	197	23	13	0	37	0	0
14	0	0	0	0	0	0	0	0
15	0	0	0	0	0	0	0	0
16	241	247	4	4	0	47	0	0
17	241	262	21	20	0	79	0	0
18	241	275	24	23	0	81	22	37
19	241	290	31	29	0	81	30	45
20	241	306	37	34	0	80	39	52
21	241	322	47	38	0	68	0	0
22	241	336	59	47	0	69	0	0
23	241	352	70	56	0	70	0	0
24	241	362	74	58	0	69	0	0
25	241	381	79	62	0	69	0	0
26	241	393	81	64	0	70	0	0
27	241	408	82	65	0	70	0	0
28	241	426	83	65	0	69	0	0
29	241	442	84	66	0	69	0	0
30	241	444	85	66	0	68	0	0
31	241	472	93	72	0	69	0	0
32	474	979	59	51	0	76	0	0

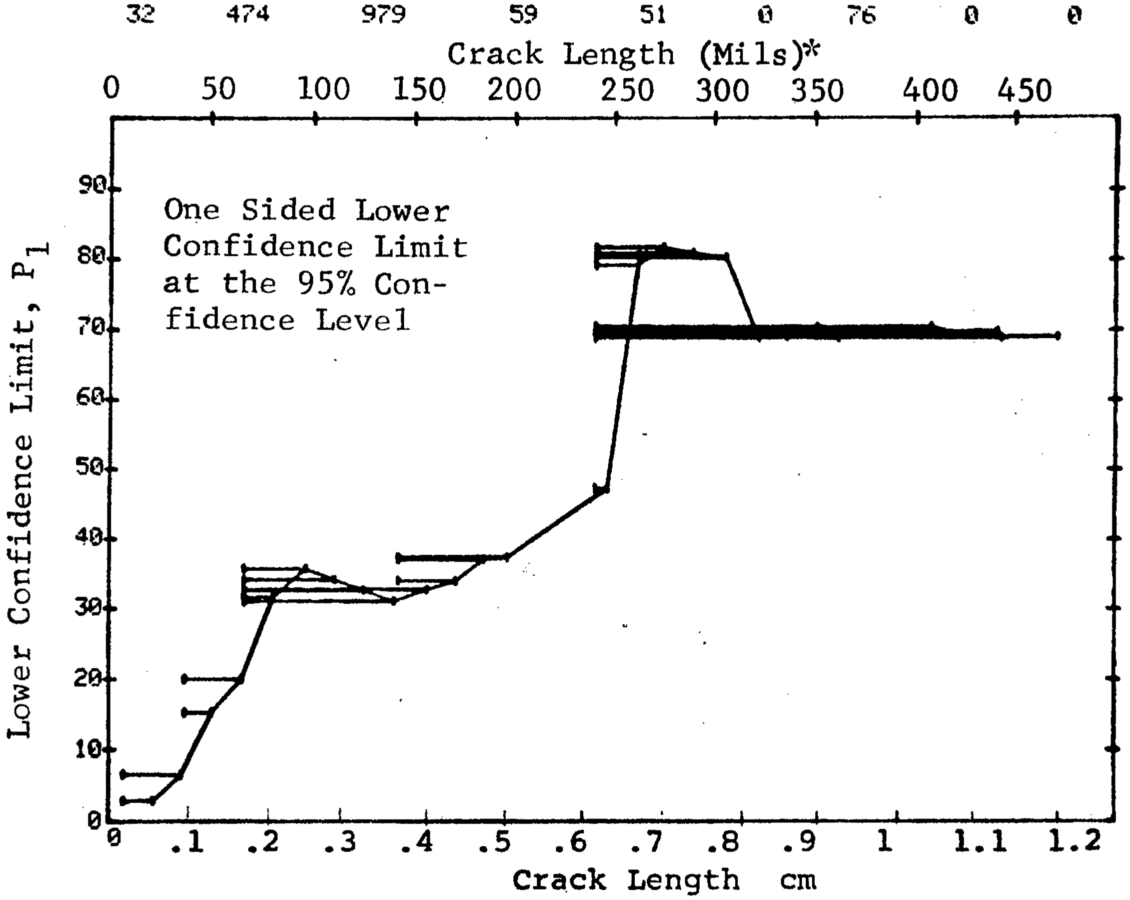

Figure D-31 (Continued)

(c) Overlapping Sixty Point Method of Data Cumulation

23-JUL-75 RADIOGRAPHY TEST 3.(31) ROCKWELL SC F

RANGE	MIN LN	MAX LN	N	DET	50%	95%	0 MISS	1 MISS
1	0*	0*	0	0	0	0	0	0
2	0	0	0	0	0	0	0	0
3	0	0	0	0	0	0	0	0
4	0	0	0	0	0	0	0	0
5	0	0	0	0	0	0	0	0
6	0	0	0	0	0	0	0	0
7	0	0	0	0	0	0	0	0
8	0	0	0	0	0	0	0	0
9	0	0	0	0	0	0	0	0
10	0	0	0	0	0	0	0	0
11	0	0	0	0	0	0	0	0
12	0	0	0	0	0	0	0	0
13	0	0	0	0	0	0	0	0
14	0	0	0	0	0	0	0	0
15	0	0	0	0	0	0	0	0
16	0	0	0	0	0	0	0	0
17	0	0	0	0	0	0	0	0
18	0	0	0	0	0	0	0	0
19	0	0	0	0	0	0	0	0
20	0	0	0	0	0	0	0	0
21	7	49	52	11	0	0	0	0
22	31	63	60	16	0	0	0	0
23	51	70	60	19	0	0	0	0
24	64	79	60	21	0	0	0	0
25	70	87	60	29	0	0	0	0
26	79	105	60	26	0	0	0	0
27	88	131	60	19	0	0	0	0
28	105	162	60	21	0	0	0	0
29	132	275	60	38	0	0	0	0
30	171	330	60	47	0	0	0	0
31	279	442	60	43	0	0	0	0
32	331	500	60	47	0	0	0	0

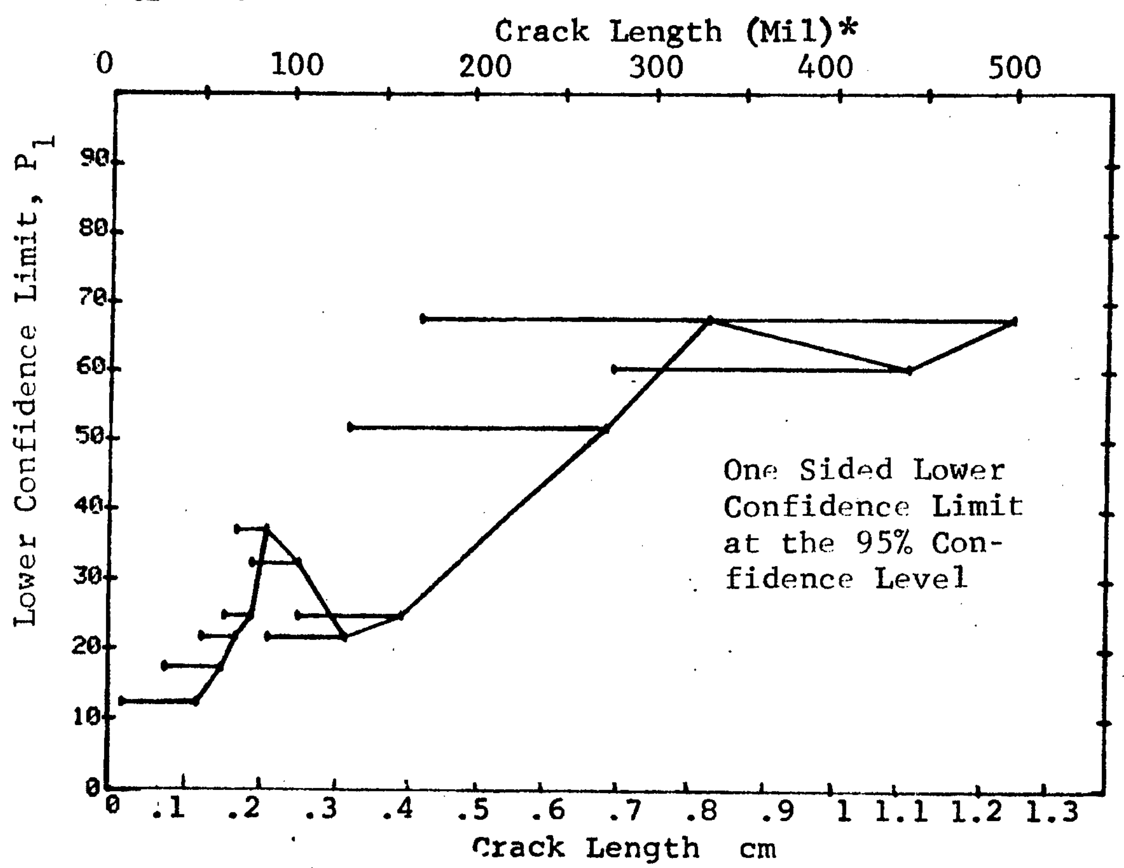

Figure D-31 (Concluded)

(a) Range Interval Method of Data Cumulation

18-SEP-75	RADIOGRAPHY			P-1,	(32)		G	
RANGE	MIN LN	MAX LN	N	DET	50%	95%	0 MISS	[illegible]
1	10 *	41 *	37	5	12	5	0	0
2	42	72	80	24	29	21	0	[illegible]
3	73	103	84	40	47	38	0	0
4	104	134	35	6	16	7	0	0
5	135	162	26	12	44	29	0	[illegible]
6	171	185	4	3	61	24	0	0
7	197	197	1	1	50	5	0	0
8	241	258	16	16	95	82	13	30
9	259	288	13	12	87	68	0	0
10	290	318	14	11	74	53	0	0
11	321	347	22	15	65	48	0	0
12	352	381	11	8	67	43	0	0
13	384	408	3	3	79	36	0	[illegible]
14	426	444	3	0	0	0	0	0
15	458	475	11	7	58	34	0	0
16	478	506	22	17	74	58	0	0
17	508	535	25	21	81	66	0	0
18	538	568	6	6	89	60	0	0
19	0	0	0	0	0	0	0	0
20	610	610	1	1	50	5	0	0
21	0	0	0	0	0	0	0	[illegible]
22	0	0	0	0	0	0	0	0
23	710	710	1	1	50	5	0	0
24	0	0	0	0	0	0	0	0
25	0	0	0	0	0	0	0	0
26	0	0	0	0	0	0	0	0
27	0	0	0	0	0	0	0	0
28	0	0	0	0	0	0	0	0
29	0	0	0	0	0	0	0	0
30	0	0	0	0	0	0	0	0
31	0	0	0	0	0	0	0	0
32	979	979	1	1	50	5	0	[illegible]

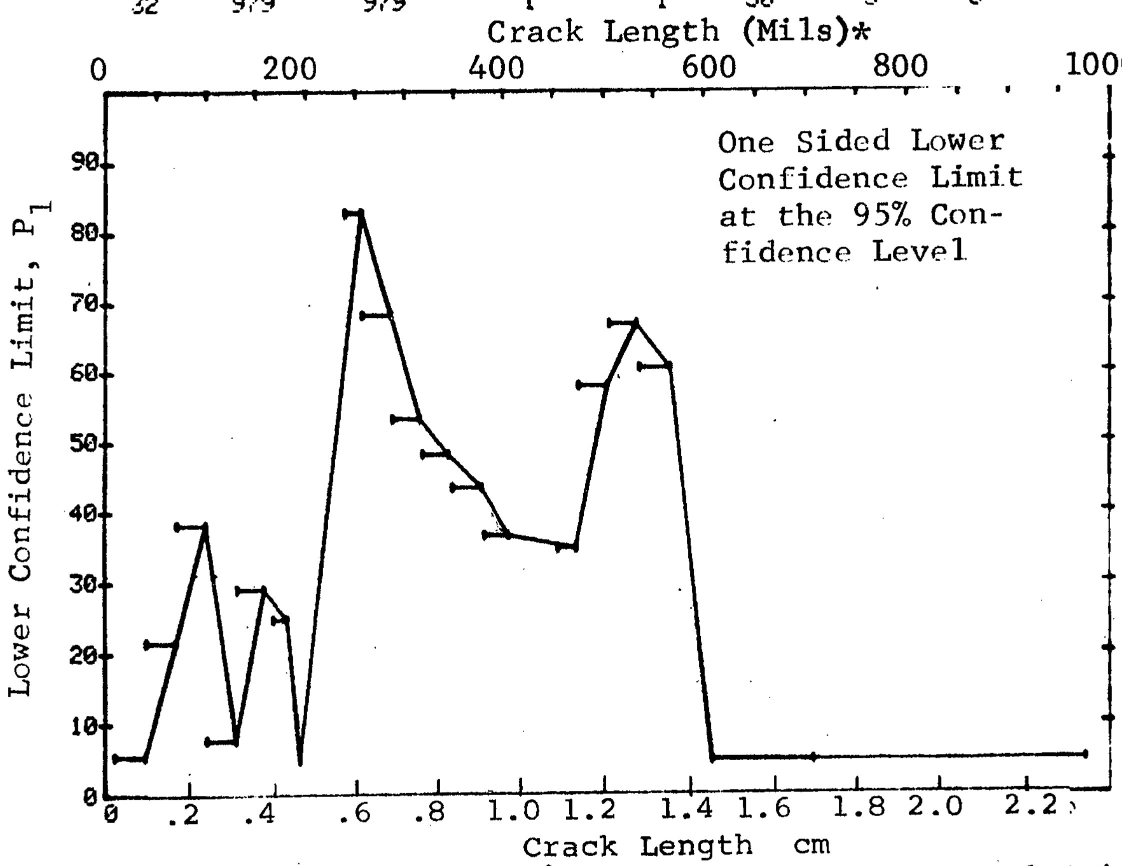

Figure D-32 Probability of Detection for 2219-T87 Al Using X-ray. Etched Fatigue Cracks in Flat Plates Measured by Operator G. Lab. Env.

(b) Optimum Probability Method of Data Cumulation

18-SEP-75 RADIOGRAPHY P-2, (32) G

RANGE	MIN LN*	MAX LN*	N	DET	50%	95%	0 MI[illegible]	[illegible]
1	10	41	37	5	0	5	[illegible]	[illegible]
2	42	72	80	24	0	21	[illegible]	[illegible]
3	73	103	84	40	0	38	[illegible]	[illegible]
4	73	134	119	46	0	31	[illegible]	[illegible]
5	73	162	145	58	0	33	[illegible]	[illegible]
6	73	185	149	61	0	34	0	[illegible]
7	135	197	31	16	0	35	0	[illegible]
8	197	258	17	17	0	83	12	[illegible]
9	197	288	30	29	0	85	15	[illegible]
10	197	318	44	40	0	80	45	[illegible]
11	197	347	66	55	0	73	0	[illegible]
12	197	381	77	63	0	73	0	[illegible]
13	197	408	80	66	0	74	0	[illegible]
14	197	444	83	66	0	70	0	[illegible]
15	171	475	98	76	0	69	0	[illegible]
16	171	506	120	93	0	70	0	[illegible]
17	197	535	141	111	0	72	0	[illegible]
18	197	568	147	117	0	73	0	[illegible]
19	0	0	0	0	0	0	0	[illegible]
20	508	610	32	28	0	73	0	[illegible]
21	0	0	0	0	0	0	0	[illegible]
22	0	0	0	0	0	0	0	[illegible]
23	508	710	33	29	0	74	0	[illegible]
24	0	0	0	0	0	0	0	[illegible]
25	0	0	0	0	0	0	0	[illegible]
26	0	0	0	0	0	0	0	0
27	0	0	0	0	0	0	0	0
28	0	0	0	0	0	0	[illegible]	[illegible]
29	0	0	0	0	0	0	[illegible]	[illegible]
30	0	0	0	0	0	0	[illegible]	[illegible]
31	0	0	0	0	0	0	[illegible]	[illegible]
32	508	979	34	30	0	75	[illegible]	[illegible]

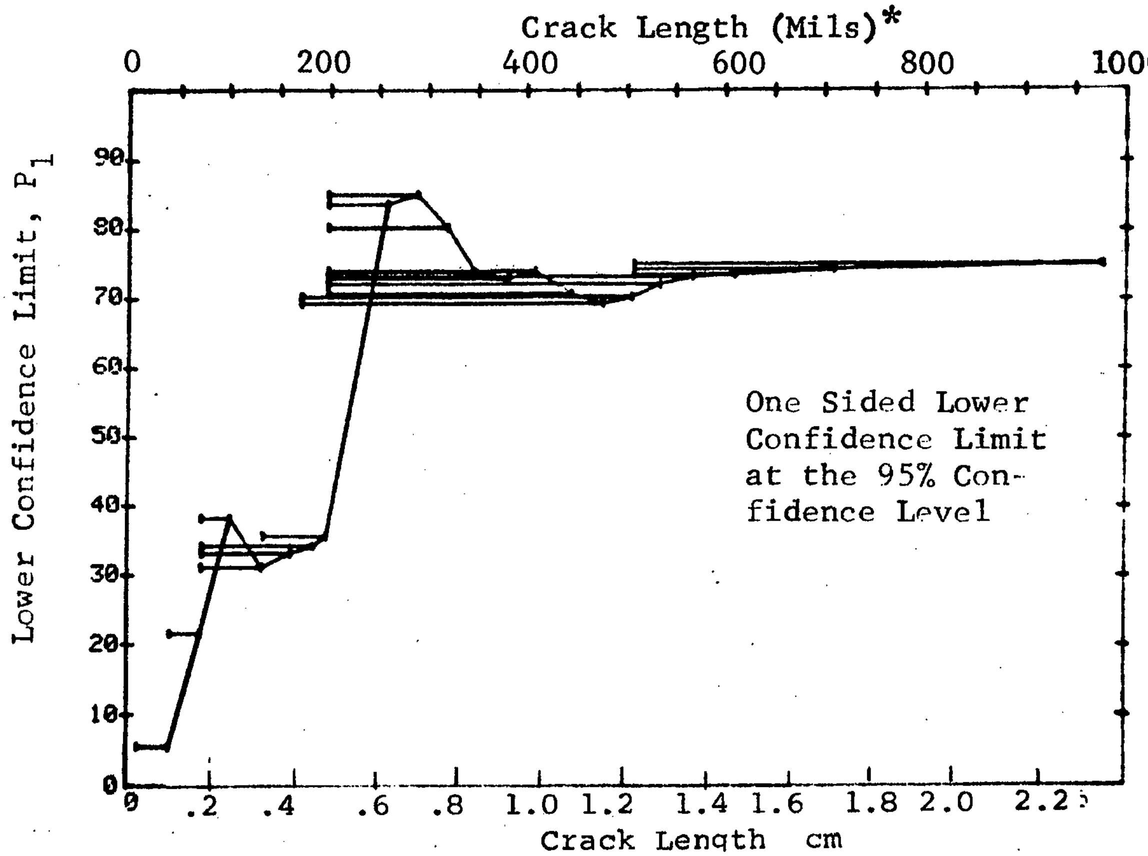

Figure D-32 (Continued)

(c) Overlapping Sixty Point Method of Data Cumulation

18-SEP-75 RADIOGRAPHY P-3 (32) G

RANGE	MIN LN *	MAX LN *	N	DET	50%	95%	[illegible]	[illegible]
1	0	0	0	0	0	0	[illegible]	[illegible]
2	0	0	0	0	0	0	[illegible]	[illegible]
3	0	0	0	0	0	0	[illegible]	[illegible]
4	0	0	0	0	0	0	[illegible]	[illegible]
5	0	0	0	0	0	0	[illegible]	[illegible]
6	0	0	0	0	0	0	0	[illegible]
7	0	0	0	0	0	0	0	[illegible]
8	0	0	0	0	0	0	0	[illegible]
9	0	0	0	0	0	0	0	[illegible]
10	0	0	0	0	0	0	[illegible]	[illegible]
11	0	0	0	0	0	0	0	[illegible]
12	0	0	0	0	0	0	0	[illegible]
13	0	0	0	0	0	0	0	[illegible]
14	0	0	0	0	0	0	0	[illegible]
15	0	0	0	0	0	0	0	[illegible]
16	0	0	0	0	0	0	0	[illegible]
17	0	0	0	0	0	0	0	[illegible]
18	0	0	0	0	0	0	0	[illegible]
19	0	0	0	0	0	0	0	[illegible]
20	10	49	51	7	12	6	0	[illegible]
21	30	63	60	17	27	18	0	[illegible]
22	51	70	60	21	34	24	0	[illegible]
23	63	79	60	18	29	20	0	[illegible]
24	70	87	60	27	44	33	0	[illegible]
25	79	103	60	32	52	41	0	[illegible]
26	88	130	60	18	29	20	0	[illegible]
27	104	158	60	17	27	18	0	0
28	131	275	60	42	69	58	0	0
29	162	333	60	52	85	[illegible]	[illegible]	[illegible]
30	279	458	60	41	67	57	[illegible]	[illegible]
31	334	506	60	41	67	57	[illegible]	[illegible]
32	459	550	60	49	80	71	[illegible]	[illegible]

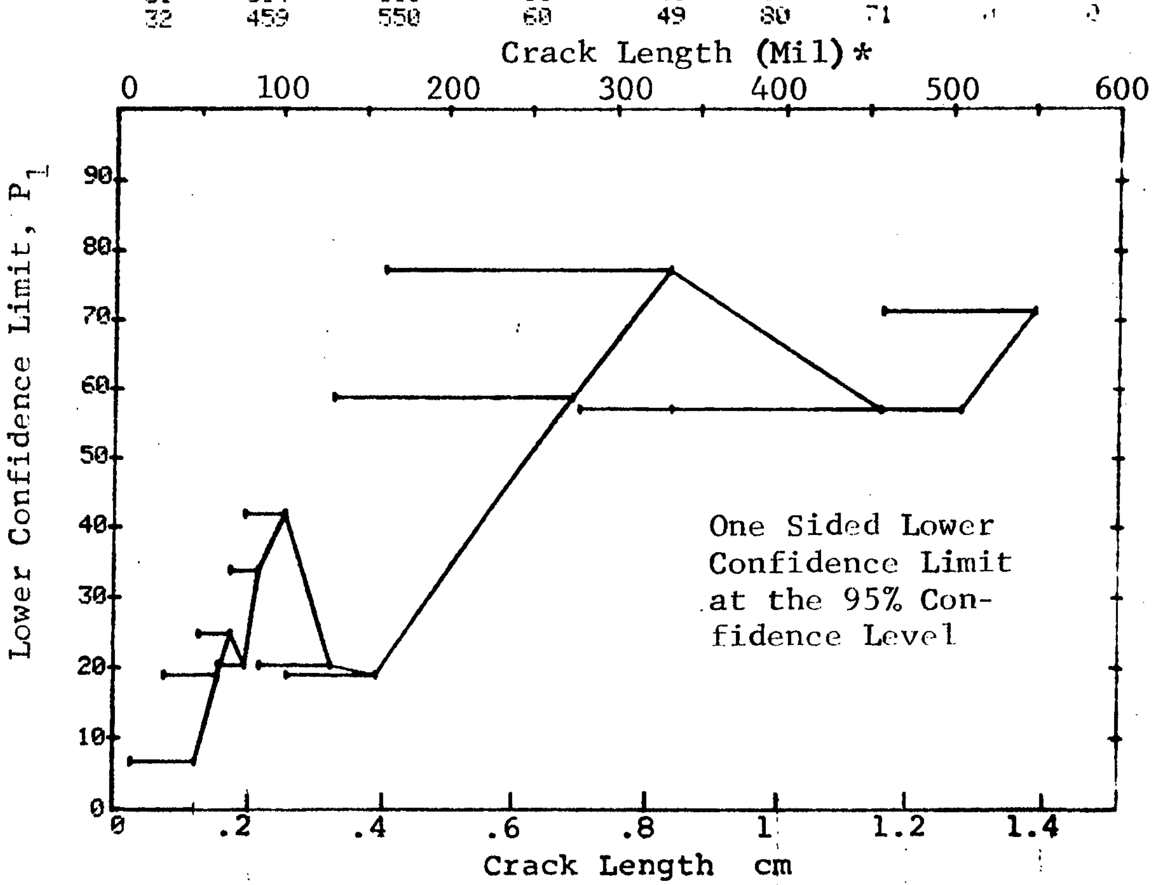

Figure D-32 (Concluded)

(a) Range Interval Method of Data Cumulation

24-JUL-75 ULTRASONIC TEST 1, MERGE, ROCKWELL SC (33)

RANGE	MIN LN *	MAX LN *	N	DET	50%	95%	0 MISS	1 MISS
1	7	22	65	21	31	22	0	0
2	25	36	90	61	67	58	0	0
3	38	52	115	91	78	71	0	0
4	54	67	231	198	81	76	0	0
5	68	82	265	232	87	83	0	0
6	83	97	195	170	86	82	0	0
7	98	111	85	74	86	79	94	100
8	115	126	85	73	91	85	44	57
9	129	141	95	85	88	82	72	94
10	143	157	75	64	84	76	100	100
11	158	171	15	13	82	63	0	0
12	182	185	15	14	89	72	0	0
13	190	197	10	9	83	60	0	0
14	207	207	1	1	50	5	0	0
15	0	0	0	0	0	0	0	0
16	241	247	20	19	91	78	26	41
17	248	262	85	85	99	96	0	0
18	268	275	15	15	95	81	14	31
19	279	290	34	33	95	86	12	27
20	295	306	30	29	94	85	16	31
21	310	322	50	48	94	87	11	26
22	323	336	60	58	95	89	1	16
23	338	352	55	49	87	79	61	74
24	356	362	20	20	96	86	9	26
25	370	381	25	22	85	71	0	0
26	384	393	10	10	93	74	0	0
27	408	408	5	4	68	34	0	0
28	426	426	5	5	87	54	0	0
29	442	442	5	5	87	54	0	0
30	444	450	6	6	89	60	0	0
31	456	472	38	38	98	92	0	8
32	474	979	295	285	96	94	0	0

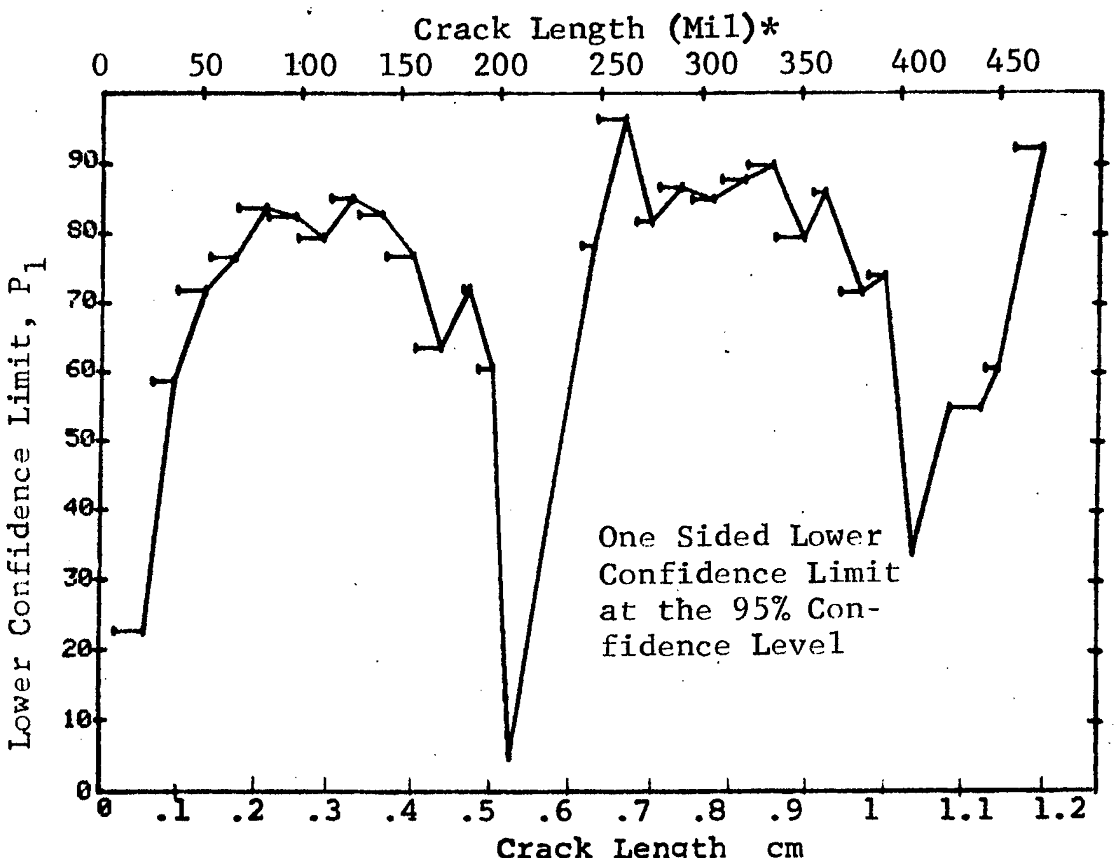

Figure D-33 Probability of Detection for 2219-T87 Al Using Ultrasonics. Etched Fatigue Cracks in Flat Plates Merged for 5 Operators. Lab. Env.

(b) Optimum Probability Method of Data Cumulation

24-JUL-75 ULTRASONIC TEST 2, MERGE, ROCKWELL SC (33)

RANGE	MIN LN	* MAX LN *	N	DET	50%	95%	0 MISS	1 MISS
1	7	22	65	21	0	22	0	0
2	25	36x	90	61	0	58	0	0
3	38	52	115	91	0	71	0	0
4	54	67	231	188	0	76	0	0
5	68	82	265	232	0	83	0	0
6	68	97	460	402	0	84	0	0
7	68	111	545	476	0	84	0	0
8	68	126	630	554	0	85	0	0
9	115	141	180	163	0	86	0	0
10	68	157	800	703	0	85	0	0
11	68	171	815	716	0	85	0	0
12	68	185	830	730	0	85	0	0
13	68	197	840	739	0	85	0	0
14	68	207	841	740	0	85	0	0
15	0	0	0	0	0	0	0	0
16	115	247	316	283	0	86	0	0
17	248	262	85	85	0	96	0	0
18	248	275	100	100	0	97	0	0
19	248	290	134	133	0	96	0	0
20	248	306	164	162	0	96	0	0
21	248	322	214	210	0	95	0	0
22	248	336	274	268	0	95	0	0
23	207	352	350	337	0	94	0	0
24	248	362	349	337	0	94	0	0
25	207	381	395	379	0	93	0	0
26	207	393	405	389	0	94	0	0
27	207	408	410	393	0	93	0	0
28	207	426	415	398	0	93	0	0
29	207	442	420	403	0	93	0	0
30	207	450	425	409	0	94	0	0
31	426	472	54	54	0	94	0	0
32	426	979	349	339	0	95	0	0

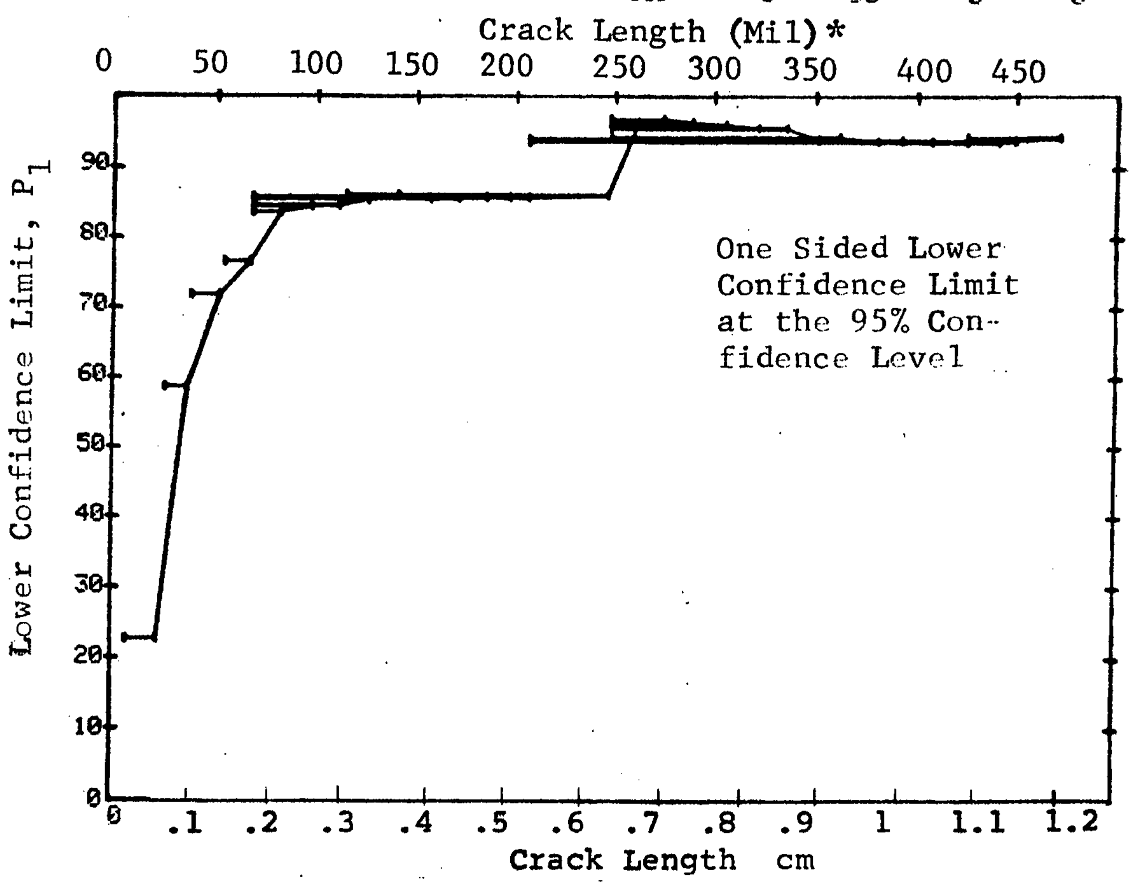

Figure D-33 (Continued

(c) Overlapping Sixty Point Method of Data Cumulation

24-JUL-75 ULTRASONIC TEST 3. MERGE, ROCKWELL SC (33)

RANGE	MIN LN	MAX LN	N	DET	50%	95%	0 MISS	1 MISS
1	95*	100*	60	51	83	75	94	100
2	97	105	60	52	85	77	82	94
3	100	109	60	54	88	81	56	69
4	105	118	60	55	90	83	43	56
5	109	123	60	55	90	83	43	56
6	118	126	60	54	88	81	56	69
7	123	131	60	53	87	79	69	82
8	126	135	60	53	87	79	69	82
9	131	140	60	54	88	81	56	69
10	135	144	60	51	83	75	94	100
11	140	151	60	50	82	73	0	0
12	144	162	60	53	87	79	69	82
13	151	197	60	56	92	85	29	43
14	162	249	60	57	93	87	16	29
15	197	257	60	58	95	89	1	16
16	249	260	60	60	98	95	0	0
17	257	275	60	60	98	95	0	0
18	260	290	60	59	97	92	0	1
19	275	304	60	59	97	92	0	1
20	290	313	60	58	95	89	1	16
21	304	323	60	57	93	87	16	29
22	313	330	60	59	97	92	0	1
23	323	338	60	57	93	87	16	29
24	330	342	60	53	87	79	69	82
25	338	362	60	55	90	83	43	56
26	342	372	60	56	92	85	29	43
27	362	442	60	56	92	85	29	43
28	372	466	60	59	97	92	0	1
29	442	475	60	59	97	92	0	1
30	466	484	60	59	97	92	0	1
31	478	495	60	58	95	89	1	16
32	489	500	60	56	92	85	29	43

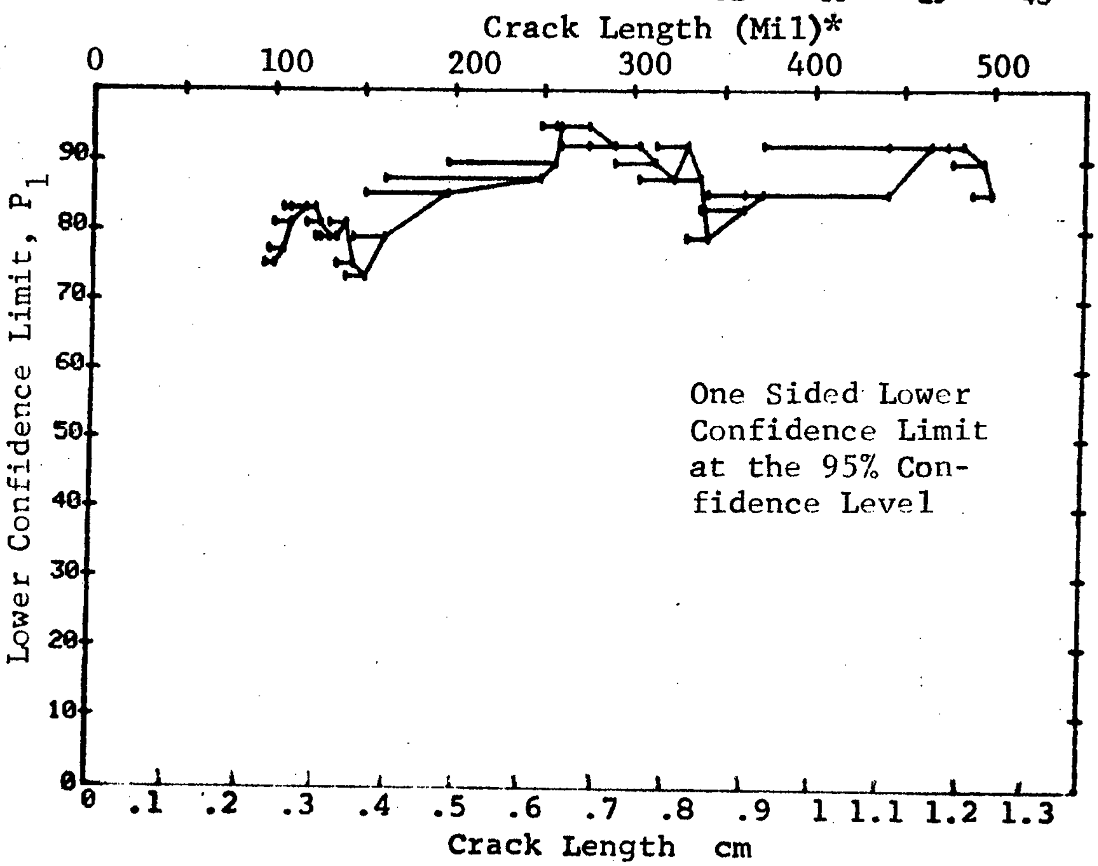

Figure D-33 (Continued)

(c) Overlapping Sixty Point Method of Data Cumulation

24-JUL-75 ULTRASONIC TEST 3, MERGE, ROCKWELLSC (33)

RANGE	MIN LN	MAX LN	N	DET	50%	95%	0 MISS	1 MISS
1	55 *	60 *	60	46	75	65	0	0
2	58	62	60	53	87	79	69	82
3	60	63	60	52	85	77	82	94
4	62	64	60	49	80	71	0	0
5	63	66	60	48	79	69	0	0
6	65	67	60	51	83	75	94	100
7	66	69	60	52	85	77	82	94
8	67	69	60	47	77	67	0	0
9	69	72	60	48	79	69	0	0
10	70	74	60	55	90	83	43	56
11	72	76	60	52	85	77	82	94
12	75	77	60	50	82	73	0	0
13	76	79	60	56	92	85	29	43
14	78	80	60	57	93	87	16	29
15	79	82	60	54	88	81	56	69
16	80	84	60	53	87	79	69	82
17	83	85	60	51	83	75	94	100
18	84	87	60	52	85	77	82	94
19	86	90	60	51	83	75	94	100
20	87	94	60	52	85	77	82	94
21	91	96	60	55	90	83	43	56
22	95	98	60	51	83	75	94	100
23	97	104	60	51	83	75	94	100
24	100	108	60	54	88	81	56	69
25	105	117	60	55	90	83	43	56
26	109	123	60	54	88	81	56	69
27	118	125	60	55	90	83	43	56
28	123	131	60	53	87	79	69	82
29	126	135	60	52	85	77	82	94
30	131	140	60	54	88	81	56	69
31	135	144	60	51	83	75	94	100
32	140	150	60	50	82	73	0	0

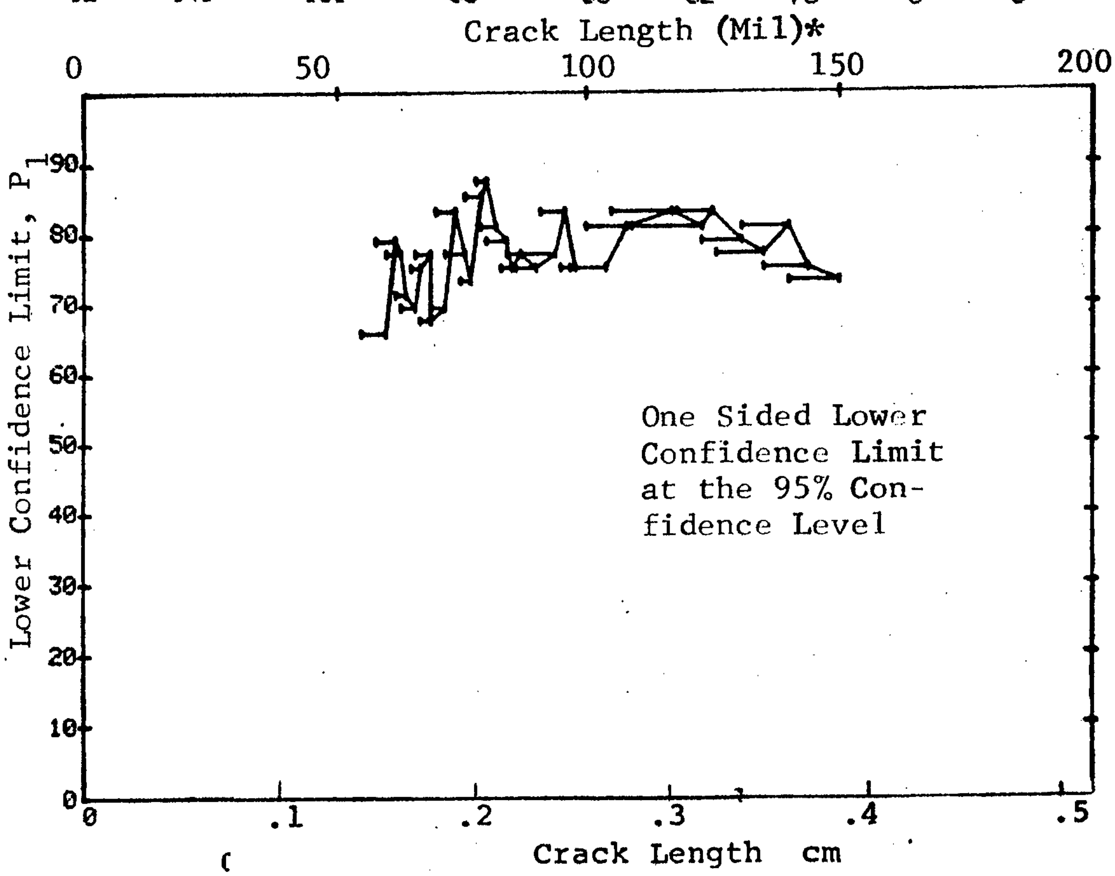

Figure D-33 (Continued)

(c) Overlapping Sixty Point Method of Data Cumulation

24-JUL-75 ULTRASONIC TEST 3, MERGE, ROCKWELL SC (33)

RANGE	MIN LN *	MAX LN *	N	DET	50%	95%	0 MISS	1 MISS
1	7	21	51	11	20	12	0	0
2	15	26	50	26	42	32	0	0
3	21	31	60	41	67	57	0	0
4	26	35	60	40	65	55	0	0
5	31	41	60	39	64	53	0	0
6	35	45	60	42	69	58	0	0
7	41	47	60	52	85	77	82	94
8	45	51	60	51	83	75	94	100
9	47	55	60	44	72	62	0	0
10	51	58	60	45	74	64	0	0
11	55	60	60	49	80	71	0	0
12	59	62	60	52	85	77	82	94
13	61	63	60	52	85	77	82	94
14	62	65	60	49	80	71	0	0
15	64	66	60	46	75	65	0	0
16	65	67	60	50	82	73	0	0
17	67	69	60	53	87	79	69	82
18	68	70	60	49	80	71	0	0
19	69	72	60	49	80	71	0	0
20	70	75	60	54	88	81	56	69
21	73	76	60	50	82	73	0	0
22	75	78	60	51	83	75	94	100
23	76	79	60	58	95	89	1	16
24	78	80	60	56	92	85	29	43
25	79	83	60	54	88	81	56	69
26	81	84	60	51	83	75	94	100
27	83	86	60	51	83	75	94	100
28	85	87	60	55	90	83	43	56
29	86	91	60	51	83	75	94	100
30	88	95	60	51	83	75	94	100
31	91	97	60	53	87	79	69	82
32	95	100	60	51	83	75	94	100

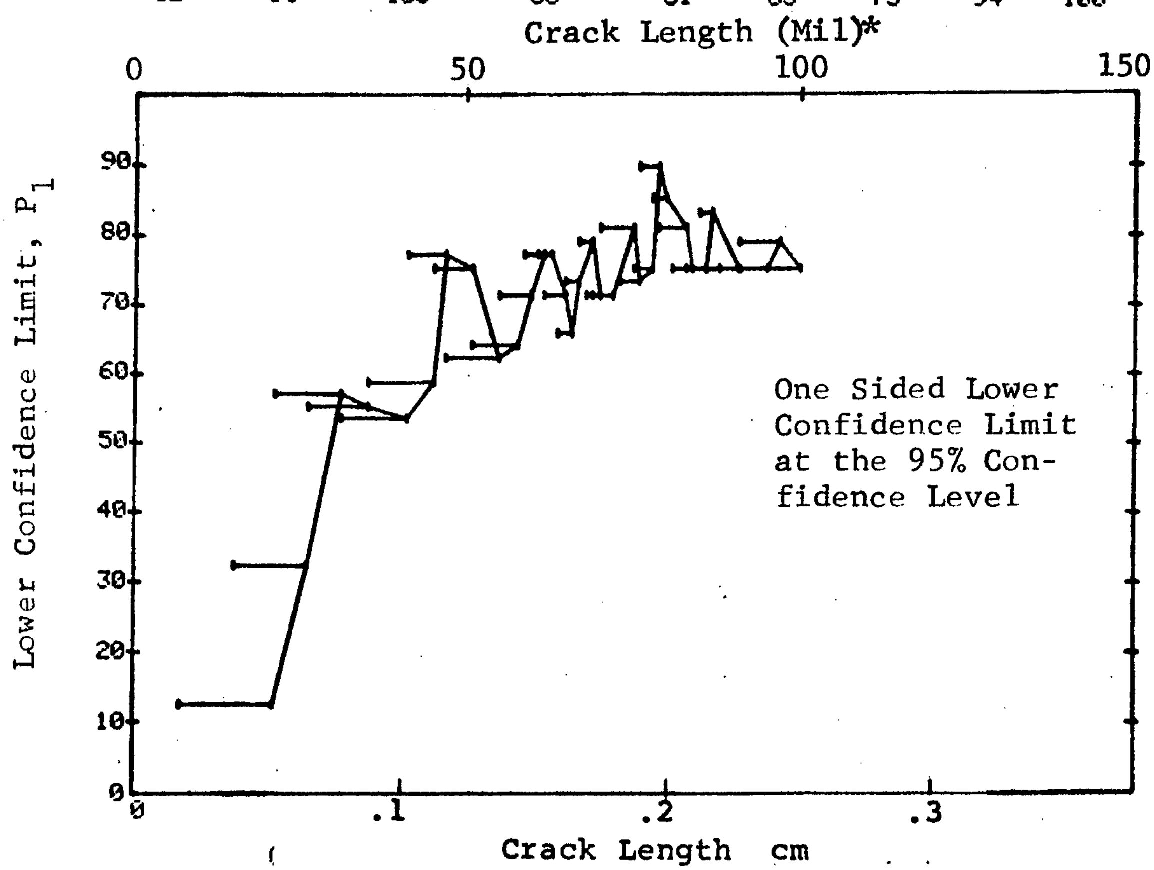

Figure D-33 (Concluded)

(a) Range Interval Method of Data Cumulation

22-JUL-75 PENETRANT MERGE PENETRANT ROCKWELL SF (34)

RANGE	MIN LN	MAX LN	N	DET	50%	95%	0 MISS	1 MISS
1	7 *	22 *	65	13	19	12	0	0
2	25	[illegible]	[illegible]	46	50	41	0	0
3	38	52	115	78	67	59	0	0
4	54	67	230	171	74	69	0	0
5	68	82	266	219	82	78	0	0
6	83	97	193	172	88	84	0	0
7	98	111	85	80	93	88	18	31
8	115	126	85	75	87	80	82	94
9	129	141	95	87	90	85	47	59
10	143	157	75	66	87	79	79	92
11	158	171	15	15	95	81	14	31
12	182	185	15	15	95	81	14	31
13	190	197	10	7	64	39	0	0
14	0	0	0	0	0	0	0	0
15	0	0	0	0	0	0	0	0
16	241	247	20	20	96	86	9	[illegible]
17	248	262	85	85	99	96	0	0
18	268	275	15	15	95	81	14	[illegible]
19	279	290	35	35	98	91	0	[illegible]
20	295	306	30	29	94	85	16	31
21	310	322	50	49	96	90	0	[illegible]
22	323	336	60	58	95	89	1	[illegible]
23	338	352	55	50	89	81	46	51
24	356	362	20	20	95	86	9	[illegible]
25	370	381	25	21	81	66	0	0
26	384	393	10	9	83	60	0	0
27	408	408	5	5	87	54	0	0
28	426	426	5	5	87	54	0	0
29	442	442	5	4	[illegible]	[illegible]	[illegible]	[illegible]
30	444	444	5	5	87	54	0	0
31	458	472	40	38	93	85	21	36
32	474	5009	297	290	97	95	0	0

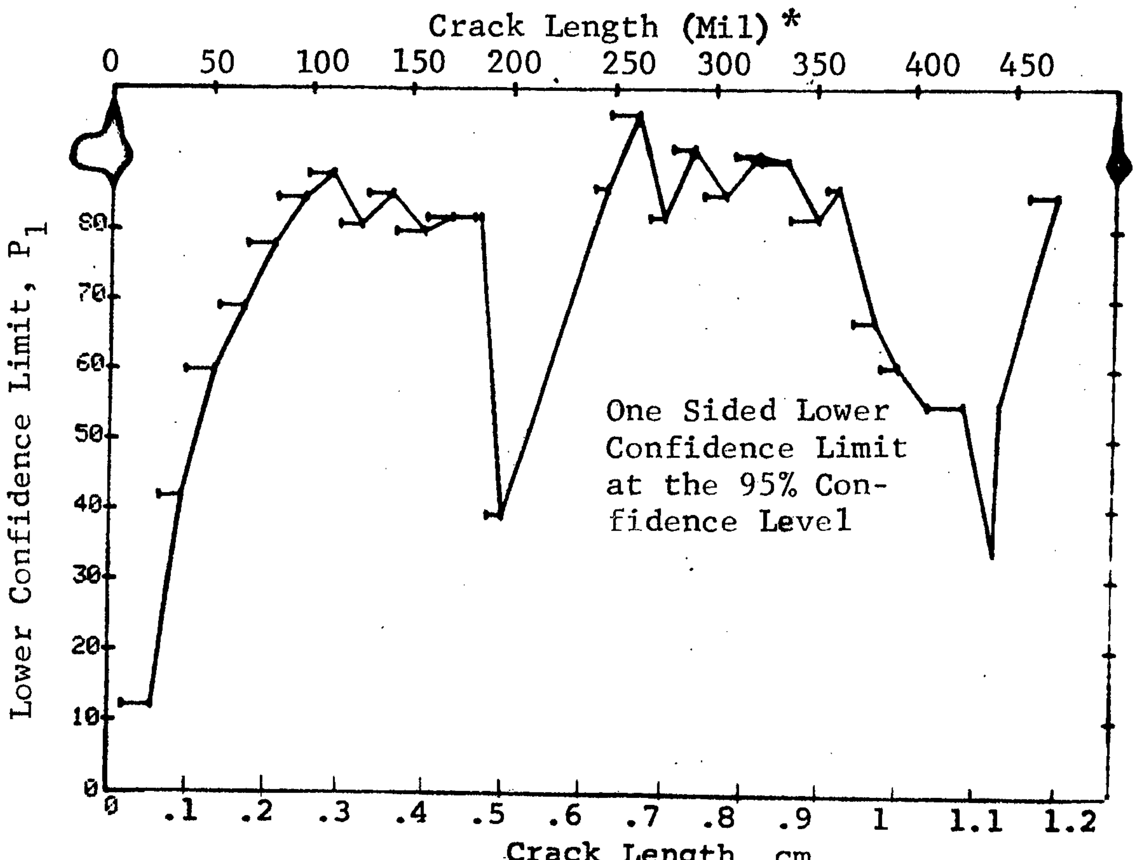

Figure D-34 Probability of Detection for 2219-T87 Al Using Liquid Penetrant. Etched Fatigue Cracks in Flat Plates Merged for 7 Operators.

Lab. Env.

(b) Optimum Probability Method of Data Cumulation

22-JUL-75 PENETRANT TEST 2, MERGE, ROCKWELL SL (34)

RANGE	MIN LN	* MAX LN *	N	DET	50%	95%	0 MISS	1 MISS
1	7	22	65	13	0	12	0	0
2	25	30	90	46	0	41	0	0
3	38	52	115	73	0	59	0	0
4	54	67	230	171	0	69	0	0
5	68	82	266	219	0	78	0	0
6	83	97	193	172	0	84	0	0
7	98	111	85	80	0	88	18	31
8	83	126	363	327	0	87	0	0
9	98	141	265	242	0	87	0	0
10	83	157	533	480	0	87	0	0
11	98	171	355	323	0	88	0	0
12	158	185	30	30	0	90	0	16
13	98	197	380	345	0	87	0	0
14	0	0	0	0	0	0	0	0
15	0	0	0	0	0	0	0	0
16	98	247	400	365	0	88	0	0
17	241	262	105	105	0	97	0	0
18	241	275	120	120	0	97	0	0
19	241	290	155	155	0	98	0	[illegible]
20	241	306	185	184	0	97	0	[illegible]
21	241	322	235	233	0	97	0	[illegible]
22	241	336	295	291	0	96	0	[illegible]
23	241	352	350	341	0	95	0	[illegible]
24	241	362	370	361	0	95	0	[illegible]
25	241	381	395	382	0	94	0	[illegible]
26	241	393	405	391	0	94	0	[illegible]
27	241	408	410	396	0	94	0	0
28	241	426	415	401	0	94	0	[illegible]
29	241	442	420	405	0	94	[illegible]	[illegible]
30	241	444	435	410	0	94	[illegible]	[illegible]
31	241	472	465	448	0	94	0	[illegible]
32	474	5009	297	290	0	95	[illegible]	[illegible]

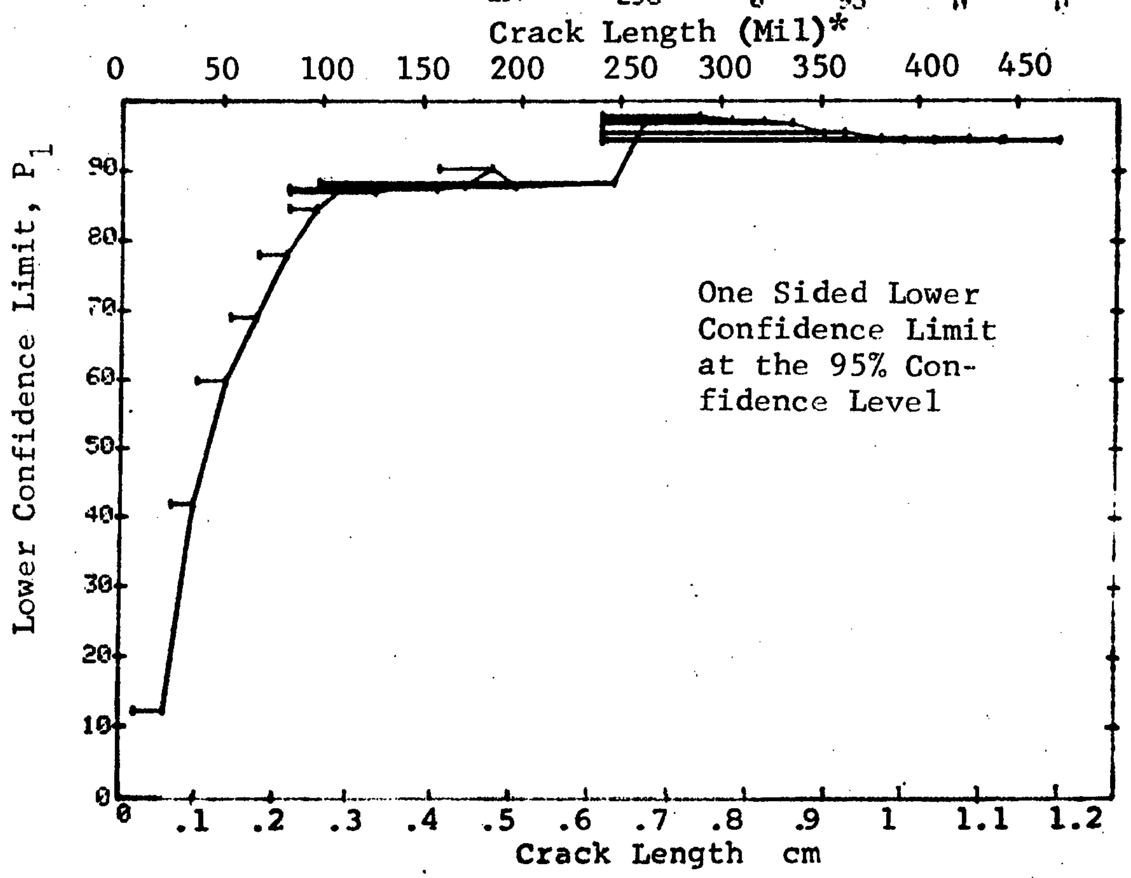

Figure D-34 (Continued)

(c) Overlapping Sixty Point Method of Data Cumulation

22-JUL-75 PENETRANT TEST 3, MERGE, ROCKWELL (34)

RANGE	MIN LN*	MAX LN*	N	DET	50%	95%	0 MISS	1 MISS
1	95	100	60	59	97	92	0	1
2	97	105	60	57	93	87	16	[illegible]
3	101	109	60	55	90	83	43	56
4	105	118	60	55	90	83	43	56
5	111	123	60	53	87	79	69	[illegible]
6	119	126	60	53	87	79	69	82
7	124	131	60	56	92	85	29	43
8	129	135	60	54	88	81	56	69
9	132	140	60	53	87	79	69	82
10	136	144	60	54	88	81	56	69
11	141	151	60	52	85	77	82	94
12	145	162	60	55	90	83	43	56
13	153	197	60	56	92	85	29	43
14	171	249	60	57	93	87	16	29
15	241	257	60	60	98	95	0	0
16	249	260	60	60	98	95	0	0
17	257	275	60	60	98	95	0	0
18	261	290	60	60	98	95	0	[illegible]
19	279	304	60	59	97	92	0	[illegible]
20	290	313	60	58	95	89	1	16
21	306	323	60	59	97	92	0	[illegible]
22	317	330	60	59	97	92	0	[illegible]
23	326	338	60	57	93	87	16	[illegible]
24	331	342	60	55	90	83	43	56
25	340	362	60	56	92	85	29	43
26	345	372	60	55	90	83	43	56
27	362	442	60	54	88	81	56	69
28	381	466	60	58	95	89	1	16
29	444	475	60	57	93	[illegible]	[illegible]	[illegible]
30	466	484	60	57	93	87	16	29
31	478	495	60	59	97	92	0	1
32	489	500	60	57	93	87	16	29

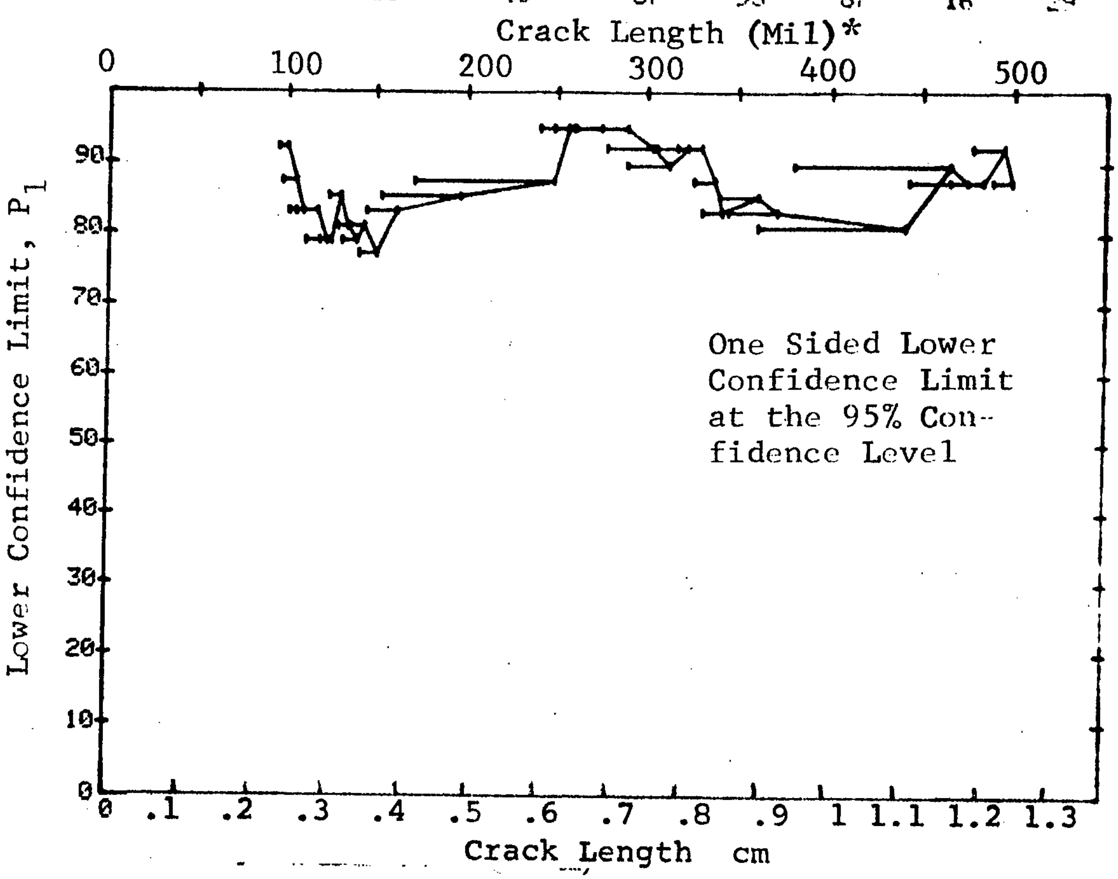

Figure D-34 (Continued)

(c) Overlapping Sixty Point Method of Data Cumulation

22-JUL-75 PENETRANT TEST 3, MERGE, ROCKWELL SC (34)

RANGE	MIN LN*	MAX LN*	N	DET	50%	95%	0 MISS	1 MISS
1	62	65	60	45	74	64	0	0
2	64	67	60	44	72	62	0	0
3	65	68	60	46	75	65	0	0
4	67	69	60	46	75	65	0	0
5	68	70	60	39	64	53	0	0
6	69	73	60	43	70	60	0	0
7	70	75	60	55	90	83	43	56
8	73	77	60	57	93	87	16	29
9	75	78	60	56	92	85	29	43
10	77	80	60	54	88	81	56	69
11	78	81	60	47	77	67	0	0
12	80	83	60	47	77	67	0	0
13	81	85	60	46	75	65	0	0
14	83	86	60	47	77	67	0	0
15	85	89	60	55	90	83	43	56
16	86	92	60	56	92	85	29	43
17	89	95	60	57	93	87	16	29
18	92	97	60	58	95	89	1	[illegible]
19	95	102	60	59	97	92	0	[illegible]
20	98	106	60	56	92	85	29	43
21	103	115	60	55	90	83	43	[illegible]
22	106	119	60	55	90	83	43	[illegible]
23	116	124	60	52	85	77	82	[illegible]
24	121	129	60	54	88	81	56	[illegible]
25	124	134	60	56	92	85	29	43
26	129	136	60	53	87	79	69	[illegible]
27	134	143	60	53	87	79	69	82
28	137	146	60	55	90	83	43	56
29	143	153	60	53	87	[illegible]	[illegible]	[illegible]
30	146	182	60	55	90	83	[illegible]	[illegible]
31	153	242	60	56	92	85	29	43
32	183	250	60	57	93	87	16	29

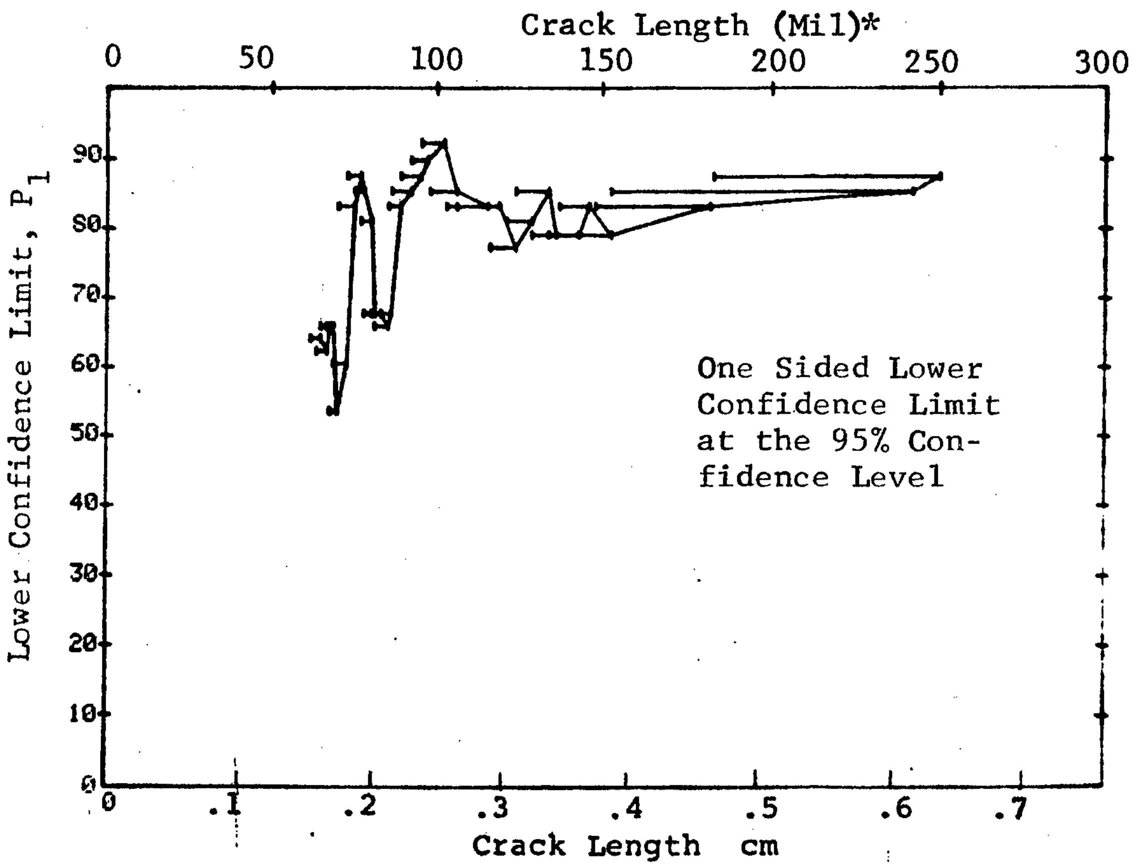

Figure D-34 (Concluded)

(a) Range Interval Method of Data Cumulation

24-JUL-75 EDDY CURRENT TEST 1, MERGE, ROCKWELL SC (35)

RANGE	MIN LN *	MAX LN *	N	DET	50%	95%	0 MISS	1 MISS
1	7	22	65	9	11	6	0	0
2	25	36	90	19	20	14	0	0
3	38	52	116	42	35	28	0	0
4	54	67	234	139	-49	-49	0	0
5	68	82	262	198	75	70	0	0
6	83	97	193	178	91	88	0	0
7	98	111	86	82	94	89	3	17
8	115	126	86	83	95	91	0	3
9	129	141	94	87	91	86	35	48
10	143	157	74	67	89	82	55	68
11	158	171	15	15	95	81	14	31
12	182	185	15	13	82	63	0	0
13	190	197	10	10	93	74	0	0
14	0	0	0	0	0	0	0	0
15	232	232	1	1	50	5	0	0
16	241	247	19	18	91	77	27	42
17	248	262	82	82	99	96	0	0
18	268	275	15	15	95	81	14	31
19	279	290	34	33	95	86	12	27
20	295	306	31	29	91	81	30	45
21	310	322	50	49	96	90	0	11
22	323	336	60	59	97	92	0	1
23	338	352	55	50	89	81	48	61
24	356	362	21	20	92	79	25	40
25	370	381	24	22	89	75	37	52
26	384	393	10	10	93	74	0	0
27	408	408	5	5	87	54	0	0
28	426	426	5	5	87	54	0	0
29	435	442	7	5	63	34	0	0
30	444	444	5	5	87	54	0	0
31	458	472	40	39	95	88	6	21
32	474	979	292	281	96	93	0	0

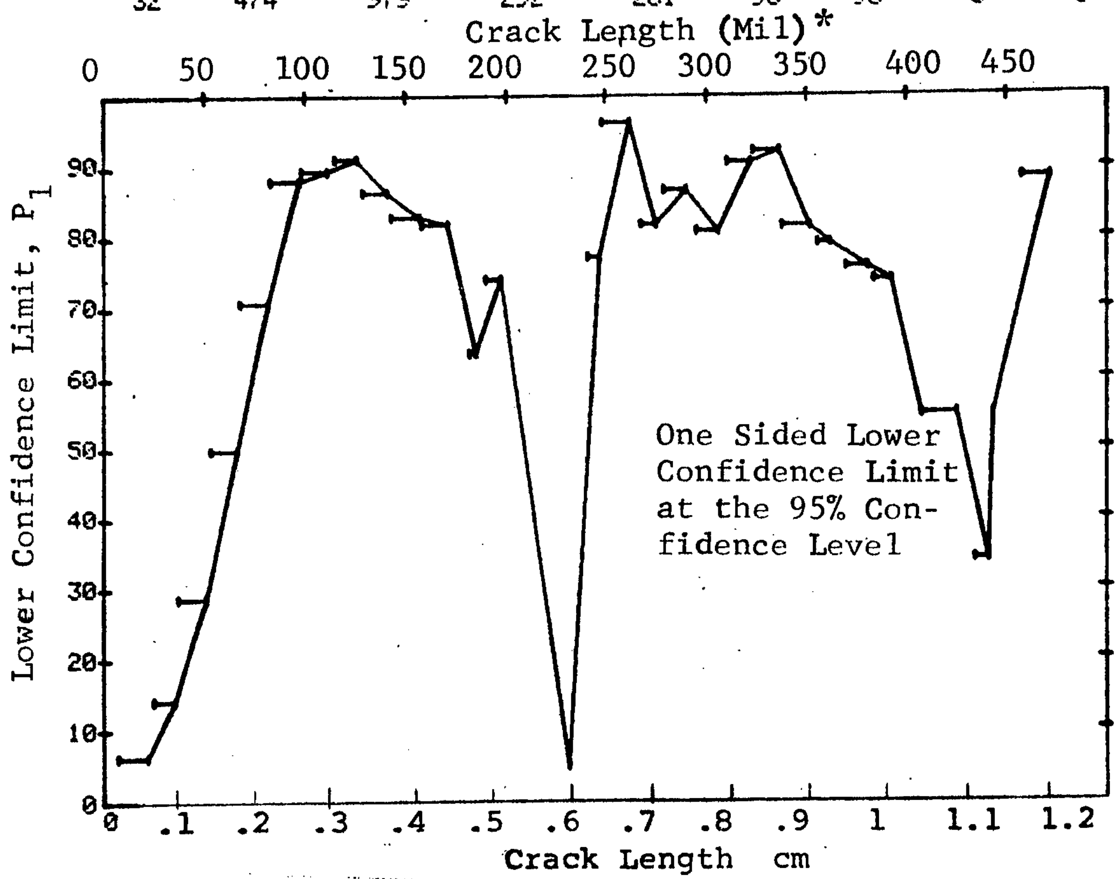

Figure D-35 Probability of Detection for 2219-T87 Al Using Eddy Current. Etched Fatigue Cracks in Flat Plates Merged for 5 Operators. D-108 Lab. Env.

(b) Optimum Probability Method of Data Cumulation

24-JUL-75 EDDY CURRENT TEST 2, MEREGE, ROCKWELL SC (35)

RANGE	MIN LN	MAX LN	N	DET	50%	95%	0 MISS	1 MISS
1	7 *	22 *	65	8	0	6	0	0
2	25	36	30	19	0	14	0	0
3	38	52	116	42	0	28	0	0
4	25	67	440	200	0	41	0	0
5	68	82	262	198	0	70	0	0
6	83	97	193	178	0	88	0	0
7	83	111	279	260	0	90	0	0
8	98	126	172	165	0	92	0	0
9	98	141	266	252	0	91	0	0
10	98	157	340	319	0	91	0	0
11	98	171	355	334	0	91	0	0
12	98	185	370	347	0	91	0	0
13	98	197	380	357	0	91	0	0
14	0	0	0	0	0	0	0	0
15	98	232	381	358	0	91	0	0
16	98	247	400	376	0	91	0	0
17	248	262	82	82	0	96	0	0
18	248	275	97	97	0	96	0	0
19	248	290	131	130	0	96	0	0
20	190	306	192	188	0	95	0	0
21	248	322	212	208	0	95	0	0
22	248	336	272	267	0	96	0	0
23	190	352	357	346	0	94	0	0
24	190	362	378	366	0	94	0	0
25	190	381	402	388	0	94	0	0
26	190	393	412	398	0	94	0	0
27	190	408	417	403	0	94	0	0
28	190	426	422	408	0	94	0	0
29	190	442	429	413	0	94	0	0
30	190	444	434	418	0	94	0	0
31	190	472	474	457	0	94	0	0
32	190	979	766	738	0	95	0	0

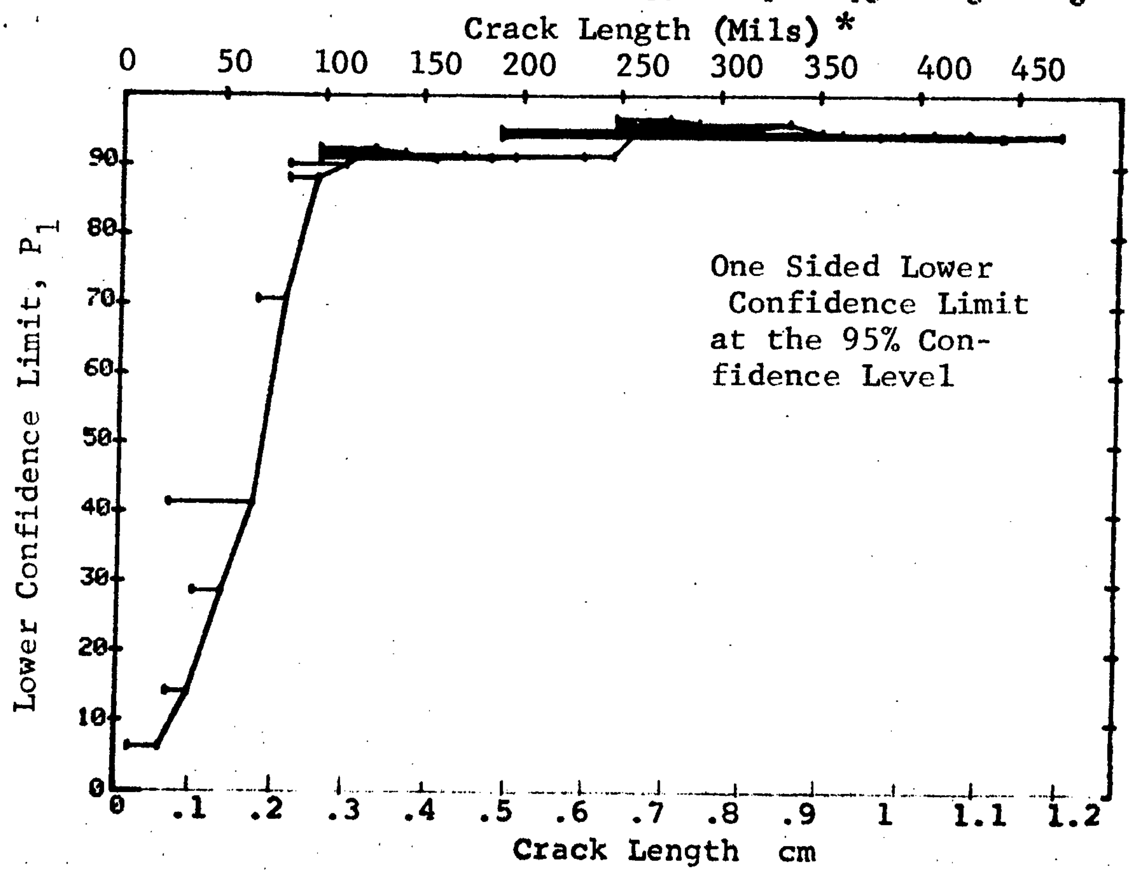

Figure D-35 (Continued)

(c) Overlapping Sixty Point Method of Data Cumulation

24-JUL-75 EDDY CURRENT TEST 3, MERGE, ROCKWELL SC (35)

RANGE	MIN LN	MAX LN	N	DET	50%	95%	0 MISS	1 MISS
1	95*	100 *	60	57	93	87	16	29
2	97	105	60	57	93	87	16	29
3	100	109	60	58	95	89	1	16
4	105	118	60	57	93	87	16	29
5	109	123	60	57	93	87	16	29
6	118	126	60	59	97	92	0	1
7	123	131	60	55	90	83	43	56
8	126	135	60	55	90	83	43	56
9	131	140	60	58	95	89	1	16
10	135	144	60	53	87	79	69	82
11	140	151	60	52	85	77	82	94
12	144	162	60	58	95	89	1	16
13	151	197	60	58	95	89	1	16
14	162	249	60	57	93	87	16	29
15	197	257	60	59	97	92	0	1
16	249	261	60	60	98	95	0	0
17	257	279	60	60	98	95	0	0
18	261	290	60	59	97	92	0	1
19	279	306	60	57	93	87	16	29
20	290	317	60	58	95	89	1	16
21	306	326	60	59	97	92	0	1
22	317	331	60	59	97	92	0	1
23	326	340	60	57	93	87	16	29
24	331	345	60	54	88	81	56	69
25	340	362	60	56	92	85	29	43
26	345	381	60	57	93	87	16	29
27	362	442	60	56	92	85	29	43
28	381	466	60	57	93	87	16	29
29	444	478	60	58	95	89	1	16
30	466	494	60	58	95	89	1	16
31	478	495	60	57	93	87	16	29
32	489	500	60	57	93	87	16	29

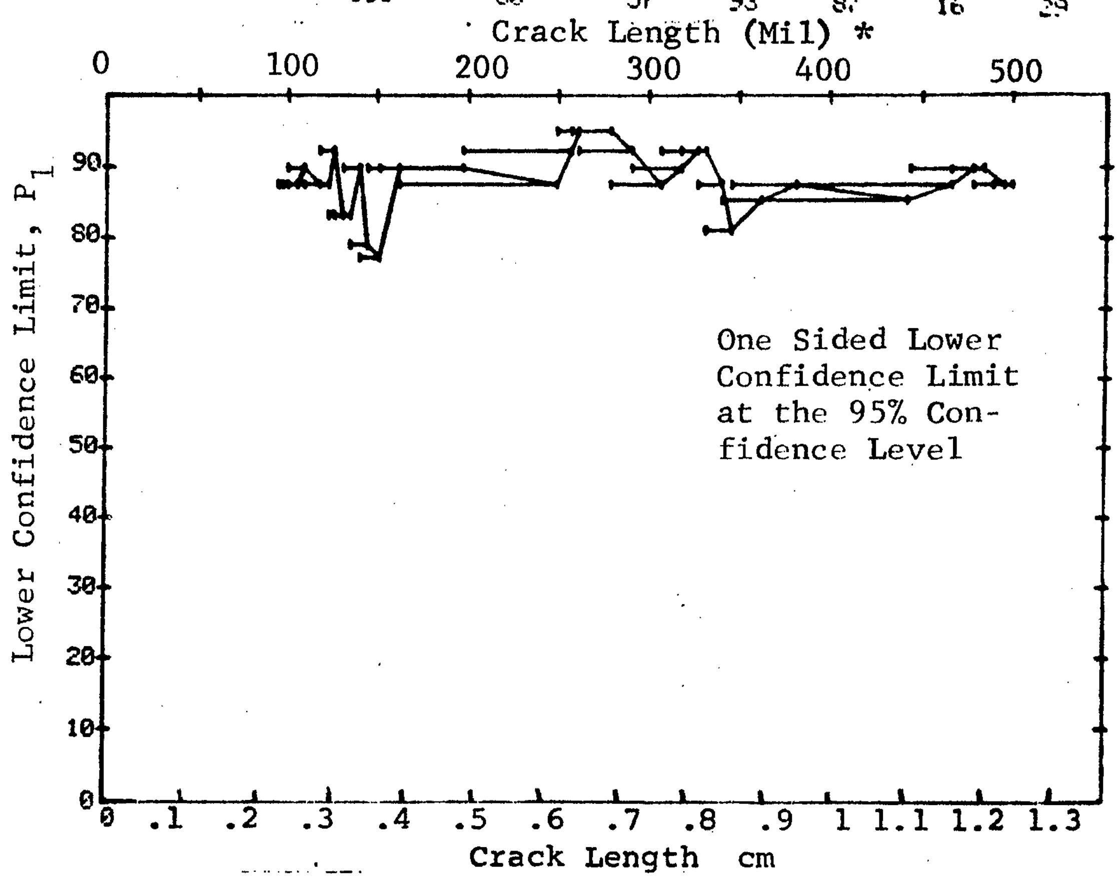

Figure D-35 (Continued)

(c) Overlapping Sixty Point Method of Data Cumulation

24-JUL-75 EDDY CURRENT TEST 3 ,MERGED, ROCKWELL SC (35)

RANGE	MIN LN	MAX LN	N	DET	50%	95%	0 MISS	1 MISS
1	7 *	21 *	51	5	9	3	0	0
2	15	26	60	10	16	9	0	0
3	21	31	60	12	19	11	0	0
4	26	35	60	12	19	11	0	0
5	31	40	60	18	29	20	0	0
6	35	45	60	19	30	21	0	0
7	41	47	60	18	29	20	0	0
8	45	49	60	21	34	24	0	0
9	47	55	60	27	44	33	0	0
10	49	58	60	25	40	30	0	0
11	55	60	60	29	47	37	0	0
12	58	62	60	33	54	43	0	0
13	60	63	60	38	62	51	0	0
14	62	65	60	44	72	62	0	0
15	63	66	60	37	60	50	0	0
16	65	67	60	37	60	50	0	0
17	66	69	60	41	67	57	0	0
18	67	70	60	39	64	53	0	0
19	69	72	60	37	60	50	0	0
20	70	75	60	42	69	58	0	0
21	72	76	60	44	72	62	0	0
22	75	78	60	44	72	62	0	0
23	76	79	60	52	85	77	82	94
24	78	80	60	57	93	87	16	29
25	79	83	60	51	83	75	94	100
26	80	84	60	48	79	69	0	0
27	83	86	60	55	90	83	43	56
28	84	87	60	58	95	89	1	16
29	86	91	60	54	88	81	56	69
30	87	95	60	55	90	83	43	56
31	91	97	60	57	93	87	16	29
32	95	100	60	57	93	87	16	29

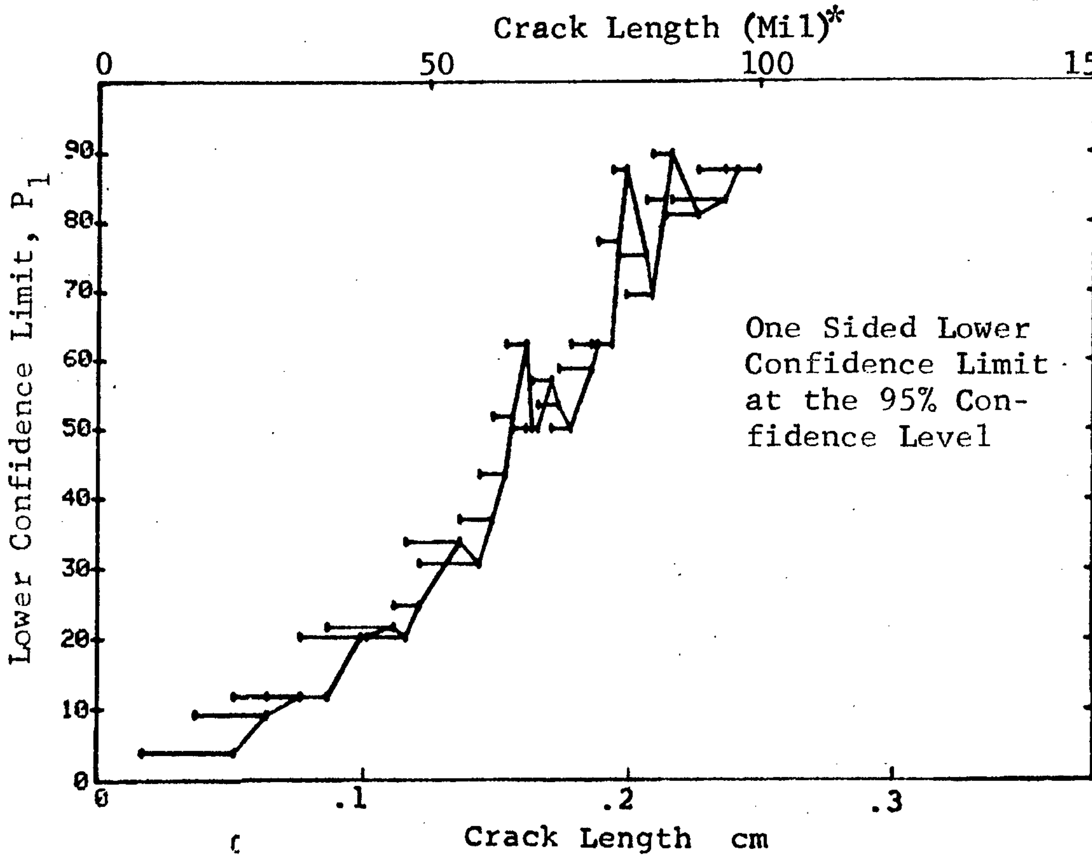

Figure D-35 (Concluded)

(a) Range Interval Method of Data Cumulation

29-JUL-75 PENETRANT TEST 1 (36) ROCKWELL B-1

RANGE	MIN LN	MAX LN	N	DET	50%	95%	0 MISS	1 MISS
1	31 *	31*	2	2	70	22	0	0
2	0	0	0	0	0	0	0	0
3	47	47	3	3	79	36	0	0
4	54	55	8	8	91	68	0	0
5	62	62	4	4	84	47	0	0
6	67	72	14	14	95	80	15	32
7	75	80	23	23	97	87	6	23
8	0	0	0	0	0	0	0	0
9	91	92	14	14	95	80	15	32
10	0	0	0	0	0	0	0	0
11	105	105	4	4	84	47	0	0
12	113	114	14	14	95	80	15	32
13	0	0	0	0	0	0	0	0
14	124	124	5	5	87	54	0	0
15	130	133	8	8	91	68	0	0
16	0	0	0	0	0	0	0	0
17	0	0	0	0	0	0	0	0
18	0	0	0	0	0	0	0	0
19	0	0	0	0	0	0	0	0
20	0	0	0	0	0	0	0	0
21	0	0	0	0	0	0	0	0
22	184	184	7	7	90	65	0	0
23	0	0	0	0	0	0	0	0
24	0	0	0	0	0	0	0	0
25	205	205	4	4	84	47	0	0
26	0	0	0	0	0	0	0	0
27	215	218	11	11	93	76	18	35
28	0	0	0	0	0	0	0	0
29	0	0	0	0	0	0	0	0
30	0	0	0	0	0	0	0	0
31	245	245	7	7	90	65	0	0
32	250	250	1	1	50	5	0	0

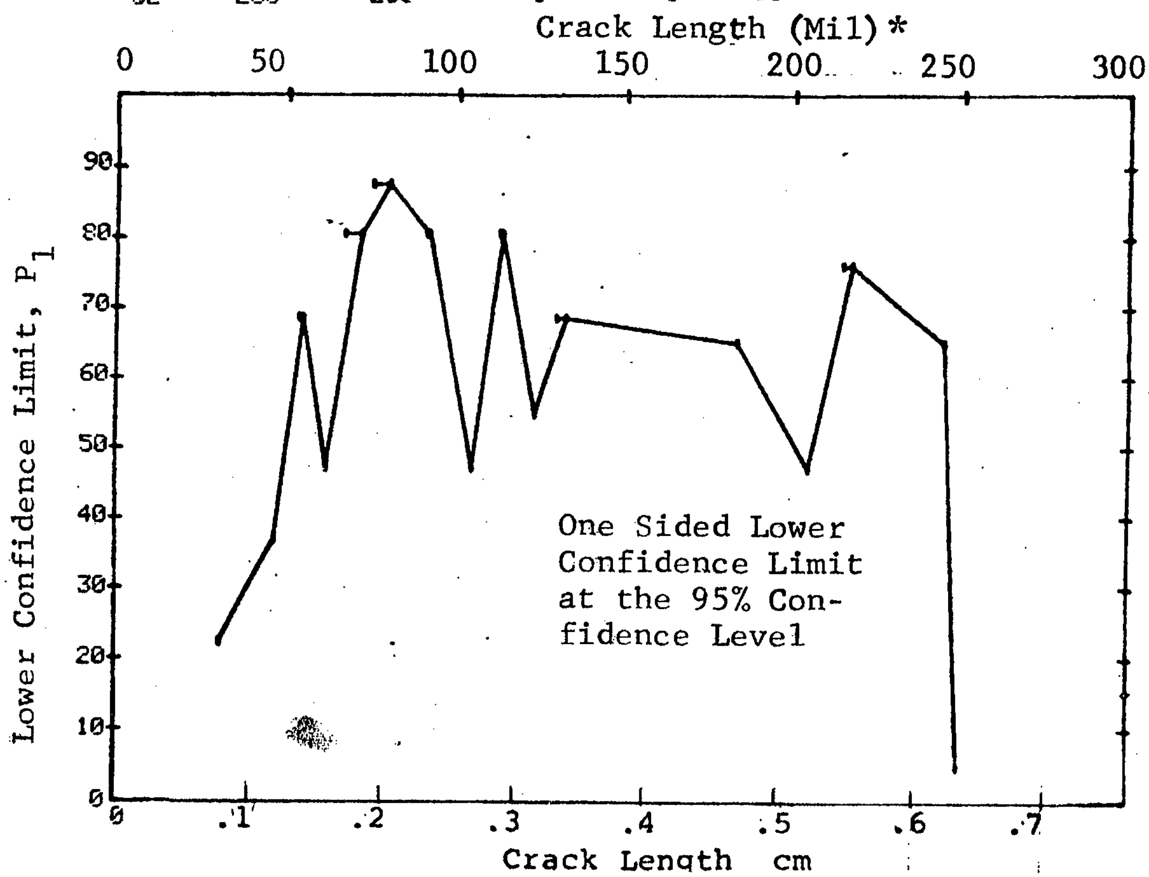

Figure D-36 Probability of Detection for Ti-6Al-4V Using Liquid Penetrant. Fatigue Cracks in Flat Plates. Prod. Env.

(b) Optimum Probability Method of Data Cumulation

29-JUL-75 PENETRANT TEST 2, (36) ROCKWELL B-1

RANGE	MIN LN*	MAX LN*	N	DET	50%	95%	0 MISS	1 MISS
1	31	31	2	2	0	22	0	0
2	0	0	0	0	0	0	0	0
3	31	47	5	5	0	54	0	0
4	31	55	13	13	0	79	0	0
5	31	62	17	17	0	83	12	29
6	31	72	31	31	0	90	0	15
7	31	80	54	54	0	94	0	0
8	0	0	0	0	0	0	0	0
9	31	92	68	68	0	95	0	0
10	0	0	0	0	0	0	0	0
11	31	105	72	72	0	95	0	0
12	31	114	86	86	0	96	0	0
13	0	0	0	0	0	0	0	0
14	31	124	91	91	0	96	0	0
15	31	133	99	99	0	97	0	0
16	0	0	0	0	0	0	0	0
17	0	0	0	0	0	0	0	0
18	0	0	0	0	0	0	0	0
19	0	0	0	0	0	0	0	0
20	0	0	0	0	0	0	0	0
21	0	0	0	0	0	0	0	0
22	31	184	106	106	0	97	0	0
23	0	0	0	0	0	0	0	0
24	0	0	0	0	0	0	0	0
25	31	205	110	110	0	97	0	0
26	0	0	0	0	0	0	0	0
27	31	218	121	121	0	97	0	0
28	0	0	0	0	0	0	0	0
29	0	0	0	0	0	0	0	0
30	0	0	0	0	0	0	0	0
31	31	245	128	128	0	97	0	0
32	31	250	129	129	0	97	0	0

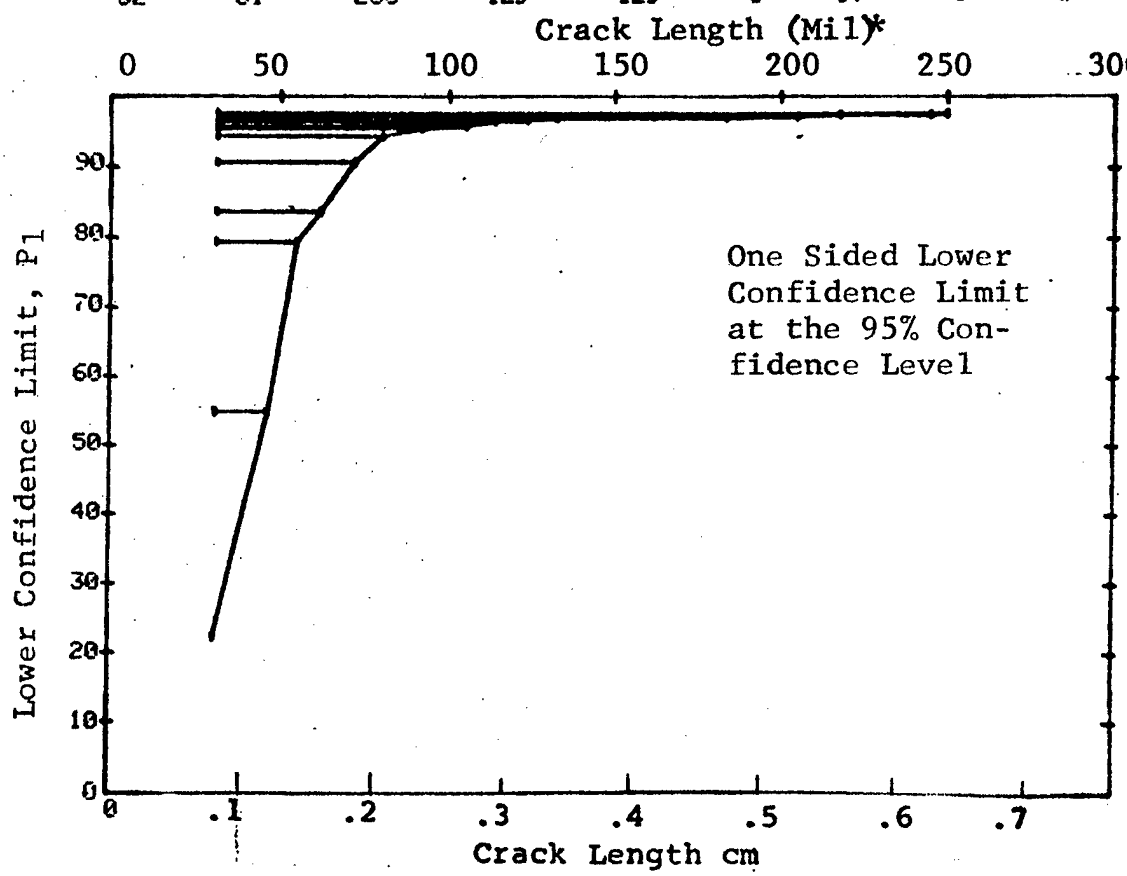

Figure D-36 (Continued)

(c) Overlapping Sixty Point Method of Data Cumulation

29-JUL-75 PENETRANT TEST 3, (36) ROCKWELL B-1

RANGE	MIN LN*	MAX LN*	N	DET	50%	95%	0 MISS	1 MISS
1	0	0	0	0	0	0	0	0
2	0	0	0	0	0	0	0	0
3	0	0	0	0	0	0	0	0
4	0	0	0	0	0	0	0	0
5	0	0	0	0	0	0	0	0
6	0	0	0	0	0	0	0	0
7	0	0	0	0	0	0	0	0
8	0	0	0	0	0	0	0	0
9	0	0	0	0	0	0	0	0
10	0	0	0	0	0	0	0	0
11	0	0	0	0	0	0	0	0
12	0	0	0	0	0	0	0	0
13	0	0	0	0	0	0	0	0
14	0	0	0	0	0	0	0	0
15	0	0	0	0	0	0	0	0
16	0	0	0	0	0	0	0	0
17	0	0	0	0	0	0	0	0
18	0	0	0	0	0	0	0	0
19	0	0	0	0	0	0	0	0
20	0	0	0	0	0	0	0	0
21	0	0	0	0	0	0	0	0
22	0	0	0	0	0	0	0	0
23	0	0	0	0	0	0	0	0
24	0	0	0	0	0	0	0	0
25	0	0	0	0	0	0	0	0
26	0	0	0	0	0	0	0	0
27	0	0	0	0	0	0	0	0
28	0	0	0	0	0	0	0	0
29	31	78	39	39	98	92	0	0
30	55	105	60	60	98	95	0	0
31	78	133	60	60	98	95	0	0
32	105	250	60	60	98	95	0	0

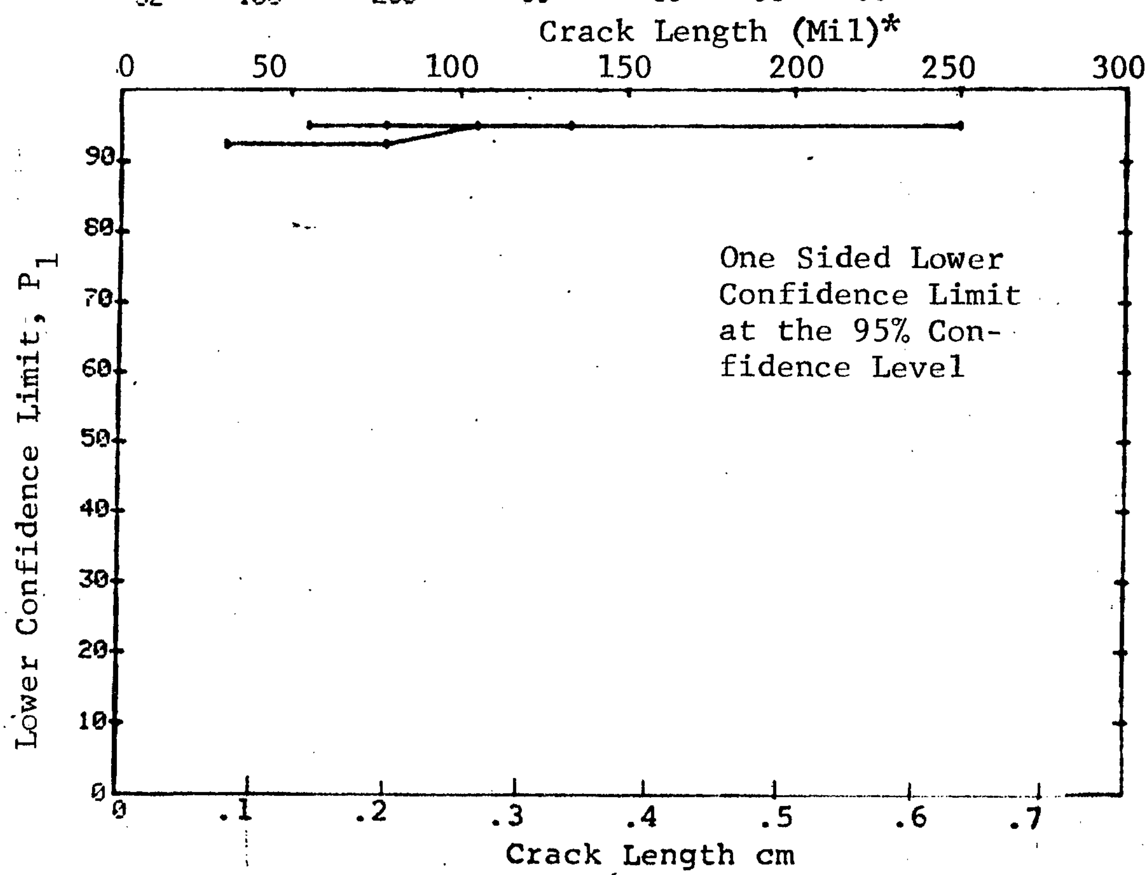

Figure D-36 (Concluded)

(a) Range Interval Method of Data Cumulation

29-JUL-75 PENETRANT TEST 1. (37) ., ROCKWELL B-1

RANGE	MIN LN	MAX LN	N	DET	50%	95%	0 MISS.	1 MISS
1	31*	31 *	4	3	61	24	0	0
2	0	0	0	0	0	0	0	0
3	47	47	9	9	92	71	0	0
4	54	55	18	18	96	84	11	28
5	0	0	0	0	0	0	0	0
6	62	67	20	20	96	86	9	26
7	70	70	10	10	93	74	0	0
8	78	78	8	8	91	63	0	0
9	80	80	7	7	90	65	0	0
10	91	91	8	8	91	68	0	0
11	92	92	8	8	91	68	0	0
12	0	0	0	0	0	0	0	0
13	0	0	0	0	0	0	0	0
14	113	114	13	13	94	79	16	33
15	0	0	0	0	0	0	0	0
16	124	124	7	7	90	65	0	0
17	130	133	11	11	93	76	18	35
18	0	0	0	0	0	0	0	0
19	0	0	0	0	0	0	0	0
20	0	0	0	0	0	0	0	0
21	0	0	0	0	0	0	0	0
22	0	0	0	0	0	0	0	0
23	0	0	0	0	0	0	0	0
24	0	0	0	0	0	0	0	0
25	0	0	0	0	0	0	0	0
26	184	184	8	8	91	68	0	0
27	0	0	0	0	0	0	0	0
28	0	0	0	0	0	0	0	0
29	205	205	5	5	87	54	0	0
30	0	0	0	0	0	0	0	0
31	215	215	5	5	87	54	0	0
32	218	245	12	12	94	77	17	34

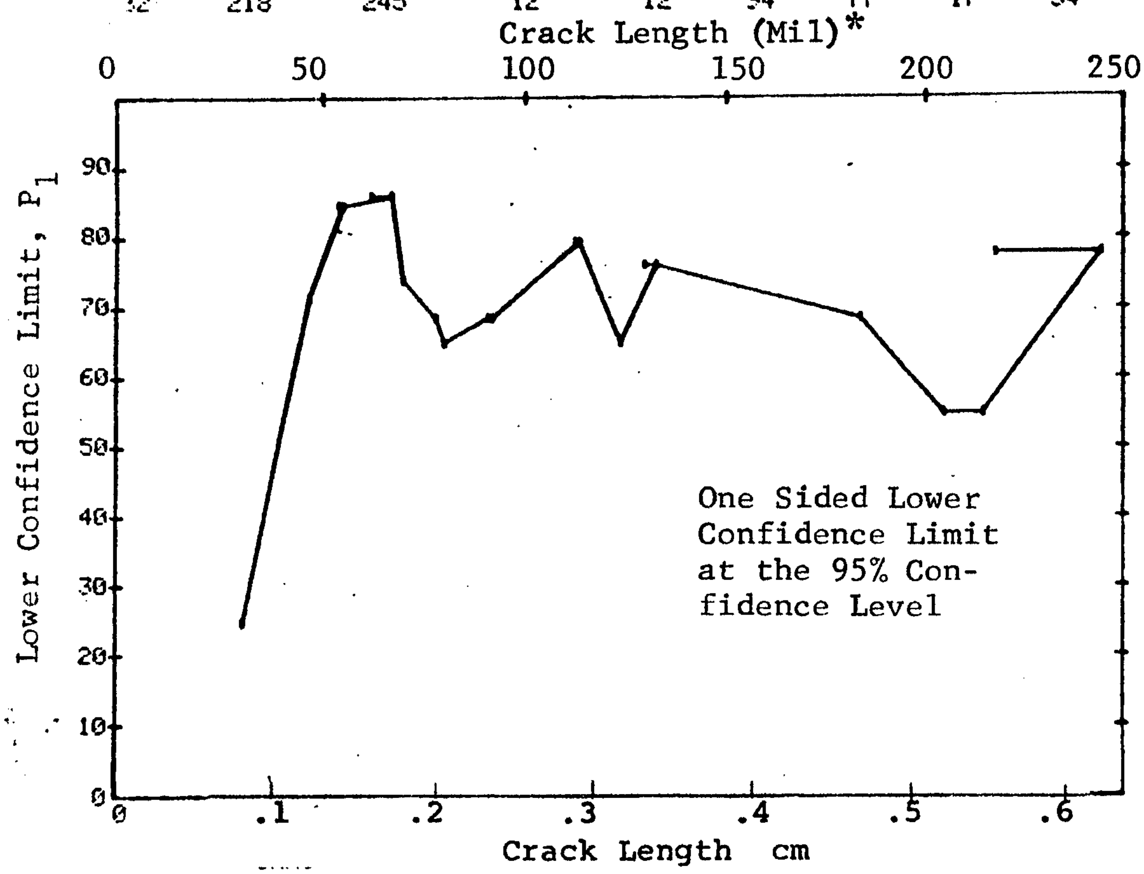

Figure D-37 Probability of Detection for Ti-6Al-4V Using Liquid Penetrant. Fatigue Cracks in Flat Plates. Prod. Env.

(b) Optimum Probability Method of Data Cumulation

29-JUL-75 PENETRANT TEST 2, (37) .. ROCKWELL I 6-1

RANGE	MIN LN	MAX LN	N	DET	50%	95%	0 MISS	1 MISS
1	31*	31*	4	3	0	24	0	0
2	0	0	0	0	0	0	0	0
3	47	47	9	9	0	71	0	0
4	47	55	27	27	0	89	2	19
5	0	0	0	0	0	0	0	0
6	47	67	47	47	0	93	0	0
7	47	70	57	57	0	94	0	0
8	47	78	65	65	0	95	0	0
9	47	80	72	72	0	95	0	0
10	47	91	80	80	0	96	0	0
11	47	92	88	88	0	96	0	0
12	0	0	0	0	0	0	0	0
13	0	0	0	0	0	0	0	0
14	47	114	101	101	0	97	0	0
15	0	0	0	0	0	0	0	0
16	47	124	108	108	0	97	0	0
17	47	133	119	119	0	97	0	0
18	0	0	0	0	0	0	0	0
19	0	0	0	0	0	0	0	0
20	0	0	0	0	0	0	0	0
21	0	0	0	0	0	0	0	0
22	0	0	0	0	0	0	0	0
23	0	0	0	0	0	0	0	0
24	0	0	0	0	0	0	0	0
25	0	0	0	0	0	0	0	0
26	47	184	127	127	0	97	0	0
27	0	0	0	0	0	0	0	0
28	0	0	0	0	0	0	0	0
29	47	205	132	132	0	97	0	0
30	0	0	0	0	0	0	0	0
31	47	215	137	137	0	97	0	0
32	47	245	149	149	0	98	0	0

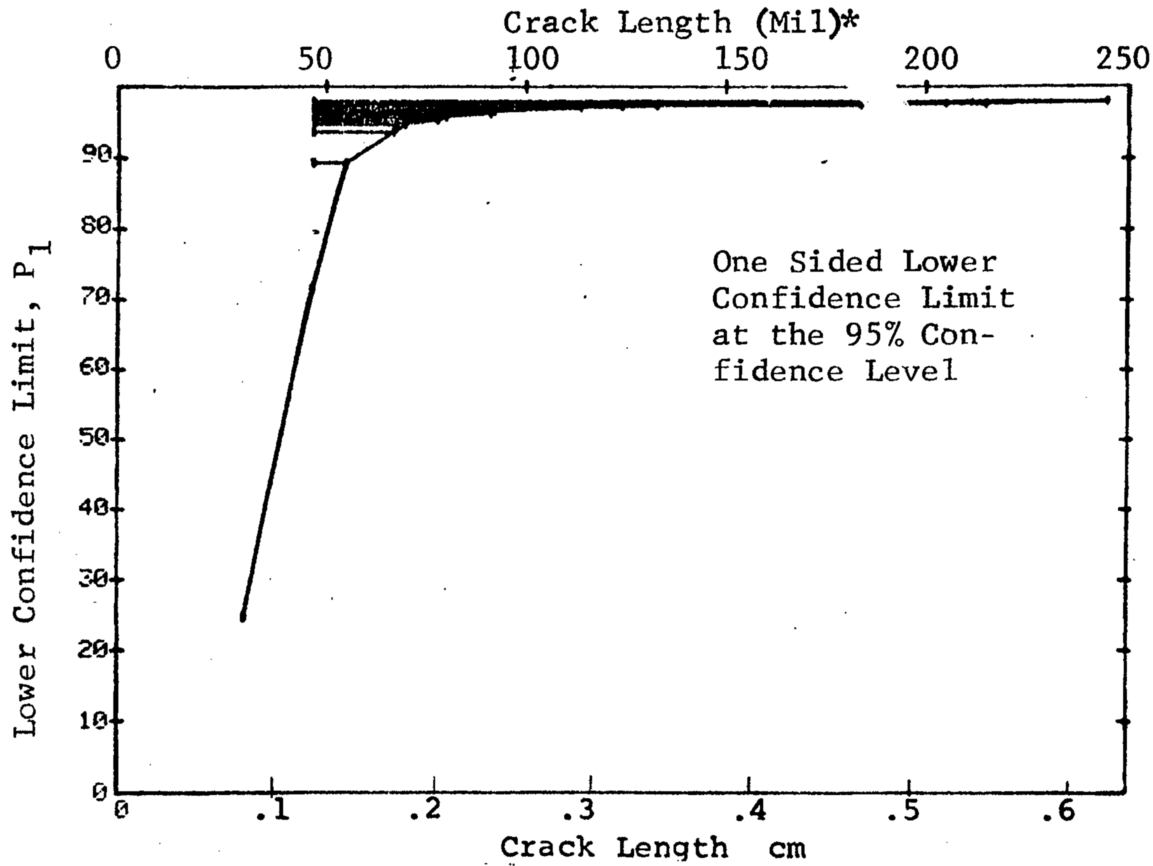

Figure D-37 (Continued)

(c) Overlapping Sixty Point Method of Data Cumulation

29-JUL-75 PENETRANT TEST 3, (37) ROCKWELL I B-1

RANGE	MIN LN *	MAX LN *	N	DET	50%	95%	0 MISS	1 MISS
1	0	0	0	0	0	0	0	0
2	0	0	0	0	0	0	0	0
3	0	0	0	0	0	0	0	0
4	0	0	0	0	0	0	0	0
5	0	0	0	0	0	0	0	0
6	0	0	0	0	0	0	0	0
7	0	0	0	0	0	0	0	0
8	0	0	0	0	0	0	0	0
9	0	0	0	0	0	0	0	0
10	0	0	0	0	0	0	0	0
11	0	0	0	0	0	0	0	0
12	0	0	0	0	0	0	0	0
13	0	0	0	0	0	0	0	0
14	0	0	0	0	0	0	0	0
15	0	0	0	0	0	0	0	0
16	0	0	0	0	0	0	0	0
17	0	0	0	0	0	0	0	0
18	0	0	0	0	0	0	0	0
19	0	0	0	0	0	0	0	0
20	0	0	0	0	0	0	0	0
21	0	0	0	0	0	0	0	0
22	0	0	0	0	0	0	0	0
23	0	0	0	0	0	0	0	0
24	0	0	0	0	0	0	0	0
25	0	0	0	0	0	0	0	0
26	0	0	0	0	0	0	0	0
27	0	0	0	0	0	0	0	0
28	31	62	33	32	94	86	13	28
29	31	78	60	59	97	92	0	1
30	62	113	60	60	98	95	0	0
31	78	133	60	60	98	95	0	0
32	113	245	60	60	98	95	0	0

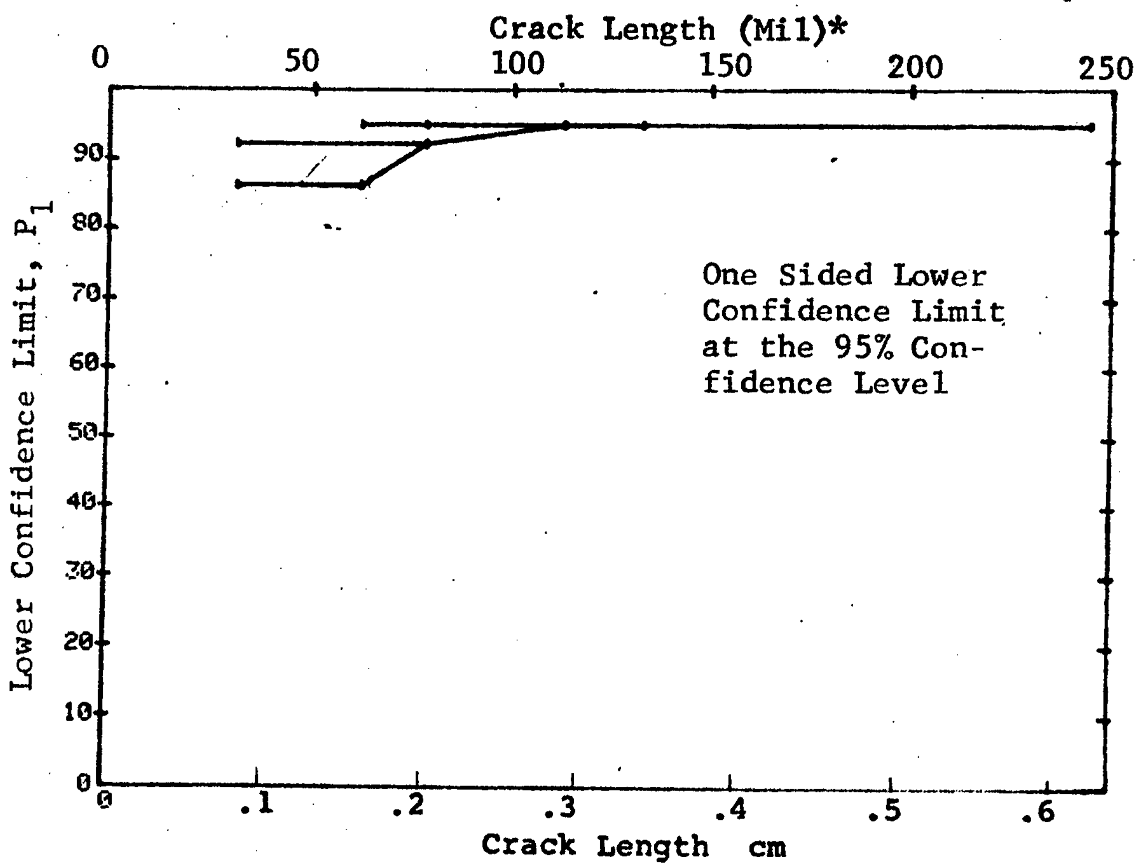

Figure D-37 (Concluded)

(a) Range Interval Method of Data Cumulation

09-OCT-75	PENETRANT			TEST 1		(38)		
RANGE	MIN LN	MAX LN	N	DET	50%	95%	0 MISS	1 MISS
1	47 *	47 *	4	4	84	47	0	0
2	0	0	0	0	0	0	0	0
3	0	0	0	0	0	0	0	0
4	0	0	0	0	0	0	0	0
5	0	0	0	0	0	0	0	0
6	0	0	0	0	0	0	0	0
7	0	0	0	0	0	0	0	0
8	0	0	0	0	0	0	0	0
9	0	0	0	0	0	0	0	0
10	0	0	0	0	0	0	0	0
11	0	0	0	0	0	0	0	0
12	0	0	0	0	0	0	0	0
13	0	0	0	0	0	0	0	0
14	0	0	0	0	0	0	0	0
15	0	0	0	0	0	0	0	0
16	0	0	0	0	0	0	0	0
17	0	0	0	0	0	0	0	0
18	0	0	0	0	0	0	0	0
19	0	0	0	0	0	0	0	0
20	0	0	0	0	0	0	0	0
21	0	0	0	0	0	0	0	0
22	0	0	0	0	0	0	0	0
23	0	0	0	0	0	0	0	0
24	0	0	0	0	0	0	0	0
25	0	0	0	0	0	0	0	0
26	0	0	0	0	0	0	0	0
27	0	0	0	0	0	0	0	0
28	0	0	0	0	0	0	0	0
29	0	0	0	0	0	0	0	0
30	0	0	0	0	0	0	0	0
31	0	0	0	0	0	0	0	0
32	54	70	26	26	97	89	3	20

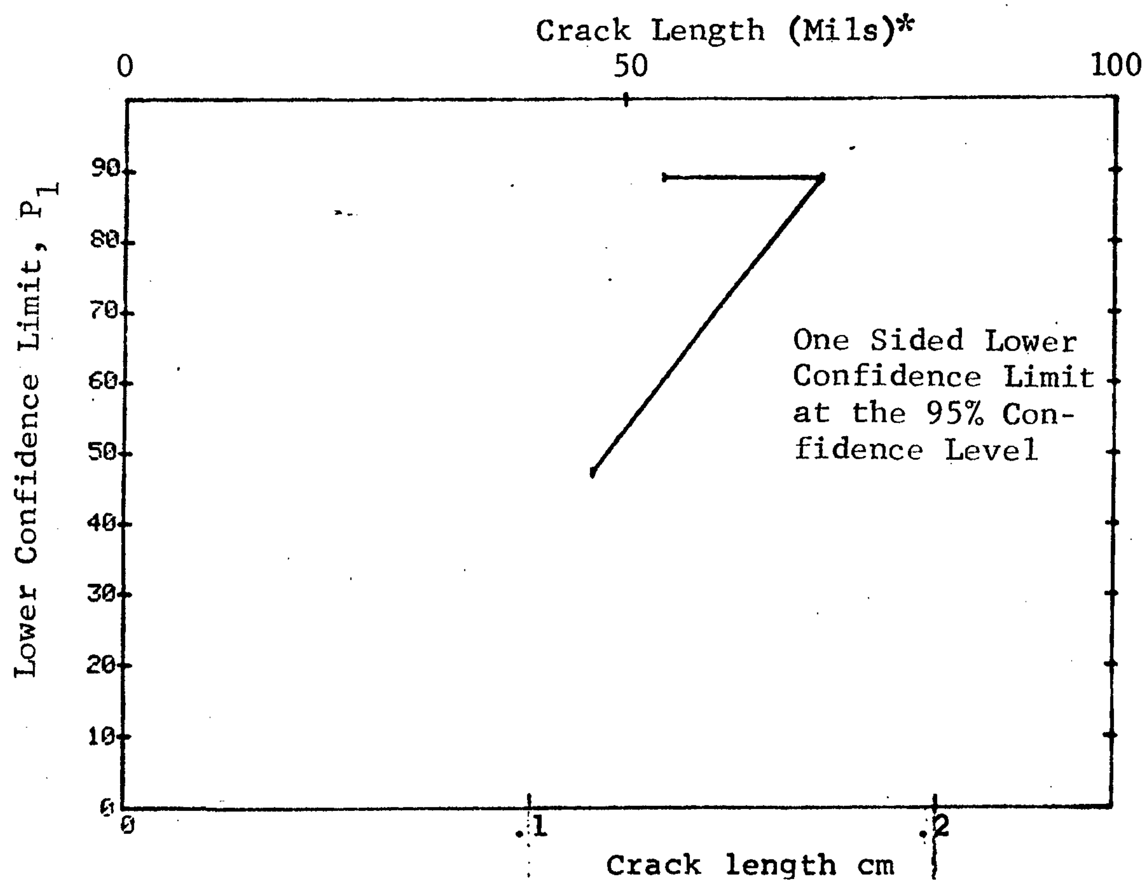

Figure D-38 Probability of Detection for Ti-6Al-4V Using Liquid Penetrant. Fatigue Cracks in Flat Plates. Prod. Env.

(b) Optimum Probability Method of Data Cumulation

09-OCT-75 PENETRANT TEST 2 (38)

RANGE	MIN LN	MAX LN	N	DET	50%	95%	0 MISS	1 MISS
1	47*	47*	4	4	0	47	0	0
2	0	0	0	0	0	0	0	0
3	0	0	0	0	0	0	0	0
4	0	0	0	0	0	0	0	0
5	0	0	0	0	0	0	0	0
6	0	0	0	0	0	0	0	0
7	0	0	0	0	0	0	0	0
8	0	0	0	0	0	0	0	0
9	0	0	0	0	0	0	0	0
10	0	0	0	0	0	0	0	0
11	0	0	0	0	0	0	0	0
12	0	0	0	0	0	0	0	0
13	0	0	0	0	0	0	0	0
14	0	0	0	0	0	0	0	0
15	0	0	0	0	0	0	0	0
16	0	0	0	0	0	0	0	0
17	0	0	0	0	0	0	0	0
18	0	0	0	0	0	0	0	0
19	0	0	0	0	0	0	0	0
20	0	0	0	0	0	0	0	0
21	0	0	0	0	0	0	0	0
22	0	0	0	0	0	0	0	0
23	0	0	0	0	0	0	0	0
24	0	0	0	0	0	0	0	0
25	0	0	0	0	0	0	0	0
26	0	0	0	0	0	0	0	0
27	0	0	0	0	0	0	0	0
28	0	0	0	0	0	0	0	0
29	0	0	0	0	0	0	0	0
30	0	0	0	0	0	0	0	0
31	0	0	0	0	0	0	0	0
32	47	70	30	30	0	90	0	16

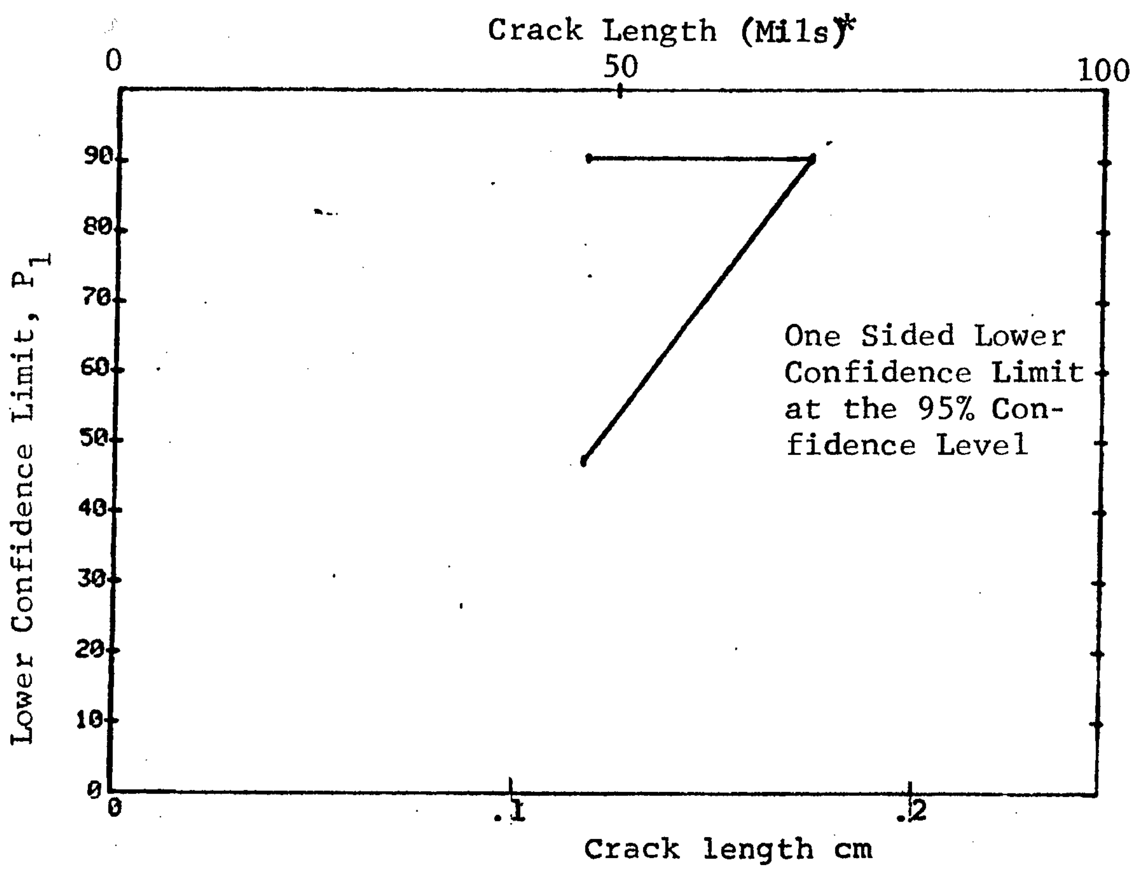

Figure D-38 (Continued)

(c) Overlapping Sixty Point Method of Data Cumulation

09-OCT-75 PENETRANT TEST 3 (38)

RANGE	MIN LN *	MAX LN *	N	DET	50%	95%	0 MISS	1 MISS
1	0	0	0	0	0	0	0	0
2	0	0	0	0	0	0	0	0
3	0	0	0	0	0	0	0	0
4	0	0	0	0	0	0	0	0
5	0	0	0	0	0	0	0	0
6	0	0	0	0	0	0	0	0
7	0	0	0	0	0	0	0	0
8	0	0	0	0	0	0	0	0
9	0	0	0	0	0	0	0	0
10	0	0	0	0	0	0	0	0
11	0	0	0	0	0	0	0	0
12	0	0	0	0	0	0	0	0
13	0	0	0	0	0	0	0	0
14	0	0	0	0	0	0	0	0
15	0	0	0	0	0	0	0	0
16	0	0	0	0	0	0	0	0
17	0	0	0	0	0	0	0	0
18	0	0	0	0	0	0	0	0
19	0	0	0	0	0	0	0	0
20	0	0	0	0	0	0	0	0
21	0	0	0	0	0	0	0	0
22	0	0	0	0	0	0	0	0
23	0	0	0	0	0	0	0	0
24	0	0	0	0	0	0	0	0
25	0	0	0	0	0	0	0	0
26	0	0	0	0	0	0	0	0
27	0	0	0	0	0	0	0	0
28	0	0	0	0	0	0	0	0
29	0	0	0	0	0	0	0	0
30	0	0	0	0	0	0	0	0
31	0	0	0	0	0	0	0	0
32	47	70	30	30	97	90	0	16

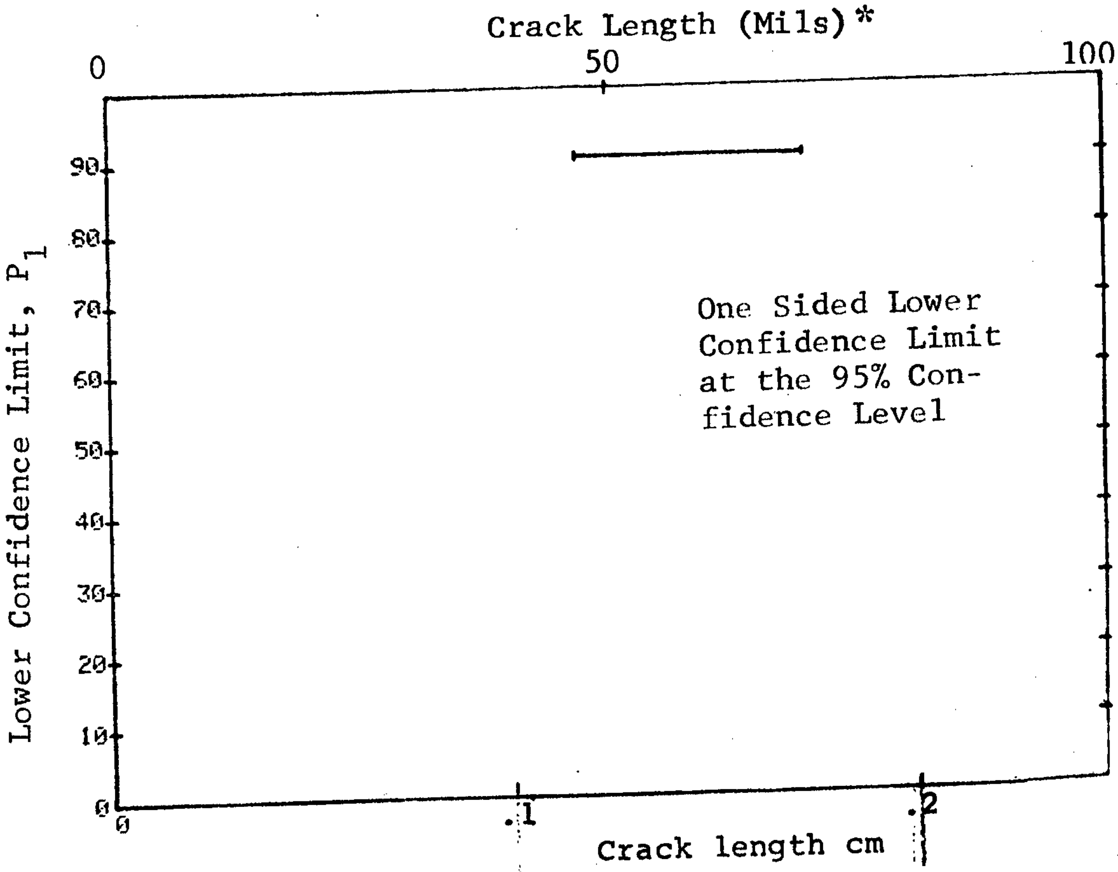

Figure D-38 (Concluded)

(a) Range Interval Method of Data Cumulation

09-OCT-75 RANGE	PENETRANT MIN LN	MAX LN	N	TEST 1 DET	50%	(39) 95%	0 MISS	1 MISS
1	8 *	8 *	3	0	0	0	0	0
2	10	10	3	2	50	13	0	0
3	0	0	0	0	0	0	0	0
4	12	12	4	1	15	1	0	0
5	13	13	2	2	70	22	0	0
6	14	14	3	3	79	36	0	0
7	15	15	3	3	79	36	0	0
8	0	0	0	0	0	0	0	0
9	17	17	3	3	79	36	0	0
10	0	0	0	0	0	0	0	0
11	19	19	3	3	79	36	0	0
12	0	0	0	0	0	0	0	0
13	21	21	6	5	73	41	0	0
14	0	0	0	0	0	0	0	0
15	23	23	4	3	61	24	0	0
16	0	0	0	0	0	0	0	0
17	25	25	14	13	88	70	0	0
18	26	26	3	3	79	36	0	0
19	27	27	3	3	79	36	0	0
20	0	0	0	0	0	0	0	0
21	0	0	0	0	0	0	0	0
22	0	0	0	0	0	0	0	0
23	31	31	7	7	90	65	0	0
24	32	32	4	3	61	24	0	0
25	33	33	4	4	84	47	0	0
26	0	0	0	0	0	0	0	0
27	35	35	2	2	70	22	0	0
28	36	36	6	6	89	60	0	0
29	0	0	0	0	0	0	0	0
30	0	0	0	0	0	0	0	0
31	39	39	7	7	90	65	0	0
32	47	50	13	13	94	79	16	33

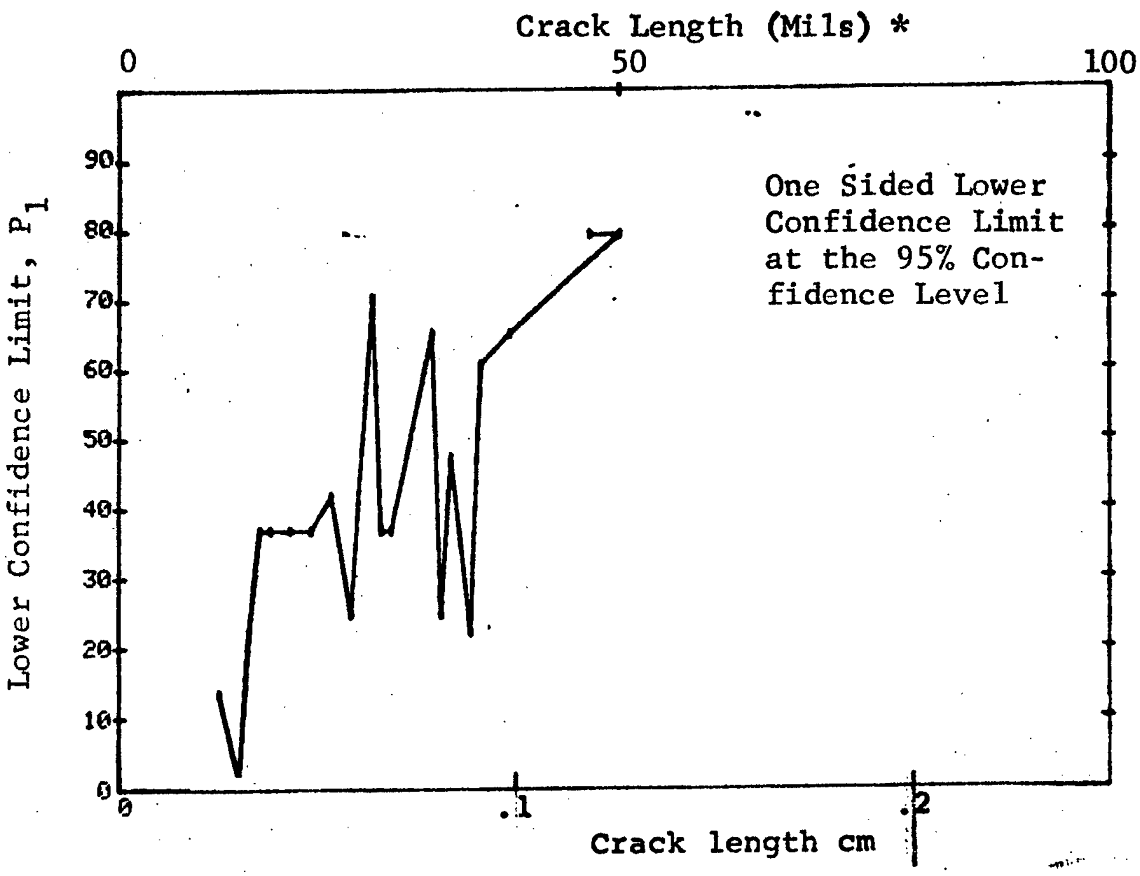

Figure D-39 Probability of Detection for Ti-6Al-4V Using Liquid Penetrant. Fatigue Cracks in Flat Plates. Prod. Env.

(b) Optimum Probability Method of Data Cumulation

09-OCT-75 PENETRANT TEST 2 (39)

RANGE	MIN LN	MAX LN	N	DET	50%	95%	0 MISS	1 MISS
1	8*	8*	3	0	0	0	0	0
2	10	10	3	2	0	13	0	0
3	0	0	0	0	0	0	0	0
4	10	12	7	3	0	12	0	0
5	10	13	9	5	0	25	0	0
6	13	14	5	5	0	54	0	0
7	13	15	8	8	0	68	0	0
8	0	0	0	0	0	0	0	0
9	13	17	11	11	0	76	0	0
10	0	0	0	0	0	0	0	0
11	13	19	14	14	0	80	15	32
12	0	0	0	0	0	0	0	0
13	13	21	20	19	0	78	0	0
14	0	0	0	0	0	0	0	0
15	13	23	24	22	0	75	0	0
16	0	0	0	0	0	0	0	0
17	13	25	38	35	0	80	38	51
18	13	26	41	38	0	82	35	48
19	13	27	44	41	0	83	32	45
20	0	0	0	0	0	0	0	0
21	0	0	0	0	0	0	0	0
22	0	0	0	0	0	0	0	0
23	13	31	51	48	0	85	25	38
24	13	32	55	51	0	84	34	48
25	13	33	59	55	0	85	30	44
26	0	0	0	0	0	0	0	0
27	13	35	61	57	0	85	28	42
28	13	36	67	63	0	86	22	36
29	0	0	0	0	0	0	0	0
30	0	0	0	0	0	0	0	0
31	13	39	74	70	0	88	15	29
32	33	50	32	32	0	91	0	14

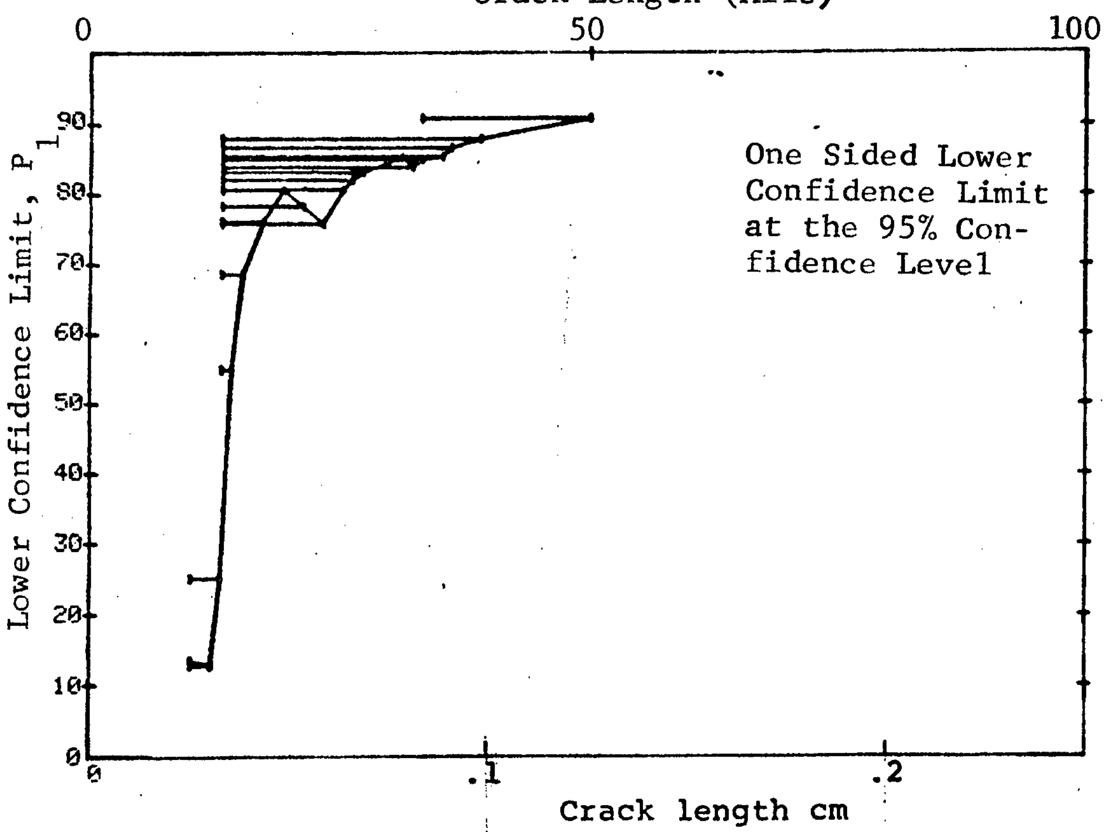

Figure D-39 (Continued)

(c) Overlapping Sixty Point Method of Data Cumulation

09-OCT-75 PENETRANT TEST 3 (39)

RANGE	MIN LN	MAX LN	N	DET	50%	95%	0 MISS	1 MISS
1	0 *	0 *	0	0	0	0	0	0
2	0	0	0	0	0	0	0	0
3	0	0	0	0	0	0	0	0
4	0	0	0	0	0	0	0	0
5	0	0	0	0	0	0	0	0
6	0	0	0	0	0	0	0	0
7	0	0	0	0	0	0	0	0
8	0	0	0	0	0	0	0	0
9	0	0	0	0	0	0	0	0
10	0	0	0	0	0	0	0	0
11	0	0	0	0	0	0	0	0
12	0	0	0	0	0	0	0	0
13	0	0	0	0	0	0	0	0
14	0	0	0	0	0	0	0	0
15	0	0	0	0	0	0	0	0
16	0	0	0	0	0	0	0	0
17	0	0	0	0	0	0	0	0
18	0	0	0	0	0	0	0	0
19	0	0	0	0	0	0	0	0
20	0	0	0	0	0	0	0	0
21	0	0	0	0	0	0	0	0
22	0	0	0	0	0	0	0	0
23	0	0	0	0	0	0	0	0
24	0	0	0	0	0	0	0	0
25	0	0	0	0	0	0	0	0
26	0	0	0	0	0	0	0	0
27	0	0	0	0	0	0	0	0
28	0	0	0	0	0	0	0	0
29	0	0	0	0	0	0	0	0
30	8	25	37	28	74	61	0	0
31	12	33	60	53	87	79	69	82
32	25	50	60	58	95	89	1	16

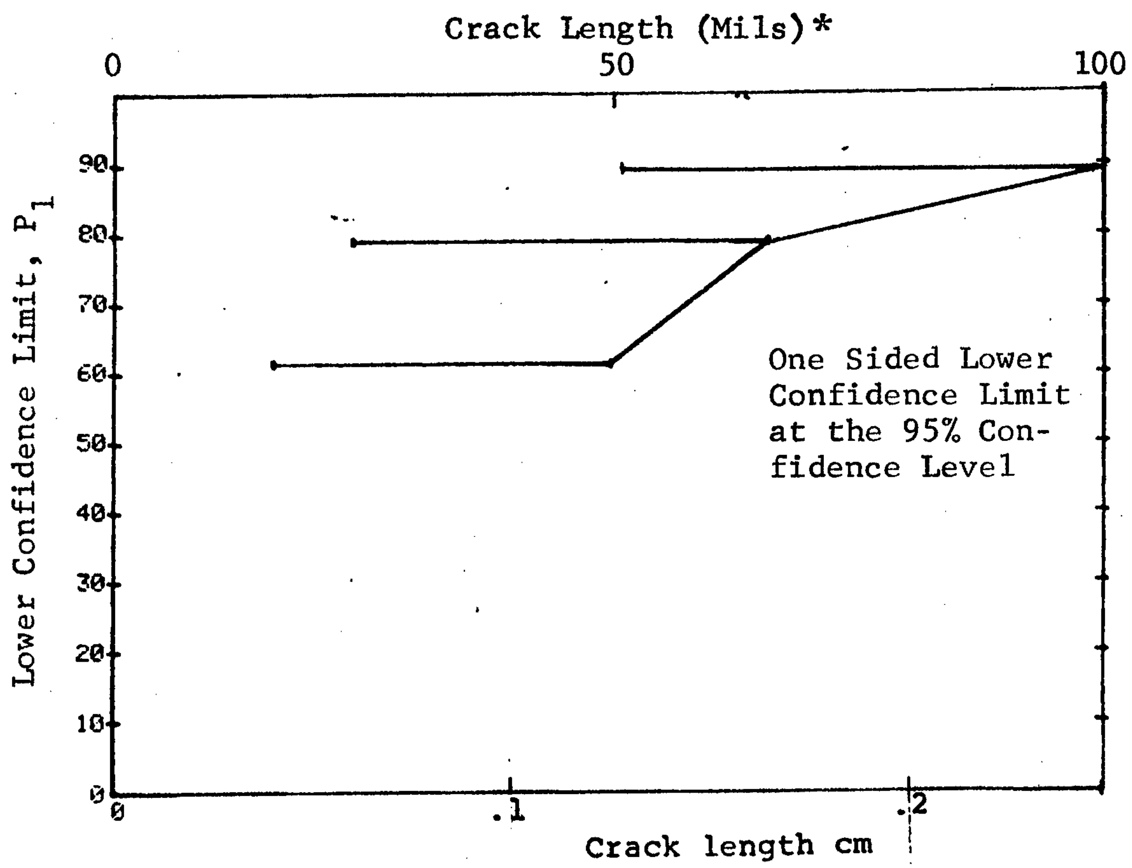

Figure D-39 (Concluded)

(a) Range Interval Method of Data Cumulation

09-OCT-75 PENETRANT TEST 1 (40)

RANGE	MIN LN	MAX LN	N	DET	50%	95%	0 MISS	1 MISS
1	37 *	37 *	5	5	87	54	0	0
2	44	44	7	7	90	65	0	0
3	51	51	7	7	90	65	0	0
4	0	0	0	0	0	0	0	0
5	60	60	5	5	87	54	0	0
6	0	0	0	0	0	0	0	0
7	68	68	7	7	90	65	0	0
8	76	76	3	3	79	36	0	0
9	0	0	0	0	0	0	0	0
10	85	86	2	2	70	22	0	0
11	88	91	12	12	94	77	17	34
12	93	97	12	12	94	77	17	34
13	99	101	7	7	90	65	0	0
14	105	105	5	5	87	54	0	0
15	110	110	5	5	87	54	0	0
16	113	115	4	4	84	47	0	0
17	0	0	0	0	0	0	0	0
18	125	125	10	10	93	74	0	0
19	0	0	0	0	0	0	0	0
20	135	135	4	4	84	47	0	0
21	0	0	0	0	0	0	0	0
22	147	147	2	2	70	22	0	0
23	0	0	0	0	0	0	0	0
24	153	156	12	12	94	77	17	34
25	162	162	3	3	79	36	0	0
26	164	164	4	4	84	47	0	0
27	0	0	0	0	0	0	0	0
28	176	176	3	3	79	36	0	0
29	0	0	0	0	0	0	0	0
30	0	0	0	0	0	0	0	0
31	189	189	5	5	87	54	0	0
32	194	194	3	3	79	36	0	0

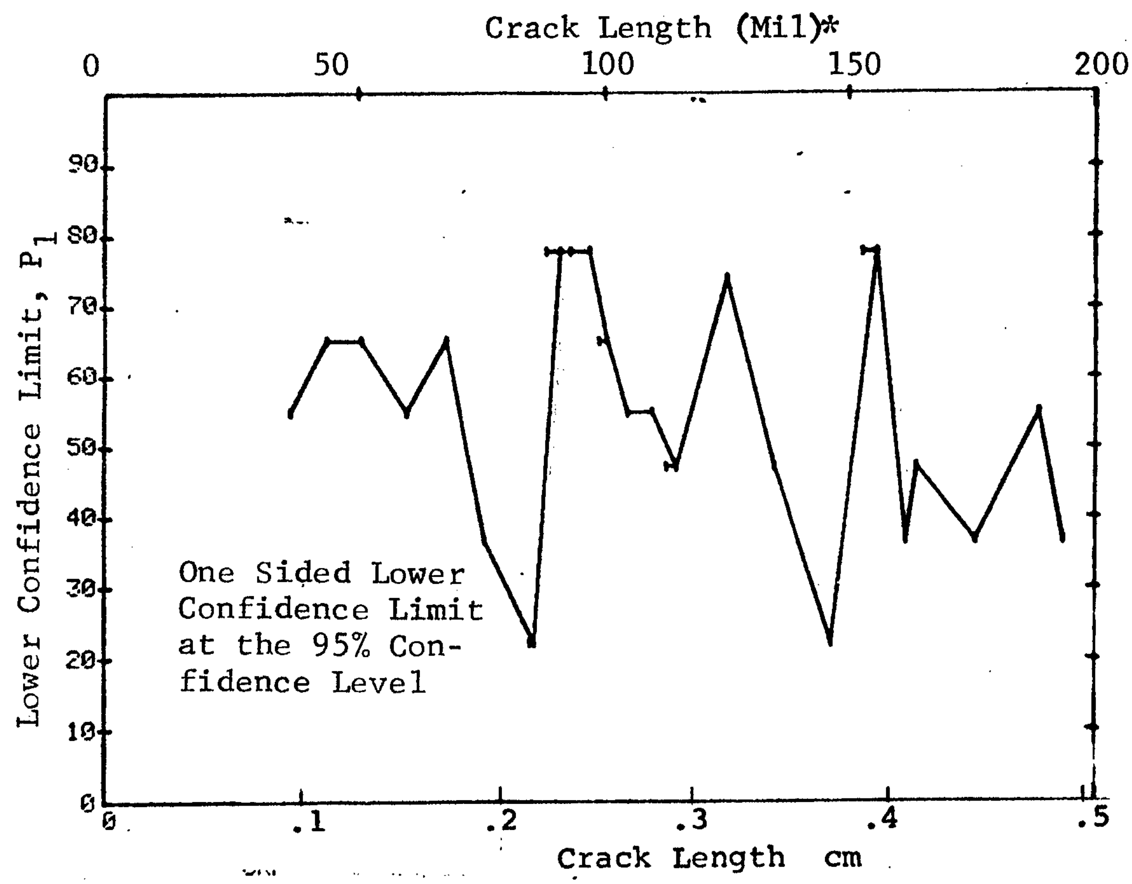

Figure D-40 Probability of Detection for 7075-T6511 Al Using Liquid Penetrant. Fatigue Cracks in Flat Plates. Prod. Env.

(b) Optimum Probability Method of Data Cumulation

09-OCT-75	PENETRANT			TEST 2		(40)		
RANGE	MIN LN	MAX LN	N	DET	50%	95%	0 MISS	1 MISS
1	37 *	37 *	5	5	0	54	0	0
2	37	44	12	12	0	77	0	0
3	37	51	19	19	0	85	10	27
4	0	0	0	0	0	0	0	0
5	37	60	24	24	0	88	5	22
6	0	0	0	0	0	0	0	0
7	37	68	31	31	0	90	0	15
8	37	76	34	34	0	91	0	12
9	0	0	0	0	0	0	0	0
10	37	86	36	36	0	92	0	10
11	37	91	48	48	0	93	0	0
12	37	97	60	60	0	95	0	0
13	37	101	67	67	0	95	0	0
14	37	105	72	72	0	95	0	0
15	37	110	77	77	0	96	0	0
16	37	115	81	81	0	96	0	0
17	0	0	0	0	0	0	0	0
18	37	125	91	91	0	96	0	0
19	0	0	0	0	0	0	0	0
20	37	135	95	95	0	96	0	0
21	0	0	0	0	0	0	0	0
22	37	147	97	97	0	96	0	0
23	0	0	0	0	0	0	0	0
24	37	156	109	109	0	97	0	0
25	37	162	112	112	0	97	0	0
26	37	164	116	116	0	97	0	0
27	0	0	0	0	0	0	0	0
28	37	176	119	119	0	97	0	0
29	0	0	0	0	0	0	0	0
30	0	0	0	0	0	0	0	0
31	37	189	124	124	0	97	0	0
32	37	194	127	127	0	97	0	0

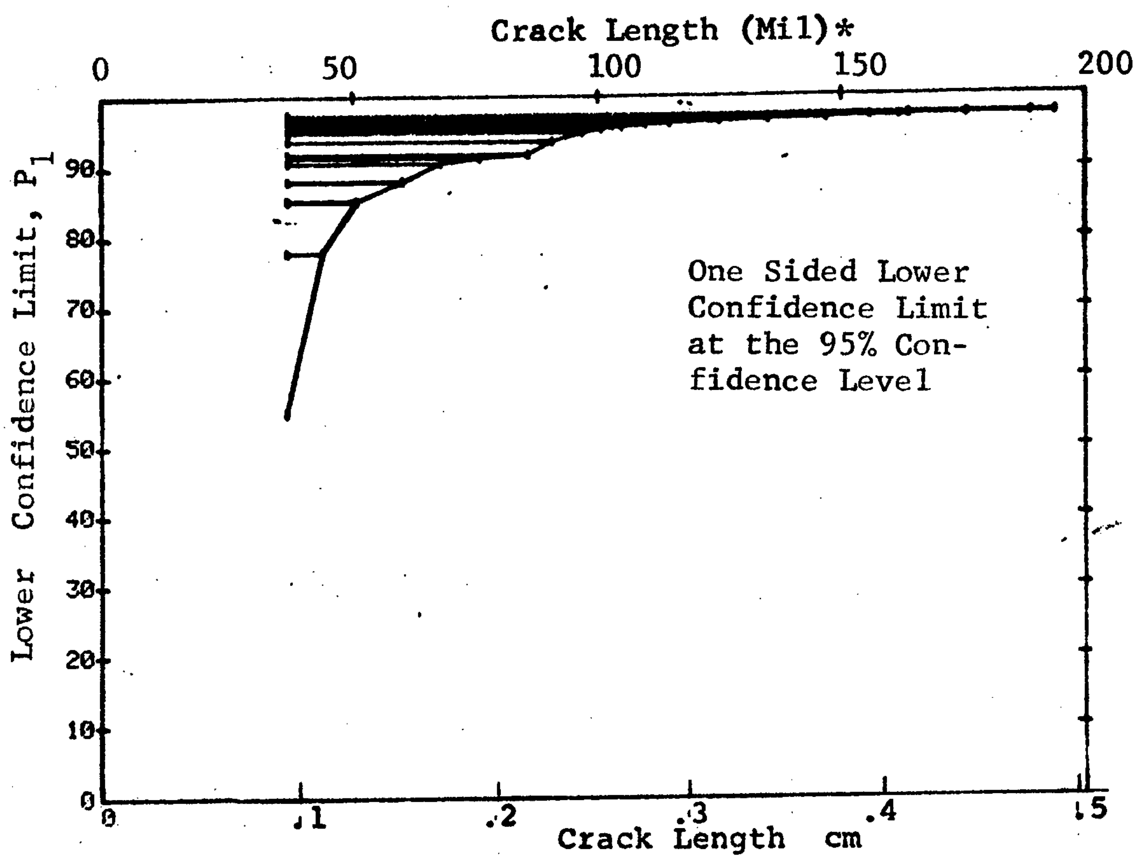

Figure D-40 (Continued)

(c) Overlapping Sixty Point Method of Data Cumulation

09-OCT-75	PENETRANT			TEST 3		(40)		
RANGE	MIN LN	MAX LN	N	DET	50%	95%	0 MISS	1 MISS
1	0 *	0 *	0	0	0	0	0	0
2	0	0	0	0	0	0	0	0
3	0	0	0	0	0	0	0	0
4	0	0	0	0	0	0	0	0
5	0	0	0	0	0	0	0	0
6	0	0	0	0	0	0	0	0
7	0	0	0	0	0	0	0	0
8	0	0	0	0	0	0	0	0
9	0	0	0	0	0	0	0	0
10	0	0	0	0	0	0	0	0
11	0	0	0	0	0	0	0	0
12	0	0	0	0	0	0	0	0
13	0	0	0	0	0	0	0	0
14	0	0	0	0	0	0	0	0
15	0	0	0	0	0	0	0	0
16	0	0	0	0	0	0	0	0
17	0	0	0	0	0	0	0	0
18	0	0	0	0	0	0	0	0
19	0	0	0	0	0	0	0	0
20	0	0	0	0	0	0	0	0
21	0	0	0	0	0	0	0	0
22	0	0	0	0	0	0	0	0
23	0	0	0	0	0	0	0	0
24	0	0	0	0	0	0	0	0
25	0	0	0	0	0	0	0	0
26	0	0	0	0	0	0	0	0
27	0	0	0	0	0	0	0	0
28	0	0	0	0	0	0	0	0
29	37	88	37	37	98	92	0	0
30	44	101	60	60	98	95	0	0
31	88	147	60	60	98	95	0	0
32	105	194	60	60	98	95	0	0

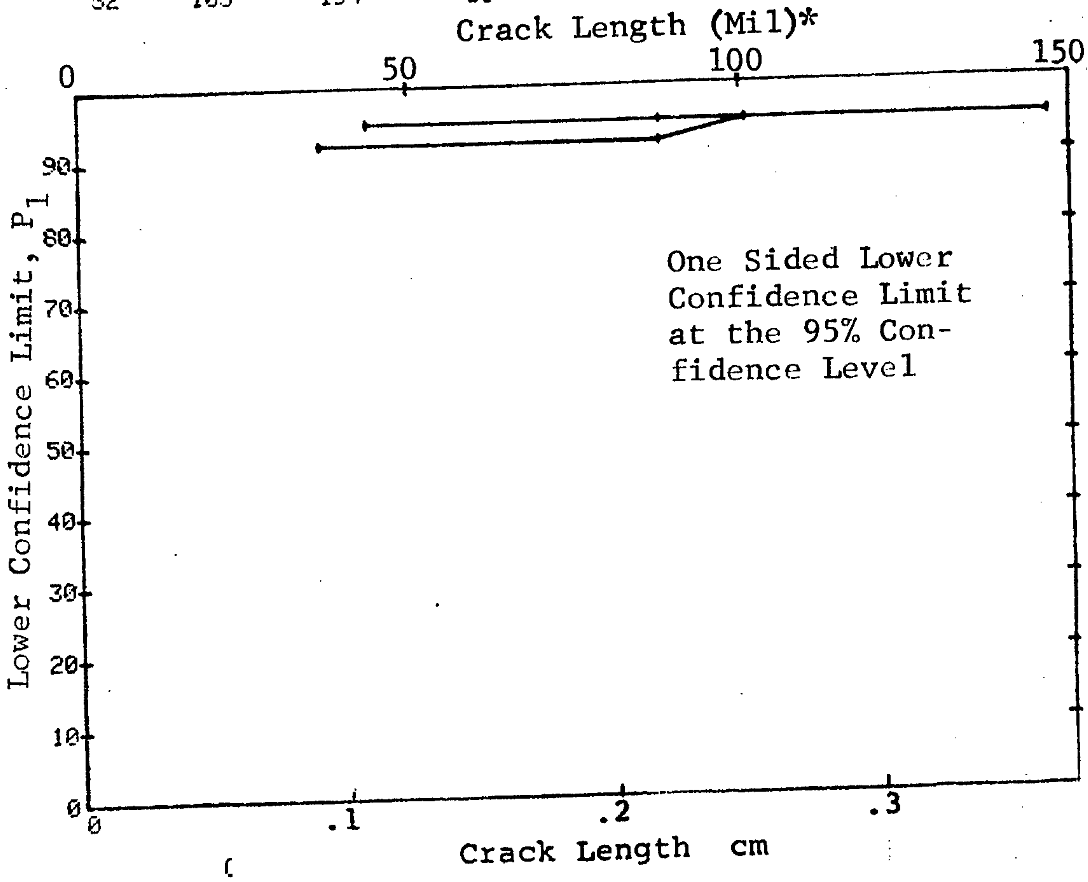

Figure D-40 (Concluded)

(a) Range Interval Method of Data Cumulation

09-OCT-75 PENETRANT TEST 1 (41)

RANGE	MIN LN	MAX LN	N	DET	50%	95%	0 MISS	1 MISS
1	44 *	44 *	10	10	93	74	0	0
2	0	0	0	0	0	0	0	0
3	0	0	0	0	0	0	0	0
4	0	0	0	0	0	0	0	0
5	0	0	0	0	0	0	0	0
6	0	0	0	0	0	0	0	0
7	0	0	0	0	0	0	0	0
8	0	0	0	0	0	0	0	0
9	0	0	0	0	0	0	0	0
10	0	0	0	0	0	0	0	0
11	0	0	0	0	0	0	0	0
12	0	0	0	0	0	0	0	0
13	0	0	0	0	0	0	0	0
14	0	0	0	0	0	0	0	0
15	0	0	0	0	0	0	0	0
16	0	0	0	0	0	0	0	0
17	0	0	0	0	0	0	0	0
18	0	0	0	0	0	0	0	0
19	0	0	0	0	0	0	0	0
20	0	0	0	0	0	0	0	0
21	0	0	0	0	0	0	0	0
22	0	0	0	0	0	0	0	0
23	0	0	0	0	0	0	0	0
24	0	0	0	0	0	0	0	0
25	0	0	0	0	0	0	0	0
26	0	0	0	0	0	0	0	0
27	0	0	0	0	0	0	0	0
28	0	0	0	0	0	0	0	0
29	0	0	0	0	0	0	0	0
30	0	0	0	0	0	0	0	0
31	0	0	0	0	0	0	0	0
32	51	68	21	21	96	86	8	25

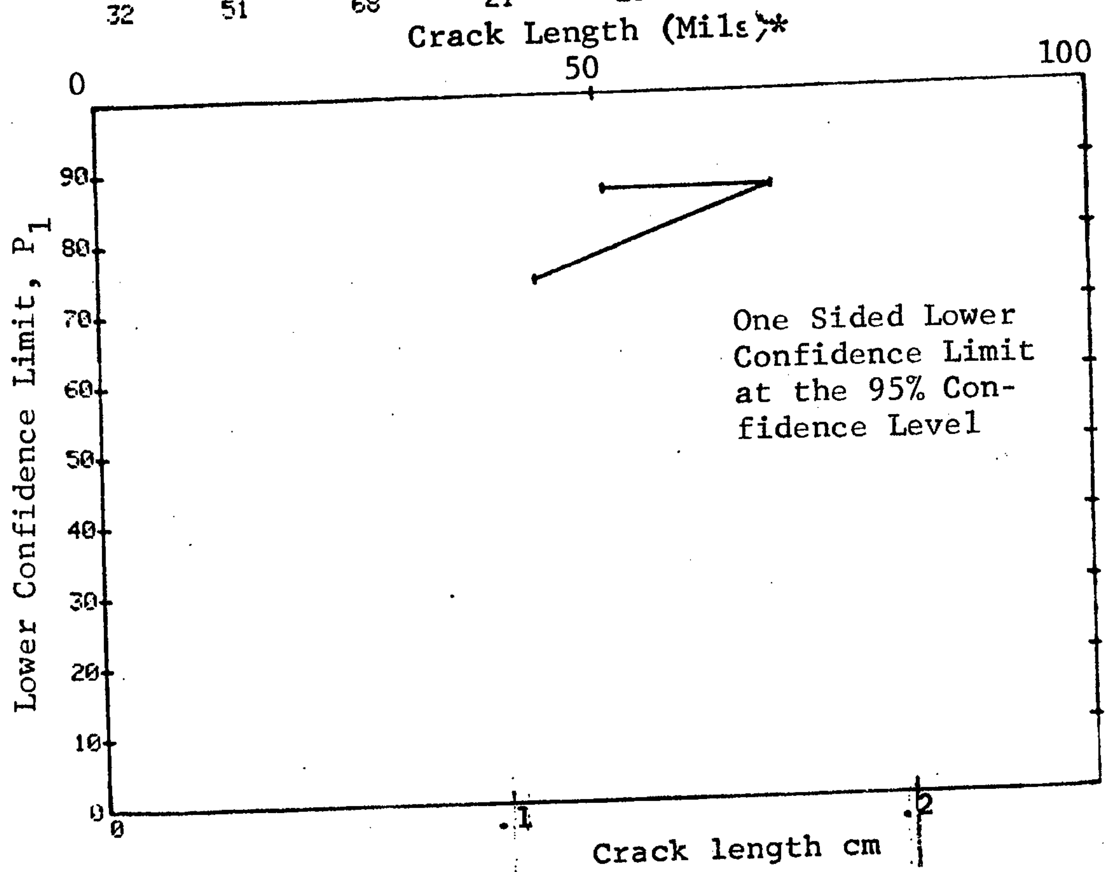

Figure D-41 Probability of Detection for 7075-T6511 Al Using Liquid Penetrant. Fatigue Cracks in Flat Plates. Prod. Env.

(b) Optimum Probability Method of Data Cumulation

09-OCT-75 PENETRANT TEST 2 (41)

RANGE	MIN LN	MAX LN	N	DET	50%	95%	0 MISS	1 MISS
1	44*	44*	10	10	0	74	0	0
2	0	0	0	0	0	0	0	0
3	0	0	0	0	0	0	0	0
4	0	0	0	0	0	0	0	0
5	0	0	0	0	0	0	0	0
6	0	0	0	0	0	0	0	0
7	0	0	0	0	0	0	0	0
8	0	0	0	0	0	0	0	0
9	0	0	0	0	0	0	0	0
10	0	0	0	0	0	0	0	0
11	0	0	0	0	0	0	0	0
12	0	0	0	0	0	0	0	0
13	0	0	0	0	0	0	0	0
14	0	0	0	0	0	0	0	0
15	0	0	0	0	0	0	0	0
16	0	0	0	0	0	0	0	0
17	0	0	0	0	0	0	0	0
18	0	0	0	0	0	0	0	0
19	0	0	0	0	0	0	0	0
20	0	0	0	0	0	0	0	0
21	0	0	0	0	0	0	0	0
22	0	0	0	0	0	0	0	0
23	0	0	0	0	0	0	0	0
24	0	0	0	0	0	0	0	0
25	0	0	0	0	0	0	0	0
26	0	0	0	0	0	0	0	0
27	0	0	0	0	0	0	0	0
28	0	0	0	0	0	0	0	0
29	0	0	0	0	0	0	0	0
30	0	0	0	0	0	0	0	0
31	0	0	0	0	0	0	0	0
32	44	68	31	31	0	90	0	15

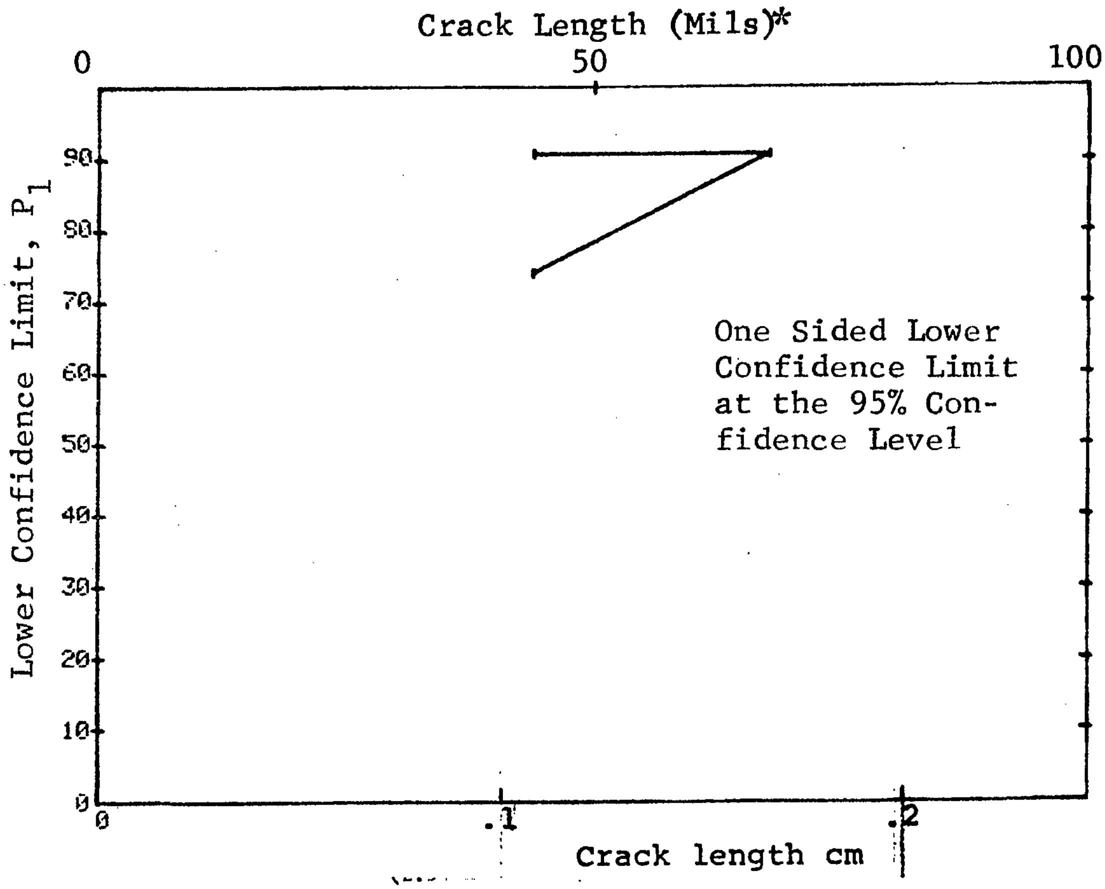

Figure D-41 (Continued)

(c) Overlapping Sixty Point Method of Data Cumulation

09-OCT-75 PENETRANT TEST 3 (41)

RANGE	MIN LN	MAX LN	N	DET	50%	95%	0 MISS	1 MISS
1	0*	0*	0	0	0	0	0	0
2	0	0	0	0	0	0	0	0
3	0	0	0	0	0	0	0	0
4	0	0	0	0	0	0	0	0
5	0	0	0	0	0	0	0	0
6	0	0	0	0	0	0	0	0
7	0	0	0	0	0	0	0	0
8	0	0	0	0	0	0	0	0
9	0	0	0	0	0	0	0	0
10	0	0	0	0	0	0	0	0
11	0	0	0	0	0	0	0	0
12	0	0	0	0	0	0	0	0
13	0	0	0	0	0	0	0	0
14	0	0	0	0	0	0	0	0
15	0	0	0	0	0	0	0	0
16	0	0	0	0	0	0	0	0
17	0	0	0	0	0	0	0	0
18	0	0	0	0	0	0	0	0
19	0	0	0	0	0	0	0	0
20	0	0	0	0	0	0	0	0
21	0	0	0	0	0	0	0	0
22	0	0	0	0	0	0	0	0
23	0	0	0	0	0	0	0	0
24	0	0	0	0	0	0	0	0
25	0	0	0	0	0	0	0	0
26	0	0	0	0	0	0	0	0
27	0	0	0	0	0	0	0	0
28	0	0	0	0	0	0	0	0
29	0	0	0	0	0	0	0	0
30	0	0	0	0	0	0	0	0
31	0	0	0	0	0	0	0	0
32	44	68	31	31	97	90	0	15

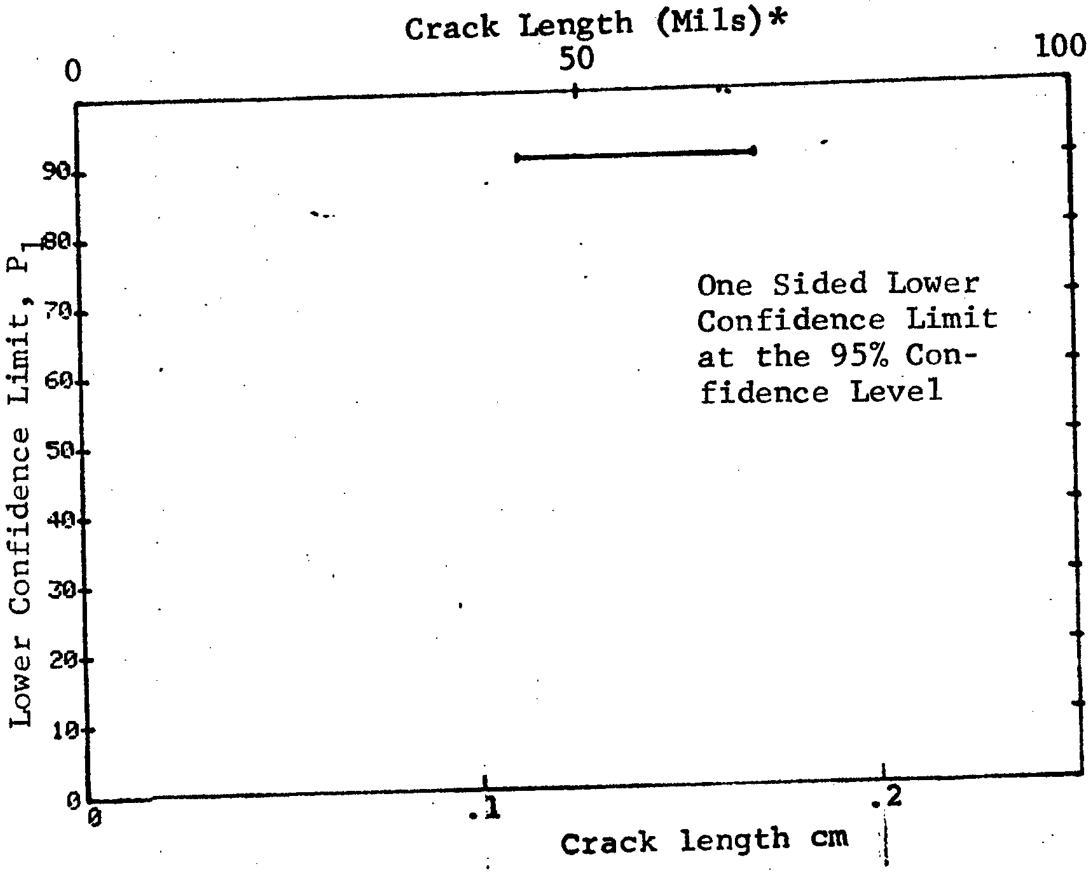

Figure D-41 (Concluded)

(a) Range Interval Method of Data Cumulation

09-OCT-75 PENETRANT TEST 1 (42)

RANGE	MIN LN	MAX LN	N	DET	50%	95%	0 MISS	1 MISS
1	44*	44*	10	10	93	74	0	0
2	0	0	0	0	0	0	0	0
3	0	0	0	0	0	0	0	0
4	0	0	0	0	0	0	0	0
5	0	0	0	0	0	0	0	0
6	0	0	0	0	0	0	0	0
7	0	0	0	0	0	0	0	0
8	0	0	0	0	0	0	0	0
9	0	0	0	0	0	0	0	0
10	0	0	0	0	0	0	0	0
11	0	0	0	0	0	0	0	0
12	0	0	0	0	0	0	0	0
13	0	0	0	0	0	0	0	0
14	0	0	0	0	0	0	0	0
15	0	0	0	0	0	0	0	0
16	0	0	0	0	0	0	0	0
17	0	0	0	0	0	0	0	0
18	0	0	0	0	0	0	0	0
19	0	0	0	0	0	0	0	0
20	0	0	0	0	0	0	0	0
21	0	0	0	0	0	0	0	0
22	0	0	0	0	0	0	0	0
23	0	0	0	0	0	0	0	0
24	0	0	0	0	0	0	0	0
25	0	0	0	0	0	0	0	0
26	0	0	0	0	0	0	0	0
27	0	0	0	0	0	0	0	0
28	0	0	0	0	0	0	0	0
29	0	0	0	0	0	0	0	0
30	0	0	0	0	0	0	0	0
31	0	0	0	0	0	0	0	0
32	51	68	21	21	96	86	8	25

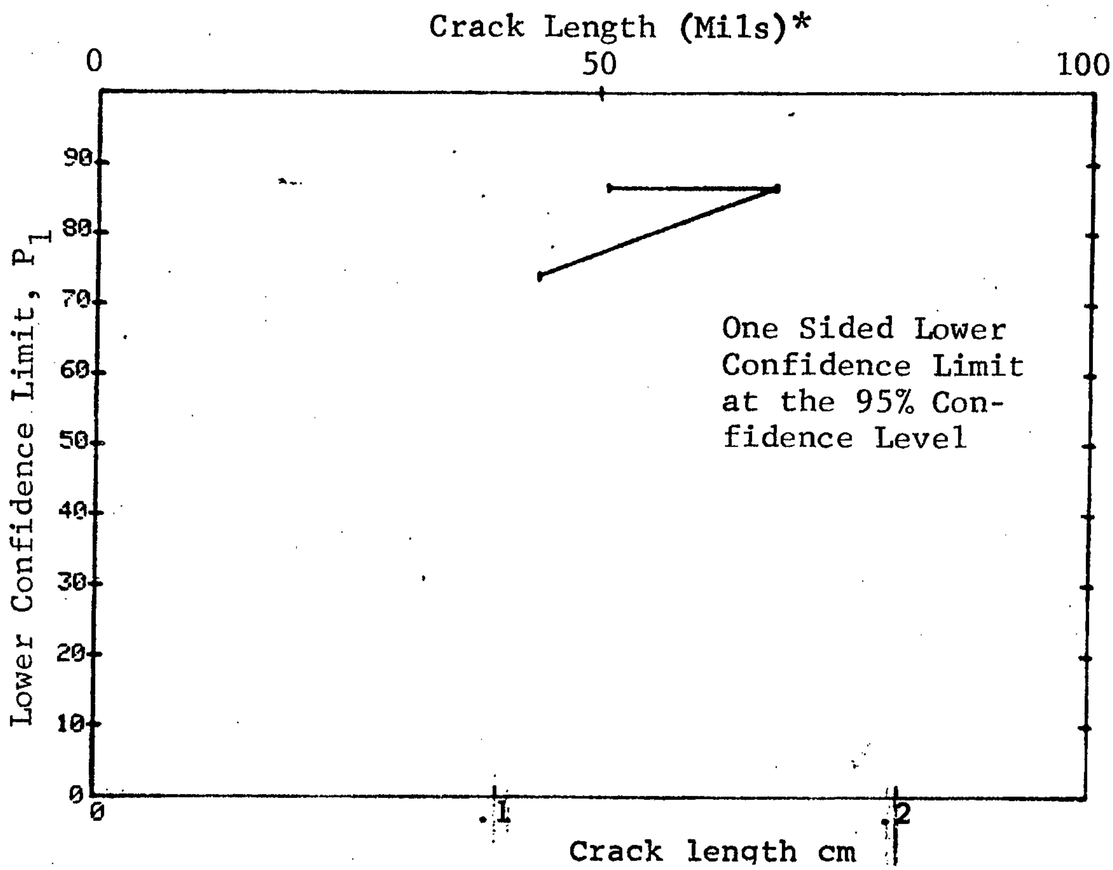

Figure D-42 Probability of Detection for 7075-T6511 Al Using Liquid Penetrant. Fatigue Cracks in Flat Plates.

Prod. Env.

(b) Optimum Probability Method of Data Cumulation

09-OCT-75 PENETRANT TEST 2 (42)

RANGE	MIN LN	MAX LN	N	DET	50%	95%	0 MISS	1 MISS
1	44*	44*	10	10	0	74	0	0
2	0	0	0	0	0	0	0	0
3	0	0	0	0	0	0	0	0
4	0	0	0	0	0	0	0	0
5	0	0	0	0	0	0	0	0
6	0	0	0	0	0	0	0	0
7	0	0	0	0	0	0	0	0
8	0	0	0	0	0	0	0	0
9	0	0	0	0	0	0	0	0
10	0	0	0	0	0	0	0	0
11	0	0	0	0	0	0	0	0
12	0	0	0	0	0	0	0	0
13	0	0	0	0	0	0	0	0
14	0	0	0	0	0	0	0	0
15	0	0	0	0	0	0	0	0
16	0	0	0	0	0	0	0	0
17	0	0	0	0	0	0	0	0
18	0	0	0	0	0	0	0	0
19	0	0	0	0	0	0	0	0
20	0	0	0	0	0	0	0	0
21	0	0	0	0	0	0	0	0
22	0	0	0	0	0	0	0	0
23	0	0	0	0	0	0	0	0
24	0	0	0	0	0	0	0	0
25	0	0	0	0	0	0	0	0
26	0	0	0	0	0	0	0	0
27	0	0	0	0	0	0	0	0
28	0	0	0	0	0	0	0	0
29	0	0	0	0	0	0	0	0
30	0	0	0	0	0	0	0	0
31	0	0	0	0	0	0	0	0
32	44	68	31	31	0	90	0	15

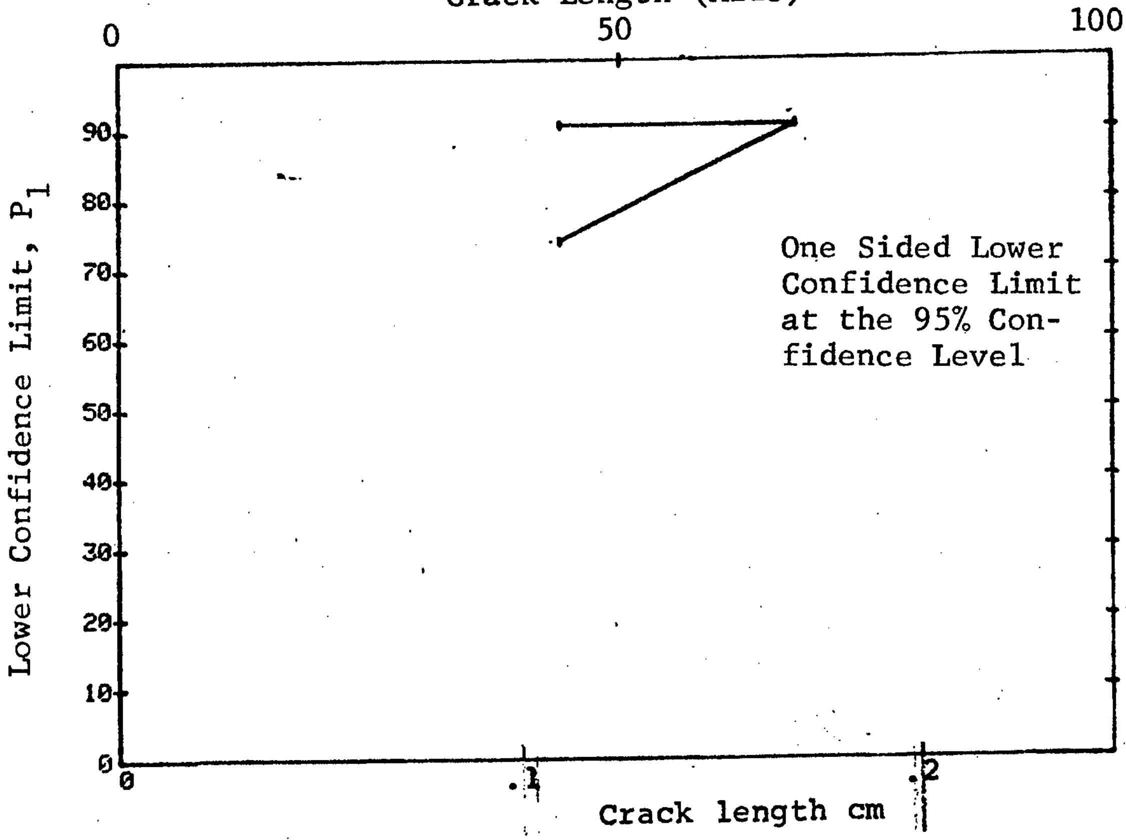

Figure D-42 (Continued)

(c) Overlapping Sixty Point Method of Data Cumulation

09-OCT-75 PENETRANT TEST 3 (42)

RANGE	MIN LN *	MAX LN *	N	DET	50%	95%	0 MISS	1 MISS
1	0	0	0	0	0	0	0	0
2	0	0	0	0	0	0	0	0
3	0	0	0	0	0	0	0	0
4	0	0	0	0	0	0	0	0
5	0	0	0	0	0	0	0	0
6	0	0	0	0	0	0	0	0
7	0	0	0	0	0	0	0	0
8	0	0	0	0	0	0	0	0
9	0	0	0	0	0	0	0	0
10	0	0	0	0	0	0	0	0
11	0	0	0	0	0	0	0	0
12	0	0	0	0	0	0	0	0
13	0	0	0	0	0	0	0	0
14	0	0	0	0	0	0	0	0
15	0	0	0	0	0	0	0	0
16	0	0	0	0	0	0	0	0
17	0	0	0	0	0	0	0	0
18	0	0	0	0	0	0	0	0
19	0	0	0	0	0	0	0	0
20	0	0	0	0	0	0	0	0
21	0	0	0	0	0	0	0	0
22	0	0	0	0	0	0	0	0
23	0	0	0	0	0	0	0	0
24	0	0	0	0	0	0	0	0
25	0	0	0	0	0	0	0	0
26	0	0	0	0	0	0	0	0
27	0	0	0	0	0	0	0	0
28	0	0	0	0	0	0	0	0
29	0	0	0	0	0	0	0	0
30	0	0	0	0	0	0	0	0
31	0	0	0	0	0	0	0	0
32	44	68	31	31	97	90	0	15

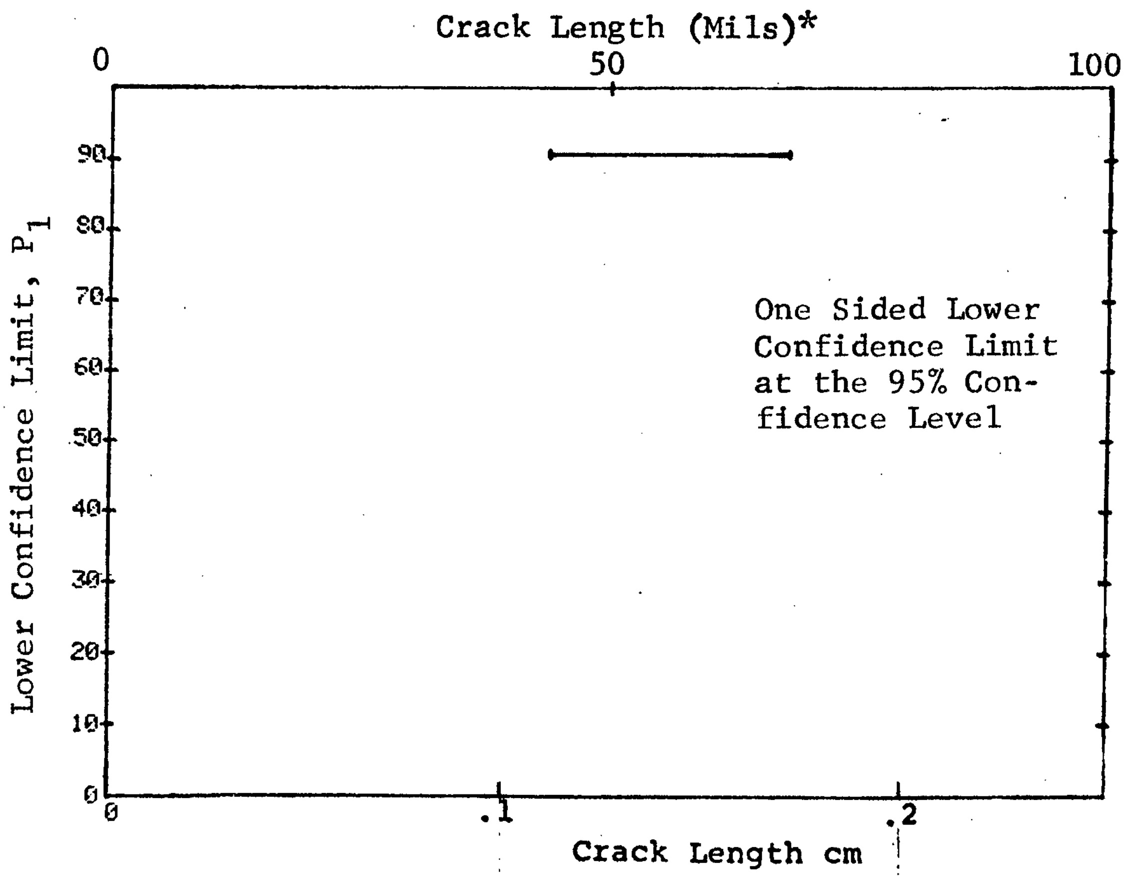

Figure D-42 (Concluded)

(a) Range Interval Method of Data Cumulation

09-OCT-75 RANGE	PENETRANT MIN LN *	MAX LN *	N	TEST 1 DET	50%	(43) 95%	0 MISS	1 MISS
1	19	19	3	0	0	0	0	0
2	0	0	0	0	0	0	0	0
3	0	0	0	0	0	0	0	0
4	0	0	0	0	0	0	0	0
5	0	0	0	0	0	0	0	0
6	0	0	0	0	0	0	0	0
7	0	0	0	0	0	0	0	0
8	0	0	0	0	0	0	0	0
9	0	0	0	0	0	0	0	0
10	0	0	0	0	0	0	0	0
11	0	0	0	0	0	0	0	0
12	0	0	0	0	0	0	0	0
13	0	0	0	0	0	0	0	0
14	0	0	0	0	0	0	0	0
15	0	0	0	0	0	0	0	0
16	0	0	0	0	0	0	0	0
17	0	0	0	0	0	0	0	0
18	0	0	0	0	0	0	0	0
19	0	0	0	0	0	0	0	0
20	39	39	5	5	87	54	0	0
21	0	0	0	0	0	0	0	0
22	0	0	0	0	0	0	0	0
23	0	0	0	0	0	0	0	0
24	0	0	0	0	0	0	0	0
25	0	0	0	0	0	0	0	0
26	0	0	0	0	0	0	0	0
27	0	0	0	0	0	0	0	0
28	0	0	0	0	0	0	[illegible]	[illegible]
29	0	0	0	0	0	[illegible]	[illegible]	[illegible]
30	49	49	7	7	90	65	0	0
31	0	0	0	0	0	0	0	0
32	60	80	24	24	97	88	5	[illegible]

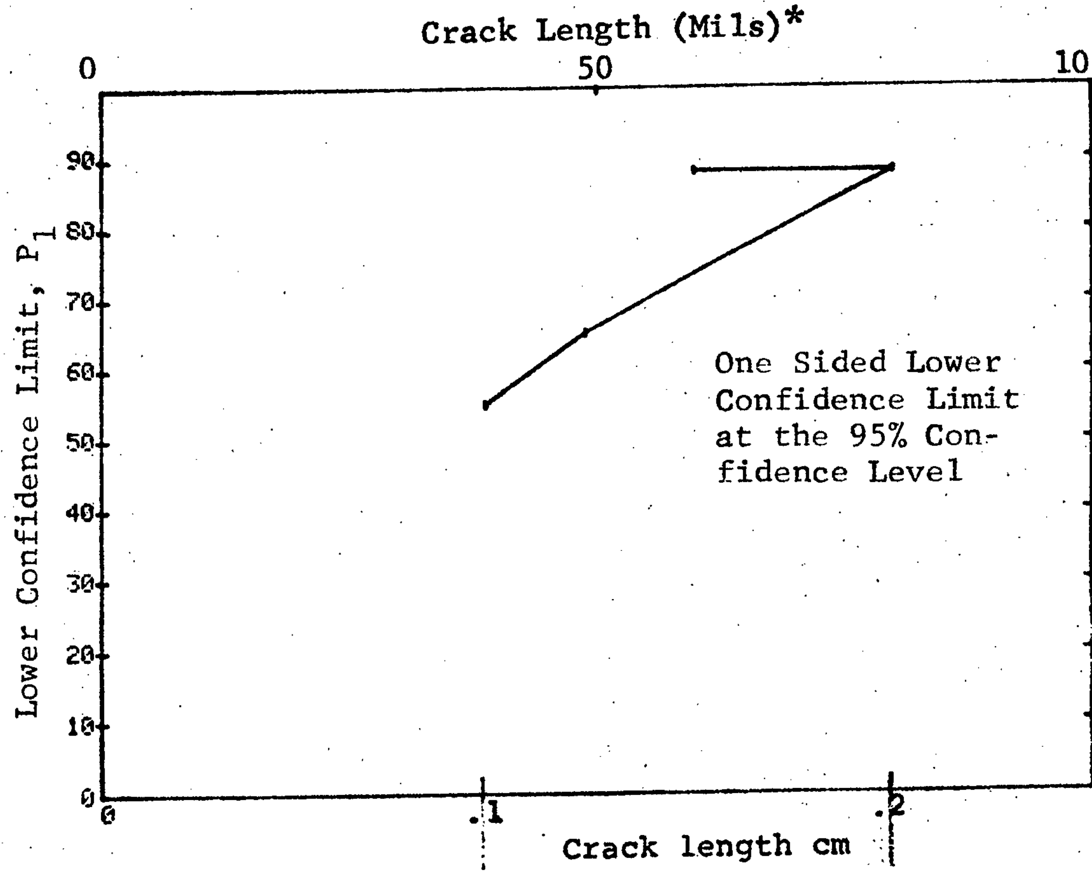

Figure D-43 Probability of Detection for PH13-8 Mo. St. Using Liquid Penetrant. Fatigue Cracks in Flat Plates. Prod. Env.

(b) Optimum Probability Method of Data Cumulation

09-OCT-75 PENETRANT

RANGE	MIN LN	MAX LN	N	TEST DET	50%	(43) 95%	0 MISS	1 MISS
1	19 *	19 *	3	0	0	0	0	0
2	0	0	0	0	0	0	0	0
3	0	0	0	0	0	0	0	0
4	0	0	0	0	0	0	0	0
5	0	0	0	0	0	0	0	0
6	0	0	0	0	0	0	0	0
7	0	0	0	0	0	0	0	0
8	0	0	0	0	0	0	0	0
9	0	0	0	0	0	0	0	0
10	0	0	0	0	0	0	0	0
11	0	0	0	0	0	0	0	0
12	0	0	0	0	0	0	0	0
13	0	0	0	0	0	0	0	0
14	0	0	0	0	0	0	0	0
15	0	0	0	0	0	0	0	0
16	0	0	0	0	0	0	0	0
17	0	0	0	0	0	0	0	0
18	0	0	0	0	0	0	0	0
19	0	0	0	0	0	0	0	0
20	39	39	5	5	0	54	0	0
21	0	0	0	0	0	0	0	0
22	0	0	0	0	0	0	0	0
23	0	0	0	0	0	0	0	0
24	0	0	0	0	0	0	0	0
25	0	0	0	0	0	0	0	0
26	0	0	0	0	0	0	0	0
27	0	0	0	0	0	0	0	0
28	0	0	0	0	0	0	0	0
29	0	0	0	0	0	0	0	0
30	39	49	12	12	0	77	0	0
31	0	0	0	0	0	0	0	0
32	39	80	36	36	0	92	0	10

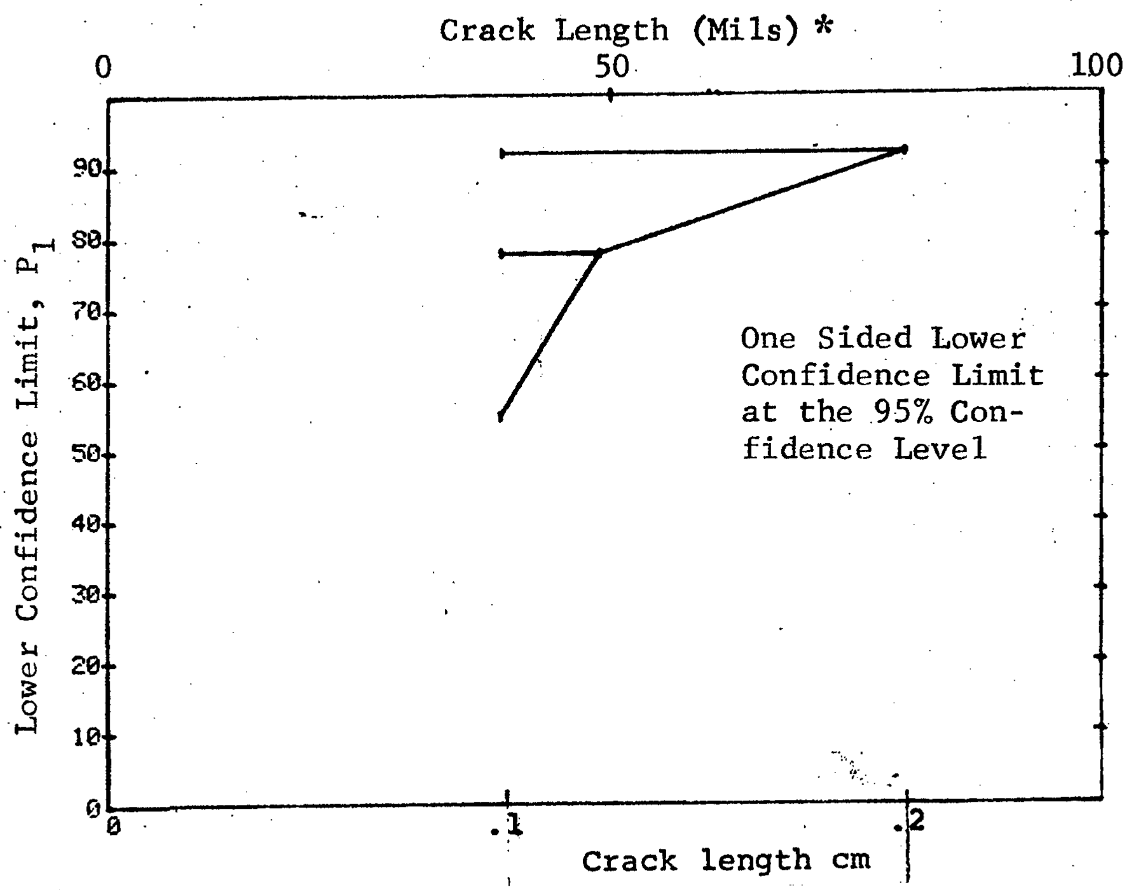

Figure D-43 (Continued)

(c) Overlapping Sixty Point Method of Data Cumulation

09-OCT-75	PENETRANT			TEST 3			(43)	
RANGE	MIN LN	MAX LN	N	DET	50%	95%	0 MISS	1 MISS
1	0 *	0 *	0	0	0	0	0	0
2	0	0	0	0	0	0	0	0
3	0	0	0	0	0	0	0	0
4	0	0	0	0	0	0	0	0
5	0	0	0	0	0	0	0	0
6	0	0	0	0	0	0	0	0
7	0	0	0	0	0	0	0	0
8	0	0	0	0	0	0	0	0
9	0	0	0	0	0	0	0	0
10	0	0	0	0	0	0	0	0
11	0	0	0	0	0	0	0	0
12	0	0	0	0	0	0	0	0
13	0	0	0	0	0	0	0	0
14	0	0	0	0	0	0	0	0
15	0	0	0	0	0	0	0	0
16	0	0	0	0	0	0	0	0
17	0	0	0	0	0	0	0	0
18	0	0	0	0	0	0	0	0
19	0	0	0	0	0	0	0	0
20	0	0	0	0	0	0	0	0
21	0	0	0	0	0	0	0	0
22	0	0	0	0	0	0	0	0
23	0	0	0	0	0	0	0	0
24	0	0	0	0	0	0	0	0
25	0	0	0	0	0	0	0	0
26	0	0	0	0	0	0	0	0
27	0	0	0	0	0	0	0	0
28	0	0	0	0	0	0	0	0
29	0	0	0	0	0	0	0	0
30	0	0	0	0	0	0	0	0
31	0	0	0	0	0	0	0	0
32	19	80	39	36	90	81	37	50

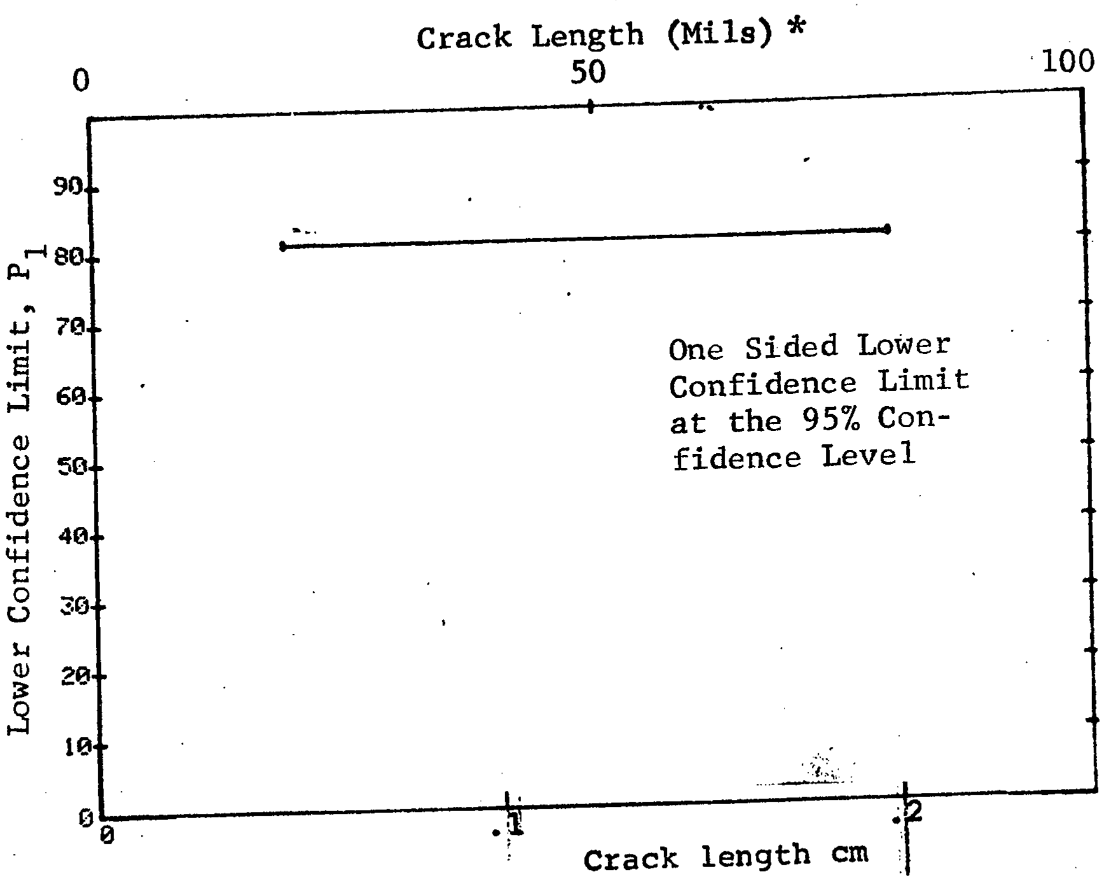

Figure D-43 (Concluded)

(a) Range Interval Method of Data Cumulation

09-OCT-75 ULTRASONIC TEST 1 (44)

RANGE	MIN LN	* MAX LN *	N	DET	50%	95%	0 MISS	1 MISS
1	48	52	29	28	94	84	17	32
2	0	0	0	0	0	0	0	0
3	60	62	16	16	95	82	13	30
4	68	68	9	9	92	71	0	0
5	0	0	0	0	0	0	0	0
6	75	75	6	6	89	60	0	0
7	0	0	0	0	0	0	0	0
8	0	0	0	0	0	0	0	0
9	90	90	11	11	93	76	18	35
10	95	98	20	20	96	86	9	26
11	102	102	4	4	84	47	0	0
12	0	0	0	0	0	0	0	0
13	110	110	7	7	90	65	0	0
14	0	0	0	0	0	0	0	0
15	0	0	0	0	0	0	0	0
16	0	0	0	0	0	0	0	0
17	0	0	0	0	0	0	0	0
18	0	0	0	0	0	0	0	0
19	142	142	5	5	87	54	0	0
20	145	148	7	7	90	65	0	0
21	0	0	0	0	0	0	0	0
22	155	158	8	8	91	68	0	0
23	160	160	4	4	84	47	0	0
24	165	165	4	4	84	47	0	0
25	0	0	0	0	0	0	0	0
26	0	0	0	0	0	0	0	0
27	0	0	0	0	0	0	0	0
28	0	0	0	0	0	0	0	0
29	0	0	0	0	0	0	0	0
30	195	195	3	3	79	36	0	0
31	0	0	0	0	0	0	0	0
32	218	218	4	4	84	47	0	0

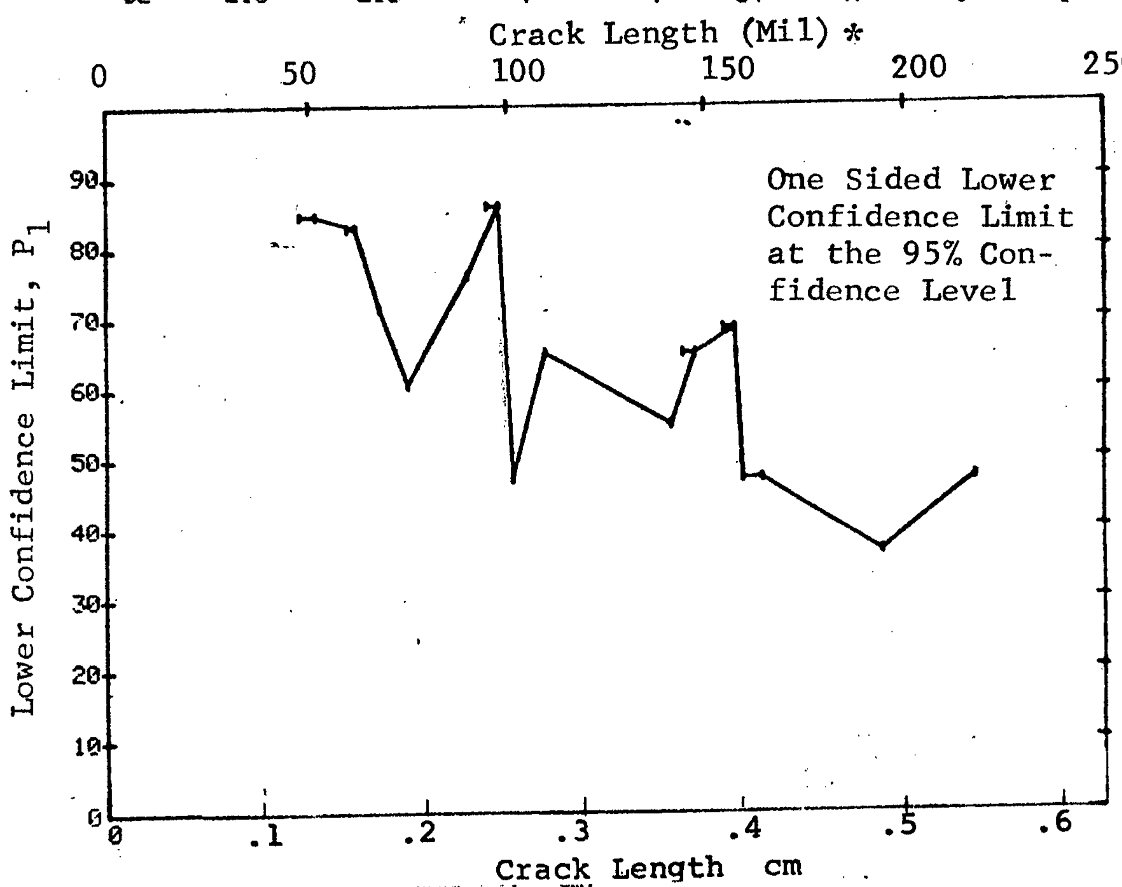

Figure D-44 Probability of Detection for Ti-6Al-4V Using Ultrasonic Shear Wave. Fatigue Cracks in Welded Flat Corroded Plates. Prod. Env.

(b) Optimum Probability Method of Data Cumulation

09-OCT-75 ULTRASONIC TEST 2 (44)

RANGE	MIN LN	MAX LN	N	DET	50%	95%	0 MISS	1 MISS
1	48 *	52 *	29	28	0	84	17	32
2	0	0	0	0	0	0	0	0
3	48	62	45	44	0	89	1	16
4	48	68	54	53	0	91	0	7
5	0	0	0	0	0	0	0	0
6	48	75	60	59	0	92	0	1
7	0	0	0	0	0	0	0	0
8	0	0	0	0	0	0	0	0
9	48	90	71	70	0	93	0	0
10	60	98	62	62	0	95	0	0
11	60	102	66	66	0	95	0	0
12	0	0	0	0	0	0	0	0
13	60	110	73	73	0	95	0	0
14	0	0	0	0	0	0	0	0
15	0	0	0	0	0	0	0	0
16	0	0	0	0	0	0	0	0
17	0	0	0	0	0	0	0	0
18	0	0	0	0	0	0	0	0
19	60	142	78	78	0	96	0	0
20	60	148	85	85	0	96	0	0
21	0	0	0	0	0	0	0	0
22	60	158	93	93	0	96	0	0
23	60	160	97	97	0	96	0	0
24	60	165	101	101	0	97	0	0
25	0	0	0	0	0	0	0	0
26	0	0	0	0	0	0	0	0
27	0	0	0	0	0	0	0	0
28	0	0	0	0	0	0	0	0
29	0	0	0	0	0	0	0	0
30	60	195	104	104	0	97	0	0
31	0	0	0	0	0	0	0	0
32	60	218	108	108	0	97	0	0

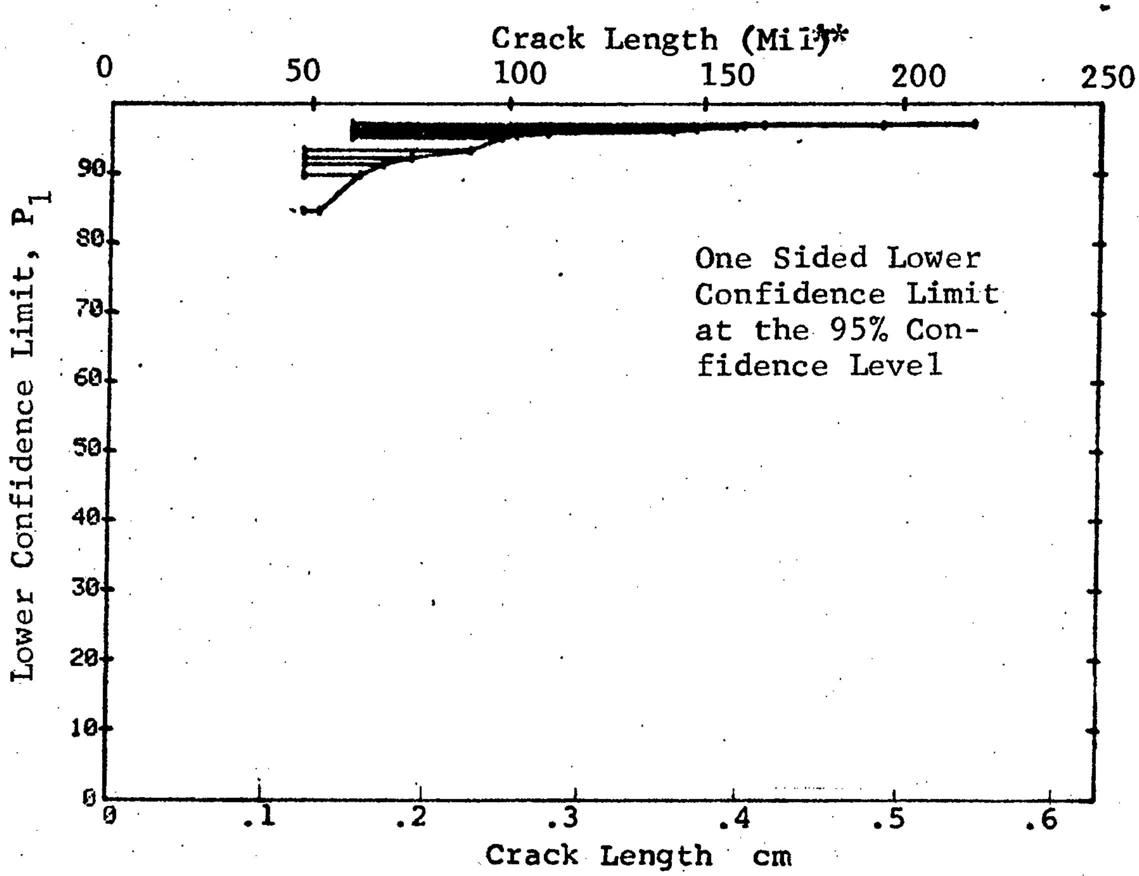

Figure D-44 (Continued)

(c) Overlapping Sixty Point Method of Data Cumulation

09-OCT-75 ULTRASONIC TEST 3 (44)

RANGE	MIN LN	MAX LN	N	DET	50%	95%	0 MISS	1 MISS
1	0*	0*	0	0	0	0	0	0
2	0	0	0	0	0	0	0	0
3	0	0	0	0	0	0	0	0
4	0	0	0	0	0	0	0	0
5	0	0	0	0	0	0	0	0
6	0	0	0	0	0	0	0	0
7	0	0	0	0	0	0	0	0
8	0	0	0	0	0	0	0	0
9	0	0	0	0	0	0	0	0
10	0	0	0	0	0	0	0	0
11	0	0	0	0	0	0	0	0
12	0	0	0	0	0	0	0	0
13	0	0	0	0	0	0	0	0
14	0	0	0	0	0	0	0	0
15	0	0	0	0	0	0	0	0
16	0	0	0	0	0	0	0	0
17	0	0	0	0	0	0	0	0
18	0	0	0	0	0	0	0	0
19	0	0	0	0	0	0	0	0
20	0	0	0	0	0	0	0	0
21	0	0	0	0	0	0	0	0
22	0	0	0	0	0	0	0	0
23	0	0	0	0	0	0	0	0
24	0	0	0	0	0	0	0	0
25	0	0	0	0	0	0	0	0
26	0	0	0	0	0	0	0	0
27	0	0	0	0	0	0	0	0
28	0	0	0	0	0	0	0	0
29	48	68	47	46	96	90	0	14
30	50	95	60	60	98	95	0	0
31	68	142	60	60	98	95	0	0
32	95	218	60	60	98	95	0	0

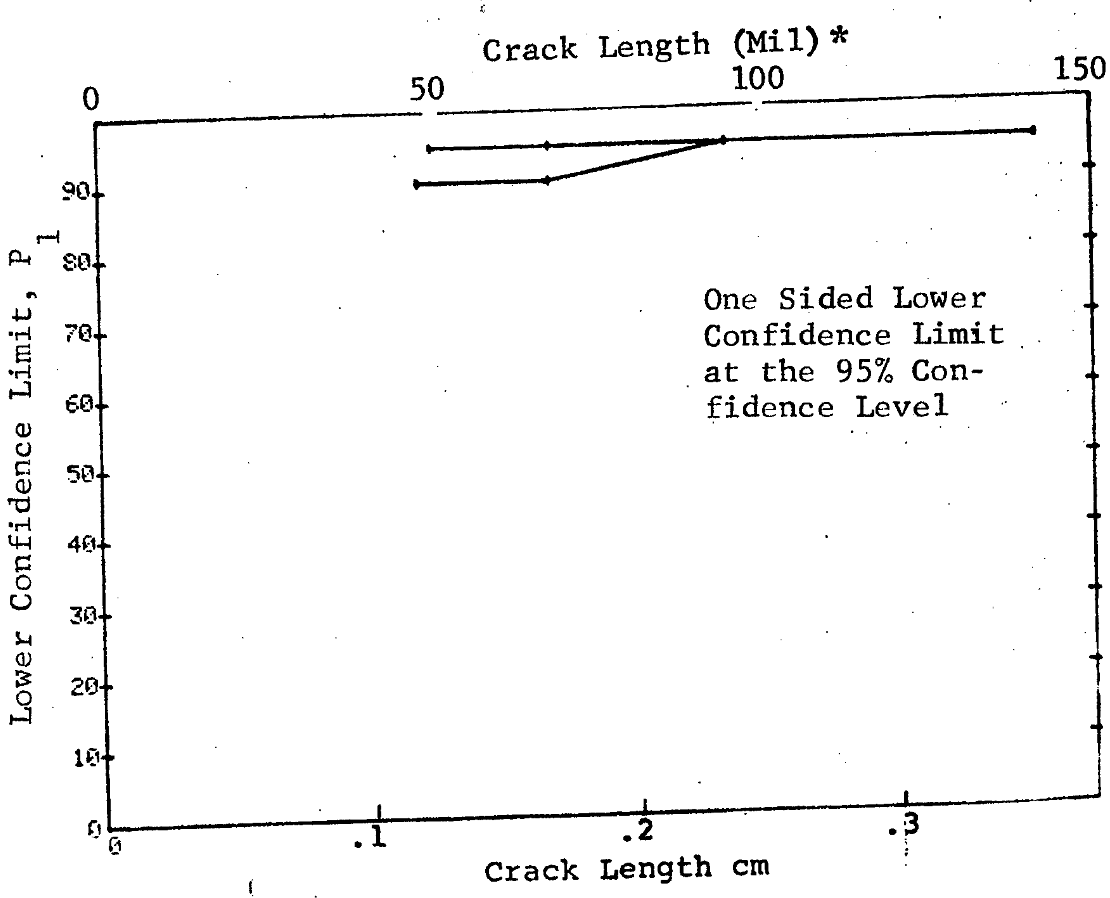

Figure D-44 (Concluded)

(a) Range Interval Method of Data Cumulation

09-OCT-75	ULTRASONIC			TEST 1			(45)	
RANGE	MIN LN	MAX LN	N	DET	50%	95%	0 MISS	1 MISS
1	58 *	62 *	11	4	32	13	0	0
2	64	67	8	9	91	68	0	0
3	72	72	5	5	87	54	0	0
4	76	76	9	9	92	71	0	0
5	83	83	13	13	94	79	16	33
6	86	86	10	10	93	74	0	0
7	90	91	14	11	74	53	0	0
8	95	97	15	15	95	81	14	31
9	99	99	14	14	95	80	15	32
10	106	108	8	8	91	68	0	0
11	109	113	11	11	93	76	18	35
12	117	118	8	8	91	68	0	0
13	119	119	3	3	79	36	0	0
14	126	126	4	4	84	47	0	0
15	0	0	0	0	0	0	0	0
16	0	0	0	0	0	0	0	0
17	0	0	0	0	0	0	0	0
18	0	0	0	0	0	0	0	0
19	0	0	0	0	0	0	0	0
20	0	0	0	0	0	0	0	0
21	161	161	4	4	84	47	0	0
22	0	0	0	0	0	0	0	0
23	0	0	0	0	0	0	0	0
24	0	0	0	0	0	0	0	0
25	0	0	0	0	0	0	0	0
26	184	184	5	5	87	54	0	0
27	0	0	0	0	0	0	0	0
28	0	0	0	0	0	0	0	0
29	199	201	11	11	93	76	[illegible]	[illegible]
30	204	204	4	4	84	47	0	0
31	0	0	0	0	0	0	0	0
32	216	216	6	6	89	60	0	0

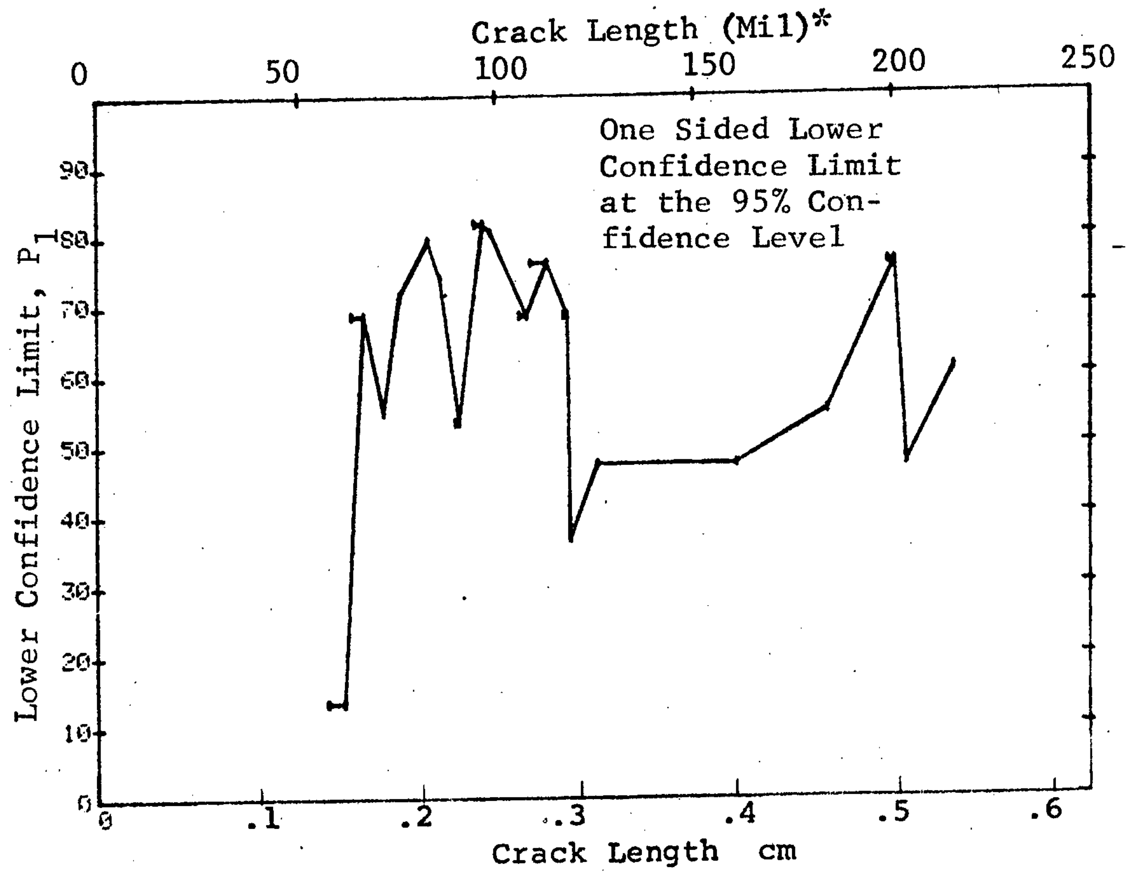

Figure D-45 Probability of Detection for 4330V Steel Using Ultrasonic Shear Wave. Simulated Weld Flaws Prod. Env.

(b) Optimum Probability Method of Data Cumulation

09-OCT-75 ULTRASONIC TEST 2

RANGE	MIN LN	* MAX LN *	N	DET	50%	95%	(45) 0 MISS	1 MISS
1	58	62	11	4	0	13	0	0
2	64	67	8	8	0	68	0	0
3	64	72	13	13	0	79	0	0
4	64	76	22	22	0	87	7	24
5	64	83	35	35	0	91	0	11
6	64	86	45	45	0	93	0	1
7	64	91	59	56	0	87	17	30
8	64	97	74	71	0	89	2	15
9	64	99	88	85	0	91	0	1
10	95	108	37	37	0	92	0	3
11	95	113	48	48	0	93	0	0
12	95	118	56	56	0	94	0	0
13	95	119	59	59	0	95	0	0
14	95	126	63	63	0	95	0	0
15	0	0	0	0	0	0	0	0
16	0	0	0	0	0	0	0	0
17	0	0	0	0	0	0	0	0
18	0	0	0	0	0	0	0	0
19	0	0	0	0	0	0	0	0
20	0	0	0	0	0	0	0	0
21	95	161	67	67	0	95	0	0
22	0	0	0	0	0	0	0	0
23	0	0	0	0	0	0	0	0
24	0	0	0	0	0	0	0	0
25	0	0	0	0	0	0	0	0
26	95	184	72	72	0	95	0	0
27	0	0	0	0	0	0	0	0
28	0	0	0	0	0	0	0	0
29	95	201	83	83	0	96	0	0
30	95	204	87	87	0	96	0	0
31	0	0	0	0	0	0	0	0
32	95	216	93	93	0	96	0	0

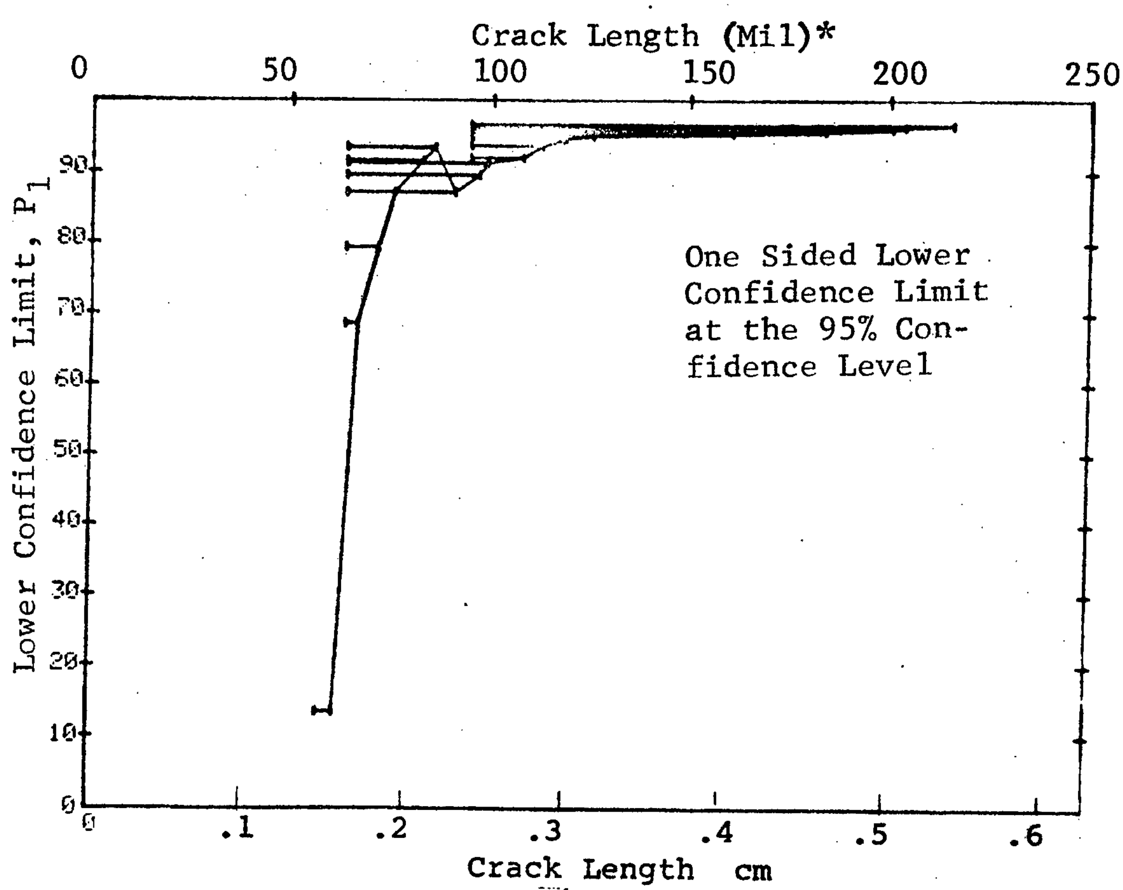

Figure D-45 (Continued)

(c) Overlapping Sixty Point Method of Data Cumulation

09-OCT-75 ULTRASONIC TEST 3 (45)

RANGE	MIN LN *	MAX LN *	N	DET	50%	95%	0 MISS	1 MISS
1	0	0	0	0	0	0	0	0
2	0	0	0	0	0	0	0	0
3	0	0	0	0	0	0	0	0
4	0	0	0	0	0	0	0	0
5	0	0	0	0	0	0	0	0
6	0	0	0	0	0	0	0	0
7	0	0	0	0	0	0	0	0
8	0	0	0	0	0	0	0	0
9	0	0	0	0	0	0	0	0
10	0	0	0	0	0	0	0	0
11	0	0	0	0	0	0	0	0
12	0	0	0	0	0	0	0	0
13	0	0	0	0	0	0	0	0
14	0	0	0	0	0	0	0	0
15	0	0	0	0	0	0	0	0
16	0	0	0	0	0	0	0	0
17	0	0	0	0	0	0	0	0
18	0	0	0	0	0	0	0	0
19	0	0	0	0	0	0	0	0
20	0	0	0	0	0	0	0	0
21	0	0	0	0	0	0	0	0
22	0	0	0	0	0	0	0	0
23	0	0	0	0	0	0	0	0
24	0	0	0	0	0	0	0	0
25	0	0	0	0	0	0	0	0
26	0	0	0	0	0	0	0	0
27	0	0	0	0	0	0	0	0
28	58	83	43	36	82	71	0	0
29	64	95	60	57	93	87	15	29
30	83	106	60	57	93	87	15	29
31	95	126	60	60	98	95	0	0
32	108	216	60	60	98	95	0	0

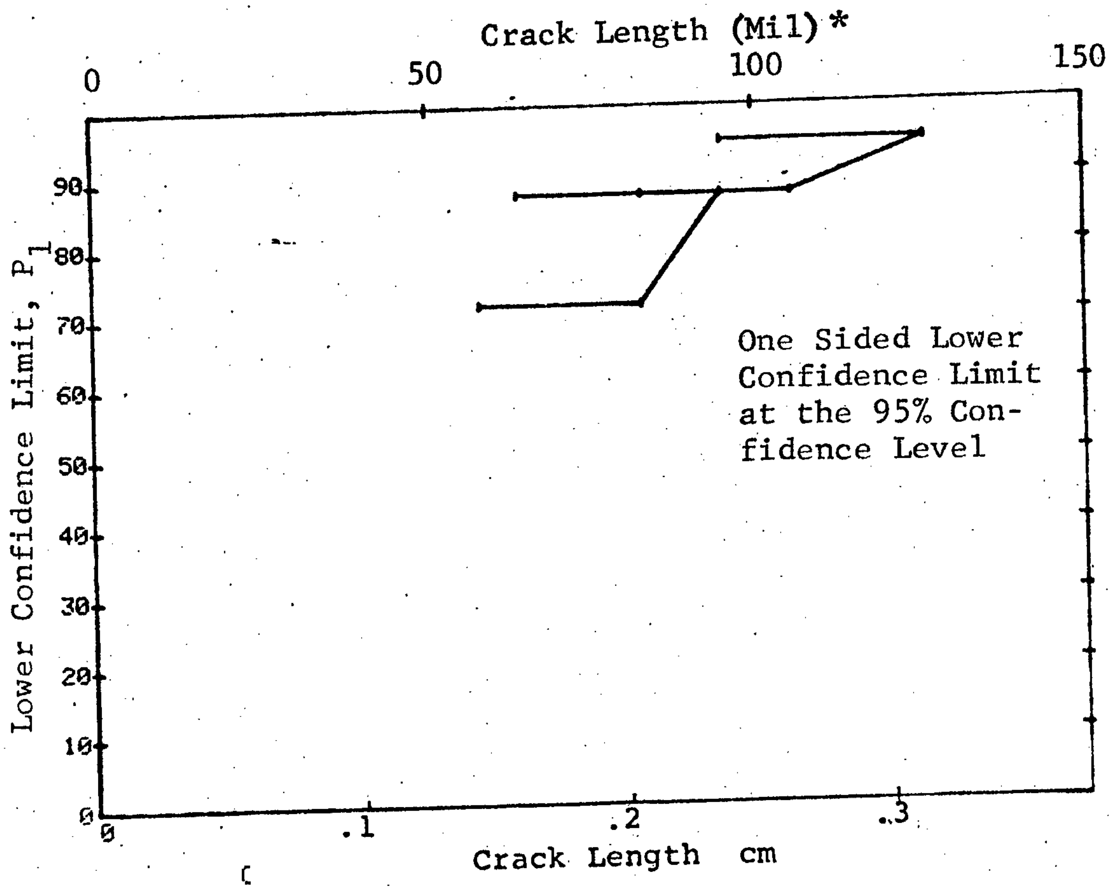

Figure D-45 Concluded)

(a) Range Interval Method of Data Cumulation

09-OCT-75		ULTRASONIC		TEST 1			(46)	
RANGE	MIN LN	MAX LN	N	DET	50%	95%	0 MISS	1 MISS
1	58 *	58 *	4	4	84	47	0	0
2	64	65	8	8	91	68	0	0
3	72	72	5	5	87	54	0	0
4	76	76	4	4	84	47	0	0
5	83	83	4	4	84	47	0	0
6	86	86	4	4	84	47	0	0
7	91	91	3	3	79	36	0	0
8	95	98	12	12	94	77	17	34
9	99	99	4	4	84	47	0	0
10	106	108	8	8	91	68	0	0
11	109	113	11	11	93	76	18	35
12	117	118	8	8	91	68	0	0
13	0	0	0	0	0	0	0	0
14	126	126	4	4	84	47	0	0
15	0	0	0	0	0	0	0	0
16	0	0	0	0	0	0	0	0
17	0	0	0	0	0	0	0	0
18	0	0	0	0	0	0	0	0
19	0	0	0	0	0	0	0	0
20	0	0	0	0	0	0	0	0
21	161	161	3	3	79	36	0	0
22	0	0	0	0	0	0	0	0
23	0	0	0	0	0	0	0	0
24	0	0	0	0	0	0	0	0
25	0	0	0	0	0	0	0	0
26	184	184	4	4	84	47	0	0
27	0	0	0	0	0	0	0	0
28	0	0	0	0	0	0	0	0
29	199	201	8	8	91	68	0	0
30	204	204	3	3	79	36	0	0
31	0	0	0	0	0	0	0	0
32	215	215	4	4	84	47	0	0

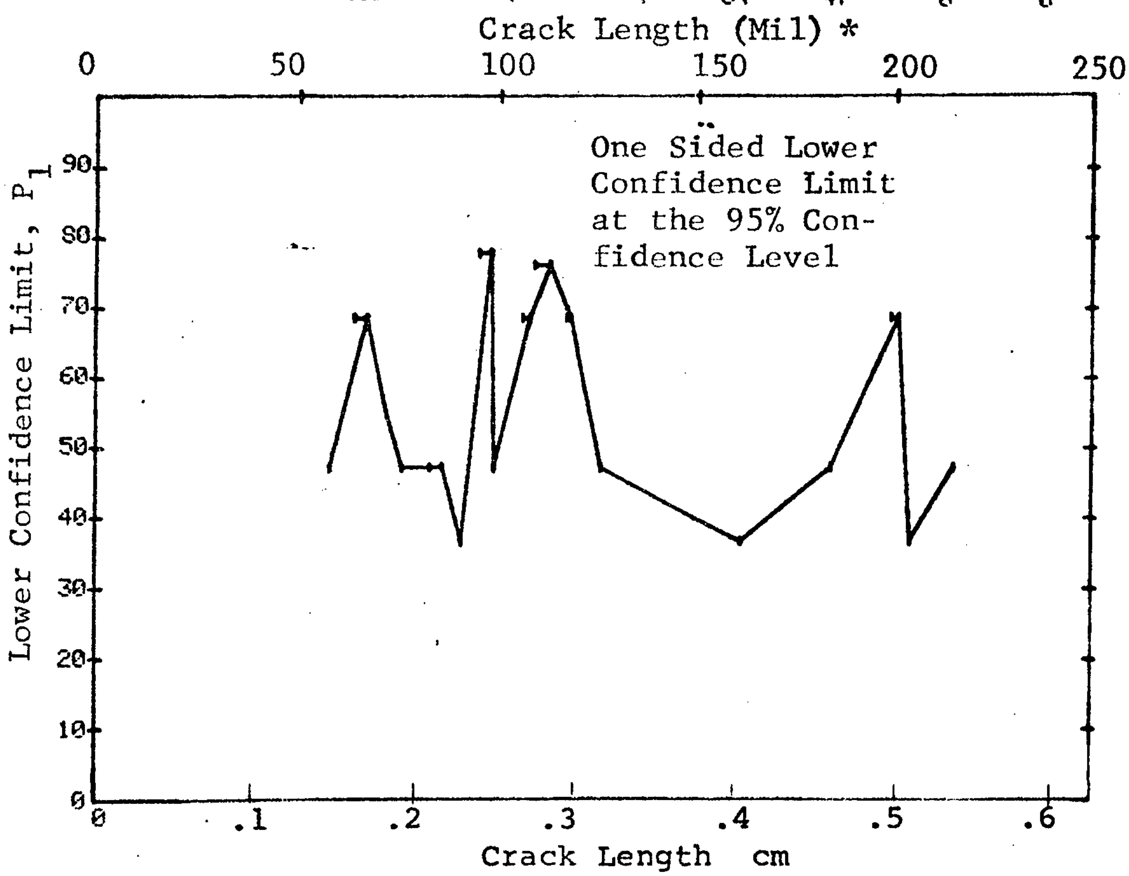

Figure D-46 Probability of Detection for PH17-4 Steel Using Ultrasonic Shear Wave. Simulated Flaws in Wrought Steel. Prod. Env.

(b) Optimum Probability Method of Data Cumulation

09-OCT-75 ULTRASONIC TEST 2 (46)

RANGE	MIN LN	MAX LN	N	DET	50%	95%	0 MISS	1 MISS
1	58*	58 *	4	4	0	47	0	0
2	58	67	12	12	0	77	0	0
3	58	72	17	17	0	83	12	29
4	58	76	21	21	0	86	8	25
5	58	83	25	25	0	88	4	21
6	58	86	29	29	0	90	0	17
7	58	91	32	32	0	91	0	14
8	58	98	44	44	0	93	0	2
9	58	99	48	48	0	93	0	0
10	58	108	56	56	0	94	0	0
11	58	113	67	67	0	95	0	0
12	58	118	75	75	0	96	0	0
13	0	0	0	0	0	0	0	0
14	58	126	79	79	0	96	0	0
15	0	0	0	0	0	0	0	0
16	0	0	0	0	0	0	0	0
17	0	0	0	0	0	0	0	0
18	0	0	0	0	0	0	0	0
19	0	0	0	0	0	0	0	0
20	0	0	0	0	0	0	0	0
21	58	161	82	82	0	96	0	0
22	0	0	0	0	0	0	0	0
23	0	0	0	0	0	0	0	0
24	0	0	0	0	0	0	0	0
25	0	0	0	0	0	0	0	0
26	58	184	86	86	0	96	0	0
27	0	0	0	0	0	0	0	0
28	0	0	0	0	0	0	0	0
29	58	201	94	94	0	96	0	0
30	58	204	97	97	0	96	0	0
31	0	0	0	0	0	0	0	0
32	58	215	101	101	0	97	0	0

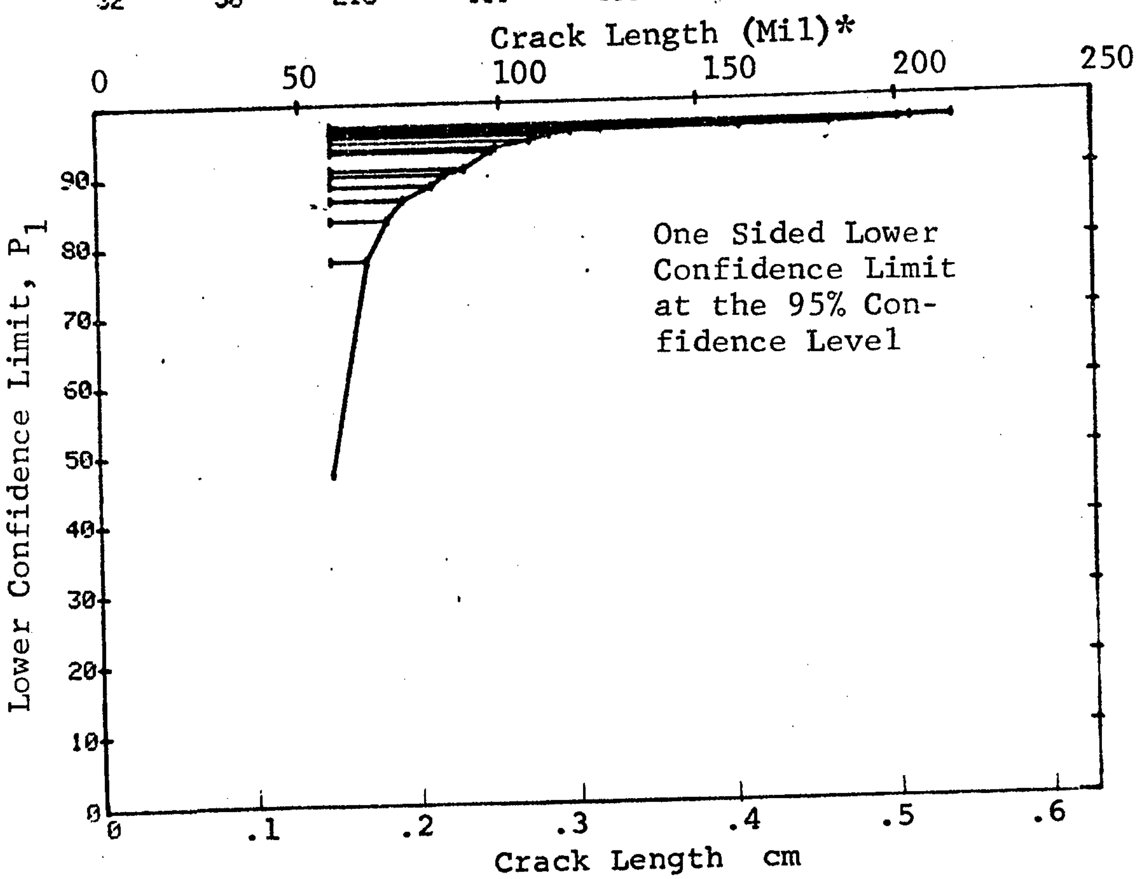

Figure D-46 (Continued)

(c) Overlapping Sixty Point Method of Data Cumulation

09-OCT-75 ULTRASONIC TEST 3 (46)

RANGE	MIN LN *	MAX LN *	N	DET	50%	95%	0 MISS	1 MISS
1	0	0	0	0	0	0	0	0
2	0	0	0	0	0	0	0	0
3	0	0	0	0	0	0	0	0
4	0	0	0	0	0	0	0	0
5	0	0	0	0	0	0	0	0
6	0	0	0	0	0	0	0	0
7	0	0	0	0	0	0	0	0
8	0	0	0	0	0	0	0	0
9	0	0	0	0	0	0	0	0
10	0	0	0	0	0	0	0	0
11	0	0	0	0	0	0	0	0
12	0	0	0	0	0	0	0	0
13	0	0	0	0	0	0	0	0
14	0	0	0	0	0	0	0	0
15	0	0	0	0	0	0	0	0
16	0	0	0	0	0	0	0	0
17	0	0	0	0	0	0	0	0
18	0	0	0	0	0	0	0	0
19	0	0	0	0	0	0	0	0
20	0	0	0	0	0	0	0	0
21	0	0	0	0	0	0	0	0
22	0	0	0	0	0	0	0	0
23	0	0	0	0	0	0	0	0
24	0	0	0	0	0	0	0	0
25	0	0	0	0	0	0	0	0
26	0	0	0	0	0	0	0	0
27	0	0	0	0	0	0	0	0
28	0	0	0	0	0	0	0	0
29	0	0	0	0	0	0	0	0
30	58	98	41	41	98	92	0	5
31	67	117	60	60	98	95	0	0
32	98	215	60	60	98	95	0	0

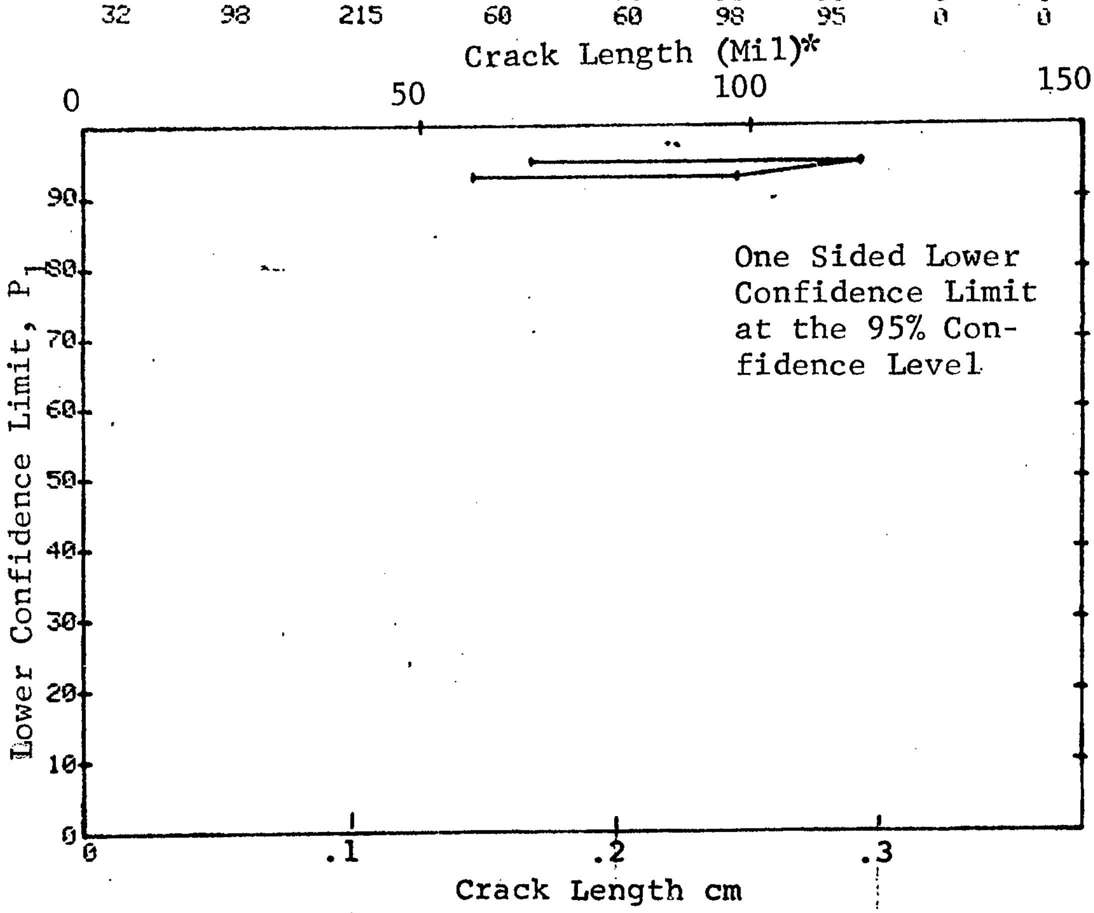

Figure D-46 (Concluded)

(a) Range Interval Method of Data Cumulation

09-OCT-75 MAGNETIC PARTICLE TEST 1 (47)

RANGE	MIN LN	* MAX LN *	N	DET	50%	95%	0 MISS	1 MISS
1	32	32	3	2	50	13	0	0
2	41	43	11	11	93	76	18	35
3	0	0	0	0	0	0	0	0
4	0	0	0	0	0	0	0	0
5	0	0	0	0	0	0	0	0
6	65	65	3	3	79	36	0	0
7	70	72	14	13	88	70	0	0
8	77	80	4	4	84	47	0	0
9	0	0	0	0	0	0	0	0
10	88	91	16	16	95	82	13	30
11	93	95	7	7	90	65	0	0
12	100	100	4	4	84	47	0	0
13	0	0	0	0	0	0	0	0
14	0	0	0	0	0	0	0	0
15	117	118	11	11	93	76	18	35
16	0	0	0	0	0	0	0	0
17	132	132	5	5	87	54	0	0
18	0	0	0	0	0	0	0	0
19	141	143	9	9	92	71	0	0
20	147	149	13	13	94	79	16	33
21	0	0	0	0	0	0	0	0
22	0	0	0	0	0	0	0	0
23	170	170	6	6	89	60	0	0
24	0	0	0	0	0	0	0	0
25	181	181	6	6	89	60	0	0
26	184	184	9	9	92	71	0	0
27	0	0	0	0	0	0	0	0
28	0	0	0	0	0	0	0	0
29	0	0	0	0	0	0	0	0
30	0	0	0	0	0	0	0	0
31	0	0	0	0	0	0	0	0
32	226	226	5	5	87	54	0	0

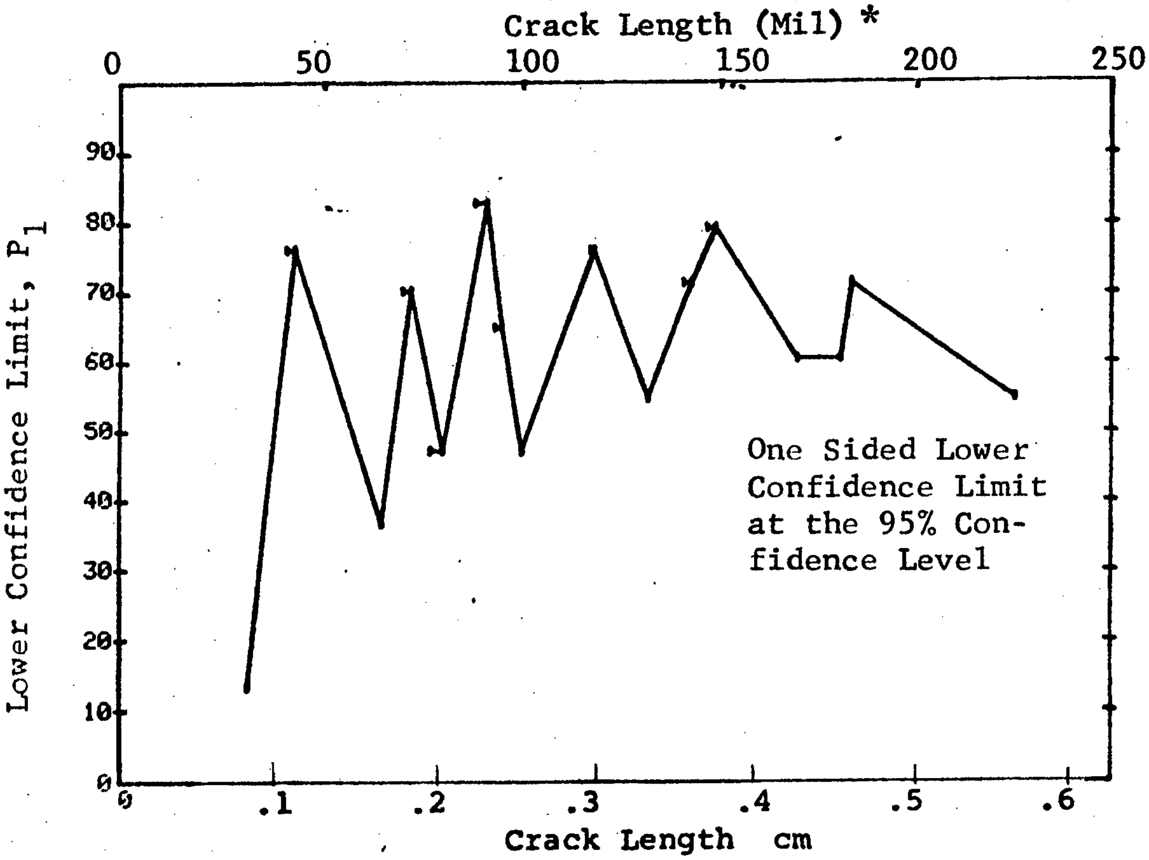

Figure D-47 Probability of Detection for PH17-4 Steel Using Ultrasonic Shear Wave. Fatigue Cracks in Flat Plates. Prod. Env.

(b) Optimum Probability Method of Data Cumulation

09-OCT-75 MAGNETIC PARTICLE TEST 2 (47)

RANGE	MIN LN	MAX LN	N	DET	50%	95%	0 MISS	1 MISS
1	32	* 32 *	3	2	0	13	0	0
2	41	43	11	11	0	76	0	0
3	0	0	0	0	0	0	0	0
4	0	0	0	0	0	0	0	0
5	0	0	0	0	0	0	0	0
6	41	65	14	14	0	80	15	32
7	41	72	28	27	0	84	18	33
8	41	80	32	31	0	86	14	29
9	0	0	0	0	0	0	0	0
10	41	91	48	47	0	90	0	13
11	41	95	55	54	0	91	0	6
12	41	100	59	58	0	92	0	2
13	0	0	0	0	0	0	0	0
14	0	0	0	0	0	0	0	0
15	41	118	70	69	0	93	0	0
16	0	0	0	0	0	0	0	0
17	77	132	47	47	0	93	0	0
18	0	0	0	0	0	0	0	0
19	77	143	56	56	0	94	0	0
20	77	149	69	69	0	95	0	0
21	0	0	0	0	0	0	0	0
22	0	0	0	0	0	0	0	0
23	77	170	75	75	0	96	0	0
24	0	0	0	0	0	0	0	0
25	77	181	81	81	0	96	0	0
26	77	184	90	90	0	96	0	0
27	0	0	0	0	0	0	0	0
28	0	0	0	0	0	0	0	0
29	0	0	0	0	0	0	0	0
30	0	0	0	0	0	0	0	0
31	0	0	0	0	0	0	0	0
32	77	226	95	95	0	96	0	0

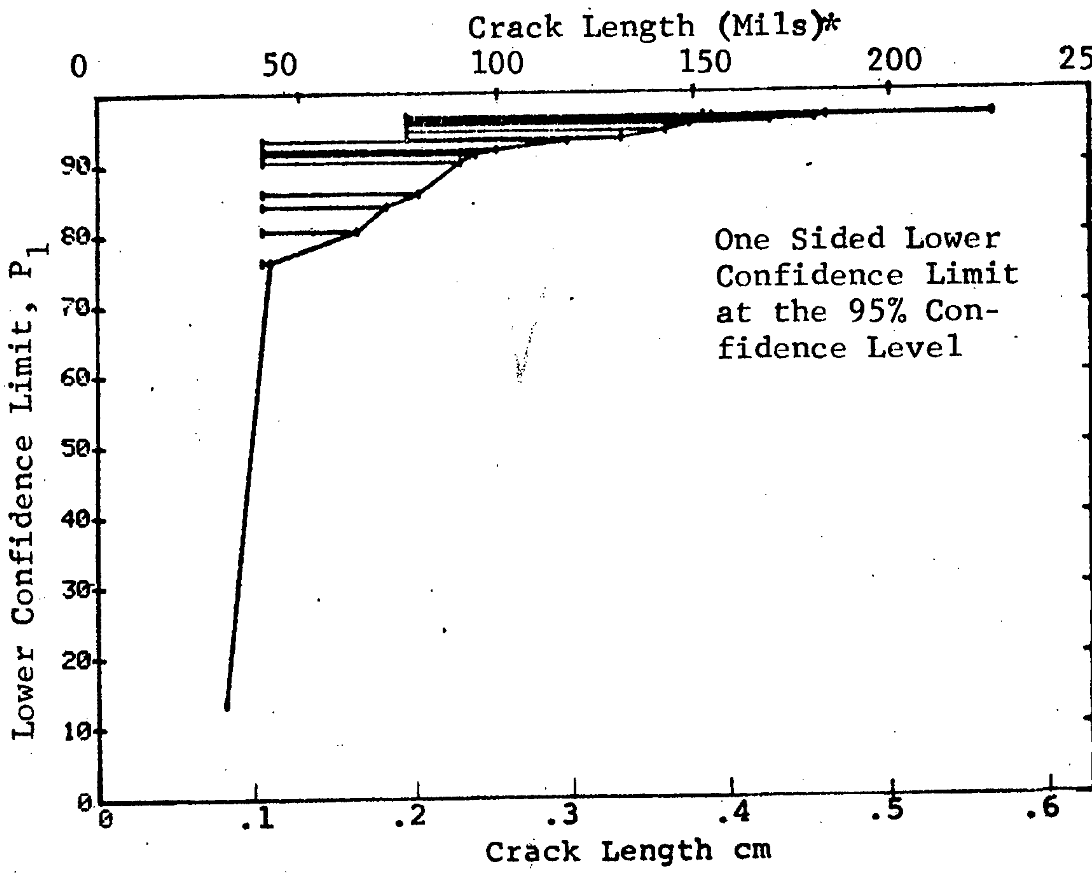

Figure D-47 (Continued)

(c) Overlapping Sixty Point Method of Data Cumulation

09-OCT-75 MAGNETIC PARTICLE TEST 3 (47)

RANGE	MIN LN*	MAX LN*	N	DET	50%	95%	0 MISS	1 MISS
1	0	0	0	0	0	0	0	0
2	0	0	0	0	0	0	0	0
3	0	0	0	0	0	0	0	0
4	0	0	0	0	0	0	0	0
5	0	0	0	0	0	0	0	0
6	0	0	0	0	0	0	0	0
7	0	0	0	0	0	0	0	0
8	0	0	0	0	0	0	0	0
9	0	0	0	0	0	0	0	0
10	0	0	0	0	0	0	0	0
11	0	0	0	0	0	0	0	0
12	0	0	0	0	0	0	0	0
13	0	0	0	0	0	0	0	0
14	0	0	0	0	0	0	0	0
15	0	0	0	0	0	0	0	0
16	0	0	0	0	0	0	0	0
17	0	0	0	0	0	0	0	0
18	0	0	0	0	0	0	0	0
19	0	0	0	0	0	0	0	0
20	0	0	0	0	0	0	0	0
21	0	0	0	0	0	0	0	0
22	0	0	0	0	0	0	0	0
23	0	0	0	0	0	0	0	0
24	0	0	0	0	0	0	0	0
25	0	0	0	0	0	0	0	0
26	0	0	0	0	0	0	0	0
27	0	0	0	0	0	0	0	0
28	0	0	0	0	0	0	0	0
29	32	88	36	34	92	83	29	40
30	41	117	60	59	97	92	0	1
31	88	149	60	60	98	95	0	0
32	117	226	60	60	98	95	0	0

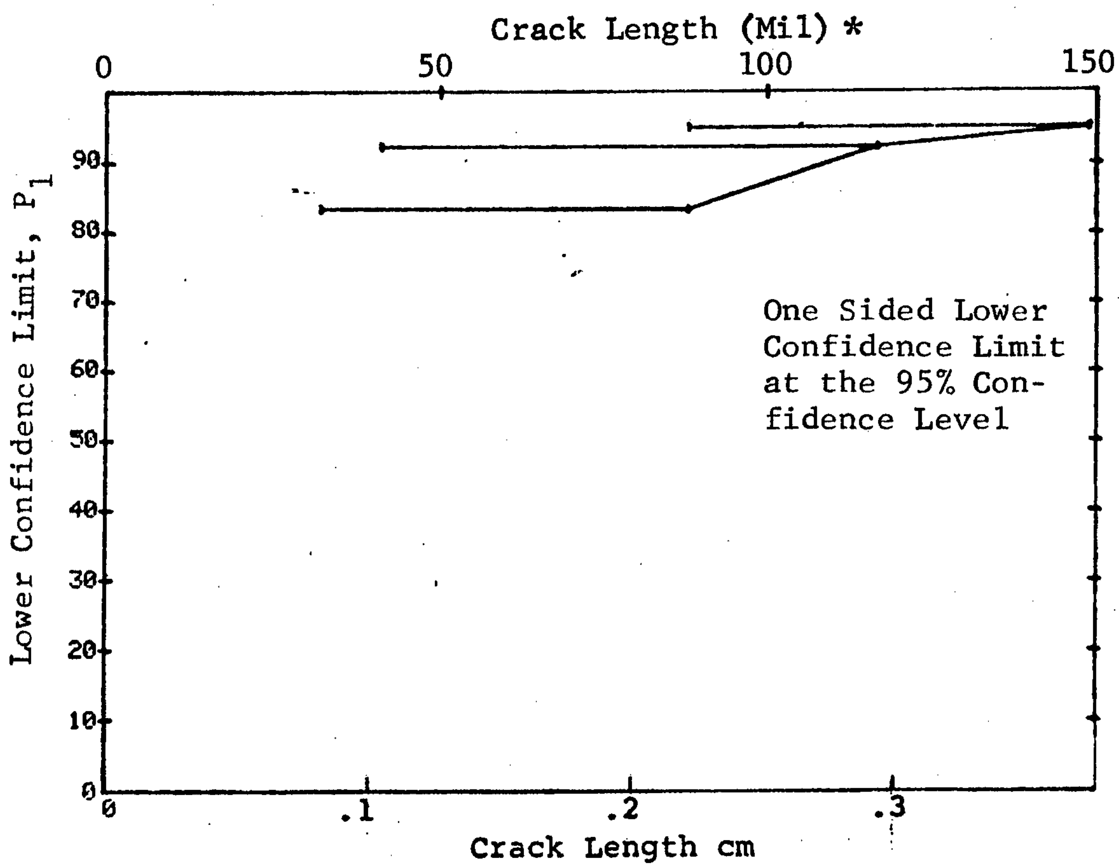

Figure D-47 (Concluded)

(a) Range Interval Method of Data Cumulation

10-OCT-75 PENETRANT TEST 1 (MERGE ALL ALUMINUM) (48)

RANGE	MIN LN	MAX LN	N	DET	90%	95%	0 MISS	1 MISS
1	7 *	39 *	226	88	39	33	0	0
2	40	69	1041	420	77	74	0	0
3	70	100	627	554	88	86	0	0
4	101	131	281	260	92	89	0	0
5	132	162	231	203	87	83	0	0
6	164	190	47	45	94	87	14	29
7	194	197	9	7	71	45	0	0
8	241	253	70	69	97	93	0	0
9	256	283	119	119	99	97	0	0
10	287	317	112	109	96	93	0	0
11	318	347	175	165	93	90	0	0
12	352	372	70	63	89	82	59	72
13	381	408	28	27	94	84	18	33
14	426	426	7	7	90	65	0	0
15	442	472	70	67	94	89	6	19
16	474	503	154	149	96	93	0	0
17	504	534	182	180	98	96	0	0
18	535	559	49	47	94	87	12	27
19	568	568	7	7	90	65	0	0
20	610	610	7	7	90	65	0	0
21	0	0	0	0	0	0	0	0
22	0	0	0	0	0	0	0	0
23	710	710	7	7	90	65	0	0
24	0	0	0	0	0	0	0	0
25	0	0	0	0	0	0	0	0
26	0	0	0	0	0	0	0	0
27	0	0	0	0	0	0	0	0
28	0	0	0	0	0	0	0	0
29	0	0	0	0	0	0	0	0
30	0	0	0	0	0	0	0	0
31	0	0	0	0	0	0	0	0
32	979	979	7	7	90	65	0	0

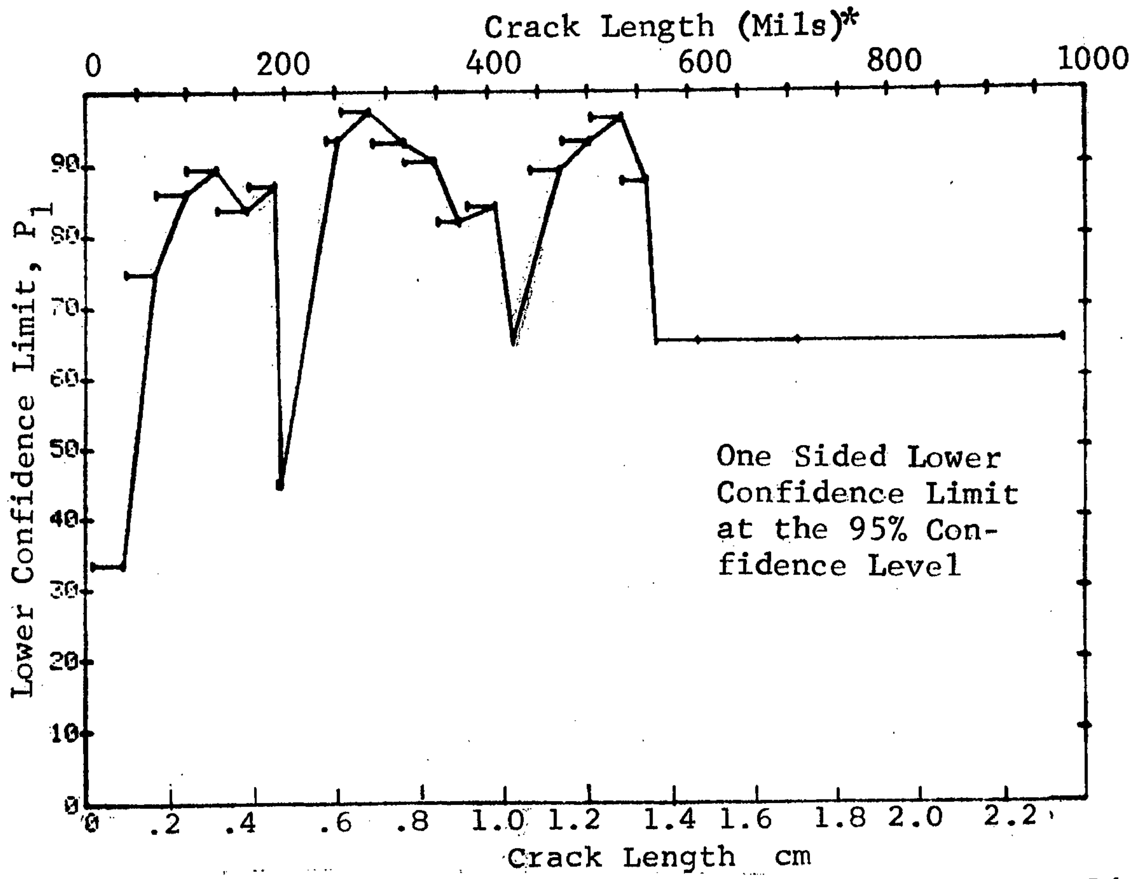

Figure D-48 Probability of Detection for Aluminum Using Liquid Penetrant Fatigue Cracks in Flat Plates.

Prod. & Lab. Env.

(b) Optimum Probability Method of Data Cumulation

10-OCT-75 PENETRANT TEST 3 (MERGE ALL ALUMINUM) (48)

RANGE	MIN LN		MAX LN		N	DET	50%	95%	0 MISS	1 MISS
1	7	*	38	*	226	88	0	33	0	0
2	40		69		441	498	0	74	0	0
3	70		100		627	554	0	86	0	0
4	101		131		281	260	0	89	0	0
5	101		162		512	463	0	88	0	0
6	101		190		559	508	0	88	0	0
7	101		197		568	515	0	88	0	0
8	241		253		70	69	0	93	0	0
9	256		283		119	119	0	97	0	0
10	241		317		301	297	0	96	0	0
11	241		347		476	462	0	95	0	0
12	241		372		546	525	0	94	0	0
13	241		408		574	552	0	94	0	0
14	241		426		581	559	0	94	0	0
15	241		472		651	626	0	94	0	0
16	241		503		805	775	0	94	0	0
17	504		534		182	180	0	96	0	0
18	504		559		231	227	0	96	0	0
19	504		568		238	234	0	96	0	0
20	504		610		245	241	0	96	0	0
21	0		0		0	0	0	0	0	0
22	0		0		0	0	0	0	0	0
23	504		710		252	248	0	96	0	0
24	0		0		0	0	0	0	0	0
25	0		0		0	0	0	0	0	0
26	0		0		0	0	0	0	0	0
27	0		0		0	0	0	0	0	0
28	0		0		0	0	0	0	0	0
29	0		0		0	0	0	0	0	0
30	0		0		0	0	0	0	0	0
31	0		0		0	0	0	0	0	0
32	504		979		259	255	0	96	0	0

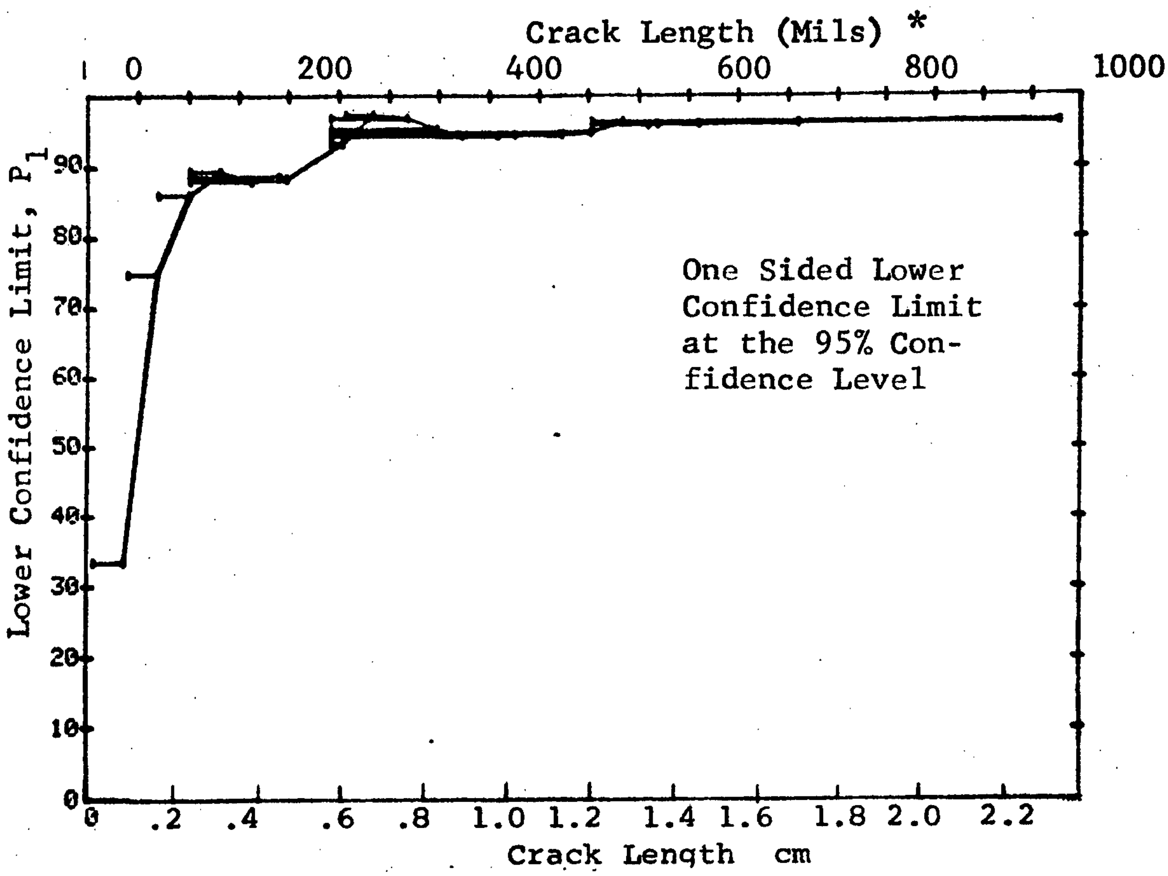

Figure D-48 (Continued)

(c) Overlapping Sixty Point Method of Data Cumulation

15-OCT-75 PENETRANT [illegible] (MERGE ALL ALUMINUM) (48)

RANGE	MIN LN	MAX LN	N	DET	50%	95%	[illegible]	[illegible]
1	143 *	149 *	60	52	85	[illegible]	[illegible]	94
2	144	153	60	52	85	[illegible]	[illegible]	94
3	149	158	60	51	83	75	94	100
4	153	182	60	57	93	87	16	[illegible]
5	158	190	60	58	95	89	1	16
6	182	247	60	55	90	83	43	56
7	190	249	60	57	93	87	16	29
8	247	257	60	60	98	95	0	0
9	249	258	60	60	98	95	0	0
10	257	261	60	60	98	95	0	0
11	258	275	60	60	98	95	0	0
12	261	288	60	60	98	95	0	0
13	279	296	60	60	98	95	0	0
14	288	306	60	59	97	92	0	1
15	296	313	60	58	95	89	1	16
16	306	321	60	58	95	89	1	16
17	313	326	60	57	93	87	16	29
18	321	330	60	58	95	89	1	16
19	326	336	60	59	97	92	0	1
20	331	340	60	54	88	81	56	69
21	336	345	60	53	87	79	69	82
22	340	362	60	57	93	87	16	29
23	345	370	60	57	93	87	16	[illegible]
24	362	384	60	54	88	81	56	[illegible]
25	370	442	60	54	88	81	56	[illegible]
26	384	460	60	58	95	89	1	16
27	444	472	60	59	97	92	0	1
28	460	478	60	57	93	87	16	[illegible]
29	472	484	60	58	95	[illegible]	[illegible]	[illegible]
30	478	492	60	59	97	[illegible]	[illegible]	1
31	484	496	60	59	97	[illegible]	[illegible]	1
32	492	500	60	57	93	[illegible]	[illegible]	[illegible]

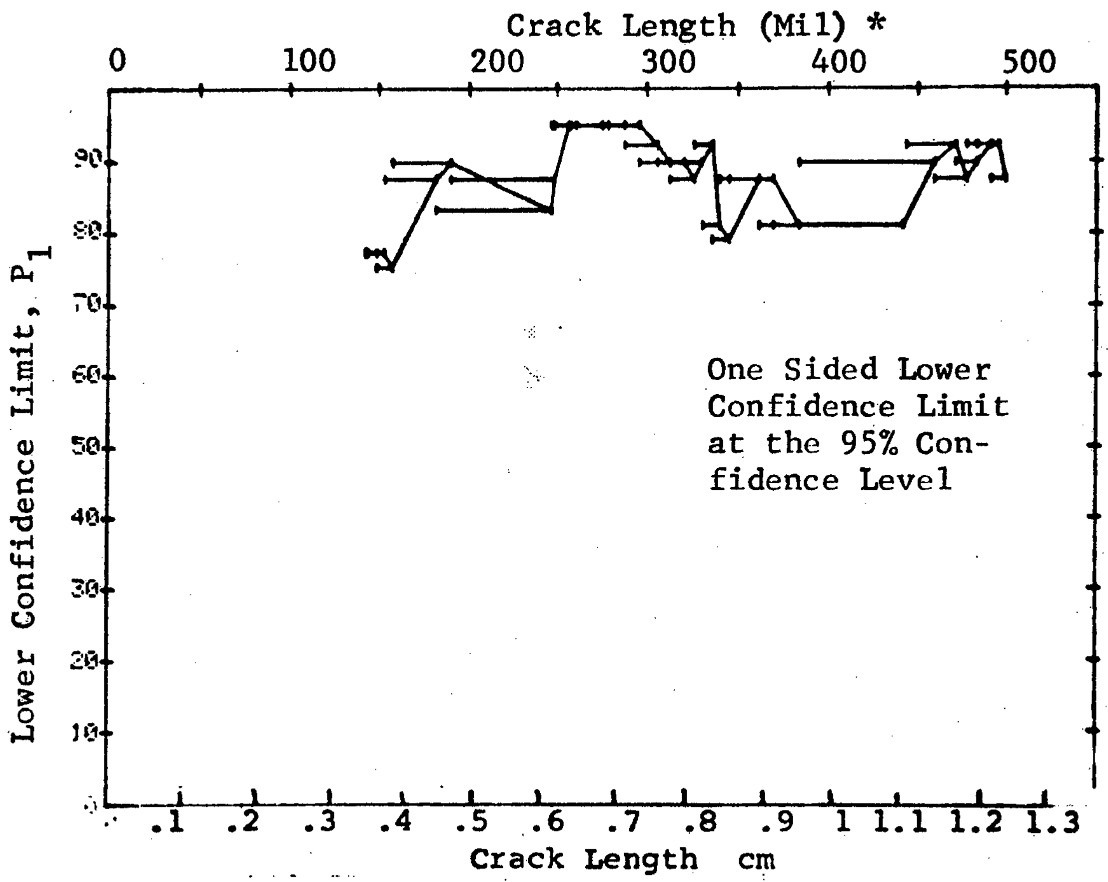

Figure D-48 (Continued)

(c) Overlapping Sixty Point Method of Data Cumulation

15-OCT-75 PENETRANT TEST 7 (MERGE ALL ALUMINUM) (48)

RANGE	MIN LN	MAX LN	N	DET	50%	95%	0 MISS	1 MISS
1	76 *	79 *	60	54	88	81	56	69
2	77	80	60	54	88	81	56	69
3	79	80	60	54	88	81	56	69
4	80	82	60	47	77	67	0	0
5	80	83	60	49	80	71	0	0
6	82	85	60	47	77	67	0	0
7	83	85	60	47	77	67	0	0
8	85	86	60	55	90	83	43	56
9	85	88	60	55	90	83	43	56
10	86	90	60	55	90	83	43	56
11	88	92	60	57	93	87	16	29
12	90	95	60	59	97	92	0	1
13	92	96	60	59	97	92	0	1
14	95	97	60	57	93	87	16	29
15	96	99	60	57	93	87	16	29
16	97	103	60	60	98	95	0	0
17	99	105	60	56	92	85	29	43
18	103	108	60	56	92	85	29	43
19	105	115	60	59	97	92	0	1
20	108	118	60	55	90	83	43	56
21	115	122	60	52	85	77	82	94
22	118	124	60	51	83	75	94	100
23	122	125	60	53	87	79	69	82
24	124	129	60	57	93	87	16	29
25	126	134	60	57	93	87	16	29
26	129	135	60	54	88	81	56	69
27	134	138	60	54	88	81	56	69
28	135	143	60	54	88	81	56	69
29	138	145	60	51	83	75	94	100
30	143	150	60	51	83	75	94	100
31	145	153	60	52	85	77	82	94
32	150	158	60	53	87	79	69	82

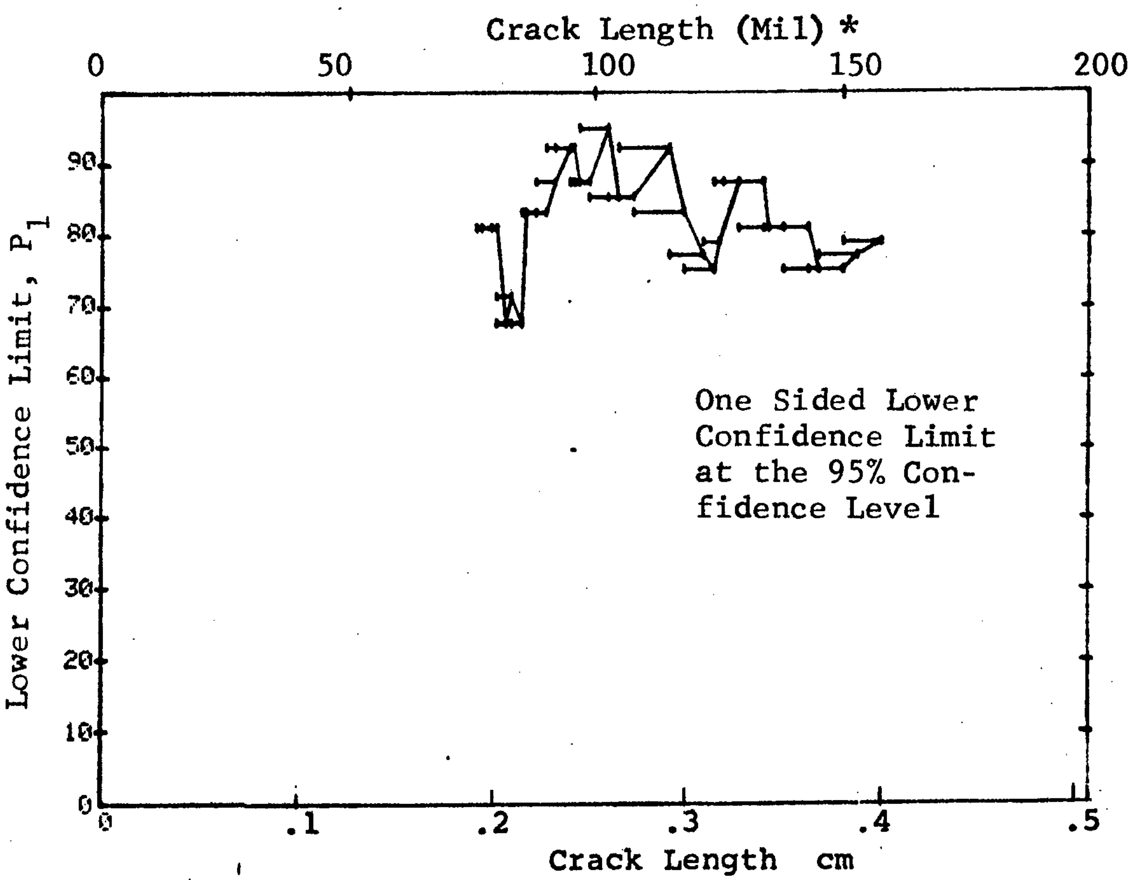

Figure D-48 (Continued)

(c) Overlapping Sixty Point Method of Data Cumulation

15-OCT-75 PENETRANT TEST [illegible] (MERGE ALL ALUMINUM) (48)

RANGE	MIN LN	MAX LN	N	DET	50%	95%	0 MISS	1 MISS
1	30*	35*	60	24	33	29	0	0
2	32	40	60	34	55	45	0	0
3	35	41	60	45	74	64	0	0
4	40	44	60	43	70	60	0	0
5	41	45	60	47	77	67	0	0
6	44	47	60	52	85	77	82	94
7	45	49	60	46	75	65	0	0
8	47	51	60	43	70	60	0	0
9	49	54	60	50	82	73	0	0
10	51	56	60	45	74	64	0	0
11	54	58	60	41	67	57	0	0
12	56	60	60	42	69	58	0	0
13	58	61	60	49	80	71	0	0
14	60	62	60	51	83	75	94	100
15	61	63	60	47	77	67	0	0
16	62	64	60	50	82	73	0	0
17	63	65	60	48	79	69	0	0
18	64	66	60	44	72	62	0	0
19	65	67	60	41	67	57	0	0
20	66	68	60	48	79	69	0	0
21	67	68	60	57	93	87	16	29
22	68	69	60	53	87	79	69	82
23	68	69	60	43	70	60	0	0
24	69	71	60	37	60	50	0	0
25	69	73	60	43	70	60	0	0
26	71	74	60	52	85	77	82	94
27	73	75	60	53	87	79	69	82
28	74	76	60	53	87	79	69	82
29	76	78	60	55	90	83	43	56
30	76	79	60	55	90	83	43	56
31	78	80	60	54	88	81	56	67
32	79	80	60	54	88	81	56	67

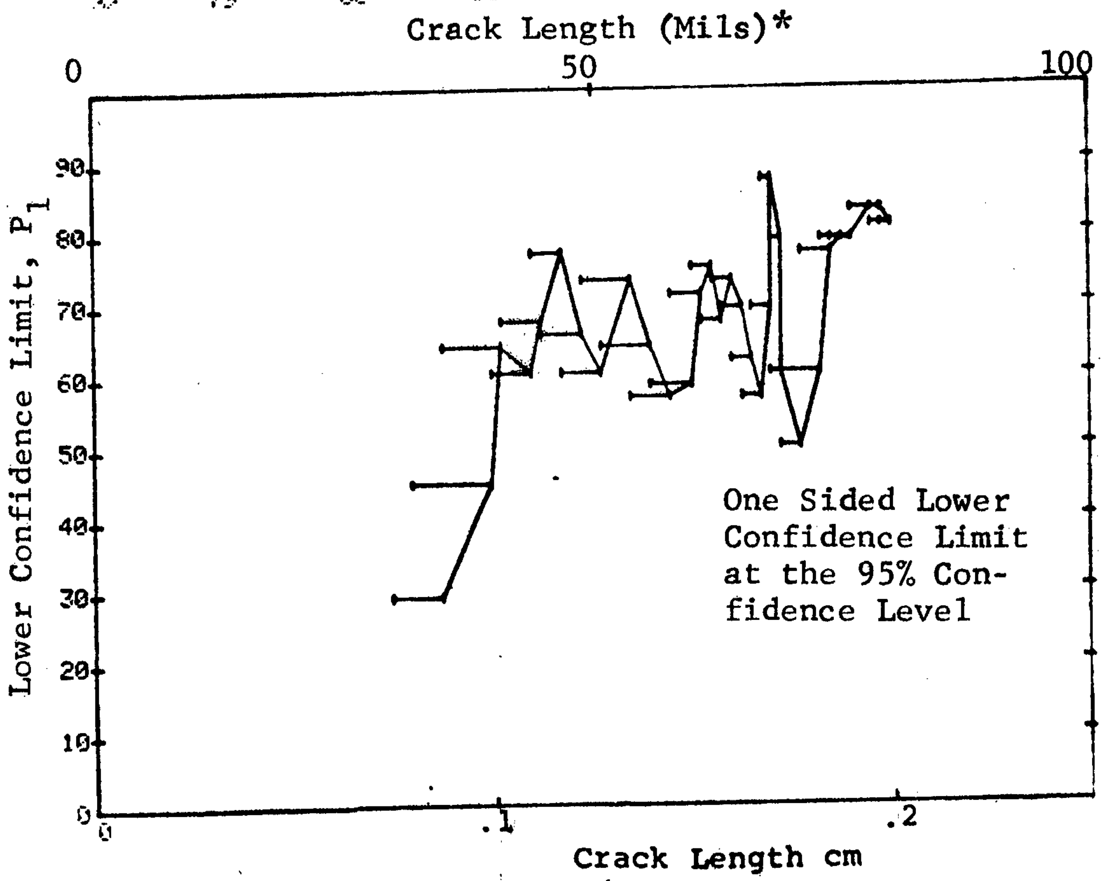

Figure D-48 (Concluded)

(a) Range Interval Method of Data Cumulation

10-OCT-75 PENETRANT TEST 1 (49)

RANGE	MIN LN	MAX LN	N	DET	50%	95%	0 MISS	1 MISS
1	70 *	70 *	1	0	0	0	0	0
2	0	0	0	0	0	0	0	0
3	100	105	4	2	38	9	0	0
4	120	120	2	0	0	0	0	0
5	130	140	11	5	41	19	0	0
6	150	150	2	0	0	0	0	0
7	157	158	5	2	31	7	0	0
8	170	170	1	0	0	0	0	0
9	184	190	3	1	20	1	0	0
10	200	200	2	0	0	0	0	0
11	212	215	2	1	29	2	0	0
12	236	236	7	5	63	34	0	0
13	0	0	0	0	0	0	0	0
14	262	264	4	3	61	24	0	0
15	0	0	0	0	0	0	0	0
16	288	292	5	4	68	34	0	0
17	0	0	0	0	0	0	0	0
18	314	315	3	3	79	36	0	0
19	0	0	0	0	0	0	0	0
20	337	344	5	2	31	7	0	0
21	0	0	0	0	0	0	0	0
22	368	368	1	1	50	5	0	0
23	0	0	0	0	0	0	0	0
24	394	394	2	2	70	22	0	0
25	420	420	1	1	50	5	0	0
26	0	0	0	0	0	0	0	0
27	446	446	1	1	50	5	0	0
28	0	0	0	0	0	0	[illegible]	0
29	472	473	2	2	70	[illegible]	[illegible]	[illegible]
30	0	0	0	0	0	0	0	0
31	499	499	1	1	50	5	[illegible]	0
32	526	526	1	1	50	5	[illegible]	[illegible]

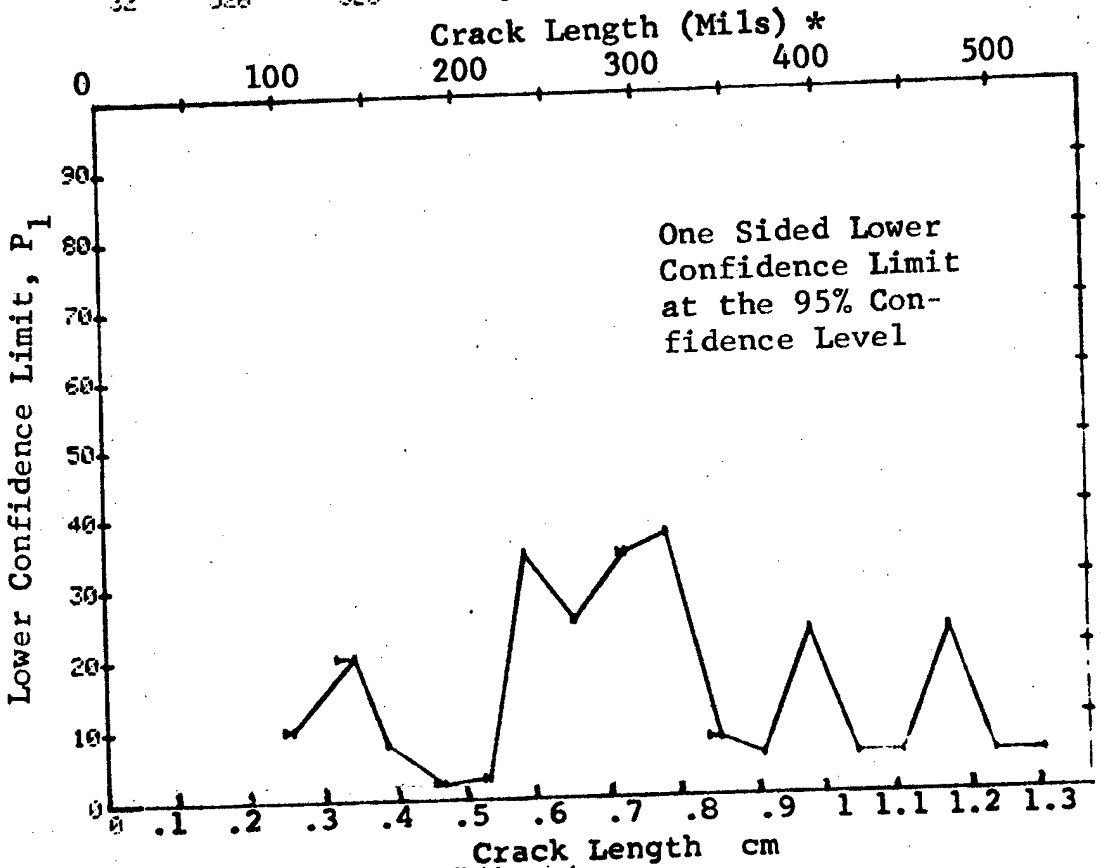

Figure D-49 Probability of Detection for 4330V Steel Using Liquid Penetrant. Fatigue Cracks in Cylindrical Shell Specimens. Lab. Env.

(b) Optimum Probability Method of Data Cumulation

10-OCT-75 PENETRANT TEST 2 (49)

RANGE	MIN LN	MAX LN	N	DET	50%	95%	0 MISS	1 MISS
1	70 *	70 *	1	0	0	0	0	0
2	0	0	0	0	0	0	0	0
3	100	105	4	2	0	9	0	0
4	100	120	6	2	0	6	0	0
5	100	140	17	7	0	21	0	0
6	100	150	19	7	0	18	0	0
7	100	158	24	9	0	21	0	0
8	100	170	25	9	0	20	0	0
9	100	190	28	10	0	20	0	0
10	100	200	30	10	0	19	0	0
11	100	215	32	11	0	20	0	0
12	212	236	9	6	0	34	0	0
13	0	0	0	0	0	0	0	0
14	236	264	11	8	0	43	0	0
15	0	0	0	0	0	0	0	0
16	236	292	16	12	0	51	0	0
17	0	0	0	0	0	0	0	0
18	236	315	19	15	0	58	0	0
19	0	0	0	0	0	0	0	0
20	236	344	24	17	0	52	0	0
21	0	0	0	0	0	0	0	0
22	236	368	25	18	0	53	0	0
23	0	0	0	0	0	0	0	0
24	236	394	27	20	0	56	0	0
25	236	420	28	21	0	58	0	0
26	0	0	0	0	0	0	0	0
27	236	446	29	22	0	59	0	0
28	0	0	0	0	0	0	0	0
29	368	473	7	7	0	65	0	0
30	0	0	0	0	0	0	0	0
31	368	499	8	8	0	68	0	0
32	368	526	9	9	0	71	0	0

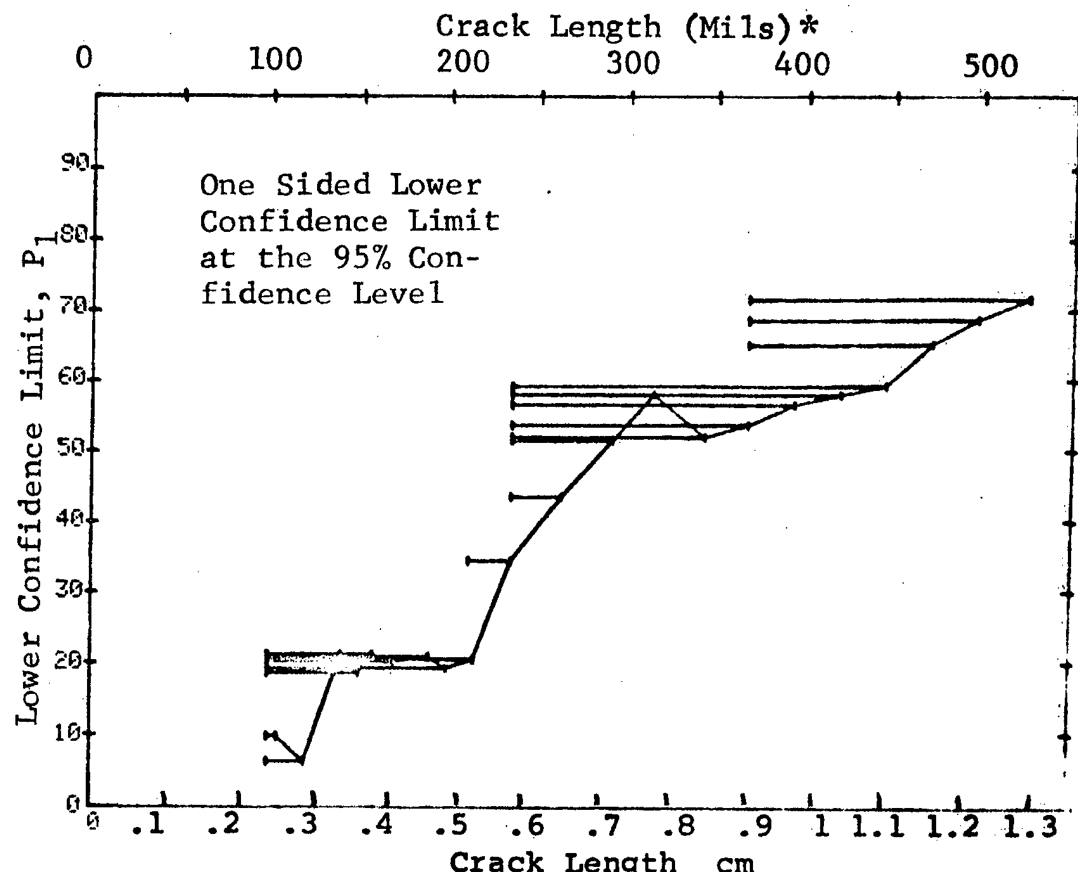

Figure D-49 (Continued)

(c) Overlapping Sixty Point Method of Data Cumulation

10-OCT-75 PENETRANT TEST 3 (49)

RANGE	MIN LN	MAX LN	N	DET	50%	95%	0 MISS	1 MISS
1	0*	0 *	0	0	0	0	0	0
2	0	0	0	0	0	0	0	0
3	0	0	0	0	0	0	0	0
4	0	0	0	0	0	0	0	0
5	0	0	0	0	0	0	0	0
6	0	0	0	0	0	0	0	0
7	0	0	0	0	0	0	0	0
8	0	0	0	0	0	0	0	0
9	0	0	0	0	0	0	0	0
10	0	0	0	0	0	0	0	0
11	0	0	0	0	0	0	0	0
12	0	0	0	0	0	0	0	0
13	0	0	0	0	0	0	0	0
14	0	0	0	0	0	0	0	0
15	0	0	0	0	0	0	0	0
16	0	0	0	0	0	0	0	0
17	0	0	0	0	0	0	0	0
18	0	0	0	0	0	0	0	0
19	0	0	0	0	0	0	0	0
20	0	0	0	0	0	0	0	0
21	0	0	0	0	0	0	0	0
22	0	0	0	0	0	0	0	0
23	0	0	0	0	0	0	0	0
24	0	0	0	0	0	0	0	0
25	0	0	0	0	0	0	0	0
26	0	0	0	0	0	0	0	0
27	0	0	0	0	0	0	0	0
28	0	0	0	0	0	0	0	0
29	0	0	0	0	0	0	0	0
30	0	0	0	0	0	0	0	0
31	70	236	35	12	33	21	0	0
32	120	499	60	34	55	45	0	0

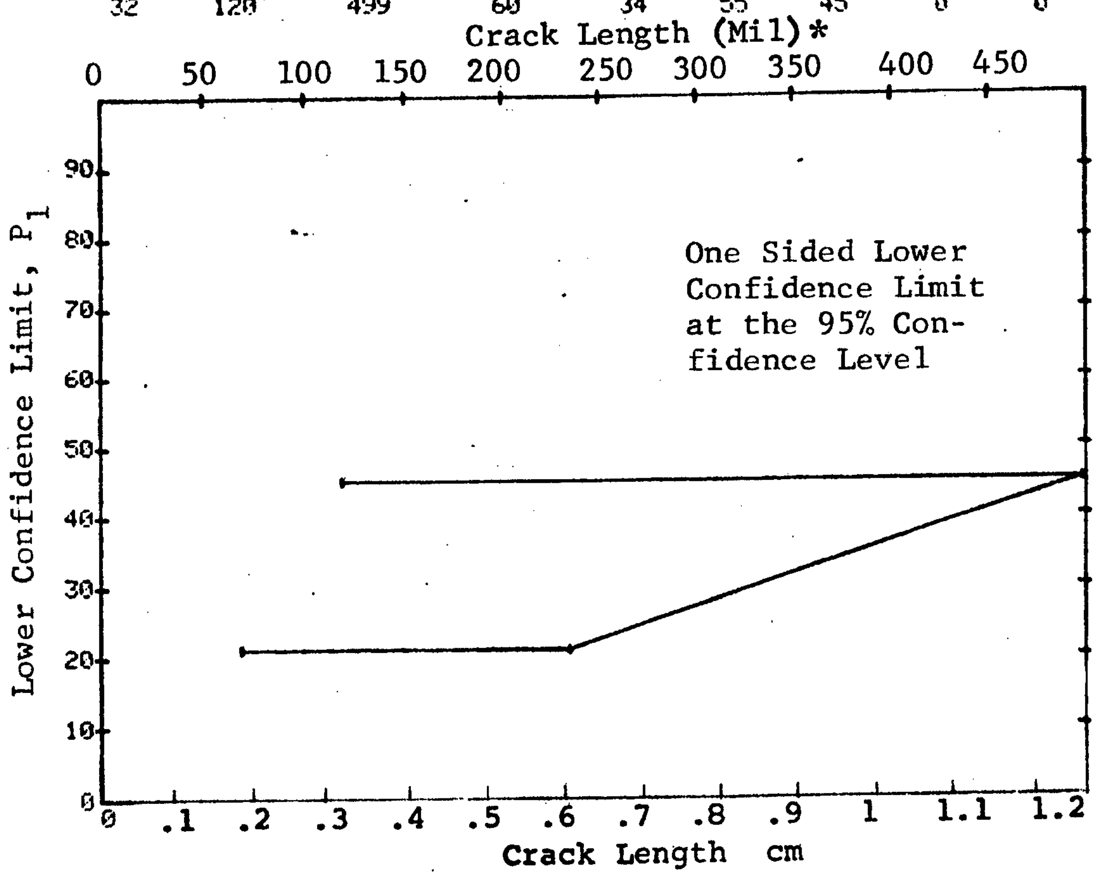

Figure D-49 (Concluded)

(a) Range Interval Method of Data Cumulation

10-OCT-75 PENETRANT TEST 1 (50)

RANGE	MIN LN*	MAX LN*	N	DET	50%	95%	0 MISS	1 MISS
1	70	70	1	1	50	5	0	0
2	0	0	0	0	0	0	0	0
3	100	105	4	0	0	0	0	0
4	120	120	2	0	0	0	0	0
5	130	140	11	1	6	0	0	0
6	150	150	2	0	0	0	0	0
7	157	158	5	1	12	1	0	0
8	170	170	1	1	50	5	0	0
9	184	190	3	0	0	0	0	0
10	200	200	2	0	0	0	0	0
11	212	215	2	0	0	0	0	0
12	236	236	7	1	9	0	0	0
13	0	0	0	0	0	0	0	0
14	262	264	4	1	15	1	0	0
15	0	0	0	0	0	0	0	0
16	288	292	5	0	0	0	0	0
17	0	0	0	0	0	0	0	0
18	314	315	3	1	20	1	0	0
19	0	0	0	0	0	0	0	0
20	337	344	5	1	12	1	0	0
21	0	0	0	0	0	0	0	0
22	368	368	1	0	0	0	0	0
23	0	0	0	0	0	0	0	0
24	394	394	2	1	29	2	0	0
25	420	420	1	0	0	0	0	0
26	0	0	0	0	0	0	0	0
27	446	446	1	0	0	0	0	0
28	0	0	0	0	0	0	0	0
29	472	473	2	0	0	0	0	0
30	0	0	0	0	0	0	0	0
31	499	499	1	1	50	5	0	0
32	526	526	1	0	0	0	0	0

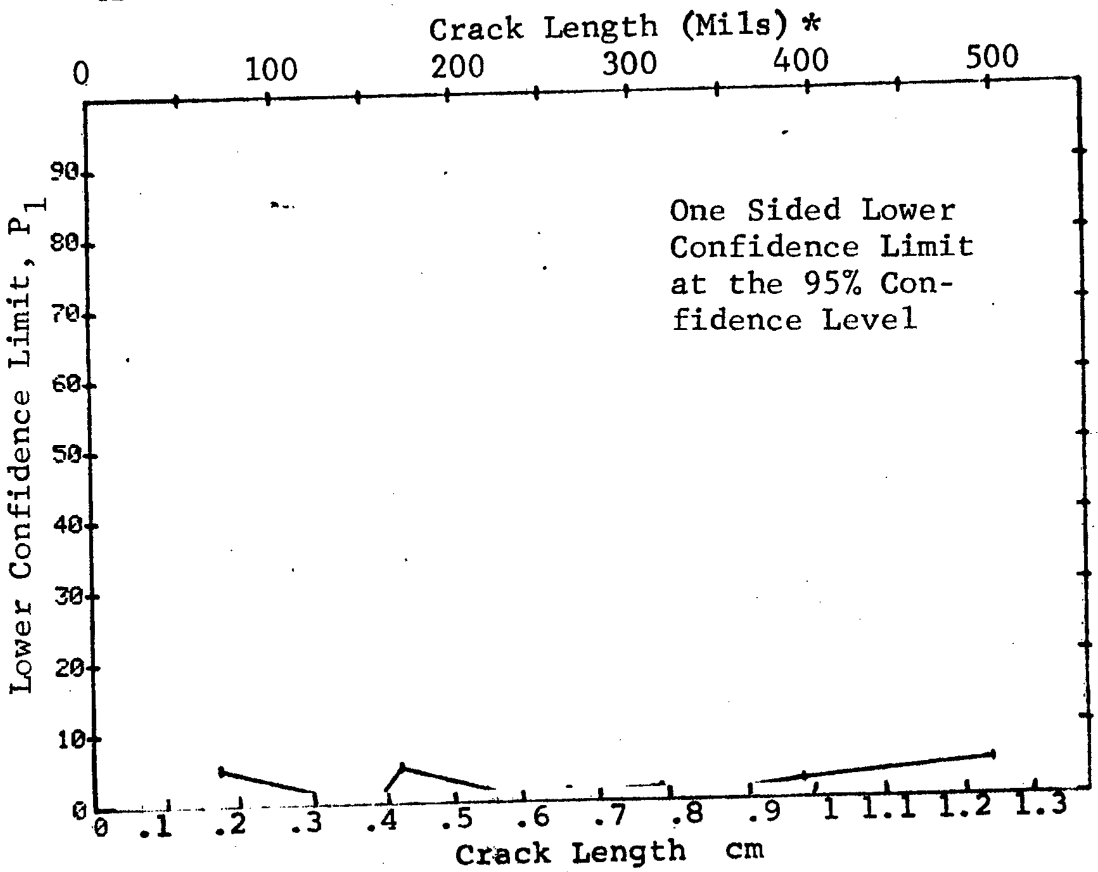

Figure D-50 Probability of Detection for 4330V Steel Using Magniflux ZL-2. Fatigue Cracks in Cylindrical Shell Specimens. Prod. Env.

(b) Optimum Probability Method of Data Cumulation

10-OCT-75 PENETRANT TEST 2 (50

RANGE	MIN LN	MAX LN	N	DET	50%	95%	0 MISS	1 MISS
1	70 *	70 *	1	1	0	5	0	0
2	0	0	0	0	0	0	0	0
3	70	105	5	1	0	1	0	0
4	70	120	7	1	0	0	0	0
5	70	140	18	2	0	2	0	0
6	70	150	20	2	0	1	0	0
7	70	158	25	3	0	3	0	0
8	157	170	6	2	0	6	0	0
9	70	190	29	4	0	4	0	0
10	70	200	31	4	0	4	0	0
11	70	215	33	4	0	4	0	0
12	70	236	40	5	0	5	0	0
13	0	0	0	0	0	0	0	0
14	70	264	44	6	0	6	0	0
15	0	0	0	0	0	0	0	0
16	70	292	49	6	0	5	0	0
17	0	0	0	0	0	0	0	0
18	70	315	52	7	0	6	0	0
19	0	0	0	0	0	0	0	0
20	157	344	37	6	0	7	0	0
21	0	0	0	0	0	0	0	0
22	157	368	38	6	0	7	0	0
23	0	0	0	0	0	0	0	0
24	157	394	40	7	0	8	0	0
25	157	420	41	7	0	8	0	0
26	0	0	0	0	0	0	0	0
27	157	446	42	7	0	8	0	0
28	0	0	0	0	0	0	0	0
29	157	473	44	7	0	[illegible]	0	0
30	0	0	0	0	0	0	0	0
31	157	499	45	8	0	9	0	0
32	157	526	46	8	0	8	0	0

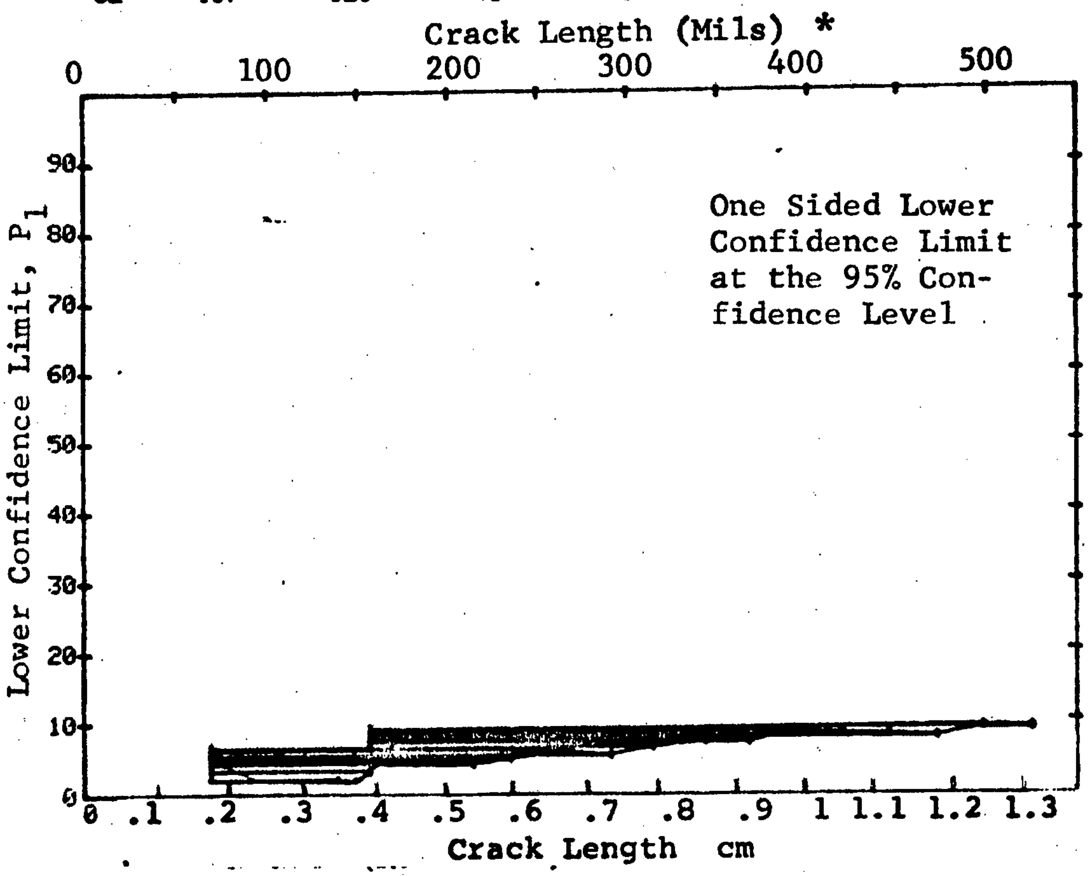

Figure D-50 (Continued)

(c) Overlapping Sixty Point Method of Data Cumulation

10-OCT-75 PENETRANT TEST 3 (50)

RANGE	MIN LN	MAX LN	N	DET	50%	95%	0 MISS	1 MISS
1	0 *	0 *	0	0	0	0	0	0
2	0	0	0	0	0	0	0	0
3	0	0	0	0	0	0	0	0
4	0	0	0	0	0	0	0	0
5	0	0	0	0	0	0	0	0
6	0	0	0	0	0	0	0	0
7	0	0	0	0	0	0	0	0
8	0	0	0	0	0	0	0	0
9	0	0	0	0	0	0	0	0
10	0	0	0	0	0	0	0	0
11	0	0	0	0	0	0	0	0
12	0	0	0	0	0	0	0	0
13	0	0	0	0	0	0	0	0
14	0	0	0	0	0	0	0	0
15	0	0	0	0	0	0	0	0
16	0	0	0	0	0	0	0	0
17	0	0	0	0	0	0	0	0
18	0	0	0	0	0	0	0	0
19	0	0	0	0	0	0	0	0
20	0	0	0	0	0	0	0	0
21	0	0	0	0	0	0	0	0
22	0	0	0	0	0	0	0	0
23	0	0	0	0	0	0	0	0
24	0	0	0	0	0	0	0	0
25	0	0	0	0	0	0	0	0
26	0	0	0	0	0	0	0	0
27	0	0	0	0	0	0	0	0
28	0	0	0	0	0	0	0	0
29	0	0	0	0	0	0	0	0
30	0	0	0	0	0	0	0	0
31	70	236	35	4	10	4	0	0
32	120	499	60	9	14	8	0	0

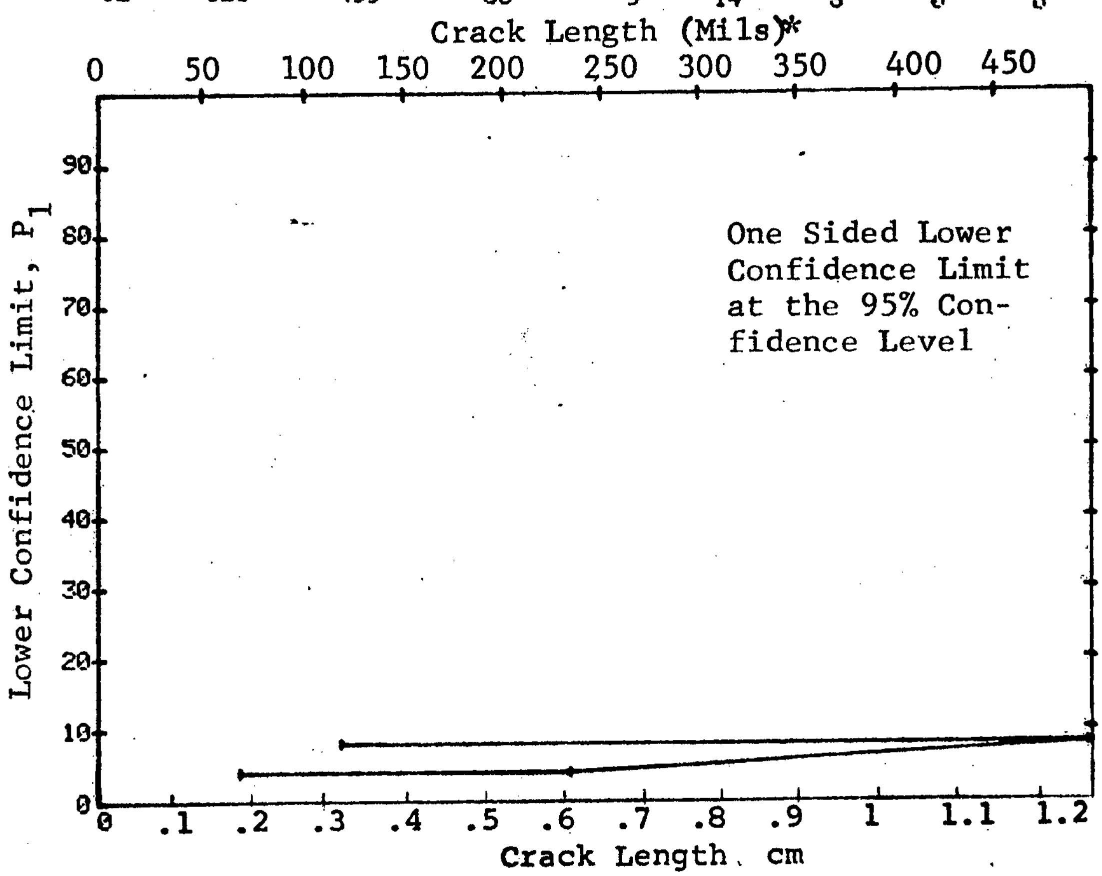

Figure D-50 (Concluded)

(a) Range Interval Method of Data Cumulation

10-OCT-75 RANGE	PENETRANT MIN LN	MAX LN	N	TEST 1 DET	50%	(51) 95%	0 MISS	1 MISS
1	52*	53 *	4	0	0	0	0	0
2	70	81	6	1	10	0	0	0
3	91	92	3	1	20	1	0	0
4	105	109	5	3	28	9	0	0
5	130	137	15	4	23	9	0	0
6	0	9	0	0	0	0	0	
7	157	162	12	2	13	3	0	
8	183	188	6	3	42	15	0	
9	190	196	3	2	50	13	0	[illegible]
10	210	212	2	2	70	22	0	0
11	236	239	2	1	29	2	0	0
12	242	248	3	3	79	36	0	0
13	262	267	2	2	70	22	0	0
14	289	290	2	2	70	22	0	0
15	0	0	0	0	0	0	0	0
16	314	321	3	3	79	36	0	0
17	327	341	3	3	79	36	0	0
18	344	358	3	3	79	36	0	0
19	362	362	1	1	50	5	0	0
20	382	389	2	2	70	22	0	0
21	0	0	0	0	0	0	0	0
22	422	423	2	2	70	22	0	0
23	428	431	2	2	70	22	0	0
24	0	0	0	0	0	0	0	0
25	461	461	1	1	50	5	0	0
26	0	0	0	0	0	0	0	0
27	498	498	1	1	50	5	0	0
28	0	0	0	0	0	0	0	0
29	0	0	0	0	0	0	0	0
30	0	0	0	0	0	0	0	0
31	576	577	2	2	70	22	0	0
32	604	604	1	1	50	5	0	0

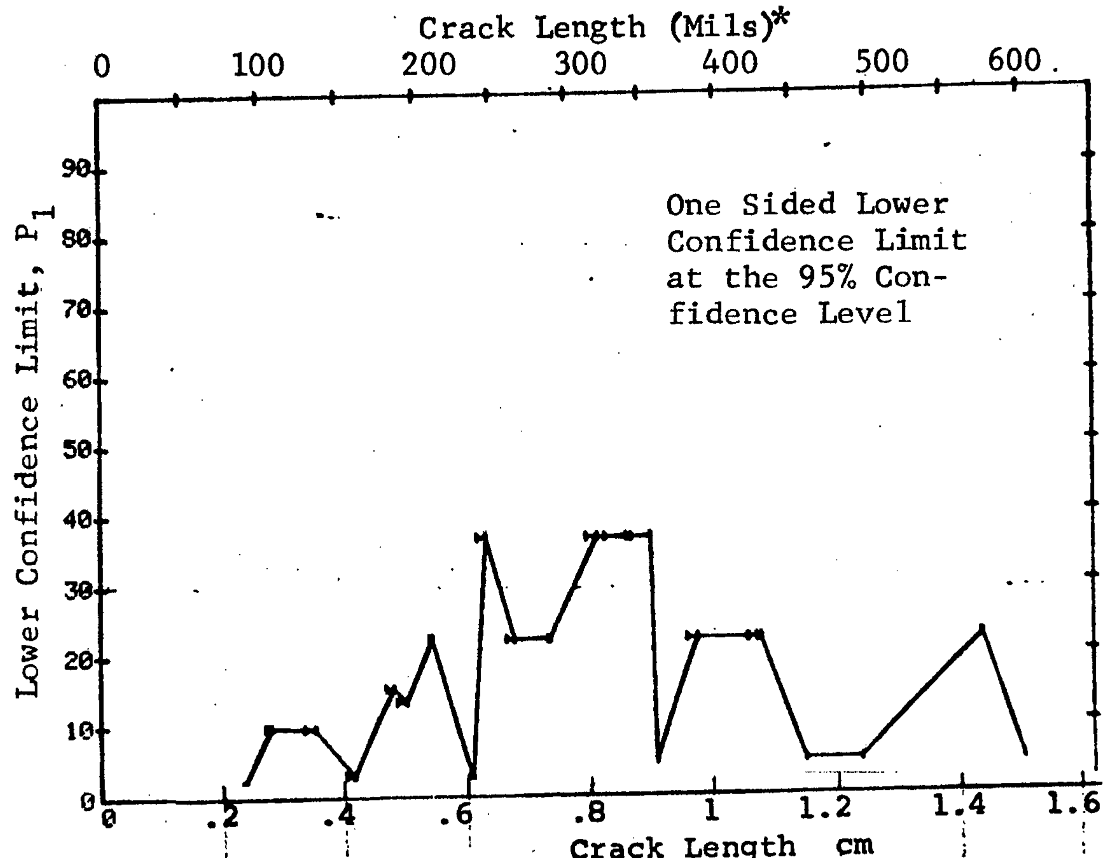

Figure D-51 Probability of Detection for 7075-T6511 Al Using Magniflux ZL-2. Fatigue Cracks in Cylindrical Shell Specimens. Lab. Env.

(b) Optimum Probability Method of Data Cumulation

10-OCT-75 PENETRANT TEST 2 (51)

RANGE	MIN LN	MAX LN	N	DET	50%	95%	0 MISS	1 MISS
1	52*	53*	4	0	0	0	0	0
2	70	[illegible]	6	1	0	0	0	0
3	70	92	9	2	0	4	0	0
4	91	109	12	4	0	12	0	0
5	91	137	27	8	0	15	0	0
6	0	0	0	0	0	0	0	0
7	91	162	39	10	0	14	0	0
8	91	188	45	13	0	18	0	0
9	183	196	9	5	0	25	0	0
10	183	212	11	7	0	34	0	0
11	183	239	13	8	0	35	0	0
12	190	248	10	8	0	49	0	0
13	210	267	9	8	0	57	0	0
14	242	290	7	7	0	65	0	0
15	0	0	0	0	0	0	0	0
16	242	321	10	10	0	74	0	0
17	242	341	13	13	0	79	0	0
18	242	358	16	16	0	82	13	30
19	242	362	17	17	0	83	12	29
20	242	389	19	19	0	85	10	27
21	0	0	0	0	0	0	0	0
22	242	423	21	21	0	86	8	25
23	242	431	23	23	0	87	6	23
24	0	0	0	0	0	0	0	0
25	242	461	24	24	0	88	5	22
26	0	0	0	0	0	0	0	0
27	242	498	25	25	0	88	4	21
28	0	0	0	0	0	0	0	0
29	0	0	0	0	0	0	0	0
30	0	0	0	0	0	0	0	0
31	242	577	27	27	0	89	2	19
32	242	604	28	28	0	89	1	18

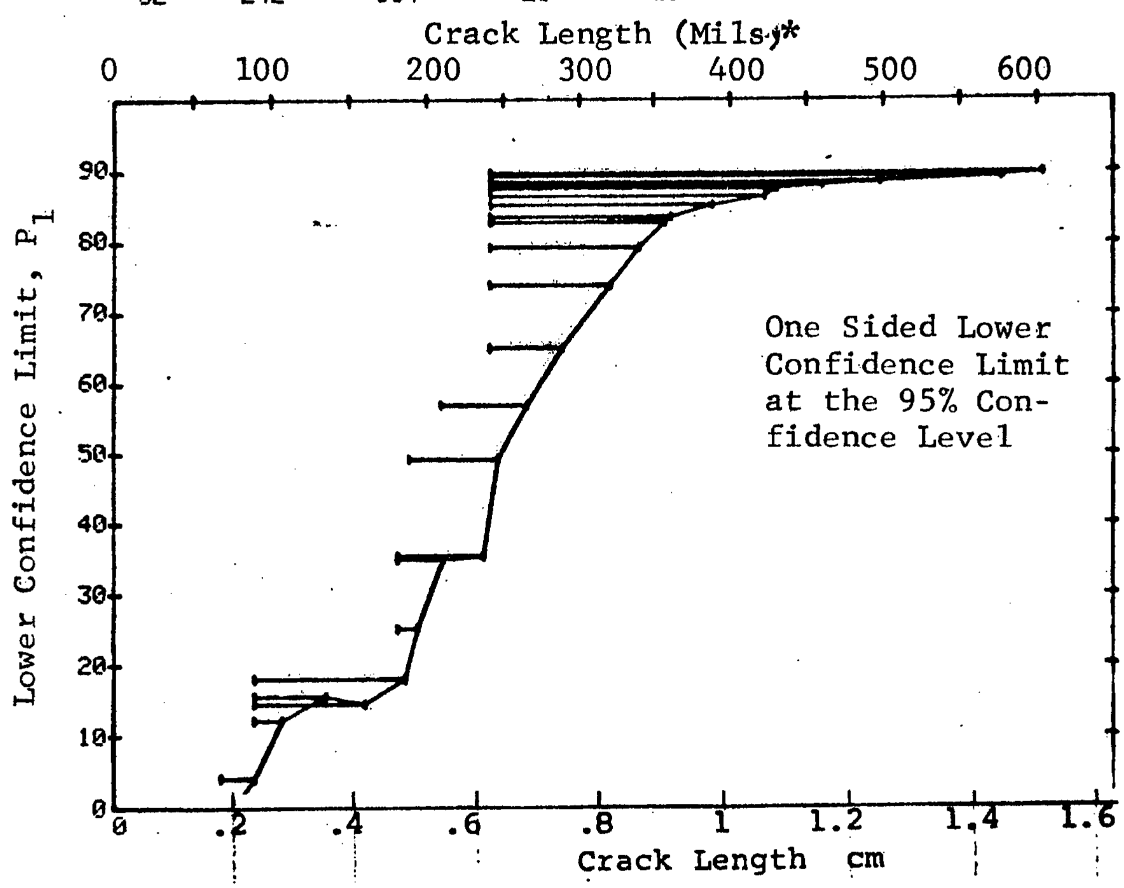

Figure D-51 (Continued)

(c) Overlapping Sixty Point Method of Data Cumulation

10-OCT-75 PENETRANT TEST 3 (51)

RANGE	MIN LN *	MAX LN *	N	DET	50%	95%	0 MISS	1 MISS
1	0	0	0	0	0	0	0	0
2	0	0	0	0	0	0	0	0
3	0	0	0	0	0	0	0	0
4	0	0	0	0	0	0	0	0
5	0	0	0	0	0	0	0	0
6	0	0	0	0	0	0	0	0
7	0	0	0	0	0	0	0	0
8	0	0	0	0	0	0	0	0
9	0	0	0	0	0	0	0	0
10	0	0	0	0	0	0	0	0
11	0	0	0	0	0	0	0	0
12	0	0	0	0	0	0	0	0
13	0	0	0	0	0	0	0	0
14	0	0	0	0	0	0	0	0
15	0	0	0	0	0	0	0	0
16	0	0	0	0	0	0	0	0
17	0	0	0	0	0	0	0	0
18	0	0	0	0	0	0	0	0
19	0	0	0	0	0	0	0	0
20	0	0	0	0	0	0	0	0
21	0	0	0	0	0	0	0	0
22	0	0	0	0	0	0	0	0
23	0	0	0	0	0	0	0	0
24	0	0	0	0	0	0	0	0
25	0	0	0	0	0	0	0	0
26	0	0	0	0	0	0	0	0
27	0	0	0	0	0	0	0	0
28	0	0	0	0	0	0	0	0
29	0	0	0	0	0	0	0	0
30	0	0	0	0	0	0	0	0
31	52	190	57	15	25	16	0	0
32	132	498	60	39	64	53	[illegible]	0

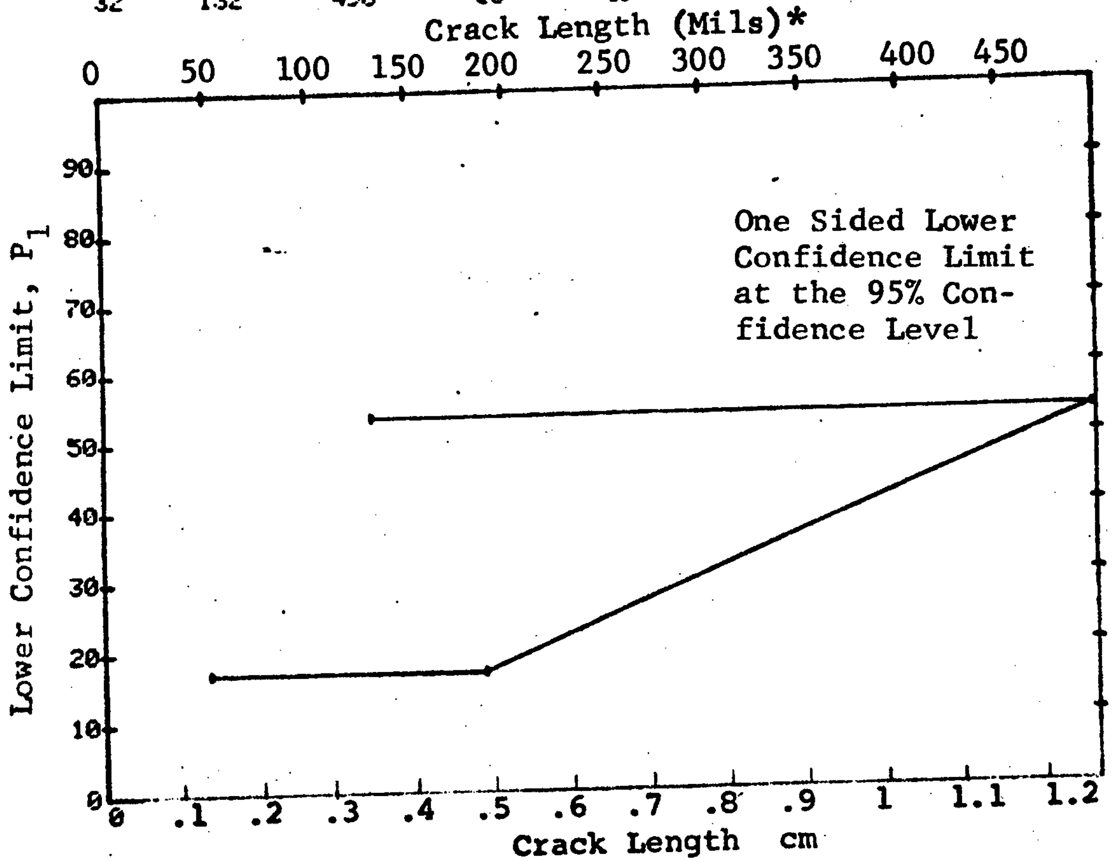

Figure D-51 (Concluded)

(a) Range Interval Method of Data Cumulation

10-OCT-75 MAGNETIC PARTICLE TEST 1 (52)

RANGE	MIN LN	MAX LN	N	DET	50%	95%	0 MISS	1 MISS
1	70 *	70 *	1	0	0	0	0	0
2	0	0	0	0	0	0	0	0
3	100	105	3	2	50	13	0	0
4	120	120	2	2	70	22	0	0
5	130	131	5	2	31	7	0	0
6	0	0	0	0	0	0	0	0
7	150	157	3	1	20	1	0	0
8	170	170	1	1	50	5	0	0
9	184	184	1	1	50	5	0	0
10	200	200	2	0	0	0	0	0
11	0	0	0	0	0	0	0	0
12	0	0	0	0	0	0	0	0
13	236	237	4	3	61	24	0	0
14	0	0	0	0	0	0	0	0
15	262	264	3	3	79	36	0	0
16	0	0	0	0	0	0	0	0
17	288	288	1	1	50	5	0	0
18	292	292	1	1	50	5	0	0
19	314	314	1	1	50	5	0	0
20	0	0	0	0	0	0	0	0
21	0	0	0	0	0	0	0	0
22	0	0	0	0	0	0	0	0
23	0	0	0	0	0	0	0	0
24	0	0	0	0	0	0	0	0
25	394	394	1	1	50	5	0	0
26	0	0	0	0	0	0	0	0
27	0	0	0	0	0	0	0	0
28	0	0	0	0	0	0	0	0
29	0	0	0	0	0	0	0	0
30	0	0	0	0	0	0	0	0
31	0	0	0	0	0	0	0	0
32	499	499	1	1	50	5	0	0

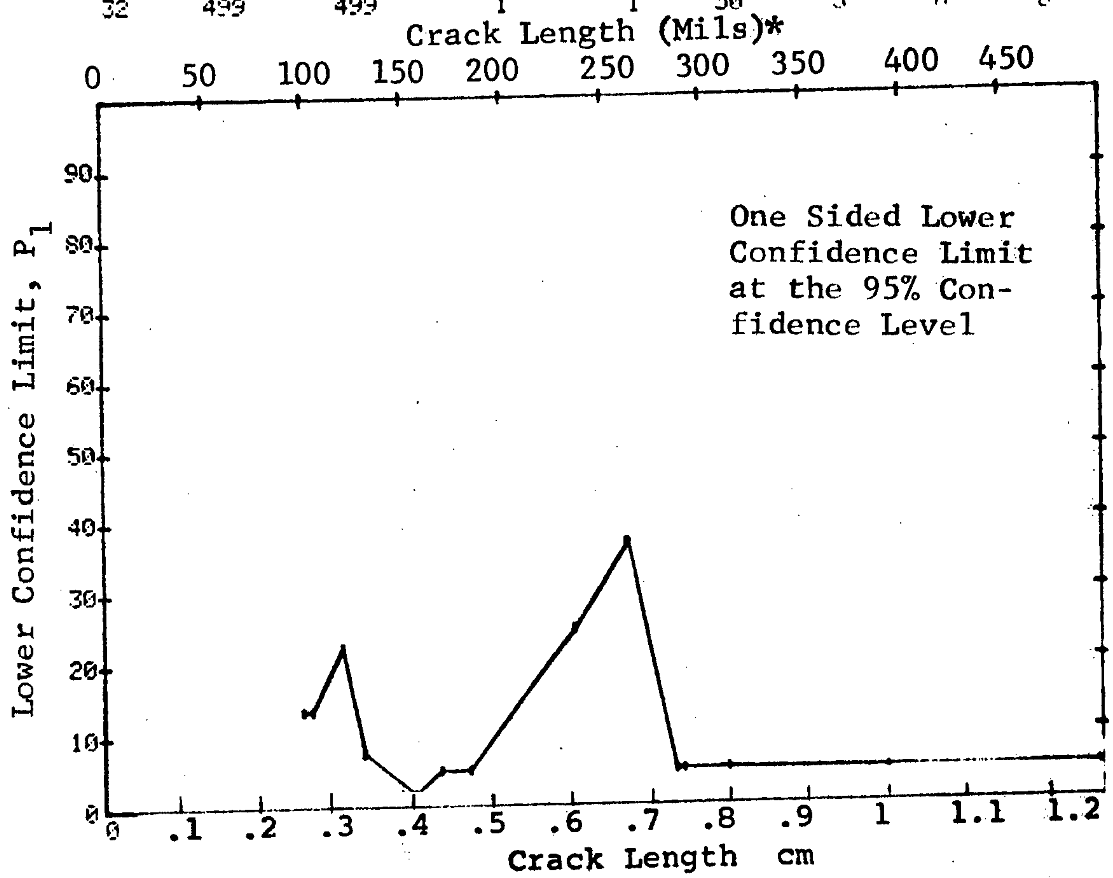

Figure D-52 Probability of Detection for 4330V Steel Using Magnetical Particle. Fatigue Cracks in Cylindrical Shell Specimens. Lab. Env.

(b) Overlapping Sixty Point Method of Data Cumulation

10-OCT-75 MAGNETIC PARTICLE TEST 2 (52)

RANGE	MIN LN	MAX LN	N	DET	50%	95%	0 MISS	1 MISS
1	70*	70*	1	0	0	0	0	0
2	0	0	0	0	0	0	0	0
3	100	105	3	2	0	13	0	0
4	100	120	5	4	0	34	0	0
5	100	131	10	6	0	30	0	0
6	0	0	0	0	0	0	0	0
7	100	157	13	7	0	28	0	0
8	100	170	14	8	0	32	0	0
9	100	184	15	9	0	35	0	0
10	100	200	17	9	0	31	0	0
11	0	0	0	0	0	0	0	0
12	0	0	0	0	0	0	0	0
13	100	237	21	12	0	37	0	0
14	0	0	0	0	0	0	0	0
15	236	264	7	6	0	47	0	0
16	0	0	0	0	0	0	0	0
17	236	288	8	7	0	52	0	0
18	236	292	9	8	0	57	0	0
19	262	314	6	6	0	60	0	0
20	0	0	0	0	0	0	0	0
21	0	0	0	0	0	0	0	0
22	0	0	0	0	0	0	0	0
23	0	0	0	0	0	0	0	0
24	0	0	0	0	0	0	0	0
25	262	394	7	7	0	65	0	0
26	0	0	0	0	0	0	0	0
27	0	0	0	0	0	0	0	0
28	0	0	0	0	0	0	0	0
29	0	0	0	0	0	0	0	0
30	0	0	0	0	0	0	0	0
31	0	0	0	0	0	0	0	0
32	262	499	8	8	0	68	0	0

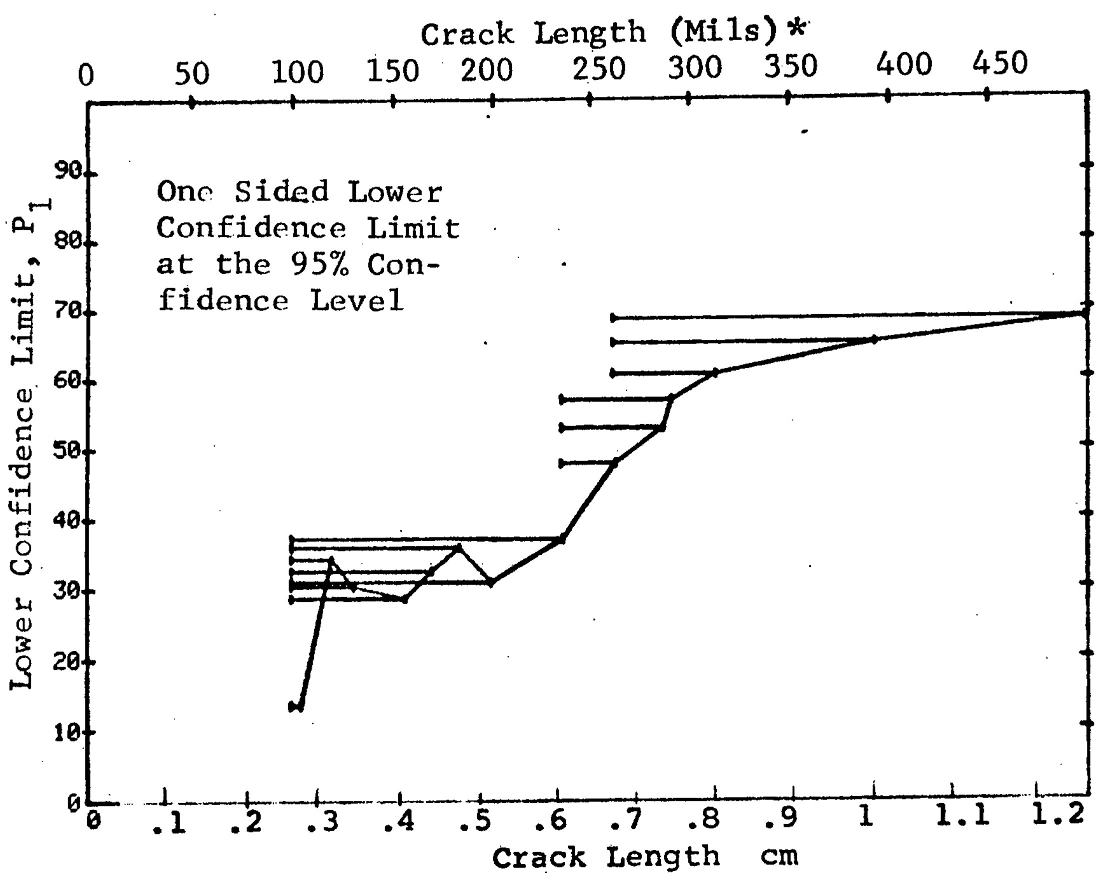

Figure D-52 (Continued)

(c) Overlapping Sixty Point Method of Data Cumulation

10-OCT-75 MAGNETIC PARTICLE TEST 3 (52)

RANGE	MIN LN	MAX LN	N	DET	50%	95%	0 MISS	1 MISS
1	0 *	0 *	0	0	0	0	0	0
2	0	0	0	0	0	0	0	0
3	0	0	0	0	0	0	0	0
4	0	0	0	0	0	0	0	0
5	0	0	0	0	0	0	0	0
6	0	0	0	0	0	0	0	0
7	0	0	0	0	0	0	0	0
8	0	0	0	0	0	0	0	0
9	0	0	0	0	0	0	0	0
10	0	0	0	0	0	0	0	0
11	0	0	0	0	0	0	0	0
12	0	0	0	0	0	0	0	0
13	0	0	0	0	0	0	0	0
14	0	0	0	0	0	0	0	0
15	0	0	0	0	0	0	0	0
16	0	0	0	0	0	0	0	0
17	0	0	0	0	0	0	0	0
18	0	0	0	0	0	0	0	0
19	0	0	0	0	0	0	0	0
20	0	0	0	0	0	0	0	0
21	0	0	0	0	0	0	0	0
22	0	0	0	0	0	0	0	0
23	0	0	0	0	0	0	0	0
24	0	0	0	0	0	0	0	0
25	0	0	0	0	0	0	0	0
26	0	0	0	0	0	0	0	0
27	0	0	0	0	0	0	0	0
28	0	0	0	0	0	0	0	0
29	0	0	0	0	0	0	0	0
30	0	0	0	0	0	0	0	0
31	0	0	0	0	0	0	0	0
32	70	499	30	20	64	50	0	0

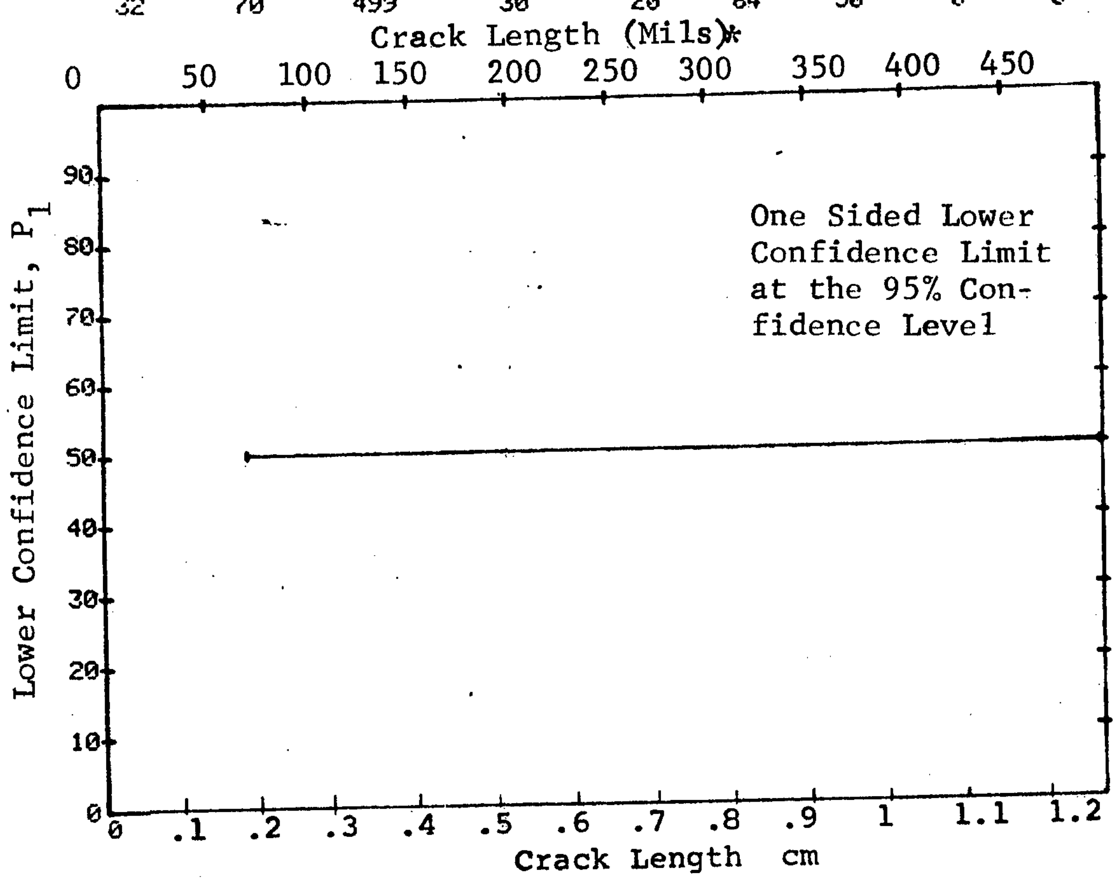

Figure D-52 (Concluded)

(a) Range Interval Method of Data Cumulation

10-OCT-75 ULTRASONIC TEST 1 (53)

RANGE	MIN LN	MAX LN	N	DET	50%	95%	0 MISS	1 MISS
1	70*	70*	1	1	50	5	0	0
2	0	0	0	0	0	0	0	0
3	100	105	4	2	38	9	0	0
4	120	120	2	1	29	2	0	0
5	130	140	10	8	74	49	0	0
6	150	150	2	2	70	22	0	0
7	157	158	5	5	87	54	0	0
8	170	170	1	1	50	5	0	0
9	184	190	3	3	79	36	0	0
10	200	200	2	1	29	2	0	0
11	212	215	2	2	70	22	0	0
12	236	236	7	7	90	65	0	0
13	0	0	0	0	0	0	0	0
14	262	264	4	4	84	47	0	0
15	0	0	0	0	0	0	0	0
16	288	292	5	5	87	54	0	0
17	0	0	0	0	0	0	0	0
18	314	315	3	3	79	36	0	0
19	0	0	0	0	0	0	0	0
20	337	344	5	4	68	34	0	0
21	0	0	0	0	0	0	0	0
22	368	368	1	1	50	5	0	0
23	0	0	0	0	0	0	0	0
24	394	394	2	2	70	22	0	0
25	420	420	1	1	50	5	0	0
26	0	0	0	0	0	0	0	0
27	0	0	0	0	0	0	0	0
28	460	460	1	1	50	5	0	0
29	472	473	2	2	70	22	0	0
30	0	0	0	0	0	0	0	0
31	499	499	1	1	50	5	0	0
32	526	526	1	1	50	5	0	0

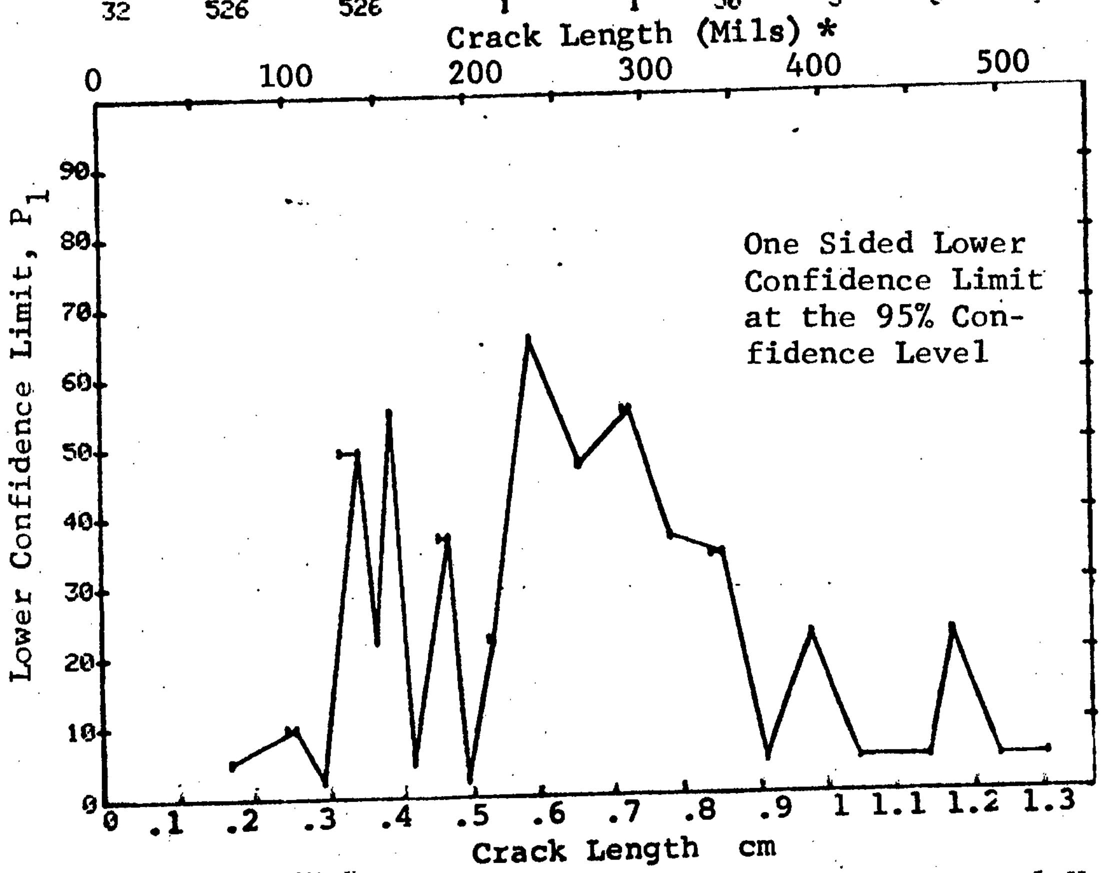

Figure D-53 Probability of Detection for 4330V Steel Using Ultrasonic Shear Wave. Fatigue Cracks in Cylindrical Shell Specimens. Lab. Env.

(b) Optimum Probability Method of Data Cumulation

10-OCT-75 ULTRASONIC TEST 2 (53)

RANGE	MIN LN *	MAX LN *	N	DET	50%	95%	0 MISS	1 MISS
1	70	70	1	1	0	5	0	0
2	0	0	0	0	0	0	0	0
3	70	105	5	3	0	18	0	0
4	70	120	7	4	0	22	0	0
5	130	140	10	6	0	49	0	0
6	130	150	12	10	0	56	0	0
7	130	158	17	15	0	67	0	0
8	130	170	18	16	0	68	0	0
9	150	190	11	11	0	76	0	0
10	130	200	23	20	0	69	0	0
11	150	215	15	14	0	72	0	0
12	150	236	22	21	0	80	24	39
13	0	0	0	0	0	0	0	0
14	150	264	26	25	0	83	20	35
15	0	0	0	0	0	0	0	0
16	150	292	31	30	0	85	15	30
17	0	0	0	0	0	0	0	0
18	150	315	34	33	0	86	12	27
19	0	0	0	0	0	0	0	0
20	150	344	39	37	0	84	22	37
21	0	0	0	0	0	0	0	0
22	150	368	40	38	0	85	21	36
23	0	0	0	0	0	0	0	0
24	150	394	42	40	0	85	19	34
25	150	420	43	41	0	86	18	33
26	0	0	0	0	0	0	0	0
27	0	0	0	0	0	0	0	0
28	150	460	44	42	0	86	17	32
29	150	473	46	44	0	86	15	30
30	0	0	0	0	0	0	0	0
31	150	499	47	45	0	87	14	29
32	150	526	48	46	0	87	13	28

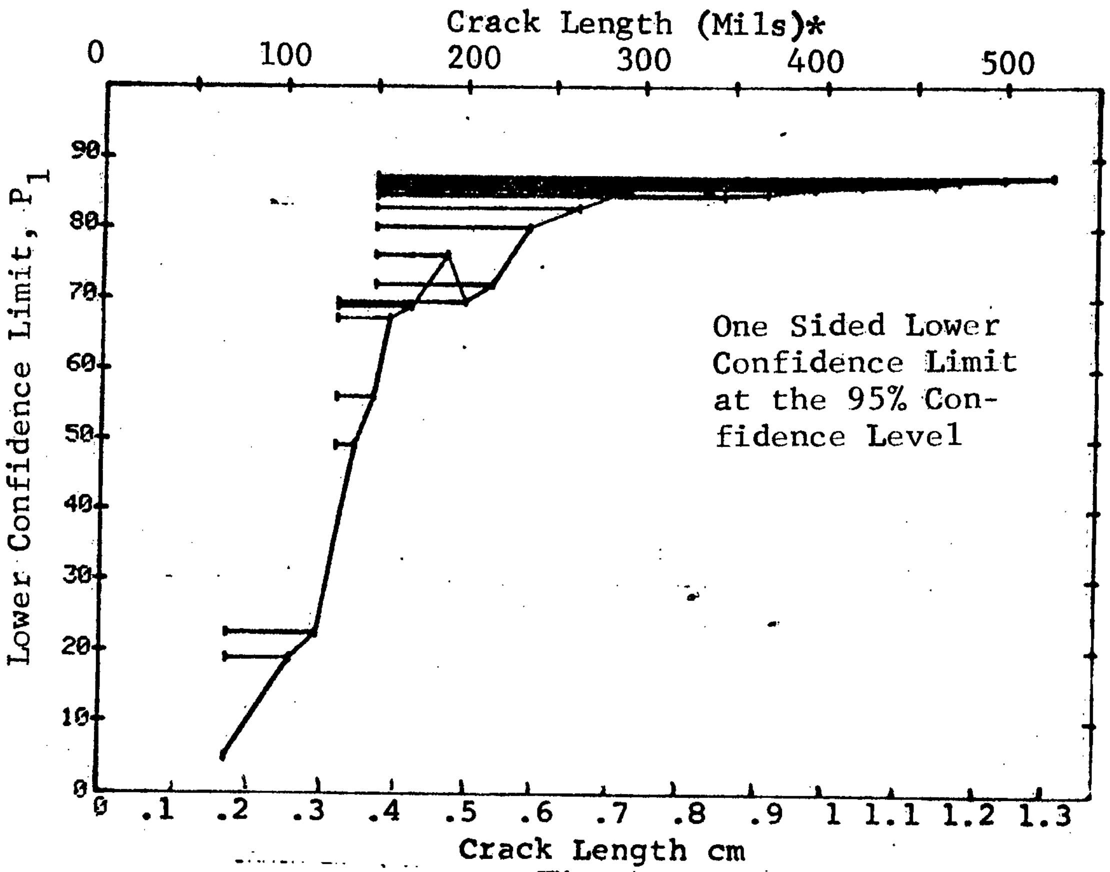

Figure D-53 (Continued)

(c) Overlapping Sixty Point Method of Data Cumulation

10-OCT-75 ULTRASONIC TEST 3 (53)

RANGE	MIN LN	MAX LN	N	DET	50%	95%	0 MISS	1 MISS
			0	0	0	0	0	0
1	0*	0*	0	0	0	0	0	0
2	0	0	0	0	0	0	0	0
3	0	0	0	0	0	0	0	0
4	0	0	0	0	0	0	0	0
5	0	0	0	0	0	0	0	0
6	0	0	0	0	0	0	0	0
7	0	0	0	0	0	0	0	0
8	0	0	0	0	0	0	0	0
9	0	0	0	0	0	0	0	0
10	0	0	0	0	0	0	0	0
11	0	0	0	0	0	0	0	0
12	0	0	0	0	0	0	0	0
13	0	0	0	0	0	0	0	0
14	0	0	0	0	0	0	0	0
15	0	0	0	0	0	0	0	0
16	0	0	0	0	0	0	0	0
17	0	0	0	0	0	0	0	0
18	0	0	0	0	0	0	0	0
19	0	0	0	0	0	0	0	0
20	0	0	0	0	0	0	0	0
21	0	0	0	0	0	0	0	0
22	0	0	0	0	0	0	0	0
23	0	0	0	0	0	0	0	0
24	0	0	0	0	0	0	0	0
25	0	0	0	0	0	0	0	0
26	0	0	0	0	0	0	0	0
27	0	0	0	0	0	0	0	0
28	0	0	0	0	0	0	0	0
29	0	0	0	0	0	0	0	0
30	0	0	0	0	0	0	0	0
31	70	236	34	28	80	68	0	0
32	105	499	60	55	90	83	43	56

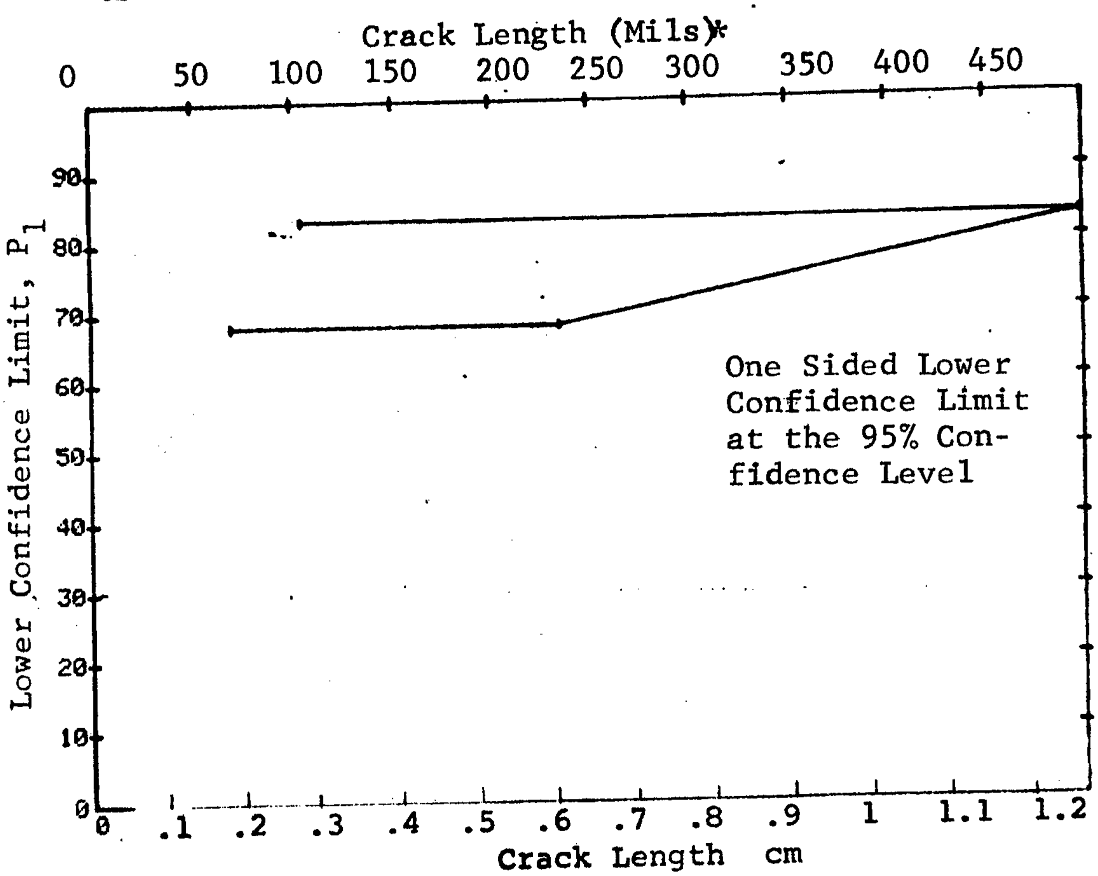

Figure D-53 (Concluded)

(a) Range Interval Method of Data Cumulation

10-OCT-75 ULTRASONIC TEST 1 (54)

RANGE	MIN LN	MAX LN	N	DET	50%	95%	0 MISS	1 MISS
1	52*	53*	4	1	15	1	0	0
2	70	81	6	2	26	6	0	0
3	91	92	3	3	79	36	0	0
4	105	109	9	6	60	34	0	0
5	130	137	15	9	56	35	0	0
6	0	0	0	0	0	0	0	0
7	157	162	12	6	45	24	0	0
8	183	188	6	4	57	27	0	0
9	190	196	3	1	20	1	0	0
10	210	212	2	2	70	22	0	0
11	234	236	2	2	70	22	0	0
12	242	248	3	3	79	36	0	0
13	262	267	2	2	70	22	0	0
14	290	290	2	2	70	22	0	0
15	0	0	0	0	0	0	0	0
16	314	322	3	3	79	36	0	0
17	327	330	2	2	70	22	0	0
18	342	358	4	3	61	24	0	0
19	362	362	1	0	0	0	0	0
20	382	389	2	2	70	22	0	0
21	0	0	0	0	0	0	0	0
22	422	423	2	2	70	22	0	0
23	428	431	2	2	70	22	0	0
24	0	0	0	0	0	0	0	0
25	461	461	1	1	50	5	0	0
26	0	0	0	0	0	0	0	0
27	498	498	1	1	50	5	0	0
28	0	0	0	0	0	0	0	0
29	0	0	0	0	0	0	0	0
30	0	0	0	0	0	0	0	0
31	576	577	2	2	70	22	0	0
32	604	604	1	1	50	5	0	0

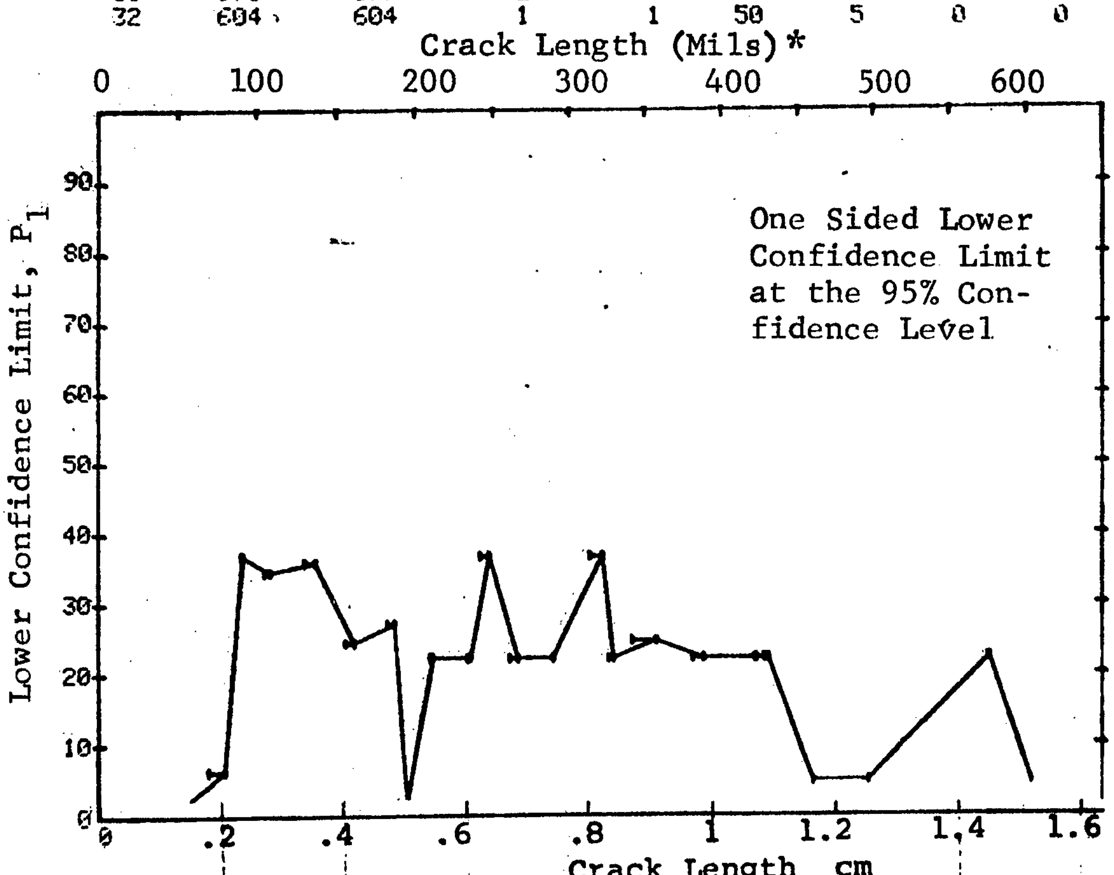

Figure D-54 Probability of Detection for 7075-T6511 Al Using Ultrasonic Shear Wave. Fatigue Cracks in Cylindrical Shell Specimens. Lab. Env..

(b) Optimum Probability Method of Data Cumulation

10-OCT-75 ULTRASONIC TEST 2 (54)

RANGE	MIN LN	MAX LN	N	DET	50%	95%	0 MISS	1 MISS
1	52 *	53*	4	1	0	1	0	0
2	52	81	10	3	0	8	0	0
3	91	92	3	3	0	36	0	0
4	91	109	12	9	0	47	0	0
5	91	137	27	18	0	49	0	0
6	0	0	0	0	0	0	0	0
7	91	162	39	24	0	47	0	0
8	91	188	45	28	0	48	0	0
9	91	196	48	29	0	47	0	0
10	91	212	50	31	0	49	0	0
11	91	236	52	33	0	51	0	0
12	210	248	7	7	0	65	0	0
13	210	267	9	9	0	71	0	0
14	210	290	11	11	0	76	0	0
15	0	0	0	0	0	0	0	0
16	210	322	14	14	0	80	15	32
17	210	330	16	16	0	82	13	30
18	210	358	20	19	0	78	0	0
19	210	362	21	19	0	72	0	0
20	210	389	23	21	0	75	0	0
21	0	0	0	0	0	0	0	0
22	210	423	25	23	0	76	0	0
23	210	431	27	25	0	78	0	0
24	0	0	0	0	0	0	0	0
25	210	461	28	26	0	79	0	0
26	0	0	0	0	0	0	0	0
27	210	498	29	27	0	79	0	0
28	0	0	0	0	0	0	0	0
29	0	0	0	0	0	0	0	0
30	0	0	0	0	0	0	0	0
31	210	577	31	29	0	81	30	45
32	210	604	32	30	0	81	29	44

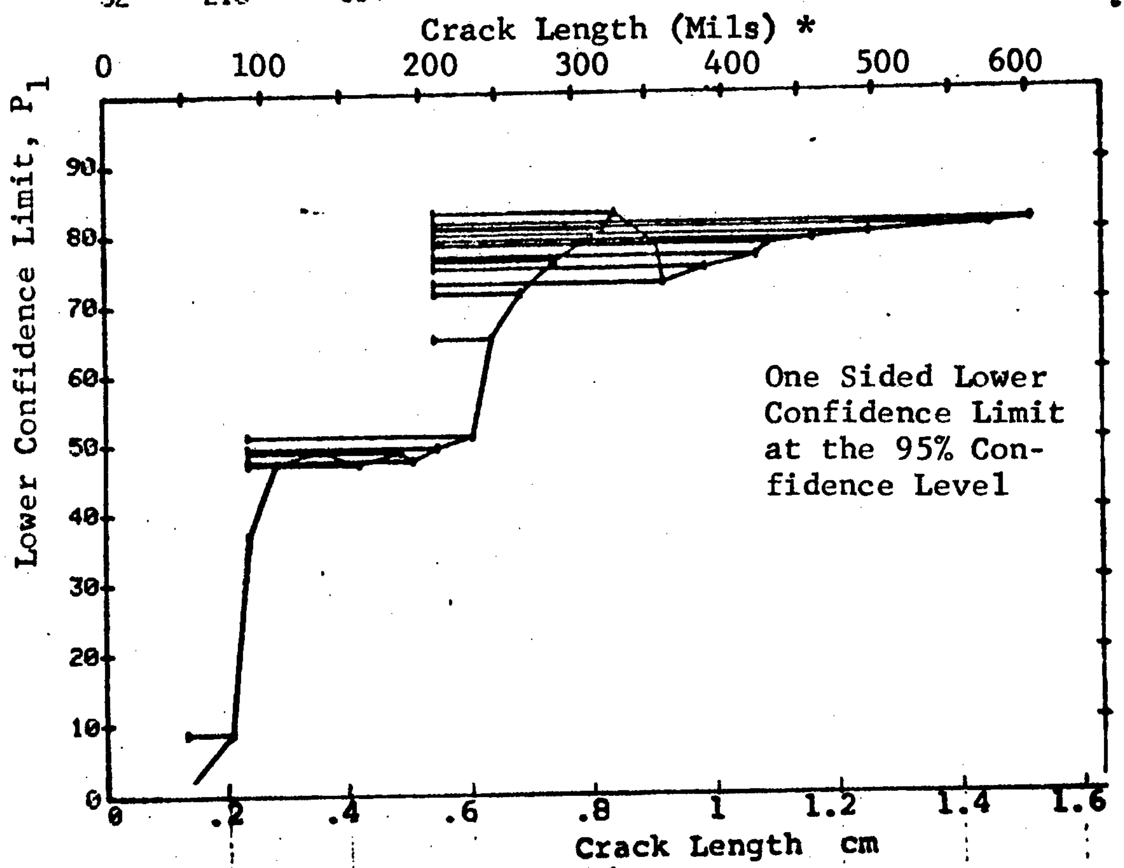

Figure D-54 (Continued)

(c) Overlapping Sixty Point Method of Data Cumulation

10-OCT-75 ULTRASONIC TEST 3 (54)

RANGE	MIN LN *	MAX LN *	N	DET	50%	95%	0 MISS	1 MISS
1	0	0	0	0	0	0	0	0
2	0	0	0	0	0	0	0	0
3	0	0	0	0	0	0	0	0
4	0	0	0	0	0	0	0	0
5	0	0	0	0	0	0	0	0
6	0	0	0	0	0	0	0	0
7	0	0	0	0	0	0	0	0
8	0	0	0	0	0	0	0	0
9	0	0	0	0	0	0	0	0
10	0	0	0	0	0	0	0	0
11	0	0	0	0	0	0	0	0
12	0	0	0	0	0	0	0	0
13	0	0	0	0	0	0	0	0
14	0	0	0	0	0	0	0	0
15	0	0	0	0	0	0	0	0
16	0	0	0	0	0	0	0	0
17	0	0	0	0	0	0	0	0
18	0	0	0	0	0	0	0	0
19	0	0	0	0	0	0	0	0
20	0	0	0	0	0	0	0	0
21	0	0	0	0	0	0	0	0
22	0	0	0	0	0	0	0	0
23	0	0	0	0	0	0	0	0
24	0	0	0	0	0	0	0	0
25	0	0	0	0	0	0	0	0
26	0	0	0	0	0	0	0	0
27	0	0	0	0	0	0	0	0
28	0	0	0	0	0	0	0	0
29	0	0	0	0	0	0	0	0
30	0	0	0	0	0	0	0	0
31	52	190	57	32	55	44	0	0
32	132	498	60	44	72	62	0	0

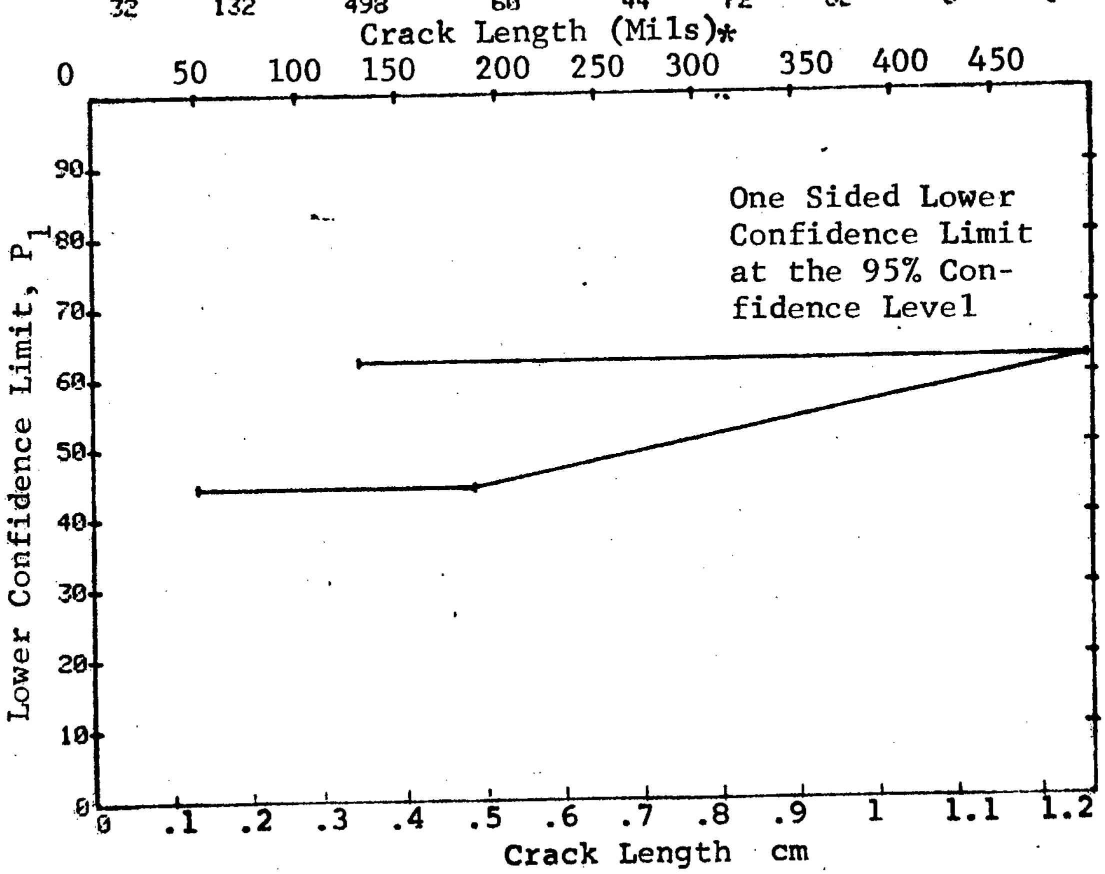

Figure D-54 (Concluded)

(a) Range Interval Method of Data Cumulation

10-OCT-75 RADIOGRAPHY TEST 1 (55)

RANGE	MIN LN	MAX LN	N	DET	50%	95%	0 MISS	1 MISS
1	52*	53*	4	0	0	0	0	0
2	70	81	6	1	10	0	0	0
3	91	92	3	0	0	0	0	0
4	105	109	9	0	0	0	0	0
5	130	137	15	0	0	0	0	0
6	0	0	0	0	0	0	0	0
7	157	162	12	0	0	0	0	0
8	183	188	6	0	0	0	0	0
9	190	196	3	0	0	0	0	0
10	210	212	2	0	0	0	0	0
11	236	236	1	0	0	0	0	0
12	240	248	4	0	0	0	0	0
13	262	267	2	0	0	0	0	0
14	290	290	2	0	0	0	0	0
15	0	0	0	0	0	0	0	0
16	314	322	3	0	0	0	0	0
17	327	330	2	0	0	0	0	0
18	342	358	4	2	38	9	0	0
19	362	362	1	0	0	0	0	0
20	382	389	2	2	70	22	0	0
21	0	0	0	0	0	0	0	0
22	422	423	2	0	0	0	0	0
23	428	431	2	1	29	2	0	0
24	0	0	0	0	0	0	0	0
25	461	461	1	1	50	5	0	0
26	0	0	0	0	0	0	0	0
27	498	498	1	1	50	5	0	0
28	0	0	0	0	0	0	0	0
29	0	0	0	0	0	0	0	0
30	0	0	0	0	0	0	0	0
31	576	577	2	2	70	22	0	0
32	604	604	1	0	0	0	0	0

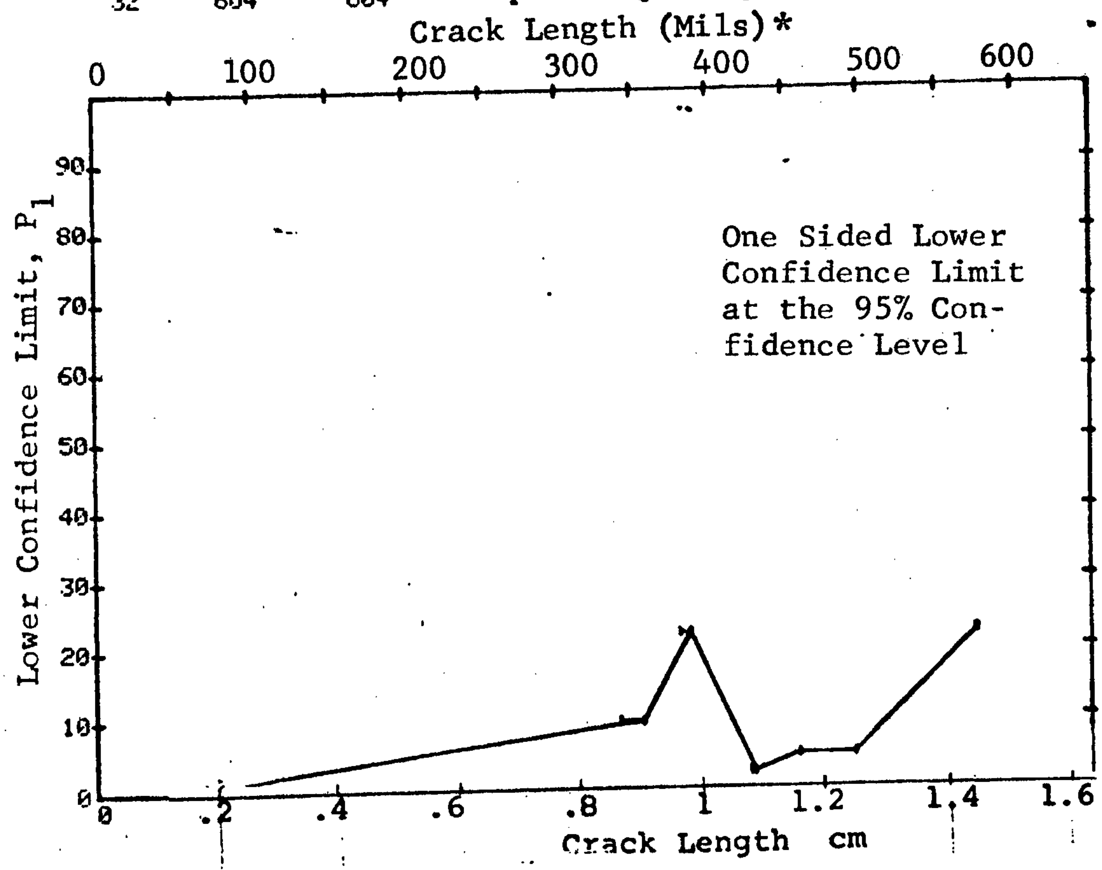

Figure D-55 Probability of Detection for 7075-T6511 Al Using X-ray. Fatigue Cracks in Cylindrical Shell. Lab. Env.

(b) Optimum Probability Method of Data Cumulation

10-OCT-75 RADIOGRAPHY TEST 2 (55)

RANGE	MIN LN *	MAX LN *	N	DET	50%	95%	0 MISS	1 MISS
1	52	53	4	0	0	0	0	0
2	70	81	6	1	0	0	0	0
3	70	92	9	1	0	0	0	0
4	70	109	18	1	0	0	0	0
5	70	137	33	1	0	0	0	0
6	0	0	0	0	0	0	0	0
7	70	162	45	1	0	0	0	0
8	70	188	51	1	0	0	0	0
9	70	196	54	1	0	0	0	0
10	70	212	56	1	0	0	0	0
11	70	236	57	1	0	0	0	0
12	70	248	61	1	0	0	0	0
13	70	267	63	1	0	0	0	0
14	70	290	65	1	0	0	0	0
15	0	0	0	0	0	0	0	0
16	70	322	68	1	0	0	0	0
17	70	330	70	1	0	0	0	0
18	342	358	4	2	0	9	0	0
19	342	362	5	2	0	7	0	0
20	342	389	7	4	0	22	0	0
21	0	0	0	0	0	0	0	0
22	342	423	9	4	0	16	0	0
23	342	431	11	5	0	19	0	0
24	0	0	0	0	0	0	0	0
25	342	461	12	6	0	24	0	0
26	0	0	0	0	0	0	0	0
27	382	498	8	5	0	28	0	0
28	0	0	0	0	0	0	0	0
29	0	0	0	0	0	0	0	0
30	0	0	0	0	0	0	0	0
31	461	577	4	4	0	47	0	0
32	382	604	11	7	0	34	0	0

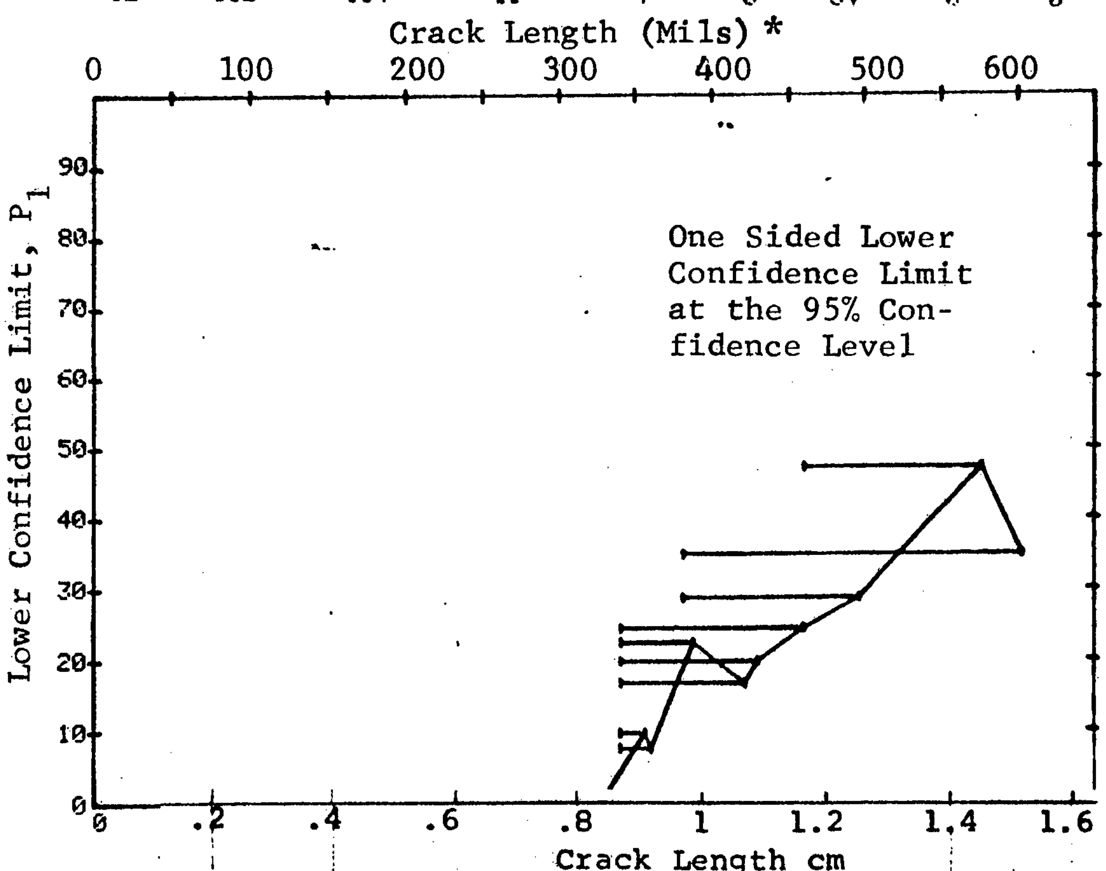

Figure D-55 (Continued)

(c) Overlapping Sixty Point Method of Data Cumulation

10-OCT-75 RADIOGRAPHY TEST 3 (55)

RANGE	MIN LN	MAX LN	N	DET	50%	95%	0 MISS	1 MISS
1	0 *	0 *	0	0	0	0	0	0
2	0	0	0	0	0	0	0	0
3	0	0	0	0	0	0	0	0
4	0	0	0	0	0	0	0	0
5	0	0	0	0	0	0	0	0
6	0	0	0	0	0	0	0	0
7	0	0	0	0	0	0	0	0
8	0	0	0	0	0	0	0	0
9	0	0	0	0	0	0	0	0
10	0	0	0	0	0	0	0	0
11	0	0	0	0	0	0	0	0
12	0	0	0	0	0	0	0	0
13	0	0	0	0	0	0	0	0
14	0	0	0	0	0	0	0	0
15	0	0	0	0	0	0	0	0
16	0	0	0	0	0	0	0	0
17	0	0	0	0	0	0	0	0
18	0	0	0	0	0	0	0	0
19	0	0	0	0	0	0	0	0
20	0	0	0	0	0	0	0	0
21	0	0	0	0	0	0	0	0
22	0	0	0	0	0	0	0	0
23	0	0	0	0	0	0	0	0
24	0	0	0	0	0	0	0	0
25	0	0	0	0	0	0	0	0
26	0	0	0	0	0	0	0	0
27	0	0	0	0	0	0	0	0
28	0	0	0	0	0	0	0	0
29	0	0	0	0	0	0	0	0
30	0	0	0	0	0	0	0	0
31	52	190	57	1	1	0	0	0
32	132	498	60	7	11	5	0	0

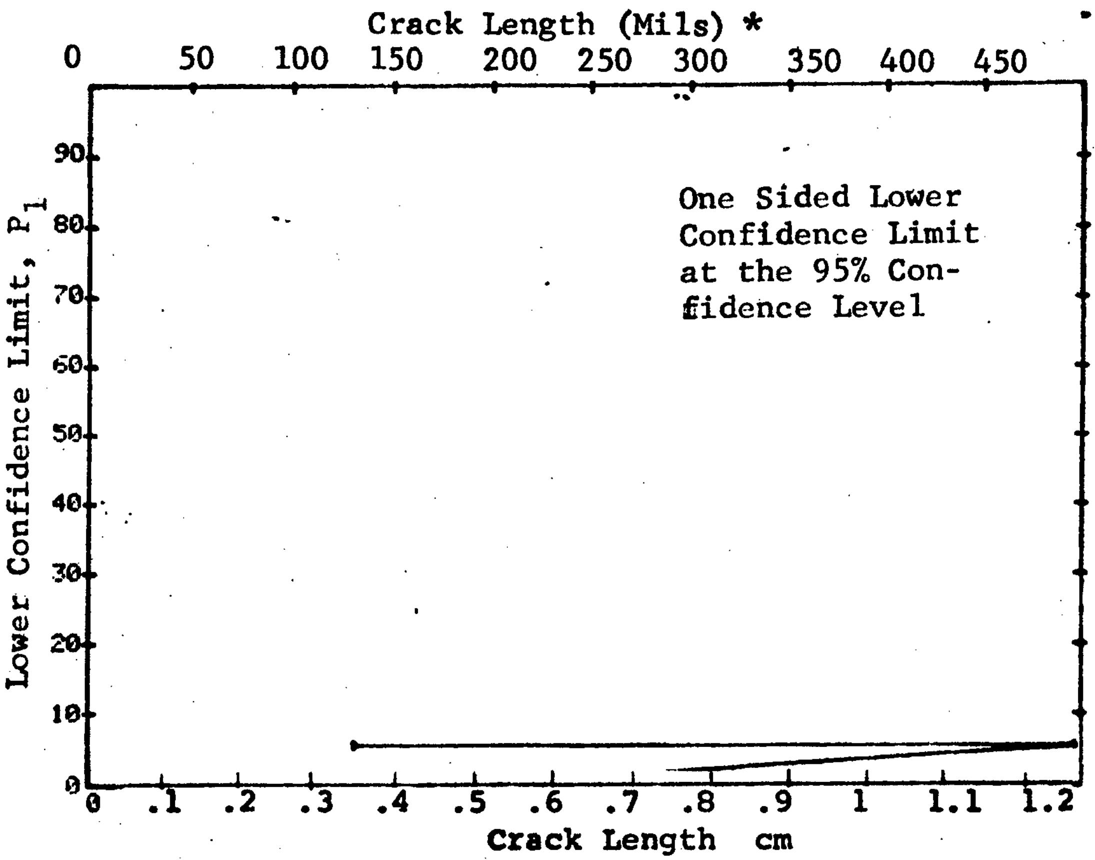

Figure D-55 (Concluded)

(a) Range Interval Method of Data Cumulation

10-OCT-75 RADIOGRAPHY TEST 1 (56)

RANGE	MIN LN *	MAX LN *	N	DET	50%	95%	0 MISS	1 MISS
1	70	70	1	0	0	0	0	0
2	0	0	0	0	0	0	0	0
3	100	105	4	0	0	0	0	0
4	120	120	2	0	0	0	0	0
5	130	140	11	0	0	0	0	0
6	150	150	2	0	0	0	0	0
7	157	158	5	0	0	0	0	0
8	170	170	1	0	0	0	0	0
9	184	190	3	0	0	0	0	0
10	200	200	2	0	0	0	0	0
11	212	215	2	0	0	0	0	0
12	236	236	7	0	0	0	0	0
13	0	0	0	0	0	0	0	0
14	262	264	4	1	15	1	0	0
15	0	0	0	0	0	0	0	0
16	288	292	5	0	0	0	0	0
17	0	0	0	0	0	0	0	0
18	314	315	3	0	0	0	0	0
19	0	0	0	0	0	0	0	0
20	337	344	5	1	12	1	0	0
21	0	0	0	0	0	0	0	0
22	368	368	1	0	0	0	0	0
23	0	0	0	0	0	0	0	0
24	394	394	2	0	0	0	0	0
25	420	420	1	0	0	0	0	0
26	0	0	0	0	0	0	0	0
27	446	446	1	0	0	0	0	0
28	0	0	0	0	0	0	0	0
29	472	473	2	1	29	2	0	0
30	0	0	0	0	0	0	0	0
31	499	499	1	1	50	5	0	0
32	526	526	1	1	50	5	0	0

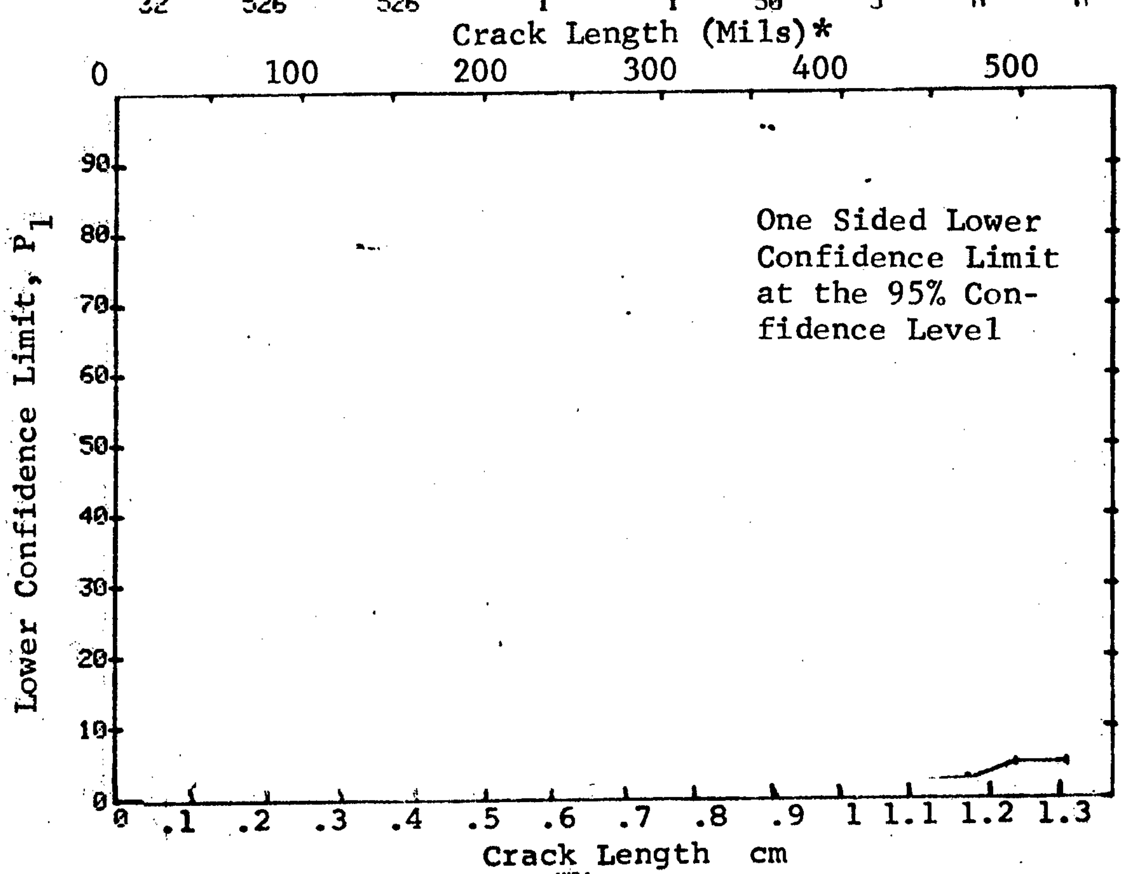

Figure D-56 Probability of Detection for 4330V Steel Using X-ray. Fatigue Cracks in Cylindrical Shell. Lab. Env.

(b) Optimum Probability Method of Data Cumulation

10-OCT-75 RADIOGRAPHY TEST 2 (56)

RANGE	MIN LN	*MAX LN*	N	DET	50%	95%	0 MISS	1 MISS
1	70	70	1	0	0	0	0	0
2	0	0	0	0	0	0	0	0
3	100	105	4	0	0	0	0	0
4	120	120	2	0	0	0	0	0
5	130	140	11	0	0	0	0	0
6	150	150	2	0	0	0	0	0
7	157	158	5	0	0	0	0	0
8	170	170	1	0	0	0	0	0
9	184	190	3	0	0	0	0	0
10	200	200	2	0	0	0	0	0
11	212	215	2	0	0	0	0	0
12	236	236	7	0	0	0	0	0
13	0	0	0	0	0	0	0	0
14	262	264	4	1	0	1	0	0
15	0	0	0	0	0	0	0	0
16	262	292	9	1	0	0	0	0
17	0	0	0	0	0	0	0	0
18	262	315	12	1	0	0	0	0
19	0	0	0	0	0	0	0	0
20	262	344	17	2	0	2	0	0
21	0	0	0	0	0	0	0	0
22	262	368	18	2	0	2	0	0
23	0	0	0	0	0	0	0	0
24	262	394	20	2	0	1	0	0
25	262	420	21	2	0	1	0	0
26	0	0	0	0	0	0	0	0
27	262	446	22	2	0	1	0	0
28	0	0	0	0	0	0	0	0
29	262	473	24	3	0	3	0	0
30	0	0	0	0	0	0	0	0
31	472	499	3	2	0	13	0	0
32	472	526	4	3	0	24	0	0

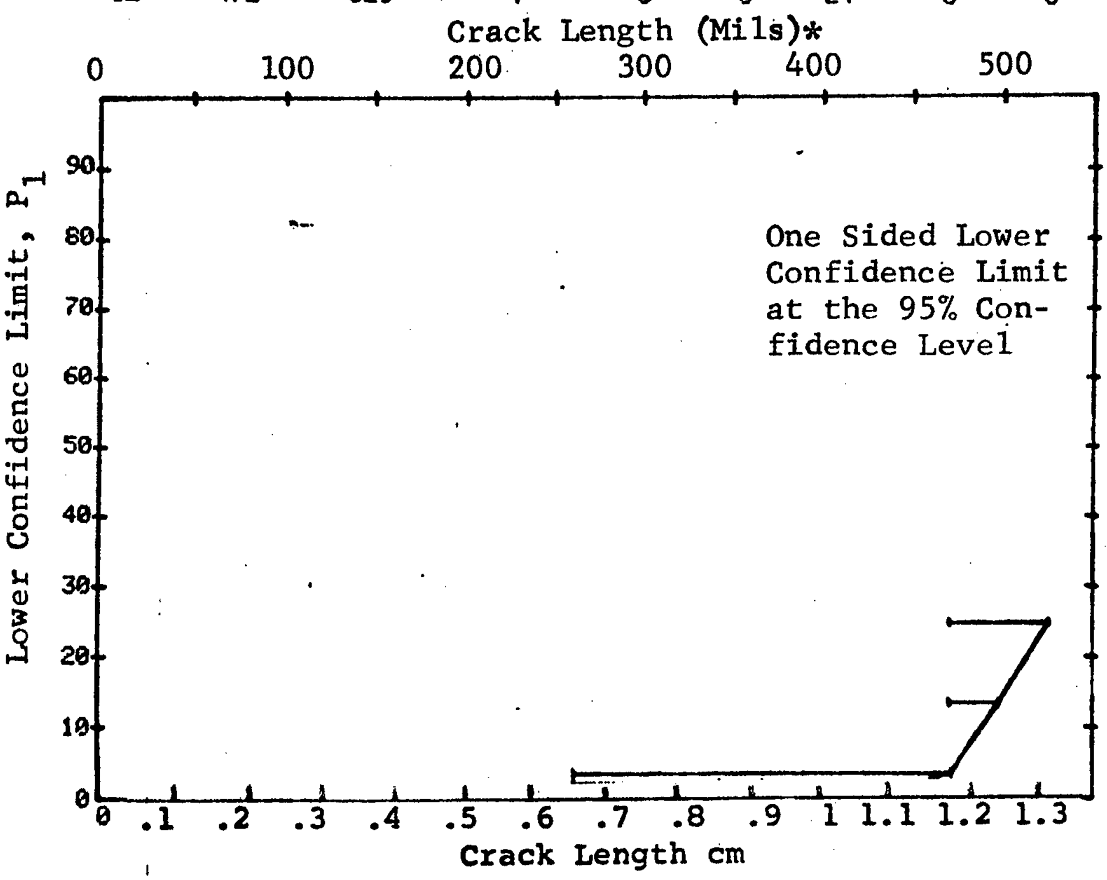

Figure D-56 (Continued)

(c) Overlapping Sixty Point Method of Data Cumulation

10-OCT-75 RADIOGRAPHY TEST 3 (56)

RANGE	MIN LN *	MAX LN *	N	DET	50%	95%	0 MISS	1 MISS
1	0	0	0	0	0	0	0	0
2	0	0	0	0	0	0	0	0
3	0	0	0	0	0	0	0	0
4	0	0	0	0	0	0	0	0
5	0	0	0	0	0	0	0	0
6	0	0	0	0	0	0	0	0
7	0	0	0	0	0	0	0	0
8	0	0	0	0	0	0	0	0
9	0	0	0	0	0	0	0	0
10	0	0	0	0	0	0	0	0
11	0	0	0	0	0	0	0	0
12	0	0	0	0	0	0	0	0
13	0	0	0	0	0	0	0	0
14	0	0	0	0	0	0	0	0
15	0	0	0	0	0	0	0	0
16	0	0	0	0	0	0	0	0
17	0	0	0	0	0	0	0	0
18	0	0	0	0	0	0	0	0
19	0	0	0	0	0	0	0	0
20	0	0	0	0	0	0	0	0
21	0	0	0	0	0	0	0	0
22	0	0	0	0	0	0	0	0
23	0	0	0	0	0	0	0	0
24	0	0	0	0	0	0	0	0
25	0	0	0	0	0	0	0	0
26	0	0	0	0	0	0	0	0
27	0	0	0	0	0	0	0	0
28	0	0	0	0	0	0	0	0
29	0	0	0	0	0	0	0	0
30	0	0	0	0	0	0	0	0
31	70	236	35	0	0	0	0	0
32	120	499	60	4	6	2	0	0

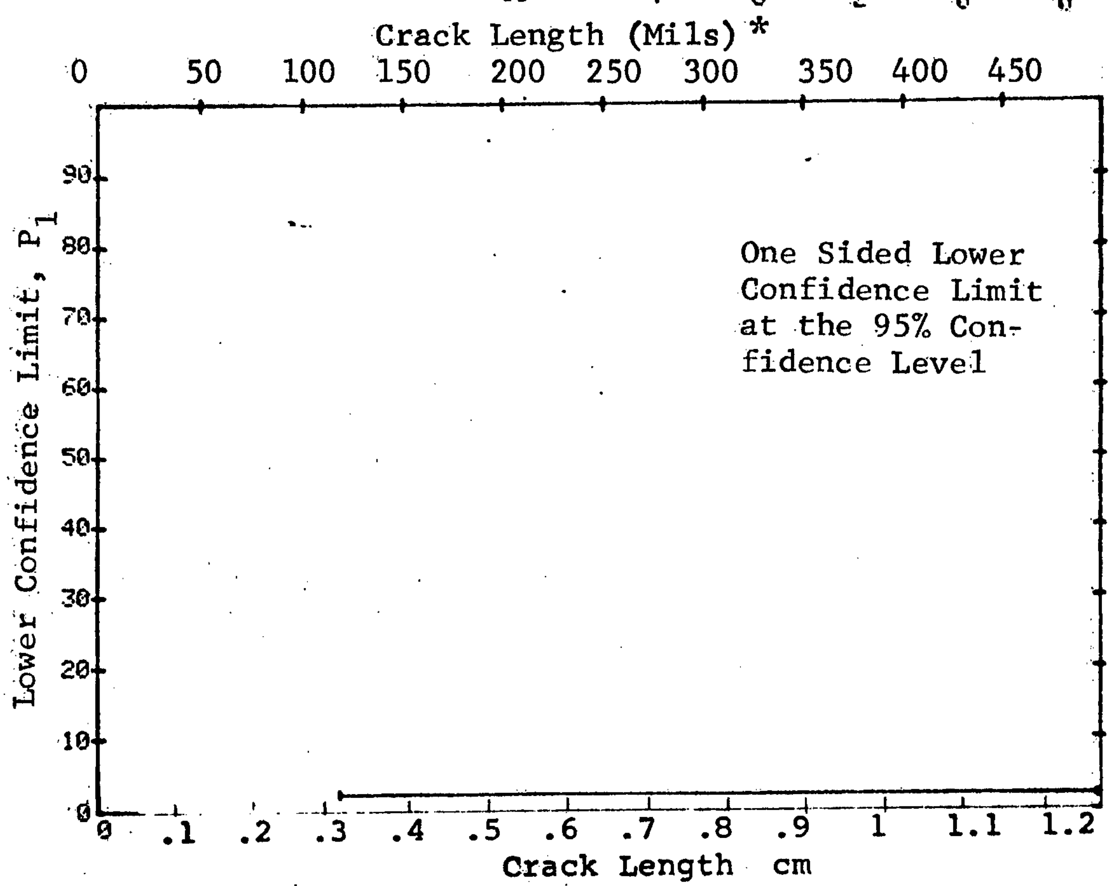

Figure D-56 (Concluded)

(a) Range Interval Method of Data Cumulation

17-OCT-75 TEST 1 (57)

RANGE	MIN LN		MAX LN		N	DET	50%	95%	0 MISS	1 MISS
1	5	*	29	*	154	19	12	8	0	0
2	30		51		87	22	24	17	0	0
3	54		74		25	14	53	37	0	0
4	78		100		19	7	34	18	0	0
5	105		125		10	9	83	60	0	0
6	127		142		8	7	79	52	0	0
7	150		168		10	6	54	30	0	0
8	179		194		4	4	84	47	0	0
9	200		220		7	6	77	47	0	0
10	230		243		3	3	79	36	0	0
11	252		265		4	4	84	47	0	0
12	271		271		1	0	0	0	0	0
13	296		307		2	1	29	2	0	0
14	320		339		2	2	70	22	0	0
15	346		353		2	2	70	22	0	0
16	0		0		0	0	0	0	0	0
17	392		408		2	1	29	2	0	0
18	0		0		0	0	0	0	0	0
19	0		0		0	0	0	0	0	0
20	0		0		0	0	0	0	0	0
21	0		0		0	0	0	0	0	0
22	533		533		1	1	50	5	0	0
23	0		0		0	0	0	0	0	0
24	0		0		0	0	0	0	0	0
25	0		0		0	0	0	0	0	0
26	0		0		0	0	0	0	0	0
27	0		0		0	0	0	0	0	0
28	0		0		0	0	0	0	0	0
29	687		687		1	1	50	5	0	0
30	0		0		0	0	0	0	0	0
31	0		0		0	0	0	0	0	0
32	774		774		1	1	50	5	0	0

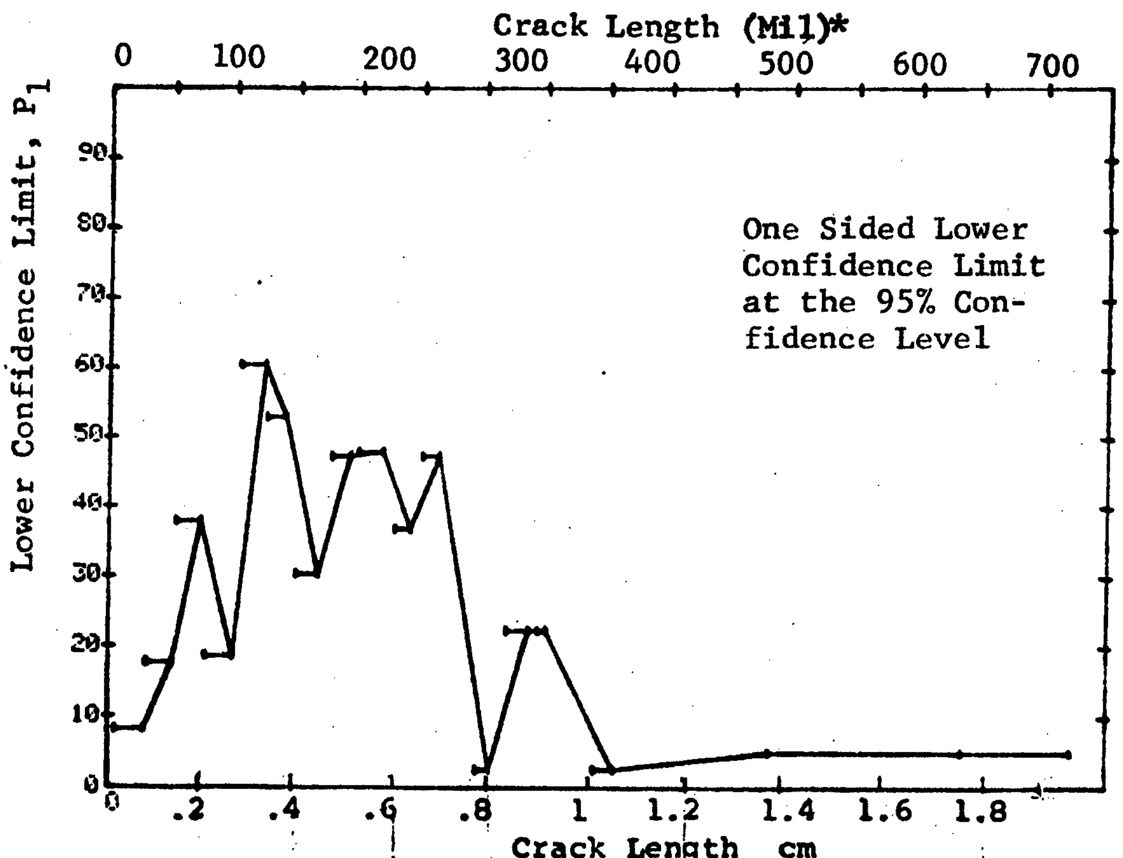

Figure D-57 Probability of Detection for 7178-T651 Al Using Eddy Current. Fatigue Cracks in Fastener Holes Measured by Team 2. Field Env.

(b) Optimum Probability Method of Data Cumulation

17-OCT-75 TEST 2 (57)

RANGE	MIN LN	MAX LN	N	DET	50%	95%	0 MISS	1 MISS
1	5	* [illegible] *	154	17	0	8	0	0
2	30	51	37	[illegible]	0	17	0	0
3	54	74	25	14	0	37	0	0
4	54	100	44	21	0	34	0	0
5	105	125	10	9	0	60	0	0
6	105	142	18	16	0	68	0	0
7	105	168	28	22	0	62	0	0
8	105	194	32	26	0	66	0	0
9	105	220	39	32	0	68	0	0
10	105	243	42	35	0	70	0	0
11	179	265	18	17	0	76	0	0
12	105	271	47	39	0	71	0	0
13	105	307	49	40	0	70	0	0
14	105	339	51	42	0	71	0	0
15	105	353	53	44	0	72	0	0
16	0	0	0	0	0	0	0	0
17	105	408	55	45	0	71	0	0
18	0	0	0	0	0	0	0	0
19	0	0	0	0	0	0	0	0
20	0	0	0	0	0	0	0	0
21	0	0	0	0	0	0	0	0
22	105	533	56	46	0	71	0	0
23	0	0	0	0	0	0	0	0
24	0	0	0	0	0	0	0	0
25	0	0	0	0	0	0	0	0
26	0	0	0	0	0	0	0	0
27	0	0	0	0	0	0	0	0
28	0	0	0	0	0	0	0	0
29	105	687	57	47	0	72	0	0
30	0	0	0	0	0	0	0	0
31	0	0	0	0	0	0	0	0
32	105	774	58	48	0	72	0	0

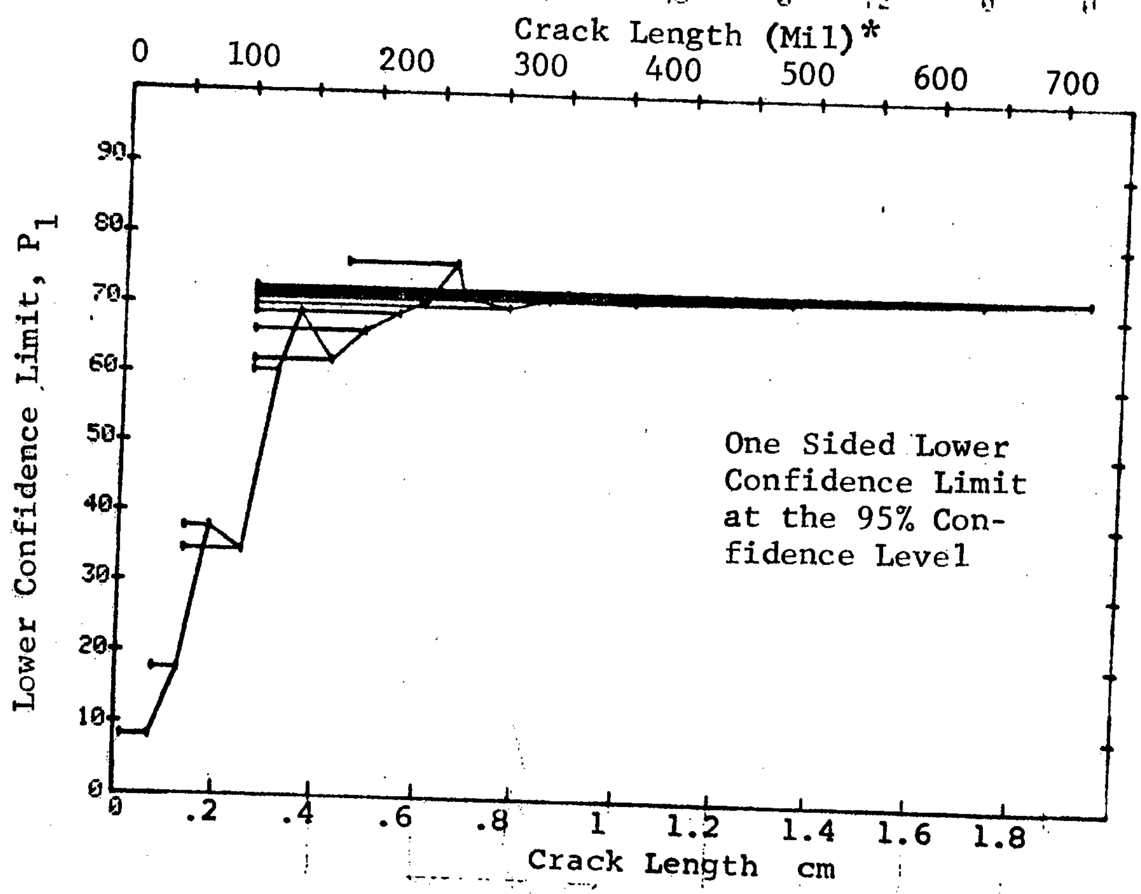

Figure D-57 (Continued)

(c) Overlapping Sixty Point Method of Data Cumulation

17-OCT-75 TEST 3 (57)

RANGE	MIN LN *	MAX LN *	N	DET	50%	95%	0 MISS	1 MISS
1	0	0	0	0	0	0	0	0
2	0	0	0	0	0	0	0	0
3	0	0	0	0	0	0	0	0
4	0	0	0	0	0	0	0	0
5	0	0	0	0	0	0	0	0
6	0	0	0	0	0	0	0	0
7	0	0	0	0	0	0	0	0
8	0	0	0	0	0	0	0	0
9	0	0	0	0	0	0	0	0
10	0	0	0	0	0	0	0	0
11	0	0	0	0	0	0	0	0
12	0	0	0	0	0	0	0	0
13	0	0	0	0	0	0	0	0
14	0	0	0	0	0	0	0	0
15	0	0	0	0	0	0	0	0
16	0	0	0	0	0	0	0	0
17	0	0	0	0	0	0	0	0
18	0	0	0	0	0	0	0	0
19	0	0	0	0	0	0	0	0
20	0	0	0	0	0	0	0	0
21	0	0	0	0	0	0	0	0
22	5	10	40	4	9	3	0	0
23	10	20	60	3	4	1	0	0
24	10	20	60	6	9	4	0	0
25	20	20	60	10	16	9	0	0
26	20	30	60	10	15	9	0	0
27	20	36	60	12	19	11	0	0
28	30	45	60	14	22	14	0	0
29	38	60	60	18	29	20	0	0
30	45	95	60	26	42	32	0	0
31	60	161	60	38	52	51	0	0
32	96	408	60	47	77	67	0	0

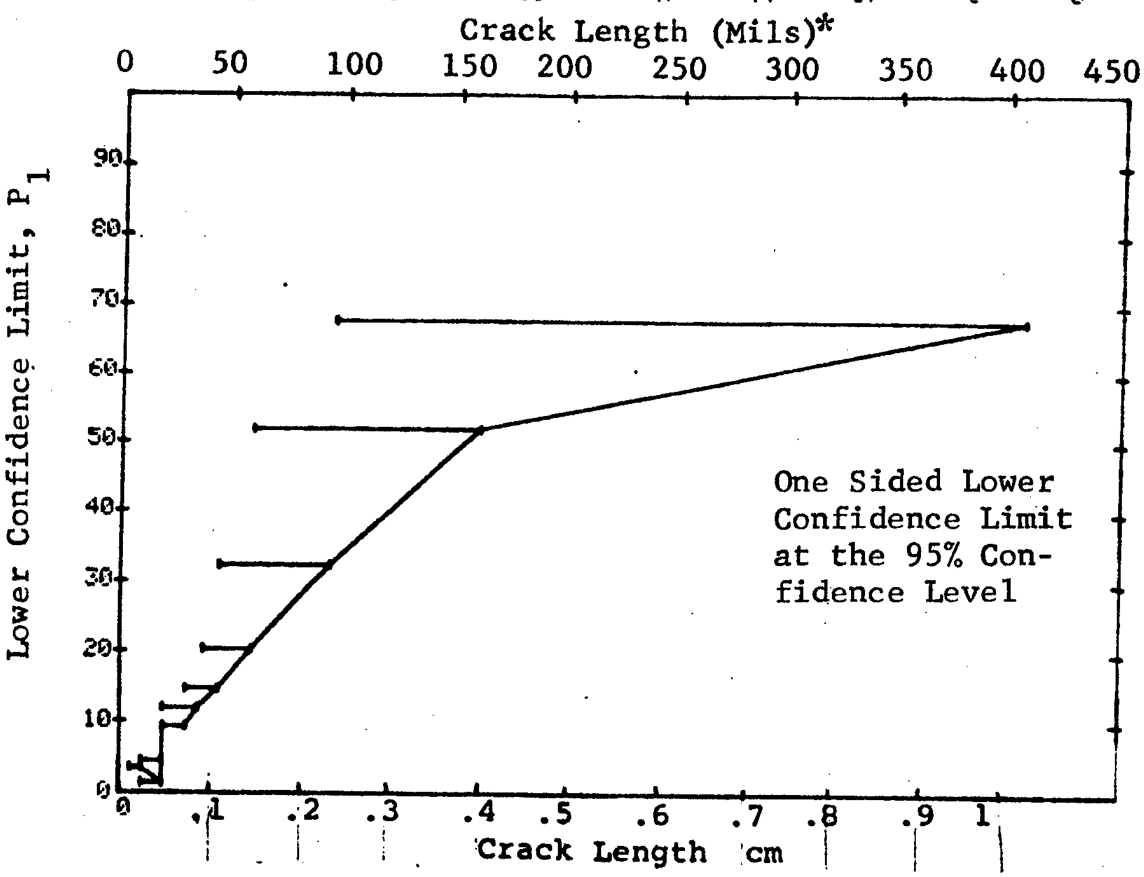

Figure D-57 (Concluded)

(a) Range Interval Method of Data Cumulation

17-OCT-75

RANGE	MIN LN	MAX LN	N	DET	50%	95% (58)	0 MISS	[illegible]
1	5 *	29 *	150	4	2	0	0	[illegible]
2	30	51	66	4	1	1	0	[illegible]
3	54	74	23	3	7	1	0	[illegible]
4	78	100	20	3	13	4	0	[illegible]
5	105	125	10	3	25	8	0	[illegible]
6	127	142	7	1	9	0	0	0
7	150	169	9	2	17	4	0	0
8	179	194	5	0	0	0	0	0
9	208	220	5	3	50	18	0	0
10	230	243	4	0	0	0	0	0
11	252	265	4	3	61	24	0	0
12	271	280	2	0	0	0	0	0
13	296	307	3	1	20	1	0	0
14	320	339	2	0	0	0	0	0
15	346	353	2	1	29	2	0	0
16	0	0	0	0	0	0	0	0
17	392	408	2	1	29	2	0	0
18	0	0	0	0	0	0	0	0
19	0	0	0	0	0	0	0	0
20	0	0	0	0	0	0	0	0
21	0	0	0	0	0	0	0	0
22	533	533	1	0	0	0	0	0
23	0	0	0	0	0	0	0	0
24	0	0	0	0	0	0	0	0
25	0	0	0	0	0	0	0	0
26	0	0	0	0	0	0	0	0
27	0	0	0	0	0	0	0	0
28	0	0	0	0	0	0	0	0
29	687	687	1	0	0	0	[illegible]	[illegible]
30	0	0	0	0	0	0	[illegible]	[illegible]
31	0	0	0	0	0	0	[illegible]	[illegible]
32	774	774	1	1	50	5	[illegible]	[illegible]

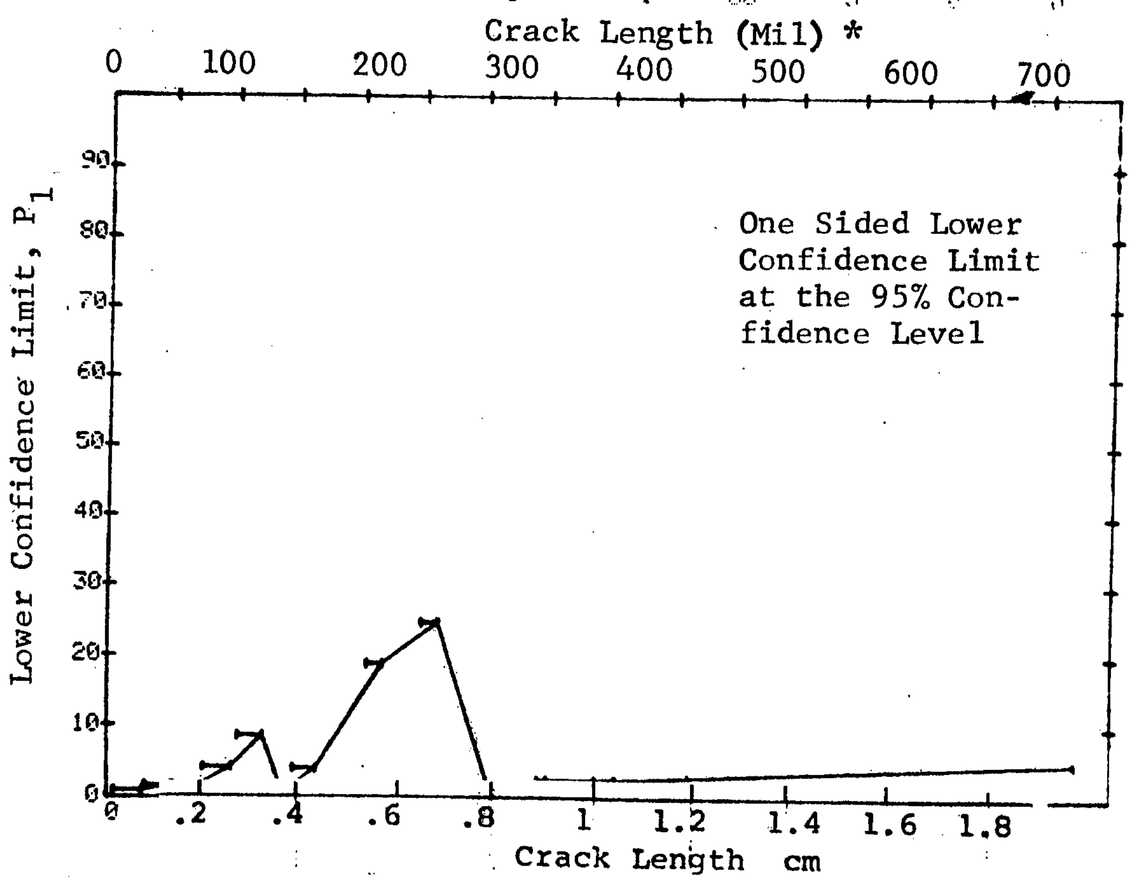

Figure D-58 Probability of Detection for 7178-T651 Al Using Eddy Current. Fatigue Cracks in Fastener Holes Measured by Team 4. Field Env.

(b) Optimum Probability Method of Data Cumulation

17-OCT-75 (58)

RANGE	MIN IN	MAX IN	[illegible]	[illegible]	[illegible]	[illegible]	[illegible]	[illegible]
1	5*	[illegible]*	150	1	0	0	0	0
2	5	[illegible]	[illegible]	[illegible]	1	1	0	[illegible]
3	30	[illegible]	109	[illegible]	0	2	0	0
4	54	100	43	[illegible]	0	4	0	0
5	78	125	30	6	0	9	0	0
6	78	142	37	7	0	9	0	0
7	78	169	46	9	0	10	0	0
8	78	194	51	9	0	9	0	0
9	208	220	5	3	0	14	0	0
10	105	243	40	9	0	12	0	0
11	252	265	4	3	0	24	0	0
12	208	280	15	6	0	19	0	0
13	208	307	18	7	0	19	0	0
14	208	339	20	7	0	17	0	0
15	208	353	22	8	0	19	0	0
16	0	0	0	0	0	0	0	0
17	208	408	24	9	0	21	0	0
18	0	0	0	0	0	0	0	0
19	0	0	0	0	0	0	0	0
20	0	0	0	0	0	0	0	0
21	0	0	0	0	0	0	0	0
22	208	537	25	9	0	20	0	0
23	0	0	0	0	0	0	0	0
24	0	0	0	0	0	0	0	0
25	0	0	0	0	0	0	0	0
26	0	0	0	0	0	0	0	0
27	0	0	0	0	0	0	0	0
28	0	0	0	0	0	0	0	0
29	208	[illegible]	26	9	0	[illegible]		
30	0	0	0	0	0	0	[illegible]	[illegible]
31	0	0	0	0	0	0	0	0
32	208	774	27	10	0	21	[illegible]	[illegible]

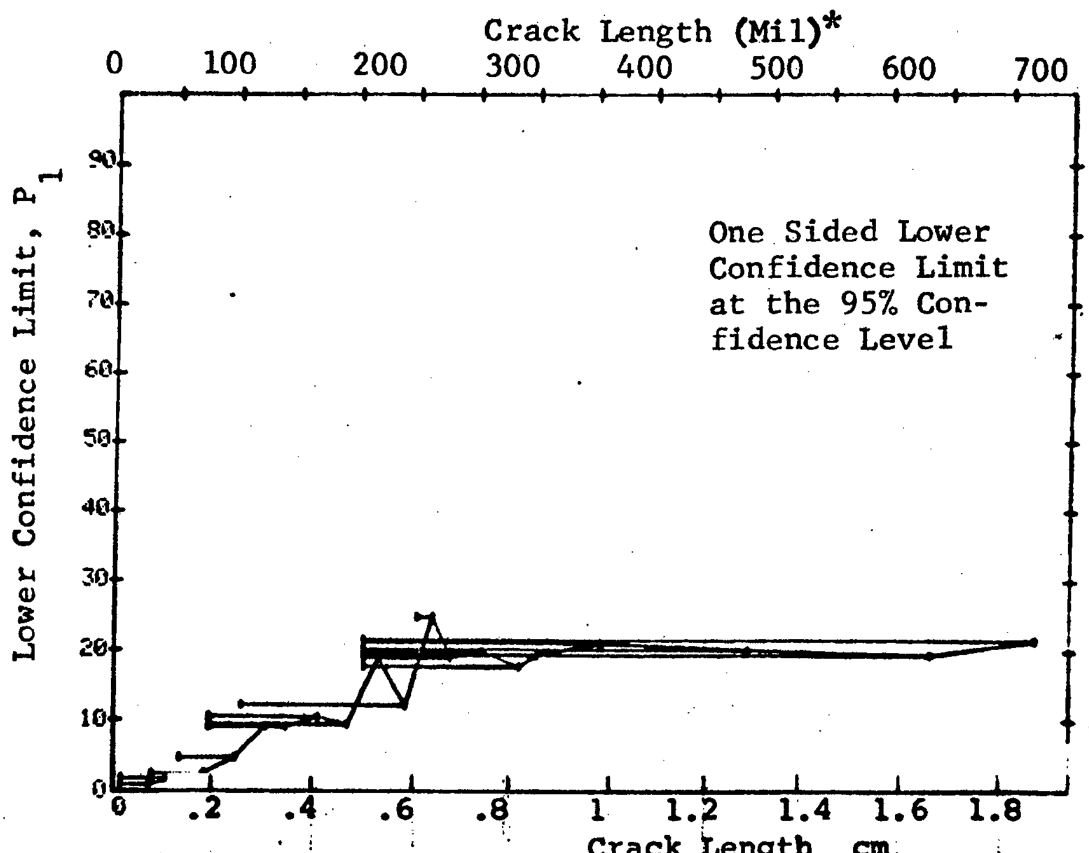

Figure D-58 (Continued)

(c) Overlapping Sixty Point Method of Data Cumulation

17-OCT-75 TEST 3

RANGE	MIN LN*	MAX LN*	N	LET	50%	95%	0 MISS	(58) 1 MISS
1	0	0	0	0	0	0	0	0
2	0	0	0	0	0	0	0	0
3	0	0	0	0	0	0	0	0
4	0	0	0	0	0	0	0	0
5	0	0	0	0	0	0	0	0
6	0	0	0	0	0	0	0	0
7	0	0	0	0	0	0	0	0
8	0	0	0	0	0	0	0	0
9	0	0	0	0	0	0	0	0
10	0	0	0	0	0	0	0	0
11	0	0	0	0	0	0	0	0
12	0	0	0	0	0	0	0	0
13	0	0	0	0	0	0	0	0
14	0	0	0	0	0	0	0	0
15	0	0	0	0	0	0	0	0
16	0	0	0	0	0	0	0	0
17	0	0	0	0	0	0	0	0
18	0	0	0	0	0	0	0	0
19	0	0	0	0	0	0	0	0
20	0	0	0	0	0	0	0	0
21	0	0	0	0	0	0	0	0
22	5	10	34	3	7	2	0	0
23	10	10	60	3	4	1	0	0
24	10	20	60	0	0	0	0	0
25	10	20	60	1	1	0	0	0
26	20	30	60	1	1	0	0	0
27	20	30	60	2	2	0	0	0
28	30	44	60	3	4	1	0	0
29	30	60	60	3	4	1	[illegible]	[illegible]
30	45	95	60	6	9	4	0	0
31	60	168	60	10	16	9	0	0
32	[illegible]	400	60	15	24	16	0	0

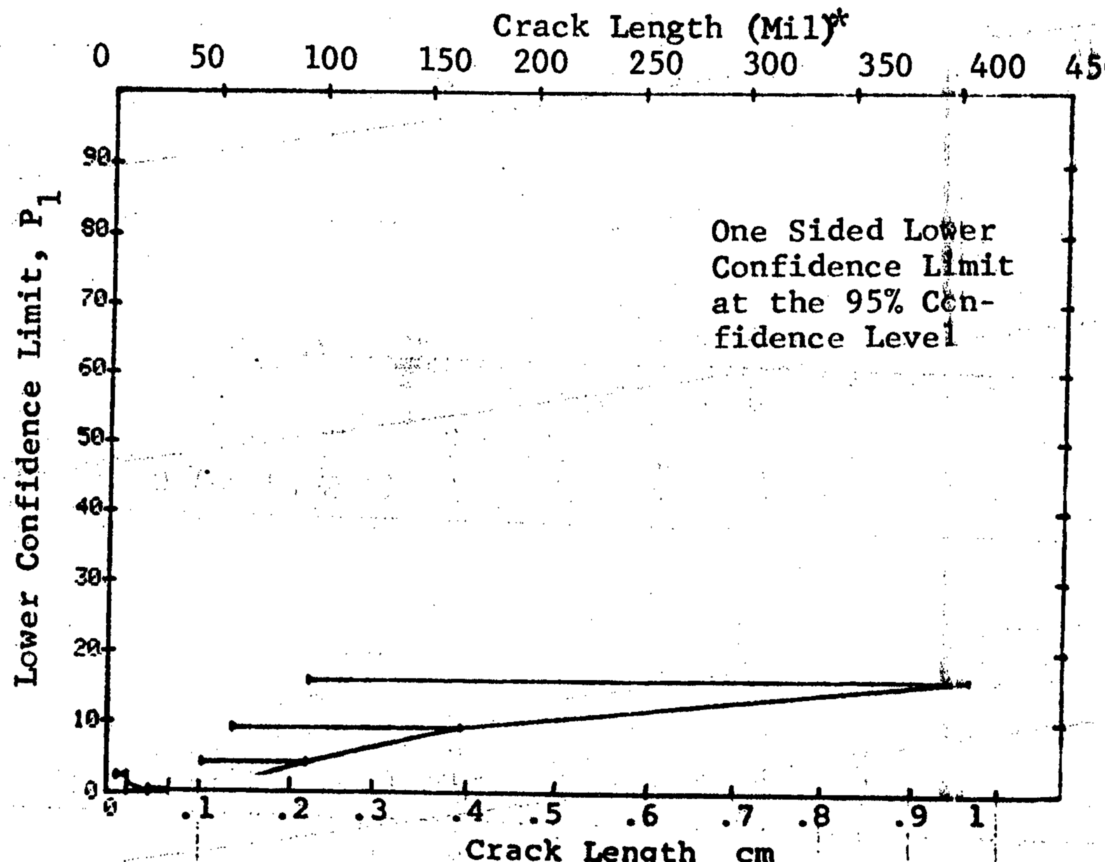

Figure D-58 (Concluded)

(a) Range Interval Method of Data Cumulation

24-OCT-75 TEST 1 MERGE ALL (59)

RANGE	MIN LN*	MAX LN*	N	DET	50%	95%	0 MISS	1 MISS
1	2	26	895	82	9	7	0	0
2	27	50	517	109	21	18	0	0
3	51	74	150	59	39	32	0	0
4	78	97	85	32	37	28	0	0
5	99	120	64	33	50	40	0	0
6	124	142	53	27	50	38	0	0
7	150	169	48	25	51	39	0	0
8	179	194	21	13	59	41	0	0
9	200	218	26	17	63	47	0	0
10	220	243	21	14	64	46	0	0
11	252	265	19	16	81	64	0	0
12	271	280	7	4	50	22	0	0
13	296	307	14	10	67	45	0	0
14	320	339	10	3	25	8	0	0
15	346	353	10	8	74	49	0	0
16	0	0	0	0	0	0	0	0
17	392	408	9	7	71	45	0	0
18	0	0	0	0	0	0	0	0
19	0	0	0	0	0	0	0	0
20	0	0	0	0	0	0	0	0
21	500	500	2	2	70	22	0	0
22	0	0	0	0	0	0	0	0
23	533	533	4	2	38	9	0	0
24	0	0	0	0	0	0	0	0
25	0	0	0	0	0	0	0	0
26	607	607	1	0	0	0	0	0
27	0	0	0	0	0	0	0	0
28	0	0	0	0	0	0	0	0
29	687	687	4	3	61	24	0	0
30	0	0	0	0	0	0	0	0
31	0	0	0	0	0	0	0	0
32	774	774	5	5	57	54	0	0

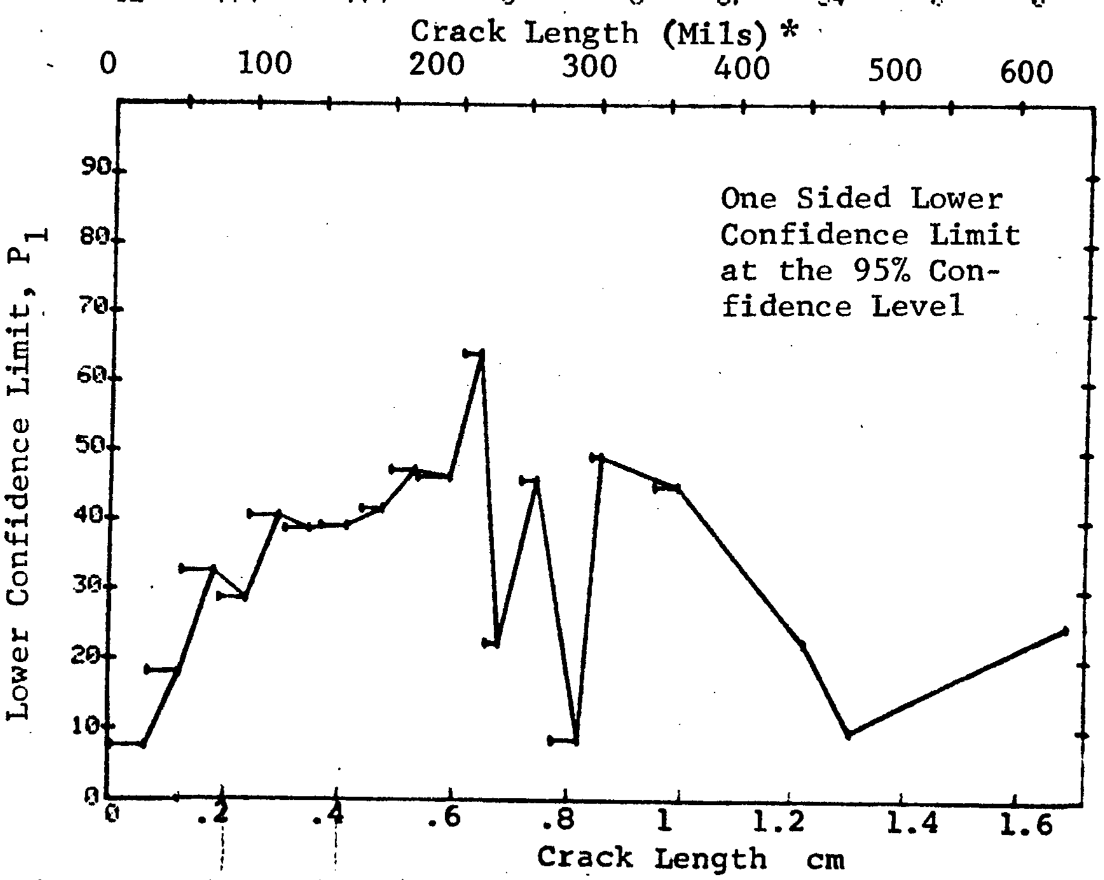

Figure D-59 Probability of Detection for 7178-T651 Al Using Eddy Current. Fatigue Cracks in Fastener Holes Measured by 5 Merged Teams. Field Env.

(b) Optimum Probability Method of Data Cumulation

24-OCT-75 TEST 2 (MERGE (59)

RANGE	MIN LN	MAX LN	N	DET	50%	95%	0 MISS	1 MISS
1	2 *	26 *	895	82	0	7	0	0
2	27	50	517	109	0	18	0	0
3	51	74	150	59	0	32	0	0
4	51	97	235	91	0	33	0	0
5	99	120	64	33	0	40	0	0
6	124	142	53	27	0	38	0	0
7	124	169	101	52	0	42	0	0
8	124	194	122	65	0	45	0	0
9	179	218	47	30	0	50	0	0
10	179	243	68	44	0	54	0	0
11	252	265	19	16	0	64	0	0
12	200	280	73	51	0	59	0	0
13	252	307	40	30	0	61	0	0
14	179	339	118	77	0	57	0	0
15	200	353	107	72	0	59	0	0
16	0	0	0	0	0	0	0	0
17	200	408	116	79	0	60	0	0
18	0	0	0	0	0	0	0	0
19	0	0	0	0	0	0	0	0
20	0	0	0	0	0	0	0	0
21	346	500	21	17	0	61	0	0
22	0	0	0	0	0	0	0	0
23	200	533	122	83	0	60	0	0
24	0	0	0	0	0	0	0	0
25	0	0	0	0	0	0	0	0
26	200	607	123	83	0	59	0	0
27	0	0	0	0	0	0	0	0
28	0	0	0	0	0	0	0	0
29	200	687	127	86	0	60	0	0
30	0	0	0	0	0	0	0	0
31	0	0	0	0	0	0	0	0
32	346	774	35	27	0	62	0	0

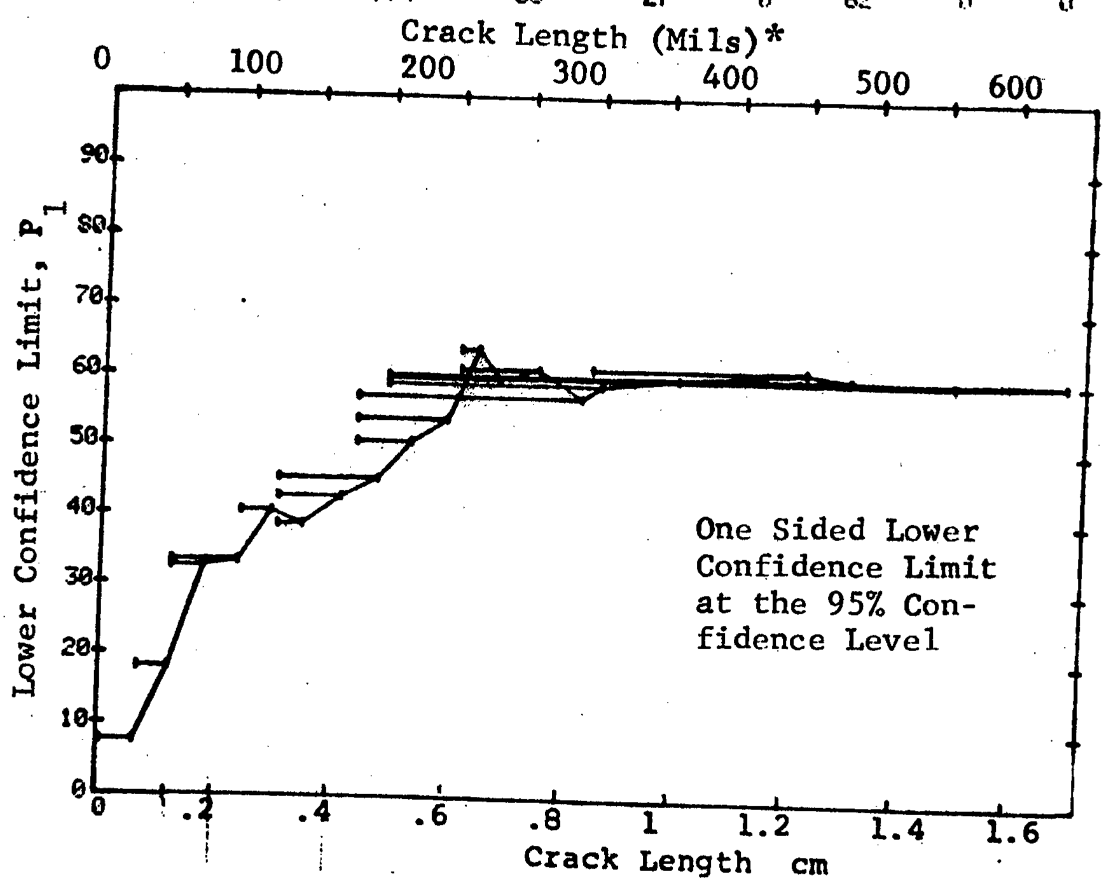

Figure D-59 (Continued)

(c) Overlapping Sixty Point Method of Data Cumulation

24-OCT-75 TEST 3 (MERGE (59)

RANGE	MIN LN *	MAX LN *	N	DET	50%	95%	0 MISS	1 MISS
1	30	30	60	9	14	8	0	0
2	30	30	60	9	14	8	0	0
3	30	30	60	8	12	6	0	0
4	30	30	60	12	19	11	0	0
5	30	40	60	12	19	11	0	0
6	30	40	60	12	19	11	0	0
7	40	40	60	16	25	17	0	0
8	40	40	60	21	34	24	0	0
9	40	42	60	15	24	16	0	0
10	40	45	60	12	19	11	0	0
11	42	50	60	14	22	14	0	0
12	45	50	60	10	16	9	0	0
13	50	50	60	8	12	6	0	0
14	50	50	60	14	22	14	0	0
15	50	60	60	22	35	26	0	0
16	50	60	60	23	37	27	0	0
17	60	64	60	24	39	29	0	0
18	60	70	60	27	44	33	0	0
19	64	74	60	24	39	29	0	0
20	70	80	60	26	42	32	0	0
21	74	90	60	22	35	26	0	0
22	80	99	60	17	27	18	0	0
23	90	108	60	30	49	38	0	0
24	99	120	60	32	52	41	0	0
25	108	132	60	28	45	35	0	0
26	124	150	60	32	52	41	0	0
27	132	166	60	32	52	41	0	0
28	150	194	60	31	50	40	0	0
29	166	220	60	36	59	48	0	0
30	194	264	60	42	69	58	0	0
31	220	320	60	43	70	60	0	0
32	264	500	60	41	67	57	0	0

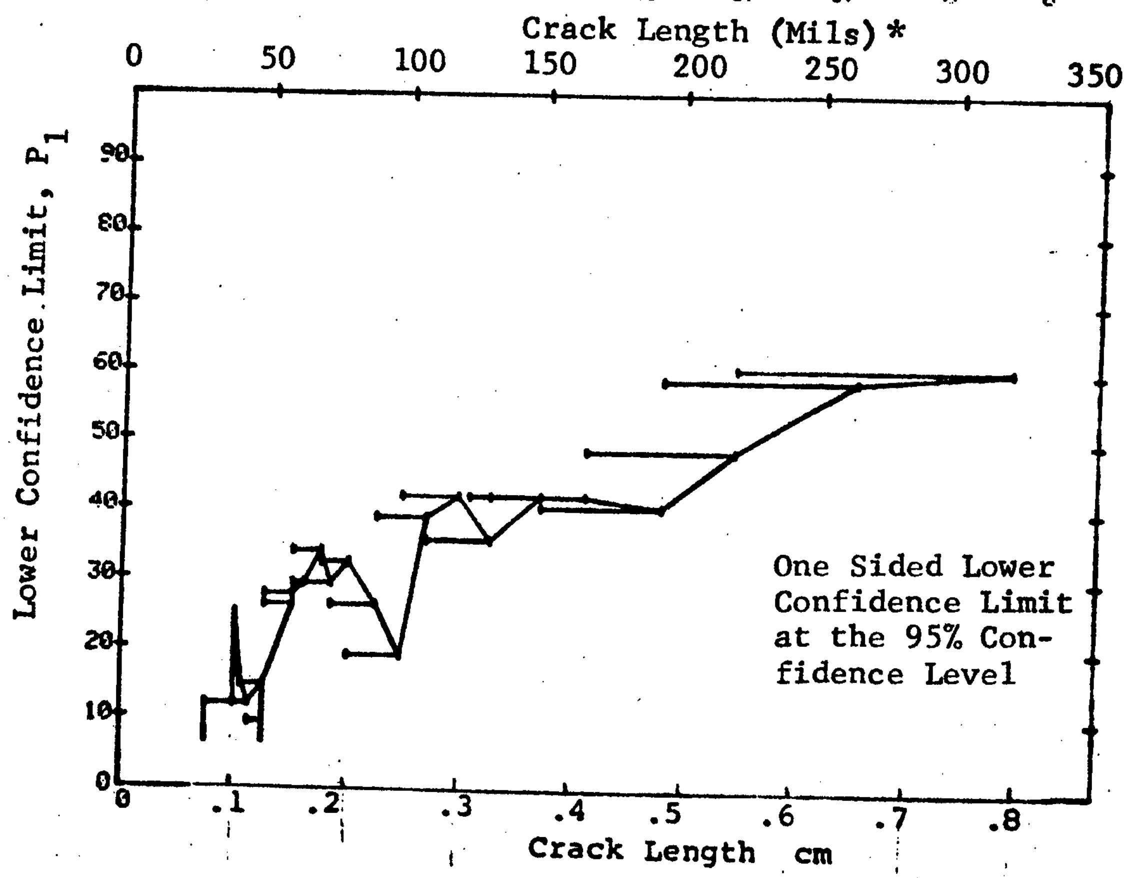

Figure D-59 (Concluded)

(a) Range Interval Method of Data Cumulation

24-OCT-75 PENETRANT TEST 1 (60)

RANGE	MIN LN	MAX LN	N	DET	50%	95%	0 MISS	1 MISS
1	10 *	10 *	2	0	0	0	0	0
2	0	0	0	0	0	0	0	0
3	30	30	5	1	12	1	0	0
4	0	0	0	0	0	0	0	0
5	40	40	10	7	64	39	0	0
6	50	50	14	8	53	32	0	0
7	0	0	0	0	0	0	0	0
8	60	60	6	4	57	27	0	0
9	70	70	4	4	84	47	0	0
10	0	0	0	0	0	0	0	0
11	80	80	8	8	91	68	0	0
12	90	90	8	7	79	52	0	0
13	0	0	0	0	0	0	0	0
14	100	100	13	9	64	42	0	0
15	110	110	18	17	90	76	28	43
16	120	120	3	3	79	36	0	0
17	0	0	0	0	0	0	0	0
18	130	130	6	2	20	4	0	0
19	140	140	9	8	82	57	0	0
20	0	0	0	0	0	0	0	0
21	150	150	11	10	85	63	0	0
22	160	160	6	6	89	60	0	0
23	0	0	0	0	0	0	0	0
24	170	170	7	4	50	22	0	0
25	180	180	15	15	95	81	14	31
26	0	0	0	0	0	0	0	0
27	190	190	7	7	90	65	0	0
28	0	0	0	0	0	0	0	0
29	0	0	0	0	0	0	0	0
30	210	210	2	1	29	2	0	0
31	220	220	3	1	20	1	0	0
32	230	230	11	11	93	76	18	35

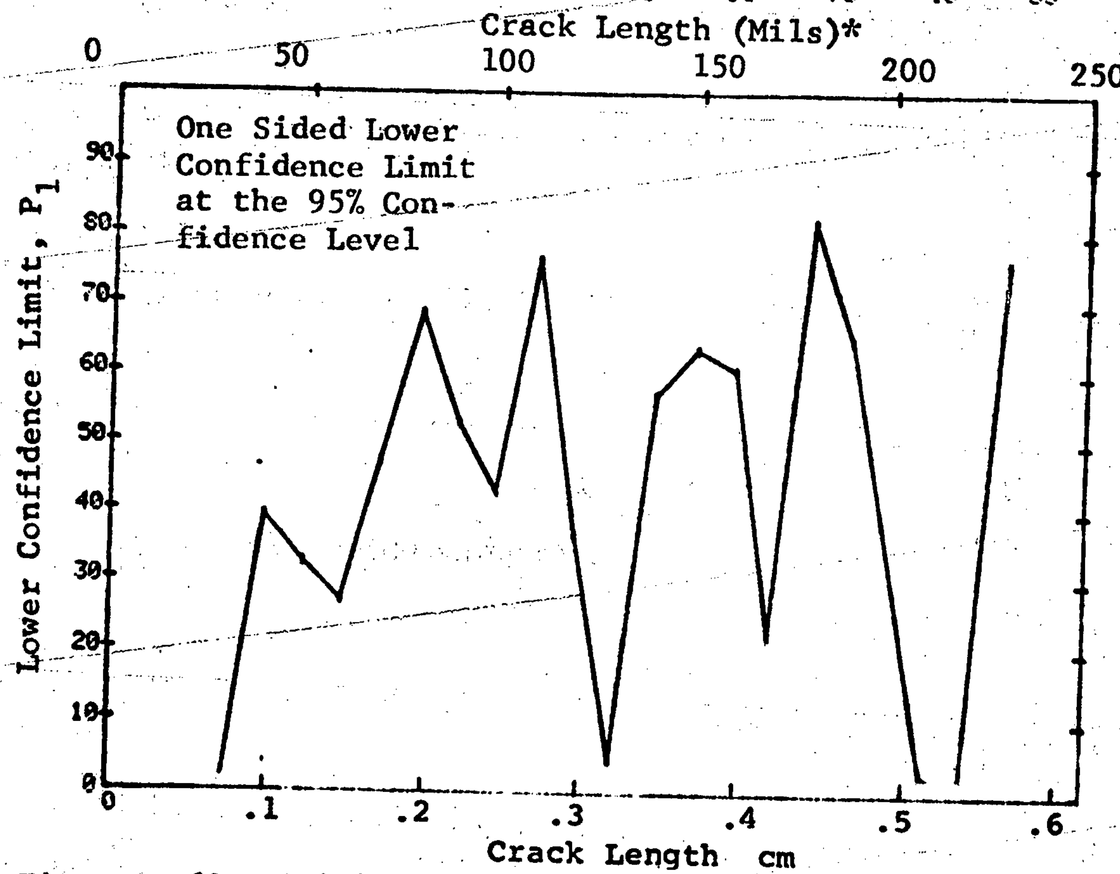

Figure D-60 Probability of Detection for 2024-T6 Al Using Liquid Penetrant. Compressed Notch Flaws in Tandem T Sections. Prod. Env.

(b) Optimum Probability Method of Data Cumulation

24-OCT-75 PENETRANT TEST 2 (60)

RANGE	MIN LN *	MAX LN *	N	DET	50%	95%	0 MISS	1 MISS
1	10	10	2	0	0	0	0	0
2	0	0	0	0	0	0	0	0
3	30	30	5	1	0	1	0	0
4	0	0	0	0	0	0	0	0
5	40	40	10	7	0	39	0	0
6	40	50	24	15	0	43	0	0
7	0	0	0	0	0	0	0	0
8	40	60	30	19	0	46	0	0
9	40	70	34	23	0	52	0	0
10	0	0	0	0	0	0	0	0
11	70	80	12	12	0	77	0	0
12	70	90	20	19	0	78	0	0
13	0	0	0	0	0	0	0	0
14	70	100	33	28	0	70	0	0
15	70	110	51	45	0	78	0	0
16	110	120	21	20	0	79	0	0
17	0	0	0	0	0	0	0	0
18	70	130	62	50	0	70	0	0
19	70	140	71	58	0	72	0	0
20	0	0	0	0	0	0	0	0
21	70	150	82	68	0	74	0	0
22	140	160	26	24	0	77	0	0
23	0	0	0	0	0	0	0	0
24	70	170	95	78	0	74	0	0
25	180	180	15	15	0	81	14	31
26	0	0	0	0	0	0	0	0
27	180	190	22	22	0	87	7	24
28	0	0	0	0	0	0	0	0
29	0	0	0	0	0	0	0	0
30	180	210	24	23	0	81	23	37
31	140	220	60	52	0	77	0	0
32	120	230	38	35	0	80	38	51

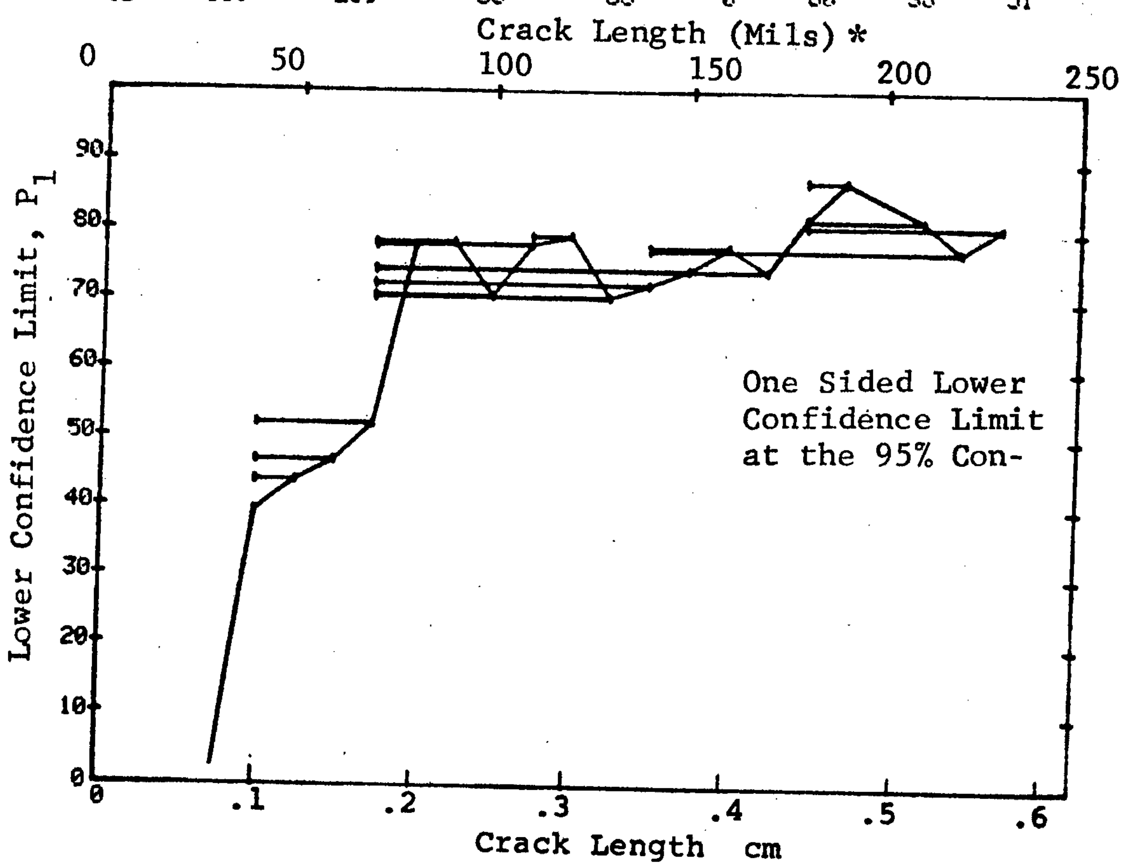

Figure D-60 (Continued)

(c) Overlapping Sixty Point Method of Data Cumulation

24-OCT-75 PENETRANT TEST 3 ( ) (60)

RANGE	MIN LN	* MAX LN *	N	DET	50%	95%	0 MISS	1 MISS
1	0	0	0	0	0	0	0	0
2	0	0	0	0	0	0	0	0
3	0	0	0	0	0	0	0	0
4	0	0	0	0	0	0	0	0
5	0	0	0	0	0	0	0	0
6	0	0	0	0	0	0	0	0
7	0	0	0	0	0	0	0	0
8	0	0	0	0	0	0	0	0
9	0	0	0	0	0	0	0	0
10	0	0	0	0	0	0	0	0
11	0	0	0	0	0	0	0	0
12	0	0	0	0	0	0	0	0
13	0	0	0	0	0	0	0	0
14	0	0	0	0	0	0	0	0
15	0	0	0	0	0	0	0	0
16	0	0	0	0	0	0	0	0
17	0	0	0	0	0	0	0	0
18	0	0	0	0	0	0	0	0
19	0	0	0	0	0	0	0	0
20	0	0	0	0	0	0	0	0
21	0	0	0	0	0	0	0	0
22	0	0	0	0	0	0	0	0
23	0	0	0	0	0	0	0	0
24	0	0	0	0	0	0	0	0
25	0	0	0	0	0	0	0	0
26	0	0	0	0	0	0	0	0
27	0	0	0	0	0	0	0	0
28	10	90	50	33	64	53	0	0
29	50	110	60	47	77	67	0	0
30	90	150	60	46	75	65	0	0
31	110	180	60	49	80	71	0	0
32	150	230	60	54	88	81	55	59

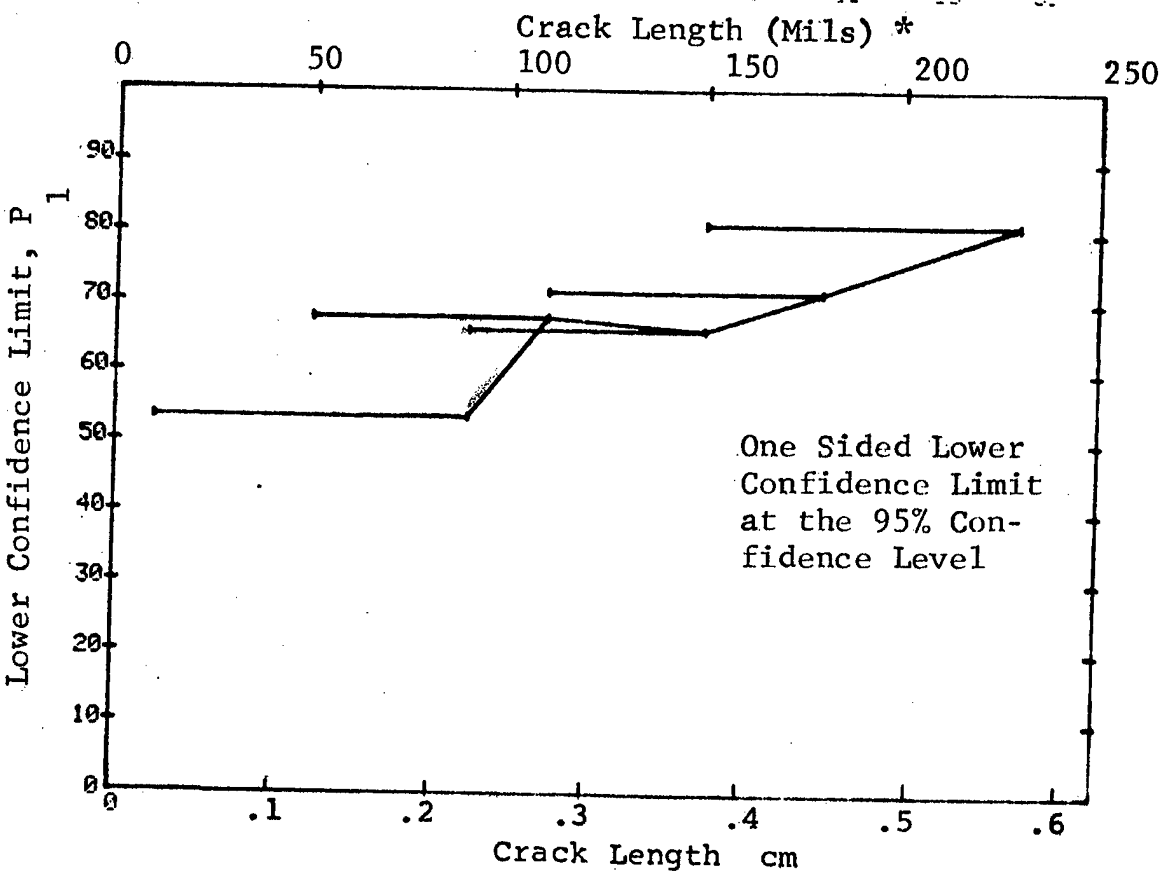

Figure D-60 (Concluded)

(a) Range Interval Method of Data Cumulation

24-OCT-75 PENETRANT TEST 1 (61)

RANGE	MIN LN *	MAX LN *	N	DET	50%	95%	0 MISS	1 MISS
1	40	40	4	0	0	0	0	0
2	70	70	3	1	20	1	0	0
3	0	0	0	0	0	0	0	0
4	100	110	18	14	74	56	0	0
5	130	130	6	4	57	27	0	0
6	0	0	0	0	0	0	0	0
7	0	0	0	0	0	0	0	0
8	190	190	1	1	50	5	0	0
9	210	210	3	1	20	1	0	0
10	230	230	3	2	50	13	0	0
11	0	0	0	0	0	0	0	0
12	250	250	6	4	57	27	0	0
13	270	270	1	1	50	5	0	0
14	300	300	3	3	79	36	0	0
15	310	310	4	4	84	47	0	0
16	0	0	0	0	0	0	0	0
17	350	350	3	3	79	36	0	0
18	380	380	3	3	79	36	0	0
19	0	0	0	0	0	0	0	0
20	410	410	1	1	50	5	0	0
21	0	0	0	0	0	0	0	0
22	450	450	3	3	79	36	0	0
23	460	460	1	1	50	5	0	0
24	480	480	3	3	79	36	0	0
25	0	0	0	0	0	0	0	0
26	0	0	0	0	0	0	0	0
27	0	0	0	0	0	0	0	0
28	0	0	0	0	0	0	0	0
29	0	0	0	0	0	0	0	0
30	0	0	0	0	0	0	0	0
31	0	0	0	0	0	0	0	0
32	650	650	3	3	79	36	0	0

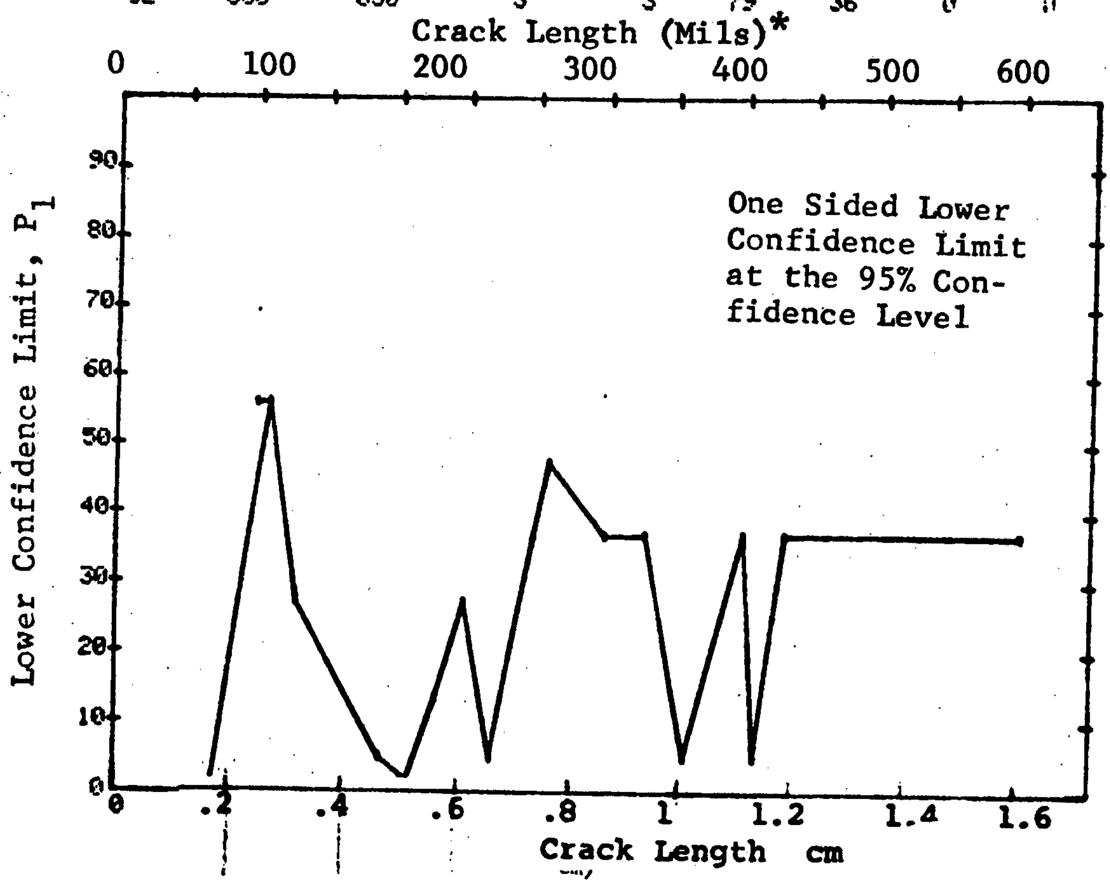

Figure D-61 Probability of Detection for 4340M Steel Using Liquid Penetrant. Compressed Notch Flaws in Solid Threaded Cylinder. Prod. Env.

(b) Optimum Probability Method of Data Cumulation

24-OCT-75 PENETRANT TEST 2 ([illegible] (61)

RANGE	MIN LN		MAX LN		N	DET	50%	95%	0 MISS	1 MISS
1	40	*	40	*	4	0	0	0	0	0
2	70		70		3	1	0	1	0	0
3	0		0		0	0	0	0	0	0
4	100		110		18	14	0	56	0	0
5	100		130		24	18	0	56	0	0
6	0		0		0	0	0	0	0	0
7	0		0		0	0	0	0	0	0
8	100		190		25	19	0	58	0	0
9	100		210		28	20	0	54	0	0
10	100		230		31	22	0	54	0	0
11	0		0		0	0	0	0	0	0
12	100		250		37	26	0	55	0	0
13	100		270		38	27	0	56	0	0
14	100		300		41	30	0	59	0	0
15	270		310		8	8	0	68	0	0
16	0		0		0	0	0	0	0	0
17	270		350		11	11	0	76	0	0
18	270		380		14	14	0	80	15	32
19	0		0		0	0	0	0	0	0
20	270		410		15	15	0	81	14	31
21	0		0		0	0	0	0	0	0
22	270		450		18	18	0	84	11	28
23	270		460		19	19	0	85	10	27
24	270		480		22	22	0	87	7	24
25	0		0		0	0	0	0	0	0
26	0		0		0	0	0	0	0	0
27	0		0		0	0	0	0	0	0
28	0		0		0	0	0	0	0	0
29	0		0		0	0	0	0	0	0
30	0		0		0	0	0	0	0	0
31	0		0		0	0	0	0	0	0
32	270		650		25	25	0	88	4	21

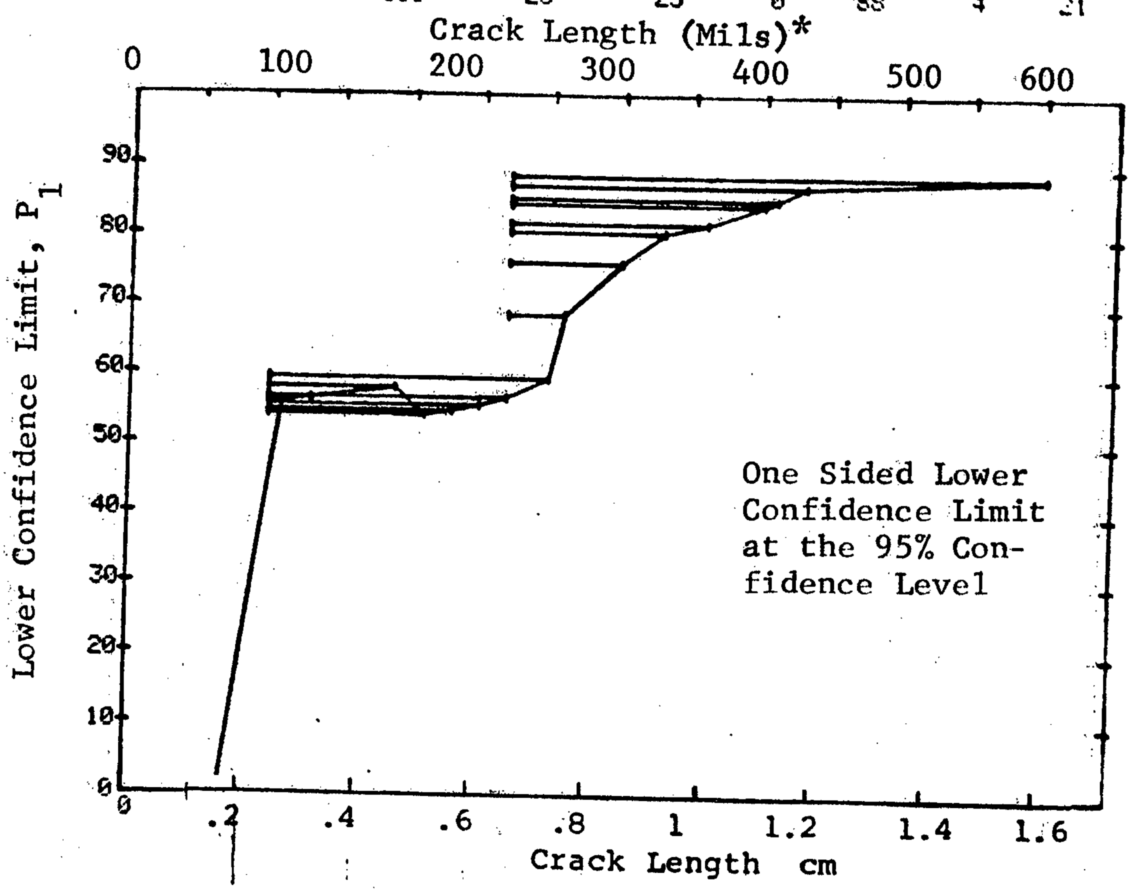

Figure D-61 (Continued)

(c) Overlapping Sixty Point Method of Data Cumulation

24-OCT-75 PENETRANT TEST 3 ([illegible]) (61)

RANGE	MIN LN *	MAX LN *	N	DET	50%	95%	0 MISS	1 MISS
1	0	0	0	0	0	0	0	0
2	0	0	0	0	0	0	0	0
3	0	0	0	0	0	0	0	0
4	0	0	0	0	0	0	0	0
5	0	0	0	0	0	0	0	0
6	0	0	0	0	0	0	0	0
7	0	0	0	0	0	0	0	0
8	0	0	0	0	0	0	0	0
9	0	0	0	0	0	0	0	0
10	0	0	0	0	0	0	0	0
11	0	0	0	0	0	0	0	0
12	0	0	0	0	0	0	0	0
13	0	0	0	0	0	0	0	0
14	0	0	0	0	0	0	0	0
15	0	0	0	0	0	0	0	0
16	0	0	0	0	0	0	0	0
17	0	0	0	0	0	0	0	0
18	0	0	0	0	0	0	0	0
19	0	0	0	0	0	0	0	0
20	0	0	0	0	0	0	0	0
21	0	0	0	0	0	0	0	0
22	0	0	0	0	0	0	0	0
23	0	0	0	0	0	0	0	0
24	0	0	0	0	0	0	0	0
25	0	0	0	0	0	0	0	0
26	0	0	0	0	0	0	0	0
27	0	0	0	0	0	0	0	0
28	0	0	0	0	0	0	0	0
29	0	0	0	0	0	0	0	0
30	0	0	0	0	0	0	0	0
31	40	230	38	21	56	43	0	0
32	70	480	60	49	80	71	0	0

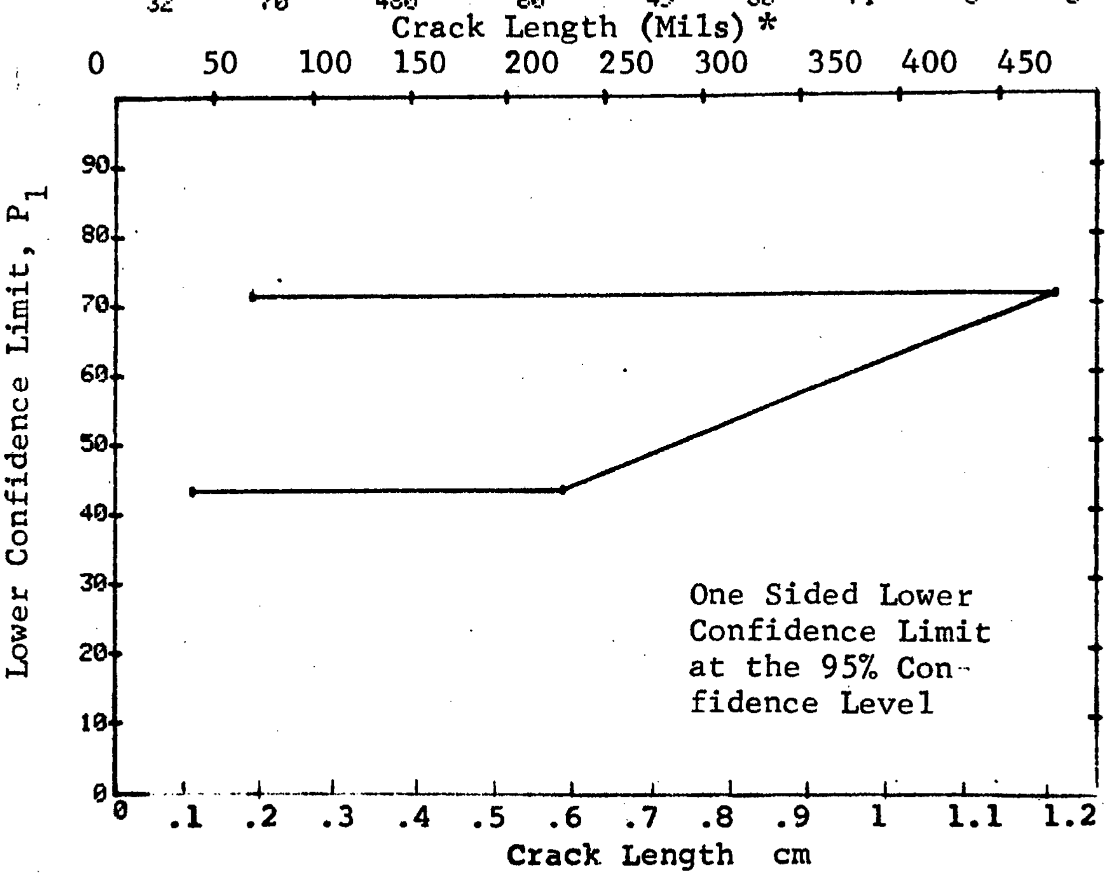

Figure D-61 (Concluded)

(a) Range Interval Method of Data Cumulation

24-OCT-75 PENETRANT TEST 1 ( ) 2 (62)

RANGE	MIN LN	*MAX LN*	N	DET	50%	95%	0 MISS	1 MISS
1	80	90	8	2	20	4	0	0
2	0	0	0	0	0	0	0	0
3	110	110	3	0	0	0	0	0
4	120	120	3	1	20	1	0	0
5	130	130	2	0	0	0	0	0
6	140	140	6	3	42	15	0	0
7	160	160	3	1	20	1	0	0
8	0	0	0	0	0	0	0	0
9	0	0	0	0	0	0	0	0
10	0	0	0	0	0	0	0	0
11	0	0	0	0	0	0	0	0
12	0	0	0	0	0	0	0	0
13	0	0	0	0	0	0	0	0
14	0	0	0	0	0	0	0	0
15	250	250	2	1	29	2	0	0
16	270	270	5	3	50	18	0	0
17	280	280	2	1	29	2	0	0
18	0	0	0	0	0	0	0	0
19	300	300	3	2	50	13	0	0
20	310	310	3	2	50	13	0	0
21	0	0	0	0	0	0	0	0
22	0	0	0	0	0	0	0	0
23	0	0	0	0	0	0	0	0
24	0	0	0	0	0	0	0	0
25	0	0	0	0	0	0	0	0
26	0	0	0	0	0	0	0	0
27	0	0	0	0	0	0	0	0
28	0	0	0	0	0	0	0	0
29	0	0	0	0	0	0	0	0
30	0	0	0	0	0	0	0	0
31	440	440	3	1	20	1	0	0
32	450	460	5	3	50	18	0	0

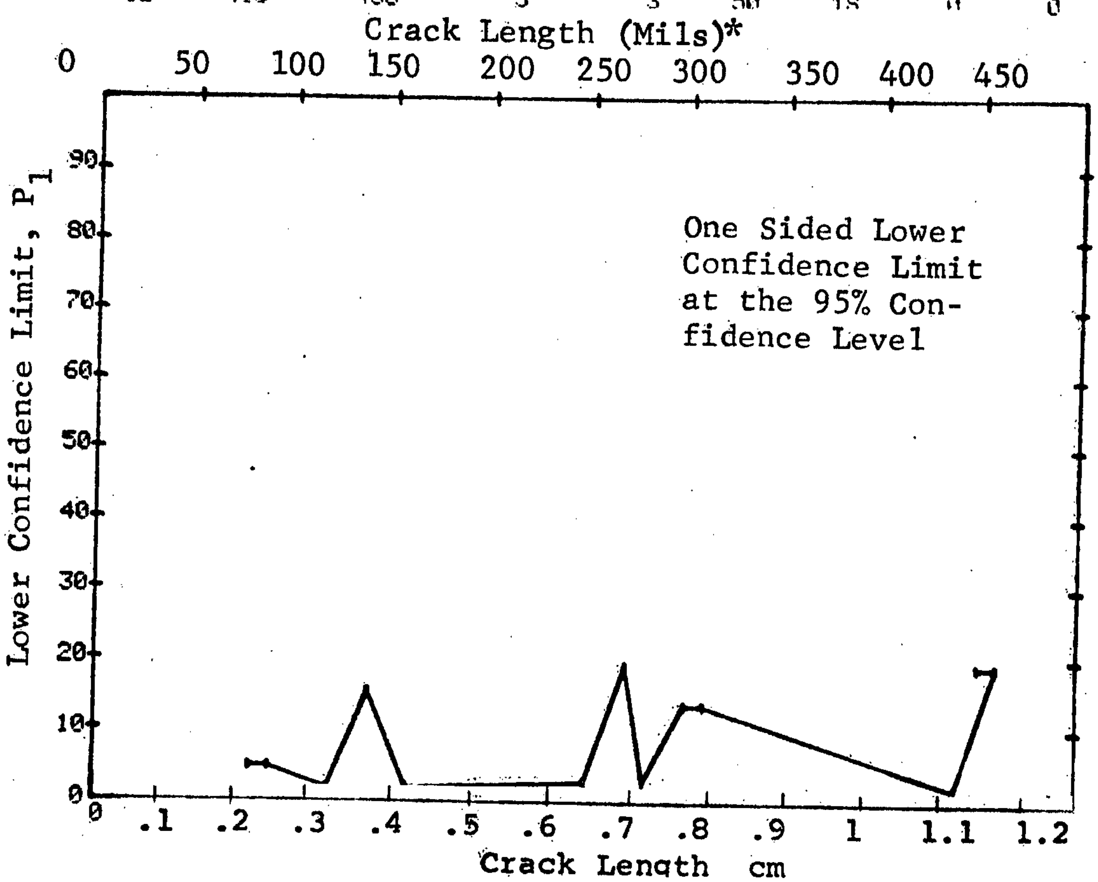

Figure D-62 Probability of Detection for 4340M Steel Using Liquid Penetrant. Compressed Notch Flaws in Hollow Cylinder. Prod. Env.

(b) Optimum Probability Method of Data Cumulation

24-OCT-75 PENETRANT TEST 2 (62)

RANGE	MIN LN	MAX LN	N	DET	50%	95%	0 MISS	1 MISS
1	80 *	90 *	8	2	0	4	0	0
2	0	0	10	0	0	0	0	0
3	80	110	11	2	0	3	0	0
4	80	120	14	3	0	6	0	0
5	80	130	16	3	0	5	0	0
6	140	140	6	3	0	15	0	0
7	140	160	9	4	0	16	0	0
8	0	0	0	0	0	0	0	0
9	0	0	0	0	0	0	0	0
10	0	0	0	0	0	0	0	0
11	0	0	0	0	0	0	0	0
12	0	0	0	0	0	0	0	0
13	0	0	0	0	0	0	0	0
14	0	0	0	0	0	0	0	0
15	140	250	11	5	0	19	0	0
16	140	270	16	8	0	27	0	0
17	140	280	18	9	0	29	0	0
18	0	0	0	0	0	0	0	0
19	140	300	21	11	0	32	0	0
20	250	310	15	9	0	35	0	0
21	0	0	0	0	0	0	0	0
22	0	0	0	0	0	0	0	0
23	0	0	0	0	0	0	0	0
24	0	0	0	0	0	0	0	0
25	0	0	0	0	0	0	0	0
26	0	0	0	0	0	0	0	0
27	0	0	0	0	0	0	0	0
28	0	0	0	0	0	0	0	0
29	0	0	0	0	0	0	0	0
30	0	0	0	0	0	0	0	0
31	140	440	27	14	0	34	0	0
32	250	460	23	13	0	37	0	0

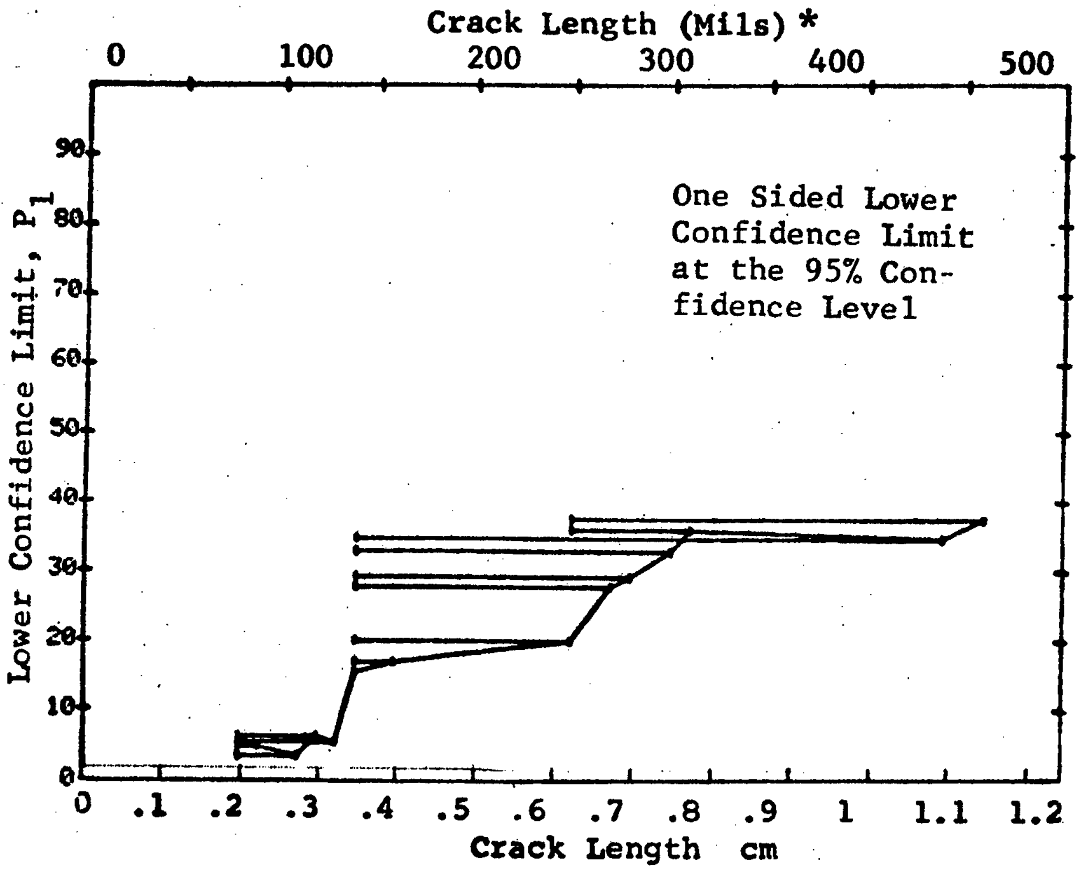

Figure D-62 (Continued)

(c) Overlapping Sixty Point Method of Data Cumulation

24-OCT-75 PENETRANT TEST 3 (62)

RANGE	MIN LN	MAX LN	N	DET	50%	95%	0 MISS	1 MISS
1	0 *	0 *	0	0	0	0	0	0
2	0	0	0	0	0	0	0	0
3	0	0	0	0	0	0	0	0
4	0	0	0	0	0	0	0	0
5	0	0	0	0	0	0	0	0
6	0	0	0	0	0	0	0	0
7	0	0	0	0	0	0	0	0
8	0	0	0	0	0	0	0	0
9	0	0	0	0	0	0	0	0
10	0	0	0	0	0	0	0	0
11	0	0	0	0	0	0	0	0
12	0	0	0	0	0	0	0	0
13	0	0	0	0	0	0	0	0
14	0	0	0	0	0	0	0	0
15	0	0	0	0	0	0	0	0
16	0	0	0	0	0	0	0	0
17	0	0	0	0	0	0	0	0
18	0	0	0	0	0	0	0	0
19	0	0	0	0	0	0	0	0
20	0	0	0	0	0	0	0	0
21	0	0	0	0	0	0	0	0
22	0	0	0	0	0	0	0	0
23	0	0	0	0	0	0	0	0
24	0	0	0	0	0	0	0	0
25	0	0	0	0	0	0	0	0
26	0	0	0	0	0	0	0	0
27	0	0	0	0	0	0	0	0
28	0	0	0	0	0	0	0	0
29	0	0	0	0	0	0	0	0
30	0	0	0	0	0	0	0	0
31	0	0	0	0	0	0	0	0
32	80	460	48	20	40	29	0	0

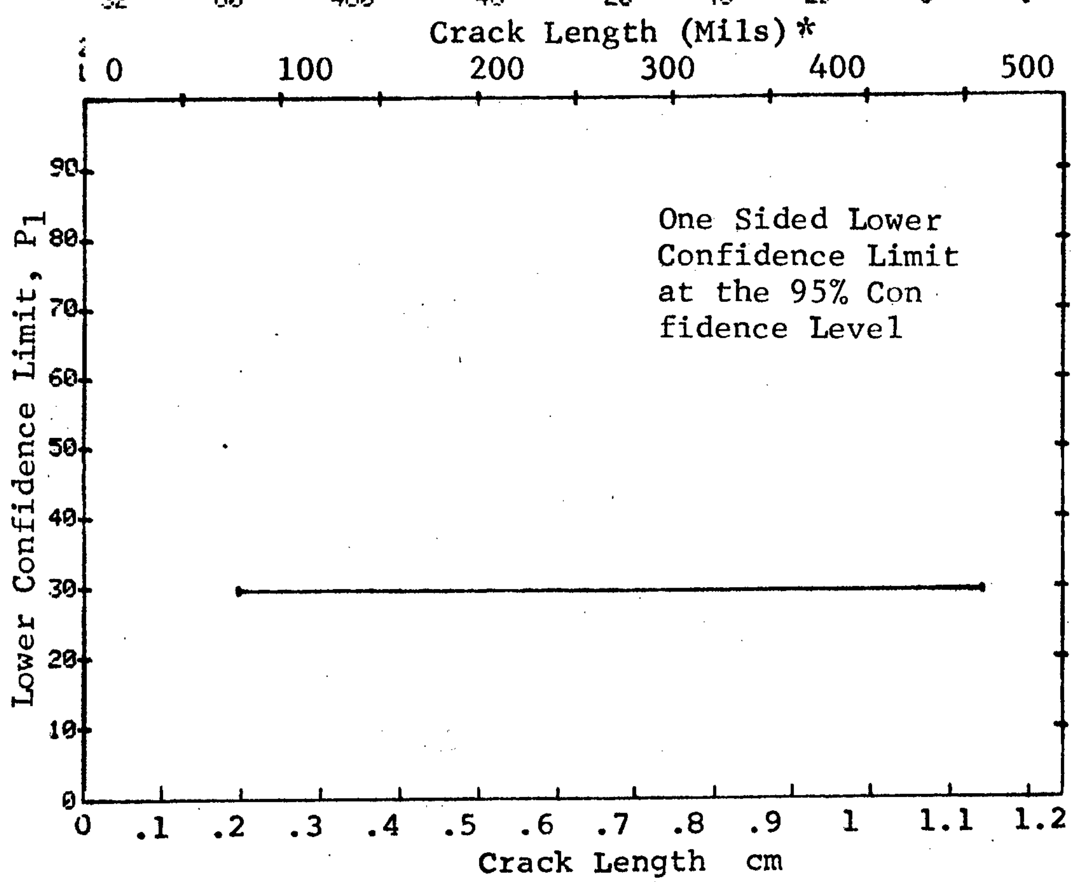

Figure D-62 (Concluded)

(a) Range Interval Method of Data Cumulation

28-OCT-75 PENETRANT TEST [illegible] (63)

RANGE	MIN LN	MAX LN	N	DET	50%	95%	0 MI[illegible]	[illegible]
1	60*	60*	2	0	0	0	0	0
2	0	[illegible]	0	0	0	0	0	[illegible]
3	100	100	13	1	5	0	0	0
4	120	120	4	0	0	0	0	[illegible]
5	130	130	1	0	0	0	0	0
6	140	140	6	2	26	6	0	0
7	160	160	2	1	29	2	0	0
8	180	180	4	0	0	0	0	0
9	0	0	0	0	0	0	0	0
10	0	0	0	0	0	0	0	0
11	230	230	2	1	29	2	0	0
12	0	0	0	0	0	0	0	0
13	0	0	0	0	0	0	0	0
14	0	0	0	0	0	0	0	0
15	0	0	0	0	0	0	0	0
16	310	310	4	3	61	24	0	0
17	0	0	0	0	0	0	0	0
18	0	0	0	0	0	0	0	0
19	350	350	11	7	58	34	0	0
20	0	0	0	0	0	0	0	0
21	390	390	4	4	84	47	0	0
22	0	0	0	0	0	0	0	0
23	0	0	0	0	0	0	0	0
24	0	0	0	0	0	0	0	[illegible]
25	0	0	0	0	0	0	0	0
26	0	0	0	0	0	0	0	0
27	0	0	0	0	0	0	0	0
28	0	0	0	0	0	0	0	0
29	0	0	0	0	0	[illegible]	[illegible]	[illegible]
30	0	0	0	0	0	0	[illegible]	[illegible]
31	0	0	0	0	0	[illegible]	[illegible]	[illegible]
32	570	570	4	4	84	47	[illegible]	[illegible]

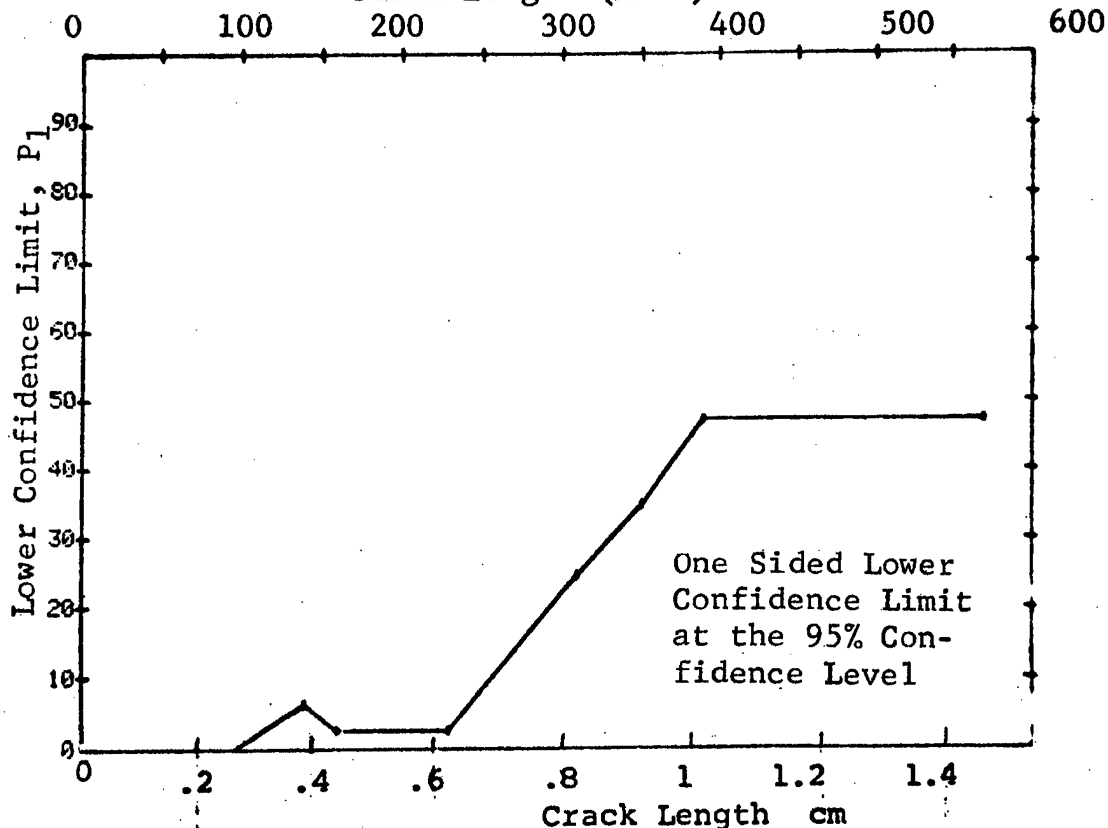

Figure D-63 Probability of Detection for 4340M Steel Using Liquid Penetrant. Compressed Notch Flaws in Filleted Hollow Cylinder. Prod. Env.

(b) Optimum Probability Method of Data Cumulation

28-OCT-75 PENETRANT TEST 2 (63)

RANGE	MIN LN	MAX LN	N	DET	50%	95%	0 MI	
1	60 *	60 *	2	0	0	0	0	[illegible]
2	0	0	0	0	0	0	0	[illegible]
3	100	100	13	1	0	0	0	[illegible]
4	100	120	17	1	0	0	0	[illegible]
5	100	130	18	1	0	0	0	[illegible]
6	140	140	6	2	0	6	0	0
7	140	160	8	3	0	11	0	0
8	140	180	12	3	0	7	0	0
9	0	0	0	0	0	0	0	0
10	0	0	0	0	0	0	0	0
11	140	230	14	4	0	10	0	0
12	0	0	0	0	0	0	0	0
13	0	0	0	0	0	0	0	0
14	0	0	0	0	0	0	0	0
15	0	0	0	0	0	0	0	0
16	230	310	6	4	0	27	0	0
17	0	0	0	0	0	0	0	0
18	0	0	0	0	0	0	0	0
19	310	350	15	10	0	42	0	0
20	0	0	0	0	0	0	0	0
21	310	390	19	14	0	52	0	0
22	0	0	0	0	0	0	0	0
23	0	0	0	0	0	0	0	0
24	0	0	0	0	0	0	0	0
25	0	0	0	0	0	0	0	0
26	0	0	0	0	0	0	0	0
27	0	0	0	0	0	0	0	0
28	0	0	0	0	0	[illegible]	[illegible]	[illegible]
29	0	0	0	0	0	0	[illegible]	[illegible]
30	0	0	0	0	0	0	[illegible]	[illegible]
31	0	0	0	0	0	0	[illegible]	[illegible]
32	390	570	8	9	0	68	[illegible]	[illegible]

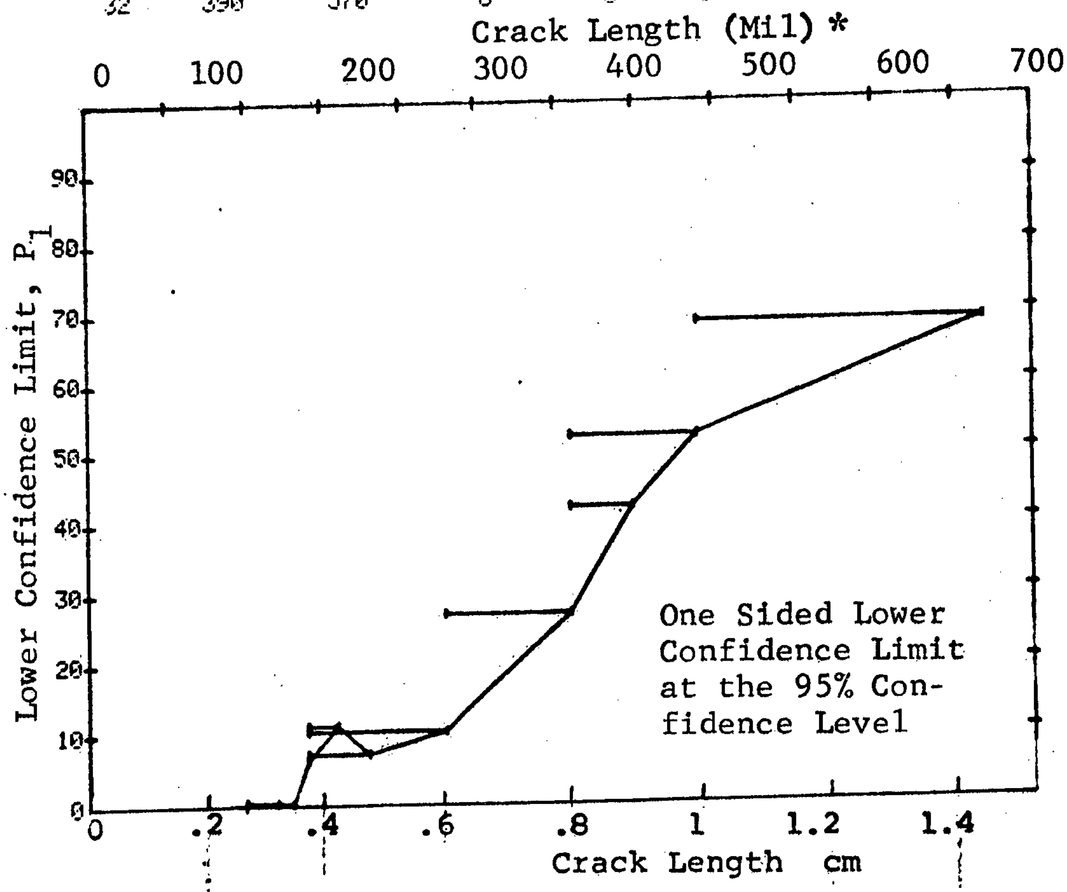

Figure D-63 (Continued)

(c) Overlapping Sixty Point Method of Data Cumulation

28-OCT-75 PENETRANT TEST 3 ✓3 (63)

RANGE	MIN LN*	MAX LN*	N	DET	50%	95%	0 MISS	1 MISS
1	0	0	0	0	0	0	0	0
2	0	0	0	0	0	0	0	0
3	0	0	0	0	0	0	0	0
4	0	0	0	0	0	0	0	0
5	0	0	0	0	0	0	0	0
6	0	0	0	0	0	0	0	0
7	0	0	0	0	0	0	0	0
8	0	0	0	0	0	0	0	0
9	0	0	0	0	0	0	0	0
10	0	0	0	0	0	0	0	0
11	0	0	0	0	0	0	0	0
12	0	0	0	0	0	0	0	0
13	0	0	0	0	0	0	0	0
14	0	0	0	0	0	0	0	0
15	0	0	0	0	0	0	0	0
16	0	0	0	0	0	0	0	0
17	0	0	0	0	0	0	0	0
18	0	0	0	0	0	0	0	0
19	0	0	0	0	0	0	0	0
20	0	0	0	0	0	0	0	0
21	0	0	0	0	0	0	0	0
22	0	0	0	0	0	0	0	0
23	0	0	0	0	0	0	0	0
24	0	0	0	0	0	0	0	0
25	0	0	0	0	0	0	0	0
26	0	0	0	0	0	0	0	0
27	0	0	0	0	0	0	0	0
28	0	0	0	0	0	0	0	0
29	0	0	0	0	0	0	0	0
30	0	0	0	0	0	0	0	0
31	0	0	0	0	0	0	0	0
32	60	390	53	19	34	24	0	0

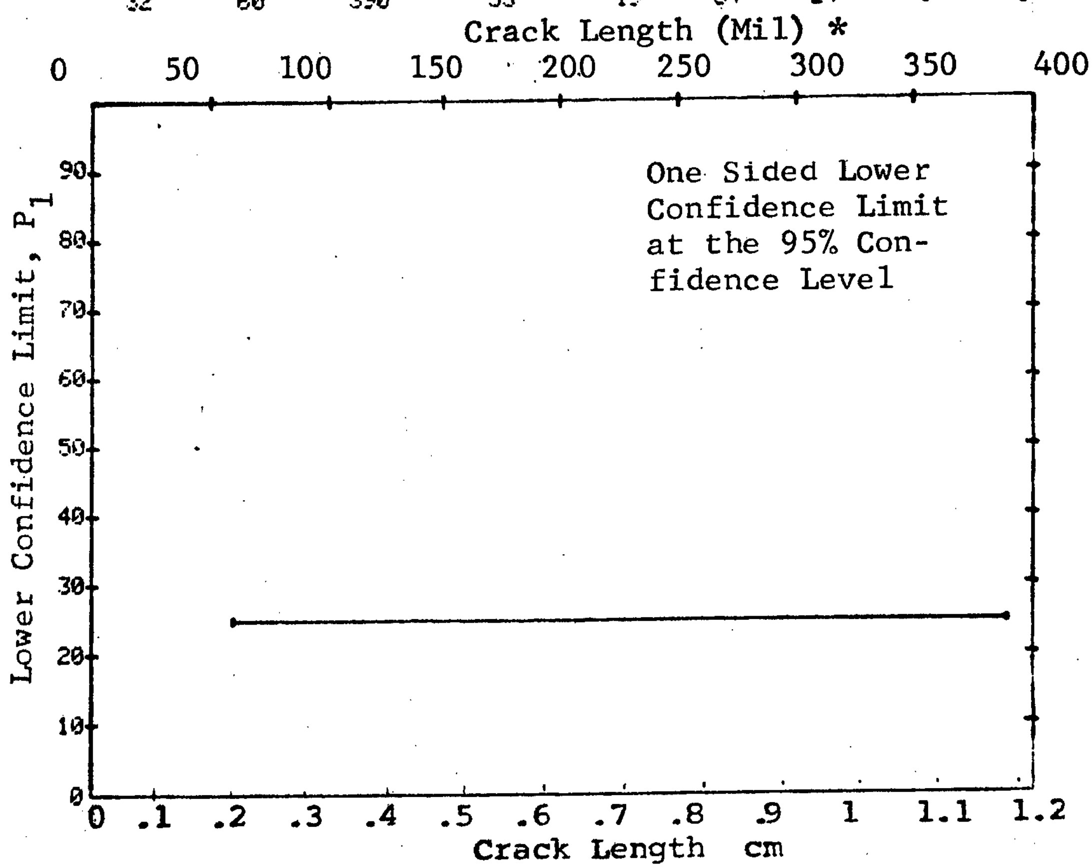

Figure D-63 (Concluded)

(a) Range Interval Method of Data Cumulation

24-OCT-75 PENETRANT TEST 1 (64)

RANGE	MIN LN *	MAX LN *	N	DET	50%	95%	0 MISS	1 MISS
1	20	40	16	2	10	2	0	0
2	50	60	30	15	48	33	0	0
3	70	70	16	13	77	58	0	0
4	90	110	24	21	84	70	0	0
5	120	130	19	16	81	64	0	0
6	140	150	44	40	89	80	45	59
7	160	160	12	11	86	66	0	0
8	200	200	3	3	79	36	0	0
9	0	0	0	0	0	0	0	0
10	0	0	0	0	0	0	0	0
11	260	260	1	1	50	5	0	0
12	0	0	0	0	0	0	0	0
13	300	300	3	3	79	36	0	0
14	0	0	0	0	0	0	0	0
15	0	0	0	0	0	0	0	0
16	370	380	5	5	87	54	0	0
17	0	0	0	0	0	0	0	0
18	0	0	0	0	0	0	0	0
19	0	0	0	0	0	0	0	0
20	0	0	0	0	0	0	0	0
21	0	0	0	0	0	0	0	0
22	0	0	0	0	0	0	0	0
23	0	0	0	0	0	0	0	0
24	0	0	0	0	0	0	0	0
25	0	0	0	0	0	0	0	0
26	0	0	0	0	0	0	0	0
27	0	0	0	0	0	0	0	0
28	0	0	0	0	0	0	0	0
29	0	0	0	0	0	0	0	0
30	0	0	0	0	0	0	0	0
31	0	0	0	0	0	0	0	0
32	750	750	2	2	70	22	0	0

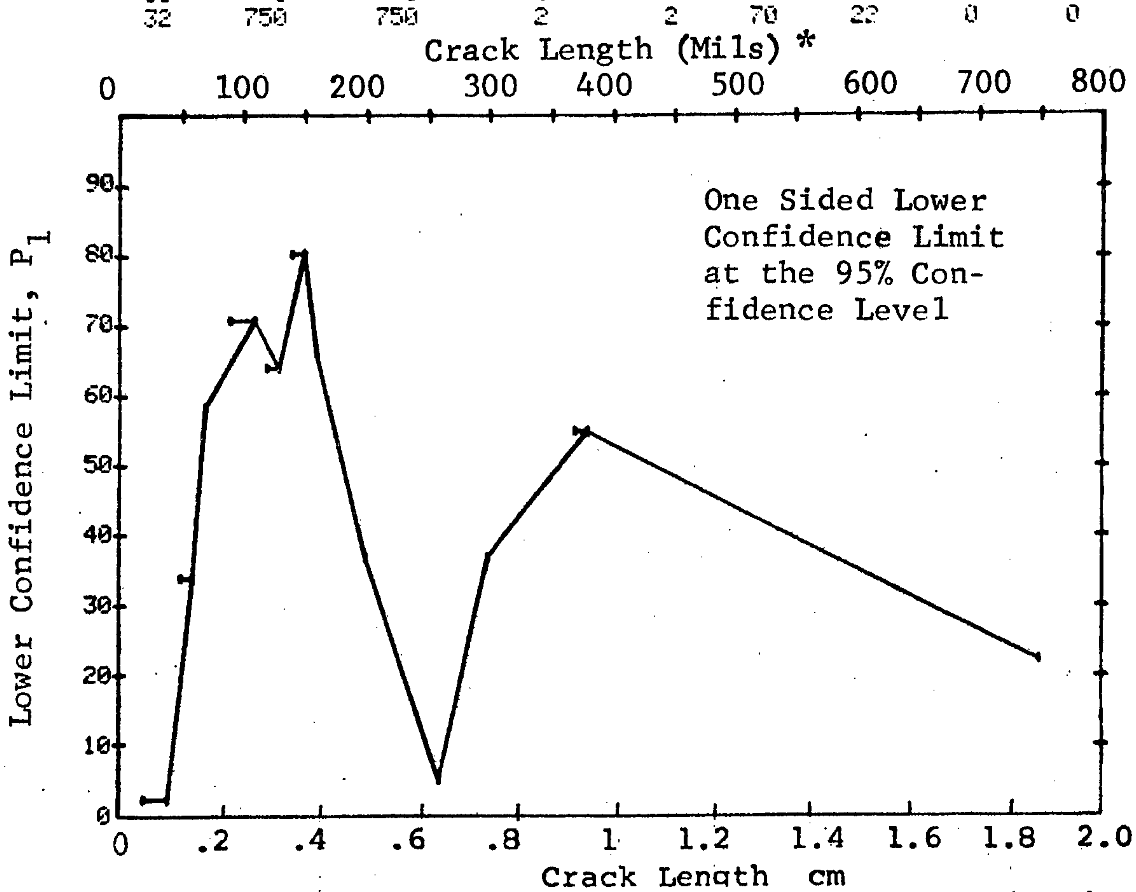

Figure D-64 Probability of Detection for 4340M Steel Using Liquid Penetrant. Compressed Notch Flaws in Solid Cylinder. Prod. Env.

(b) Optimum Probability Method of Data Cumulation

24-OCT-75 PENETRANT TEST 2 ( ) % (64)

RANGE	MIN LN	MAX LN	N	DET	50%	95%	0 MISS	1 MISS
1	20	* 40 *	16	2	0	2	0	0
2	50	60	30	15	0	33	0	0
3	70	70	16	13	0	58	0	0
4	70	110	40	34	0	72	0	0
5	70	130	59	50	0	74	0	0
6	90	150	87	77	0	81	80	92
7	90	160	99	88	0	82	80	92
8	140	200	59	54	0	83	44	57
9	0	0	0	0	0	0	0	0
10	0	0	0	0	0	0	0	0
11	140	260	60	55	0	83	43	56
12	0	0	0	0	0	0	0	0
13	140	300	63	58	0	84	40	53
14	0	0	0	0	0	0	0	0
15	0	0	0	0	0	0	0	0
16	140	380	68	63	0	85	35	48
17	0	0	0	0	0	0	0	0
18	0	0	0	0	0	0	0	0
19	0	0	0	0	0	0	0	0
20	0	0	0	0	0	0	0	0
21	0	0	0	0	0	0	0	0
22	0	0	0	0	0	0	0	0
23	0	0	0	0	0	0	0	0
24	0	0	0	0	0	0	0	0
25	0	0	0	0	0	0	0	0
26	0	0	0	0	0	0	0	0
27	0	0	0	0	0	0	0	0
28	0	0	0	0	0	0	0	0
29	0	0	0	0	0	0	0	0
30	0	0	0	0	0	0	0	0
31	0	0	0	0	0	0	0	0
32	140	750	70	65	0	85	33	46

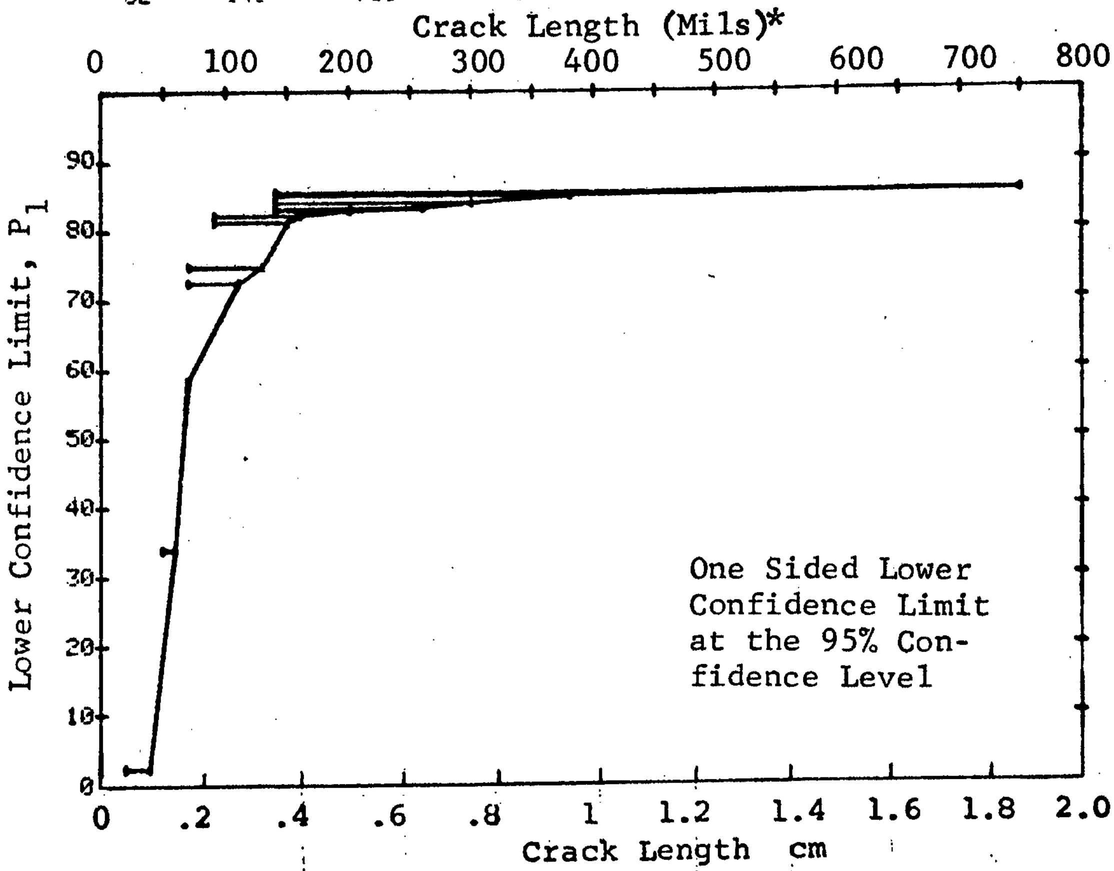

Figure D-64 (Continued)

(c) Overlapping Sixty Point Method of Data Cumulation

24-OCT-75 PENETRANT TEST 3 (64)

RANGE	MIN LN *	MAX LN *	N	DET	50%	95%	0 MISS	1 MISS
1	0	0	0	0	0	0	0	0
2	0	0	0	0	0	0	0	0
3	0	0	0	0	0	0	0	0
4	0	0	0	0	0	0	0	0
5	0	0	0	0	0	0	0	0
6	0	0	0	0	0	0	0	0
7	0	0	0	0	0	0	0	0
8	0	0	0	0	0	0	0	0
9	0	0	0	0	0	0	0	0
10	0	0	0	0	0	0	0	0
11	0	0	0	0	0	0	0	0
12	0	0	0	0	0	0	0	0
13	0	0	0	0	0	0	0	0
14	0	0	0	0	0	0	0	0
15	0	0	0	0	0	0	0	0
16	0	0	0	0	0	0	0	0
17	0	0	0	0	0	0	0	0
18	0	0	0	0	0	0	0	0
19	0	0	0	0	0	0	0	0
20	0	0	0	0	0	0	0	0
21	0	0	0	0	0	0	0	0
22	0	0	0	0	0	0	0	0
23	0	0	0	0	0	0	0	0
24	0	0	0	0	0	0	0	0
25	0	0	0	0	0	0	0	0
26	0	0	0	0	0	0	0	0
27	0	0	0	0	0	0	0	0
28	20	70	53	21	38	28	0	0
29	50	110	60	43	70	60	[illegible]	[illegible]
30	70	140	60	54	88	81	56	59
31	110	150	60	53	87	79	69	82
32	140	380	60	55	90	83	43	56

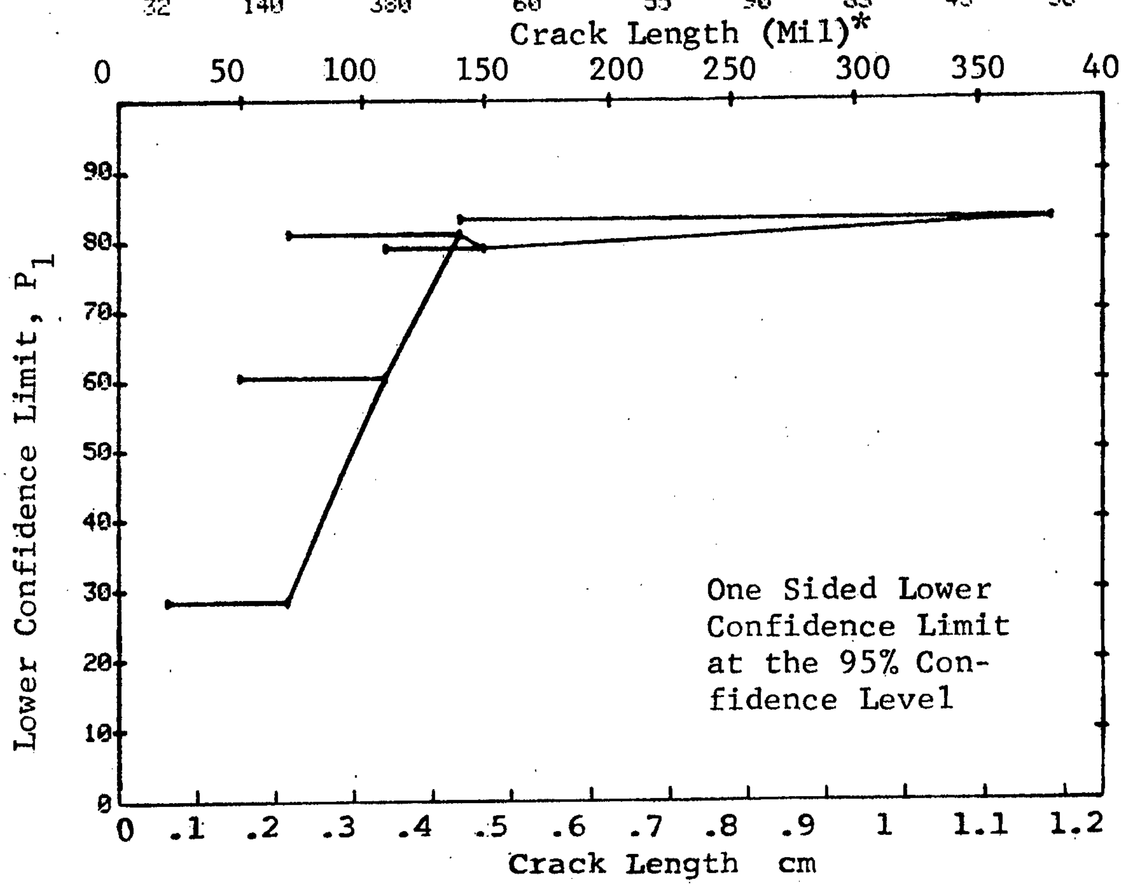

Figure D-64 (Concluded)

(a) Range Interval Method of Data Cumulation

24-OCT-75		PENETRANT	N	TEST 1			(65)	
RANGE	MIN LN *	MAX LN *	N	DET	50%	95%	0 MISS	1 MISS
1	10	10	6	1	10	0	0	0
2	0	0	0	0	0	0	0	0
3	30	30	3	3	79	36	0	0
4	0	0	0	0	0	0	0	0
5	40	40	11	11	93	76	18	35
6	50	50	34	32	92	82	27	42
7	0	0	0	0	0	0	0	0
8	60	60	12	12	94	77	17	34
9	70	70	2	2	70	22	0	0
10	0	0	0	0	0	0	0	0
11	80	80	9	9	92	71	0	0
12	90	90	14	14	95	80	15	32
13	0	0	0	0	0	0	0	0
14	100	100	1	1	50	5	0	0
15	110	110	22	22	96	87	7	24
16	120	120	2	2	70	22	0	0
17	0	0	0	0	0	0	0	0
18	130	130	8	5	55	28	0	0
19	140	140	7	7	90	65	0	0
20	0	0	0	0	0	0	0	0
21	150	150	18	18	96	84	11	28
22	160	160	2	2	70	22	0	0
23	0	0	0	0	0	0	0	0
24	170	170	11	11	93	76	18	35
25	180	180	11	11	93	76	18	35
26	0	0	0	0	0	0	0	0
27	190	190	1	1	50	5	0	0
28	0	0	0	0	0	0	0	0
29	0	0	0	0	0	0	0	0
30	210	210	3	3	79	36	0	0
31	220	220	2	2	70	22	0	0
32	230	230	9	8	91	68	0	0

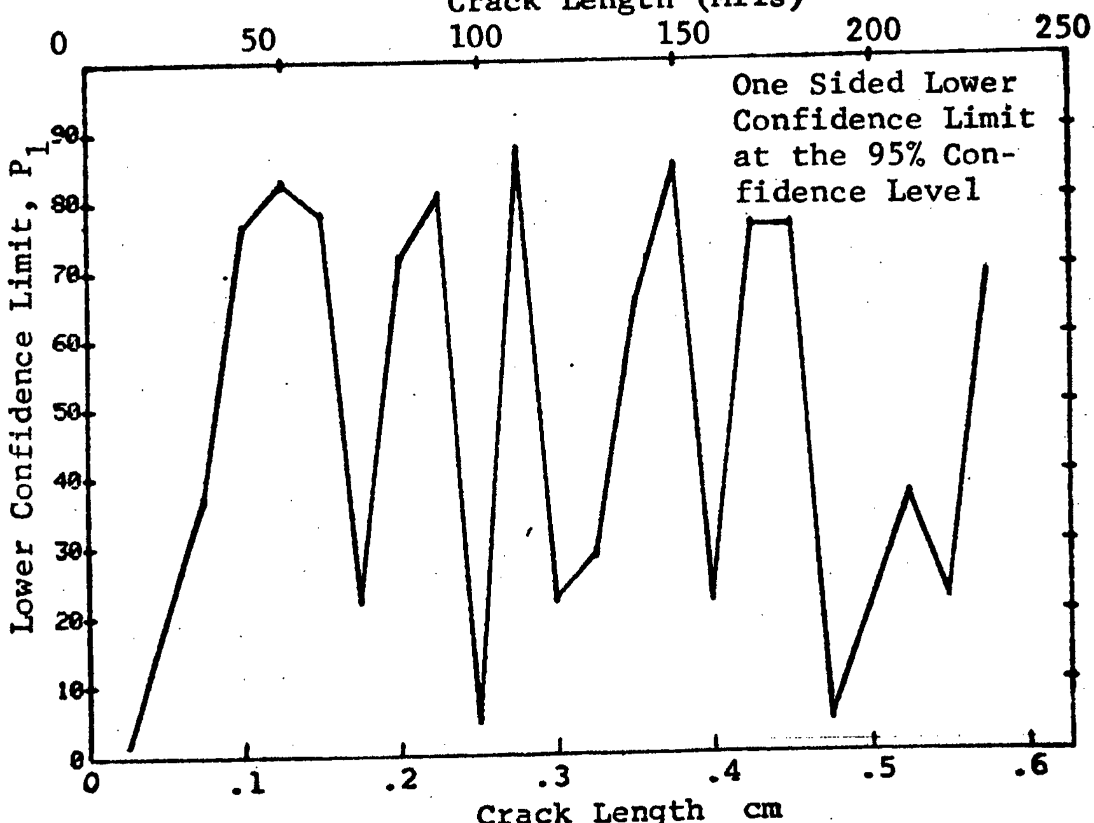

Figure D-65 Probability of Detection for 2024-T6 Al Using Liquid Penetrant. Compressed Notch Flaws in Tandem T Specimen. Lab. Env.

(b) Optimum Probability Method of Data Cumulation

24-OCT-75 PENETRANT TEST 2 (65)

RANGE	MIN LN *	MAX LN *	N	DET	50%	95%	0 MISS	1 MISS
1	10	10	5	1	0	0	0	0
2	0	0	3	0	0	0	0	0
3	30	30	3	3	0	36	0	0
4	0	0	0	0	0	0	0	0
5	30	40	14	14	0	80	15	32
6	30	50	48	46	0	87	13	28
7	0	0	0	0	0	0	0	0
8	30	60	60	58	0	89	1	16
9	30	70	62	60	0	90	0	14
10	0	0	0	0	0	0	0	0
11	30	80	71	69	0	91	0	5
12	30	90	85	83	0	92	0	0
13	0	0	0	0	0	0	0	0
14	30	100	86	84	0	92	0	0
15	60	110	60	60	0	95	0	0
16	60	120	62	62	0	95	0	0
17	0	0	0	0	0	0	0	0
18	30	130	118	113	0	91	0	0
19	30	140	125	120	0	91	0	0
20	0	0	0	0	0	0	0	0
21	30	150	143	138	0	92	0	0
22	30	160	145	140	0	92	0	0
23	0	0	0	0	0	0	0	0
24	30	170	156	151	0	93	0	0
25	140	180	49	49	0	94	0	0
26	0	0	0	0	0	0	0	0
27	140	190	50	50	0	94	0	0
28	0	0	0	0	0	0	0	0
29	0	0	0	0	0	0	0	0
30	140	210	53	53	0	94	0	0
31	140	220	55	55	0	94	0	0
32	140	230	63	63	0	95	0	0

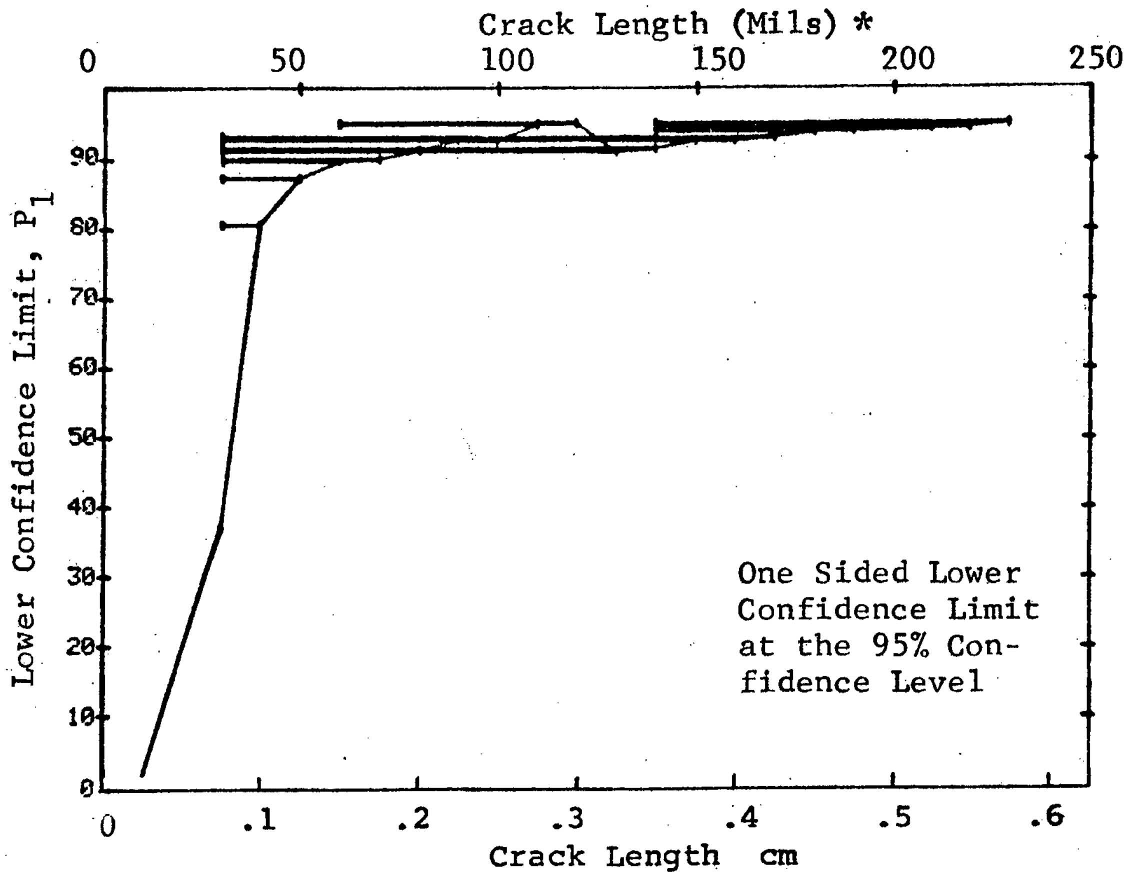

Figure D-65 (Continued)

(c) Overlapping Sixty Point Method of Data Cumulation

24-OCT-75 PENETRANT TEST 3 ( ) (65)

RANGE	MIN LN	MAX LN	N	DET	50%	95%	0 MISS	1 MISS
1	0 *	0 *	0	0	0	0	0	0
2	0	0	0	0	0	0	0	0
3	0	0	0	0	0	0	0	0
4	0	0	0	0	0	0	0	0
5	0	0	0	0	0	0	0	0
6	0	0	0	0	0	0	0	0
7	0	0	0	0	0	0	0	0
8	0	0	0	0	0	0	0	0
9	0	0	0	0	0	0	0	0
10	0	0	0	0	0	0	0	0
11	0	0	0	0	0	0	0	0
12	0	0	0	0	0	0	0	0
13	0	0	0	0	0	0	0	0
14	0	0	0	0	0	0	0	0
15	0	0	0	0	0	0	0	0
16	0	0	0	0	0	0	0	0
17	0	0	0	0	0	0	0	0
18	0	0	0	0	0	0	0	0
19	0	0	0	0	0	0	0	0
20	0	0	0	0	0	0	0	0
21	0	0	0	0	0	0	0	0
22	0	0	0	0	0	0	0	0
23	0	0	0	0	0	0	0	0
24	0	0	0	0	0	0	0	0
25	0	0	0	0	0	0	0	0
26	0	0	0	0	0	0	0	0
27	10	50	37	32	84	73	0	0
28	30	70	60	58	95	89	1	16
29	50	110	60	58	95	89	1	16
30	70	140	60	57	93	87	16	29
31	110	170	60	57	93	87	16	29
32	140	230	60	60	98	95	0	0

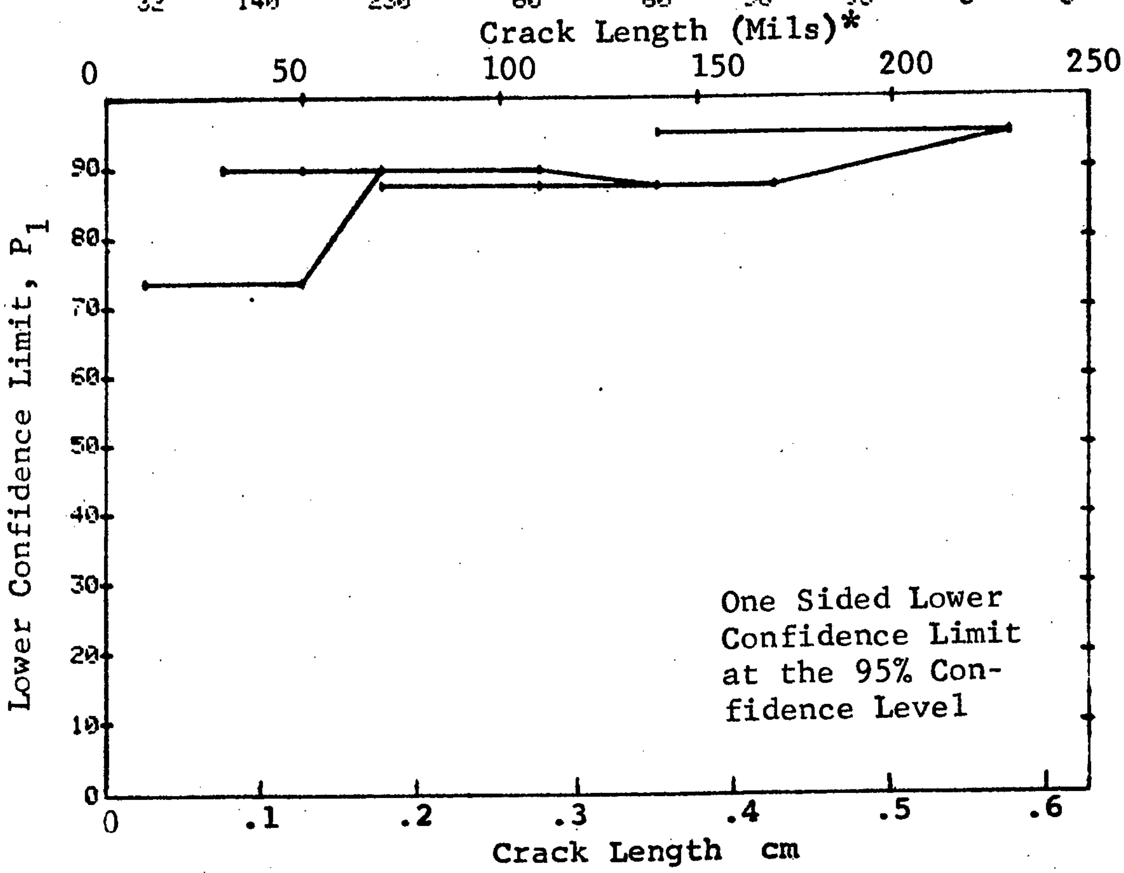

Figure D-65 (Concluded)

(a) Range Interval Method of Data Cumulation

27-OCT-75 PENETRANT TEST 1 (66)

RANGE	MIN LN	MAX LN	N	DET	50%	95%	0 MISS	1 MISS
1	40	40	4	4	84	47	0	0
2	70	70	4	4	84	47	0	0
3	0	0	0	0	0	0	0	0
4	100	110	29	25	84	71	0	0
5	130	130	16	16	95	82	13	30
6	0	0	0	0	0	0	0	0
7	0	0	0	0	0	0	0	0
8	190	190	4	4	84	47	0	0
9	210	210	4	4	84	47	0	0
10	230	230	5	5	87	54	0	0
11	0	0	0	0	0	0	0	0
12	250	250	5	5	87	54	0	0
13	270	270	4	4	84	47	0	0
14	300	300	4	4	84	47	0	0
15	310	310	4	4	84	47	0	0
16	340	340	4	4	84	47	0	0
17	350	350	4	4	84	47	0	0
18	380	380	4	4	84	47	0	0
19	0	0	0	0	0	0	0	0
20	410	410	4	4	84	47	0	0
21	0	0	0	0	0	0	0	0
22	450	450	5	5	87	54	0	0
23	460	460	4	4	84	47	0	0
24	480	480	4	4	84	47	0	0
25	0	0	0	0	0	0	0	0
26	0	0	0	0	0	0	0	0
27	0	0	0	0	0	0	0	0
28	0	0	0	0	0	0	0	0
29	0	0	0	0	0	0	0	0
30	0	0	0	0	0	0	0	0
31	0	0	0	0	0	0	0	0
32	650	650	4	4	84	47	0	0

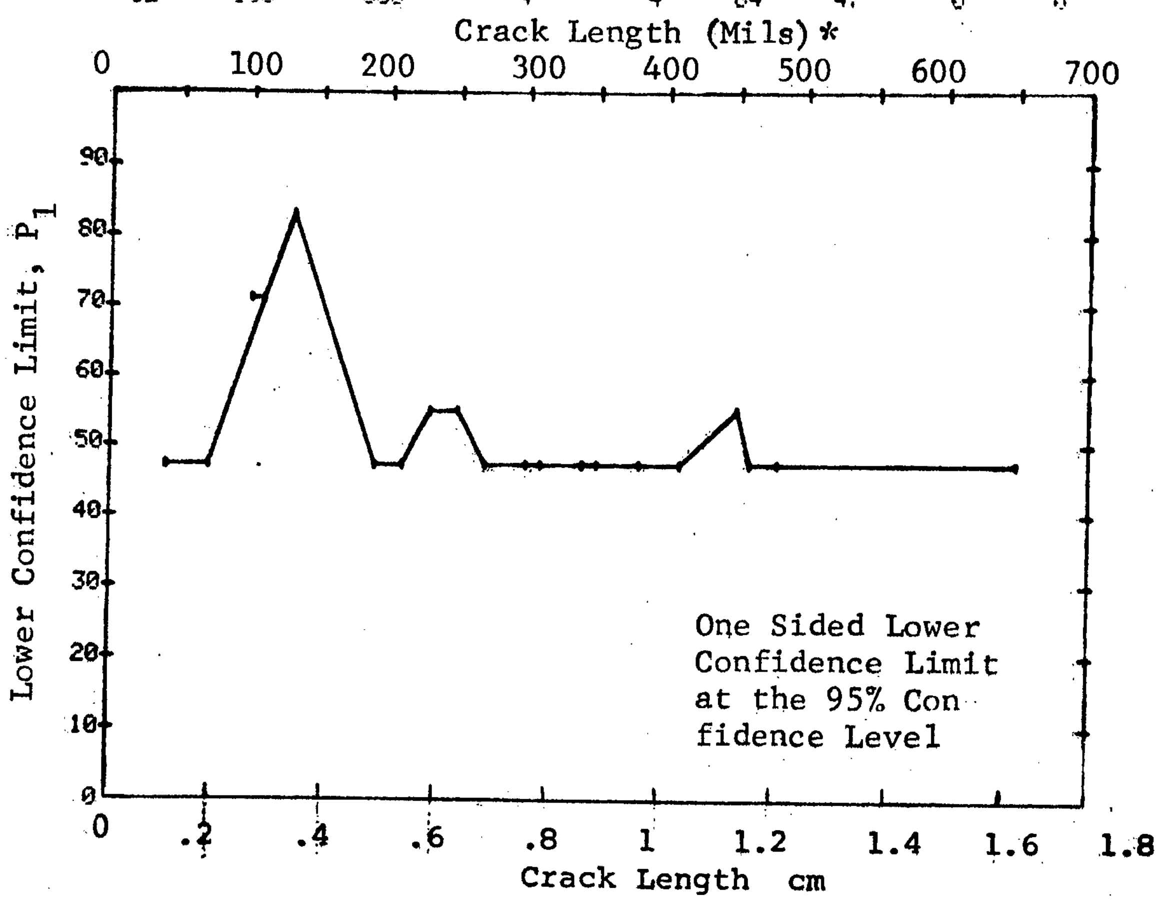

Figure D-66 Probability of Detection for 4340M Steel Using Liquid Penetrant. Compressed Notch Flaws in Solid Cylinder. Lab. Env.

(b) Optimum Probability Method of Data Cumulation

27-OCT-75	PENETRANT			TEST 2 (		(66)		
RANGE	MIN LN	MAX LN	N	DET	50%	95%	0 MISS	1 MISS
1	40 *	40*	4	4	0	47	0	0
2	40	70	8	8	0	68	0	0
3	0	0	0	0	0	0	0	0
4	40	110	37	33	0	76	0	0
5	40	130	53	49	0	83	36	50
6	0	0	0	0	0	0	0	0
7	0	0	0	0	0	0	0	0
8	130	190	20	20	0	86	9	26
9	130	210	24	24	0	88	5	22
10	130	230	29	29	0	90	0	17
11	0	0	0	0	0	0	0	9
12	130	250	34	34	0	91	0	12
13	130	270	38	38	0	92	0	8
14	130	300	42	42	0	93	0	4
15	130	310	46	46	0	93	0	0
16	130	340	50	50	0	94	0	0
17	130	350	54	54	0	94	0	0
18	130	380	58	58	0	94	0	0
19	0	0	0	0	0	0	0	0
20	130	410	62	62	0	95	0	0
21	0	0	0	0	0	0	0	0
22	130	450	67	67	0	95	0	0
23	130	460	71	71	0	95	0	0
24	130	480	75	75	0	96	0	0
25	0	0	0	0	0	0	0	0
26	0	0	0	0	0	0	0	0
27	0	0	0	0	0	0	0	0
28	0	0	0	0	0	0	0	0
29	0	0	0	0	0	0	0	0
30	0	0	0	0	0	0	0	0
31	0	0	0	0	0	0	0	0
32	130	[illegible]	79	79	0	96	0	0

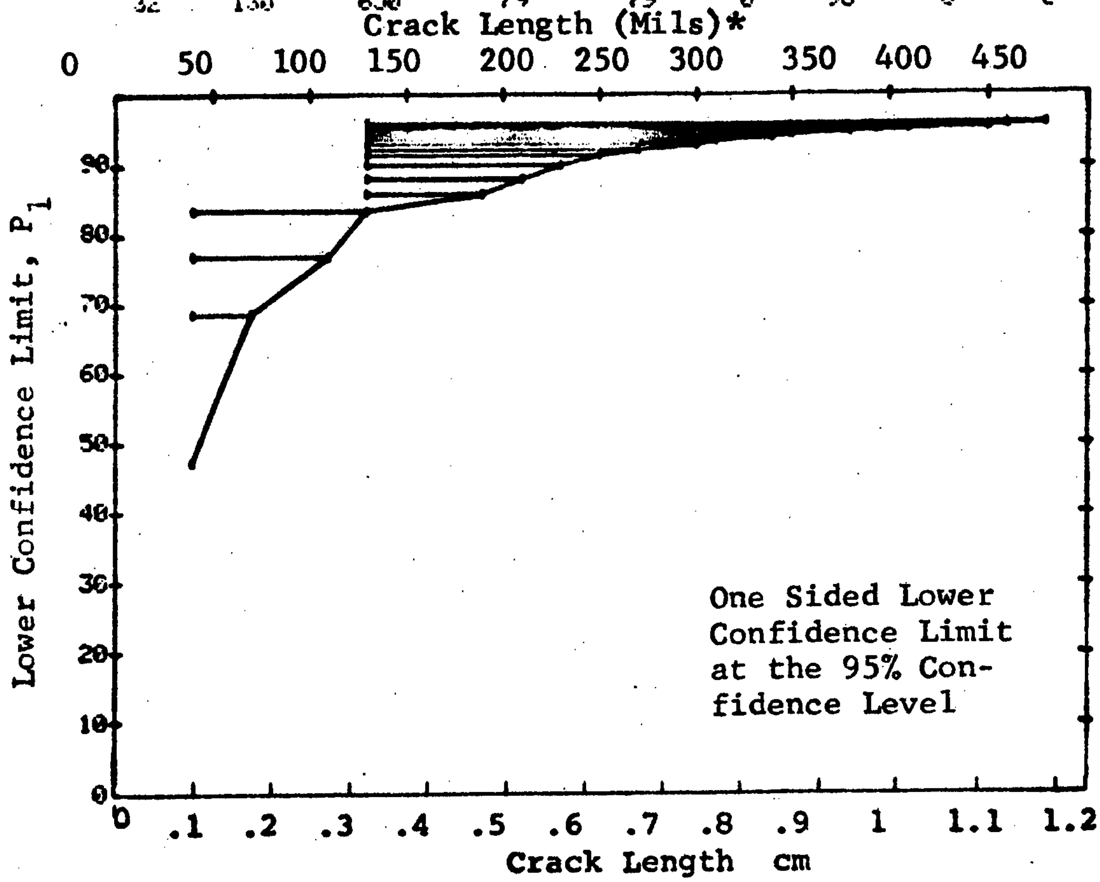

Figure D-66 (Continued)

(c) Overlapping Sixty Point Method of Data Cumulation

27-OCT-75 PENETRANT TEST 3 266 (66)

RANGE	MIN LN	MAX LN	N	DET	50%	95%	0 MISS	1 MISS
1	0 *	0 *	0	0	0	0	0	0
2	0	0	0	0	0	0	0	0
3	0	0	0	0.	0	0	0	0
4	0	0	0	0	0	0	0	0
5	0	0	0	0	0	0	0	0
6	0	0	0	0	0	0	0	0
7	0	0	0	0	0	0	0	0
8	0	0	0	0	0	0	0	0
9	0	0	0	0	0	0	0	0
10	0	0	0	0	0	0	0	0
11	0	0	0	0	0	0	0	0
12	0	0	0	0	0	0	0	0
13	0	0	0	0	0	0	0	0
14	0	0	0	0	0	0	0	0
15	0	0	0	0	0	0	0	0
16	0	0	0	0	0	0	0	0
17	0	0	0	0	0	0	0	0
18	0	0	0	0	0	0	0	0
19	0	0	0	0	0	0	0	0
20	0	0	0	0	0	0	0	0
21	0	0	0	0	0	0	0	0
22	0	0	0	0	0	0	0	0
23	0	0	0	0	0	0	0	0
24	0	0	0	0	0	0	0	0
25	0	0	0	0	0	0	0	0
26	0	0	0	0	0	0	0	0
27	0	0	0	0	0	0	0	0
28	0	0	0	0	0	0	0	0
29	0	0	0	0	0	0	0	0
30	40	130	52	48	91	83	37	51
31	110	310	59	60	99	95	0	0
32	130	480	60	60	98	95	0	0

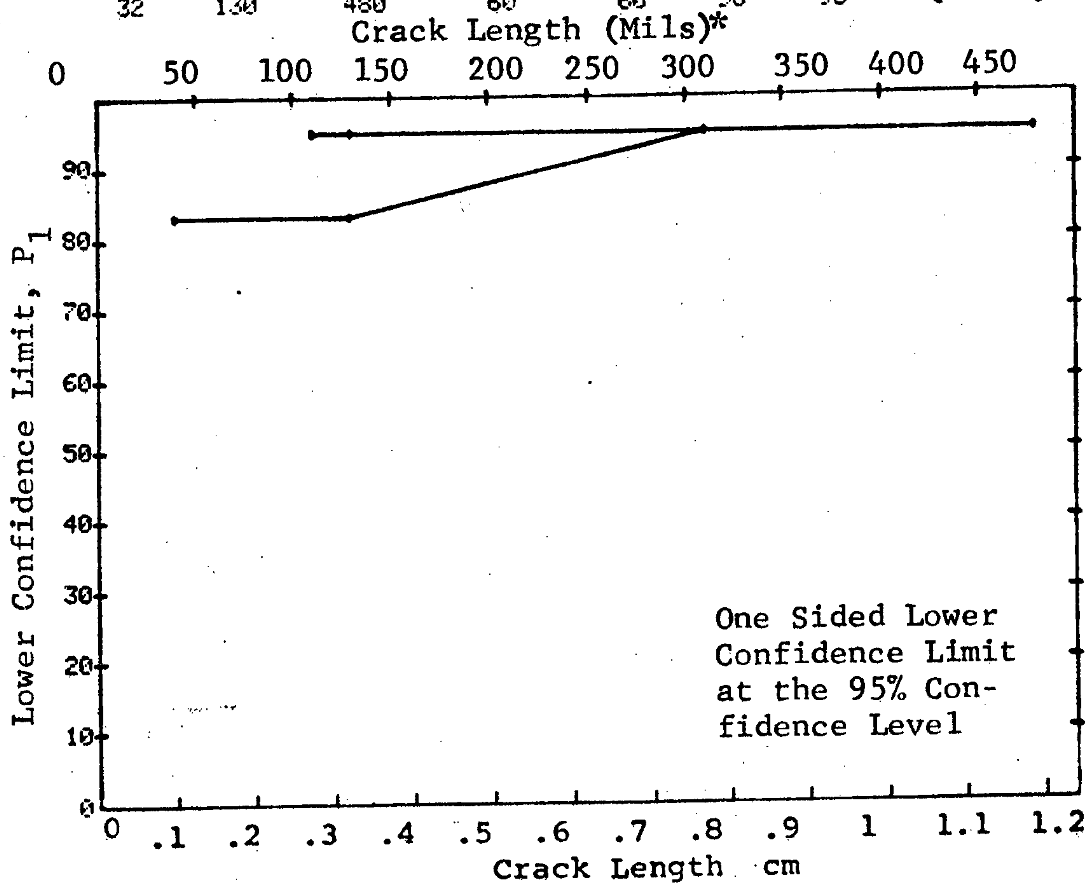

Figure D-66 (Concluded)

(a) Range Interval Method of Data Cumulation

27-OCT-75 PENETRANT TEST (67)

RANGE	MIN LN		MAX LN		N	DET	50%	95%	0 MISS	1 MISS
1	80	*	90	*	33	19	53	38	0	0
2	0		0		0	0	0	0	0	0
3	110		110		8	2	20	4	0	0
4	120		120		4	4	84	47	0	0
5	130		130		10	5	45	22	0	0
6	140		140		16	16	95	82	13	30
7	160		160		3	3	79	36	0	0
8	0		0		0	0	0	0	0	0
9	0		0		0	0	0	0	0	0
10	0		0		0	0	0	0	0	0
11	0		0		0	0	0	0	0	0
12	0		0		0	0	0	0	0	0
13	0		0		0	0	0	0	0	0
14	0		0		0	0	0	0	0	0
15	250		250		1	1	50	5	0	0
16	270		270		1	1	50	5	0	0
17	280		280		2	2	70	22	0	0
18	0		0		0	0	0	0	0	0
19	300		300		4	4	84	47	0	0
20	310		310		4	4	84	47	0	0
21	0		0		0	0	0	0	0	0
22	0		0		0	0	0	0	0	0
23	0		0		0	0	0	0	0	0
24	0		0		0	0	0	0	0	0
25	0		0		0	0	0	0	0	0
26	0		0		0	0	0	0	0	0
27	390		390		4	4	84	47	0	0
28	0		0		0	0	0	0	0	0
29	0		0		0	0	0	0	0	0
30	0		0		0	0	0	0	0	0
31	0		0		0	0	0	0	0	0
32	450		460		5	5	87	54	0	0

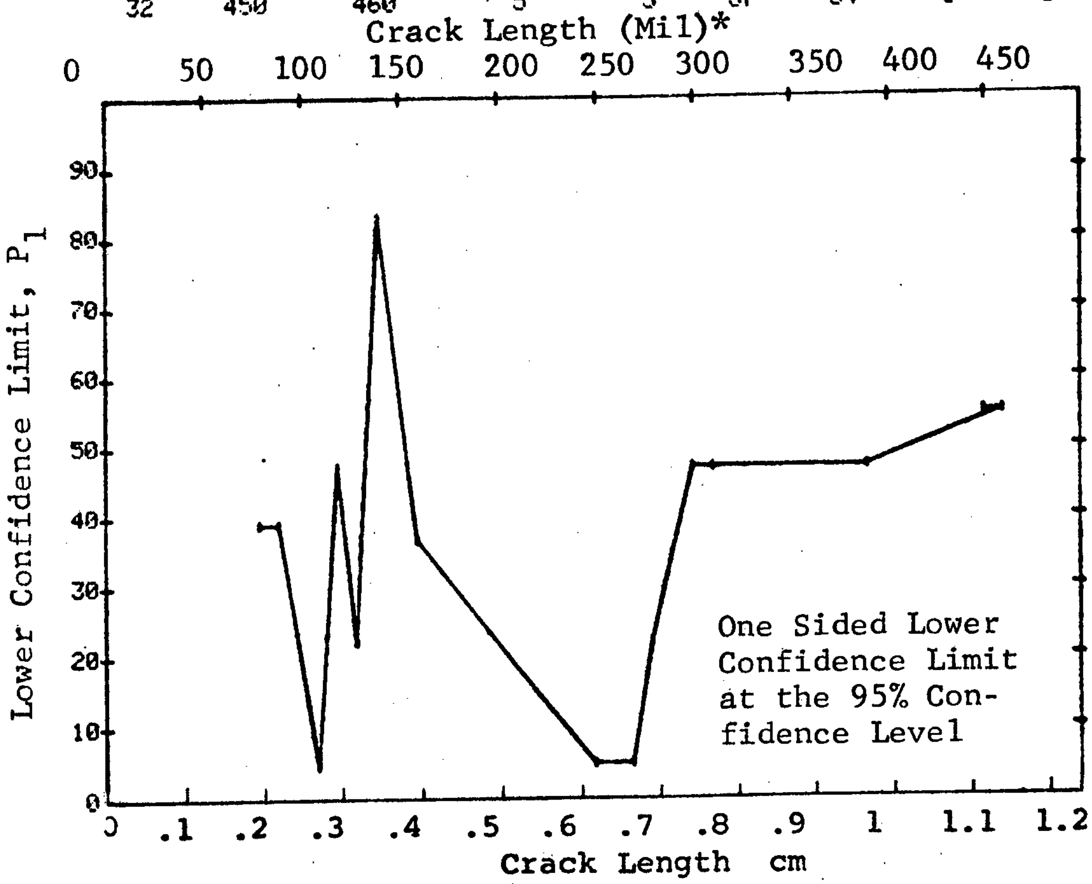

Figure D-67 Probability of Detection for 4340M Steel Using Liquid Penetrant. Compressed Notch Flaws in Hollow Cylinder. Lab. Env.

(b) Optimum Probability Method of Data Cumulation

27-OCT-75 PENETRANT TEST 2 ( )C2 (67)

RANGE	MIN LN	MAX LN	N	DET	50%	95%	0 MISS	1 MISS
1	80 *	90 *	33	18	0	38	0	0
2	0	0	0	0	0	0	0	0
3	80	110	41	20	0	35	0	0
4	120	120	4	4	0	47	0	0
5	80	130	55	29	0	40	0	0
6	140	140	16	16	0	82	13	30
7	140	160	19	19	0	85	10	27
8	0	0	0	0	0	0	0	0
9	0	0	0	0	0	0	0	0
10	0	0	0	0	0	0	0	0
11	0	0	0	0	0	0	0	0
12	0	0	0	0	0	0	0	0
13	0	0	0	0	0	0	0	0
14	0	0	0	0	0	0	0	0
15	140	250	20	20	0	86	9	26
16	140	270	21	21	0	86	8	25
17	140	280	23	23	0	87	6	23
18	0	0	0	0	0	0	0	0
19	140	300	27	27	0	89	2	19
20	140	310	31	31	0	90	0	15
21	0	0	0	0	0	0	0	0
22	0	0	0	0	0	0	0	0
23	0	0	0	0	0	0	0	0
24	0	0	0	0	0	0	0	0
25	0	0	0	0	0	0	0	0
26	0	0	0	0	0	0	0	0
27	140	390	35	35	0	91	0	11
28	0	0	0	0	0	0	0	0
29	0	0	0	0	0	0	0	0
30	0	0	0	0	0	0	0	0
31	0	0	0	0	0	0	0	0
32	140	460	40	40	0	92	0	6

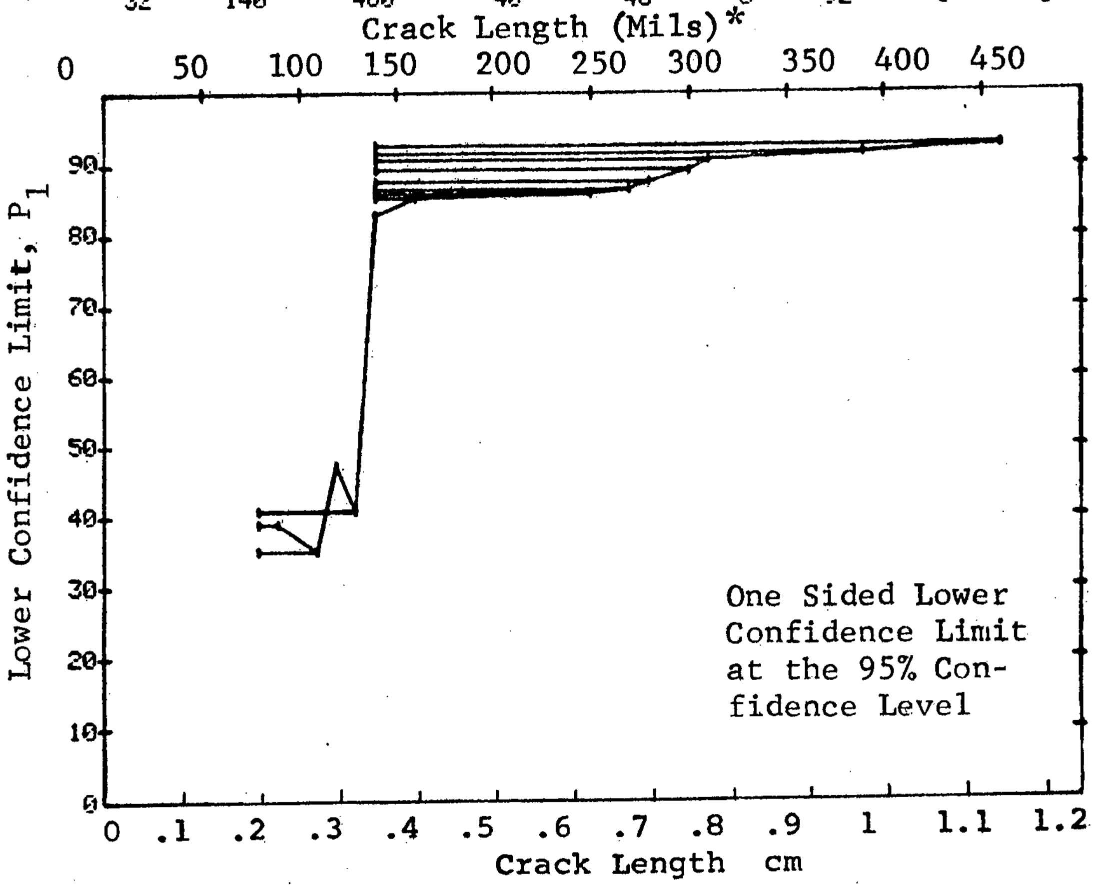

Figure D-67 (Continued)

(c) Overlapping Sixty Point Method of Data Cumulation

27-OCT-75 PENETRANT TEST 3 ( ) 7 (67)

RANGE	MIN LN	* MAX LN *	N	DET	50%	95%	0 MISS	1 MISS
1	0	0	0	0	0	0	0	0
2	0	0	0	0	0	0	0	0
3	0	0	0	0	0	0	0	0
4	0	0	0	0	0	0	0	0
5	0	0	0	0	0	0	0	0
6	0	0	0	0	0	0	0	0
7	0	0	0	0	0	0	0	0
8	0	0	0	0	0	0	0	0
9	0	0	0	0	0	0	0	0
10	0	0	0	0	0	0	0	0
11	0	0	0	0	0	0	0	0
12	0	0	0	0	0	0	0	0
13	0	0	0	0	0	0	0	0
14	0	0	0	0	0	0	0	0
15	0	0	0	0	0	0	0	0
16	0	0	0	0	0	0	0	0
17	0	0	0	0	0	0	0	0
18	0	0	0	0	0	0	0	0
19	0	0	0	0	0	0	0	0
20	0	0	0	0	0	0	0	0
21	0	0	0	0	0	0	0	0
22	0	0	0	0	0	0	0	0
23	0	0	0	0	0	0	0	0
24	0	0	0	0	0	0	0	0
25	0	0	0	0	0	0	0	0
26	0	0	0	0	0	0	0	0
27	0	0	0	0	0	0	0	0
28	0	0	0	0	0	0	0	0
29	0	0	0	0	0	0	0	0
30	80	110	35	20	55	41	0	0
31	80	140	60	38	62	51	0	0
32	110	460	60	49	80	71	0	0

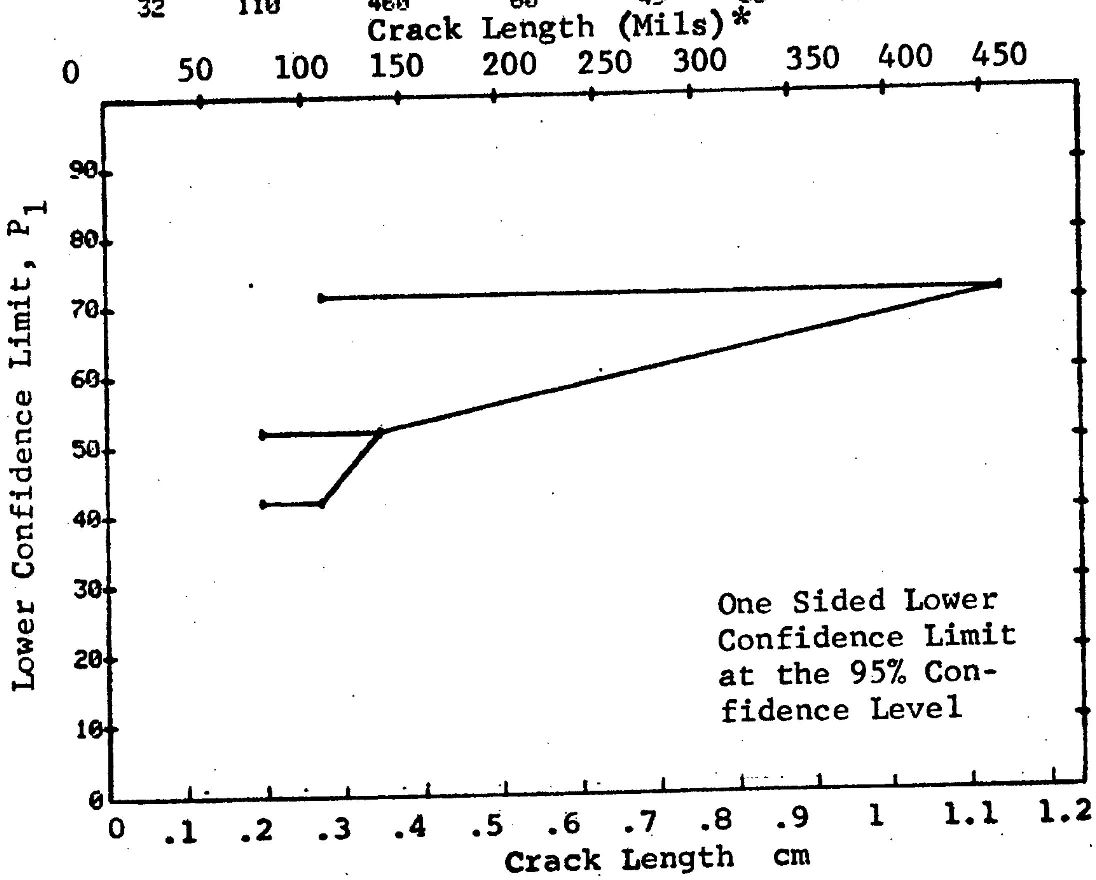

Figure D-67 (Concluded)

(a) Range Interval Method of Data Cumulation

27-OCT-75 PENETRANT TEST 1 ⟨. 568 (68)

RANGE	MIN LN *	MAX LN *	N	DET	50%	95%	0 MISS	1 MISS
1	60	60	10	2	16	3	0	0
2	0	0	0	0	0	0	0	0
3	0	0	0	0	0	0	0	0
4	0	0	0	0	0	0	0	0
5	0	0	0	0	0	0	0	0
6	0	0	0	0	0	0	0	0
7	0	0	0	0	0	0	0	0
8	100	100	9	5	50	25	0	0
9	0	0	0	0	0	0	0	0
10	0	0	0	0	0	0	0	0
11	0	0	0	0	0	0	0	0
12	120	120	2	0	0	0	0	0
13	0	0	0	0	0	0	0	0
14	130	130	5	2	31	7	0	0
15	0	0	0	0	0	0	0	0
16	140	140	3	3	79	36	0	0
17	0	0	0	0	0	0	0	0
18	0	0	0	0	0	0	0	0
19	0	0	0	0	0	0	0	0
20	0	0	0	0	0	0	0	0
21	0	0	0	0	0	0	0	0
22	0	0	0	0	0	0	0	0
23	180	180	2	0	0	0	0	0
24	0	0	0	0	0	0	0	0
25	0	0	0	0	0	0	0	0
26	0	0	0	0	0	0	0	0
27	0	0	0	0	0	0	0	0
28	0	0	0	0	0	0	0	0
29	0	0	0	0	0	0	0	0
30	0	0	0	0	0	0	0	0
31	0	0	0	0	0	0	0	0
32	230	230	1	1	50	5	0	0

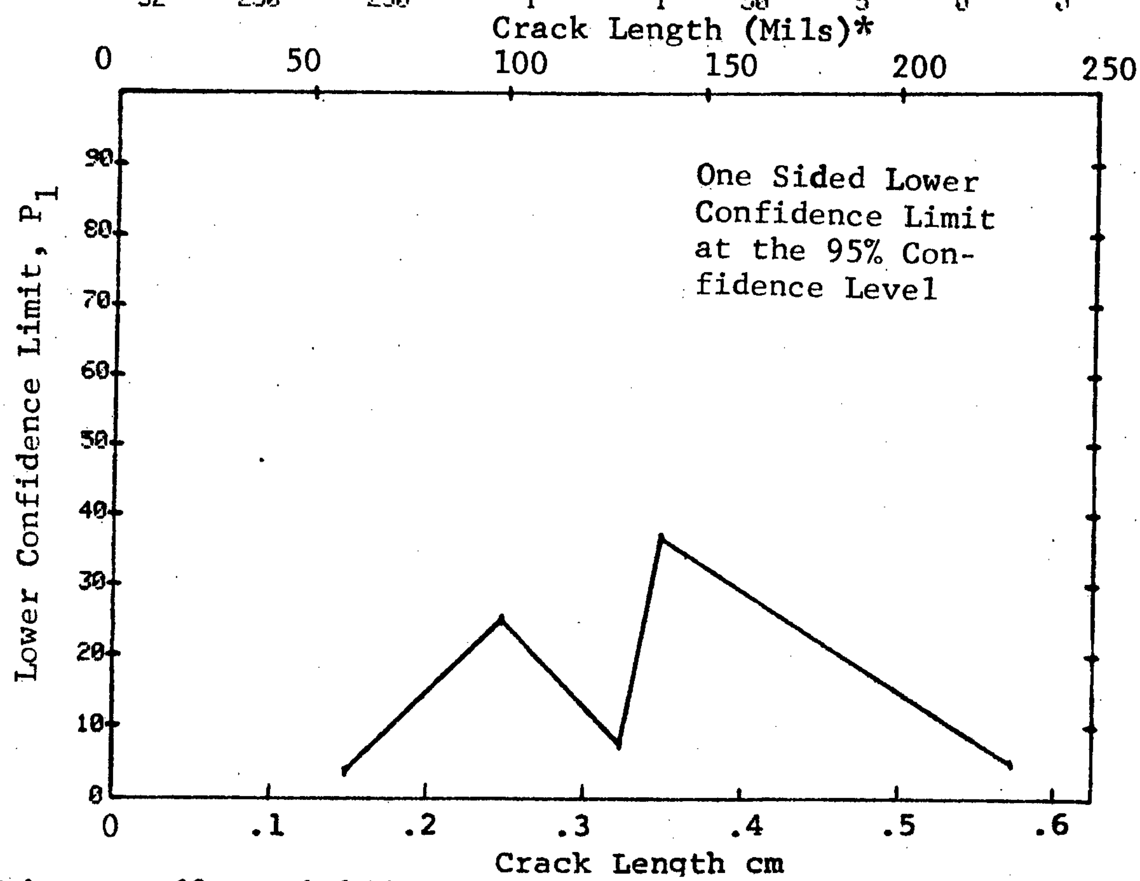

Figure D-68 Probability of Detection for 4340M Steel Using Liquid Penetrant. Compressed Notch Flaws in Filleted Hollow Cylinder. Lab. Env.

(b) Optimum Probability Method of Data Cumulation

27-OCT-75 PENETRANT TEST 2 (.)<8 (68)

RANGE	MIN LN	MAX LN	N	DET	50%	95%	0 MISS	1 MISS
1	60 *	50 *	10	2	0	3	0	0
2	0	0	0	0	0	0	0	0
3	0	0	0	0	0	0	0	0
4	0	0	0	0	0	0	0	0
5	0	0	0	0	0	0	0	0
6	0	0	0	0	0	0	0	0
7	0	0	0	0	0	0	0	0
8	100	100	9	5	0	25	0	0
9	0	0	0	0	0	0	0	0
10	0	0	0	0	0	0	0	0
11	0	0	0	0	0	0	0	0
12	100	120	11	5	0	19	0	0
13	0	0	0	0	0	0	0	0
14	100	130	16	7	0	22	0	0
15	0	0	0	0	0	0	0	0
16	140	140	3	3	0	36	0	0
17	0	0	0	0	0	0	0	0
18	0	0	0	0	0	0	0	0
19	0	0	0	0	0	0	0	0
20	0	0	0	0	0	0	0	0
21	0	0	0	0	0	0	0	0
22	0	0	0	0	0	0	0	0
23	100	180	21	10	0	28	0	0
24	0	0	0	0	0	0	0	0
25	0	0	0	0	0	0	0	0
26	0	0	0	0	0	0	0	0
27	0	0	0	0	0	0	0	0
28	0	0	0	0	0	0	0	0
29	0	0	0	0	0	0	0	0
30	0	0	0	0	0	0	0	0
31	0	0	0	0	0	0	0	0
32	100	230	22	11	0	31	0	0

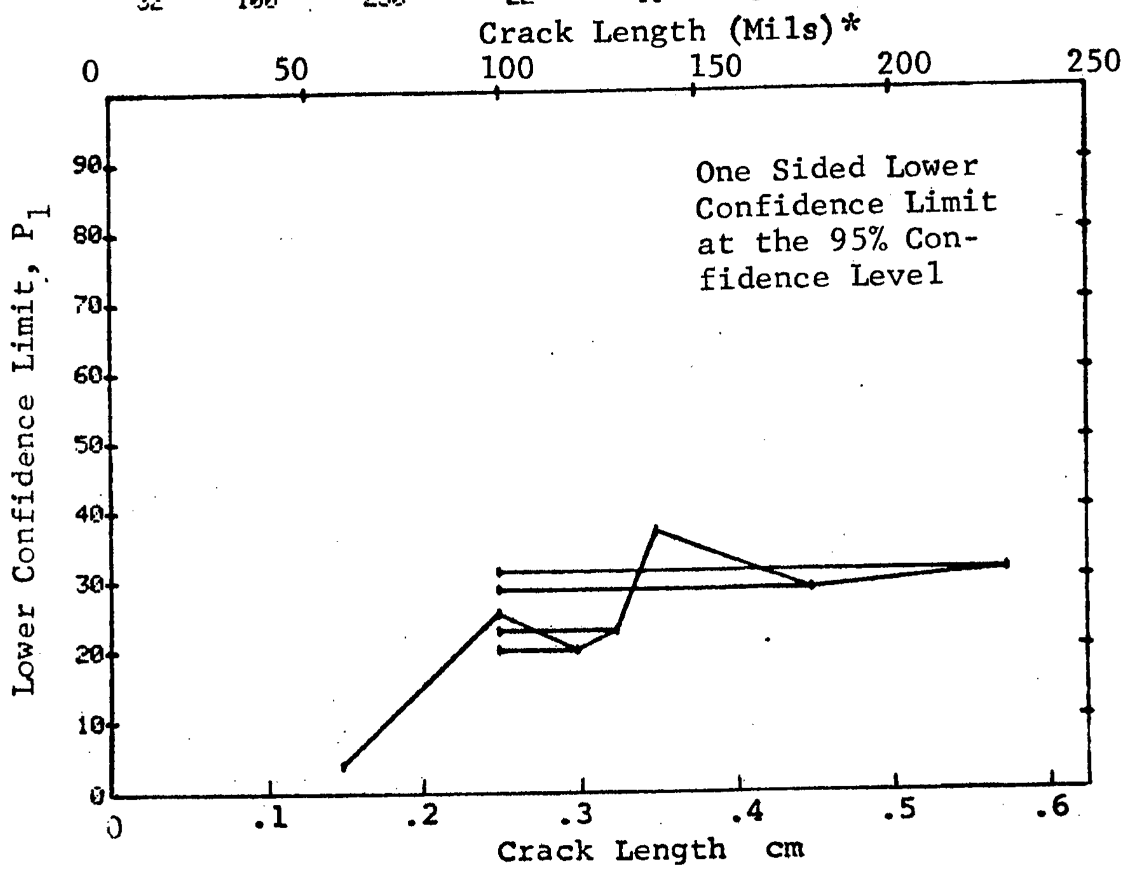

Figure D-68 (Continued)

(c) Overlapping Sixty Point Method of Data Cumulation

27-OCT-75 PENETRANT TEST 3 ((68)

RANGE	MIN LN *	MAX LN *	N	DET	50%	95%	0 MISS	1 MISS
1	0	0	0	0	0	0	0	0
2	0	0	0	0	0	0	0	0
3	0	0	0	0	0	0	0	0
4	0	0	0	0	0	0	0	0
5	0	0	0	0	0	0	0	0
6	0	0	0	0	0	0	0	0
7	0	0	0	0	0	0	0	0
8	0	0	0	0	0	0	0	0
9	0	0	0	0	0	0	0	0
10	0	0	0	0	0	0	0	0
11	0	0	0	0	0	0	0	0
12	0	0	0	0	0	0	0	0
13	0	0	0	0	0	0	0	0
14	0	0	0	0	0	0	0	0
15	0	0	0	0	0	0	0	0
16	0	0	0	0	0	0	0	0
17	0	0	0	0	0	0	0	0
18	0	0	0	0	0	0	0	0
19	0	0	0	0	0	0	0	0
20	0	0	0	0	0	0	0	0
21	0	0	0	0	0	0	0	0
22	0	0	0	0	0	0	0	0
23	0	0	0	0	0	0	0	0
24	0	0	0	0	0	0	0	0
25	0	0	0	0	0	0	0	0
26	0	0	0	0	0	0	0	0
27	0	0	0	0	0	0	0	0
28	0	0	0	0	0	0	0	0
29	0	0	0	0	0	0	0	0
30	0	0	0	0	0	0	0	0
31	0	0	0	0	0	0	0	0
32	60	230	32	13	39	25	0	0

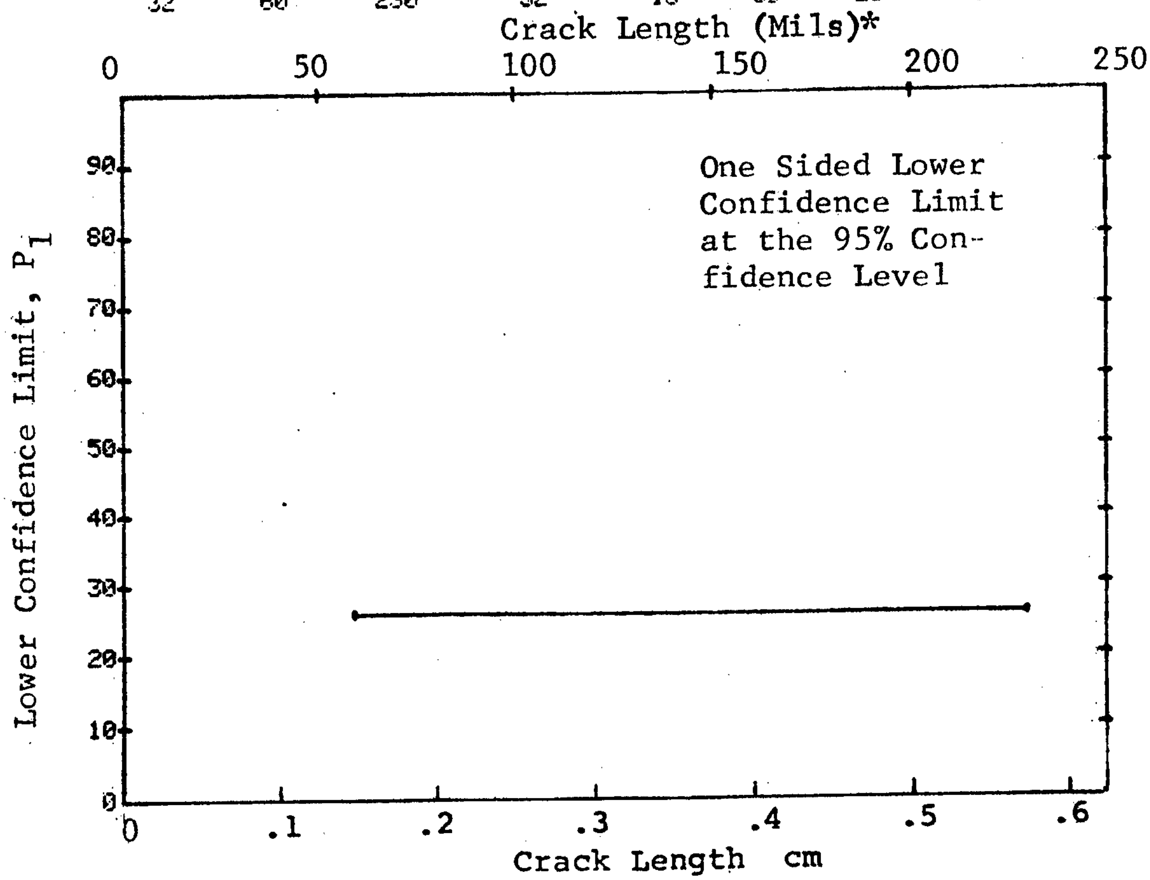

Figure D-68 (Concluded)

(a) Range Interval Method of Data Cumulation

27-OCT-75 PENETRANT TEST [illegible] (69)

RANGE	MIN LN *	MAX LN *	N	DET	50%	95%	0 MISS	1 MISS
1	20	30	20	17	81	65	0	0
2	0	0	0	0	0	0	0	0
3	0	0	0	0	0	0	0	0
4	60	60	7	7	90	65	0	0
5	70	70	15	15	95	81	14	31
6	0	0	0	0	0	0	0	0
7	90	90	8	8	91	68	0	0
8	100	100	5	5	87	54	0	0
9	0	0	0	0	0	0	0	0
10	0	0	0	0	0	0	0	0
11	130	140	13	13	94	79	16	33
12	150	150	7	7	90	65	0	0
13	0	0	0	0	0	0	0	0
14	0	0	0	0	0	0	0	0
15	0	0	0	0	0	0	0	0
16	0	0	0	0	0	0	0	0
17	0	0	0	0	0	0	0	0
18	0	0	0	0	0	0	0	0
19	0	0	0	0	0	0	0	0
20	0	0	0	0	0	0	0	0
21	0	0	0	0	0	0	0	0
22	0	0	0	0	0	0	0	0
23	0	0	0	0	0	0	0	0
24	0	0	0	0	0	0	0	0
25	0	0	0	0	0	0	0	0
26	300	300	6	6	89	60	0	0
27	0	0	0	0	0	0	0	0
28	0	0	0	0	0	0	0	0
29	0	0	0	0	0	0	0	0
30	0	0	0	0	0	0	0	0
31	0	0	0	0	0	0	0	0
32	370	370	6	6	89	60	0	0

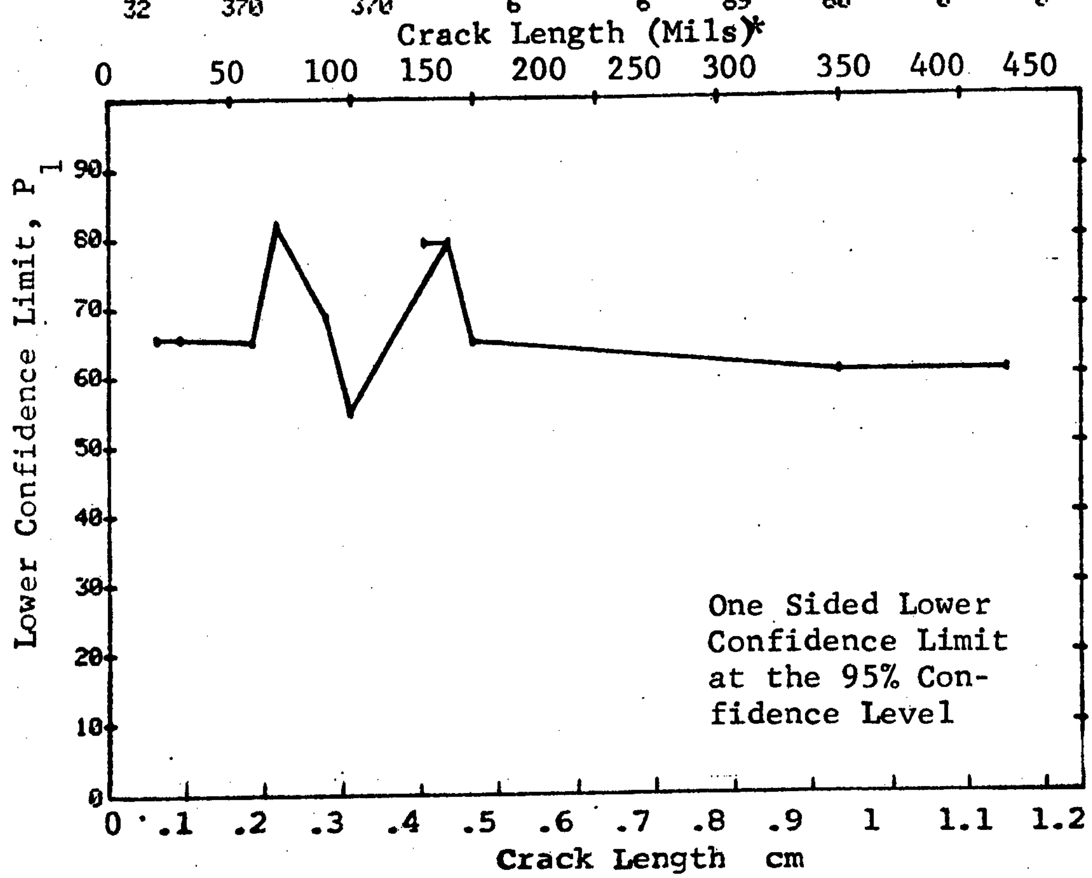

Figure D-69 Probability of Detection for 4340M Steel Using Liquid Penetrant. Compressed Notch Flaws in Filleted Solid Cylinder. Lab. Env.

(b) Optimum Probability Method of Data Cumulation

27-OCT-75 PENETRANT TEST 2 ([illegible]) (69)

RANGE	MIN LN	MAX LN	N	DET	50%	95%	0 MISS	1 MISS
1	20 *	30 *	29	17	0	65	0	0
2	0	0	0	0	0	0	0	0
3	0	0	0	0	0	0	0	0
4	20	60	27	24	0	73	0	0
5	60	70	22	22	0	87	7	24
6	0	0	0	0	0	0	0	0
7	60	90	30	30	0	90	0	16
8	60	100	35	35	0	91	0	11
9	0	0	0	0	0	0	0	0
10	0	0	0	0	0	0	0	0
11	60	140	48	48	0	93	0	0
12	60	150	55	55	0	94	0	0
13	0	0	0	0	0	0	0	0
14	0	0	0	0	0	0	0	0
15	0	0	0	0	0	0	0	0
16	0	0	0	0	0	0	0	0
17	0	0	0	0	0	0	0	0
18	0	0	0	0	0	0	0	0
19	0	0	0	0	0	0	0	0
20	0	0	0	0	0	0	0	0
21	0	0	0	0	0	0	0	0
22	0	0	0	0	0	0	0	0
23	0	0	0	0	0	0	0	0
24	0	0	0	0	0	0	0	0
25	0	0	0	0	0	0	0	0
26	60	300	61	61	0	95	0	0
27	0	0	0	0	0	0	0	0
28	0	0	0	0	0	0	0	0
29	0	0	0	0	0	0	0	0
30	0	0	0	0	0	0	0	0
31	0	0	0	0	0	0	0	0
32	60	370	67	67	0	95	0	0

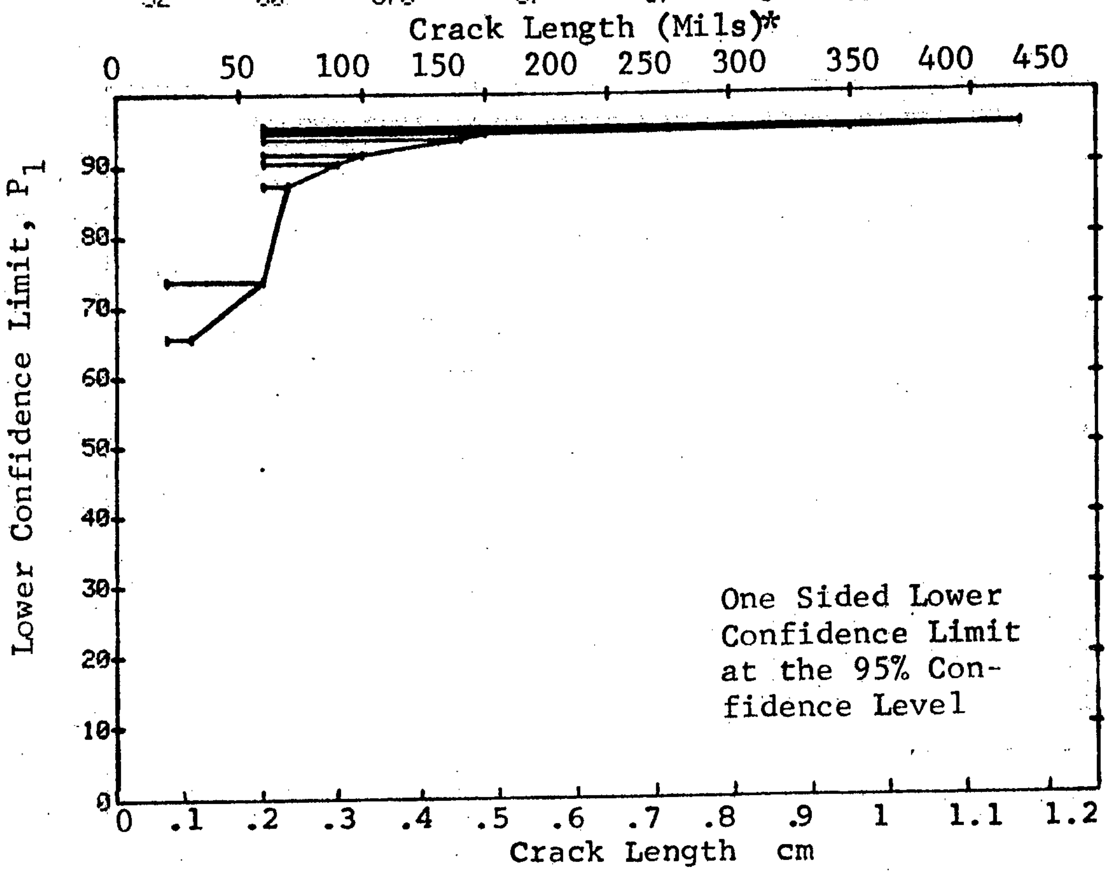

Figure D-69 (Continued)

(c) Overlapping Sixty Point Method of Data Cumulation

27-OCT-75 PENETRANT TEST 3 (69)

RANGE	MIN LN	* MAX LN *	N	DET	50%	95%	0 MISS	1 MISS
1	0	0	0	0	0	0	0	0
2	0	0	0	0	0	0	0	0
3	0	0	0	0	0	0	0	0
4	0	0	0	0	0	0	0	0
5	0	0	0	0	0	0	0	0
6	0	0	0	0	0	0	0	0
7	0	0	0	0	0	0	0	0
8	0	0	0	0	0	0	0	0
9	0	0	0	0	0	0	0	0
10	0	0	0	0	0	0	0	0
11	0	0	0	0	0	0	0	0
12	0	0	0	0	0	0	0	0
13	0	0	0	0	0	0	0	0
14	0	0	0	0	0	0	0	0
15	0	0	0	0	0	0	0	0
16	0	0	0	0	0	0	0	0
17	0	0	0	0	0	0	0	0
18	0	0	0	0	0	0	0	0
19	0	0	0	0	0	0	0	0
20	0	0	0	0	0	0	0	0
21	0	0	0	0	0	0	0	0
22	0	0	0	0	0	0	0	0
23	0	0	0	0	0	0	0	0
24	0	0	0	0	0	0	0	0
25	0	0	0	0	0	0	0	0
26	0	0	0	0	0	0	0	0
27	0	0	0	0	0	0	0	0
28	0	0	0	0	0	0	0	0
29	0	0	0	0	0	0	0	0
30	0	0	0	0	0	0	0	0
31	20	130	57	54	93	86	19	32
32	70	370	60	60	98	95	0	0

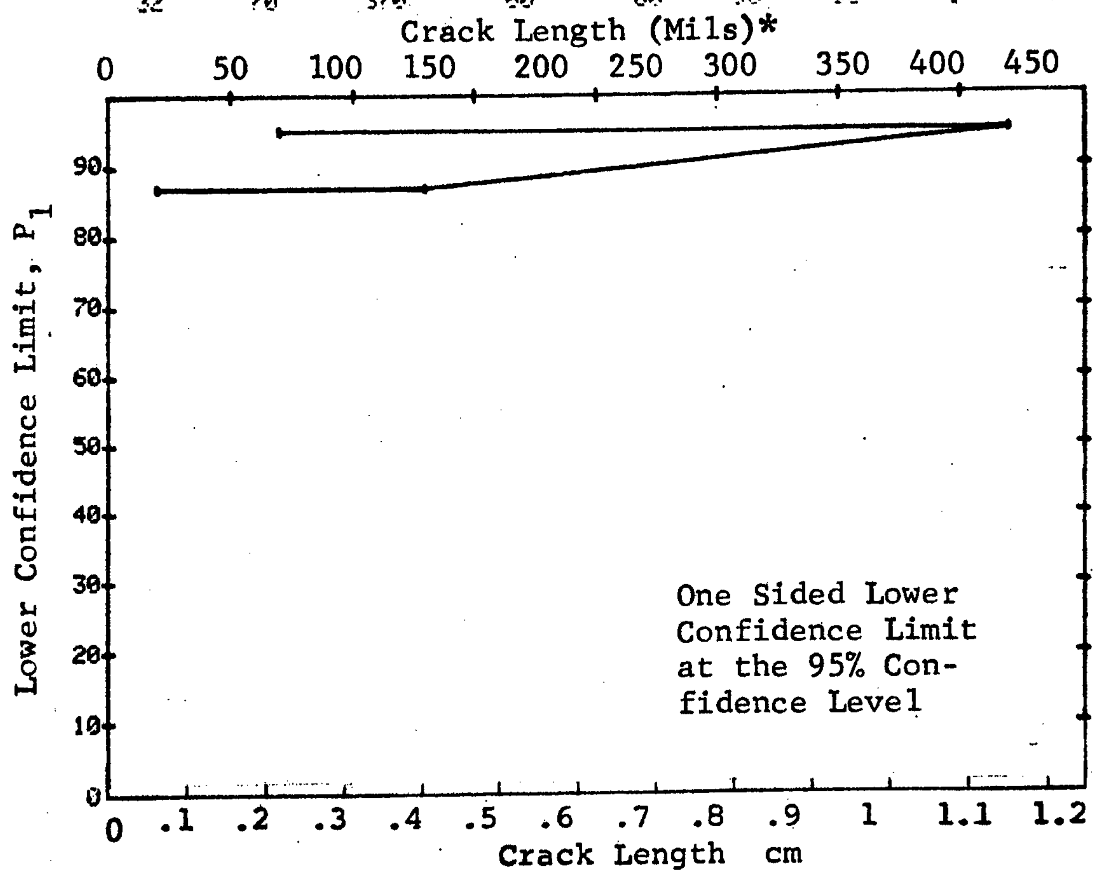

Figure D-69 (Concluded)

(a) Range Interval Method of Data Cumulation

27-OCT-75 PENETRANT TEST 1 ( ) 70 (70)

RANGE	MIN LN	MAX LN	N	DET	50%	95%	0 MISS	1 MISS
1	30*	50*	22	6	25	12	0	0
2	60	70*	15	12	76	56	0	0
3	0	0	0	0	0	0	0	0
4	110	120	12	10	79	56	0	0
5	140	140	21	21	96	86	8	25
6	150	160	14	14	95	80	15	32
7	0	0	0	0	0	0	0	0
8	200	200	1	1	50	5	0	0
9	0	0	0	0	0	0	0	0
10	0	0	0	0	0	0	0	0
11	0	0	0	0	0	0	0	0
12	0	0	0	0	0	0	0	0
13	0	0	0	0	0	0	0	0
14	0	0	0	0	0	0	0	0
15	0	0	0	0	0	0	0	0
16	0	0	0	0	0	0	0	0
17	0	0	0	0	0	0	0	0
18	0	0	0	0	0	0	0	0
19	0	0	0	0	0	0	0	0
20	0	0	0	0	0	0	0	0
21	0	0	0	0	0	0	0	0
22	0	0	0	0	0	0	0	0
23	0	0	0	0	0	0	0	0
24	0	0	0	0	0	0	0	0
25	0	0	0	0	0	0	0	0
26	0	0	0	0	0	0	0	0
27	0	0	0	0	0	0	0	0
28	0	0	0	0	0	0	0	0
29	0	0	0	0	0	0	0	0
30	0	0	0	0	0	0	0	0
31	0	0	0	0	0	0	0	0
32	750	750	7	7	90	65	0	0

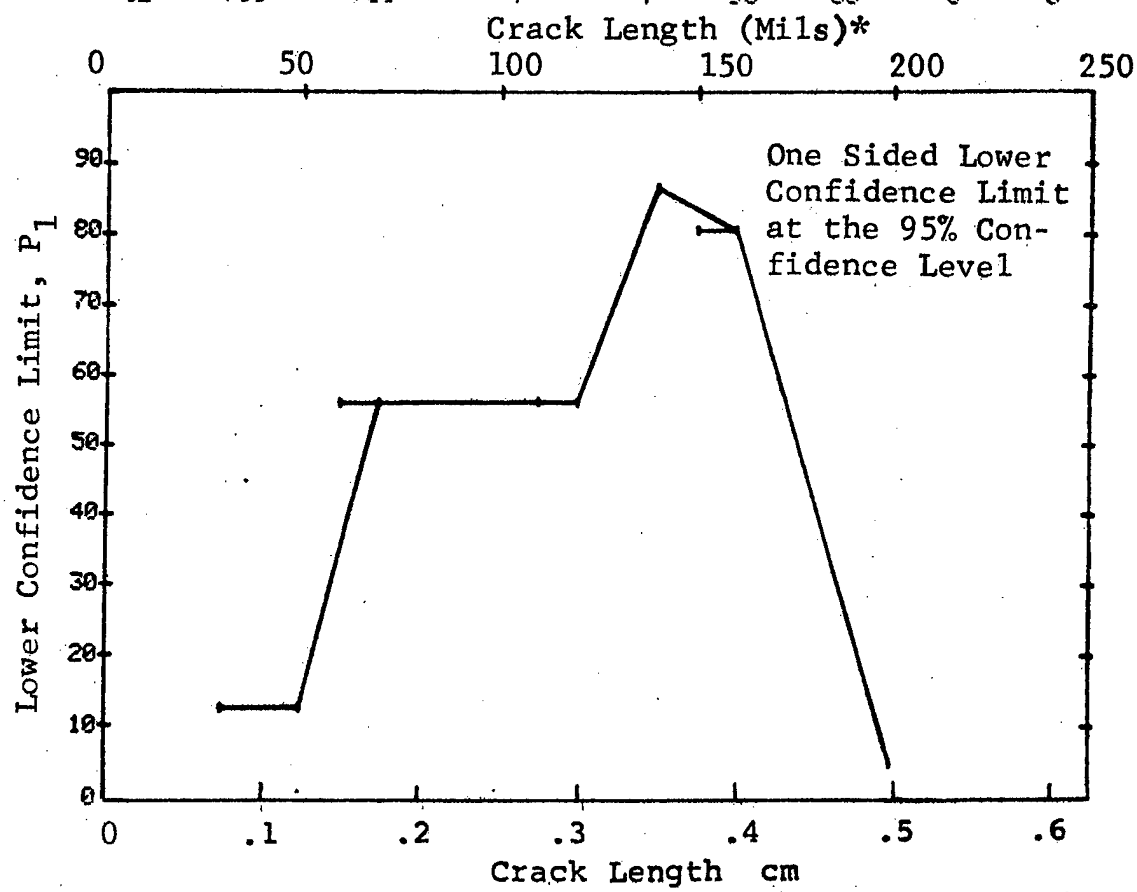

Figure D-70 Probability of Detection for 4340M Steel Using Liquid Penetrant. Compressed Notch Flaws in Filleted Solid Cylinder. Lab. Env.

(b) Optimum Probability Method of Data Cumulation

27-OCT-75 PENETRANT TEST 2 ( ) 70 (70)

RANGE	MIN LN	MAX LN	N	DET	50%	95%	0 MISS	1 MISS
1	30	50	22	6	0	12	0	0
2	60	70	15	12	0	56	0	0
3	0	0	0	0	0	0	0	0
4	60	120	27	22	0	64	0	0
5	140	140	21	21	0	86	8	25
6	140	160	35	35	0	91	0	11
7	0	0	0	0	0	0	0	0
8	140	200	36	36	0	92	0	10
9	0	0	0	0	0	0	0	0
10	0	0	0	0	0	0	0	0
11	0	0	0	0	0	0	0	0
12	0	0	0	0	0	0	0	0
13	0	0	0	0	0	0	0	0
14	0	0	0	0	0	0	0	0
15	0	0	0	0	0	0	0	0
16	0	0	0	0	0	0	0	0
17	0	0	0	0	0	0	0	0
18	0	0	0	0	0	0	0	0
19	0	0	0	0	0	0	0	0
20	0	0	0	0	0	0	0	0
21	0	0	0	0	0	0	0	0
22	0	0	0	0	0	0	0	0
23	0	0	0	0	0	0	0	0
24	0	0	0	0	0	0	0	0
25	0	0	0	0	0	0	0	0
26	0	0	0	0	0	0	0	0
27	0	0	0	0	0	0	0	0
28	0	0	0	0	0	0	0	0
29	0	0	0	0	0	0	0	0
30	0	0	0	0	0	0	0	0
31	0	0	0	0	0	0	0	0
32	140	750	43	43	0	93	0	3

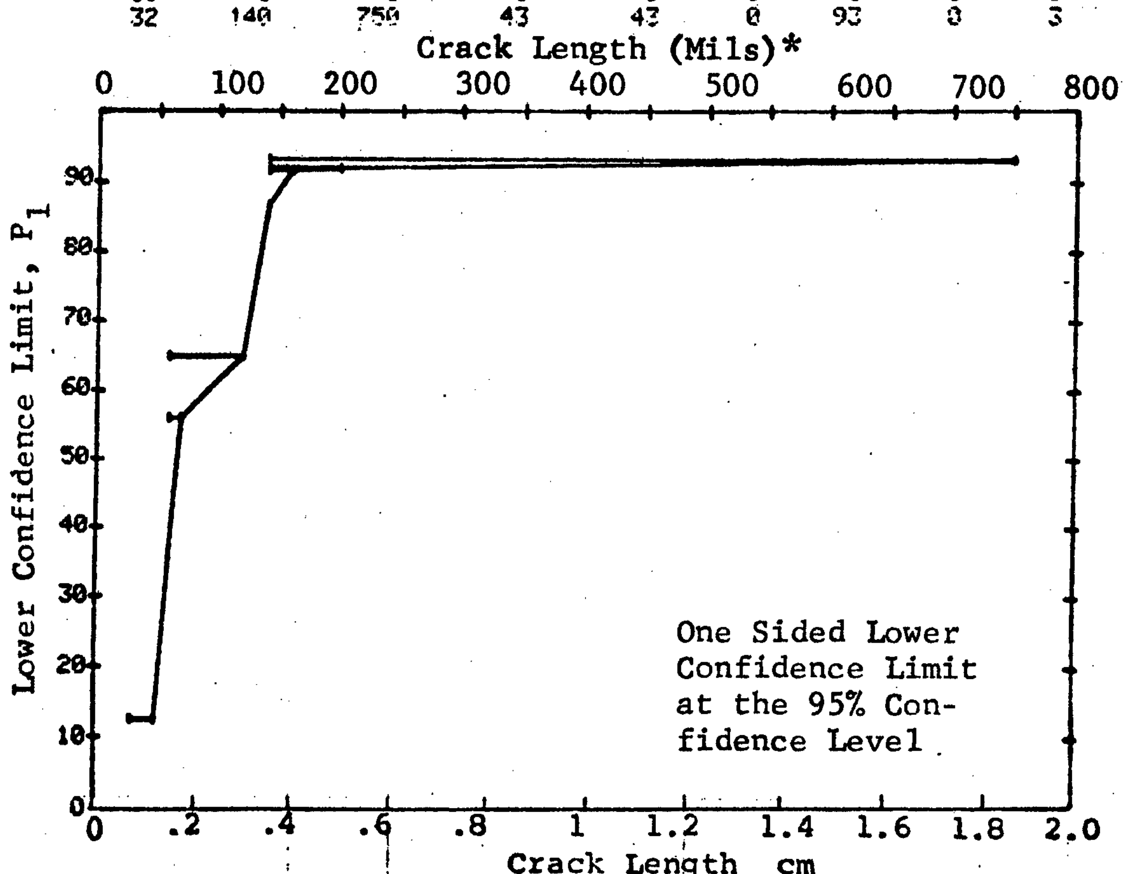

Figure D-70 (Continued)

(c) Overlapping Sixty Point Method of Data Cumulation

27-OCT-75 PENETRANT TEST 3 ( ) 70 (70)

RANGE	MIN LN	MAX LN	N	DET	50%	95%	0 MISS	1 MISS
1	0*	0*	0	0	0	0	0	0
2	0	0	0	0	0	0	0	0
3	0	0	0	0	0	0	0	0
4	0	0	0	0	0	0	0	0
5	0	0	0	0	0	0	0	0
6	0	0	0	0	0	0	0	0
7	0	0	0	0	0	0	0	0
8	0	0	0	0	0	0	0	0
9	0	0	0	0	0	0	0	0
10	0	0	0	0	0	0	0	0
11	0	0	0	0	0	0	0	0
12	0	0	0	0	0	0	0	0
13	0	0	0	0	0	0	0	0
14	0	0	0	0	0	0	0	0
15	0	0	0	0	0	0	0	0
16	0	0	0	0	0	0	0	0
17	0	0	0	0	0	0	0	0
18	0	0	0	0	0	0	0	0
19	0	0	0	0	0	0	0	0
20	0	0	0	0	0	0	0	0
21	0	0	0	0	0	0	0	0
22	0	0	0	0	0	0	0	0
23	0	0	0	0	0	0	0	0
24	0	0	0	0	0	0	0	0
25	0	0	0	0	0	0	0	0
26	0	0	0	0	0	0	0	0
27	0	0	0	0	0	0	0	0
28	0	0	0	0	0	0	0	0
29	0	0	0	0	0	0	0	0
30	0	0	0	0	0	0	0	0
31	30	140	55	34	60	49	0	0
32	60	200	60	55	90	83	43	58

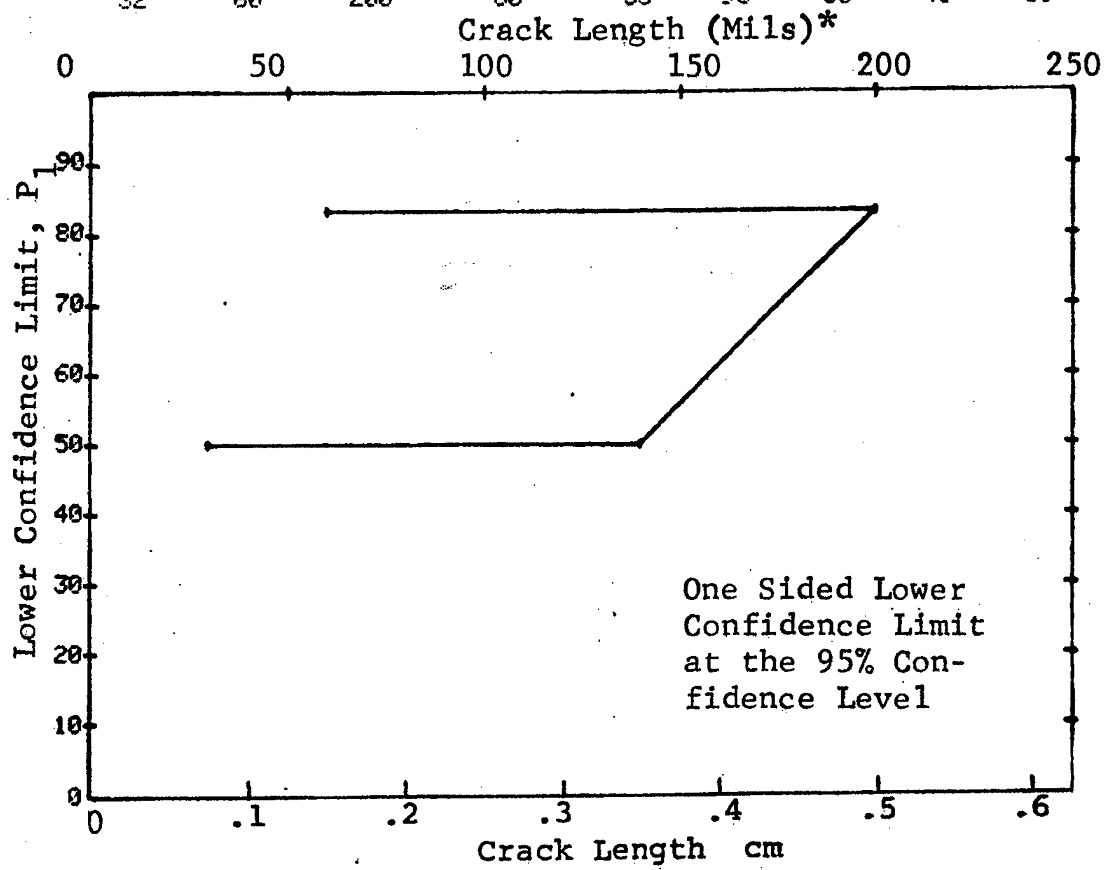

Figure D-70 (Concluded)

(a) Range Interval Method of Data Cumulation

27-OCT-75 ULTRASONIC TEST 1 (71)

RANGE	MIN LN	MAX LN	N	DET	50%	95%	0 MISS	1 MISS
1	30	30	2	1	29	2	0	0
2	40	40	7	4	50	22	0	0
3	0	0	0	0	0	0	0	0
4	50	50	9	6	60	34	0	0
5	0	0	0	0	0	0	0	0
6	0	0	0	0	0	0	0	0
7	70	70	3	3	79	36	0	0
8	80	80	10	9	83	60	0	0
9	0	0	0	0	0	0	0	0
10	90	90	12	10	78	56	0	0
11	0	0	0	0	0	0	0	0
12	100	100	9	8	82	57	0	0
13	110	110	22	20	88	74	0	0
14	0	0	0	0	0	0	0	0
15	120	120	9	9	92	71	0	0
16	130	130	9	9	92	71	0	0
17	0	0	0	0	0	0	0	0
18	140	140	7	6	77	47	0	0
19	0	0	0	0	0	0	0	0
20	150	150	16	14	83	65	0	0
21	160	160	6	5	73	41	0	0
22	0	0	0	0	0	0	0	0
23	170	170	16	16	95	82	13	30
24	180	180	8	8	91	68	0	0
25	0	0	0	0	0	0	0	0
26	190	190	4	4	84	47	0	0
27	0	0	0	0	0	0	0	0
28	0	0	0	0	0	0	0	0
29	210	210	2	2	70	22	0	0
30	0	0	0	0	0	0	0	0
31	220	220	9	9	92	71	0	0
32	230	230	10	9	83	60	0	0

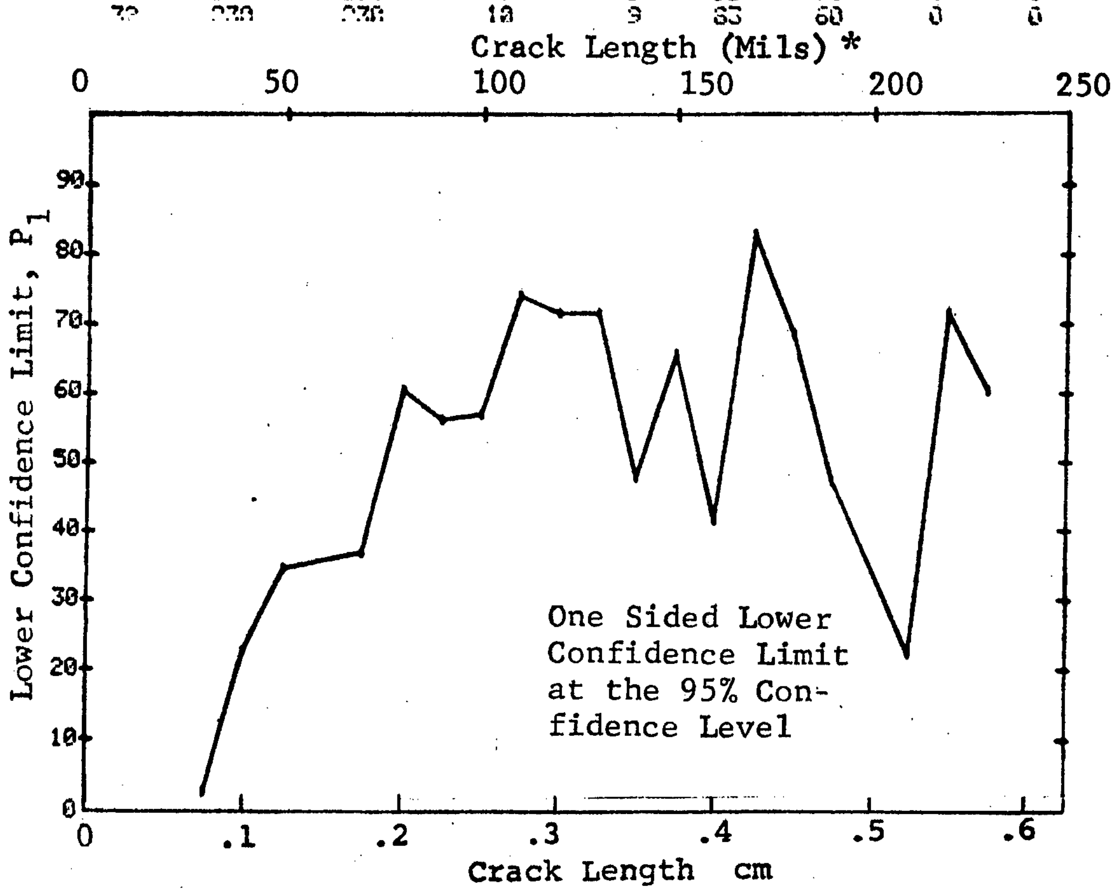

Figure D-71 Probability of Detection for 2024-T6 Al for Ultrasonic Shear and Surface Waves. Compressed Notch Flaws in Tandem T. Prod. Env.

(b) Optimum Probability Method of Data Cumulation

27-OCT-75 ULTRASONIC TEST 2 ? 7/ (71)

RANGE	MIN LN	MAX LN	N	DET	50%	95%	0 MISS	1 MISS
1	30 *	30 *	2	1	0	2	0	0
2	30	40	9	5	0	25	0	0
3	0	0	0	0	0	0	0	0
4	30	50	18	11	0	39	0	0
5	0	0	0	0	0	0	0	0
6	0	0	0	0	0	0	0	0
7	50	70	12	9	0	47	0	0
8	70	80	13	12	0	68	0	0
9	0	0	0	0	0	0	0	0
10	70	90	25	22	0	71	0	0
11	0	0	0	0	0	0	0	0
12	70	100	34	30	0	75	0	0
13	70	110	56	50	0	79	0	0
14	0	0	0	0	0	0	0	0
15	70	120	65	59	0	82	51	64
16	110	130	40	38	0	85	21	36
17	0	0	0	0	0	0	0	0
18	100	140	56	52	0	84	33	47
19	0	0	0	0	0	0	0	0
20	70	150	97	88	0	84	57	70
21	70	160	103	93	0	84	0	0
22	0	0	0	0	0	0	0	0
23	110	170	85	79	0	86	31	44
24	170	180	24	24	0	88	5	22
25	0	0	0	0	0	0	0	0
26	170	190	28	28	0	89	1	18
27	0	0	0	0	0	0	0	0
28	0	0	0	0	0	0	0	0
29	170	210	30	30	0	90	3	16
30	0	0	0	0	0	0	0	0
31	170	220	39	39	0	92	0	7
32	170	230	49	48	0	90 *	0	12

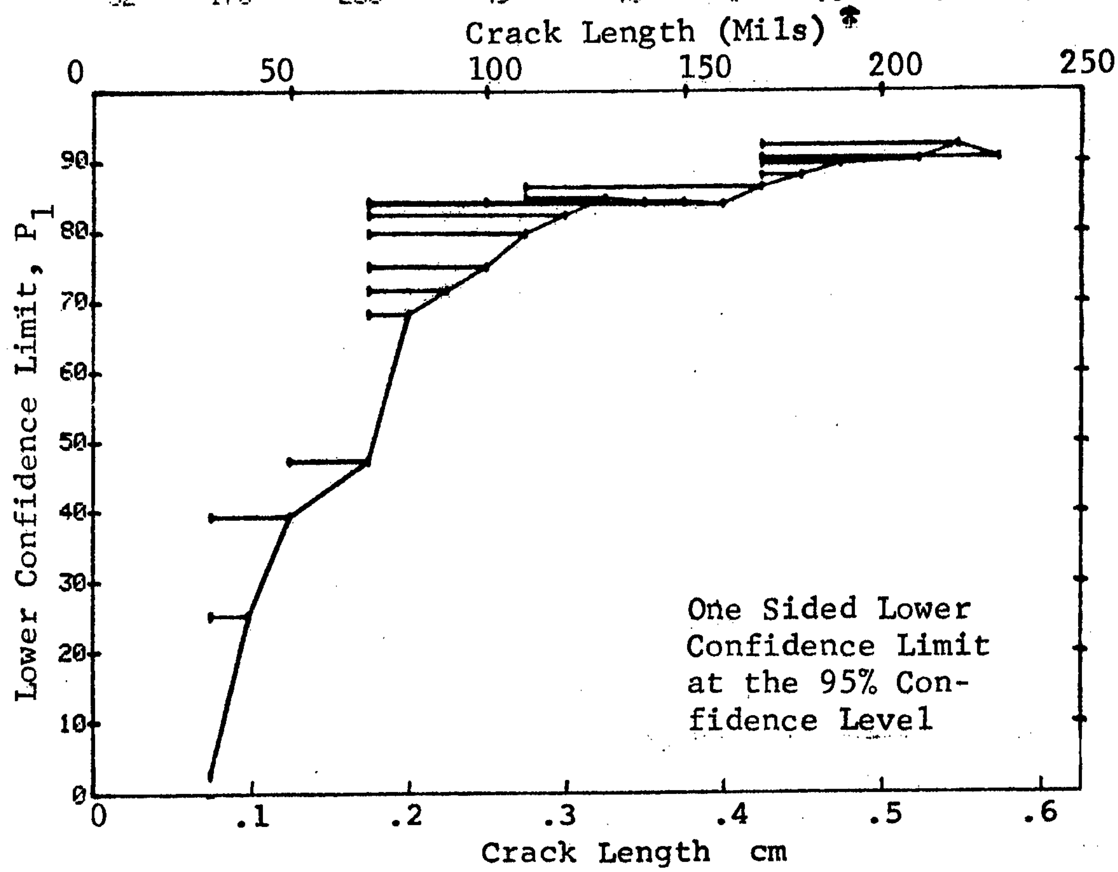

Figure D-71 (Continued)

(c) Overlapping Sixty Point Method of Data Cumulation

27-OCT-75 ULTRASONIC TEST 3 .) 7/ (71)

RANGE	MIN LN*	MAX LN*	N	DET	50%	95%	0 MISS	1 MISS
1	0	0	0	0	0	0	0	0
2	0	0	0	0	0	0	0	0
3	0	0	0	0	0	0	0	0
4	0	0	0	0	0	0	0	0
5	0	0	0	0	0	0	0	0
6	0	0	0	0	0	0	0	0
7	0	0	0	0	0	0	0	0
8	0	0	0	0	0	0	0	0
9	0	0	0	0	0	0	0	0
10	0	0	0	0	0	0	0	0
11	0	0	0	0	0	0	0	0
12	0	0	0	0	0	0	0	0
13	0	0	0	0	0	0	0	0
14	0	0	0	0	0	0	0	0
15	0	0	0	0	0	0	0	0
16	0	0	0	0	0	0	0	0
17	0	0	0	0	0	0	0	0
18	0	0	0	0	0	0	0	0
19	0	0	0	0	0	0	0	0
20	0	0	0	0	0	0	0	0
21	0	0	0	0	0	0	0	0
22	0	0	0	0	0	0	0	0
23	0	0	0	0	0	0	0	0
24	0	0	0	0	0	0	0	0
25	0	0	0	0	0	0	0	0
26	0	0	0	0	0	0	0	0
27	0	0	0	0	0	0	0	0
28	30	100	50	39	76	66	0	0
29	70	120	60	54	88	81	[illegible]	[illegible]
30	100	150	60	55	90	83	43	57
31	120	180	60	56	92	85	29	43
32	150	230	60	58	95	89	1	16

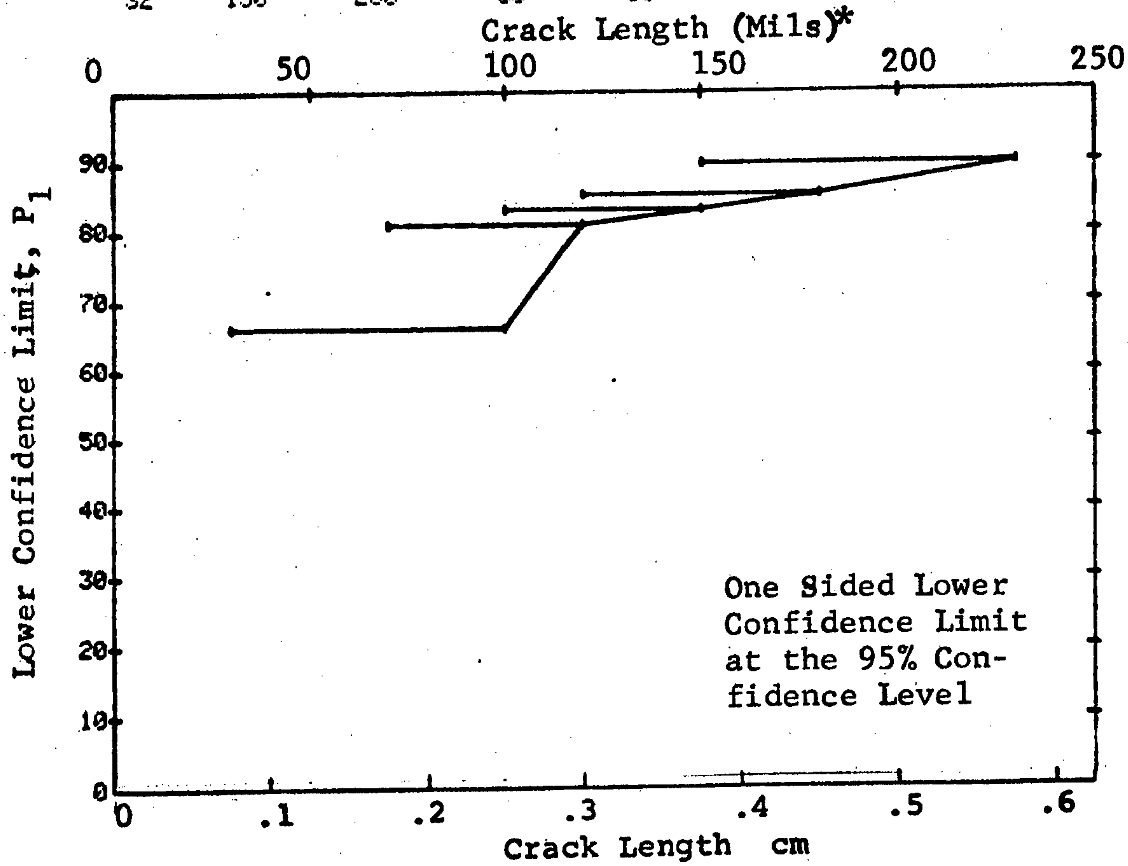

Figure D-71 (Concluded)

(a) Range Interval Method of Data Cumulation

27-OCT-75 ULTRASONIC TEST ! ( )72 (72)

RANGE	MIN LN *	MAX LN *	N	DET	50%	95%	0 MISS	1 MISS
1	40	40	2	0	0	0	0	0
2	70	70	1	0	0	0	0	0
3	0	0	0	0	0	0	0	0
4	100	110	11	2	14	3	0	0
5	130	130	4	1	15	1	0	0
6	0	0	0	0	0	0	0	0
7	0	0	0	0	0	0	0	0
8	190	190	1	1	50	5	0	0
9	210	210	1	0	0	0	0	0
10	230	230	2	2	70	22	0	0
11	0	0	0	0	0	0	0	0
12	250	250	3	3	79	36	0	0
13	0	0	0	0	0	0	0	0
14	300	300	2	2	70	22	0	0
15	310	310	2	2	70	22	0	0
16	0	0	0	0	0	0	0	0
17	350	350	2	2	70	22	0	0
18	380	380	2	2	70	22	0	0
19	0	0	0	0	0	0	0	0
20	0	0	0	0	0	0	0	0
21	0	0	0	0	0	0	0	0
22	450	450	2	2	70	22	0	0
23	460	460	1	1	50	5	0	0
24	480	480	2	2	70	22	0	0
25	0	0	0	0	0	0	0	0
26	0	0	0	0	0	0	0	0
27	0	0	0	0	0	0	0	0
28	0	0	0	0	0	0	0	0
29	0	0	0	0	0	0	0	0
30	0	0	0	0	0	0	0	0
31	0	0	0	0	0	0	0	0
32	650	650	2	2	70	22	0	0

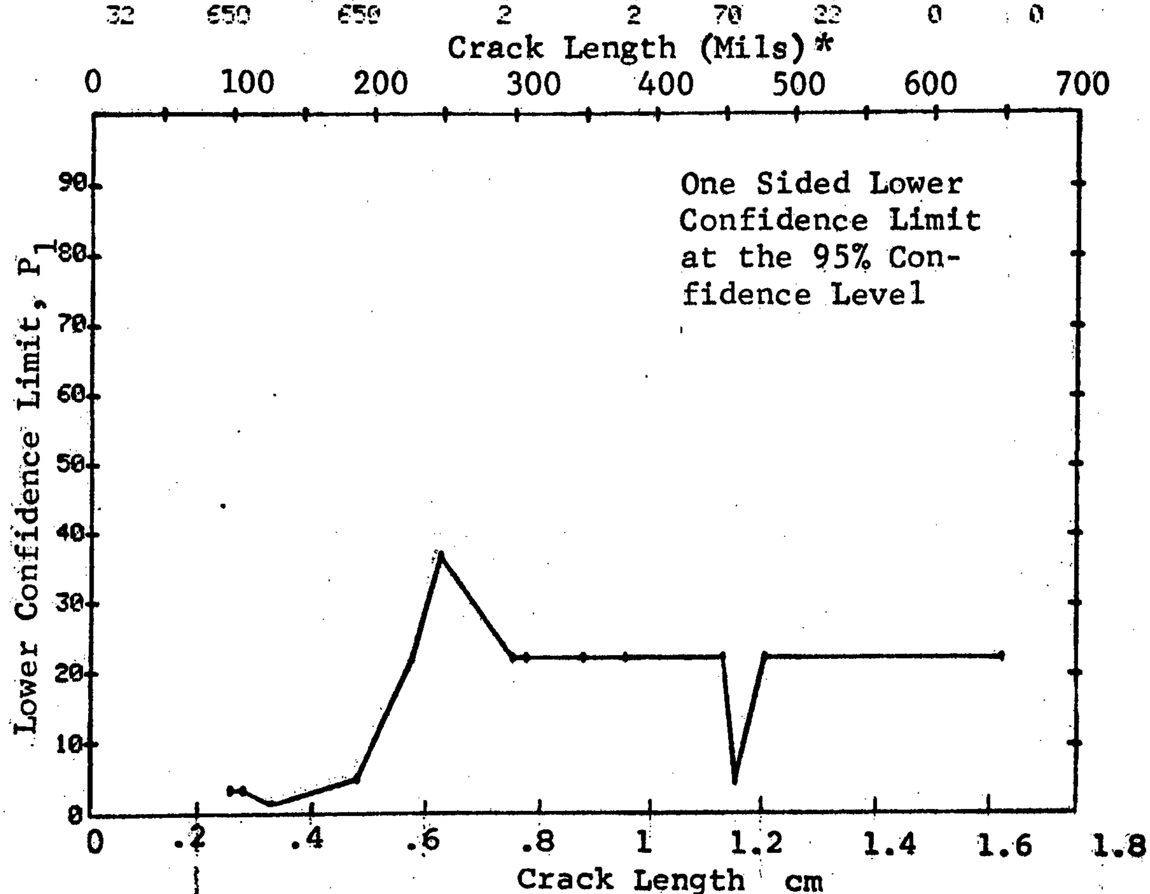

Figure D-72 Probability of Detection for 4340M Steel Using Ultrasonic Shear and Surface Waves. Compressed Notch Flaws in Solid Threaded Cylinder. Prod. Env.

(b) Optimum Probability Method of Data Cumulation

27-OCT-75 ULTRASONIC TEST 2 ((72)

RANGE	MIN LN *	MAX LN *	N	DET	50%	95%	0 MISS	1 MISS
1	40	40	2	0	0	0	0	0
2	70	70	1	0	0	0	0	0
3	0	0	0	0	0	0	0	0
4	100	110	11	2	0	3	0	0
5	100	130	15	3	0	5	0	0
6	0	0	0	0	0	0	0	0
7	0	0	0	0	0	0	0	0
8	100	190	16	4	0	9	0	0
9	100	210	17	4	0	8	0	0
10	190	230	4	3	0	24	0	0
11	0	0	0	0	0	0	0	0
12	230	250	5	5	0	54	0	0
13	0	0	0	0	0	0	0	0
14	230	300	7	7	0	65	0	0
15	230	310	9	9	0	71	0	0
16	0	0	0	0	0	0	0	0
17	230	350	11	11	0	76	0	0
18	230	380	13	13	0	79	0	0
19	0	0	0	0	0	0	0	0
20	0	0	0	0	0	0	0	0
21	0	0	0	0	0	0	0	0
22	230	450	15	15	0	81	14	31
23	230	460	16	16	0	82	13	30
24	230	480	18	18	0	84	11	29
25	0	0	0	0	0	0	0	0
26	0	0	0	0	0	0	0	0
27	0	0	0	0	0	0	0	0
28	0	0	0	0	0	0	0	0
29	0	0	0	0	0	0	0	0
30	0	0	0	0	0	0	0	0
31	0	0	0	0	0	0	0	0
32	230	650	20	20	0	86	9	26

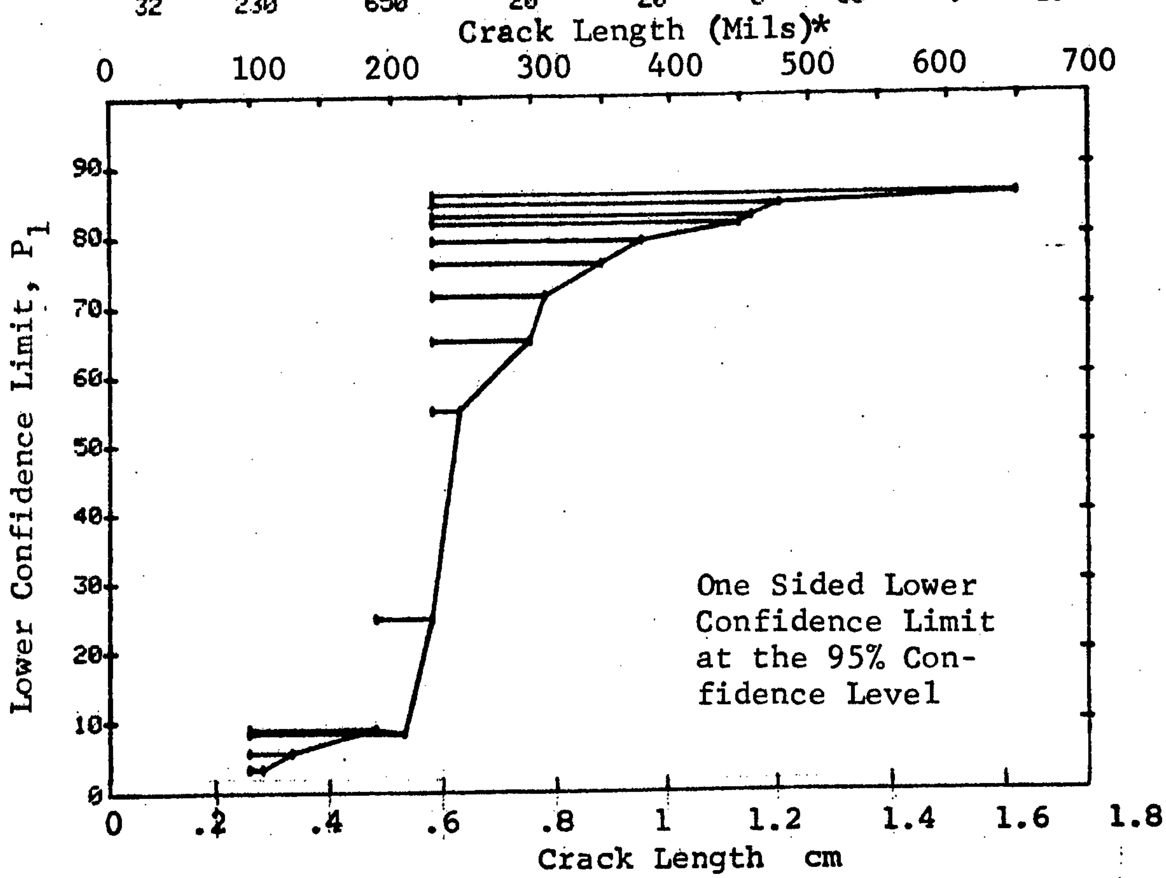

Figure D-72 (Continued)

(c) Overlapping Sixty Point Method of Data Cumulation

27-OCT-75 ULTRASONIC TEST 3 (272 (72)

RANGE	MIN LN*	MAX LN*	N	DET	50%	95%	0 MISS	1 MISS
1	0	0	0	0	0	0	0	0
2	0	0	0	0	0	0	0	0
3	0	0	0	0	0	0	0	0
4	0	0	0	0	0	0	0	0
5	0	0	0	0	0	0	0	0
6	0	0	0	0	0	0	0	0
7	0	0	0	0	0	0	0	0
8	0	0	0	0	0	0	0	0
9	0	0	0	0	0	0	0	0
10	0	0	0	0	0	0	0	0
11	0	0	0	0	0	0	0	0
12	0	0	0	0	0	0	0	0
13	0	0	0	0	0	0	0	0
14	0	0	0	0	0	0	0	0
15	0	0	0	0	0	0	0	0
16	0	0	0	0	0	0	0	0
17	0	0	0	0	0	0	0	0
18	0	0	0	0	0	0	0	0
19	0	0	0	0	0	0	0	0
20	0	0	0	0	0	0	0	0
21	0	0	0	0	0	0	0	0
22	0	0	0	0	0	0	0	0
23	0	0	0	0	0	0	0	0
24	0	0	0	0	0	0	0	0
25	0	0	0	0	0	0	0	0
26	0	0	0	0	0	0	0	0
27	0	0	0	0	0	0	0	0
28	0	0	0	0	0	0	0	0
29	0	0	0	0	0	0	0	0
30	0	0	0	0	0	0	0	0
31	0	0	0	0	0	0	0	0
32	40	480	38	22	56	43	0	0

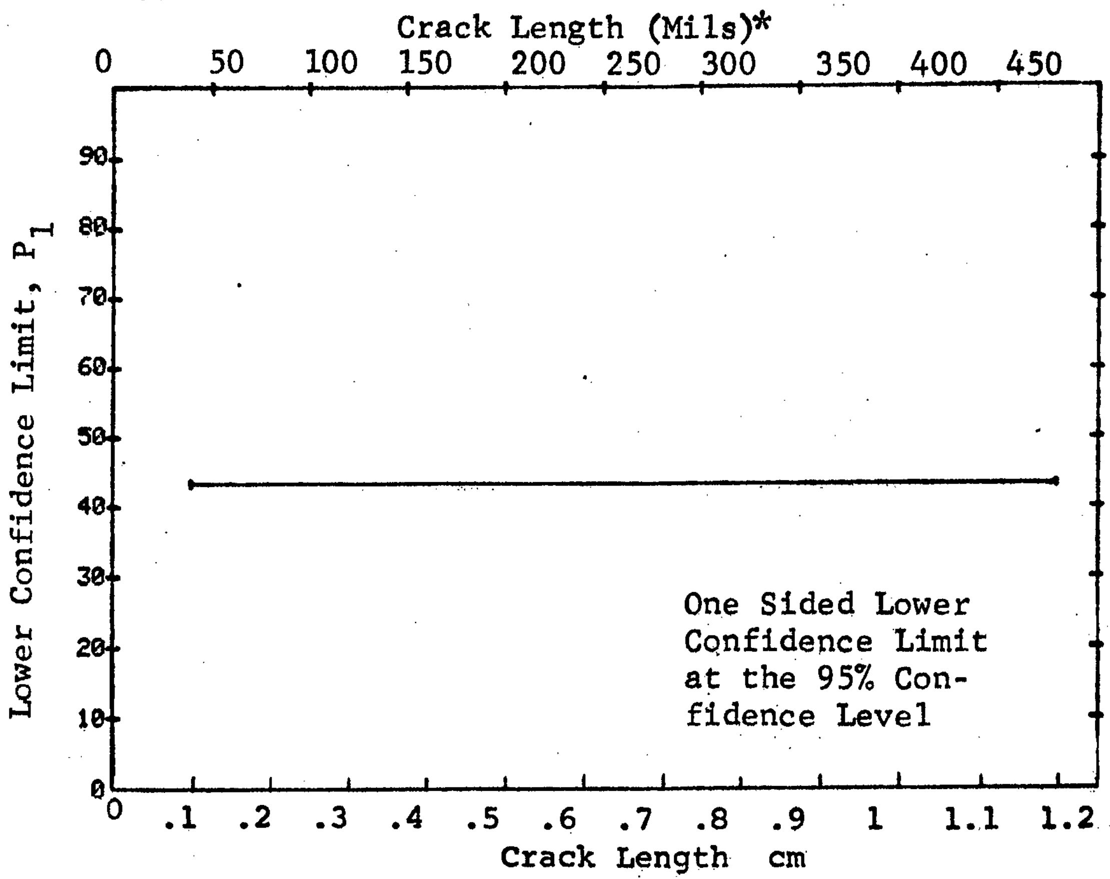

Figure D-72 (Concluded)

(a) Range Interval Method of Data Cumulation

27-OCT-75 ULTRASONIC TEST 1 (73)

RANGE	MIN LN	MAX LN	N	DET	50%	95%	0 MISS	1 MISS
1	80 *	80 *	8	8	91	68	0	0
2	90	90	7	7	90	65	0	0
3	0	0	0	0	0	0	0	0
4	0	0	0	0	0	0	0	0
5	110	110	3	3	79	36	0	0
6	120	120	5	5	87	54	0	0
7	130	130	8	8	91	68	0	0
8	0	0	0	0	0	0	0	0
9	140	140	4	4	84	47	0	0
10	0	0	0	0	0	0	0	0
11	0	0	0	0	0	0	0	0
12	160	160	1	1	50	5	0	0
13	0	0	0	0	0	0	0	0
14	0	0	0	0	0	0	0	0
15	0	0	0	0	0	0	0	0
16	0	0	0	0	0	0	0	0
17	0	0	0	0	0	0	0	0
18	0	0	0	0	0	0	0	0
19	0	0	0	0	0	0	0	0
20	0	0	0	0	0	0	0	0
21	0	0	0	0	0	0	0	0
22	0	0	0	0	0	0	0	0
23	0	0	0	0	0	0	0	0
24	0	0	0	0	0	0	0	0
25	0	0	0	0	0	0	0	0
26	0	0	0	0	0	0	0	0
27	0	0	0	0	0	0	0	0
28	0	0	0	0	0	0	0	0
29	0	0	0	0	0	0	0	0
30	0	0	0	0	0	0	0	0
31	300	300	1	1	50	5	0	0
32	310	310	5	5	87	54	0	0

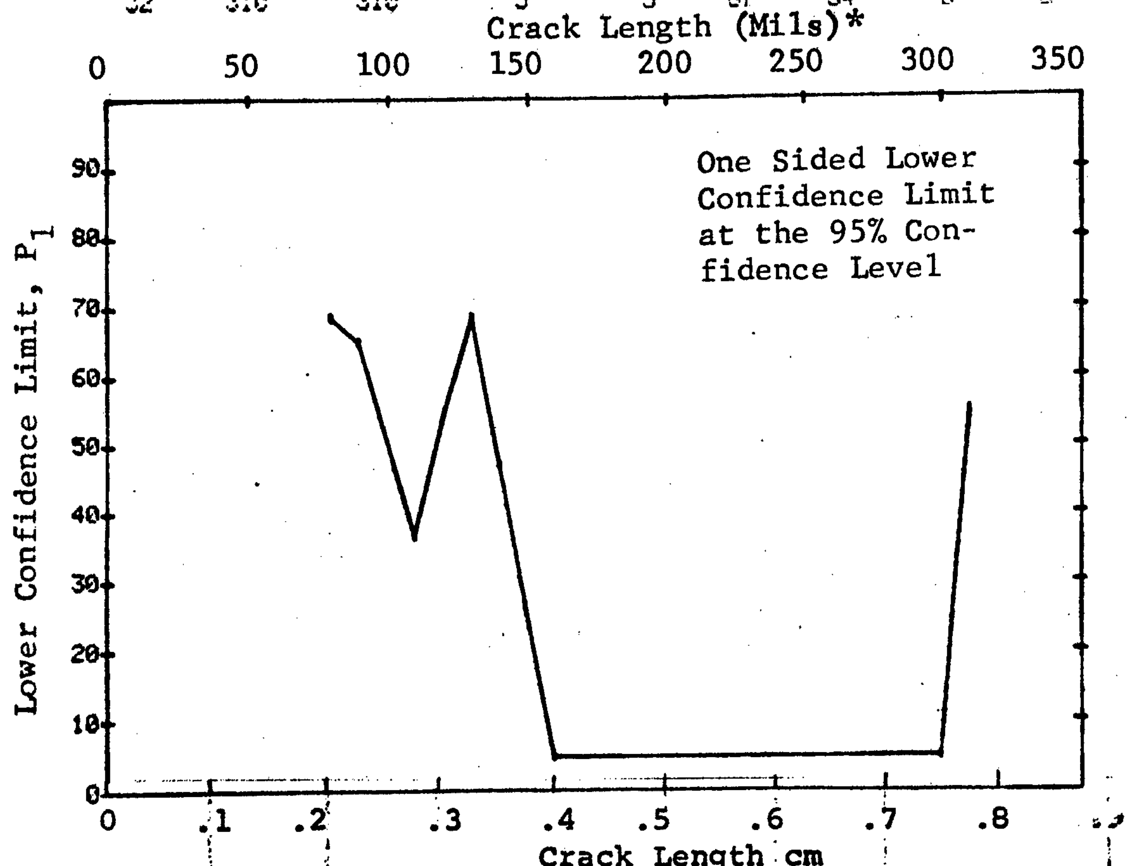

Figure D-73 Probability of Detection for 4340M Steel Using Ultrasonic Shear and Surface Waves. Compressed Notch Flaws in Hollow Cylinder. Prod. Env.

(b) Optimum Probability Method of Data Cumulation

27-OCT-75 ULTRASONIC TEST 2 (273 (73)

RANGE	MIN LN	MAX LN	N	DET	50%	95%	0 MISS	1 MISS
1	80*	80*	8	8	0	68	0	0
2	80	90	15	15	0	81	14	31
3	0	0	0	0	0	0	0	0
4	0	0	0	0	0	0	0	0
5	80	110	18	18	0	84	11	23
6	80	120	23	23	0	87	6	23
7	80	130	31	31	0	90	0	15
8	0	0	0	0	0	0	0	0
9	80	140	35	35	0	91	0	11
10	0	0	0	0	0	0	0	0
11	0	0	0	0	0	0	0	0
12	80	160	36	36	0	92	0	10
13	0	0	0	0	0	0	0	0
14	0	0	0	0	0	0	0	0
15	0	0	0	0	0	0	0	0
16	0	0	0	0	0	0	0	0
17	0	0	0	0	0	0	0	0
18	0	0	0	0	0	0	0	0
19	0	0	0	0	0	0	0	0
20	0	0	0	0	0	0	0	0
21	0	0	0	0	0	0	0	0
22	0	0	0	0	0	0	0	0
23	0	0	0	0	0	0	0	0
24	0	0	0	0	0	0	0	0
25	0	0	0	0	0	0	0	0
26	0	0	0	0	0	0	0	0
27	0	0	0	0	0	0	0	0
28	0	0	0	0	0	0	0	0
29	0	0	0	0	0	0	0	0
30	0	0	0	0	0	0	0	0
31	80	300	37	37	0	92	0	9
32	80	310	42	42	0	93	0	4

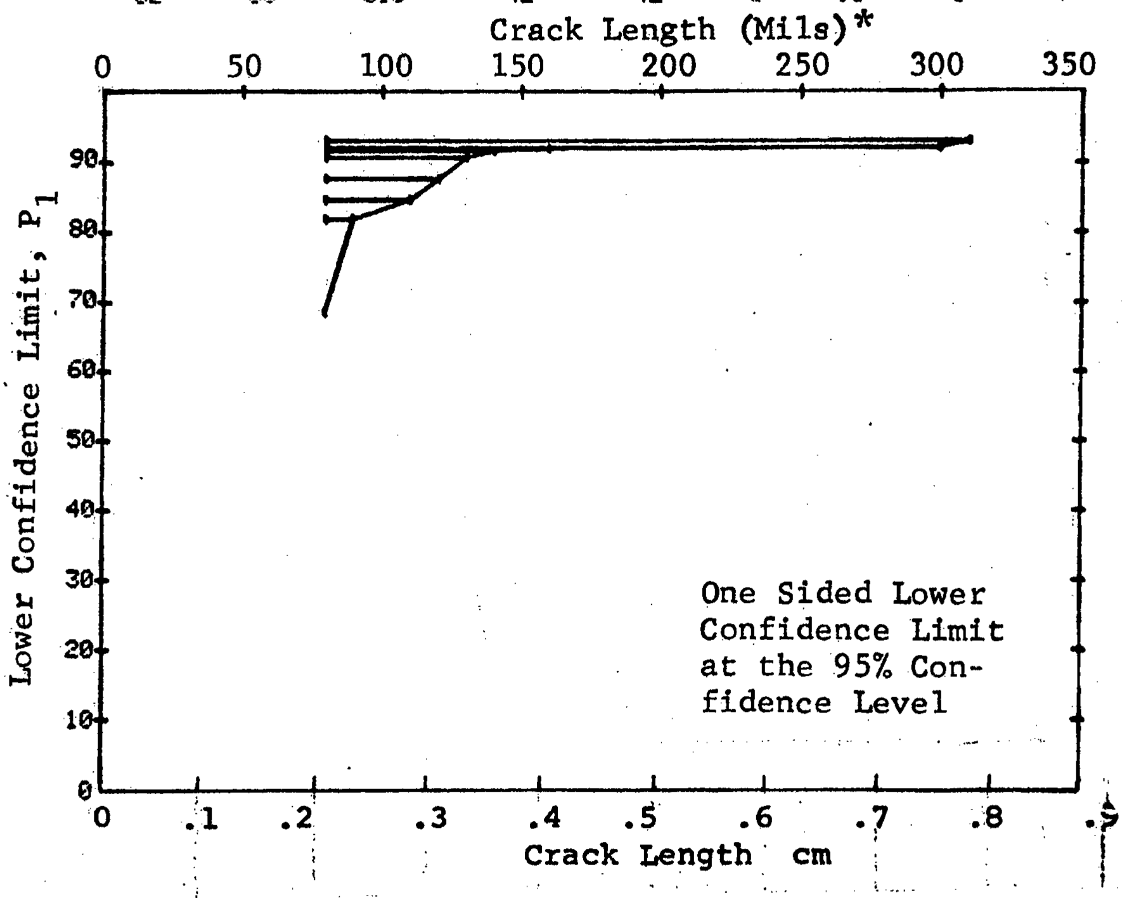

Figure D-73 (Continued)

(c) Overlapping Sixty Point Method of Data Cumulation

27-OCT-75 ULTRASONIC TEST 3 C (73)

RANGE	MIN LN	MAX LN	N	DET	50%	95%	0 MISS	1 MISS
1	0 *	0 *	0	0	0	0	0	0
2	0	0	0	0	0	0	0	0
3	0	0	0	0	0	0	0	0
4	0	0	0	0	0	0	0	0
5	0	0	0	0	0	0	0	0
6	0	0	0	0	0	0	0	0
7	0	0	0	0	0	0	0	0
8	0	0	0	0	0	0	0	0
9	0	0	0	0	0	0	0	0
10	0	0	0	0	0	0	0	0
11	0	0	0	0	0	0	0	0
12	0	0	0	0	0	0	0	0
13	0	0	0	0	0	0	0	0
14	0	0	0	0	0	0	0	0
15	0	0	0	0	0	0	0	0
16	0	0	0	0	0	0	0	0
17	0	0	0	0	0	0	0	0
18	0	0	0	0	0	0	0	0
19	0	0	0	0	0	0	0	0
20	0	0	0	0	0	0	0	0
21	0	0	0	0	0	0	0	0
22	0	0	0	0	0	0	0	0
23	0	0	0	0	0	0	0	0
24	0	0	0	0	0	0	0	0
25	0	0	0	0	0	0	0	0
26	0	0	0	0	0	0	0	0
27	0	0	0	0	0	0	0	0
28	0	0	0	0	0	0	0	0
29	0	0	0	0	0	0	0	0
30	0	0	0	0	0	0	0	0
31	0	0	0	0	0	0	0	0
32	80	310	42	42	98	93	0	4

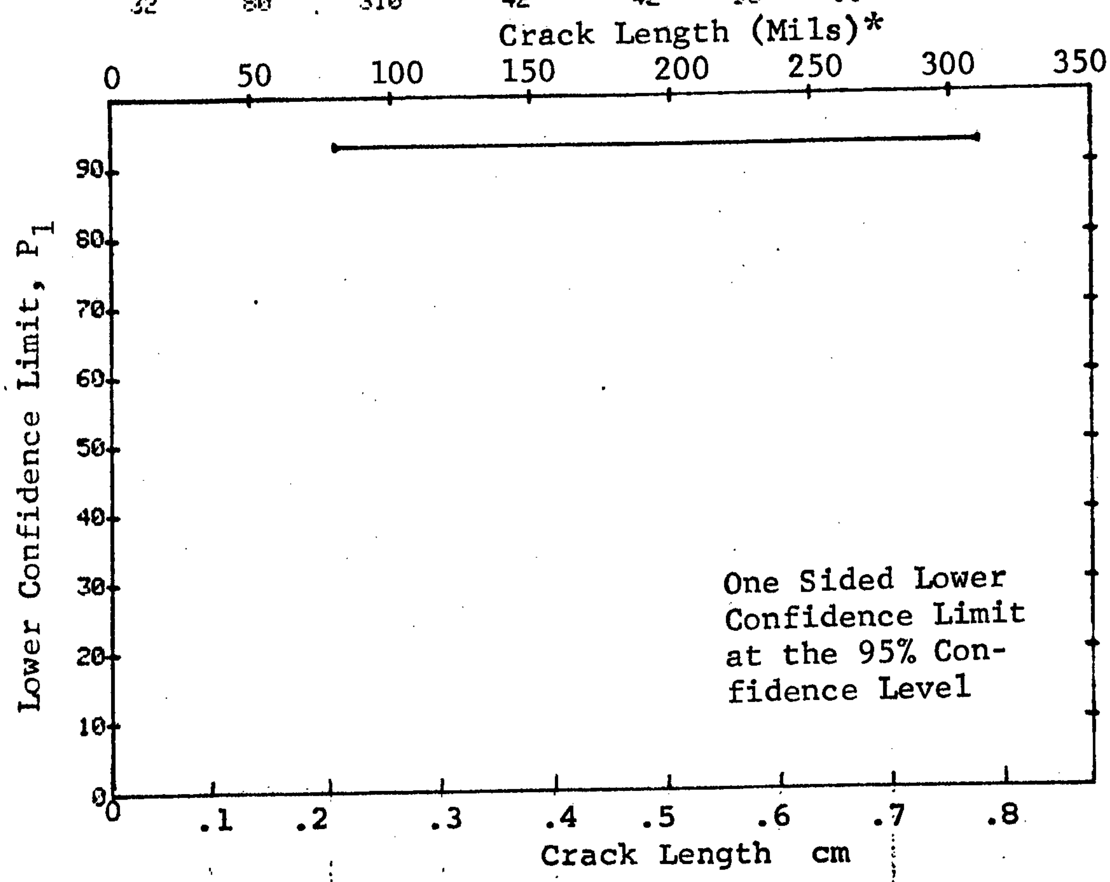

Figure D-73 (Concluded)

(a) Range Interval Method of Data Cumulation

27-OCT-75 ULTRASONIC TEST 1 (74)

RANGE	MIN LN *	MAX LN *	N	DET	50%	95%	0 MISS	1 MISS
1	60	60	12	10	78	56	0	0
2	0	0	0	0	0	0	0	0
3	0	0	0	0	0	0	0	0
4	100	100	23	22	92	80	23	38
5	0	0	0	0	0	0	0	0
6	120	120	6	6	89	60	0	0
7	130	130	5	5	87	54	0	0
8	140	140	5	5	87	54	0	0
9	0	0	0	0	0	0	0	0
10	160	160	3	2	50	13	0	0
11	0	0	0	0	0	0	0	0
12	180	180	6	6	89	60	0	0
13	0	0	0	0	0	0	0	0
14	0	0	0	0	0	0	0	0
15	0	0	0	0	0	0	0	0
16	0	0	0	0	0	0	0	0
17	230	230	1	1	50	5	0	0
18	0	0	0	0	0	0	0	0
19	0	0	0	0	0	0	0	0
20	0	0	0	0	0	0	0	0
21	0	0	0	0	0	0	0	0
22	0	0	0	0	0	0	0	0
23	0	0	0	0	0	0	0	0
24	0	0	0	0	0	0	0	0
25	310	310	1	1	50	5	0	0
26	0	0	0	0	0	0	0	0
27	0	0	0	0	0	0	0	0
28	0	0	0	0	0	0	0	0
29	350	350	2	2	70	21	0	0
30	0	0	0	0	0	0	0	0
31	0	0	0	0	0	0	0	0
32	390	390	1	1	50	5	0	0

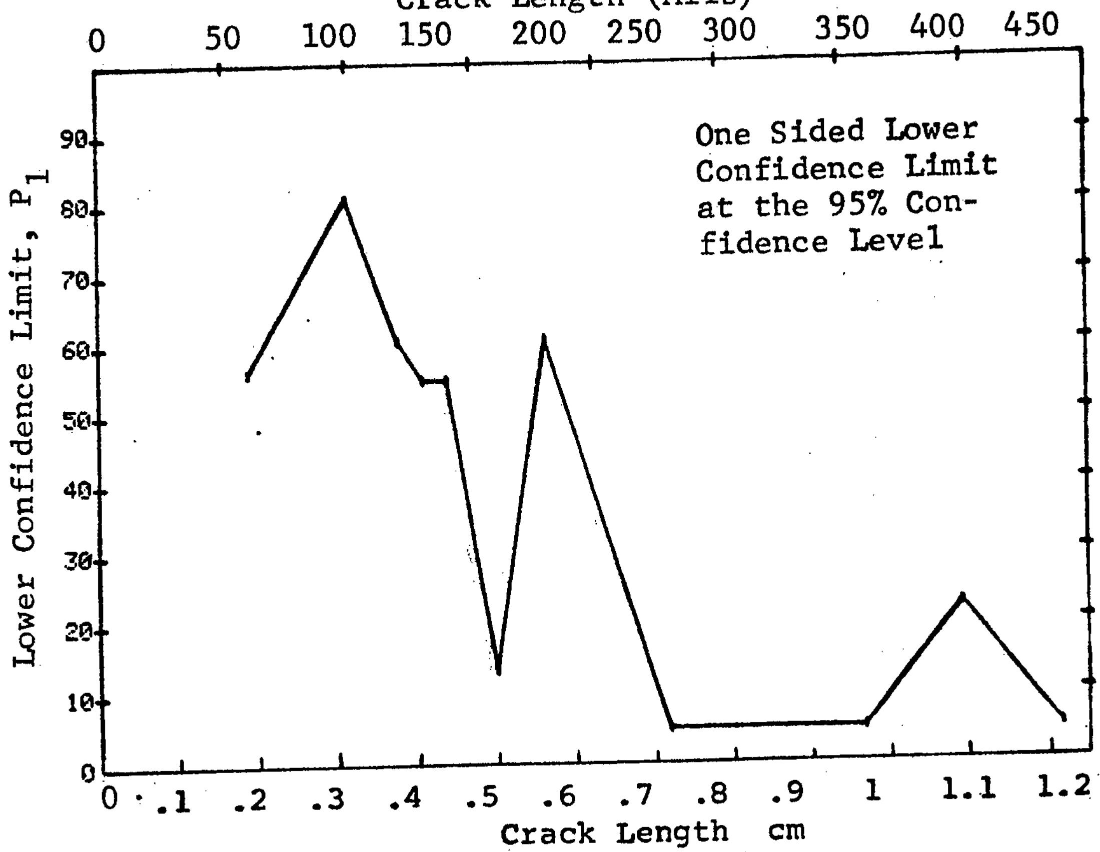

Figure D-74 Probability of Detection for 4340M Steel Using Ultrasonic Shear and Surface Waves. Compressed Notch Flaws in Filleted Hollow Cylinder. Prod. Env.

(b) Optimum Probability Method of Data Cumulation

27-OCT-75 ULTRASONIC TEST 2 (74)

RANGE	MIN LN	MAX LN	N	DET	50%	95%	0 MISS	1 MISS
1	60 *	60 *	12	10	0	56	0	0
2	0	0	0	0	0	0	0	0
3	0	0	0	0	0	0	0	0
4	100	100	23	22	0	80	23	38
5	0	0	0	0	0	0	0	0
6	100	120	29	28	0	84	17	32
7	100	130	34	33	0	86	12	27
8	100	140	39	38	0	88	7	22
9	0	0	0	0	0	0	0	0
10	100	160	42	40	0	85	19	34
11	0	0	0	0	0	0	0	0
12	100	180	48	46	0	87	13	28
13	0	0	0	0	0	0	0	0
14	0	0	0	0	0	0	0	0
15	0	0	0	0	0	0	0	0
16	0	0	0	0	0	0	0	0
17	100	230	49	47	0	87	12	27
18	0	0	0	0	0	0	0	0
19	0	0	0	0	0	0	0	0
20	0	0	0	0	0	0	0	0
21	0	0	0	0	0	0	0	0
22	0	0	0	0	0	0	0	0
23	0	0	0	0	0	0	0	0
24	0	0	0	0	0	0	0	0
25	100	310	50	48	0	87	11	26
26	0	0	0	0	0	0	0	0
27	0	0	0	0	0	0	0	0
28	0	0	0	0	0	0	0	0
29	100	350	52	50	0	88	[illegible]	24
30	0	0	0	0	0	0	0	0
31	0	0	0	0	0	0	0	0
32	100	390	53	51	0	88	8	23

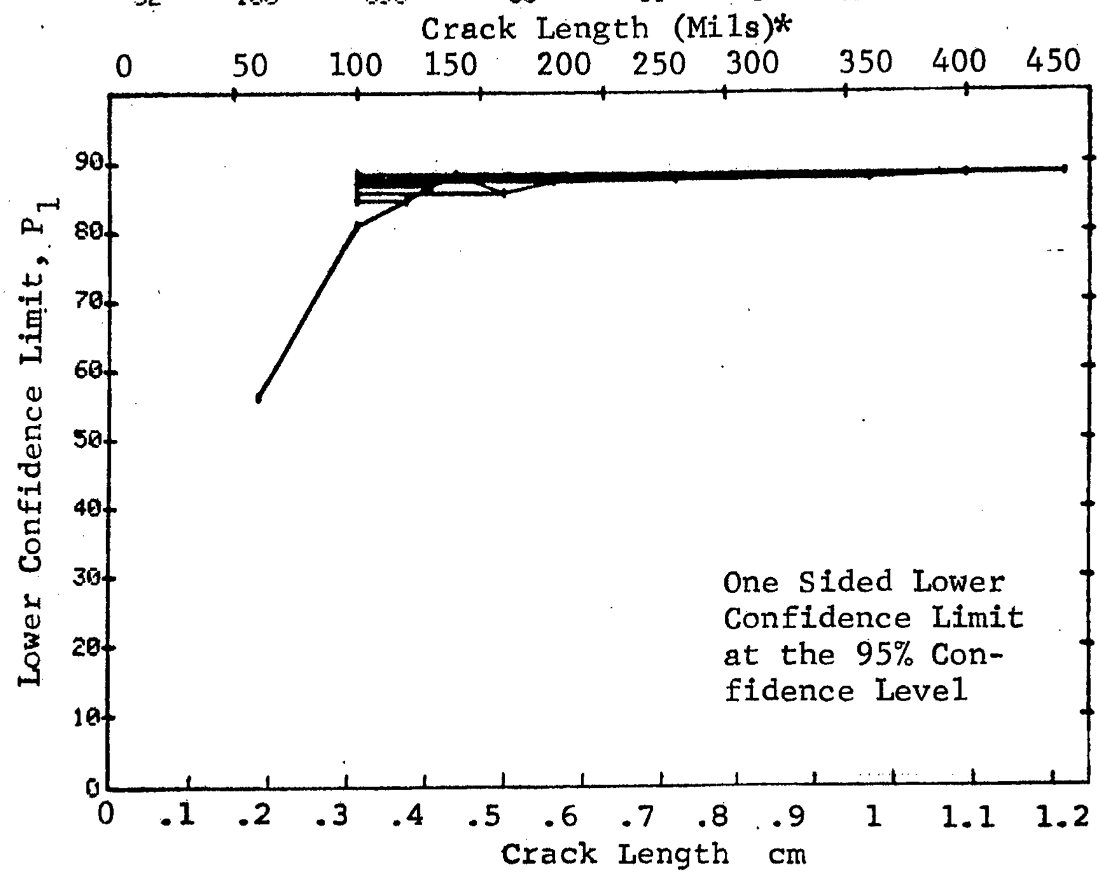

Figure D-74 (Continued)

(c) Overlapping Sixty Point Method of Data Cumulation

27-OCT-75 ULTRASONIC TEST 3 (74)

RANGE	MIN LN *	MAX LN *	N	DET	50%	95%	0 MISS	1 MISS
1	0	0	0	0	0	0	0	0
2	0	0	0	0	0	0	0	0
3	0	0	0	0	0	0	0	0
4	0	0	0	0	0	0	0	0
5	0	0	0	0	0	0	0	0
6	0	0	0	0	0	0	0	0
7	0	0	0	0	0	0	0	0
8	0	0	0	0	0	0	0	0
9	0	0	0	0	0	0	0	0
10	0	0	0	0	0	0	0	0
11	0	0	0	0	0	0	0	0
12	0	0	0	0	0	0	0	0
13	0	0	0	0	0	0	0	0
14	0	0	0	0	0	0	0	0
15	0	0	0	0	0	0	0	0
16	0	0	0	0	0	0	0	0
17	0	0	0	0	0	0	0	0
18	0	0	0	0	0	0	0	0
19	0	0	0	0	0	0	0	0
20	0	0	0	0	0	0	0	0
21	0	0	0	0	0	0	0	0
22	0	0	0	0	0	0	0	0
23	0	0	0	0	0	0	0	0
24	0	0	0	0	0	0	0	0
25	0	0	0	0	0	0	0	0
26	0	0	0	0	0	0	0	0
27	0	0	0	0	0	0	0	0
28	0	0	0	0	0	0	0	0
29	0	0	0	0	0	0	0	0
30	0	0	0	0	0	0	0	0
31	60	100	35	32	89	79	41	54
32	60	390	60	58	95	89	1	16

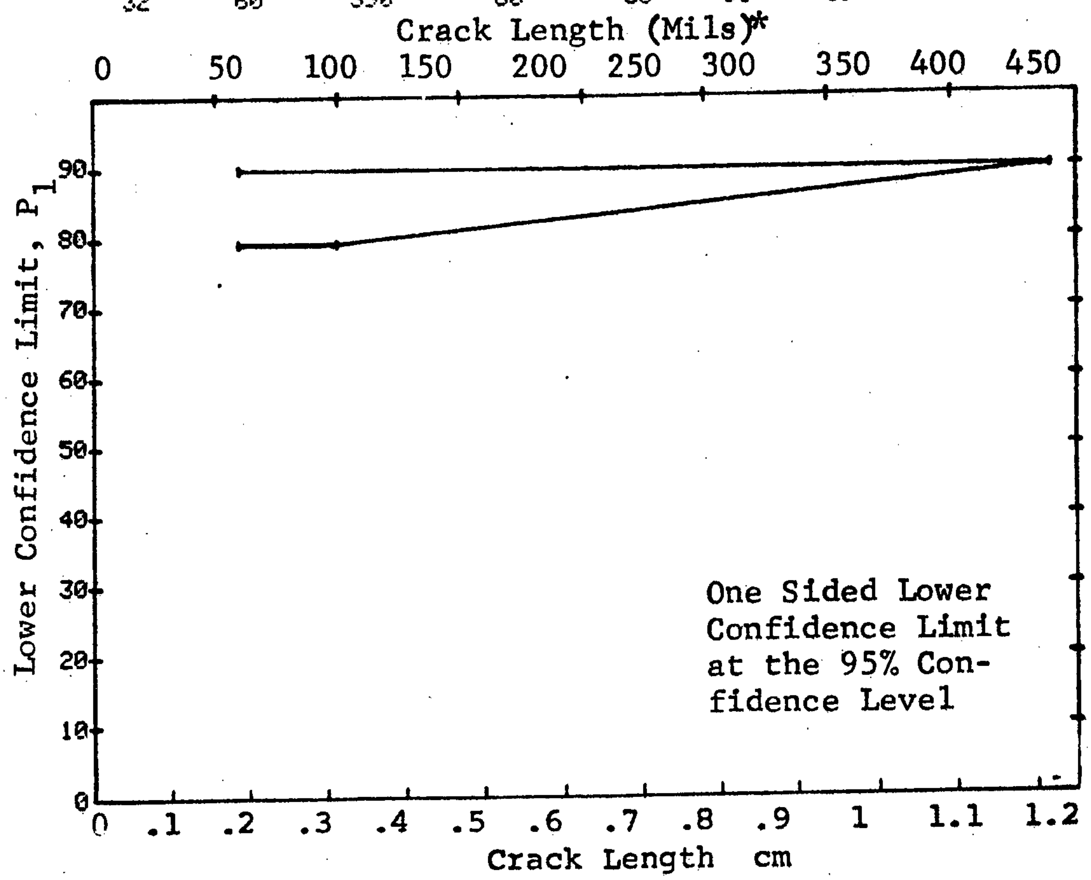

Figure D-74 (Concluded)

(a) Range Interval Method of Data Cumulation

27-OCT-75 ULTRASONIC TEST 1 (75)

RANGE	MIN LN *	MAX LN *	N	DET	50%	95%	0 MISS	1 MISS
1	20	30	12	4	29	12	0	0
2	0	0	0	0	0	0	0	0
3	0	0	0	0	0	0	0	0
4	60	60	12	12	94	77	17	34
5	70	70	21	21	96	86	8	25
6	0	0	0	0	0	0	0	0
7	90	90	12	12	94	77	17	34
8	100	100	11	11	93	76	18	35
9	0	0	0	0	0	0	0	0
10	130	130	1	1	50	5	0	0
11	140	140	3	3	79	36	0	0
12	150	150	12	12	94	77	17	34
13	0	0	0	0	0	0	0	0
14	0	0	0	0	0	0	0	0
15	0	0	0	0	0	0	0	0
16	0	0	0	0	0	0	0	0
17	0	0	0	0	0	0	0	0
18	0	0	0	0	0	0	0	0
19	0	0	0	0	0	0	0	0
20	0	0	0	0	0	0	0	0
21	0	0	0	0	0	0	0	0
22	0	0	0	0	0	0	0	0
23	0	0	0	0	0	0	0	0
24	0	0	0	0	0	0	0	0
25	300	300	3	3	79	36	0	0
26	0	0	0	0	0	0	0	0
27	0	0	0	0	0	0	0	0
28	0	0	0	0	0	0	0	0
29	0	0	0	0	0	0	0	0
30	0	0	0	0	0	0	0	0
31	0	0	0	0	0	0	0	0
32	370	380	2	2	70	22	0	0

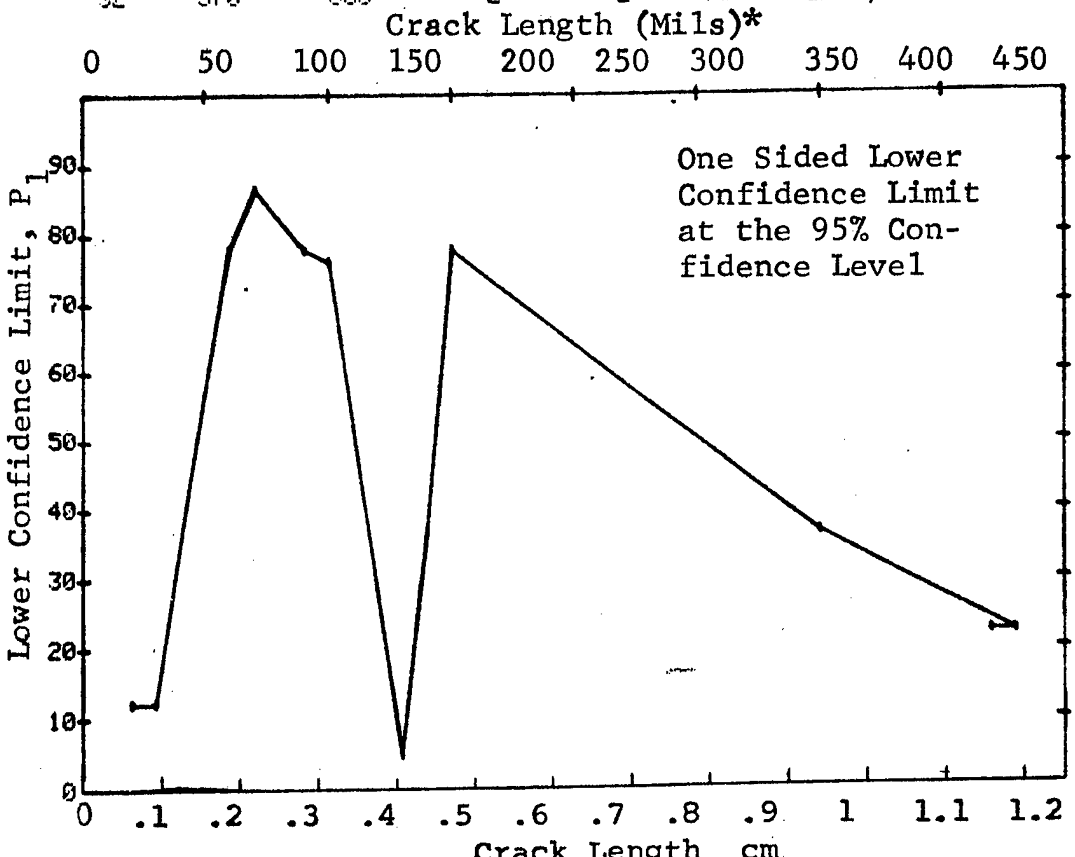

Figure D-75 Probability of Detection for 4340M Steel Using Ultrasonic Shear and Surface Waves. Compressed Notch Flaws in Filleted Solid Cylinder. Prod Env.

(b) Optimum Probability Method of Data Cumulation

27-OCT-75 ULTRASONIC TEST 2 C. 75 (75)

RANGE	MIN LN	MAX LN	N	DET	50%	95%	0 MISS	1 MISS
1	20 *	30 *	12	4	0	12	0	0
2	0	0	0	0	0	0	0	0
3	0	0	0	0	0	0	0	0
4	60	60	12	12	0	77	0	0
5	60	70	33	33	0	91	0	13
6	0	0	0	0	0	0	0	0
7	60	90	45	45	0	93	0	1
8	60	100	56	56	0	94	0	0
9	0	0	0	0	0	0	0	0
10	60	130	57	57	0	94	0	0
11	60	140	60	60	0	95	0	0
12	60	150	72	72	0	95	0	0
13	0	0	0	0	0	0	0	0
14	0	0	0	0	0	0	0	0
15	0	0	0	0	0	0	0	0
16	0	0	0	0	0	0	0	0
17	0	0	0	0	0	0	0	0
18	0	0	0	0	0	0	0	0
19	0	0	0	0	0	0	0	0
20	0	0	0	0	0	0	0	0
21	0	0	0	0	0	0	0	0
22	0	0	0	0	0	0	0	0
23	0	0	0	0	0	0	0	0
24	0	0	0	0	0	0	0	0
25	60	300	75	75	0	96	0	0
26	0	0	0	0	0	0	0	0
27	0	0	0	0	0	0	0	0
28	0	0	0	0	0	0	0	0
29	0	0	0	0	0	0	0	0
30	0	0	0	0	0	0	0	0
31	0	0	0	0	0	0	0	0
32	60	330	77	77	0 *	96	0	0

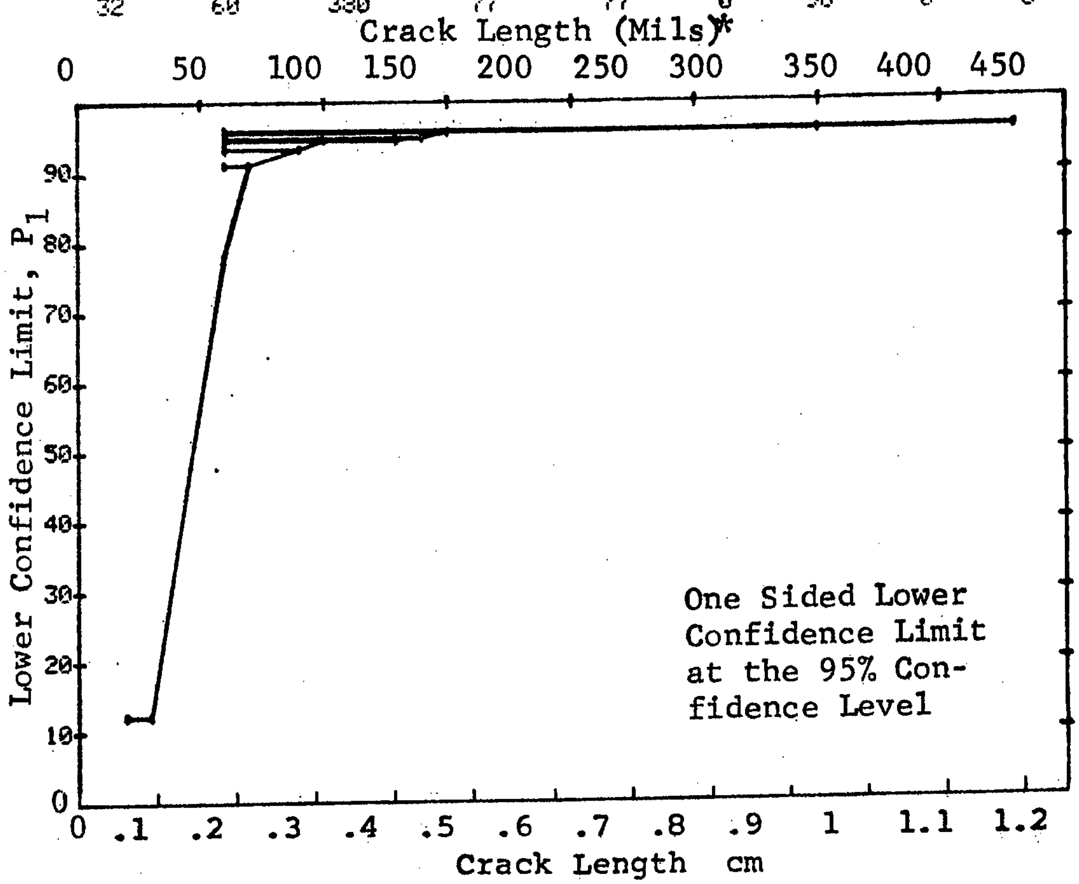

Figure D-75 (Continued)

(c) Overlapping Sixty Point Method of Data Cumulation

27-OCT-75 ULTRASONIC TEST 3 ( )7.5 (75)

RANGE	MIN LN	MAX LN	N	DET	50%	95%	0 MISS	1 MISS
1	0 *	0 *	0	0	0	0	0	0
2	0	0	0	0	0	0	0	0
3	0	0	0	0	0	0	0	0
4	0	0	0	0	0	0	0	0
5	0	0	0	0	0	0	0	0
6	0	0	0	0	0	0	0	0
7	0	0	0	0	0	0	0	0
8	0	0	0	0	0	0	0	0
9	0	0	0	0	0	0	0	0
10	0	0	0	0	0	0	0	0
11	0	0	0	0	0	0	0	0
12	0	0	0	0	0	0	0	0
13	0	0	0	0	0	0	0	0
14	0	0	0	0	0	0	0	0
15	0	0	0	0	0	0	0	0
16	0	0	0	0	0	0	0	0
17	0	0	0	0	0	0	0	0
18	0	0	0	0	0	0	0	0
19	0	0	0	0	0	0	0	0
20	0	0	0	0	0	0	0	0
21	0	0	0	0	0	0	0	0
22	0	0	0	0	0	0	0	0
23	0	0	0	0	0	0	0	0
24	0	0	0	0	0	0	0	0
25	0	0	0	0	0	0	0	0
26	0	0	0	0	0	0	0	0
27	0	0	0	0	0	0	0	0
28	0	0	0	0	0	0	0	0
29	0	0	0	0	0	0	0	0
30	0	0	0	0	0	0	0	0
31	20	100	59	51	85	76	83	95
32	70	380	60	60	98	95	0	0

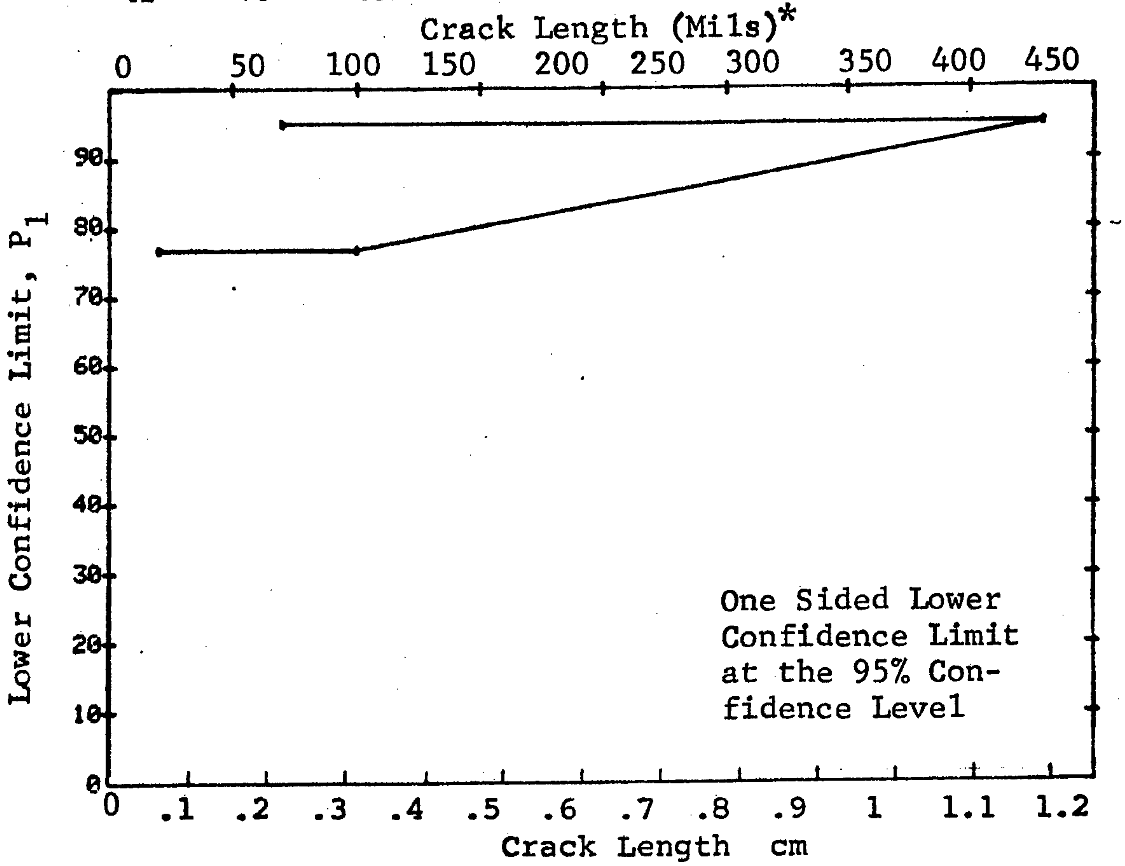

Figure D-75 (Concluded)

(a) Range Interval Method of Data Cumulation

27-OCT-75 ULTRASONIC TEST 1 ( ) 76 (76)

RANGE	MIN LN	MAX LN	N	DET	50%	95%	0 MISS	1 MISS
1	30 *	50 *	19	17	86	70	0	0
2	60	70	35	33	92	83	26	41
3	0	0	0	0	0	0	0	0
4	110	120	14	14	95	80	15	32
5	140	140	29	29	97	90	0	17
6	150	160	14	14	95	80	15	32
7	0	0	0	0	0	0	0	0
8	200	200	8	8	91	63	0	0
9	0	0	0	0	0	0	0	0
10	0	0	0	0	0	0	0	0
11	0	0	0	0	0	0	0	0
12	0	0	0	0	0	0	0	0
13	0	0	0	0	0	0	0	0
14	0	0	0	0	0	0	0	0
15	0	0	0	0	0	0	0	0
16	0	0	0	0	0	0	0	0
17	0	0	0	0	0	0	0	0
18	0	0	0	0	0	0	0	0
19	0	0	0	0	0	0	0	0
20	0	0	0	0	0	0	0	0
21	0	0	0	0	0	0	0	0
22	0	0	0	0	0	0	0	0
23	0	0	0	0	0	0	0	0
24	0	0	0	0	0	0	0	0
25	0	0	0	0	0	0	0	0
26	0	0	0	0	0	0	0	0
27	0	0	0	0	0	0	0	0
28	0	0	0	0	0	0	0	0
29	0	0	0	0	0	0	0	0
30	0	0	0	0	0	0	0	0
31	0	0	0	0	0	0	0	0
32	750	750	3	3	79	36	0	0

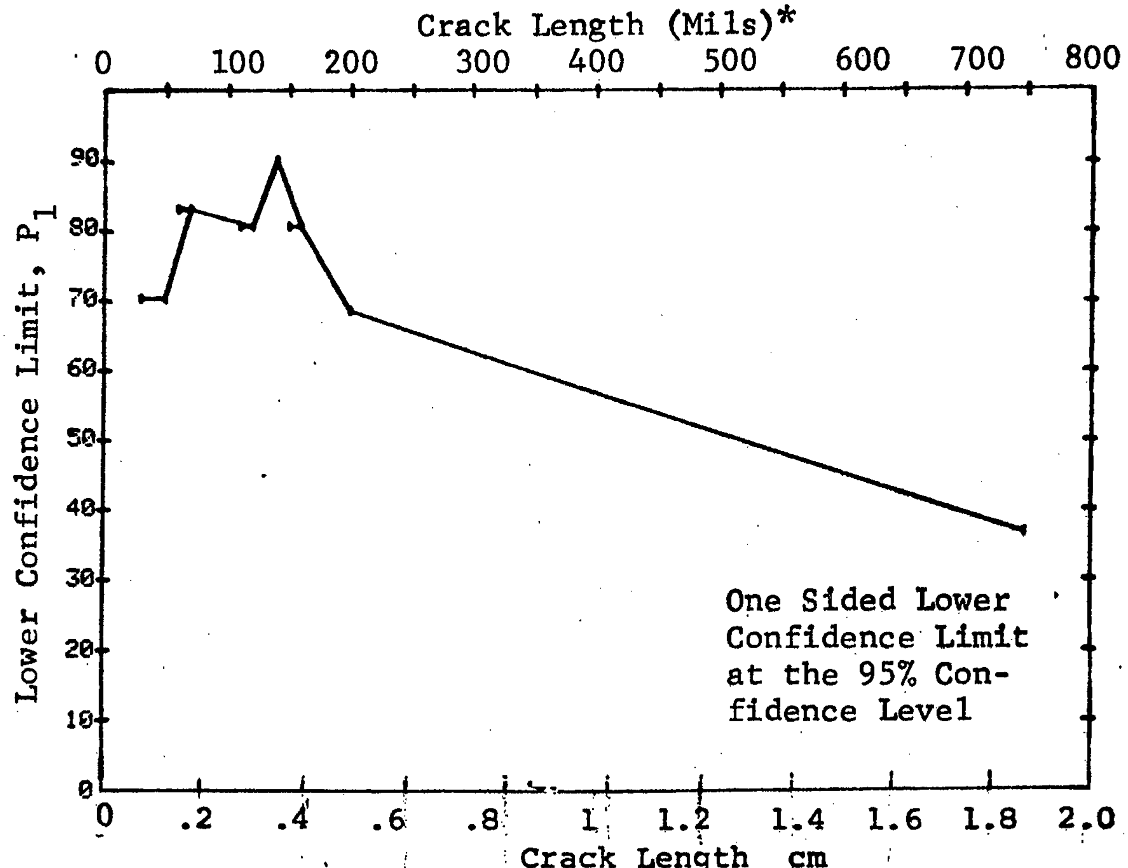

Figure D-76 Probability of Detection for 4340M Steel Using Ultrasonic Shear and Surface Waves. Compressed Notch Flaws in Filleted Solid Cylinder. Prod. Env.

(b) Optimum Probability Method of Data Cumulation

27-OCT-75 ULTRASONIC TEST 2 (76)

RANGE	MIN LN	MAX LN	N	DET	50%	95%	0 MISS	1 MISS
1	30 *	50 *	19	17	0	70	0	0
2	30	70	54	50	0	83	35	49
3	0	0	0	0	0	0	0	0
4	60	120	49	47	0	87	12	27
5	110	140	43	43	0	93	0	3
6	110	160	57	57	0	94	0	0
7	0	0	0	0	0	0	0	0
8	110	200	65	65	0	95	0	0
9	0	0	0	0	0	0	0	0
10	0	0	0	0	0	0	0	0
11	0	0	0	0	0	0	0	0
12	0	0	0	0	0	0	0	0
13	0	0	0	0	0	0	0	0
14	0	0	0	0	0	0	0	0
15	0	0	0	0	0	0	0	0
16	0	0	0	0	0	0	0	0
17	0	0	0	0	0	0	0	0
18	0	0	0	0	0	0	0	0
19	0	0	0	0	0	0	0	0
20	0	0	0	0	0	0	0	0
21	0	0	0	0	0	0	0	0
22	0	0	0	0	0	0	0	0
23	0	0	0	0	0	0	0	0
24	0	0	0	0	0	0	0	0
25	0	0	0	0	0	0	0	0
26	0	0	0	0	0	0	0	0
27	0	0	0	0	0	0	0	0
28	0	0	0	0	0	0	0	0
29	0	0	0	0	0	0	0	0
30	0	0	0	0	0	0	0	0
31	0	0	0	0	0	0	0	0
32	110	750	68	68	0	95	0	0

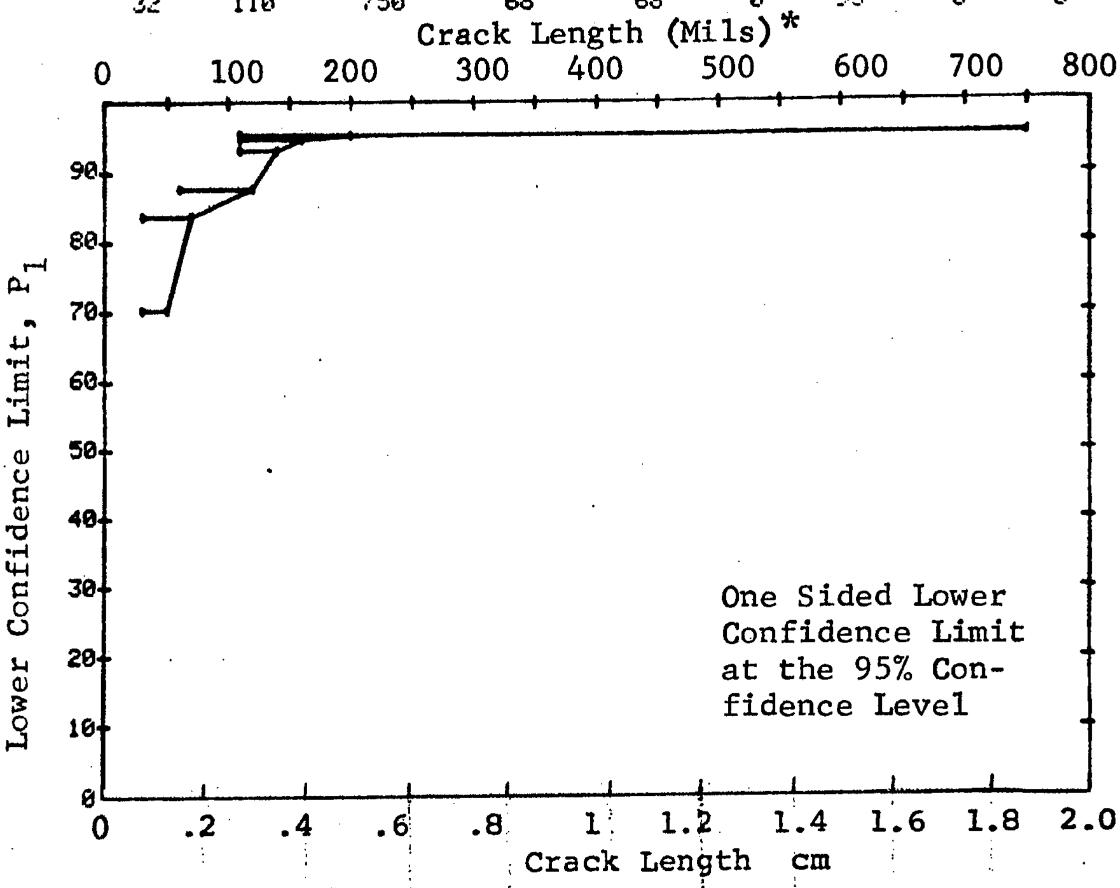

Figure D-76 (Continued)

(c) Overlapping Sixty Point Method of Data Cumulation

27-OCT-75 ULTRASONIC TEST 3 (76 (76)

RANGE	MIN LN *	MAX LN *	N	DET	50%	95%	0 MISS	1 MISS
1	0	0	0	0	0	0	0	0
2	0	0	0	0	0	0	0	0
3	0	0	0	0	0	0	0	0
4	0	0	0	0	0	0	0	0
5	0	0	0	0	0	0	0	0
6	0	0	0	0	0	0	0	0
7	0	0	0	0	0	0	0	0
8	0	0	0	0	0	0	0	0
9	0	0	0	0	0	0	0	0
10	0	0	0	0	0	0	0	0
11	0	0	0	0	0	0	0	0
12	0	0	0	0	0	0	0	0
13	0	0	0	0	0	0	0	0
14	0	0	0	0	0	0	0	0
15	0	0	0	0	0	0	0	0
16	0	0	0	0	0	0	0	0
17	0	0	0	0	0	0	0	0
18	0	0	0	0	0	0	0	0
19	0	0	0	0	0	0	0	0
20	0	0	0	0	0	0	0	0
21	0	0	0	0	0	0	0	0
22	0	0	0	0	0	0	0	0
23	0	0	0	0	0	0	0	0
24	0	0	0	0	0	0	0	0
25	0	0	0	0	0	0	0	0
26	0	0	0	0	0	0	0	0
27	0	0	0	0	0	0	0	0
28	0	0	0	0	0	0	0	0
29	0	0	0	0	0	0	0	0
30	30	120	59	55	92	85	30	44
31	60	140	60	59	97	92	0	1
32	120	200	60	60	98	95	0	0

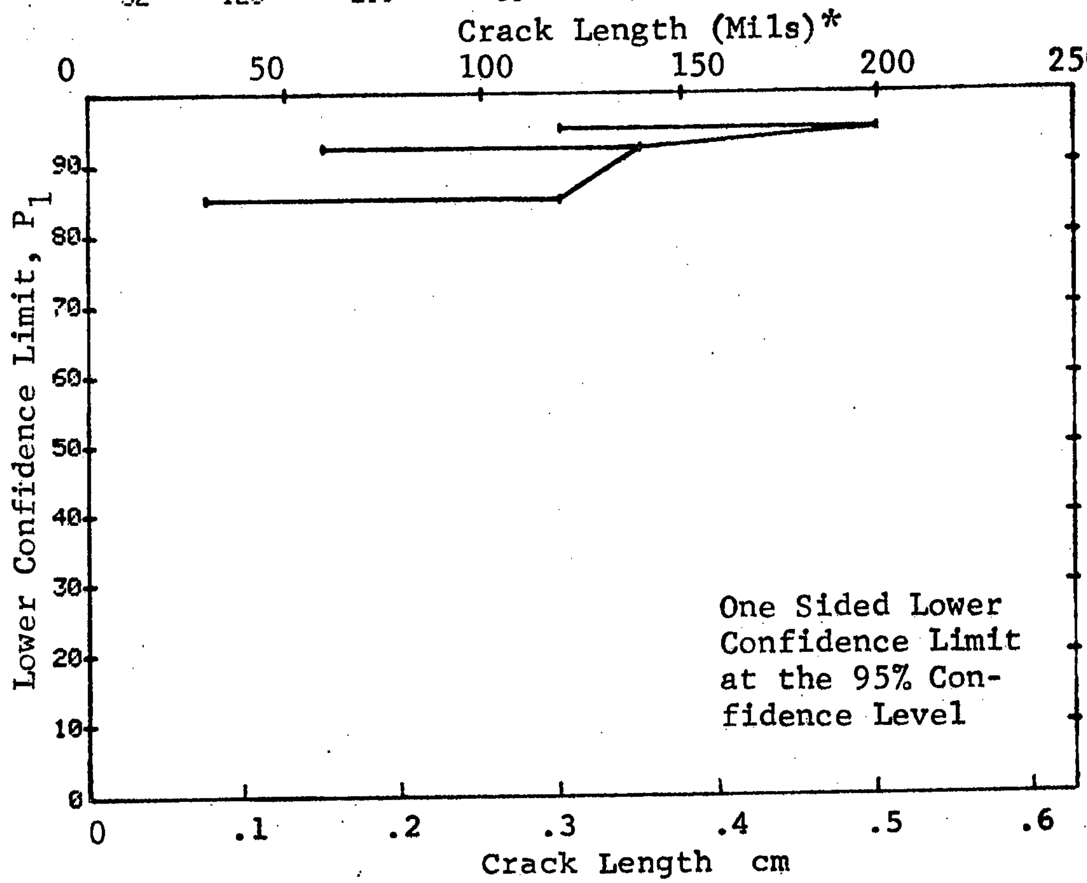

Figure D-76 (Concluded)

(a) Range Interval Method of Data Cumulation

27-OCT-75 ULTRASONIC TEST 1 (.) 77 (77)

RANGE	MIN LN	*	MAX LN	*	N	DET	50%	95%	0 MISS	1 MISS
1	30		50		26	23	86	72	0	0
2	60		70		41	39	93	85	20	35
3	0		0		0	0	0	0	0	0
4	110		120		18	18	96	84	11	28
5	130		140		33	33	97	91	0	13
6	150		160		13	13	94	79	16	33
7	0		0		0	0	0	0	0	0
8	200		200		11	11	93	76	18	35
9	0		0		0	0	0	0	0	0
10	0		0		0	0	0	0	0	0
11	0		0		0	0	0	0	0	0
12	0		0		0	0	0	0	0	0
13	0		0		0	0	0	0	0	0
14	0		0		0	0	0	0	0	0
15	0		0		0	0	0	0	0	0
16	0		0		0	0	0	0	0	0
17	0		0		0	0	0	0	0	0
18	0		0		0	0	0	0	0	0
19	0		0		0	0	0	0	0	0
20	0		0		0	0	0	0	0	0
21	0		0		0	0	0	0	0	0
22	0		0		0	0	0	0	0	0
23	0		0		0	0	0	0	0	0
24	0		0		0	0	0	0	0	0
25	0		0		0	0	0	0	0	0
26	0		0		0	0	0	0	0	0
27	0		0		0	0	0	0	0	0
28	0		0		0	0	0	0	0	0
29	0		0		0	0	0	0	0	0
30	0		0		0	0	0	0	0	0
31	0		0		0	0	0	0	0	0
32	750		750		2	2	70	22	0	0

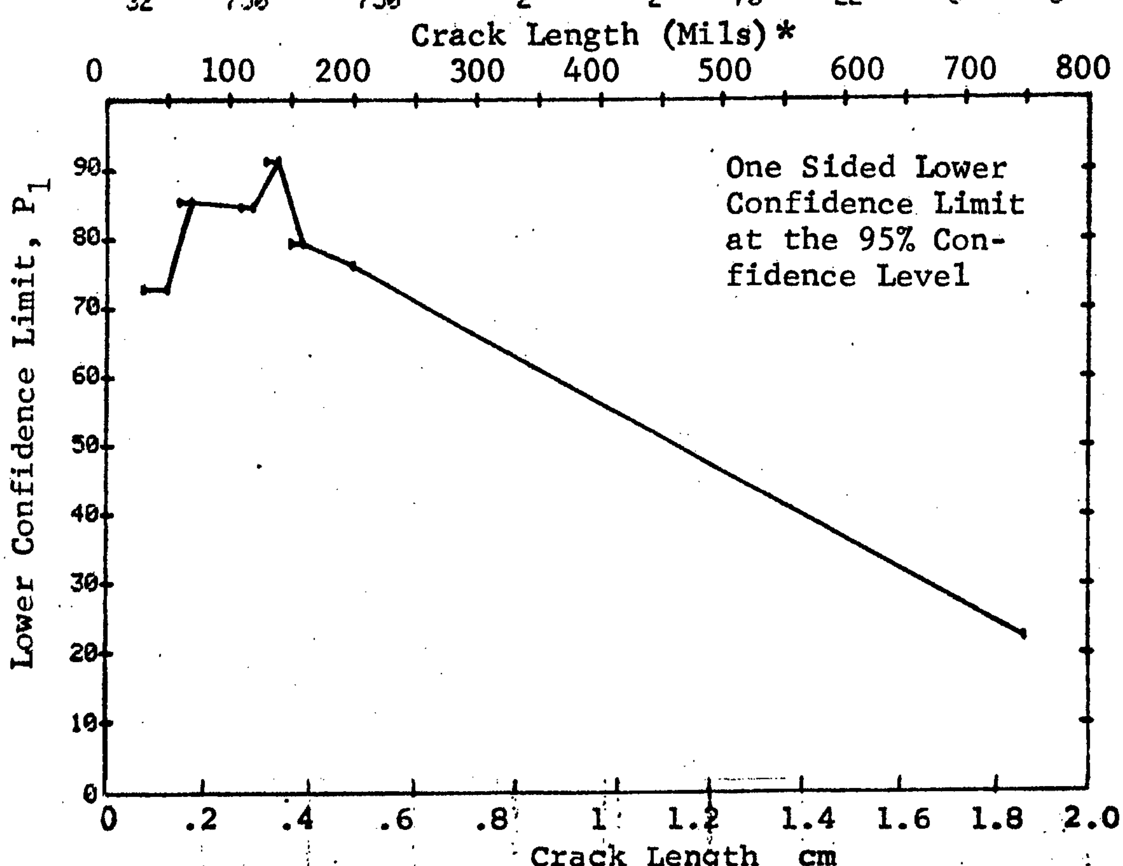

Figure D-77 Probability of Detection for 4340M Steel Using Ultrasonic Shear and Surface Waves, Compressed Notch Flaws in Filleted Solid Cylinder. Lab. Env.

(b) Optimum Probability Method of Data Cumulation

27-OCT-75 ULTRASONIC TEST 2 ( )77 (77)

RANGE	MIN LN	MAX LN	N	DET	50%	95%	0 MISS	1 MISS
1	30 *	50 *	26	23	0	72	0	0
2	60	70	41	39	0	85	20	35
3	0	0	0	0	0	0	0	0
4	60	120	59	57	0	89	2	17
5	110	140	51	51	0	94	0	0
6	110	160	64	64	0	95	0	0
7	0	0	0	0	0	0	0	0
8	110	200	75	75	0	96	0	0
9	0	0	0	0	0	0	0	0
10	0	0	0	0	0	0	0	0
11	0	0	0	0	0	0	0	0
12	0	0	0	0	0	0	0	0
13	0	0	0	0	0	0	0	0
14	0	0	0	0	0	0	0	0
15	0	0	0	0	0	0	0	0
16	0	0	0	0	0	0	0	0
17	0	0	0	0	0	0	0	0
18	0	0	0	0	0	0	0	0
19	0	0	0	0	0	0	0	0
20	0	0	0	0	0	0	0	0
21	0	0	0	0	0	0	0	0
22	0	0	0	0	0	0	0	0
23	0	0	0	0	0	0	0	0
24	0	0	0	0	0	0	0	0
25	0	0	0	0	0	0	0	0
26	0	0	0	0	0	0	0	0
27	0	0	0	0	0	0	0	0
28	0	0	0	0	0	0	0	0
29	0	0	0	0	0	0	0	0
30	0	0	0	0	0	0	0	0
31	0	0	0	0	0	0	0	0
32	110	750	77	77	0	96	0	0

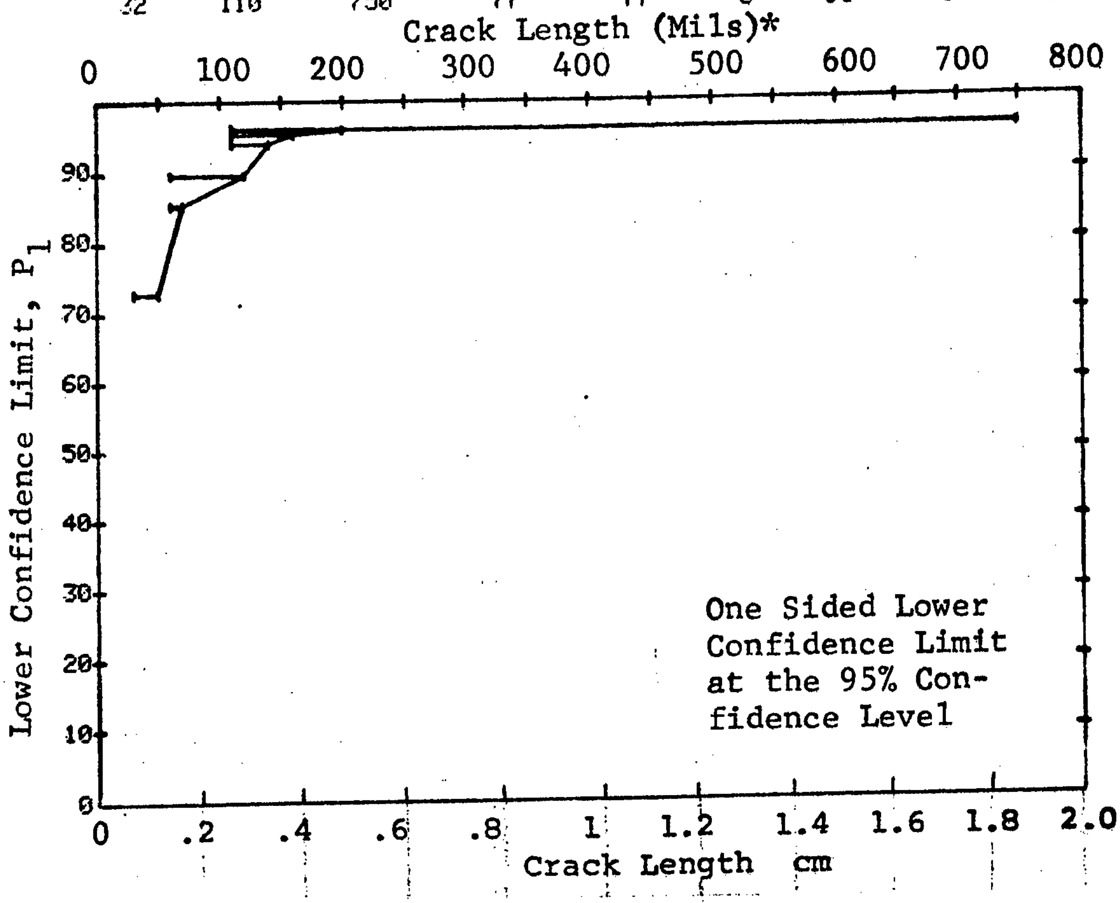

Figure D-77(Continued)

(c) Overlapping Sixty Point Method of Data Cumulation

27-OCT-75 ULTRASONIC TEST 3 (77 (77)

RANGE	MIN LN *	MAX LN *	N	DET	50%	95%	0 MISS	1 MISS
1	0	0	0	0	0	0	0	0
2	0	0	0	0	0	0	0	0
3	0	0	0	0	0	0	0	0
4	0	0	0	0	0	0	0	0
5	0	0	0	0	0	0	0	0
6	0	0	0	0	0	0	0	0
7	0	0	0	0	0	0	0	0
8	0	0	0	0	0	0	0	0
9	0	0	0	0	0	0	0	0
10	0	0	0	0	0	0	0	0
11	0	0	0	0	0	0	0	0
12	0	0	0	0	0	0	0	0
13	0	0	0	0	0	0	0	0
14	0	0	0	0	0	0	0	0
15	0	0	0	0	0	0	0	0
16	0	0	0	0	0	0	0	0
17	0	0	0	0	0	0	0	0
18	0	0	0	0	0	0	0	0
19	0	0	0	0	0	0	0	0
20	0	0	0	0	0	0	0	0
21	0	0	0	0	0	0	0	0
22	0	0	0	0	0	0	0	0
23	0	0	0	0	0	0	0	0
24	0	0	0	0	0	0	0	0
25	0	0	0	0	0	0	0	0
26	0	0	0	0	0	0	0	0
27	0	0	0	0	0	0	0	0
28	0	0	0	0	0	0	0	0
29	30	60	52	48	91	83	37	51
30	50	120	60	58	95	89	1	16
31	60	140	60	59	97	92	0	1
32	120	200	60	60	98	95	0	0

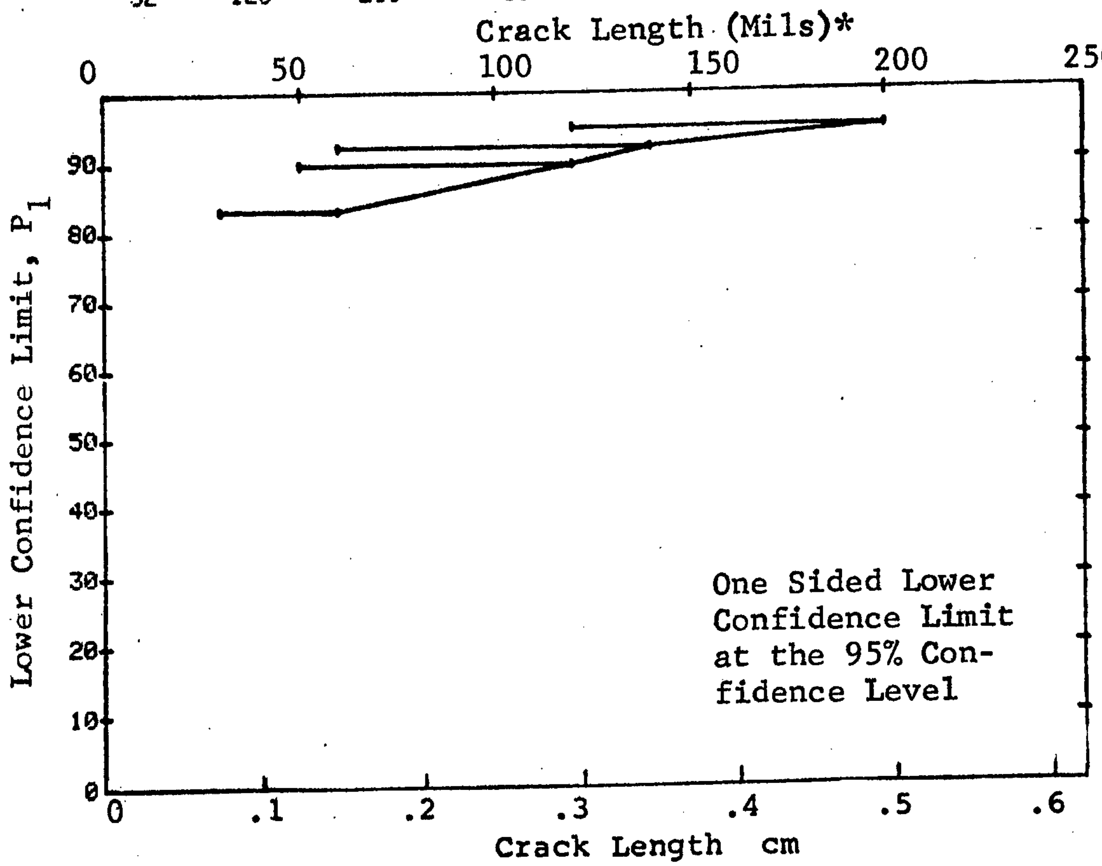

Figure D-77 (Concluded)

(a) Range Interval Method of Data Cumulation

27-OCT-75 ULTRASONIC TEST 1 (... 278 (78)

RANGE	MIN LN	MAX LN	N	DET	50%	95%	0 MISS	1 MISS
1	20*	30*	15	8	50	29	0	0
2	0	0	0	0	0	0	0	0
3	60	60	7	7	90	65	0	0
4	70	70	15	15	95	81	14	31
5	90	90	14	14	95	80	15	32
6	100	100	6	6	89	60	0	0
7	0	0	0	0	0	0	0	0
8	130	140	7	7	90	65	0	0
9	150	150	8	8	91	68	0	0
10	0	0	0	0	0	0	0	0
11	0	0	0	0	0	0	0	0
12	200	200	1	1	50	5	0	0
13	0	0	0	0	0	0	0	0
14	230	230	2	2	70	22	0	0
15	240	240	1	1	50	5	0	0
16	250	260	2	2	70	22	0	0
17	0	0	0	0	0	0	0	0
18	280	280	1	1	50	5	0	0
19	300	300	2	2	70	22	0	0
20	0	0	0	0	0	0	0	0
21	0	0	0	0	0	0	0	0
22	0	0	0	0	0	0	0	0
23	0	0	0	0	0	0	0	0
24	370	370	2	2	70	22	0	0
25	390	390	2	2	70	22	0	0
26	410	410	1	1	50	5	0	0
27	0	0	0	0	0	0	0	0
28	0	0	0	0	0	0	0	0
29	0	0	0	0	0	0	0	0
30	0	0	0	0	0	0	0	0
31	0	0	0	0	0	0	0	0
32	500	500	1	1	50	5	0	0

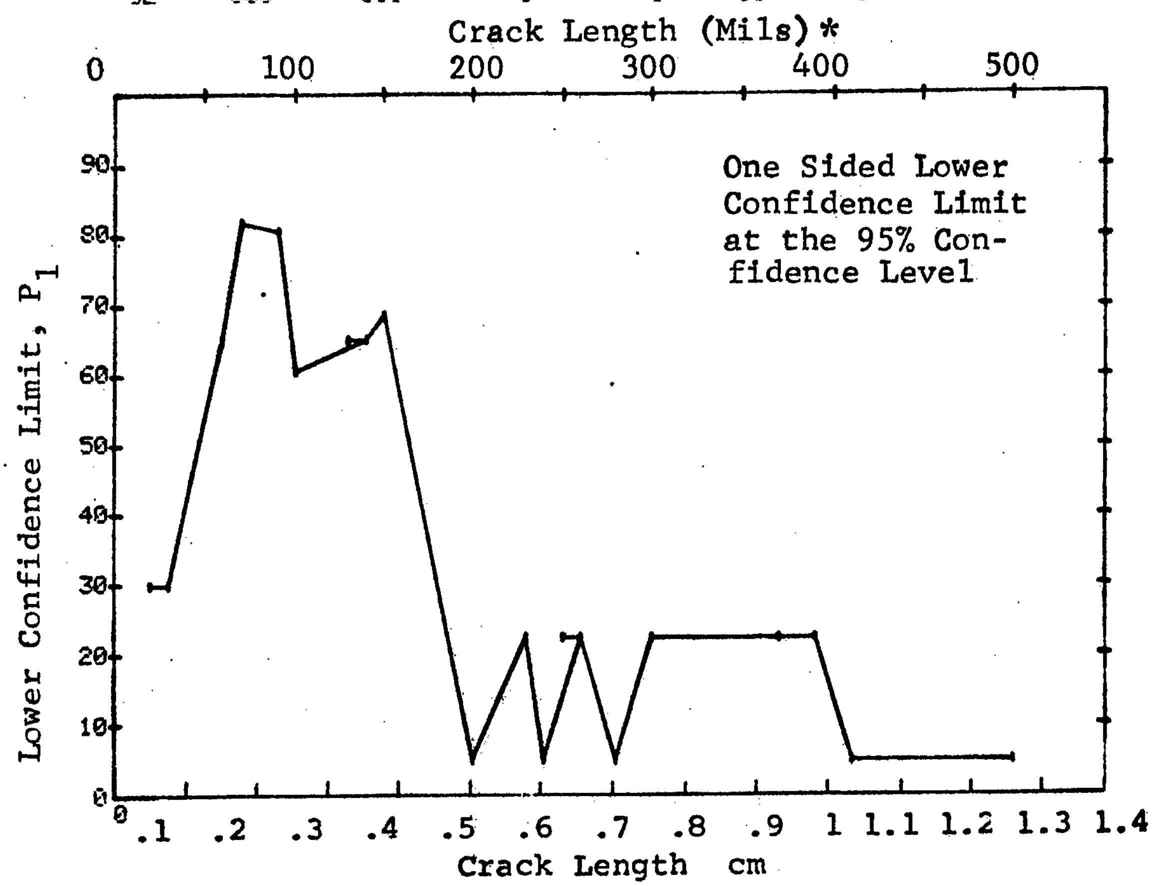

Figure D-78 Probability of Detection for 4340M Steel Using Ultrasonic Shear and Surface Waves. Compressed Notch Flaws in Filleted Solid Cylinder. Lab. Env.

(b) Optimum Probability Method of Data Cumulation

27-OCT-75 ULTRASONIC TEST 2 (. .) (78)

RANGE	MIN LN *	MAX LN *	N	DET	50%	95%	0 MISS	1 MISS
1	20	30	15	8	0	29	0	0
2	0	0	0	0	0	0	0	0
3	60	60	7	7	0	65	0	0
4	60	70	22	22	0	87	7	24
5	60	90	36	36	0	92	0	10
6	60	100	42	42	0	93	0	4
7	0	0	0	0	0	0	0	0
8	60	140	49	49	0	94	0	0
9	60	150	57	57	0	94	0	0
10	0	0	0	0	0	0	0	0
11	0	0	0	0	0	0	0	0
12	60	200	58	58	0	94	0	0
13	0	0	0	0	0	0	0	0
14	60	230	60	60	0	95	0	0
15	60	240	61	61	0	95	0	0
16	60	260	63	63	0	95	0	0
17	0	0	0	0	0	0	0	0
18	60	280	64	64	0	95	0	0
19	60	300	66	66	0	95	0	0
20	0	0	0	0	0	0	0	0
21	0	0	0	0	0	0	0	0
22	0	0	0	0	0	0	0	0
23	0	0	0	0	0	0	0	0
24	60	370	68	68	0	95	0	0
25	60	390	70	70	0	95	0	0
26	60	410	71	71	0	95	0	0
27	0	0	0	0	0	0	0	0
28	0	0	0	0	0	0	0	0
29	0	0	0	0	0	0	0	0
30	0	0	0	0	0	0	0	0
31	0	0	0	0	0	0	0	0
32	60	500	72	72	0	95	0	0

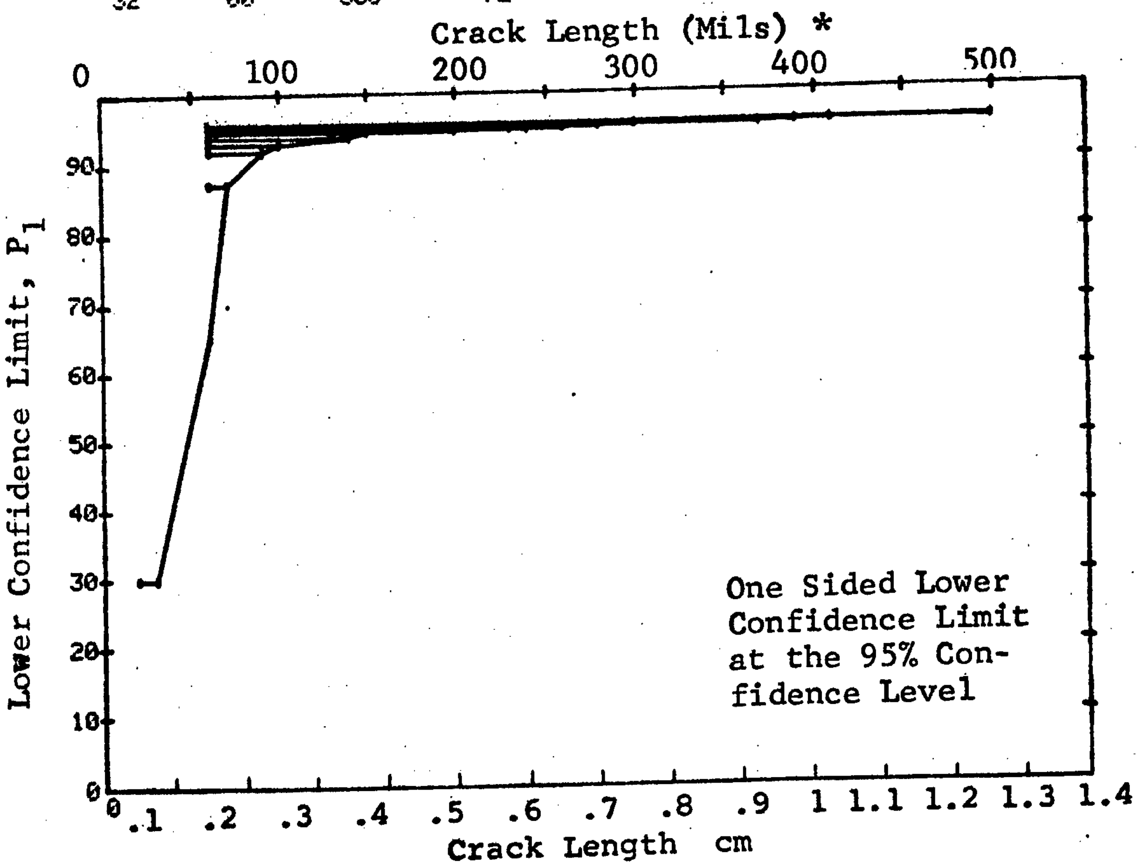

Figure D-78 (Continued)

(c) Overlapping Sixty Point Method of Data Cumulation

27-OCT-75 ULTRASONIC TEST 3 (J (78)

RANGE	MIN LN	MAX LN	N	DET	50%	95%	0 MISS	1 MISS
1	0 *	0 *	0	0	0	0	0	0
2	0	0	0	0	0	0	0	0
3	0	0	0	0	0	0	0	0
4	0	0	0	0	0	0	0	0
5	0	0	0	0	0	0	0	0
6	0	0	0	0	0	0	0	0
7	0	0	0	0	0	0	0	0
8	0	0	0	0	0	0	0	0
9	0	0	0	0	0	0	0	0
10	0	0	0	0	0	0	0	0
11	0	0	0	0	0	0	0	0
12	0	0	0	0	0	0	0	0
13	0	0	0	0	0	0	0	0
14	0	0	0	0	0	0	0	0
15	0	0	0	0	0	0	0	0
16	0	0	0	0	0	0	0	0
17	0	0	0	0	0	0	0	0
18	0	0	0	0	0	0	0	0
19	0	0	0	0	0	0	0	0
20	0	0	0	0	0	0	0	0
21	0	0	0	0	0	0	0	0
22	0	0	0	0	0	0	0	0
23	0	0	0	0	0	0	0	0
24	0	0	0	0	0	0	0	0
25	0	0	0	0	0	0	0	0
26	0	0	0	0	0	0	0	0
27	0	0	0	0	0	0	0	0
28	0	0	0	0	0	0	0	0
29	0	0	0	0	0	0	0	0
30	0	0	0	0	0	0	0	0
31	20	100	57	50	86	78	72	65
32	70	500	60	60	98	95	0	0

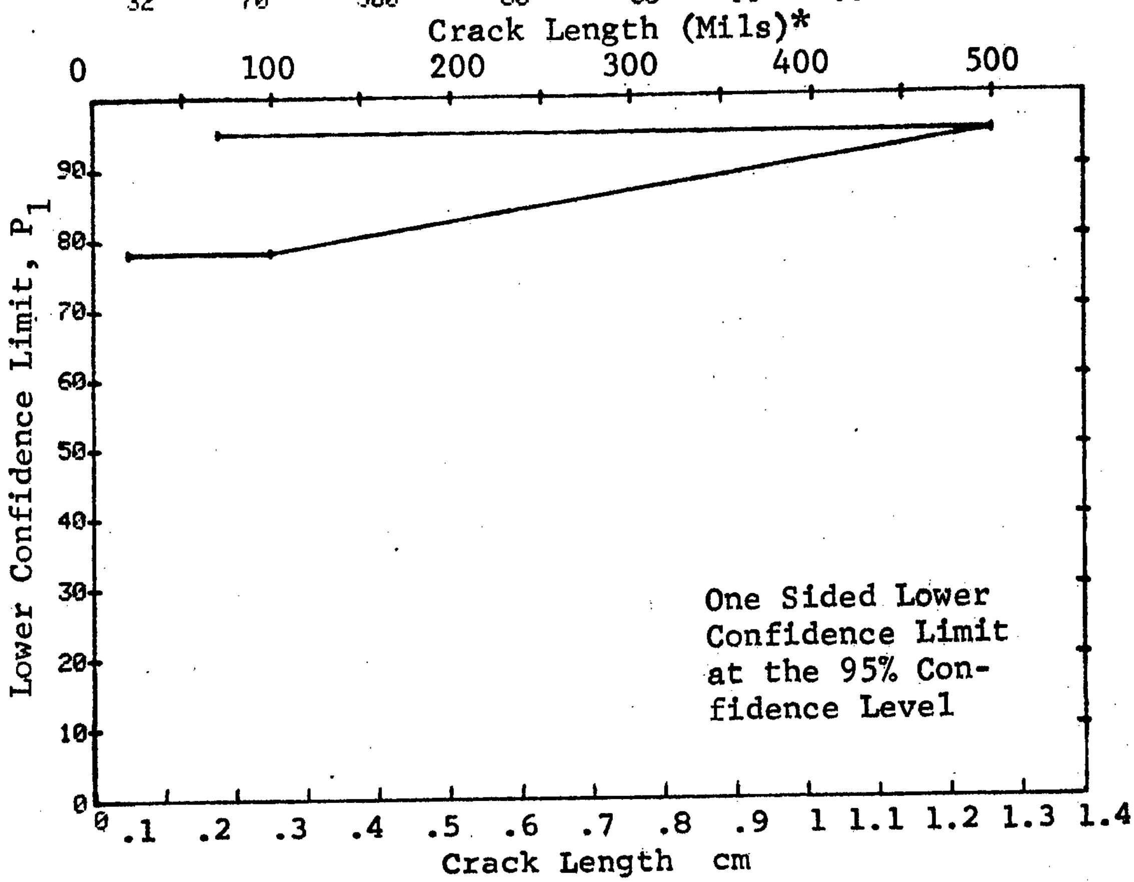

Figure D-78 (Concluded)

(a) Range Interval Method of Data Cumulation

27-OCT-75 ULTRASONIC TEST 1 (-? (79)

RANGE	MIN LN*	MAX LN*	N	DET	50%	95%	0 MISS	1 MISS
1	60	60	17	17	96	83	12	29
2	0	0	0	0	0	0	0	0
3	0	0	0	0	0	0	0	0
4	0	0	0	0	0	0	0	0
5	0	0	0	0	0	0	0	0
6	0	0	0	0	0	0	0	0
7	0	0	0	0	0	0	0	0
8	0	0	0	0	0	0	0	0
9	0	0	0	0	0	0	0	0
10	0	0	0	0	0	0	0	0
11	0	0	0	0	0	0	0	0
12	0	0	0	0	0	0	0	0
13	0	0	0	0	0	0	0	0
14	0	0	0	0	0	0	0	0
15	0	0	0	0	0	0	0	0
16	100	100	23	23	97	87	6	23
17	0	0	0	0	0	0	0	0
18	0	0	0	0	0	0	0	0
19	0	0	0	0	0	0	0	0
20	0	0	0	0	0	0	0	0
21	0	0	0	0	0	0	0	0
22	0	0	0	0	0	0	0	0
23	0	0	0	0	0	0	0	0
24	0	0	0	0	0	0	0	0
25	0	0	0	0	0	0	0	0
26	0	0	0	0	0	0	0	0
27	0	0	0	0	0	0	0	0
28	130	130	6	6	89	60	0	0
29	0	0	0	0	0	0	0	0
30	0	0	0	0	0	0	0	0
31	0	0	0	0	0	0	0	0
32	140	140	1	1	50	5	0	0

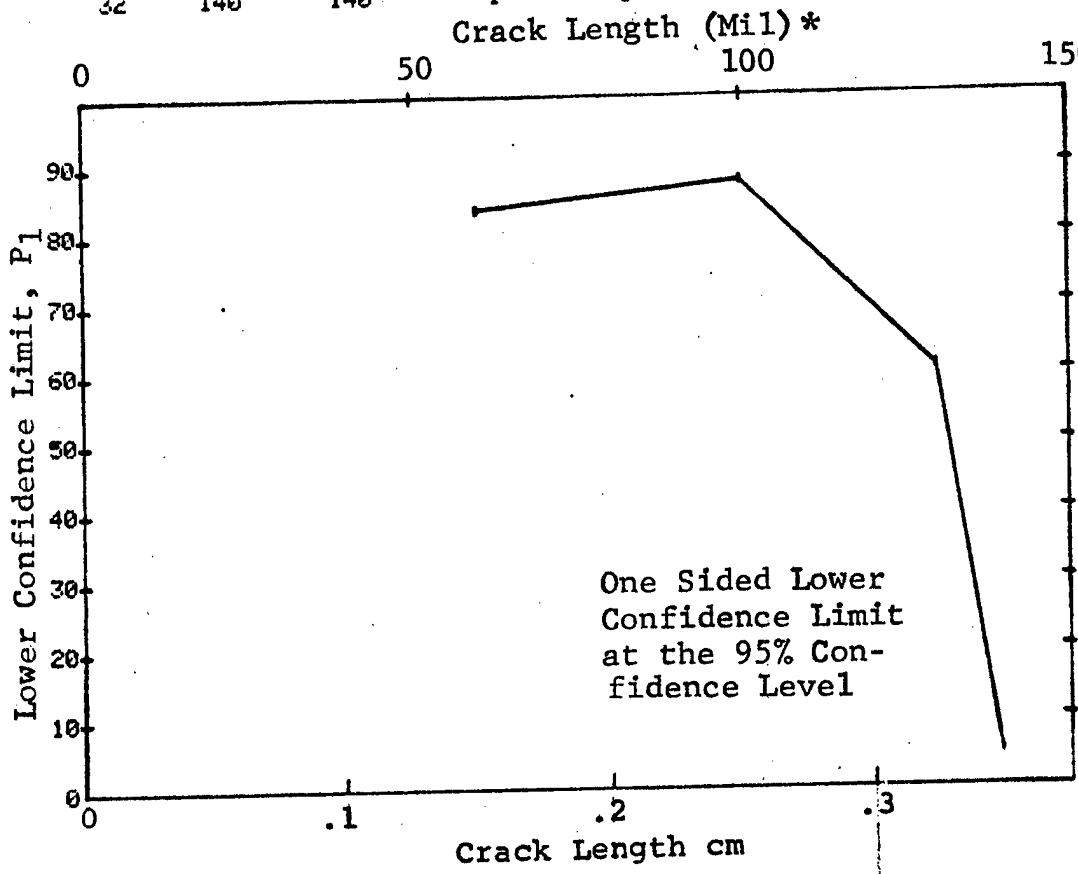

Figure D-79 Probability of Detection for 4340M Steel Using Ultrasonic Shear and Surface Waves. Compressed Notch Flaws in Hollow Cylinder. Lab. Env.

(b) Optimum Probability Method of Data Cumulation

27-OCT-75 ULTRASONIC TEST 2 (79)

RANGE	MIN LN	MAX LN	N	DET	50%	95%	0 MISS	1 MISS
1	60*	60*	17	17	0	83	12	29
2	0	0	0	0	0	0	0	0
3	0	0	0	0	0	0	0	0
4	0	0	0	0	0	0	0	0
5	0	0	0	0	0	0	0	0
6	0	0	0	0	0	0	0	0
7	0	0	0	0	0	0	0	0
8	0	0	0	0	0	0	0	0
9	0	0	0	0	0	0	0	0
10	0	0	0	0	0	0	0	0
11	0	0	0	0	0	0	0	0
12	0	0	0	0	0	0	0	0
13	0	0	0	0	0	0	0	0
14	0	0	0	0	0	0	0	0
15	0	0	0	0	0	0	0	0
16	60	100	40	40	0	92	0	6
17	0	0	0	0	0	0	0	0
18	0	0	0	0	0	0	0	0
19	0	0	0	0	0	0	0	0
20	0	0	0	0	0	0	0	0
21	0	0	0	0	0	0	0	0
22	0	0	0	0	0	0	0	0
23	0	0	0	0	0	0	0	0
24	0	0	0	0	0	0	0	0
25	0	0	0	0	0	0	0	0
26	0	0	0	0	0	0	0	0
27	0	0	0	0	0	0	0	0
28	60	130	46	46	0	93	0	0
29	0	0	0	0	0	0	0	0
30	0	0	0	0	0	0	0	0
31	0	0	0	0	0	0	0	0
32	60	140	47	47	0	93	0	0

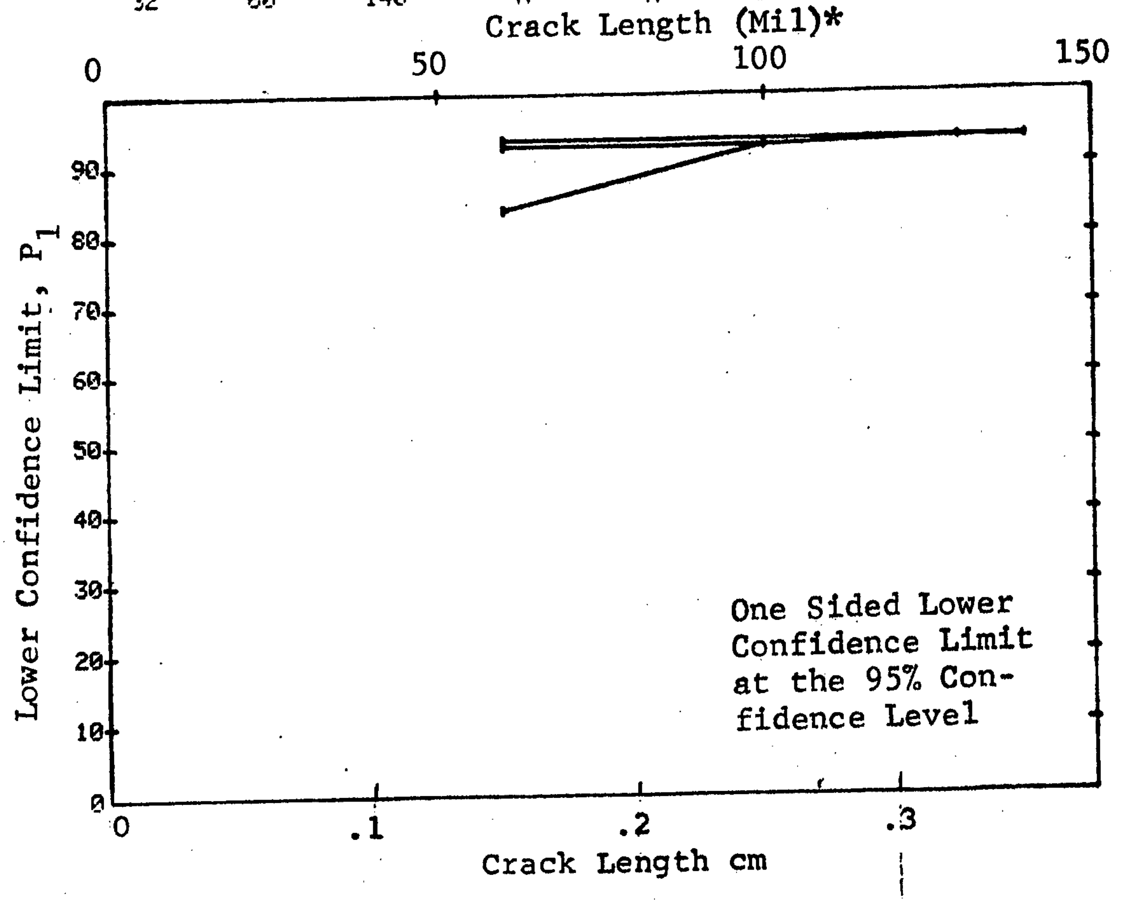

Figure D-79 (Continued)

(c) Overlapping Sixty Point Method of Data Cumulation

27-OCT-75 ULTRASONIC TEST 3 (79)

RANGE	MIN LN	MAX LN	N	DET	50%	95%	0 MISS	1 MISS
1	0	0	0	0	0	0	0	0
2	0	0	0	0	0	0	0	0
3	0	0	0	0	0	0	0	0
4	0	0	0	0	0	0	0	0
5	0	0	0	0	0	0	0	0
6	0	0	0	0	0	0	0	0
7	0	0	0	0	0	0	0	0
8	0	0	0	0	0	0	0	0
9	0	0	0	0	0	0	0	0
10	0	0	0	0	0	0	0	0
11	0	0	0	0	0	0	0	0
12	0	0	0	0	0	0	0	0
13	0	0	0	0	0	0	0	0
14	0	0	0	0	0	0	0	0
15	0	0	0	0	0	0	0	0
16	0	0	0	0	0	0	0	0
17	0	0	0	0	0	0	0	0
18	0	0	0	0	0	0	0	0
19	0	0	0	0	0	0	0	0
20	0	0	0	0	0	0	0	0
21	0	0	0	0	0	0	0	0
22	0	0	0	0	0	0	0	0
23	0	0	0	0	0	0	0	0
24	0	0	0	0	0	0	0	0
25	0	0	0	0	0	0	0	0
26	0	0	0	0	0	0	0	0
27	0	0	0	0	0	0	0	0
28	0	0	0	0	0	0	0	0
29	0	0	0	0	0	0	0	0
30	0	0	0	0	0	0	0	0
31	0	0	0	0	0	0	0	0
32	60	140	47	47	98	93	0	0

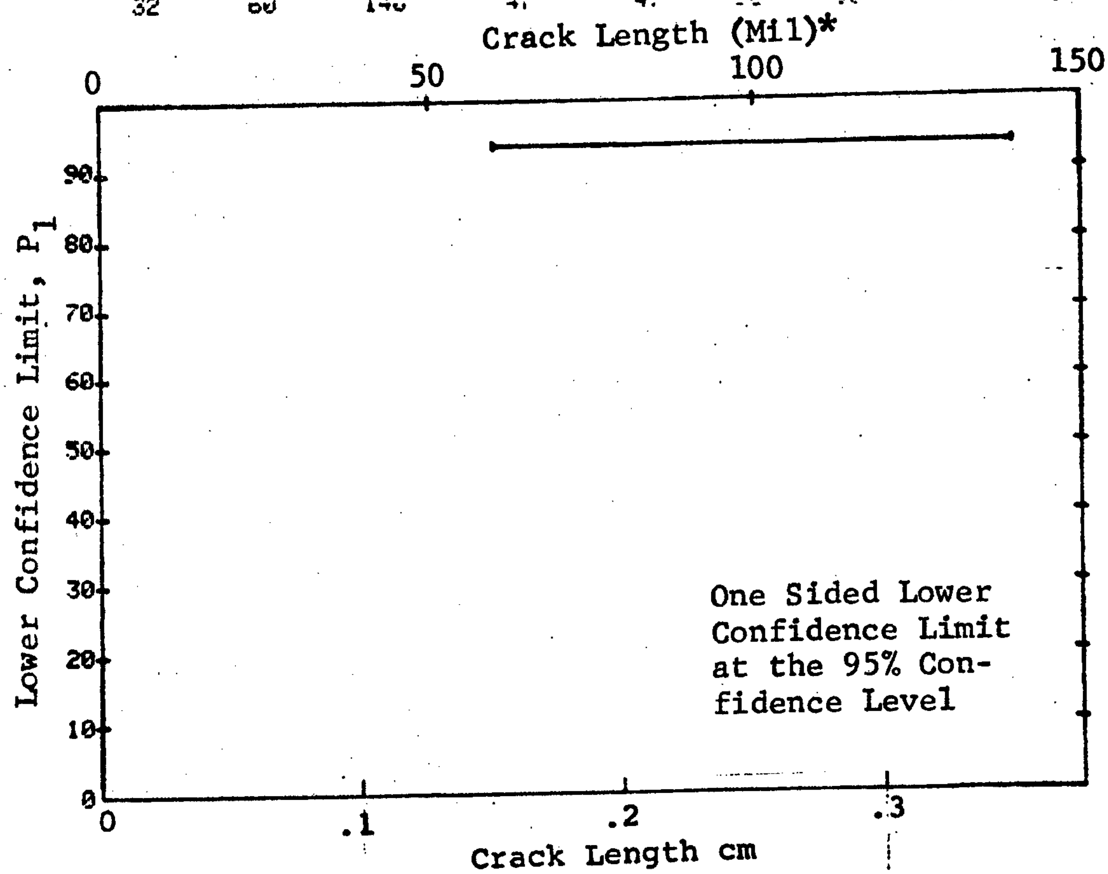

Figure D-79 (Concluded)

(a) Range Interval Method of Data Cumulation

29-OCT-75 ULTRASONIC TEST 1 (80)

RANGE	MIN LN	* MAX LN *	N	DET	50%	95%	0 MISS	1 MISS
1	80	80	7	7	90	65	0	0
2	90	90	17	17	94	79	16	37
3	0	0	0	0	0	0	0	0
4	0	0	0	0	0	0	0	0
5	110	110	4	4	84	47	0	0
6	120	120	4	4	84	47	0	0
7	130	130	7	7	90	65	0	0
8	0	0	0	0	0	0	0	0
9	140	140	9	9	92	71	0	0
10	0	0	0	0	0	0	0	0
11	0	0	0	0	0	0	0	0
12	0	0	0	0	0	0	0	0
13	0	0	0	0	0	0	0	0
14	0	0	0	0	0	0	0	0
15	0	0	0	0	0	0	0	0
16	0	0	0	0	0	0	0	0
17	0	0	0	0	0	0	0	0
18	0	0	0	0	0	0	0	0
19	0	0	0	0	0	0	0	0
20	0	0	0	0	0	0	0	0
21	0	0	0	0	0	0	0	0
22	0	0	0	0	0	0	0	0
23	0	0	0	0	0	0	0	0
24	0	0	0	0	0	0	0	0
25	0	0	0	0	0	0	0	0
26	0	0	0	0	0	0	0	0
27	0	0	0	0	0	0	0	0
28	0	0	0	0	0	0	0	0
29	0	0	0	0	0	0	[illegible]	[illegible]
30	0	0	0	0	0	0	0	[illegible]
31	300	300	1	1	50	5	0	0
32	310	310	3	3	79	36	0	0

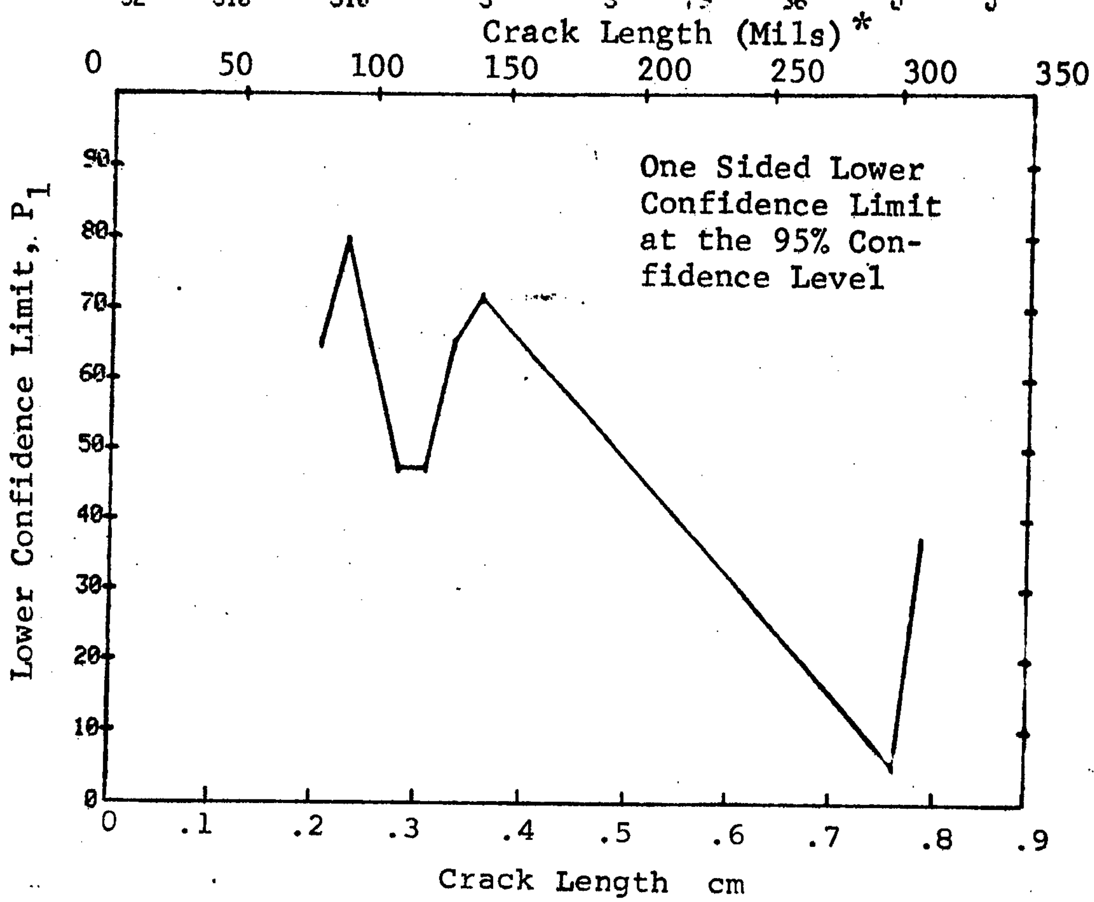

Figure D-80 Probability of Detection for 4340M Steel Using Ultrasonic Shear and Surface Waves. Compressed Notch Flaws in Filleted Hollow Cylinder. Lab. Env.

(b) Optimum Probability Method of Data Cumulation

29-OCT-75 ULTRASONIC TEST [illegible] (80)

RANGE	MIN LN	MAX LN	N	DET	50%	95%	0 MISS	[illegible]
1	80 *	80 *	7	7	0	65	0	[illegible]
2	80	90	20	20	0	86	3	[illegible]
3	0	0	0	0	0	0	0	0
4	0	0	0	0	0	0	0	0
5	80	110	24	24	0	88	5	22
6	80	120	28	28	0	89	1	13
7	80	130	35	35	0	91	0	11
8	0	0	0	0	0	0	0	0
9	80	140	44	44	0	93	0	[illegible]
10	0	0	0	0	0	0	0	0
11	0	0	0	0	0	0	0	0
12	0	0	0	0	0	0	0	0
13	0	0	0	0	0	0	0	0
14	0	0	0	0	0	0	0	0
15	0	0	0	0	0	0	0	0
16	0	0	0	0	0	0	0	0
17	0	0	0	0	0	0	0	0
18	0	0	0	0	0	0	0	0
19	0	0	0	0	0	0	0	0
20	0	0	0	0	0	0	0	0
21	0	0	0	0	0	0	0	0
22	0	0	0	0	0	0	0	0
23	0	0	0	0	0	0	0	0
24	0	0	0	0	0	0	0	[illegible]
25	0	0	0	0	0	0	0	0
26	0	0	0	0	0	0	0	[illegible]
27	0	0	0	0	0	0	0	0
28	0	0	0	0	0	0	0	0
29	0	0	0	0	0	0	[illegible]	[illegible]
30	0	0	0	0	0	0	[illegible]	[illegible]
31	80	300	45	45	0	93	0	1
32	80	310	48	48	0	93	[illegible]	[illegible]

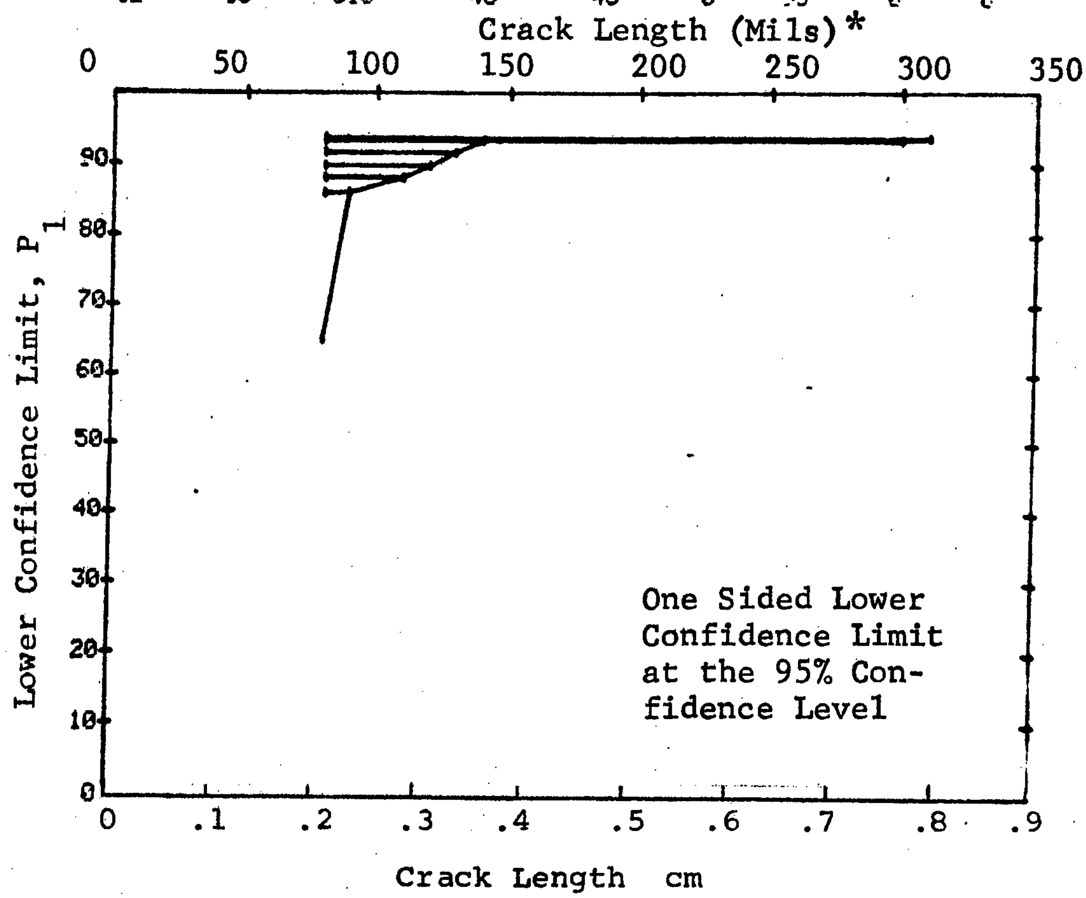

Figure D-80 (Continued)

(c) Overlapping Sixty Point Method of Data Cumulation

29-OCT-75 ULTRASONIC TEST 3 [illegible] (80)

RANGE	MIN LN	MAX LN	N	DET	50%	95%	0 MISS	1 MISS
1	0*	0*	0	0	0	0	0	0
2	0	0	0	0	0	0	0	0
3	0	0	0	0	0	0	0	0
4	0	0	0	0	0	0	0	0
5	0	0	0	0	0	0	0	0
6	0	0	0	0	0	0	0	0
7	0	0	0	0	0	0	0	0
8	0	0	0	0	0	0	0	0
9	0	0	0	0	0	0	0	0
10	0	0	0	0	0	0	0	0
11	0	0	0	0	0	0	0	0
12	0	0	0	0	0	0	0	0
13	0	0	0	0	0	0	0	0
14	0	0	0	0	0	0	0	0
15	0	0	0	0	0	0	0	0
16	0	0	0	0	0	0	0	0
17	0	0	0	0	0	0	0	0
18	0	0	0	0	0	0	0	0
19	0	0	0	0	0	0	0	0
20	0	0	0	0	0	0	0	0
21	0	0	0	0	0	0	0	0
22	0	0	0	0	0	0	0	0
23	0	0	0	0	0	0	0	0
24	0	0	0	0	0	0	0	0
25	0	0	0	0	0	0	0	0
26	0	0	0	0	0	0	0	0
27	0	0	0	0	0	0	0	0
28	0	0	0	0	0	0	0	0
29	0	0	0	0	0	0	[illegible]	[illegible]
30	0	0	0	0	0	0	[illegible]	[illegible]
31	0	0	0	0	0	0	0	0
32	80	310	46	46	98	[illegible]	[illegible]	[illegible]

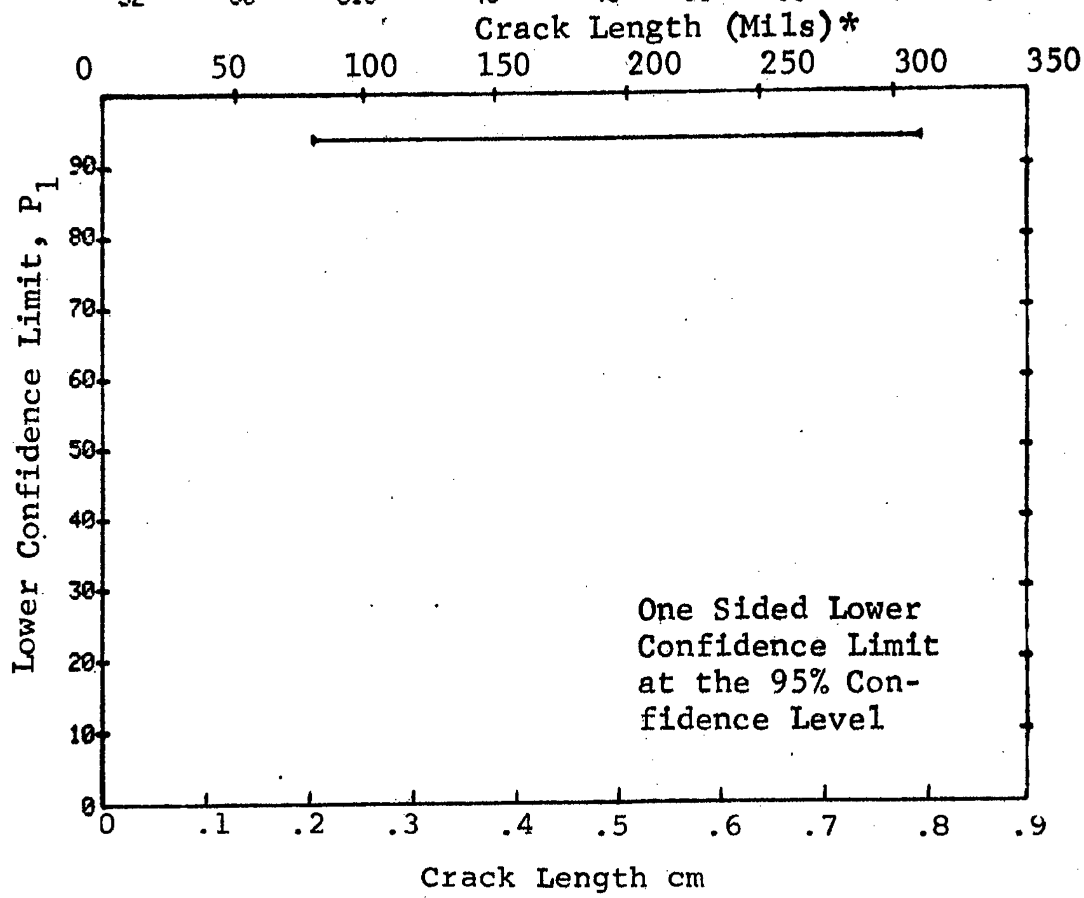

Figure D-80 (Concluded)

(a) Range Interval Method of Data Cumulation

27-OCT-75 ULTRASONIC TEST 1 (.) 7/(81)

RANGE	MIN LN	MAX LN	N	DET	50%	95%	0 MISS	1 MISS
1	10 *	10*	6	4	57	27	0	0
2	0	0	0	0	0	0	0	0
3	30	30	3	0	0	0	0	0
4	0	0	0	0	0	0	0	0
5	40	40	11	8	67	43	0	0
6	50	50	21	11	50	32	0	0
7	0	0	0	0	0	0	0	0
8	60	60	11	7	58	34	0	0
9	70	70	6	6	89	60	0	0
10	0	0	0	0	0	0	0	0
11	80	80	7	7	90	65	0	0
12	90	90	13	10	72	50	0	0
13	0	0	0	0	0	0	0	0
14	100	100	9	9	92	71	0	0
15	110	110	22	19	83	68	0	0
16	120	120	2	1	29	2	0	0
17	0	0	0	0	0	0	0	0
18	130	130	9	9	92	71	0	0
19	140	140	10	8	74	49	0	0
20	0	0	0	0	0	0	0	0
21	150	150	21	21	96	86	8	25
22	160	160	4	4	84	47	0	0
23	0	0	0	0	0	0	0	0
24	170	170	8	8	91	68	0	0
25	180	180	12	12	94	77	17	34
26	0	0	0	0	0	0	0	0
27	190	190	5	5	87	54	0	0
28	0	0	0	0	0	0	0	0
29	0	0	0	0	0	0	0	0
30	210	210	1	1	50	5	0	0
31	220	220	2	2	70	22	0	0
32	230	230	11	9	76	52	0	0

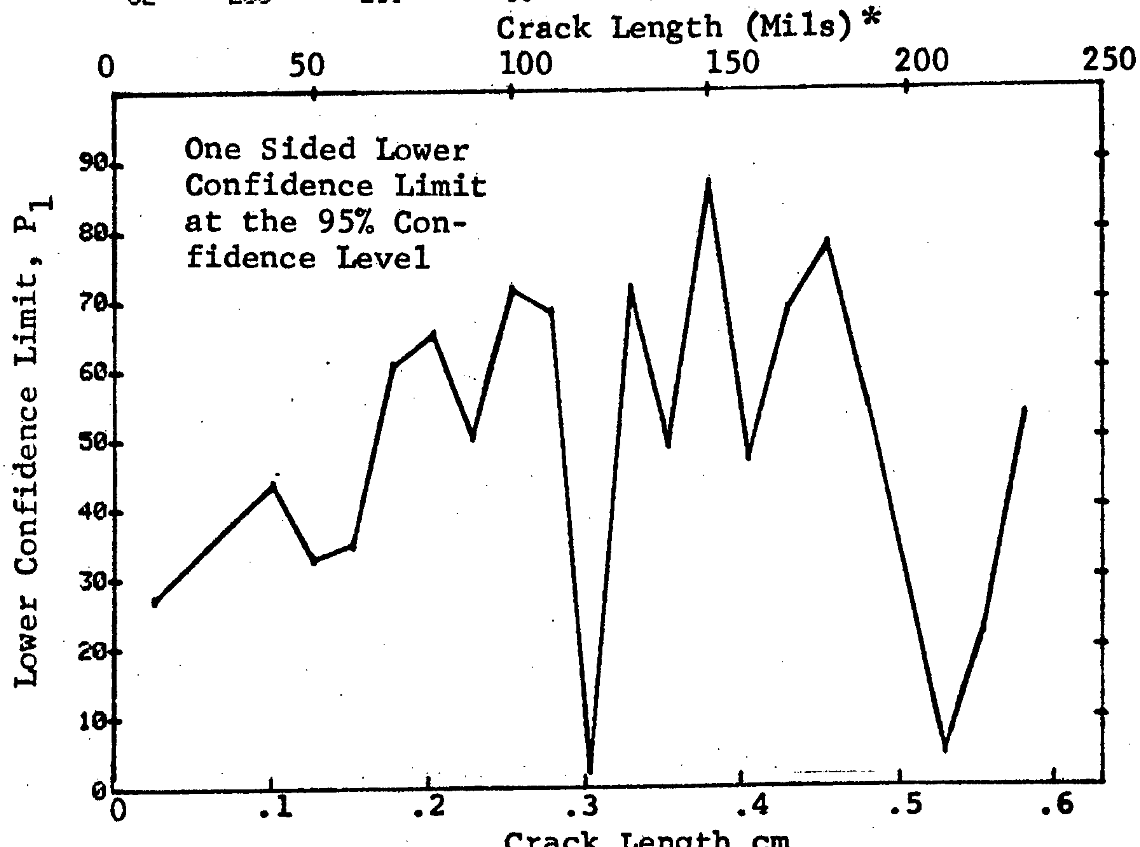

Figure D-81 Probability of Detection for 2024-T6 Al Using Ultrasonic Shear and Surface Waves. Compressed Notch Flaws in Tandem T Specimen. Lab. Env.

(b) Optimum Probability Method of Data Cumulation

27-OCT-75 ULTRASONIC TEST 2 ( ) (81)

RANGE	MIN LN	MAX LN	N	DFT	50%	95%	0 MISS	1 MISS
1	10*	10*	6	4	0	27	0	0
2	0	0	0	0	0	0	0	0
3	10	30	9	4	0	16	0	0
4	0	0	0	0	0	0	0	0
5	40	40	11	8	0	43	0	0
6	40	50	32	19	0	43	0	0
7	0	0	0	0	0	0	0	0
8	40	60	43	26	0	46	0	0
9	70	70	6	6	0	60	0	0
10	0	0	0	0	0	0	0	0
11	70	80	13	13	0	79	0	0
12	70	90	26	23	0	72	0	0
13	0	0	0	0	0	0	0	0
14	70	100	35	32	0	79	0	0
15	70	110	57	51	0	80	59	72
16	70	120	59	52	0	78	0	0
17	0	0	0	0	0	0	0	0
18	70	130	68	61	0	81	61	74
19	70	140	78	69	0	80	76	89
20	0	0	0	0	0	0	0	0
21	150	150	21	21	0	86	8	25
22	150	160	25	25	0	88	4	21
23	0	0	0	0	0	0	0	0
24	150	170	33	33	0	91	0	13
25	150	180	45	45	0	93	0	1
26	0	0	0	0	0	0	0	0
27	150	190	50	50	0	94	0	0
28	0	0	0	0	0	0	0	0
29	0	0	0	0	0	0	0	0
30	150	210	51	51	0	94	0	0
31	150	220	53	53	0	94	0	0
32	150	230	64	62	0	90	0	12

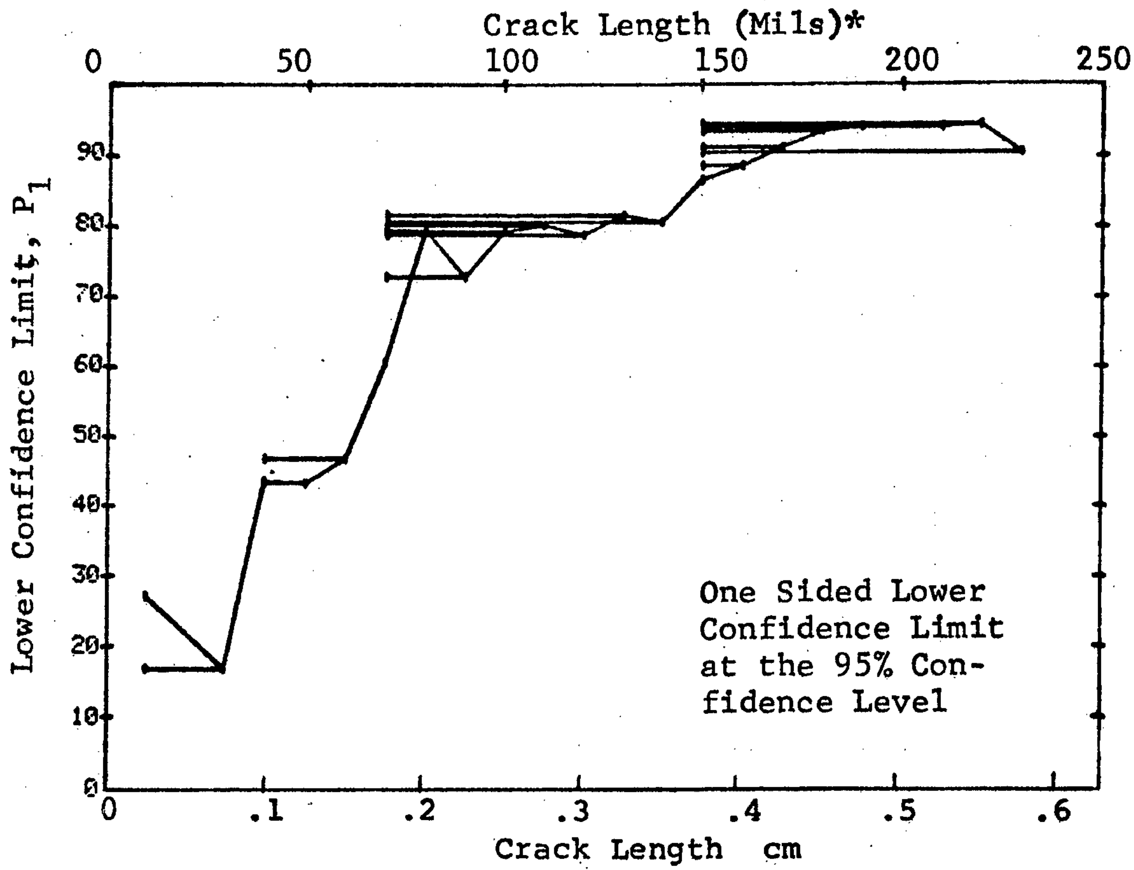

Figure D-81 (Continued)

(c) Overlapping Sixty Point Method of Data Cumulation

27-OCT-75	ULTRASONIC			TEST 3 (		)	(81)	
RANGE	MIN LN	MAX LN	N	DET	50%	95%	0 MISS	1 MISS
1	0*	0*	0	0	0	0	0	0
2	0	0	0	0	0	0	0	0
3	0	0	0	0	0	0	0	0
4	0	0	0	0	0	0	0	0
5	0	0	0	0	0	0	0	0
6	0	0	0	0	0	0	0	0
7	0	0	0	0	0	0	0	0
8	0	0	0	0	0	0	0	0
9	0	0	0	0	0	0	0	0
10	0	0	0	0	0	0	0	0
11	0	0	0	0	0	0	0	0
12	0	0	0	0	0	0	0	0
13	0	0	0	0	0	0	0	0
14	0	0	0	0	0	0	0	0
15	0	0	0	0	0	0	0	0
16	0	0	0	0	0	0	0	0
17	0	0	0	0	0	0	0	0
18	0	0	0	0	0	0	0	0
19	0	0	0	0	0	0	0	0
20	0	0	0	0	0	0	0	0
21	0	0	0	0	0	0	0	0
22	0	0	0	0	0	0	0	0
23	0	0	0	0	0	0	0	0
24	0	0	0	0	0	0	0	0
25	0	0	0	0	0	0	0	0
26	0	0	0	0	0	0	0	0
27	10	60	44	23	51	38	0	0
28	40	90	60	43	70	60	0	0
29	60	110	60	53	87	79	[illegible]	[illegible]
30	90	150	60	54	88	81	55	[illegible]
31	110	180	60	57	93	97	[illegible]	[illegible]
32	150	230	60	58	95	89	1	16

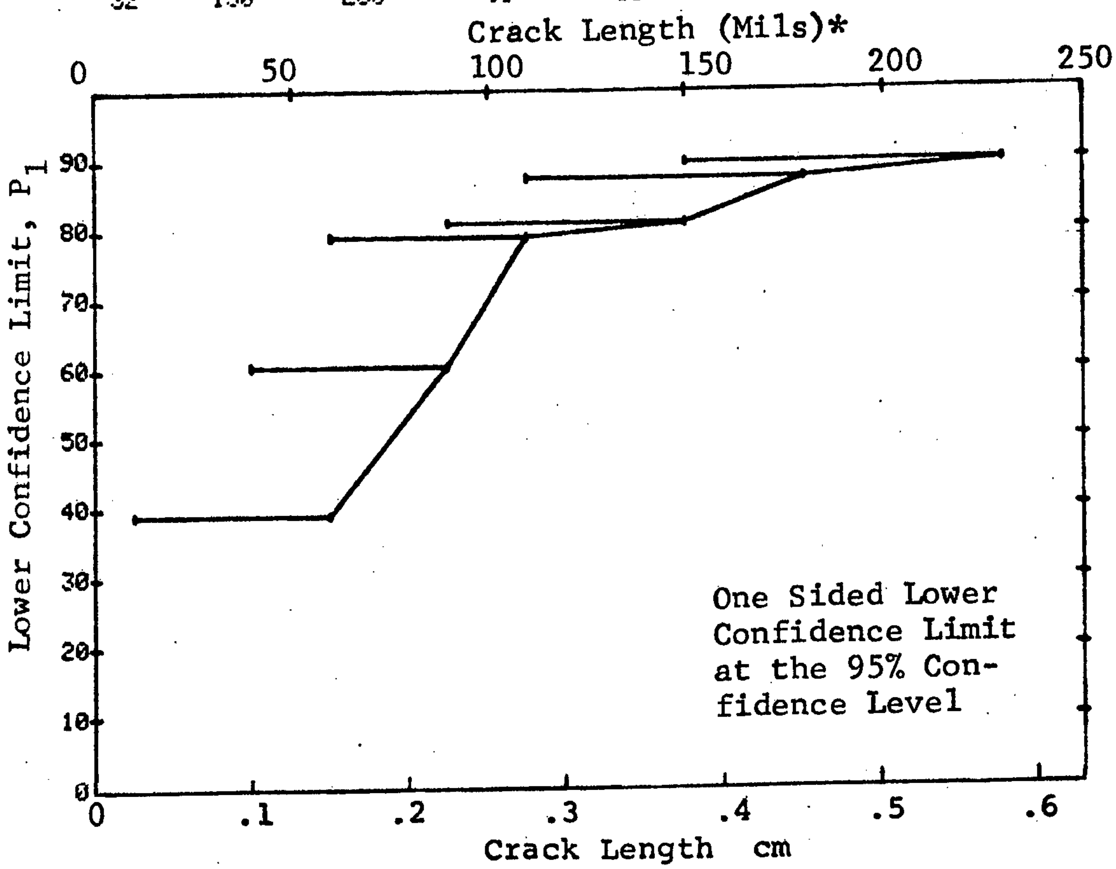

Figure D-81 (Concluded)

(a) Range Interval Method of Data Cumulation

27-OCT-75 RADIOGRAPHY TEST (82)

RANGE	MIN LN *	MAX LN *	N	DET	50%	95%	0 MISS	1 MISS
1	30	50	10	0	0	0	0	0
2	60	70	12	0	0	0	0	0
3	0	0	0	0	0	0	0	0
4	110	120	8	0	0	0	0	0
5	130	140	10	0	0	0	0	0
6	150	160	4	1	15	1	0	0
7	0	0	0	0	0	0	0	0
8	200	200	4	0	0	0	0	0
9	0	0	0	0	0	0	0	0
10	0	0	0	0	0	0	0	0
11	0	0	0	0	0	0	0	0
12	0	0	0	0	0	0	0	0
13	0	0	0	0	0	0	0	0
14	0	0	0	0	0	0	0	0
15	0	0	0	0	0	0	0	0
16	0	0	0	0	0	0	0	0
17	0	0	0	0	0	0	0	0
18	0	0	0	0	0	0	0	0
19	0	0	0	0	0	0	0	0
20	0	0	0	0	0	0	0	0
21	0	0	0	0	0	0	0	0
22	0	0	0	0	0	0	0	0
23	0	0	0	0	0	0	0	0
24	0	0	0	0	0	0	0	0
25	0	0	0	0	0	0	0	0
26	0	0	0	0	0	0	0	0
27	0	0	0	0	0	0	0	0
28	0	0	0	0	0	0	0	0
29	0	0	0	0	0	0	0	0
30	0	0	0	0	0	0	0	0
31	0	0	0	0	0	0	0	0
32	750	750	3	0	0	0	0	0

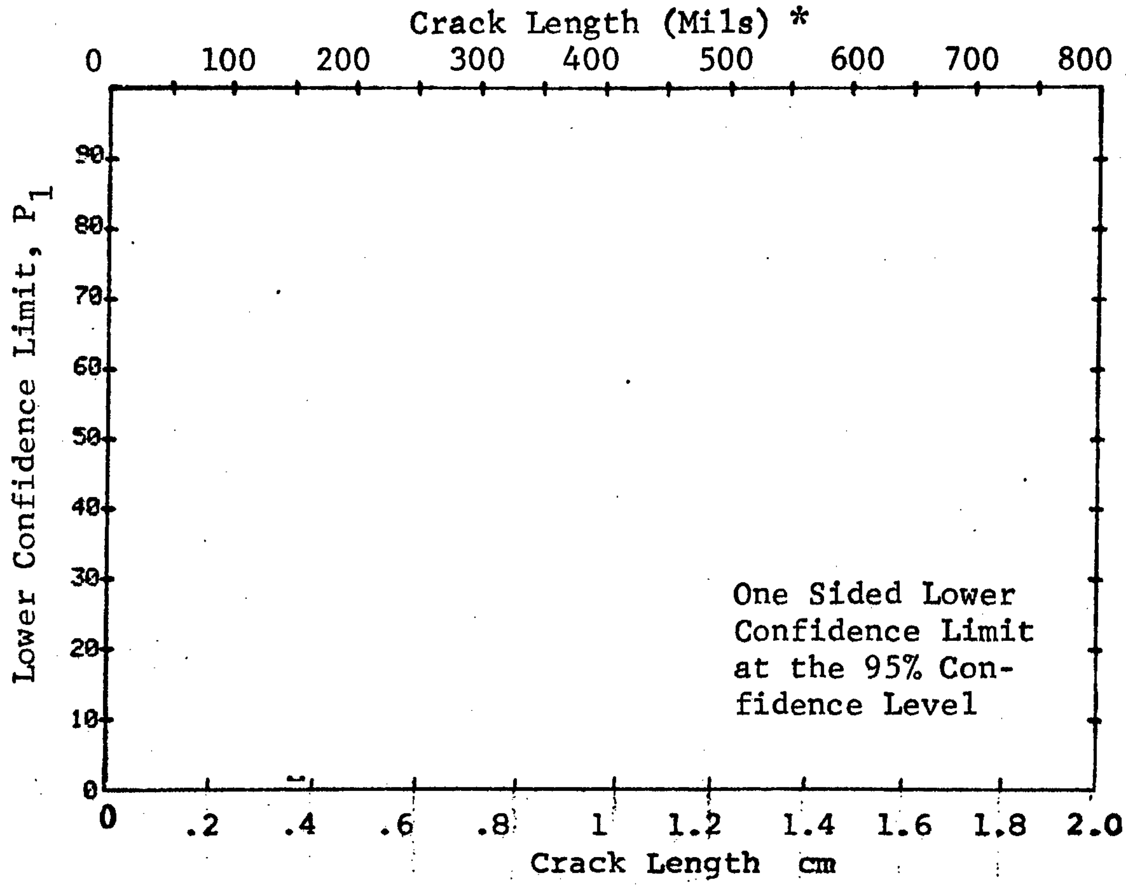

Figure D-82 Probability of Detection for 4340M Steel Using X-ray. Compressed Notch Flaws in Solid Cylinder. Prod. Env.

(b) Optimum Probability Method of Data Cumulation

27-OCT-75 RADIOGRAPHY TEST 2 (..) 72 (82)

RANGE	MIN LN	MAX LN	N	DET	50%	95%	0 MISS	1 MISS
1	30 *	50*	10	0	0	0	0	0
2	60	70	12	0	0	0	0	0
3	0	0	0	0	0	0	0	0
4	110	120	8	0	0	0	0	0
5	130	140	10	0	0	0	0	0
6	150	160	4	1	0	1	0	0
7	0	0	0	0	0	0	0	0
8	150	200	8	1	0	0	0	0
9	0	0	0	0	0	0	0	0
10	0	0	0	0	0	0	0	0
11	0	0	0	0	0	0	0	0
12	0	0	0	0	0	0	0	0
13	0	0	0	0	0	0	0	0
14	0	0	0	0	0	0	0	0
15	0	0	0	0	0	0	0	0
16	0	0	0	0	0	0	0	0
17	0	0	0	0	0	0	0	0
18	0	0	0	0	0	0	0	0
19	0	0	0	0	0	0	0	0
20	0	0	0	0	0	0	0	0
21	0	0	0	0	0	0	0	0
22	0	0	0	0	0	0	0	0
23	0	0	0	0	0	0	0	0
24	0	0	0	0	0	0	0	0
25	0	0	0	0	0	0	0	0
26	0	0	0	0	0	0	0	0
27	0	0	0	0	0	0	0	0
28	0	0	0	0	0	0	0	0
29	0	0	0	0	0	0	0	0
30	0	0	0	0	0	0	0	0
31	0	0	0	0	0	0	0	0
32	150	750	11	1	0	0	0	0

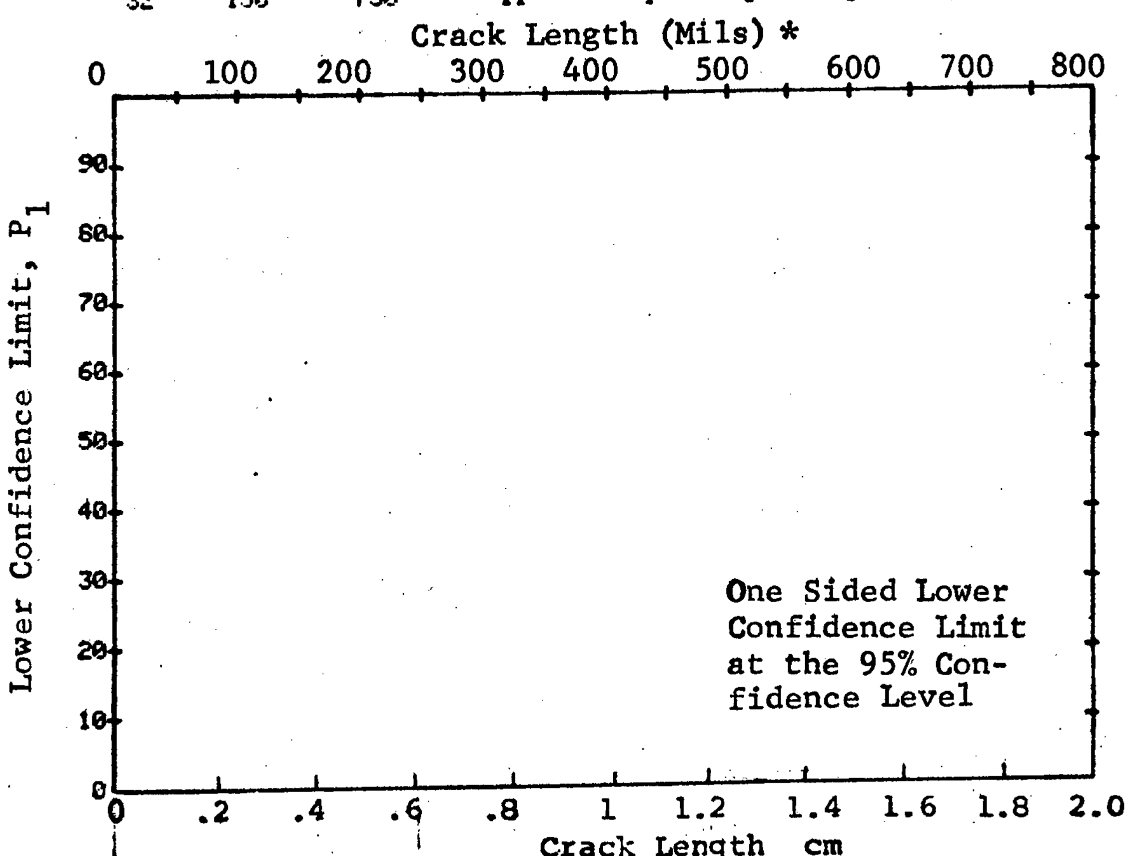

Figure D-82 (Continued)

(c) Overlapping Sixty Point Method of Data Cumulation

27-OCT-75 RADIOGRAPHY TEST 3 ( ) (82)

RANGE	MIN LN *	MAX LN *	N	DET	50%	95%	0 MISS	1 MISS
1	0	0	0	0	0	0	0	0
2	0	0	0	0	0	0	0	0
3	0	0	0	0	0	0	0	0
4	0	0	0	0	0	0	0	0
5	0	0	0	0	0	0	0	0
6	0	0	0	0	0	0	0	0
7	0	0	0	0	0	0	0	0
8	0	0	0	0	0	0	0	0
9	0	0	0	0	0	0	0	0
10	0	0	0	0	0	0	0	0
11	0	0	0	0	0	0	0	0
12	0	0	0	0	0	0	0	0
13	0	0	0	0	0	0	0	0
14	0	0	0	0	0	0	0	0
15	0	0	0	0	0	0	0	0
16	0	0	0	0	0	0	0	0
17	0	0	0	0	0	0	0	0
18	0	0	0	0	0	0	0	0
19	0	0	0	0	0	0	0	0
20	0	0	0	0	0	0	0	0
21	0	0	0	0	0	0	0	0
22	0	0	0	0	0	0	0	0
23	0	0	0	0	0	0	0	0
24	0	0	0	0	0	0	0	0
25	0	0	0	0	0	0	0	0
26	0	0	0	0	0	0	0	0
27	0	0	0	0	0	0	0	0
28	0	0	0	0	0	0	0	0
29	0	0	0	0	0	0	0	0
30	0	0	0	0	0	0	0	0
31	0	0	0	0	0	0	0	0
32	30	200	48	1	1	0	0	0

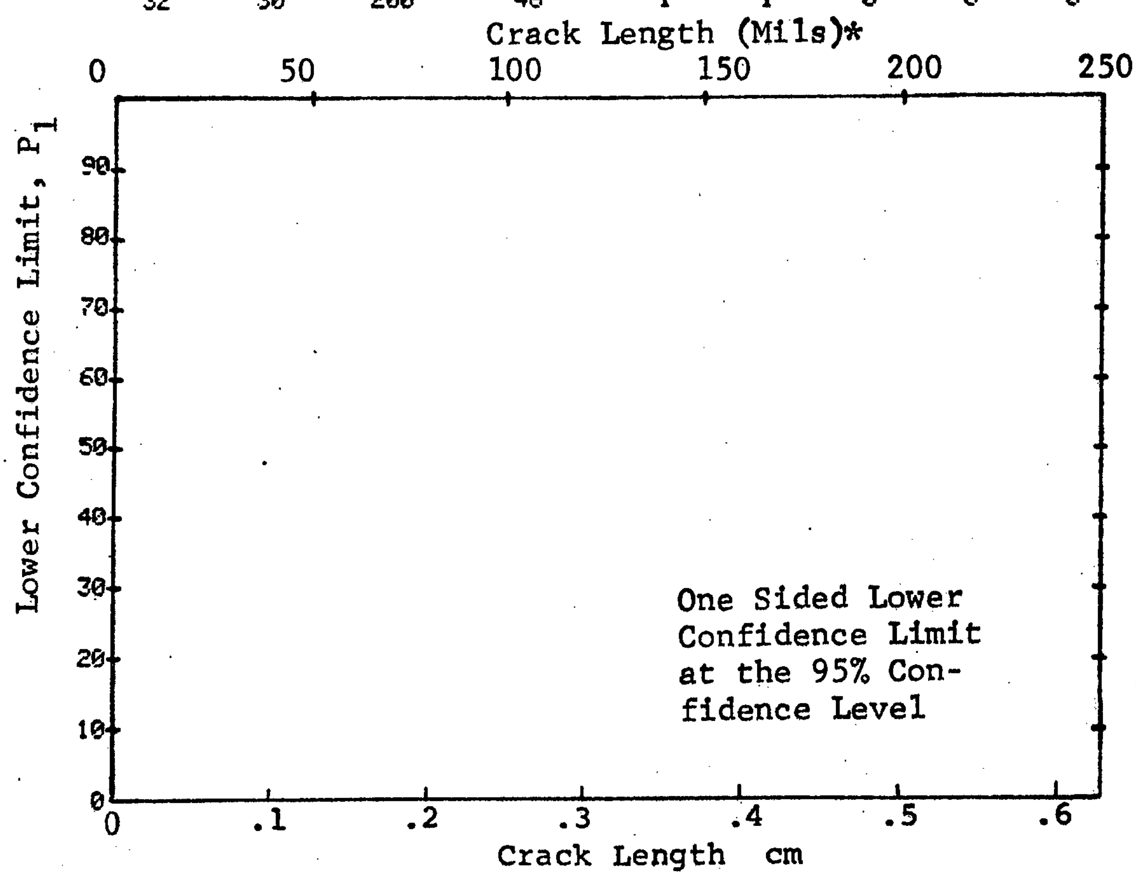

Figure D-82 (Concluded)

(a) Range Interval Method of Data Cumulation

27-OCT-75 RANGE	RADIOGRAPHY MIN LN	MAX LN	N	TEST 1 (DET	50%	) 95%	,83) 0 MISS	1 MISS
1	20*	30*	3	0	0	0	0	0
2	0	0	0	0	0	0	0	0
3	60	60	1	0	0	0	0	0
4	70	70	2	0	0	0	0	0
5	90	90	2	0	0	0	0	0
6	100	100	1	0	0	0	0	0
7	0	0	0	0	0	0	0	0
8	130	140	4	0	0	0	0	0
9	150	150	1	0	0	0	0	0
10	0	0	0	0	0	0	0	0
11	0	0	0	0	0	0	0	0
12	0	0	0	0	0	0	0	0
13	0	0	0	0	0	0	0	0
14	0	0	0	0	0	0	0	0
15	0	0	0	0	0	0	0	0
16	250	250	1	0	0	0	0	0
17	0	0	0	0	0	0	0	0
18	0	0	0	0	0	0	0	0
19	300	300	1	1	50	5	0	0
20	0	0	0	0	0	0	0	0
21	0	0	0	0	0	0	0	0
22	0	0	0	0	0	0	0	0
23	0	0	0	0	0	0	0	0
24	370	370	2	2	70	22	0	0
25	0	0	0	0	0	0	0	0
26	0	0	0	0	0	0	0	0
27	0	0	0	0	0	0	0	0
28	0	0	0	0	0	0	0	0
29	0	0	0	0	0	0	0	0
30	0	0	0	0	0	0	0	0
31	0	0	0	0	0	0	0	0
32	500	500	1	1	50	5	0	0

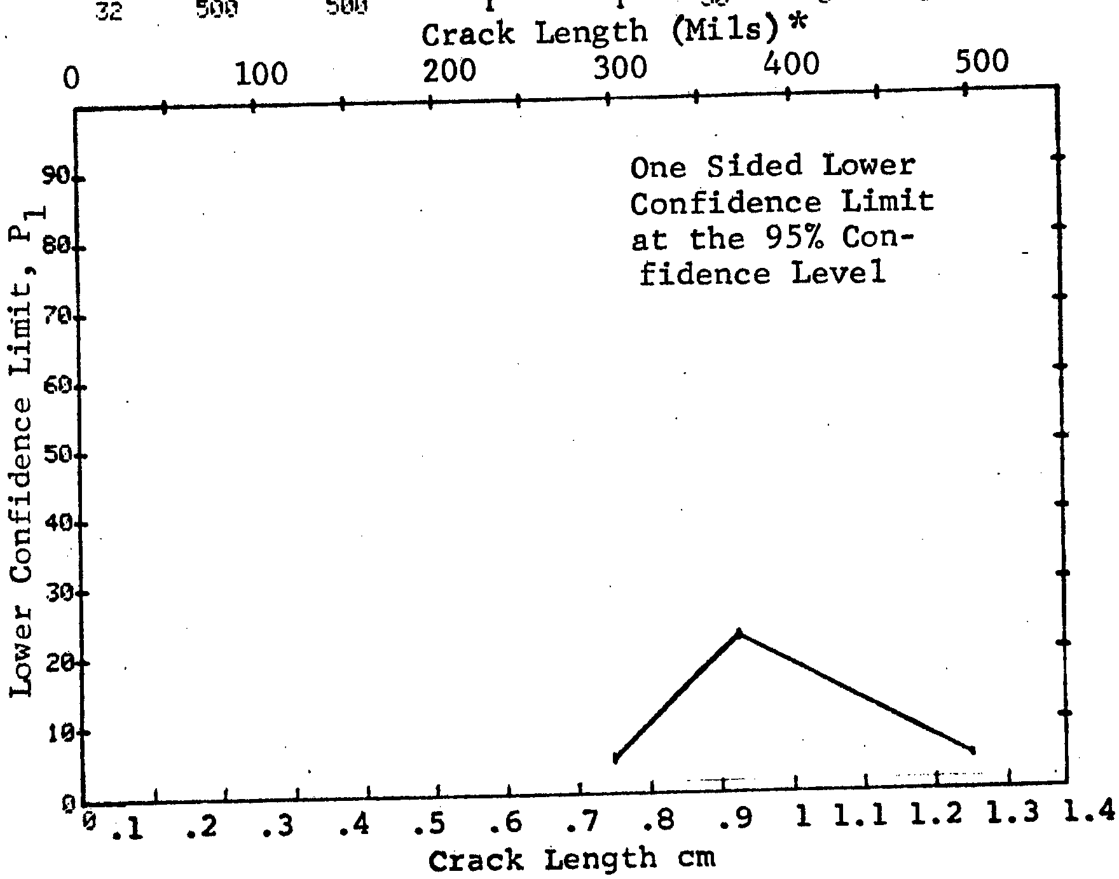

Figure D-83 Probability of Detection for 4340M Steel Using X-ray. Compressed Notch Flaws in Filleted Solid Cylinder.

 Prod. Env.

(b) Optimum Probability Method of Data Cumulation

27-OCT-75 RADIOGRAPHY TEST 2 ( )8.3 (83)

RANGE	MIN LN	MAX LN	N	DET	50%	95%	0 MISS	1 MISS
1	20 *	30 *	3	0	0	0	0	0
2	0	0	0	0	0	0	0	0
3	60	60	1	0	0	0	0	0
4	70	70	2	0	0	0	0	0
5	90	90	2	0	0	0	0	0
6	100	100	1	0	0	0	0	0
7	0	0	0	0	0	0	0	0
8	130	140	4	0	0	0	0	0
9	150	150	1	0	0	0	0	0
10	0	0	0	0	0	0	0	0
11	0	0	0	0	0	0	0	0
12	0	0	0	0	0	0	0	0
13	0	0	0	0	0	0	0	0
14	0	0	0	0	0	0	0	0
15	0	0	0	0	0	0	0	0
16	250	250	1	0	0	0	0	0
17	0	0	0	0	0	0	0	0
18	0	0	0	0	0	0	0	0
19	300	300	1	1	0	5	0	0
20	0	0	0	0	0	0	0	0
21	0	0	0	0	0	0	0	0
22	0	0	0	0	0	0	0	0
23	0	0	0	0	0	0	0	0
24	300	370	3	3	0	36	0	0
25	0	0	0	0	0	0	0	0
26	0	0	0	0	0	0	0	0
27	0	0	0	0	0	0	0	0
28	0	0	0	0	0	0	0	0
29	0	0	0	0	0	0	0	0
30	0	0	0	0	0	0	0	0
31	0	0	0	0	0	0	0	0
32	300	500	4	4	0	47	0	0

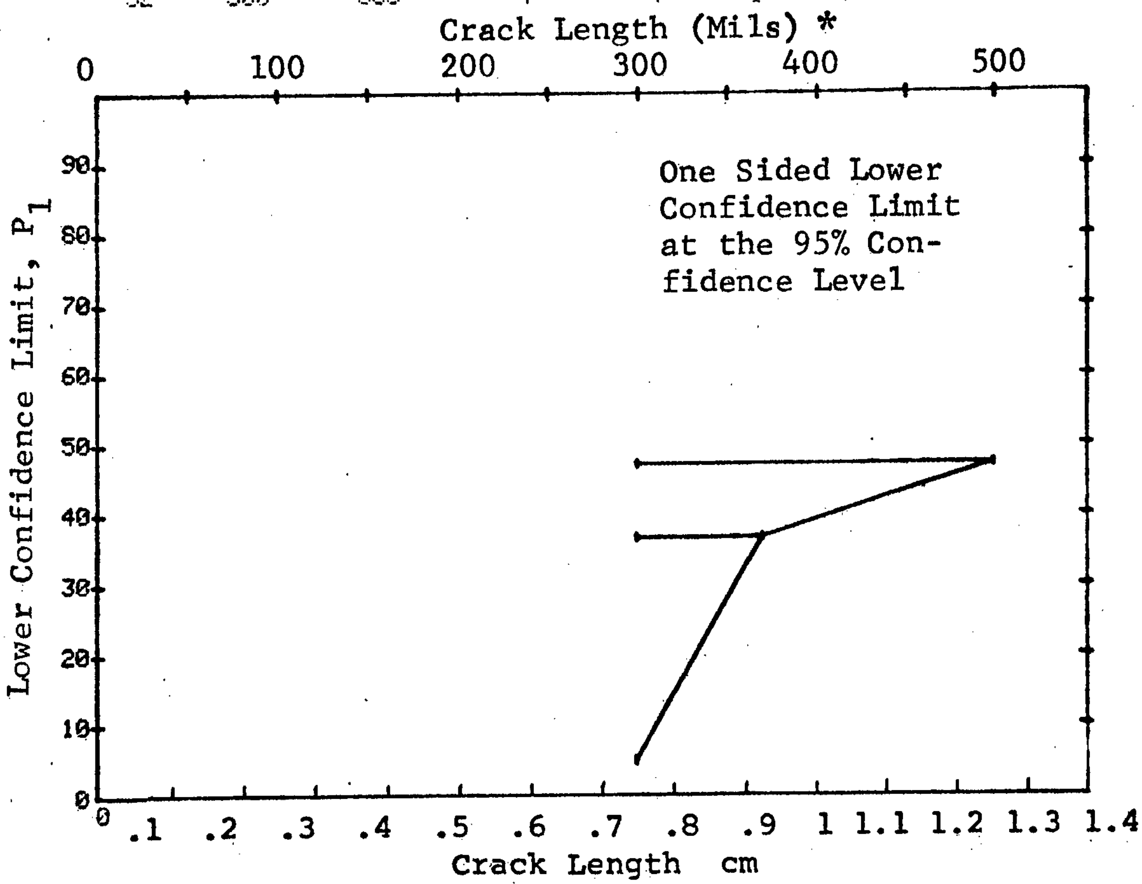

Figure D-83 (Continued)

(c) Overlapping Sixty Point Method of Data Cumulation

27-OCT-75 RADIOGRAPHY TEST 3 (.) (83)

RANGE	MIN LN *	MAX LN *	N	DET	50%	95%	0 MISS	1 MISS
1	0	0	0	0	0	0	0	0
2	0	0	0	0	0	0	0	0
3	0	0	0	0	0	0	0	0
4	0	0	0	0	0	0	0	0
5	0	0	0	0	0	0	0	0
6	0	0	0	0	0	0	0	0
7	0	0	0	0	0	0	0	0
8	0	0	0	0	0	0	0	0
9	0	0	0	0	0	0	0	0
10	0	0	0	0	0	0	0	0
11	0	0	0	0	0	0	0	0
12	0	0	0	0	0	0	0	0
13	0	0	0	0	0	0	0	0
14	0	0	0	0	0	0	0	0
15	0	0	0	0	0	0	0	0
16	0	0	0	0	0	0	0	0
17	0	0	0	0	0	0	0	0
18	0	0	0	0	0	0	0	0
19	0	0	0	0	0	0	0	0
20	0	0	0	0	0	0	0	0
21	0	0	0	0	0	0	0	0
22	0	0	0	0	0	0	0	0
23	0	0	0	0	0	0	0	0
24	0	0	0	0	0	0	0	0
25	0	0	0	0	0	0	0	0
26	0	0	0	0	0	0	0	0
27	0	0	0	0	0	0	0	0
28	0	0	0	0	0	0	0	0
29	0	0	0	0	0	0	0	0
30	0	0	0	0	0	0	0	0
31	0	0	0	0	0	0	0	0
32	20	500	19	4	16	7	0	0

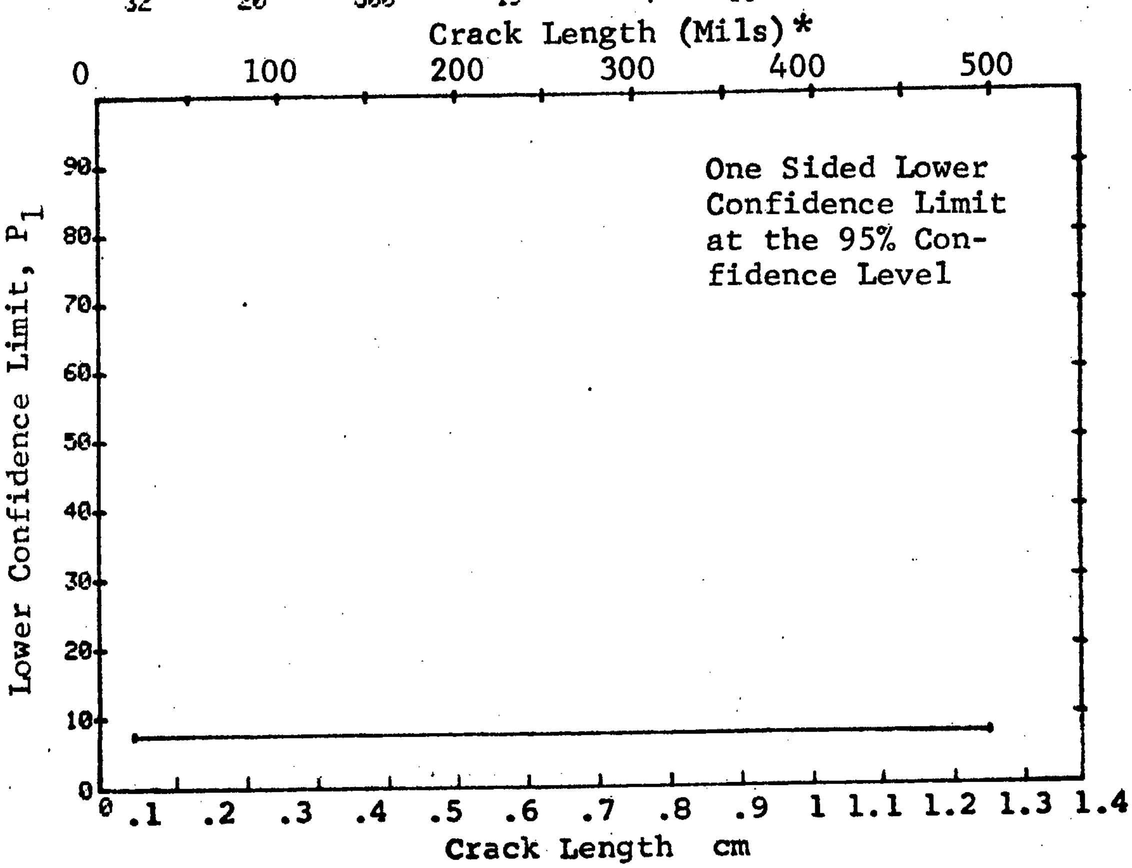

Figure D-83 (Concluded)

(a) Range Interval Method of Data Cumulation

27-OCT-75 RADIOGRAPHY TEST 1 (84)

RANGE	MIN LN*	MAX LN*	N	DET	50%	95%	0 MISS	1 MISS
1	100	100	8	0	0	0	0	0
2	120	120	4	0	0	0	0	0
3	140	140	6	3	42	15	0	0
4	0	0	0	0	0	0	0	0
5	160	160	3	0	0	0	0	0
6	180	180	4	0	0	0	0	0
7	0	0	0	0	0	0	0	0
8	0	0	0	0	0	0	0	0
9	230	230	2	2	70	22	0	0
10	0	0	0	0	0	0	0	0
11	0	0	0	0	0	0	0	0
12	0	0	0	0	0	0	0	0
13	0	0	0	0	0	0	0	0
14	0	0	0	0	0	0	0	0
15	310	310	3	3	79	36	0	0
16	0	0	0	0	0	0	0	0
17	0	0	0	0	0	0	0	0
18	350	350	5	5	87	54	0	0
19	0	0	0	0	0	0	0	0
20	390	390	3	3	79	36	0	0
21	0	0	0	0	0	0	0	0
22	0	0	0	0	0	0	0	0
23	0	0	0	0	0	0	0	0
24	0	0	0	0	0	0	0	0
25	0	0	0	0	0	0	0	0
26	0	0	0	0	0	0	0	0
27	0	0	0	0	0	0	0	0
28	0	0	0	0	0	0	0	0
29	0	0	0	0	0	0	0	0
30	0	0	0	0	0	0	0	0
31	0	0	0	0	0	0	0	0
32	570	570	2	2	70	22	0	0

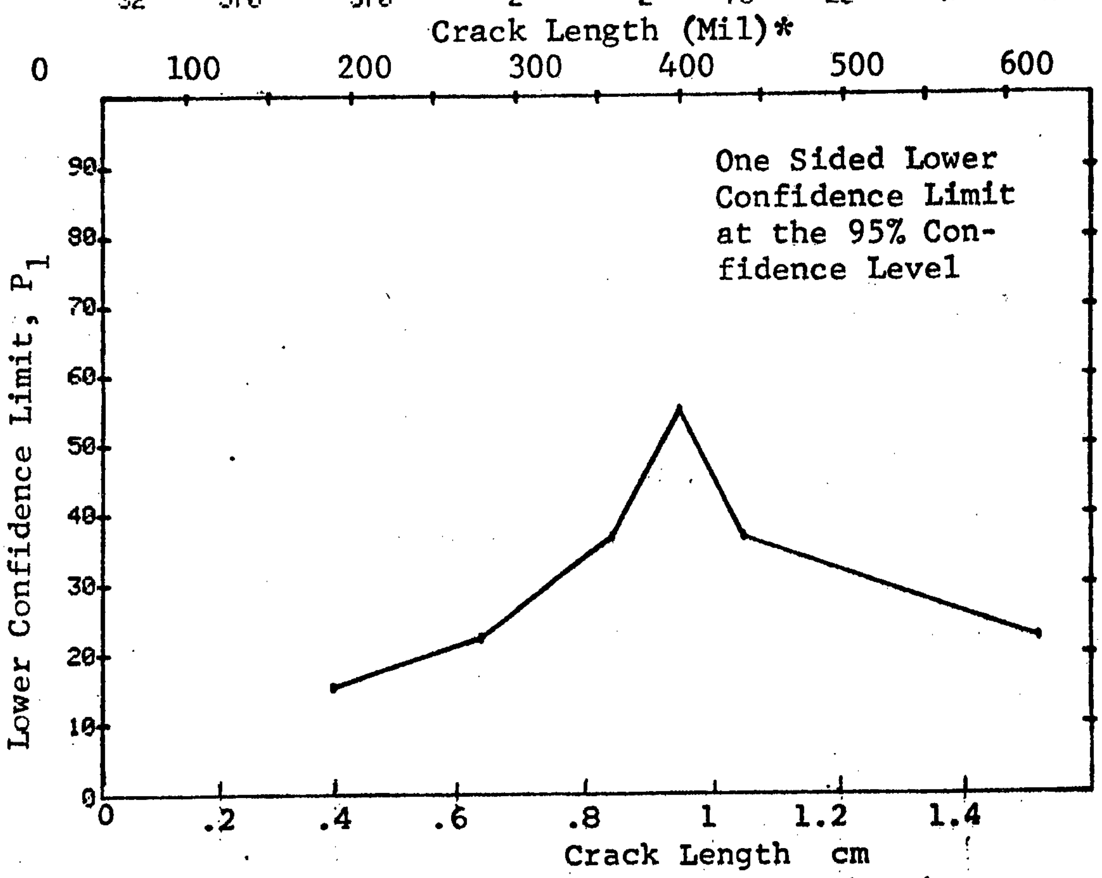

Figure D-84 Probability of Detection for 4340M Steel Using X-ray. Compressed Notch Flaws in Hollow Filleted Cylinder. Prod. Env.

(b) Optimum Probability Method of Data Cumulation

27-OCT-75 RADIOGRAPHY TEST 2 (84)

RANGE	MIN LN*	MAX LN*	N	DET	50%	95%	0 MISS	1 MISS
1	100	100	0	0	0	0	0	0
2	120	120	4	0	0	0	0	0
3	140	140	6	3	0	15	0	0
4	0	0	0	0	0	0	0	0
5	140	160	9	3	0	9	0	0
6	140	180	13	3	0	6	0	0
7	0	0	0	0	0	0	0	0
8	0	0	0	0	0	0	0	0
9	230	230	2	2	0	22	0	0
10	0	0	0	0	0	0	0	0
11	0	0	0	0	0	0	0	0
12	0	0	0	0	0	0	0	0
13	0	0	0	0	0	0	0	0
14	0	0	0	0	0	0	0	0
15	230	310	5	5	0	54	0	0
16	0	0	0	0	0	0	0	0
17	0	0	0	0	0	0	0	0
18	230	350	10	10	0	74	0	0
19	0	0	0	0	0	0	0	0
20	230	390	13	13	0	79	0	0
21	0	0	0	0	0	0	0	0
22	0	0	0	0	0	0	0	0
23	0	0	0	0	0	0	0	0
24	0	0	0	0	0	0	0	0
25	0	0	0	0	0	0	0	0
26	0	0	0	0	0	0	0	0
27	0	0	0	0	0	0	0	0
28	0	0	0	0	0	0	0	0
29	0	0	0	0	0	0	0	0
30	0	0	0	0	0	0	0	0
31	0	0	0	0	0	0	0	0
32	230	570	15	15	0	81	14	31

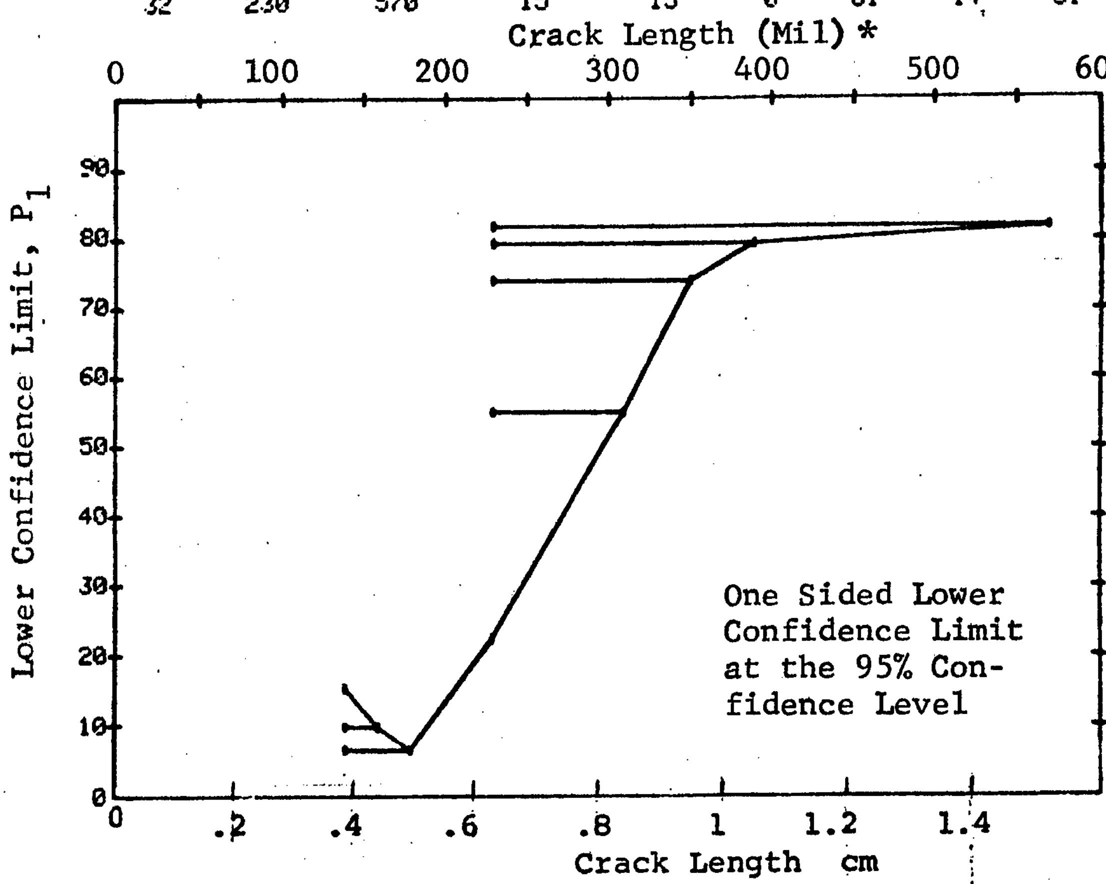

Figure D-84 (Continued)

(c) Overlapping Sixty Point Method of Data Cumulation

27-OCT-75 RADIOGRAPHY TEST 3 (84)

RANGE	MIN LN*	MAX LN*	N	DET	50%	95%	0 MISS	1 MISS
1	0	0	0	0	0	0	0	0
2	0	0	0	0	0	0	0	0
3	0	0	0	0	0	0	0	0
4	0	0	0	0	0	0	0	0
5	0	0	0	0	0	0	0	0
6	0	0	0	0	0	0	0	0
7	0	0	0	0	0	0	0	0
8	0	0	0	0	0	0	0	0
9	0	0	0	0	0	0	0	0
10	0	0	0	0	0	0	0	0
11	0	0	0	0	0	0	0	0
12	0	0	0	0	0	0	0	0
13	0	0	0	0	0	0	0	0
14	0	0	0	0	0	0	0	0
15	0	0	0	0	0	0	0	0
16	0	0	0	0	0	0	0	0
17	0	0	0	0	0	0	0	0
18	0	0	0	0	0	0	0	0
19	0	0	0	0	0	0	0	0
20	0	0	0	0	0	0	0	0
21	0	0	0	0	0	0	0	0
22	0	0	0	0	0	0	0	0
23	0	0	0	0	0	0	0	0
24	0	0	0	0	0	0	0	0
25	0	0	0	0	0	0	0	0
26	0	0	0	0	0	0	0	0
27	0	0	0	0	0	0	0	0
28	0	0	0	0	0	0	0	0
29	0	0	0	0	0	0	0	0
30	0	0	0	0	0	0	0	0
31	0	0	0	0	0	0	0	0
32	100	390	38	16	40	28	0	0

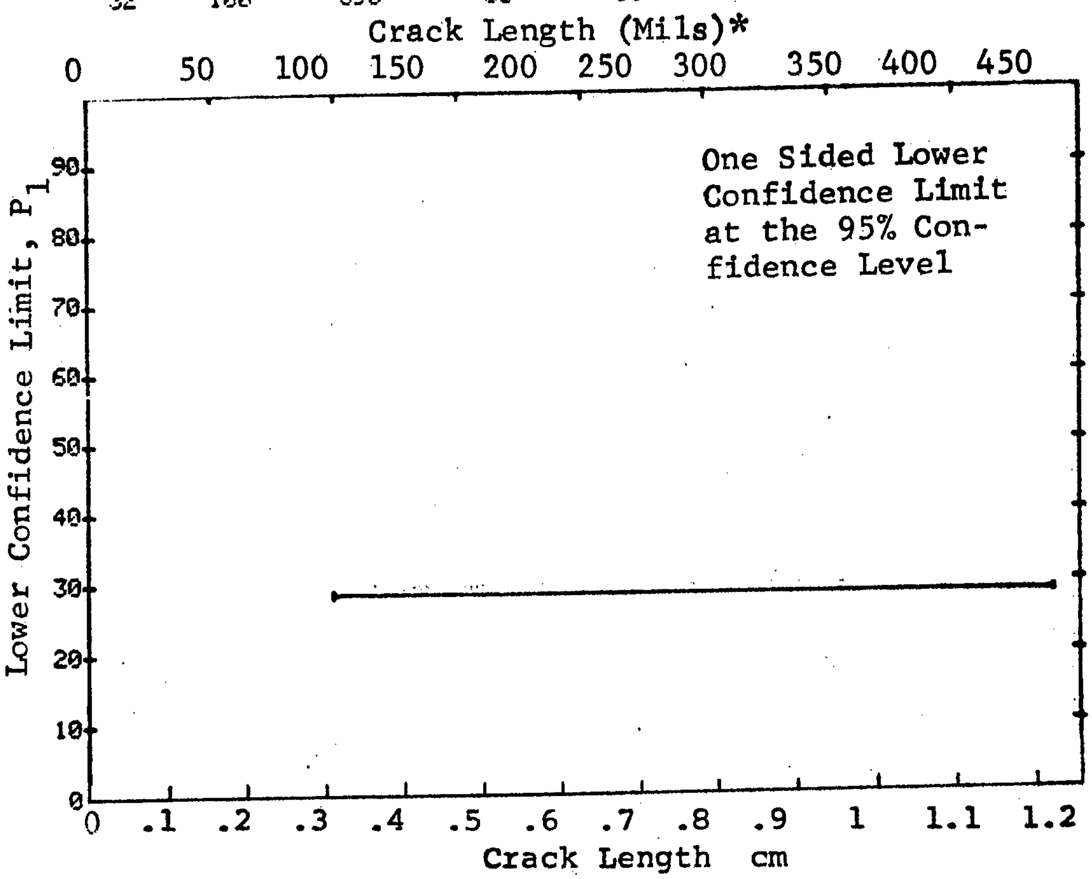

Figure D-84 (Concluded)

27-OCT-75 RADIOGRAPHY TEST 1 (85)

RANGE	MIN LN *	MAX LN *	N	DET	50%	95%	0 MISS	1 MISS
1	80	90	7	2	22	5	0	0
2	0	0	0	0	0	0	0	0
3	110	110	2	0	0	0	0	0
4	0	0	0	0	0	0	0	0
5	130	130	2	1	29	2	0	0
6	140	140	3	1	20	1	0	0
7	160	160	1	0	0	0	0	0
8	0	0	0	0	0	0	0	0
9	0	0	0	0	0	0	0	0
10	0	0	0	0	0	0	0	0
11	0	0	0	0	0	0	0	0
12	0	0	0	0	0	0	0	0
13	0	0	0	0	0	0	0	0
14	0	0	0	0	0	0	0	0
15	250	250	3	2	50	13	0	0
16	270	270	1	0	0	0	0	0
17	280	280	3	3	79	36	0	0
18	0	0	0	0	0	0	0	0
19	300	300	3	3	79	36	0	0
20	0	0	0	0	0	0	0	0
21	0	0	0	0	0	0	0	0
22	0	0	0	0	0	0	0	0
23	0	0	0	0	0	0	0	0
24	0	0	0	0	0	0	0	0
25	0	0	0	0	0	0	0	0
26	0	0	0	0	0	0	0	0
27	0	0	0	0	0	0	0	0
28	0	0	0	0	0	0	0	0
29	0	0	0	0	0	0	0	0
30	0	0	0	0	0	0	0	0
31	0	0	0	0	0	0	0	0
32	450	460	4	3	61	24	0	0

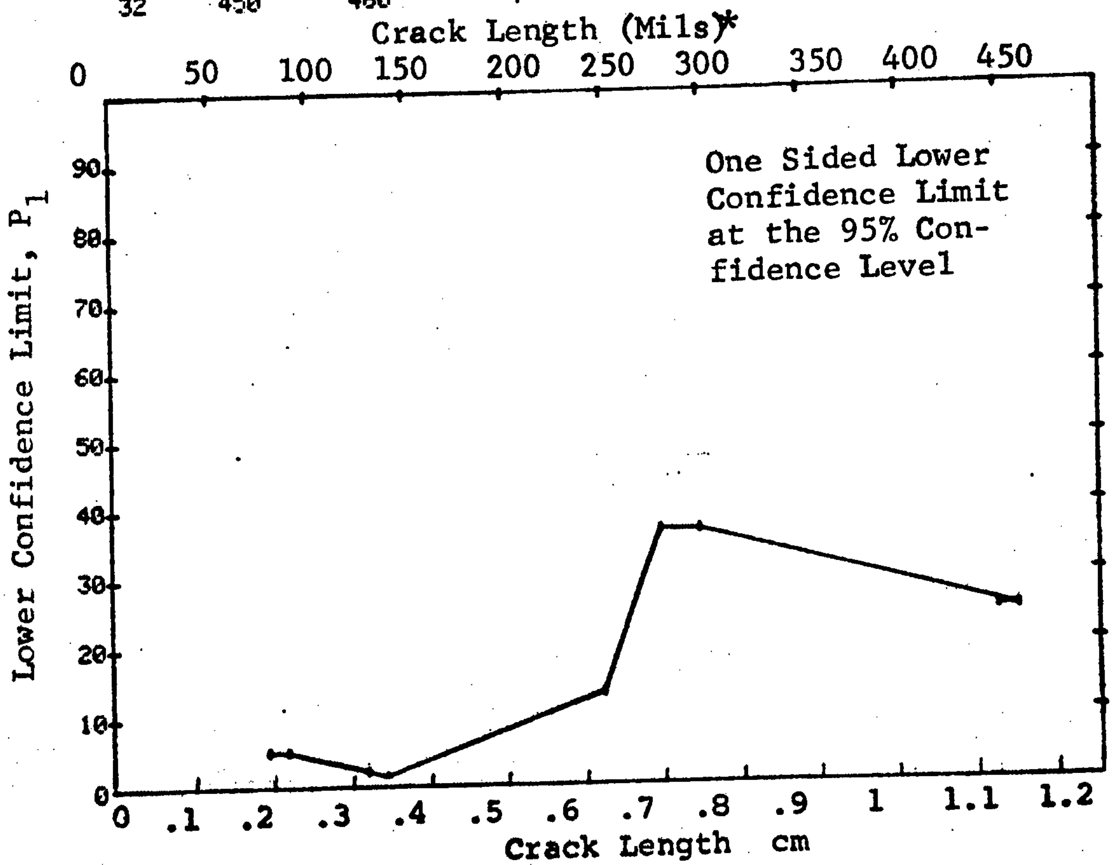

Figure D-85 Probability of Detection for 4340M Steel Using X-ray. Compressed Notch Flaws in Hollow Filleted Cylinder. Prod. Env.

(b) Optimum Probability Method of Data Cumulation

27-OCT-75 RADIOGRAPHY TEST 2 ( ) (85)

RANGE	MIN LN	MAX LN	N	DET	50%	95%	0 MISS	1 MISS
1	80 *	90 *	7	2	0	5	0	0
2	0	0	0	0	0	0	0	0
3	80	110	9	2	0	4	0	0
4	0	0	0	0	0	0	0	0
5	80	130	11	3	0	7	0	0
6	80	140	14	4	0	10	0	0
7	80	160	15	4	0	9	0	0
8	0	0	0	0	0	0	0	0
9	0	0	0	0	0	0	0	0
10	0	0	0	0	0	0	0	0
11	0	0	0	0	0	0	0	0
12	0	0	0	0	0	0	0	0
13	0	0	0	0	0	0	0	0
14	0	0	0	0	0	0	0	0
15	130	250	9	4	0	16	0	0
16	130	270	10	4	0	15	0	0
17	280	280	3	3	0	36	0	0
18	0	0	0	0	0	0	0	0
19	280	300	6	6	0	60	0	0
20	0	0	0	0	0	0	0	0
21	0	0	0	0	0	0	0	0
22	0	0	0	0	0	0	0	0
23	0	0	0	0	0	0	0	0
24	0	0	0	0	0	0	0	0
25	0	0	0	0	0	0	0	0
26	0	0	0	0	0	0	0	0
27	0	0	0	0	0	0	0	0
28	0	0	0	0	0	0	0	0
29	0	0	0	0	0	0	0	0
30	0	0	0	0	0	0	0	0
31	0	0	0	0	0	0	0	0
32	280	460	10	9	0	60	0	0

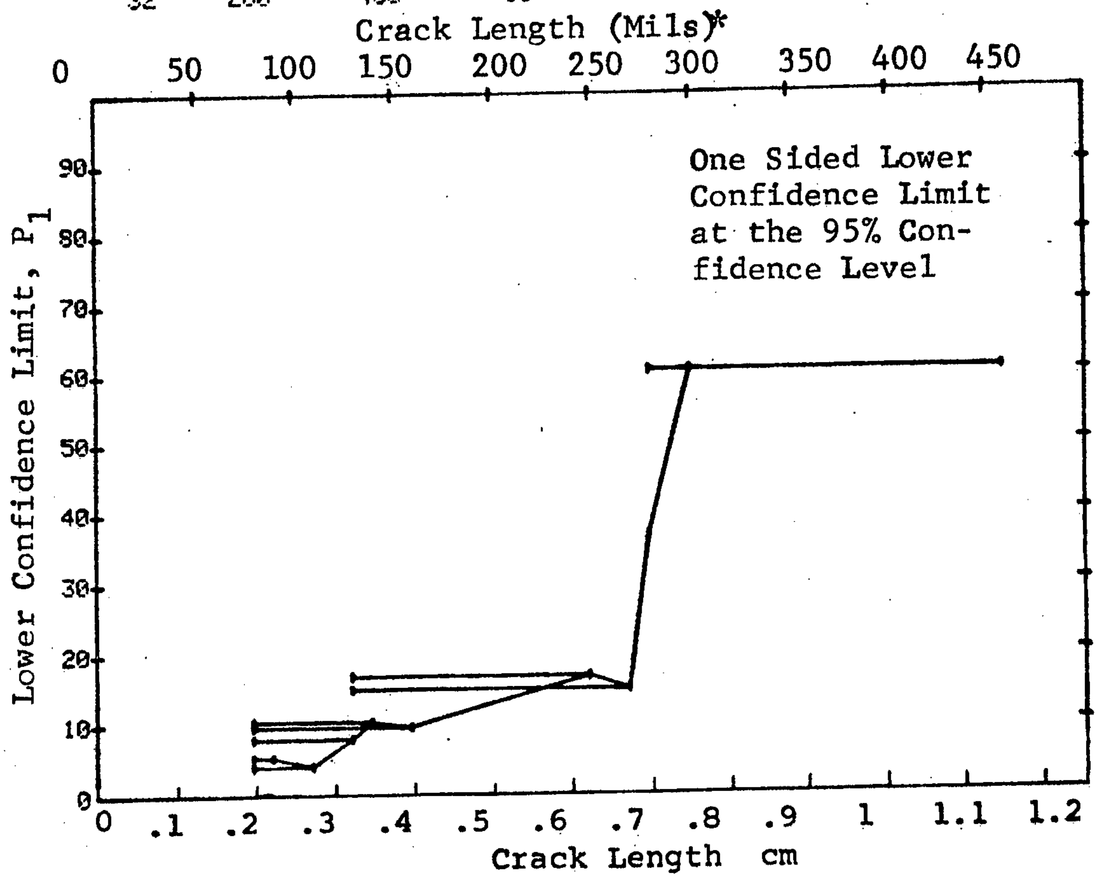

Figure D-85 (Continued)

(c) Overlapping Sixty Point Method of Data Cumulation

27-OCT-75 RADIOGRAPHY TEST 3 (.75 (85)

RANGE	MIN LN *	MAX LN *	N	DET	50%	95%	0 MISS	1 MISS
1	0	0	0	0	0	0	0	0
2	0	0	0	0	0	0	0	0
3	0	0	0	0	0	0	0	0
4	0	0	0	0	0	0	0	0
5	0	0	0	0	0	0	0	0
6	0	0	0	0	0	0	0	0
7	0	0	0	0	0	0	0	0
8	0	0	0	0	0	0	0	0
9	0	0	0	0	0	0	0	0
10	0	0	0	0	0	0	0	0
11	0	0	0	0	0	0	0	0
12	0	0	0	0	0	0	0	0
13	0	0	0	0	0	0	0	0
14	0	0	0	0	0	0	0	0
15	0	0	0	0	0	0	0	0
16	0	0	0	0	0	0	0	0
17	0	0	0	0	0	0	0	0
18	0	0	0	0	0	0	0	0
19	0	0	0	0	0	0	0	0
20	0	0	0	0	0	0	0	0
21	0	0	0	0	0	0	0	0
22	0	0	0	0	0	0	0	0
23	0	0	0	0	0	0	0	0
24	0	0	0	0	0	0	0	0
25	0	0	0	0	0	0	0	0
26	0	0	0	0	0	0	0	0
27	0	0	0	0	0	0	0	0
28	0	0	0	0	0	0	0	0
29	0	0	0	0	0	0	0	0
30	0	0	0	0	0	0	0	0
31	0	0	0	0	0	0	0	0
32	80	460	29	15	50	35	0	0

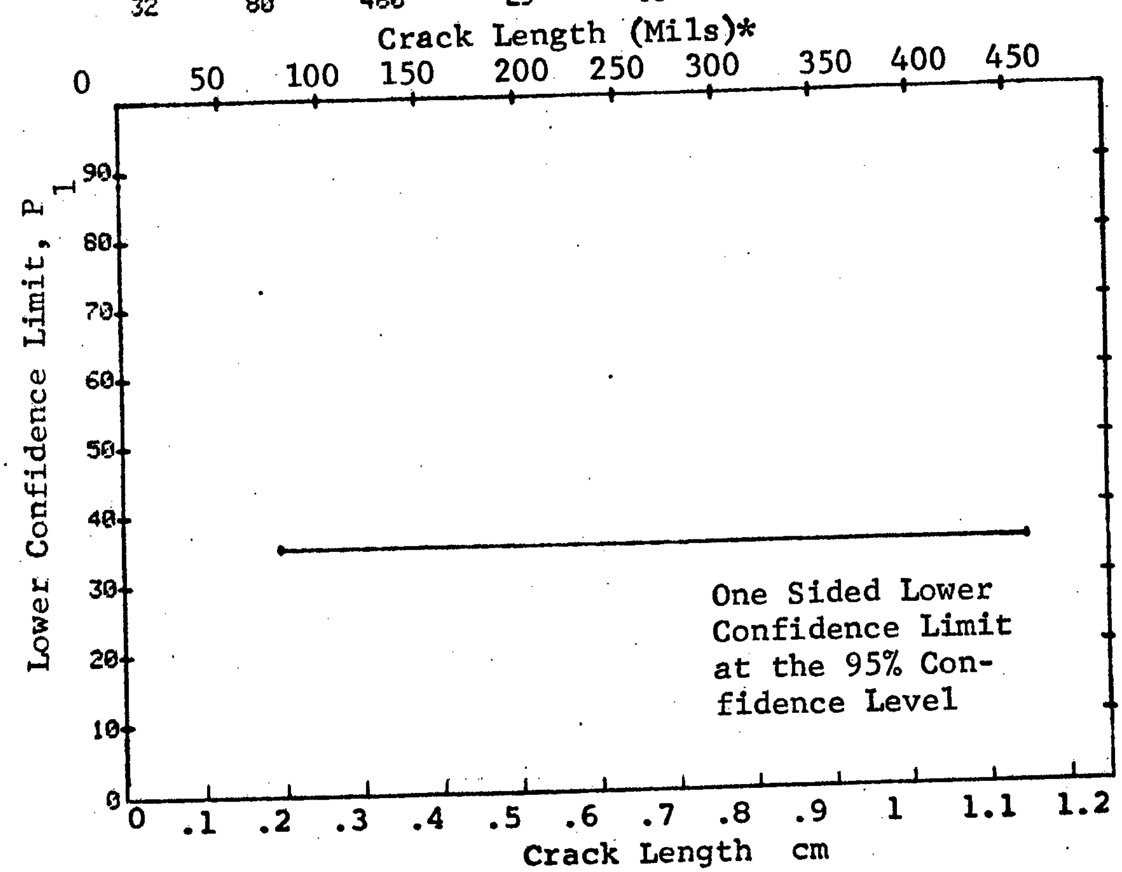

Figure D-85 (Concluded)

(a) Range Interval Method of Data Cumulation

27-OCT-75 RADIOGRAPHY TEST 1 ([illegible])76 (86)

RANGE	MIN LN	MAX LN	N	DET	50%	95%	0 MISS	1 MISS
1	100 *	110 *	3	1	20	1	0	0
2	0	0	0	0	0	0	0	0
3	0	0	0	0	0	0	0	0
4	0	0	0	0	0	0	0	0
5	0	0	0	0	0	0	0	0
6	190	190	1	1	50	5	0	0
7	0	0	0	0	0	0	0	0
8	230	230	1	0	0	0	0	0
9	250	250	1	0	0	0	0	0
10	0	0	0	0	0	0	0	0
11	0	0	0	0	0	0	0	0
12	0	0	0	0	0	0	0	0
13	0	0	0	0	0	0	0	0
14	0	0	0	0	0	0	0	0
15	350	350	1	0	0	0	0	0
16	0	0	0	0	0	0	0	0
17	380	380	1	1	50	5	0	0
18	0	0	0	0	0	0	0	0
19	0	0	0	0	0	0	0	0
20	0	0	0	0	0	0	0	0
21	450	460	2	1	29	2	0	0
22	0	0	0	0	0	0	0	0
23	0	0	0	0	0	0	0	0
24	0	0	0	0	0	0	0	0
25	0	0	0	0	0	0	0	0
26	0	0	0	0	0	0	0	0
27	0	0	0	0	0	0	0	0
28	0	0	0	0	0	0	0	0
29	0	0	0	0	0	0	0	0
30	0	0	0	0	0	0	0	0
31	0	0	0	0	0	0	0	0
32	650	650	1	1	50	5	0	0

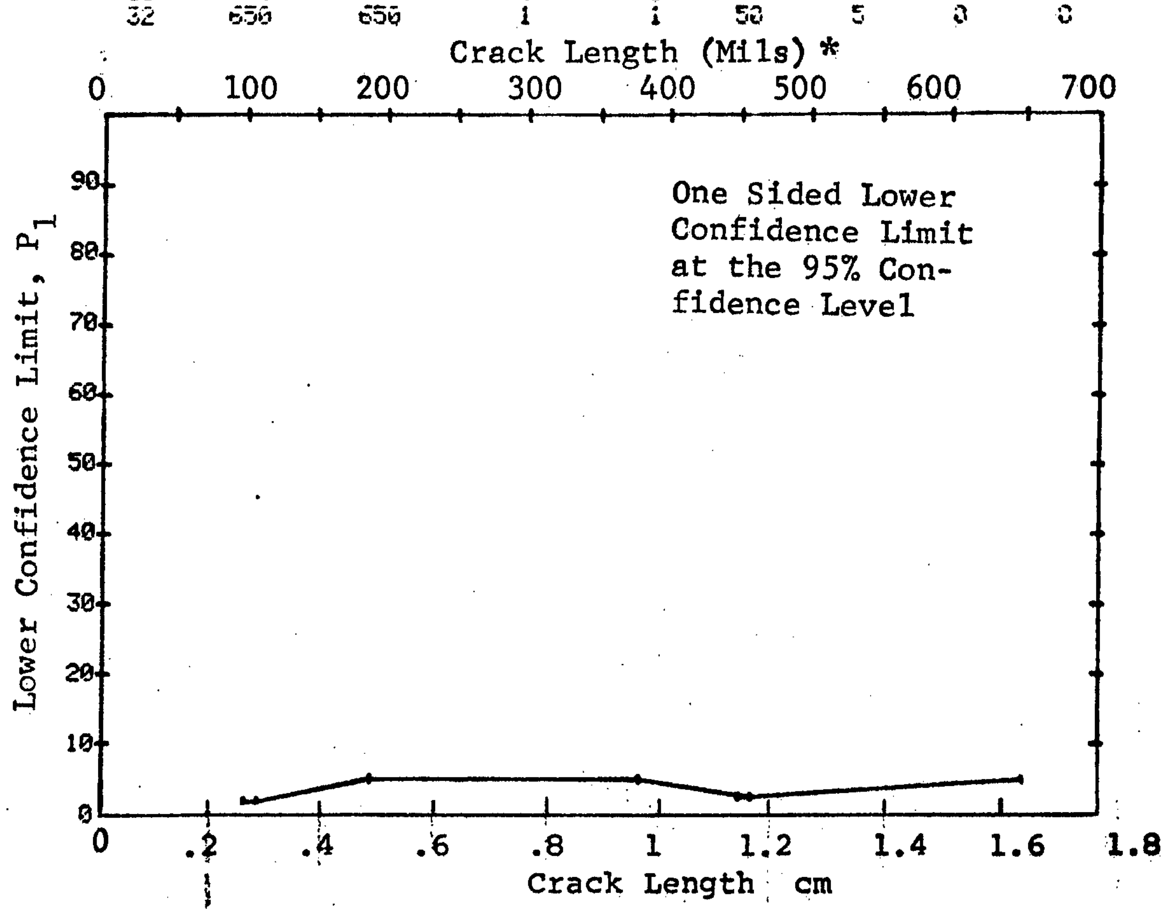

Figure D-86 Probability of Detection for 4340M Steel Using X-ray. Compressed Notch Flaws in Solid Threaded Cylinder. Prod. Env.

(b) Optimum Probability Method of Data Cumulation

27-OCT-75 RADIOGRAPHY TEST 2 (96 (86)

RANGE	MIN LN	MAX LN	N	DET	50%	95%	0 MISS	1 MISS
1	100 *	110 *	3	1	0	1	0	0
2	0	0	0	0	0	0	0	0
3	0	0	0	0	0	0	0	0
4	0	0	0	0	0	0	0	0
5	0	0	0	0	0	0	0	0
6	100	190	4	2	0	9	0	0
7	0	0	0	0	0	0	0	0
8	100	230	5	2	0	7	0	0
9	100	250	6	2	0	6	0	0
10	0	0	0	0	0	0	0	0
11	0	0	0	0	0	0	0	0
12	0	0	0	0	0	0	0	0
13	0	0	0	0	0	0	0	0
14	0	0	0	0	0	0	0	0
15	100	350	7	2	0	5	0	0
16	0	0	0	0	0	0	0	0
17	100	380	8	3	0	11	0	0
18	0	0	0	0	0	0	0	0
19	0	0	0	0	0	0	0	0
20	0	0	0	0	0	0	0	0
21	100	460	10	4	0	15	0	0
22	0	0	0	0	0	0	0	0
23	0	0	0	0	0	0	0	0
24	0	0	0	0	0	0	0	0
25	0	0	0	0	0	0	0	0
26	0	0	0	0	0	0	0	0
27	0	0	0	0	0	0	0	0
28	0	0	0	0	0	0	0	0
29	0	0	0	0	0	0	0	0
30	0	0	0	0	0	0	0	0
31	0	0	0	0	0	0	0	0
32	380	650	4	3	0	24	0	0

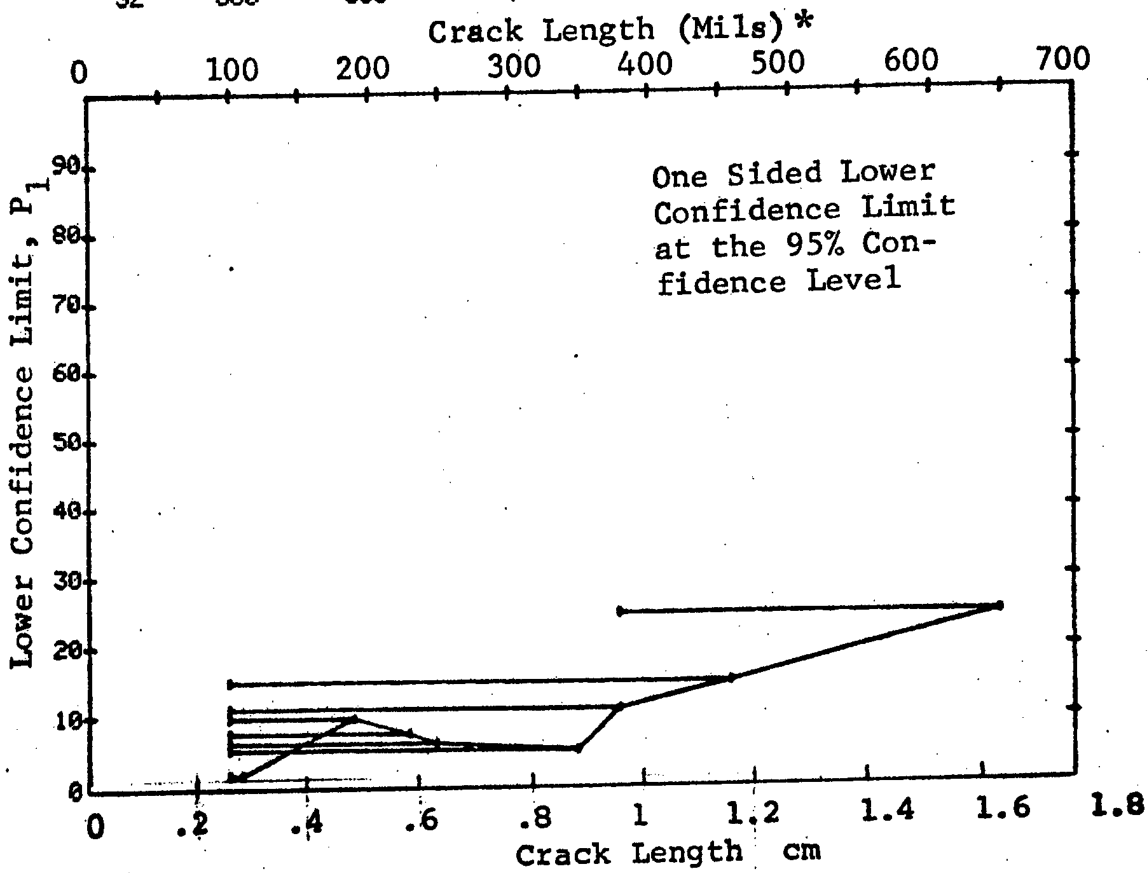

Figure D-86 (Continued)

(c) Overlapping Sixty Point Method of Data Cumulation

27-OCT-75 RADIOGRAPHY TEST 3 ([illegible] (86)

RANGE	MIN LN *	MAX LN *	N	DET	50%	95%	0 MISS	1 MISS
1	0	0	0	0	0	0	0	0
2	0	0	0	0	0	0	0	0
3	0	0	0	0	0	0	0	0
4	0	0	0	0	0	0	0	0
5	0	0	0	0	0	0	0	0
6	0	0	0	0	0	0	0	0
7	0	0	0	0	0	0	0	0
8	0	0	0	0	0	0	0	0
9	0	0	0	0	0	0	0	0
10	0	0	0	0	0	0	0	0
11	0	0	0	0	0	0	0	0
12	0	0	0	0	0	0	0	0
13	0	0	0	0	0	0	0	0
14	0	0	0	0	0	0	0	0
15	0	0	0	0	0	0	0	0
16	0	0	0	0	0	0	0	0
17	0	0	0	0	0	0	0	0
18	0	0	0	0	0	0	0	0
19	0	0	0	0	0	0	0	0
20	0	0	0	0	0	0	0	0
21	0	0	0	0	0	0	0	0
22	0	0	0	0	0	0	0	0
23	0	0	0	0	0	0	0	0
24	0	0	0	0	0	0	0	0
25	0	0	0	0	0	0	0	0
26	0	0	0	0	0	0	0	0
27	0	0	0	0	0	0	0	0
28	0	0	0	0	0	0	0	0
29	0	0	0	0	0	0	0	0
30	0	0	0	0	0	0	0	0
31	0	0	0	0	0	0	0	0
32	100	460	10	4	35	15	0	0

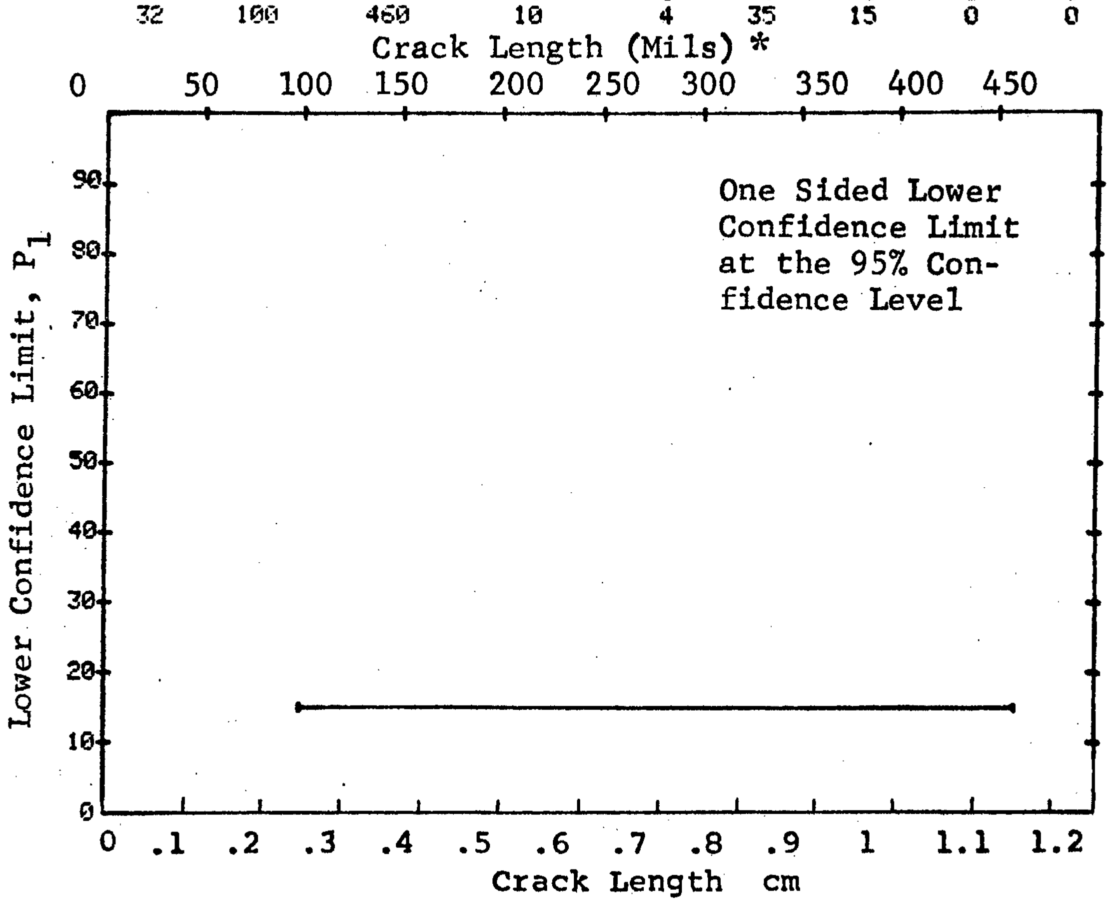

Figure D-86 (Concluded)

(a) Range Interval Method of Data Cumulation

27-OCT-75 RADIOGRAPHY TEST 1 ([illegible] (87)

RANGE	MIN LN	MAX LN	N	DET	50%	95%	0 MISS	1 MISS
1	10 *	10 *	5	0	0	0	0	0
2	0	0	0	0	0	0	0	0
3	30	30	3	3	79	36	0	0
4	0	0	0	0	0	0	0	0
5	40	40	9	6	60	34	0	0
6	50	50	19	17	86	70	0	0
7	0	0	0	0	0	0	0	0
8	60	60	8	8	91	68	0	0
9	70	70	1	1	50	5	0	0
10	0	0	0	0	0	0	0	0
11	80	80	6	4	57	27	0	0
12	90	90	5	4	68	34	0	0
13	0	0	0	0	0	0	0	0
14	100	100	4	2	38	9	0	0
15	110	110	7	6	77	47	0	0
16	120	120	3	3	79	36	0	0
17	0	0	0	0	0	0	0	0
18	130	130	4	4	84	47	0	0
19	140	140	2	1	29	2	0	0
20	0	0	0	0	0	0	0	0
21	150	150	9	9	92	71	0	0
22	160	160	1	0	0	0	0	0
23	0	0	0	0	0	0	0	0
24	170	170	5	5	87	54	0	0
25	180	180	9	8	82	57	0	0
26	0	0	0	0	0	0	0	0
27	190	190	1	0	0	0	0	0
28	0	0	0	0	0	0	0	0
29	0	0	0	0	0	0	0	0
30	0	0	0	0	0	0	0	0
31	220	220	3	3	79	36	0	0
32	230	230	5	4	68	34	0	0

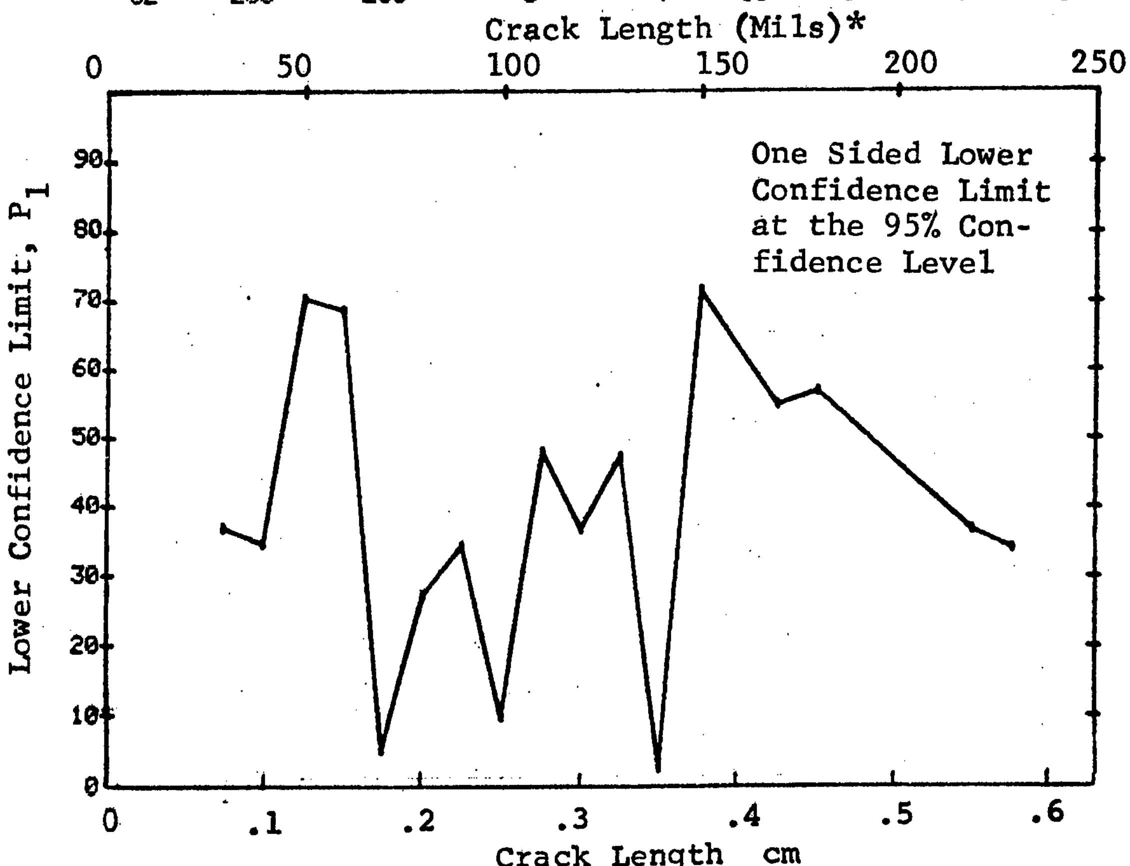

Figure D-87 Probability of Detection for 2024-T6 Al Using X-ray. Compressed Notch Flaws in Tandem-T Specimen. Prod. Env.

(b) Optimum Probability Method of Data Cumulation

27-OCT-75 RADIOGRAPHY TEST 3 (7 (87)

RANGE	MIN LN *	MAX LN *	N	DET	50%	95%	0 MISS	1 MISS
1	10	10	5	0	0	0	0	0
2	0	0	0	0	0	0	0	0
3	30	30	3	3	0	36	0	0
4	0	0	0	0	0	0	0	0
5	30	40	12	9	0	47	0	0
6	50	50	19	17	0	70	0	0
7	0	0	0	0	0	0	0	0
8	50	60	27	25	0	73	0	0
9	50	70	28	26	0	79	0	0
10	0	0	0	0	0	0	0	0
11	50	80	34	30	0	75	0	0
12	50	90	39	34	0	74	0	0
13	0	0	0	0	0	0	0	0
14	50	100	43	36	0	71	0	0
15	50	110	50	42	0	72	0	0
16	50	120	53	45	0	74	0	0
17	0	0	0	0	0	0	0	0
18	50	130	57	49	0	76	0	0
19	50	140	59	50	0	74	0	0
20	0	0	0	0	0	0	0	0
21	50	150	68	59	0	78	0	0
22	50	160	69	59	0	76	0	0
23	0	0	0	0	0	0	0	0
24	50	170	74	64	0	78	0	0
25	50	180	83	72	0	79	0	0
26	0	0	0	0	0	0	0	0
27	50	190	84	72	0	77	0	0
28	0	0	0	0	0	0	0	0
29	0	0	0	0	0	0	0	0
30	0	0	0	0	0	0	0	0
31	50	220	87	75	0	78	0	0
32	50	230	92	79	0	78	0	0

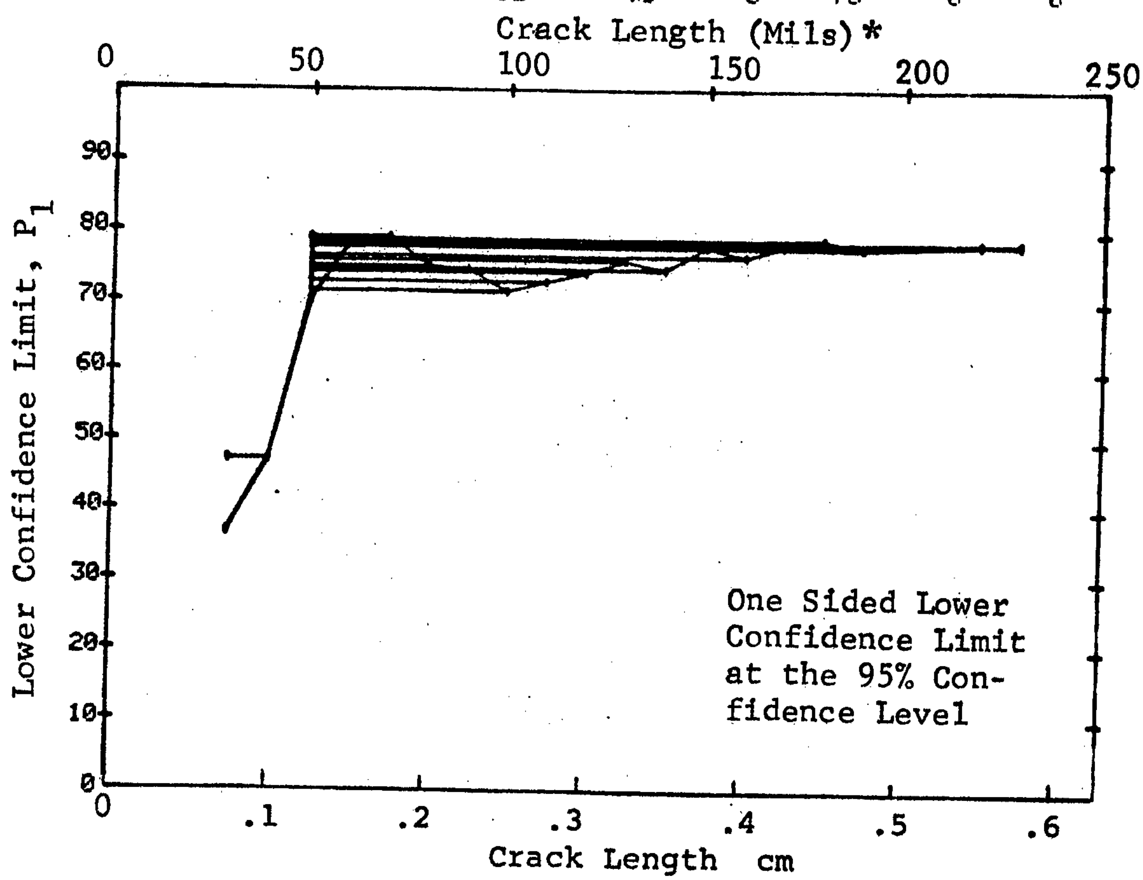

Figure D-87 (Continued)

(c) Overlapping Sixty Point Method of Data Cumulation

27-OCT-75 RADIOGRAPHY TEST 3 (87)

RANGE	MIN LN *	MAX LN *	N	DET	50%	95%	0 MISS	1 MISS
1	0	0	0	0	0	0	0	0
2	0	0	0	0	0	0	0	0
3	0	0	0	0	0	0	0	0
4	0	0	0	0	0	0	0	0
5	0	0	0	0	0	0	0	0
6	0	0	0	0	0	0	0	0
7	0	0	0	0	0	0	0	0
8	0	0	0	0	0	0	0	0
9	0	0	0	0	0	0	0	0
10	0	0	0	0	0	0	0	0
11	0	0	0	0	0	0	0	0
12	0	0	0	0	0	0	0	0
13	0	0	0	0	0	0	0	0
14	0	0	0	0	0	0	0	0
15	0	0	0	0	0	0	0	0
16	0	0	0	0	0	0	0	0
17	0	0	0	0	0	0	0	0
18	0	0	0	0	0	0	0	0
19	0	0	0	0	0	0	0	0
20	0	0	0	0	0	0	0	0
21	0	0	0	0	0	0	0	0
22	0	0	0	0	0	0	0	0
23	0	0	0	0	0	0	0	0
24	0	0	0	0	0	0	0	0
25	0	0	0	0	0	0	0	0
26	0	0	0	0	0	0	0	0
27	0	0	0	0	0	0	0	0
28	0	0	0	0	0	0	0	0
29	0	0	0	0	0	0	0	0
30	10	80	49	37	74	63	0	0
31	50	150	60	51	83	75	94	100
32	80	230	60	51	83	75	94	100

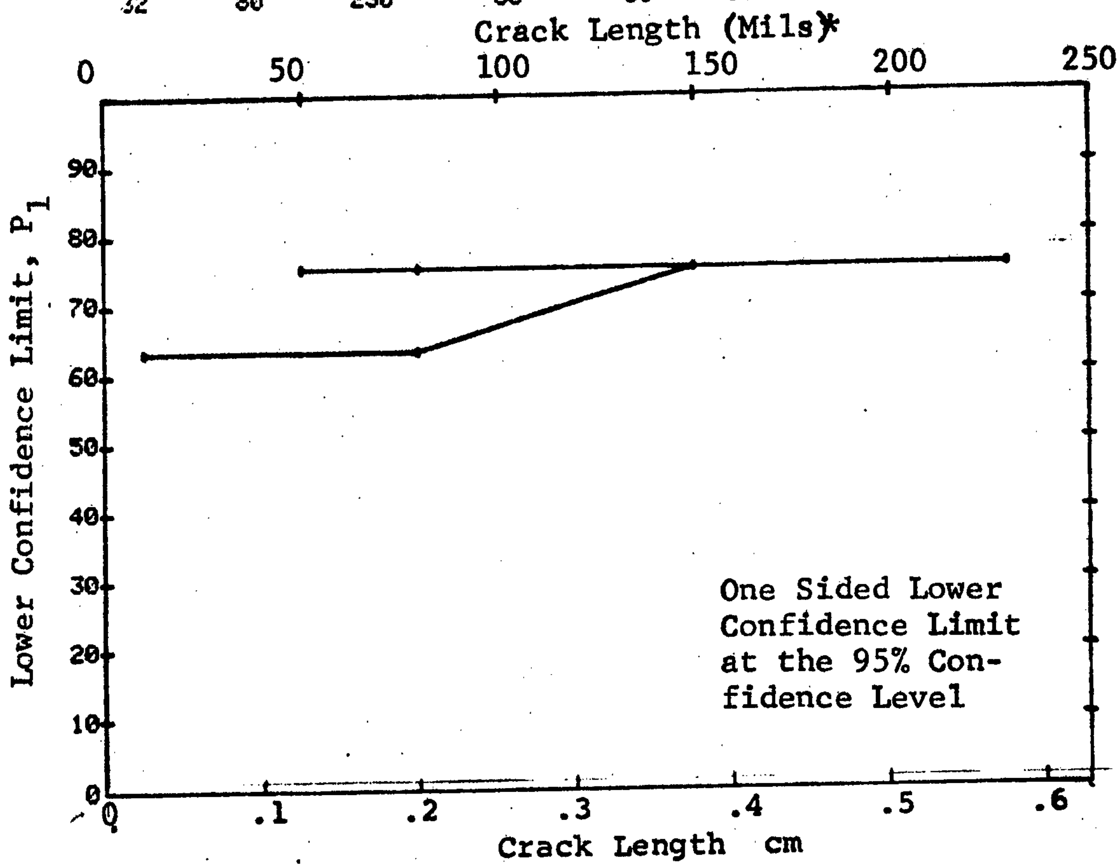

Figure D-87 (Concluded)

(a) Range Interval Method of Data Cumulation

27-OCT-75 RADIOGRAPHY TEST 1 (88)

RANGE	MIN LN	MAX LN	N	DET	50%	95%	0 MISS	1 MISS
1	50*	70*	6	0	0	0	0	0
2	0	0	0	0	0	0	0	0
3	110	110	1	0	0	0	0	0
4	120	120	2	0	0	0	0	0
5	140	150	5	2	31	7	0	0
6	160	160	1	1	50	5	0	0
7	200	200	1	0	0	0	0	0
8	0	0	0	0	0	0	0	0
9	0	0	0	0	0	0	0	0
10	0	0	0	0	0	0	0	0
11	0	0	0	0	0	0	0	0
12	0	0	0	0	0	0	0	0
13	0	0	0	0	0	0	0	0
14	0	0	0	0	0	0	0	0
15	0	0	0	0	0	0	0	0
16	0	0	0	0	0	0	0	0
17	0	0	0	0	0	0	0	0
18	0	0	0	0	0	0	0	0
19	0	0	0	0	0	0	0	0
20	0	0	0	0	0	0	0	0
21	0	0	0	0	0	0	0	0
22	0	0	0	0	0	0	0	0
23	0	0	0	0	0	0	0	0
24	0	0	0	0	0	0	0	0
25	0	0	0	0	0	0	0	0
26	0	0	0	0	0	0	0	0
27	0	0	0	0	0	0	0	0
28	0	0	0	0	0	0	0	0
29	0	0	0	0	0	0	0	0
30	0	0	0	0	0	0	0	0
31	0	0	0	0	0	0	0	0
32	750	750	2	2	70	22	0	0

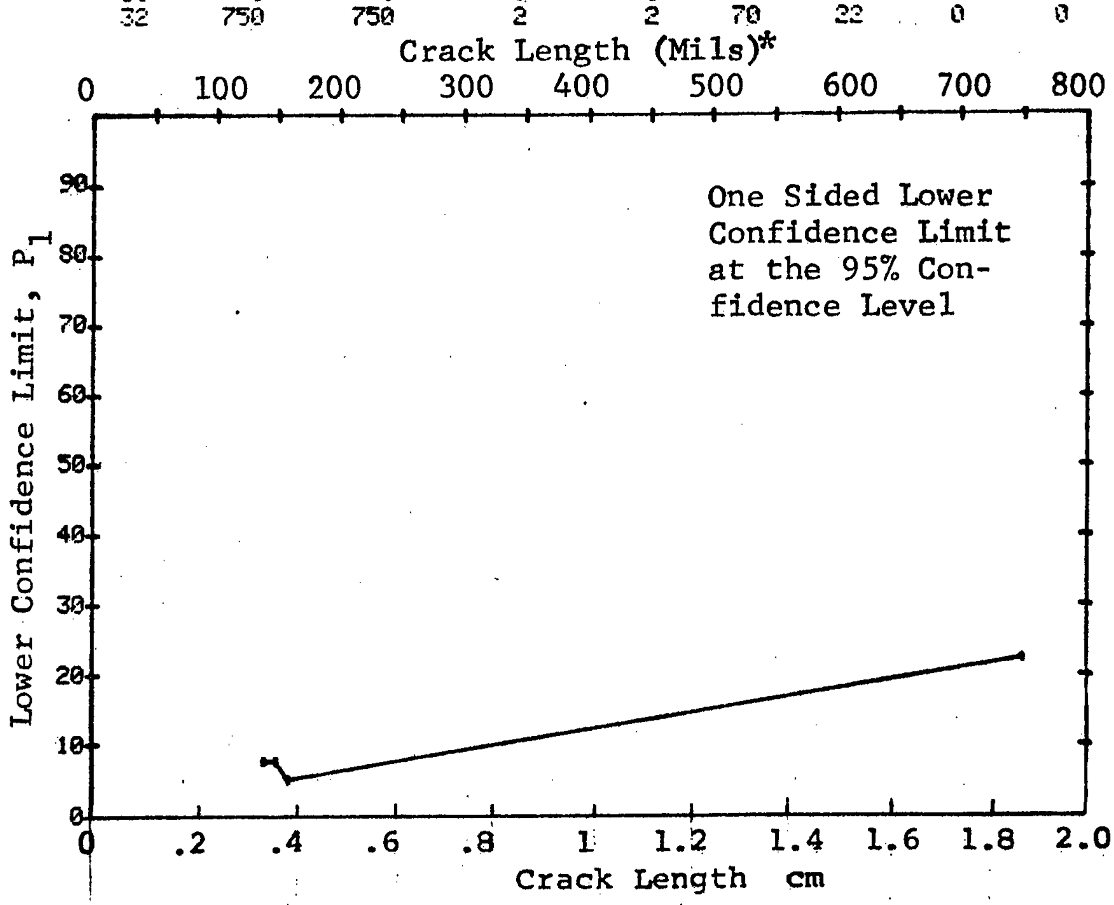

Figure D-88 Probability of Detection for 4340M Steel Using X-ray. Compressed Notch Flaws in Solid Cylinder. Lab. Env.

(b) Optimum Probability Method of Data Cumulation

27-OCT-75 RADIOGRAPHY TEST 2 (88)

RANGE	MIN LN	MAX LN	N	DET	50%	95%	0 MISS	1 MISS
1	50 *	70 *	6	0	0	0	0	0
2	0	0	0	0	0	0	0	0
3	110	110	1	0	0	0	0	0
4	120	120	2	0	0	0	0	0
5	140	150	5	2	0	7	0	0
6	140	160	6	3	0	15	0	0
7	140	200	7	3	0	12	0	0
8	0	0	0	0	0	0	0	0
9	0	0	0	0	0	0	0	0
10	0	0	0	0	0	0	0	0
11	0	0	0	0	0	0	0	0
12	0	0	0	0	0	0	0	0
13	0	0	0	0	0	0	0	0
14	0	0	0	0	0	0	0	0
15	0	0	0	0	0	0	0	0
16	0	0	0	0	0	0	0	0
17	0	0	0	0	0	0	0	0
18	0	0	0	0	0	0	0	0
19	0	0	0	0	0	0	0	0
20	0	0	0	0	0	0	0	0
21	0	0	0	0	0	0	0	0
22	0	0	0	0	0	0	0	0
23	0	0	0	0	0	0	0	0
24	0	0	0	0	0	0	0	0
25	0	0	0	0	0	0	0	0
26	0	0	0	0	0	0	0	0
27	0	0	0	0	0	0	0	0
28	0	0	0	0	0	0	0	0
29	0	0	0	0	0	0	0	0
30	0	0	0	0	0	0	0	0
31	0	0	0	0	0	0	0	0
32	140	750	9	5	0	25	0	0

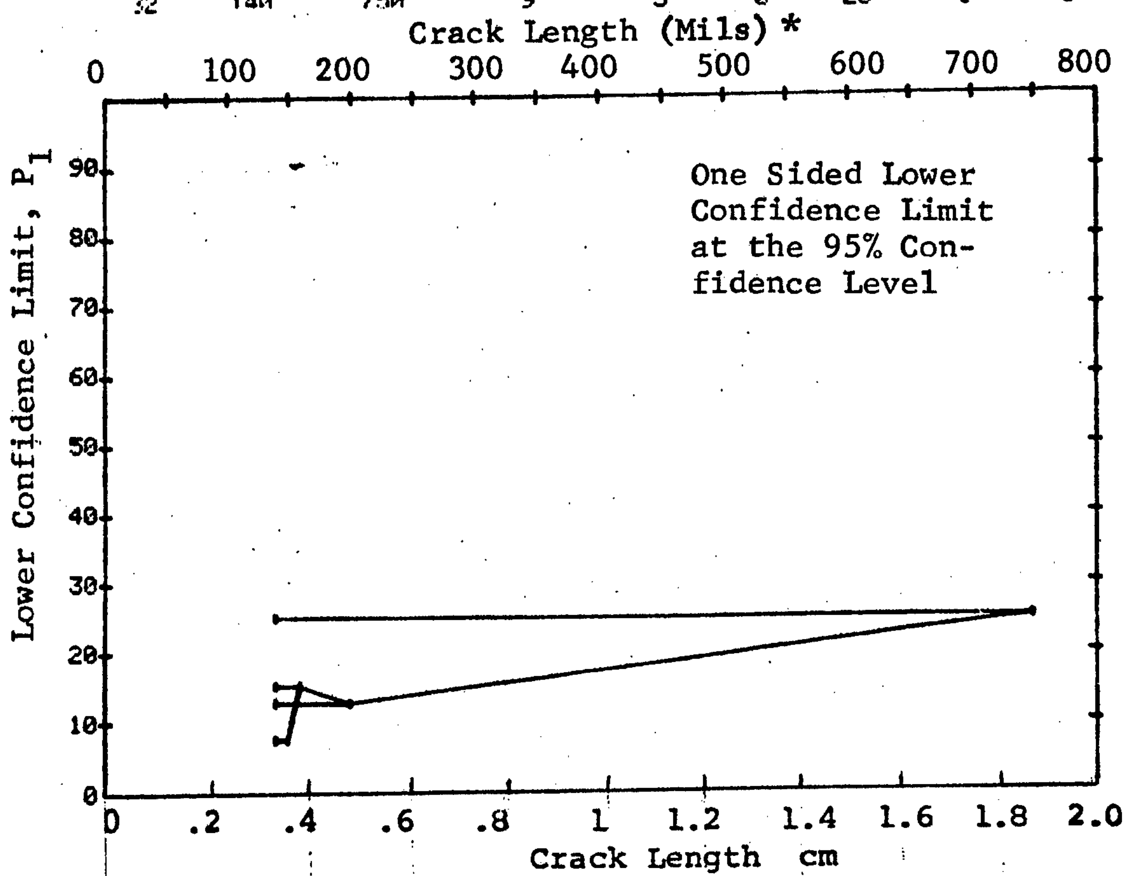

Figure D-88 (Continued)

(c) Overlapping Sixty Point Method of Data Cumulation

27-OCT-75 RADIOGRAPHY TEST 3 ((88)

RANGE	MIN LN	MAX LN	N	DET	50%	95%	0 MISS	1 MISS
1	0 *	0 *	0	0	0	0	0	0
2	0	0	0	0	0	0	0	0
3	0	0	0	0	0	0	0	0
4	0	0	0	0	0	0	0	0
5	0	0	0	0	0	0	0	0
6	0	0	0	0	0	0	0	0
7	0	0	0	0	0	0	0	0
8	0	0	0	0	0	0	0	0
9	0	0	0	0	0	0	0	0
10	0	0	0	0	0	0	0	0
11	0	0	0	0	0	0	0	0
12	0	0	0	0	0	0	0	0
13	0	0	0	0	0	0	0	0
14	0	0	0	0	0	0	0	0
15	0	0	0	0	0	0	0	0
16	0	0	0	0	0	0	0	0
17	0	0	0	0	0	0	0	0
18	0	0	0	0	0	0	0	0
19	0	0	0	0	0	0	0	0
20	0	0	0	0	0	0	0	0
21	0	0	0	0	0	0	0	0
22	0	0	0	0	0	0	0	0
23	0	0	0	0	0	0	0	0
24	0	0	0	0	0	0	0	0
25	0	0	0	0	0	0	0	0
26	0	0	0	0	0	0	0	0
27	0	0	0	0	0	0	0	0
28	0	0	0	0	0	0	0	0
29	0	0	0	0	0	0	0	0
30	0	0	0	0	0	0	0	0
31	0	0	0	0	0	0	0	0
32	50	200	16	3	16	5	0	0

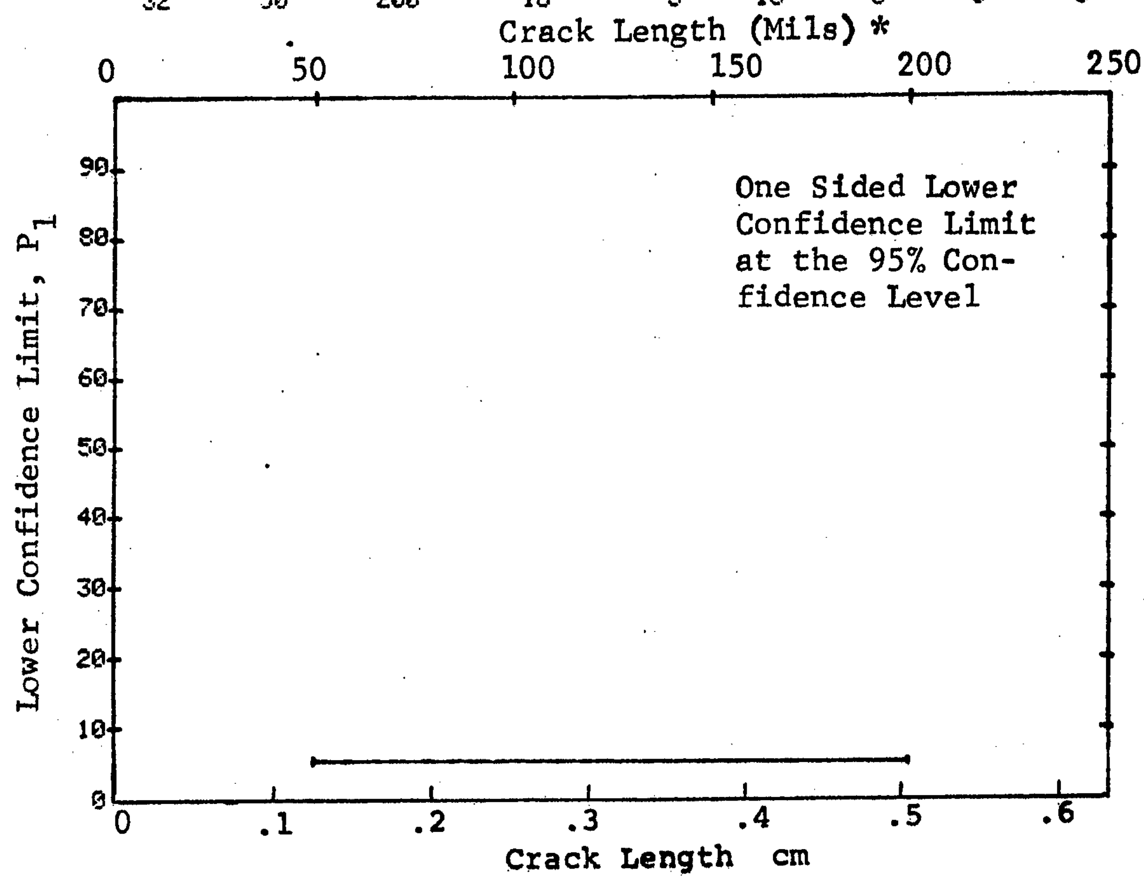

Figure D-88 (Concluded)

(a) Range Interval Method of Data Cumulation

27-OCT-75 RADIOGRHPHY TEST 1 (89)

RANGE	MIN LN*	MAX LN*	N	DET	50%	95%	0 MISS	1 MISS
1	70	70	1	1	50	5	0	0
2	0	0	0	0	0	0	0	0
3	0	0	0	0	0	0	0	0
4	0	0	0	0	0	0	0	0
5	0	0	0	0	0	0	0	0
6	140	140	1	1	50	5	0	0
7	0	0	0	0	0	0	0	0
8	160	160	1	1	50	5	0	0
9	0	0	0	0	0	0	0	0
10	180	180	1	1	50	5	0	0
11	0	0	0	0	0	0	0	0
12	0	0	0	0	0	0	0	0
13	0	0	0	0	0	0	0	0
14	0	0	0	0	0	0	0	0
15	250	250	1	1	50	5	0	0
16	0	0	0	0	0	0	0	0
17	270	270	1	1	50	5	0	0
18	280	280	2	2	70	22	0	0
19	300	300	1	1	50	5	0	0
20	0	0	0	0	0	0	0	0
21	0	0	0	0	0	0	0	0
22	0	0	0	0	0	0	0	0
23	0	0	0	0	0	0	0	0
24	0	0	0	0	0	0	0	0
25	0	0	0	0	0	0	0	0
26	0	0	0	0	0	0	0	0
27	390	390	2	2	70	22	0	0
28	0	0	0	0	0	0	0	0
29	0	0	0	0	0	0	0	0
30	0	0	0	0	0	0	0	0
31	440	440	1	1	50	5	0	0
32	450	460	4	4	84	47	0	0

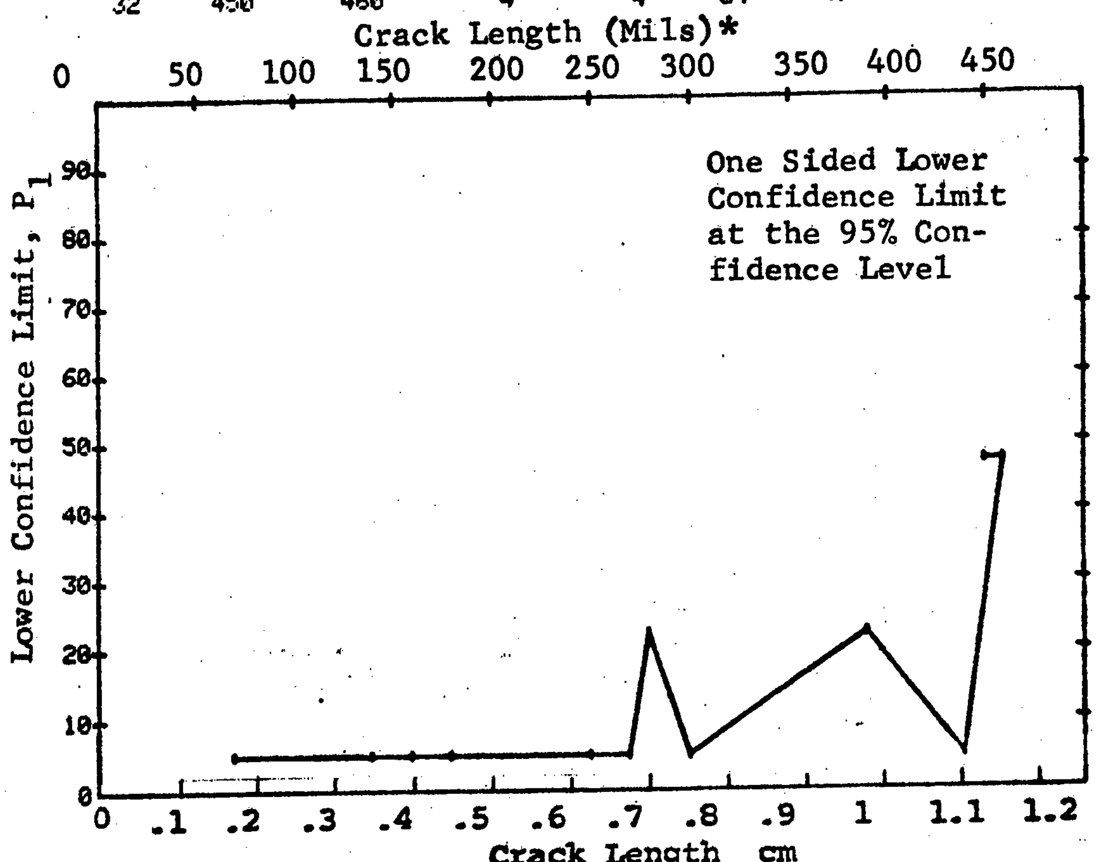

Figure D-89 Probability of Detection for 4340M Steel Using X-ray. Compressed Notch Flaws in Hollow Filleted Cylinder. Lab. Env.

(b) Optimum Probability Method of Data Cumulation

27-OCT-75 RADIOGRAPHY TEST 2 (89)

RANGE	MIN LN *	MAX LN *	N	DET	50%	95%	0 MISS	1 MISS
1	70	70	1	1	0	5	0	0
2	0	0	0	0	0	0	0	0
3	0	0	0	0	0	0	0	0
4	0	0	0	0	0	0	0	0
5	0	0	0	0	0	0	0	0
6	70	140	2	2	0	22	0	0
7	0	0	0	0	0	0	0	0
8	70	160	3	3	0	36	0	0
9	0	0	0	0	0	0	0	0
10	70	180	4	4	0	47	0	0
11	0	0	0	0	0	0	0	0
12	0	0	0	0	0	0	0	0
13	0	0	0	0	0	0	0	0
14	0	0	0	0	0	0	0	0
15	70	250	5	5	0	54	0	0
16	0	0	0	0	0	0	0	0
17	70	270	6	6	0	60	0	0
18	70	280	8	8	0	68	0	0
19	70	300	9	9	0	71	0	0
20	0	0	0	0	0	0	0	0
21	0	0	0	0	0	0	0	0
22	0	0	0	0	0	0	0	0
23	0	0	0	0	0	0	0	0
24	0	0	0	0	0	0	0	0
25	0	0	0	0	0	0	0	0
26	0	0	0	0	0	0	0	0
27	70	390	11	11	0	76	0	0
28	0	0	0	0	0	0	0	0
29	0	0	0	0	0	0	0	0
30	0	0	0	0	0	0	0	0
31	70	440	12	12	0	77	0	0
32	70	460	16	16	0	82	13	30

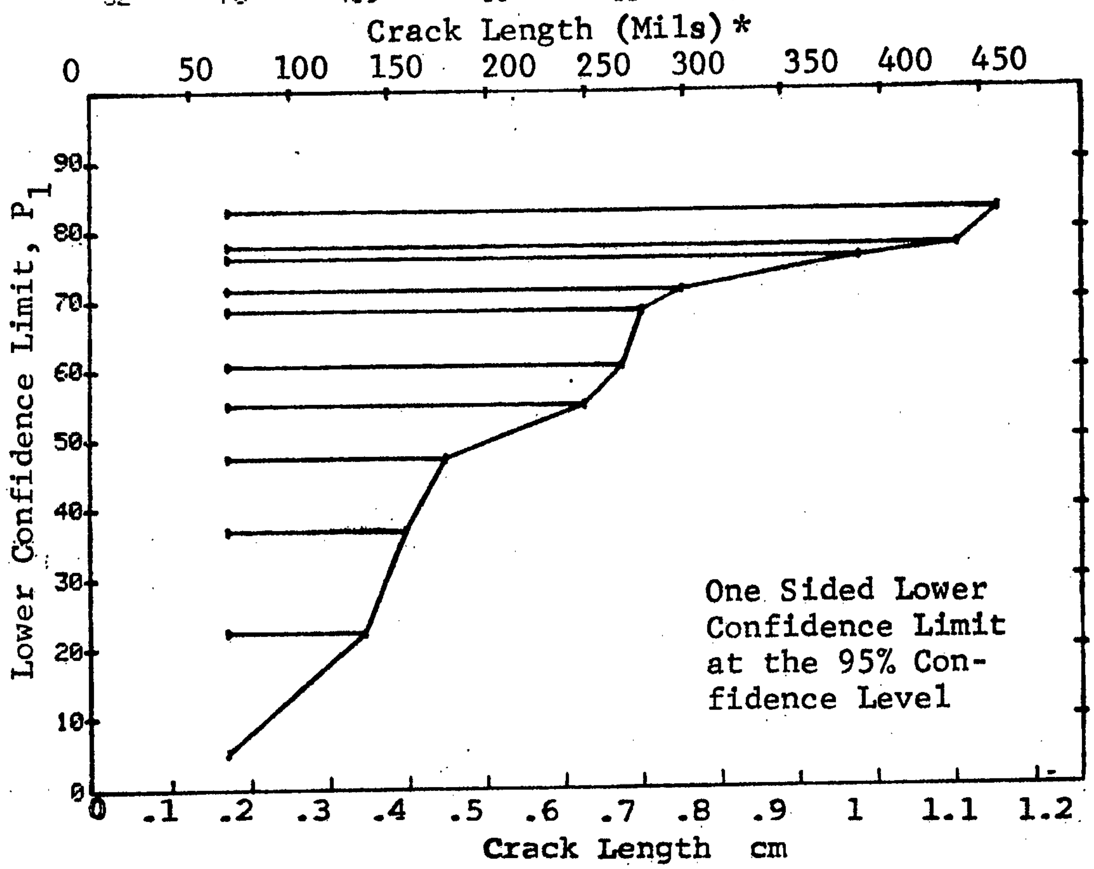

Figure D-89 (Continued)

(c) Overlapping Sixty Point Method of Data Cumulation

27-OCT-75 RADIOGRAPHY TEST 3 ([illegible]) (89)

RANGE	MIN LN *	MAX LN *	N	DET	50%	95%	0 MISS	1 MISS
1	0	0	0	0	0	0	0	0
2	0	0	0	0	0	0	0	0
3	0	0	0	0	0	0	0	0
4	0	0	0	0	0	0	0	0
5	0	0	0	0	0	0	0	0
6	0	0	0	0	0	0	0	0
7	0	0	0	0	0	0	0	0
8	0	0	0	0	0	0	0	0
9	0	0	0	0	0	0	0	0
10	0	0	0	0	0	0	0	0
11	0	0	0	0	0	0	0	0
12	0	0	0	0	0	0	0	0
13	0	0	0	0	0	0	0	0
14	0	0	0	0	0	0	0	0
15	0	0	0	0	0	0	0	0
16	0	0	0	0	0	0	0	0
17	0	0	0	0	0	0	0	0
18	0	0	0	0	0	0	0	0
19	0	0	0	0	0	0	0	0
20	0	0	0	0	0	0	0	0
21	0	0	0	0	0	0	0	0
22	0	0	0	0	0	0	0	0
23	0	0	0	0	0	0	0	0
24	0	0	0	0	0	0	0	0
25	0	0	0	0	0	0	0	0
26	0	0	0	0	0	0	0	0
27	0	0	0	0	0	0	0	0
28	0	0	0	0	0	0	0	0
29	0	0	0	0	0	0	0	0
30	0	0	0	0	0	0	0	0
31	0	0	0	0	0	0	0	0
32	70	460	16	16	95	82	13	30

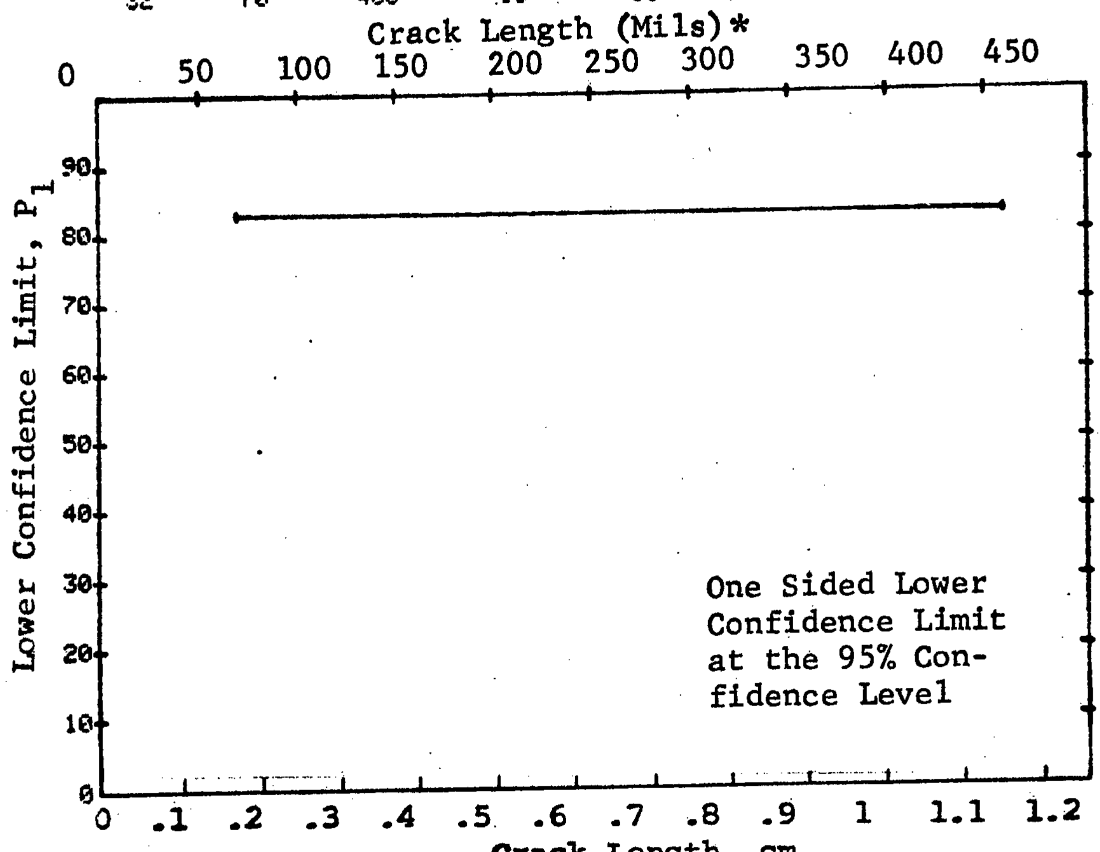

Figure D-89 (Concluded)

(a) Range Interval Method of Data Cumulation

27-OCT-75 RADIOGRAPHY TEST 1 (90)

RANGE	MIN LN*	MAX LN*	N	DET	50%	95%	0 MISS	1 MISS
1	60	70	2	0	0	0	0	0
2	0	0	0	0	0	0	0	0
3	90	100	2	0	0	0	0	0
4	0	0	0	0	0	0	0	0
5	0	0	0	0	0	0	0	0
6	130	140	3	0	0	0	0	0
7	150	150	1	0	0	0	0	0
8	0	0	0	0	0	0	0	0
9	0	0	0	0	0	0	0	0
10	0	0	0	0	0	0	0	0
11	0	0	0	0	0	0	0	0
12	0	0	0	0	0	0	0	0
13	230	230	1	0	0	0	0	0
14	250	250	1	1	50	5	0	0
15	0	0	0	0	0	0	0	0
16	0	0	0	0	0	0	0	0
17	0	0	0	0	0	0	0	0
18	300	300	1	0	0	0	0	0
19	0	0	0	0	0	0	0	0
20	0	0	0	0	0	0	0	0
21	0	0	0	0	0	0	0	0
22	0	0	0	0	0	0	0	0
23	370	370	1	1	50	5	0	0
24	390	390	1	1	50	5	0	0
25	0	0	0	0	0	0	0	0
26	0	0	0	0	0	0	0	0
27	0	0	0	0	0	0	0	0
28	0	0	0	0	0	0	0	0
29	0	0	0	0	0	0	0	0
30	0	0	0	0	0	0	0	0
31	0	0	0	0	0	0	0	0
32	500	500	1	1	[illegible]	[illegible]	[illegible]	[illegible]

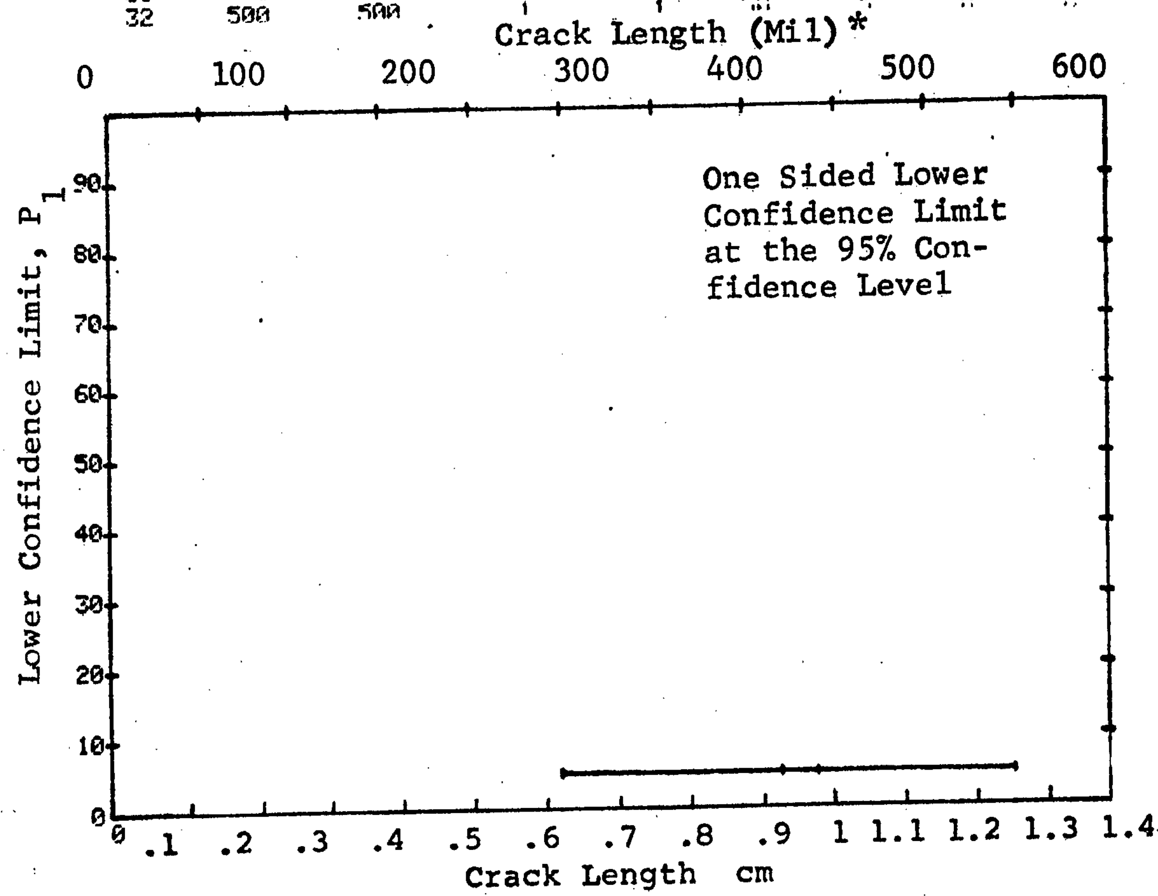

Figure D-90 Probability of Detection for 4340M Steel Using X-ray. Compressed Notch Flaws in Solid Filleted Cylinder. Lab. Env.

(b) Optimum Probability Method of Data Cumulation

27-OCT-75 RADIOGRAPHY TEST 2 (90)

RANGE	MIN LN *	MAX LN *	N	DET	50%	95%	0 MISS	1 MISS
1	60	70	2	0	0	0	0	0
2	0	0	0	0	0	0	0	0
3	90	100	2	0	0	0	0	0
4	0	0	0	0	0	0	0	0
5	0	0	0	0	0	0	0	0
6	130	140	3	0	0	0	0	0
7	150	150	1	0	0	0	0	0
8	0	0	0	0	0	0	0	0
9	0	0	0	0	0	0	0	0
10	0	0	0	0	0	0	0	0
11	0	0	0	0	0	0	0	0
12	0	0	0	0	0	0	0	0
13	230	230	1	0	0	0	0	0
14	250	250	1	1	0	5	0	0
15	0	0	0	0	0	0	0	0
16	0	0	0	0	0	0	0	0
17	0	0	0	0	0	0	0	0
18	250	300	2	1	0	2	0	0
19	0	0	0	0	0	0	0	0
20	0	0	0	0	0	0	0	0
21	0	0	0	0	0	0	0	0
22	0	0	0	0	0	0	0	0
23	250	370	3	2	0	13	0	0
24	250	390	4	3	0	24	0	0
25	0	0	0	0	0	0	0	0
26	0	0	0	0	0	0	0	0
27	0	0	0	0	0	0	0	0
28	0	0	0	0	0	0	0	0
29	0	0	0	0	0	0	0	0
30	0	0	0	0	0	0	0	0
31	0	0	0	0	0	0	0	0
32	370	500	3	3	0	36	0	0

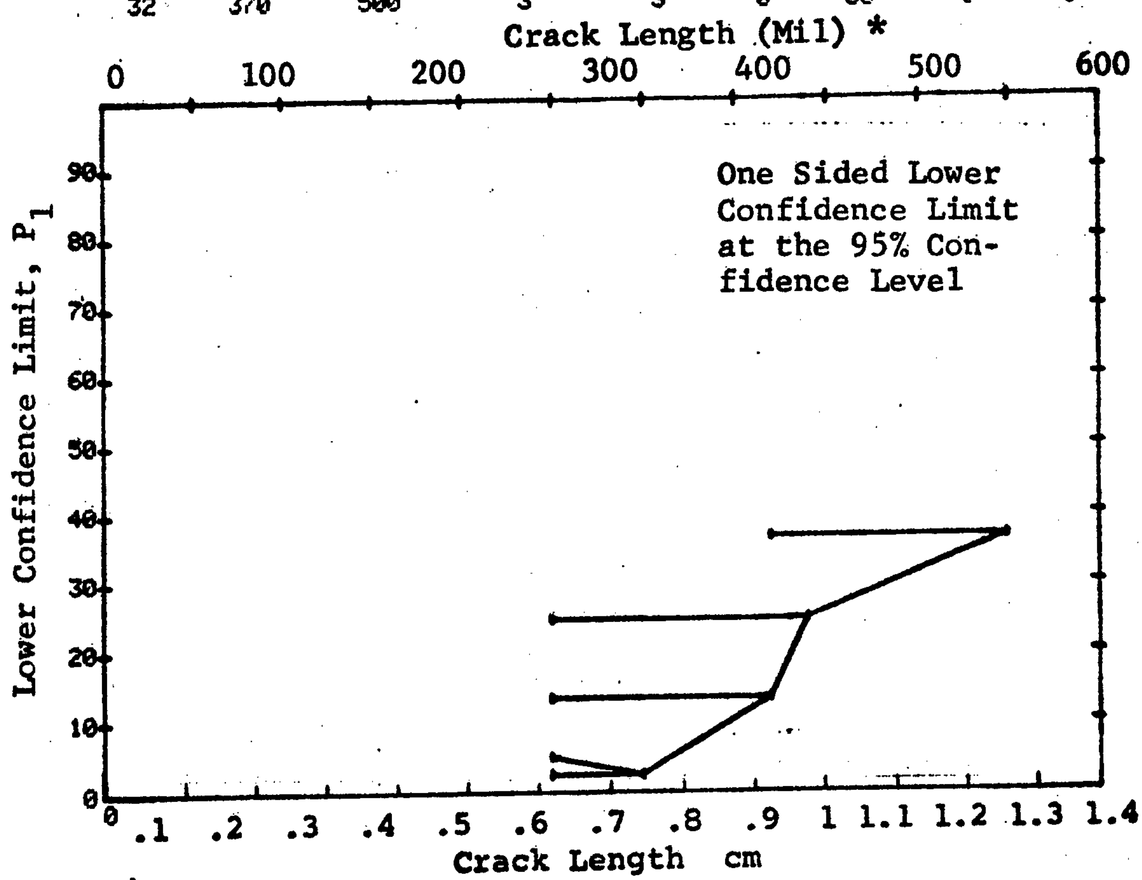

Figure D-90 (Continued)

(c) Overlapping Sixty Point Method of Data Cumulation

27-OCT-75 RADIOGRAPHY TEST 3 (90)

RANGE	MIN LN *	MAX LN *	N	DET	50%	95%	0 MISS	1 MISS
1	0	0	0	0	0	0	0	0
2	0	0	0	0	0	0	0	0
3	0	0	0	0	0	0	0	0
4	0	0	0	0	0	0	0	0
5	0	0	0	0	0	0	0	0
6	0	0	0	0	0	0	0	0
7	0	0	0	0	0	0	0	0
8	0	0	0	0	0	0	0	0
9	0	0	0	0	0	0	0	0
10	0	0	0	0	0	0	0	0
11	0	0	0	0	0	0	0	0
12	0	0	0	0	0	0	0	0
13	0	0	0	0	0	0	0	0
14	0	0	0	0	0	0	0	0
15	0	0	0	0	0	0	0	0
16	0	0	0	0	0	0	0	0
17	0	0	0	0	0	0	0	0
18	0	0	0	0	0	0	0	0
19	0	0	0	0	0	0	0	0
20	0	0	0	0	0	0	0	0
21	0	0	0	0	0	0	0	0
22	0	0	0	0	0	0	0	0
23	0	0	0	0	0	0	0	0
24	0	0	0	0	0	0	0	0
25	0	0	0	0	0	0	0	0
26	0	0	0	0	0	0	0	0
27	0	0	0	0	0	0	0	0
28	0	0	0	0	0	0	0	0
29	0	0	0	0	0	0	0	0
30	0	0	0	0	0	0	0	0
31	0	0	0	0	0	0	0	0
32	60	500	14	4	25	10	0	0

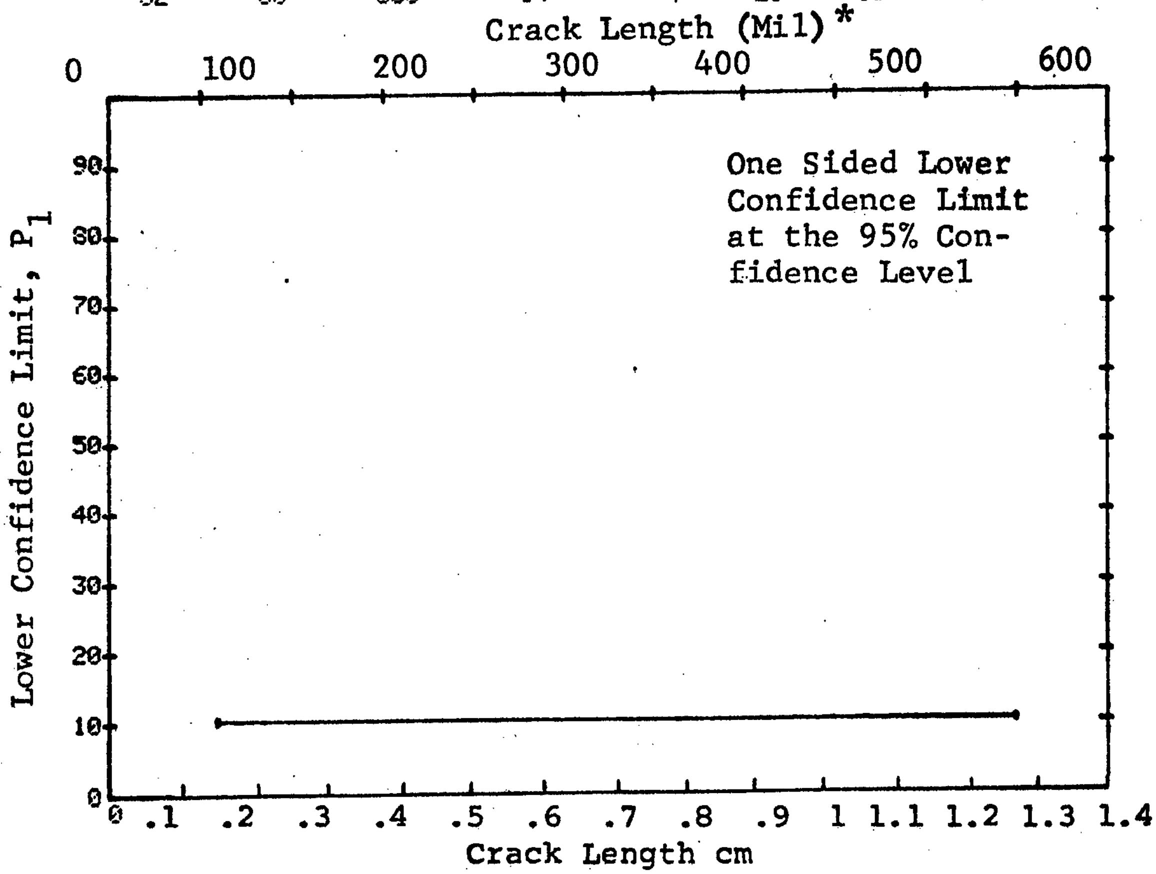

Figure D-90 (Concluded)

(a) Range Interval Method of Data Cumulation

27-OCT-75 RADIOGRAPHY TEST 1 (91)

RANGE	MIN LN*	MAX LN*	N	DET	50%	95%	0 MISS	1 MISS
1	100	100	4	0	0	0	0	0
2	0	0	0	0	0	0	0	0
3	120	120	1	0	0	0	0	0
4	0	0	0	0	0	0	0	0
5	140	140	2	1	29	2	0	0
6	0	0	0	0	0	0	0	0
7	160	160	1	0	0	0	0	0
8	0	0	0	0	0	0	0	0
9	180	180	1	0	0	0	0	0
10	0	0	0	0	0	0	0	0
11	0	0	0	0	0	0	0	0
12	0	0	0	0	0	0	0	0
13	0	0	0	0	0	0	0	0
14	0	0	0	0	0	0	0	0
15	230	230	1	1	50	5	0	0
16	0	0	0	0	0	0	0	0
17	0	0	0	0	0	0	0	0
18	0	0	0	0	0	0	0	0
19	0	0	0	0	0	0	0	0
20	0	0	0	0	0	0	0	0
21	0	0	0	0	0	0	0	0
22	0	0	0	0	0	0	0	0
23	0	0	0	0	0	0	0	0
24	310	310	1	1	50	5	0	0
25	0	0	0	0	0	0	0	0
26	0	0	0	0	0	0	0	0
27	0	0	0	0	0	0	0	0
28	350	350	2	2	70	22	0	0
29	0	0	0	0	0	0	0	0
30	0	0	0	0	0	0	0	0
31	0	0	0	0	0	0	0	0
32	390	390	1	1	50	5	0	0

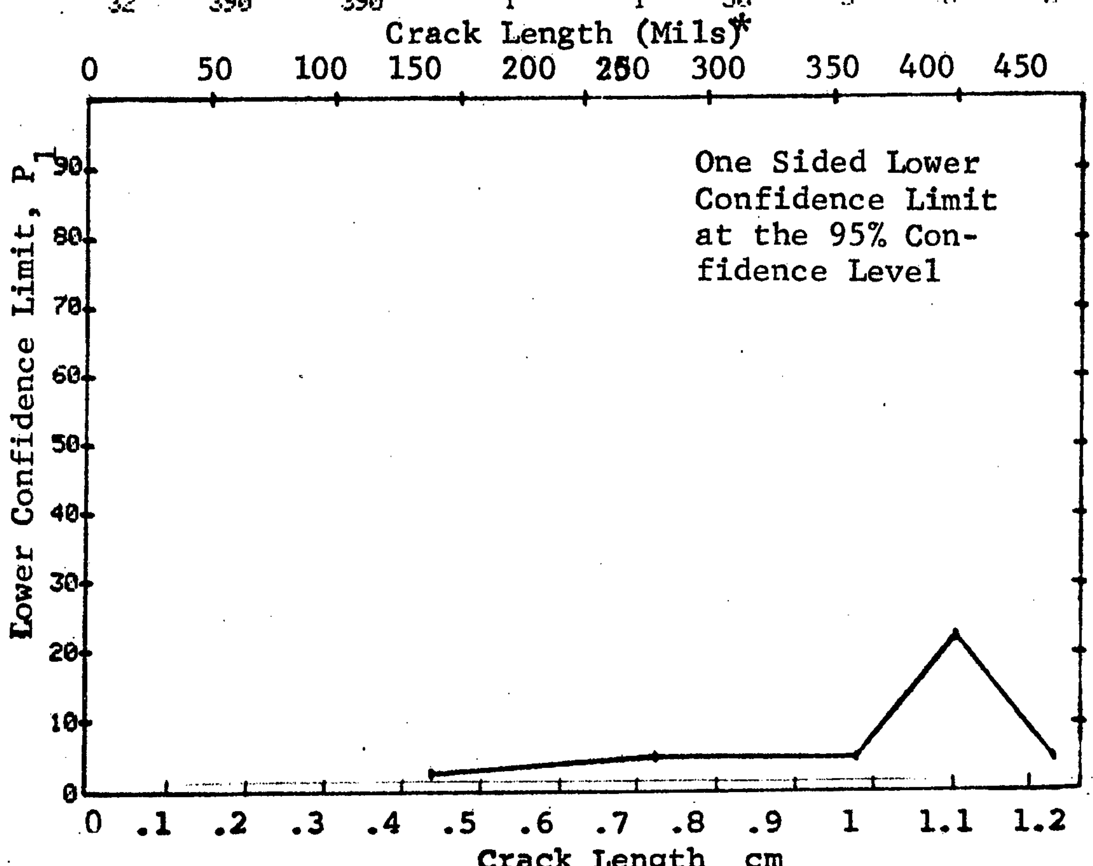

Figure D-91 Probability of Detection for 4340M Steel Using X-ray. Compressed Notch Flaws in Hollow Filleted Cylinder. Lab. Env.

(b) Optimum Probability Method of Data Cumulation

27-OCT-75 RADIOGRAPHY TEST 2 ([illegible] 5/(91)

RANGE	MIN LN *	MAX LN *	N	DET	50%	95%	0 MISS	1 MISS
1	100	100	4	0	0	0	0	0
2	0	0	0	0	0	0	0	0
3	120	120	1	0	0	0	0	0
4	0	0	0	0	0	0	0	0
5	140	140	2	1	0	2	0	0
6	0	0	0	0	0	0	0	0
7	140	160	3	1	0	1	0	0
8	0	0	0	0	0	0	0	0
9	140	180	4	1	0	1	0	0
10	0	0	0	0	0	0	0	0
11	0	0	0	0	0	0	0	0
12	0	0	0	0	0	0	0	0
13	0	0	0	0	0	0	0	0
14	0	0	0	0	0	0	0	0
15	140	230	5	2	0	7	0	0
16	0	0	0	0	0	0	0	0
17	0	0	0	0	0	0	0	0
18	0	0	0	0	0	0	0	0
19	0	0	0	0	0	0	0	0
20	0	0	0	0	0	0	0	0
21	0	0	0	0	0	0	0	0
22	0	0	0	0	0	0	0	0
23	0	0	0	0	0	0	0	0
24	230	310	2	2	0	22	0	0
25	0	0	0	0	0	0	0	0
26	0	0	0	0	0	0	0	0
27	0	0	0	0	0	0	0	0
28	230	350	4	4	0	47	0	0
29	0	0	0	0	0	0	0	0
30	0	0	0	0	0	0	0	0
31	0	0	0	0	0	0	0	0
32	230	390	5	5	0	54	0	0

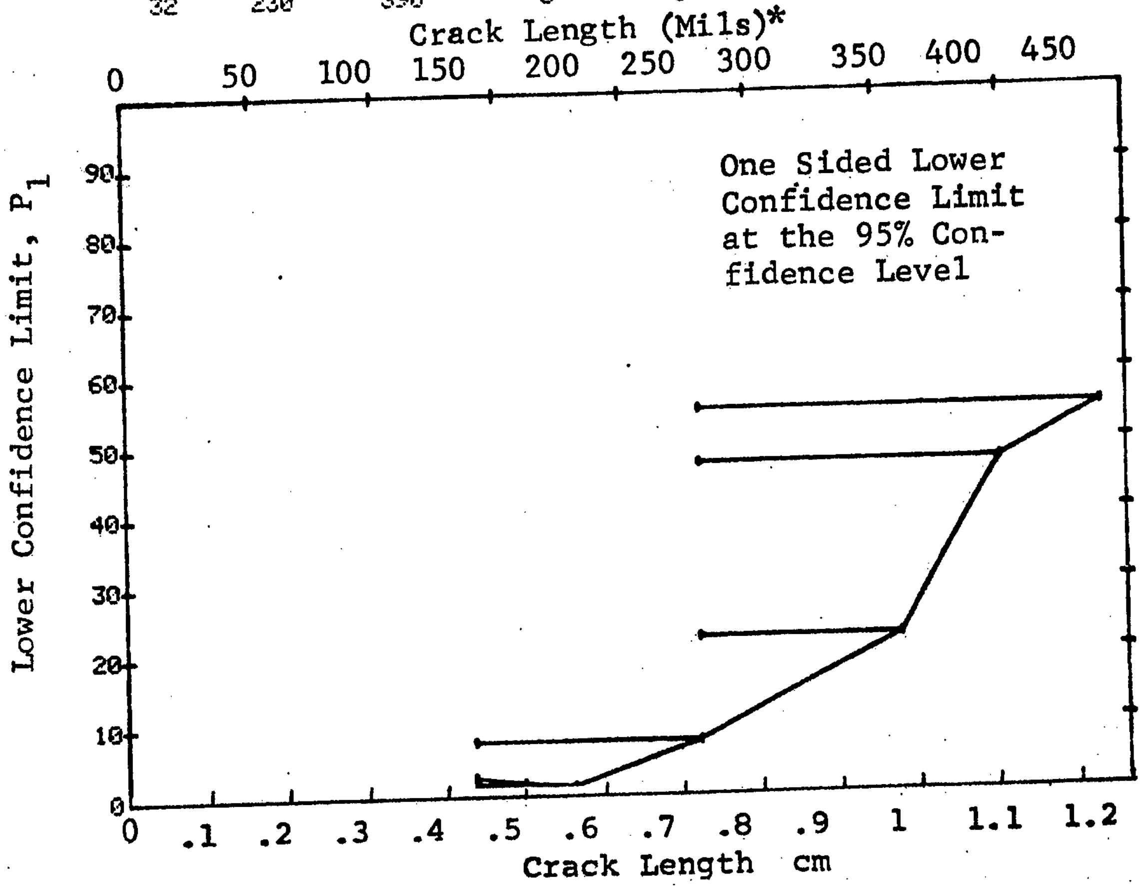

Figure D-91 (Continued)

(c) Overlapping Sixty Point Method of Data Cumulation

27-OCT-75 RADIOGRAPHY TEST 3 (... 95% (91)

RANGE	MIN LN*	MAX LN*	N	DET	50%	95%	0 MISS	1 MISS
1	0	0	0	0	0	0	0	0
2	0	0	0	0	0	0	0	0
3	0	0	0	0	0	0	0	0
4	0	0	0	0	0	0	0	0
5	0	0	0	0	0	0	0	0
6	0	0	0	0	0	0	0	0
7	0	0	0	0	0	0	0	0
8	0	0	0	0	0	0	0	0
9	0	0	0	0	0	0	0	0
10	0	0	0	0	0	0	0	0
11	0	0	0	0	0	0	0	0
12	0	0	0	0	0	0	0	0
13	0	0	0	0	0	0	0	0
14	0	0	0	0	0	0	0	0
15	0	0	0	0	0	0	0	0
16	0	0	0	0	0	0	0	0
17	0	0	0	0	0	0	0	0
18	0	0	0	0	0	0	0	0
19	0	0	0	0	0	0	0	0
20	0	0	0	0	0	0	0	0
21	0	0	0	0	0	0	0	0
22	0	0	0	0	0	0	0	0
23	0	0	0	0	0	0	0	0
24	0	0	0	0	0	0	0	0
25	0	0	0	0	0	0	0	0
26	0	0	0	0	0	0	0	0
27	0	0	0	0	0	0	0	0
28	0	0	0	0	0	0	0	0
29	0	0	0	0	0	0	0	0
30	0	0	0	0	0	0	0	0
31	0	0	0	0	0	0	0	0
32	100	390	14	6	39	20	0	0

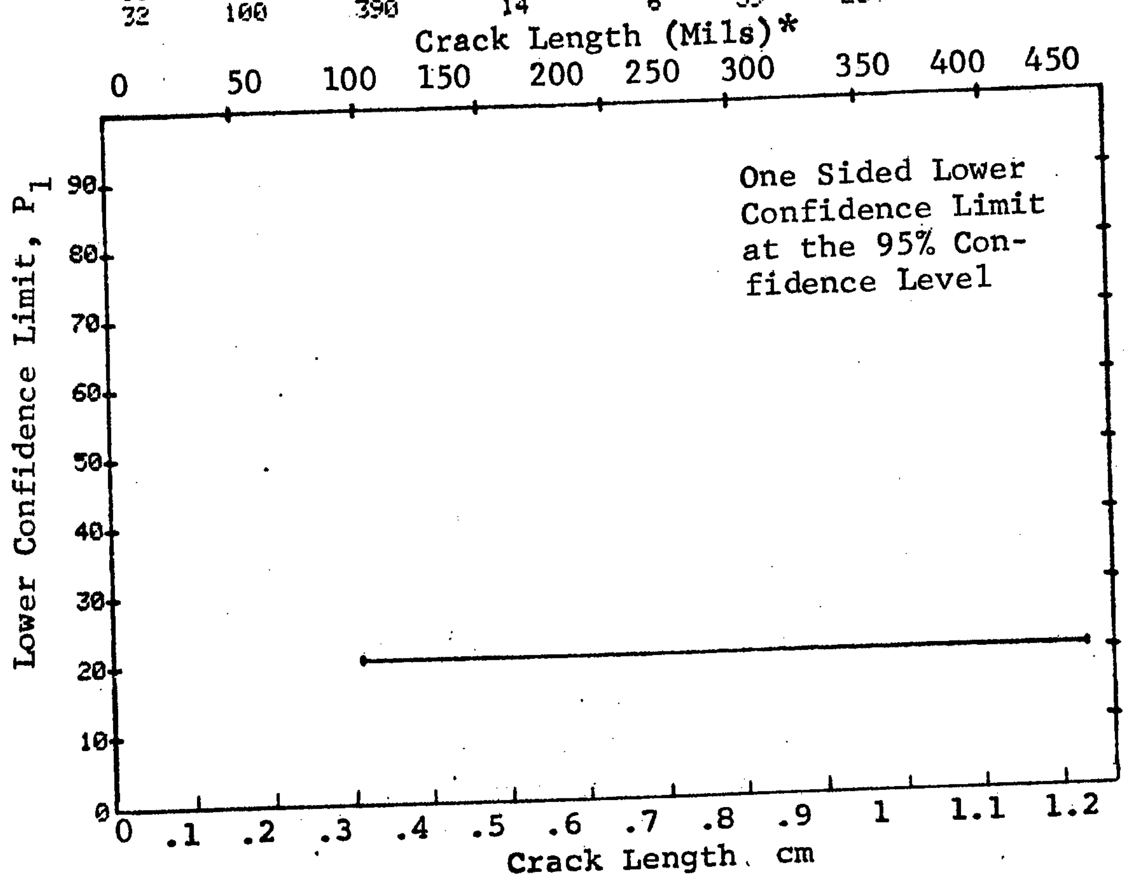

Figure D-91 (Concluded)

(a) Range Interval Method of Data Cumulation

27-OCT-75 RADIOGRAPHY TEST 1 (92)

RANGE	MIN LN *	MAX LN *	N	DET	50%	95%	0 MISS	1 MISS
1	10	10	3	0	0	0	0	0
2	0	0	0	0	0	0	0	0
3	30	30	2	1	29	2	0	0
4	0	0	0	0	0	0	0	0
5	40	40	11	8	67	43	0	0
6	50	50	24	23	93	81	22	37
7	0	0	0	0	0	0	0	0
8	60	60	8	8	91	68	0	0
9	70	70	1	1	50	5	0	0
10	0	0	0	0	0	0	0	0
11	80	80	6	6	89	60	0	0
12	90	90	11	10	85	63	0	0
13	0	0	0	0	0	0	0	0
14	100	100	4	4	84	47	0	0
15	110	110	12	12	94	77	17	34
16	120	120	1	1	50	5	0	0
17	0	0	0	0	0	0	0	0
18	130	130	3	3	79	36	0	0
19	140	140	6	6	89	60	0	0
20	0	0	0	0	0	0	0	0
21	150	150	11	11	93	76	18	35
22	160	160	2	2	70	22	0	0
23	0	0	0	0	0	0	0	0
24	170	170	5	5	87	54	0	0
25	180	180	11	10	85	63	0	0
26	0	0	0	0	0	0	0	0
27	190	190	3	3	79	36	0	0
28	0	0	0	0	0	0	0	0
29	0	0	0	0	0	0	0	0
30	210	210	1	1	50	5	0	0
31	220	220	1	1	50	5	0	0
32	230	230	6	6	89	60	0	0

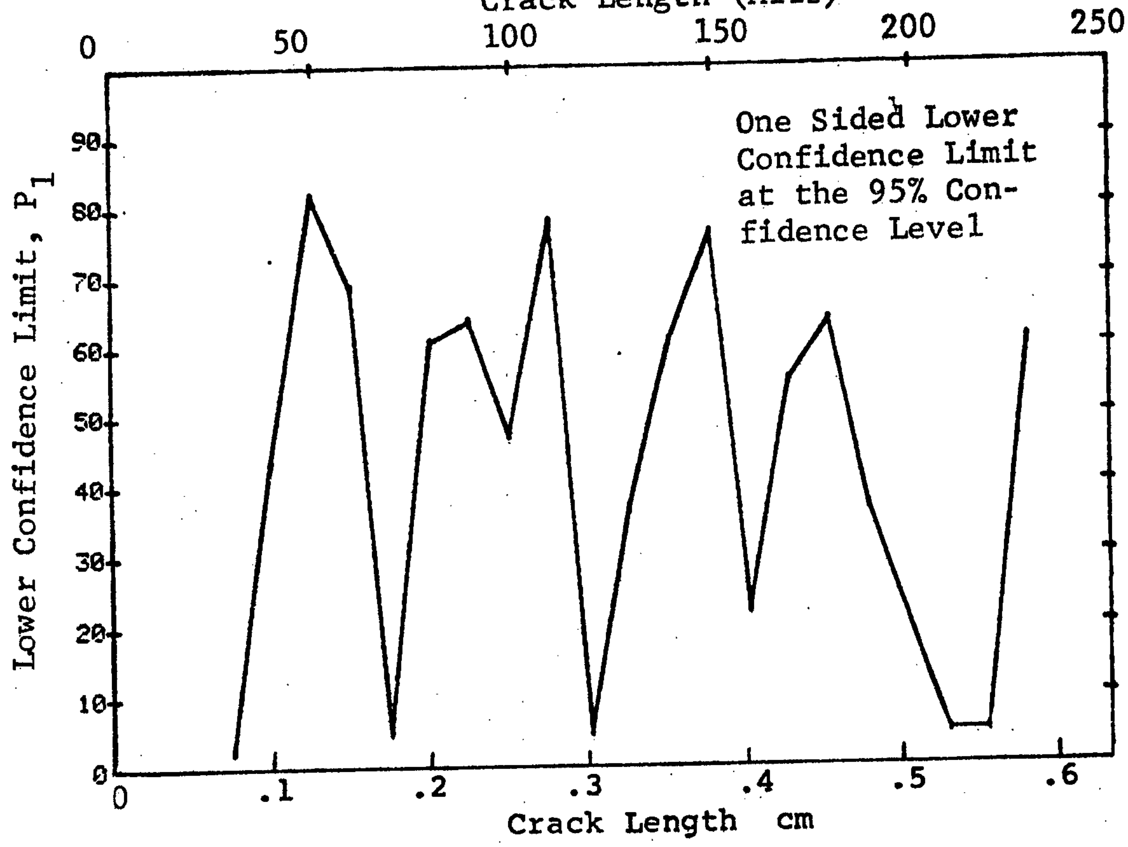

Figure D-92 Probability of Detection for 2024-T6 Al Using X-ray. Compressed Notch Flaws in Tandem T Specimen. Lab. Env.

(b) Optimum Probability Method of Data Cumulation

27-OCT-75 RADIOGRAPHY TEST 2 (92)

RANGE	MIN LN	MAX LN *	N	DET	50%	95%	0 MISS	1 MISS
1	10	10	3	0	0	0	0	0
2	0	0	0	0	0	0	0	0
3	30	30	2	1	0	2	0	0
4	0	0	0	0	0	0	0	0
5	40	40	11	8	0	43	0	0
6	50	50	24	23	0	81	22	37
7	0	0	0	0	0	0	0	0
8	50	60	32	31	0	86	14	29
9	50	70	33	32	0	86	13	28
10	0	0	0	0	0	0	0	0
11	50	80	39	38	0	88	7	22
12	50	90	50	48	0	87	11	26
13	0	0	0	0	0	0	0	0
14	50	100	54	52	0	88	7	22
15	50	110	66	64	0	90	0	10
16	50	120	67	65	0	90	0	9
17	0	0	0	0	0	0	0	0
18	50	130	70	68	0	91	0	6
19	50	140	76	74	0	91	0	0
20	0	0	0	0	0	0	0	0
21	50	150	87	85	0	92	0	0
22	50	160	89	87	0	93	0	0
23	0	0	0	0	0	0	0	0
24	50	170	94	92	0	93	0	0
25	50	180	105	102	0	92	0	0
26	0	0	0	0	0	0	0	0
27	50	190	108	105	0	92	0	0
28	0	0	0	0	0	0	0	0
29	0	0	0	0	0	0	0	0
30	50	210	109	106	0	93	0	0
31	50	220	110	107	0	93	0	0
32	50	230	116	113	0	93	0	0

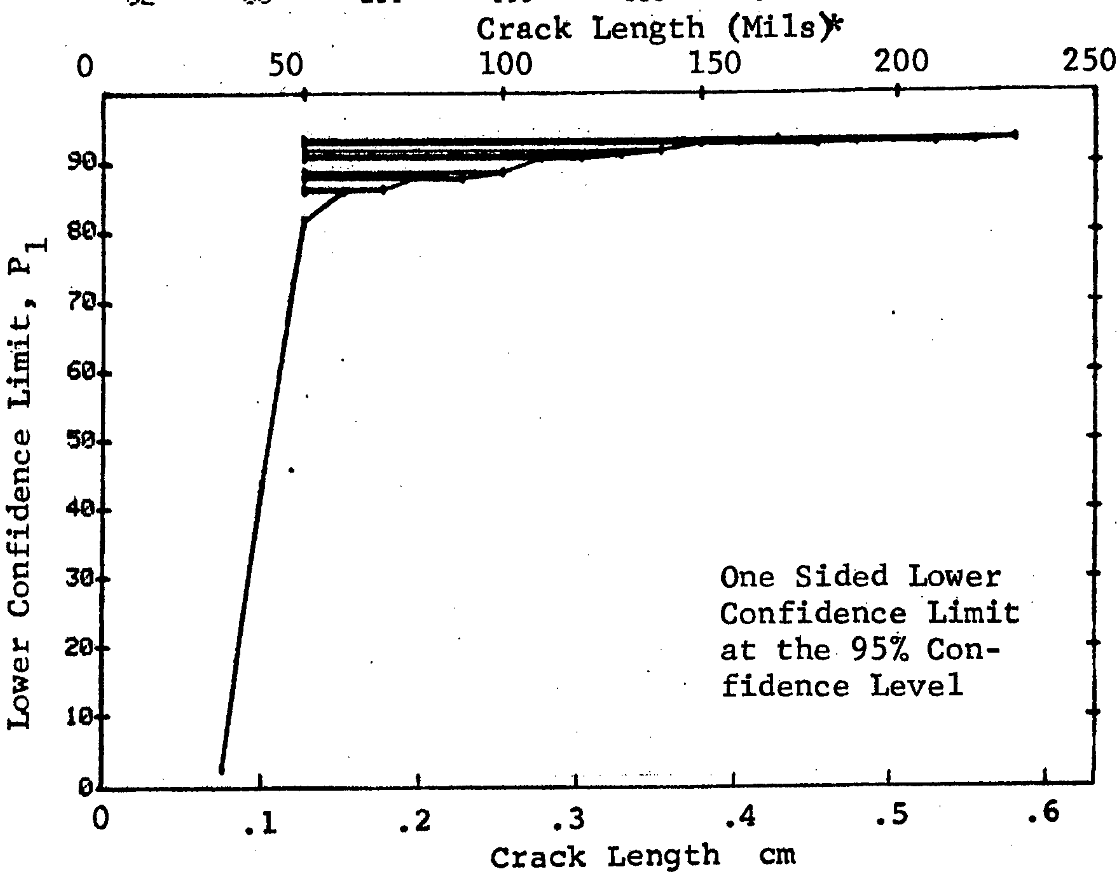

Figure D-92 (Continued)

(c) Overlapping Sixty Point Method of Data Cumulation

27-OCT-75 RADIOGRAPHY TEST 3 (152 (92)

RANGE	MIN LN	MAX LN	N	DET	50%	95%	0 MISS	1 MISS
1	0 *	0 *	0	0	0	0	0	0
2	0	0	0	0	0	0	0	0
3	0	0	0	0	0	0	0	0
4	0	0	0	0	0	0	0	0
5	0	0	0	0	0	0	0	0
6	0	0	0	0	0	0	0	0
7	0	0	0	0	0	0	0	0
8	0	0	0	0	0	0	0	0
9	0	0	0	0	0	0	0	0
10	0	0	0	0	0	0	0	0
11	0	0	0	0	0	0	0	0
12	0	0	0	0	0	0	0	0
13	0	0	0	0	0	0	0	0
14	0	0	0	0	0	0	0	0
15	0	0	0	0	0	0	0	0
16	0	0	0	0	0	0	0	0
17	0	0	0	0	0	0	0	0
18	0	0	0	0	0	0	0	0
19	0	0	0	0	0	0	0	0
20	0	0	0	0	0	0	0	0
21	0	0	0	0	0	0	0	0
22	0	0	0	0	0	0	0	0
23	0	0	0	0	0	0	0	0
24	0	0	0	0	0	0	0	0
25	0	0	0	0	0	0	0	0
26	0	0	0	0	0	0	0	0
27	0	0	0	0	0	0	0	0
28	0	0	0	0	0	0	0	0
29	10	60	42	34	79	68	0	0
30	40	110	60	56	92	85	29	43
31	60	150	60	59	97	92	0	1
32	110	230	60	59	97	92	0	1

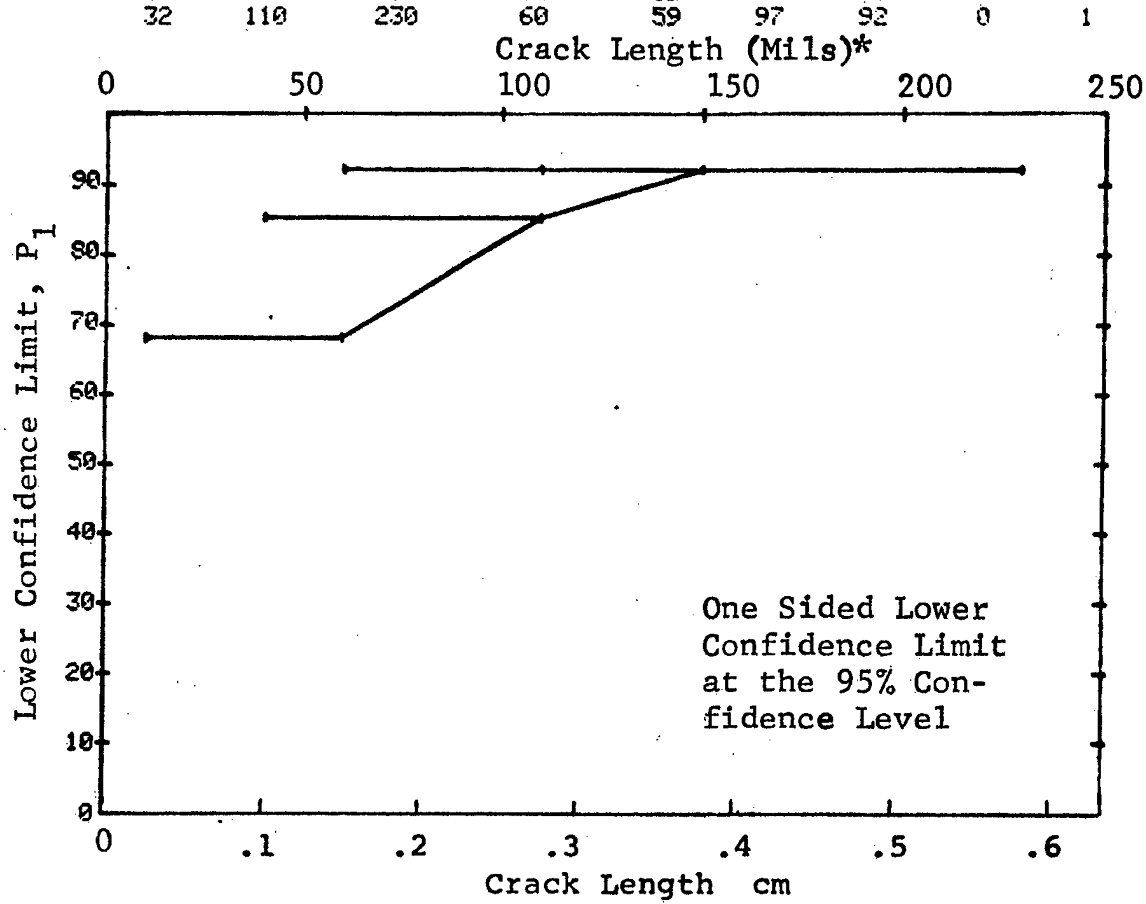

Figure D-92 (Concluded)

(a) Range Interval Method of Data Cumulation

27-OCT-75 MAGNETIC PARTICLE TEST/((93)

RANGE	MIN LN *	MAX LN *	N	DET	50%	95%	0 MISS	1 MISS
1	30	50	20	15	72	54	0	0
2	60	70	27	26	93	83	19	34
3	0	0	0	0	0	0	0	0
4	110	120	23	23	97	87	6	23
5	130	140	34	34	97	91	0	12
6	150	160	23	23	97	87	6	23
7	0	0	0	0	0	0	0	0
8	200	200	5	5	87	54	0	0
9	0	0	0	0	0	0	0	0
10	0	0	0	0	0	0	0	0
11	0	0	0	0	0	0	0	0
12	0	0	0	0	0	0	0	0
13	0	0	0	0	0	0	0	0
14	0	0	0	0	0	0	0	0
15	0	0	0	0	0	0	0	0
16	0	0	0	0	0	0	0	0
17	0	0	0	0	0	0	0	0
18	0	0	0	0	0	0	0	0
19	0	0	0	0	0	0	0	0
20	0	0	0	0	0	0	0	0
21	0	0	0	0	0	0	0	0
22	0	0	0	0	0	0	0	0
23	0	0	0	0	0	0	0	0
24	0	0	0	0	0	0	0	0
25	0	0	0	0	0	0	0	0
26	0	0	0	0	0	0	0	0
27	0	0	0	0	0	0	0	0
28	0	0	0	0	0	0	0	0
29	0	0	0	0	0	0	0	0
30	0	0	0	0	0	0	0	0
31	0	0	0	0	0	0	0	0
32	750	750	3	3	79	36	0	0

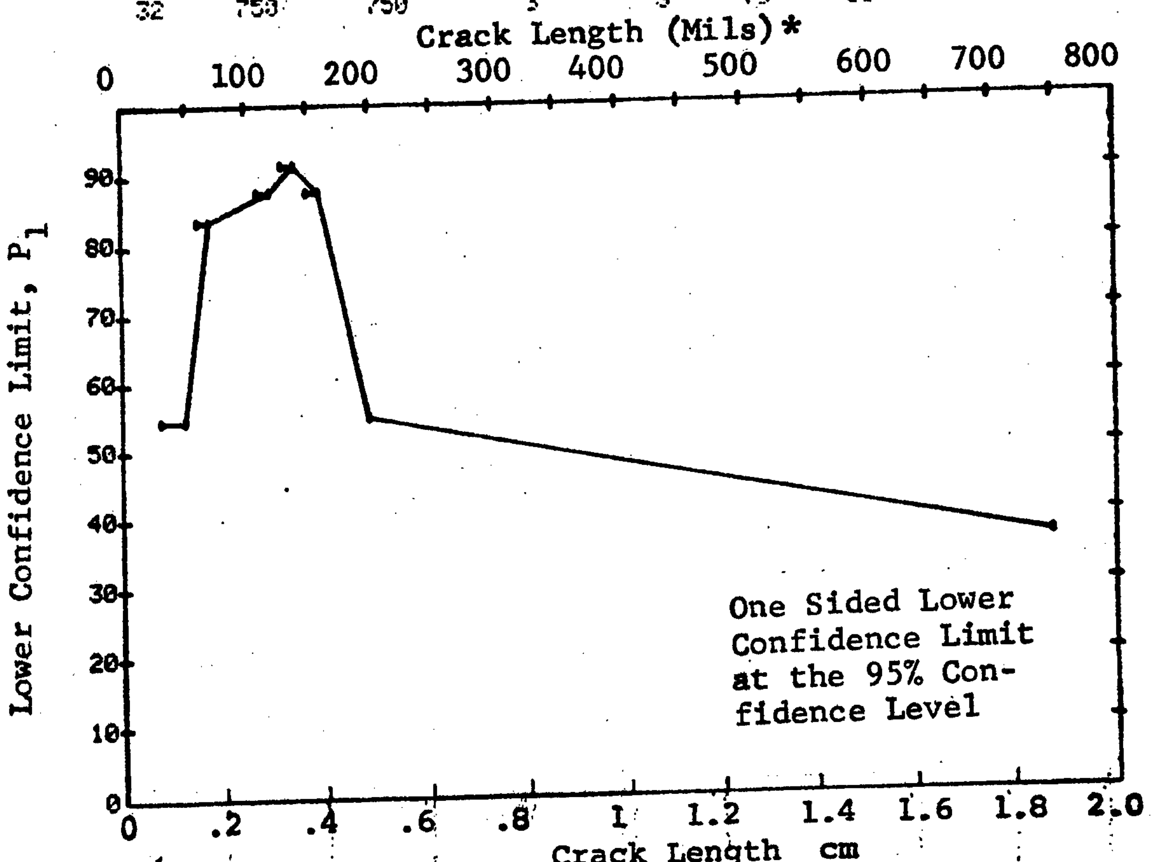

Figure D-93 Probability of Detection for 4340M Steel Using Magnetic Particles. Compressed Notch Flaws in Solid Cylinder. Prod. Env.

(b) Optimum Probability Method of Data Cumulation

27-OCT-75 MAGNETIC PARTICLE TEST 2 ( ) (93)

RANGE	MIN LN *	MAX LN *	N	DET	50%	95%	0 MISS	1 MISS
1	30	50	20	15	0	54	0	0
2	60	70	27	26	0	83	19	34
3	0	0	0	0	0	0	0	0
4	60	120	50	49	0	90	0	11
5	110	140	57	57	0	94	0	0
6	110	160	80	80	0	96	0	0
7	0	0	0	0	0	0	0	0
8	110	200	85	85	0	96	0	0
9	0	0	0	0	0	0	0	0
10	0	0	0	0	0	0	0	0
11	0	0	0	0	0	0	0	0
12	0	0	0	0	0	0	0	0
13	0	0	0	0	0	0	0	0
14	0	0	0	0	0	0	0	0
15	0	0	0	0	0	0	0	0
16	0	0	0	0	0	0	0	0
17	0	0	0	0	0	0	0	0
18	0	0	0	0	0	0	0	0
19	0	0	0	0	0	0	0	0
20	0	0	0	0	0	0	0	0
21	0	0	0	0	0	0	0	0
22	0	0	0	0	0	0	0	0
23	0	0	0	0	0	0	0	0
24	0	0	0	0	0	0	0	0
25	0	0	0	0	0	0	0	0
26	0	0	0	0	0	0	0	0
27	0	0	0	0	0	0	0	0
28	0	0	0	0	0	0	0	0
29	0	0	0	0	0	0	0	0
30	0	0	0	0	0	0	0	0
31	0	0	0	0	0	0	0	0
32	110	750	88	88	0	96	0	0

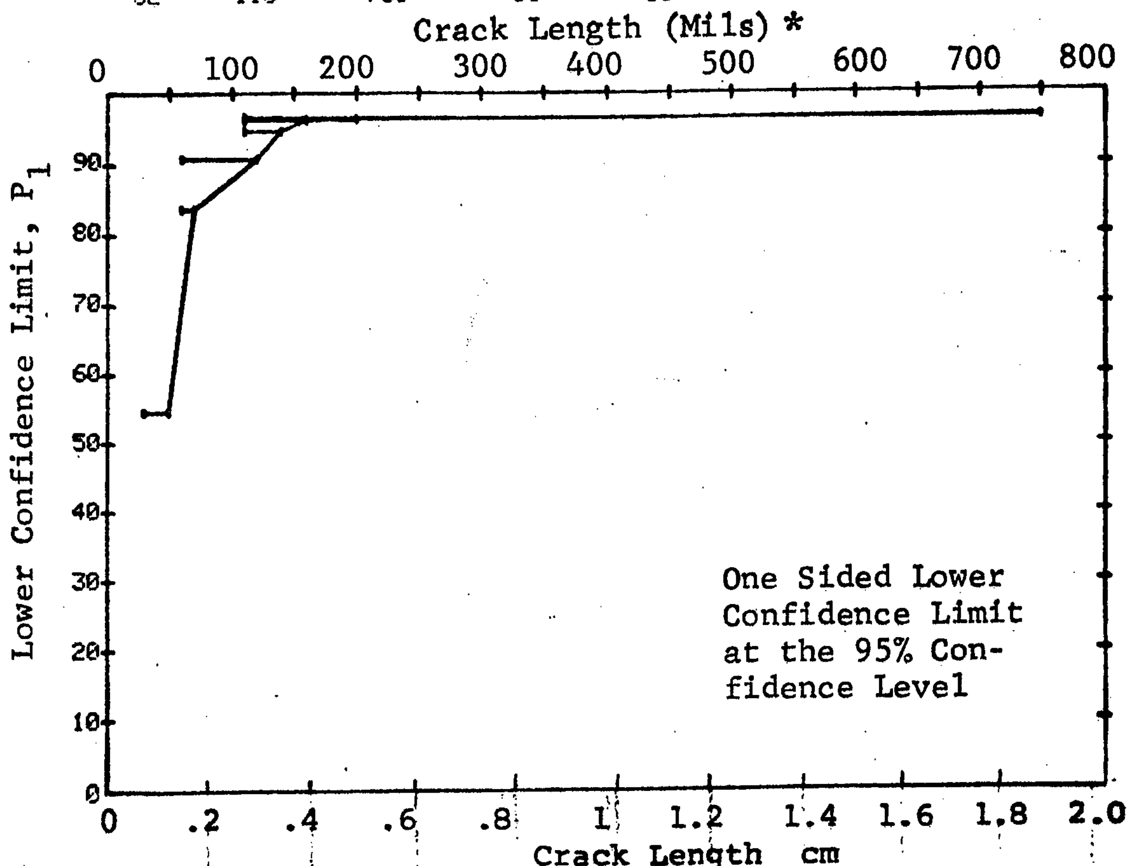

Figure D-93 (Continued)

(c) Overlapping Sixty Point Method of Data Cumulation

27-OCT-75 MAGNETIC PARTICLE TEST 3 (93)

RANGE	MIN LN*	MAX LN*	N	DET	50%	95%	0 MISS	1 MISS
1	0	0	0	0	0	0	0	0
2	0	0	0	0	0	0	0	0
3	0	0	0	0	0	0	0	0
4	0	0	0	0	0	0	0	0
5	0	0	0	0	0	0	0	0
6	0	0	0	0	0	0	0	0
7	0	0	0	0	0	0	0	0
8	0	0	0	0	0	0	0	0
9	0	0	0	0	0	0	0	0
10	0	0	0	0	0	0	0	0
11	0	0	0	0	0	0	0	0
12	0	0	0	0	0	0	0	0
13	0	0	0	0	0	0	0	0
14	0	0	0	0	0	0	0	0
15	0	0	0	0	0	0	0	0
16	0	0	0	0	0	0	0	0
17	0	0	0	0	0	0	0	0
18	0	0	0	0	0	0	0	0
19	0	0	0	0	0	0	0	0
20	0	0	0	0	0	0	0	0
21	0	0	0	0	0	0	0	0
22	0	0	0	0	0	0	0	0
23	0	0	0	0	0	0	0	0
24	0	0	0	0	0	0	0	0
25	0	0	0	0	0	0	0	0
26	0	0	0	0	0	0	0	0
27	0	0	0	0	0	0	0	0
28	0	0	0	0	0	0	0	0
29	30	70	42	36	84	73	0	0
30	50	130	60	58	95	89	1	16
31	70	140	60	60	98	95	0	0
32	130	200	60	60	98	95	0	0

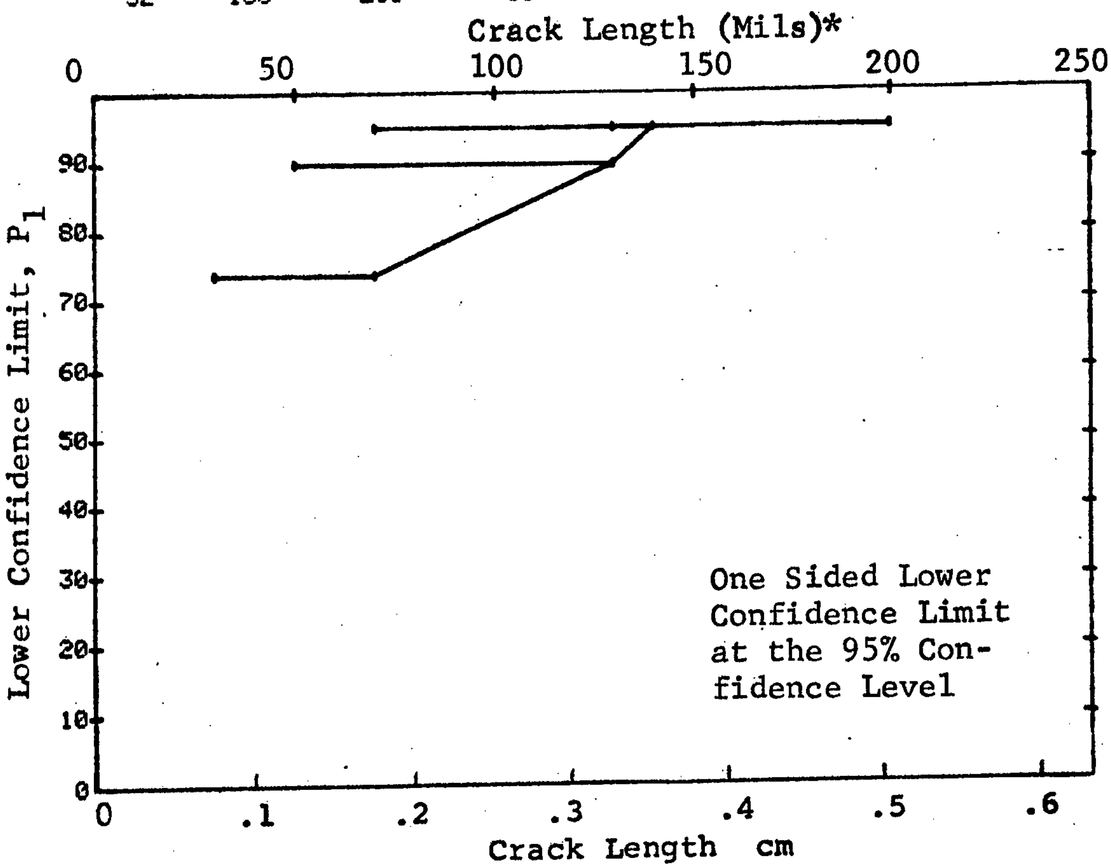

Figure D-93 (Concluded)

(a) Range Interval Method of Data Cumulation

27-OCT-75 MAGNETIC PARTICLE TEST 1 ( ), (94)

RANGE	MIN LN *	MAX LN *	N	DET	50%	95%	0 MISS	1 MISS
1	20	30	13	3	20	6	0	0
2	0	0	0	0	0	0	0	0
3	0	0	0	0	0	0	0	0
4	60	60	9	9	92	71	0	0
5	70	70	16	15	89	73	0	0
6	0	0	0	0	0	0	0	0
7	90	90	11	11	93	76	18	35
8	100	100	8	8	91	68	0	0
9	0	0	0	0	0	0	0	0
10	130	130	4	4	84	47	0	0
11	140	140	7	7	90	65	0	0
12	150	150	9	9	92	71	0	0
13	0	0	0	0	0	0	0	0
14	0	0	0	0	0	0	0	0
15	0	0	0	0	0	0	0	0
16	0	0	0	0	0	0	0	0
17	0	0	0	0	0	0	0	0
18	0	0	0	0	0	0	0	0
19	0	0	0	0	0	0	0	0
20	0	0	0	0	0	0	0	0
21	0	0	0	0	0	0	0	0
22	260	260	2	2	70	22	0	0
23	0	0	0	0	0	0	0	0
24	0	0	0	0	0	0	0	0
25	300	300	5	5	87	54	0	0
26	0	0	0	0	0	0	0	0
27	0	0	0	0	0	0	0	0
28	0	0	0	0	0	0	0	0
29	0	0	0	0	0	0	0	0
30	0	0	0	0	0	0	0	0
31	0	0	0	0	0	0	0	0
32	370	380	5	5	87	54	0	0

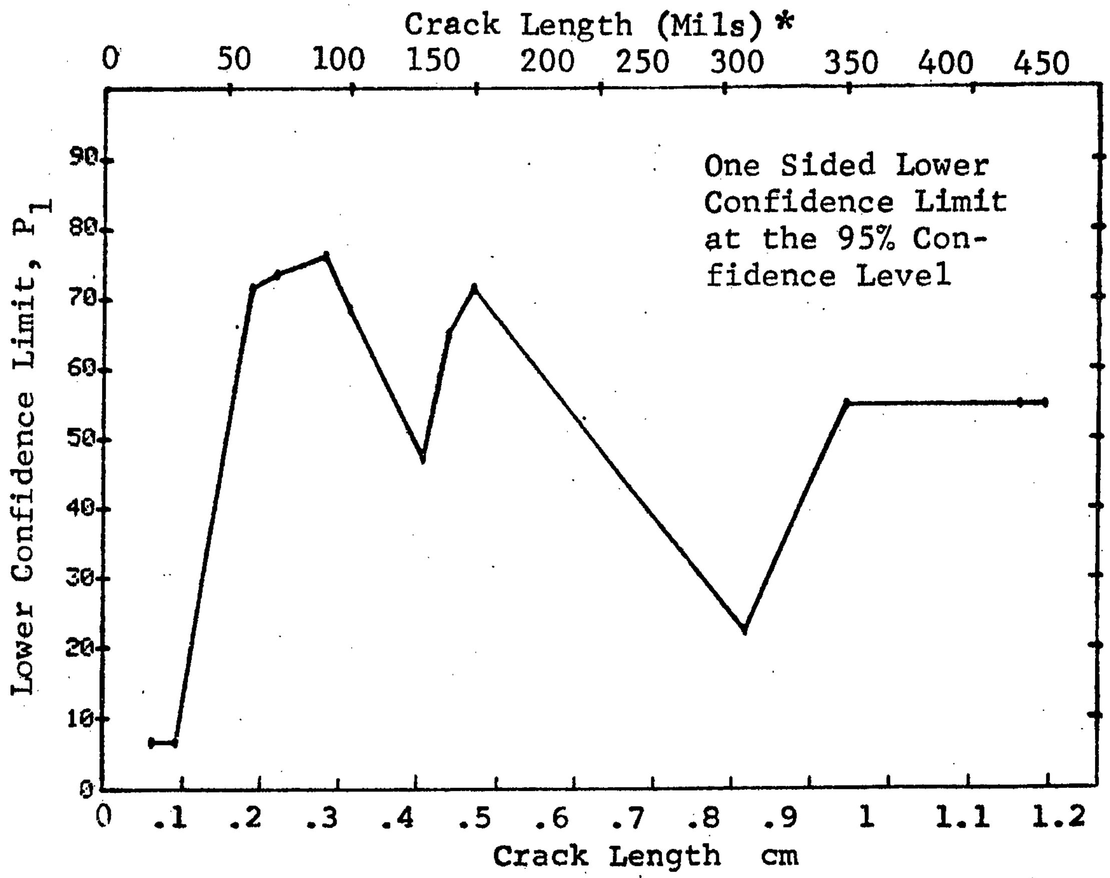

Figure D-94 Probability of Detection for 4340M Steel Using Magnetic Particles. Compressed Notch Flaws in Hollow Filleted Cylinder. Prod. Env.

(b) Optimum Probability Method of Data Cumulation

27-OCT-75 MAGNETIC PARTICLE TEST 2 .: (94)).7Y

RANGE	MIN LN *	MAX LN *	N	DET	50%	95%	0 MISS	1 MISS
1	20	30	13	3	0	6	0	0
2	0	0	0	0	0	0	0	0
3	0	0	0	0	0	0	0	0
4	60	60	9	9	0	71	0	0
5	60	70	25	24	0	82	21	36
6	0	0	0	0	0	0	0	0
7	60	90	36	35	0	87	10	25
8	60	100	44	43	0	89	2	17
9	0	0	0	0	0	0	0	0
10	60	130	48	47	0	90	0	13
11	60	140	55	54	0	91	0	5
12	60	150	64	63	0	92	0	0
13	0	0	0	0	0	0	0	0
14	0	0	0	0	0	0	0	0
15	0	0	0	0	0	0	0	0
16	0	0	0	0	0	0	0	0
17	0	0	0	0	0	0	0	0
18	0	0	0	0	0	0	0	0
19	0	0	0	0	0	0	0	0
20	0	0	0	0	0	0	0	0
21	0	0	0	0	0	0	0	0
22	60	260	66	65	0	93	0	0
23	0	0	0	0	0	0	0	0
24	0	0	0	0	0	0	0	0
25	90	300	46	46	0	93	0	0
26	0	0	0	0	0	0	0	0
27	0	0	0	0	0	0	0	0
28	0	0	0	0	0	0	0	0
29	0	0	0	0	0	0	0	0
30	0	0	0	0	0	0	0	0
31	0	0	0	0	0	0	0	0
32	90	380	51	51	0	94	0	0

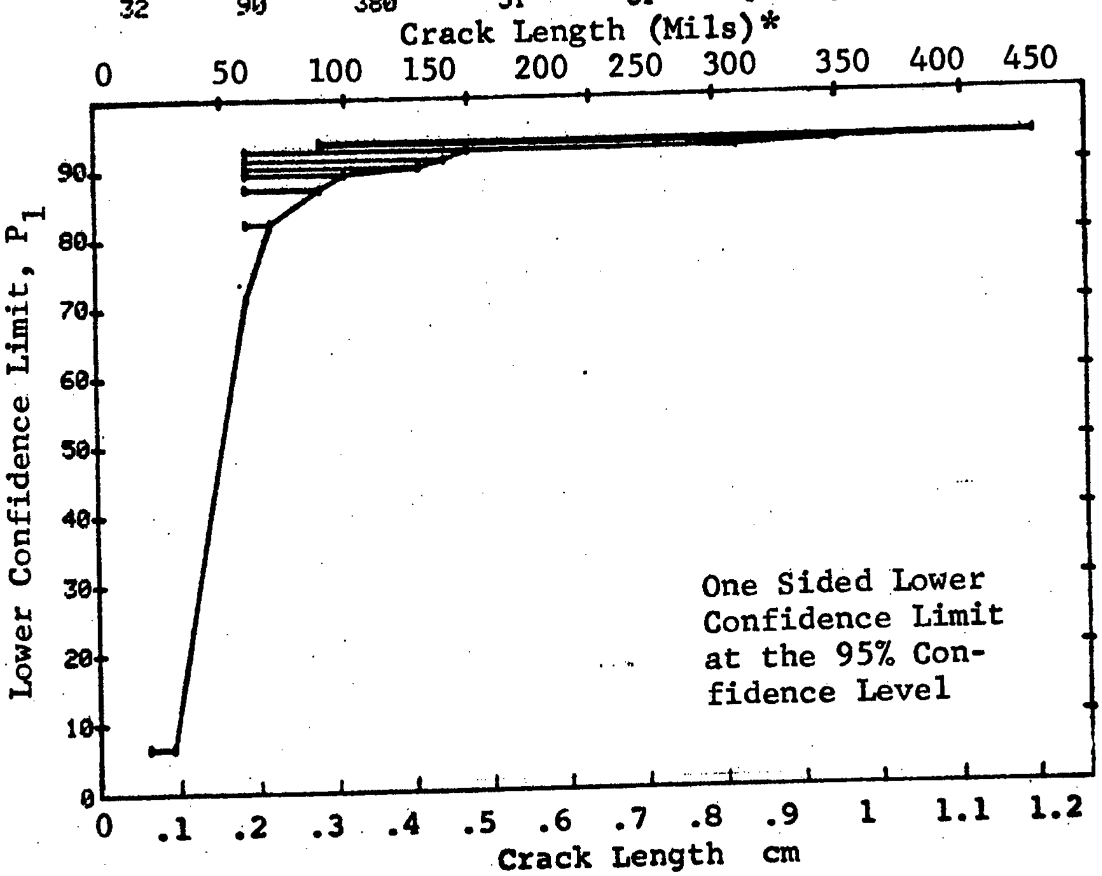

Figure D-94 (Continued)

(c) Overlapping Sixty Point Method of Data Cumulation

27-OCT-75 MAGNETIC PARTICLE TEST 3 (. (94)

RANGE	MIN LN	MAX LN	N	DET	50%	95%	0 MISS	1 MISS
1	0 *	0*	0	0	0	0	0	0
2	0	0	0	0	0	0	0	0
3	0	0	0	0	0	0	0	0
4	0	0	0	0	0	0	0	0
5	0	0	0	0	0	0	0	0
6	0	0	0	0	0	0	0	0
7	0	0	0	0	0	0	0	0
8	0	0	0	0	0	0	0	0
9	0	0	0	0	0	0	0	0
10	0	0	0	0	0	0	0	0
11	0	0	0	0	0	0	0	0
12	0	0	0	0	0	0	0	0
13	0	0	0	0	0	0	0	0
14	0	0	0	0	0	0	0	0
15	0	0	0	0	0	0	0	0
16	0	0	0	0	0	0	0	0
17	0	0	0	0	0	0	0	0
18	0	0	0	0	0	0	0	0
19	0	0	0	0	0	0	0	0
20	0	0	0	0	0	0	0	0
21	0	0	0	0	0	0	0	0
22	0	0	0	0	0	0	0	0
23	0	0	0	0	0	0	0	0
24	0	0	0	0	0	0	0	0
25	0	0	0	0	0	0	0	0
26	0	0	0	0	0	0	0	0
27	0	0	0	0	0	0	0	0
28	0	0	0	0	0	0	0	0
29	0	0	0	0	0	0	0	0
30	0	0	0	0	0	0	0	0
31	20	130	59	48	80	71	0	0
32	70	380	60	59	97	92	0	1

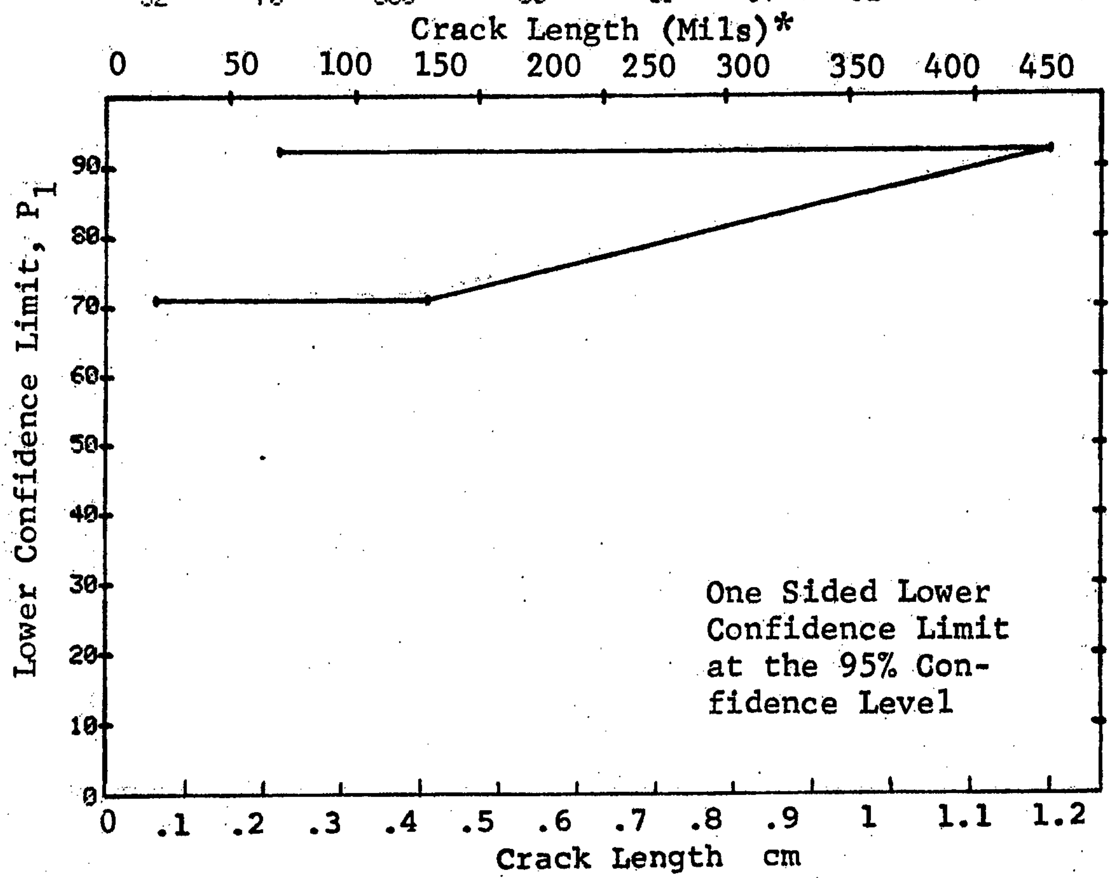

Figure D-94 (Concluded)

(a) Range Interval Method of Data Cumulation

27-OCT-75 MAGNETIC PARTICLE TEST 1 75 (95)

RANGE	MIN LN	MAX LN	N	DET	50%	95%	0 MISS	1 MISS
1	60 *	60 *	3	0	0	0	0	0
2	0	0	0	0	0	0	0	0
3	100	100	13	5	35	16	0	0
4	120	120	4	1	15	1	0	0
5	130	130	2	1	29	2	0	0
6	140	140	6	3	42	15	0	0
7	160	160	3	1	20	1	0	0
8	180	180	4	2	38	9	0	0
9	0	0	0	0	0	0	0	0
10	0	0	0	0	0	0	0	0
11	230	230	2	1	29	2	0	0
12	0	0	0	0	0	0	0	0
13	0	0	0	0	0	0	0	0
14	0	0	0	0	0	0	0	0
15	0	0	0	0	0	0	0	0
16	310	310	4	3	61	24	0	0
17	0	0	0	0	0	0	0	0
18	0	0	0	0	0	0	0	0
19	350	350	10	9	83	60	0	0
20	0	0	0	0	0	0	0	0
21	390	390	4	4	84	47	0	0
22	0	0	0	0	0	0	0	0
23	0	0	0	0	0	0	0	0
24	0	0	0	0	0	0	0	0
25	0	0	0	0	0	0	0	0
26	0	0	0	0	0	0	0	0
27	0	0	0	0	0	0	0	0
28	0	0	0	0	0	0	0	0
29	0	0	0	0	0	0	0	0
30	0	0	0	0	0	0	0	0
31	0	0	0	0	0	0	0	0
32	570	570	4	4	84	47	0	0

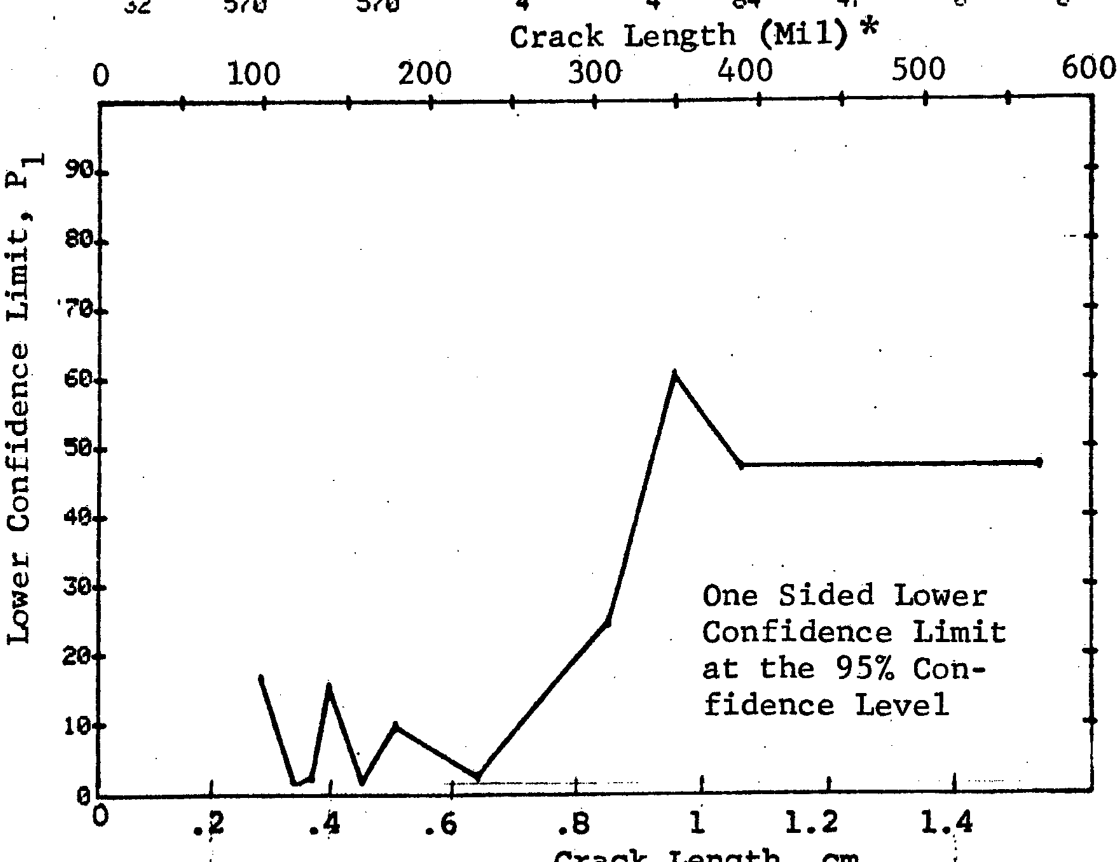

Figure D-95 Probability of Detection for 4340M Steel Using Magnetic Particles. Compressed Notch Flaws in Hollow Filleted Cylinder. Prod. Env.

(b) Optimum Probability Method of Data Cumulation

27-OCT-75 MAGNETIC PARTICLE TEST 2 (A5) 175

RANGE	MIN LN	MAX LN	N	DET	50%	95%	0 MISS	1 MISS
1	60 *	60 *	3	0	0	0	0	0
2	0*	0*	0	0	0	0	0	0
3	100	100	13	5	0	16	0	0
4	100	120	17	6	0	16	0	0
5	100	130	19	7	0	18	0	0
6	100	140	25	10	0	23	0	0
7	100	160	28	11	0	23	0	0
8	100	180	32	13	0	25	0	0
9	0	0	0	0	0	0	0	0
10	0	0	0	0	0	0	0	0
11	100	230	34	14	0	26	0	0
12	0	0	0	0	0	0	0	0
13	0	0	0	0	0	0	0	0
14	0	0	0	0	0	0	0	0
15	0	0	0	0	0	0	0	0
16	130	310	21	11	0	32	0	0
17	0	0	0	0	0	0	0	0
18	0	0	0	0	0	0	0	0
19	310	350	14	12	0	61	0	0
20	0	0	0	0	0	0	0	0
21	350	390	14	13	0	70	0	0
22	0	0	0	0	0	0	0	0
23	0	0	0	0	0	0	0	0
24	0	0	0	0	0	0	0	0
25	0	0	0	0	0	0	0	0
26	0	0	0	0	0	0	0	0
27	0	0	0	0	0	0	0	0
28	0	0	0	0	0	0	0	0
29	0	0	0	0	0	0	0	0
30	0	0	0	0	0	0	0	0
31	0	0	0	0	0	0	0	0
32	350	570	19	17	0	76	0	0

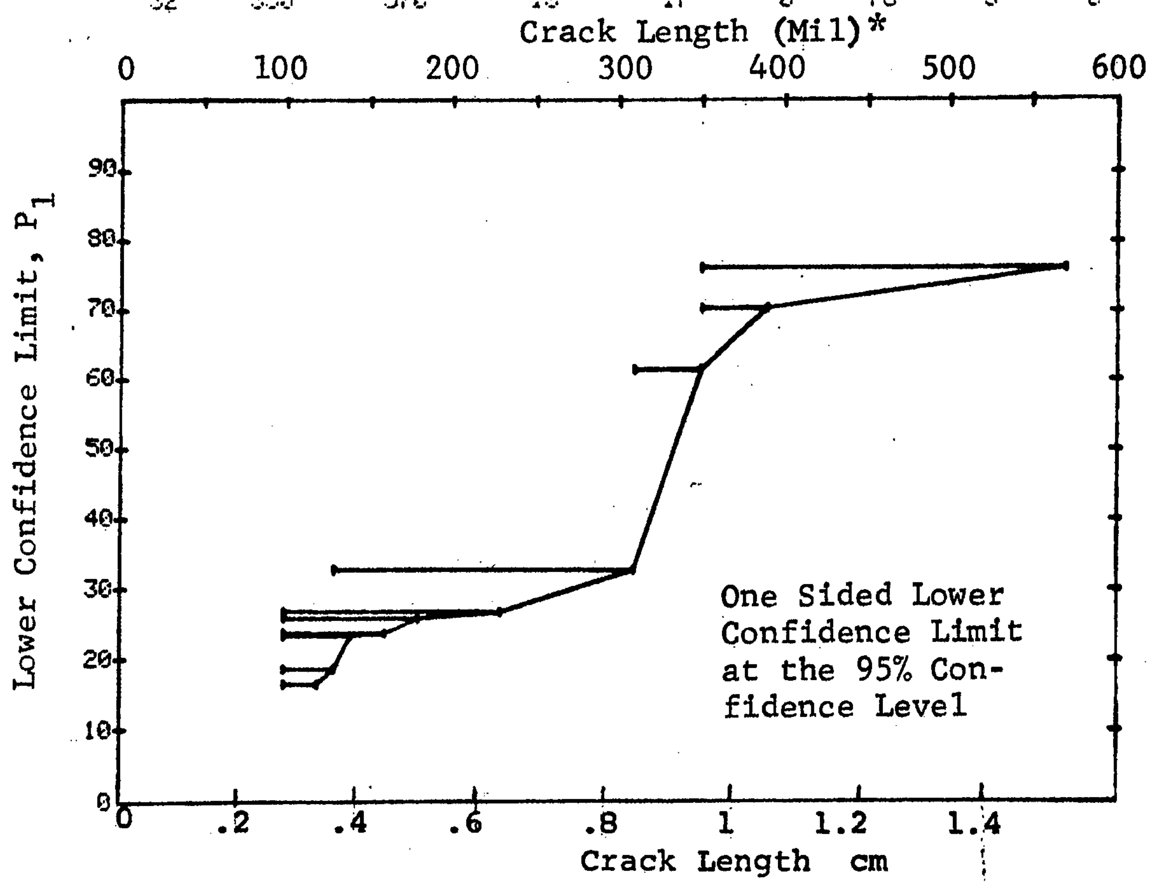

Figure D-95 (Continued)

(c) Overlapping Sixty Point Method of Data Cumulation

27-OCT-75 MAGNETIC PARTICLE TEST 3 (95)

RANGE	MIN LN	MAX LN	N	DET	50%	95%	0 MISS	1 MISS
1	0 *	0 *	0	0	0	0	0	0
2	0	0	0	0	0	0	0	0
3	0	0	0	0	0	0	0	0
4	0	0	0	0	0	0	0	0
5	0	0	0	0	0	0	0	0
6	0	0	0	0	0	0	0	0
7	0	0	0	0	0	0	0	0
8	0	0	0	0	0	0	0	0
9	0	0	0	0	0	0	0	0
10	0	0	0	0	0	0	0	0
11	0	0	0	0	0	0	0	0
12	0	0	0	0	0	0	0	0
13	0	0	0	0	0	0	0	0
14	0	0	0	0	0	0	0	0
15	0	0	0	0	0	0	0	0
16	0	0	0	0	0	0	0	0
17	0	0	0	0	0	0	0	0
18	0	0	0	0	0	0	0	0
19	0	0	0	0	0	0	0	0
20	0	0	0	0	0	0	0	0
21	0	0	0	0	0	0	0	0
22	0	0	0	0	0	0	0	0
23	0	0	0	0	0	0	0	0
24	0	0	0	0	0	0	0	0
25	0	0	0	0	0	0	0	0
26	0	0	0	0	0	0	0	0
27	0	0	0	0	0	0	0	0
28	0	0	0	0	0	0	0	0
29	0	0	0	0	0	0	0	0
30	0	0	0	0	0	0	0	0
31	0	0	0	0	0	0	0	0
32	60	390	55	30	53	42	0	0

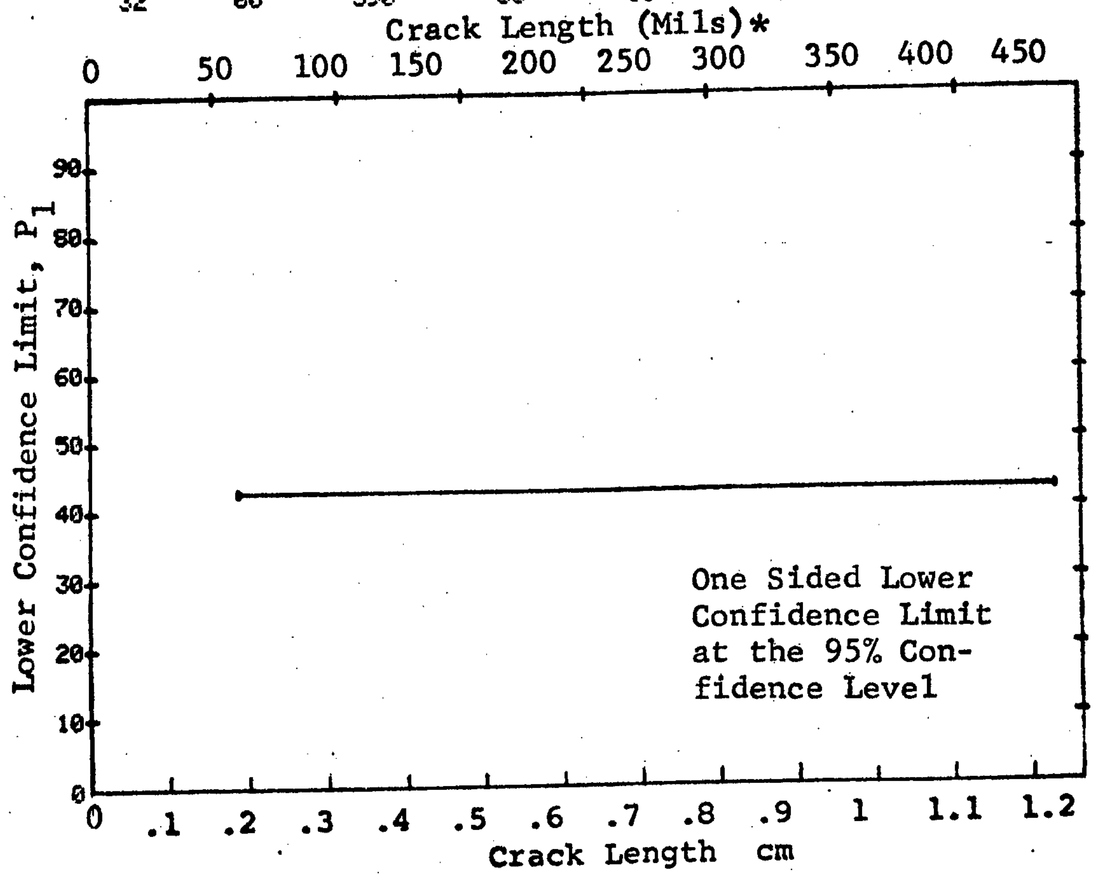

Figure D-95 (Concluded)

(a) Range Interval Method of Data Cumulation

28-OCT-75 MAGNETIC PARTICLE TEST 1 ( ) (96)

RANGE	MIN LN	MAX LN	N	DET	50%	95%	0 MISS	1 MISS
1	80 *	90 *	10	2	16	3	0	0
2	0	0	0	0	0	0	0	0
3	110	110	4	0	0	0	0	0
4	120	120	3	2	50	13	0	0
5	130	130	3	0	0	0	0	0
6	140	140	8	1	8	0	0	0
7	160	160	3	1	20	1	0	0
8	0	0	0	0	0	0	0	0
9	0	0	0	0	0	0	0	0
10	0	0	0	0	0	0	0	0
11	0	0	0	0	0	0	0	0
12	0	0	0	0	0	0	0	0
13	0	0	0	0	0	0	0	0
14	0	0	0	0	0	0	0	0
15	250	250	2	1	29	2	0	0
16	270	270	5	2	31	7	0	0
17	280	280	2	1	29	2	0	0
18	0	0	0	0	0	0	0	0
19	300	300	3	2	50	13	0	0
20	310	310	3	2	50	13	0	0
21	0	0	0	0	0	0	0	0
22	0	0	0	0	0	0	0	0
23	0	0	0	0	0	0	0	0
24	0	0	0	0	0	0	0	0
25	0	0	0	0	0	0	0	0
26	0	0	0	0	0	0	0	0
27	0	0	0	0	0	0	0	0
28	0	0	0	0	0	0	[illegible]	[illegible]
29	0	0	0	0	0	[illegible]	[illegible]	[illegible]
30	0	0	0	0	0	0	0	0
31	440	440	3	3	79	36	0	0
32	450	460	5	2	31	[illegible]	[illegible]	0

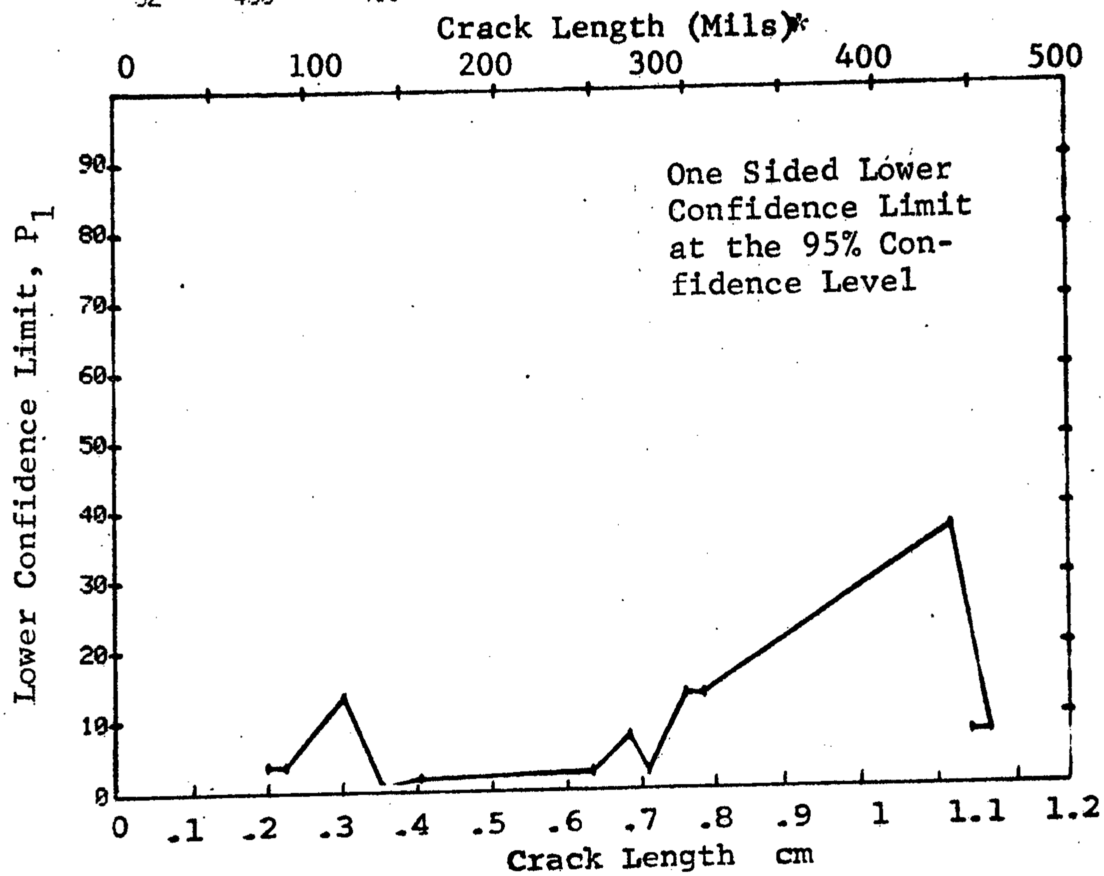

Figure D-96 Probability of Detection for 4340M Steel Using Magnetic Particles. Compressed Notch Flaws in Hollow Filleted Cylinder Prod. Env.

(b) Optimum Probability Method of Data Cumulation

28-OCT-75 MAGNETIC PARTICLE TEST 2 (96)

RANGE	MIN LN	MAX LN	N	DET	50%	95%	0 MISS	1 MISS
1	80*	90*	10	2	0	3	0	0
2	0	0	0	0	0	0	0	0
3	80	110	14	2	0	2	0	0
4	120	120	3	2	0	13	0	0
5	80	130	20	4	0	7	0	0
6	80	140	28	5	0	7	0	0
7	80	160	31	6	0	8	0	0
8	0	0	0	0	0	0	0	0
9	0	0	0	0	0	0	0	0
10	0	0	0	0	0	0	0	0
11	0	0	0	0	0	0	0	0
12	0	0	0	0	0	0	0	0
13	0	0	0	0	0	0	0	0
14	0	0	0	0	0	0	0	0
15	120	250	19	5	0	10	0	0
16	160	270	10	4	0	15	0	0
17	160	280	12	5	0	18	0	0
18	0	0	0	0	0	0	0	0
19	250	300	12	6	0	24	0	0
20	250	310	15	8	0	29	0	0
21	0	0	0	0	0	0	0	0
22	0	0	0	0	0	0	0	0
23	0	0	0	0	0	0	0	0
24	0	0	0	0	0	0	0	0
25	0	0	0	0	0	0	0	0
26	0	0	0	0	0	0	0	0
27	0	0	0	0	0	0	0	0
28	0	0	0	0	0	0	0	0
29	0	0	0	0	0	0	0	0
30	0	0	0	0	0	0	0	0
31	300	440	9	7	0	45	0	0
32	300	460	14	9	0	39	0	0

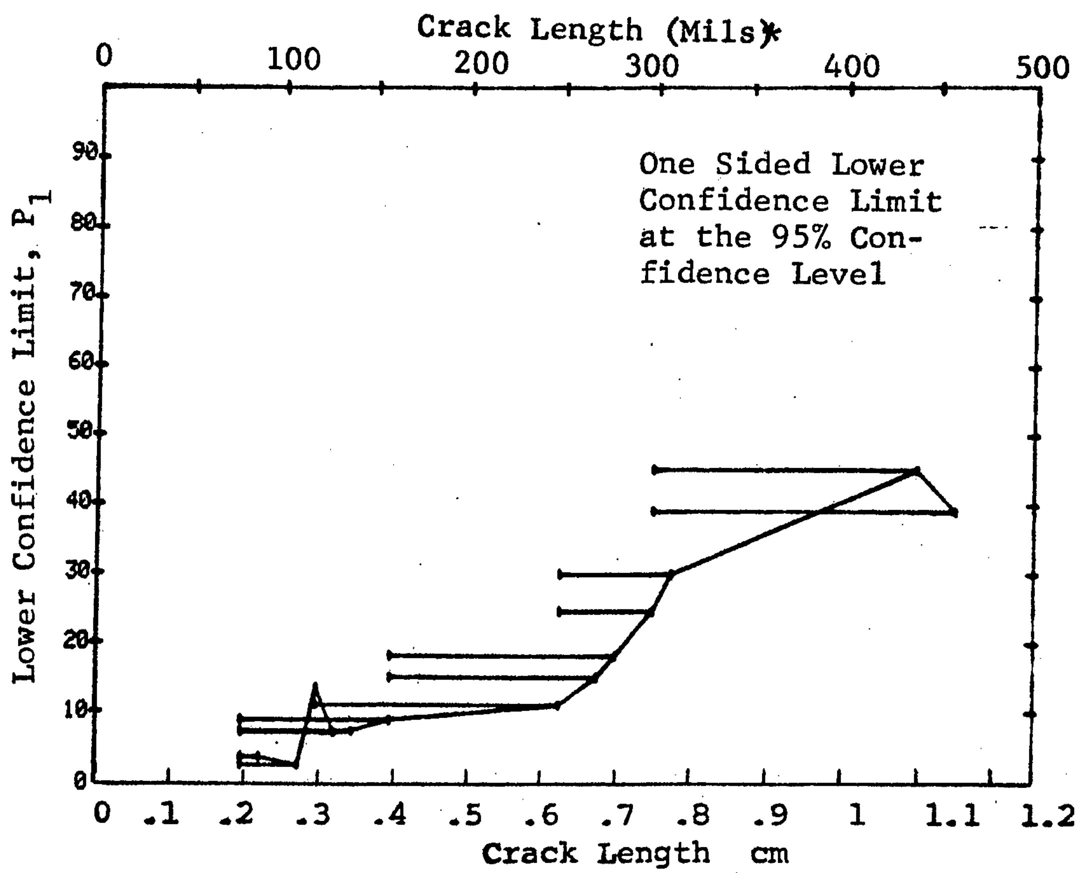

Figure D-96 (Continued)

(c) Overlapping Sixty Point Method of Data Cumulation

28-OCT-75 MAGNETIC PARTICLE TEST 3 (96)

RANGE	MIN LN *	MAX LN *	N	DET	50%	95%	0 MISS	1 MISS
1	0	0	0	0	0	0	0	0
2	0	0	0	0	0	0	0	0
3	0	0	0	0	0	0	0	0
4	0	0	0	0	0	0	0	0
5	0	0	0	0	0	0	0	0
6	0	0	0	0	0	0	0	0
7	0	0	0	0	0	0	0	0
8	0	0	0	0	0	0	0	0
9	0	0	0	0	0	0	0	0
10	0	0	0	0	0	0	0	0
11	0	0	0	0	0	0	0	0
12	0	0	0	0	0	0	0	0
13	0	0	0	0	0	0	0	0
14	0	0	0	0	0	0	0	0
15	0	0	0	0	0	0	0	0
16	0	0	0	0	0	0	0	0
17	0	0	0	0	0	0	0	0
18	0	0	0	0	0	0	0	0
19	0	0	0	0	0	0	0	0
20	0	0	0	0	0	0	0	0
21	0	0	0	0	0	0	0	0
22	0	0	0	0	0	0	0	0
23	0	0	0	0	0	0	0	0
24	0	0	0	0	0	0	0	0
25	0	0	0	0	0	0	0	0
26	0	0	0	0	0	0	0	0
27	0	0	0	0	0	0	0	0
28	0	0	0	0	0	0	0	0
29	0	0	0	0	0	0	0	0
30	0	0	0	0	0	0	0	0
31	0	0	0	0	0	0	0	0
32	80	460	54	19	34	24	0	0

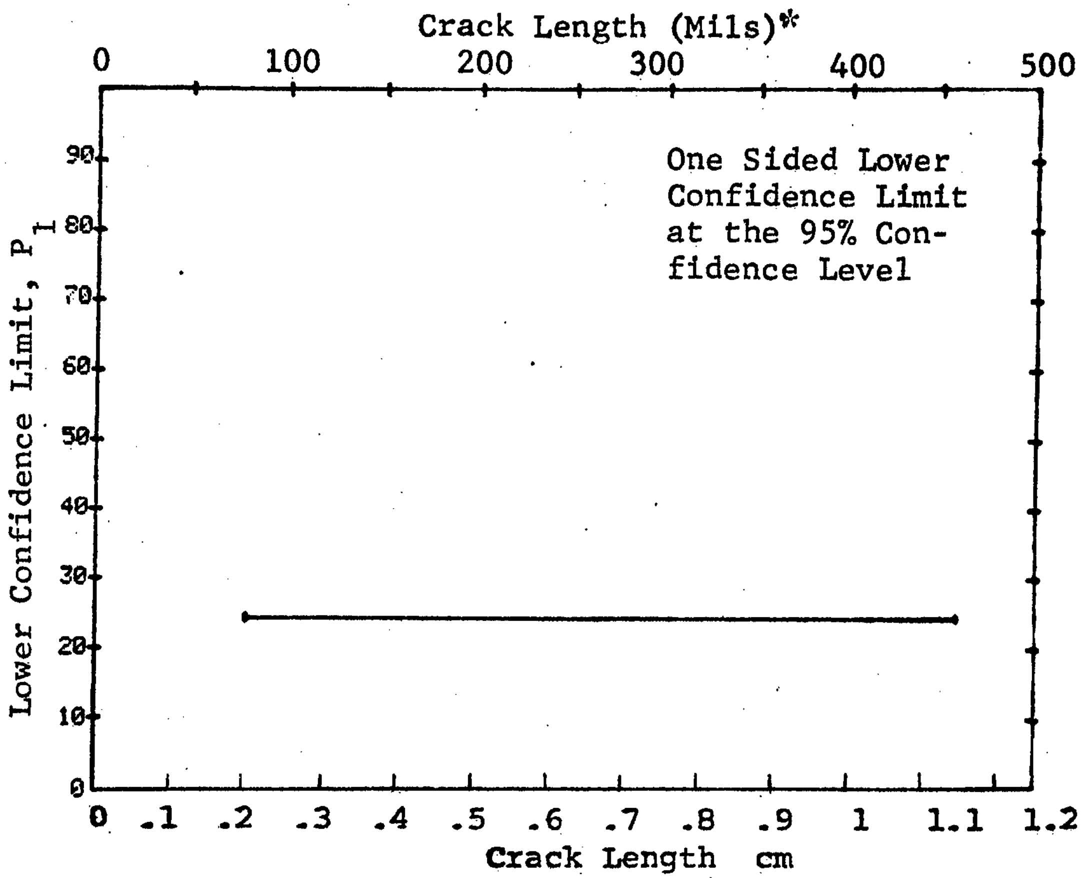

Figure D-96 (Concluded)

(a) Range Interval Method of Data Cumulation

27-OCT-75 MAGNETIC PARTICLE TEST 1 (97)

RANGE	MIN LN *	MAX LN *	N	DET	50%	95%	0 MISS	1 MISS
1	40	40	3	2	50	13	0	0
2	70	70	3	0	0	0	0	0
3	0	0	0	0	0	0	0	0
4	100	110	14	8	53	32	0	0
5	130	130	7	2	22	5	0	0
6	0	0	0	0	0	0	0	0
7	0	0	0	0	0	0	0	0
8	190	190	1	0	0	0	0	0
9	210	210	3	2	50	13	0	0
10	230	230	2	2	70	22	0	0
11	0	0	0	0	0	0	0	0
12	250	250	5	5	87	54	0	0
13	270	270	2	2	70	22	0	0
14	300	300	3	3	79	36	0	0
15	310	310	3	3	79	36	0	0
16	0	0	0	0	0	0	0	0
17	350	350	2	2	70	22	0	0
18	380	380	2	2	70	22	0	0
19	0	0	0	0	0	0	0	0
20	410	410	2	2	70	22	0	0
21	0	0	0	0	0	0	0	0
22	450	450	2	2	70	22	0	0
23	460	460	1	1	50	5	0	0
24	480	480	2	2	70	22	0	0
25	0	0	0	0	0	0	0	0
26	0	0	0	0	0	0	0	0
27	0	0	0	0	0	0	0	0
28	0	0	0	0	0	0	0	0
29	0	0	0	0	0	0	0	0
30	0	0	0	0	0	0	0	0
31	0	0	0	0	0	0	0	0
32	650	650	1	1	50	5	0	0

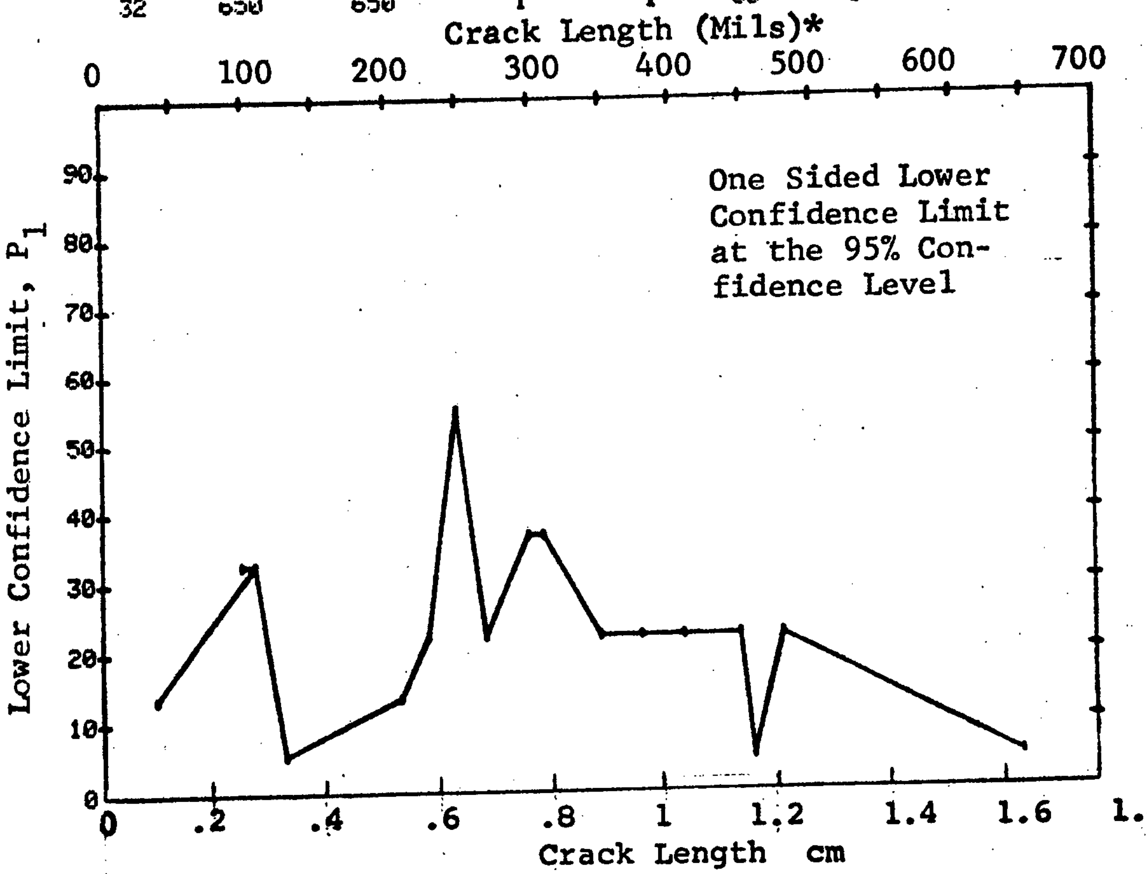

Figure D-97 Probability of Detection for 4340M Steel Using Magnetic Particles. Compressed Notch Flaws in Solid Threaded Cylinder. Prod. Env.

(b) Optimum Probability Method of Data Cumulation

27-OCT-75 MAGNETIC PARTICLE TEST 2 (97)

RANGE	MIN LN	MAX LN	N	DET	50%	95%	0 MISS	1 MISS
1	40*	40 *	3	2	0	13	0	0
2	40	70	6	2	0	6	0	0
3	0	0	0	0	0	0	0	0
4	100	110	14	8	0	32	0	0
5	100	130	21	10	0	28	0	0
6	0	0	0	0	0	0	0	0
7	0	0	0	0	0	0	0	0
8	100	190	22	10	0	27	0	0
9	100	210	25	12	0	30	0	0
10	100	230	27	14	0	34	0	0
11	0	0	0	0	0	0	0	0
12	230	250	7	7	0	65	0	0
13	230	270	9	9	0	71	0	0
14	230	300	12	12	0	77	0	0
15	230	310	15	15	0	81	14	31
16	0	0	0	0	0	0	0	0
17	230	350	17	17	0	83	12	29
18	230	380	19	19	0	85	10	27
19	0	0	0	0	0	0	0	0
20	230	410	21	21	0	86	8	25
21	0	0	0	0	0	0	0	0
22	230	450	23	23	0	87	6	23
23	230	460	24	24	0	88	5	22
24	230	480	26	26	0	89	3	20
25	0	0	0	0	0	0	0	0
26	0	0	0	0	0	0	0	0
27	0	0	0	0	0	0	0	0
28	0	0	0	0	0	0	0	0
29	0	0	0	0	0	0	0	0
30	0	0	0	0	0	0	0	0
31	0	0	0	0	0	0	0	0
32	230	650	27	27	0	89	2	19

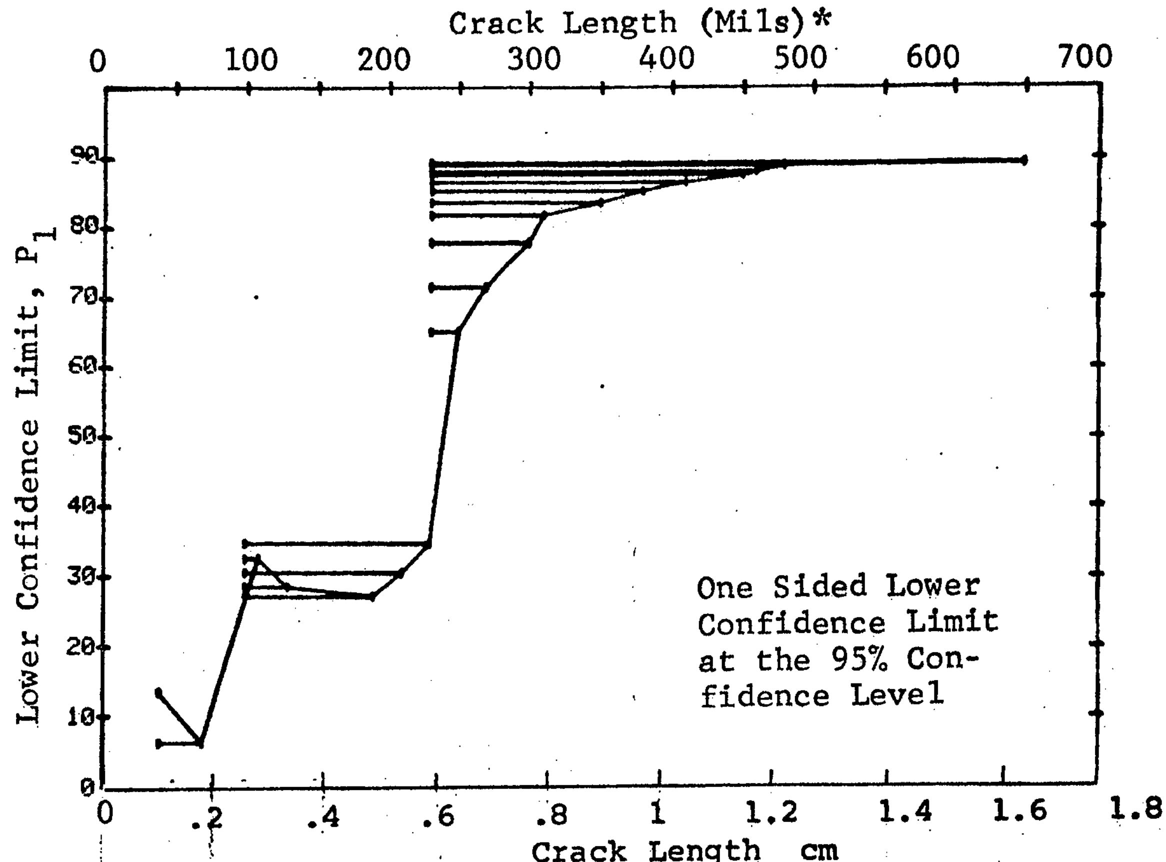

Figure D-97 (Continued)

(c) Overlapping Sixty Point Method of Data Cumulation

27-OCT-75 MAGNETIC PARTICLE TEST 3 ( ) (97)

RANGE	MIN LN *	MAX LN *	N	DET	50%	95%	0 MISS	1 MISS
1	0	0	0	0	0	0	0	0
2	0	0	0	0	0	0	0	0
3	0	0	0	0	0	0	0	0
4	0	0	0	0	0	0	0	0
5	0	0	0	0	0	0	0	0
6	0	0	0	0	0	0	0	0
7	0	0	0	0	0	0	0	0
8	0	0	0	0	0	0	0	0
9	0	0	0	0	0	0	0	0
10	0	0	0	0	0	0	0	0
11	0	0	0	0	0	0	0	0
12	0	0	0	0	0	0	0	0
13	0	0	0	0	0	0	0	0
14	0	0	0	0	0	0	0	0
15	0	0	0	0	0	0	0	0
16	0	0	0	0	0	0	0	0
17	0	0	0	0	0	0	0	0
18	0	0	0	0	0	0	0	0
19	0	0	0	0	0	0	0	0
20	0	0	0	0	0	0	0	0
21	0	0	0	0	0	0	0	0
22	0	0	0	0	0	0	0	0
23	0	0	0	0	0	0	0	0
24	0	0	0	0	0	0	0	0
25	0	0	0	0	0	0	0	0
26	0	0	0	0	0	0	0	0
27	0	0	0	0	0	0	0	0
28	0	0	0	0	0	0	0	0
29	0	0	0	0	0	0	0	0
30	0	0	0	0	0	0	0	0
31	0	0	0	0	0	0	0	0
32	40	480	57	40	69	58	0	0

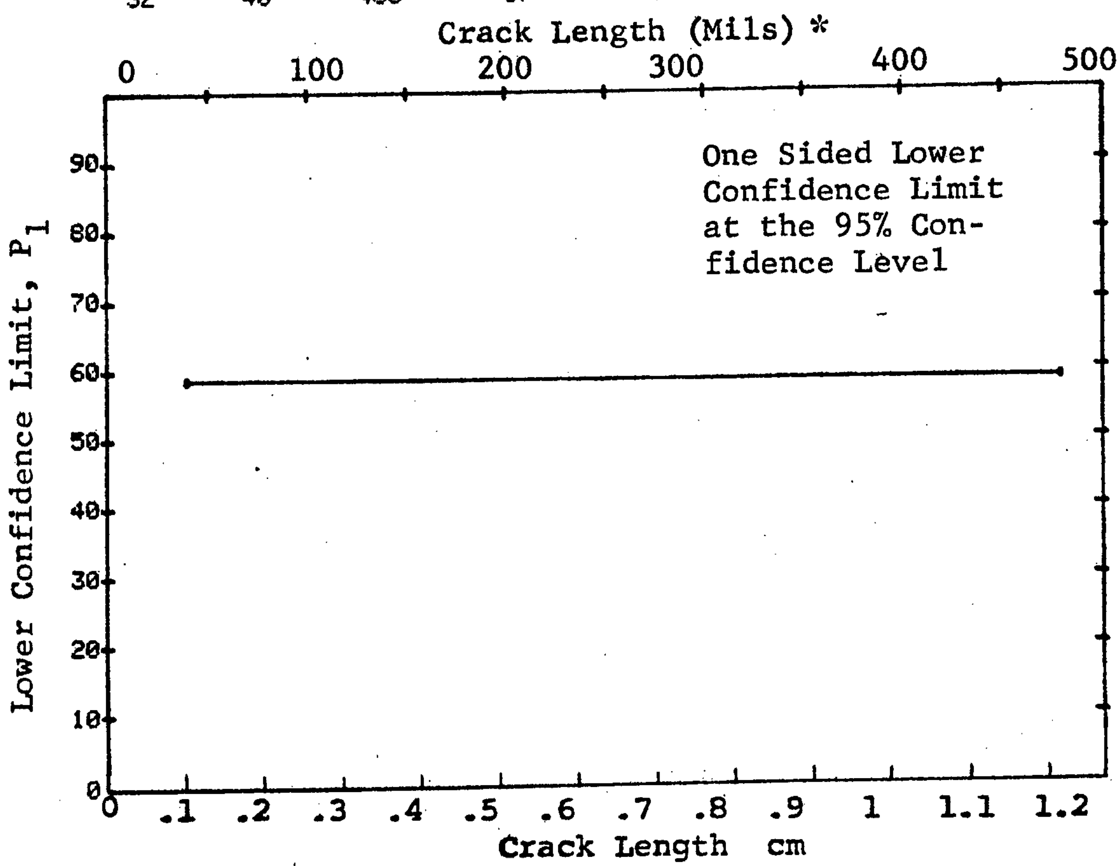

Figure D-97(Concluded)

(a) Range Interval Method of Data Cumulation

28-OCT-75 MAGNETIC PARTICLE TEST 1 (98)

RANGE	MIN LN*	MAX LN*	N	DET	50%	95%	0 MISS	1 MISS
1	30	50	31	24	75	61	0	0
2	60	70	27	27	97	89	2	19
3	0	0	0	0	0	0	0	0
4	110	120	25	25	97	88	4	21
5	130	140	38	38	98	92	0	8
6	150	160	13	13	94	79	16	33
7	0	0	0	0	0	0	0	0
8	200	200	3	3	79	36	0	0
9	0	0	0	0	0	0	0	0
10	0	0	0	0	0	0	0	0
11	0	0	0	0	0	0	0	0
12	0	0	0	0	0	0	0	0
13	0	0	0	0	0	0	0	0
14	0	0	0	0	0	0	0	0
15	0	0	0	0	0	0	0	0
16	0	0	0	0	0	0	0	0
17	0	0	0	0	0	0	0	0
18	0	0	0	0	0	0	0	0
19	0	0	0	0	0	0	0	0
20	0	0	0	0	0	0	0	0
21	0	0	0	0	0	0	0	0
22	0	0	0	0	0	0	0	0
23	0	0	0	0	0	0	0	0
24	0	0	0	0	0	0	0	0
25	0	0	0	0	0	0	0	0
26	0	0	0	0	0	0	0	0
27	0	0	0	0	0	0	0	0
28	0	0	0	0	0	0	0	0
29	0	0	0	0	0	0	0	0
30	0	0	0	0	0	0	0	0
31	0	0	0	0	0	0	0	0
32	750	750	6	6	89	60	0	0

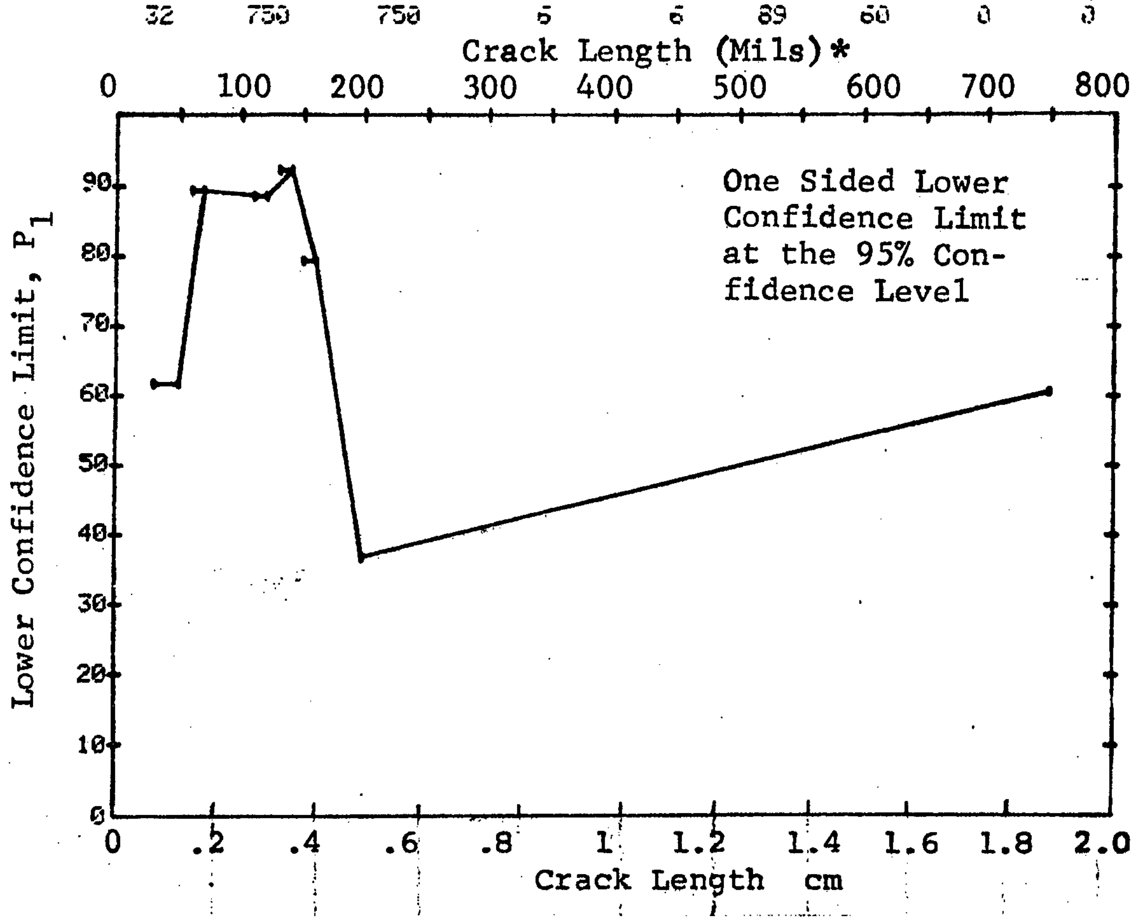

Figure D-98 Probability of Detection for 4340M Steel Using Magnetic Particles. Compressed Notch Flaws in Solid Cylinder. Lab. Env.

(b) Optimum Probability Method of Data Cumulation

28-OCT-75 MAGNETIC PARTICLE TEST 2 (98)

RANGE	MIN LN	* MAX LN	* N	DET	50%	95%	0 MISS	1 MISS
1	30	50	31	24	0	61	0	0
2	60	70	27	27	0	89	2	19
3	0	0	0	0	0	0	0	0
4	60	120	52	52	0	94	0	0
5	60	140	90	90	0	96	0	0
6	60	160	103	103	0	97	0	0
7	0	0	0	0	0	0	0	0
8	60	200	106	106	0	97	0	0
9	0	0	0	0	0	0	0	0
10	0	0	0	0	0	0	0	0
11	0	0	0	0	0	0	0	0
12	0	0	0	0	0	0	0	0
13	0	0	0	0	0	0	0	0
14	0	0	0	0	0	0	0	0
15	0	0	0	0	0	0	0	0
16	0	0	0	0	0	0	0	0
17	0	0	0	0	0	0	0	0
18	0	0	0	0	0	0	0	0
19	0	0	0	0	0	0	0	0
20	0	0	0	0	0	0	0	0
21	0	0	0	0	0	0	0	0
22	0	0	0	0	0	0	0	0
23	0	0	0	0	0	0	0	0
24	0	0	0	0	0	0	0	0
25	0	0	0	0	0	0	0	0
26	0	0	0	0	0	0	0	0
27	0	0	0	0	0	0	0	0
28	0	0	0	0	0	0	0	0
29	0	0	0	0	0	0	0	0
30	0	0	0	0	0	0	0	0
31	0	0	0	0	0	0	0	0
32	60	750	112	112	0	97	0	0

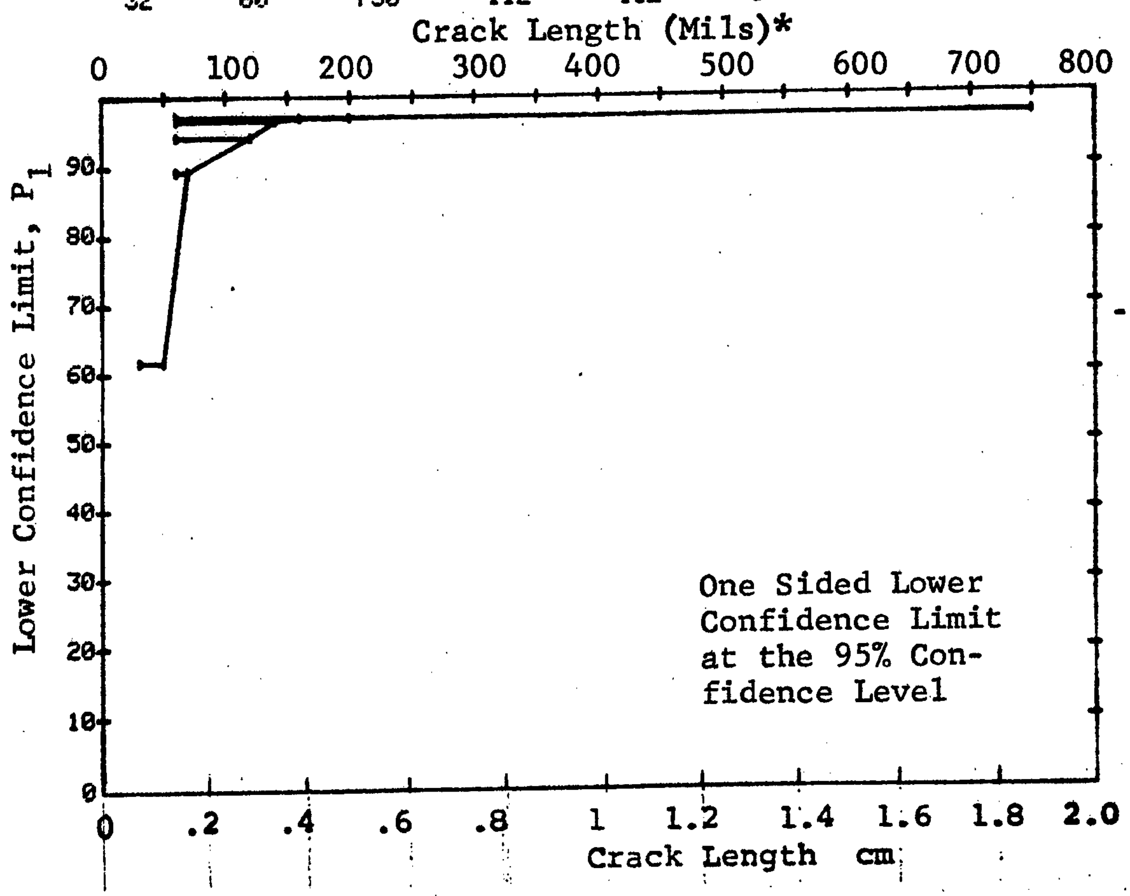

Figure D-98 (Continued)

(c) Overlapping Sixty Point Method of Data Cumulation

28-OCT-75 MAGNETIC PARTICLE TEST 3 C (98)

RANGE	MIN LN	MAX LN	N	DET	50%	95%	0 MISS	1 MISS
1	0	0	0	0	0	0	0	0
2	0	0	0	0	0	0	0	0
3	0	0	0	0	0	0	0	0
4	0	0	0	0	0	0	0	0
5	0	0	0	0	0	0	0	0
6	0	0	0	0	0	0	0	0
7	0	0	0	0	0	0	0	0
8	0	0	0	0	0	0	0	0
9	0	0	0	0	0	0	0	0
10	0	0	0	0	0	0	0	0
11	0	0	0	0	0	0	0	0
12	0	0	0	0	0	0	0	0
13	0	0	0	0	0	0	0	0
14	0	0	0	0	0	0	0	0
15	0	0	0	0	0	0	0	0
16	0	0	0	0	0	0	0	0
17	0	0	0	0	0	0	0	0
18	0	0	0	0	0	0	0	0
19	0	0	0	0	0	0	0	0
20	0	0	0	0	0	0	0	0
21	0	0	0	0	0	0	0	0
22	0	0	0	0	0	0	0	0
23	0	0	0	0	0	0	0	0
24	0	0	0	0	0	0	0	0
25	0	0	0	0	0	0	0	0
26	0	0	0	0	0	0	0	0
27	0	0	0	0	0	0	0	0
28	0	0	0	0	0	0	0	0
29	30	60	47	40	83	73	0	0
30	50	120	60	60	98	95	0	0
31	60	140	60	60	98	95	0	0
32	120	200	60	60	98	95	0	0

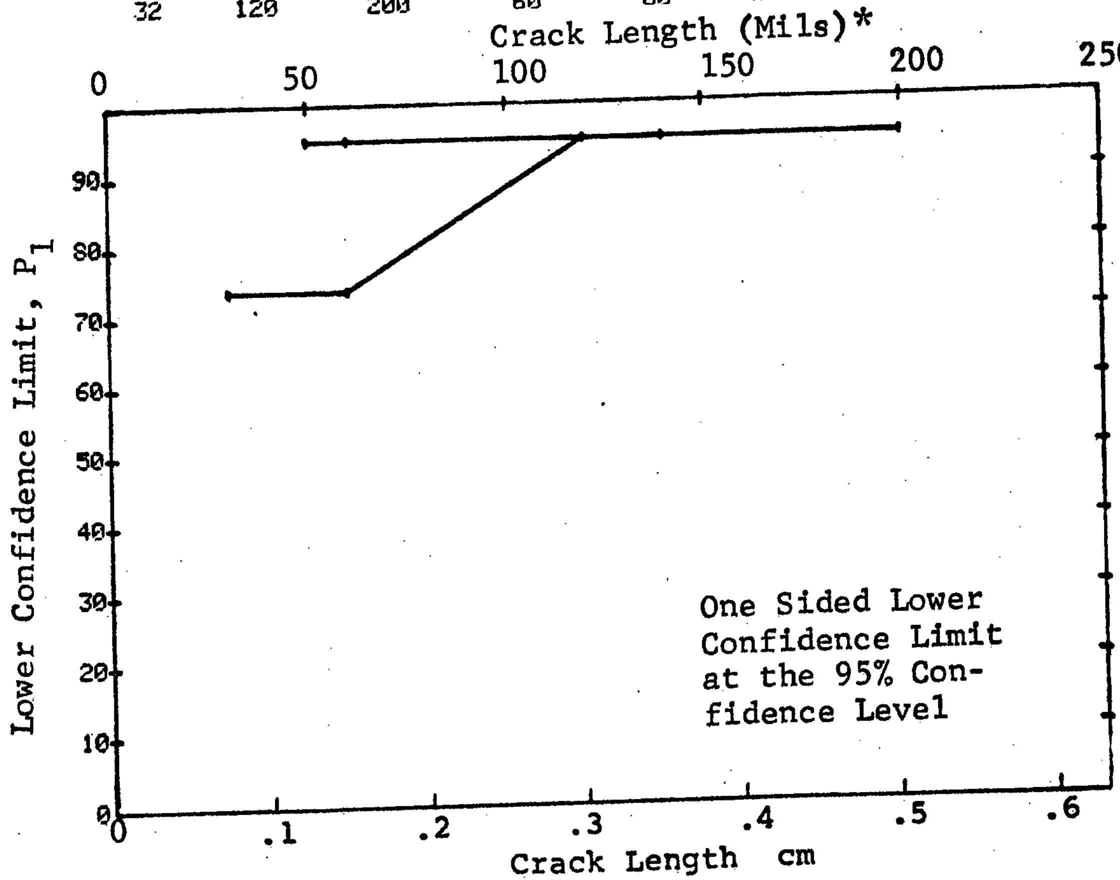

Figure D-98 (Concluded)

(a) Range Interval Method of Data Cumulation

28-OCT-75 MAGNETIC PARTICLE TEST 1 (99)

RANGE	MIN LN *	MAX LN *	N	DET	50%	95%	0 MISS	1 MISS
1	70	80	20	20	96	86	9	26
2	90	90	19	19	96	85	10	27
3	0	0	0	0	0	0	0	0
4	110	110	8	6	67	40	0	0
5	120	130	12	12	94	77	17	34
6	140	140	16	16	95	82	13	30
7	0	0	0	0	0	0	0	0
8	160	160	2	2	70	22	0	0
9	0	0	0	0	0	0	0	0
10	180	180	9	9	92	71	0	0
11	0	0	0	0	0	0	0	0
12	0	0	0	0	0	0	0	0
13	0	0	0	0	0	0	0	0
14	0	0	0	0	0	0	0	0
15	250	250	1	1	50	5	0	0
16	0	0	0	0	0	0	0	0
17	270	270	2	2	70	22	0	0
18	280	280	1	1	50	5	0	0
19	300	300	11	11	93	76	18	35
20	310	310	1	1	50	5	0	0
21	0	0	0	0	0	0	0	0
22	0	0	0	0	0	0	0	0
23	0	0	0	0	0	0	0	0
24	0	0	0	0	0	0	0	0
25	0	0	0	0	0	0	0	0
26	0	0	0	0	0	0	0	0
27	390	390	1	1	50	5	0	0
28	0	0	0	0	0	0	0	0
29	0	0	0	0	0	0	0	0
30	0	0	0	0	0	0	0	0
31	0	0	0	0	0	0	0	0
32	450	460	3	3	79	36	0	0

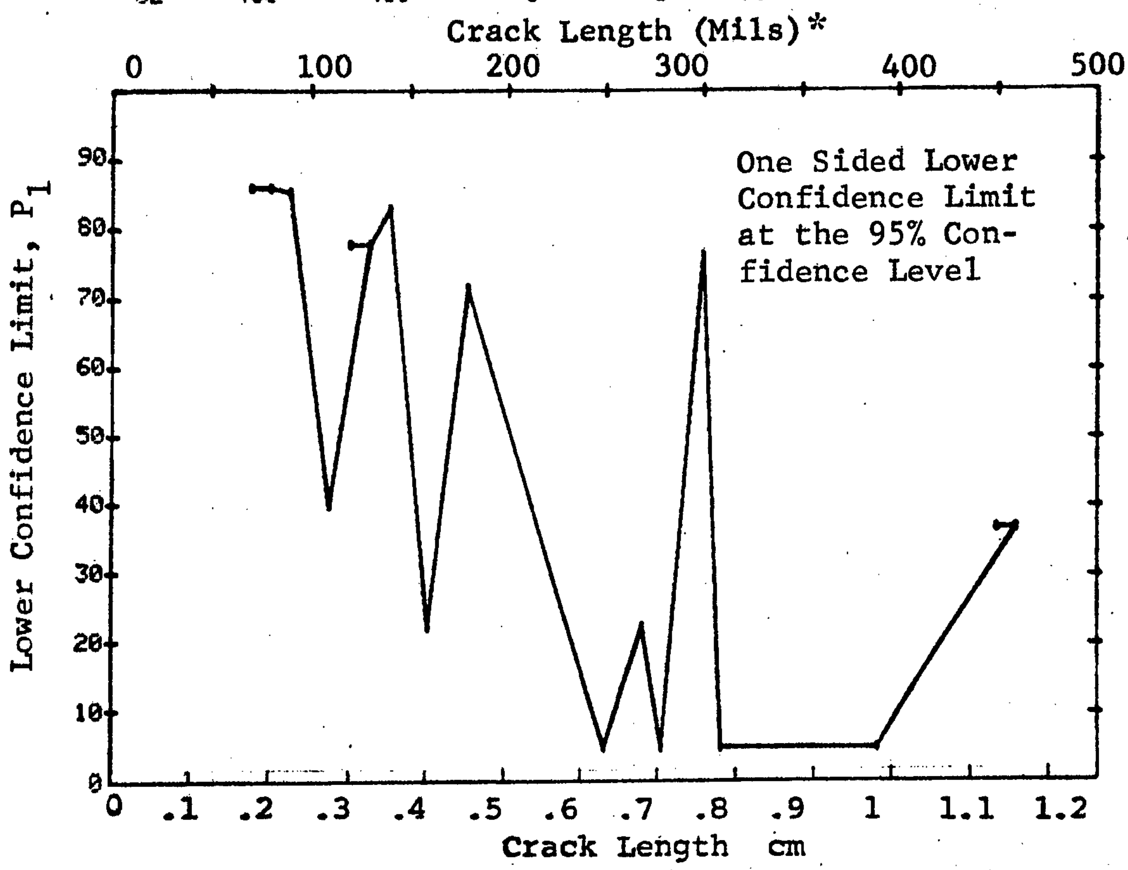

Figure D-99 Probability of Detection for 4340M Steel Using Magnetic Particles. Compressed Notch Flaws in Hollow Filleted Cylinder. Lab. Env.

(b) Optimum Probability Method of Data Cumulation

28-OCT-75 MAGNETIC PARTICLE TEST 2 ( ).(99)

RANGE	MIN LN	* MAX LN	* N	DET	50%	95%	0 MISS	1 MISS
1	70	80	20	20	0	86	9	26
2	70	90	39	39	0	92	0	7
3	0	0	0	0	0	0	0	0
4	70	110	47	45	0	87	14	29
5	70	130	59	57	0	89	2	17
6	70	140	75	73	0	91	0	1
7	0	0	0	0	0	0	0	0
8	70	160	77	75	0	92	0	0
9	0	0	0	0	0	0	0	0
10	70	180	86	84	0	92	0	0
11	0	0	0	0	0	0	0	0
12	0	0	0	0	0	0	0	0
13	0	0	0	0	0	0	0	0
14	0	0	0	0	0	0	0	0
15	70	250	87	85	0	92	0	0
16	0	0	0	0	0	0	0	0
17	120	270	42	42	0	93	0	4
18	120	280	43	43	0	93	0	3
19	120	300	54	54	0	94	0	0
20	120	310	55	55	0	94	0	0
21	0	0	0	0	0	0	0	0
22	0	0	0	0	0	0	0	0
23	0	0	0	0	0	0	0	0
24	0	0	0	0	0	0	0	0
25	0	0	0	0	0	0	0	0
26	0	0	0	0	0	0	0	0
27	120	390	56	56	0	94	0	0
28	0	0	0	0	0	0	0	0
29	0	0	0	0	0	0	0	0
30	0	0	0	0	0	0	0	0
31	0	0	0	0	0	0	0	0
32	120	460	59	59	0	95	0	0

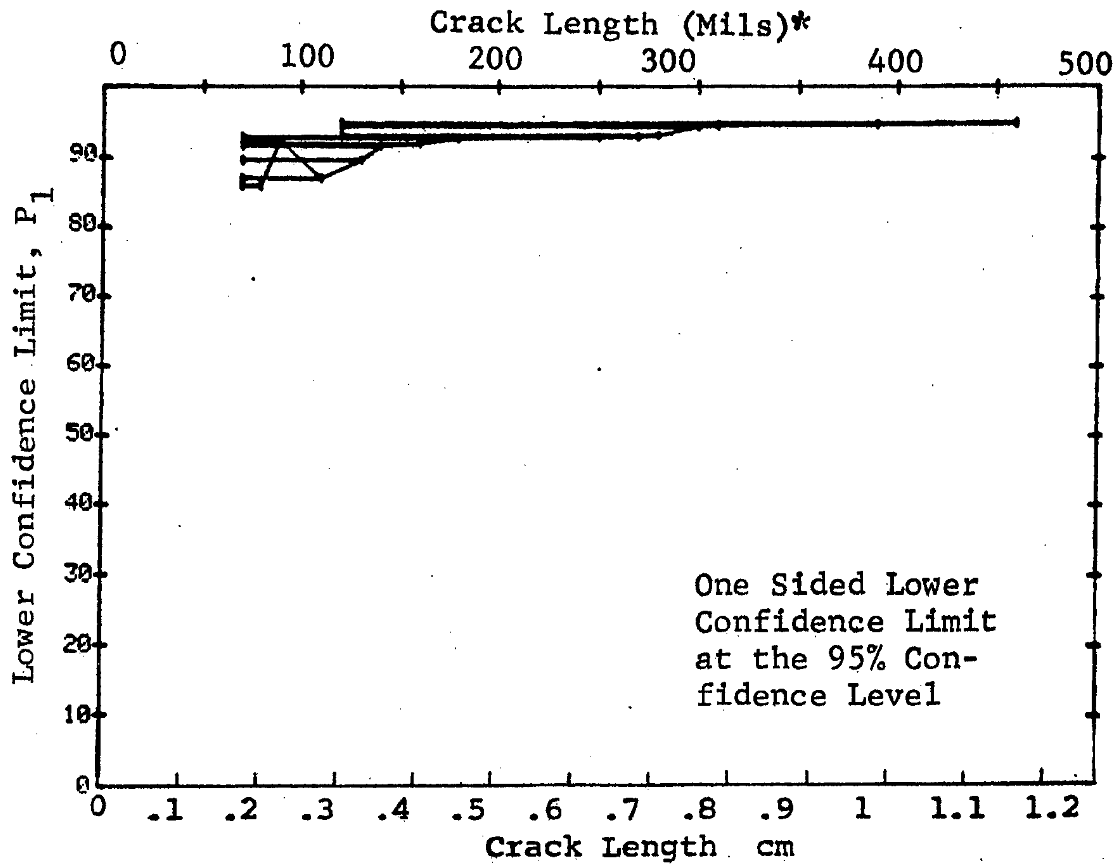

Figure D-99 (Continued)

(c) Overlapping Sixty Point Method of Data Cumulation

28-OCT-75 MAGNETIC PARTICLE TEST 3 ( ) (99)

RANGE	MIN LN	*MAX LN*	N	DET	50%	95%	0 MISS	1 MISS
1	0	0	0	0	0	0	0	0
2	0	0	0	0	0	0	0	0
3	0	0	0	0	0	0	0	0
4	0	0	0	0	0	0	0	0
5	0	0	0	0	0	0	0	0
6	0	0	0	0	0	0	0	0
7	0	0	0	0	0	0	0	0
8	0	0	0	0	0	0	0	0
9	0	0	0	0	0	0	0	0
10	0	0	0	0	0	0	0	0
11	0	0	0	0	0	0	0	0
12	0	0	0	0	0	0	0	0
13	0	0	0	0	0	0	0	0
14	0	0	0	0	0	0	0	0
15	0	0	0	0	0	0	0	0
16	0	0	0	0	0	0	0	0
17	0	0	0	0	0	0	0	0
18	0	0	0	0	0	0	0	0
19	0	0	0	0	0	0	0	0
20	0	0	0	0	0	0	0	0
21	0	0	0	0	0	0	0	0
22	0	0	0	0	0	0	0	0
23	0	0	0	0	0	0	0	0
24	0	0	0	0	0	0	0	0
25	0	0	0	0	0	0	0	0
26	0	0	0	0	0	0	0	0
27	0	0	0	0	0	0	0	0
28	0	0	0	0	0	0	0	0
29	0	0	0	0	0	0	0	0
30	70	110	46	44	94	86	15	30
31	80	160	60	58	95	89	1	16
32	110	460	60	60	98	95	0	0

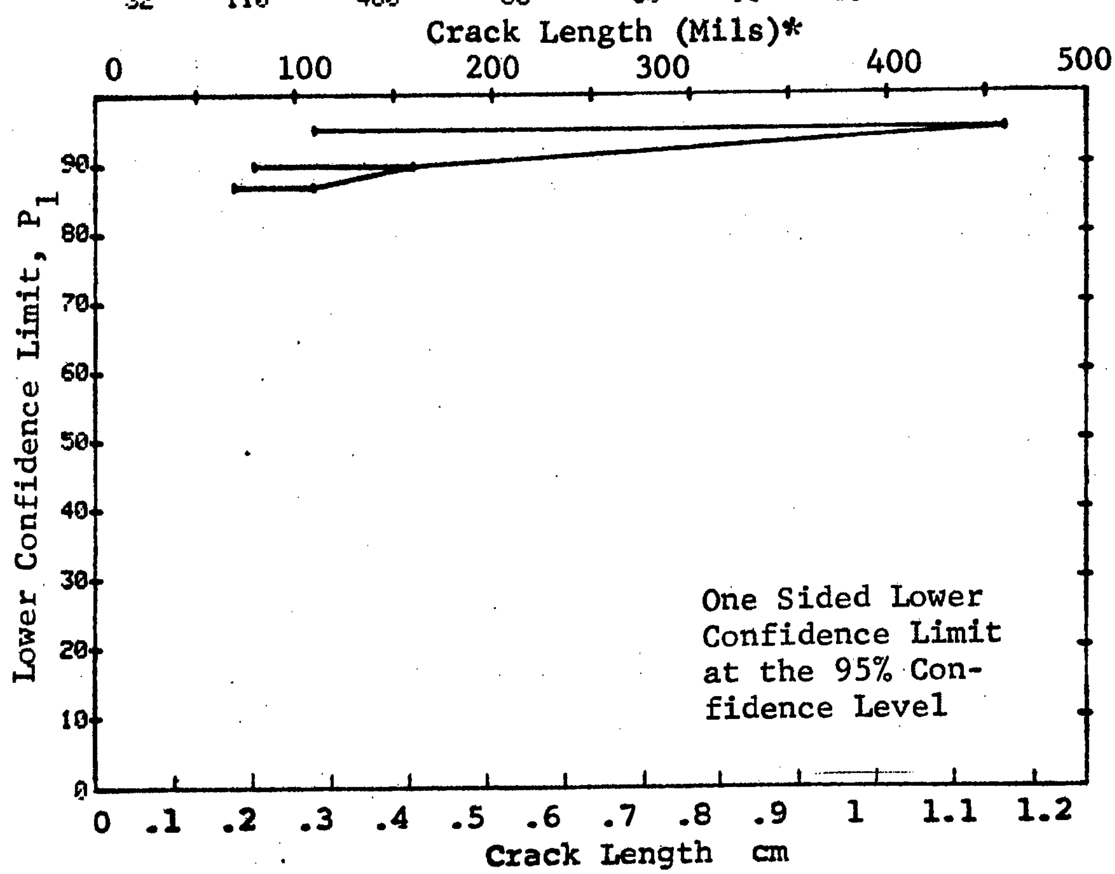

Figure D-99 (Concluded)

(a) Range Interval Method of Data Cumulation

28-OCT-75 MAGNETIC PARTICLE TEST 1 ( ) (100)

RANGE	MIN LN *	MAX LN *	N	DET	50%	95%	0 MISS	1 MISS
1	40	40	1	1	50	5	0	0
2	70	70	1	0	0	0	0	0
3	0	0	0	0	0	0	0	0
4	100	110	7	3	36	12	0	0
5	130	130	4	1	15	1	0	0
6	0	0	0	0	0	0	0	0
7	0	0	0	0	0	0	0	0
8	190	190	1	1	50	5	0	0
9	210	210	1	1	50	5	0	0
10	230	230	1	1	50	5	0	0
11	0	0	0	0	0	0	0	0
12	250	250	2	2	70	22	0	0
13	270	270	1	1	50	5	0	0
14	300	300	1	1	50	5	0	0
15	310	310	1	1	50	5	0	0
16	0	0	0	0	0	0	0	0
17	350	350	1	1	50	5	0	0
18	380	380	1	1	50	5	0	0
19	0	0	0	0	0	0	0	0
20	410	410	1	1	50	5	0	0
21	0	0	0	0	0	0	0	0
22	450	450	1	1	50	5	0	0
23	460	460	1	1	50	5	0	0
24	480	480	1	1	50	5	0	0
25	0	0	0	0	0	0	0	0
26	0	0	0	0	0	0	0	0
27	0	0	0	0	0	0	0	0
28	0	0	0	0	0	0	0	0
29	0	0	0	0	0	0	0	0
30	0	0	0	0	0	0	0	0
31	0	0	0	0	0	0	0	0
32	650	650	1	1	50	5	0	0

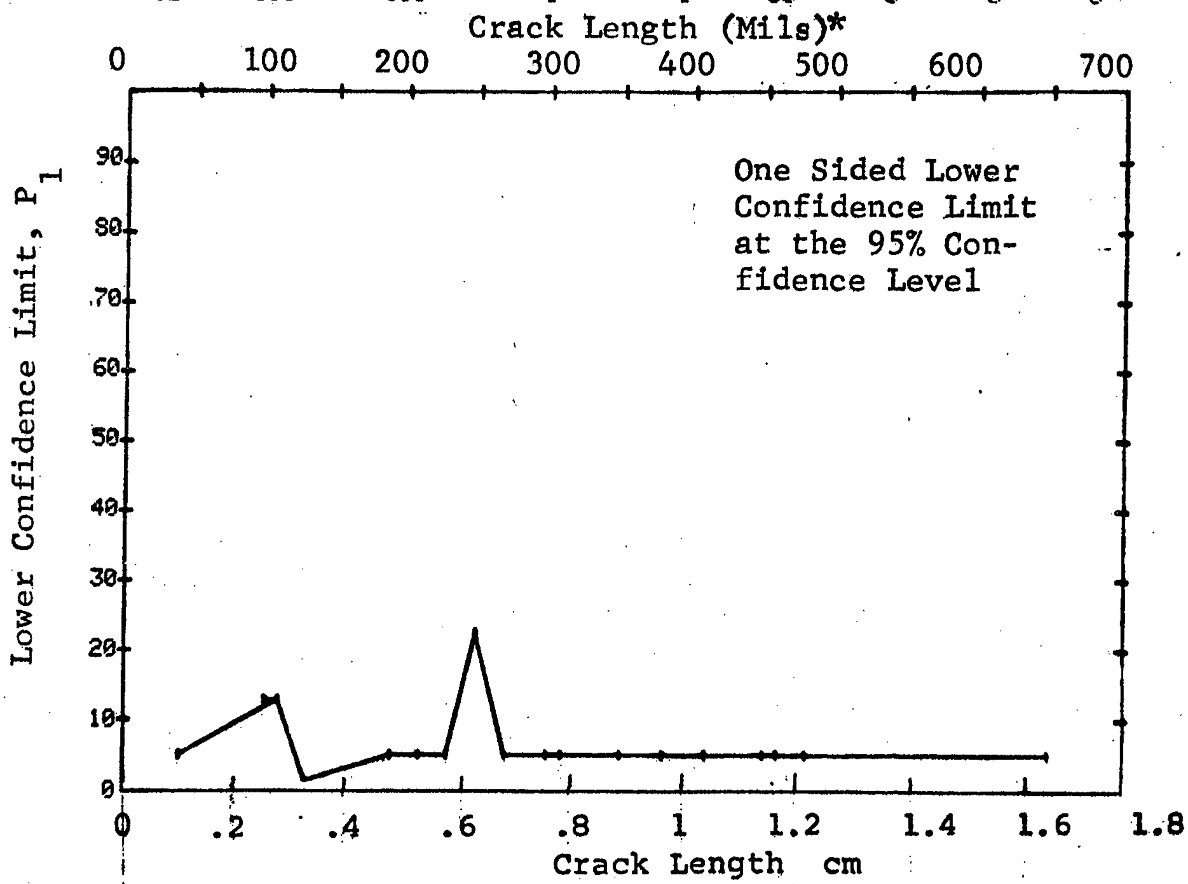

Figure D-100 Probability of Detection for 4340M Steel Using Magnetic Particles. Compressed Notch Flaws in Solid Threaded Cylinder. Lab. Env.

(b) Optimum Probability Method of Data Cumulation

28-OCT-75 MAGNETIC PARTICLE TEST 2 ([illegible]) (100)

RANGE	MIN LN *	MAX LN *	N	DET	50%	95%	0 MISS	1 MISS
1	40	40	1	1	0	5	0	0
2	40	70	2	1	0	2	0	0
3	0	0	0	0	0	0	0	0
4	40	110	9	4	0	16	0	0
5	40	130	13	5	0	16	0	0
6	0	0	0	0	0	0	0	0
7	0	0	0	0	0	0	0	0
8	40	190	14	6	0	20	0	0
9	40	210	15	7	0	24	0	0
10	190	230	3	3	0	36	0	0
11	0	0	0	0	0	0	0	0
12	190	250	5	5	0	54	0	0
13	190	270	6	6	0	60	0	0
14	190	300	7	7	0	65	0	0
15	190	310	8	8	0	69	0	0
16	0	0	0	0	0	0	0	0
17	190	350	9	9	0	71	0	0
18	190	380	10	10	0	74	0	0
19	0	0	0	0	0	0	0	0
20	190	410	11	11	0	76	0	0
21	0	0	0	0	0	0	0	0
22	190	450	12	12	0	77	0	0
23	190	460	13	13	0	79	0	0
24	190	480	14	14	0	80	15	32
25	0	0	0	0	0	0	0	0
26	0	0	0	0	0	0	0	0
27	0	0	0	0	0	0	0	0
28	0	0	0	0	0	0	0	0
29	0	0	0	0	0	0	0	0
30	0	0	0	0	0	0	0	0
31	0	0	0	0	0	0	0	0
32	190	650	15	15	0	81	14	31

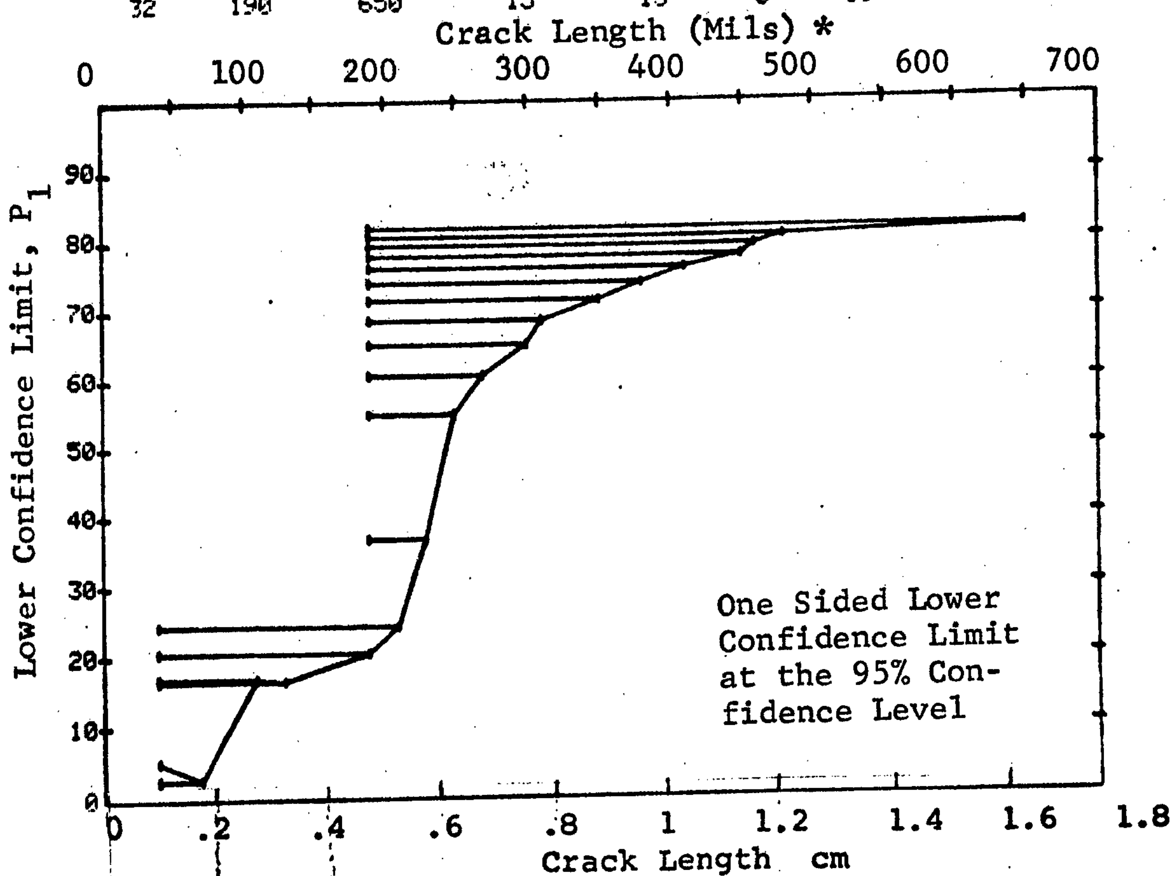

Figure D-100 (Continued)

(c) Overlapping Sixty Point Method of Data Cumulation

28-OCT-75 MAGNETIC PARTICLE TEST 3)(100)

RANGE	MIN LN	MAX LN	N	DET	50%	95%	0 MISS	1 MISS
1	0	0	0	0	0	0	0	0
2	0	0	0	0	0	0	0	0
3	0	0	0	0	0	0	0	0
4	0	0	0	0	0	0	0	0
5	0	0	0	0	0	0	0	0
6	0	0	0	0	0	0	0	0
7	0	0	0	0	0	0	0	0
8	0	0	0	0	0	0	0	0
9	0	0	0	0	0	0	0	0
10	0	0	0	0	0	0	0	0
11	0	0	0	0	0	0	0	0
12	0	0	0	0	0	0	0	0
13	0	0	0	0	0	0	0	0
14	0	0	0	0	0	0	0	0
15	0	0	0	0	0	0	0	0
16	0	0	0	0	0	0	0	0
17	0	0	0	0	0	0	0	0
18	0	0	0	0	0	0	0	0
19	0	0	0	0	0	0	0	0
20	0	0	0	0	0	0	0	0
21	0	0	0	0	0	0	0	0
22	0	0	0	0	0	0	0	0
23	0	0	0	0	0	0	0	0
24	0	0	0	0	0	0	0	0
25	0	0	0	0	0	0	0	0
26	0	0	0	0	0	0	0	0
27	0	0	0	0	0	0	0	0
28	0	0	0	0	0	0	0	0
29	0	0	0	0	0	0	0	0
30	0	0	0	0	0	0	0	0
31	0	0	0	0	0	0	0	0
32	40	480	27	19	68	52	0	0

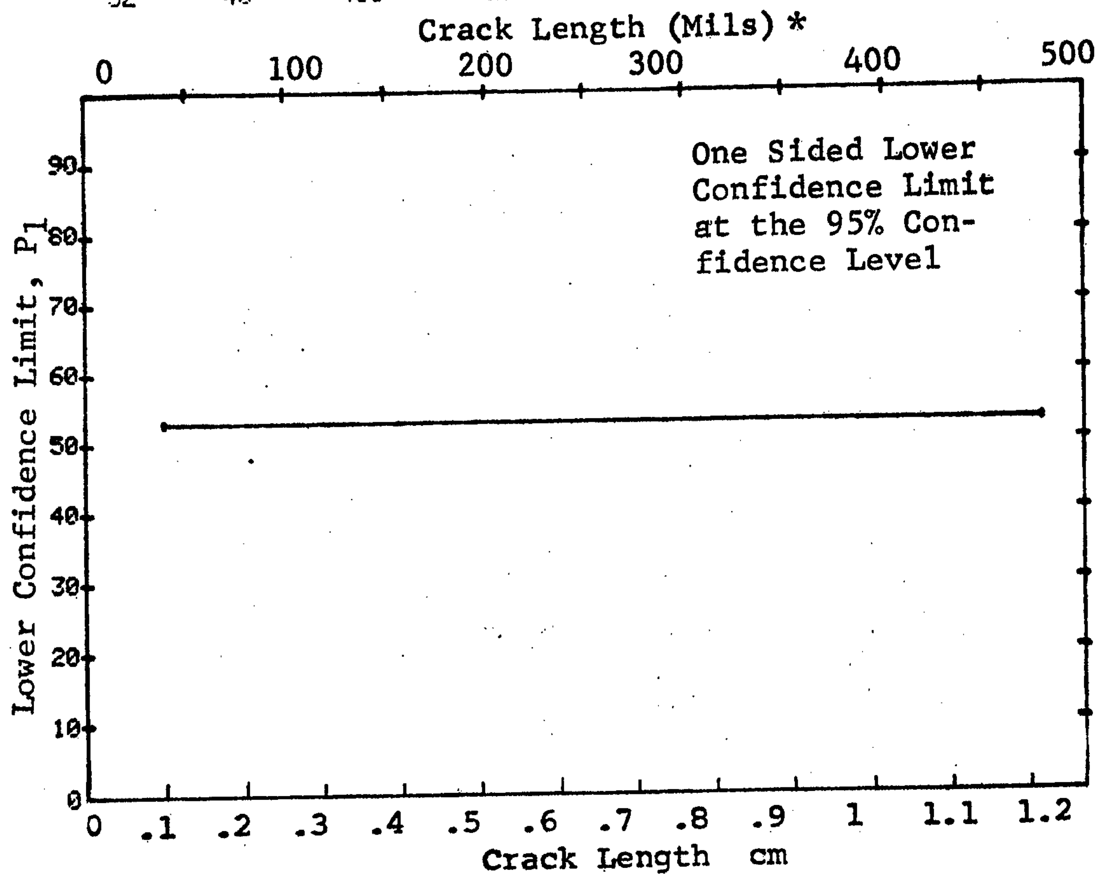

Figure D-100 (Concluded)

(a) Range Interval Method of Data Cumulation

28-OCT-75 MAGNETIC PARTICLE TEST 1 ( ) (101)

RANGE	MIN LN	MAX LN	N	DET	50%	95%	0 MISS	1 MISS
1	20 *	30 *	23	16	67	50	0	0
2	0	0	0	0	0	0	0	0
3	60	60	11	11	93	76	18	35
4	70	70	18	18	96	84	11	28
5	90	90	13	13	94	79	16	33
6	100	100	10	10	93	74	0	0
7	0	0	0	0	0	0	0	0
8	130	140	26	25	93	83	20	35
9	150	150	13	12	87	68	0	0
10	0	0	0	0	0	0	0	0
11	0	0	0	0	0	0	0	0
12	200	200	2	2	70	22	0	0
13	0	0	0	0	0	0	0	0
14	230	230	3	3	79	36	0	0
15	240	240	2	2	70	22	0	0
16	250	260	4	4	84	47	0	0
17	0	0	0	0	0	0	0	0
18	280	280	2	2	70	22	0	0
19	300	300	10	10	93	74	0	0
20	0	0	0	0	0	0	0	0
21	0	0	0	0	0	0	0	0
22	0	0	0	0	0	0	0	0
23	0	0	0	0	0	0	0	0
24	370	380	11	11	93	76	18	35
25	390	390	4	4	84	47	0	0
26	410	410	2	2	70	22	0	0
27	0	0	0	0	0	0	0	0
28	0	0	0	0	0	0	0	0
29	0	0	0	0	0	0	0	0
30	0	0	0	0	0	0	0	0
31	0	0	0	0	0	0	0	0
32	500	500	2	2	70	22	0	0

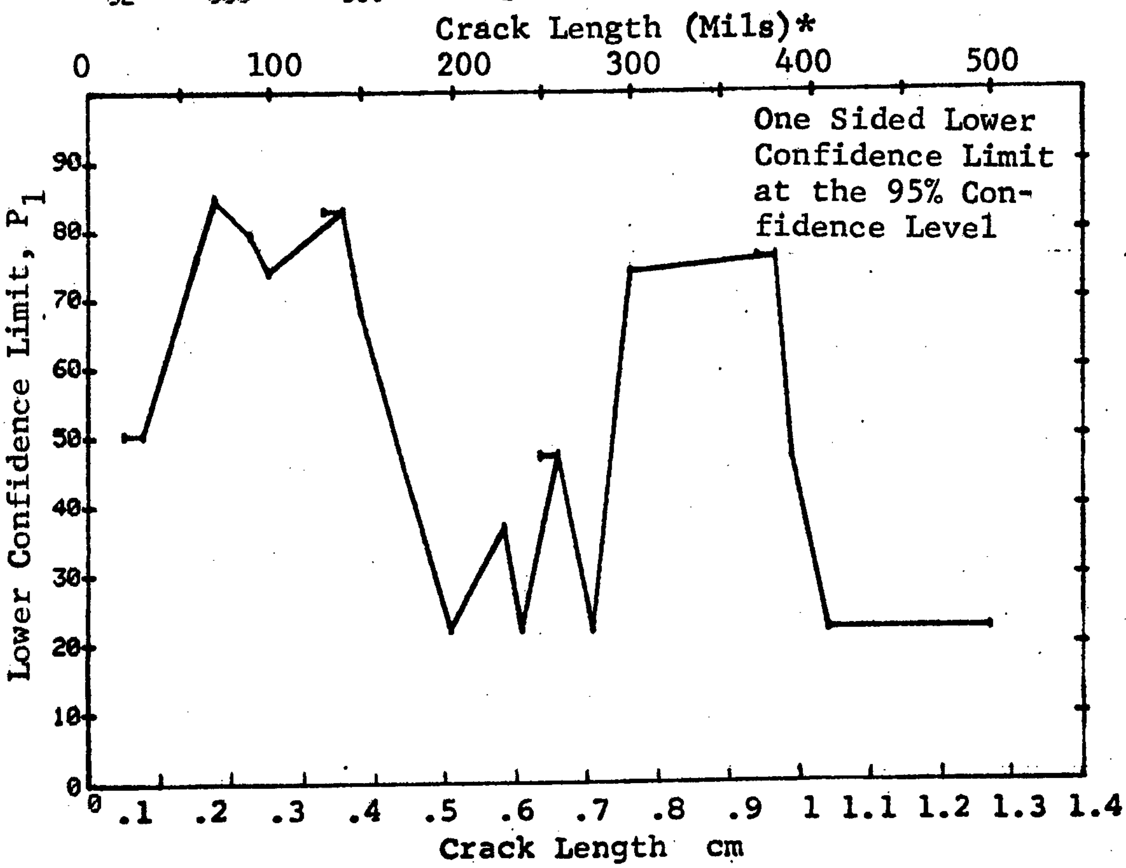

Figure D-101 Probability of Detection for 4340M Steel Using Magnetic Particles. Compressed Notch Flaws in Solid Filleted Cylinder . Lab. Env.

(b) Optimum Probability Method of Data Cumulation

28-OCT-75 MAGNETIC PARTICLE TEST [illegible] (101)

RANGE	MIN LN *	MAX LN *	N	DET	50%	95%	0 MISS	1 MISS
1	20	30	23	16	0	50	0	0
2	0	0	0	0	0	0	0	0
3	60	60	11	11	0	76	0	0
4	60	70	29	29	0	90	0	17
5	60	90	42	42	0	93	0	4
6	60	100	52	52	0	94	0	0
7	0	0	0	0	0	0	0	0
8	60	140	78	77	0	94	0	0
9	60	150	91	89	0	93	0	0
10	0	0	0	0	0	0	0	0
11	0	0	0	0	0	0	0	0
12	60	200	93	91	0	93	0	0
13	0	0	0	0	0	0	0	0
14	60	230	96	94	0	93	0	0
15	60	240	98	96	0	93	0	0
16	60	260	102	100	0	93	0	0
17	0	0	0	0	0	0	0	0
18	60	280	104	102	0	94	0	0
19	60	300	114	112	0	94	0	0
20	0	0	0	0	0	0	0	0
21	0	0	0	0	0	0	0	0
22	0	0	0	0	0	0	0	0
23	0	0	0	0	0	0	0	0
24	60	380	125	123	0	95	0	0
25	60	390	129	127	0	95	0	0
26	60	410	131	129	0	95	0	0
27	0	0	0	0	0	0	0	0
28	0	0	0	0	0	0	0	0
29	0	0	0	0	0	0	0	0
30	0	0	0	0	0	0	0	0
31	0	0	0	0	0	0	0	0
32	60	500	133	131	0	95	0	0

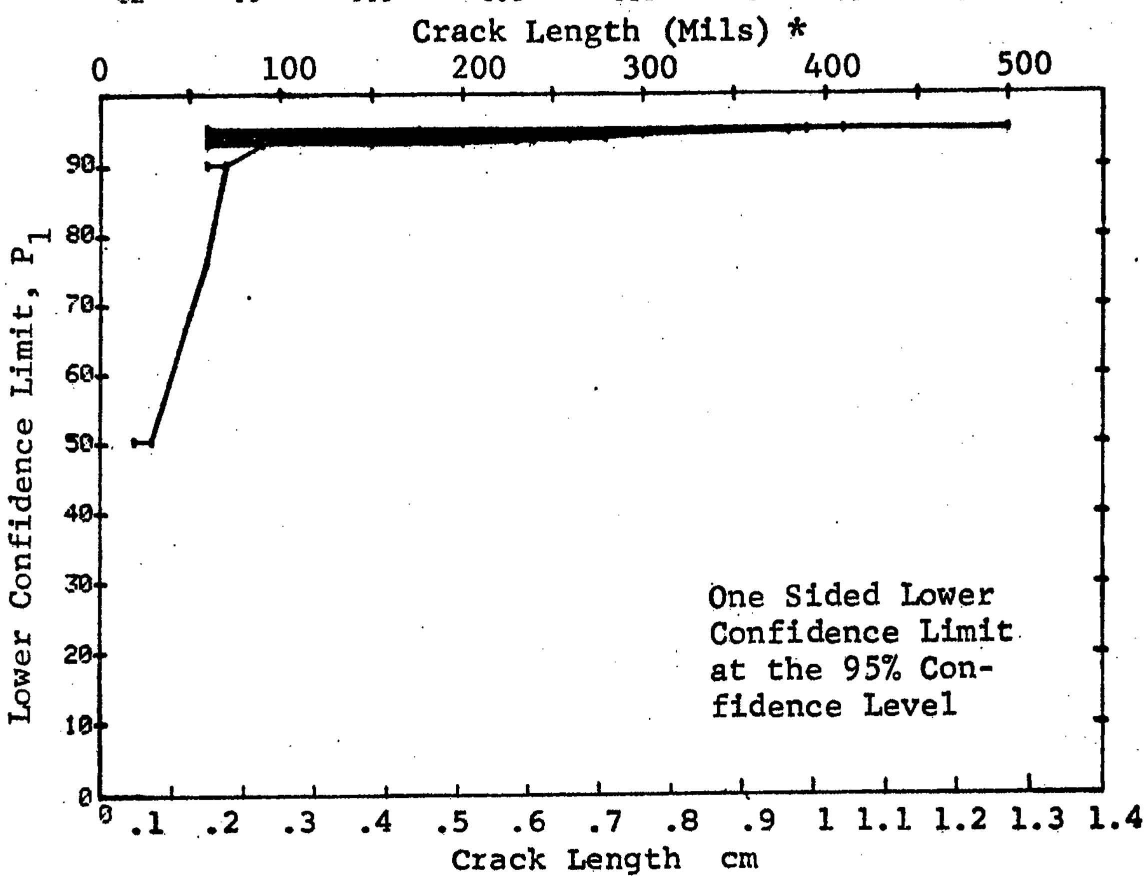

Figure D-101 (Continued)

(c) Overlapping Sixty Point Method of Data Cumulation

28-OCT-75 MAGNETIC PARTICLE TEST 3 ( ) (101)

RANGE	MIN LN	MAX LN	N	DET	50%	95%	0 MISS	1 MISS
1	0*	0*	0	0	0	0	0	0
2	0	0	0	0	0	0	0	0
3	0	0	0	0	0	0	0	0
4	0	0	0	0	0	0	0	0
5	0	0	0	0	0	0	0	0
6	0	0	0	0	0	0	0	0
7	0	0	0	0	0	0	0	0
8	0	0	0	0	0	0	0	0
9	0	0	0	0	0	0	0	0
10	0	0	0	0	0	0	0	0
11	0	0	0	0	0	0	0	0
12	0	0	0	0	0	0	0	0
13	0	0	0	0	0	0	0	0
14	0	0	0	0	0	0	0	0
15	0	0	0	0	0	0	0	0
16	0	0	0	0	0	0	0	0
17	0	0	0	0	0	0	0	0
18	0	0	0	0	0	0	0	0
19	0	0	0	0	0	0	0	0
20	0	0	0	0	0	0	0	0
21	0	0	0	0	0	0	0	0
22	0	0	0	0	0	0	0	0
23	0	0	0	0	0	0	0	0
24	0	0	0	0	0	0	0	0
25	0	0	0	0	0	0	0	0
26	0	0	0	0	0	0	0	0
27	0	0	0	0	0	0	0	0
28	20	70	36	29	78	66	69	92
29	20	100	60	53	87	79	0	1
30	70	140	60	59	97	92	1	16
31	100	200	60	58	95	89	0	1
32	140	500	60	59	97	92		

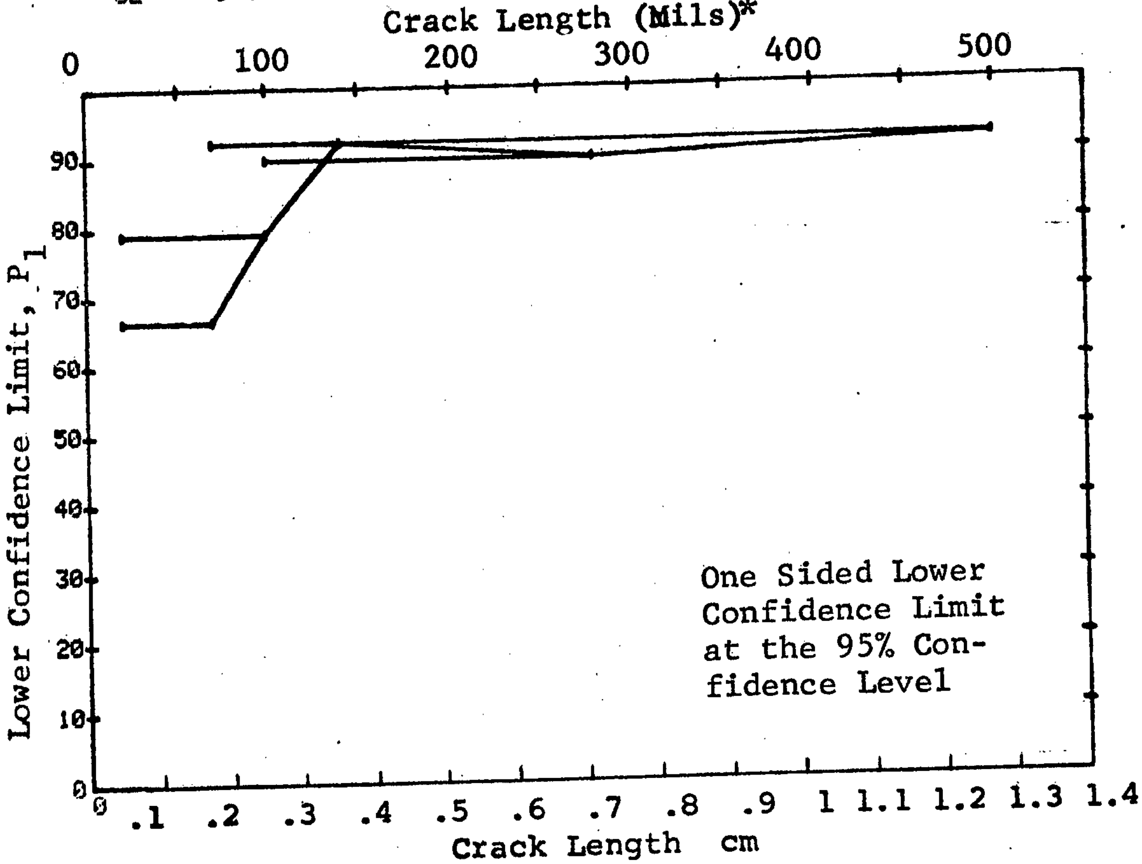

Figure D-101 (Concluded)

(a) Range Interval Method of Data Cumulation

28-OCT-75 MAGNETIC PARTICLE TEST 1 (102)

RANGE	MIN LN *	MAX LN *	N	DET	50%	95%	0 MISS	1 MISS
1	60	60	17	17	96	83	12	29
2	90	90	1	1	50	5	0	0
3	100	100	17	17	96	83	12	29
4	120	120	2	2	70	22	0	0
5	130	130	9	9	92	71	0	0
6	140	140	8	8	91	68	0	0
7	160	170	2	2	70	22	0	0
8	180	180	2	2	70	22	0	0
9	0	0	0	0	0	0	0	0
10	0	0	0	0	0	0	0	0
11	230	230	3	3	79	36	0	0
12	0	0	0	0	0	0	0	0
13	0	0	0	0	0	0	0	0
14	0	0	0	0	0	0	0	0
15	0	0	0	0	0	0	0	0
16	310	310	1	1	50	5	0	0
17	0	0	0	0	0	0	0	0
18	0	0	0	0	0	0	0	0
19	350	350	4	4	84	47	0	0
20	0	0	0	0	0	0	0	0
21	390	390	1	1	50	5	0	0
22	0	0	0	0	0	0	0	0
23	0	0	0	0	0	0	0	0
24	0	0	0	0	0	0	0	0
25	0	0	0	0	0	0	0	0
26	0	0	0	0	0	0	0	0
27	0	0	0	0	0	0	0	0
28	0	0	0	0	0	0	0	0
29	0	0	0	0	0	0	0	0
30	0	0	0	0	0	0	0	0
31	0	0	0	0	0	0	0	0
32	570	570	1	1	50	5	0	0

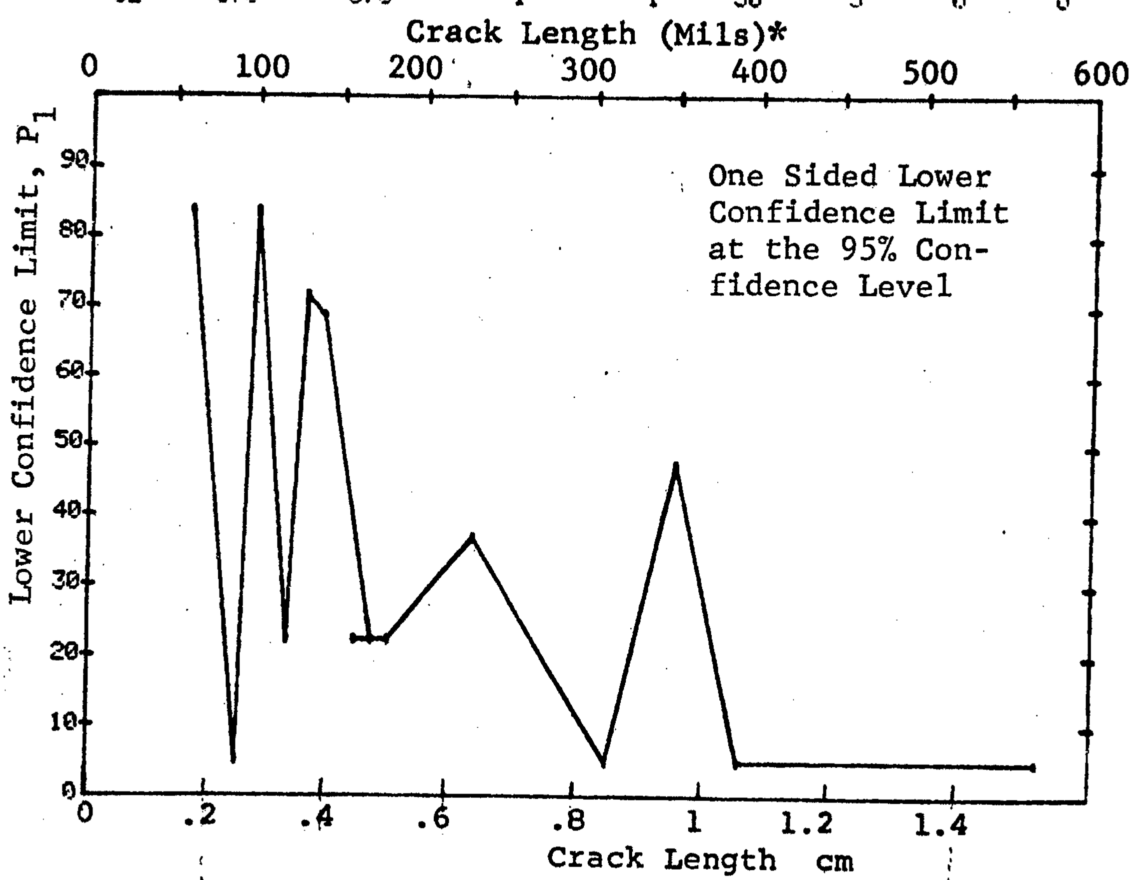

Figure D-102 Probability of Detection for 4340M Steel Using Magnetic Particles. Compressed Notch Flaws in Hollow Cylinder. Lab. Env.

(b) Optimum Probability Method of Data Cumulation

28-OCT-75 MAGNETIC PARTICLE TEST 2 ((402))

RANGE	MIN LN	* MAX LN *	N	DET	50%	95%	0 MISS	1 MISS
1	60	60	17	17	0	83	12	29
2	60	90	18	18	0	84	11	28
3	60	100	35	35	0	91	0	11
4	60	120	37	37	0	92	0	9
5	60	130	46	46	0	93	0	0
6	60	140	54	54	0	94	0	0
7	60	170	56	56	0	94	0	0
8	60	180	58	58	0	94	0	0
9	0	0	0	0	0	0	0	0
10	0	0	0	0	0	0	0	0
11	60	230	61	61	0	95	0	0
12	0	0	0	0	0	0	0	0
13	0	0	0	0	0	0	0	0
14	0	0	0	0	0	0	0	0
15	0	0	0	0	0	0	0	0
16	60	310	62	62	0	95	0	0
17	0	0	0	0	0	0	0	0
18	0	0	0	0	0	0	0	0
19	60	350	66	66	0	95	0	0
20	0	0	0	0	0	0	0	0
21	60	390	67	67	0	95	0	0
22	0	0	0	0	0	0	0	0
23	0	0	0	0	0	0	0	0
24	0	0	0	0	0	0	0	0
25	0	0	0	0	0	0	0	0
26	0	0	0	0	0	0	0	0
27	0	0	0	0	0	0	0	0
28	0	0	0	0	0	0	0	0
29	0	0	0	0	0	0	0	0
30	0	0	0	0	0	0	0	0
31	0	0	0	0	0	0	0	0
32	60	570	68	68	0	95	0	0

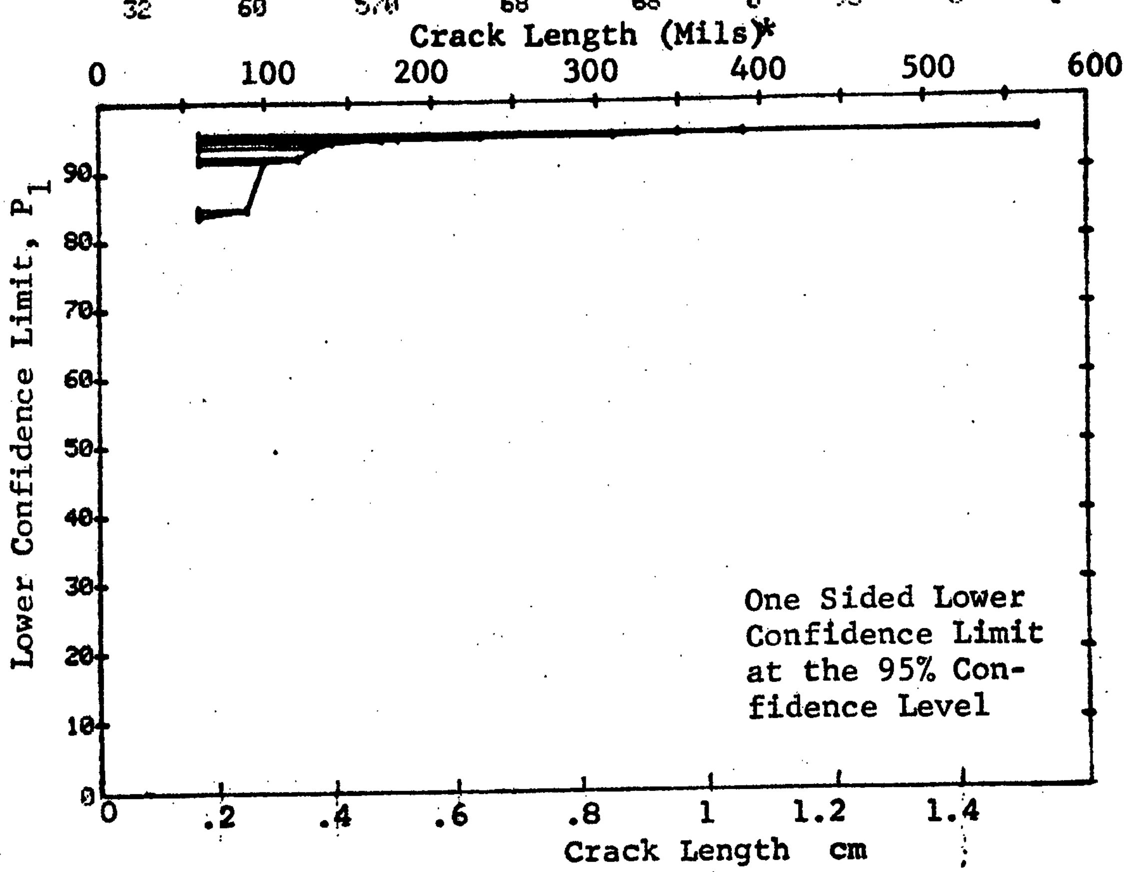

Figure D-102 (Continued)

(c) Overlapping Sixty Point Method of Data Cumulation

28-OCT-75 MAGNETIC PARTICLE TEST 3 (102)

RANGE	MIN LN *	MAX LN *	N	DET	50%	95%	0 MISS	1 MISS
1	0	0	0	0	0	0	0	0
2	0	0	0	0	0	0	0	0
3	0	0	0	0	0	0	0	0
4	0	0	0	0	0	0	0	0
5	0	0	0	0	0	0	0	0
6	0	0	0	0	0	0	0	0
7	0	0	0	0	0	0	0	0
8	0	0	0	0	0	0	0	0
9	0	0	0	0	0	0	0	0
10	0	0	0	0	0	0	0	0
11	0	0	0	0	0	0	0	0
12	0	0	0	0	0	0	0	0
13	0	0	0	0	0	0	0	0
14	0	0	0	0	0	0	0	0
15	0	0	0	0	0	0	0	0
16	0	0	0	0	0	0	0	0
17	0	0	0	0	0	0	0	0
18	0	0	0	0	0	0	0	0
19	0	0	0	0	0	0	0	0
20	0	0	0	0	0	0	0	0
21	0	0	0	0	0	0	0	0
22	0	0	0	0	0	0	0	0
23	0	0	0	0	0	0	0	0
24	0	0	0	0	0	0	0	0
25	0	0	0	0	0	0	0	0
26	0	0	0	0	0	0	0	0
27	0	0	0	0	0	0	0	0
28	0	0	0	0	0	0	0	0
29	0	0	0	0	0	0	0	0
30	0	0	0	0	0	0	0	0
31	60	120	37	37	98	92	0	0
32	60	390	60	60	98	95	0	0

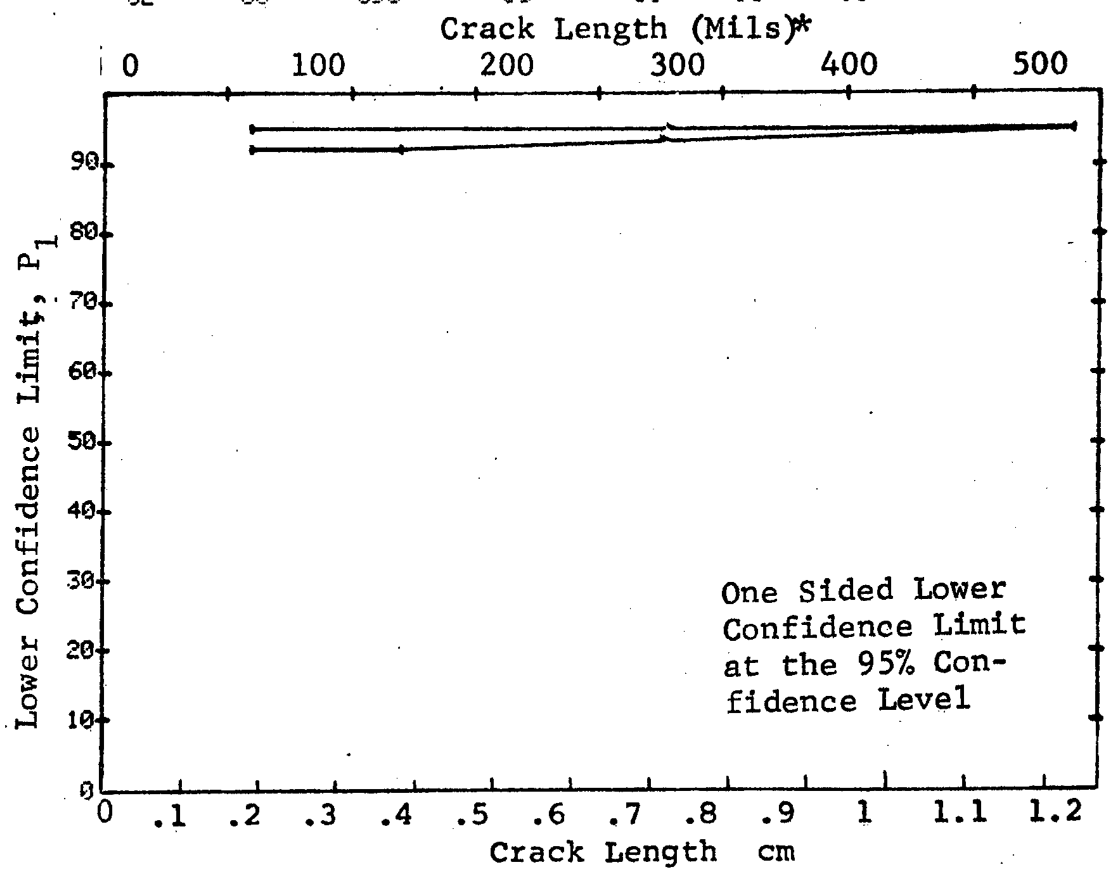

Figure D-102 (Concluded)

(a) Range Interval Method of Data Cumulation

28-OCT-75 EDDY CURRENT TEST 1 (103)

RANGE	MIN LN	MAX LN	N	DET	50%	95%	0 MISS	1 MISS
1	30	50	21	12	54	37	0	0
2	60	70	15	11	69	48	0	0
3	0	0	0	0	0	0	0	0
4	110	120	17	17	96	83	12	29
5	130	140	22	21	92	80	24	39
6	150	160	12	12	94	77	17	34
7	0	0	0	0	0	0	0	0
8	200	200	2	2	70	22	0	0
9	0	0	0	0	0	0	0	0
10	0	0	0	0	0	0	0	0
11	0	0	0	0	0	0	0	0
12	0	0	0	0	0	0	0	0
13	0	0	0	0	0	0	0	0
14	0	0	0	0	0	0	0	0
15	0	0	0	0	0	0	0	0
16	0	0	0	0	0	0	0	0
17	0	0	0	0	0	0	0	0
18	0	0	0	0	0	0	0	0
19	0	0	0	0	0	0	0	0
20	0	0	0	0	0	0	0	0
21	0	0	0	0	0	0	0	0
22	0	0	0	0	0	0	0	0
23	0	0	0	0	0	0	0	0
24	0	0	0	0	0	0	0	0
25	0	0	0	0	0	0	0	0
26	0	0	0	0	0	0	0	0
27	0	0	0	0	0	0	0	0
28	0	0	0	0	0	0	0	0
29	0	0	0	0	0	0	0	0
30	0	0	0	0	0	0	0	0
31	0	0	0	0	0	0	0	0
32	750	750	4	4	84	47	0	0

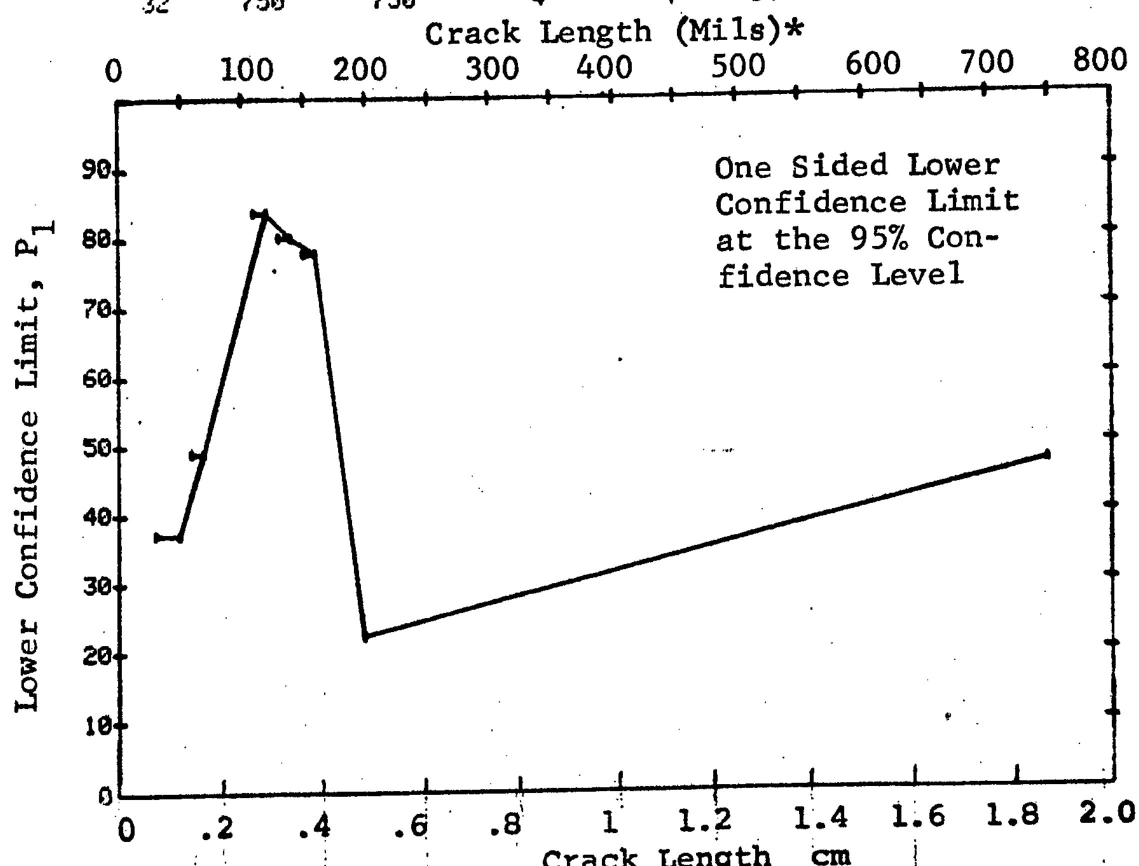

Figure D-103 Probability of Detection for 4340M Steel Using Eddy Current. Compressed Notch Flaws in Solid Cylinder. Prod. Env.

(b) Optimum Probability Method of Data Cumulation

28-OCT-75 EDDY CURRENT TEST 2 CL(103)

RANGE	MIN LN	* MAX LN *	N	DET	50%	95%	0 MISS	1 MISS
1	30	50	21	12	0	37	0	0
2	60	70	15	11	0	48	0	0
3	0	0	0	0	0	0	0	0
4	110	120	17	17	0	83	12	29
5	110	140	39	38	0	89	7	22
6	110	160	51	50	0	91	0	10
7	0	0	0	0	0	0	0	0
8	110	200	53	52	0	91	0	8
9	0	0	0	0	0	0	0	0
10	0	0	0	0	0	0	0	0
11	0	0	0	0	0	0	0	0
12	0	0	0	0	0	0	0	0
13	0	0	0	0	0	0	0	0
14	0	0	0	0	0	0	0	0
15	0	0	0	0	0	0	0	0
16	0	0	0	0	0	0	0	0
17	0	0	0	0	0	0	0	0
18	0	0	0	0	0	0	0	0
19	0	0	0	0	0	0	0	0
20	0	0	0	0	0	0	0	0
21	0	0	0	0	0	0	0	0
22	0	0	0	0	0	0	0	0
23	0	0	0	0	0	0	0	0
24	0	0	0	0	0	0	0	0
25	0	0	0	0	0	0	0	0
26	0	0	0	0	0	0	0	0
27	0	0	0	0	0	0	0	0
28	0	0	0	0	0	0	0	0
29	0	0	0	0	0	0	0	0
30	0	0	0	0	0	0	0	0
31	0	0	0	0	0	0	0	0
32	110	750	57	56	0	91	0	4

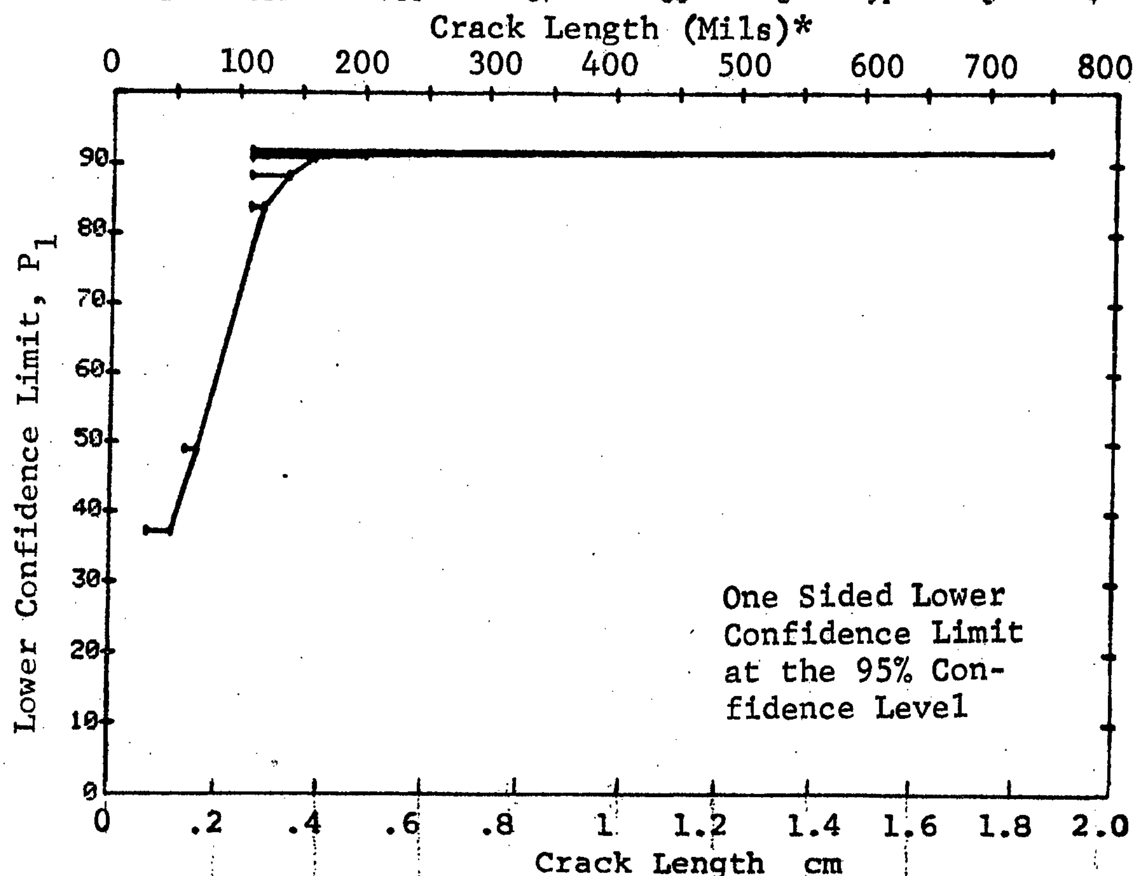

Figure D-103 (Continued)

(c) Overlapping Sixty Point Method of Data Cumulation

28-OCT-75 EDDY CURRENT TEST 3 (103)

RANGE	MIN LN*	MAX LN*	N	DET	50%	95%	0 MISS	1 MISS
1	0	0	0	0	0	0	0	0
2	0	0	0	0	0	0	0	0
3	0	0	0	0	0	0	0	0
4	0	0	0	0	0	0	0	0
5	0	0	0	0	0	0	0	0
6	0	0	0	0	0	0	0	0
7	0	0	0	0	0	0	0	0
8	0	0	0	0	0	0	0	0
9	0	0	0	0	0	0	0	0
10	0	0	0	0	0	0	0	0
11	0	0	0	0	0	0	0	0
12	0	0	0	0	0	0	0	0
13	0	0	0	0	0	0	0	0
14	0	0	0	0	0	0	0	0
15	0	0	0	0	0	0	0	0
16	0	0	0	0	0	0	0	0
17	0	0	0	0	0	0	0	0
18	0	0	0	0	0	0	0	0
19	0	0	0	0	0	0	0	0
20	0	0	0	0	0	0	0	0
21	0	0	0	0	0	0	0	0
22	0	0	0	0	0	0	0	0
23	0	0	0	0	0	0	0	0
24	0	0	0	0	0	0	0	0
25	0	0	0	0	0	0	0	0
26	0	0	0	0	0	0	0	0
27	0	0	0	0	0	0	0	0
28	0	0	0	0	0	0	0	0
29	0	0	0	0	0	0	0	0
30	0	0	0	0	0	0	0	0
31	30	140	59	46	76	67	0	0
32	60	200	60	56	92	85	29	43

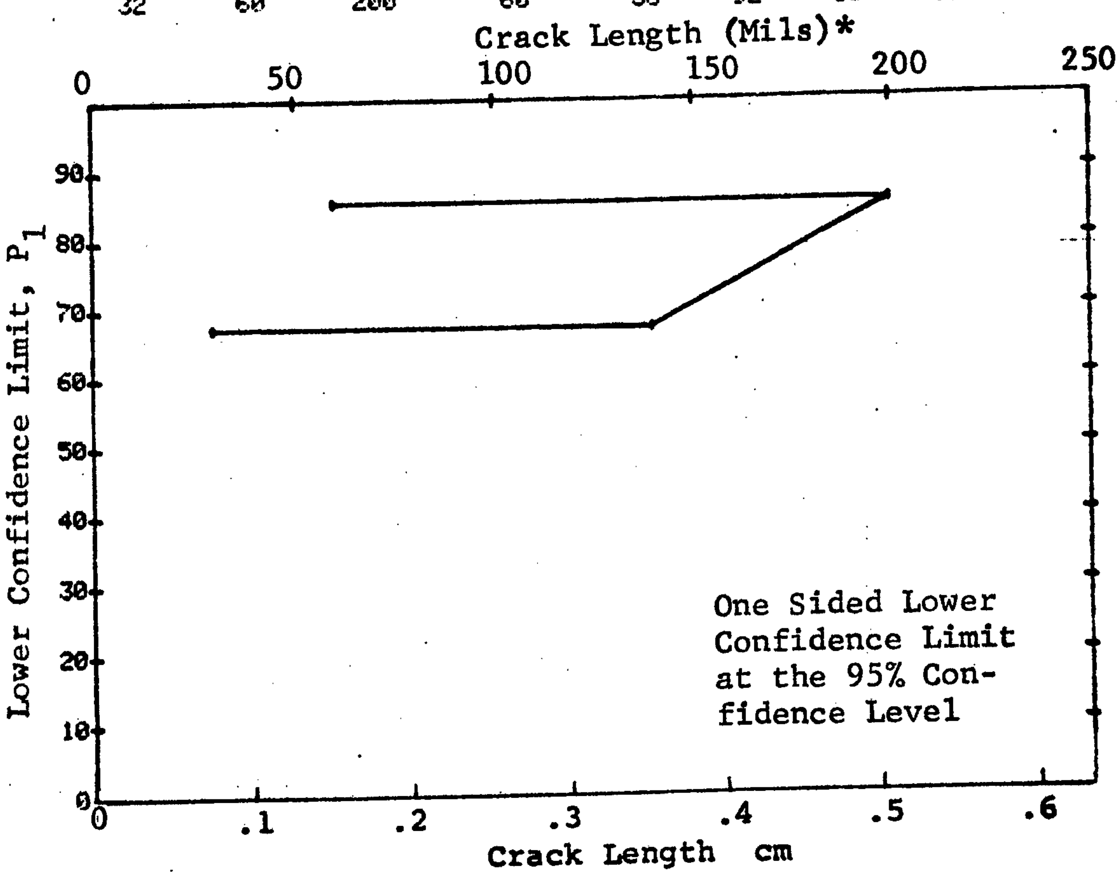

Figure D-103 (Concluded)

(a) Range Interval Method of Data Cumulation

28-OCT-75 EDDY CURRENT TEST 1 (104)

RANGE	MIN LN	MAX LN	N	DET	50%	95%	0 MISS	1 MISS
1	20 *	20 *	5	0	0	0	0	0
2	0	0	0	0	0	0	0	0
3	60	60	7	6	77	47	0	0
4	70	70	11	9	76	52	0	0
5	90	90	7	6	77	47	0	0
6	100	100	9	9	92	71	0	0
7	0	0	0	0	0	0	0	0
8	130	140	9	9	92	71	0	0
9	150	150	7	7	90	65	0	0
10	0	0	0	0	0	0	0	0
11	0	0	0	0	0	0	0	0
12	0	0	0	0	0	0	0	0
13	0	0	0	0	0	0	0	0
14	0	0	0	0	0	0	0	0
15	0	0	0	0	0	0	0	0
16	250	260	3	3	79	36	0	0
17	0	0	0	0	0	0	0	0
18	0	0	0	0	0	0	0	0
19	300	300	5	5	87	54	0	0
20	0	0	0	0	0	0	0	0
21	0	0	0	0	0	0	0	0
22	0	0	0	0	0	0	0	0
23	0	0	0	0	0	0	0	0
24	370	370	1	1	50	5	0	0
25	0	0	0	0	0	0	0	0
26	0	0	0	0	0	0	0	0
27	0	0	0	0	0	0	0	0
28	0	0	0	0	0	0	0	0
29	0	0	0	0	0	0	0	0
30	0	0	0	0	0	0	0	0
31	0	0	0	0	0	0	0	0
32	500	500	1	1	50	5	0	0

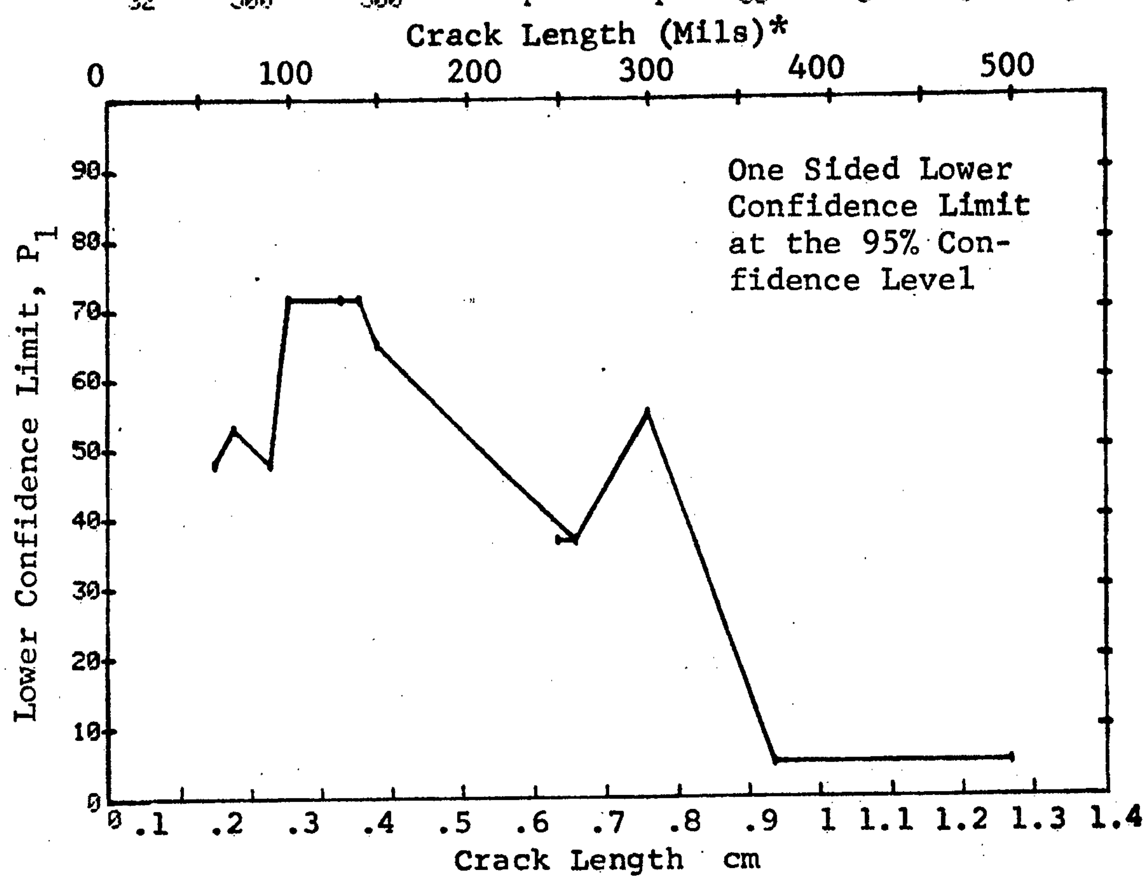

Figure D-104 Probability of Detection for 4340M Steel Using Eddy Current. Compressed Notch Flaws in Solid Filleted Cylinder. Prod. Env.

(b) Optimum Probability Method of Data Cumulation

28-OCT-75 EDDY CURRENT TEST 2 ((104)

RANGE	MIN LN	MAX LN	N	DFT	50%	95%	0 MISS	1 MISS
1	20 *	20 *	5	0	0	0	0	0
2	0	0	0	0	0	0	0	0
3	60	60	7	6	0	47	0	0
4	60	70	18	15	0	62	0	0
5	60	90	25	21	0	66	0	0
6	60	100	34	30	0	75	0	0
7	0	0	0	0	0	0	0	0
8	100	140	18	18	0	84	11	28
9	100	150	25	25	0	88	4	21
10	0	0	0	0	0	0	0	0
11	0	0	0	0	0	0	0	0
12	0	0	0	0	0	0	0	0
13	0	0	0	0	0	0	0	0
14	0	0	0	0	0	0	0	0
15	0	0	0	0	0	0	0	0
16	100	260	28	28	0	89	1	18
17	0	0	0	0	0	0	0	0
18	0	0	0	0	0	0	0	0
19	100	300	33	33	0	91	0	13
20	0	0	0	0	0	0	0	0
21	0	0	0	0	0	0	0	0
22	0	0	0	0	0	0	0	0
23	0	0	0	0	0	0	0	0
24	100	370	34	34	0	91	0	12
25	0	0	0	0	0	0	0	0
26	0	0	0	0	0	0	0	0
27	0	0	0	0	0	0	0	0
28	0	0	0	0	0	0	0	0
29	0	0	0	0	0	0	0	0
30	0	0	0	0	0	0	0	0
31	0	0	0	0	0	0	0	0
32	100	500	35	35	0	91	0	11

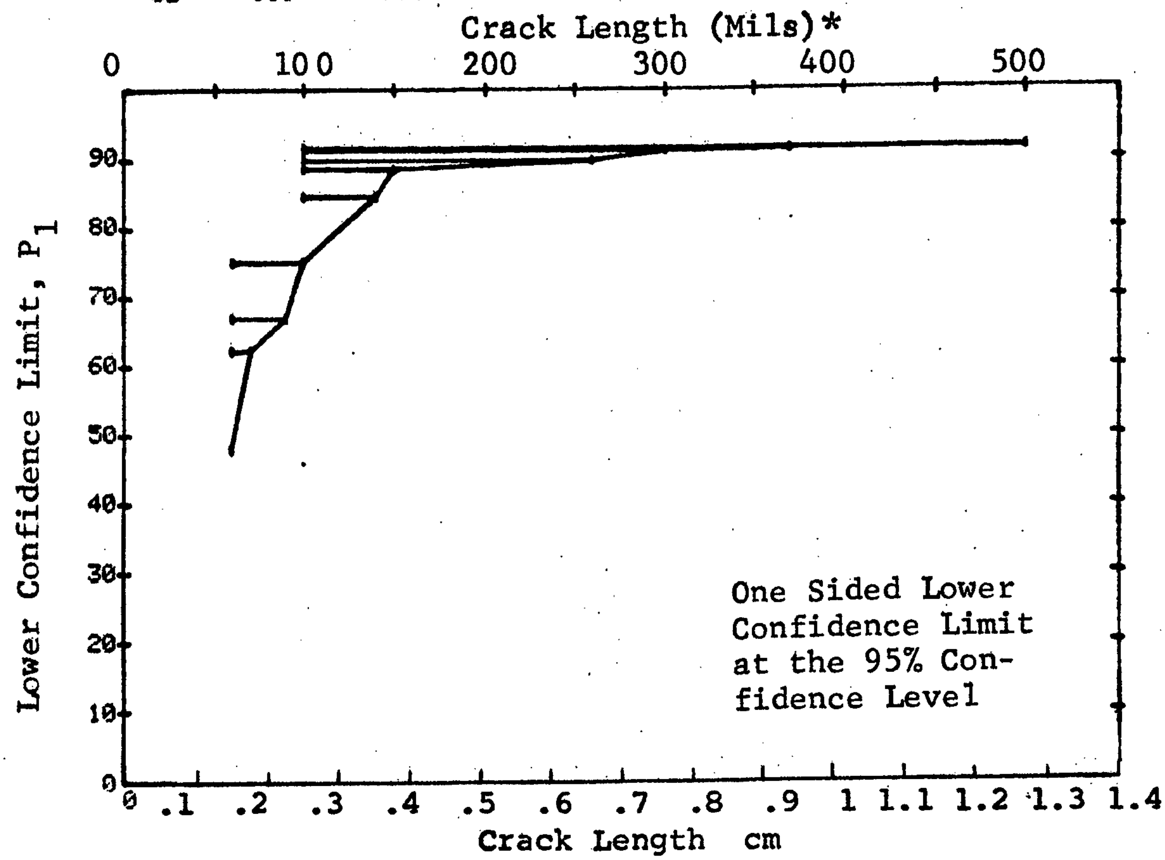

Figure D-104 (Continued)

(c) Overlapping Sixty Point Method of Data Cumulation

28-OCT-75 EDDY CURRENT TEST 3 (104)

RANGE	MIN LN *	MAX LN *	N	DET	50%	95%	0 MISS	1 MISS
1	0	0	0	0	0	0	0	0
2	0	0	0	0	0	0	0	0
3	0	0	0	0	0	0	0	0
4	0	0	0	0	0	0	0	0
5	0	0	0	0	0	0	0	0
6	0	0	0	0	0	0	0	0
7	0	0	0	0	0	0	0	0
8	0	0	0	0	0	0	0	0
9	0	0	0	0	0	0	0	0
10	0	0	0	0	0	0	0	0
11	0	0	0	0	0	0	0	0
12	0	0	0	0	0	0	0	0
13	0	0	0	0	0	0	0	0
14	0	0	0	0	0	0	0	0
15	0	0	0	0	0	0	0	0
16	0	0	0	0	0	0	0	0
17	0	0	0	0	0	0	0	0
18	0	0	0	0	0	0	0	0
19	0	0	0	0	0	0	0	0
20	0	0	0	0	0	0	0	0
21	0	0	0	0	0	0	0	0
22	0	0	0	0	0	0	0	0
23	0	0	0	0	0	0	0	0
24	0	0	0	0	0	0	0	0
25	0	0	0	0	0	0	0	0
26	0	0	0	0	0	0	0	0
27	0	0	0	0	0	0	0	0
28	0	0	0	0	0	0	0	0
29	0	0	0	0	0	0	0	0
30	0	0	0	0	0	0	0	0
31	20	100	35	26	72	59	0	0
32	60	500	60	56	93	85	29	43

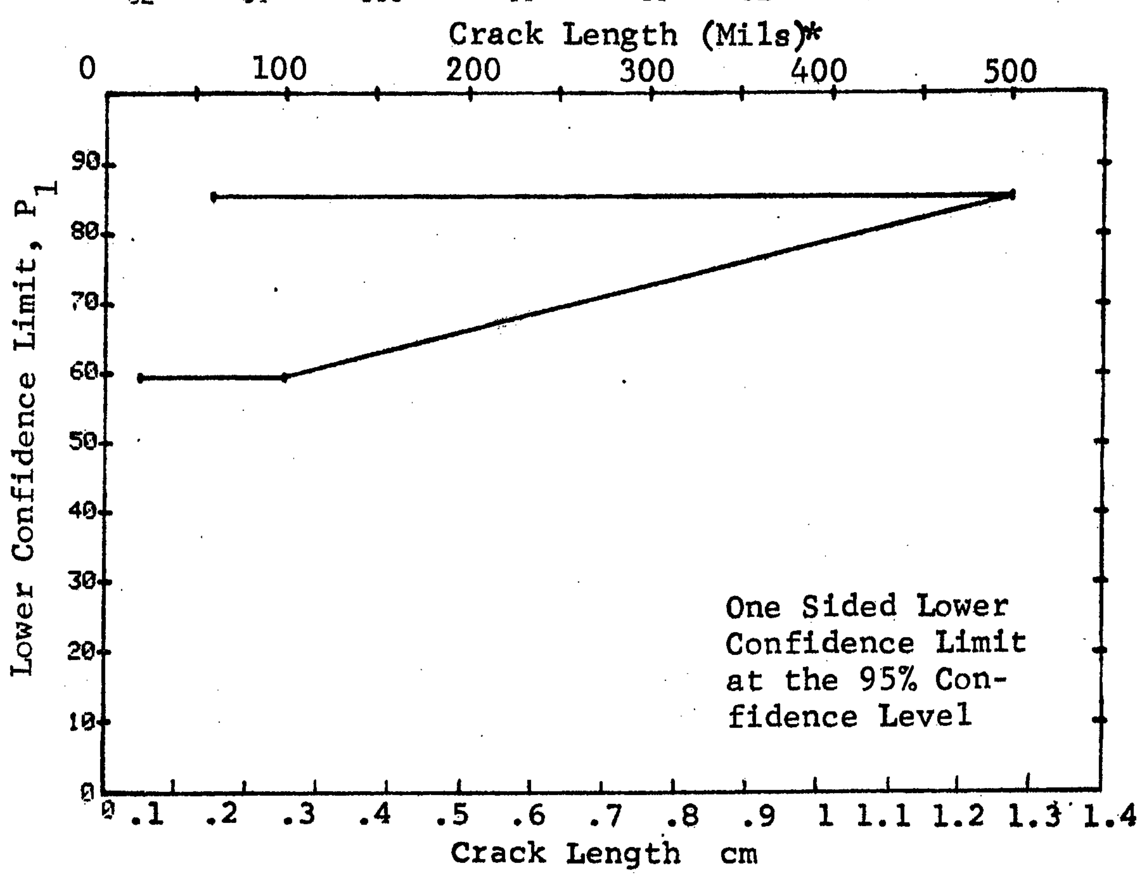

Figure D-104 (Concluded)

(a) Range Interval Method of Data Cumulation

28-OCT-75 EDDY CURRENT TEST 1 (105)

RANGE	MIN LN	MAX LN	N	DET	50%	95%	0 MISS	1 MISS
1	60 *	60 *	4	4	84	47	0	0
2	0	0	0	0	0	0	0	0
3	0	0	0	0	0	0	0	0
4	0	0	0	0	0	0	0	0
5	0	0	0	0	0	0	0	0
6	0	0	0	0	0	0	0	0
7	0	0	0	0	0	0	0	0
8	0	0	0	0	0	0	0	0
9	0	0	0	0	0	0	0	0
10	0	0	0	0	0	0	0	0
11	100	100	8	8	91	68	0	0
12	0	0	0	0	0	0	0	0
13	0	0	0	0	0	0	0	0
14	0	0	0	0	0	0	0	0
15	0	0	0	0	0	0	0	0
16	120	120	2	2	70	22	0	0
17	0	0	0	0	0	0	0	0
18	0	0	0	0	0	0	0	0
19	0	0	0	0	0	0	0	0
20	0	0	0	0	0	0	0	0
21	0	0	0	0	0	0	0	0
22	140	140	2	2	70	22	0	0
23	0	0	0	0	0	0	0	0
24	0	0	0	0	0	0	0	0
25	0	0	0	0	0	0	0	0
26	0	0	0	0	0	0	0	0
27	160	160	3	2	50	13	0	0
28	0	0	0	0	0	0	0	0
29	0	0	0	0	0	0	0	0
30	0	0	0	0	0	0	0	0
31	0	0	0	0	0	0	0	0
32	180	180	2	2	70	22	0	0

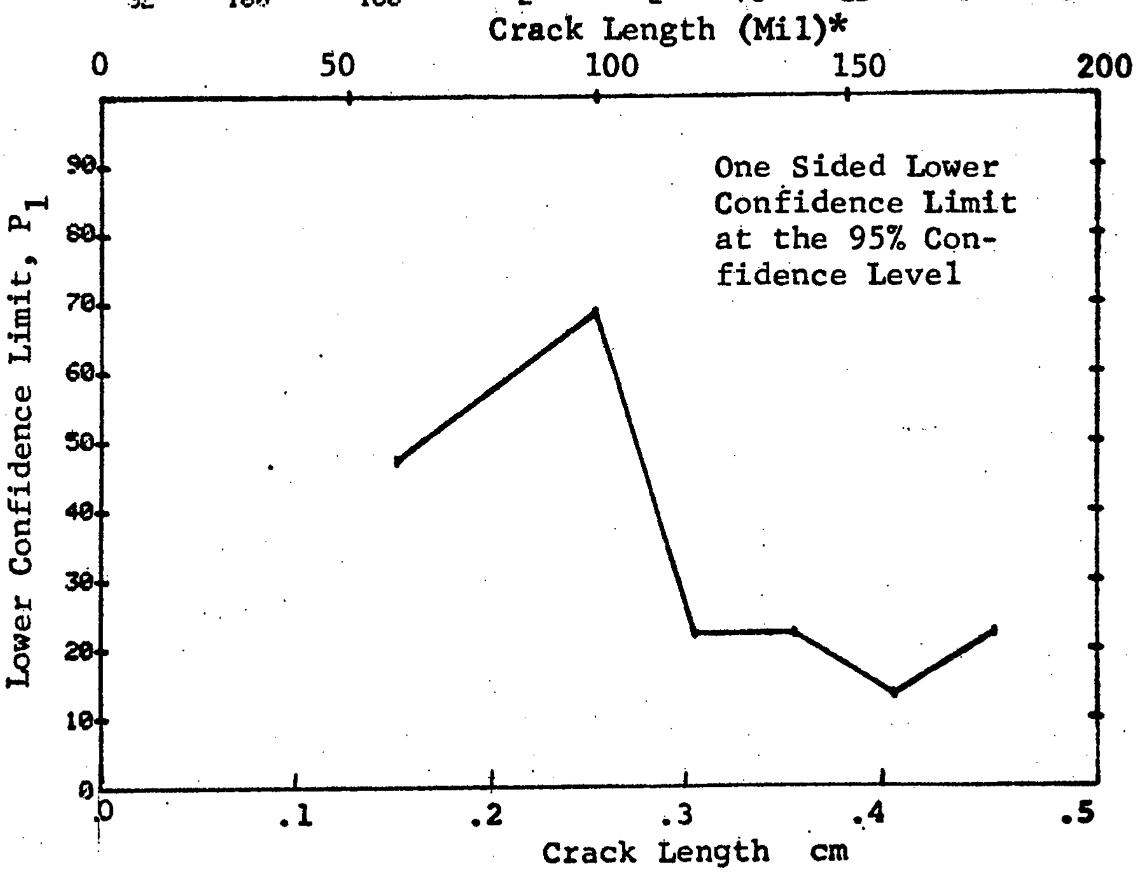

Figure D-105 Probability of Detection for 4340M Steel Using Eddy Current. Compressed Notch Flaws in Hollow Cylinder. Prod. Env.

(b) Optimum Probability Method of Data Cumulation

28-OCT-75 EDDY CURRENT TEST (105)

RANGE	MIN LN	MAX LN	N	DET	50%	95%	0 MISS	1 MISS
1	60*	60*	4	4	0	47	0	0
2	0	0	0	0	0	0	0	0
3	0	0	0	0	0	0	0	0
4	0	0	0	0	0	0	0	0
5	0	0	0	0	0	0	0	0
6	0	0	0	0	0	0	0	0
7	0	0	0	0	0	0	0	0
8	0	0	0	0	0	0	0	0
9	0	0	0	0	0	0	0	0
10	0	0	0	0	0	0	0	0
11	60	100	12	12	0	77	0	0
12	0	0	0	0	0	0	0	0
13	0	0	0	0	0	0	0	0
14	0	0	0	0	0	0	0	0
15	0	0	0	0	0	0	0	0
16	60	120	14	14	0	80	15	32
17	0	0	0	0	0	0	0	0
18	0	0	0	0	0	0	0	0
19	0	0	0	0	0	0	0	0
20	0	0	0	0	0	0	0	0
21	0	0	0	0	0	0	0	0
22	60	140	16	16	0	82	13	30
23	0	0	0	0	0	0	0	0
24	0	0	0	0	0	0	0	0
25	0	0	0	0	0	0	0	0
26	0	0	0	0	0	0	0	0
27	60	160	19	18	0	77	0	0
28	0	0	0	0	0	0	0	0
29	0	0	0	0	0	0	0	0
30	0	0	0	0	0	0	0	0
31	0	0	0	0	0	0	0	0
32	60	180	21	20	0	79	0	0

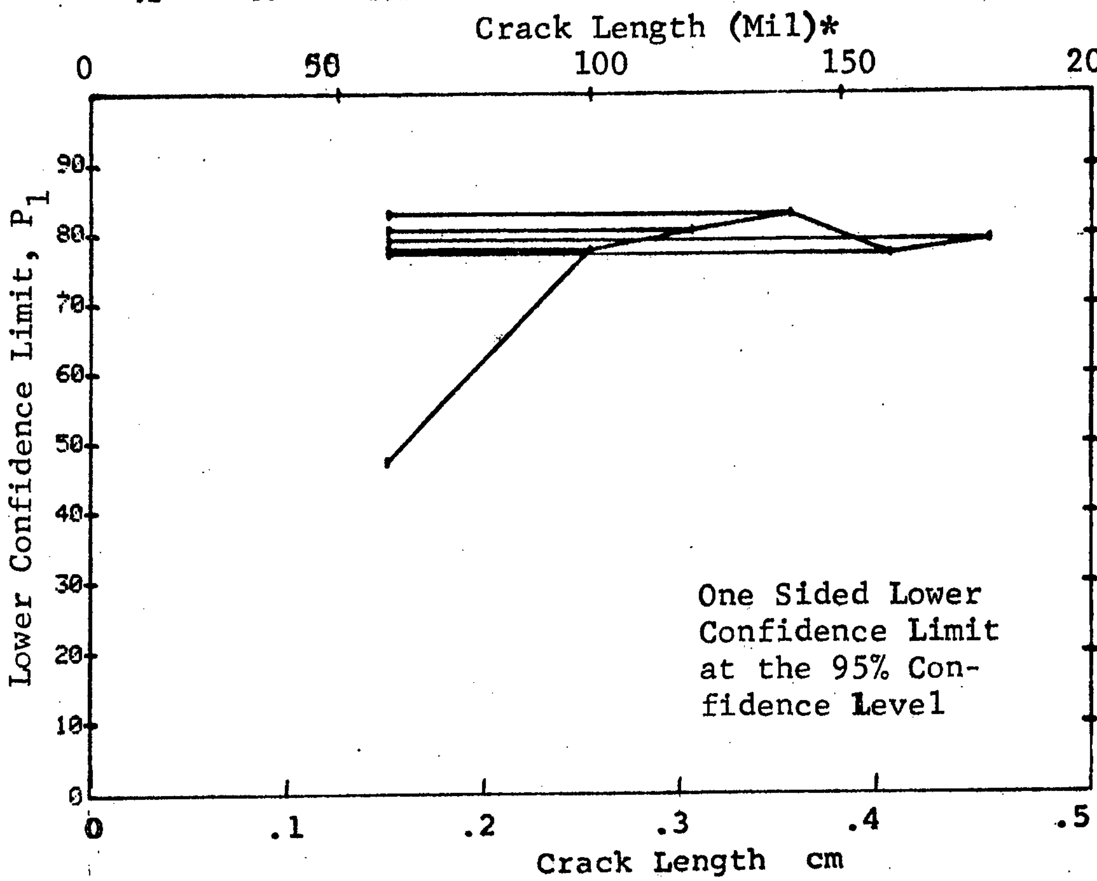

Figure D-105 (Continued)

(c) Overlapping Sixty Point Method of Data Cumulation

28-OCT-75 EDDY CURRENT TEST 3 (105)

RANGE	MIN LN	*MAX LN	N	DET	50%	95%	0 MISS	1 MISS
1	0	0*	0	0	0	0	0	0
2	0	0	0	0	0	0	0	0
3	0	0	0	0	0	0	0	0
4	0	0	0	0	0	0	0	0
5	0	0	0	0	0	0	0	0
6	0	0	0	0	0	0	0	0
7	0	0	0	0	0	0	0	0
8	0	0	0	0	0	0	0	0
9	0	0	0	0	0	0	0	0
10	0	0	0	0	0	0	0	0
11	0	0	0	0	0	0	0	0
12	0	0	0	0	0	0	0	0
13	0	0	0	0	0	0	0	0
14	0	0	0	0	0	0	0	0
15	0	0	0	0	0	0	0	0
16	0	0	0	0	0	0	0	0
17	0	0	0	0	0	0	0	0
18	0	0	0	0	0	0	0	0
19	0	0	0	0	0	0	0	0
20	0	0	0	0	0	0	0	0
21	0	0	0	0	0	0	0	0
22	0	0	0	0	0	0	0	0
23	0	0	0	0	0	0	0	0
24	0	0	0	0	0	0	0	0
25	0	0	0	0	0	0	0	0
26	0	0	0	0	0	0	0	0
27	0	0	0	0	0	0	0	0
28	0	0	0	0	0	0	0	0
29	0	0	0	0	0	0	0	0
30	0	0	0	0	0	0	0	0
31	0	0	0	0	0	0	0	0
32	60	180	21	20	92	79	25	40

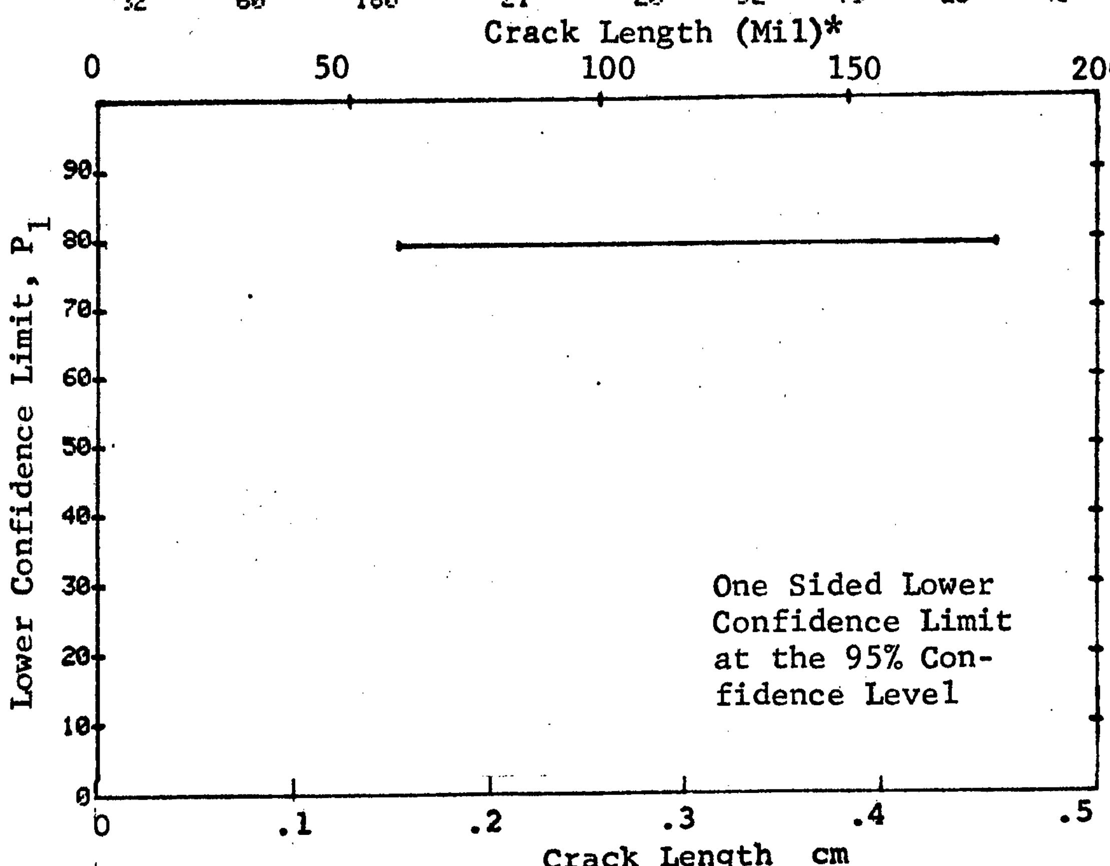

Figure D-105 (Concluded)

(a) Range Interval Method of Data Cumulation

28-OCT-75 EDDY CURRENT TEST 1 (106)

RANGE	MIN LN	MAX LN	N	DFT	50%	95%	0 MISS	1 MISS
1	80 *	80 *	1	1	50	5	0	0
2	90	90	8	8	91	68	0	0
3	0	0	0	0	0	0	0	0
4	0	0	0	0	0	0	0	0
5	110	110	4	4	84	47	0	0
6	120	120	1	1	50	5	0	0
7	0	0	0	0	0	0	0	0
8	130	130	1	1	50	5	0	0
9	140	140	7	7	90	65	0	0
10	0	0	0	0	0	0	0	0
11	0	0	0	0	0	0	0	0
12	0	0	0	0	0	0	0	0
13	0	0	0	0	0	0	0	0
14	0	0	0	0	0	0	0	0
15	0	0	0	0	0	0	0	0
16	0	0	0	0	0	0	0	0
17	0	0	0	0	0	0	0	0
18	0	0	0	0	0	0	0	0
19	0	0	0	0	0	0	0	0
20	0	0	0	0	0	0	0	0
21	0	0	0	0	0	0	0	0
22	0	0	0	0	0	0	0	0
23	0	0	0	0	0	0	0	0
24	0	0	0	0	0	0	0	0
25	0	0	0	0	0	0	0	0
26	0	0	0	0	0	0	0	0
27	0	0	0	0	0	0	0	0
28	0	0	0	0	0	0	0	0
29	0	0	0	0	0	0	0	0
30	0	0	0	0	0	0	0	0
31	0	0	0	0	0	0	0	0
32	300	300	3	3	79	36	0	0

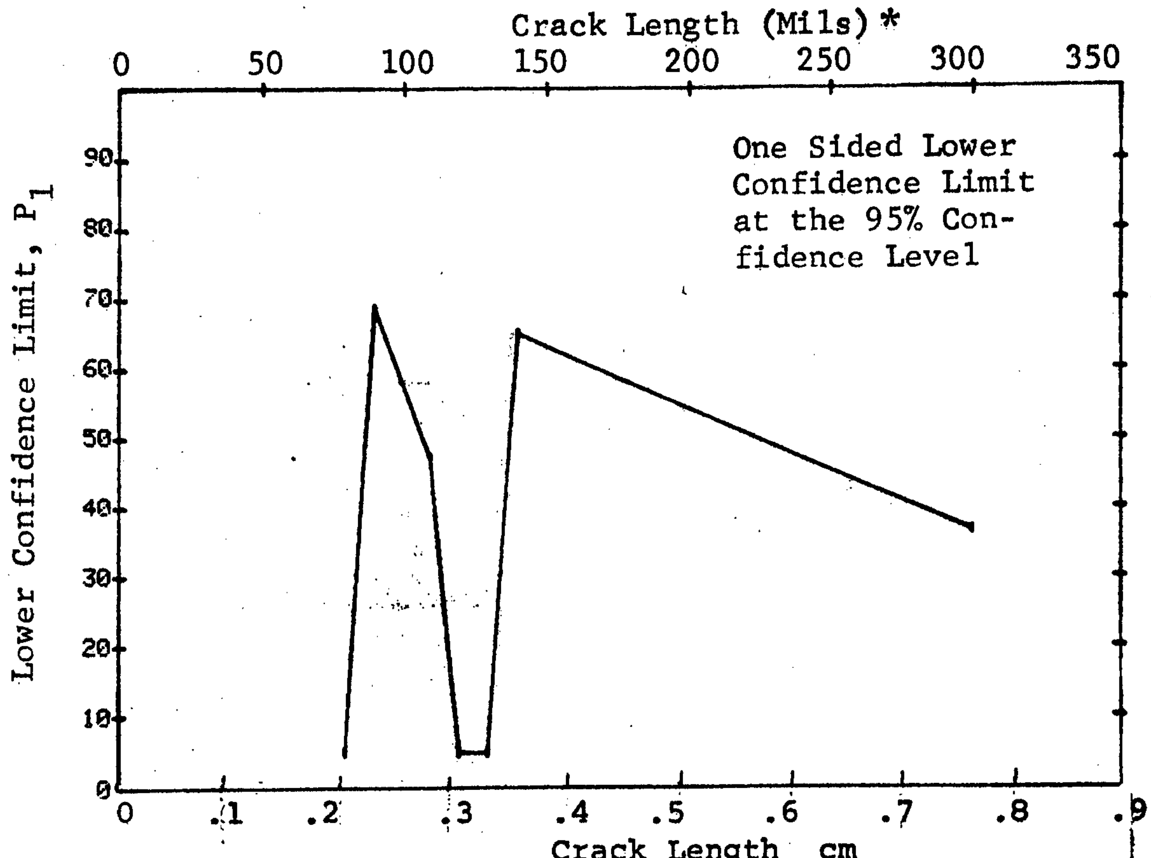

Figure D-106 Probability of Detection for 4340M Steel Using Eddy Current Compressed Notch Flaws in Hollow Cylinder. Prod. Env.

(b) Optimum Probability Method of Data Cumulation

28-OCT-75 EDDY CURRENT TEST 2 (106)

RANGE	MIN LN	MAX LN	N	DET	50%	95%	0 MISS	1 MISS
1	80 *	80 *	1	1	0	5	0	0
2	80	90	9	9	0	71	0	0
3	0	0	0	0	0	0	0	0
4	0	0	0	0	0	0	0	0
5	80	110	13	13	0	79	0	0
6	80	120	14	14	0	80	15	32
7	0	0	0	0	0	0	0	0
8	80	130	15	15	0	81	14	31
9	80	140	22	22	0	87	7	24
10	0	0	0	0	0	0	0	0
11	0	0	0	0	0	0	0	0
12	0	0	0	0	0	0	0	0
13	0	0	0	0	0	0	0	0
14	0	0	0	0	0	0	0	0
15	0	0	0	0	0	0	0	0
16	0	0	0	0	0	0	0	0
17	0	0	0	0	0	0	0	0
18	0	0	0	0	0	0	0	0
19	0	0	0	0	0	0	0	0
20	0	0	0	0	0	0	0	0
21	0	0	0	0	0	0	0	0
22	0	0	0	0	0	0	0	0
23	0	0	0	0	0	0	0	0
24	0	0	0	0	0	0	0	0
25	0	0	0	0	0	0	0	0
26	0	0	0	0	0	0	0	0
27	0	0	0	0	0	0	0	0
28	0	0	0	0	0	0	0	0
29	0	0	0	0	0	0	0	0
30	0	0	0	0	0	0	0	0
31	0	0	0	0	0	0	0	0
32	80	300	25	25	0	88	4	21

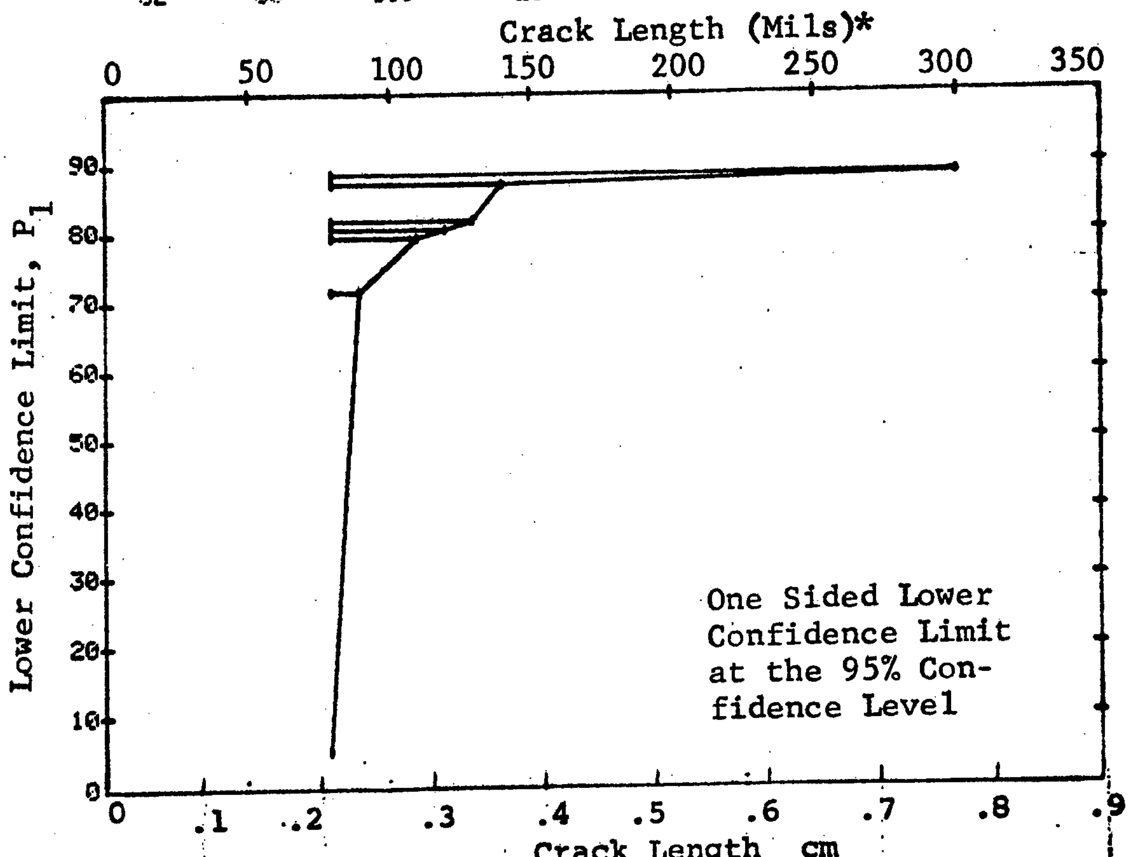

Figure D-106 (Continued)

(c) Overlapping Sixty Point Method of Data Cumulation

28-OCT-75 EDDY CURRENT TEST 3 ((106)) :

RANGE	MIN LN *	MAX LN *	N	DET	50%	95%	0 MISS	1 MISS
1	0	0	0	0	0	0	0	0
2	0	0	0	0	0	0	0	0
3	0	0	0	0	0	0	0	0
4	0	0	0	0	0	0	0	0
5	0	0	0	0	0	0	0	0
6	0	0	0	0	0	0	0	0
7	0	0	0	0	0	0	0	0
8	0	0	0	0	0	0	0	0
9	0	0	0	0	0	0	0	0
10	0	0	0	0	0	0	0	0
11	0	0	0	0	0	0	0	0
12	0	0	0	0	0	0	0	0
13	0	0	0	0	0	0	0	0
14	0	0	0	0	0	0	0	0
15	0	0	0	0	0	0	0	0
16	0	0	0	0	0	0	0	0
17	0	0	0	0	0	0	0	0
18	0	0	0	0	0	0	0	0
19	0	0	0	0	0	0	0	0
20	0	0	0	0	0	0	0	0
21	0	0	0	0	0	0	0	0
22	0	0	0	0	0	0	0	0
23	0	0	0	0	0	0	0	0
24	0	0	0	0	0	0	0	0
25	0	0	0	0	0	0	0	0
26	0	0	0	0	0	0	0	0
27	0	0	0	0	0	0	0	0
28	0	0	0	0	0	0	0	0
29	0	0	0	0	0	0	0	0
30	0	0	0	0	0	0	0	0
31	0	0	0	0	0	0	0	0
32	80	300	25	25	97	88	4	21

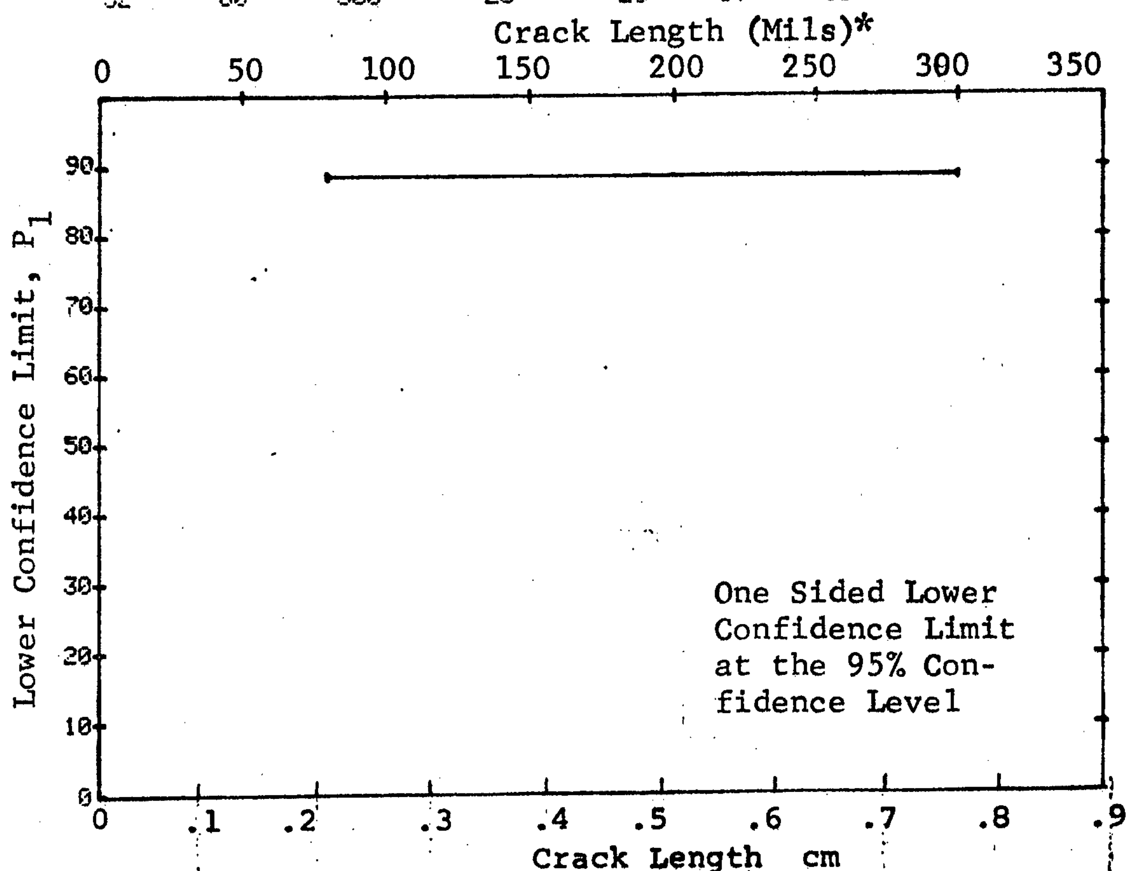

Figure D-106 (Concluded)

(a) Range Interval Method of Data Cumulation

28-OCT-75 EDDY CURRENT TEST 1 ((107)

RANGE	MIN LN	MAX LN	N	DET	50%	95%	0 MISS	1 MISS
1	10 *	10 *	1	0	0	0	0	0
2	0	0	0	0	0	0	0	0
3	30	30	5	4	68	34	0	0
4	0	0	0	0	0	0	0	0
5	40	40	7	2	22	5	0	0
6	50	50	14	12	81	61	0	0
7	0	0	0	0	0	0	0	0
8	60	60	3	2	50	13	0	0
9	70	70	6	6	89	60	0	0
10	0	0	0	0	0	0	0	0
11	80	80	13	12	87	68	0	0
12	90	90	11	11	93	76	18	35
13	0	0	0	0	0	0	0	0
14	100	100	14	11	74	53	0	0
15	110	110	26	25	93	83	20	35
16	120	120	9	9	92	71	0	0
17	0	0	0	0	0	0	0	0
18	130	130	11	11	93	76	18	35
19	140	140	13	11	79	58	0	0
20	0	0	0	0	0	0	0	0
21	150	150	19	15	75	58	0	0
22	160	160	10	10	93	74	0	0
23	0	0	0	0	0	0	0	0
24	170	170	15	15	95	81	14	31
25	180	180	11	11	93	76	18	35
26	0	0	0	0	0	0	0	0
27	190	190	7	6	77	47	0	0
28	0	0	0	0	0	0	0	0
29	0	0	0	0	0	0	0	0
30	210	210	2	2	70	22	0	0
31	220	220	9	9	92	71	0	0
32	230	230	13	13	94	79	16	33

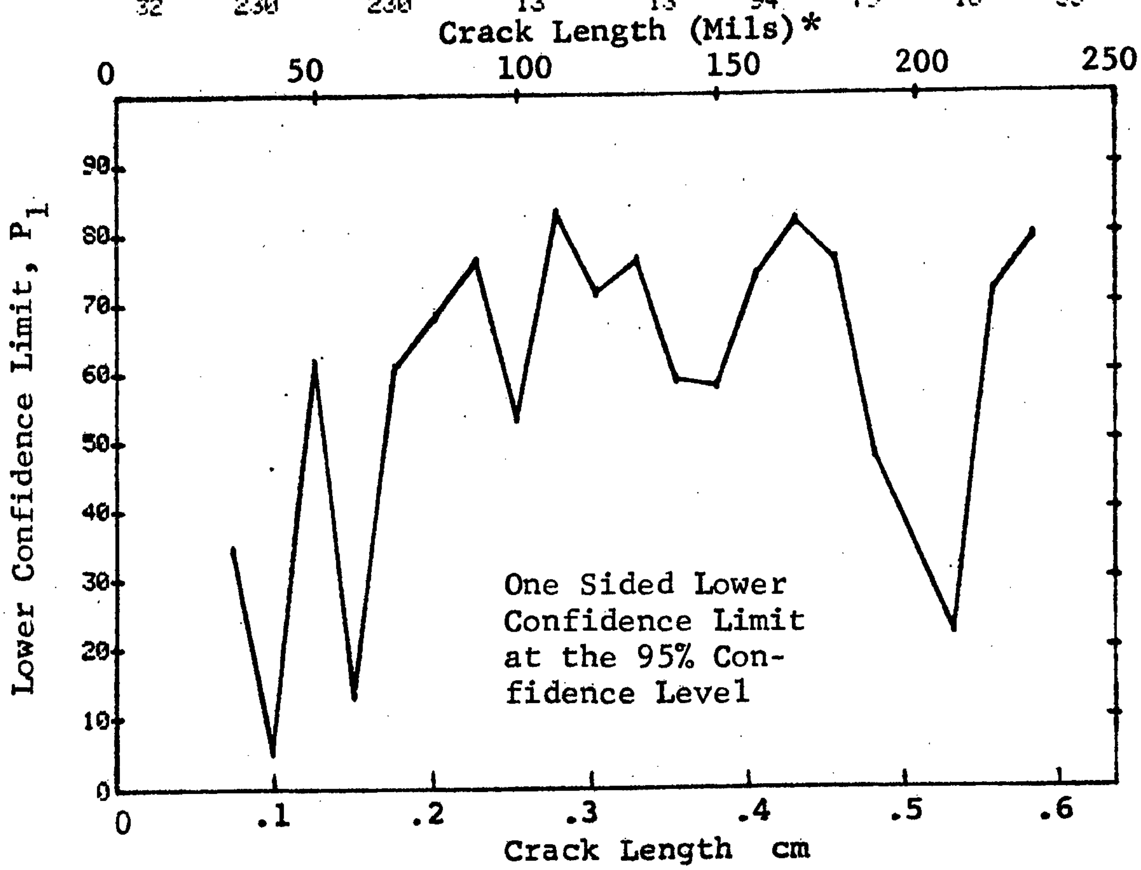

Figure D-107 Probability of Detection for 2024-T6 Al Using Eddy Current. Compressed Notch Flaws in Tandem T Specimens. Production Environment.

(b) Optimum Probability Method of Data Cumulation

28-OCT-75	EDDY CURRENT			TEST 2 (107)				
RANGE	MIN LN	MAX LN	N	DET	50%	95%	0 MISS	1 MISS
1	10 *	10 *	1	0	0	0	0	0
2	0	0	0	0	0	0	0	0
3	30	30	5	4	0	34	0	0
4	0	0	0	0	0	0	0	0
5	30	40	12	6	0	24	0	0
6	50	50	14	12	0	61	0	0
7	0	0	0	0	0	0	0	0
8	50	60	17	14	0	60	0	0
9	50	70	23	20	0	69	0	0
10	0	0	0	0	0	0	0	0
11	70	80	19	18	0	77	0	0
12	70	90	30	29	0	85	16	31
13	0	0	0	0	0	0	0	0
14	70	100	44	40	0	80	45	59
15	70	110	70	65	0	85	33	46
16	110	120	35	34	0	87	11	26
17	0	0	0	0	0	0	0	0
18	110	130	46	45	0	90	0	15
19	70	140	103	96	0	87	0	0
20	0	0	0	0	0	0	0	0
21	70	150	122	111	0	85	0	0
22	70	160	132	121	0	86	0	0
23	0	0	0	0	0	0	0	0
24	160	170	25	25	0	88	4	21
25	160	180	36	36	0	92	0	10
26	0	0	0	0	0	0	0	0
27	160	190	43	42	0	89	3	18
28	0	0	0	0	0	0	0	0
29	0	0	0	0	0	0	0	0
30	160	210	45	44	0	89	1	[illegible]
31	160	220	54	53	0	91	0	0
32	160	230	67	66	0	93	0	0

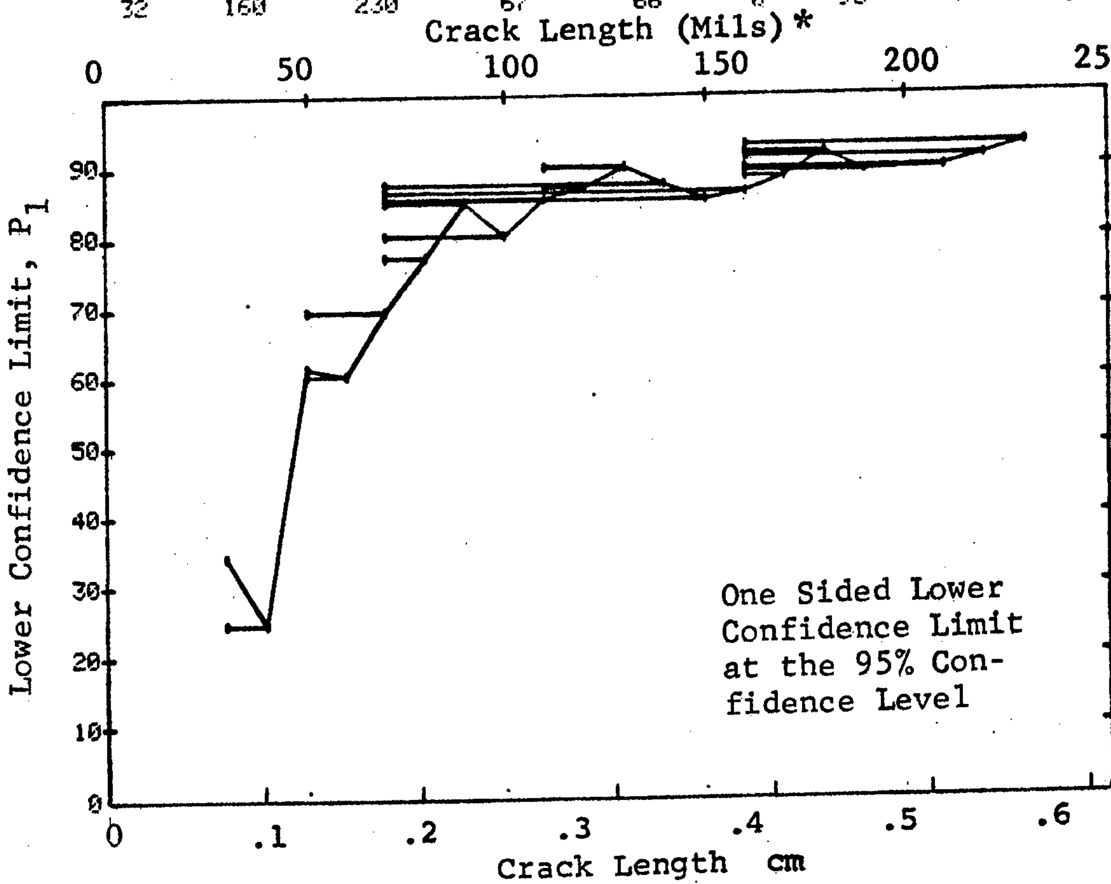

Figure D-107 (Continued)

(c) Overlapping Sixty Point Method of Data Cumulation

28-OCT-75 EDDY CURRENT T[illegible] 3 (107)

RANGE	MIN LN	MAX LN	N	DET	50%	95%	0 MISS	1 MISS
1	0	0	0	0	0	0	0	0
2	0	0	0	0	0	0	0	0
3	0	0	0	0	0	0	0	0
4	0	0	0	0	0	0	0	0
5	0	0	0	0	0	0	0	0
6	0	0	0	0	0	0	0	0
7	0	0	0	0	0	0	0	0
8	0	0	0	0	0	0	0	0
9	0	0	0	0	0	0	0	0
10	0	0	0	0	0	0	0	0
11	0	0	0	0	0	0	0	0
12	0	0	0	0	0	0	0	0
13	0	0	0	0	0	0	0	0
14	0	0	0	0	0	0	0	0
15	0	0	0	0	0	0	0	0
16	0	0	0	0	0	0	0	0
17	0	0	0	0	0	0	0	0
18	0	0	0	0	0	0	0	0
19	0	0	0	0	0	0	0	0
20	0	0	0	0	0	0	0	0
21	0	0	0	0	0	0	0	0
22	0	0	0	0	0	0	0	0
23	0	0	0	0	0	0	0	0
24	0	0	0	0	0	0	0	0
25	0	0	0	0	0	0	0	0
26	10	80	39	29	72	60	0	0
27	40	100	60	51	83	75	94	100
28	80	110	60	55	90	83	43	56
29	100	140	60	57	93	87	[illegible]	[illegible]
30	110	160	60	54	88	81	56	[illegible]
31	140	190	59	54	98	81	56	69
32	160	230	60	59	97	92	0	[illegible]

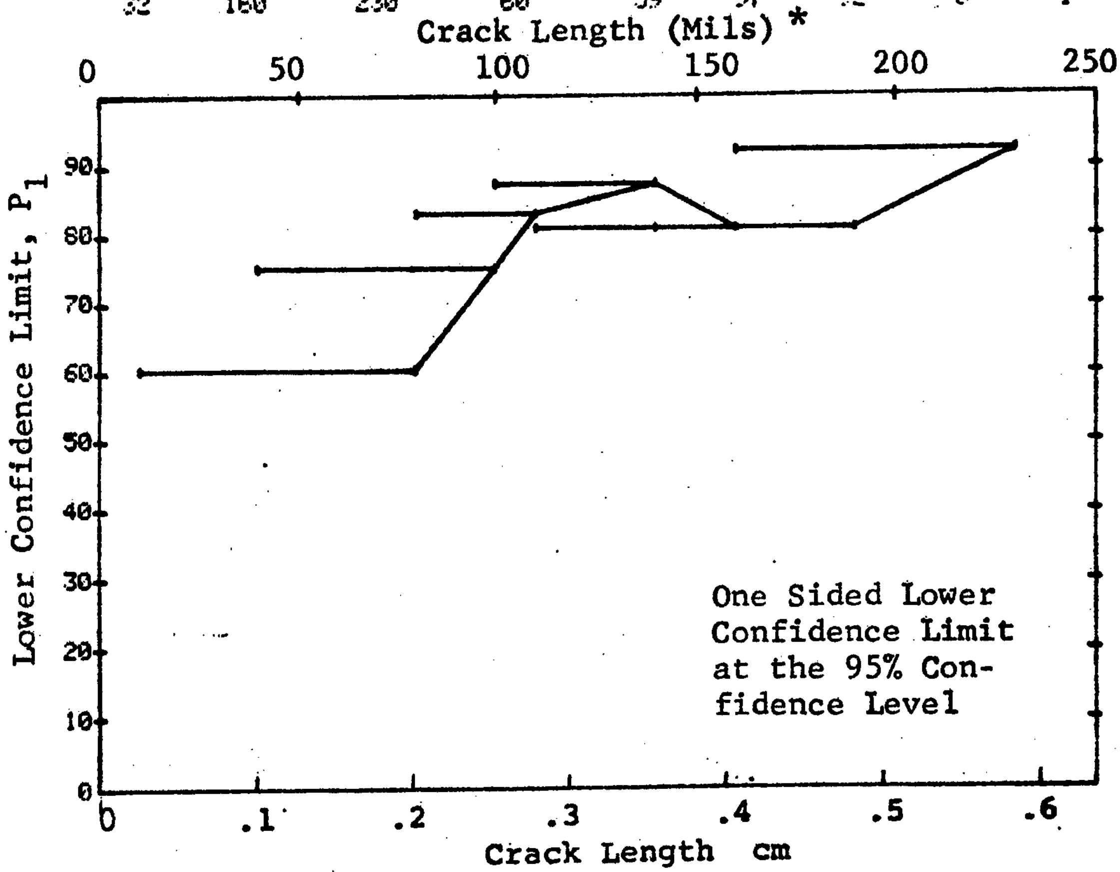

Figure D-107 (Concluded)

(a) Range Interval Method of Data Cumulation

28-OCT-7[illegible] EDC [illegible] (108)

RANGE	MIN LN	[illegible] LN	[illegible]	[illegible]	[illegible]	[illegible]	[illegible]	[illegible]
1	10	10	[illegible]	2	70	22	0	
2	0	[illegible]	0	0	0	0	0	[illegible]
3	30	30	2	0	0	0	0	[illegible]
4	0	0	0	0	0	0	0	[illegible]
5	40	40	8	6	67	40	0	[illegible]
6	50	50	10	6	54	30	0	0
7	0	0	0	0	0	0	0	0
8	60	60	4	4	84	47	0	0
9	70	70	4	3	61	24	0	0
10	0	0	0	0	0	0	0	0
11	80	80	14	9	60	39	0	0
12	90	90	15	8	50	29	0	0
13	0	0	0	0	0	0	0	0
14	100	100	9	6	60	34	0	0
15	110	110	23	18	75	59	0	0
16	120	120	3	3	79	36	0	0
17	0	0	0	0	0	0	0	0
18	130	130	4	4	84	47	0	0
19	140	140	12	10	78	56	0	0
20	0	0	0	0	0	0	0	0
21	150	150	14	14	95	80	15	32
22	160	160	5	5	87	54	0	0
23	0	0	0	0	0	0	0	0
24	170	170	8	8	91	68	0	[illegible]
25	180	180	14	14	95	80	15	[illegible]
26	0	0	0	0	0	0	[illegible]	[illegible]
27	190	190	4	4	84	47	0	[illegible]
28	0	0	0	0	0	0	0	[illegible]
29	0	0	0	0	0	[illegible]		[illegible]
30	210	210	2	2	70	22	[illegible]	[illegible]
31	220	220	3	3	79	36	[illegible]	[illegible]
32	230	230	14	14	95	[illegible]	[illegible]	[illegible]

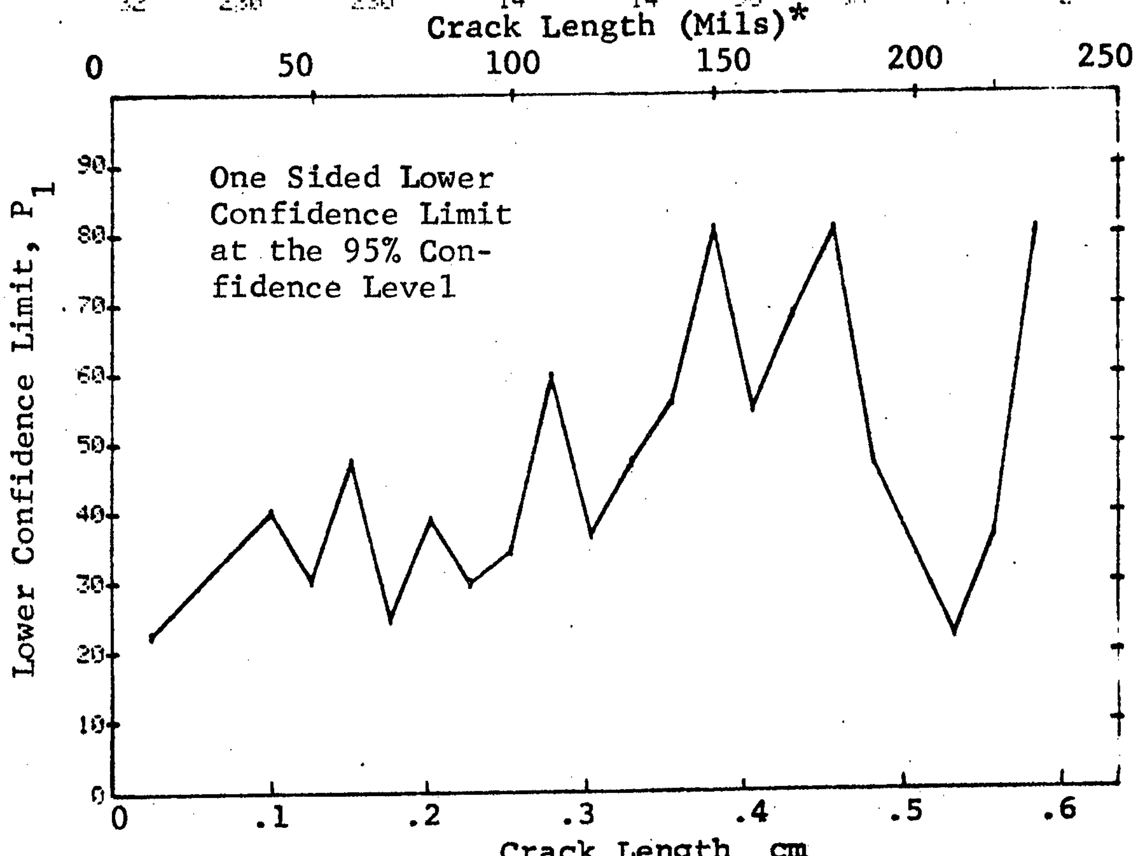

Figure D-108 Probability of Detection for 2024-T6 Al Using Eddy Current. Compressed Notch Flaws in Tandem T Specimen. Laboratory Environment.

(b) Optimum Probability Method of Data Cumulation

28-OCT-75 EDDY CURRENT TEST (108)

RANGE	MIN LN	MAX LN	N	HIT	[illegible]	[illegible]	[illegible]	[illegible]
1	10	10	[illegible]	2	0	[illegible]	[illegible]	[illegible]
2	0	[illegible]	0	0	[illegible]	[illegible]	[illegible]	[illegible]
3	10	30	4	2	0	[illegible]	[illegible]	[illegible]
4	0	0	0	0	0	0	[illegible]	[illegible]
5	40	40	8	6	0	40	[illegible]	[illegible]
6	40	50	18	12	0	44	[illegible]	0
7	0	0	0	0	0	0	0	0
8	40	60	22	16	0	53	0	0
9	40	70	26	19	0	55	0	0
10	0	0	0	0	0	0	0	0
11	40	80	40	28	0	55	0	0
12	40	90	55	36	0	53	0	0
13	0	0	0	0	0	0	0	0
14	40	100	64	42	0	54	0	0
15	40	110	87	60	0	59	0	0
16	110	120	26	21	0	63	0	0
17	0	0	0	0	0	0	0	0
18	110	130	30	25	0	68	0	0
19	110	140	42	35	0	70	0	0
20	0	0	0	0	0	0	0	0
21	120	150	33	31	0	82	28	43
22	150	160	19	19	0	85	10	[illegible]
23	0	0	0	0	0	0	0	[illegible]
24	150	170	27	27	0	89	0	[illegible]
25	150	180	41	41	0	92	0	[illegible]
26	0	0	0	0	0	0	0	[illegible]
27	150	190	45	45	0	93	0	0
28	0	0	0	0	0	0	0	0
29	0	0	0	0	0	[illegible]		
30	150	210	47	47	0	93	[illegible]	[illegible]
31	150	220	50	50	0	94	[illegible]	[illegible]
32	150	230	54	54	0	95	[illegible]	[illegible]

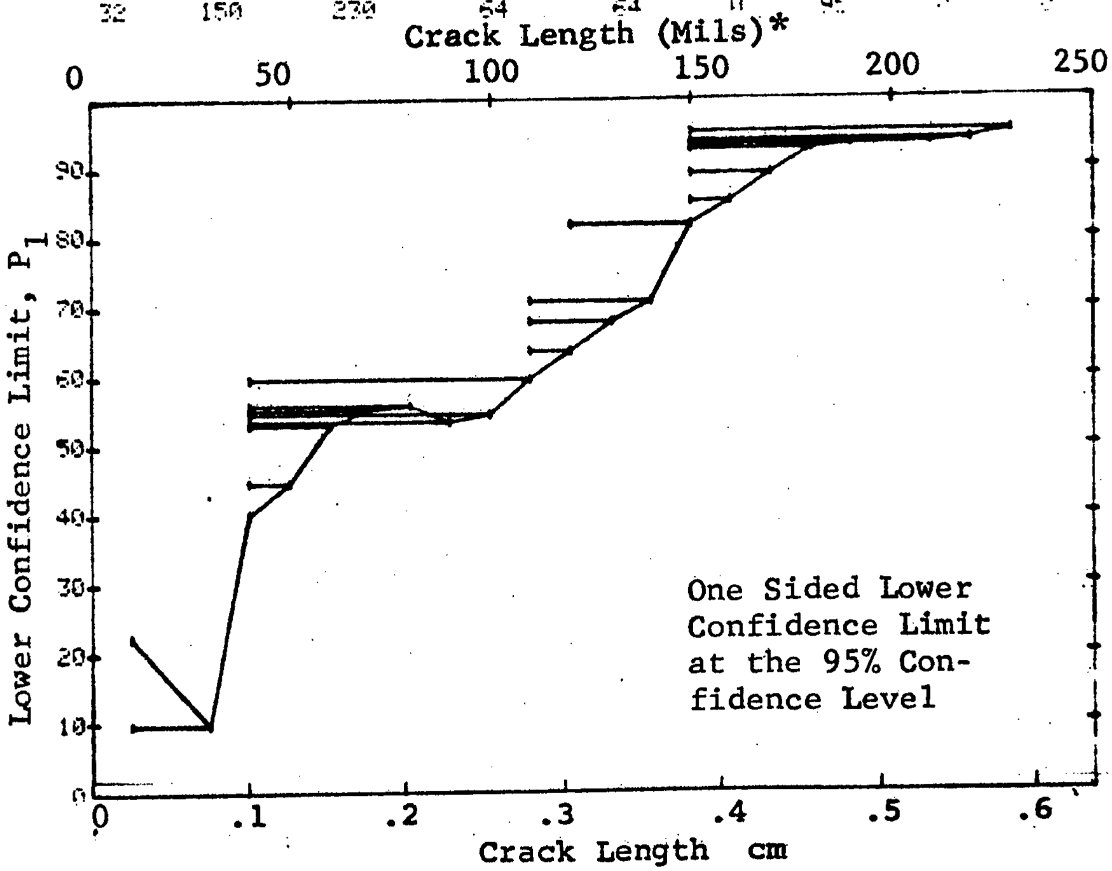

Figure D-108. (Continued)

(c) Overlapping Sixty Point Method of Data Cumulation

RANGE	MIN LN	MAX LN	[illegible]	[illegible]	[illegible] (108)	[illegible]	[illegible]	[illegible]
1	0	[illegible]	[illegible]	[illegible]	[illegible]	[illegible]	[illegible]	
2	0	[illegible]	[illegible]	[illegible]	[illegible]	[illegible]	0	
3	0	[illegible]	[illegible]	[illegible]	[illegible]	[illegible]	0	
4	0	[illegible]	[illegible]	[illegible]	[illegible]	[illegible]	0	
5	0	0	0	0	0	0	0	[illegible]
6	0	0	0	0	0	0	0	[illegible]
7	0	0	0	0	0	0	0	[illegible]
8	0	0	0	0	0	0	0	[illegible]
9	0	0	0	0	0	0	0	[illegible]
10	0	0	0	0	0	0	0	[illegible]
11	0	0	0	0	0	0	0	[illegible]
12	0	0	0	0	0	0	0	[illegible]
13	0	0	0	0	0	0	0	[illegible]
14	0	0	0	0	0	0	0	[illegible]
15	0	0	0	0	0	0	0	[illegible]
16	0	0	0	0	0	0	0	[illegible]
17	0	0	0	0	0	0	0	[illegible]
18	0	0	0	0	0	0	0	[illegible]
19	0	0	0	0	0	0	0	0
20	0	0	0	0	0	0	0	[illegible]
21	0	0	0	0	0	0	0	0
22	0	0	0	0	0	0	0	[illegible]
23	0	0	0	0	0	0	0	[illegible]
24	0	0	0	0	0	0	0	[illegible]
25	0	0	0	0	0	0	0	[illegible]
26	0	0	0	0	0	0	0	[illegible]
27	0	0	0	0	0	0	0	[illegible]
28	10	90	54	33	60	49	0	[illegible]
29	60	110	60	40	65	73	[illegible]	
30	90	150	60	50	82	87	16	[illegible]
31	110	180	60	57	93	95	[illegible]	[illegible]
32	150	230	60	60	98			

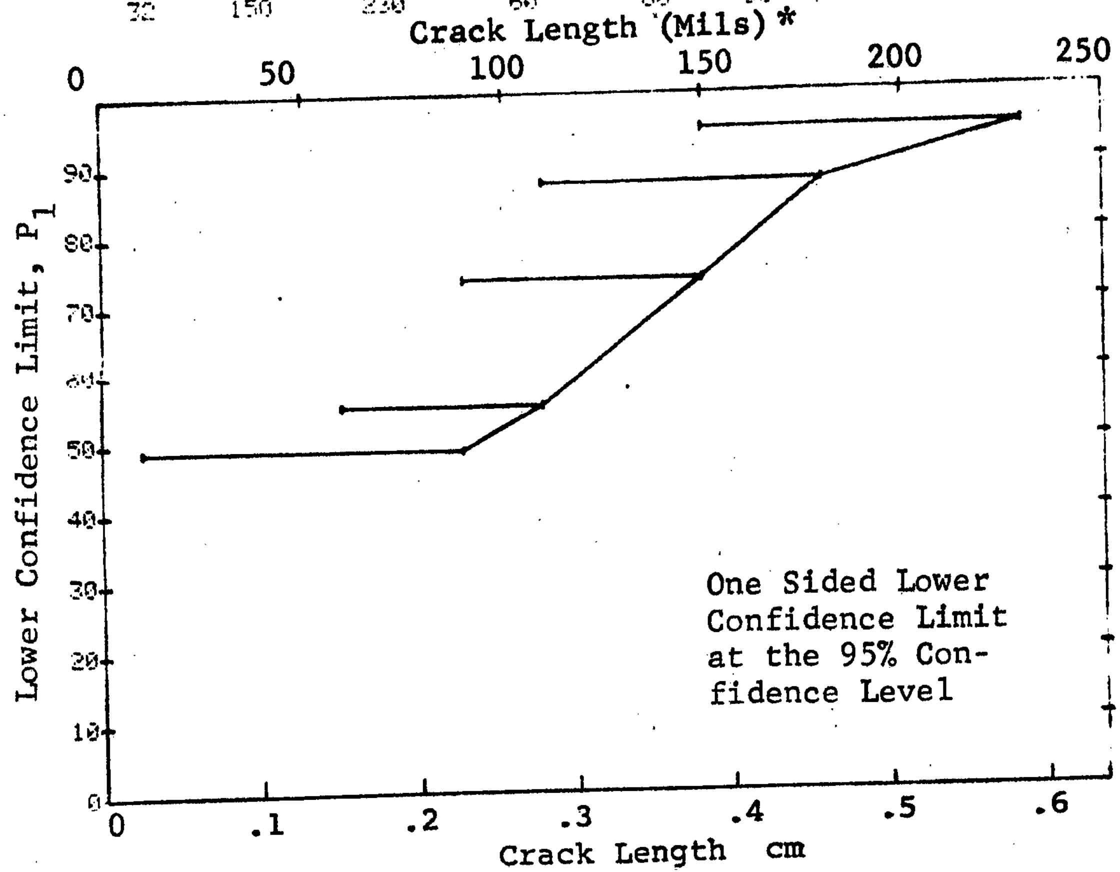

Figure D-108 (Concluded)

(a) Range Interval Method of Data Cumulation

(109)

RANGE	MIN	MAX						
1	[illegible]	[illegible]	[illegible]	[illegible]	56	[illegible]	[illegible]	
2	[illegible]	[illegible]	[illegible]	[illegible]	[illegible]	[illegible]	[illegible]	
3	0	0	0	0	0	[illegible]	0	
4	110	131	12	[illegible]	86	[illegible]	[illegible]	[illegible]
5	130	140	34	[illegible]	[illegible]	82	13	[illegible]
6	150	160	16	16	95	[illegible]	0	[illegible]
7	170	170	5	5	[illegible]	54	[illegible]	[illegible]
8	190	200	22	22	96	[illegible]	0	[illegible]
9	0	0	0	0	0	0	0	[illegible]
10	250	250	5	5	87	54	0	[illegible]
11	0	0	0	0	0	0	0	[illegible]
12	0	0	0	0	0	0	0	[illegible]
13	0	0	0	0	0	0	0	[illegible]
14	0	0	0	0	0	0	0	[illegible]
15	0	0	0	0	0	0	0	[illegible]
16	0	0	0	0	0	0	0	[illegible]
17	0	0	0	0	0	0	0	[illegible]
18	0	0	0	0	0	0	0	[illegible]
19	0	0	0	0	0	0	0	[illegible]
20	0	0	0	0	0	0	0	[illegible]
21	0	0	0	0	0	0	0	[illegible]
22	0	0	0	0	0	0	0	[illegible]
23	0	0	0	0	0	0	0	[illegible]
24	0	0	0	0	0	0	0	[illegible]
25	0	0	0	0	0	0	0	[illegible]
26	0	0	0	0	0	0	0	[illegible]
27	0	0	0	0	0	0	0	[illegible]
28	0	0	0	0	0	[illegible]	[illegible]	[illegible]
29	0	0	0	0	0	0	[illegible]	[illegible]
30	0	0	0	0	0	0	[illegible]	[illegible]
31	0	0	0	0	0	[illegible]	[illegible]	[illegible]
32	750	750	2	2	70	[illegible]	[illegible]	[illegible]

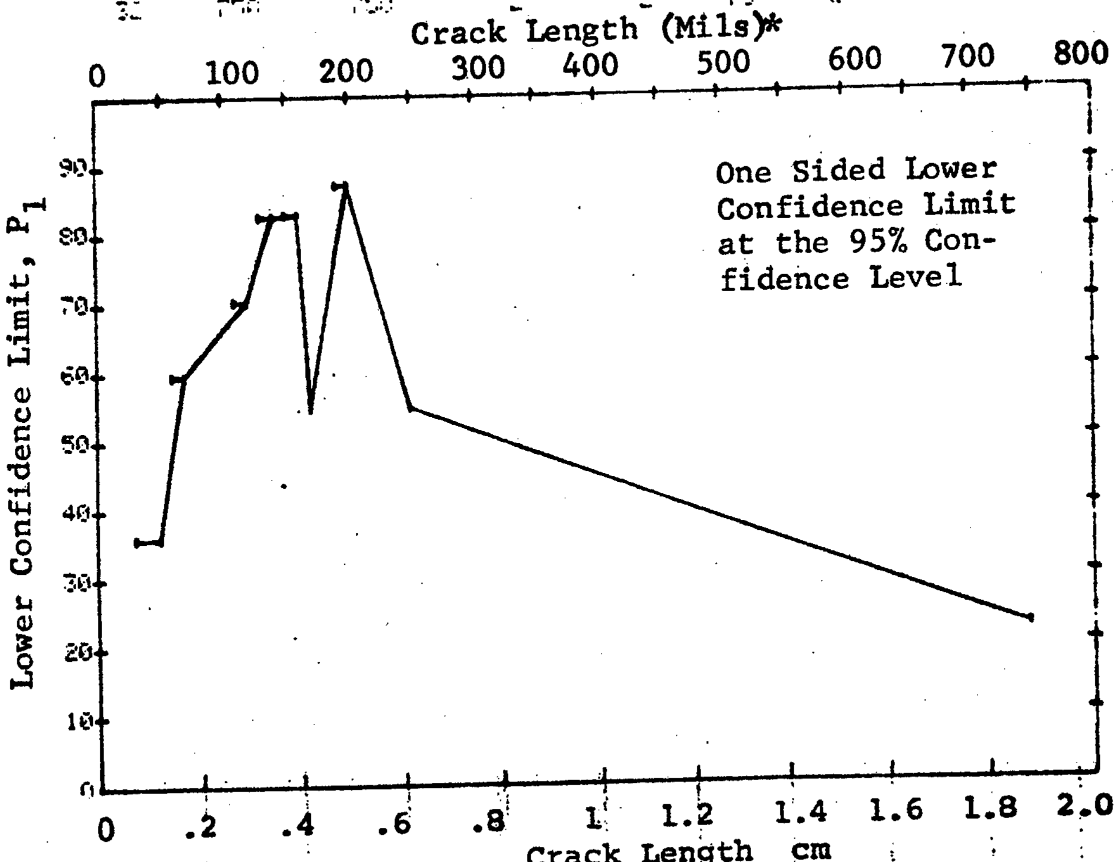

Figure D-109 Probability of Detection for 4340M Steel Using Eddy Current. Compressed Notch Flaws in Solid Cylinder. Laboratory Environment.

(b) Optimum Probability Method of Data Cumulation

28-OCT-75 [illegible] TEST 2 (109)

RANGE	MIN LN	MAX LN	N	HIT	50%	90%	0 MIS	[illegible]
1	30*	50*	15	3	0	35	0	[illegible]
2	60*	[illegible]	22	13	0	53	0	[illegible]
3	0	0	0	0	0	0	0	[illegible]
4	60	120	42	35	0	70	0	[illegible]
5	110	140	53	49	0	83	36	[illegible]
6	130	160	50	48	0	87	11	[illegible]
7	130	170	55	53	0	89	6	[illegible]
8	150	200	43	43	0	93	0	[illegible]
9	0	0	0	0	0	0	0	0
10	150	250	48	48	0	93	0	0
11	0	0	0	0	0	0	0	[illegible]
12	0	0	0	0	0	0	0	0
13	0	0	0	0	0	0	0	0
14	0	0	0	0	0	0	0	0
15	0	0	0	0	0	0	0	0
16	0	0	0	0	0	0	0	0
17	0	0	0	0	0	0	0	0
18	0	0	0	0	0	0	0	0
19	0	0	0	0	0	0	0	0
20	0	0	0	0	0	0	0	0
21	0	0	0	0	0	0	0	0
22	0	0	0	0	0	0	0	0
23	0	0	0	0	0	0	0	0
24	0	0	0	0	0	0	0	0
25	0	0	0	0	0	0	0	0
26	0	0	0	0	0	0	0	0
27	0	0	0	0	0	0	0	0
28	0	0	0	0	0	0	0	0
29	0	0	0	0	0	0	[illegible]	[illegible]
30	0	0	0	0	0	0	0	[illegible]
31	0	0	0	0	0	0	0	0
32	150	750	50	50	0	94	0	0

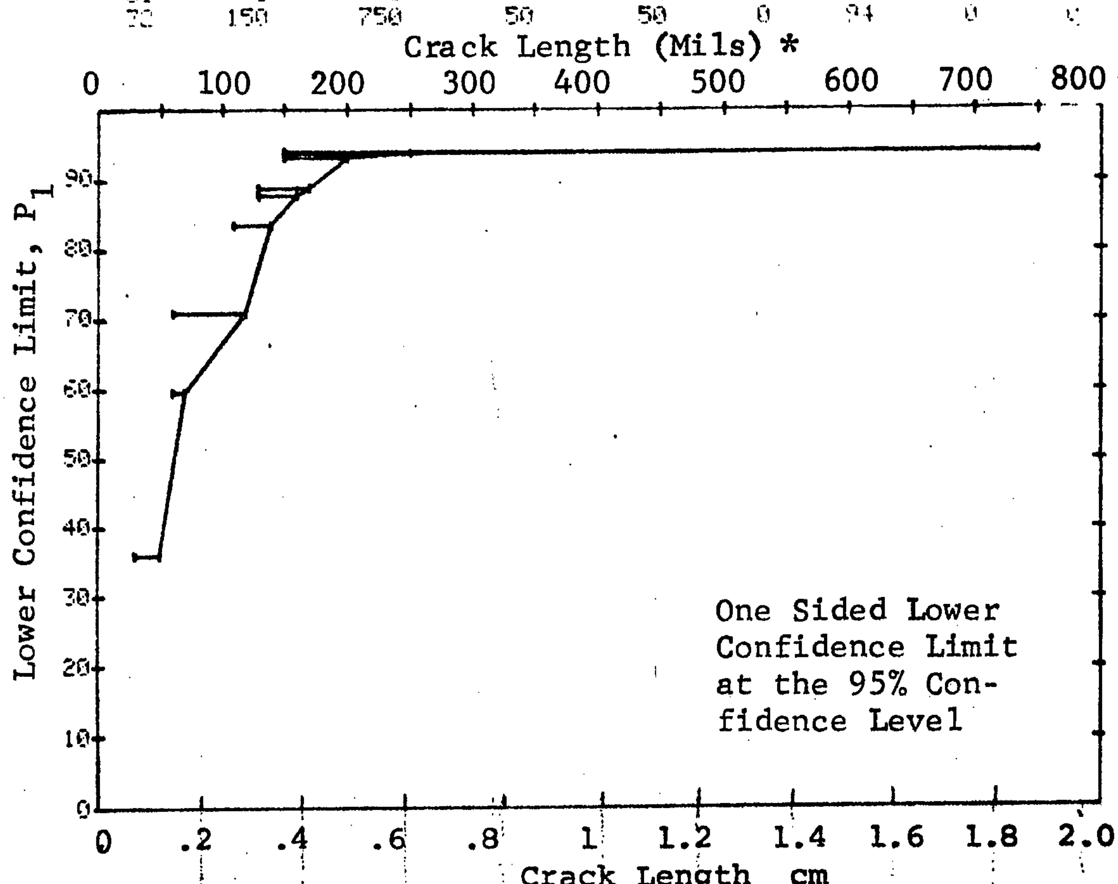

Figure D-109 (Continued)

(c) Overlapping Sixty Point Method of Data Cumulation

28-OCT-7? EDDY [illegible] (109)

RANGE	MIN LN*	MAX LN*	[illegible]	[illegible]	[illegible]	[illegible]	[illegible]	[illegible]
1	0	0	0	0	0	0	0	
2	0	0	0	0	0	0	0	
3	0	0	0	0	0	0	0	
4	0	0	0	0	0	0	0	
5	0	0	0	0	0	0	0	
6	0	0	0	0	0	0	0	[illegible]
7	0	0	0	0	0	0	0	[illegible]
8	0	0	0	0	0	0	0	[illegible]
9	0	0	0	0	0	0	0	[illegible]
10	0	0	0	0	0	0	0	[illegible]
11	0	0	0	0	0	0	0	[illegible]
12	0	0	0	0	0	0	0	[illegible]
13	0	0	0	0	0	0	0	[illegible]
14	0	0	0	0	0	0	0	[illegible]
15	0	0	0	0	0	0	0	[illegible]
16	0	0	0	0	0	0	0	[illegible]
17	0	0	0	0	0	0	0	[illegible]
18	0	0	0	0	0	0	0	[illegible]
19	0	0	0	0	0	0	0	[illegible]
20	0	0	0	0	0	0	0	[illegible]
21	0	0	0	0	0	0	0	[illegible]
22	0	0	0	0	0	0	0	[illegible]
23	0	0	0	0	0	0	0	[illegible]
24	0	0	0	0	0	0	0	
25	0	0	0	0	0	0	0	
26	0	0	0	0	0	0	0	[illegible]
27	0	0	0	0	0	0	0	[illegible]
28	0	0	0	0	0	0	0	[illegible]
29	30	120	43	37	74	[illegible]	[illegible]	
30	60	140	60	55	90	83	[illegible]	
31	120	170	60	57	93	87	16	[illegible]
32	140	250	60	59	97	92	[illegible]	

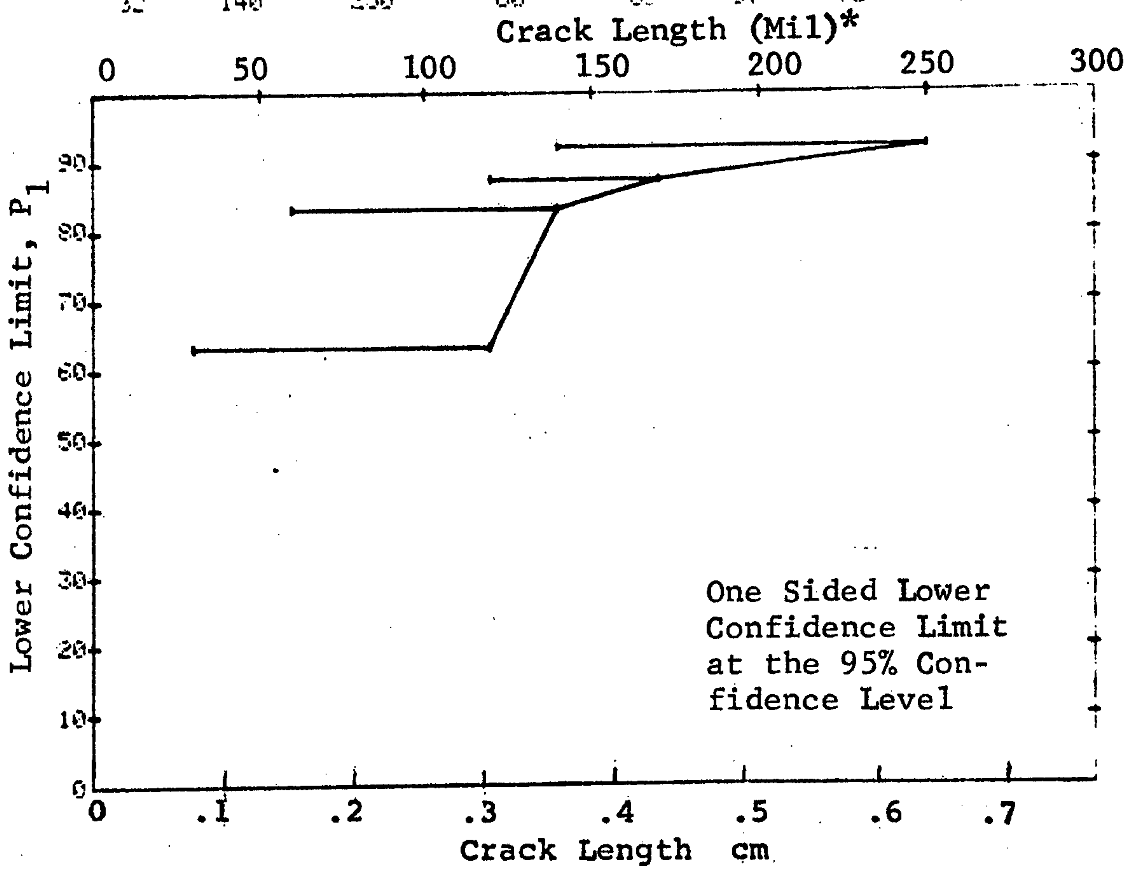

Figure D-109 (Concluded)

(a) Range Interval Method of Data Cumulation

28-OCT-75	EDDY CURRENT			TEST 1		(110)		
RANGE	MIN LN	MAX LN	N	DET	50%	95%	0 MISS	[illegible]
1	70*	80*	[illegible]	7	71	45	0	[illegible]
2	90	90	13	13	94	79	16	[illegible]
3	0	0	0	0	0	0	0	[illegible]
4	110	110	10	10	93	74	0	[illegible]
5	120	120	5	4	68	34	0	[illegible]
6	130	140	30	30	97	90	0	[illegible]
7	0	0	0	0	0	0	0	[illegible]
8	160	160	5	5	87	54	0	[illegible]
9	0	0	0	0	0	0	0	[illegible]
10	180	180	1	1	50	5	0	0
11	0	0	0	0	0	0	0	[illegible]
12	0	0	0	0	0	0	0	0
13	0	0	0	0	0	0	0	[illegible]
14	0	0	0	0	0	0	0	[illegible]
15	0	0	0	0	0	0	0	0
16	0	0	0	0	0	0	0	[illegible]
17	270	270	2	2	70	22	0	[illegible]
18	0	0	0	0	0	0	0	[illegible]
19	0	0	0	0	0	0	0	[illegible]
20	300	300	4	4	84	47	0	0
21	310	310	5	5	87	54	0	0
22	0	0	0	0	0	0	0	0
23	0	0	0	0	0	0	0	[illegible]
24	0	0	0	0	0	0	0	[illegible]
25	0	0	0	0	0	0	0	[illegible]
26	0	0	0	0	0	0	0	[illegible]
27	0	0	0	0	0	0	0	[illegible]
28	0	0	0	0	0	0	[illegible]	[illegible]
29	0	0	0	0	0	0		
30	0	0	0	0	0	0	[illegible]	
31	0	0	0	0	0	0	[illegible]	[illegible]
32	450	450	5	5	87	54	[illegible]	

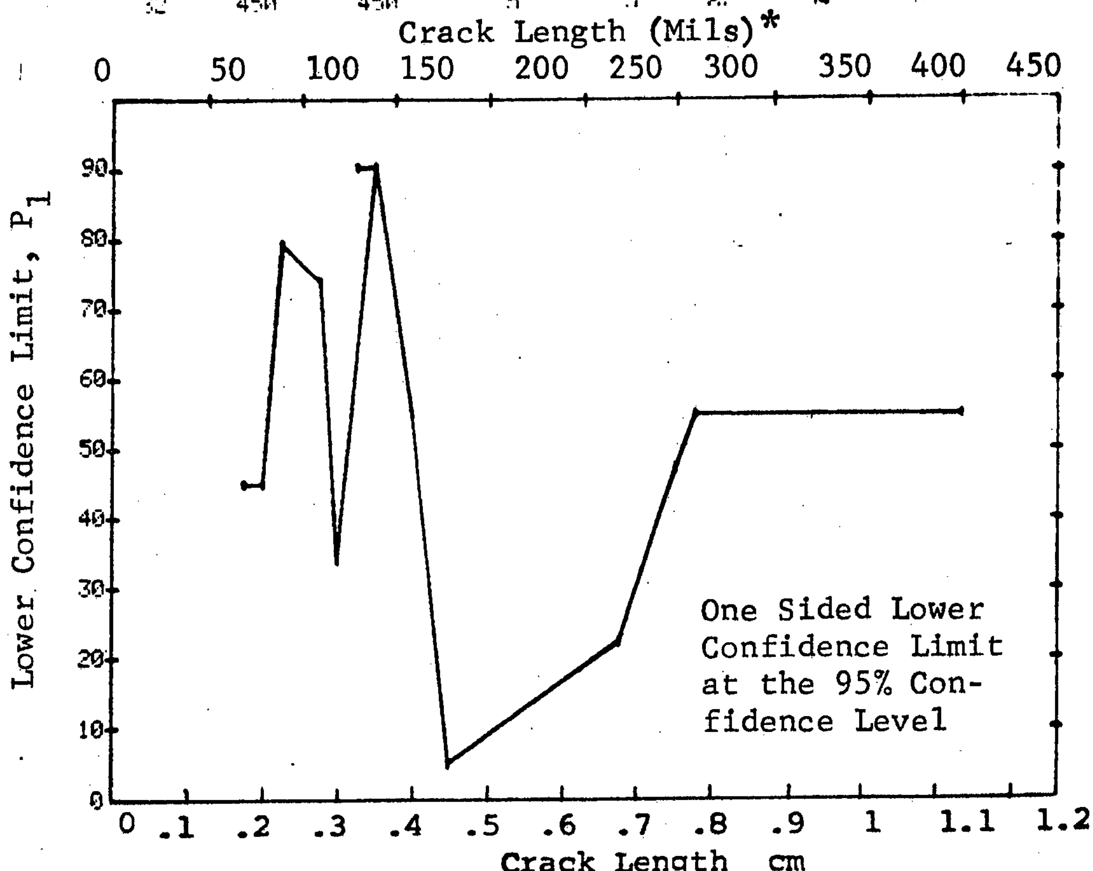

Figure D-110 Probability of Detection for 4340M Steel Using Eddy Current. Compressed Notch Flaws in Hollow Filleted Cylinder. Laboratory Environment.

(b) Optimum Probability Method of Data Cumulation

28-OCT-75 EDDY CURRENT TEST 2 (110)

RANGE	MIN LN	MAX LN	N	NFT	50%	95%	0 M[illegible]	
1	70	90	3	[illegible]	0	45	[illegible]	
2	90	90	13	1[illegible]	0	79	[illegible]	
3	0	0	0	0	0	0	[illegible]	[illegible]
4	90	110	23	23	0	87	[illegible]	[illegible]
5	90	120	28	27	0	84	1[illegible]	[illegible]
6	90	140	58	57	0	92	0	[illegible]
7	0	0	0	0	0	0	0	[illegible]
8	90	160	63	62	0	92	0	[illegible]
9	0	0	0	0	0	0	0	[illegible]
10	90	180	64	63	0	92	0	0
11	0	0	0	0	0	0	0	0
12	0	0	0	0	0	0	0	0
13	0	0	0	0	0	0	0	0
14	0	0	0	0	0	0	0	0
15	0	0	0	0	0	0	0	0
16	0	0	0	0	0	0	0	0
17	90	270	66	65	0	93	0	0
18	0	0	0	0	0	0	0	0
19	0	0	0	0	0	0	0	0
20	90	300	70	69	0	93	0	0
21	130	310	47	47	0	93	0	0
22	0	0	0	0	0	0	0	0
23	0	0	0	0	0	0	0	0
24	0	0	0	0	0	0	0	[illegible]
25	0	0	0	0	0	0	0	[illegible]
26	0	0	0	0	0	0	0	[illegible]
27	0	0	0	0	0	0	0	[illegible]
28	0	0	0	0	0	[illegible]		
29	0	0	0	0	0	[illegible]	[illegible]	
30	0	0	0	0	0	0	[illegible]	
31	0	0	0	0	0	0		
32	130	450	52	52	0	94		

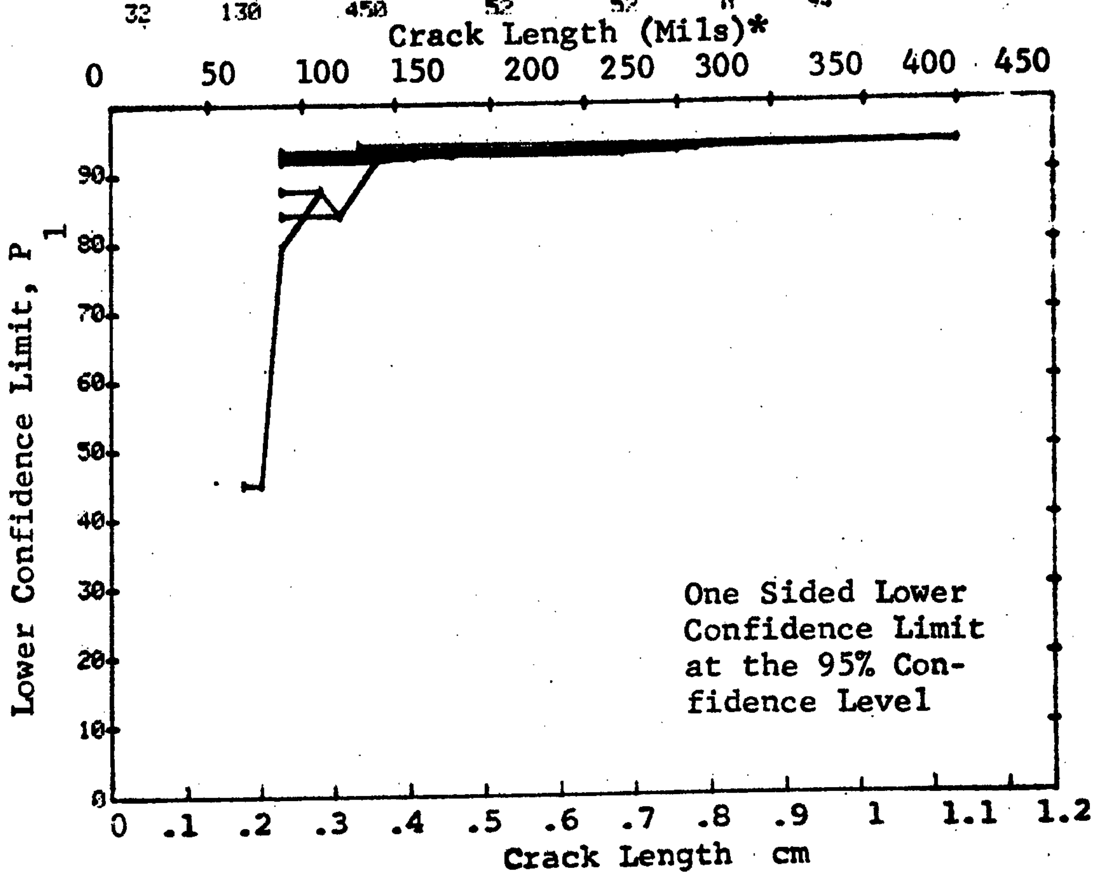

Figure D-110 (Continued)

(c) Overlapping Sixty Point Method of Data Cumulation

28-OCT-75 EDDY CURRENT TEST 3 [illegible] (110)

RANGE	MIN LN	MAX LN	[illegible]	DET	50%	95%	0 MI	
1	0	0	0	0	0	0	0	
2	0	[illegible]	0	0	0	0	0	
3	0	0	0	0	0	0	0	[illegible]
4	0	0	0	0	0	0	0	[illegible]
5	0	0	0	0	0	0	0	
6	0	0	0	0	0	0	0	[illegible]
7	0	0	0	0	0	0	0	[illegible]
8	0	0	0	0	0	0	0	
9	0	0	0	0	0	0	0	[illegible]
10	0	0	0	0	0	0	0	[illegible]
11	0	0	0	0	0	0	0	[illegible]
12	0	0	0	0	0	0	0	[illegible]
13	0	0	0	0	0	0	0	[illegible]
14	0	0	0	0	0	0	0	[illegible]
15	0	0	0	0	0	0	0	[illegible]
16	0	0	0	0	0	0	0	[illegible]
17	0	0	0	0	0	0	0	[illegible]
18	0	0	0	0	0	0	0	[illegible]
19	0	0	0	0	0	0	0	[illegible]
20	0	0	0	0	0	0	0	0
21	0	0	0	0	0	0	0	0
22	0	0	0	0	0	0	0	0
23	0	0	0	0	0	0	0	[illegible]
24	0	0	0	0	0	0	0	[illegible]
25	0	0	0	0	0	0	0	[illegible]
26	0	0	0	0	0	0	[illegible]	[illegible]
27	0	0	0	0	0	0	0	[illegible]
28	0	0	0	0	0	0	0	
29	0	0	0	0	0	[illegible]	[illegible]	
30	0	0	0	0	0	[illegible]		
31	70	140	59	56	93	87	[illegible]	[illegible]
32	110	450	60	59	97	[illegible]		

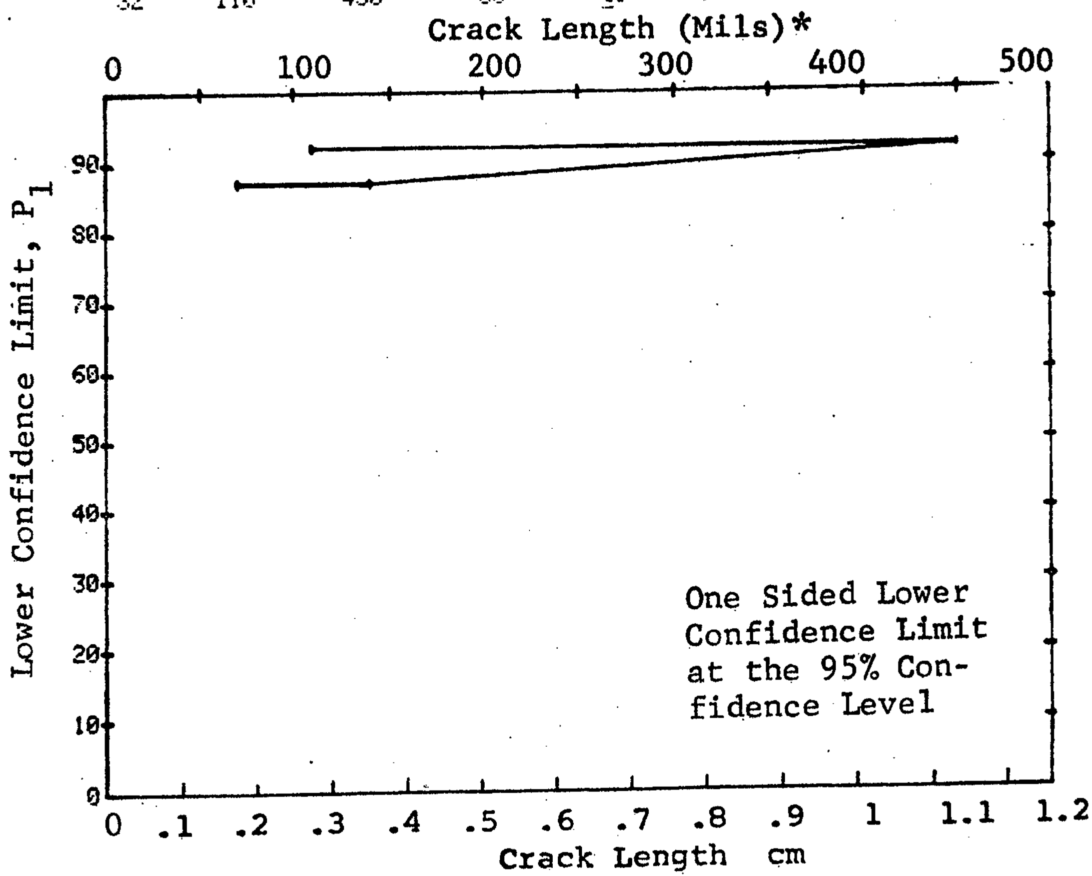

Figure D-110 (Concluded)

(a) Range Interval Method of Data Cumulation

28-OCT-75 EDDY CURRENT TEST 1 (111)

RANGE	MIN LN	*MAX LN*	N	DET	50%	95%	0 MI
1	20	30	10	2	15	3	0
2	0	0	0	0	0	0	0
3	60	60	8	3	32	11	0
4	70	70	6	5	73	41	0
5	90	90	8	8	91	69	0
6	100	100	5	5	87	54	0
7	0	0	0	0	0	0	0
8	130	140	20	19	91	78	26
9	150	150	11	11	93	76	18
10	0	0	0	0	0	0	0
11	0	0	0	0	0	0	0
12	0	0	0	0	0	0	0
13	0	0	0	0	0	0	0
14	230	230	3	3	79	36	0
15	0	0	0	0	0	0	0
16	250	260	8	8	91	68	0
17	0	0	0	0	0	0	0
18	280	280	3	3	79	36	0
19	300	300	7	7	90	65	0
20	0	0	0	0	0	0	0
21	0	0	0	0	0	0	0
22	0	0	0	0	0	0	0
23	0	0	0	0	0	0	0
24	370	380	7	7	90	65	0
25	0	0	0	0	0	0	0
26	0	0	0	0	0	0	0
27	0	0	0	0	0	0	0
28	0	0	0	0	0	0	0
29	0	0	0	0	0	0	[illegible]
30	0	0	0	0	0	0	[illegible]
31	0	0	0	0	0	0	[illegible]
32	500	500	3	3	79	36	[illegible]

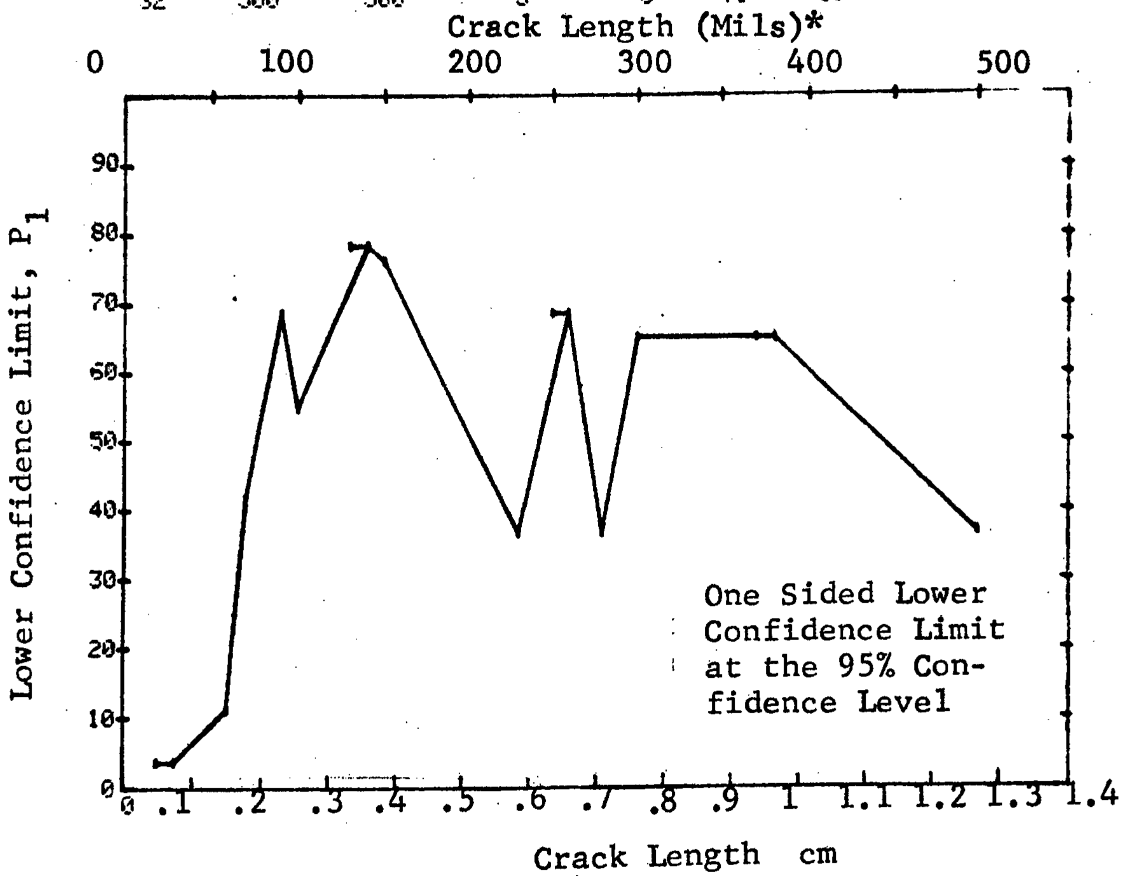

Figure D-111 Probability of Detection for 4340M Steel Using Eddy Current. Compressed Notch Flaws in Solid Filleted Cylinder. Laboratory Environment

(b) Optimum Probability Method of Data Cumulation

28-OCT-75 EDDY CURRENT TEST 2 ( ) (111)

RANGE	MIN LN	MAX LN	N	DET	50%	95%	[illegible]	[illegible]
1	20 *	30 *	10	2	0	3	0	0
2	0	0	0	0	0	0	0	[illegible]
3	20	60	18	5	0	11	0	[illegible]
4	70	70	6	5	0	41	0	[illegible]
5	70	90	14	13	0	70	0	[illegible]
6	90	100	13	13	0	79	0	[illegible]
7	0	0	0	0	0	0	0	[illegible]
8	90	140	33	32	0	86	17	[illegible]
9	90	150	44	43	0	89	2	1
10	0	0	0	0	0	0	0	0
11	0	0	0	0	0	0	0	0
12	0	0	0	0	0	0	0	0
13	0	0	0	0	0	0	0	0
14	90	230	47	46	0	90	0	14
15	0	0	0	0	0	0	0	0
16	90	260	55	54	0	91	0	0
17	0	0	0	0	0	0	0	0
18	90	280	58	57	0	92	0	0
19	90	300	65	64	0	92	0	0
20	0	0	0	0	0	0	0	0
21	0	0	0	0	0	0	0	0
22	0	0	0	0	0	0	0	0
23	0	0	0	0	0	0	0	0
24	90	380	72	71	0	93	0	0
25	0	0	0	0	0	0	0	0
26	0	0	0	0	0	0	0	0
27	0	0	0	0	0	0	0	[illegible]
28	0	0	0	0	0	0	[illegible]	[illegible]
29	0	0	0	0	0	0	[illegible]	[illegible]
30	0	0	0	0	0	0	[illegible]	[illegible]
31	0	0	0	0	0	0	[illegible]	[illegible]
32	90	500	75	74	0	93	[illegible]	[illegible]

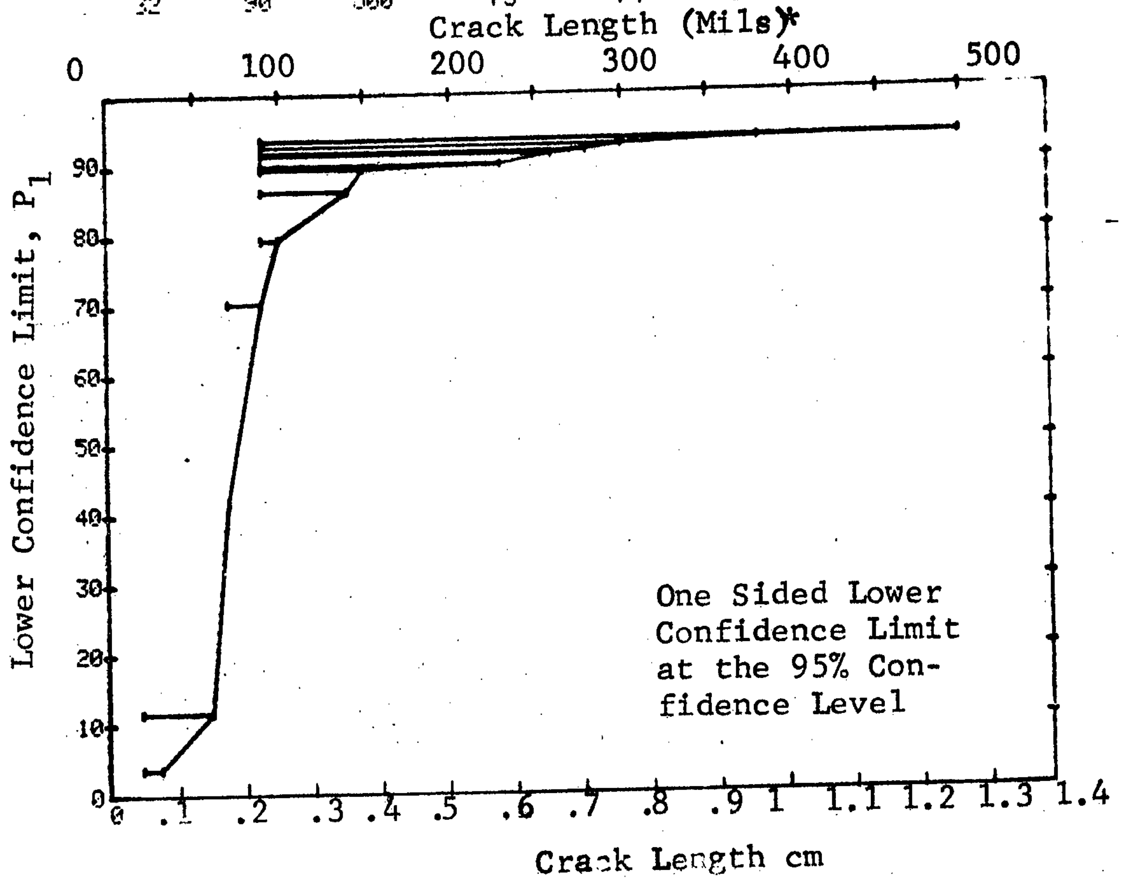

Figure D-111 (Continued)

(c) Overlapping Sixty Point Method of Data Cumulation

28-OCT-75 EDDY CURRENT TEST 3 (111)

RANGE	MIN LN	MAX LN	N	DET	50%	95%	0 MI[illegible]	[illegible]
1	0 *	0 *	0	0	0	0	0	
2	0	0	0	0	0	0	0	0
3	0	0	0	0	0	0	0	0
4	0	0	0	0	0	0	0	0
5	0	0	0	0	0	0	0	0
6	0	0	0	0	0	0	0	0
7	0	0	0	0	0	0	0	0
8	0	0	0	0	0	0	0	0
9	0	0	0	0	0	0	0	0
10	0	0	0	0	0	0	0	0
11	0	0	0	0	0	0	0	0
12	0	0	0	0	0	0	0	0
13	0	0	0	0	0	0	0	0
14	0	0	0	0	0	0	0	0
15	0	0	0	0	0	0	0	0
16	0	0	0	0	0	0	0	0
17	0	0	0	0	0	0	0	0
18	0	0	0	0	0	0	0	0
19	0	0	0	0	0	0	0	0
20	0	0	0	0	0	0	0	0
21	0	0	0	0	0	0	0	0
22	0	0	0	0	0	0	0	0
23	0	0	0	0	0	0	0	0
24	0	0	0	0	0	0	0	0
25	0	0	0	0	0	0	0	0
26	0	0	0	0	0	0	0	0
27	0	0	0	0	0	0	0	0
28	0	0	0	0	0	0		
29	0	0	0	0	0	0		
30	20	130	39	25	62	49	[illegible]	[illegible]
31	30	230	60	53	87	79		
32	130	500	60	59	97	92		

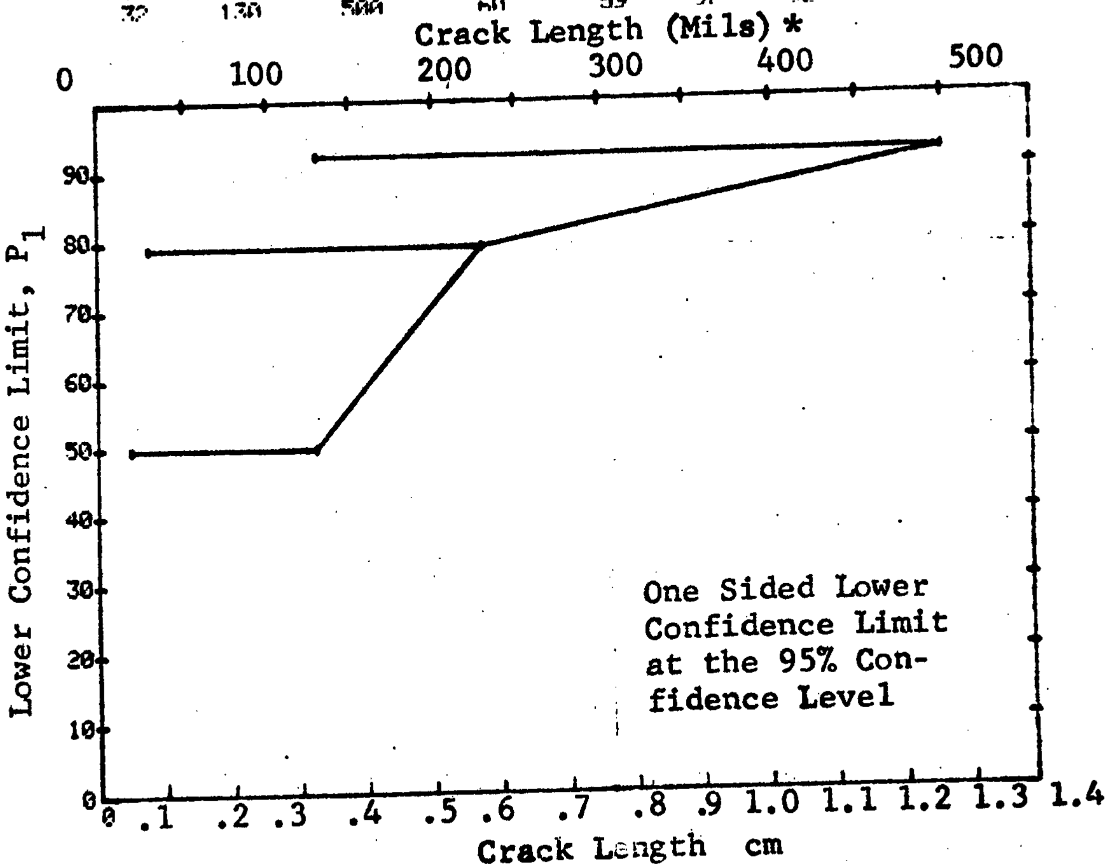

Figure D-111 (Concluded)

(a) Range Interval Method of Data Cumulation

28-OCT-75 EDDY CURRENT TEST 1 . (112)

RANGE	MIN LN	MAX LN	N	DET	50%	95%	0 MI	
1	60 *	60 *	4	0	0	0	0	[illegible]
2	0	0	0	0	0	0	0	[illegible]
3	0	0	0	0	0	0	0	[illegible]
4	0	0	0	0	0	0	0	[illegible]
5	0	0	0	0	0	0	0	[illegible]
6	0	0	0	0	0	0	0	[illegible]
7	0	0	0	0	0	0	0	[illegible]
8	100	100	16	10	59	39	0	0
9	0	0	0	0	0	0	0	0
10	0	0	0	0	0	0	0	0
11	0	0	0	1	15	1	0	0
12	120	120	4	0	0	0	0	0
13	0	0	0	2	50	13	0	0
14	130	130	3	0	0	0	0	0
15	0	0	0	12	87	68	0	0
16	140	140	13	0	0	0	0	0
17	0	0	0	0	0	0	0	0
18	0	0	0	2	70	22	0	0
19	160	160	2	0	0	0	0	0
20	0	0	0	0	0	0	0	0
21	0	0	0	0	0	0	0	0
22	0	0	0	3	61	24	0	0
23	180	180	4	0	0	0	0	0
24	0	0	0	0	0	0	0	0
25	0	0	0	0	0	0	0	0
26	0	0	0	0	0	0	0	0
27	0	0	0	0	0	0	0	0
28	0	0	0	0	0	0		
29	0	0	0	0	0	0		
30	0	0	0	0	0	0		
31	0	0	0	0	0	[illegible]		
32	230	230	4	4	[illegible]	[illegible]		

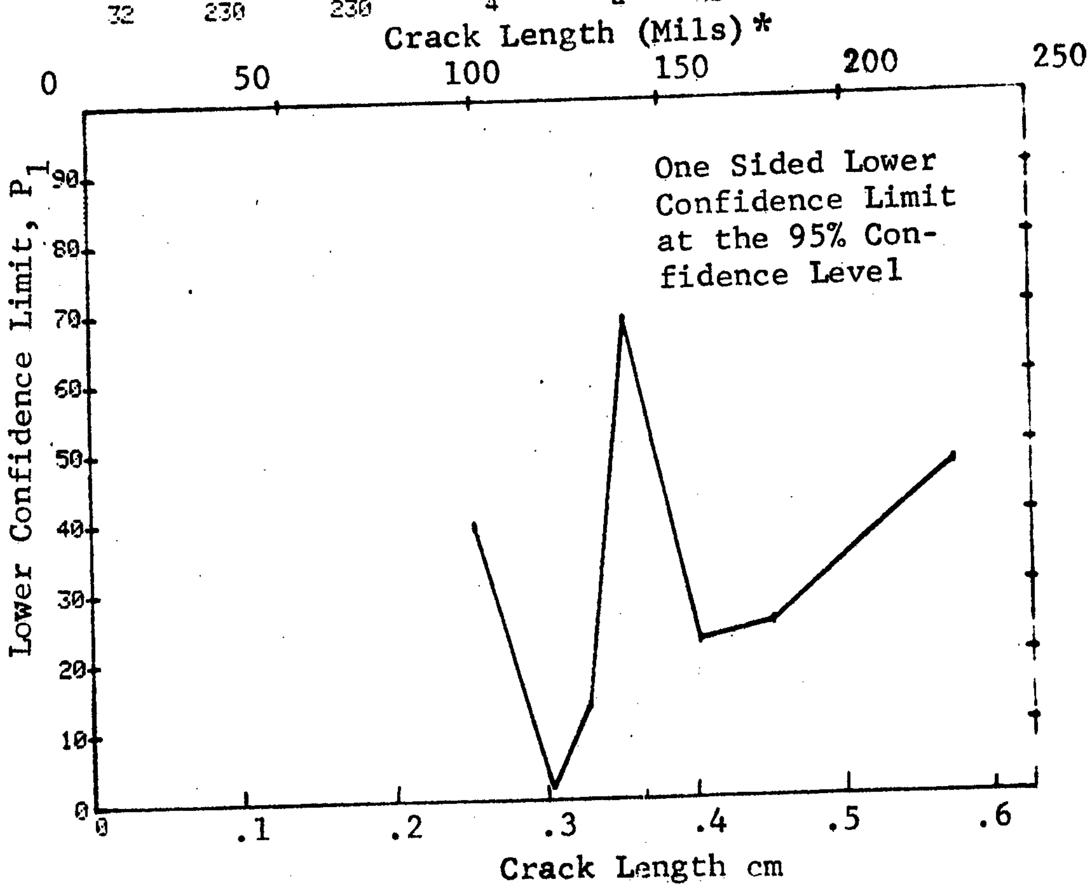

Figure D-112 Probability of Detection for 4340M Steel Using Eddy Current. Compressed Notch Flaws in Hollow Cylinder. Laboratory Environment.

(b) Optimum Probability Method of Data Cumulation

28-OCT-75 EDDY CURRENT TEST 2 (112)

RANGE	MIN LN *	MAX LN *	N	DET	50%	95%	0 MISS	
1	60	60	4	0	0	0	0	[illegible]
2	0	[illegible]	0	0	0	0	0	[illegible]
3	0	0	0	0	0	0	0	[illegible]
4	0	0	0	0	0	0	0	[illegible]
5	0	0	0	0	0	0	0	0
6	0	0	0	0	0	0	0	0
7	0	0	0	0	0	0	0	0
8	100	100	16	10	0	39	0	0
9	0	0	0	0	0	0	0	0
10	0	0	0	0	0	0	0	0
11	0	0	0	0	0	0	0	0
12	100	120	20	11	0	34	0	0
13	0	0	0	0	0	0	0	0
14	100	130	23	13	0	37	0	0
15	0	0	0	0	0	0	0	0
16	140	140	13	12	0	68	0	0
17	0	0	0	0	0	0	0	0
18	0	0	0	0	0	0	0	0
19	140	160	15	14	0	72	0	0
20	0	0	0	0	0	0	0	0
21	0	0	0	0	0	0	0	0
22	0	0	0	0	0	0	0	0
23	140	180	19	17	0	70	0	0
24	0	0	0	0	0	0	0	0
25	0	0	0	0	0	0	0	0
26	0	0	0	0	0	0	0	0
27	0	0	0	0	0	0	0	0
28	0	0	0	0	0	0	[illegible]	[illegible]
29	0	0	0	0	0	0	[illegible]	[illegible]
30	0	0	0	0	0	0	[illegible]	[illegible]
31	0	0	0	0	0	0	[illegible]	[illegible]
32	140	230	23	21	0	75	[illegible]	[illegible]

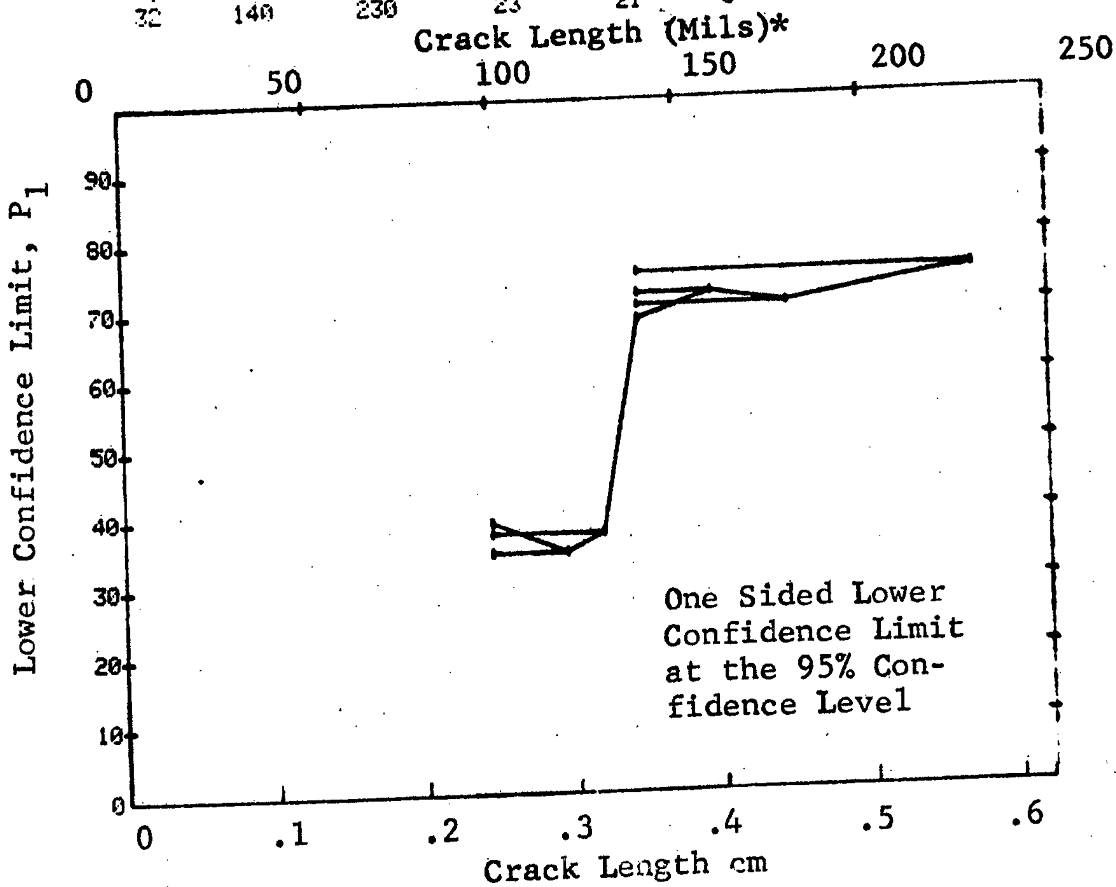

Figure D-112 (Continued)

(c) Overlapping Sixty Point Method of Data Cumulation

28-OCT-75 EDDY CURRENT TEST 3 ( ) (112)

RANGE	MIN LN *	MAX LN *	N	DET	50%	95%	0 MIS
1	0	0	0	0	0	0	0
2	0	0	0	0	0	0	0
3	0	0	0	0	0	0	0
4	0	0	0	0	0	0	0
5	0	0	0	0	0	0	0
6	0	0	0	0	0	0	0
7	0	0	0	0	0	0	0
8	0	0	0	0	0	0	0
9	0	0	0	0	0	0	0
10	0	0	0	0	0	0	0
11	0	0	0	0	0	0	0
12	0	0	0	0	0	0	0
13	0	0	0	0	0	0	0
14	0	0	0	0	0	0	0
15	0	0	0	0	0	0	0
16	0	0	0	0	0	0	0
17	0	0	0	0	0	0	0
18	0	0	0	0	0	0	0
19	0	0	0	0	0	0	0
20	0	0	0	0	0	0	0
21	0	0	0	0	0	0	0
22	0	0	0	0	0	0	0
23	0	0	0	0	0	0	0
24	0	0	0	0	0	0	0
25	0	0	0	0	0	0	0
26	0	0	0	0	0	0	0
27	0	0	0	0	0	0	0
28	0	0	0	0	0	0	0
29	0	0	0	0	0	[illegible]	[illegible]
30	0	0	0	0	0	0	[illegible]
31	0	0	0	0	0	0	0
32	60	230	56	34	66	55	

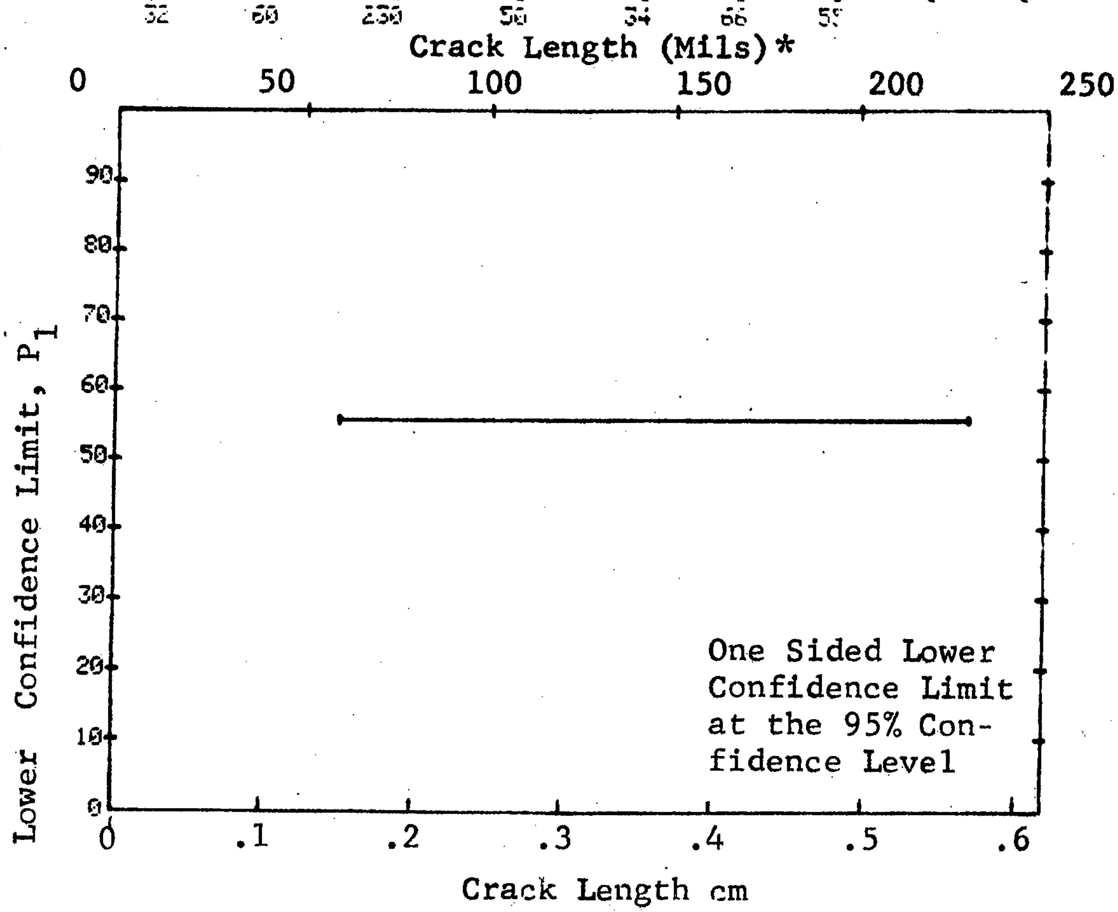

Figure D-112 (Concluded)

DISTRIBUTION LIST

Contract NAS3-18907
Final Contractor Report

NASA-Lewis Research Center
Cleveland, OH 44135
Attn: *T. Gulko, MS 49-3
*R.L. Davies, MS 106-1
*N.T. Saunders, MS 105-1
*Audit Branch, MS 500-303
*S.J. Klima, MS 106-1 (22 copies)
*J.E. Dilley, MS 500-313

G.T. Smith, MS 49-3
W.F. Brown, MS 105-1
Library, MS 60-3 (2 copies)
Technology Utilization, MS 3-9
Report Control, MS 5-5
R.W. Hall, MS 49-1

National Aeronautics and Space Administration
Washington, DC 20546
Attn: RW/G.C. Deutsch

RWS/ M. Salkind
Library

MHQ/G. Eriksen
MQ/P. Wood

National Aeronautics and Space Administration
George C. Marshall Space Flight Center
Marshall Space Flight Center, AL 35812
Attn: J. M. Knadler, III, Code EH13
R. C. Crockett, Code EL44
Library

National Aeronautics and Space Administration
Lyndon B. Johnson Space Center
Houston, TX 77058
Attn: ES-5/R.E. Johnson
ES-5/W.L. Castner
Library

National Aeronautics and Space Administration
Langley Research Center
Hampton, VA 23365
Attn: R.W. Leonard, MS 188
Library

D-345

National Aeronautics and Space Administration
John F. Kennedy Space Center
Kennedy Space Center, FL 32899
Attn: R. Sannicandro, DD-SED-4
Library

National Aeronautics and Space Administration
Goddard Space Flight Center
Greenbelt, MD 20771
Attn: Library

Jet Propulsion Laboratory
4800 Oak Grove Drive
Pasadena, CA 91103
Attn: Library

U. S. Air Force
Wright Patterson AFB, OH 45433
Attn: T.D. Cooper, AFML/MXA
M.J. Warrick, AMRL/HE
N. Tupper, AFFDL/FBA
W.R. Luebben, AFLC/MAUT
D. Fourney, AFML/LLP

Scientific and Technical Information Facility
Box 8757
Baltimore-Washington Int. Airport
Baltimore, MD 21240
Attn: NASA Representative (6 copies)

Lockheed Georgia Company
Marietta, GA 30063
Attn: W.H. Lewis, D/73-30, Z-285

TRW Inc.
23555 Euclid Ave.
Cleveland, OH 44117
Attn: I.M. Matay TM-2966

North American Rockwell
Quality Assurance
12214 Lakewood Boulevard
Downey, CA 90241
Attn: C.R. Bishop

U. S. Air Force
Hq. SAAMA/MMEW-4
Kelly Air Force Base, TX 78241
Attn: B.W. Boisvert

Pratt & Whitney Aircraft
P. O. Box 2691
West Palm Beach, FL 33402
Attn: C. Biddle

D-346

McDonnell Douglas Corp.
P.O. Box 516
St. Louis, MO 63166
Attn: R. J. Roehrs

Lockheed-California Company
Dept. 74-44, Bldg. 243, Plant 2
Burbank, CA 91503
Attn: D.E. Pettit

Martin-Marietta Corporation
P.O. Box 179
Denver, CO 80201
Attn: W. Rummel, MS 1620

LTV Aerospace Division
P.O. Box 5907
Dallas, TX 75222
Attn: B.W. Staff

Naval Air Development Center
Warminster, PA 18974
Attn: F.S. Williams, Code 302

Northrop Corporation
A/C Division
3901 West Broadway
Hawthorne, CA 90250
Attn: W.R. Sturrock, 7620/23

Fairchild Republic Company
Quality Assurance Laboratory
Bldg. 32
Farmingdale, NY 11735
Attn: R. Brousseau

Grumman Aerospace Corp.
Q.C.A.D.
Bethpage, NY 11714
Attn: S. Chance

Systems Research Laboratory
2800 Indian Ripple Road
Dayton, OH 45440
Attn: W. Dirkes

Pratt & Whitney Aircraft
East Hartford, CT
Attn: F. Vick

Rockwell International
Los Angeles Division
Los Angeles, CA
Attn: E. L. Caustin

D-347

Army Materials & Mechanics Research Center
Mechanics of Materials
Watertown, MA 02172
Attn: G. A. Darcy

General American Research Division
7449 North Natchez Avenue
Niles, IL 60642
Attn: W. Lichodziejewski

U. S. Air Force
Tinker AFB
Oklahoma City, OK 73145
Attn: M. Mizell, ALC/MMET

Boeing Commercial Airplane Company
P.O. Box 3707
Seattle, WA 98124
Attn: H. Southworth, MS 73-05

Rockwell International
Science Center
1049 Camino Dos Rios
Thousand Oaks, CA 91360
Attn: D. Thompson

U. S. Air Force
Hill AFB
Ogden, UT 84401
Attn: C. Thomson, ALC/MMET

General Electric Company
Aircraft Engine Group
Evendale, OH 45215
Attn: H. Truscott, M/L M-87
R. Wagner

National Bureau of Standards
Materials Building, Rm. B354
Washington, DC 20234
Attn: H. Berger

Transportation Systems Center
Kendall Square
Cambridge, MA 02142
Attn: I. Litant

Sandia Laboratories
Dept. 9350
Albuquerque, NM 87115
Attn: F.W. Neilson

D-348

National Science Foundation
Division of Materials Research
1800 G Street, N.W.
Washington, DC 20550
Attn: J. R. Lane

Shannon Luminous Materials Company
Tracer-Tech Division
7356 Santa Monica Blvd.
Los Angeles, CA 90046
Attn: J.R. Alburger

Bucyrus-Erie Company
Construction Machinery
Milwaukee, WI
Attn: K.V. Johnson

Babcock & Wilcox Company
Hwy. 69 S
Mt. Vernon, IN 47620
Attn: P.J. Kovach

Schlumberger Well Services
P.O. Box 2175
Houston, TX 77C01
Attn: E. Moser

Wyman-Gordon Company
14600 S. Wood Street
Harvey, IL 60426
Attn: J. Sekerka

Combustion Engineering
911 West Main Street
Chattanooga, TN 37401
Attn: R.M. Stone

Office of The Secretary of Transportation
Office of Pipeline Safety
Washington, DC 2C590
Attn: J.C. Caldwell

Westinghouse Electric Corporation
Gas Turbine Engine Division
Building A 603
Philadelphia, PA 19113
Attn: T. Sherlock

NASA-Ames Research Center
Moffett Field, CA 94035
Attn: R. Hampton, MS213-4

Martin Marietta
P. O. Box 29304
New Orleans, LA 70189
Attn: V. Clisham

D-349

General Dynamics Letter
18907-FW#11-29
dated 1 November 1976

DOCUMENT RELEASE AUTHORIZATION

NASA Scientific and Technical Information Facility
P.O. Box 8757, Balt/Wash International Airport, Maryland 21240

Control No.
Date:

DOCUMENT DESCRIPTION

TITLE: Assessment of NDE Reliability Data

AUTHOR(S): B. G. W. Yee, F. H. Chang, J. C. Couchman, G. H. Lemon, and P. F. Packman

ORIGINATING ORGANIZATION: General Dynamics, Fort Worth Division

CONTRACT NO: NAS3-18907

SECURITY CLASSIFICATION: TITLE: U DOCUMENT: U

REPORT NO.

DATE:

COGNIZANT NASA CENTER
NASA Lewis Research Center
Mail Stop 106-1
21000 Brookpark Rd.
Cleveland, OH 44135

NASA CR NO 134991
NASA TMX NO.

WORK UNIT NO: YHG6780

NASA TECHNICAL MONITOR: S. J. Klima

OFFICE CODE: 5532

THE FOLLOWING TO BE COMPLETED BY THE RESPONSIBLE NASA PROGRAM OFFICER OR HIS DESIGNEE

(Further information is available in SP-7034 entitled R & D Reporting Guidance for Technical Monitoring of NASA Contracts)

I. Document may be processed into the NASA Information System as follows:

- [x] May be announced in STAR (or CSTAR if a limited availability is checked below)
- [ ] May not be announced (The attached letter may be consulted for information pertaining to the NASA non-announcement series)
- [ ] May not be entered into the System because ______

(Provide a brief statement to be quoted in answering requests for the referenced document)

II. Document may be made available as checked below:

- [x] Publicly Available
- [ ] Classified but Unlimited to Security Qualified Requesters
- [ ] U.S. Government Agencies and Contractors Only
- [ ] U.S. Government Agencies Only
- [ ] U.S. Government Agencies, NASA and NASA Contractors Only
- [ ] NASA and NASA Contractors Only
- [ ] NASA Headquarters and Centers Only
- [ ] Other Limitations (Specify) ______

Signature (Program Officer or Designee):

Office Code: 5532
Telephone No: 216/433-4000 X357

Date Signed:

MAILING LABEL
Use open window envelope
or
Clip out and paste

TO:

NASA Scientific and Technical
Information Facility
Attn: Accessioning Department
P.O. Box 8757
Balt/Wash International Airport
Maryland 21240

FF 427 FEB 75

76 10227